BNL-99088-2013

# RIKEN/RBRC Workshop
## Thermal Radiation
## December 5-7, 2012

**Proceedings of RIKEN BNL Research Center Workshop**

Volume 113

RBRC
RIKEN BNL Research Center

## DISCLAIMER

This work was prepared as an account of work sponsored by an agency of the United States Government. Neither the United States Government nor any agency thereof, nor any of their employees, nor any of their contractors, subcontractors or their employees, makes any warranty, express or implied, or assumes any legal liability or responsibility for the accuracy, completeness, or any third party's use or the results of such use of any information, apparatus, product, or process disclosed, or represents that its use would not infringe privately owned rights. Reference herein to any specific commercial product, process, or service by trade name, trademark, manufacturer, or otherwise, does not necessarily constitute or imply its endorsement, recommendation, or favoring by the United States Government or any agency thereof or its contractors or subcontractors. The views and opinions of authors expressed herein do not necessarily state or reflect those of the United States Government or any agency thereof.

Notice: This manuscript has been authored by employees of Brookhaven Science Associates, LLC under Contract No. DE-AC02-98CH10886 with the U.S. Department of Energy. The publisher by accepting the manuscript for publication acknowledges that the United States Government retains a non-exclusive, paid-up, irrevocable, world-wide license to publish or reproduce the published form of this manuscript, or allow others to do so, for United States Government purposes.

# Preface to the Series

The RIKEN BNL Research Center (RBRC) was established in April 1997 at Brookhaven National Laboratory. It is funded by the "Rikagaku Kenkyusho" (RIKEN, The Institute of Physical and Chemical Research) of Japan. The Memorandum of Understanding between RIKEN and BNL, initiated in 1997, has been renewed in 2002, 2007 and again in 2012. The Center is dedicated to the study of strong interactions, including spin physics, lattice QCD, and RHIC physics through the nurturing of a new generation of young physicists.

The RBRC has both a theory and experimental component. The RBRC Theory Group and the RBRC Experimental Group consists of a total of 25-30 researchers. Positions include the following: full time RBRC Fellow, half-time RHIC Physics Fellow, and full-time post-doctoral Research Associate. The RHIC Physics Fellows hold joint appointments with RBRC and other institutions and have tenure track positions at their respective universities or BNL. To date, RBRC has over 95 graduates (Fellows and Post- docs) of which approximately 40 theorists and 20 experimenters have already attained tenure positions at major institutions worldwide.

Beginning in 2001 a new RIKEN Spin Program (RSP) category was implemented at RBRC. These appointments are joint positions of RBRC and RIKEN and include the following positions in theory and experiment: RSP Researchers, RSP Research Associates, and Young Researchers, who are mentored by senior RBRC Scientists. A number of RIKEN Jr. Research Associates and Visiting Scientists also contribute to the physics program at the Center.

RBRC has an active workshop program on strong interaction physics with each workshop focused on a specific physics problem. In most cases all the talks are made available on the RBRC website. In addition, highlights to each speaker's presentation are collected to form proceedings which can therefore be made available within a short time after the workshop. To date there are over one hundred proceeding volumes available.

A 10 teraflops RBRC QCDOC computer funded by RIKEN, Japan, was unveiled at a dedication ceremony at BNL on May 26, 2005. This supercomputer was designed and built by individuals from Columbia University, IBM, BNL, RBRC, and the University of Edinburgh, with the U.S. D.O.E. Office of Science providing infrastructure support at BNL. Physics results were reported at the RBRC QCDOC Symposium following the dedication. QCDSP, a 0.6 teraflops parallel processor, dedicated to lattice QCD, was begun at the Center on February 19, 1998, was completed on August 28, 1998, and was decommissioned in 2006. It was awarded the Gordon Bell Prize for price performance in 1998. QCDOC was decommissioned in May 2012. The next generation computer in this sequence, QCDCQ (600 Teraflops), is currently operational and is expected to produce many more interesting discoveries in the future.

N. P. Samios, Director
December 2012

*Work performed under the auspices of U.S.D.O.E. Contract No. DE-AC02-98CH10886.

# Contents

## Presentations


***R. Averbeck*** ..... Dielectron measurement with ALICE at the LHC

***G. Chen*** ..... Dileptons and photons from the hadronization process

***X. Cui*** ..... Di-electron elliptic flow in 200 GeV Au+Au collisions at STAR

***H.-T. Ding*** ..... Lattice QCD calculation of vector spectral functions and EM emission rates

***A. Drees*** ..... Thermal dileptons from NA60 and possible future opportunities at SPS

***K. Dusling*** ..... Viscosity and thermal photon production

***T. Galatyuk*** ..... Results on virtual-photon production at SIS: resume and prospects

***P. Hohler*** ..... Connections between dilepton data and chiral symmetry restoration

***B. Huang*** ..... Di-electron spectra in p+p and Au+Au at 200 GeV from STAR

***P. Huck*** ..... Dielectron production in Au+Au collisions at BES energies and its energy dependence from SPS to top RHIC energies

***Z. Kang*** ..... Cold nuclear matter effects on dilepton and photon production

***O. Linnyk*** ..... Probing hot QCD matter with dileptons using PHSD approach
Short Movie: PHSD: Au+Au @ 21300 AGeV, b=1fm

***L. McLerran*** ..... The space-time evolution of heavy ion collisions

***A. Mocsy*** ..... Hydrogen-like atoms from ultrarelativistic nuclear collisions

***R. Petti*** ..... Thermal photon yield and elliptic flow in 200 GeV Au+Au collisions from PHENIX

***R. Rapp*** ..... Thermal dileptons + photons: baseline approach

***I. Ravinovich*** ..... Di-electron spectra from 200 GeV p+p and Au+Au with the HBD from PHENIX

***B. Schenke*** ..... Initial state fluctuations and hydrodynamics

***D. Sharma*** ..... Dielectron spectrum in d + Au Collisions at $\sqrt{s}_{NN}$=200 GeV

***E. Shuryak*** ..... New ideas on the penetrating probes

***V. Skokov*** ..... Anisotropy of photon production in magnetic field

***D. Teaney*** ..... Photon production at NLO in hot QCD

***G. Torrieri*** ..... Detecting quarkyonic matter via EM probes?

***I. Tserruya*** ..... Future dilepton experiments

***K. Tuchin*** ..... Photons and di-leptons in strong magnetic field in heavy-ion collisions

***G. Vujanovic*** ..... Thermal dileptons at RHIC

***Q. Wang*** ..... Some aspects of dilepton production in HIC

***M. Wilde*** ..... Direct photon spectra and elliptic flow in 2.76 TeV Pb-Pb collisions from ALICE

***Z. Xu*** ..... Future dilepton measurements from STAR upgrades


## Agenda
## Registered List of Participants
## Additional RIKEN BNL Research Center Proceeding Volumes

# Dielectron measurements with ALICE at the LHC

**Ralf Averbeck**
**ExtreMe Matter Institute EMMI and Research Division**
**GSI Helmholtzzentrum für Schwerionenforschung**
**Darmstadt, Germany**

**on behalf of the ALICE Collaboration**

## Thermal Radiation Workshop

**RIKEN BNL Research Center**
**December 5-7, 2012**
**Brookhaven National Laboratory, NY, USA**

# Outline

- introduction
- ALICE
- dielectron measurements with ALICE
  - pp collisions
  - Pb-Pb collisions
- summary of current status
- future perspectives
  - dielectron performance with ALICE upgrade

# Dielectrons

- measurement of dielectrons from AA collisions
  - electromagnetic probe
    → negligible final state interaction
  - information from all phases of the collision
  - sensitivity to
    - electromagnetic structure of the hot and dense medium
    - in-medium modification of low-mass vector mesons
    - thermal radiation
    - heavy-flavor hadron decays (at intermediate mass)
    - heavy quarkonia suppression/enhancement

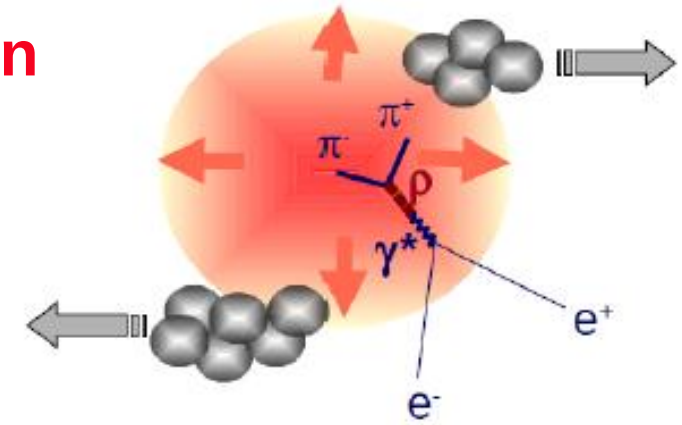


- measurement of dielectrons from pp collisions
  - provides necessary baseline for AA studies

# A Large Ion Collider Experiment

ALICE

**Inner Tracking System**
**tracking/vertexing**
**(particle ID)**

**Time Projection Chamber**
**tracking**
**particle ID**

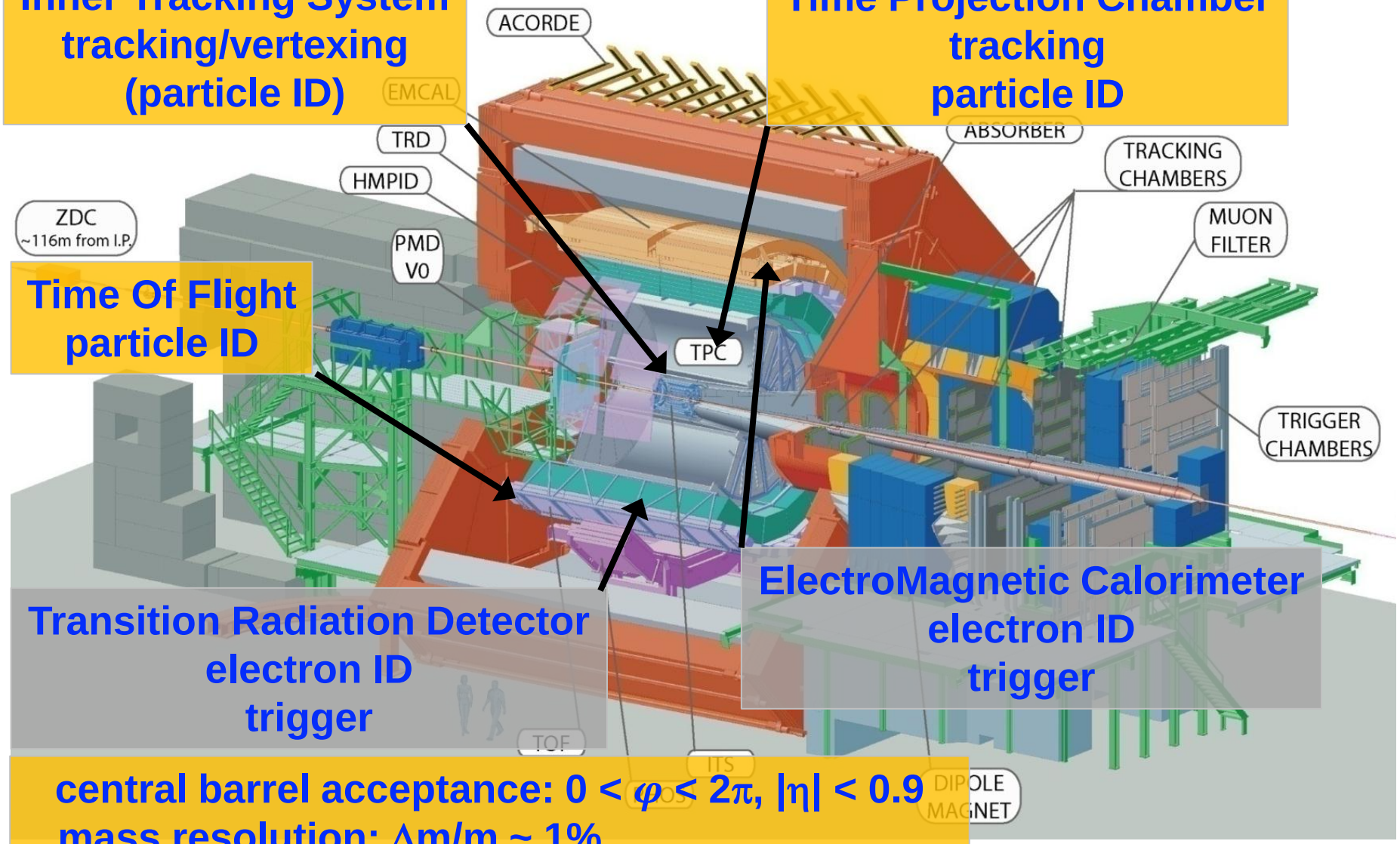


**Time Of Flight**
**particle ID**

**Transition Radiation Detector**
**electron ID**
**trigger**

**ElectroMagnetic Calorimeter**
**electron ID**
**trigger**

**central barrel acceptance: $0 < \varphi < 2\pi$, $|\eta| < 0.9$**
**mass resolution: $\Delta m/m \sim 1\%$**

# Inner Tracking System (ITS)

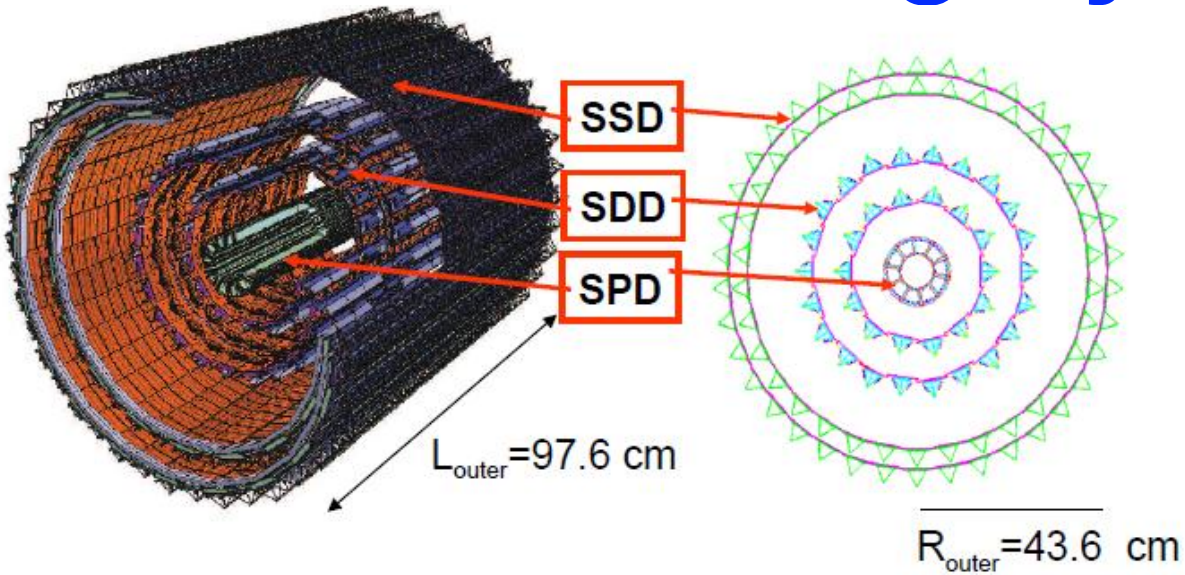


- 2 silicon pixel detector (SPD) layers
  - $X/X_0$ = 1.14 %
  - $R_{inner}$ = 3.9 cm
  - 9.8M channels, 0.2 $m^2$
- 2 silicon drift detector (SDD) layers
  - 133k channels, 1.3 $m^2$
- 2 silicon strip detector (SSD) layers
  - 2.6M channels, 4.75 $m^2$

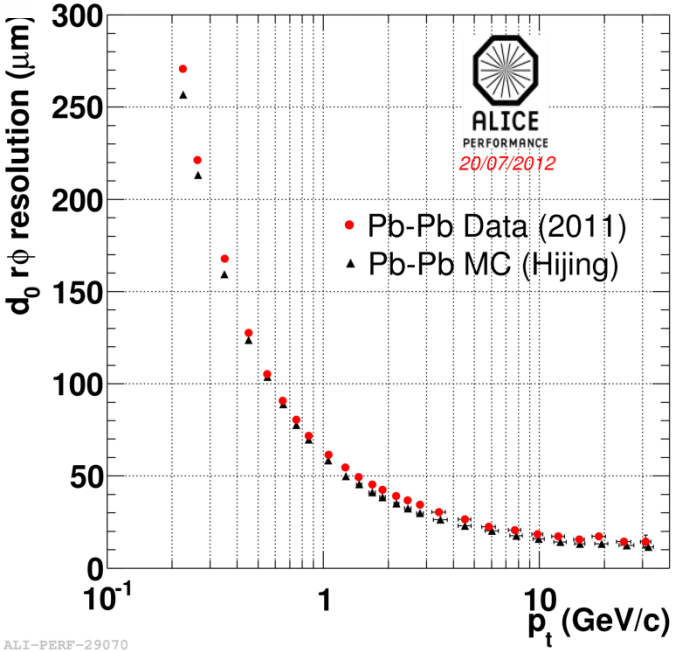

# Time Projection Chamber (TPC)

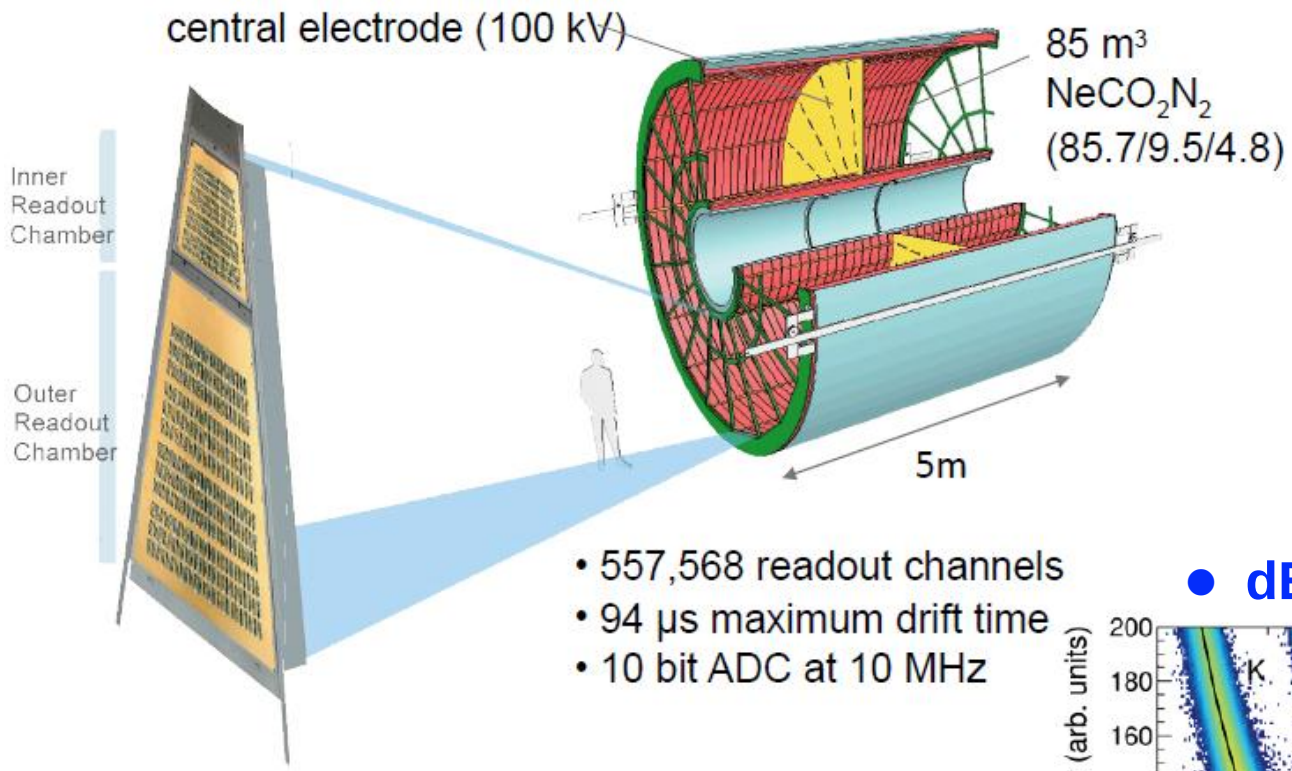


- 557,568 readout channels
- 94 μs maximum drift time
- 10 bit ADC at 10 MHz

- **dE/dx resolution ~6 %**

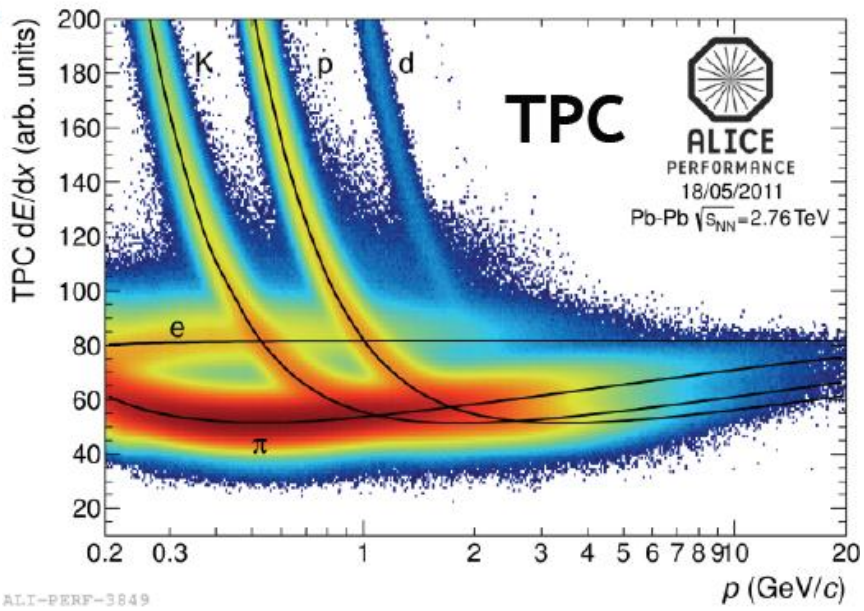

# Time of Flight (TOF)

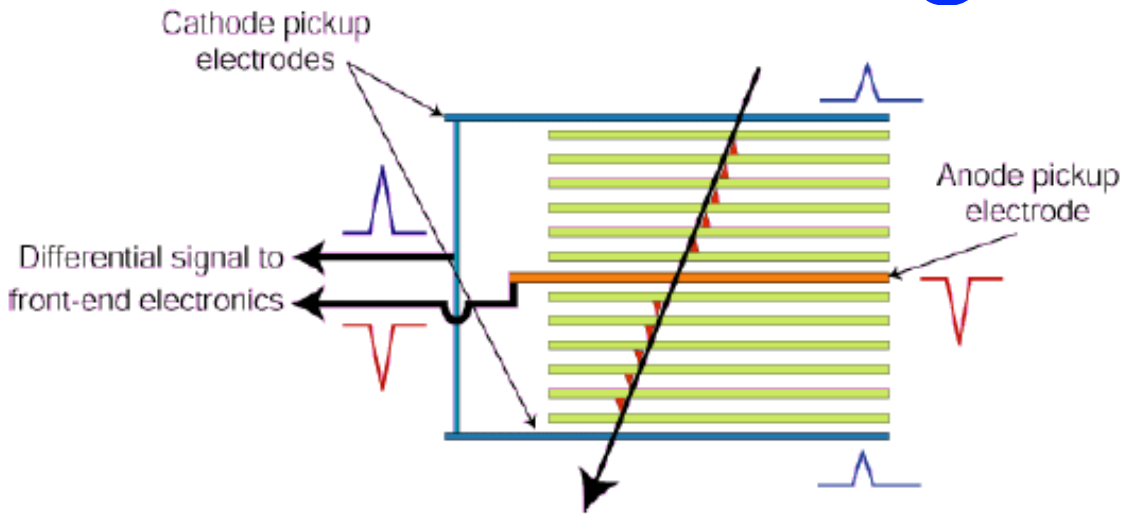


- **hadron rejection at low momenta**

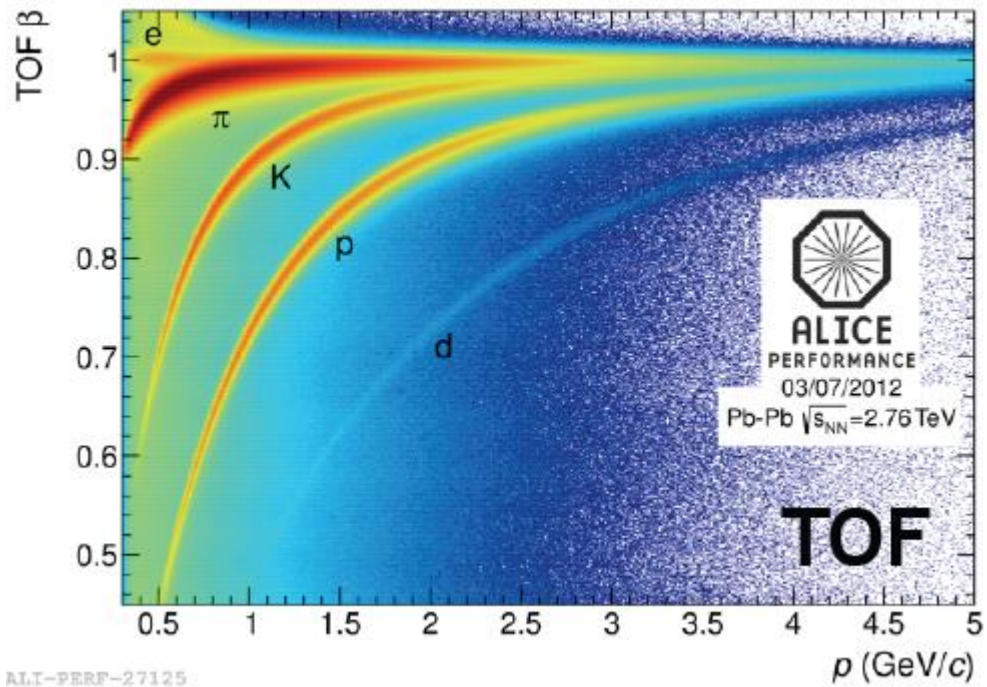

# Transition Radiation Detector (TRD)

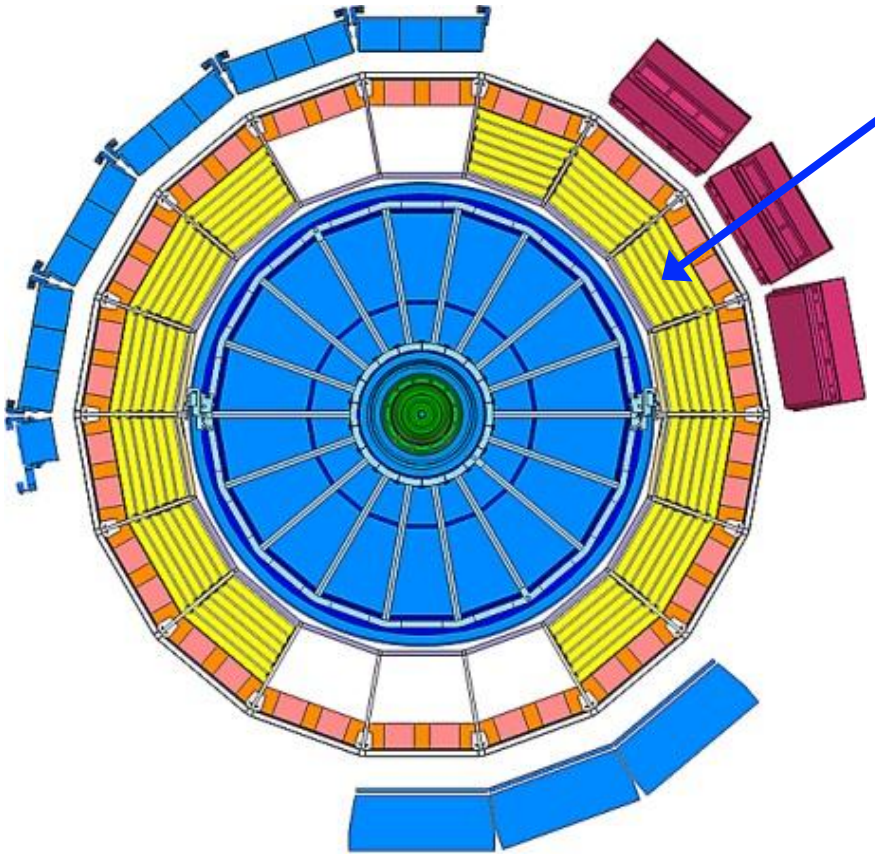

- TRD modules currently installed: 13
  (7 in 2010, 10 in 2011)
  → currently not used in dielectron analysis due to limited acceptance
  (same is true for EMCal)

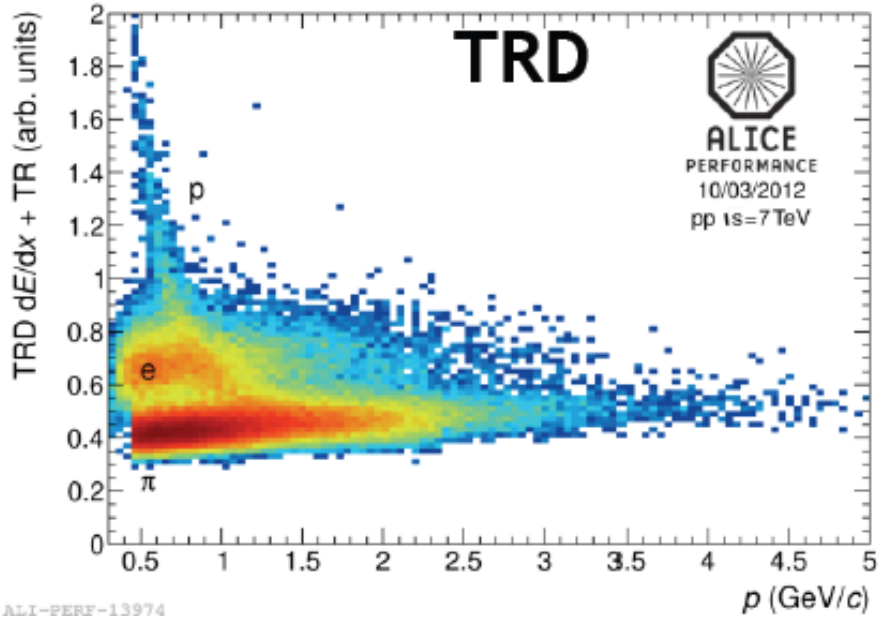

# Triggers and data sets

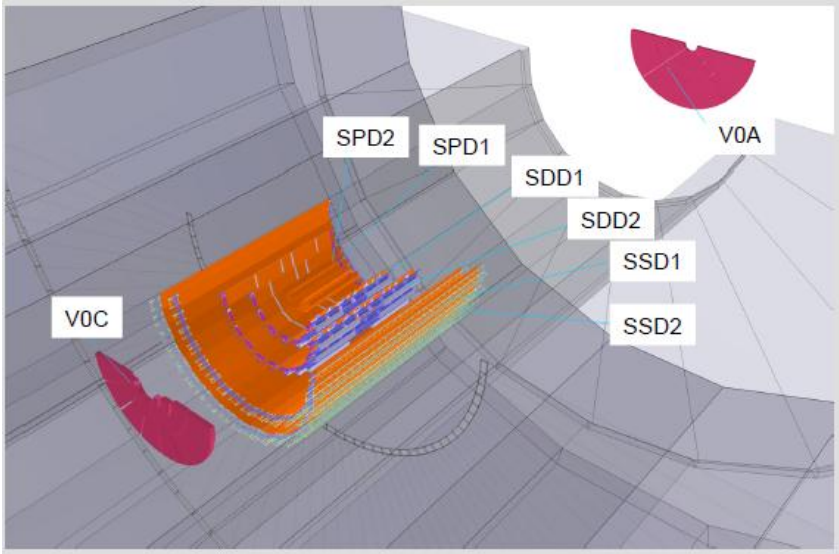


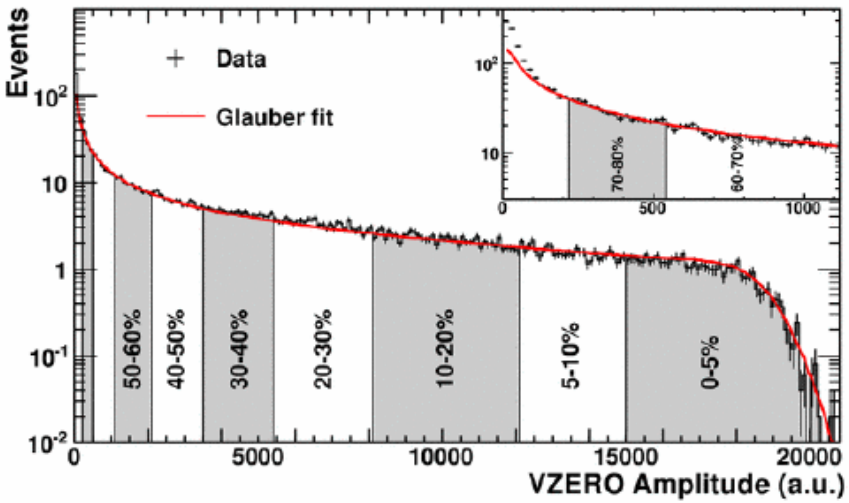


- **minimum bias pp collisions**
  - **coincidence of beam pick-ups and a signal in either the SPD or one of the V0 scintillator arrays**
  - **efficiency: ~95% of $\sigma_{inel.}$**
  - **~350M events (2010 data set)**
- **Pb-Pb collisions**
  - **minimum bias trigger: coincidence of V0 arrays and Zero Degree Calorimeters**
  - **in addition: centrality triggers defined via total charge measured in V0**
  - **2010: ~12M MB events**
  - **2011: ~8M MB, ~27M central, ~32M semicentral events**

# Dielectrons in pp collisions at $\sqrt{s}$ = 7 TeV

# Electron candidate selection

- electron identification is crucial
  - start with high quality tracks
    - $p_T > 0.2$ GeV/c, $|\eta| < 0.8$
    - 'long' tracks in the TPC without 'kinks'
  - require associated hit in the first SPD layer (to minimize contribution from photon conversions)
  - require electron Time of Flight (within $3\sigma$) to reject K, p
  - require electron dE/dx ($-1.5 < \sigma < 3$) and reject tracks with pion dE/dx (within $4\sigma$) to reject pions
- how well does this work?

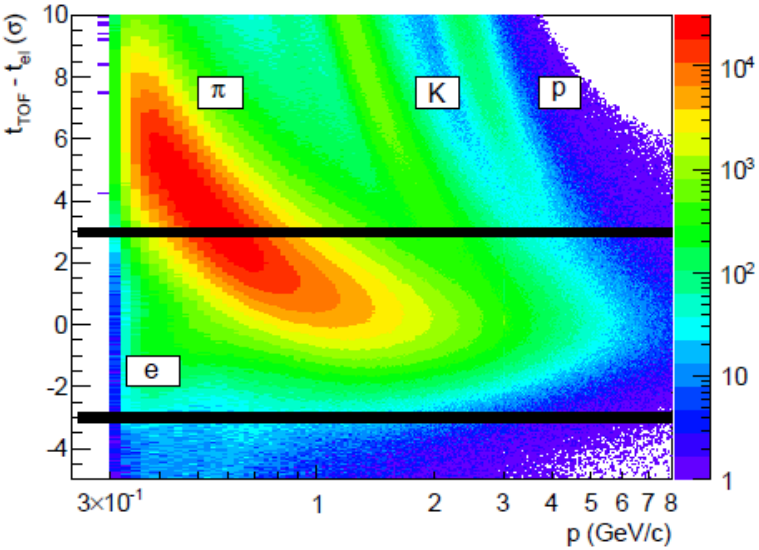


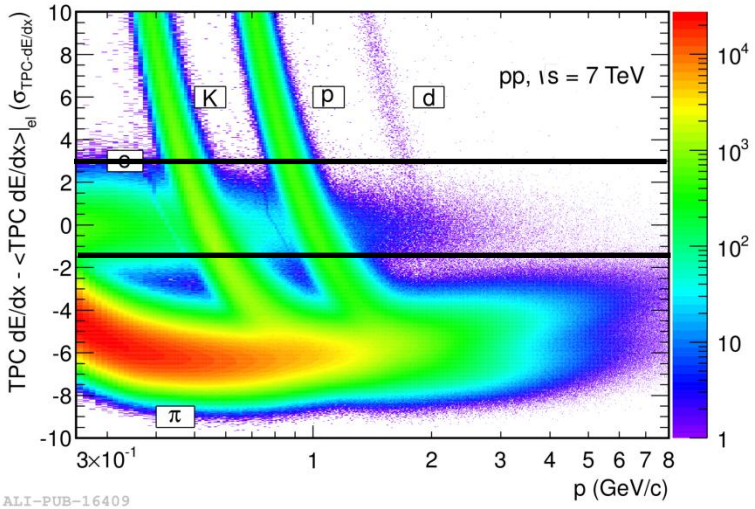

# Purity of candidate sample

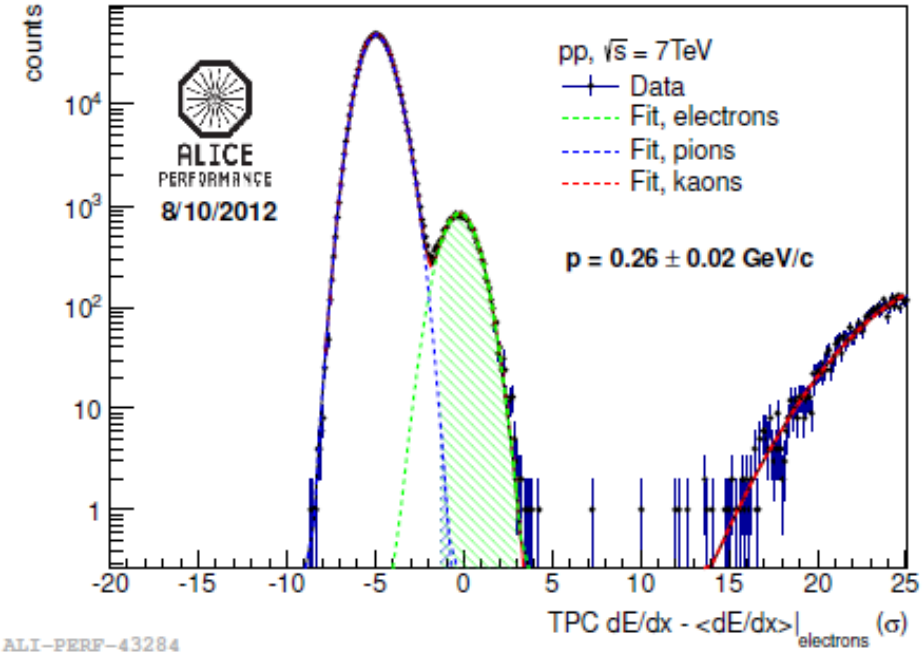


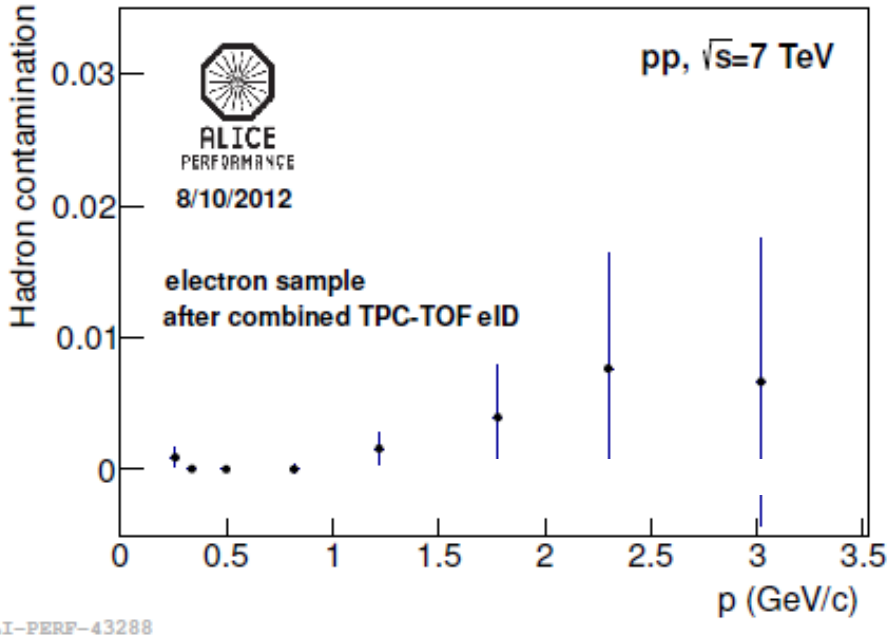


- **fit TPC dE/dx in momentum slices**

**→ remaining hadron contamination for p < 3 GeV/c: <~ 1%**

# Contamination from γ conversions

- how to identify photon conversion candidates
  - displaced secondary vertex
  - orientation of the 'pair plane' with respect to the magnetic field direction

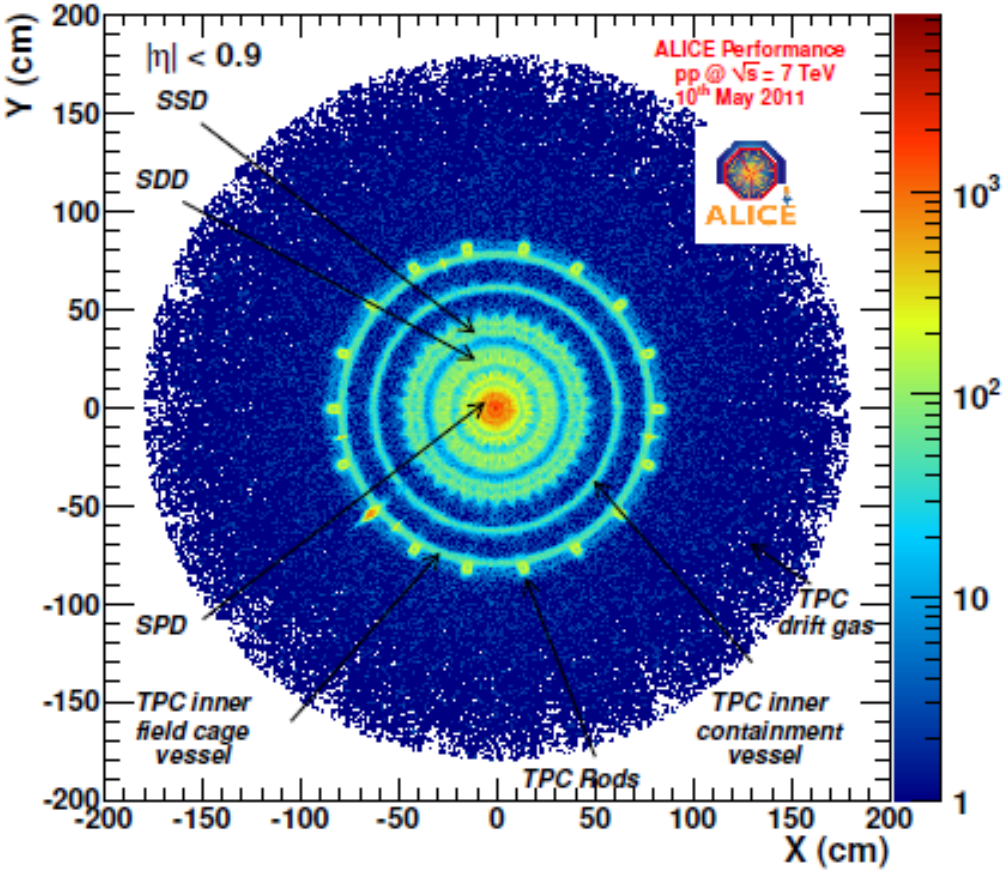


- remaining contamination from photon conversions: few percent at low mass ($m_{ee}$ < 0.1 GeV/$c^2$)

# Combinatorial background

- pairing of all electrons and positrons gives rise to combinatorial background

$$\underbrace{N_{+-}}_{\text{measured}} = S_{+-} + N_{+-}^{\text{CombBkg}}$$

- methods to determine this background
  - mixed event subtraction
  - same-event like-sign subtraction
  - same-event track rotation

$$N_{+-}^{\text{CombBkg}} = \underbrace{2 \times \sqrt{N_{++}N_{--}}}_{\text{Like-sign}} * \overbrace{R_{Acc}}^{\text{from mixed events}}$$

- current approach: like-sign subtraction

# Raw mass spectra

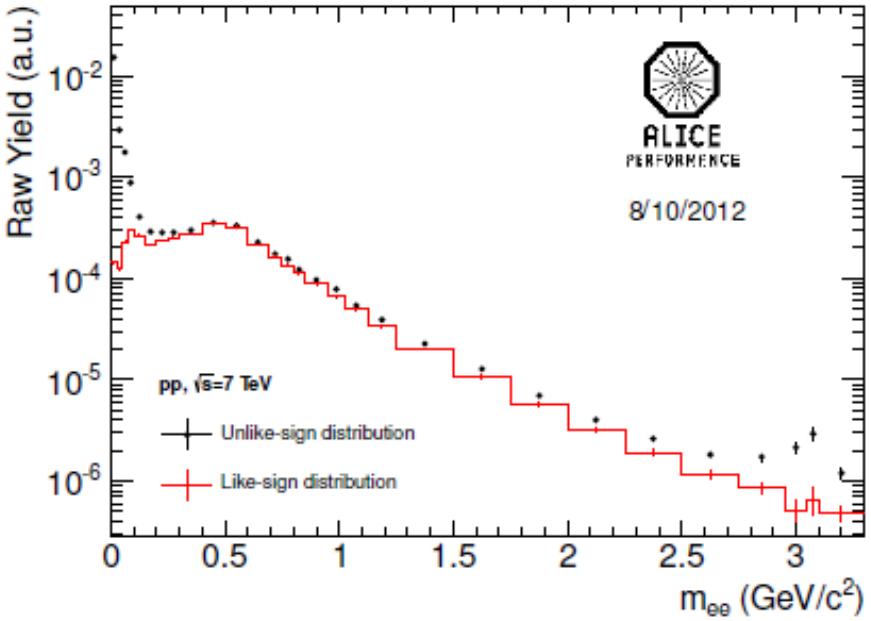


ALI-PERF-43276

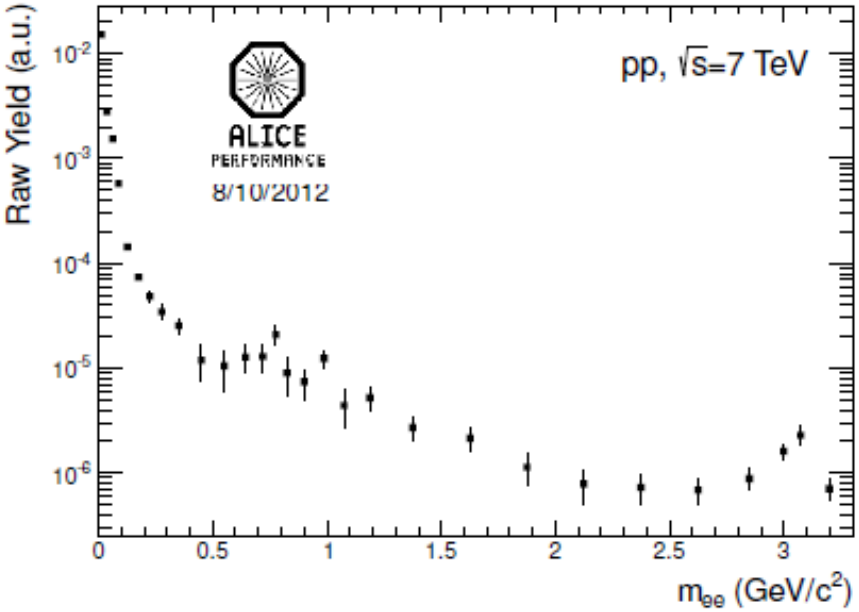


ALI-PERF-43272

- **large background from uncorrelated pairs**
- **subtraction of like-sign combinatorial background**
  **→ raw signal of correlated pairs**

# Correction for efficiency

- efficiency correction for detector effects (including Bremsstrahlung in material)
- no acceptance correction into unmeasured region of phase space
- correction based on full MonteCarlo simulations
- efficiency determined for single electron tracks as function of ($p_T$, $\eta$, $\varphi$)

# Systematic uncertainties

- relevant sources
  - track selection
  - electron ID
  - efficiency correction
  - normalization
  - most important: combinatorial background

$$\frac{dS}{S} = \frac{dB}{B} \times \frac{B}{S}$$

→ currently NO significant measurement close to $m_{ee}$ = 0.5 GeV/c²!

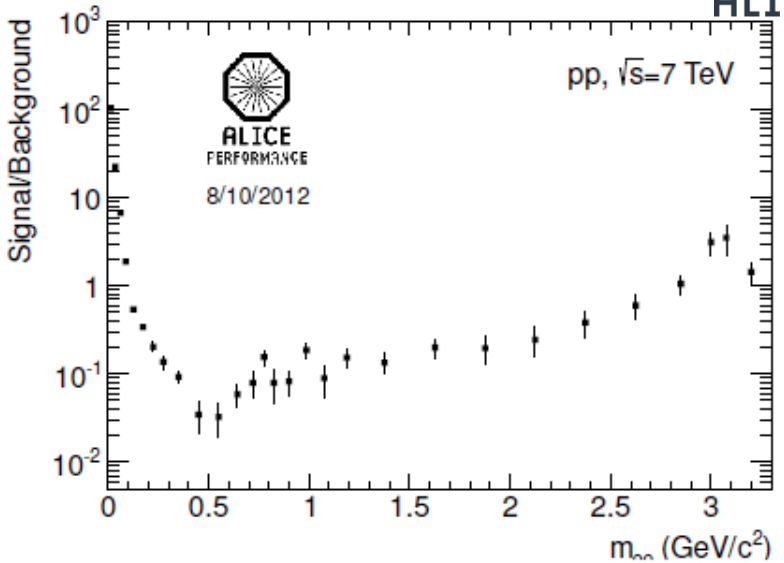


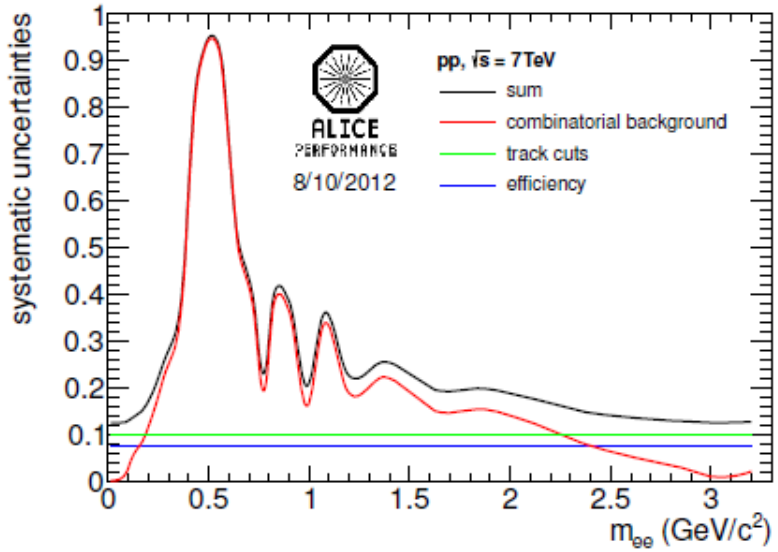


ALI-PERF-43375

# Known hadronic $e^+e^-$ sources

- calculation of hadronic cocktail
  - based on:
    measured $p_T$-differential invariant cross section of $\pi^0$
  - contributions from other hadron decays:
    from data ($\eta$, $\phi$, $J/\psi$ ) or via $m_T$ scaling
  - contribution from correlated charm decays:
    from measured charm cross section and
    PYTHIA decay kinematics
- ALICE data used as input
  - $\pi^0$, $\eta$: Phys. Lett. B717 (2012) 162
  - $\phi$: arXiv:1208.5717
  - $\sigma_{cc}$: arXiv:1205.4007
  - $J/\psi$: Phys. Lett. B704 (2011) 442

# Cocktail versus data

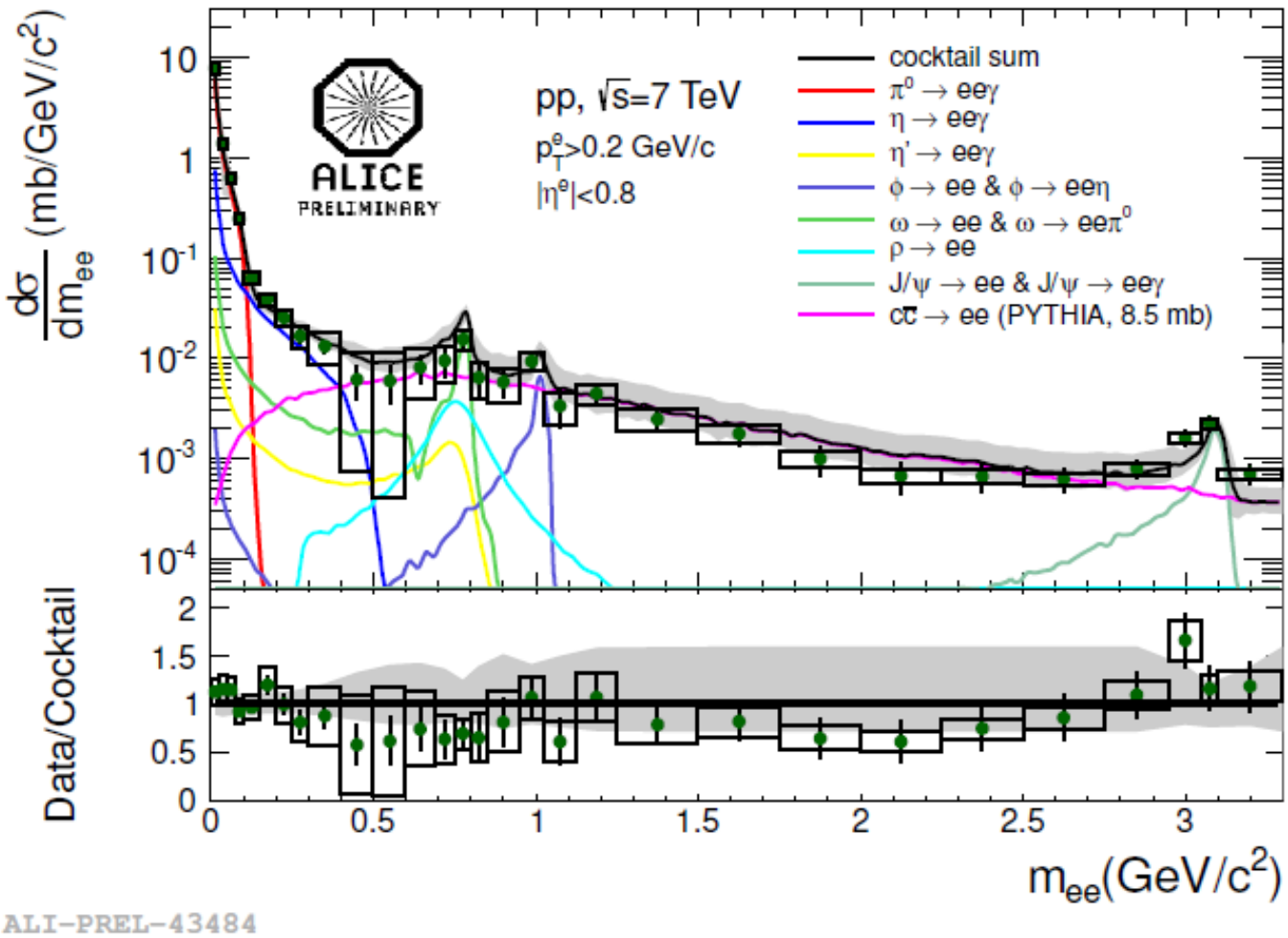


- **cocktail in reasonable agreement with data**

# Outlook for Pb-Pb collisions at $\sqrt{s_{NN}}$ = 2.76 TeV

# Signal extraction

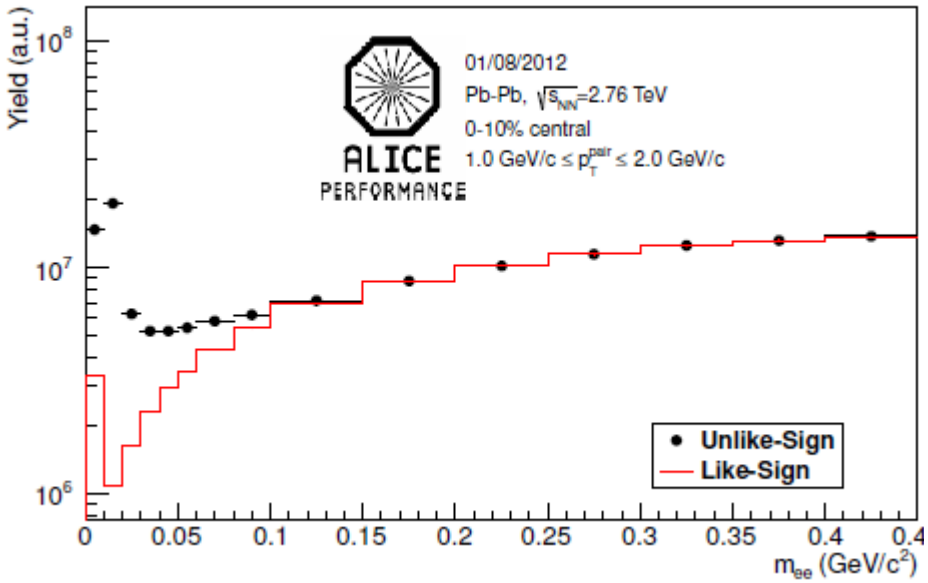


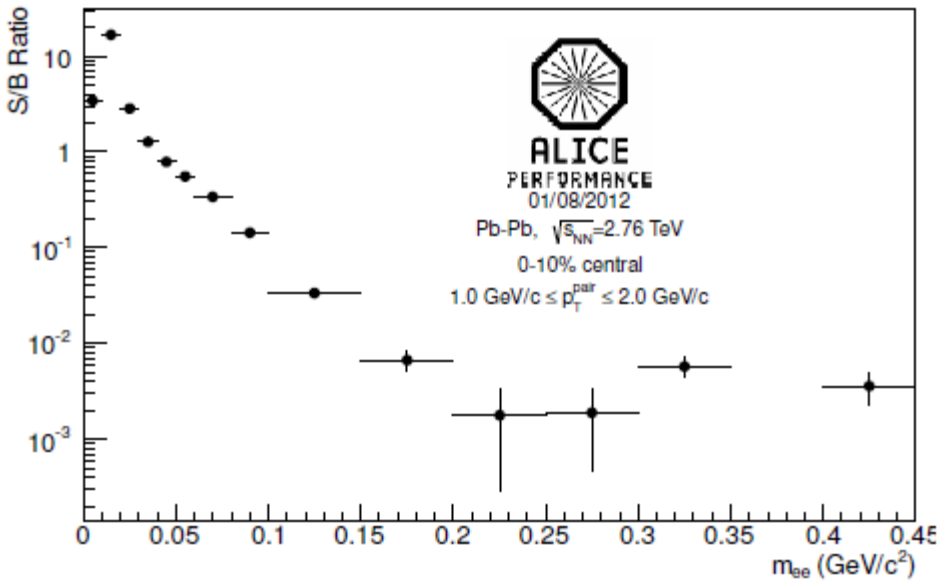


- similar analysis as for pp collisions at $\sqrt{s}$ = 7 TeV (but: $p_T^e > 0.4\ GeV/c$)
- S/B ratio few $10^{-3}$ at low mass (0.2 – 0.4 MeV/$c^2$)
- detailed study of background systematics ongoing

# Summary I

- first dielectron continuum measurement with ALICE for pp collisions at $\sqrt{s}$ = 7 TeV
- hadronic cocktail calculation agrees within errors with data in the range $0 < m_{ee} < 3.3$ GeV/$c^2$
- analysis is difficult for Pb-Pb collisions
  → requires improved knowledge of background
- unique strength of ALICE at the LHC
  - access to the low mass & low $p_T$ region!
  - how can this be improved further?

# ALICE upgrade - LOI

http://cdsweb.cern.ch/record/1475243

http://cdsweb.cern.ch/record/1475244

# Dielectron strategy

- reduction of central barrel magnetic field from 0.5 T to 0.2 T
  - extend tracking efficiency and electron PID to lower $p_T$
- high rate upgrade of the TPC
  - improve the data taking rate by a factor 100
- upgrade of the ITS
  - reduced material budget
  - improve tracking efficiency at very low $p_T$
  - improve capability to identify electrons originating from secondary vertices (DCA cut)

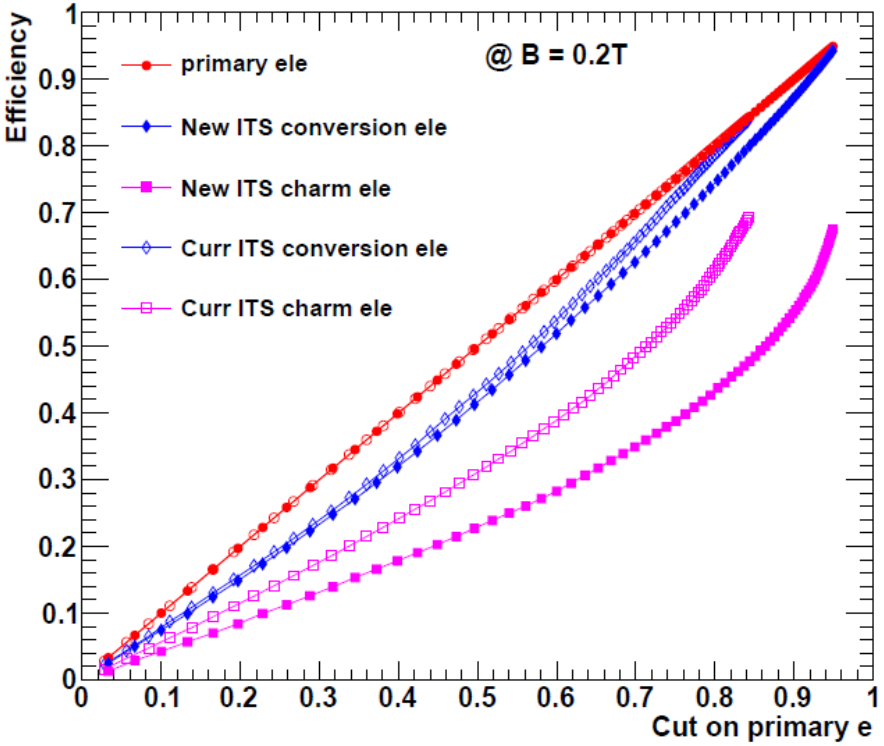

# Dielectron performance study

- here: focus on 10% most central Pb-Pb collisions ($\langle dN_{ch}/d\eta \rangle = 1750$ ) at $\sqrt{s_{NN}} = 5.5$ TeV (peripheral case was studied as well)
- dielectron signal
  - hadronic cocktail
  - open charm decays based on PYTHIA, interpolated total charm production cross sections for pp collisions, and binary collision scaling
  - thermal signal (R. Rapp & J. Wambach, EPJA 6(1999)425)

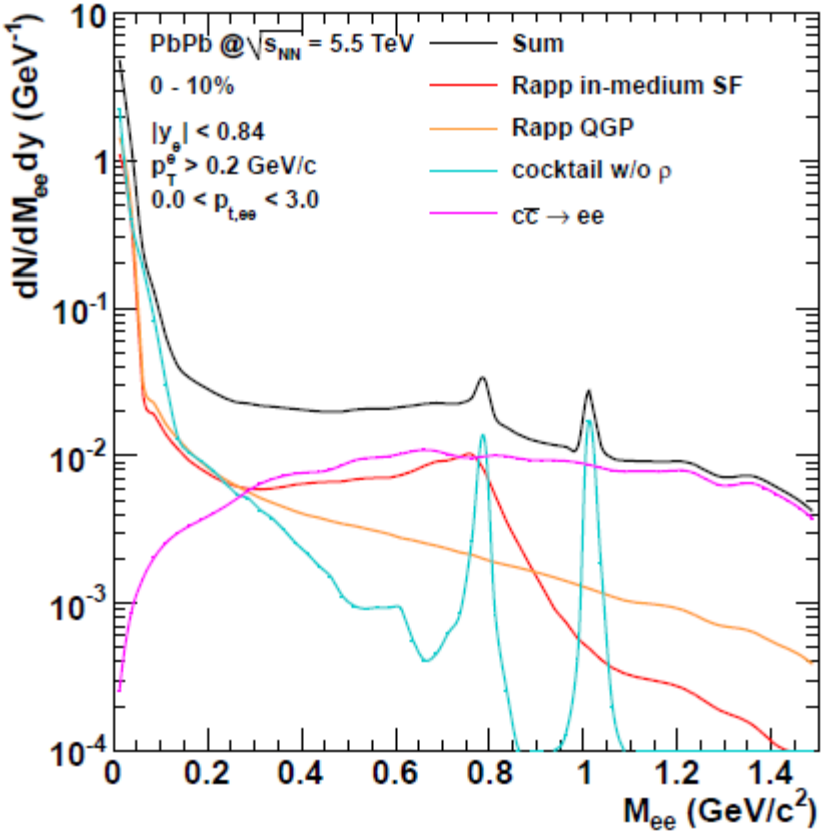

# Dielectron performance study

- background
  - PYTHIA pp events superimposed to Pb-Pb $\langle dN_{ch}/d\eta \rangle$
  - photon conversions from GEANT3
- kinematic cuts
  - $|\eta_e| < 0.84$, $p_{T,e} > 0.2$ (0.06) GeV/c for global (ITS) tracking
- conversion and Dalitz rejection
  - $m_{ee} < 50$ MeV/c$^2$, opening angle < 100 mrad

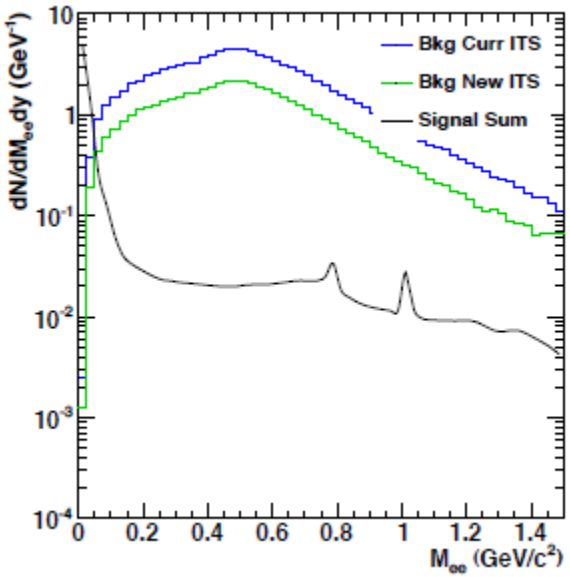


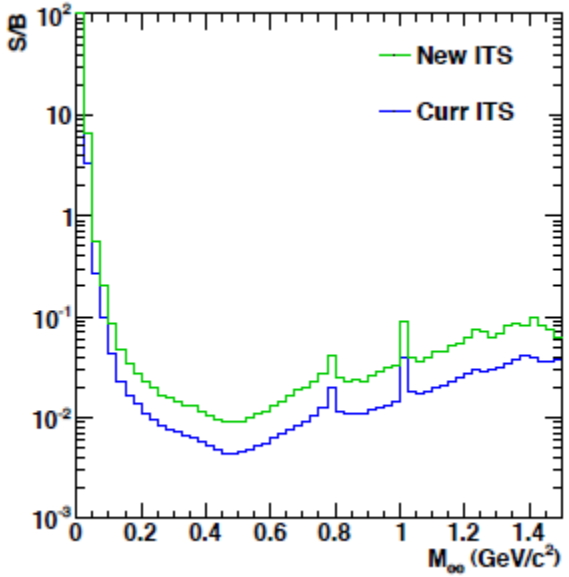


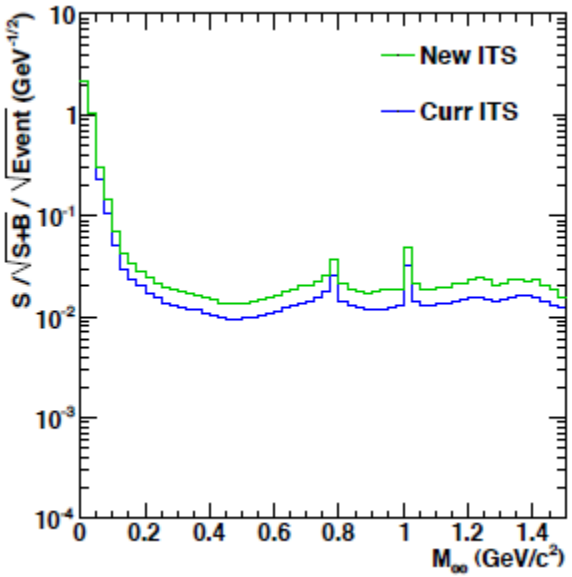

# Current ITS, no DCA cut

- 2.5 x $10^7$ Pb-Pb collisions at 5.5 TeV
- precision of comb. background measurement: 0.25%
- background precision: 10% (20%) for cocktail (charm)

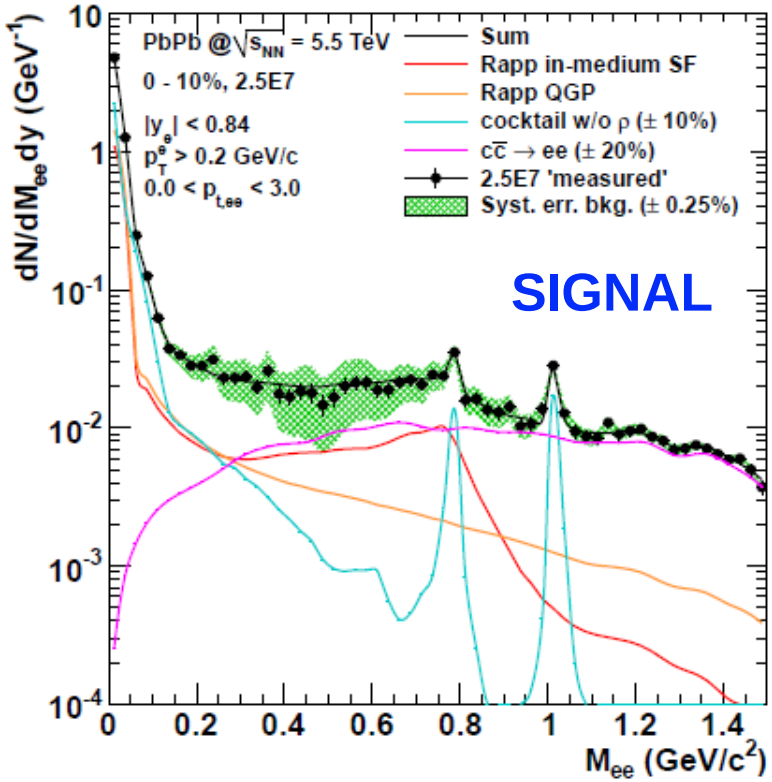


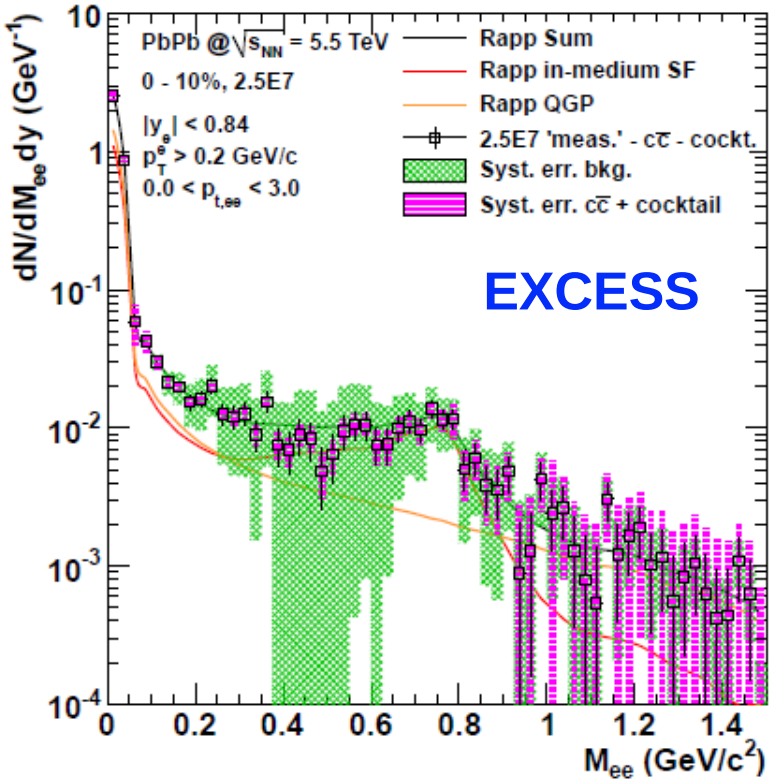


→ no quantitative access to in-medium spectral functions and thermal dielectron emission

# Current ITS, tight DCA cut

- 2.5 x $10^7$ Pb-Pb collisions at 5.5 TeV
- precision of comb. background measurement: 0.25%
- background precision: 10% (20%) for cocktail (charm)

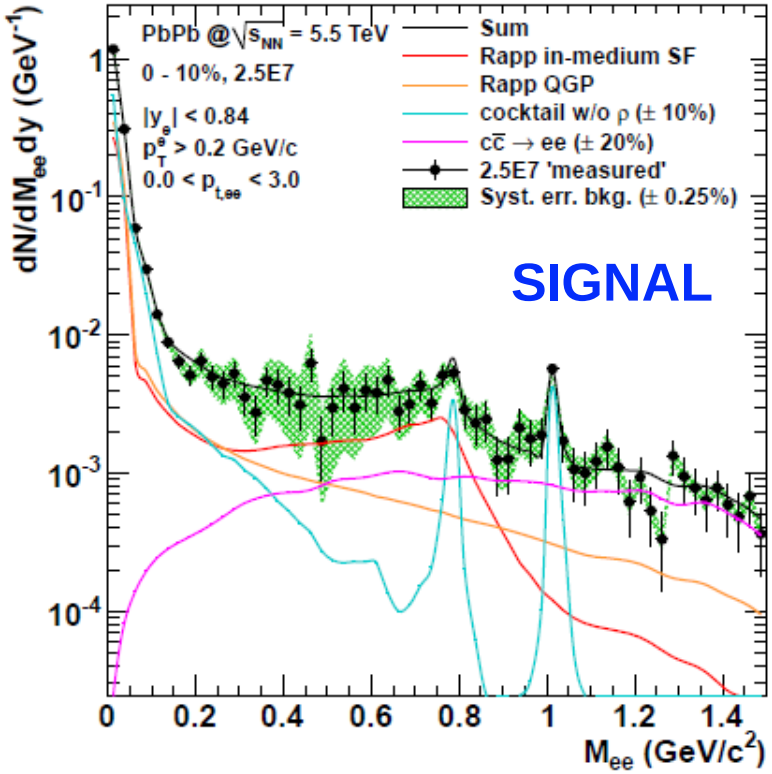


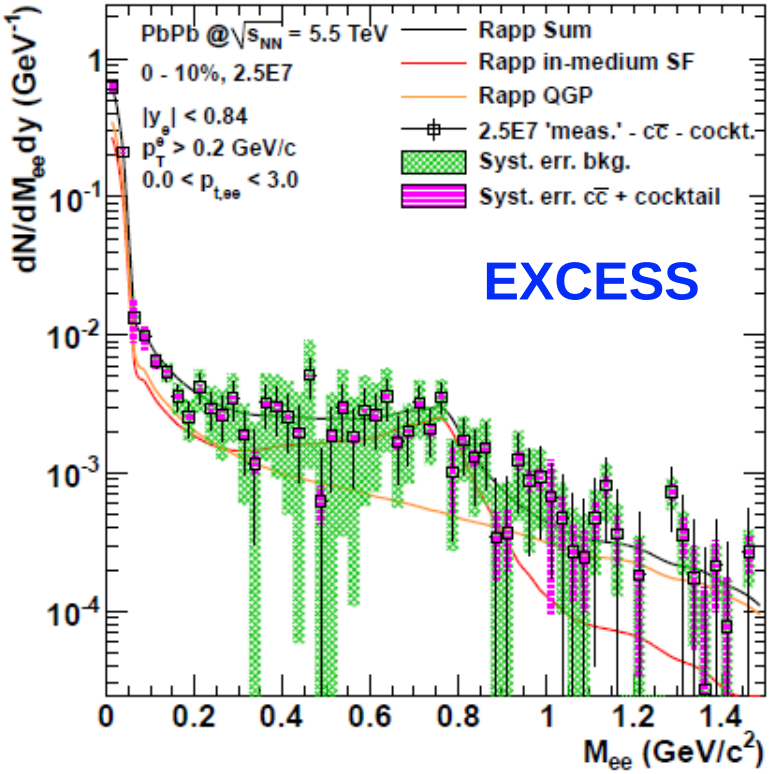


→ marginal improvement only

# New ITS, DCA cut

- 2.5 x $10^7$ Pb-Pb collisions at 5.5 TeV
- precision of comb. background measurement: 0.25%
- background precision: 10% (20%) for cocktail (charm)

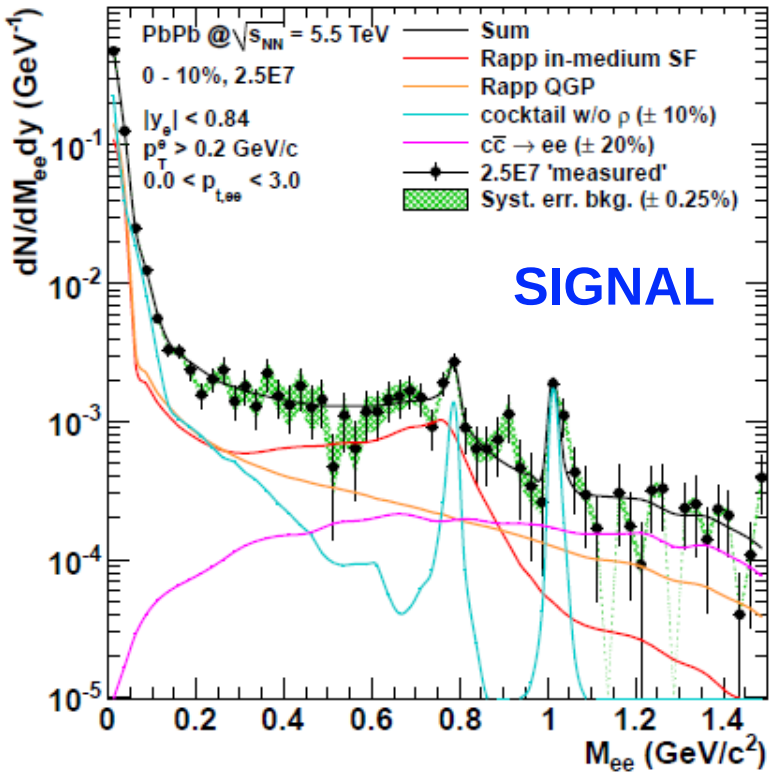


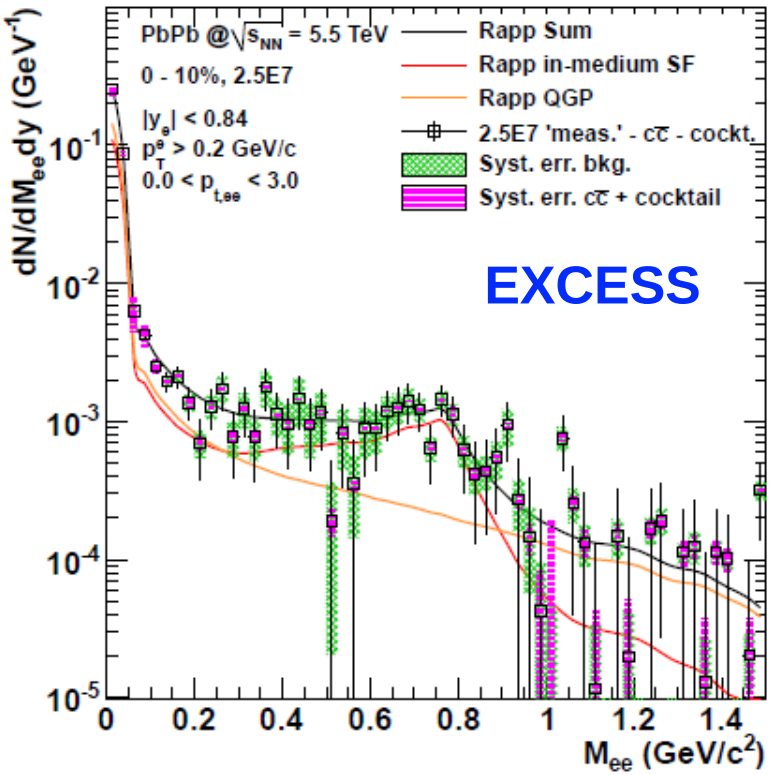


→ significantly reduced systematics, but statistics limited

# New ITS, DCA cut, high rate

- 2.5 x $10^9$ Pb-Pb collisions at 5.5 TeV
- precision of comb. background measurement: 0.25%
- background precision: 10% (20%) for cocktail (charm)

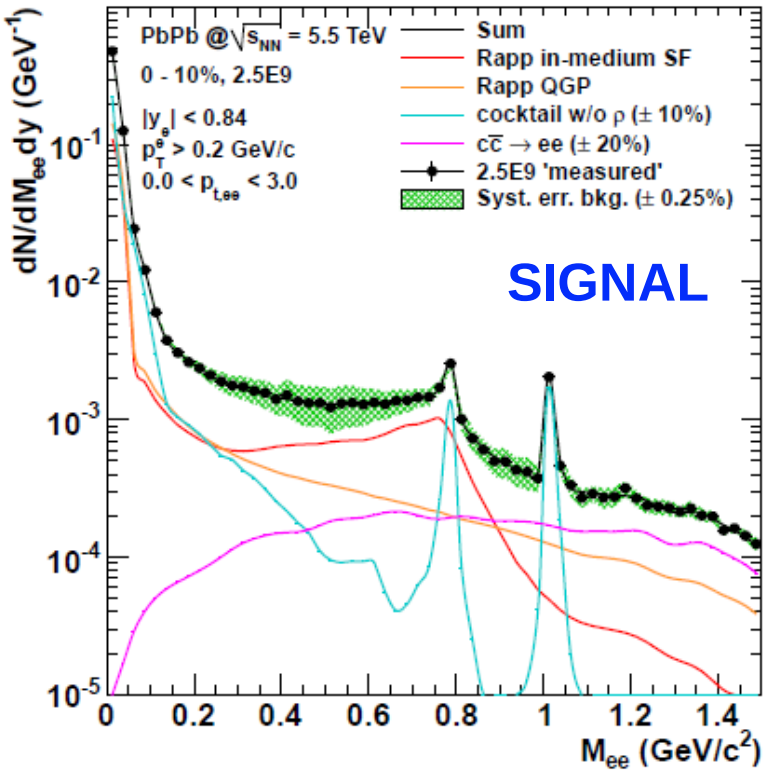


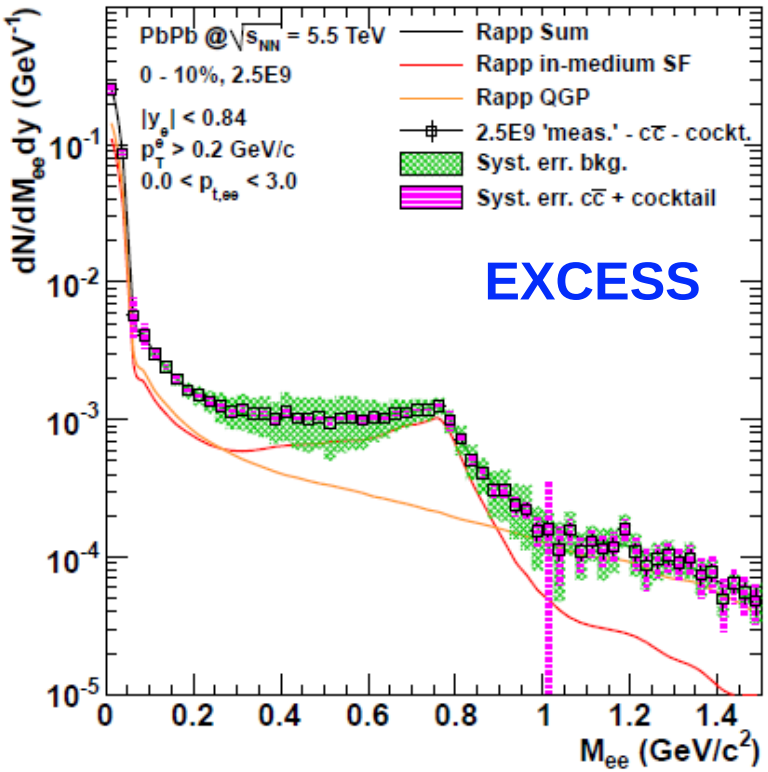


→ quantitative access to dielectron production beyond hadronic cocktail and correlated charm decays!

# Summary II

- precision measurement of dielectron poduction in Pb-Pb collisions at the LHC beyond the hadronic cocktail and correlated charm decays: **NOT possible with the current ALICE setup!**
  (even with increased kinematic coverage due to a reduced B field)
- current limitations: addressed by ALICE upgrade
- new ITS
  → improved Signal/Background ratio
  → reduced sys. uncertainty of $e^+e^-$ measurement
- high rate upgrade of the TPC
  → reduced stat. uncertainty of $e^+e^-$ measurement

**ALICE upgrade**
**→ precision low-mass dielectron measurement**

# Dileptons and photons from the Hadronization Process

Guangyao Chen
Rainer J. Fries
Department of Physics and Astronomy & Cyclotron Institute
Texas A&M University

RIKEN Thermal Radiation Workshop, Dec 5-7,2012

# Sources of E&M Probes

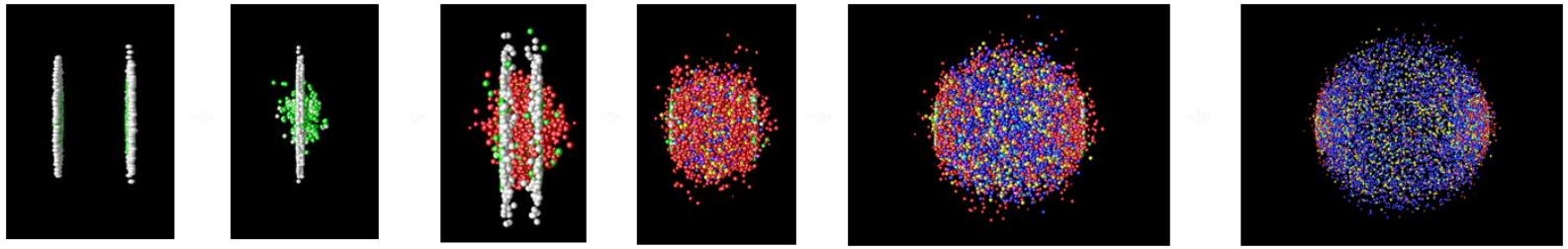

- Initial Hard Scattering and fragmentation of jets
- Pre-equilibrium phase/Glasma?
- QGP
- Hadronic Gas
- Jet-medium interaction
- Phase transition?

Hadronization involves charged particles, should be a source of EM radiation!
Q: Is it large?

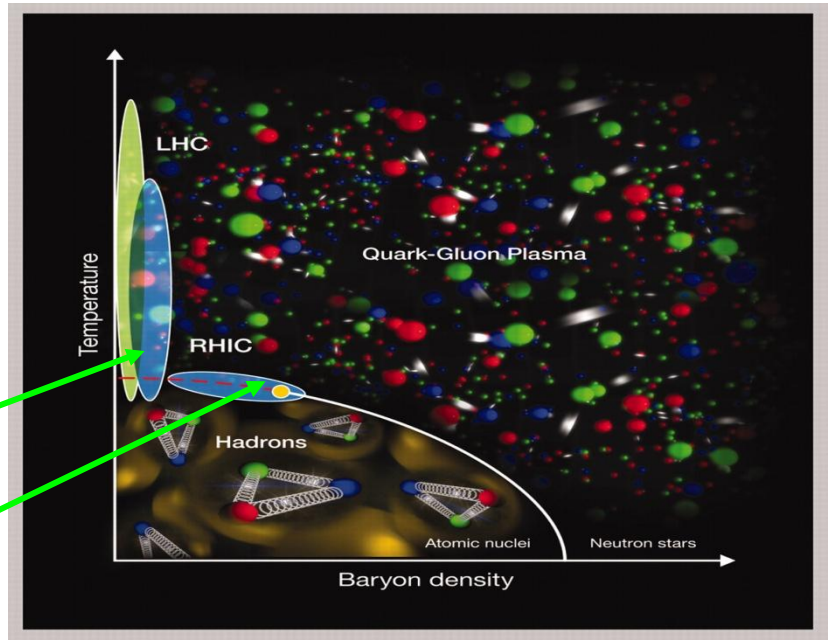

# State of Art

- Dilepton/Photon production: clear separation between QGP and Hadronic Phase

1. QGP ( $q+\bar{q}\rightarrow\gamma^{*}\rightarrow e^{+}+e^{-}$ , $q+g\rightarrow\gamma^{*}+q\rightarrow e^{+}+e^{-}+q$ )
2. Hadronic Gas ( $\pi^{+}+\pi^{-}\rightarrow\rho\rightarrow e^{+}+e^{-}$ )

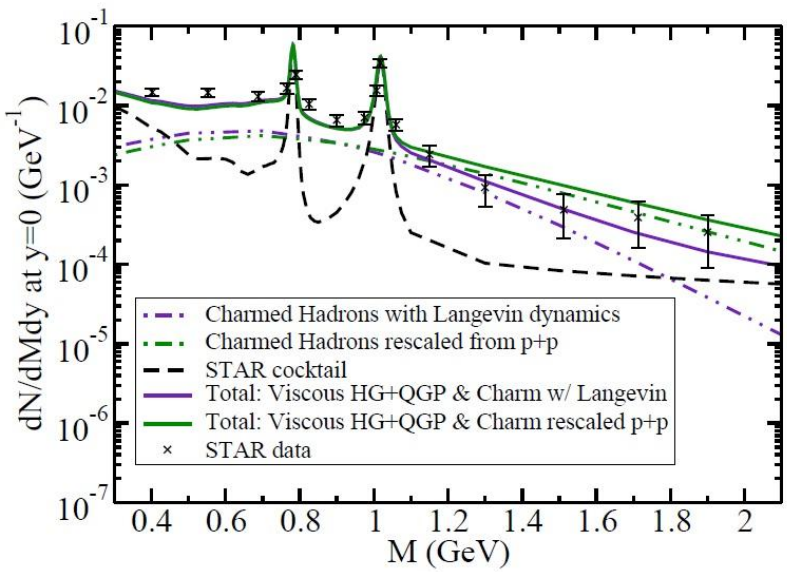


Vujanovic, G et al, QM 2012

Questions: Large photon v2, dilepton enhancement……

# First Order v.s. Crossover Phase Transition

- Typical 1st order phase transition.

Ice and water are well separated during a 1st order phase transition.

$$fR_{Hadron} + (1-f)R_{qgp}$$

Good for 1st order.

- Lattice: Hadron $\longleftrightarrow$ QGP is a crossover.

WB Collaboration & hotQCD Collaboration

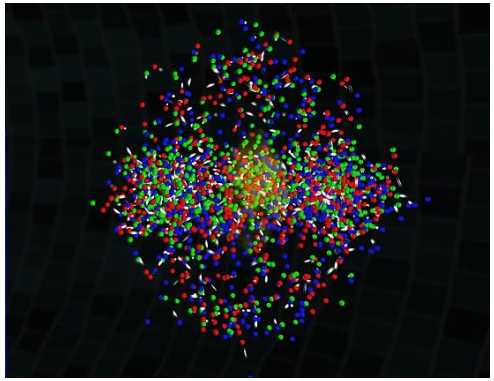

Q: Can hadrons or resonance states coexist with partons in a finite temperature window around Tc?

A: Maybe.

Shuryak, E et al, 2003

# Our Approach

- Assume coexistence of q,g,π and rho; or coexistence of q,g and HRG in a temperature range around Tc.

i. Use vacuum quark meson coupling;
ii. No strangeness yet;
iii. No baryons yet.

- Include photon/dilepton production channels through "quark recombination" like graphs.

# Quark Pion Coupling

- Pseudo scalar meson interaction Lagrangian

$$L_{int} = ig_{qq\pi}\bar{\psi}\gamma^5\vec{\tau}\cdot\vec{\phi}\psi$$

Suzuki and R.~K.~Bhaduri, 1983

- Quark recombination into pion with photon/dilepton.

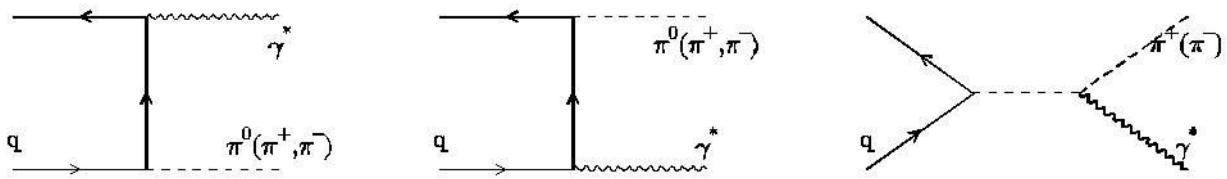


- Compton scattering of quark and pion.

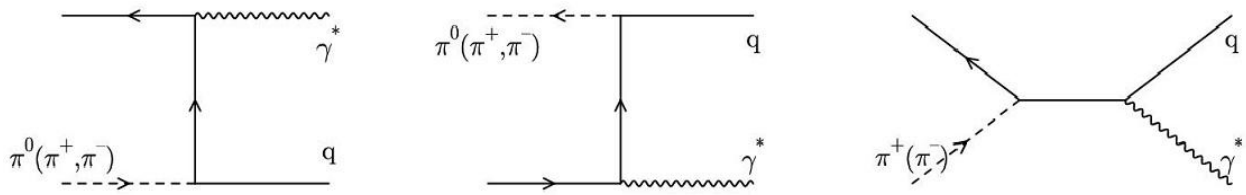

# Quark Rho Coupling

- Vector meson interaction Lagrangian

$$L_{int} = ig_{qq\rho}\bar{\psi}\gamma^{\mu}\vec{\tau}\cdot\vec{\phi}_{\mu}\psi$$

Polleri et al, 1997

- Quark recombination into rho with photon/dilepton.

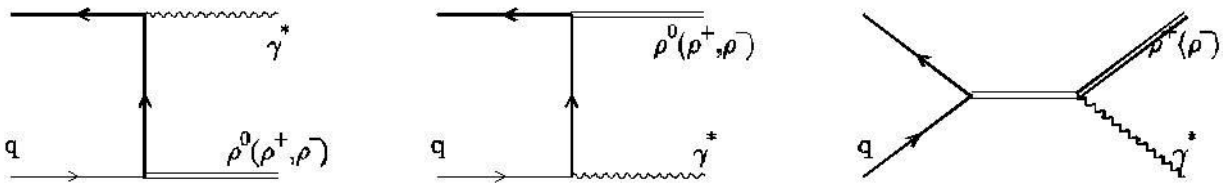


- Compton scattering of quark and rho.

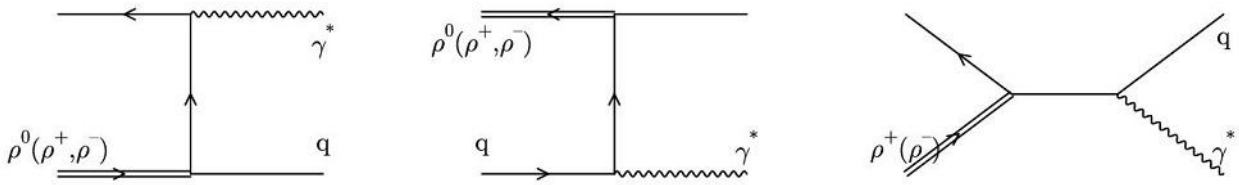


- Quark annihilation via intermediate rho.

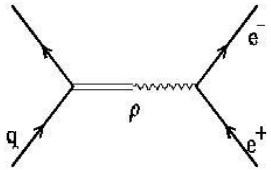


Thoma, M et al, 2001

Greiner, C et al, 2010

# Dilepton/Photon Production Rate

Dilepton rate at T=180 MeV

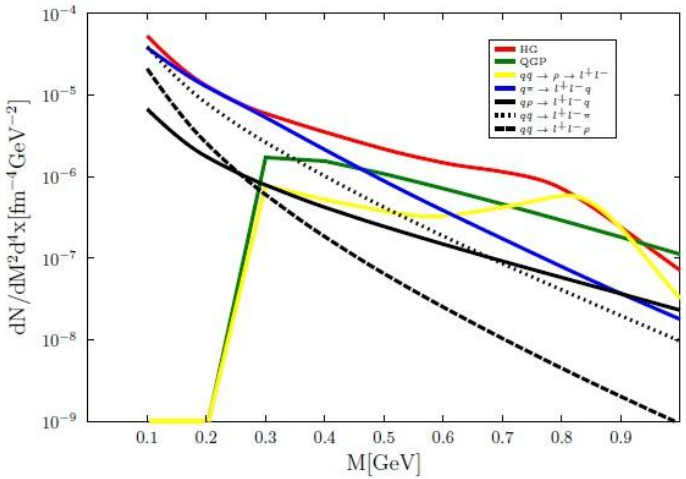


Rapp and Wambach, 1999

Greiner, C et al, 2010

Photon rate at T=164 MeV

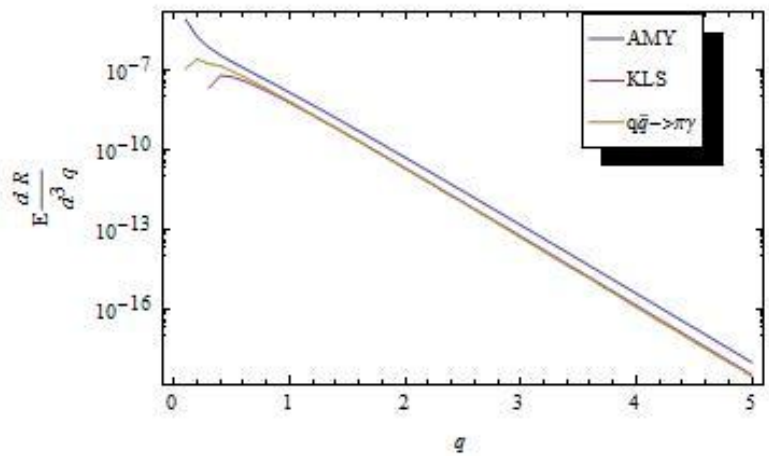


Arnold et al, 2001

Kapusta et al, 1991

- Quark-meson interactions are significant for dilepton.
- Photon production rates are at the order of 1st order QCD rate, less than AMY.

# Counting Degrees of Freedom

- Constraint from lQCD

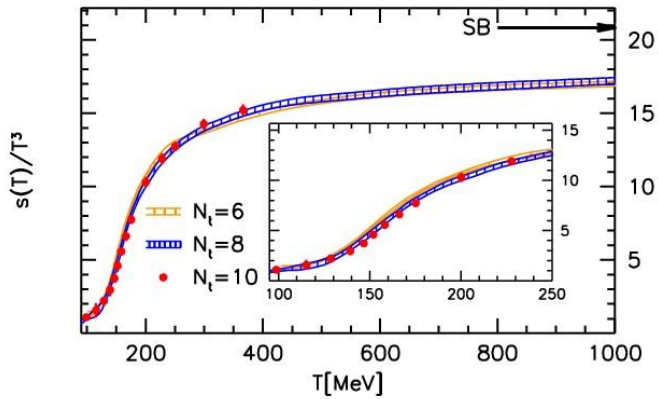


WB Collaboration, 2010

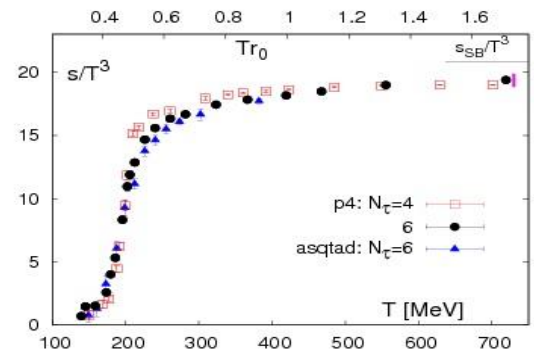


hotQCD Collaboration, 2008

$$C_q(T)s_{parton}(T)+C_\pi(T)s_{hadron}(T)=s_{lattice}(T)$$

- Quasi Particle description of QGP

$$s_{qgp}(T)=\frac{v_g}{2\pi^2 T}\int_0^\infty dkk^2[f_B(E_k^g)\frac{4k^2/3+m_g^2(T)}{E_k^g}+\frac{v_q}{2\pi^2 T}\int_0^\infty dkk^2[f_D(E_k^g)\frac{4k^2/3+m_q^2(T)}{E_k^q}$$

Peshier et al, PLB,1994 Renk et al, PRC, (2002) Rapp, PRC, (2002)

# Counting Degrees of Freedom

- Constraint from lQCD

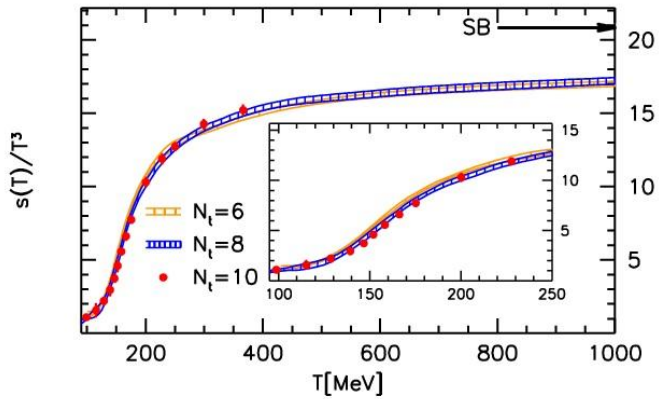


WB Collaboration, 2010

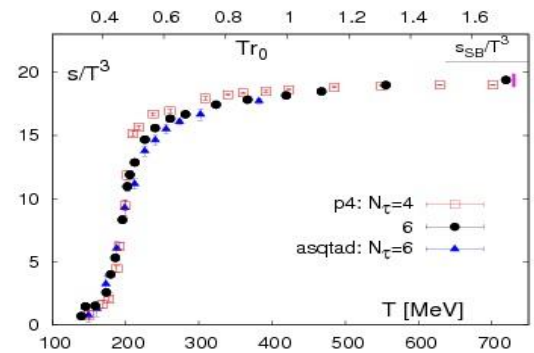


hotQCD Collaboration, 2008

$$C_q(T)s_{parton}(T)+C_\pi(T)s_{hadron}(T)=s_{lattice}(T)$$

- Quasi Particle description of QGP

$$s_{qgp}(T)=\frac{v_g}{2\pi^2T}\int_0^\infty dkk^2[f_B(E_k^g)\frac{4k^2/3+m_g^2(T)}{E_k^g}+\frac{v_q}{2\pi^2T}\int_0^\infty dkk^2[f_D(E_k^g)\frac{4k^2/3+m_q^2(T)}{E_k^q}$$

Peshier et al, PLB,1994 Renk et al, PRC, (2002) Rapp, PRC, (2002)

# A Possible Scenario (I)

| Temperature | Ingredients | Dilepton Source |
|---|---|---|
| T>200MeV | QGP with thermal mass | $q+\bar{q}\rightarrow\gamma^{*}\rightarrow e^{+}+e^{-}$ |
| 170MeV<T<200MeV | Pion,Rho,QGP. | $q+\bar{q}\rightarrow\rho\rightarrow e^{+}+e^{-}$<br>$\pi^{+}+\pi^{-}\rightarrow\rho\rightarrow e^{+}+e^{-}$<br>quark meson interaction. |
| T<170 | HRG. | Hadronic rate from Rapp&Wambach. |

Fraction of QGP and HG

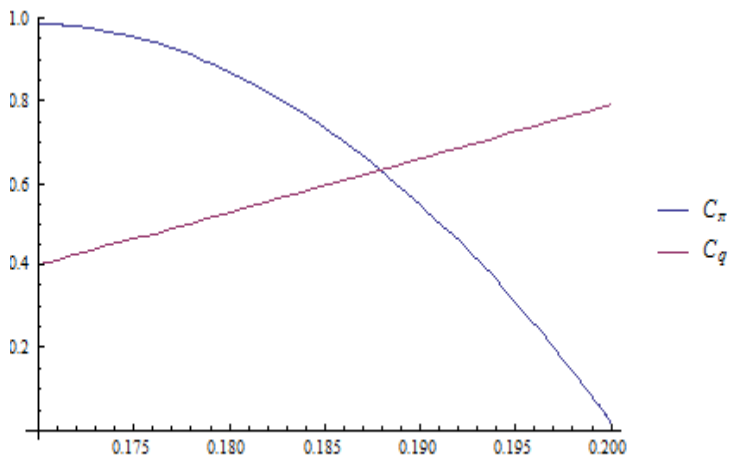


Weight of interaction channels

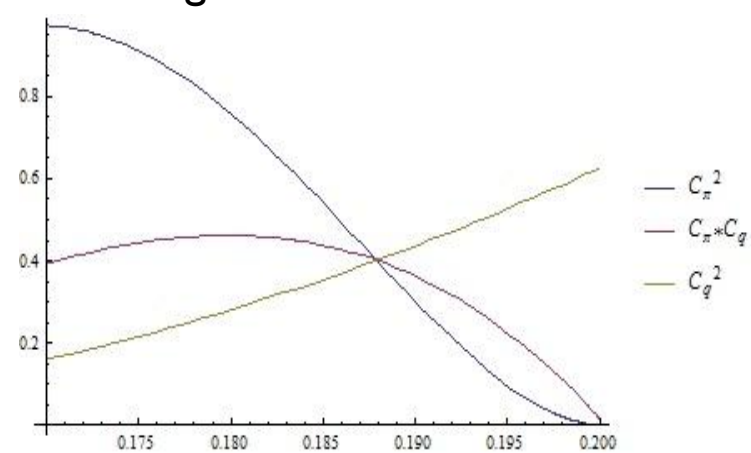

# Rates from Scenario I

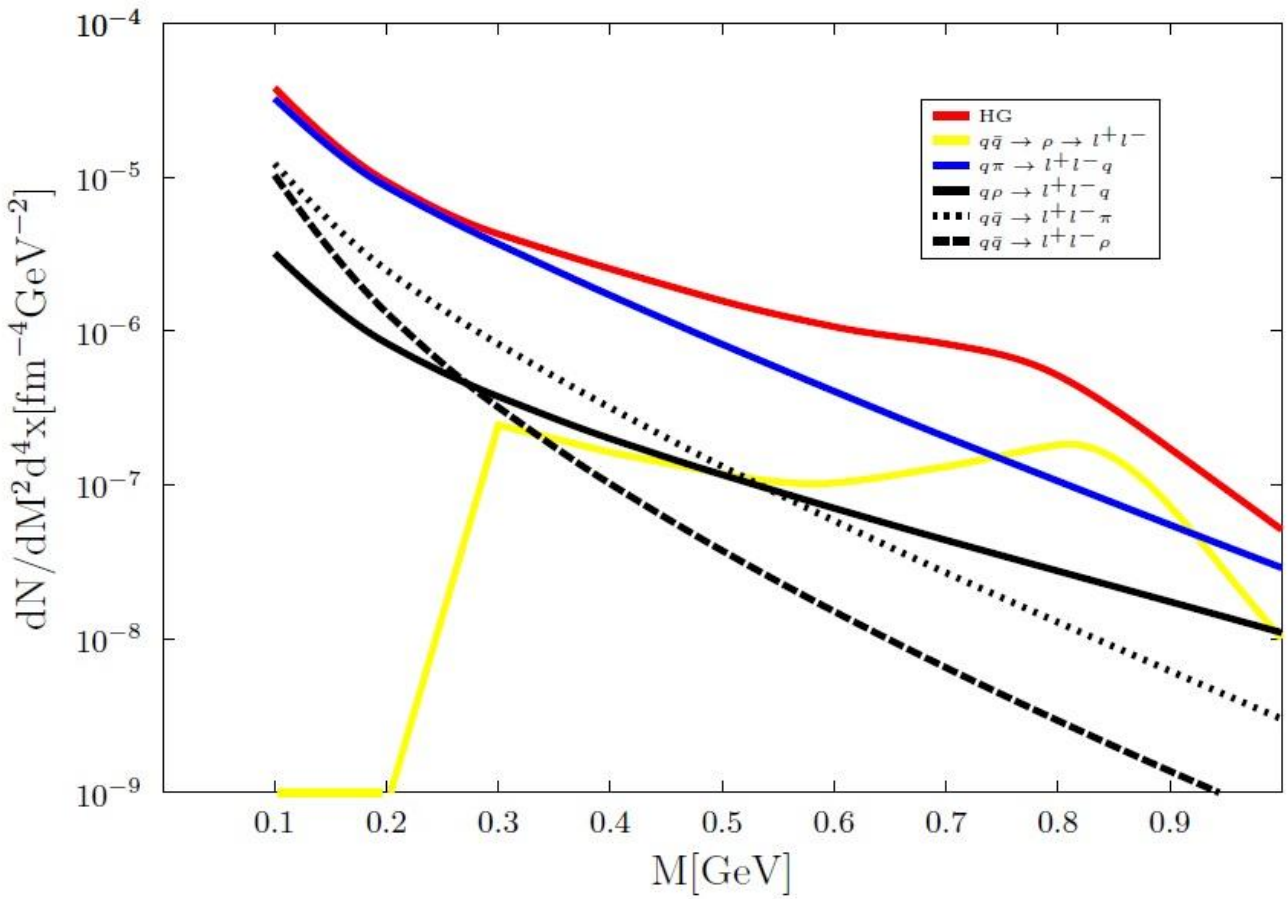

# Dilepton Yields from Scenario I

Include quark meson interaction

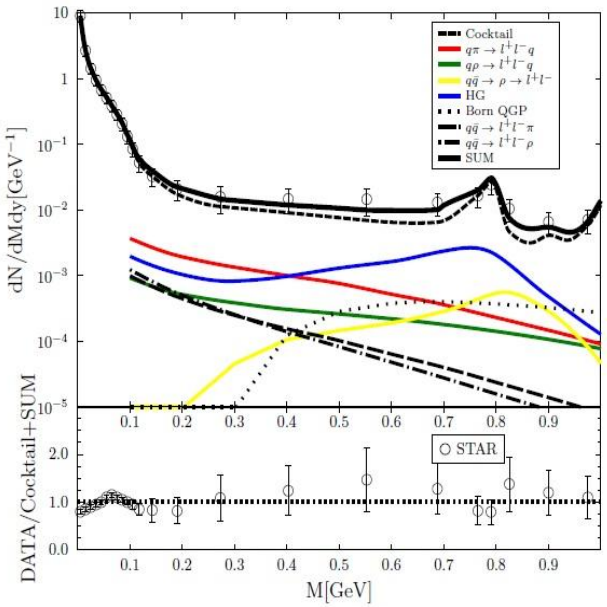


State of art calculation

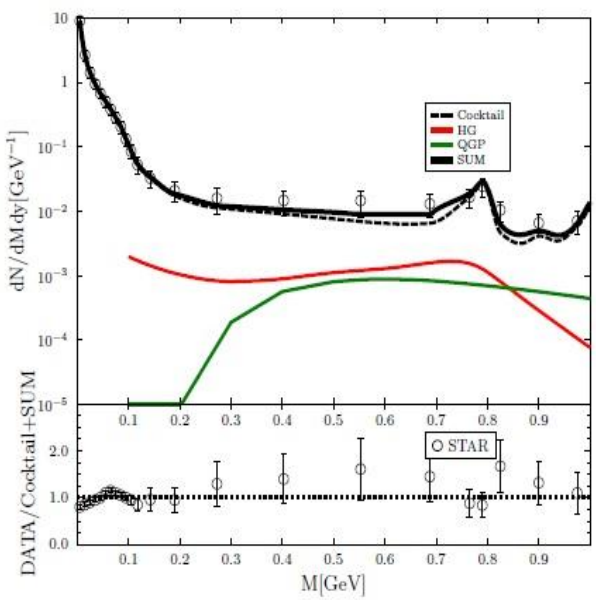


He, Fries and Rapp, priv. comm.

- Have 20% more than just HG+QGP.
- Hydro: He, Fries and Rapp, 2011.
- STAR Data: QM11, J. Zhao; QM12, B. Huang

# v2 from Scenario I

M=400 MeV

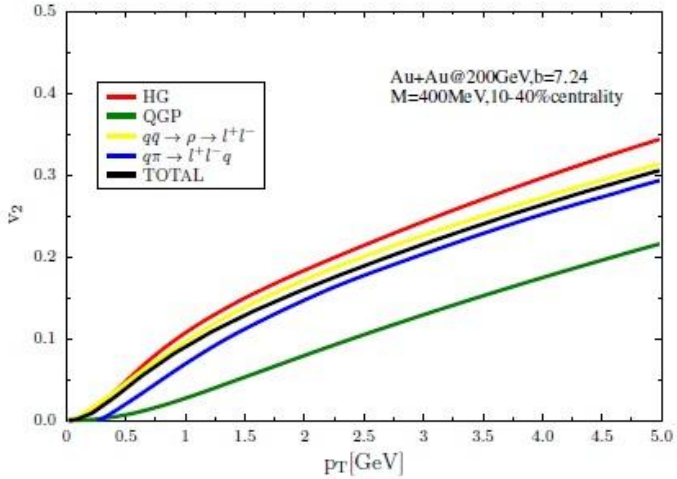


- Dilepton from hadronization has large v2;
- Total thermal v2 from scenario I very close to hadronic v2.

# v2 from Scenario I

M=800 MeV

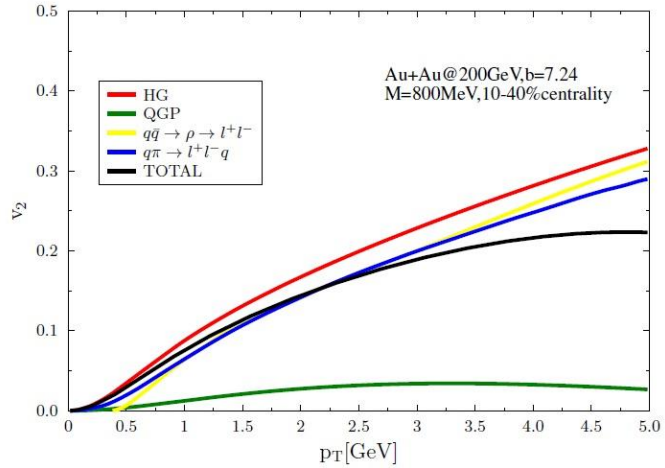


- Total v2 is slightly larger than if we only considered HG+QGP.

Compare to HG+QGP

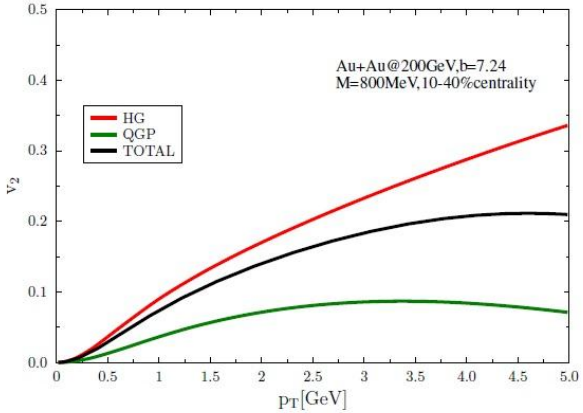


He, Fries and Rapp

# Another Possible Scenario (II)

| Temperature | Ingredients | Dilepton Source |
|---|---|---|
| T>200MeV | QGP with thermal mass | $q+\bar{q}\rightarrow\gamma^{*}\rightarrow e^{+}+e^{-}$ |
| 150MeV<T<200MeV | QGP and HRG. | Quark meson interaction; Hadronic(RW) with weight; $q+\bar{q}\rightarrow\rho\rightarrow e^{+}+e^{-}$ |
| T<150 | HRG. | Full Hadronic rate(RW). |

Fraction of QGP and HG

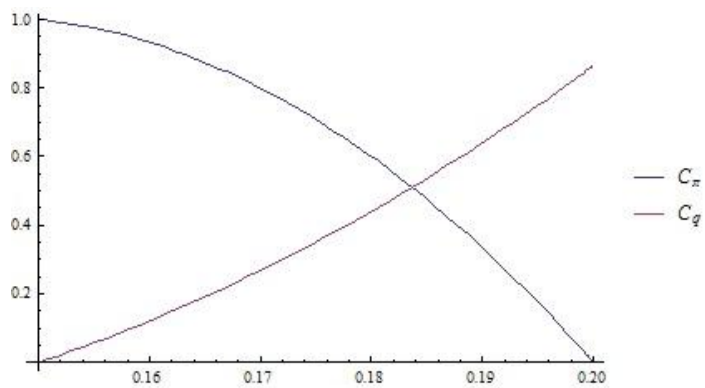


Weight of interaction channels

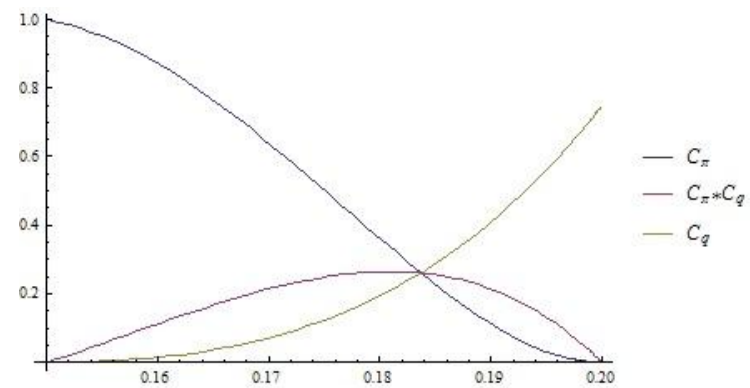

# Dilepton Yields from Scenario II

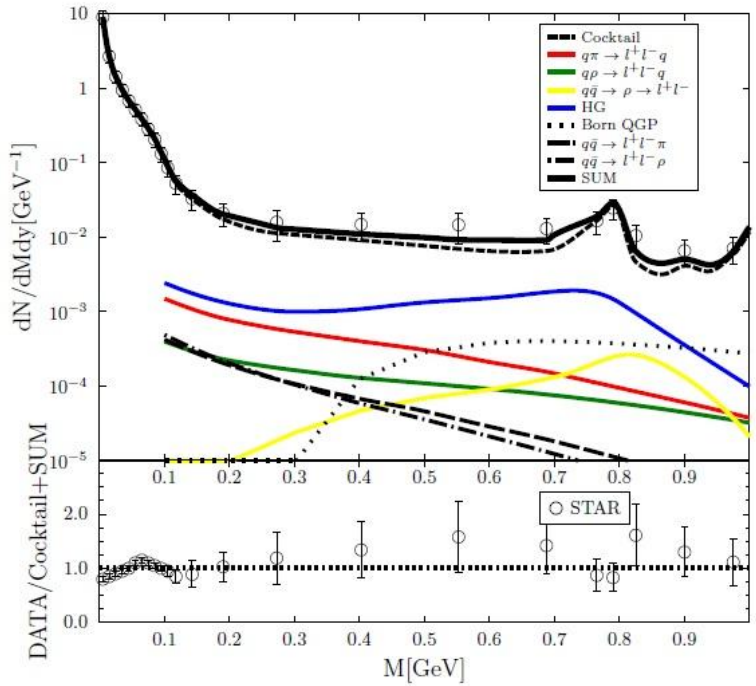


- Less yield than scenario I.
- Quark meson interaction are less important than hadronic contribution.

# Summary

- First attempt to calculate dilepton production through quark hadron interaction during phase transition;
- Calculations of dilepton yields in two different scenarios during crossover phase transition are carried out;
- Dilepton spectrum and v2 are found to be modestly different from mixed phase results.

# Thank You!


- Acknowledgements
- Dr. Ralf Rapp
- Dr. Min He
- J. Zhao, B. Huang……

# Backup

# Integrated v2

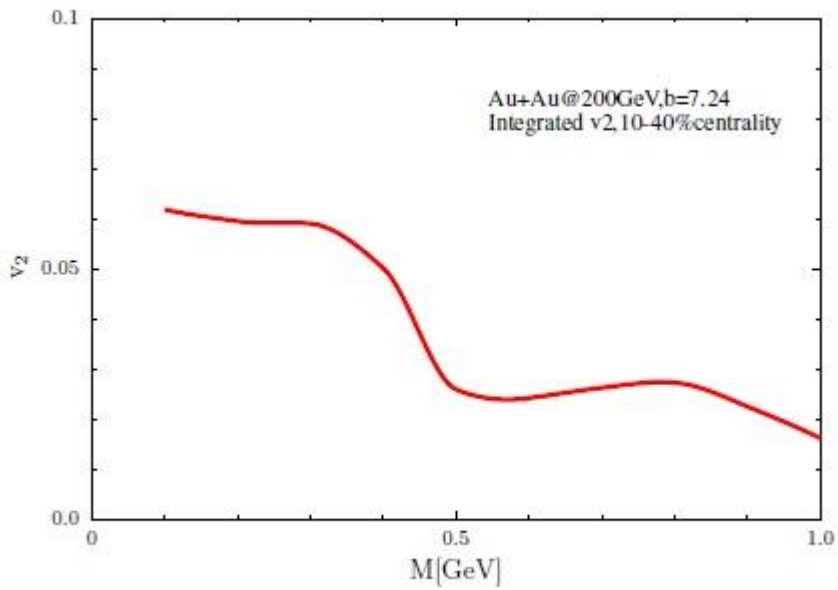

# Di-electron elliptic flow in 200 GeV Au+Au collisions at STAR

**Xiangli Cui** *(for the STAR Collaboration)*
*University of Science and Technology of China (USTC)*
*Brookhaven National Laboratory (BNL)*

# Outline

- **Introduction**
- **Electron identification**
- **Analysis technique**
- **Centrality, mass and $p_T$ dependence of $v_2$**
- **Summary**

# Introduction

***NA60:*** *Eur. Phys. J.C 61(2009) 711-720*

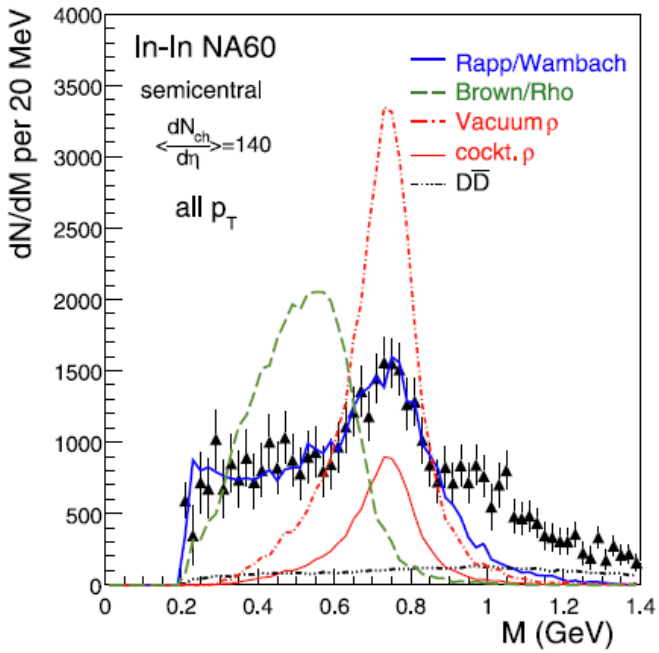


***R. Rapp, et al .,****Phys.Rev. C63 (2001) 054907.*

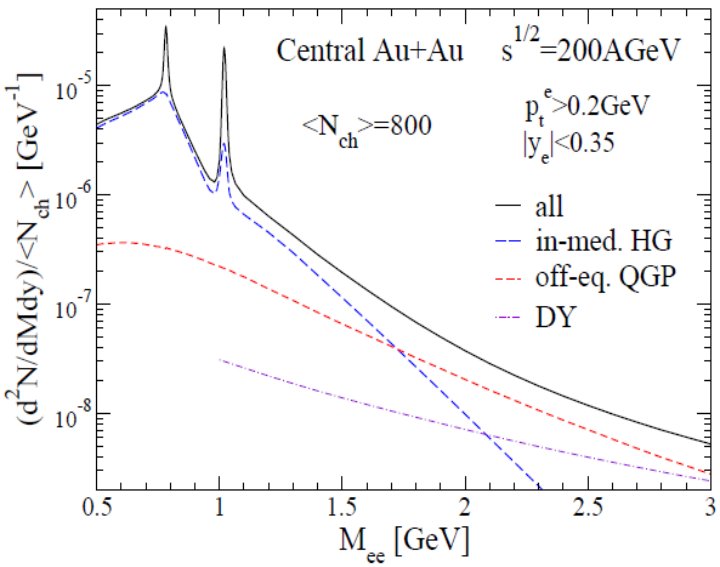


***Low mass region ($M_{ll}$ <1.1 GeV/c$^2$):***
*In-medium modifications of vector mesons.*
*Chiral symmetry restoration?*

***Intermediate mass region (1.1< $M_{ll}$ <3.0 GeV/c$^2$ ):***
*QGP thermal radiation.*

# Introduction

***Rupa Chatterjee , et al.,*** *Phys Rev C 75, 054909 (2007)*

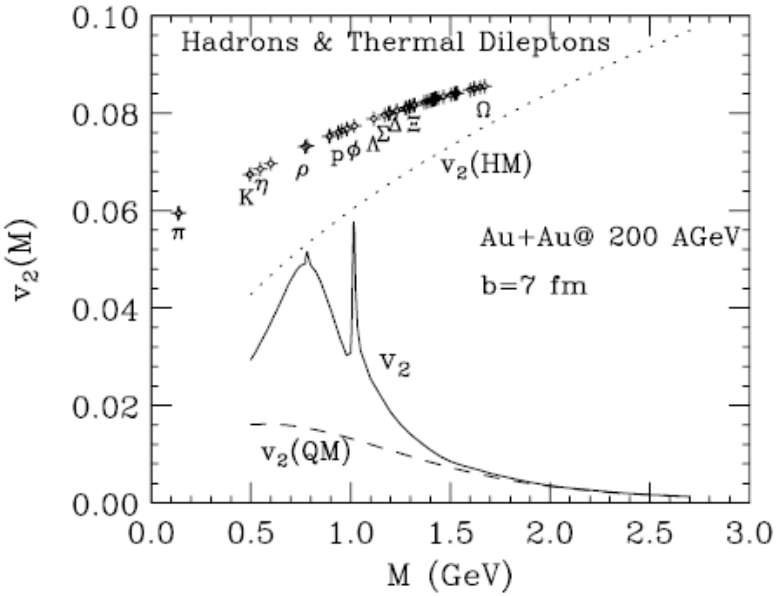


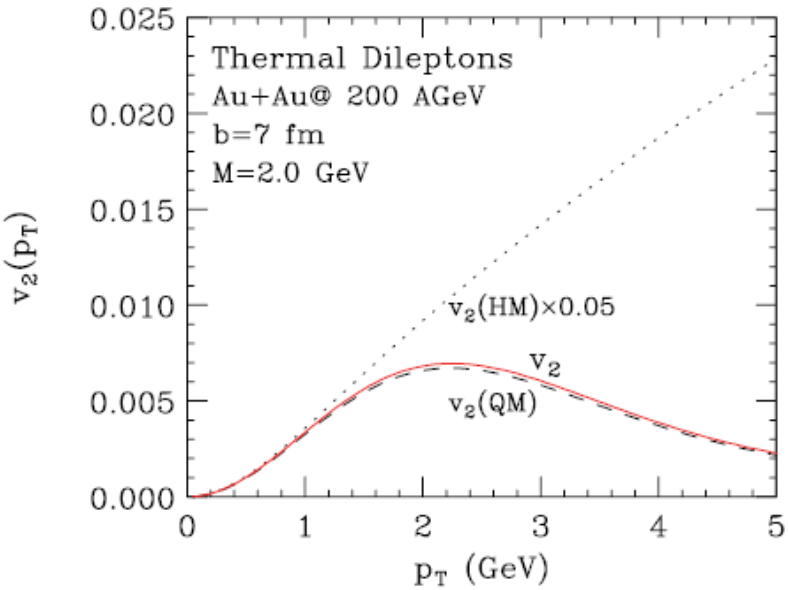


- ***The mass and $p_T$ dependences of di-lepton $v_2$ could give very rich information on specific stages of the fireball expansion***

- ***Measurements of $v_2$ of thermal di-lepton could distinguish partonic and hadronic radiation sources***

# STAR detector

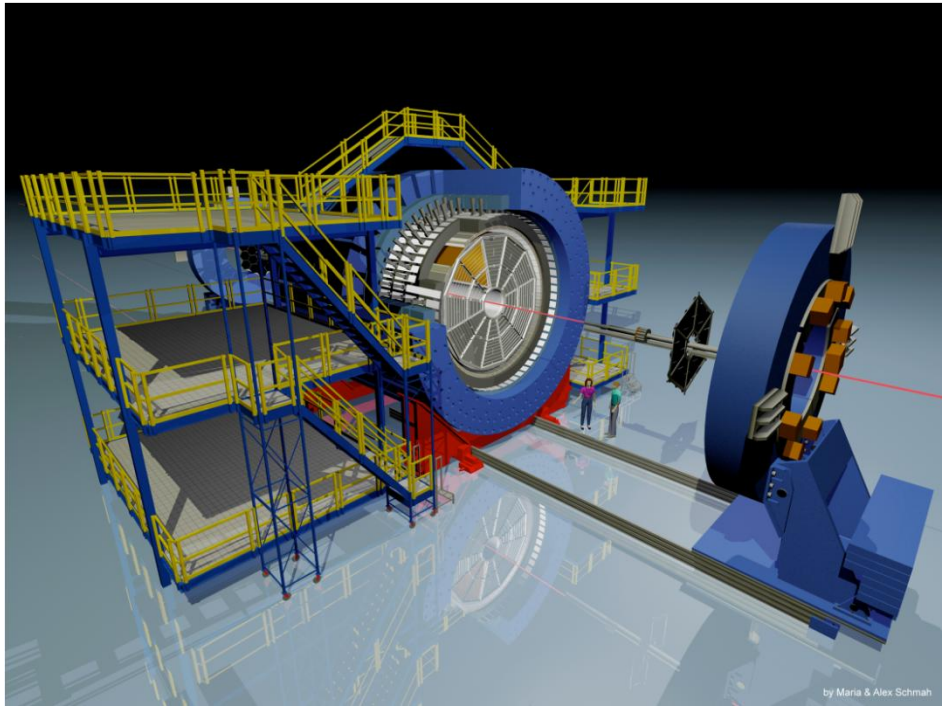


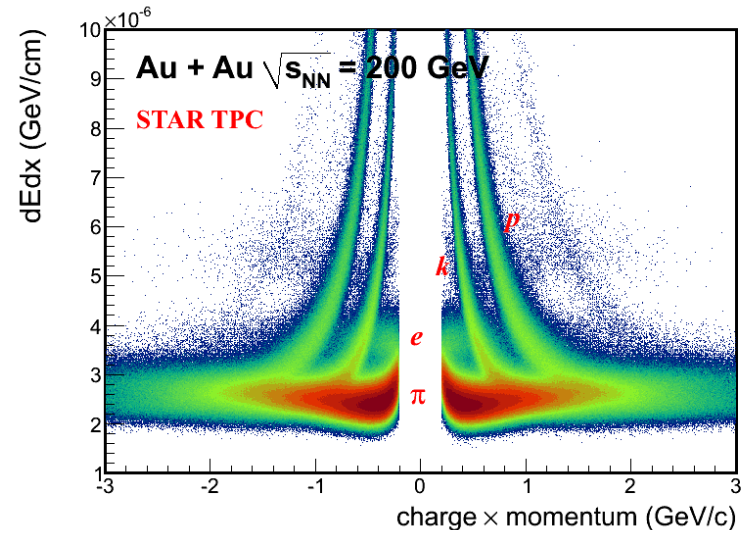


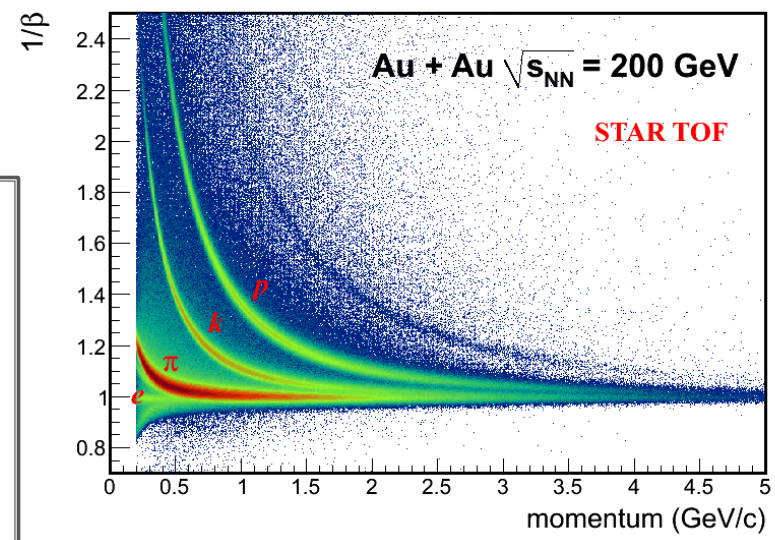


- **Time Projection Chamber** (0<ϕ<2π, |η|<1 )
  *Tracking – momentum*
  *Ionization energy loss (dE/dx, PID)*
- **Time Of Flight** (0<ϕ<2π, |η|<0.9)
  *Timing resolution <100ps - significant improvement for PID*

# Electron identification

**TOF velocity cut to remove slow hadrons**

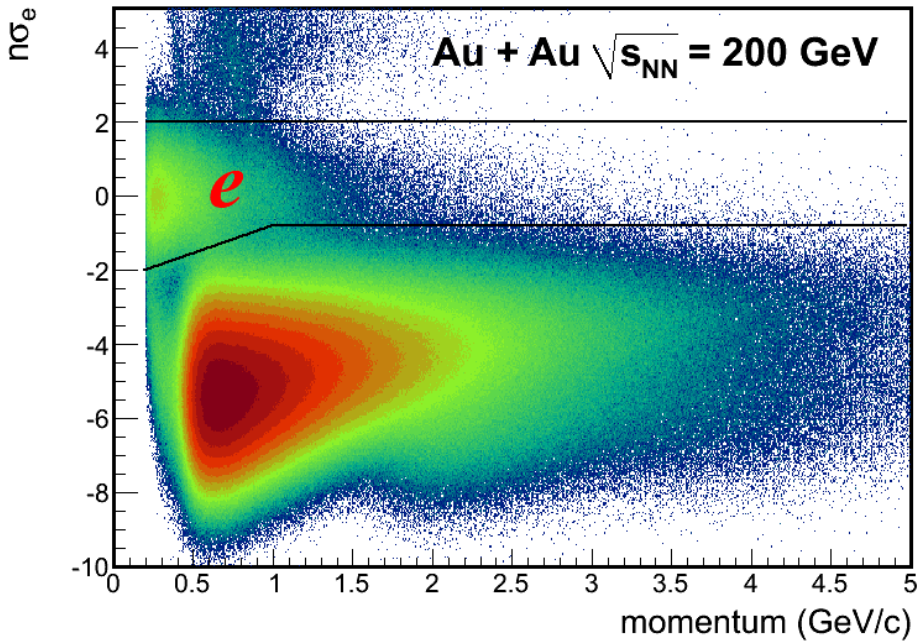


$$n\sigma_e = \frac{\log(\frac{dE/dx}{B_e})}{\sigma_e}$$

- **Clean electron PID Au+Au collisions with a combination of TPC dE/dx and TOF velocity**
  - ✓ *electron purity ~97% in Au + Au Min Bias collision.*
- **Combine data sets of year 2010 and 2011 ~ 720M**

# Invariant mass distribution

*Au+Au 0-80%@200GeV*

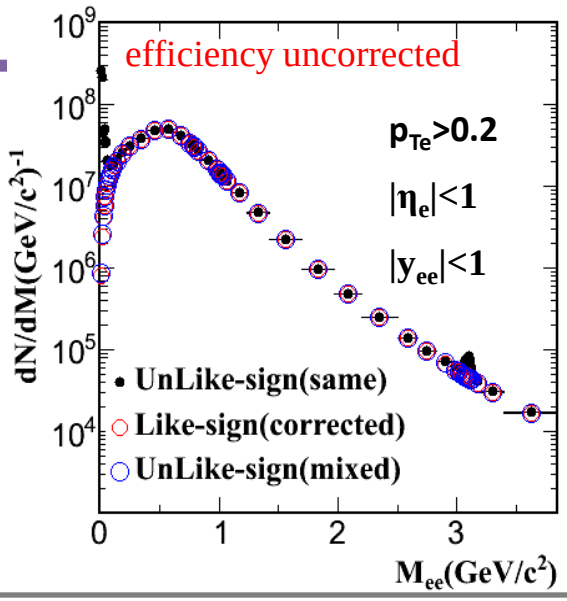


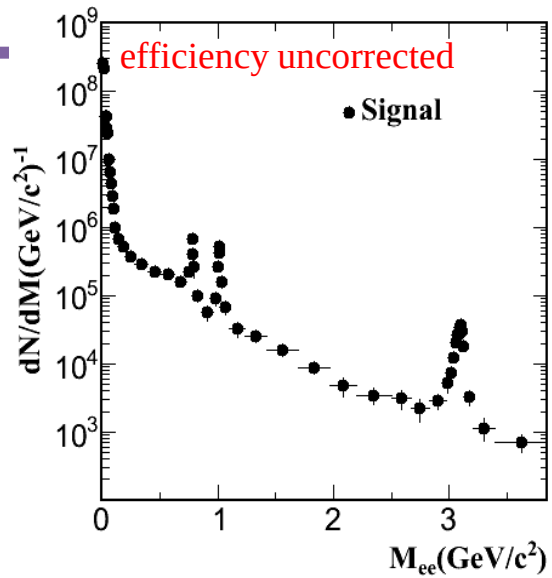


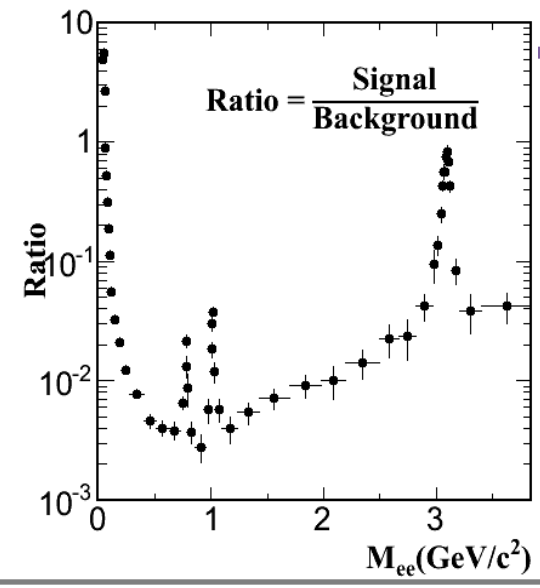


***Background:*** *Like-sign (same) or Unlike-sign (mixed);* ***Signal:*** *Unlike-sign(same) – Background;*
***Signal + Background:*** *Unlike-sign(same)*

*$M_{ee}$<=0.7 GeV/c$^2$ :*
*Subtract the like-sign background*
*$M_{ee}$>0.7 GeV/c$^2$ :*
*Subtract the normalized mixed-event background (normalized to like-sign background at $M_{ee}$(0.7,3) GeV/c$^2$ and $p_T$ (0,4)) GeV/c.*

*We mix events which are in the same centrality bin (9), vertex z bin (10) and event plane angle bin (100), same magnetic field.*

# Dominant particle contribution in different mass ranges

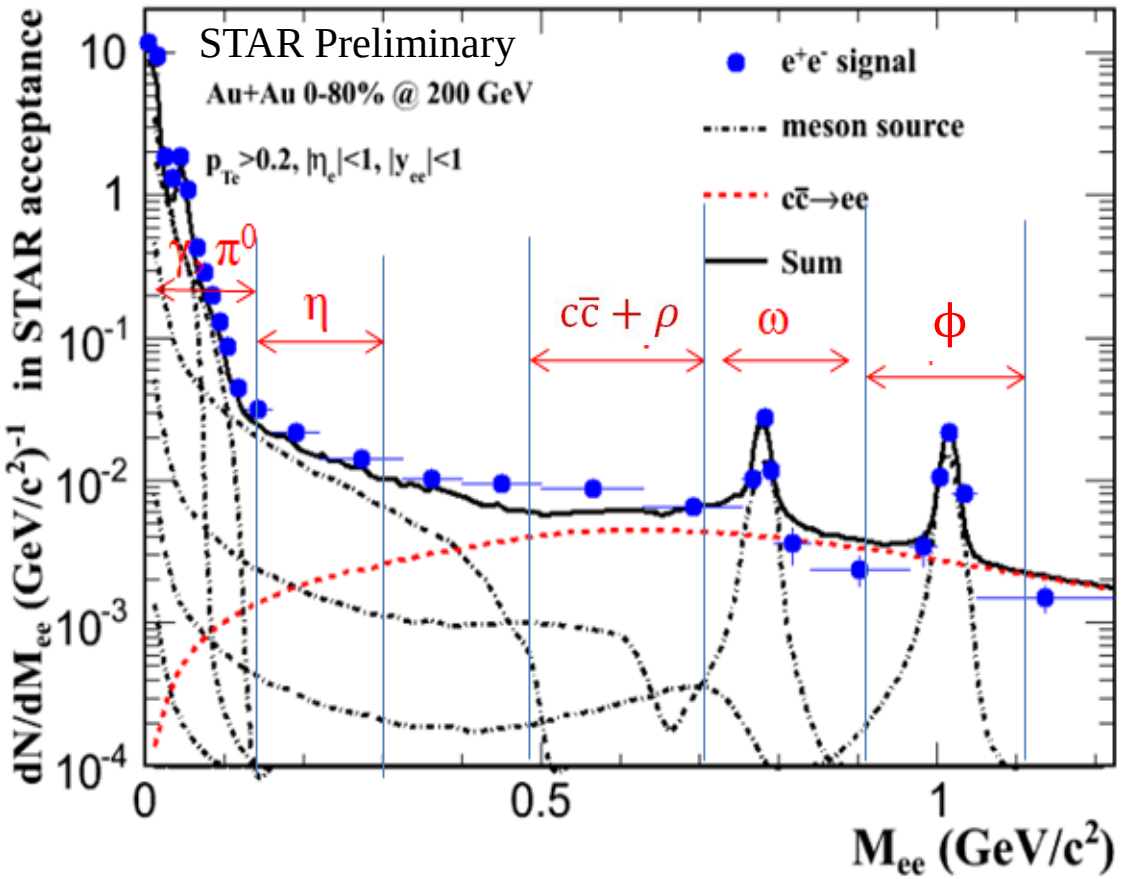


$M_{ee}$(0-0.14) : $\pi^0$+others

$M_{ee}$(0.14,0.3): η+others

$M_{ee}$(0.5,0.7) : charm+ρ+ others

$M_{ee}$(0.7,0.9): ω+others

$M_{ee}$(0.9,1.1): ϕ+others

$M_{ee}$(1.1,2.9): charm+other

# Analysis technique

$$v_2^S \times \frac{N_S}{N_{(S+B)}} = v_2^T - v_2^B \times (1 - \frac{N_S}{N_{(S+B)}})$$

$$v_2 = < \cos(2(\phi_i - \psi_2)) > / r_j$$

***Background:*** ***Like-sign (same) or Unlike-sign (mixed).***
***Signal + Background:*** ***Unlike-sign(same).***
***Signal:*** ***Unlike-sign(same) – Background.***

$v_2^T$ **:** *Signal + Background* $v_2$,
$v_2^B$**:** *Background* $v_2$,
$v_2^S$**:** *Signal* $v_2$
$N_S/N_{(S+B)}$**:** *Signal/(Signal + Background)*
$r_j$ **:** *Resolution of event plane in centrality j*
*<>: average over all di-electron pairs in all events*

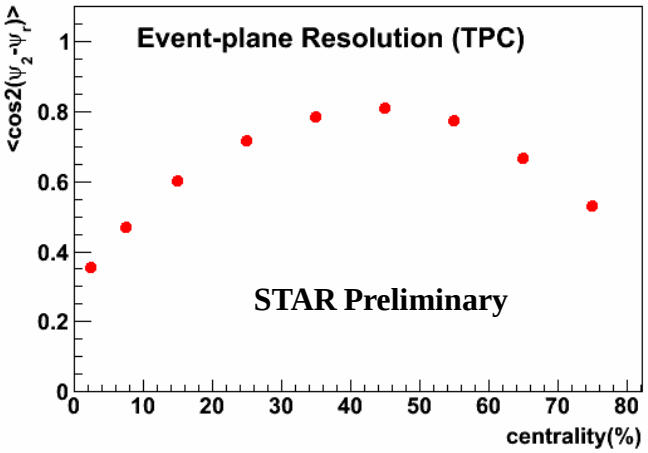

# Unlike-sign and background $v_2$

*Au+Au 0-80%@200GeV*

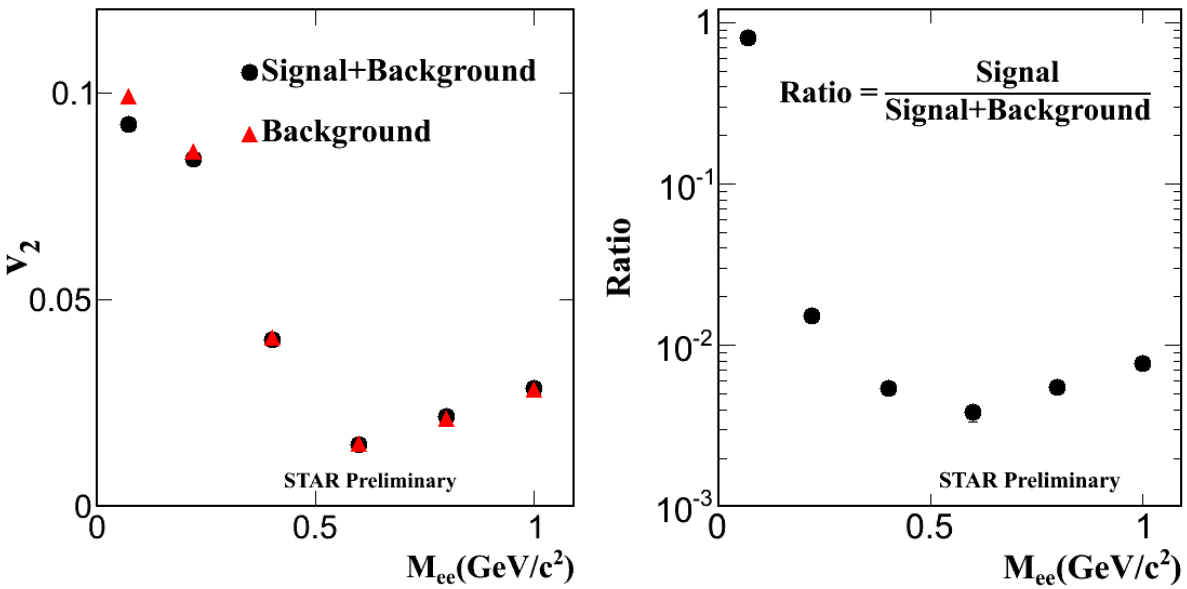


**In each mass bin:** $$v_2^S \times \frac{N_S}{N_{(S+B)}} = v_2^T - v_2^B \times (1 - \frac{N_S}{N_{(S+B)}})$$

*Calculated the* $v_2^T$, $v_2^B$ *and* $N_S/N_{(S+B)}$ *, use above formula to get* $v_2^S$

***Background:*** $M_{ee}$ ***<=0.7 GeV/c²: Like-sign same event,***

$M_{ee}$ ***>0.7 GeV/c² : Unlike-sign mixed-event***

# Cocktail $v_2$ and $p_T$ input ($M_{ee}$<1.1GeV/$c^2$)

http://drupal.star.bnl.gov/STAR/files/Bai_Yuting.pdf *(Ph.D thesis)*

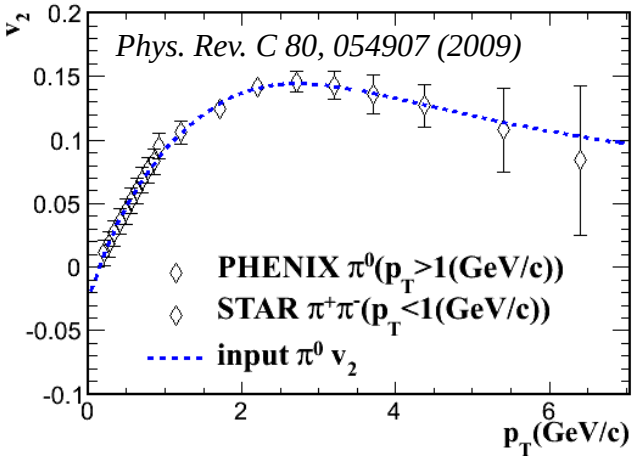


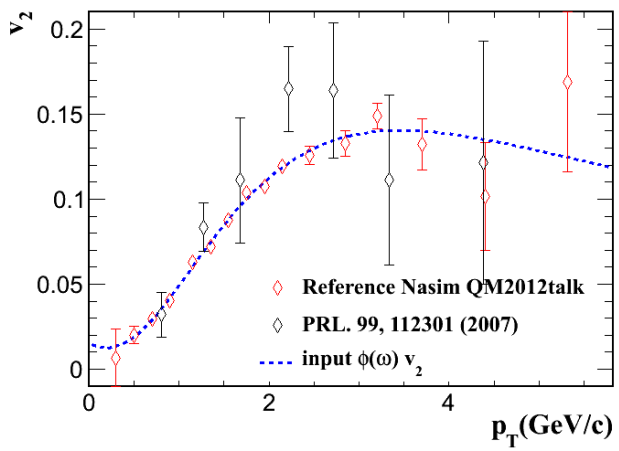


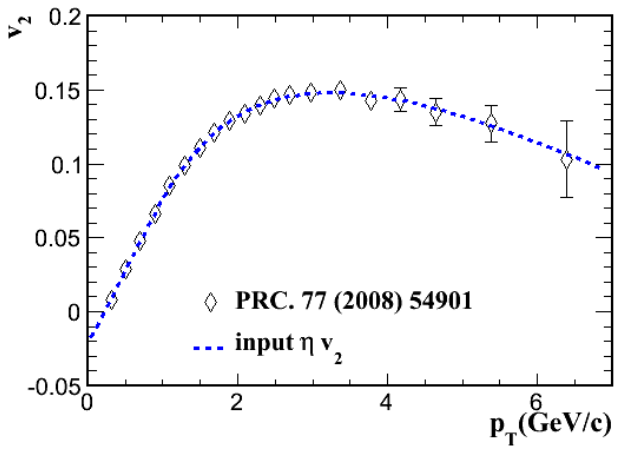


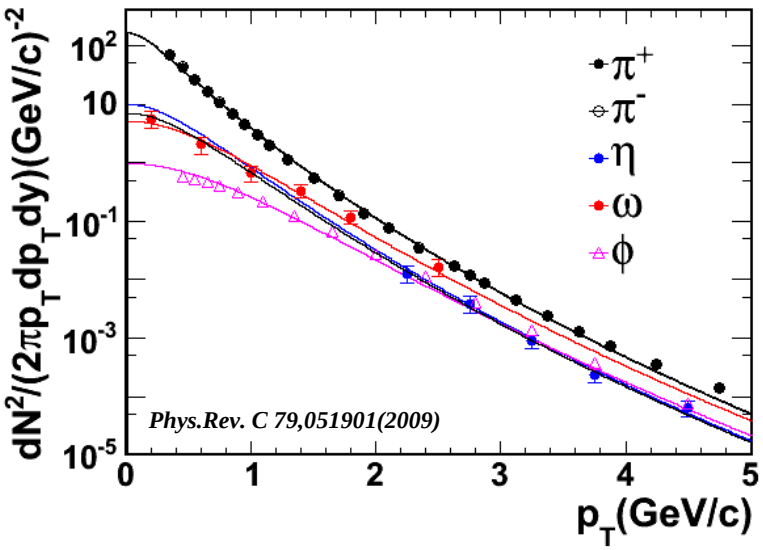


- ***components : $\pi^0$, $\eta$, $\omega$, $\phi$***
- ***Input:*** *flat rapidity (-1,1);*

  *$p_T$: Tsallis function;*

  *$\varphi$:1+ $2v_2\cos(2\varphi)$.*

# Cocktail simulation results ($M_{ee}$<1.1GeV/$c^2$)

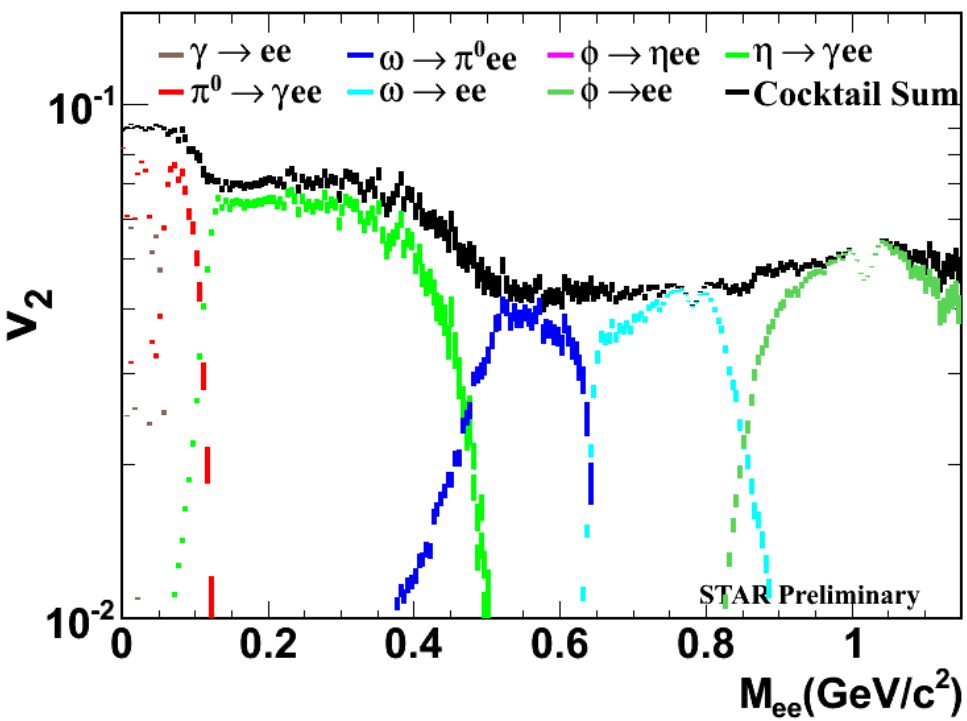


- *1. Reconstruct $e^+e^-$ pairs after they decay in the STAR simulators.*
- *2. Same acceptance cuts applied as in data.*
- *3.obtain each component $v_2$ and yield.*
- *4. The cocktail $v_2$ obtained by combining each component $v_2$ (weight by its yield).*
- *5.The cocktail $v_2$ and each component contribution (weighted by the yield) are shown in the plot.*

# $M_{ee}$ dependence of $v_2$ in Au+Au 200 GeV

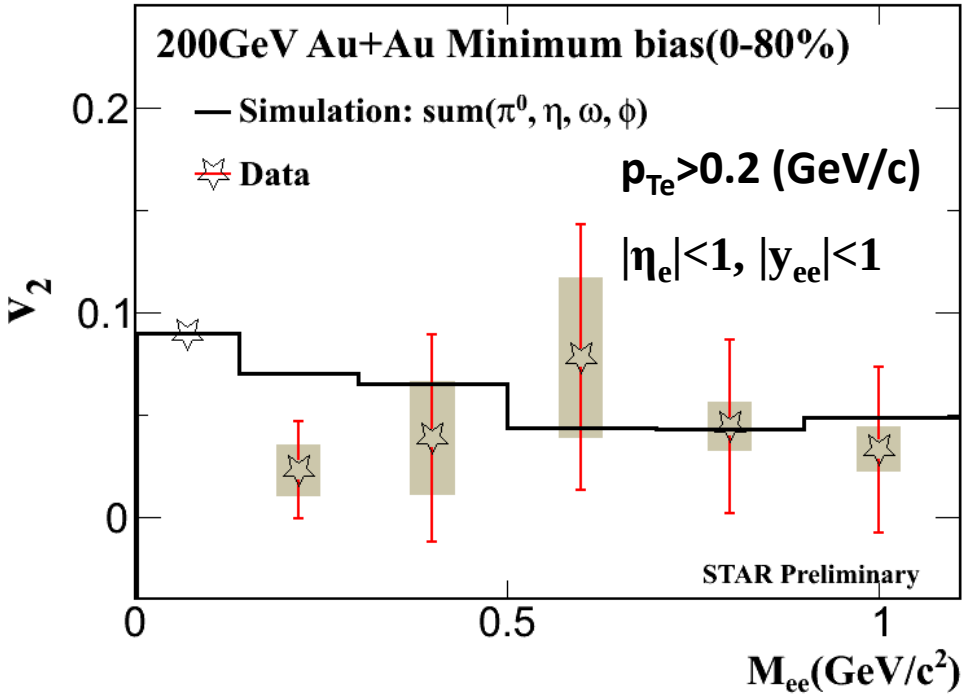


- ***Di-electron $v_2$ is consistent with simulation using the measured meson $v_2$ as input in Au+Au at 200 GeV.***
- ***Work in progress to include intermediate mass region $v_2$***

# $P_T$ dependence of $v_2$ in Au+Au 200 GeV

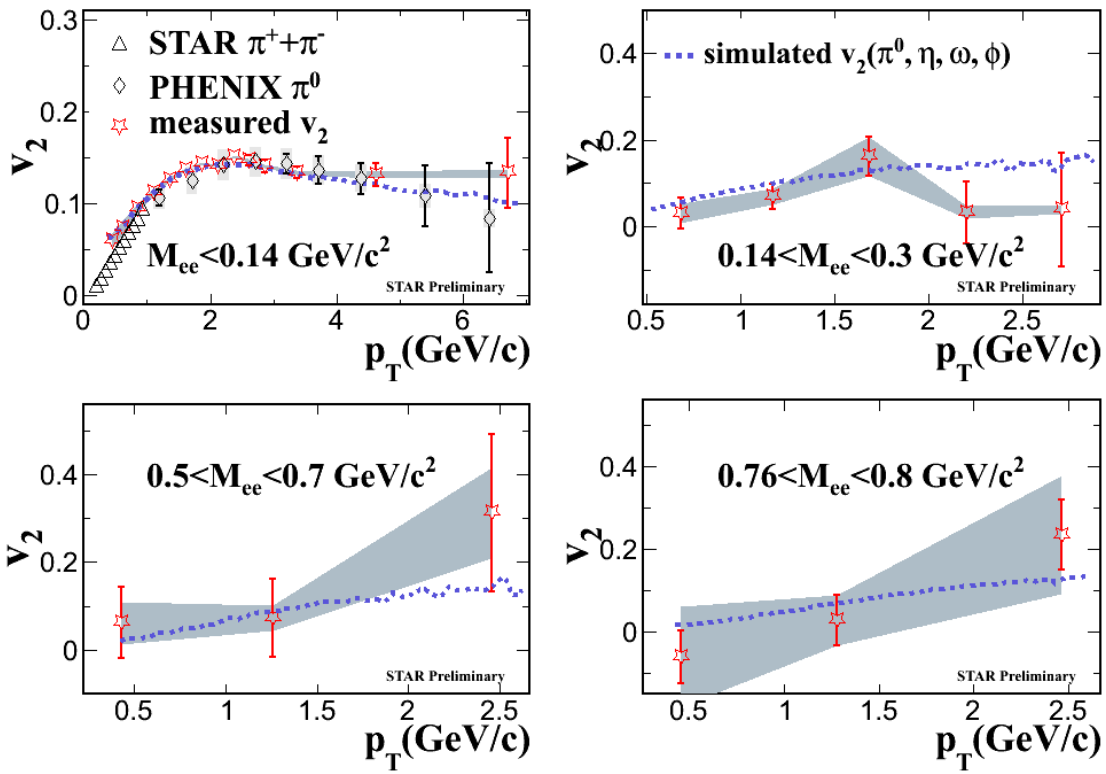


*Au+Au 0-80%@200GeV*

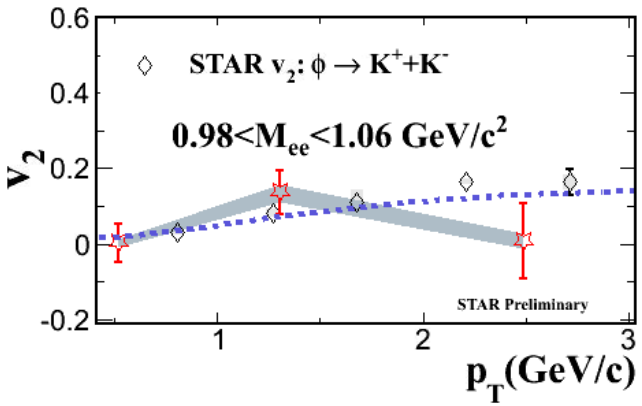


- ***Simulated $v_2$ is consistent with measured di-electron $v_2$ within uncertainties in 0-80% Au+Au collisions.***
- ***The $v_2$ of di-electrons in the $\phi$ mass region is consistent with the results of $\phi \rightarrow KK$ within error***

# $\pi^0$ Dalitz decay $v_2$ and $p_T$ Input in different centralities ($M_{ee}$<0.14 GeV/$c^2$ )

PHYSICAL REVIEW C 80, 054907 (2009)
http://arxiv.org/abs/1203.2644v1

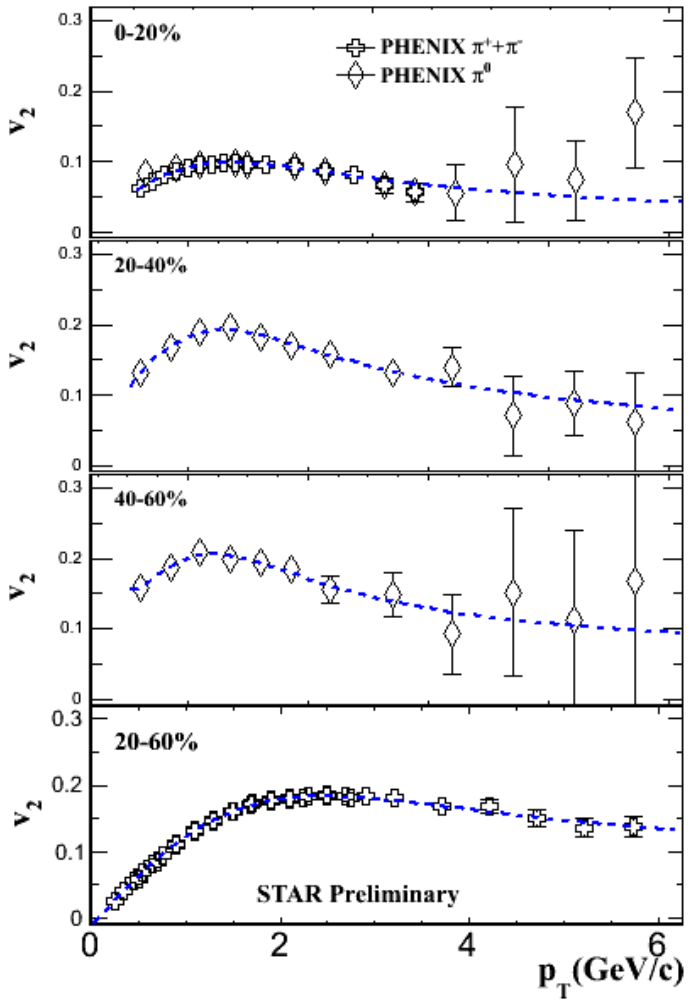


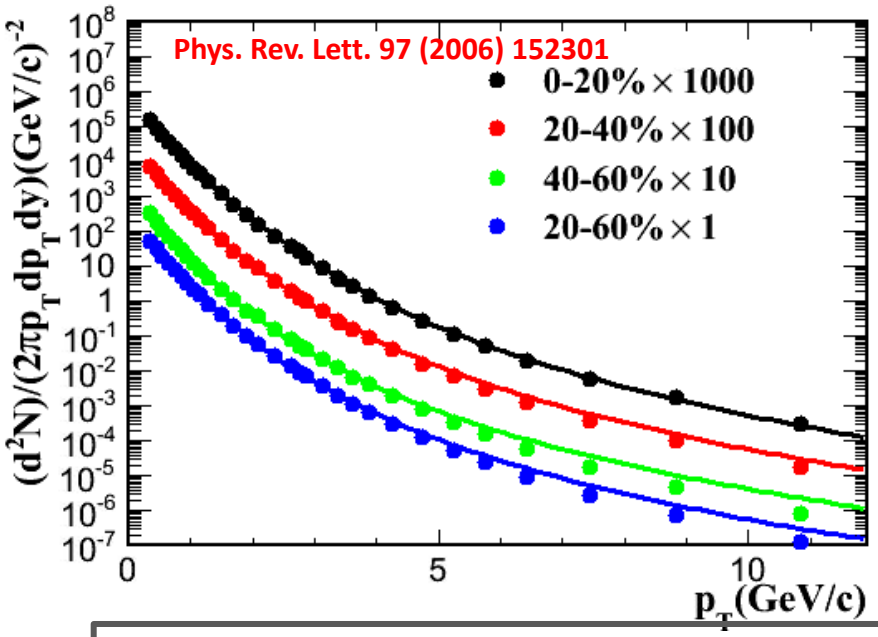


- ***components : $\pi^0$***
- **Input:** flat rapidity (-1,1);

  $p_T$: $M_T$ scaling;

  $\varphi$: $1+2v_2\cos(2\varphi)$.

# Centrality dependence of $v_2$ ($M_{ee}$<0.14 GeV/$c^2$ )

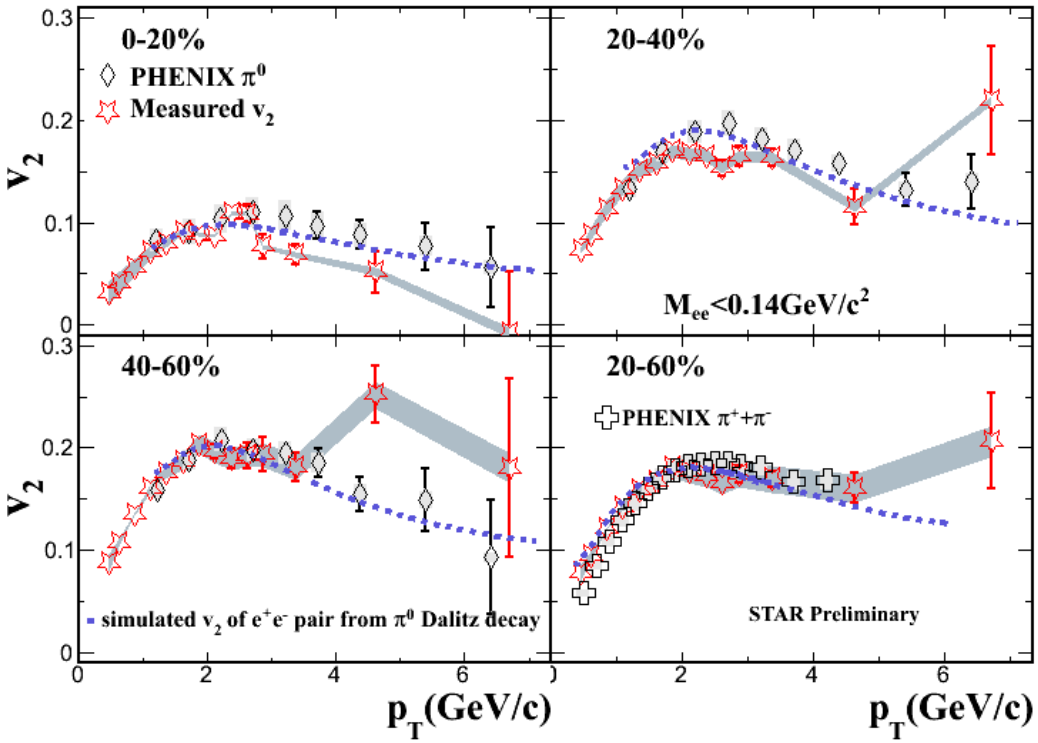


➢**For each centrality:**

➢*1. Reconstruct $e^+e^-$ pairs after $\pi^0$ decay in the STAR simulators.*

➢*2. Same acceptance cuts applied as in data.*

➢3. *obtain $e^+e^-$ pairs $v_2$*

➢ ***Di-electron $v_2$ is consistent with simulated results for different centralities in Au+Au at 200 GeV.***

# Summary

- ***For $M_{ee}$ <1.1 GeV/$c^2$, the simulated cocktail $v_2$ are consistent with the measured di-electron $v_2$***

- ***For $M_{ee}$ <0.14 GeV/$c^2$, the simulated $e^+e^-$ $v_2$ are consistent with the measured di-electron $v_2$ in different centralities.***

- ***Work in progress to include intermediate mass region $v_2$***

*Thanks!*

# Lattice QCD calculation of vector spectral functions and EM emission rates

Heng-Tong Ding

Brookhaven National Laboratory

based on work with

Anthony Francis(Mainz), Olaf Kaczmarek (Bielefeld), Frithjof Karsch (Bielefeld+BNL),
Edwin Laermann (Bielefeld), Marcel Müller (Bielefeld) and Wolfgang Söldner (Regensburg)

**Phys.Rev.D83:034504,2011, arXiv:1012.4963,**

**J.Phys.G38:124178,2011, arXiv:1109.4054**

# Outline

- Introduction & Motivation
  - thermal dilepton & photon emission rates, electrical conductivity
  - Euclidean correlation and spectral functions
- Vector correlation functions on the lattice
  - finite volume & cut-off effects
  - continuum extrapolation
- Thermal dilepton emission rate and electric conductivity
  - continuum extrapolated results at $T \simeq 1.45 T_c$
  - preliminary results at $T \simeq 1.1 T_c$
- Thermal photon emission rate
  - continuum extrapolated vector correlators at finite p at $T \simeq 1.1 T_c$
- Conclusions & Outlook

# Electromagnetic observables in HIC

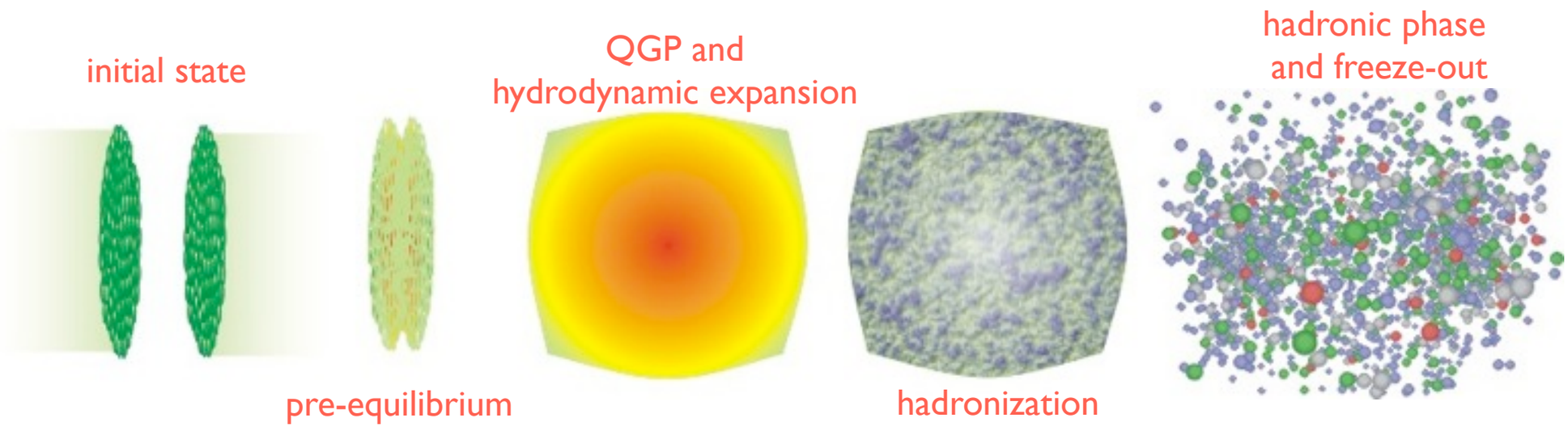


- dileptons/photons: penetrating probes
- produced in the all stages of HIC
- models needed to describe the evolution of the system
- understanding of contributions from all sources

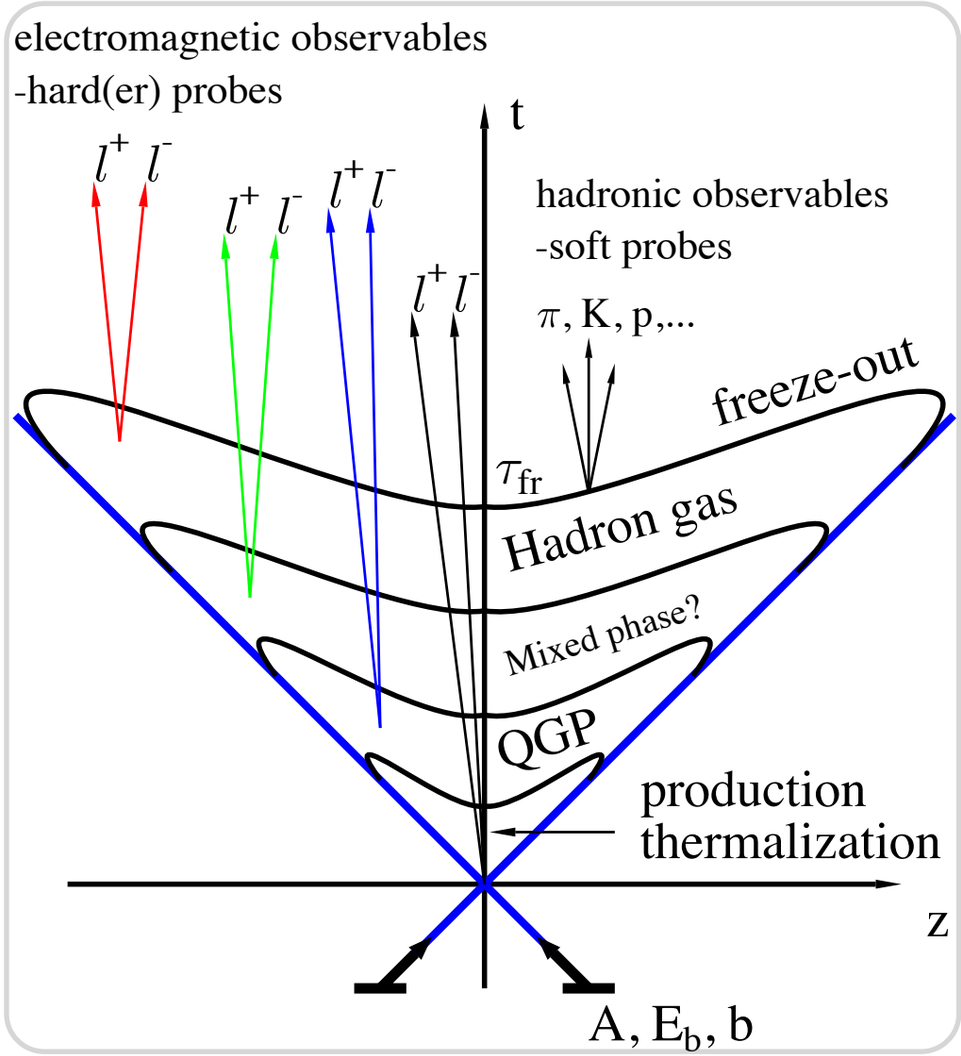

# photon/dilepton production rates

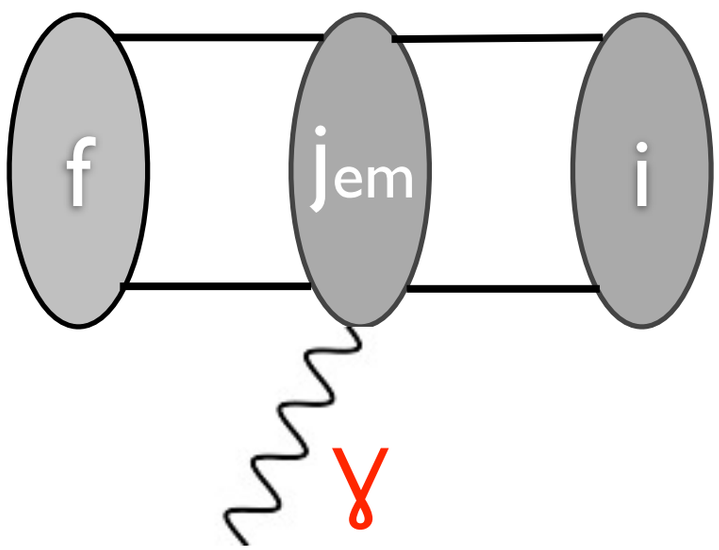


Transition amplitude between |i> and |f> with a on shell photon

$$S_{fi}^{(\lambda)} = -ie \int \mathrm{d}^4x \, \exp(ipx) \, \epsilon_\mu^{(\lambda)}(p) \, \langle f | j_{em}^\mu(x) | i \rangle$$

Electromagnetic current operator

$$j_{em}^\mu = \frac{2}{3}\bar{u}\gamma_\mu u - \frac{1}{3}\bar{d}\gamma_\mu d - \frac{1}{3}\bar{s}\gamma_\mu s + \cdots$$

Number of photons emitted per unit proper volume

$$R_\gamma = \frac{\mathrm{d}^4 N_\gamma}{\mathrm{d}^4 x} = \frac{1}{\int \mathrm{d}^4 x} \int \frac{\mathrm{d}^3 p}{2\omega(2\pi)^3} \frac{1}{Z} \sum_{f,i,\lambda} e^{-(E_i - \mu N_i)/T} \left| S_{fi}^{(\lambda)} \right|^2$$

Photon emission rate

$$\omega \frac{\mathrm{d}R_\gamma}{\mathrm{d}^3 p} = \sum_f Q_f^2 \, \frac{\alpha_{em}}{4\pi^2} \, \frac{\rho_T(\omega = |\vec{p}|, \vec{p})}{\exp(\omega/T) - 1}$$

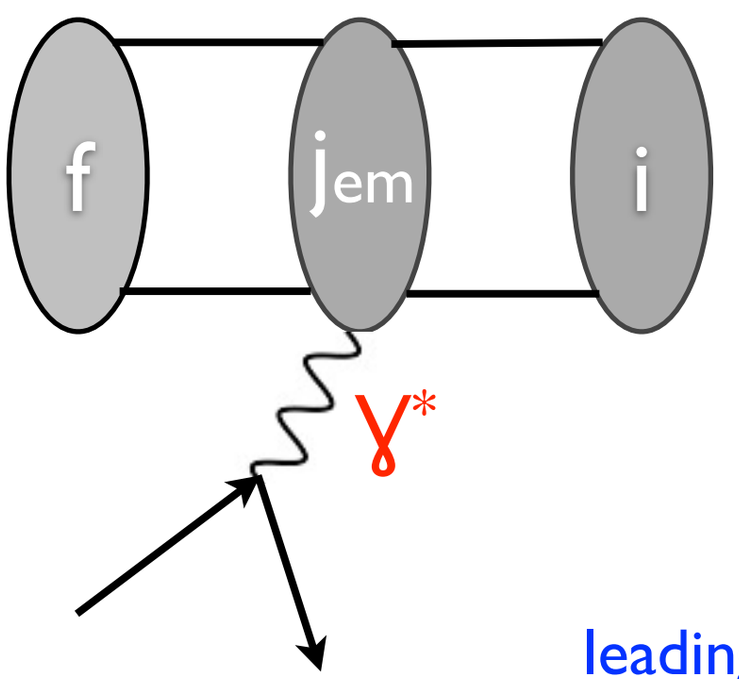


Emission rate of dilepton from virtual photons

$$\frac{\mathrm{d}R_{l^+l^-}}{\mathrm{d}\omega \mathrm{d}^3 p} = \sum_f Q_f^2 \, \frac{\alpha_{em}^2}{6\pi^3} \, \frac{2\rho_T(\omega, \vec{p}) + \rho_L(\omega, \vec{p})}{(\omega^2 - \vec{p}^2)(\exp(\omega/T) - 1)}$$

Above EM emission rate formulae are valid in leading order of $\alpha_{em}$ and exact to all orders in strong coupling

# Experimental results on dilepton rates

- dilepton rates: $$\frac{\mathrm{d}N_{l^+l^-}}{\mathrm{d}\omega \mathrm{d}^3p} = C_{em}\frac{\alpha_{em}^2}{6\pi^3}\frac{\rho_V(\omega,\vec{p},T)}{(\omega^2-\vec{p}^2)(\mathrm{e}^{\omega/T}-1)} \qquad C_{em} = e^2\sum_{f=1}^{n_f} Q_f^2$$

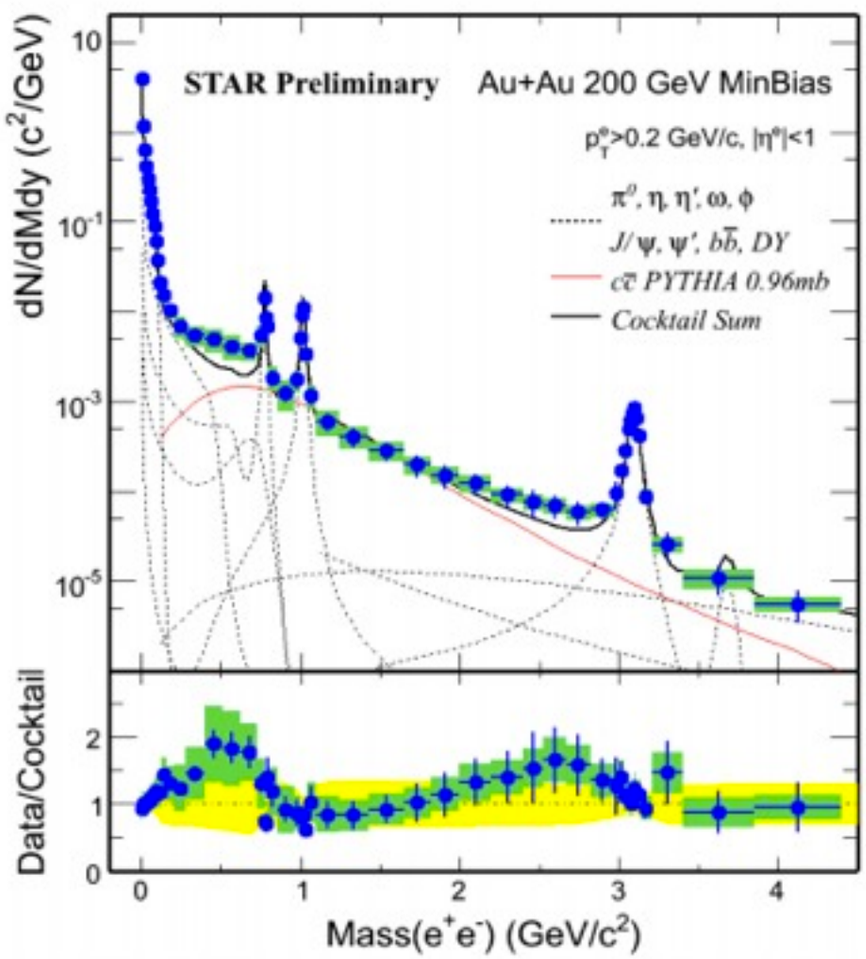


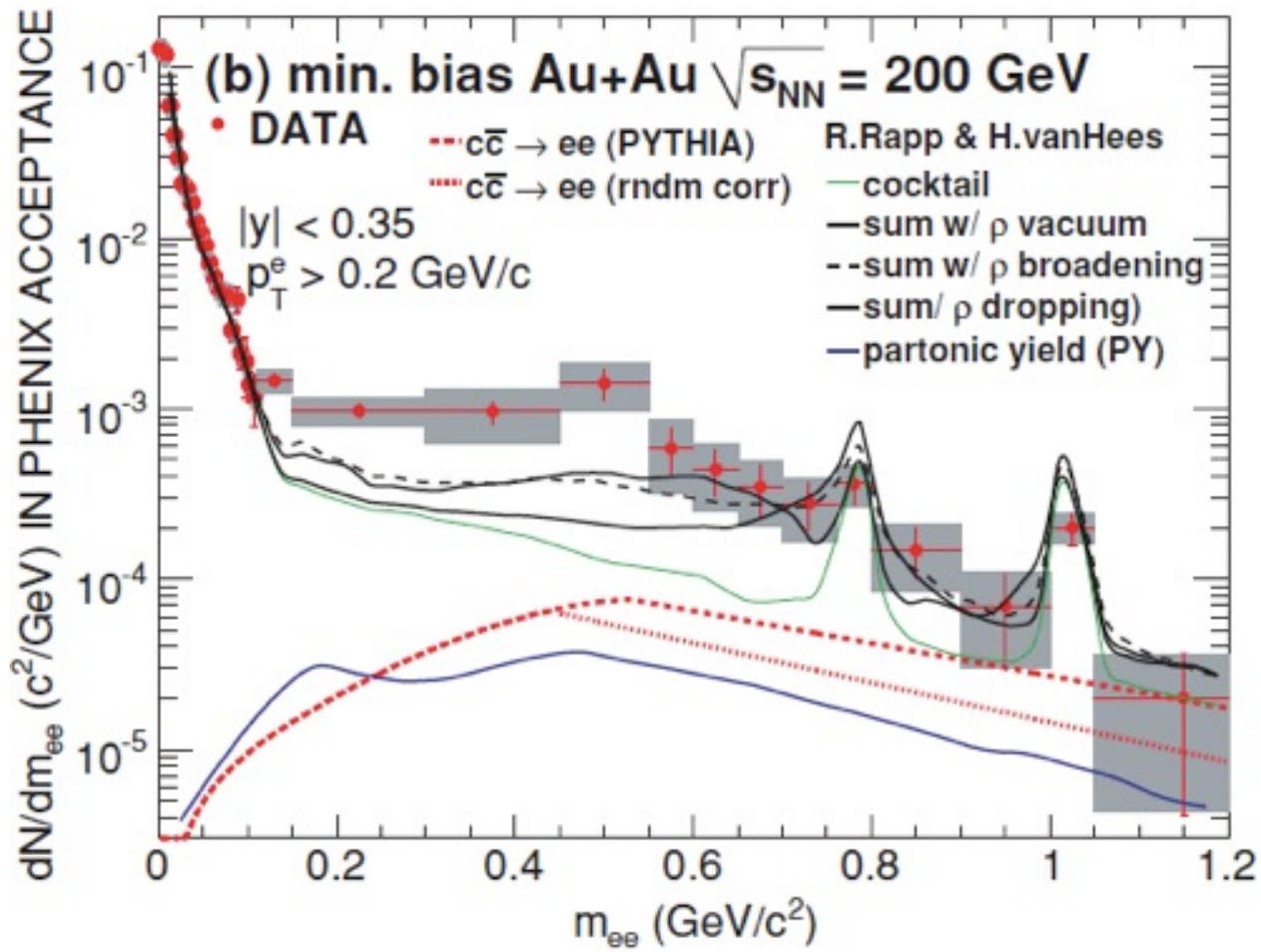


PHENIX: Phys. Rev. C 81 (2010) 034911

- Controversy between STAR and PHENIX in the low mass low pt region
- If PHENIX is right it may imply new mechanism for dilepton production

# Direct photon spectra

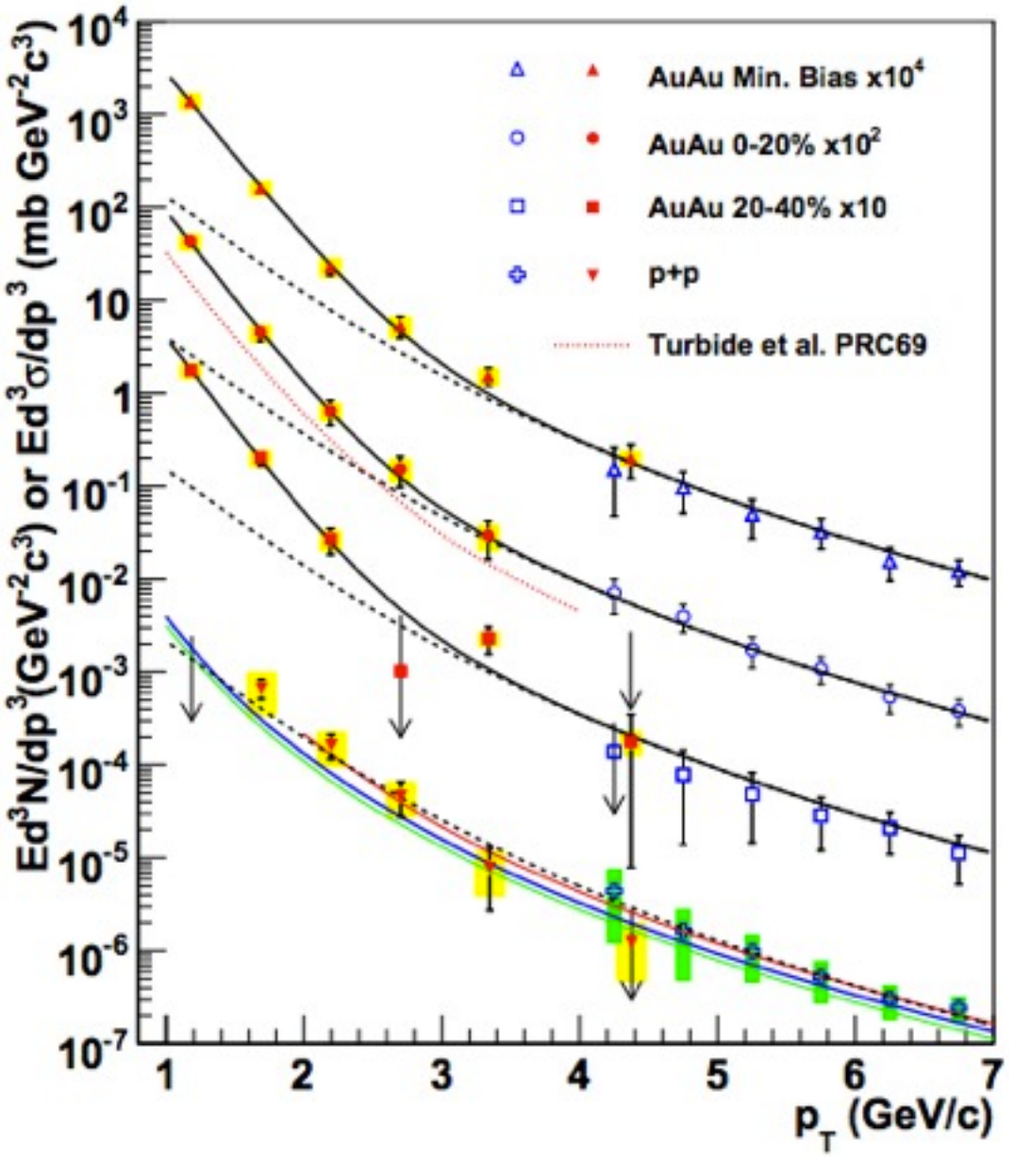


PHENIX: Phys.Rev.Lett.104:132301,2010

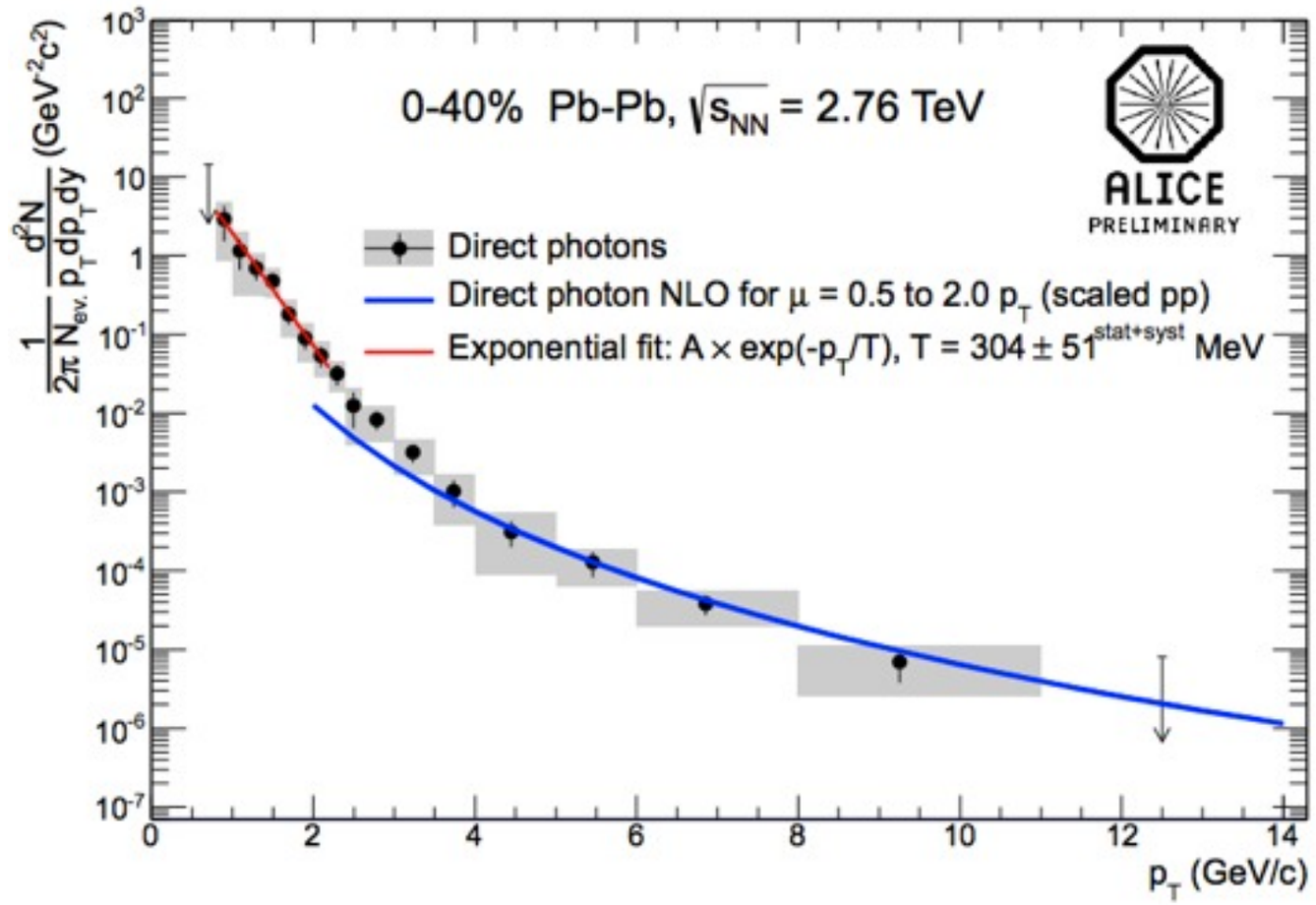


ALICE, M. Wilde, arXiv:1210.5958

- Enhanced direct photon production in AuAu/PbPb collisions at pt<2.5 GeV/c
- photon emission rate:

$$\omega \frac{\mathrm{d}R_\gamma}{\mathrm{d}^3p} = C_{em}\,\frac{\alpha_{em}}{4\pi^2}\,\frac{\rho_T(\omega = |\vec{p}|, T)}{\exp(\omega/T) - 1}$$

# Vector correlation & spectral functions

## Euclidean correlation function

$$G_{\mu\nu}(\tau,\vec{p}) = \int \mathrm{d}^3x \langle J_\mu(\tau,\vec{x}) J_\nu^\dagger(0,\vec{0})\rangle \, e^{i\vec{p}\cdot\vec{x}}$$

$$J_\mu(\tau,\vec{x}) \equiv \bar{q}(\tau,\vec{x})\gamma_\mu q(\tau,\vec{x})$$

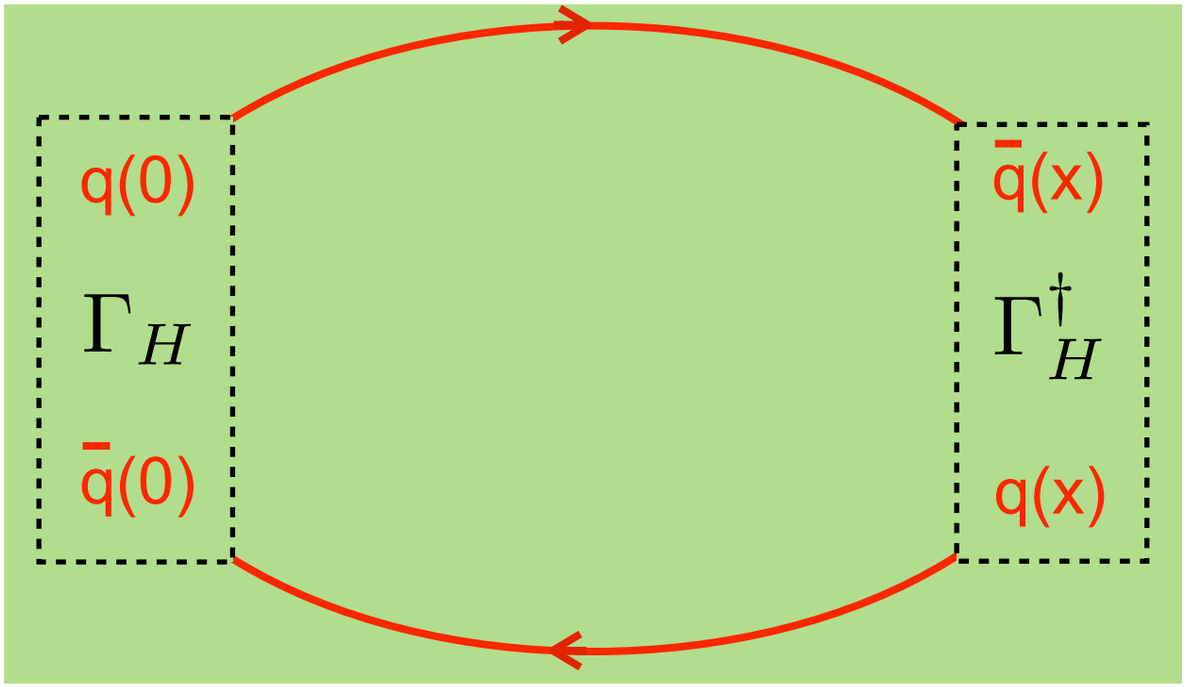


## Spectral function

$$\rho(\omega,\vec{p}) = D^+(\omega,\vec{p}) - D^-(\omega,\vec{p}) = 2\,\mathrm{Im}D_R(\omega,\vec{p})$$

## Relation between spectral function and correlator

$$G(\tau,\vec{p}) = \int \mathrm{d}^3x\, e^{-i\vec{p}\cdot\vec{x}}\, D^+(-i\tau,\vec{x}) \,, \qquad D^+(t,\vec{x}) = D^-(t+i\beta,\vec{x})$$

$$\boxed{G_H(\tau,\vec{p},T) = \int_0^\infty \frac{\mathrm{d}\omega}{2\pi}\, \rho_H(\omega,\vec{p},T)\, \frac{\cosh(\omega(\tau-1/2T))}{\sinh(\omega/2T)} \quad , \quad H = 00,\ ii,\ V\ .}$$

# Vector correlation function

$$G_H(\tau,\vec{p},T) = \int_0^\infty \frac{\mathrm{d}\omega}{2\pi}\,\rho_H(\omega,\vec{p},T)\,\frac{\cosh(\omega(\tau-1/2T))}{\sinh(\omega/2T)} \quad , \quad H = 00,\ ii,\ V\ .$$

time like correlator $G_{00}$ and space like correlator $G_{ii}$

$$G_V(\tau,\vec{p},T) = G_{ii}(\tau,\vec{p},T) + G_{00}(\tau,\vec{p},T)$$

conserved current, $J_0$, gives $\tau$-independent correlator $G_{00}$

$$G_{00}(T) \equiv -\chi_q T + \mathcal{O}(a^2)$$

the local, non-conserved current needs to be renormalized

$$J_\mu(\tau,\vec{x}) = 2\kappa Z_V \bar{\psi}(\tau,\vec{x})\gamma_\mu\psi(\tau,\vec{x})$$

avoid ambiguities of renormalization

$$R(\tau) \equiv \frac{G_V(\tau)}{G_{00}(\tau)} \quad ; \quad R(\tau) \equiv \frac{G_V(\tau)}{G_{00}(\tau)G_V^{free}(\tau T)}$$

# Prior information on spectral functions

- free vector spectral function (in the infinite temperature limit)

$$\rho_{00}^{free}(\omega) = -2\pi T^2 \omega \delta(\omega)$$

$$\rho_{ii}^{free}(\omega) = 2\pi T^2 \omega \delta(\omega) + \frac{3}{2\pi}\omega^2 \tanh(\frac{\omega}{4T})$$

  - $\delta$-functions cancel in $\rho_V(\omega) \equiv \rho_{00}(\omega) + \rho_{ii}(\omega)$

- vector spectral function at T<∞
  - $\delta$-function in $\rho_{00}$ is protected

$$\rho_{00}(\omega, T) = -2\pi \chi_q \omega \delta(\omega)$$

  - $\delta$-function in $\rho_{ii}$ is smeared out

possible form: Breit-Wigner (BW) form + modified continuum

$$\rho_{ii}(\omega, T) = \chi_q c_{BW} \frac{\omega\Gamma}{\omega^2 + (\Gamma/2)^2} + \frac{3}{2\pi}\left(1 + \frac{\alpha_s}{\pi}\right) \omega^2 \tanh(\frac{\omega}{4T})$$

3-4 parameters: $(\chi_q), c_{BW}, \Gamma, \alpha_s$

# previous lattice results on electrical conductivity

Electrical conductivity: $$\frac{\sigma}{T} = \frac{C_{em}}{6} \lim_{\omega \to 0} \frac{\rho_{ii}(\omega)}{\omega T}$$

The emission rate of soft photons: $$\lim_{\omega \to 0} \omega \frac{\mathrm{d}R_\gamma}{\mathrm{d}^3 p} = \lim_{\omega \to 0} C_{em} \frac{\alpha_{em}}{4\pi^2} \frac{\rho_T(\omega = |\vec{p}|, T)}{e^{\omega/T} - 1} = \frac{3}{2\pi^2} \sigma(T) T \alpha_{em}$$

Lattice calculations with unrenormalized currents produced unrenormalized electrical conductivity:

$$\sigma/T \simeq 7 C_{em}$$

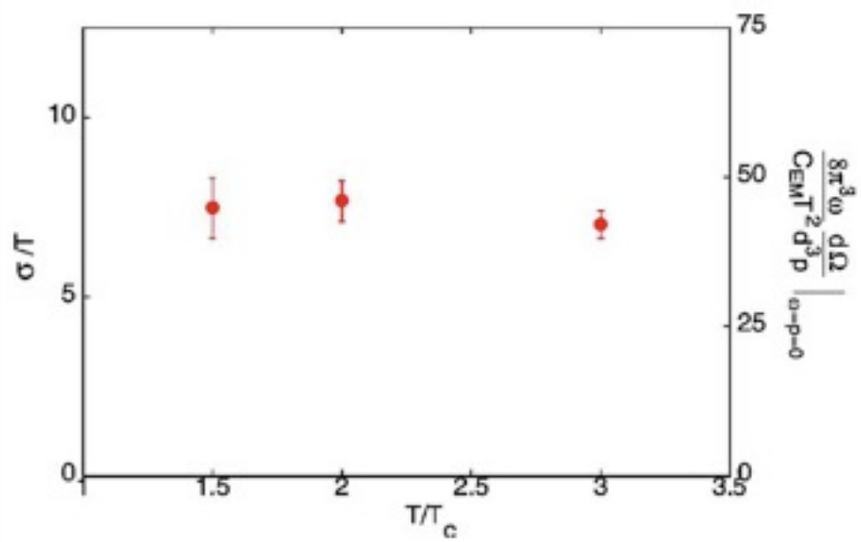


S. Gupta PLB 597(2004)

$N_\tau = 8 - 14,\ N_\sigma \leq 44$

$$\sigma/T \simeq (0.4 \pm 0.1) C_{em}$$

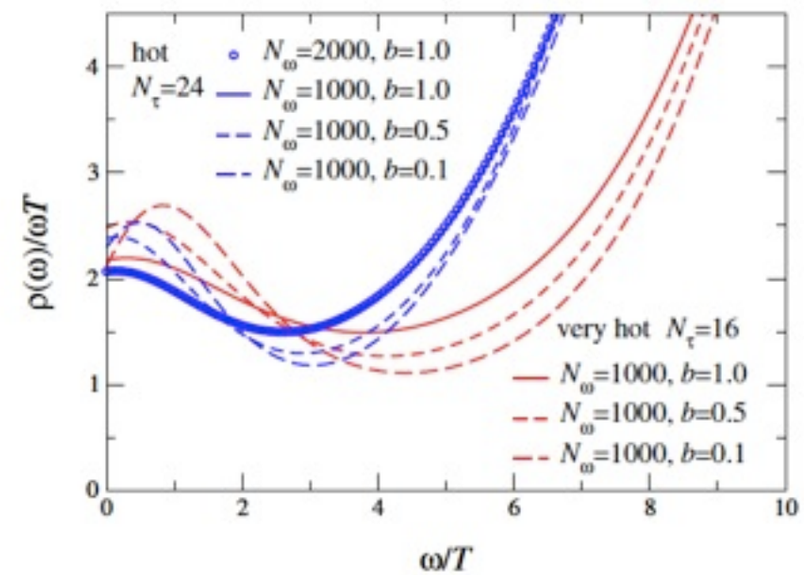


G. Aarts et al., PRL 99(2007)

$N_\tau = 16, 24,\ N_\sigma = 64$

staggered fermions used

$\rho_{even}$ and $\rho_{odd}$ need to be distinguished

# Vector correlation functions on large & fine lattices at 1.45Tc

- SU(3) gauge configurations at $T/T_c \simeq 1.45$
- lattice size $N_\sigma^3 \times N_\tau$ with $N_\sigma$ = 32-128 & $N_\tau$=16,24,32,48
- Non-perturbatively clover O(a) improved Wilson fermions
- Quark masses close to chiral limit $\kappa \simeq \kappa_c$

volume dependence

| $N_\tau$ | $N_\sigma$ | $\beta$ | $c_{SW}$ | $\kappa$ | $Z_V$ | $a^{-1}$[GeV] | a[fm] | #conf |
|---|---|---|---|---|---|---|---|---|
| 16 | 32 | 6.872 | 1.4125 | 0.13495 | 0.829 | 6.43 | 0.031 | 251 |
| 16 | 48 | 6.872 | 1.4125 | 0.13495 | 0.829 | 6.43 | 0.031 | 229 |
| 16 | 64 | 6.872 | 1.4125 | 0.13495 | 0.829 | 6.43 | 0.031 | 191 |
| 16 | 128 | 6.872 | 1.4125 | 0.13495 | 0.829 | 6.43 | 0.031 | 191 |
| 24 | 128 | 7.192 | 1.3673 | 0.13431 | 0.842 | 9.65 | 0.020 | 340 |
| | 128 | 7.192 | 1.3673 | 0.13440 | 0.842 | 9.65 | 0.020 | 156 |
| 32 | 128 | 7.457 | 1.3389 | 0.13390 | 0.851 | 12.86 | 0.015 | 255 |
| 48 | 128 | 7.793 | 1.3104 | 0.13340 | 0.861 | 18.97 | 0.010 | 451 |

cut-off dep. & continuum extrapolation

close to continuum

# Volume & cut-off dep. of vector corr. function

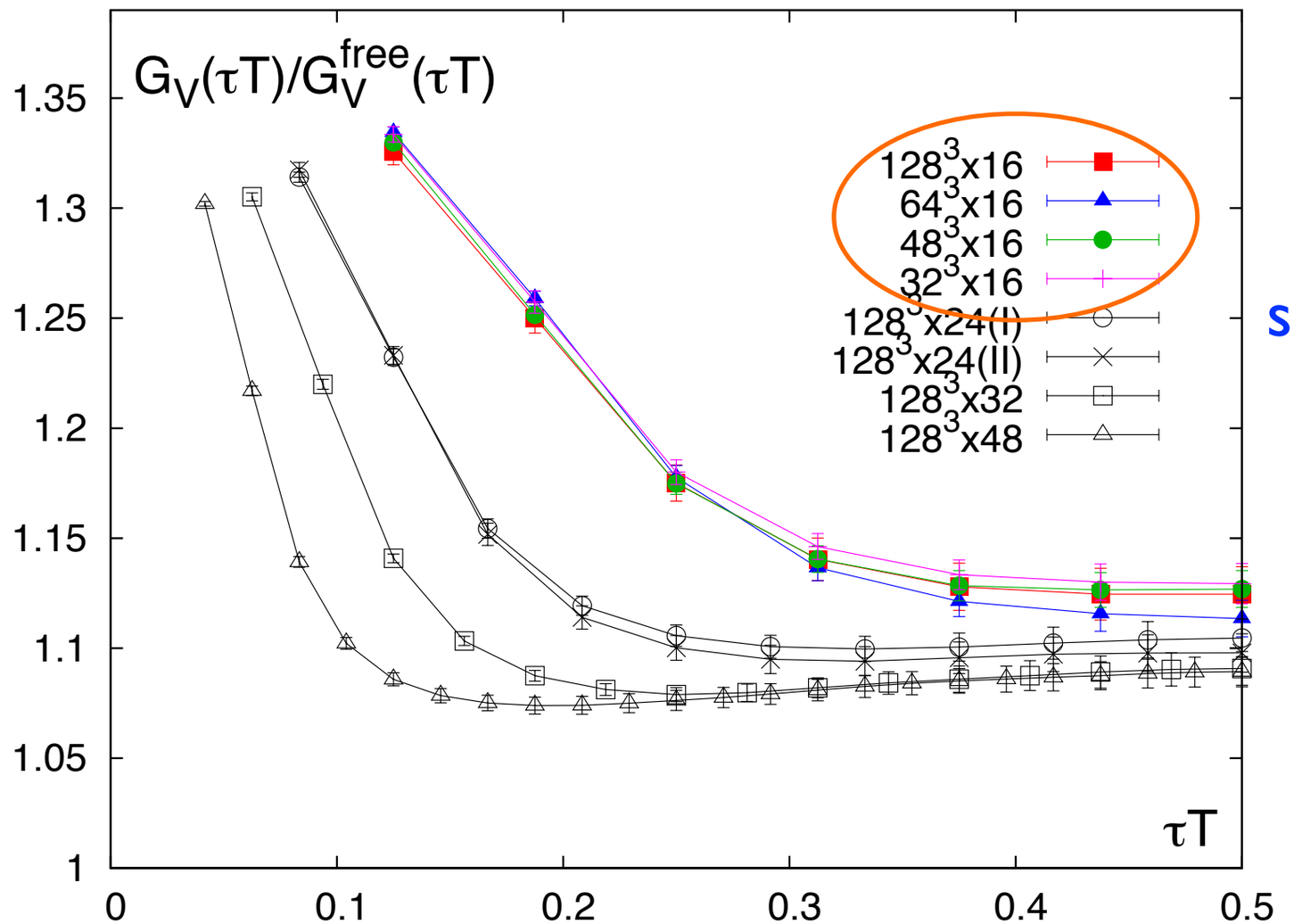


small volume dependence

weak τT dep. near 1/2

Normalized by free correlators in the continuum $G_V^{free}(\tau T)$

$$G_V^{free}(\tau T) = 6T^3 \left( \pi \, (1 - 2\tau T) \frac{1 + \cos^2(2\pi\tau T)}{\sin^3(2\pi\tau T)} + 2 \, \frac{\cos(2\pi\tau T)}{\sin^2(2\pi\tau T)} \right)$$

# Volume & cut-off dep. of vector corr. function

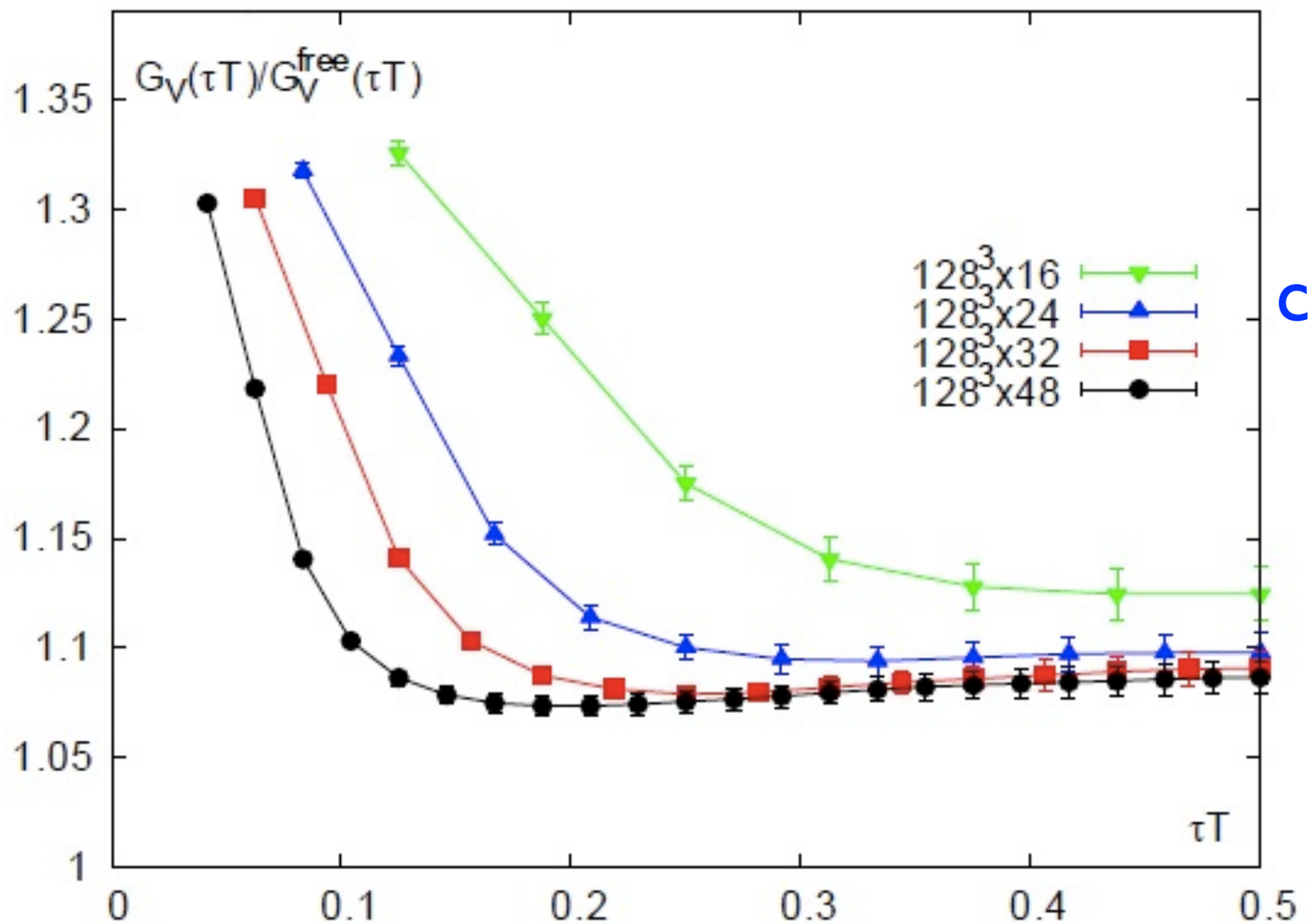


cut-off effects are more server than finite volume effects

large $N_\tau$ needed to perform continuum extrapolation

$G_V(\tau T)$ is close to the free case at large $\tau T$

incomplete cancelation between $G_{00}(\tau T)$ and BW-contribution to $G_{ii}(\tau T)$ ?

# Continuum extrapolation

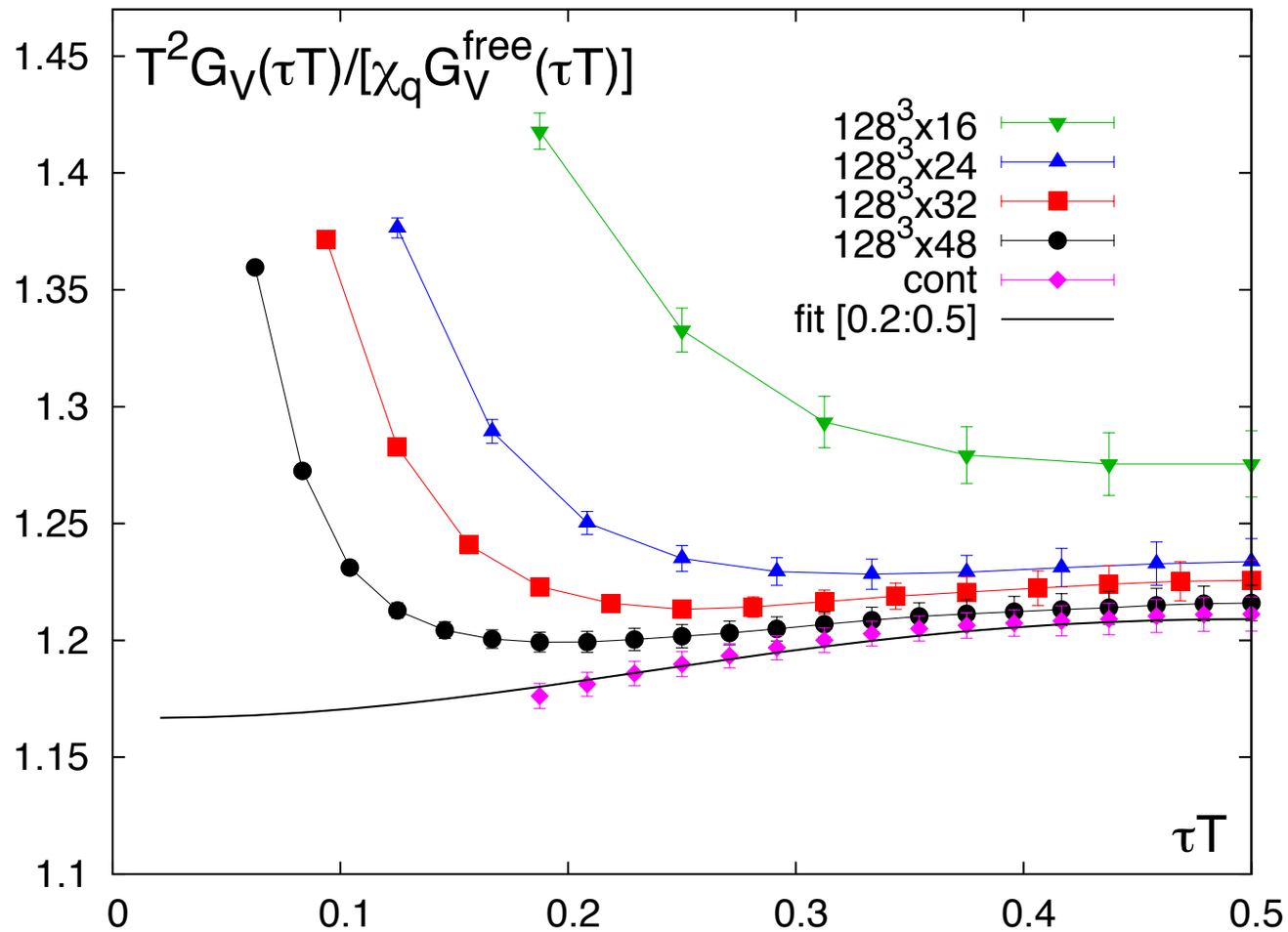


$$\frac{G_V(1/2)}{G_V^{free}(1/2)} = 1.086 \pm 0.008 \,,$$

$$\frac{G_V(1/4)}{G_V^{free}(1/4)} = (0.982 \pm 0.005)\frac{G_V(1/2)}{G_V^{free}(1/2)}$$

- Increase of $G_V(\tau T)/G_V^{free}(\tau T)$ with τT is obvious
- The rise with τT indicates that vector spectral function in the low frequency region is different from the free case
- Motivation for the Breit-Wigner type ansatz fitting

# Breit-Wigner + continuum Ansatz

$$\widetilde{\rho}_{ii}(\widetilde{\omega}) = \frac{2c_{BW}\widetilde{\chi}_q}{\widetilde{\Gamma}} \frac{2\widetilde{\omega}(\widetilde{\Gamma}/2)^2}{\widetilde{\omega}^2 + (\widetilde{\Gamma}/2)^2} + \frac{3}{2\pi}(1+k)\ \widetilde{\omega}^2\ \tanh(\frac{\widetilde{\omega}}{4})$$

$$k = 0.0465(30)\ ,\ \widetilde{\Gamma} = 2.235(75)\ ,\ 2c_{BW}\widetilde{\chi}_q/\widetilde{\Gamma} = 1.098(27)$$

→ vary width Γ with the other two parameters fixed

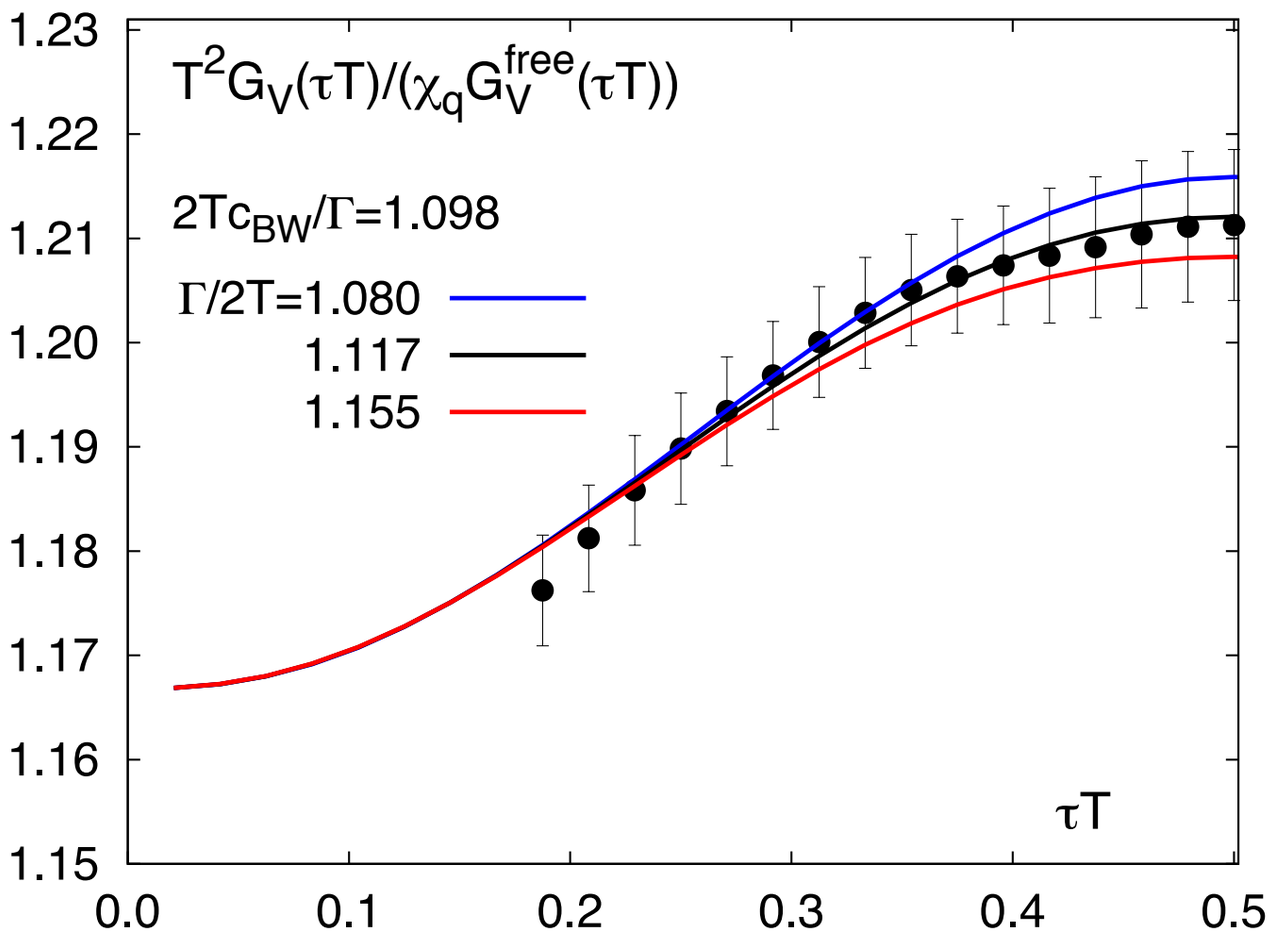


- vector correlation function is sensitive to the low energy, Breit-Wigner contribution only for distance $\tau T \gtrsim 0.25$

# Estimate of electrical conductivity

$$\widetilde{\rho}_{ii}(\widetilde{\omega}) = \frac{2c_{BW}\widetilde{\chi}_q}{\widetilde{\Gamma}} \frac{2\widetilde{\omega}(\widetilde{\Gamma}/2)^2}{\widetilde{\omega}^2 + (\widetilde{\Gamma}/2)^2} + \frac{3}{2\pi}(1+k)\ \widetilde{\omega}^2\ \tanh(\frac{\widetilde{\omega}}{4})$$

$k = 0.0465(30)$ , $\widetilde{\Gamma} = 2.235(75)$ , $2c_{BW}\widetilde{\chi}_q/\widetilde{\Gamma} = 1.098(27)$

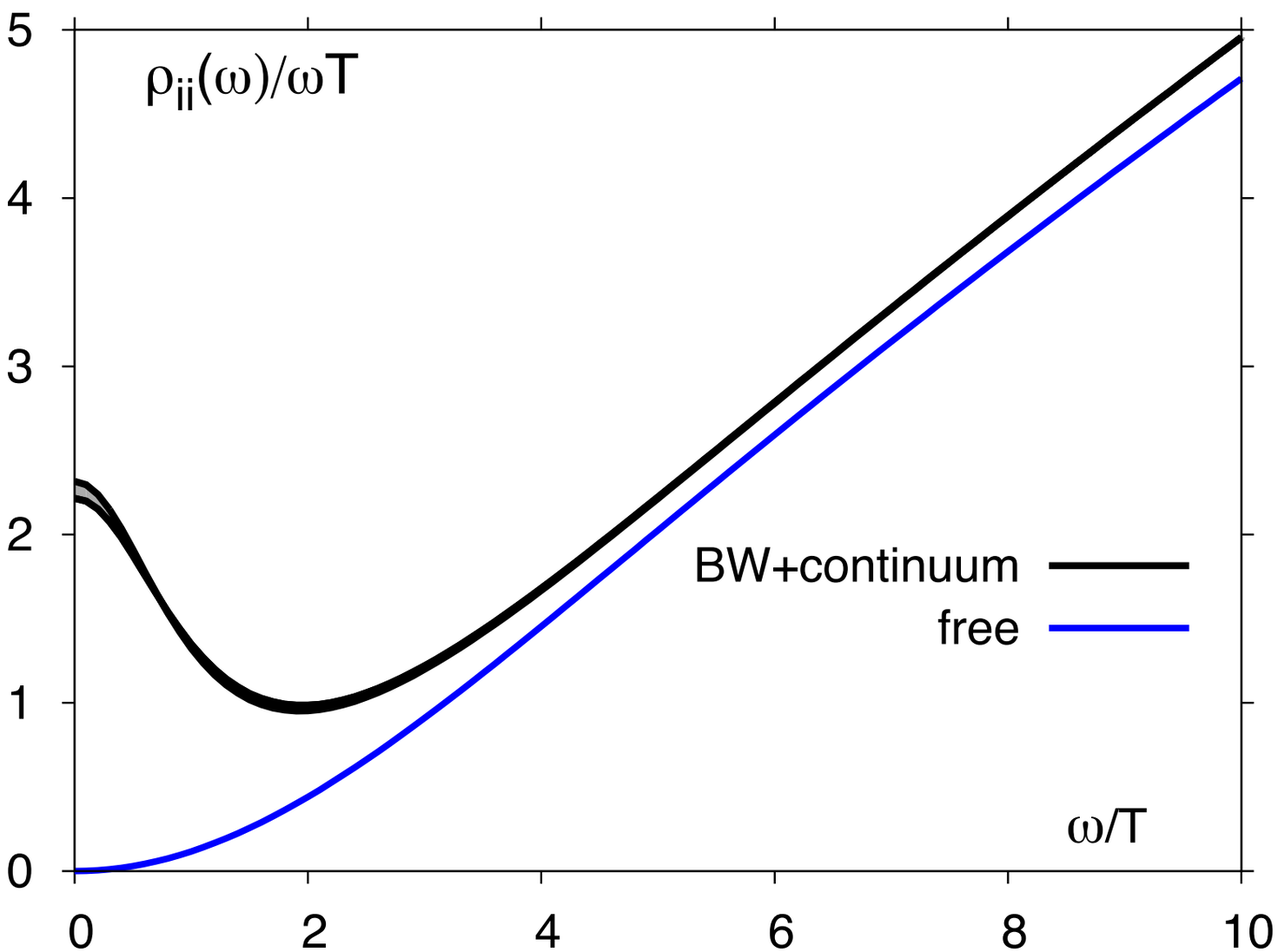


$$\frac{\sigma}{T} = \frac{C_{em}}{6} \lim_{\omega\to 0} \frac{\rho_{ii}(\omega)}{\omega T}$$

$$= \frac{C_{em}}{3} \frac{2c_{BW}\widetilde{\chi}_q}{\widetilde{\Gamma}}$$

$$= (0.37 \pm 0.01) C_{em}$$

# Breit-Wigner + truncated continuum Ansatz

$$\rho_{ii}(\omega) = 2\chi_q c_{BW} \frac{\omega\Gamma/2}{\omega^2 + (\Gamma/2)^2} + \frac{3}{2\pi}(1+k)\ \omega^2\ \tanh(\frac{\omega}{4T})\ \Theta(\omega_0, \Delta_\omega)$$

$$\Theta(\omega_0, \Delta_\omega) = \left(1 + \mathrm{e}^{(\omega_0^2 - \omega^2)/\omega\Delta_\omega}\right)^{-1}$$

delay the onset ($\omega_0$) of the continuum part

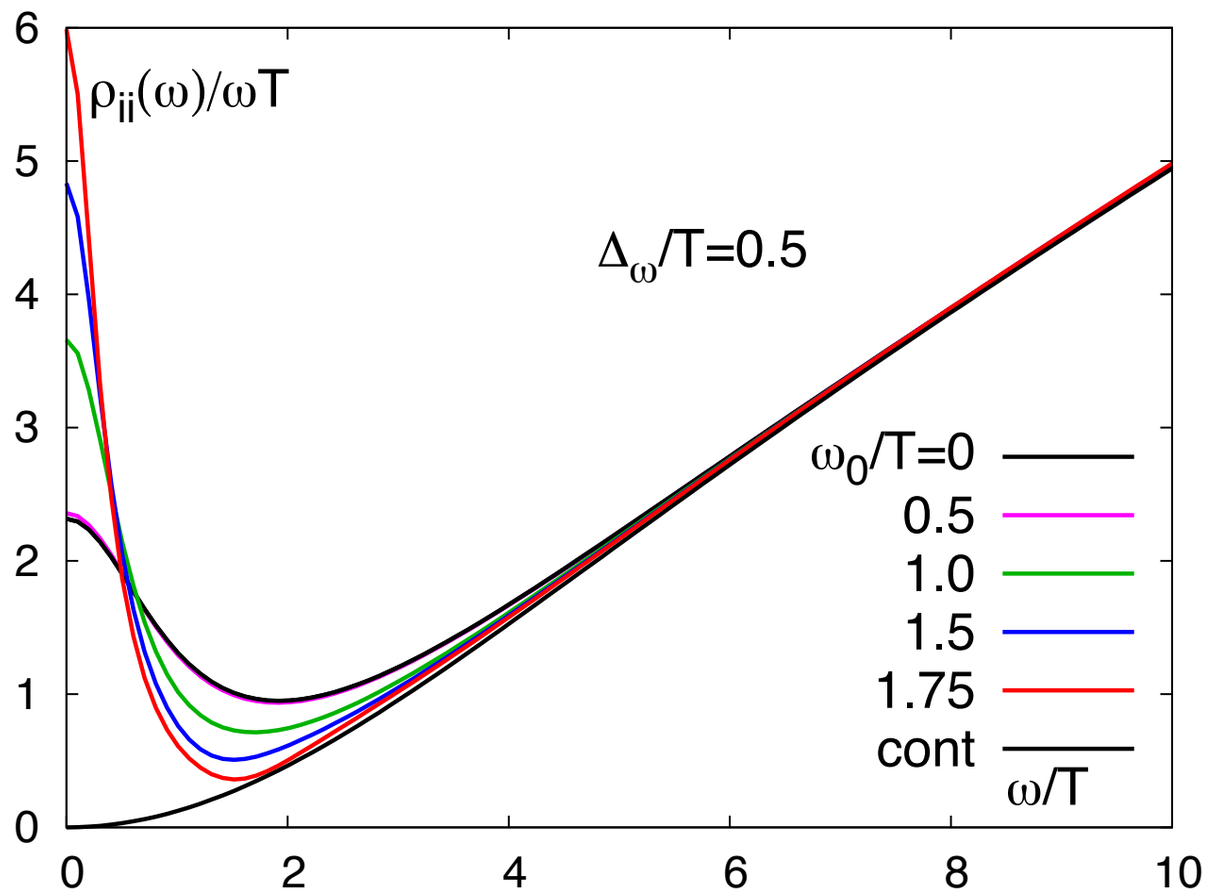


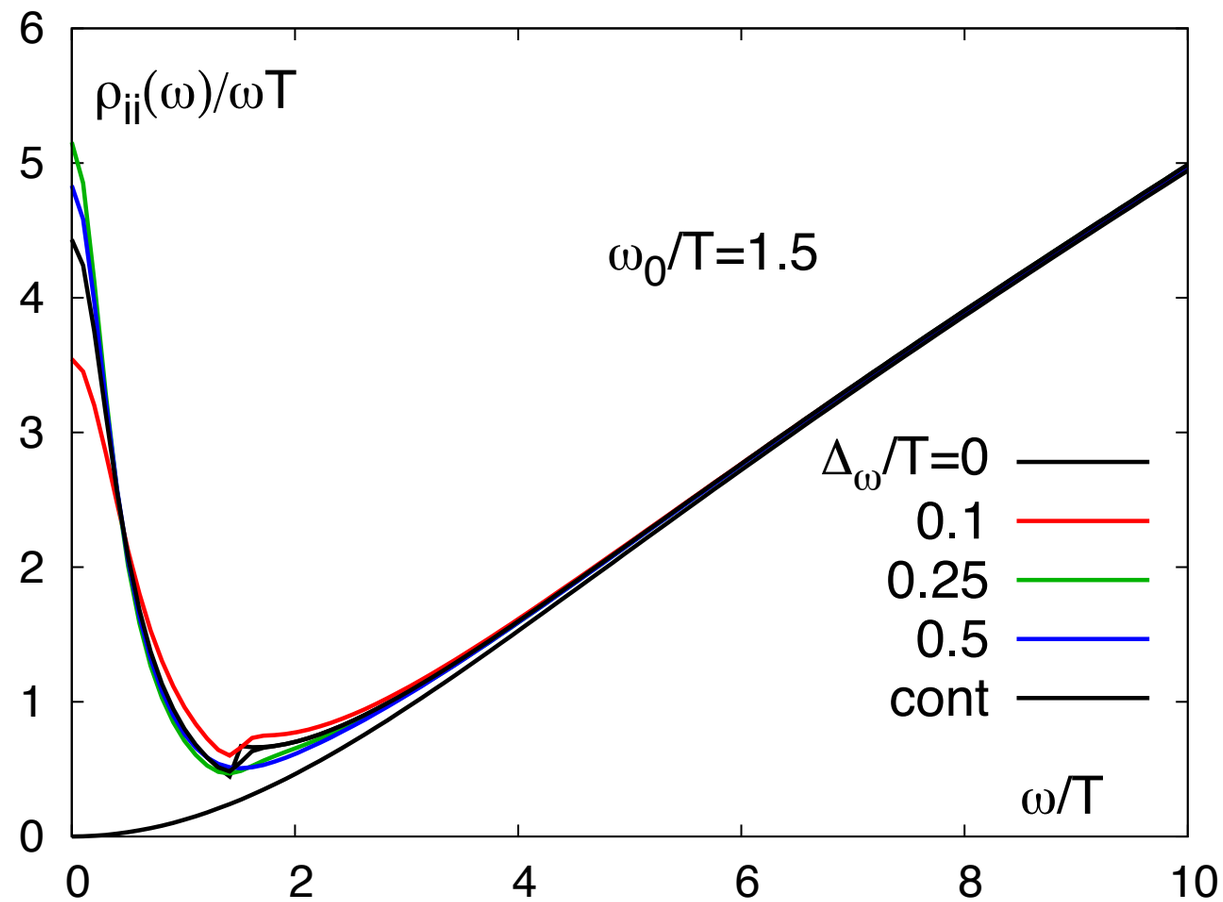


- Rise of BW peaks compensate for the cut from continuum parts
- Fits become worse with increasing $\omega_0$ and/or increasing $\Delta_\omega$

# Electrical conductivity at 1.45 Tc

$$\rho_{ii}(\omega) = 2\chi_q c_{BW} \frac{\omega\Gamma/2}{\omega^2 + (\Gamma/2)^2} + \frac{3}{2\pi}(1+k)\ \omega^2\ \tanh(\frac{\omega}{4T})\ \Theta(\omega_0, \Delta_\omega)$$

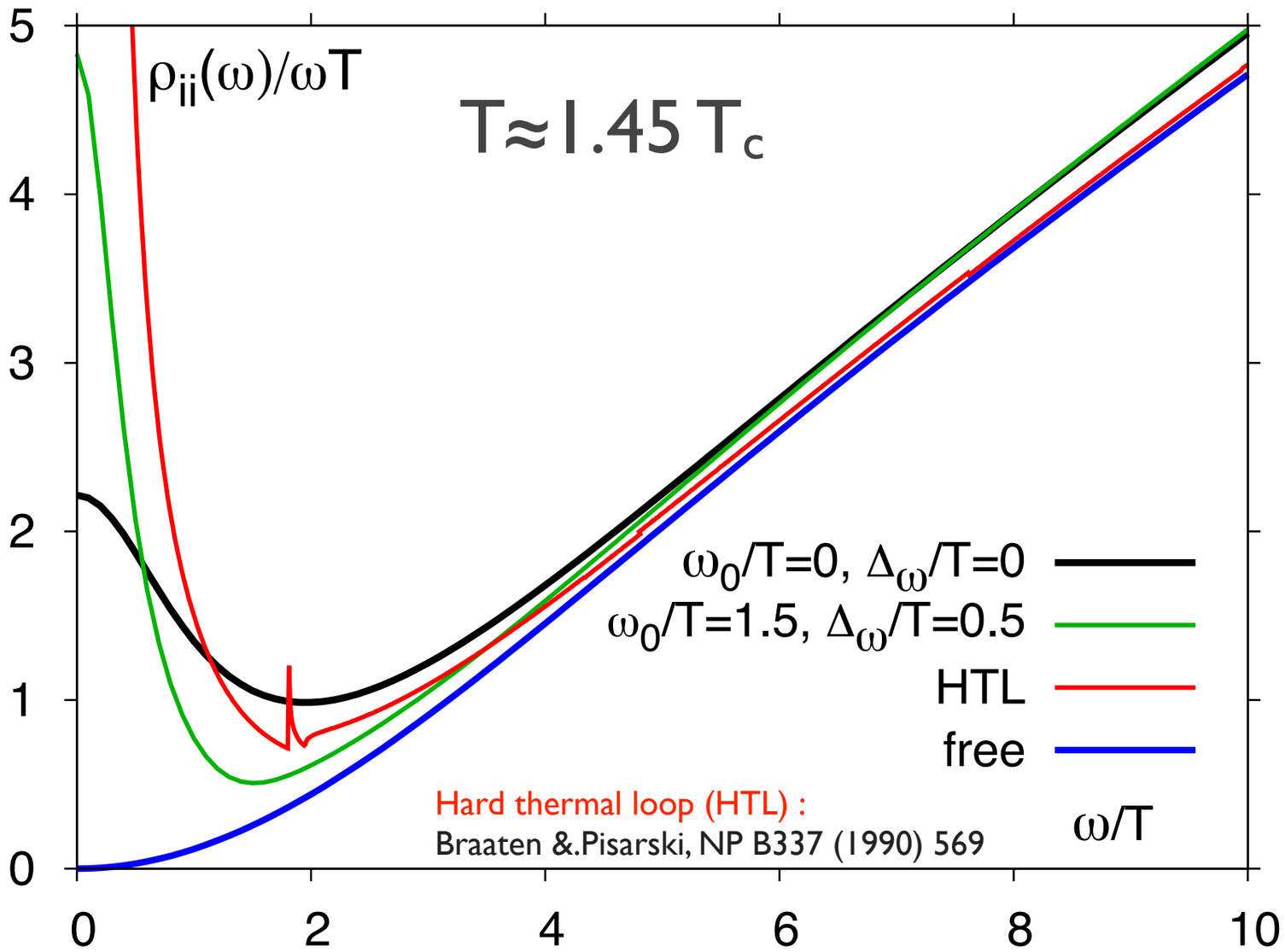


$$\Theta(\omega_0, \Delta_\omega) = \left(1 + e^{(\omega_0^2 - \omega^2)/\omega\Delta_\omega}\right)^{-1}$$

electrical conductivity

$$1/3 \lesssim \frac{1}{C_{em}} \frac{\sigma}{T} \lesssim 1$$

Soft photon emission rate

$$\lim_{\omega \to 0} \omega \frac{dR_\gamma}{d^3p} = (0.0004 - 0.0013)\, T_c^2$$

HTL conductivity is divergent at w~0

# Thermal dilepton rates at 1.45 $T_c$

$$\frac{\mathrm{d}N_{l^+l^-}}{\mathrm{d}\omega \mathrm{d}^3p} = C_{em}\frac{\alpha_{em}^2}{6\pi^3}\frac{\rho_V(\omega,\vec{p},T)}{(\omega^2-\vec{p}^2)(\mathrm{e}^{\omega/T}-1)}$$

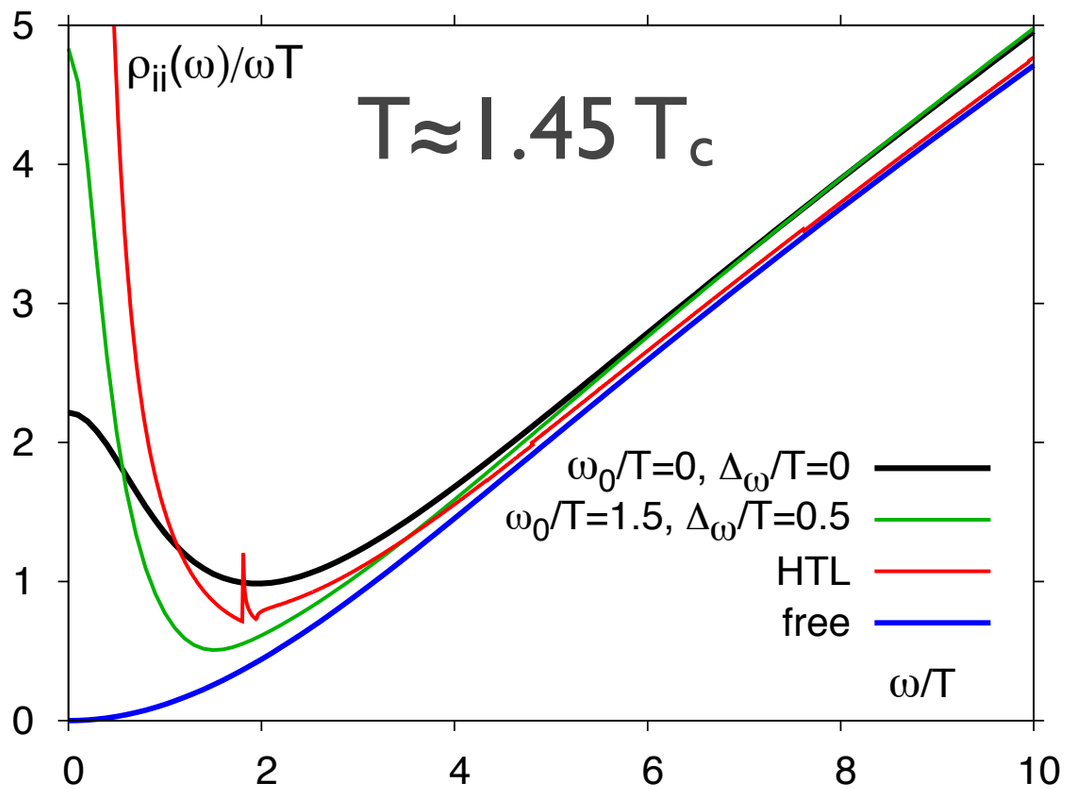


Hard thermal loop (HTL): Braaten &.Pisarski, NP B337 (1990) 569

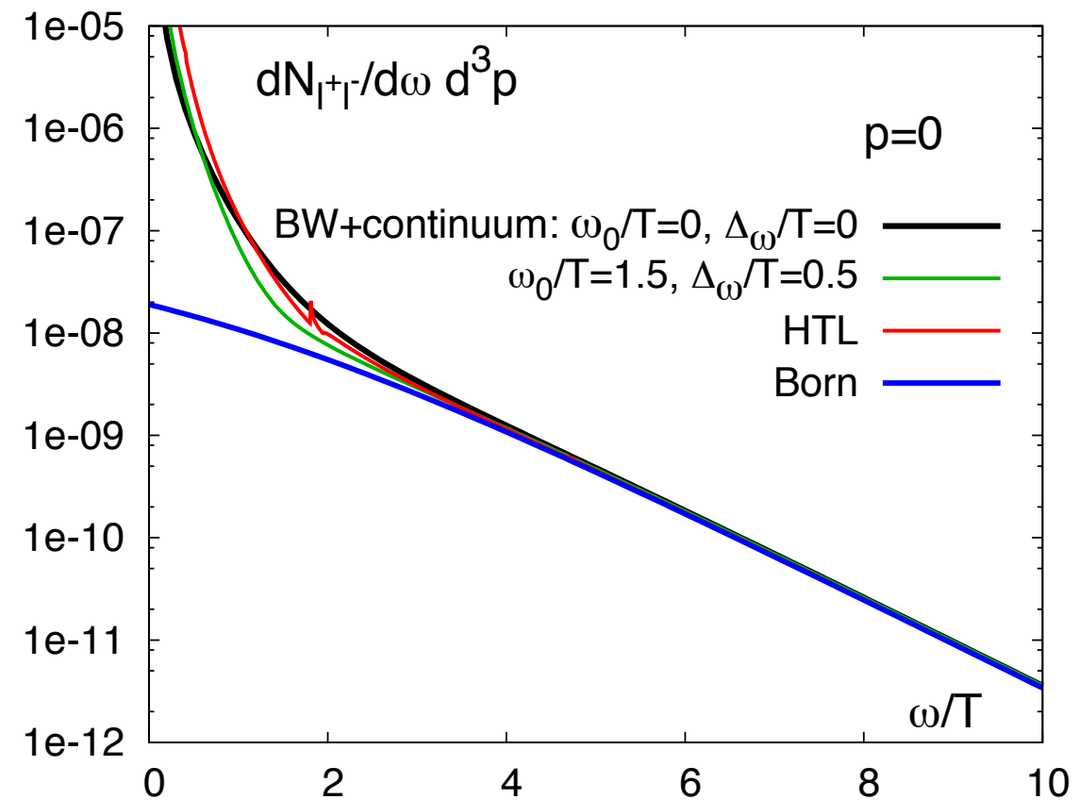


HTD, Francis, Kaczmarek,Karsch, Laermann, Soeldner, Phys.Rev. D83 (2011) 034504

- thermal dilepton rate approaches leading order Born rate at w/T ≳ 4
- enhancement at small w/T

# Vector correlation function at $T=1.1T_c$

- SU(3) gauge configurations at $T/T_c \simeq 1.1$

| $N_\tau$ | $N_\sigma$ | $\beta$ | $\kappa$ | $1/a$[GeV] | $a$[fm] | #conf |
|---|---|---|---|---|---|---|
| 32 | 96 | 7.192 | 0.13440 | 9.65 | 0.020 | 223 |
| 48 | 144 | 7.544 | 0.13383 | 14.21 | 0.15 | 226 |
| 64 | 192 | 7.793 | 0.13345 | 19.30 | 0.010 | 165 |

- Allows to study the T-dependence of thermal dilepton and electrical conductivity
- Fixed aspect ratio $N_\sigma/N_\tau=3$ allows the continuum extrapolation of the correlation function at finite momentum

$$\frac{\vec{p}}{T} = 2\pi \frac{N_\tau}{N_\sigma} \vec{n}$$

- 15 values of p from 0 up to 3.5 GeV allow the extraction of the thermal photon rate

# continuum extrapolation of vector corr. at 1.1 $T_c$

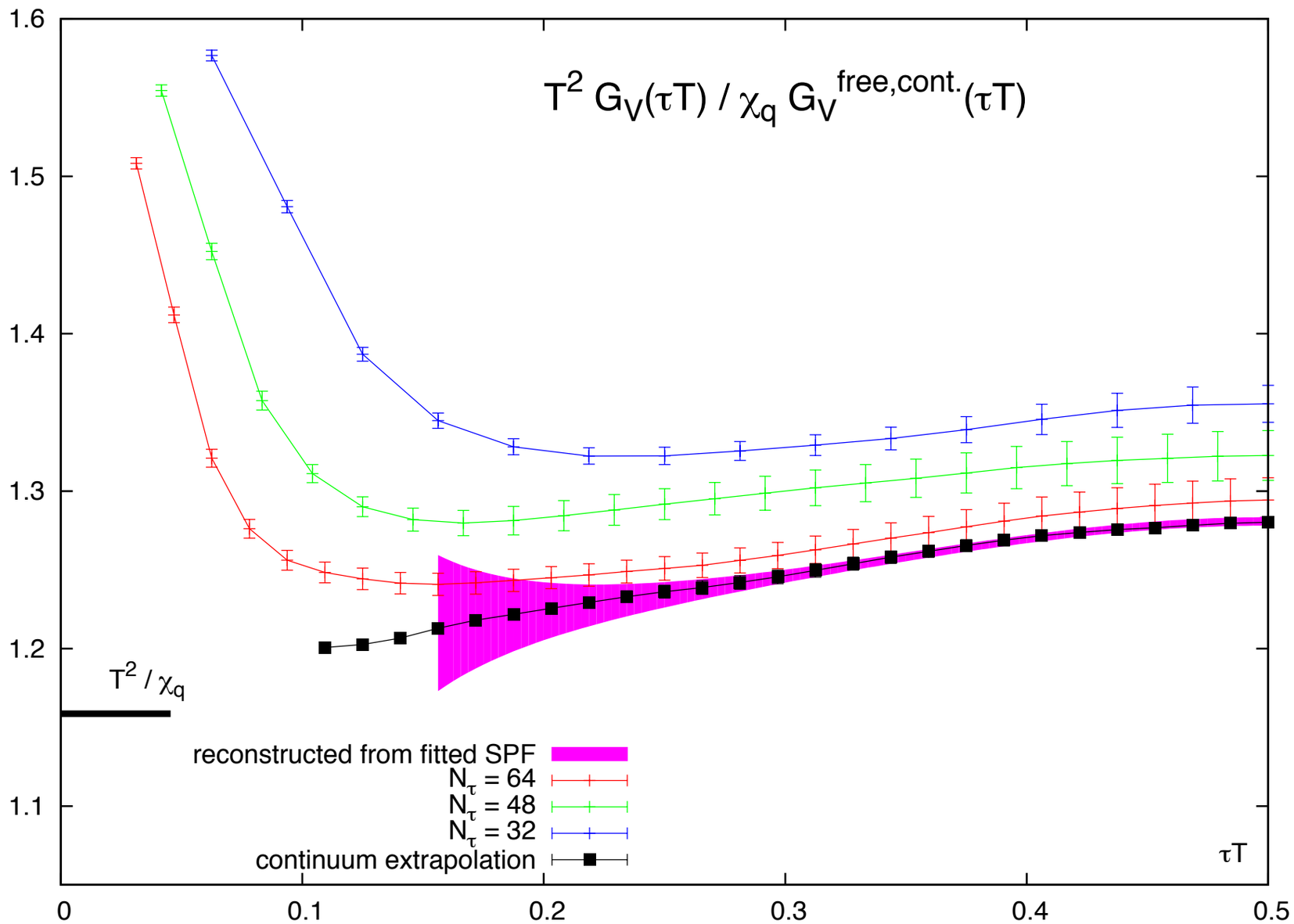


- reliable continuum extrapolation from $\tau T$ larger than 0.2
- used to extract vector spectral function at 1.1 $T_c$

# vector spectral functions

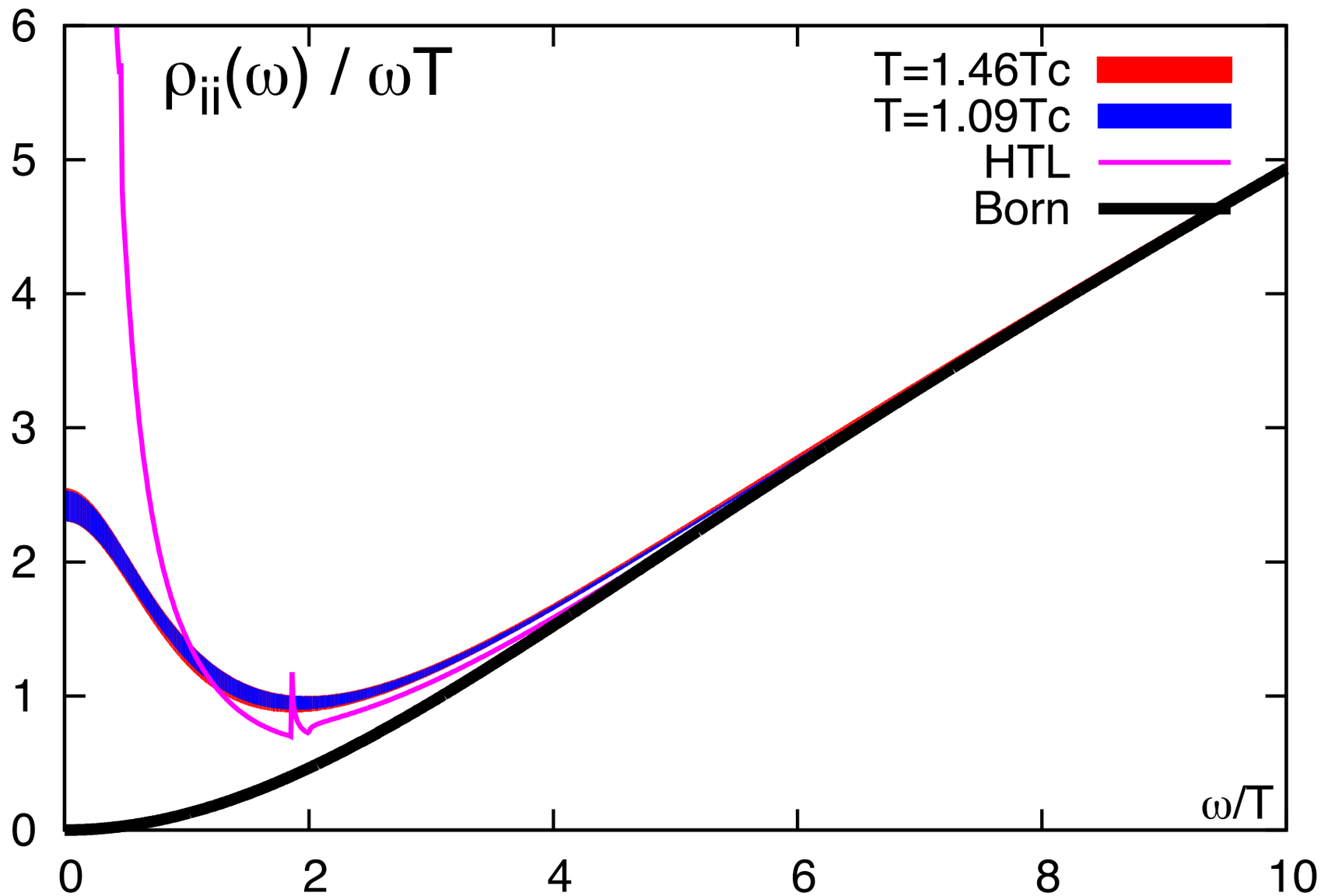


Preliminary

- spf at 1.1 $T_c$: use the same ansatz as at $T=1.45T_c$
- almost no change from $1.45T_c$ to $1.1T_c$, e.g. similar $\sigma/T$
- uncertainties of spf at 1.1 $T_c$ need to be checked

# thermal dilepton emission rate

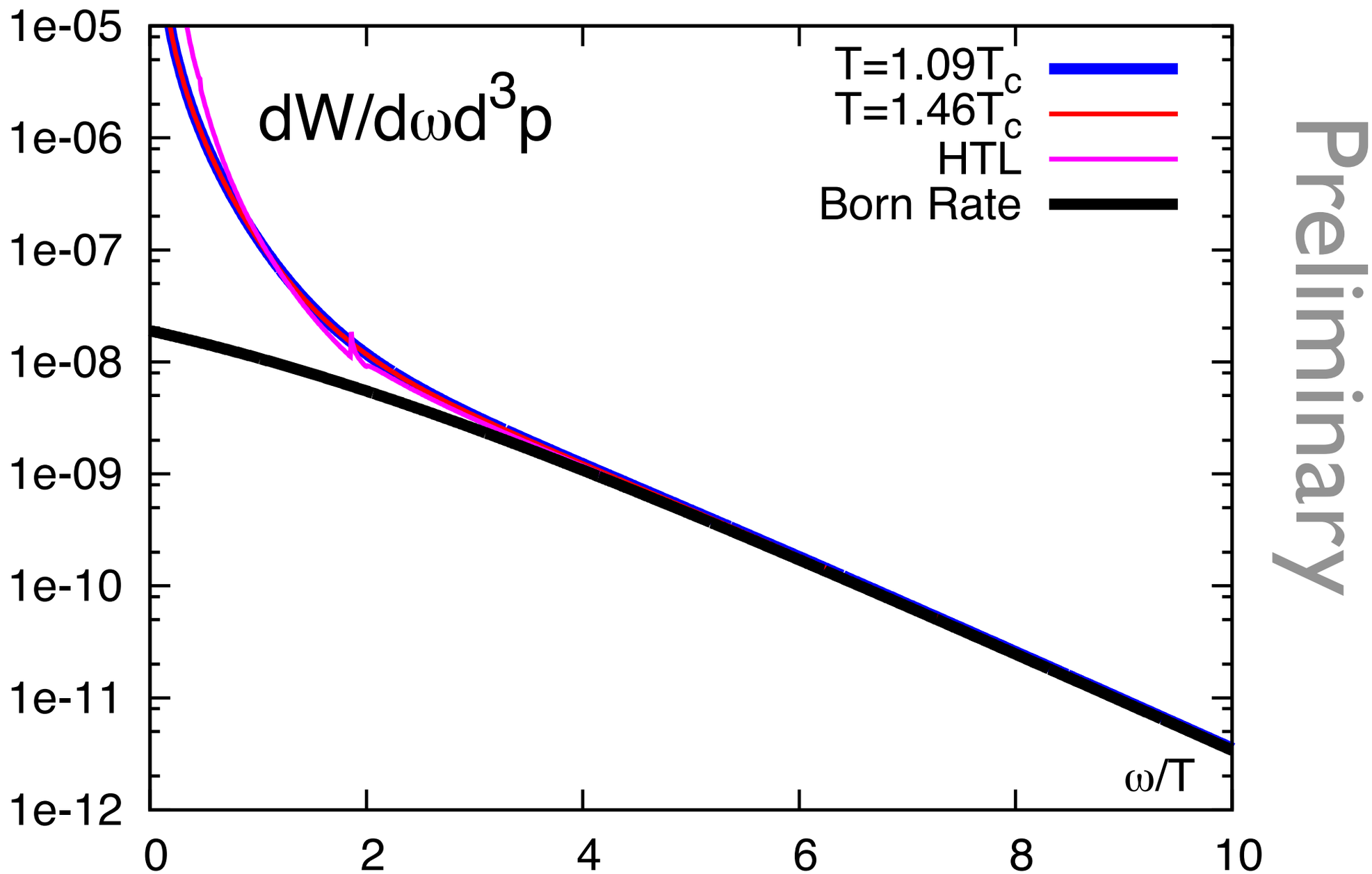


Preliminary

- uncertainties of spf at 1.1 $T_c$ need to be checked

# Polarized vector correlation function at finite p

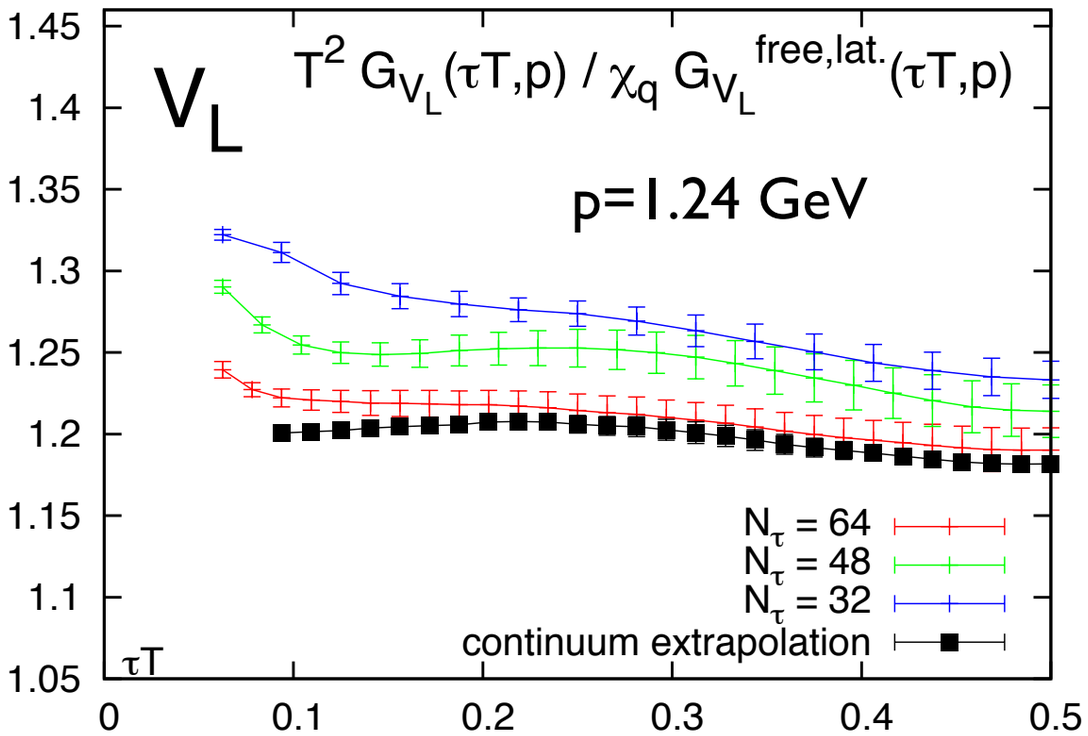


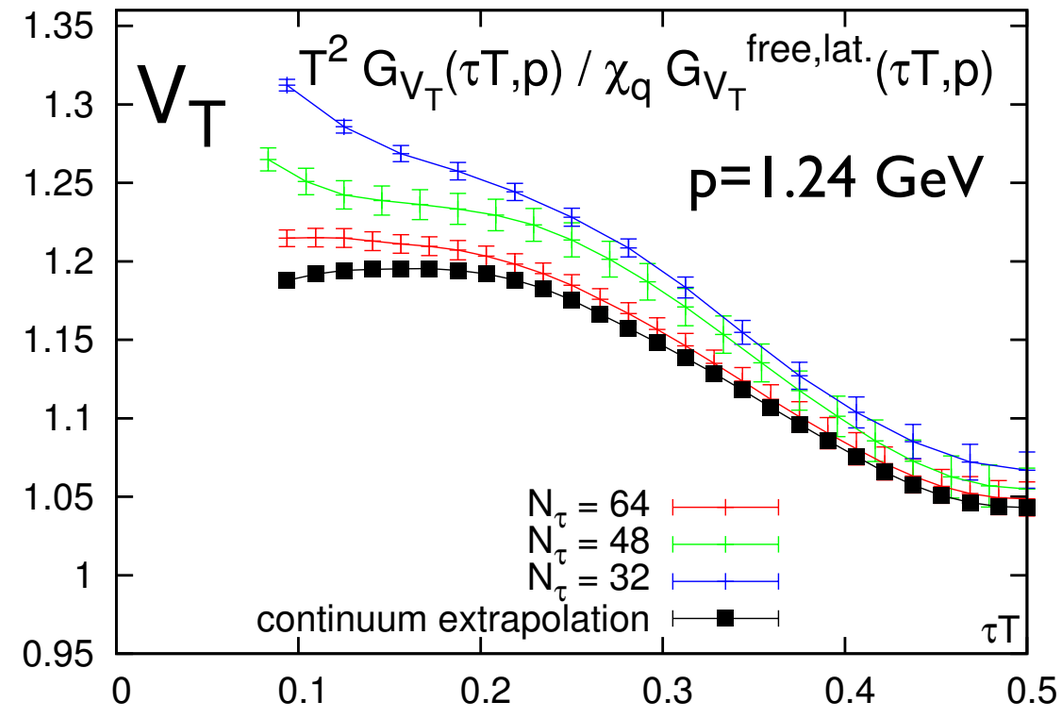


Nontrivial structure seen in the low energy region of finite p spectral function

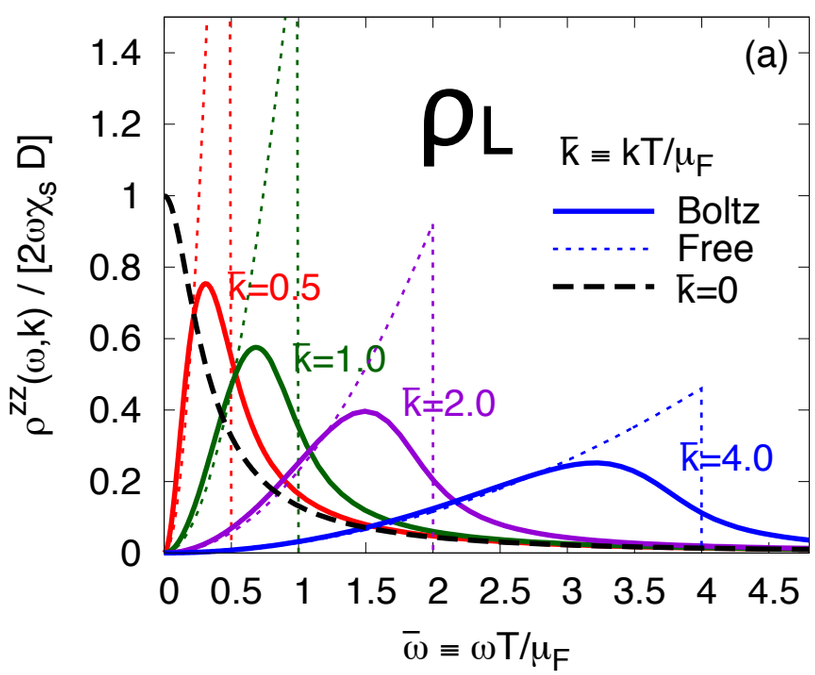


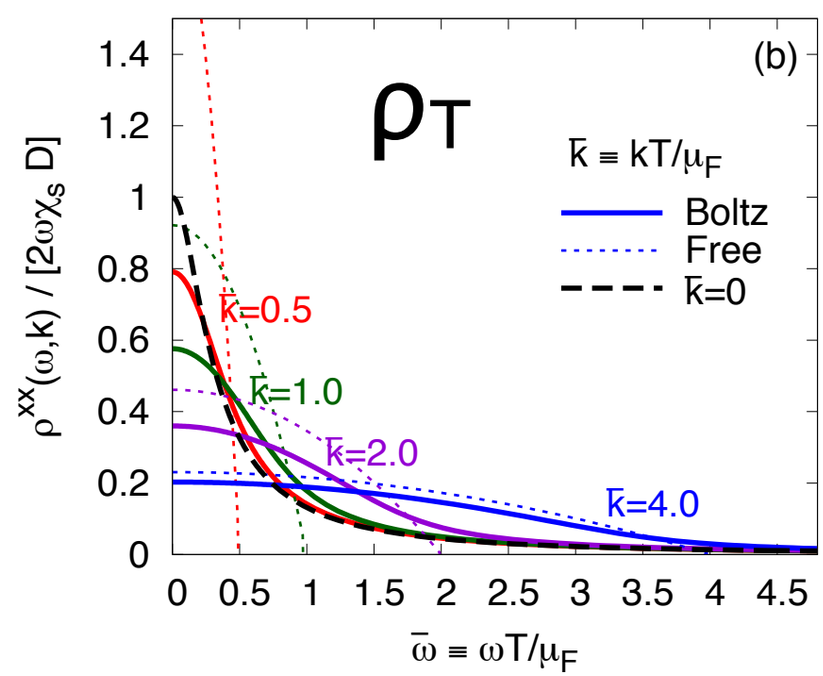


J. Hong and D. Teaney, PRC 82(2010)044908

# Thermal photon rate

continuum extrapolated transverse vector correlation functions at $1.1T_c$

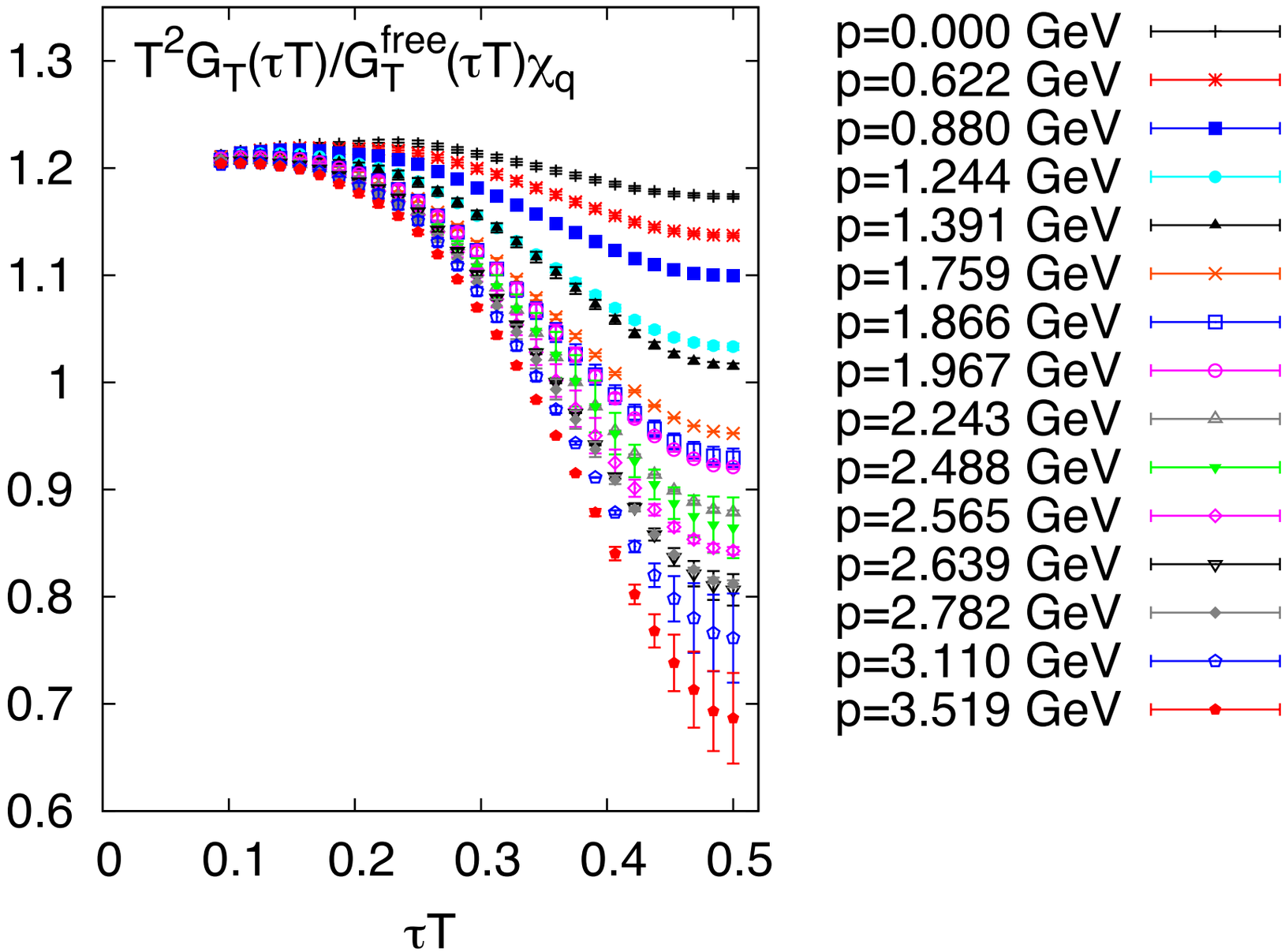


$$\omega \frac{\mathrm{d}R_\gamma}{\mathrm{d}^3p} = C_{em}\,\frac{\alpha_{em}}{4\pi^2}\,\frac{\rho_T(\omega = |\vec{p}|, T)}{\exp(\omega/T) - 1}$$

# Conclusions & Outlook

- We calculated the vector correlation function at T≃1.45Tc and 1.1 Tc in quenched lattice QCD and performed a continuum extrapolation

T≃1.45Tc

- Electrical conductivity $1/3 \lesssim \frac{1}{C_{em}} \frac{\sigma}{T} \lesssim 1$
- Dilepton rate approaches leading order Born rate at $\omega/T \gtrsim 4$

T≃1.1Tc

- Similar thermal dilepton rate and electrical cond. as that at 1.45 $T_c$
- Uncertainties need to be checked
- Continuum extrapolated results for vector correlator at finite p
- Extraction of thermal photon rate is on the way...

# comparison of corr. at 1.1 and 1.5 $T_c$

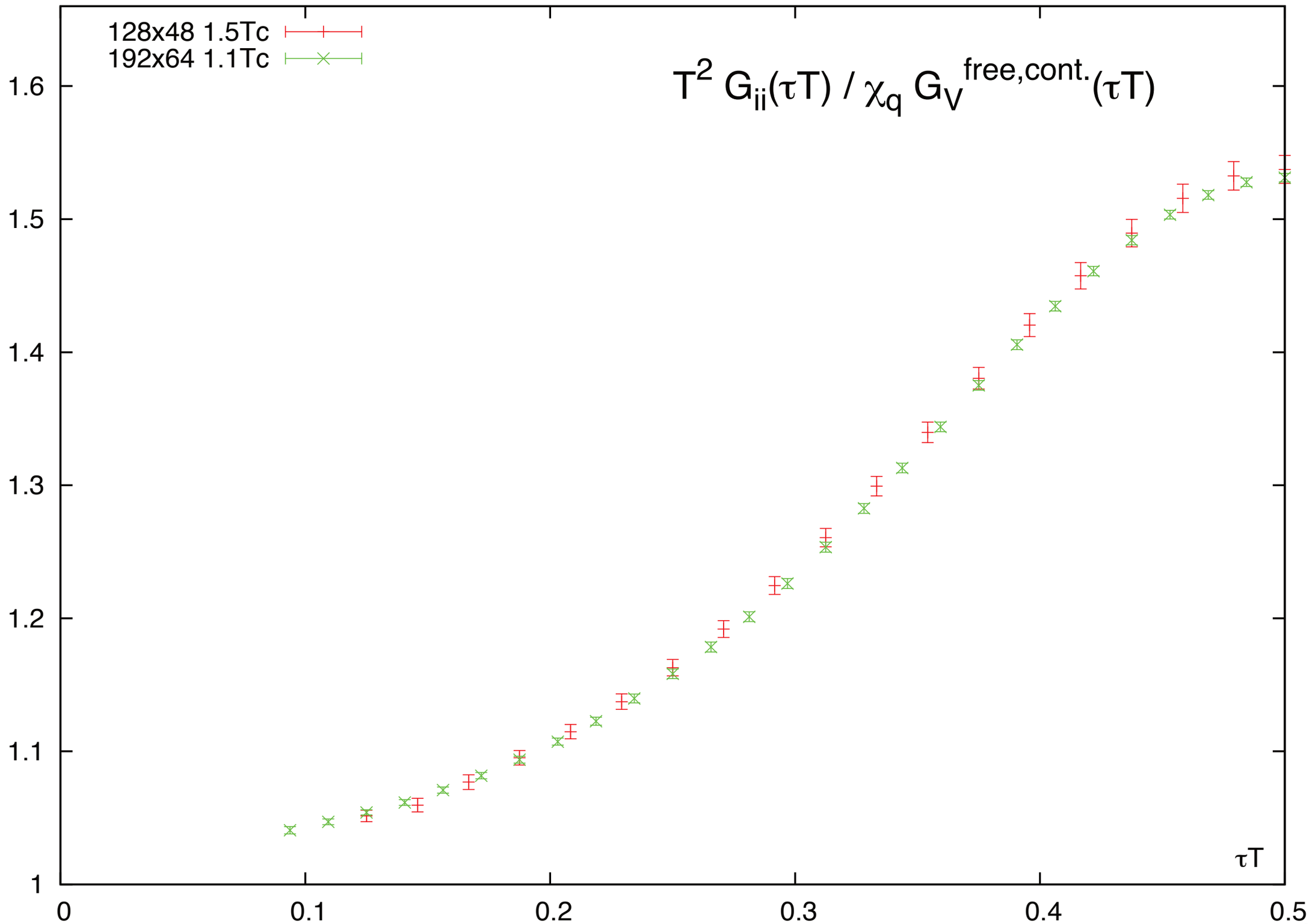

# Thermal dileptons from NA60 and possible future opportunities at SPS

**Axel Drees, Stony Brook University --- for Gianluca Usai who could not attend**

**Most slides mostly derived from talks given by Sanja Damjanovic and Hans Specht**

- **Introduction**
  - **“thermal” radiation**
  - **Experimental Challenges**
- **State of the art experiment NA60**
  - **Experimental method**
  - **Thermal radiation**
  - **ρ spectral function**
  - **Angular distribution**
- **Remarks on future perspectives**

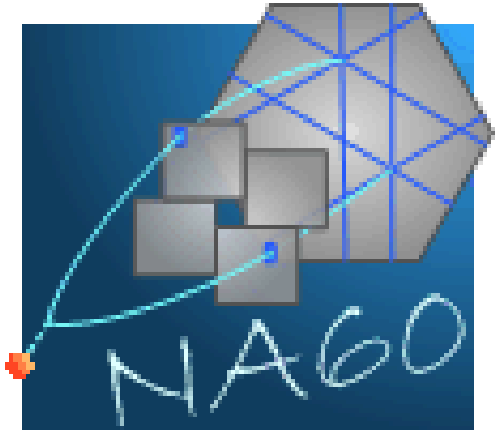

# Thermal Radiation from Heavy Ion Collisions

- **Thermal radiation ($\gamma$, $\ell^+\ell^-$ ) sensitive to temperature and collective motion of source**
  - **Planck spectrum → yield ∝ $T^4$ , mean ∝ T**
  - **Transverse and longitudinal expansion → blue and/or red shift**
  - **integrated over space-time evolution**

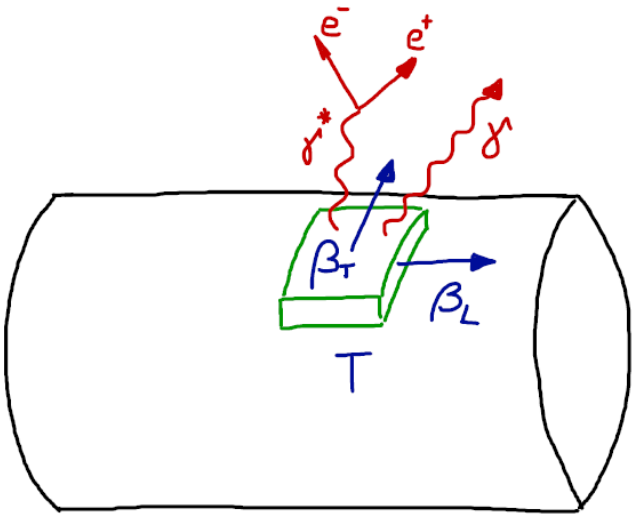


- **Photons and dilepton momentum spectrum**
  - **Sensitive to temperature**
  - **Sensitive to collective expansion (pressure)**

- **Dilepton $\ell^+\ell^-$ mass spectrum is Lorentz invariant**
  - **Sensitive to Temperature**

**Dilepton dN/dM is the thermometer of the source**

$$dN/dM \propto M^{3/2} \times \exp(-M/T)$$

**$d^4N/dMdp^3$ maps the space time evolution**

# Microscopic View of Thermal Radiation

**Production process: real or virtual photons (lepton pairs)**

**hadron gas:**

**photons**

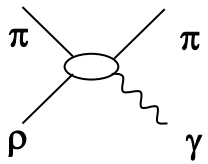


**low mass lepton pairs**

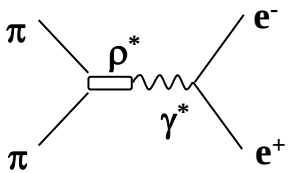


**Key issues:**
**In medium modifications of mesons**

R. Rapp and J. Wambach, EPJA 6 (1999) 415

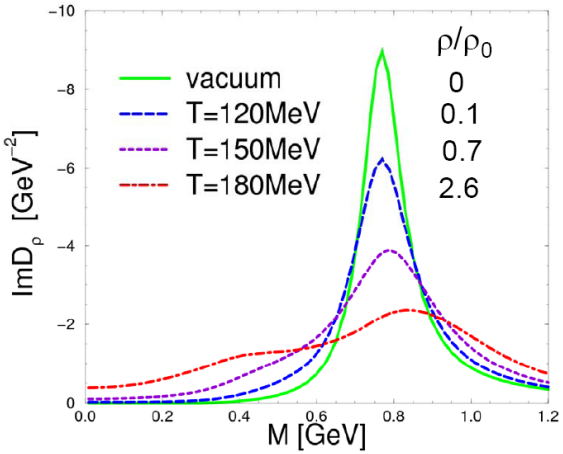


**QGP:**

**photons**

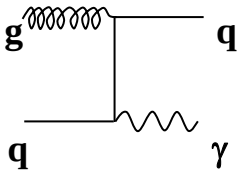


**medium mass lepton pairs**

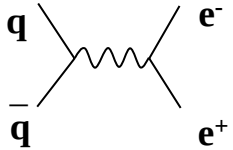


**pQCD base picture requires small $\alpha_s$**

**Rates not well established for strongly coupled plasma**

**Equilibrium of strong interaction →**
**Thermal radiation sensitive to constituents**

# Experimental Issue: Isolate Thermal Radiation

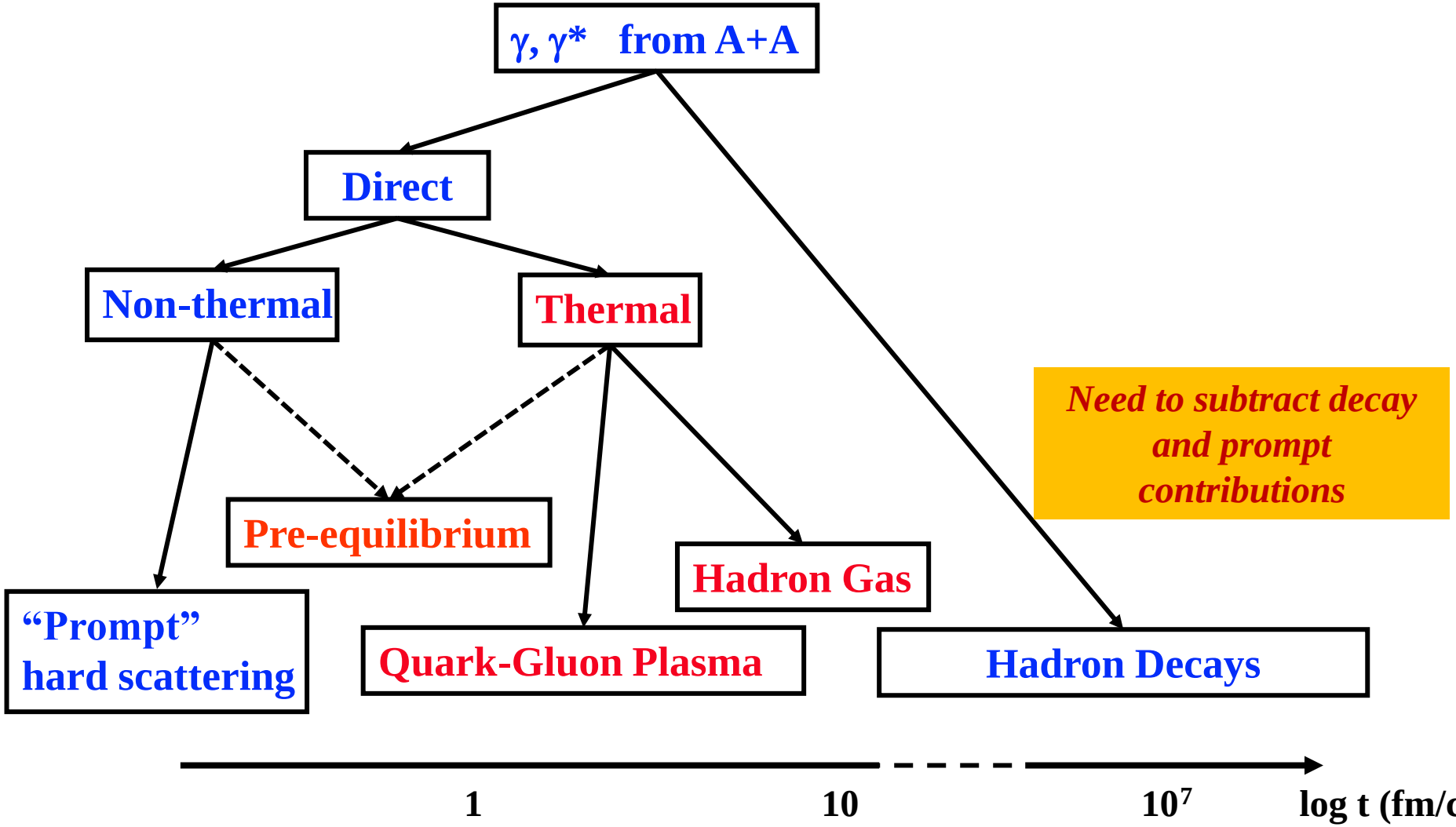


*Need to subtract decay and prompt contributions*

**Sensitive to temperature and space-time evolution**

# State of the Art Measurements with NA60

*Next slides mostly derived from talks given by Sanja Damjanovic*

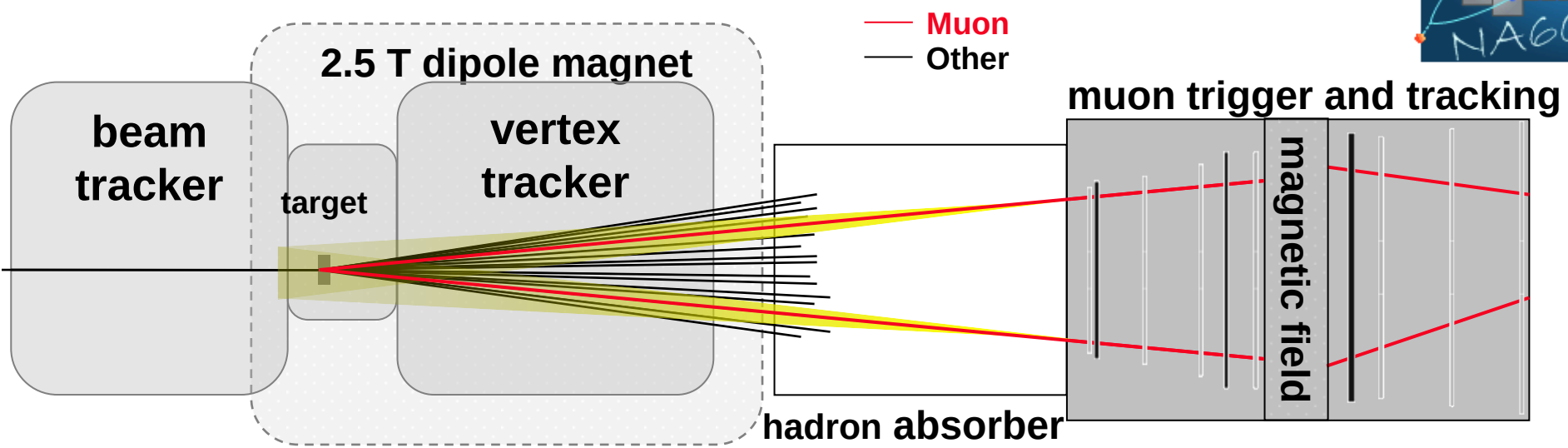


- **NA60 features**
  - **Classic muon spectrometer**
  - **Precision silicon pixel vertex tracker**

    **tagging of heavy flavor decay muons**

    **Reduction of combinatorial background by vetoing π, K decay muons**

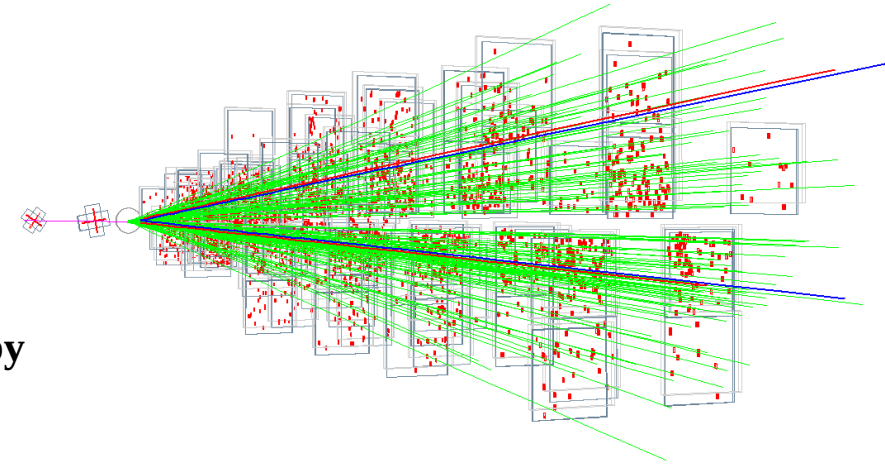

# Low Mass Data Sample for 158 AGeV In-In

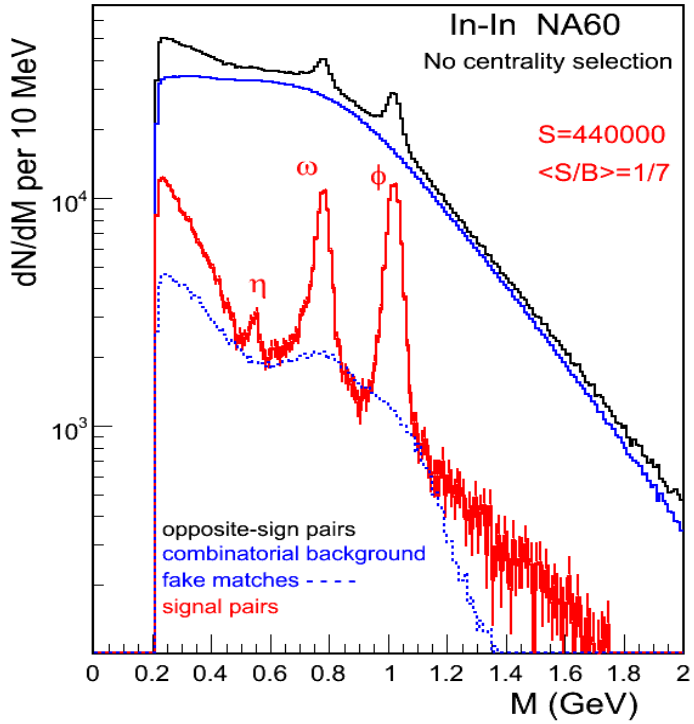


- **Experimental advance**
  - **High statistics**
  - **Excellent background rejection**
  - **Precision control of meson decay cocktail and open heavy flavor**

*Phys. Rev. Lett. 96 (2006) 162302*

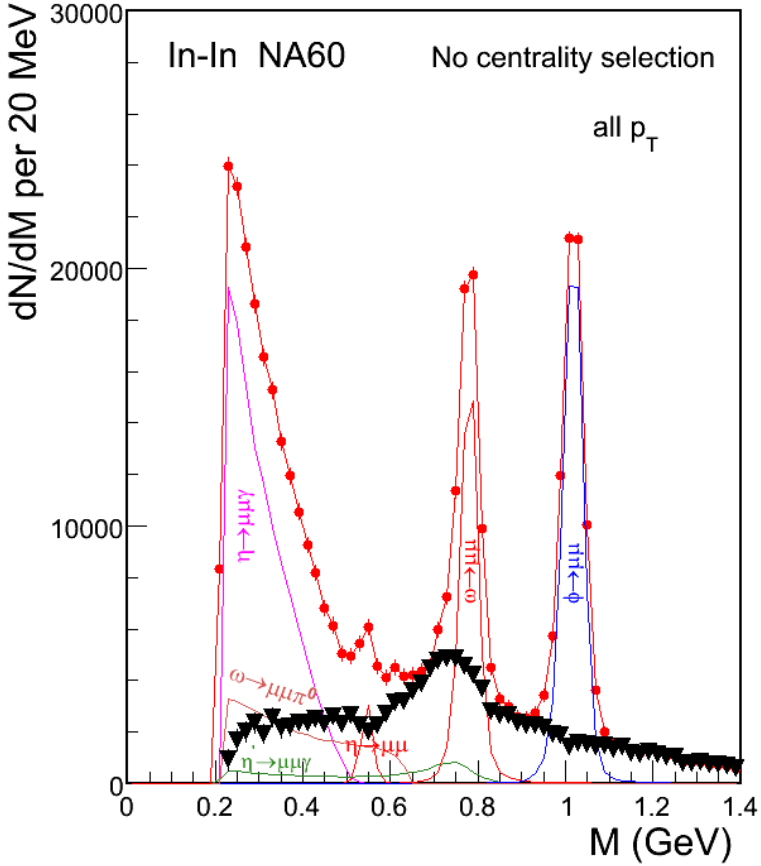


**NA60 can isolate continuum excess (including ρ meson) from decay background**

# Open Heavy Flavor Contribution

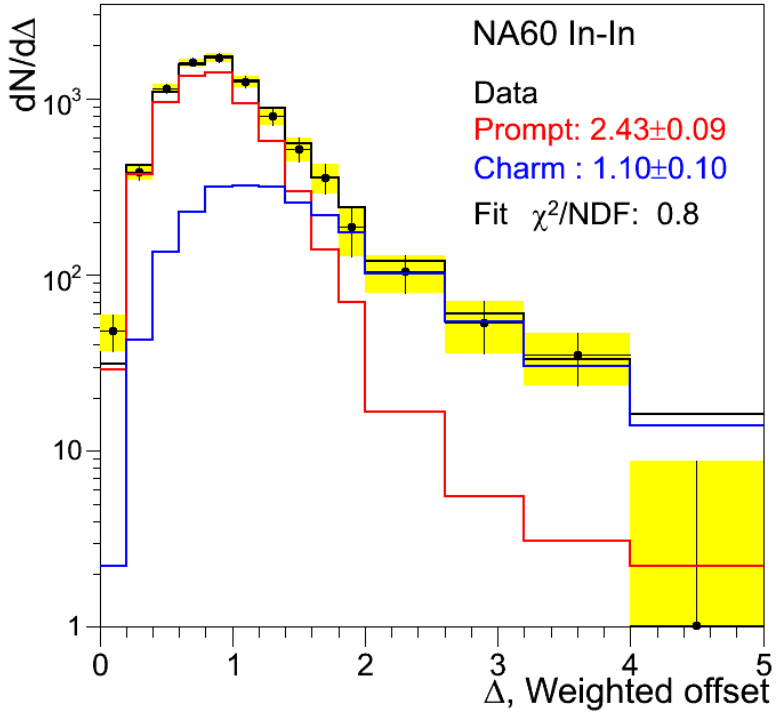


- **Experimental Breakthrough**
  - **Separate prompt from heavy flavor muons**
  - **Heavy flavor production consistent with PYTHIA**

*Eur.Phys.J. C 59 (2009) 607*

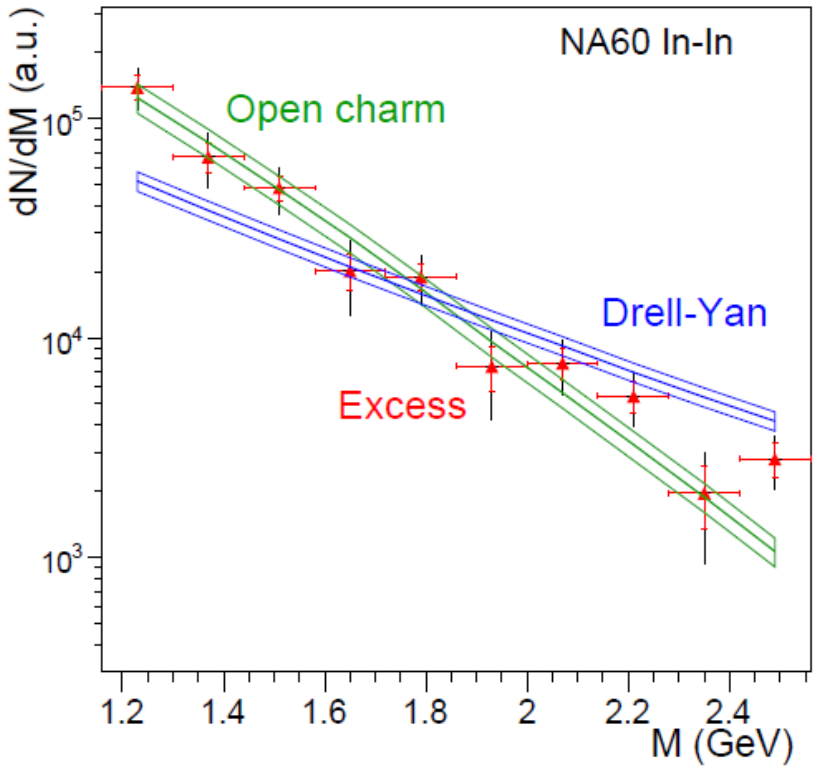


**Intermediate Mass Range prompt continuum excess 2.4 x Drell-Yan**

# Isolating the Dimuon Excess

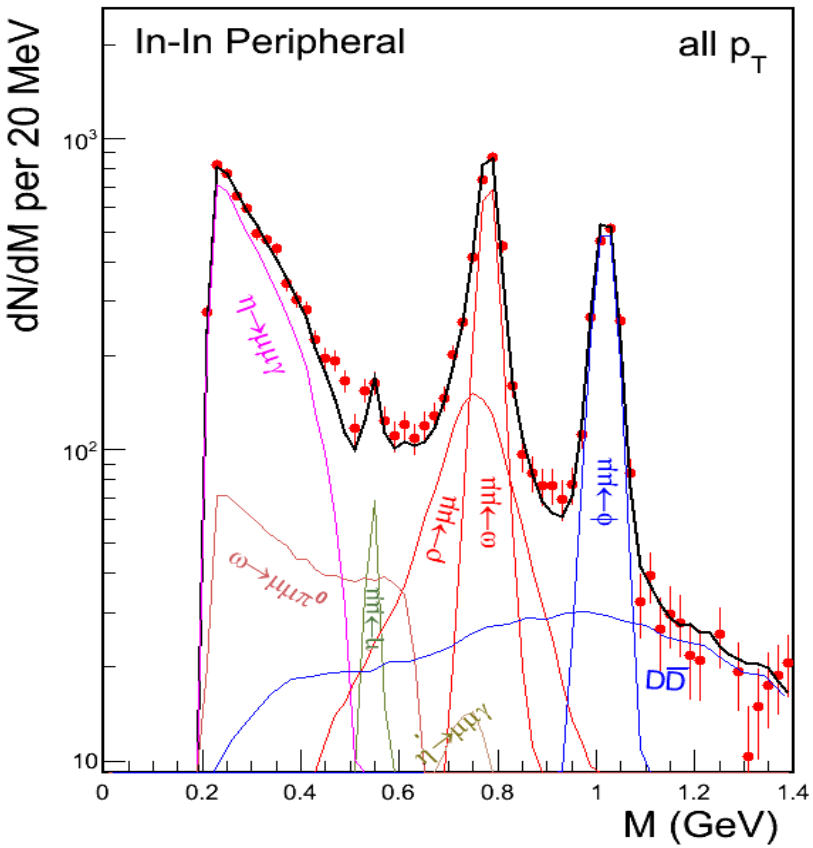


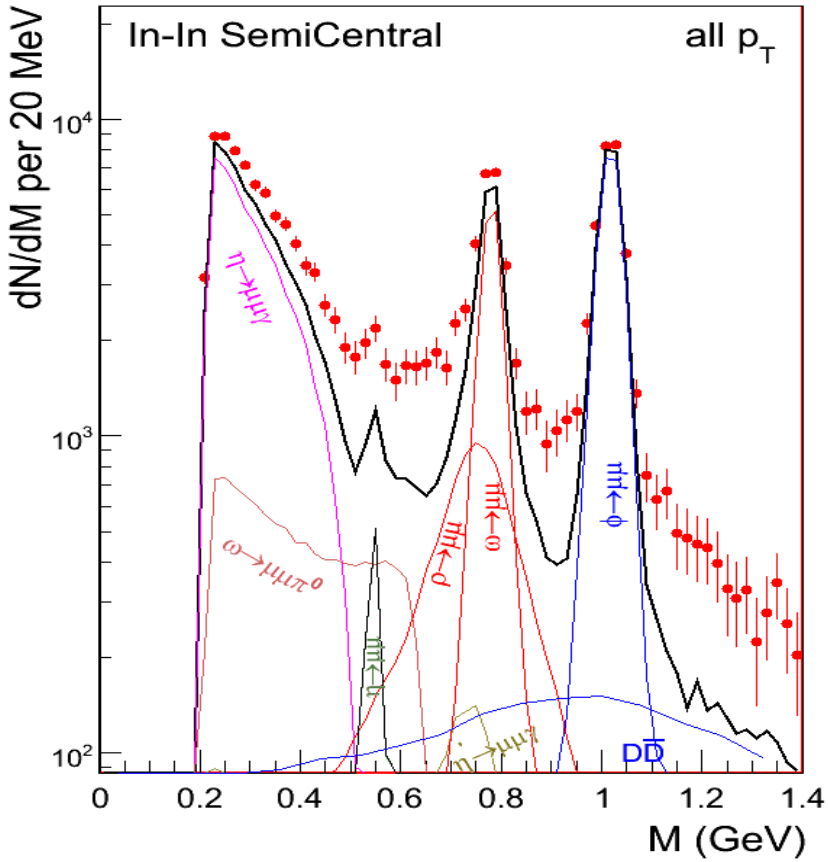


- **Tune meson decay cocktail (η, ω, ϕ) to M-$p_T$ spectra**
- **DD determined by binary scaled PYTHIA**
- **Extract excess dimuons (including ρ meson) by subtracting tuned cocktail and DD contribution**

# Acceptance Correction

- **Individual contributions identified can now be acceptance corrected**
  - **Meson yields (η, ρ, ω, ϕ)**
  - **Dimuon excess (assume γ*)**
  - **open heavy flavor**

- **Acceptance correction with separate treatment of individual sources**
  - **in 4-dimensional M-$p_T$-y-cos$\Theta_{CS}$**
  - **Project to 2-dimensional corrections**
    **Example M-$p_T$**
  - **Data driven iterative procedure**

**Example dimuon excess**

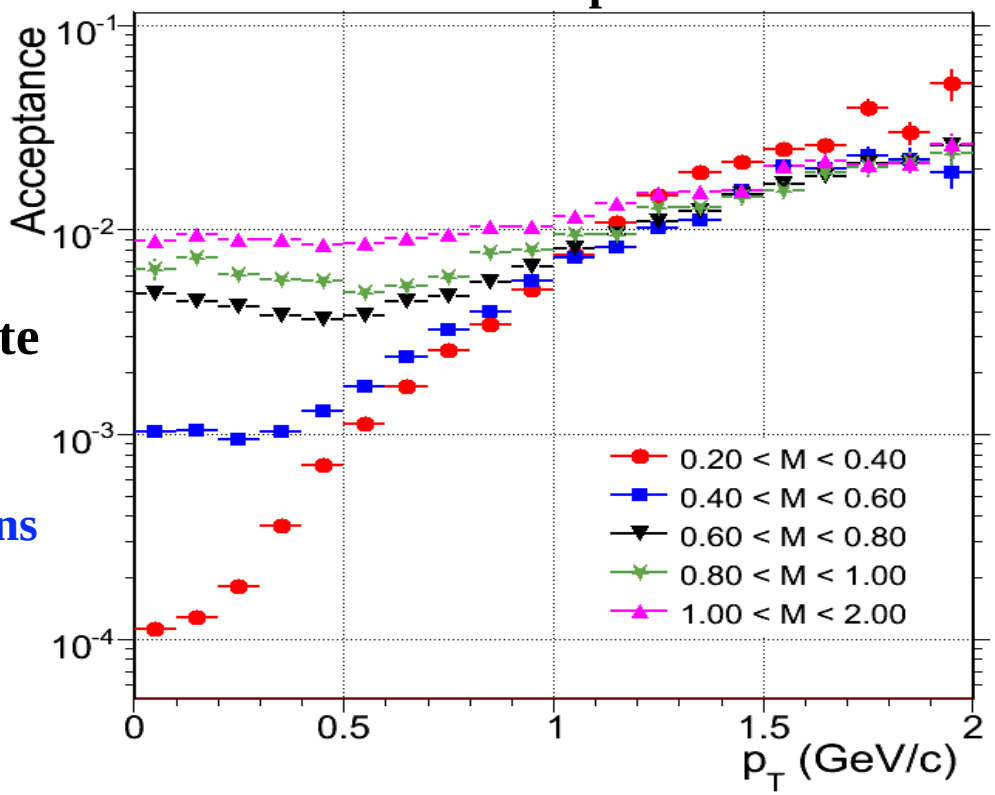


- **acceptance vs. M, $p_T$, y, and cosΘ understood to within <10%, based on a detailed study of the peripheral**

# Electromagnetic Transition Form Factors

*Phys. Lett. B 677 (2009) 260*

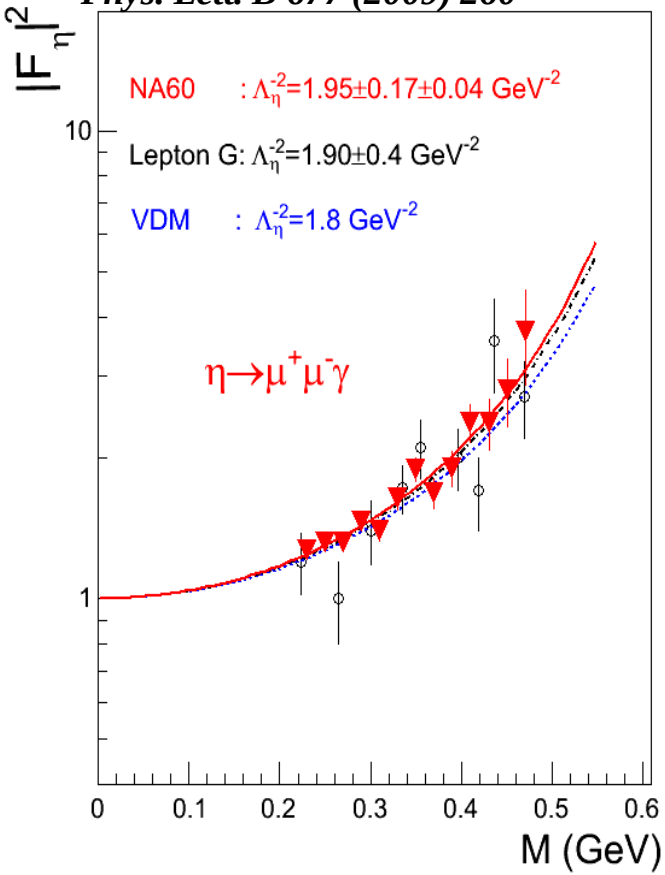


**data corrected for acceptance**

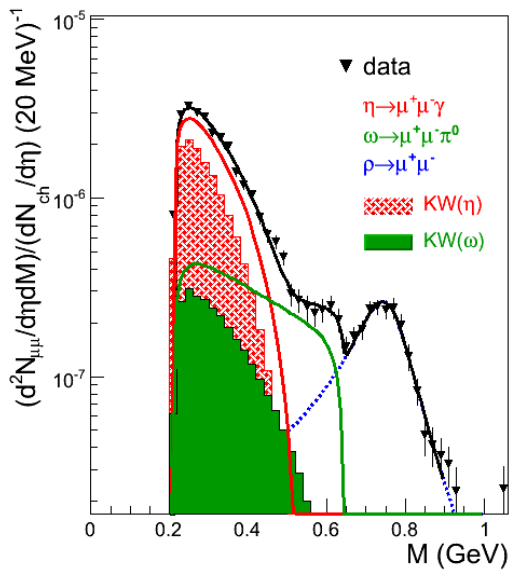


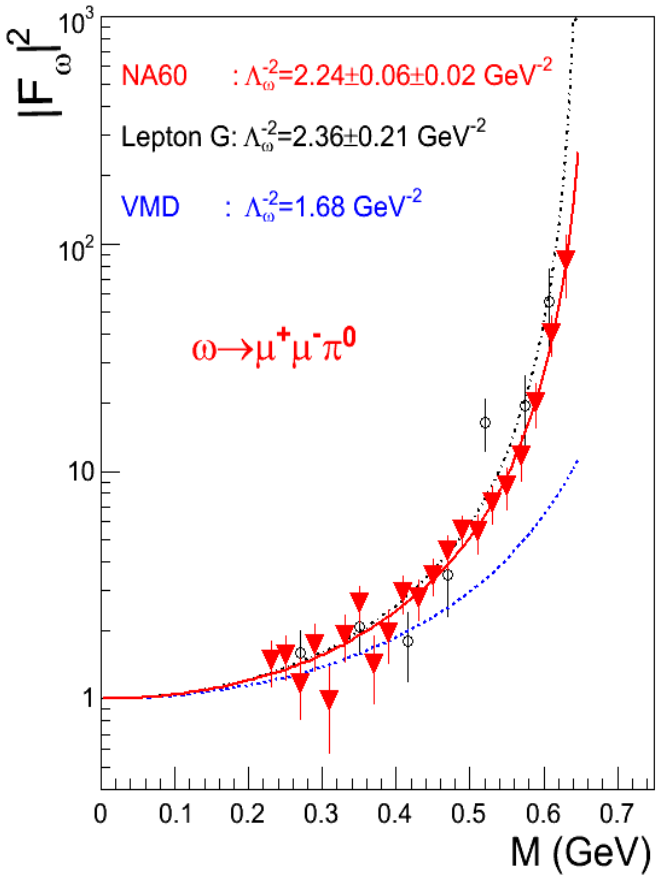


- **Large statistics data set**
  - **Excellent agreement with Lepton G experiment**
  - **Deviation from Vector Dominance Model 10 σ**
  - **p-Au data still higher accuracy**

**anomaly of ω transition formfactor confirmed**

# Transition Formfactor in PDG since 2010

## LIGHT UNFLAVORED MESONS
## $(S = C = B = 0)$

For $I = 1$ ($\pi$, $b$, $\rho$, $a$): $u\overline{d}$, $(u\overline{u}-d\overline{d})/\sqrt{2}$, $d\overline{u}$;
for $I = 0$ ($\eta$, $\eta'$, $h$, $h'$, $\omega$, $\phi$, $f$, $f'$): $c_1(u\overline{u} + d\overline{d}) + c_2(s\overline{s})$

### $\omega(782)$

$I^G(J^{PC}) = 0^-(1^{--})$

**$\omega(782)$ BRANCHING RATIOS**

**$\Gamma(\pi^0\mu^+\mu^-)/\Gamma_{total}$** — $\Gamma_7/\Gamma$

| VALUE (units $10^{-4}$) | EVTS | DOCUMENT ID | | TECN | COMMENT |
|---|---|---|---|---|---|
| **1.3 ±0.4 OUR NEW AVERAGE** | | Error includes scale factor of 2.1. [(0.96 ± 0.23) × $10^{-4}$ OUR 2009 AVERAGE] | | | |
| 1.72±0.25±0.14 | 3k | ARNALDI | 09 | NA60 | 158*A* In–In collisions |
| 0.96±0.23 | | DZHELYADIN | 81B | CNTR | 25–33 $\pi^- p \to \omega n$ |

**PARAMETER Λ IN $\omega \to \pi^0\mu^+\mu^-$ DECAY**

In the pole approximation the electromagnetic transition form factor for a resonance of mass $M$ is given by the expression:

$$|F|^2 = (1 - M^2/\Lambda^2)^{-2},$$

where for the parameter Λ vector dominance predicts $\Lambda = M_p \approx 0.770$ GeV. The ARNALDI 09 measurement is in obvious conflict with this expectation. Note that for $\eta \to \mu^+\mu^-\gamma$ decay ARNALDI 09 and DZHELYADIN 80 obtain the value of Λ consistent with vector dominance.

| VALUE (GeV) | EVTS | DOCUMENT ID | | TECN | COMMENT |
|---|---|---|---|---|---|
| **0.668±0.009±0.003** | 3k | ARNALDI | 09 | NA60 | 158*A* In–In collisions |
| • • • We do not use the following data for averages, fits, limits, etc. • • • | | | | | |
| 0.65 ±0.03 | | DZHELYADIN | 81B | CNTR | 25–33 $\pi^- p \to \omega n$ |

**First result from a heavy-ion experiment in the PDG ever**

**$\omega(782)$ REFERENCES**


ARNALDI 09 PL B677 260 R. Amaldi *et al.* (NA60 Collab.)
DZHELYADIN 81B PL 102B 296 R.I. Dzhelyadin *et al.* (SERP)
DZHELYADIN 80 PL 94B 548 R.I. Dzhelyadin *et al.* (SERP)

# Acceptance-Corrected M-$p_T$ Matrix of Excess

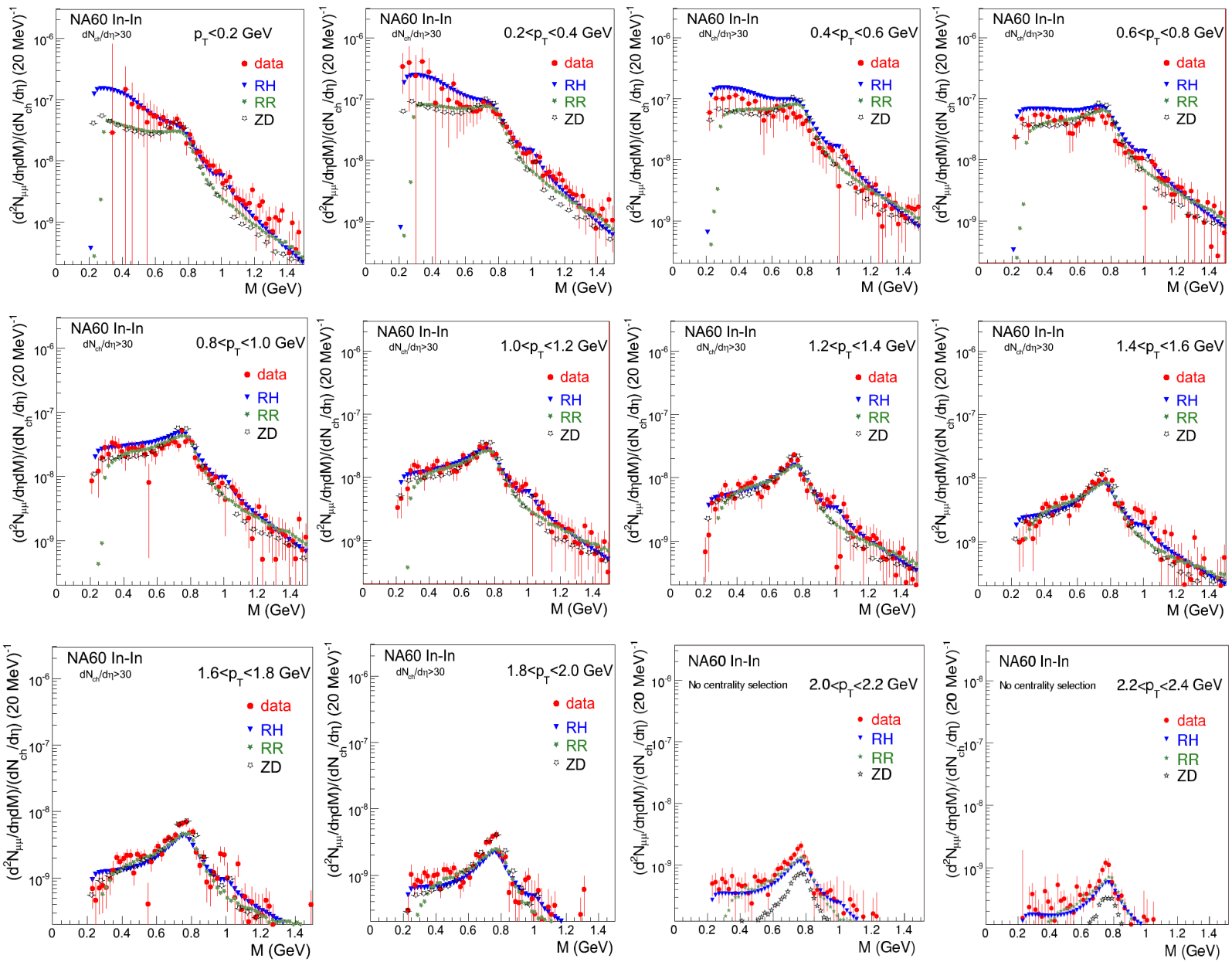

# Continuum Excess Measured by NA60

*Eur. Phys. J. C 59 (2009) 607; CERN Courier 11/2009*

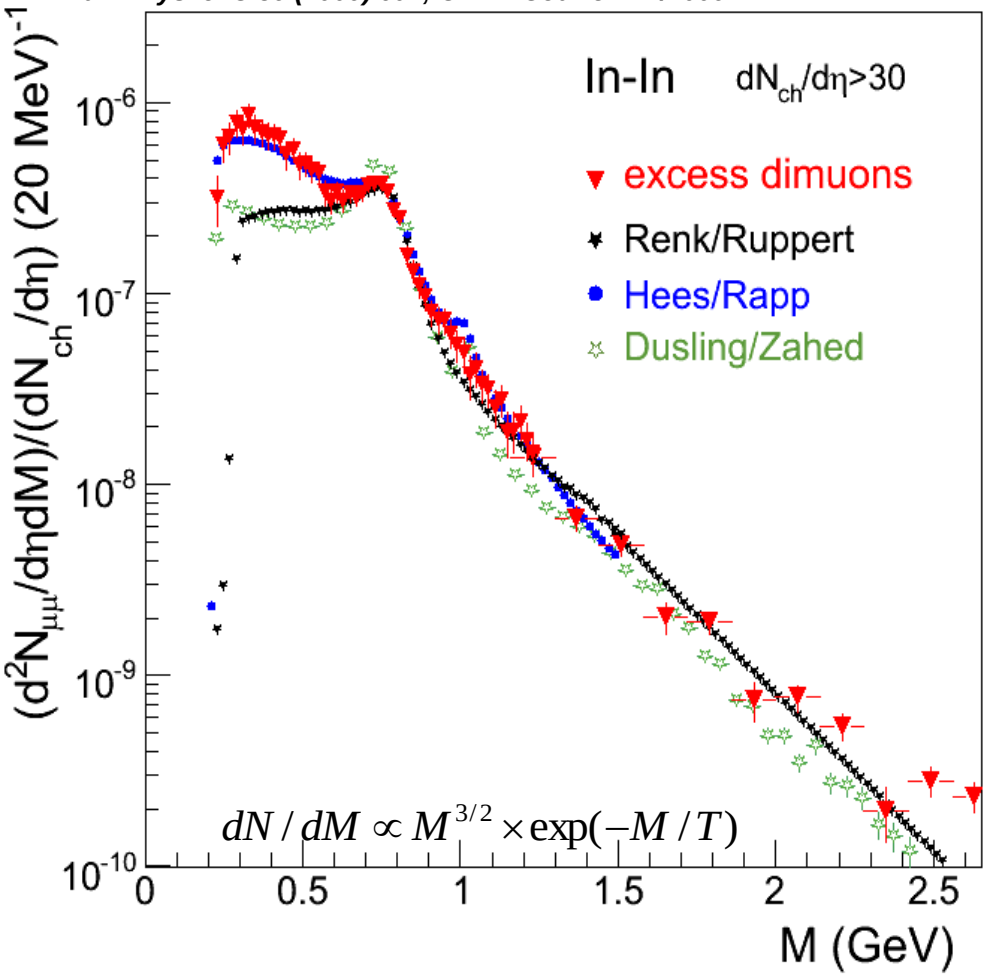


**Dileptons for M >1 GeV dominantly of partonic origin**

- **Planck-like mass spectrum m > 1 GeV**
  - **1.1-2.0 GeV: T=205±12 MeV**
  - **1.1-2.4 GeV: T=230±10 MeV**

**Thermal dilepton radiation**
**$T_{eff}$ ~ 220 MeV > $T_C$**

- **Model comparison**
  - **Main Sources m < 1 GeV**
    $\pi^+\pi^- \rightarrow \rho \rightarrow \mu^+\mu^-$
    **broadening spectral function**
  - **Main sources m > 1 GeV**
    $qq \rightarrow \mu^+\mu^-$
    $\pi\, a_1 \rightarrow \mu^+\mu^-$ **(consistent up to 1.5 GeV)**
- **Systematic uncertainties**
  - **Fits to theory (RR and DZ)**

| | |
|---|---|
| **Global fit:** | **T = 215 MeV** |
| **Local fit 1.2 GeV:** | **T = 205 MeV** |
| **2.5 GeV:** | **T = 225 MeV** |

- **20-30% Drell Yan oversubtraction**
  **10-20 MeV reduction in T**

# Transverse Mass Distributions of Excess Dimuon

**transverse mass: $m_T = (p_T^2 + m^2)^{1/2}$**

*Phys. Rev. Lett. 100 (2008) 022302*

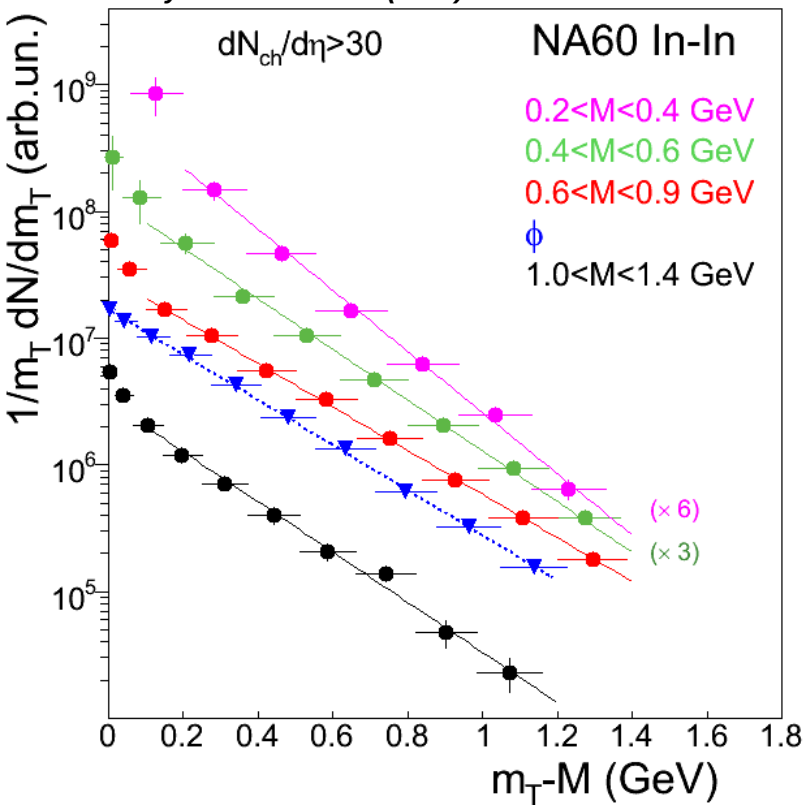


*Eur. Phys. J. C 59 (2009) 607*

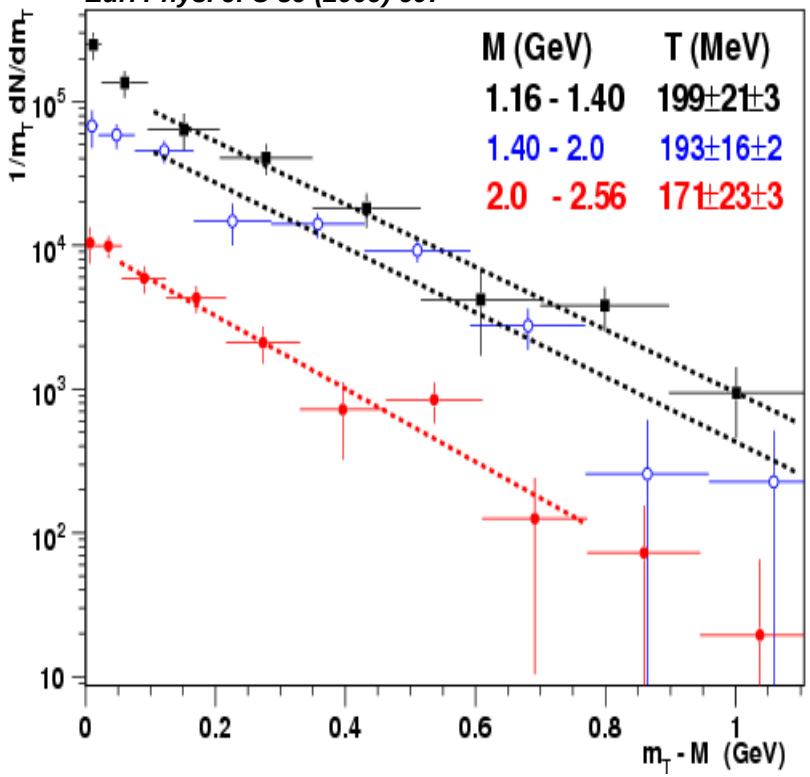


- **All $m_T$ spectra exponential for $m_T$-m > 0.1 GeV**
  - **Fit with exponential in $1/m_T\ dN/dm_T \sim \exp(-m_T/T_{eff})$**
- **Soft component for <0.1 GeV ??**
  - **Only in dileptons not in hadrons**

# Unfolding Time-Evolution Using m-$p_T$ Dependence

- **Inverse slope verses mass for thermal radiation**
  - **Mass < 1 GeV from hadronic phase**

$$T_{eff} \sim \langle T_{th} \rangle + M \langle v_T \rangle^2$$

$\langle T_{th} \rangle = 130–140$ MeV $< T_c$

  - **Mass > 1 GeV from partonic phase**

$\langle T_{th} \rangle = 200$ MeV $> T_c$

- **Schematic hydrodynamic evolution**
  - **Partonic phase**
    **early emission: high T, low $v_T$**
  - **Hadronic phase**
    **late emission: low T, high $v_T$**

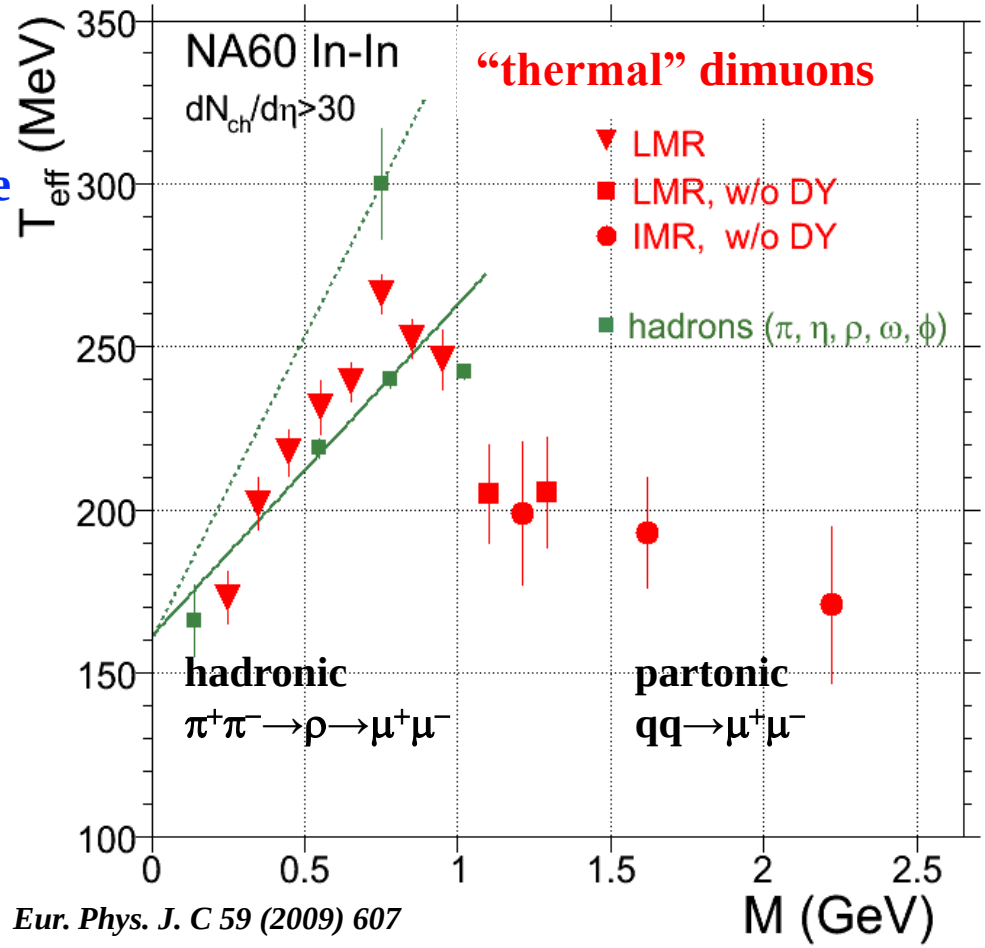


*Eur. Phys. J. C 59 (2009) 607*

**Dileptons for M >1 GeV dominantly of partonic origin**

# Combined Conclusions from Mass and $p_T$ Spectra

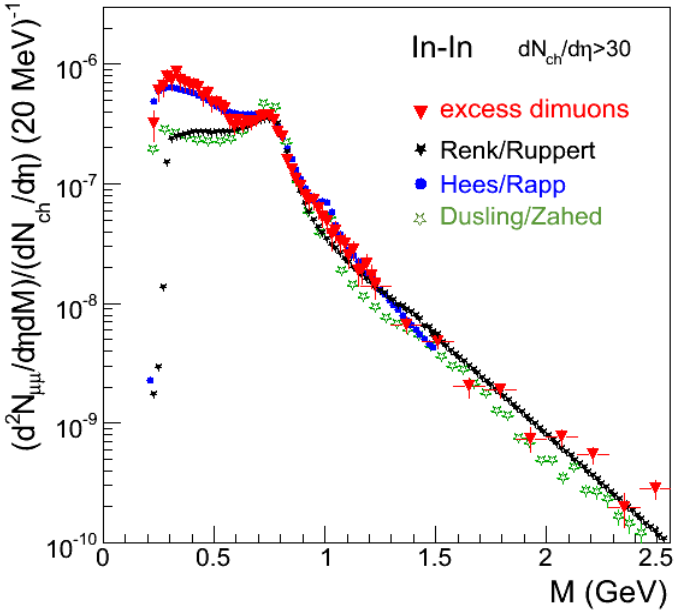


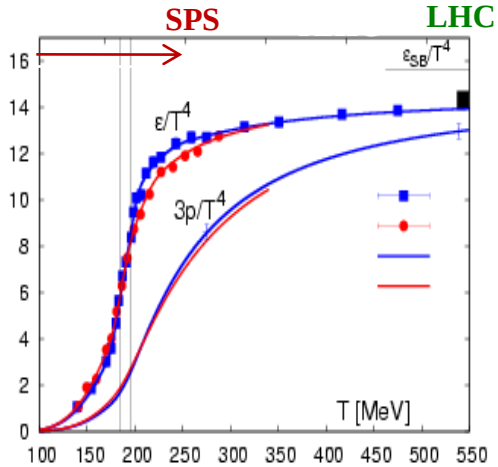


**rapid rise of energy density ε, slow rise of pressure p (not ideal gas)**

**→ EoS above $T_c$ very soft initially ($c_S$ minimal)**

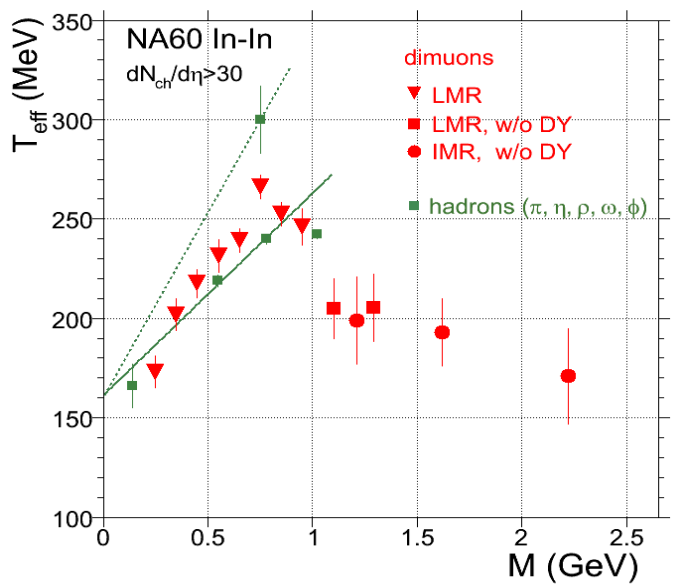


**M >1 GeV**

**- $T_{eff}$ independent of mass within errors**

**mass spectrum: T = 205 12 MeV**

**$p_T$ spectra: $\langle T_{eff} \rangle$ = 190 12 MeV**

**- same values within errors**

**T = 205 MeV > $T_c$ = 170 (MeV)**

**negligible flow → soft EoS above $T_c$**

**all consistent with partonic phase**

# Angular Distributions

$$\frac{1}{\sigma}\frac{d\sigma}{d\cos\theta\, d\phi} = \left(1+\lambda\cos^2\theta+\mu\sin 2\theta\cos\phi+\frac{\nu}{2}\sin^2\theta\cos 2\phi\right)$$

**$\lambda$, $\mu$, $\nu$ : structure functions related to helicity structure functions and the spin density matrix elements of the virtual photon**

**Choice of reference frame: Collins-Soper (CS)**

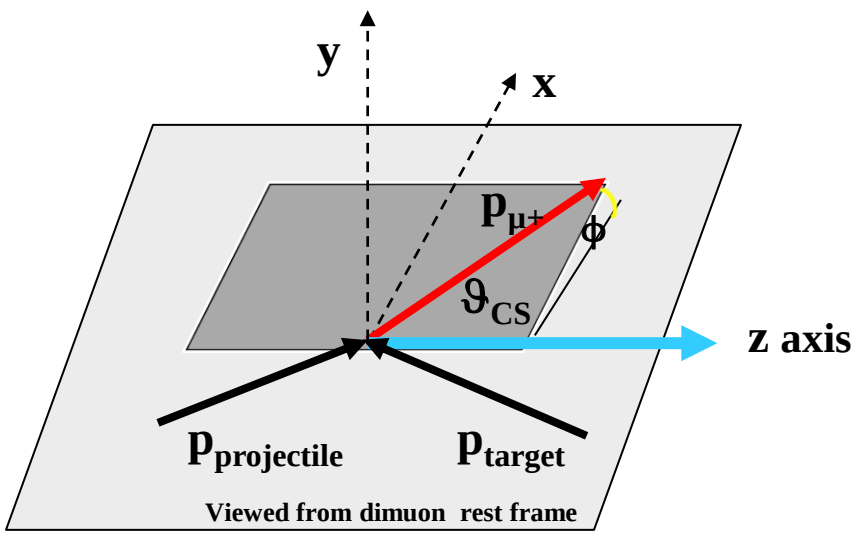


**In rest frame of virtual photon:**

**$\theta$ : angle between the positive muon $p_{\mu+}$ and the z-axis.**

**z axis : bisector between $p_{proj}$ and $-p_{target}$**

**Expectation: completely random orientation of annihilating particles (pions or quarks) in 3 dimensions would lead to $\lambda$, $\mu$, $\nu$ = 0**

# Results on structure coefficients λ, μ, ν

*Phys. Rev. Lett. 102 (2009) 222301*

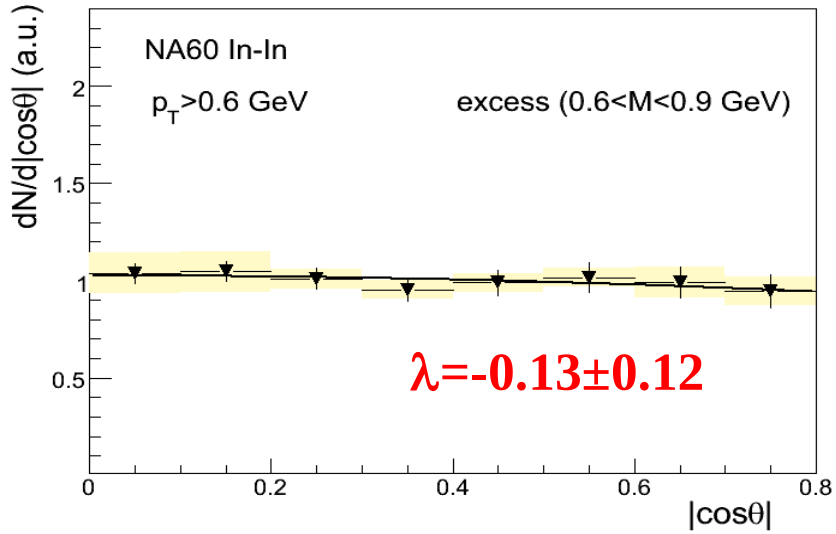


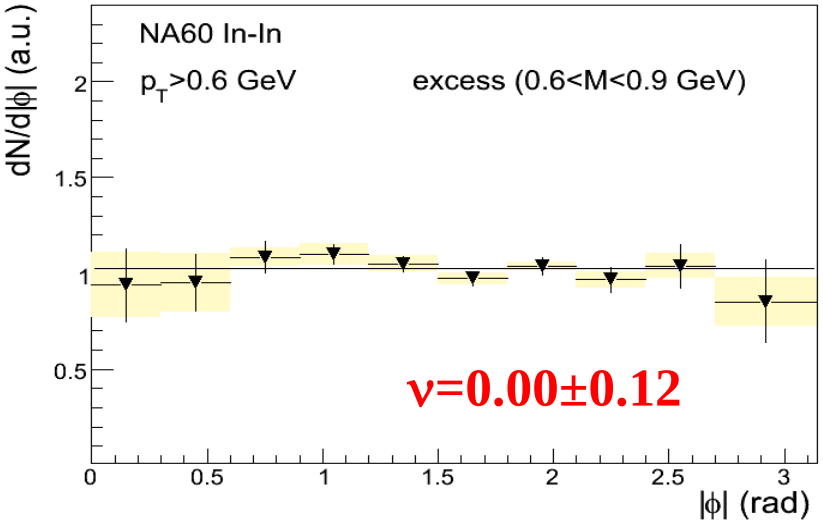


**example:**
**excess 0.6<M<0.9 GeV**

***μ* = 0.05 ± 0.03 (~0 as expected)**
**set μ = 0 and fit projections**

**fit function for polar angle**

$$\frac{dN}{d|\cos\theta|} \propto \left(1+\lambda\cos^2\theta\right)$$

**fit function for azimuth angle**

$$\frac{dN}{d|\phi|} \propto \left(1+\frac{1}{3}\lambda+\frac{\nu}{3}\cos 2\phi\right)$$

**Zero polarization within errors**

# Sensitivity to Spectral Function

*Phys. Rev. Lett. 96 (2006) 162302*

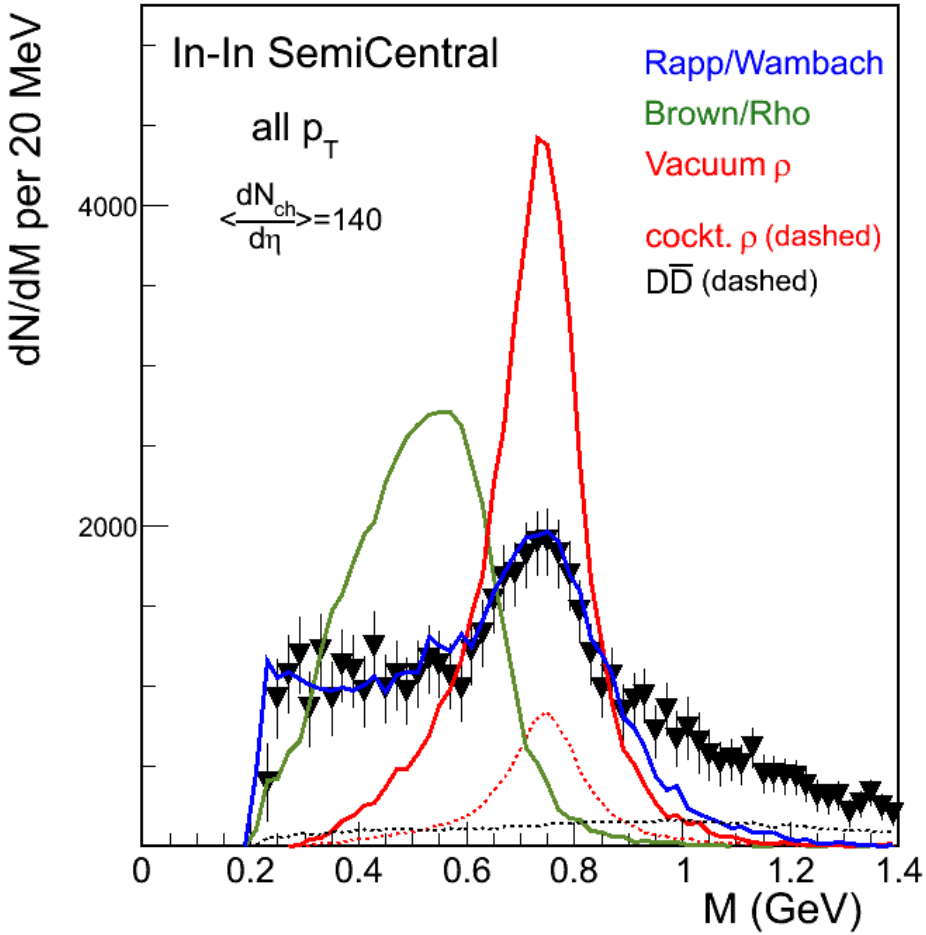


**Not acceptance corrected**

- **Models for contributions from hot medium (mostly ππ from hadronic phase)**
  - **Vacuum spectral functions**
  - **Dropping mass scenarios**
  - **Broadening of spectral function**
- **Broadening of spectral functions clearly favored!**

**ππ annihilation with medium modified ρ works very well at SPS energies!**

# Role of Baryons in Broadening the ρ

*van Hees and Rapp, Phys.Rev.Lett. 97 (2006) 102301*

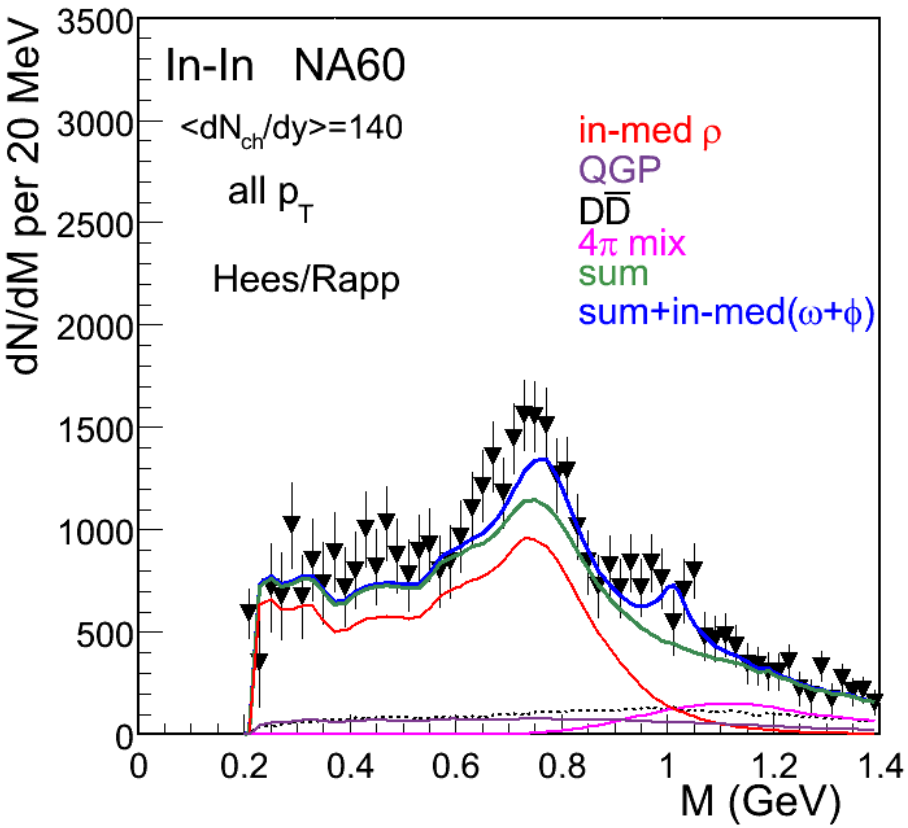


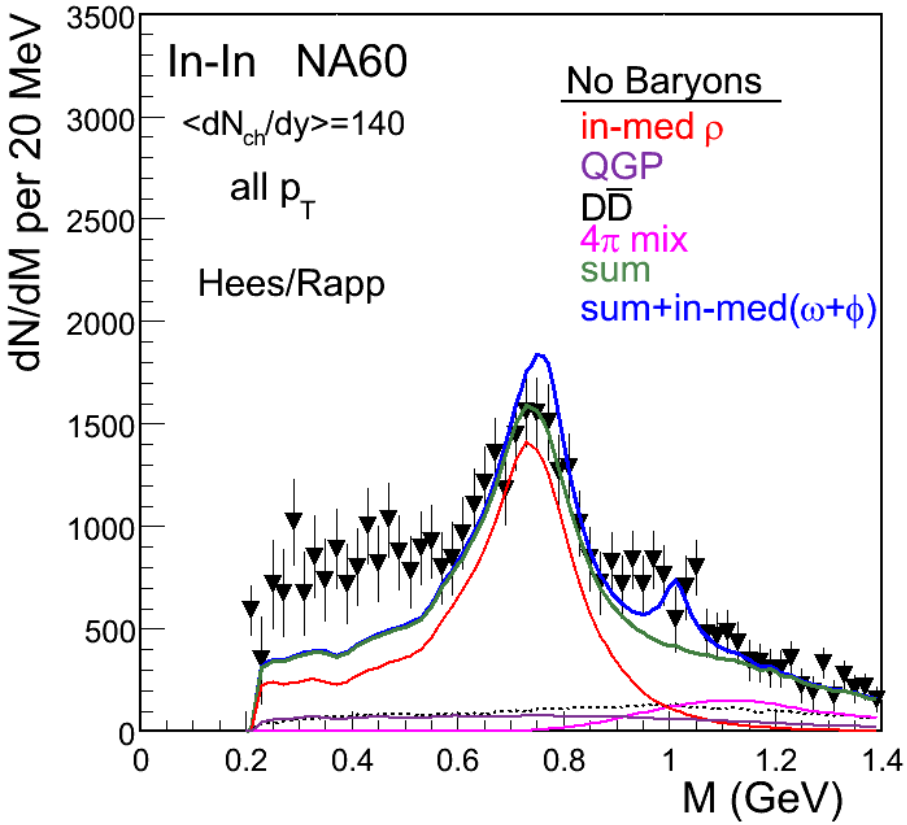


**Whole spectrum reasonably well described, even in absolute terms**

**In this model, low-mass tail requires baryon interactions**

**Role of baryons important at SPS energies!**

# New facilities and fixed-target - conclusions

Conclusions of the Heavy-Ion Town Meeting:

***„2. At lower center of mass energies where the highest baryon densities are reached, advances in accelerator and detector technologies provide opportunities for a new generation of precision measurements that address central questions about the QCD phase diagram"***

„The town meeting also observed that the CERN SPS would be well-positioned to contribute decisevely and at a competetive time scale to central open physics issues at large baryon density. In particular, the CERN SPS will remain also in the future the only machine capable of delivering heavy-ion beams with energies exceeding 30 AGeV, and the potential of investigating rare probes at this machine is very attractive."

# SPS Energy Range

**Prime physics goal:**

**systematic measurement of EM radiation and charm over the full energy range from SIS-100 (11 AGeV) to top SPS (160 AGeV)**

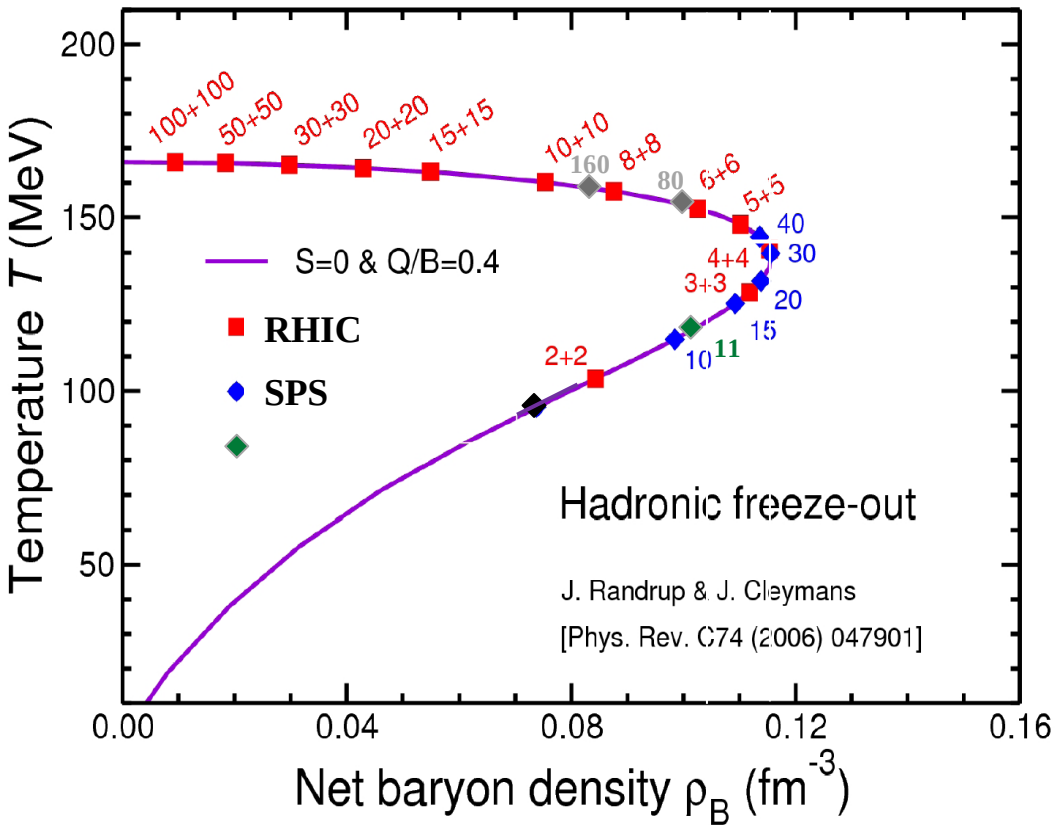


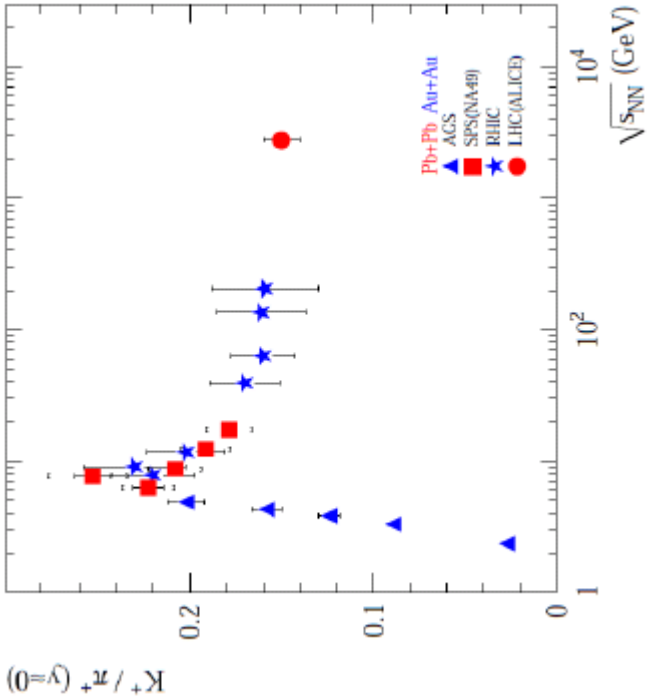


**SPS covers full range above and below maximum baryon density**

# Assessing Performance of Experiment

- **Decisive parameter for data quality:**
  - **Sample size N and Signal/Background**

**effective signal: $N_{eff} \sim N \times S/B$**

- **Choose data for B and cocktail at 0.6 GeV for S**
  - **Independent of excess**
  - **Unambiguous scaling between experiments by $dN_{ch}/dy$**

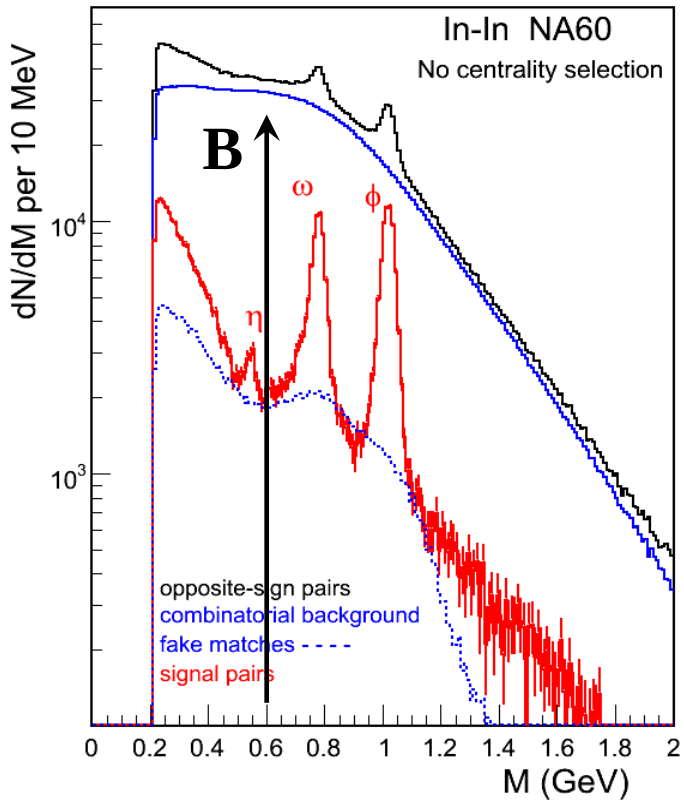


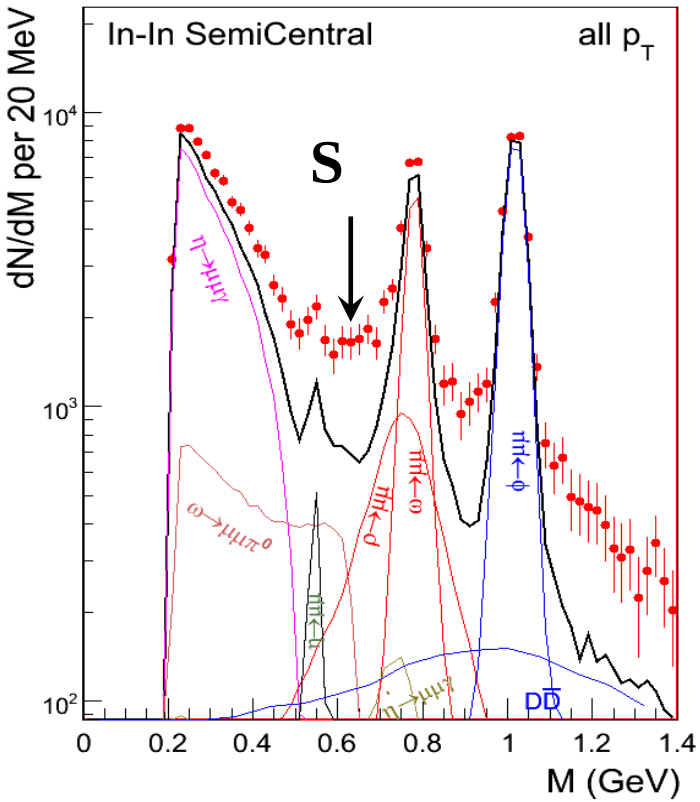

# Combinatorial Background/Signal in Dilepton Experiments

Reference: hadron cocktail at masses of 0.5-0.6 GeV

| Experiment | Centrality | Lepton flavor | B/S as meas. or simul. | B/S rescaled to $dN_{ch}/dy=300$ | B/S field data ×1/3 | B-field at vertex |
|---|---|---|---|---|---|---|
| HADES-SIS100 | semicentr | $e^+e^-$ | 20 | → 60 | 60 | – |
| CERES DR | semicentr | $e^+e^-$ | 80 | 100 | 100 | – |
| CERES SR/TPC | c | | | | 0 | – |
| PHENIX with HBD | c | | | | 0 | – |
| PHENIX w/o HBD | c | | | | 0 | + |
| STAR | c | | | | 0 | + |
| ALICE Upg ITS | c | | | | 0 | + |
| CBM-SIS100 | c | | | | 0 | + |
| CBM-SIS300 | central | $e^+e^-$ | 200 | 200 | 70 | + |
| NA60 | semicentr | $\mu^+\mu^-$ | 55 | 80 | 80 | |
| CBM-SIS300 | central | $\mu^+\mu^-$ | 600 | 600 | 600 | |

**NA60 setup already optimized and proven concept**

**Need scalability for beam energy**

→ 'penalty' factor 3 (4) for B-field, hindering optimal rejection of low-mass pairs

→ 'reduced' values 80 20 (w/o red) → only small influences of experimental details

# Low energy apparatus layout

G. Usai, CERN
Town Meeting 2012

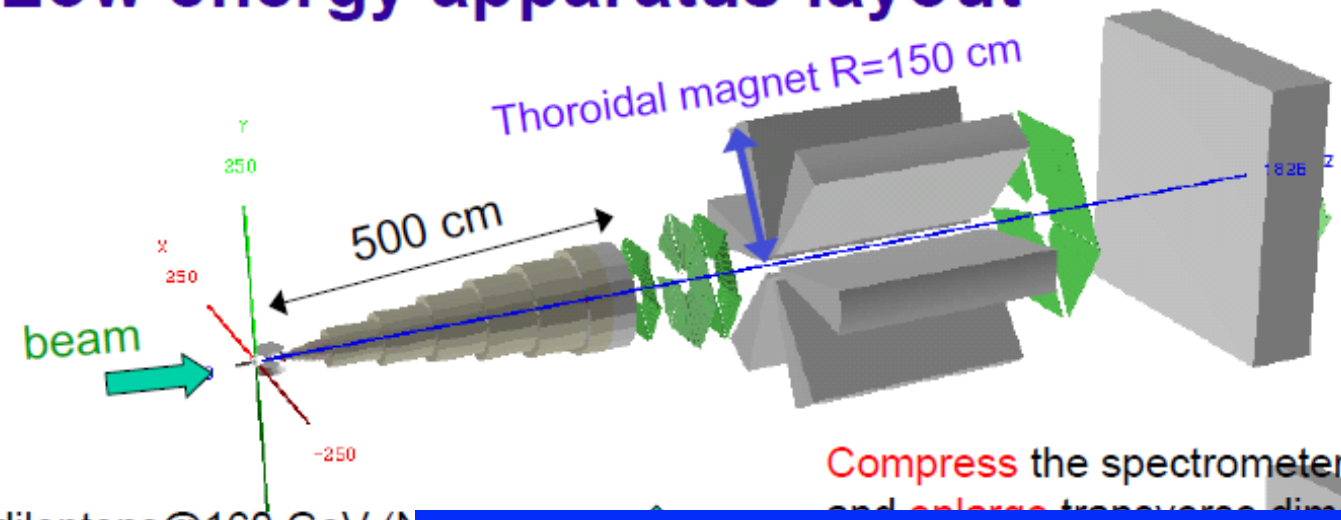


Compress the spectrometer reducing the absorber

dileptons@160 GeV (N
160 mrad angular
coverage

**Setup under intensive MC investigation**
**watch out for future presentations by Gianluca**

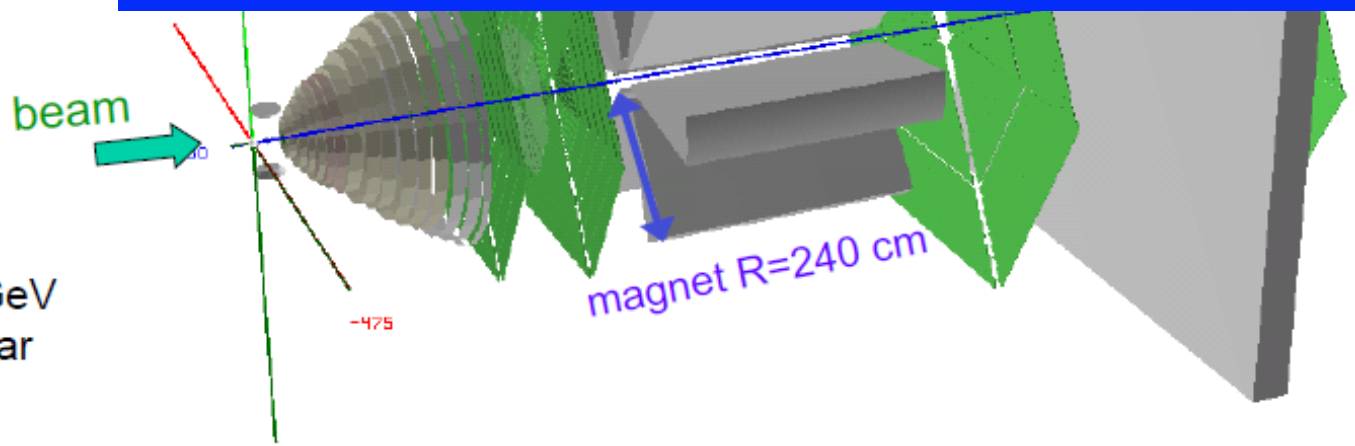


dileptons@30 GeV
240 mrad angular
coverage

Longitudinally scalable setup for running at different energies

# Beam conditions: CERN vs. GSI/FAIR

| | SPS | | | SIS100/300 |
|---|---|---|---|---|
| Energy range: [AGeV] | 10 – 158 | | | < 11 – 35 (45) |
| | beam intensity [Hz] | target thickness [$\lambda_i$] | interaction rate [Hz] | interaction rate [Hz] |
| NA60 (20 | | | | |
| ne inje sche | | | | |
| LHC | | | | |

**SPS beam intensity increased by factor 40**
**Increase of sample size by >>10 possible**
**4/6 years from now**

**Ideas about LHC fixed target under discussion**
**would reach RHIC energies**

No lo

RP limits at CERN in EHN1, not in (former) NA60 cave

Pb beams scheduled for the SPS in 2016-2017, 2019-2021

# Conclusion from NA60 at SPS and Outlook

- **Interpretation of excess dimuons as thermal radiation**
  - Planck-like exponential mass spectra
  - exponential $m_T$ spectra
  - zero polarization
  - general agreement with thermal models

- **Excess directly connected to deconfinement**
  - M < 1 GeV consistent with emission from $\pi^+\pi^-$ annihilation
  - M > 1 GeV consistent with mostly partonic emission
  - associated temperatures quantified
  - hints at soft EoS close to $T_c$

- **Excess (indirectly) connected to chiral symmetry restoration**
  - In-medium $\rho$ spectral function identified
  - no significant mass shift of the intermediate $\rho$, only broadening

- **Future opportunities at CERN SPS**
  - NA60 like experiment at 40x beam intensity
  - Scan beam energies → baryon density
  - Map out phase boundary

# The NA60 experiment

http://cern.ch/na60

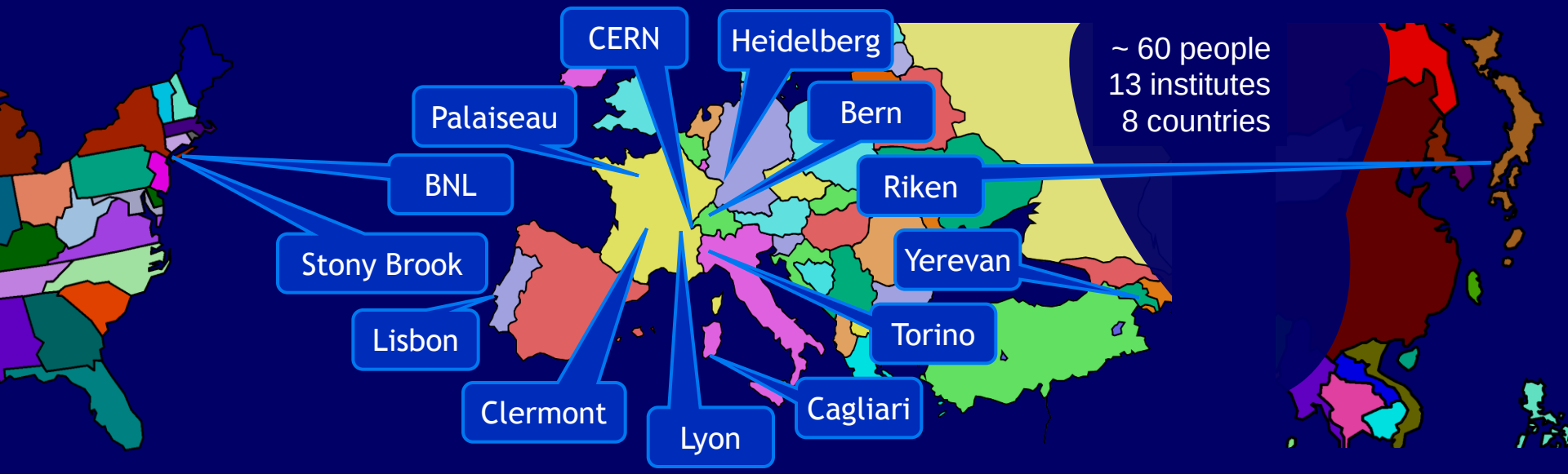


R. Arnaldi, K. Banicz, K. Borer, J. Buytaert, J. Castor, B. Chaurand, W. Chen,B. Cheynis, C. Cicalò, A. Colla, P. Cortese, S. Damjanovic, A. David, A. de Falco, N. de Marco, A. Devaux, A. Drees, L. Ducroux, H. En'yo, A. Ferretti, M. Floris, A. Förster, P. Force, A. Grigorian, J.Y. Grossiord, N. Guettet, A. Guichard, H. Gulkanian, J. Heuser, M. Keil, L. Kluberg, Z. Li, C. Lourenço, J. Lozano, F. Manso, P. Martins, A. Masoni, A. Neves, H. Ohnishi, C. Oppedisano, P. Parracho, P. Pillot, G. Puddu, E. Radermacher, P. Ramalhete, P. Rosinsky, E. Scomparin, J. Seixas, S. Serci, R. Shahoyan, P. Sonderegger, H.J. Specht, R. Tieulent, E. Tveiten, G. Usai, H. Vardanyan, R. Veenhof and H. Wöhri

# Backup

# Centrality Dependence of Spectral Shape

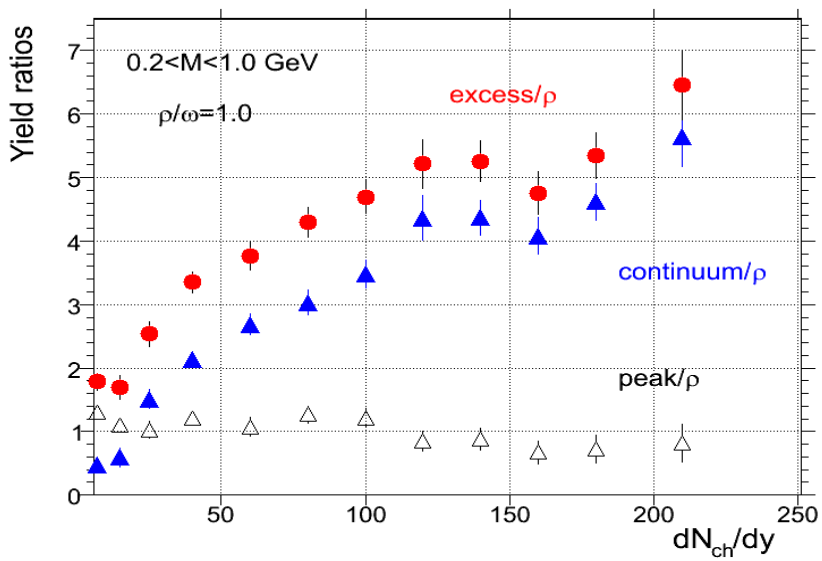


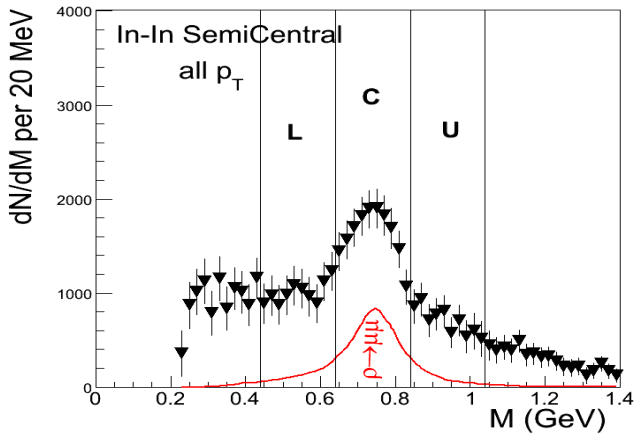


**peak:** R=C-1/2(L+U)
**continuum:** 3/2(L+U)

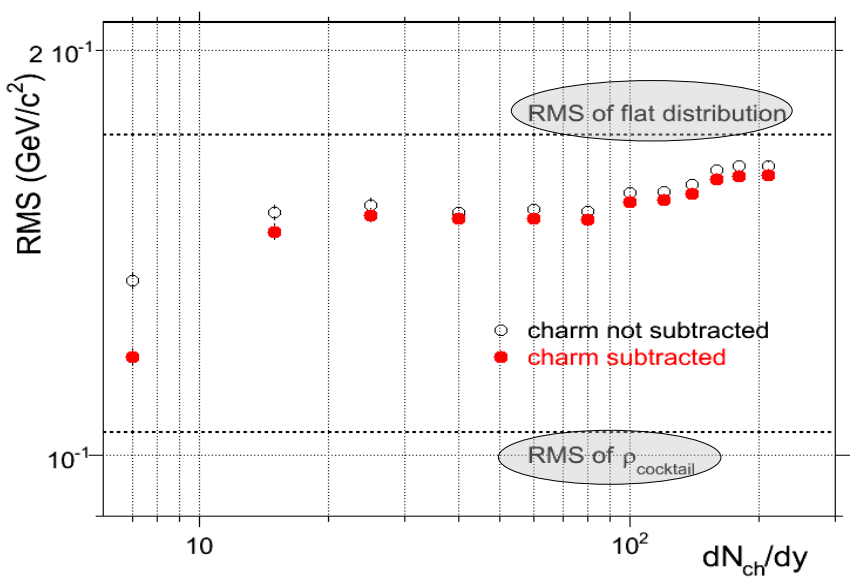


- **rapid increase of relative yield reflects the number of ρ's regenerated in $\pi^+\pi^- \rightarrow \rho^* \rightarrow \mu^+\mu^-$**

  → **'ρ clock'**

- **near divergence of the width**

  → **'melting' of the ρ**

# Experimental Issue: Combinatorial Background

$\pi^0 \rightarrow e^+ e^- \gamma$ $\qquad$ $\pi^+ \rightarrow \mu^+ \nu$

$\gamma \rightarrow e^+ e^-$ $\qquad$ $\pi^- \rightarrow \mu^- \nu$

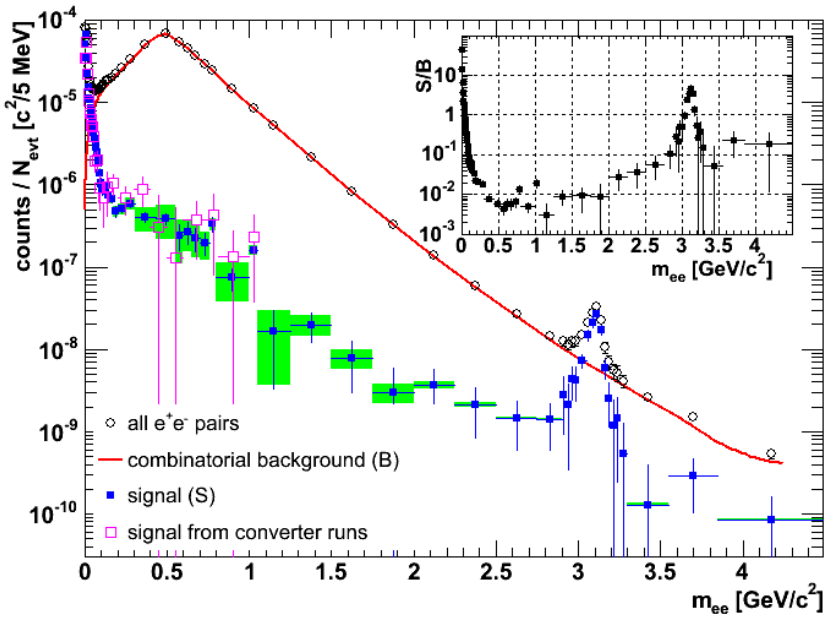


- **Performance in terms of Background/Signal**

  **signal = known sources**

  **Typical values ~ 500 MeV**

| | |
|---|---|
| HADES | 20 |
| CERES | 100 |
| NA60 (μμ) | 55 |
| PHENIX | >1000 |
| PHENIX – HBD | ~ 250 |
| STAR | 400 |

- **Decisive parameter for data quality: Sample size N and Signal/Background**

  **effective signal:** $N_{eff} \sim N \times S/B$

- **Dilepton measurement requirements:**
  - **active/passive background rejection**
  - **high rate**
  - **vertex tracking**

# Viscosity and thermal photon production

Kevin Dusling
North Carolina State University

December $7^{\text{th}}$, 2012

# Contents


- Reminder on shear viscosity and photons
- Bulk viscosity and hadronic observables
- Bulk viscosity and electromagnetic observables

# Elliptic flow from dissipative hydrodynamics

State of the art fits suggest $\eta/s \sim 0.2$

Gale, Jeon, Schenke, Tribedy, Venugopalan (2012)

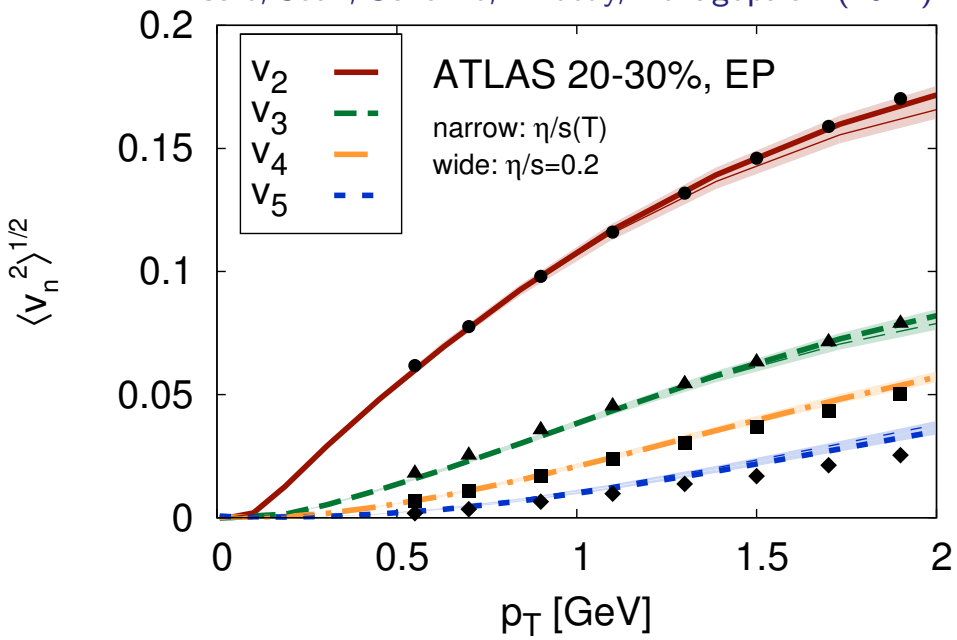


Still a number of uncertainties (two that will be addressed here)

- Need for kinetics
- Bulk viscosity

# Elliptic flow from dissipative hydrodynamics

Spectra computed with Cooper-Frye:

$$E_{\mathbf{p}} \frac{dN}{d^3p} = \frac{1}{(2\pi)^3} \int_\sigma f(E_{\mathbf{p}})\, p^\mu d\sigma_\mu$$

Expand $f = f_o + \delta f$ with constraint:

$$\delta T^{\mu\nu} = \int \frac{d^3\mathbf{p}}{(2\pi)^3 E_{\mathbf{p}}}\, p^\mu p^\nu \delta f(E_{\mathbf{p}})$$

Only moments of $\delta f$ fixed by hydro; leaving a need for kinetic models.

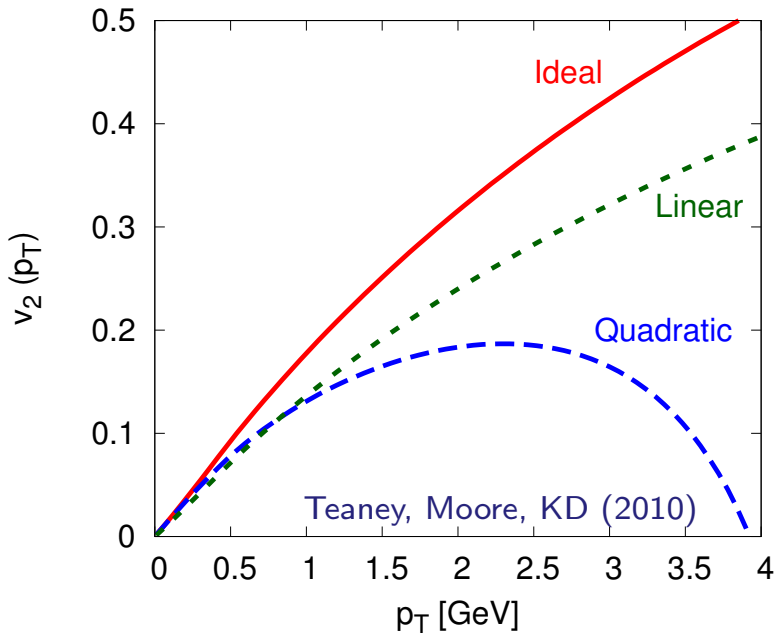

# QGP distribution functions

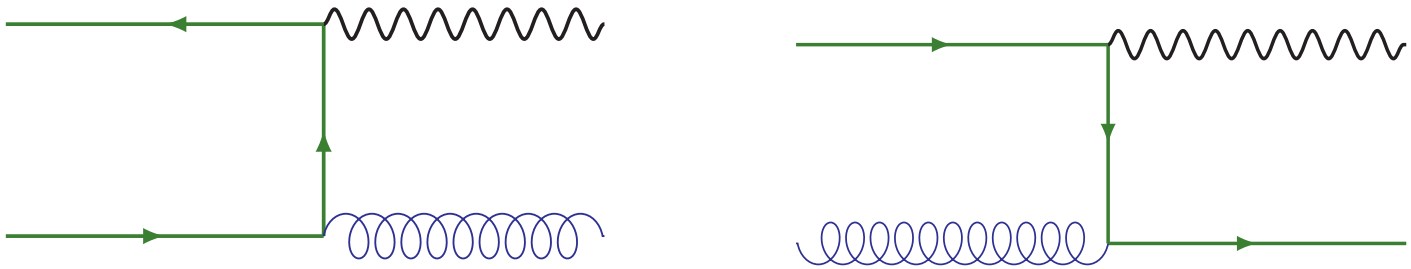

- Photons are completely out of equilibrium (contrast to early universe)
- Photon spectra only appears thermal because quarks / gluons creating photons are thermal
- This is very clear at leading log where $P^{\mu}_{\text{quark}} \approx Q^{\mu}_{\text{photon}}$

# QGP distribution functions

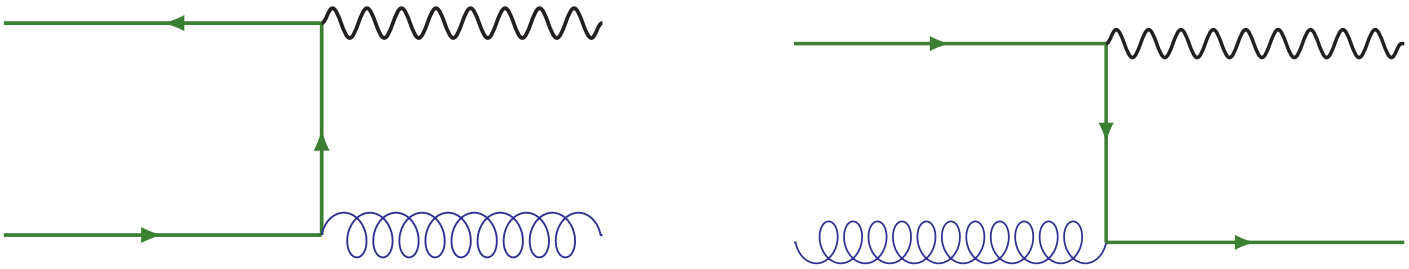

At leading log:

$$E\frac{dN_\gamma}{d^3q} \sim \alpha_{\rm em}\alpha_S f_{\rm quark}(Q_\gamma)T^2 \log\left(\#\frac{E_\gamma}{g^2T}\right)$$

Out of equilbrium:

$$f_{\rm quark} = f_0\left(1 - \chi^{\rm shear}_{\rm quark}(q)\cdot q^i q^j \partial_{\langle i}u_{j\rangle} - \chi^{\rm bulk}_{\rm quark}(q)\cdot \partial_i u^i\right)$$

# QGP photons

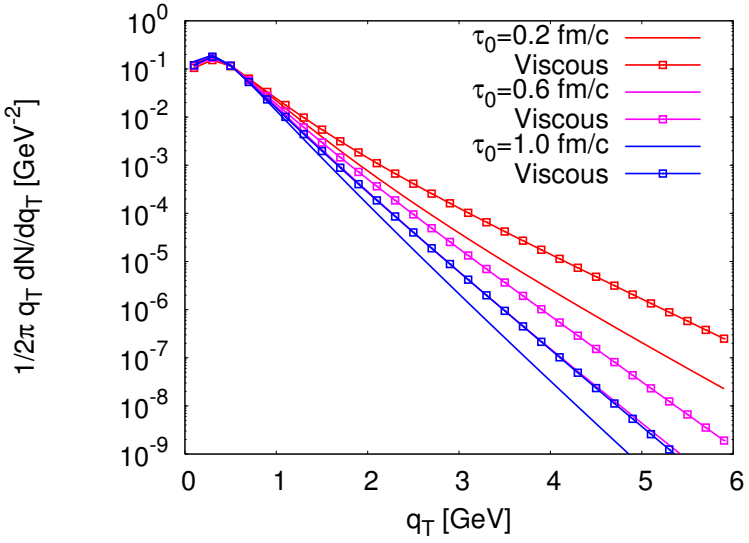


Dusling (2009); Dusling, Lin (2008)

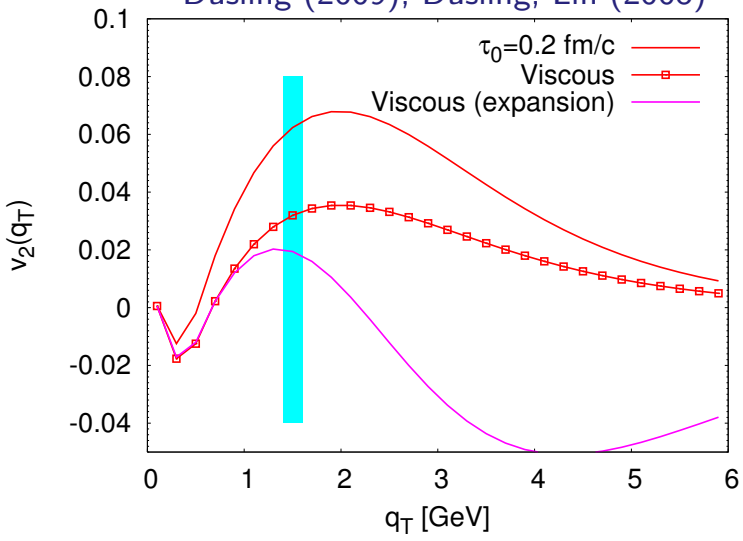


Above calculation shows the kinetic $\delta f$ correction.

See the more sophisticated work by the McGill group.

# Why bulk viscosity?

QCD is clearly not scale invariant and $\zeta \neq 0$.

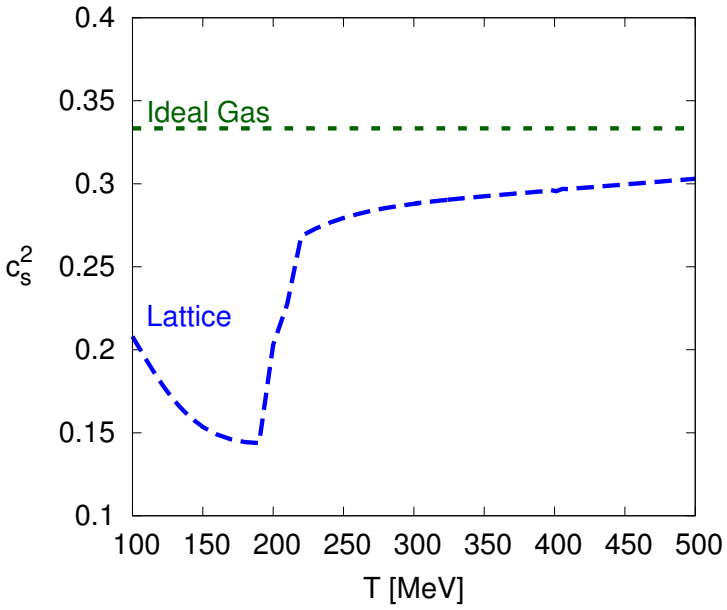


So, do we need to understand bulk viscosity if we want to extract $\eta/s$?
Yes, but bulk viscosity is interesting in its own right.
Has implications for cosmology (*e.g.* relic abundances).

# Relaxation Time Approximation

Approximate collision operator by single relaxation time:

$$\mathcal{C}[\delta f] \simeq -\frac{\delta f}{\tau_R(E_{\mathbf{p}})}$$

Bulk visocisity goes as $2^{\mathrm{nd}}$ power of conformal breaking

$$\zeta \sim \eta \left(\frac{1}{3} - c_s^2\right)^2$$

Weinberg (1972)

while distribution function goes as $1^{\mathrm{st}}$ power

$$\frac{\delta f}{f_o} \sim p_T^2 \left(\frac{1}{3} - c_s^2\right)(\partial \cdot u)$$

Bulk viscous correction dominated by $\delta f$

# QGP distribution functions

QCD: Elastic vs. Inelastic

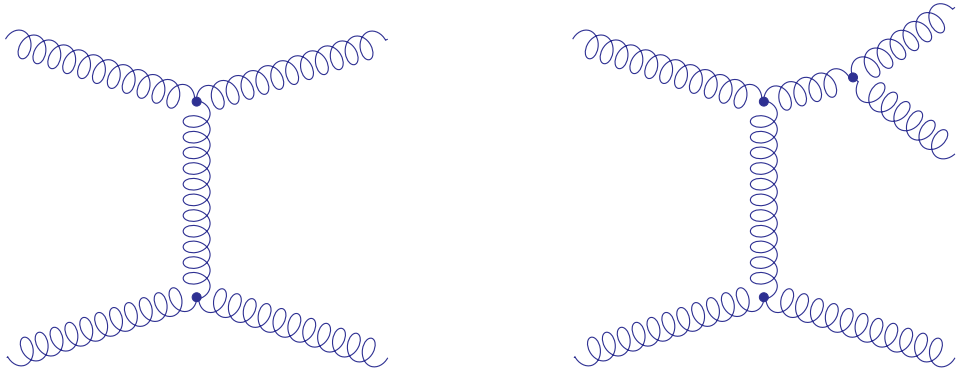

Arnold, Dogan, Moore (2006)

For elastic $2 \leftrightarrow 2$ recast as Fokker-Planck

$$(\partial \cdot u)\left(\frac{p^2}{3} - c_s^2 E_{\mathbf{p}} \frac{\partial\left(\beta E_{\mathbf{p}}\right)}{\partial \beta}\right) = \frac{T\mu_A}{n_{\mathbf{p}}} \frac{\partial}{\partial p^i}\left(n_{\mathbf{p}} \frac{\partial}{\partial p^i}\left[\frac{\delta f_{\mathbf{p}}}{n_{\mathbf{p}}}\right]\right) + \cdots$$

Drag coefficient:

$$\mu_A = \frac{g^2 C_A m_D^2}{8\pi} \ln\left(\frac{T}{m_D}\right)$$

# QGP distribution functions

Result:

$$\delta f_{\text{bulk}} \sim \left(\frac{1}{3} - c_s^2\right) \delta f_{\text{shear}} \qquad \zeta \sim 50 \left(\frac{1}{3} - c_s^2\right)^2 \eta$$

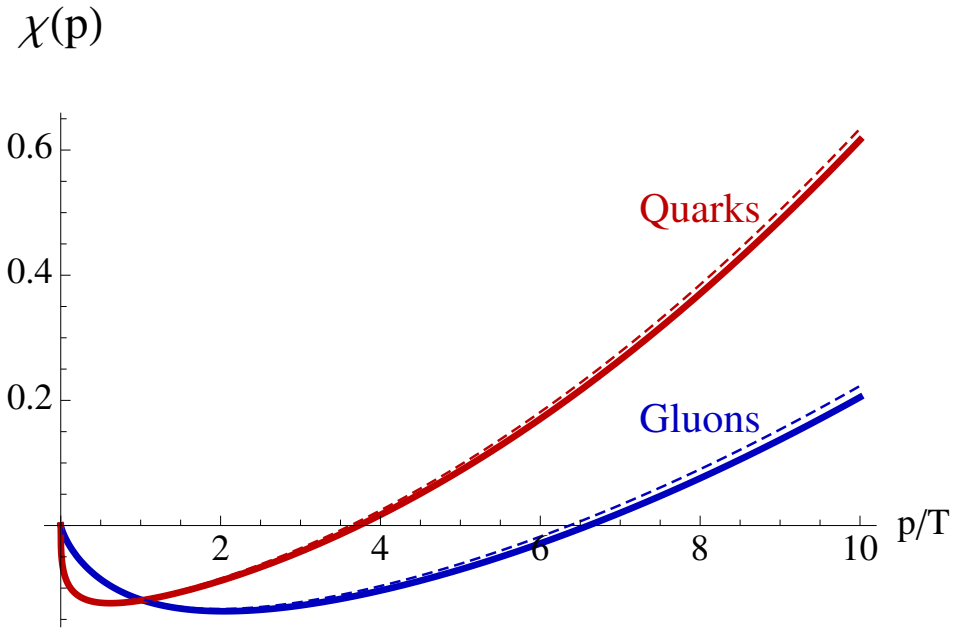


$$\text{where} \quad \delta f = -f_o \, (\partial \cdot u) \, \chi(p)$$

# Pion Gas:

Pion Gas: Elastic vs. Inelastic

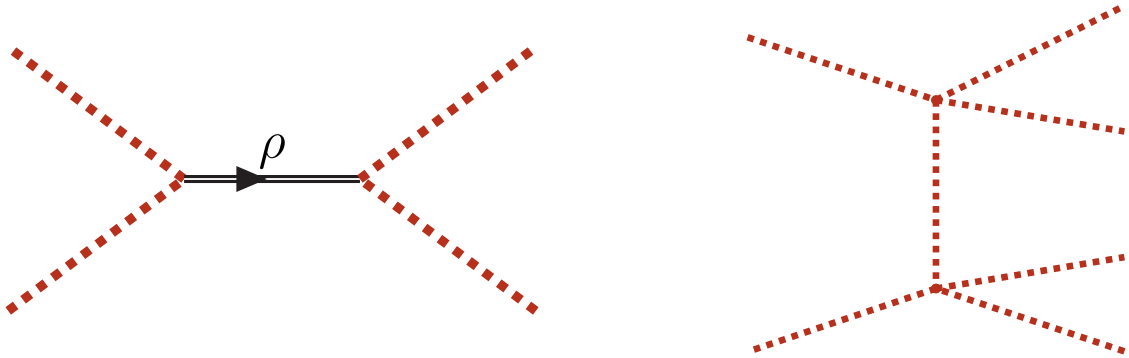


Bulk viscosity governed by chemical non-equilibrium

$\delta f$ takes form of zero mode which dominates $\mathcal{C}^{-1}$

$$\begin{aligned} \delta f &= -f_o\left(\chi_0 - \chi_1 E_{\mathbf{p}}\right)(\partial \cdot u) \\ &= f_o\left(\frac{\delta\mu}{T} + \frac{\delta T}{T^2} E_{\mathbf{p}}\right) \end{aligned}$$

Lu, Moore (2011); Jeon, Yaffe (1995)

# Pion Gas:

Bulk viscosity governed by chemical non-equilibrium

$$\delta f = -f_o \left(\partial \cdot u\right)\left(\chi_0 - \chi_1 E_{\mathbf{p}}\right)$$

Chemical equilibration rate determines $\chi_0$, energy conservation fixed $\chi_1$

$$\chi_0 = \frac{\beta \mathcal{F}}{4\Gamma_{2\pi\to 4\pi}}, \qquad \zeta = \frac{\mathcal{F}^2}{4\Gamma_{2\pi\to 4\pi}}$$

where $\mathcal{F}$ characterizes conformal breaking

$$\mathcal{F} \equiv \int \frac{d^3\mathbf{p}}{(2\pi)^3 E_{\mathbf{p}}}\left(\frac{p^2}{3} - c_s^2 E_{\mathbf{p}}^2\right) f_o$$

# Hadron Resonance Gas: A model

Assume slowest process is chemical relaxation:

$$\delta f^a = -f_o \left(\partial \cdot u\right) \left(\chi_0^a - \chi_1 E_{\mathbf{p}}\right)$$

where $a = \pi, K, \rho, K^*, p, n, \Delta, \cdots$

Slowest rate determines $\zeta$, other rates fix the relative $\delta f^a$:

$$\chi_0^a \simeq \chi_0^\pi \times \begin{cases} 2 & \text{Mesons} \\ 2.5 & \text{Baryons} \end{cases}$$

Motivated by $\mu_\rho = 2\mu_\pi$ and $2\mu_N = 5\mu_\pi$:

Goity (1993); Pratt, Haglin (1999)

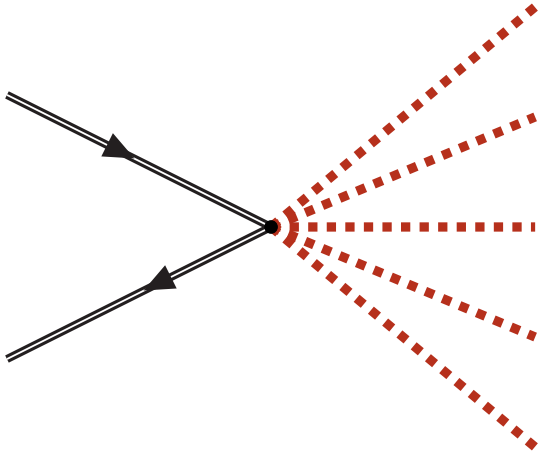

# Hadron Resonance Gas: A model

Hadron Gas: $\zeta$ determined by chemical non-equilibration

Bottom line for $\delta f$:

- $\delta\mu \sim \frac{\zeta}{s}\left(\partial \cdot u\right)$
- temperature shift $\delta T \approx 0.25\delta\mu$ to conserve energy

A new (dynamical) way to look at fugacity factors

# Pion / Proton $p_T$ spectra

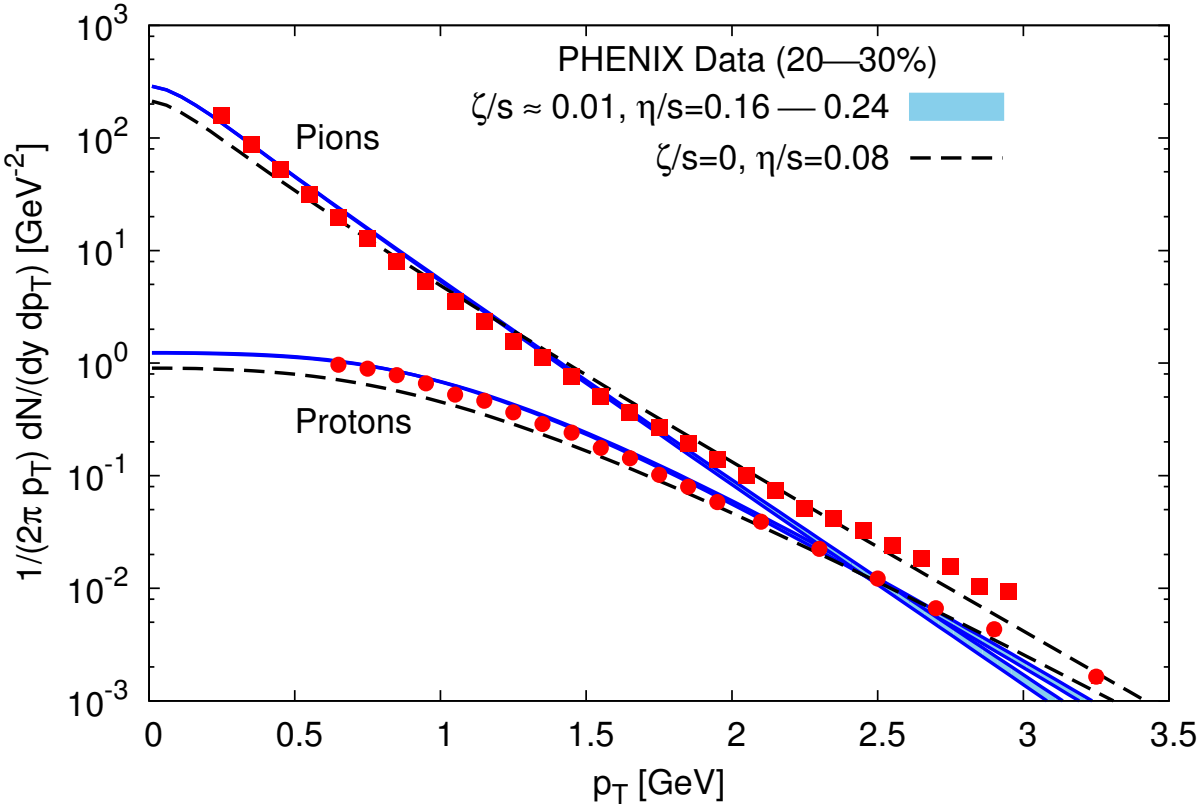


Data: PHENIX nucl-ex/0307022.

LHC: Bozek & Wyskiel arxiv:1203.6513

# Pion / Proton differential $v_2(p_T)$ spectra

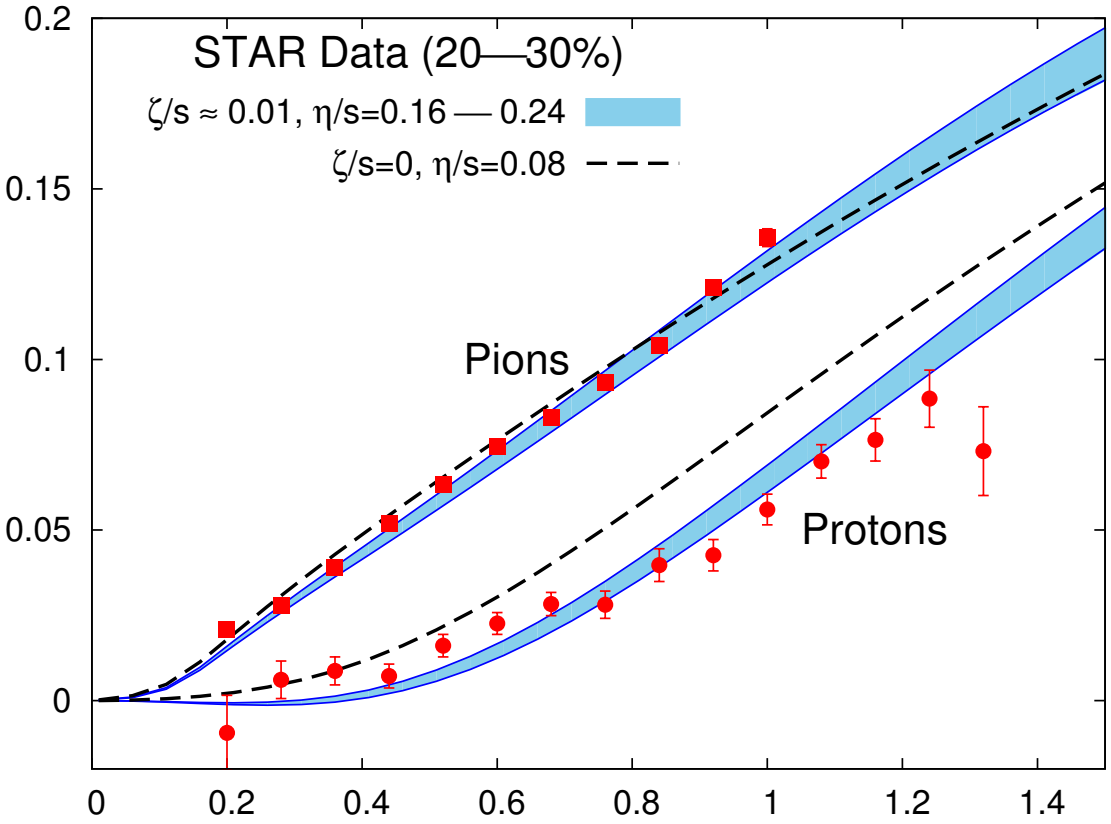


Data: STAR, nucl-ex/0409033.

# Bulk viscosity and EM probes

As for shear viscosity, bulk $\delta f$ modifies photon rates

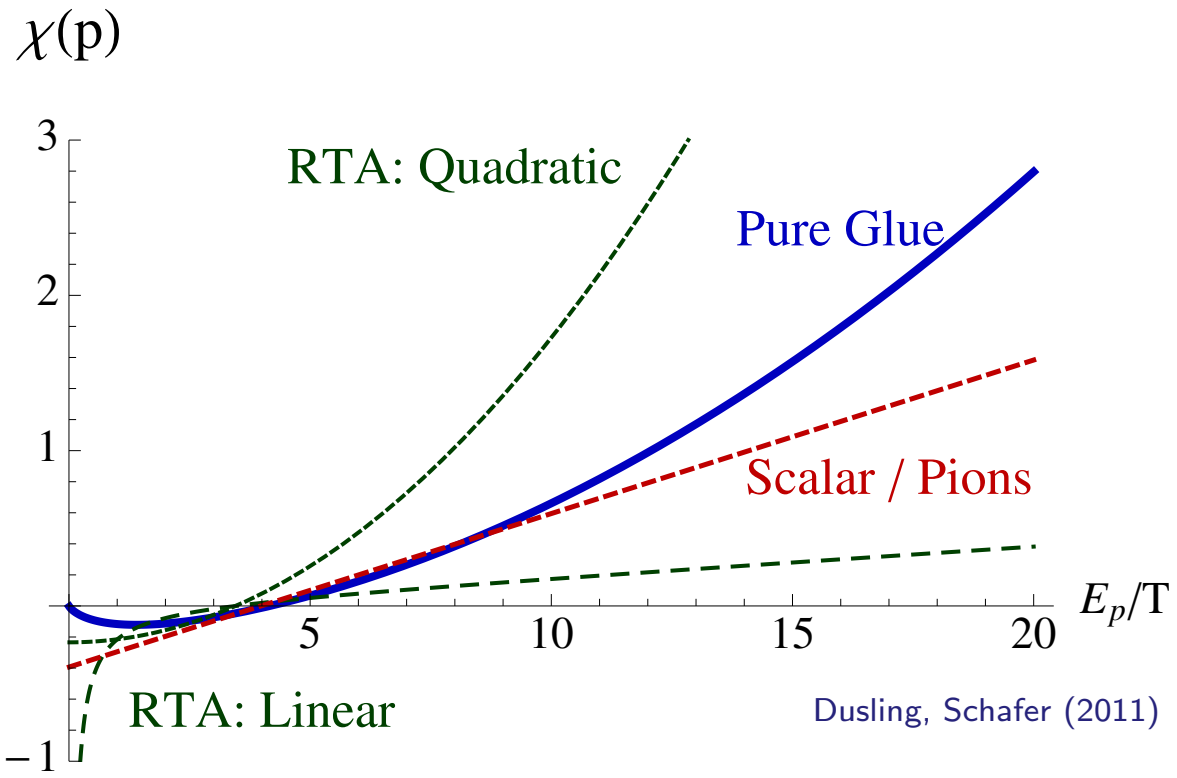


Dusling, Schafer (2011)

# Bulk viscosity and EM probes

First shot:

- Using AMY rates with $f \to f + \delta f$ and pQCD $\delta f$
- Using $\chi$RF (Steele, Yamagishi, Zahed) with
  - $z_\pi^3$ enhancement with $\mu_\pi \sim \zeta/s\,(\partial \cdot u)$
  - $T \to T - \delta T$
- Results preliminary: Need to
  - include shear viscosity
  - fine-tune initial condition
  - worry about pQCD at high $q_T$
  - $\ldots$

# Ideal photon $v_2(q_T)$

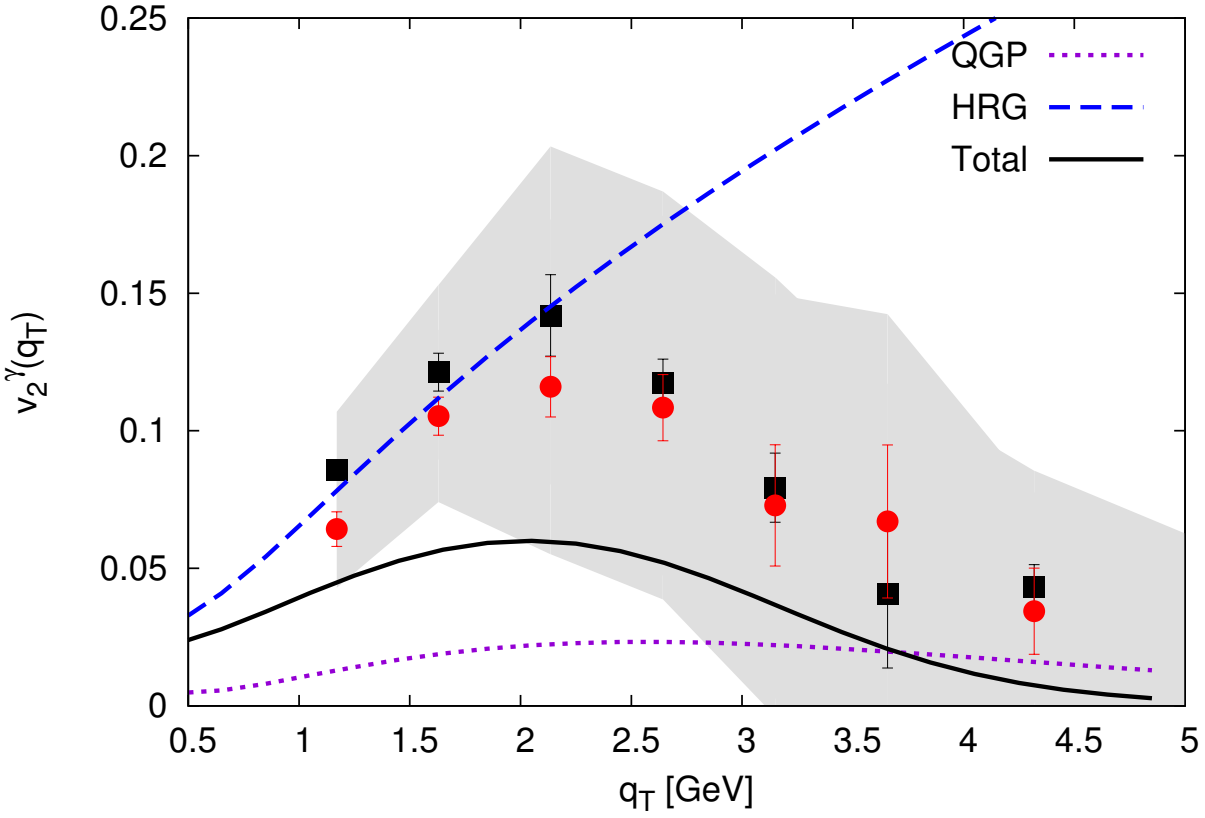

# Viscous photon $v_2(q_T)$

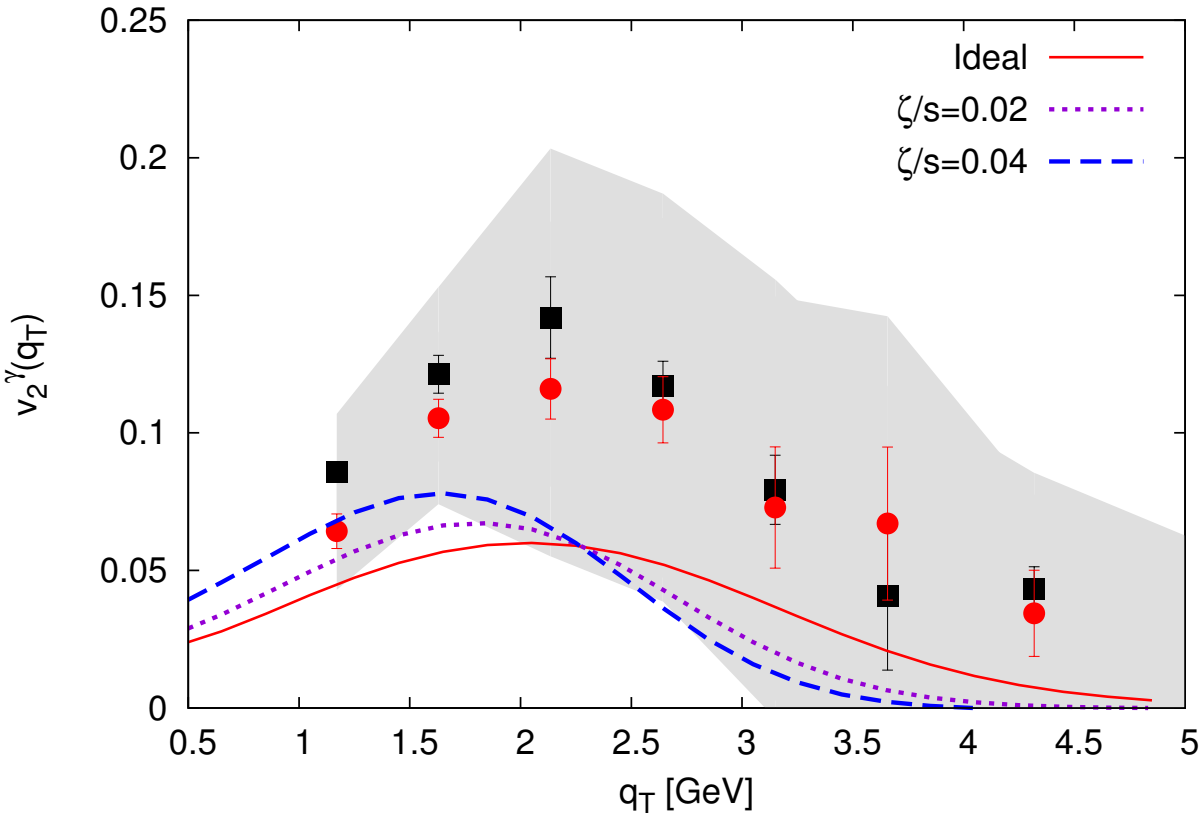


Only including bulk viscosity – no fine-tuning.

# Summary

Bulk viscosity is not zero:

- fine structure of spectra improves
- may help with photon $v_2$
- dynamical mechanism for fugacity factors

# Backup Slides

# Ideal photon $q_T$ spectra

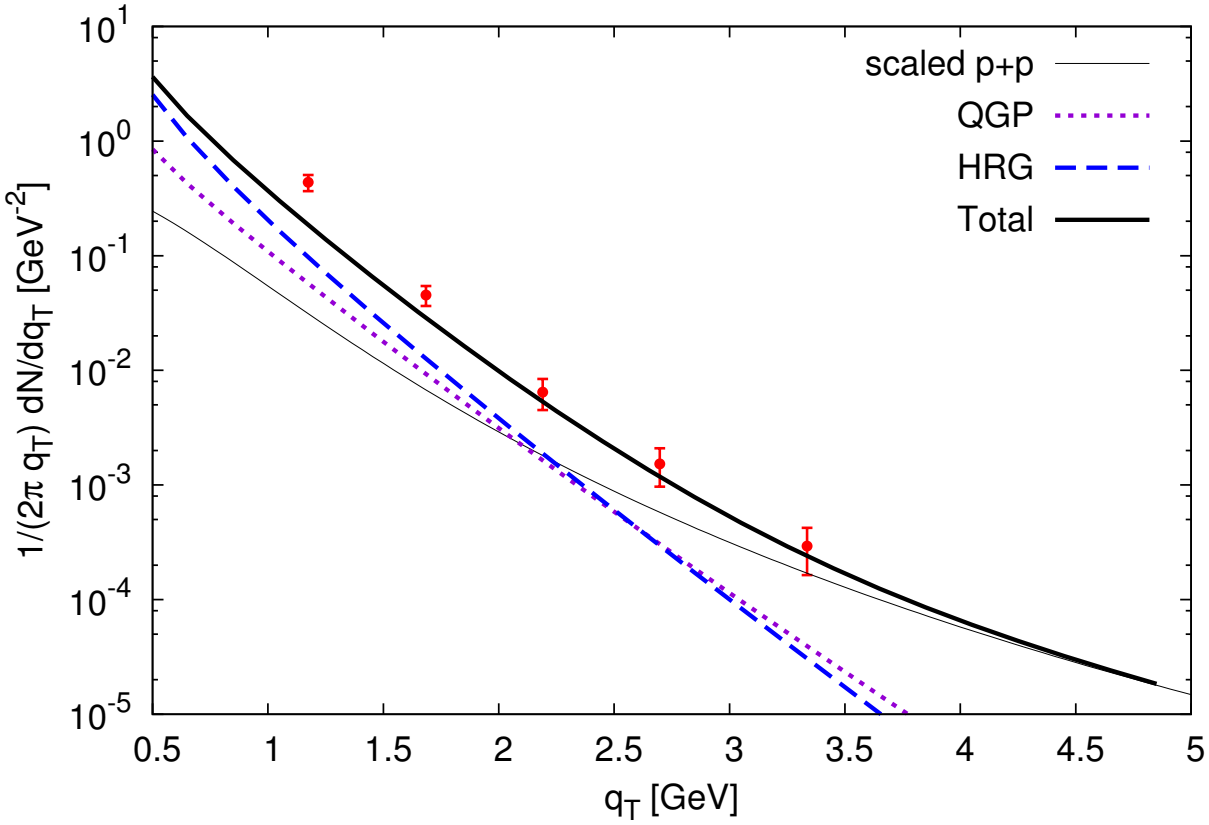

# Viscous photon $q_T$ spectra

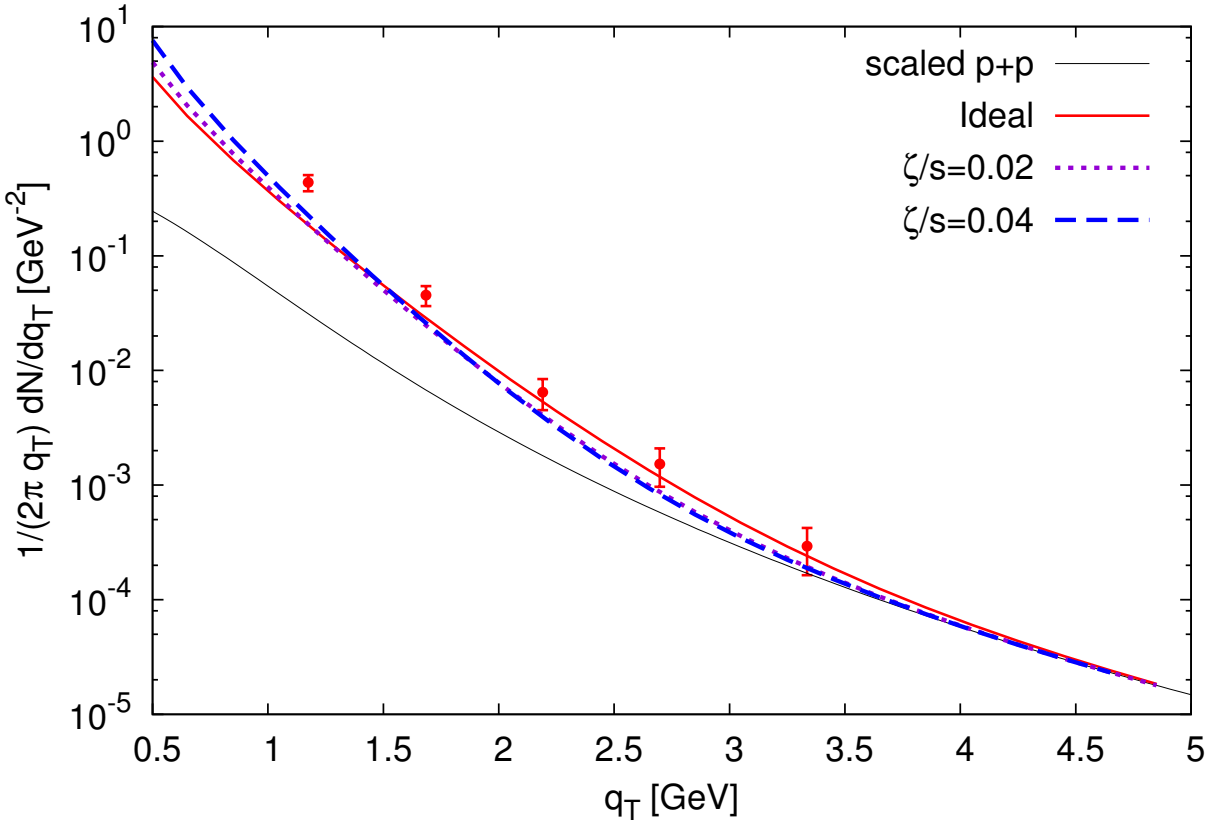


Only including bulk viscosity – no fine-tuning.

# Thermal photon production

At leading order in $\alpha_{\rm em}$ but all orders in $\alpha_{\rm s}$

$$\frac{dN}{d^4Q} = \frac{\alpha_{\rm em}^2}{6\pi^3}\frac{1}{Q^4}\left(Q^\mu Q^\nu - Q^2 g^{\mu\nu}\right) W_{\mu\nu}(Q)$$

where

$$W_{\mu\nu}(Q) \equiv \int d^4x\, e^{-iQ\cdot X} \langle J_\mu^{\rm em}(X) J_\nu^{\dagger,{\rm em}}(0)\rangle_\beta$$

Evaluate $W_{\mu\nu}$ in two different ways

- Vacuum spectral functions
- Kinetic Theory

# Thermal photon production

Kinetic theory (all processes $I \to F + l^+ l^-$):

$$W_{\mu\nu}(Q) = \sum_F \sum_I \int d^4x \; e^{-iQ\cdot X} \langle I | J_\mu^{\rm em}(X) | F \rangle \langle F | J_\nu^{\dagger,{\rm em}}(0) | F \rangle \frac{e^{-\beta E_I}}{\mathcal{Z}}$$

using $E_I = E_F + Q_0$ and $\sum_I |I\rangle\langle I| = 1$

$$W_{\mu\nu}(Q) = e^{-\beta Q_0} \sum_F \int d^4x \; e^{+iQ\cdot X} \langle F | J_\mu^{\dagger,{\rm em}}(X) J_\nu^{\rm em}(0) | F \rangle \frac{e^{-\beta E_F}}{\mathcal{Z}}$$

McLerran & Toimela, 1985

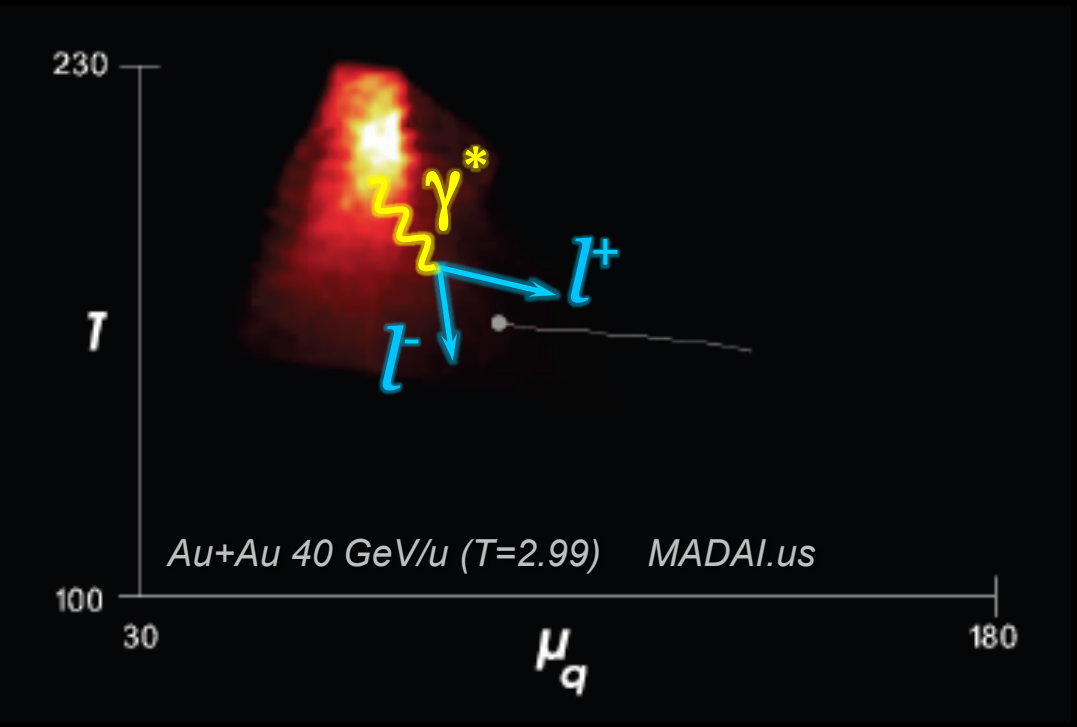


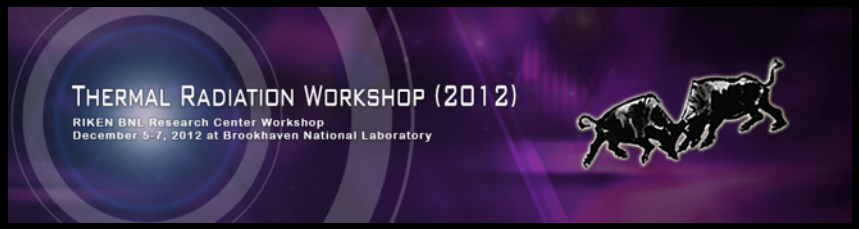


# Results on virtual-photon production at SIS: resume and prospects

*Tetyana Galatyuk*
*TU Darmstadt / GSI*
*for the HADES and CBM Collaborations*

TECHNISCHE UNIVERSITÄT DARMSTADT

GSI

EMMI

# High Acceptance DiElectron Spectrometer

# The HADES mission





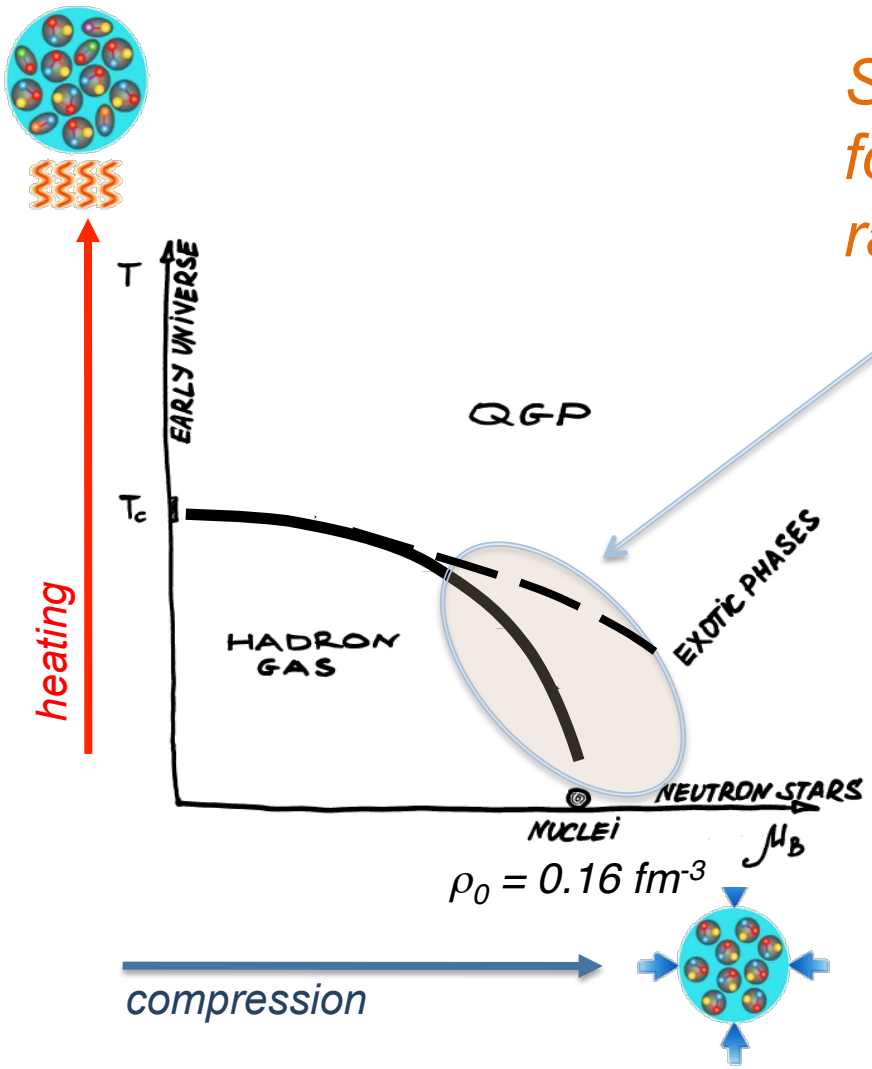


*Search (in this region) for new states of matter with rare and penetrating probes*

- Stage I (2002 - 2008)
  - Limited granularity of time-of-flight system → light collision systems
- Stage II (2012 - 2015)
  - Heavy collision-systems
  - $\pi$-induced reactions
- Stage III (2018 - …)
  - Lepton pair excitation function up to 8 GeV/u (medium-heavy systems) and (multi-)strange particle

*+ Various aspects of baryon-resonances physics*

# Dileptons and the phase diagram of matter

„I wonder if it finally will turn into a bluff...“





## Use ρ as a probe for the restoration of χ symmetry

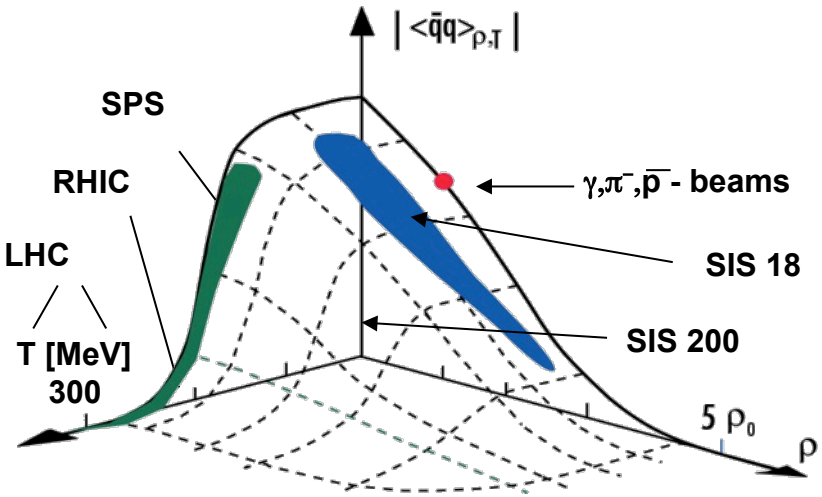


Robert D. Pisarski, PLB 110 (1982),

…

## Dileptons from exotic phases…

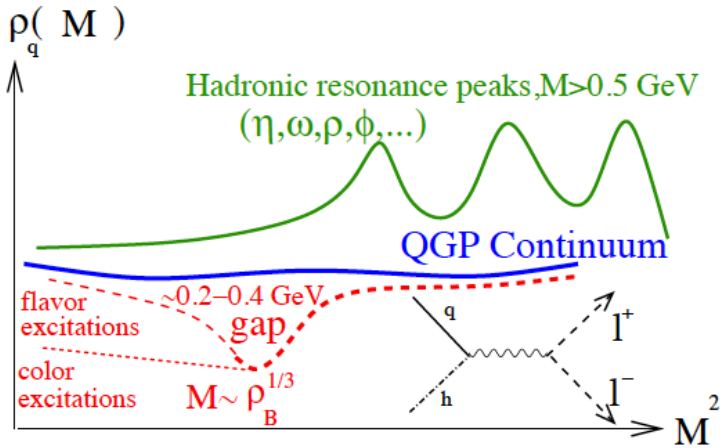


S. Lottini and G. Torrieri, ***PRL 107***, 152301 (2011)
S. Lottini and G. Torrieri, arXiv:1204.3272v1 [nucl-th]

…

→ Experimental test

# The experimental challenge…



- Lepton pairs are rare probes (branching ratio O($10^{-4}$))
- at SIS18 energies vector mesons are produced sub-threshold (NN)

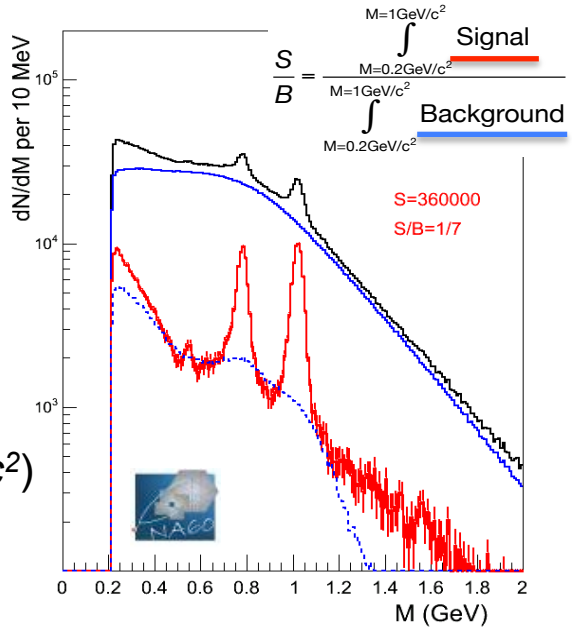


- Large combinatorial background from:
  - **$e^+e^-$:** Dalitz decays ($\pi^0$) and conversion pairs
  - **$\mu^+\mu^-$:** weak $\pi$, K decays
- Isolate the contribution to the spectrum from the dense stage (***X Factor*** = *excess yield above hadronic cocktail in $0.2<M_{ll}<0.6$ GeV/$c^2$*)

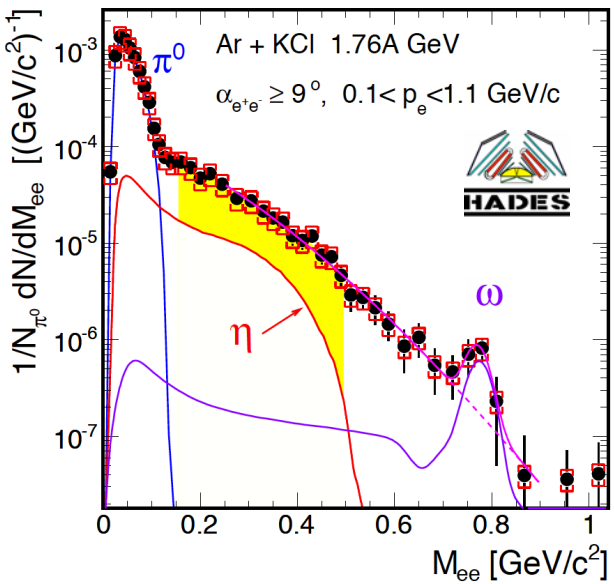


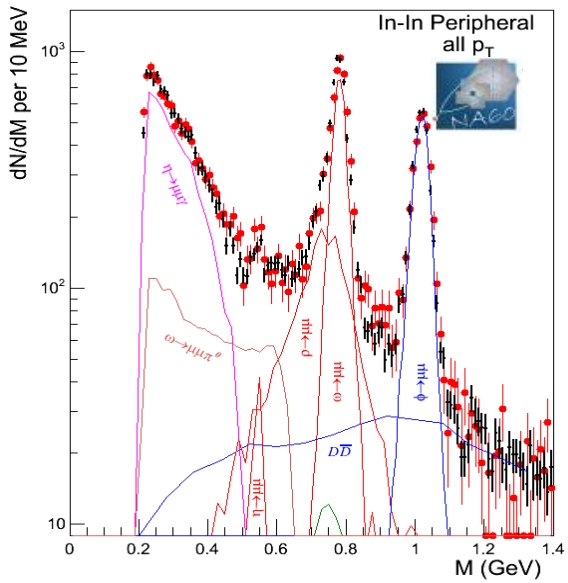

# High Acceptance Di-Electron Spectrometer





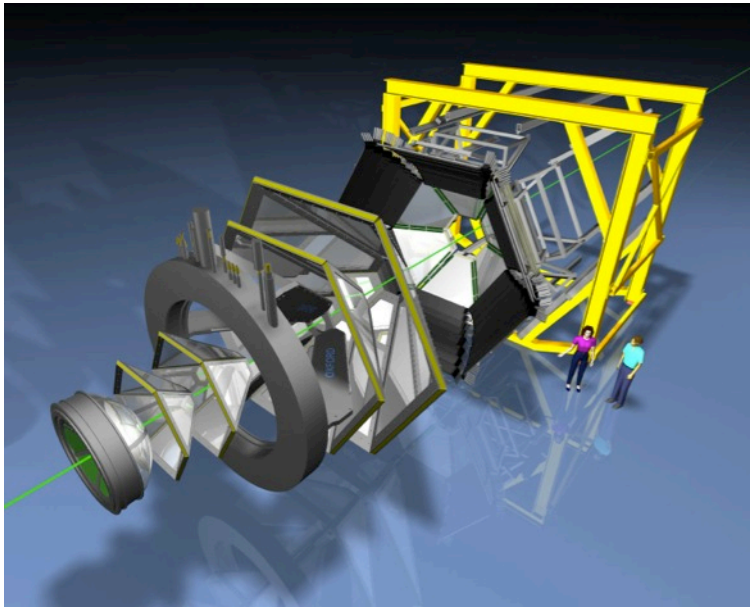

**HADES strategy:**
Systematic di-electron and strangeness measurements in NN, AA, pA, πN and πA collisions

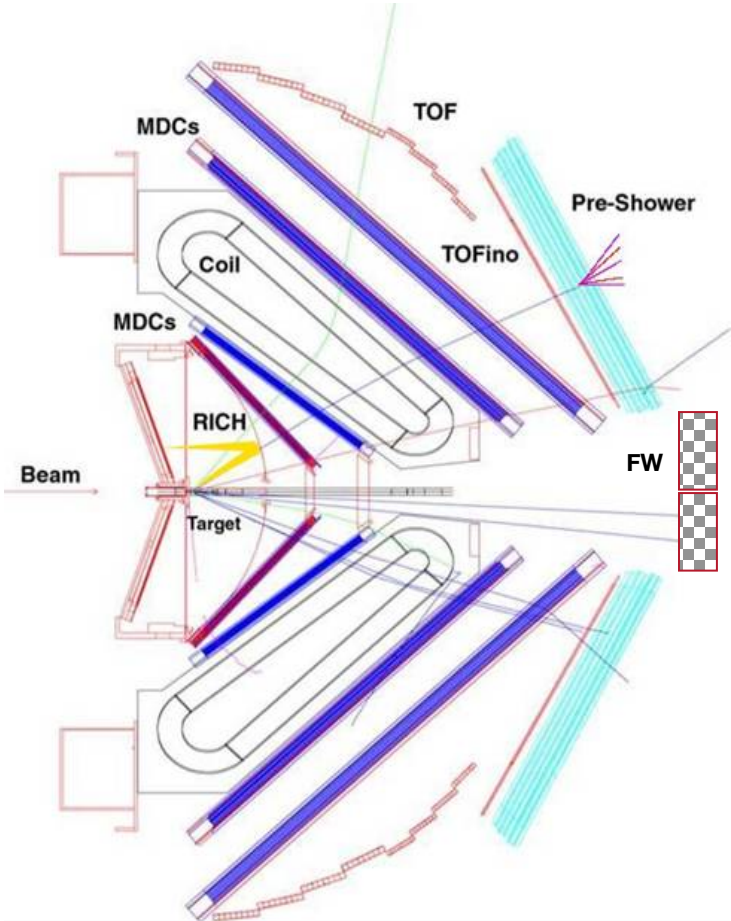


- Beams provided by SIS18: π, p, ions

- Full azimuthal coverage
- Hadron and lepton identification

- $e^+e^-$ pair acceptance 0.35
- **Mass resolution 2 % (ρ/ω region)**

- ~ 80.000 channels
- now: **up to 50 kHz event rate (400 Mbyte/s peak data rate)**

# NN Reference: $e^+e^-$ in p+p collisions at 1.25 GeV

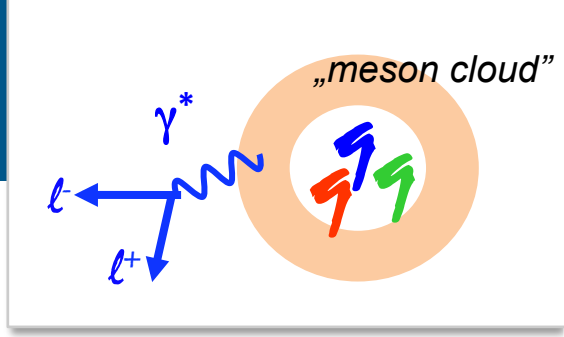






HADES : PLB 690 (2010) 118

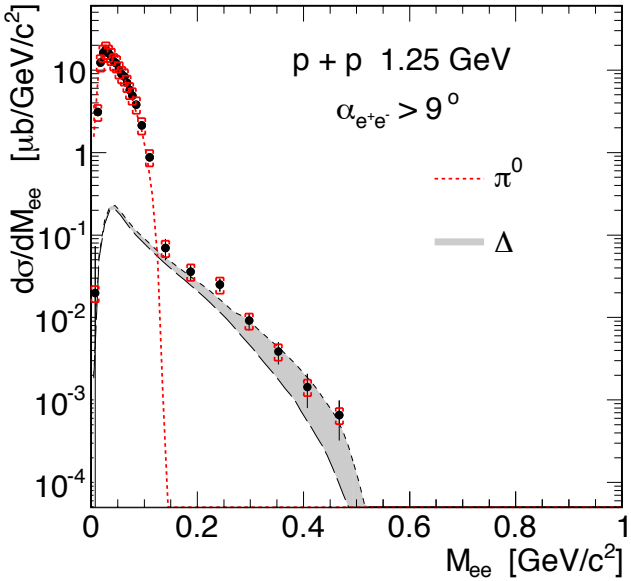


HADES : PLB 690 (2010) 118

*time-like region $q^2 > 0$*

**Goal**

- Understand Δ → N γ* transition
  - **Known from γN → Δ → πN**
    *(exact QED calculation, Krivoruchenko et al. PRD 65 (2001) 017502)*
  - **Unknown at $q^2$ >0!**

  → use models fitted to the space-like data

  *G. Ramalho and T. Pena arxiv: 1205.2575v1 (2012)*
  *Wan and Iachello, int. J. Mod. Phys. A20 (2005) 1846*

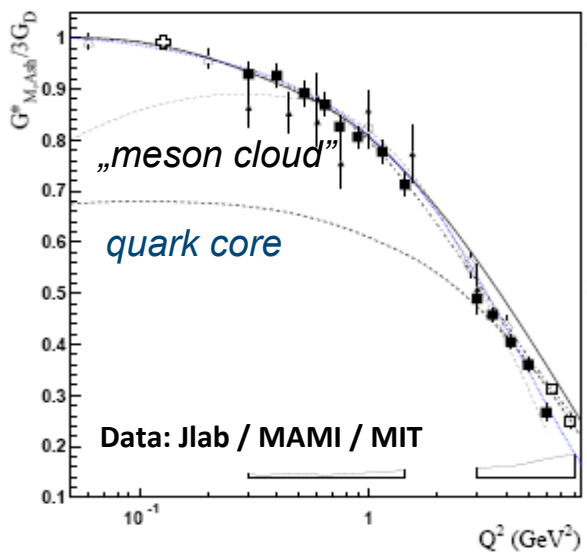


*space-like region $q^2 < 0$*

- Excitation of a baryon can be carried by the meson cloud
  - Precise data from Jlab / MAMI / MIT
  - **Strong hint for dominant contribution to the $G_M(Q^2)$ from the meson cloud (30% at $G_M(0)$)**
    *I.G. Aznauryan, V.D. Burkert Prog. Part. Nucl. Phys. 67, 1 (2012)*

# NN Reference: exclusive analysis $pp \rightarrow ppe^+e^-$





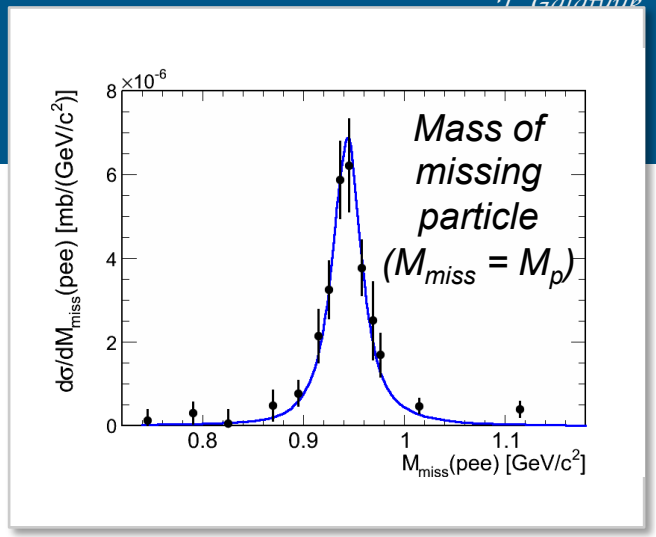


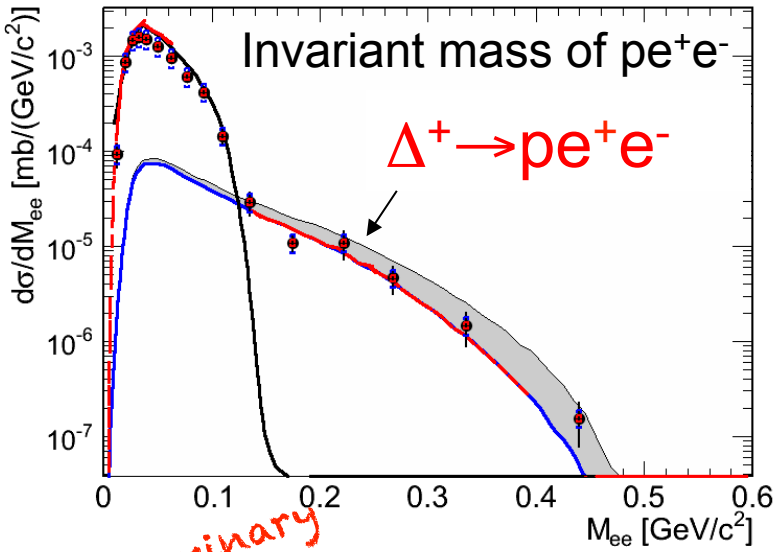


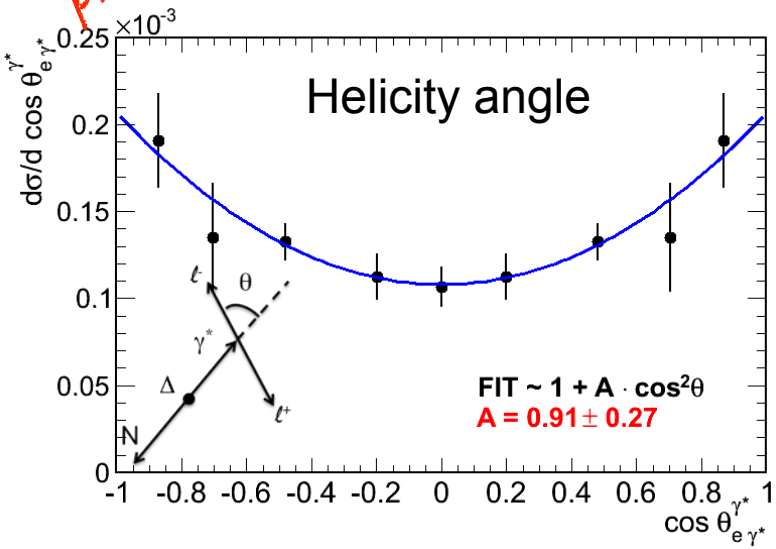


- **First direct access to the Δ transition form factor in the time-like region**
  - Data agree with QED calculation!
  - Branching ratio ($\Delta^+ \rightarrow pe^+e^-$) = $4.2 \times 10^{-5}$

# NN Reference: $e^+e^-$ in QF n+p collisions $\sqrt{s} - 2m_N \approx m_\eta$

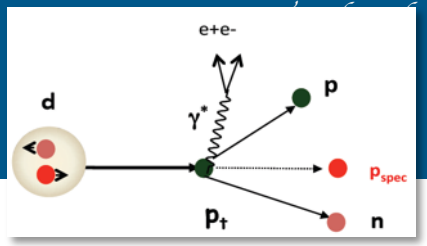






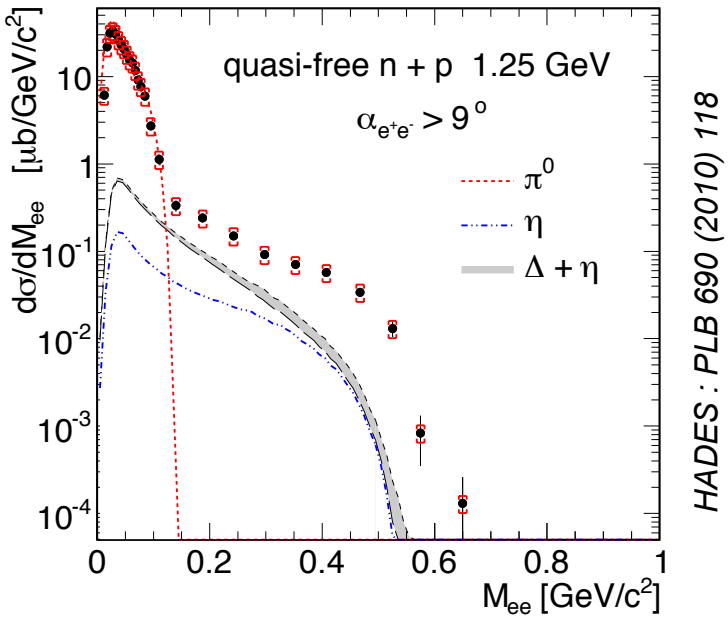


HADES : PLB 690 (2010) 118

- Large isospin dependence in dilepton production!
  - Role of the momentum distribution of the neutron inside the deuteron?
  - NN bremsstrahlung?

→ Check with One Boson Exchange effective Lagrangian based approach

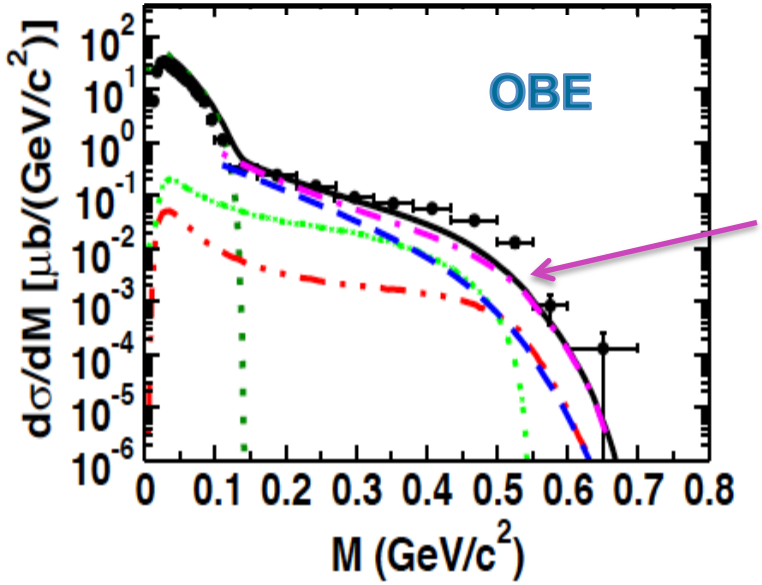


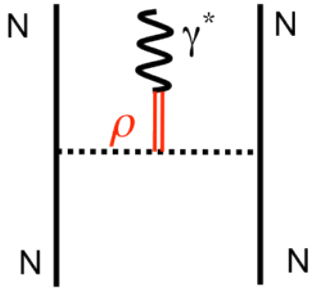


Much better agreement with data when including π em form factor

→

**Sensitivity to hadronic electromagnetic structure**

*R. Shyam and U. Mosel, PRC 82:062201, 2010*

# NN Reference: $e^+e^-$ in p+p collisions at 2.2 GeV and 3.5 GeV





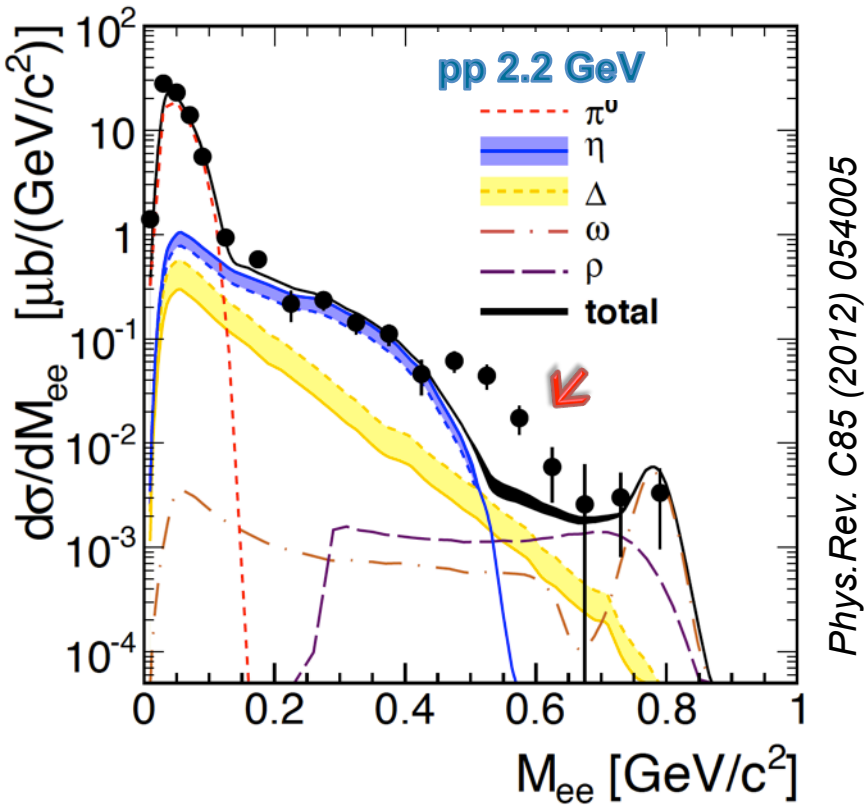


Phys.Rev. C85 (2012) 054005

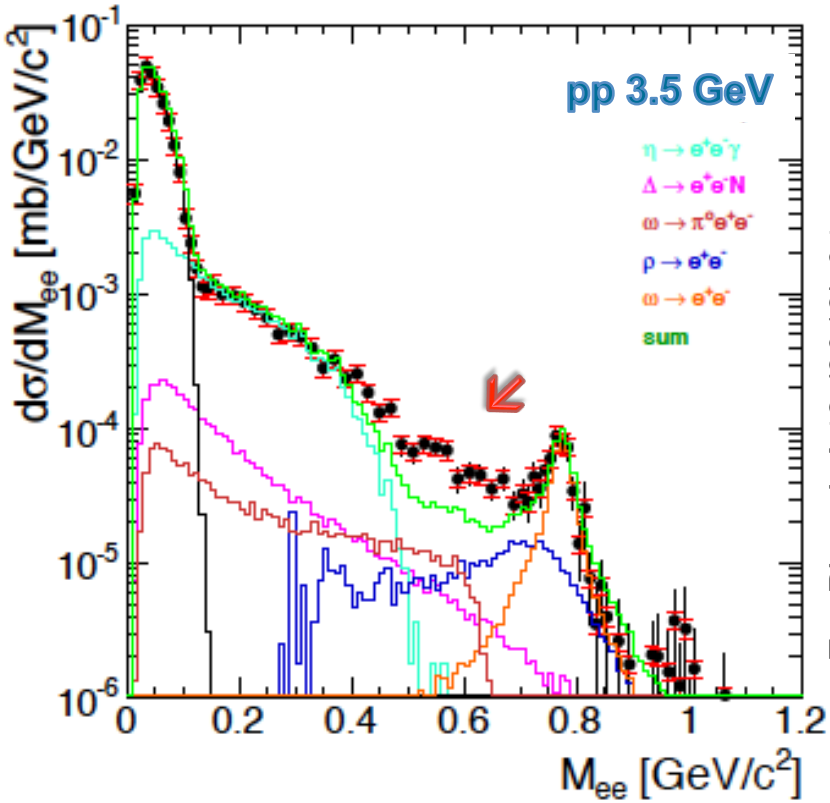


Eur.Phys.J. A48 (2012) 64

**PDG Enrty 2012**
**BR(η→e+e-) < 5.6x10$^{-6}$ (90% CL)**

- Effect of electromagnetic form factor?
  → Dalitz decays of broad resonances is not well understood theoretically

- Coupling of ρ to baryonic resonances
  → Cross check with hadronic final states needed!

# Reconstruction of contributing baryonic resonances: exclusive analysis of pp → pnπ⁺ ans pp → ppπ⁰





*nπ⁺ invariant mass*

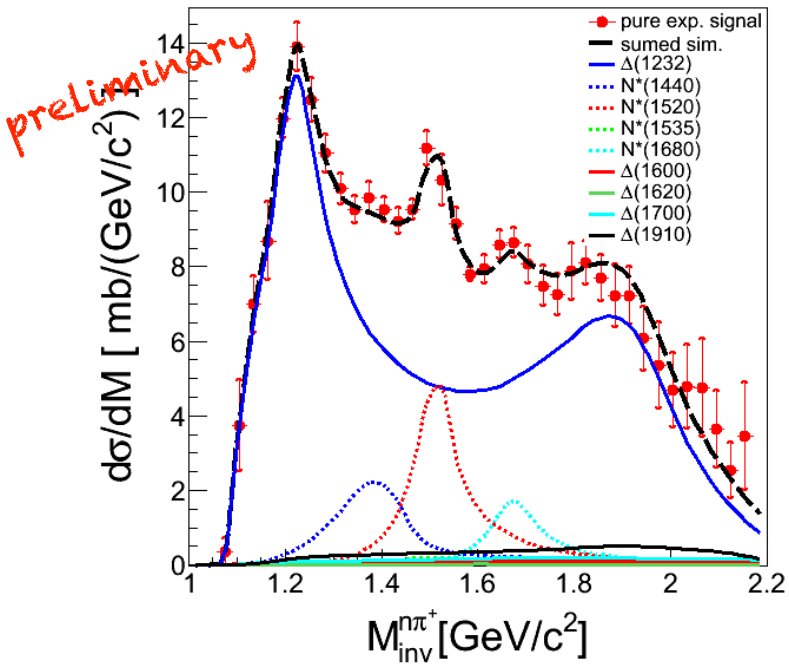


*pπ⁺ angular distribution*

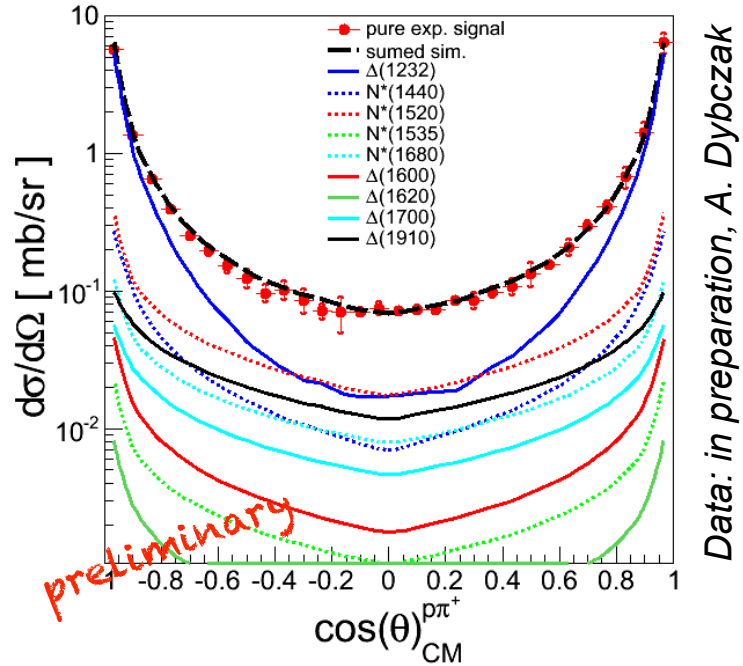


- 14 baryonic resonances are included in the analysis (N*1535 constrained by pp → ppη channel)
  *K. Teilab Int.J.Mod.Phys.A26:694-696,2011*

→ *pp → ppe⁺e⁻*

- Cross section for resonance production via exclusive analysis of pp → pnπ⁺ and pp → ppπ⁰

# Exclusive dilepton production





## Exclusive analysis: pp → ppe⁺e⁻

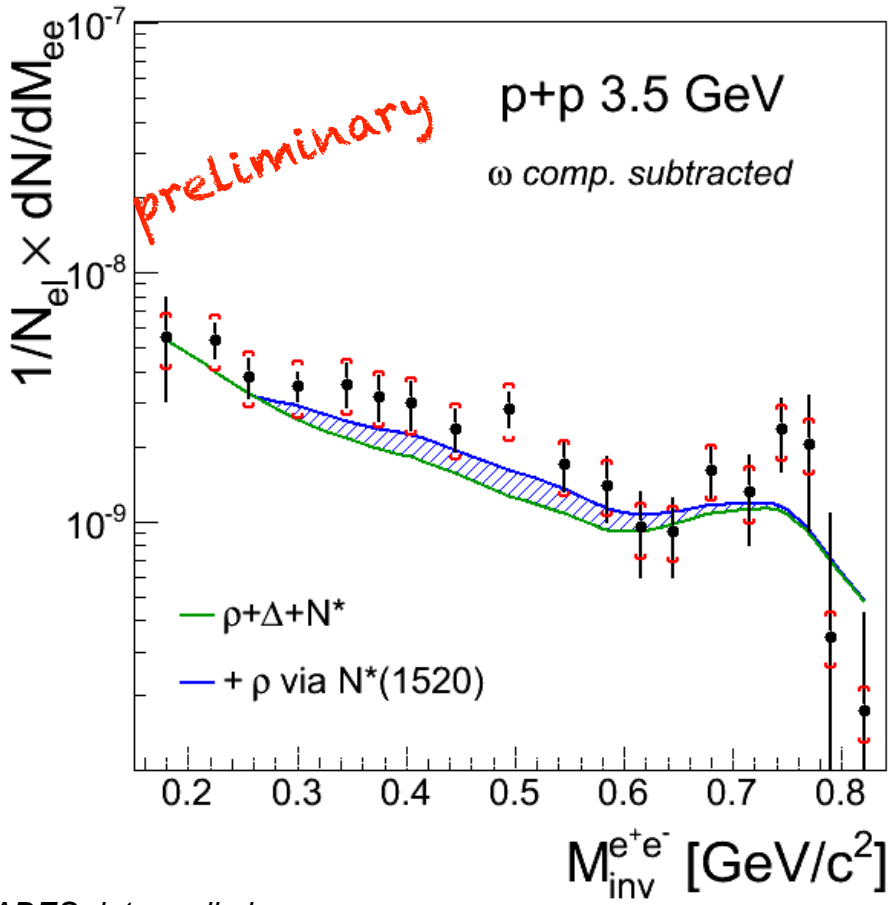


*HADES data preliminary*
*Model: M. Zetenyi and Gy. Wolf*
*Phys. Rev. C 67, 044002 (2003).*

- Relative contribution is fixed through exclusive pion production
- ω contribution subtracted, η contribution suppressed by kinematics

**Dalitz decays of baryonic resonances – are the dominant source at low beam energies.**

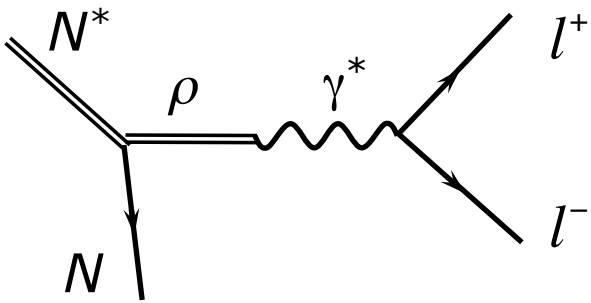

# Electron pairs from cold nuclear matter

*"if you are out to describe the truth, leave elegance to the tailor" (A. Einstein)*





*HADES: Phys.Lett. B715 (2012) 304-309*

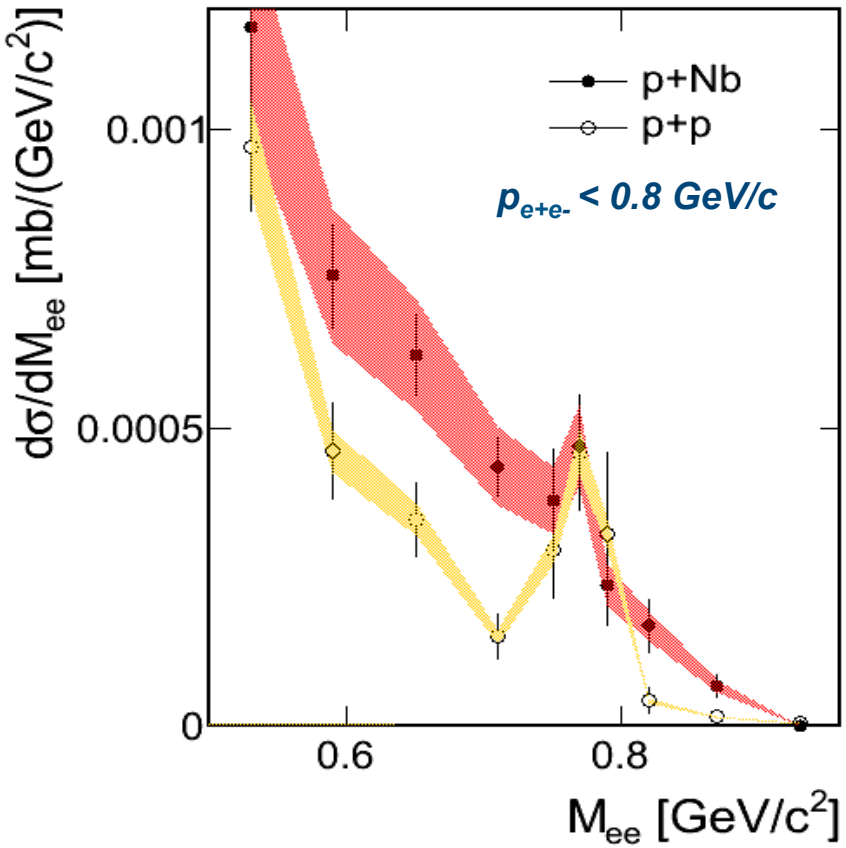


- **First measurement of lepton pairs with $p_{e+e-}$ < 0.8 GeV/c radiated from cold matter**
  → not measured in this region by CLAS, KEK-E325
- Mass resolution: $\sigma_{M\omega}$ **= 16 MeV/c$^2$**
- Clear **excess over p+p**
  → role of the secondary ρ from N(1520), Δ (1700)…?
- **Reduced ω yield** → strong broadening?

# Virtual photon emission in A+A collisions





Ar+KCl compared to reference
after subtraction of contributions from η

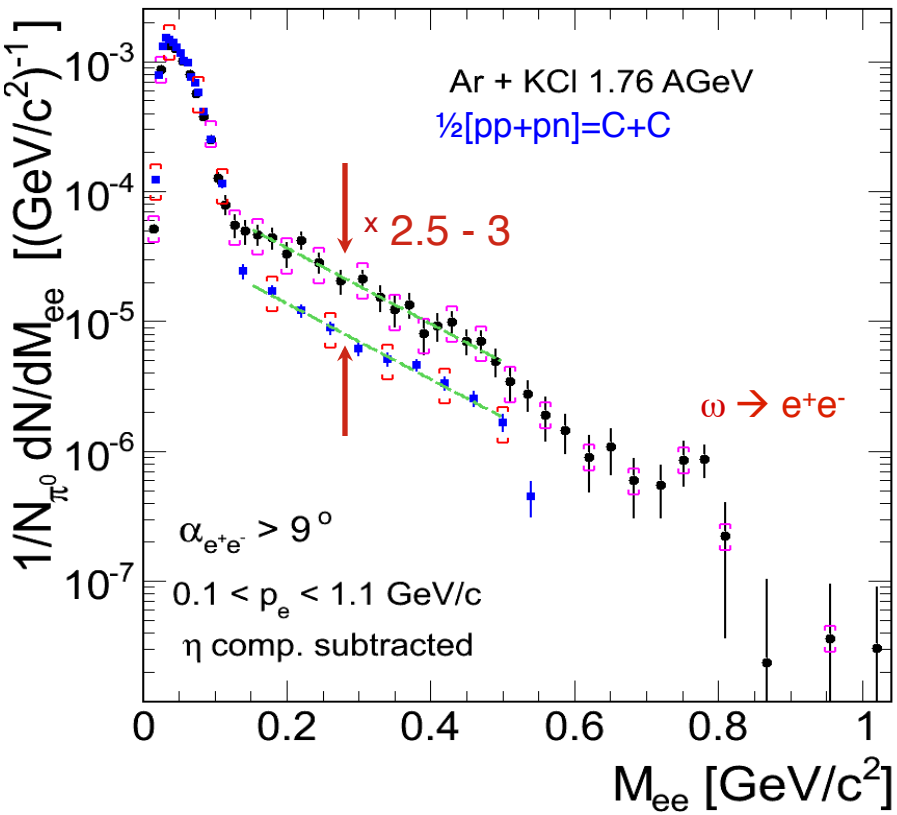


- **First evidence for radiation from the "medium"!**
- Excess yield scales with system size like $A_{part}^{1.4}$

*Quest for heavier systems!*

*HADES: Phys.Rev.C84:014902,2011*

# Isolation of excess by a comparison with a measured decay cocktail





## Excess $e^+e^-$ yield in p+Nb 3.5 GeV

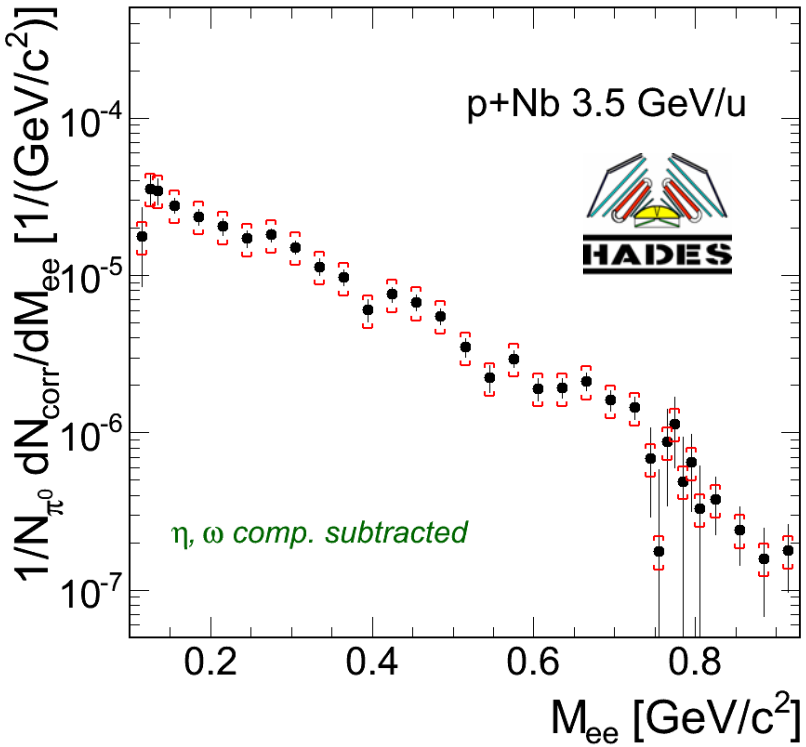


**In medium ρ modification?**
→ will be answered only after pp reference is understood!

- Full reconstruction of $\pi^0$ and η decays (meson → $e^+e^-e^+e^-$)

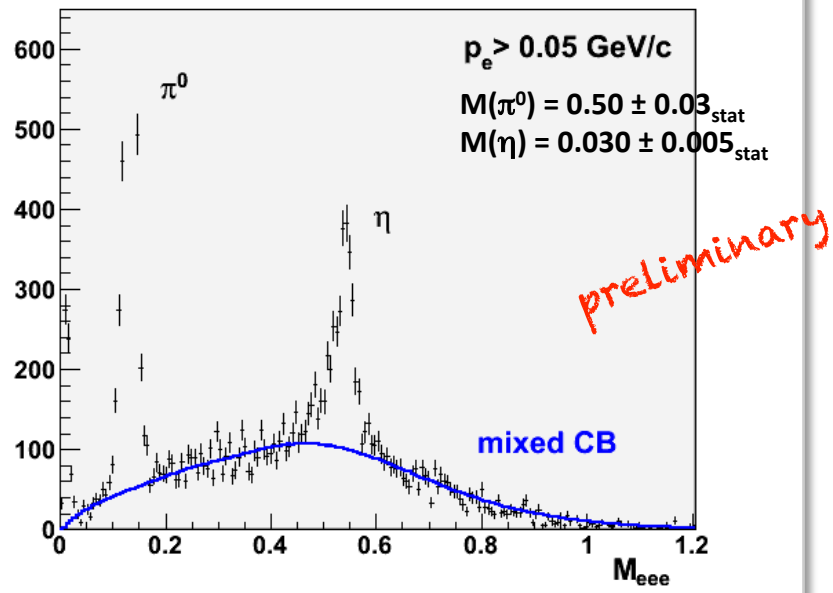


- HADES η cross section provides constraint on Δ and N* contributions!
- Critical test for theoretical input!

# The ρ meson in a hot and/or dense fireballs: from SIS18 to SPS





## Acc.-corrected $\mu^+\mu^-$ excess spectrum

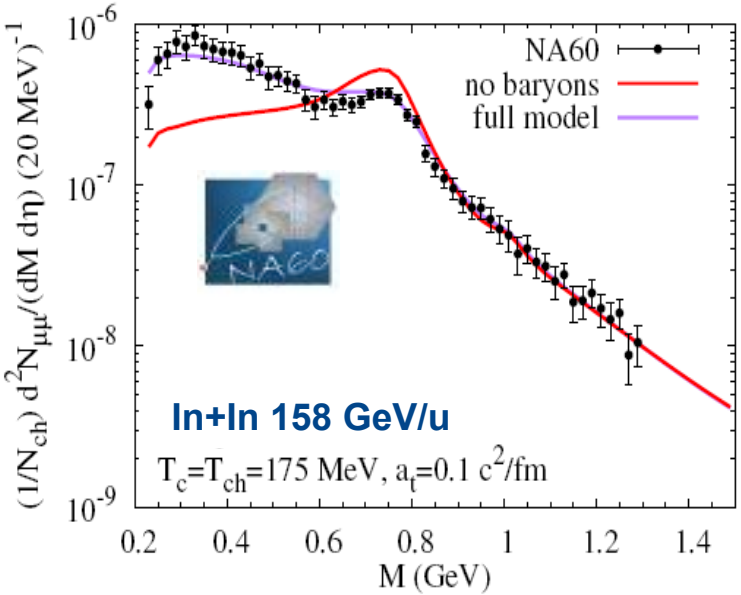


*Data: EPJC 59 (2009) 607*
*R.Rapp: NPA806 (2008) 339*

- Main source: $\pi^+\pi^- \rightarrow \rho \rightarrow e^+e^-$
- Low mass enhancement is **due to coupling of the VM to baryons**!

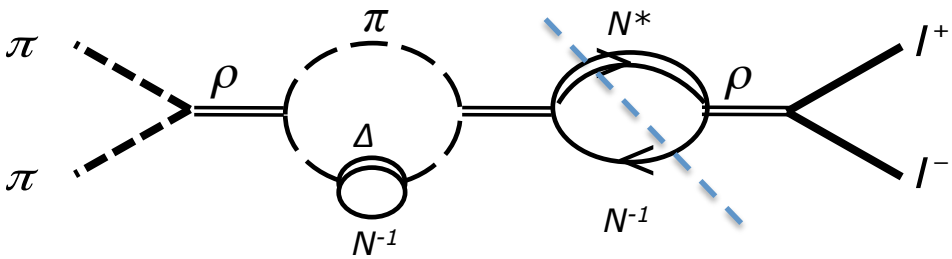


## Excess $e^+e^-$ yield, Ar+KCl 1.76 GeV/u

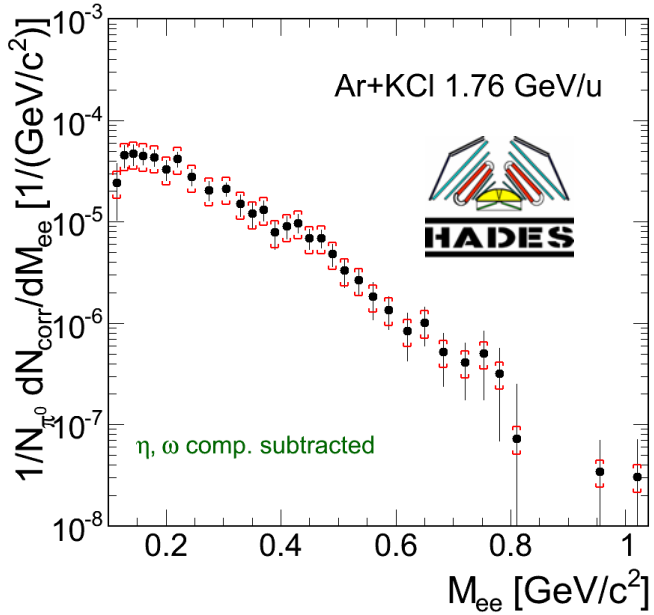


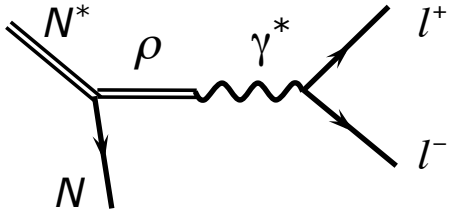


**Dalitz decays of baryonic resonances – dominant source at SIS18!**

# Dileptons, baryonic resonances and the phase diagram of matter





R. Rapp, Acta Phys. Polon. B 42, 2823, 2011

**In-medium ρ spectral function**

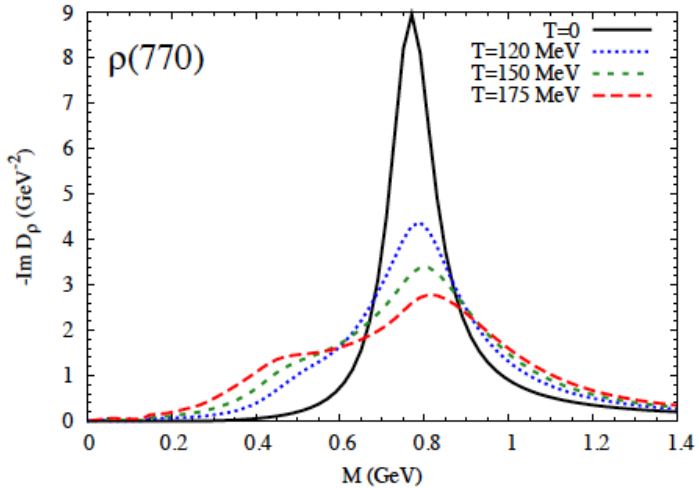


**Temperature dependence of the chiral quark condensate**

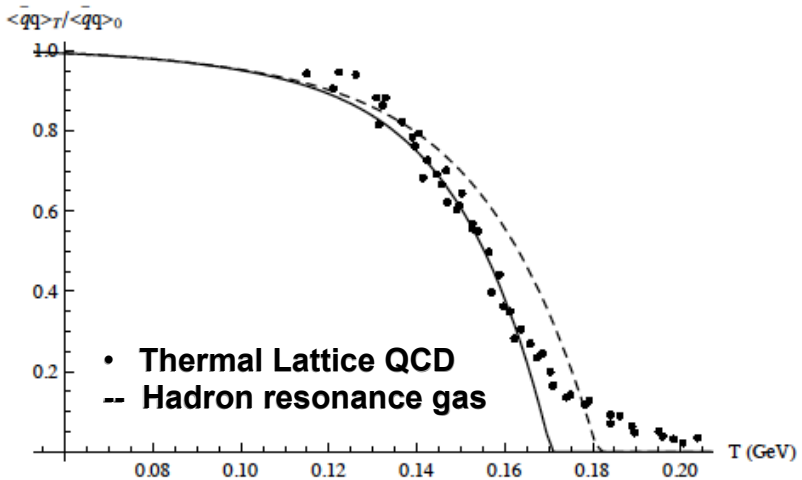


S. Borsanyi et al., JHEP 1009, 073 (2010)

**effective hadronic theory** ⟺ $\frac{\langle\bar{q}q\rangle(T,\mu_B)}{\langle\bar{q}q\rangle_0} = 1 - \sum_h \frac{\varrho_h^s \Sigma_h}{m_\pi^2 f_\pi^2}$

***1.*** $\Sigma_h = m_q \langle h|q\bar{q}|h\rangle > 0$ contains ***quark core + "pion cloud"***

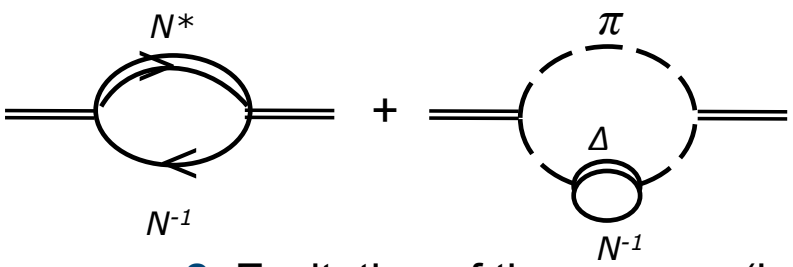


⟺

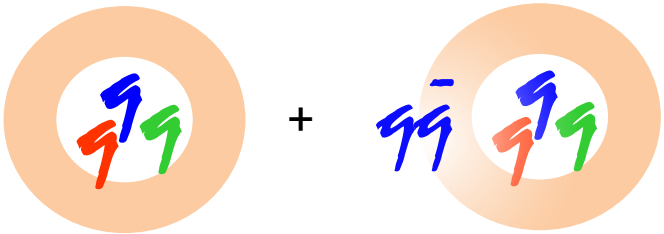


**2.** Excitation of the vacuum (i.e. melting of the condensate) influences the modification of the spectral properties

# Virtual photon radiation from hot and/or dense QCD matter

T

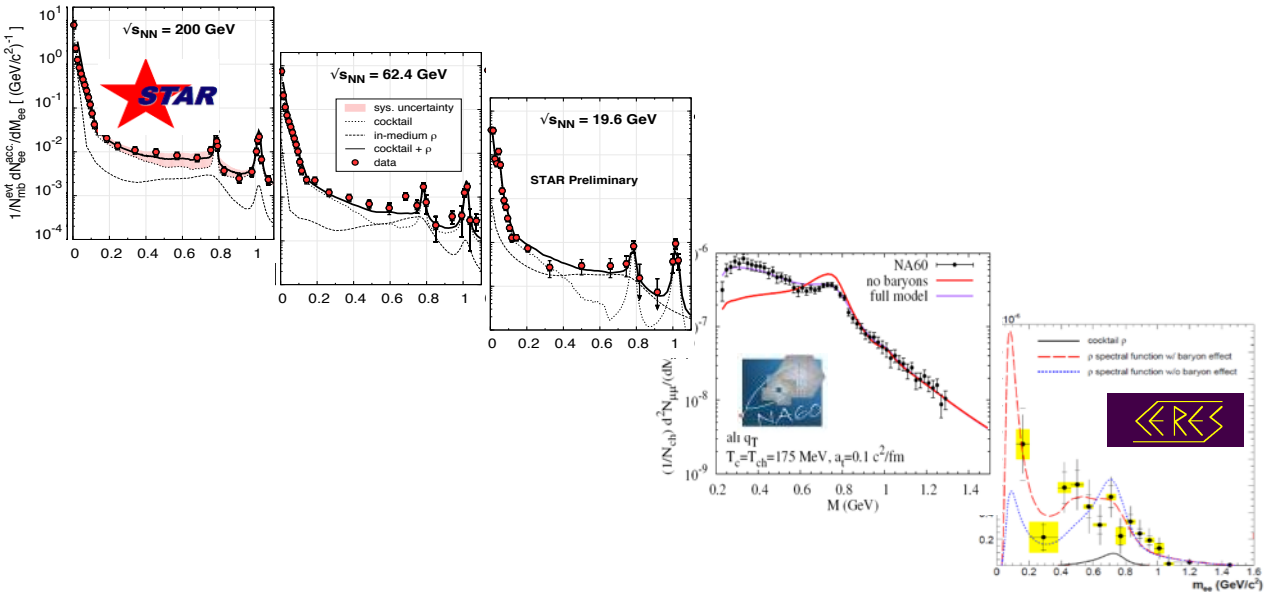


*Model: Ralf Rapp*
*STAR: QM2012,*
*NA60: EPJC 59 (2009) 607,*
*CERES: Phys. Lett. B 666 (2006) 425,*
*HADES: Phys.Rev.C84 (2011) 014902*

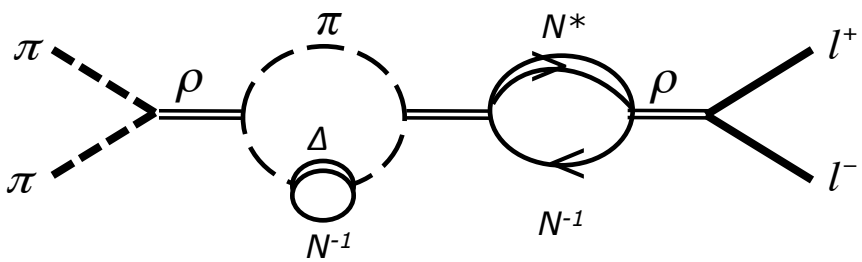


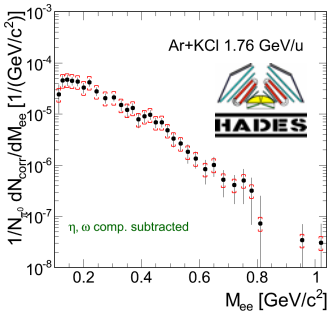


**Highly interesting results from RHIC, SPS, SIS18 → importance of baryons!**

$\mu_B$

# Quest: explore the regime of baryon dominated matter





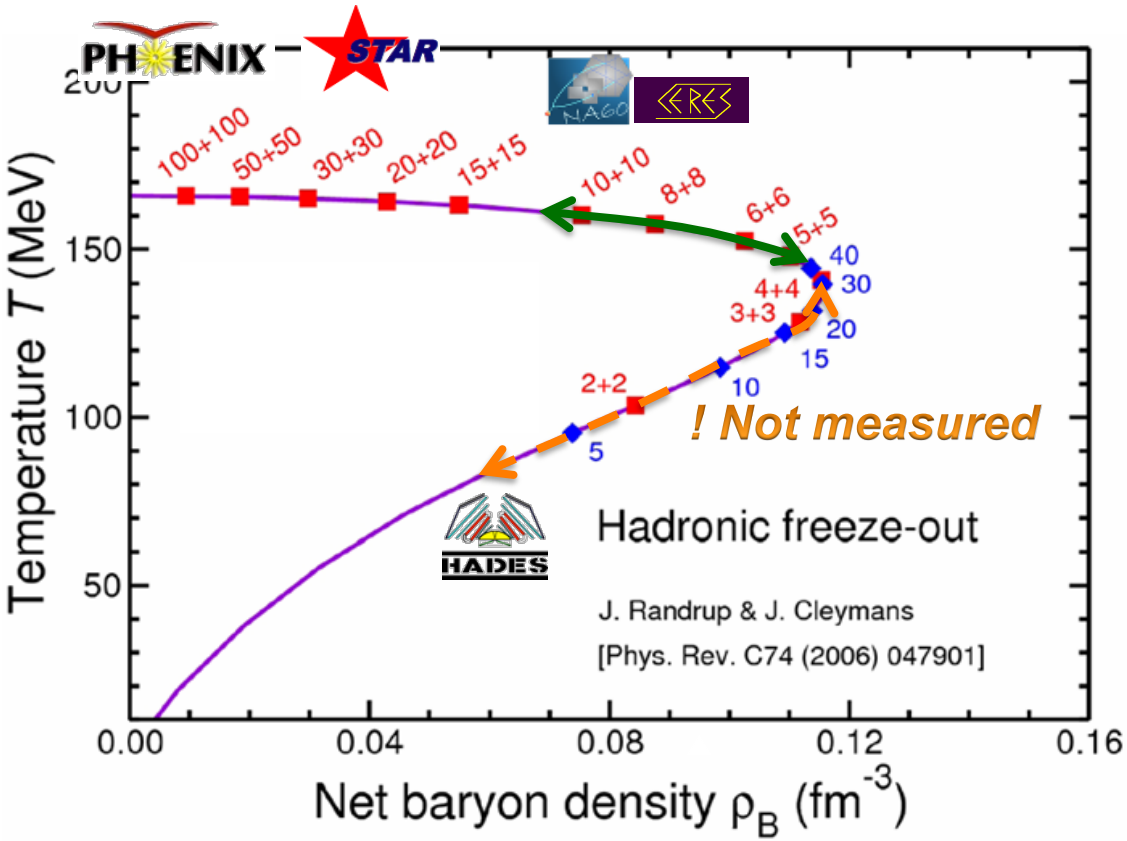


**Composition of a hot πΔN gas (T)**

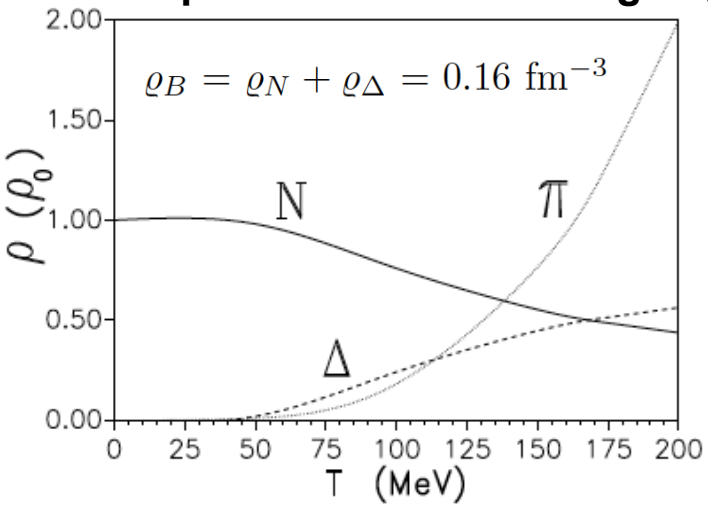


R. Rapp, J. Wambach, Adv.Nucl.Phys. 25 (2000) 1

**Published low-mass enhancement factors**

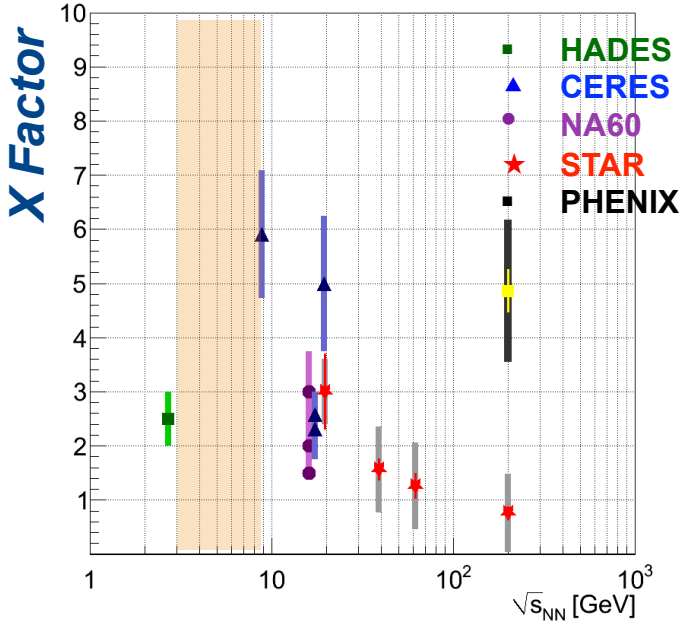


**No measurement for beam energies of 2-40 GeV/u**

→ **HADES/CBM at SIS100**

→ **CBM at SIS300**

# HADES at SIS100: phase space coverage for $e^+e^-$





## The "sweet spot" is at mid-rapidity and low $p_t$!

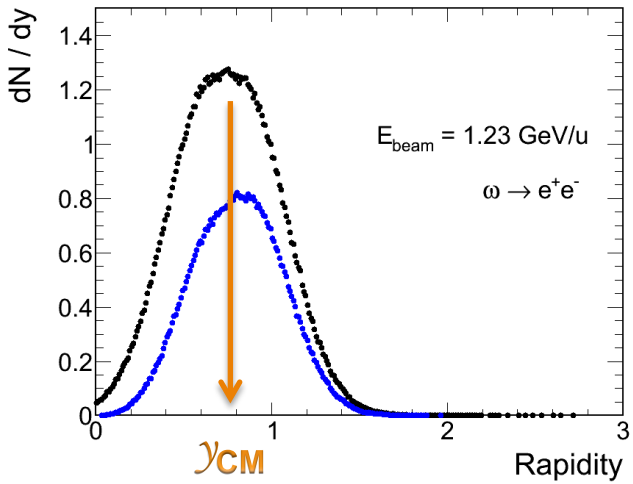


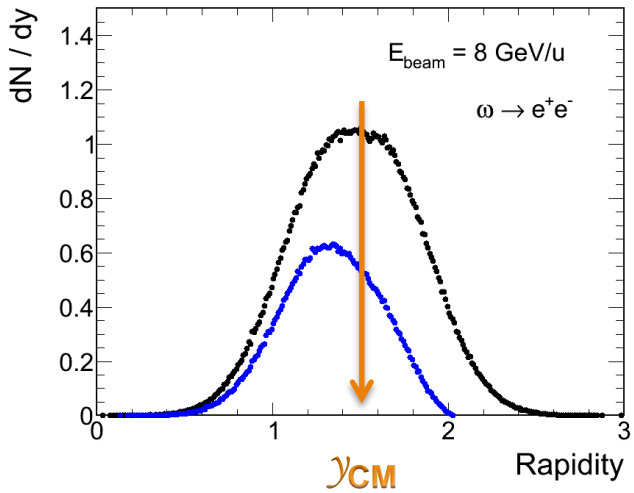


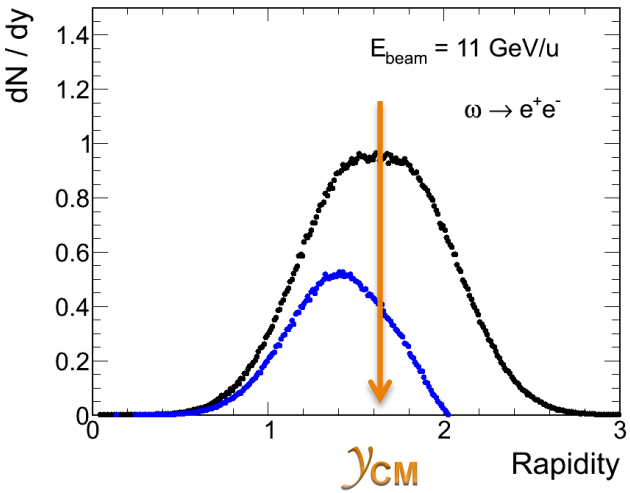


**$E_{beam}$ = 1 GeV/u**

- overall acceptance for di-electron pairs Acc ≈ 35%
- with nice mid-rapidity coverage

**$E_{beam}$ = 8 GeV/u**

- Acc ≈ 20%
- (natural) shift towards backward rapidity

**$E_{beam}$ = 11 GeV/u**

- … still HADES → Acc ≈ 20%
- **but…**

# HADES at SIS100: problems, challenges, opportunities

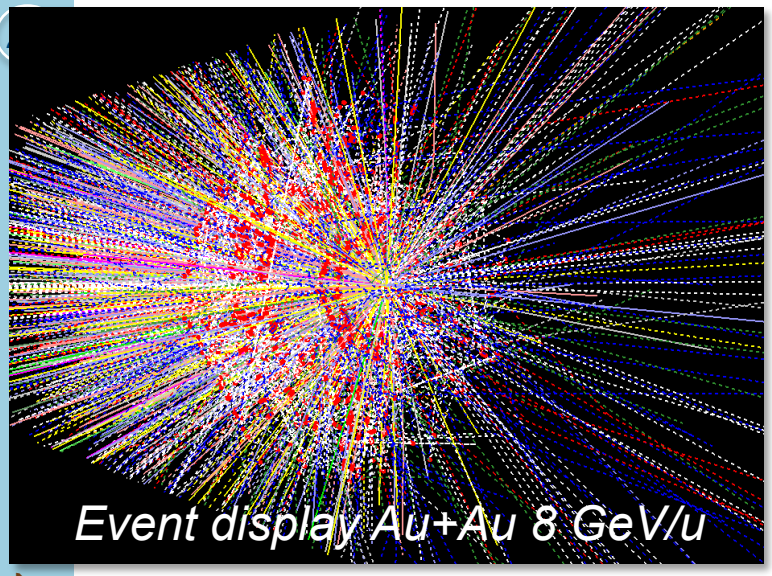


- **Challenge:** limited granularity →
  - sophisticated tracking algorithm

- Au+Au 1.23 GeV/u successfully measured in May 2012
- Ni+Ni 8 GeV/u ≈ Au+Au at 1.23 GeV/u
- Au+Au 8 GeV/u occupancy increases by factor of 4-5!

→ **CBM kicks in**

**Occupancy in tracking chambers ($b_{max}$ = 1 fm)**

*Cell size is factor of 2 larger*

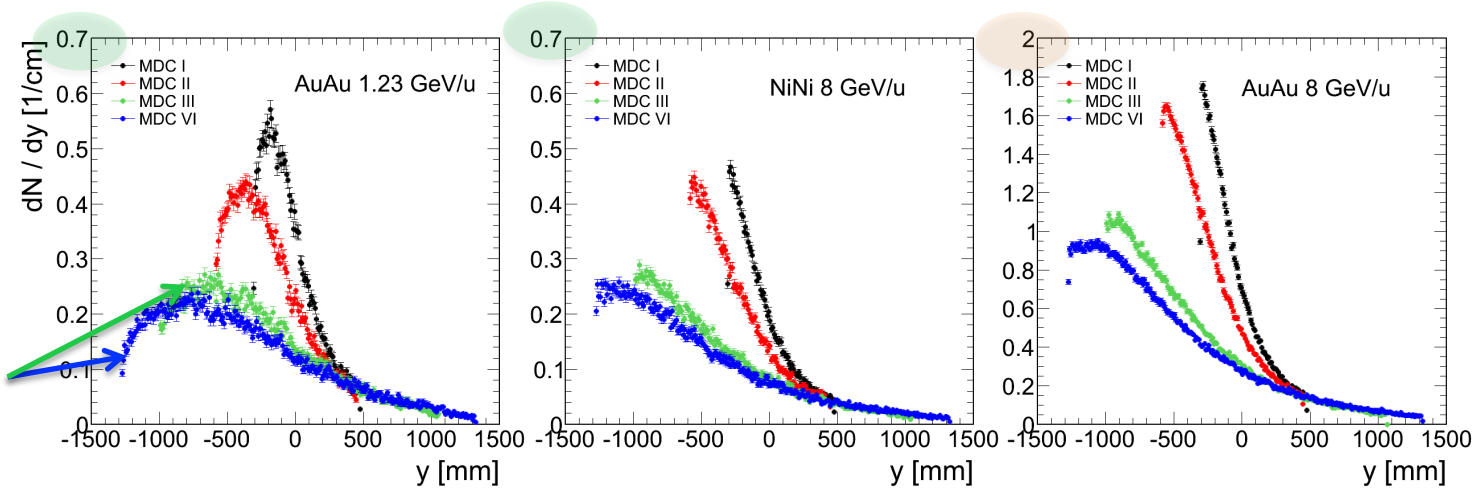


*y – radial coordinate in drift chamber*

# Di-electron reconstruction in CBM

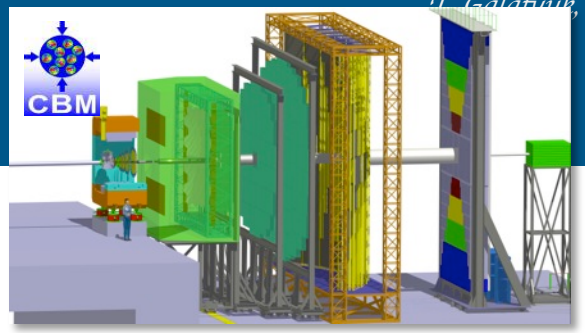


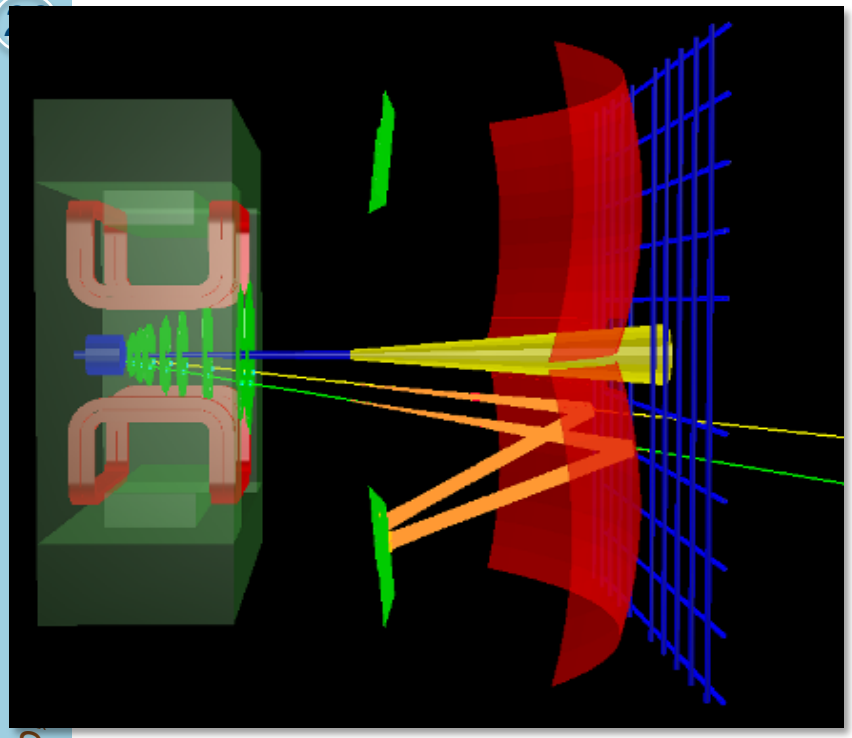

- **Challenge:**
  - No electron identification before tracking
  - Background due to material budget of the STS
  - Sufficient $\pi$ discrimination (600 $\pi^{+/-}$/event, misidentification $10^{-4}$)
- **Strategy:**
  - Reduction of background by reconstructing pairs from $\gamma$-conversion (~3 $\gamma$) and $\pi^0$ Dalitz decay (8 $\pi^0$/event)
  - Excellent double-hit resolution in MAPS (<100$\mu$m) provides substantial close pair rejection capability

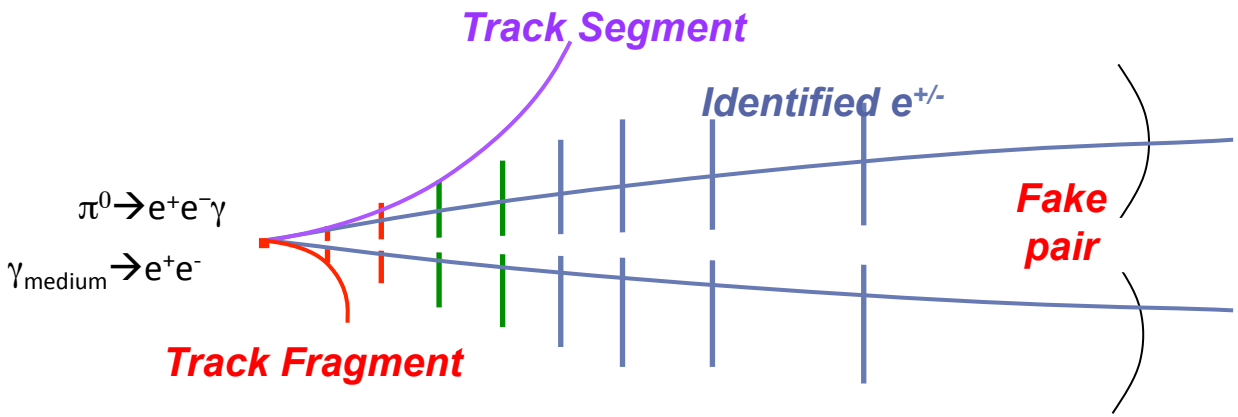

# Electron identification





## Track reconstruction efficiency

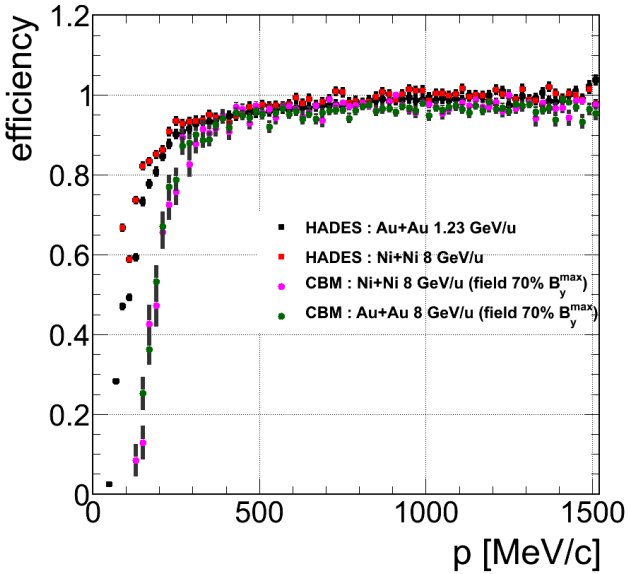


- Momentum distribution of conversion pairs are very soft
- High reconstruction efficiency is required for rejection of conversion pairs

## Ring radius vs. momentum

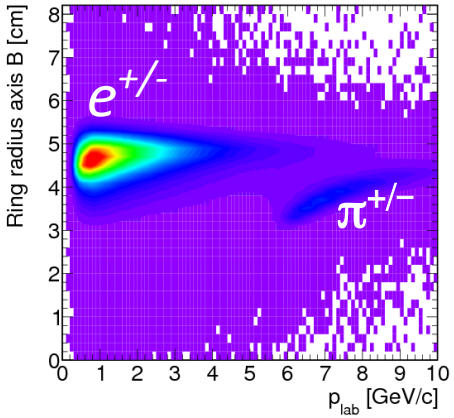


## RICH identified $e^{+/-}$ in TOF

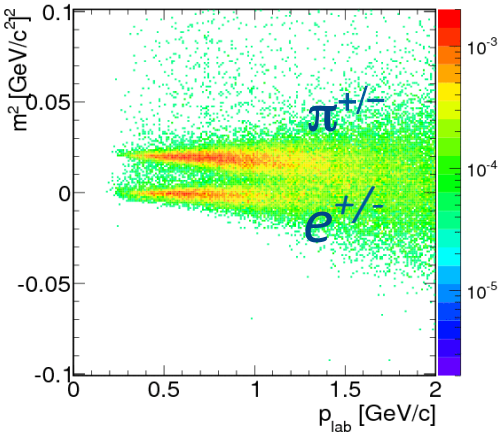


**$\pi$ suppression factor of $10^4$ (for p < 1 GeV/c) is in reach with RICH and ToF**

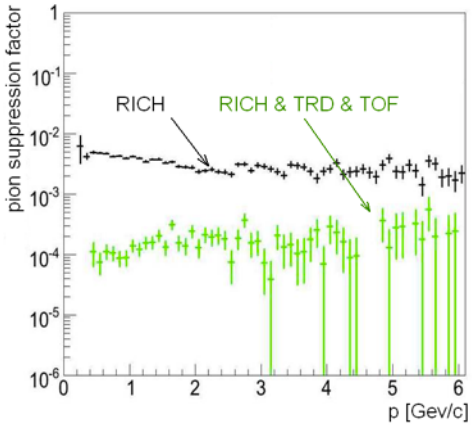

# Detector R&D



## RICH

- Conventional design based on commercial products (Germany, Russia, Korea)
  - Float glass mirror (carbon as backup)
  - Multi-anode PMT photo detector

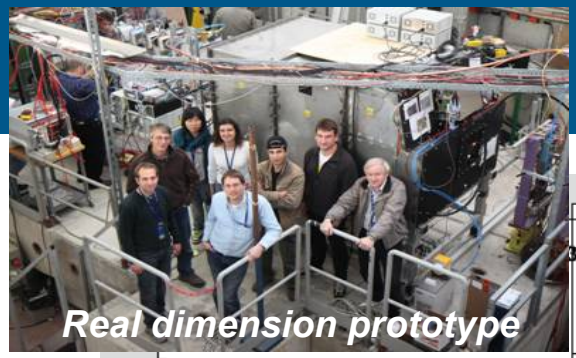


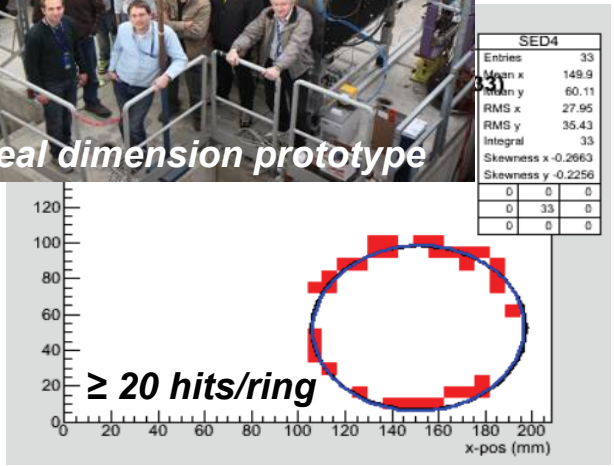


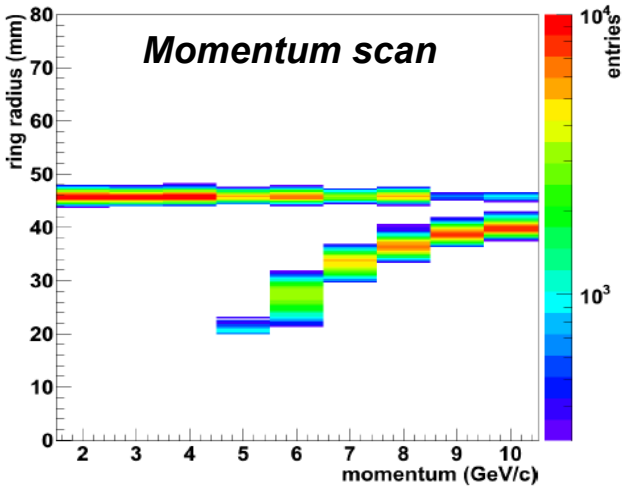


- **Test Beam at CERN T9, October 2011**
- **Mixed electron / pion beam of 2 – 10 GeV/c**

## TRD

- Thin gap design based on ALICE TRD (Germany, Russia, Romania)

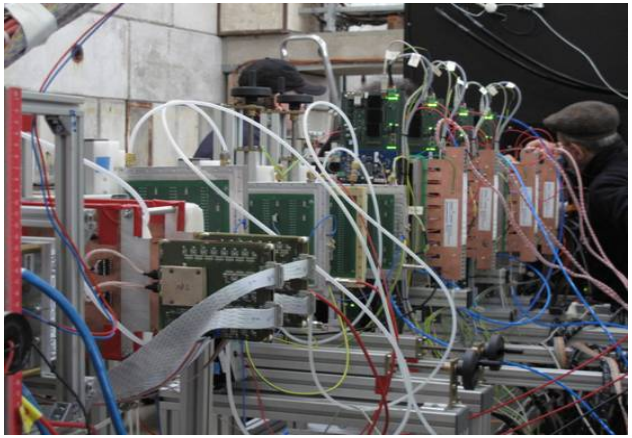

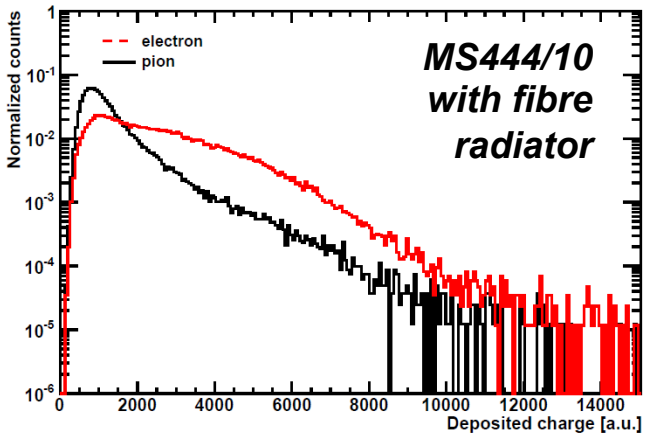

# Detector R&D : Micro-Vertex Detector

## Detector module:

- Two thinned (50 μm) sensors mounted to either side of a 200 μm CVD diamond carrierer.
- ***Total thickness = 0.3% x/X0***

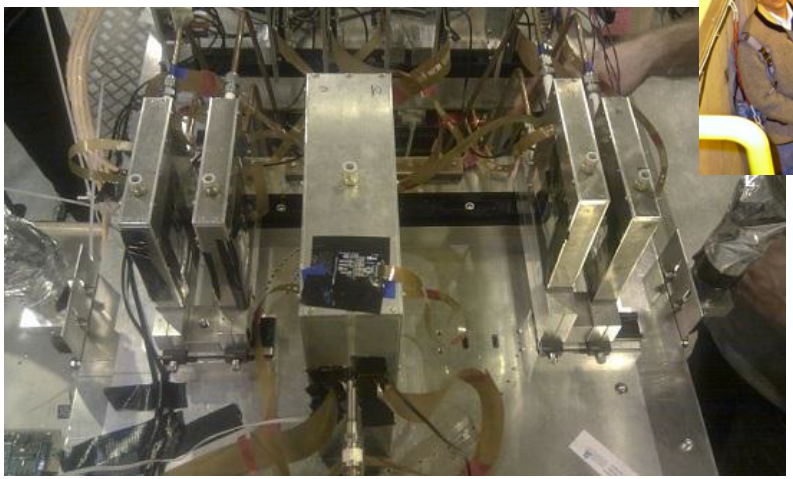

- **Test Beam at CERN T9, 26-30 November 2012**
- **Pion beam of 20, 60, 120 GeV/c**

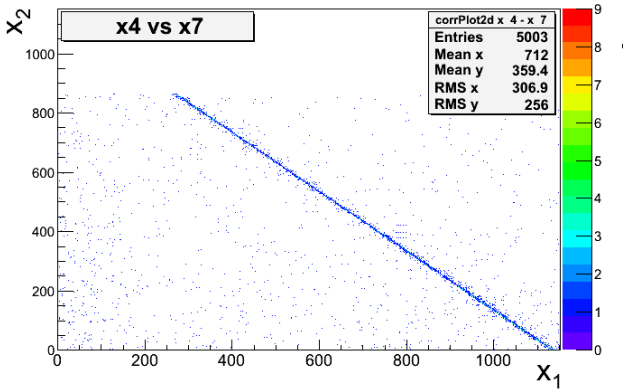


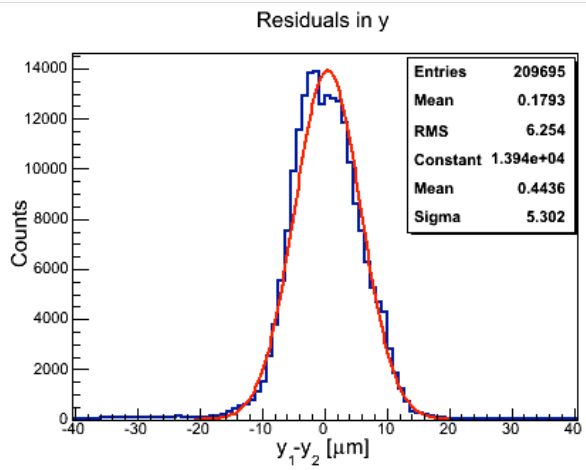


***Spatial Resolution***

$\sigma_x = 3.3\ \mu m$

$\sigma_y = 3.7\ \mu m$

# Low mass electron pairs reconstruction





Au+Au 25 GeV/u, b = 0 fm!

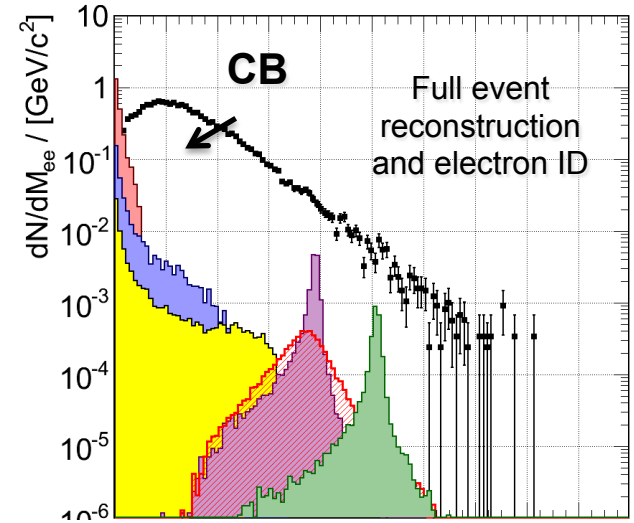


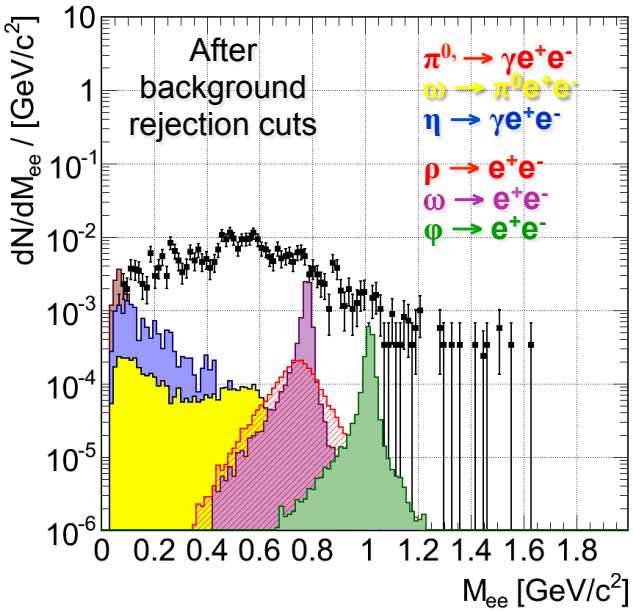


## Phase space coverage

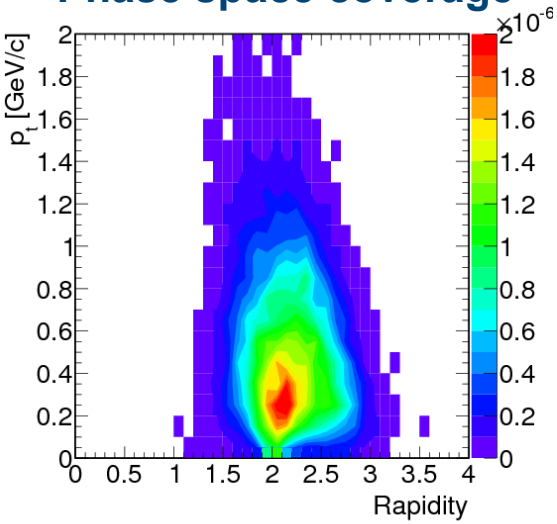


*after all cuts*

## Coverage in pair $p_t$-$m_{inv}$ plane

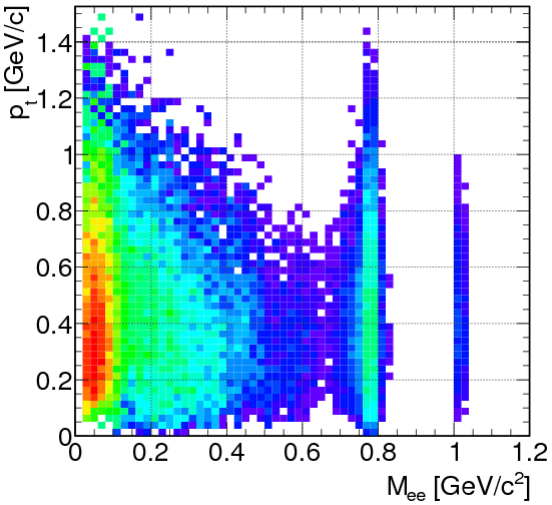


*after all cuts*
*excluding single leg $p_t$ cut*

# Dilepton emission rates in theory





## Thermal emission...

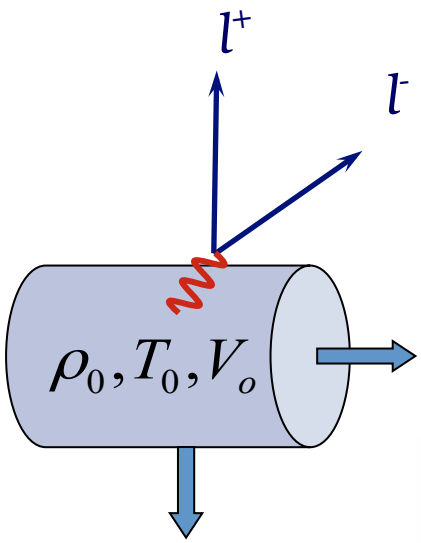


isentropic expansion

$$\frac{d^3N}{dMdydp_t} \equiv \int_{t=0}^{\infty} \frac{d^4\varepsilon}{d\mathbf{p}} \left[T(\mathbf{x}), \mu_B(\mathbf{x}), \vec{v}_{coll}(\mathbf{x}), ..\right] d\mathbf{x}$$

R. Rapp, J. Wambach and H. Hees : arXiv:0901.3289

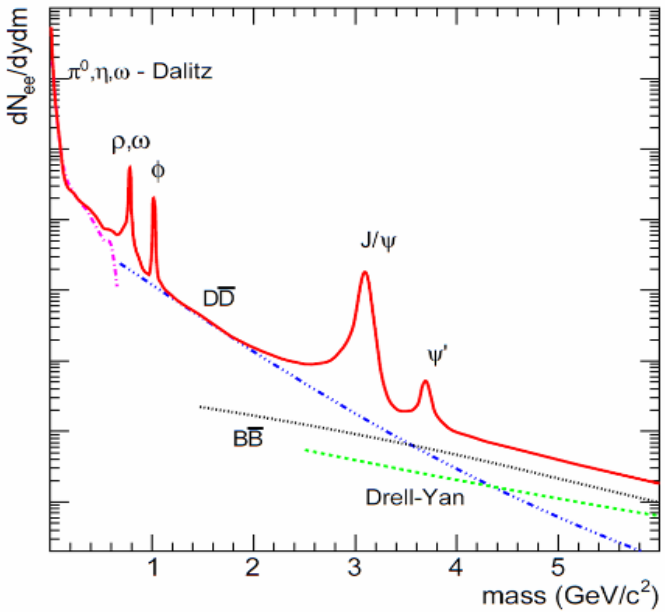


## ...or from transport

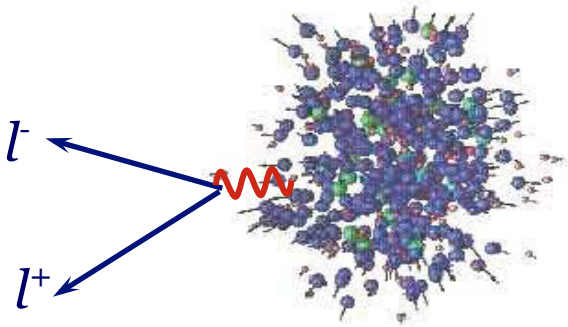

# Radiation from dense matter





- Schematic illustration of ρ meson propagation within "shining" approach.
- Resonance can continuously emit dileptons over its whole lifetime.

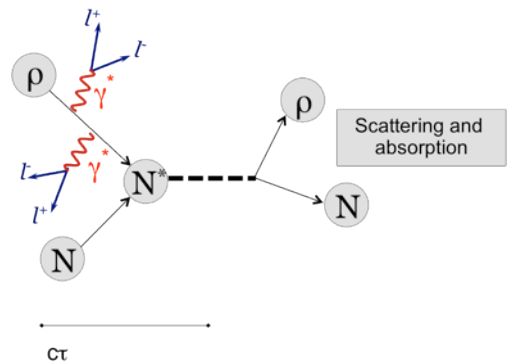


- Isolate the contribution to the spectrum from the dense stage
- Couple transport and a **thermal model**

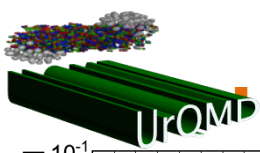


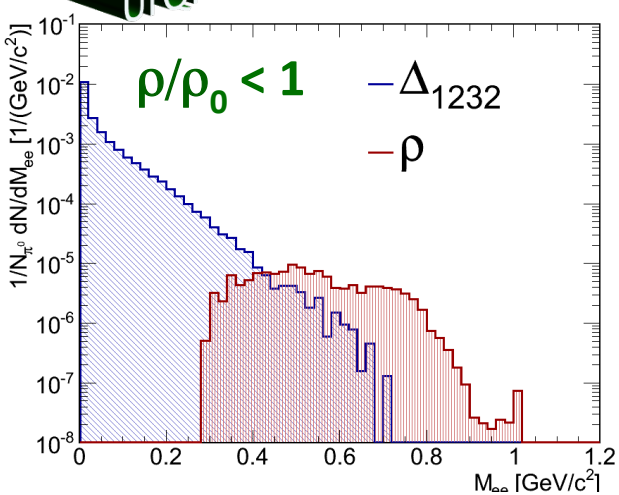


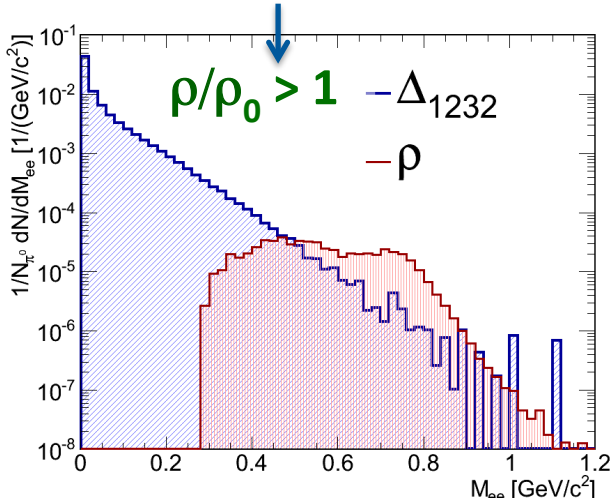


## Emission density evolution

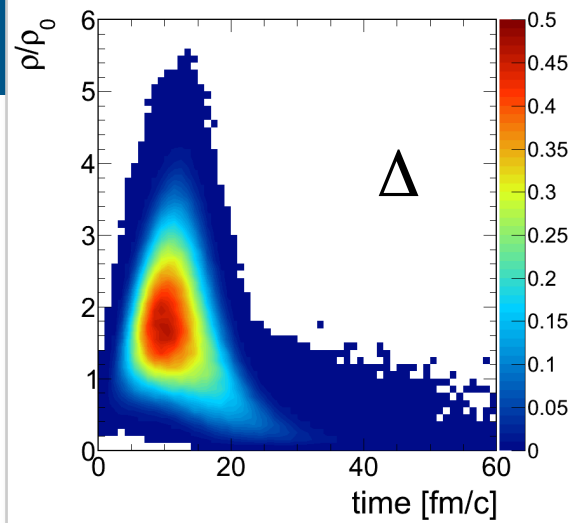


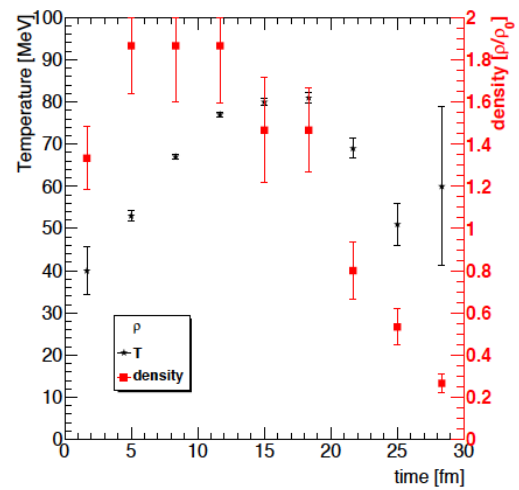


- First (points) and second (errors) moment of the density profile at a given τ.
- T – Boltzmann fit to the particle $m_T$ spectra

# $\pi$ beam experiments with HADES





- **Physics with $\pi$N experiments:**
  - New precision data are of enormous importance for understanding of baryon resonance physics
  - Special interest to sub-threshold production
- **Challenges:**
  - Determine $\pi$ momentum with $\Delta p/p$ ~1-5%
  - Beam spot of 6x6 cm$^2$ at dispersive plane
    → detector with sufficient active area
  - Beam intensity ~$10^8$ part./s
    → radiation hard detector
    → fast readout electronics

*Primary beam:*
*$10^{11}$ N (2 AGeV) /spill*

*SIS fast ramping*

*Spill: 4s cycle*

*Stable run for 3 weeks!*

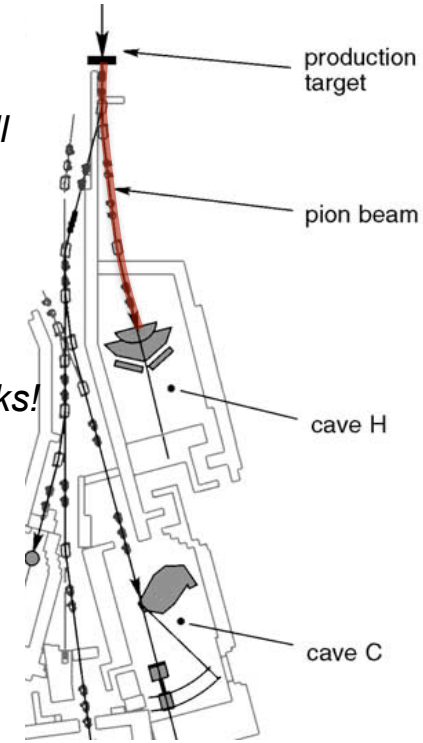


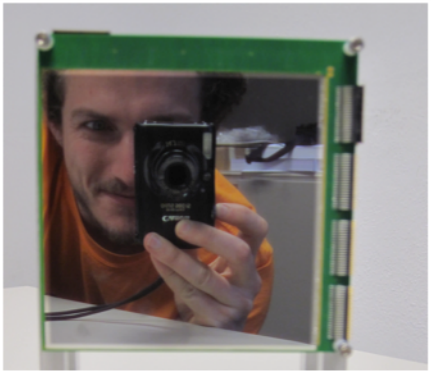

- **Strategy:**
  - Use 10×10cm$^2$ silicon strip detector
  - 2×128 channels - double sided
  - Radiation hard
  - Profit from n-xyter developments for CBM
    - ✓ Self-triggered architecture
    - ✓ 128 channels
    - ✓ Average hit per channel rate 160 kHz

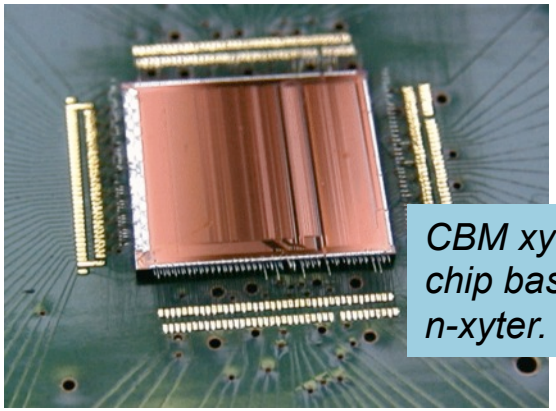

*CBM xyter FE chip based on n-xyter.*

# HADES explores Quarkyonic matter





April-May 2012 Au+Au run, 1.23 GeV/u 7 Billion events in 4 weeks, 140 T Bytes of data

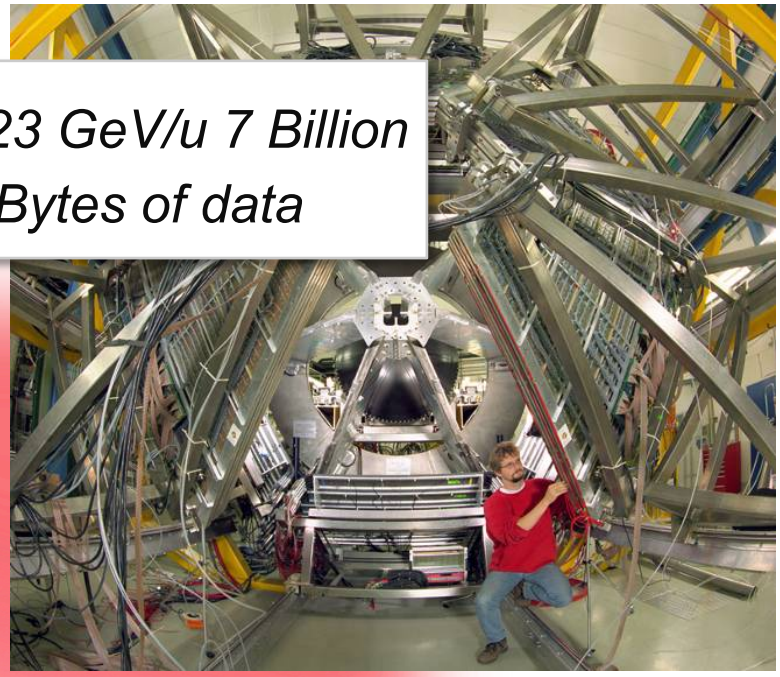

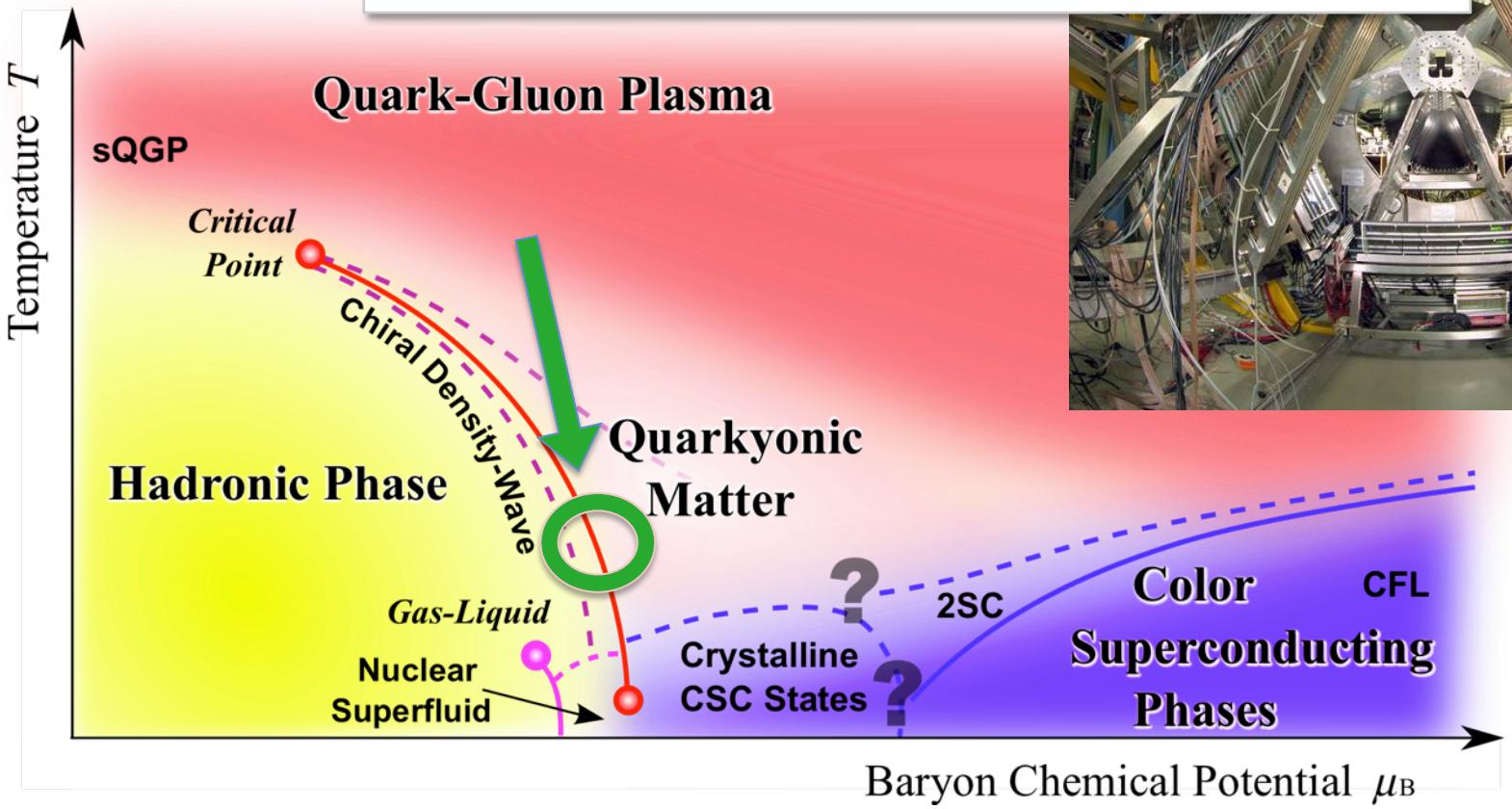

# Au+Au at 1.23 GeV/u (beam time April – May '2012)

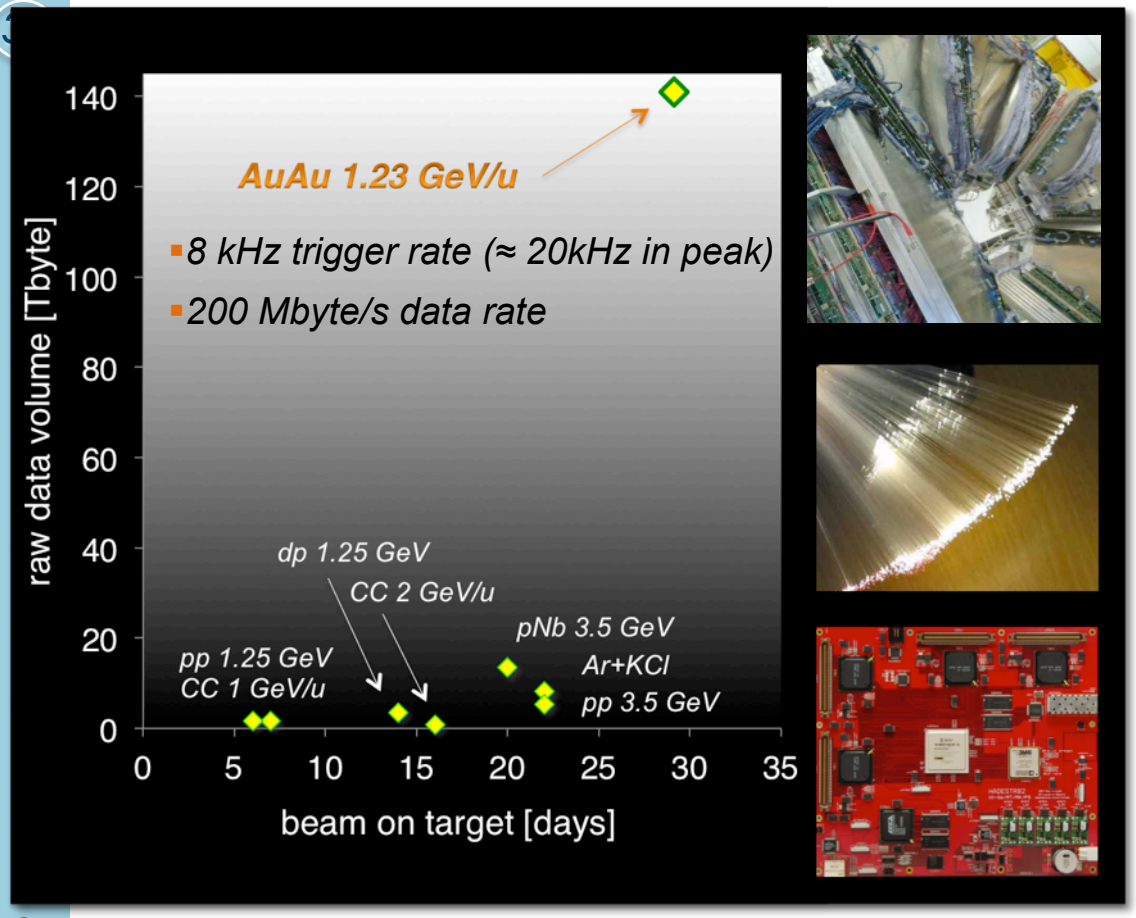








**Track reconstruction efficiency in high track density environment**

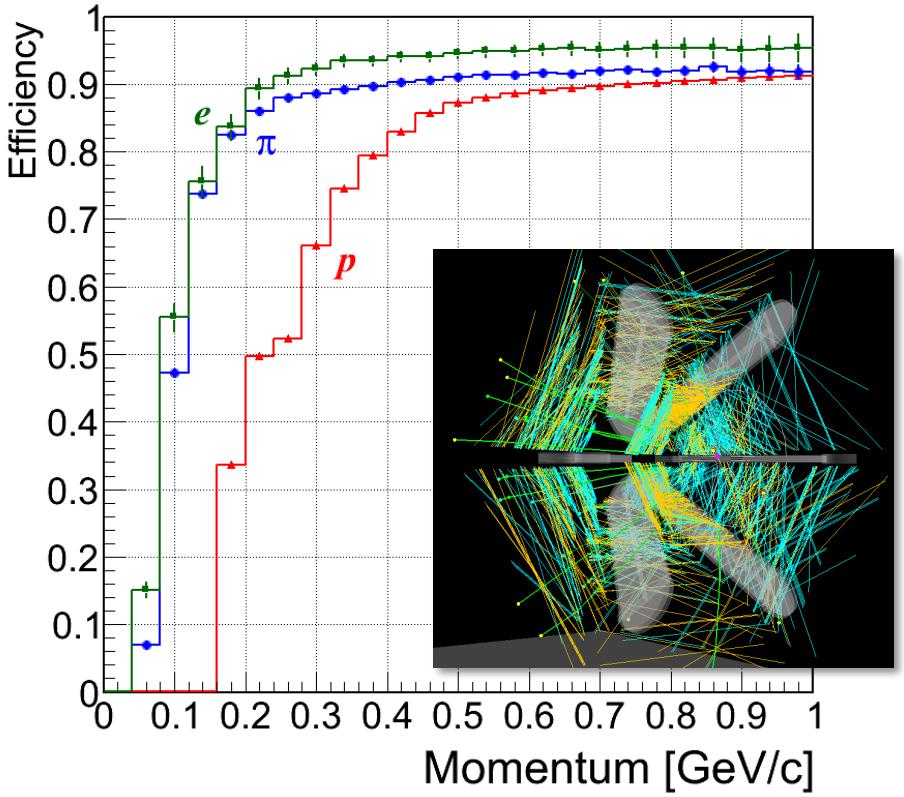


***HADES DAQ:***

*Versatile, FPGA board based system using dedicated add-on boards and data/trigger/slow-control transport via serial optical links (TRBnet)*

# Strangeness





*NN excess energy 0.44 GeV only!*
*Strong constraints on production mechanism*

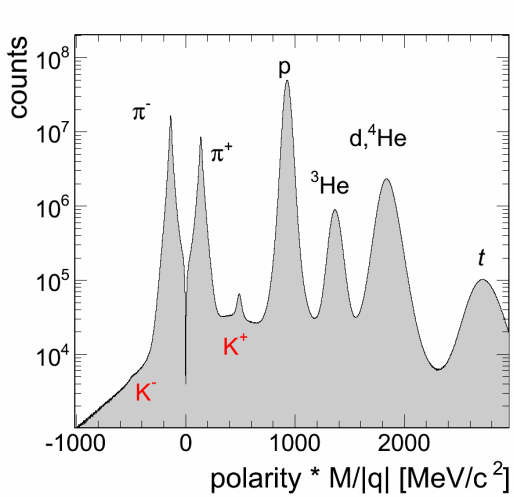


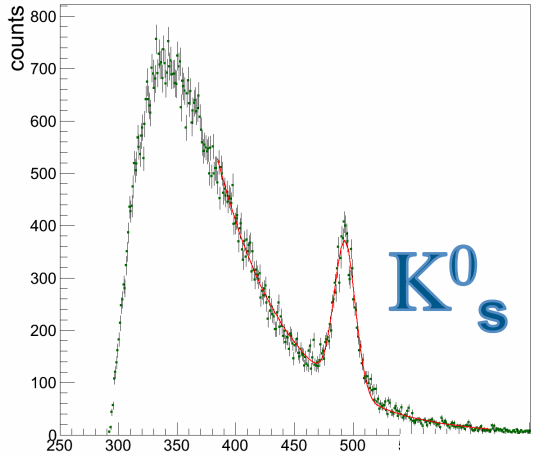


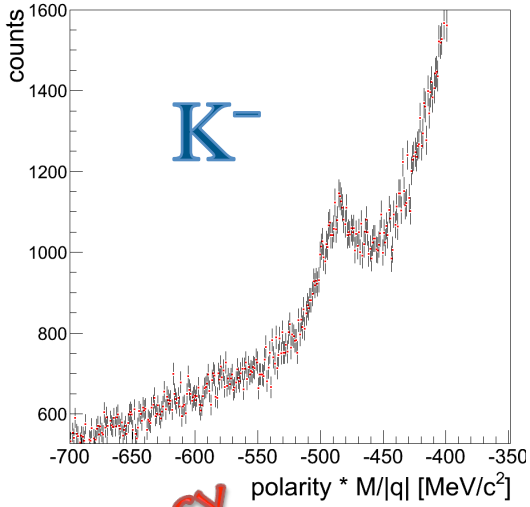


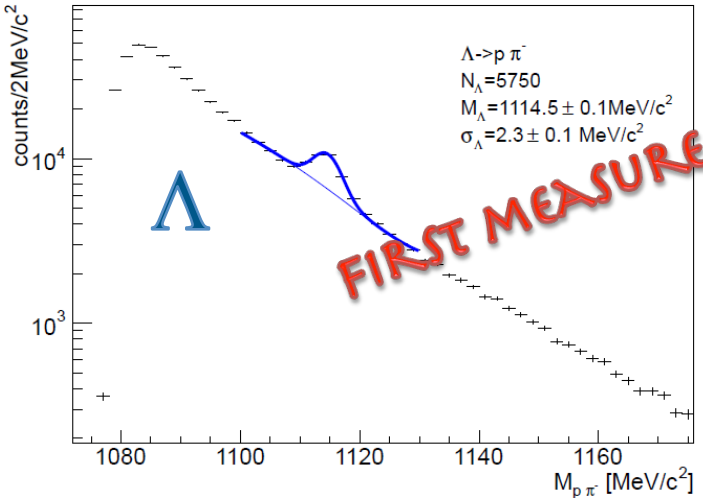


FIRST MEASUREMENT AT SUCH LOW BEAM ENERGY

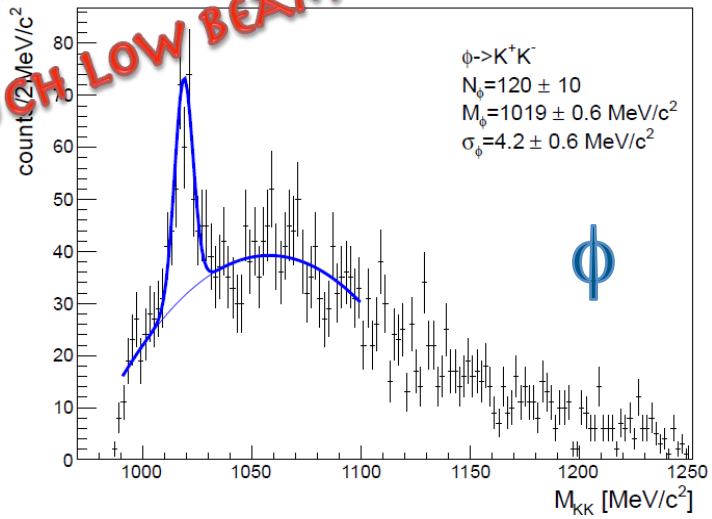

# Leptons





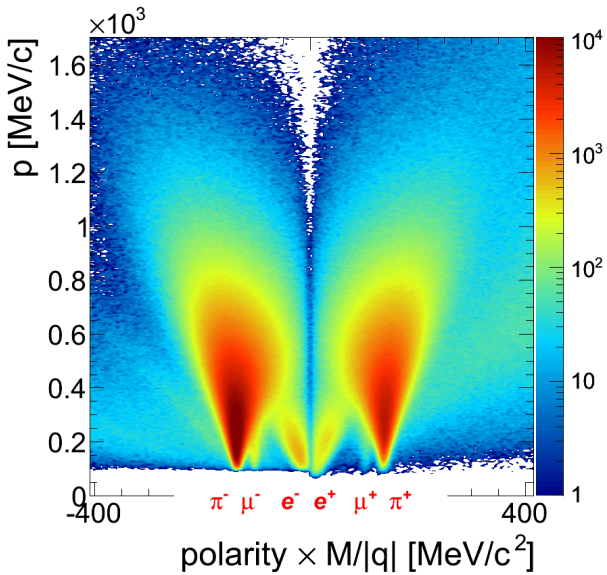
×10^3
p [MeV/c]
1.6
1.4
1.2
1
0.8
0.6
0.4
0.2
0
-400
400
π⁻ μ⁻ e⁻ e⁺ μ⁺ π⁺
polarity × M/|q| [MeV/c²]
10⁴
10³
10²
10
1

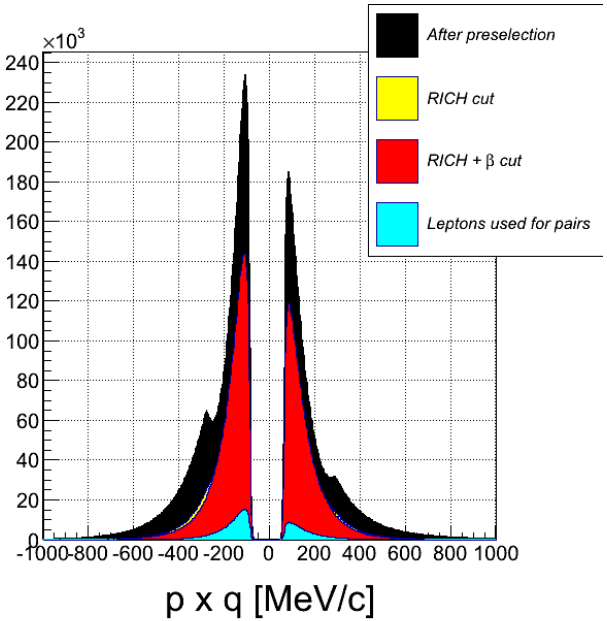
×10^3
After preselection
RICH cut
RICH + β cut
Leptons used for pairs
p x q [MeV/c]

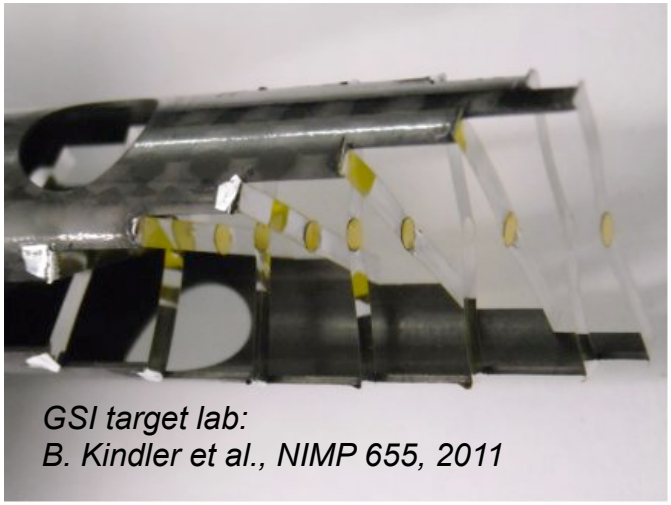
GSI target lab:
B. Kindler et al., NIMP 655, 2011

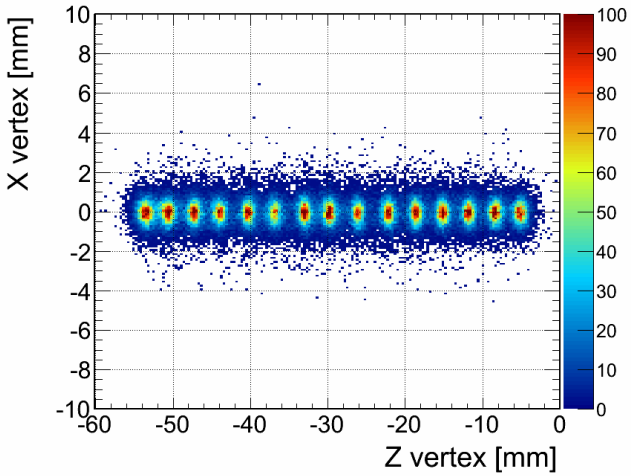
X vertex [mm]
Z vertex [mm]

# Summary





**Encouraging prospects for studying QCD matter in the region of compressed baryonic matter (finite $\mu_B$)**

- Explore “unknown” territory of the nuclear matter phase diagram with HADES and CBM :
  - **Unique possibility of characterizing properties of baryon dominated matter with rare probes:**
    - long-lived states of compressed nuclear matter are produced in heavy-ion collisions at few GeV energy regime
    - this state of matter might be much more exotic than a hadron gas (Quarkyonic metter?)
  - **Establish a complete excitation function of dilepton production up to energies of 40 GeV/u:**
    - baryon dominated to meson dominated fireballs!
    - from "transport" to "thermal expansion" models!
    - from "no QGP" to "QGP”?

***The results presented is the work of many …***

… THE HADES AND CBM COLLABORATIONS

# BONUS SLIDES

# NN Reference : $e^+e^-$ in QF n+p collisions





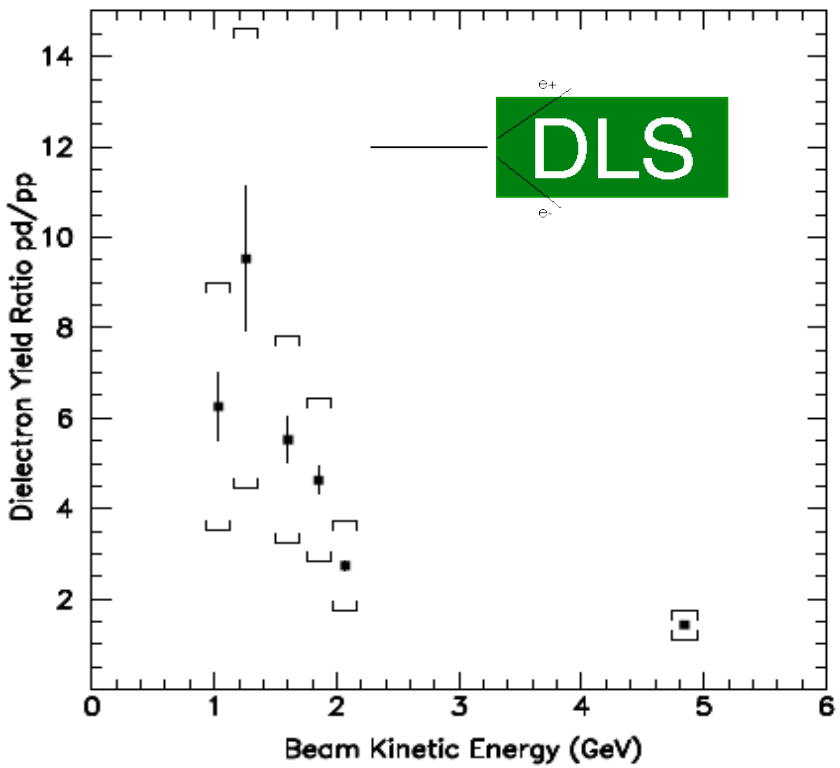


*W. Wilson et al., Phys. Rev. C 57 (1998)*

- Large isospin effects in dilepton production!
  - Role of the momentum distribution of the neutron inside the deuteron?
  - NN bremsstrahlung?

# Virtual photon emission in A+A collisions



Origin of the low-mass pair excess in C+C collisions

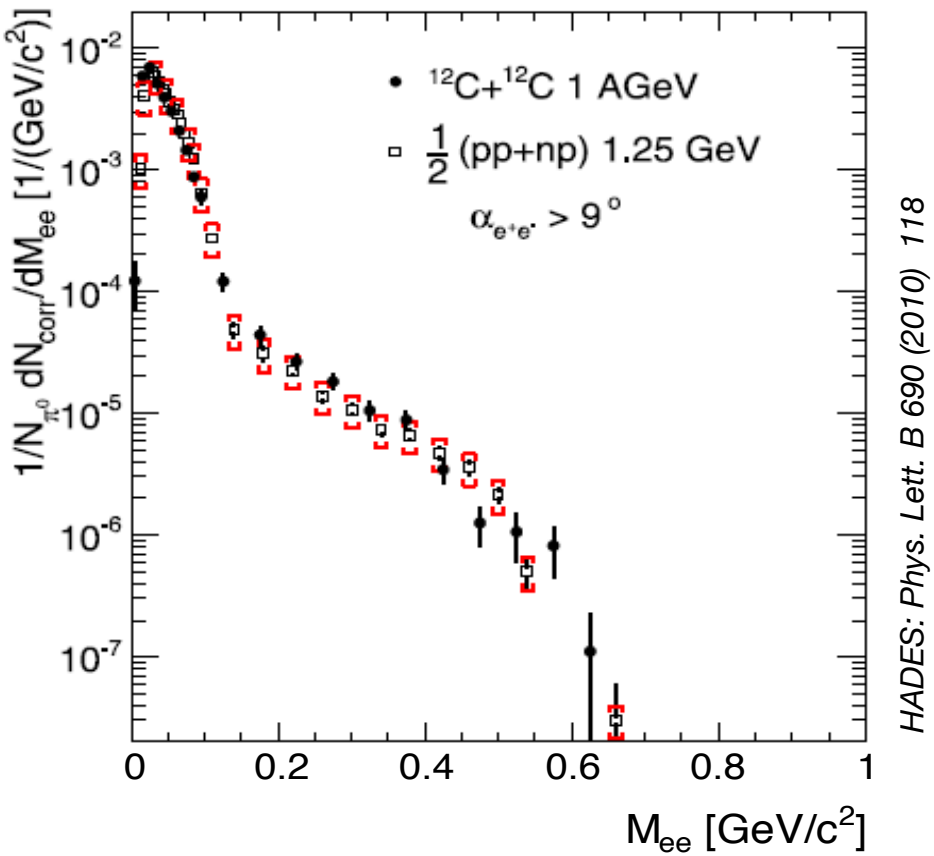


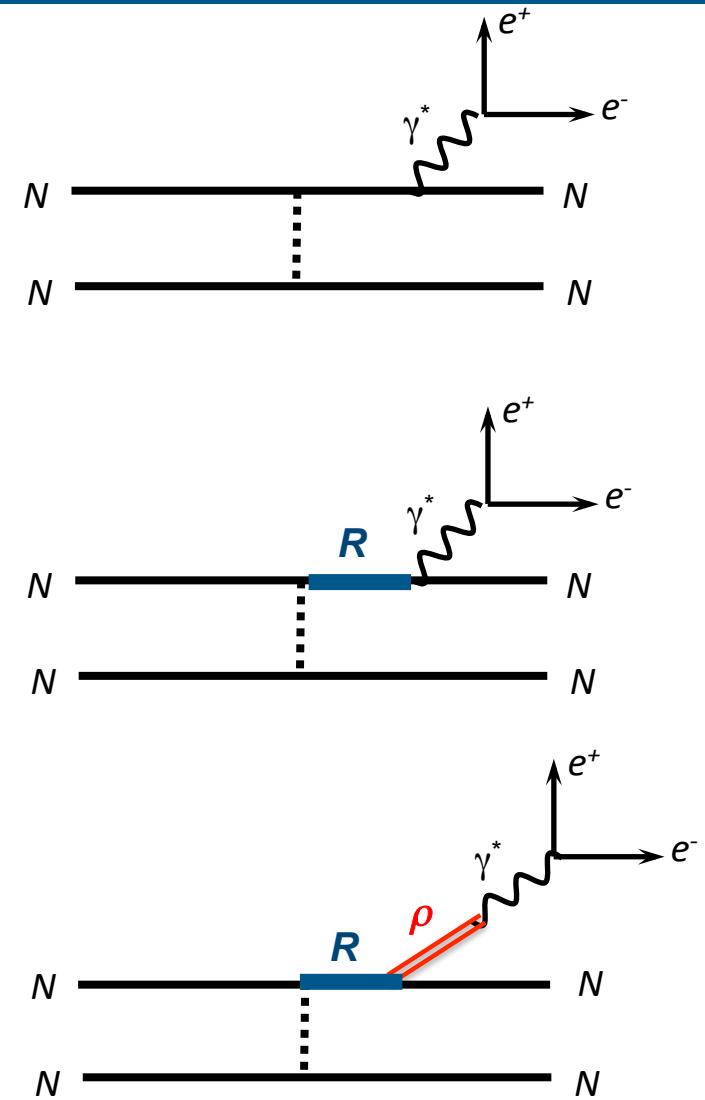


**Baryonic contributions from NN "reference"**

***R = Δ, N****

# Centrality dependence of spectral shape





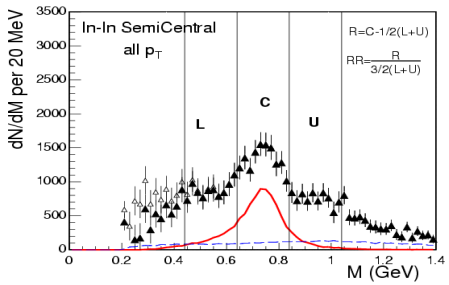

## "ρ clock"

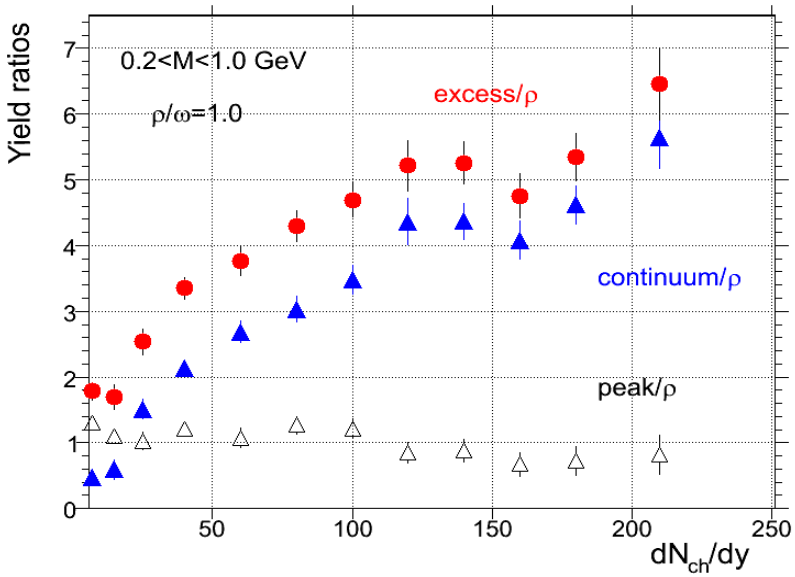


- Rapid increase of relative yield reflects the number of ρ's regenerated in fireball

*Na60 data: EPJC 61 (2009) 711*

## "Δ clock"

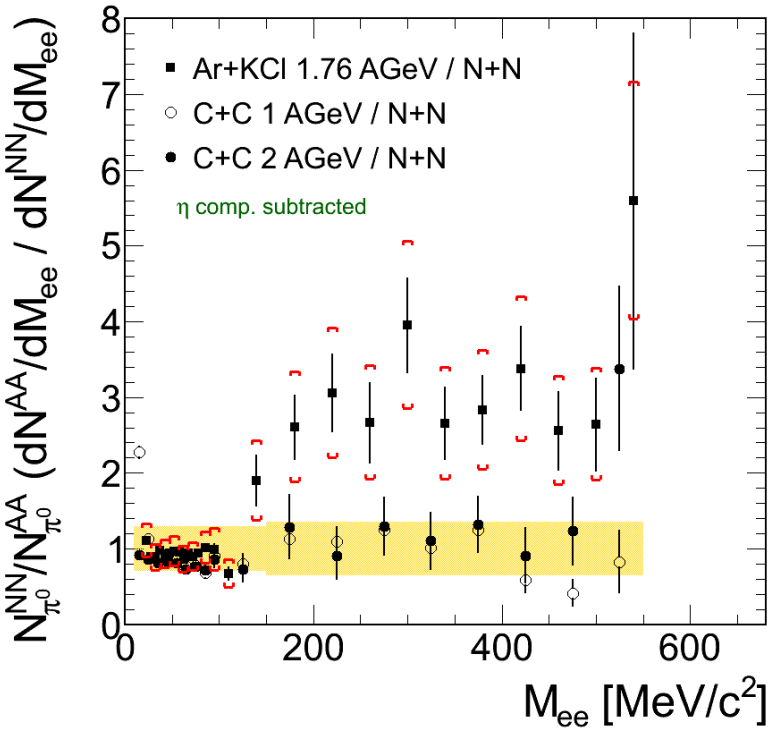


*HADES: Phys.Rev.C84:014902,2011*

- 34% most central collisions ($A_{part}$=38)
- Δ regeneration

# Electron pairs from cold nuclear matter





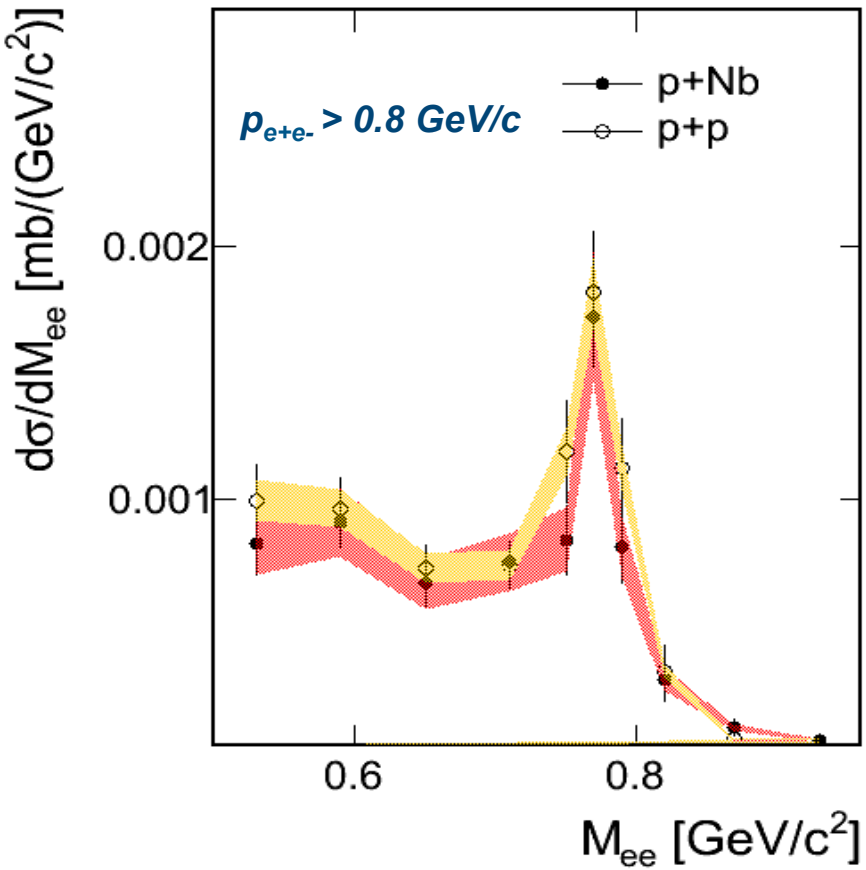


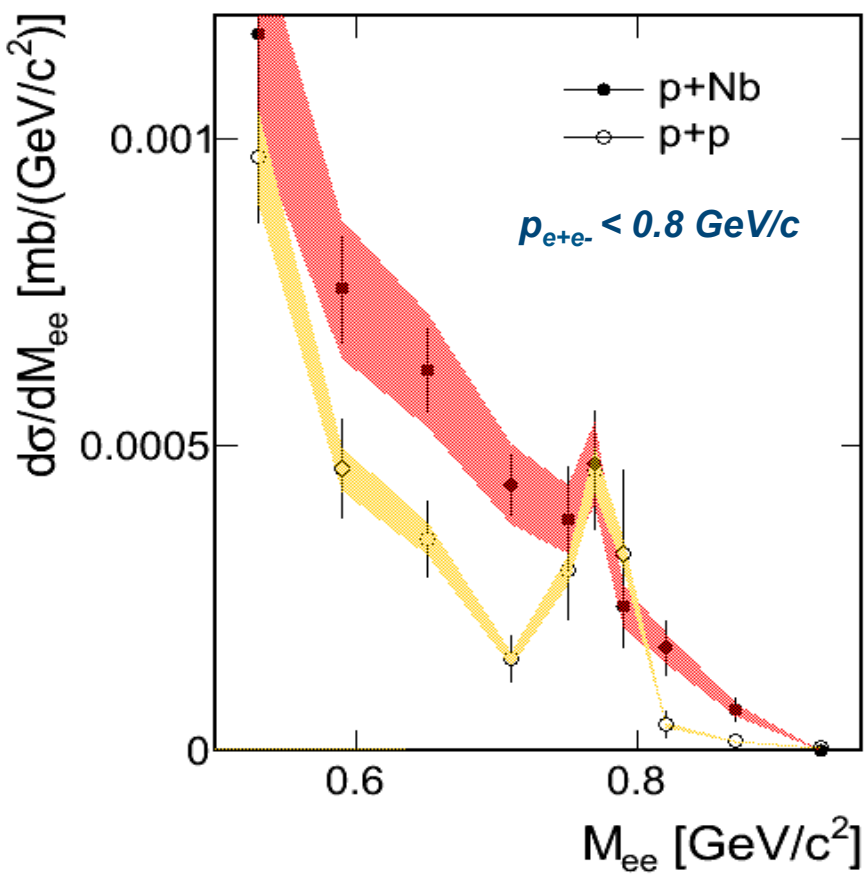

# Virtual photon emission in A+A collisions - transport

J. Weil at al., arXiv:1106.1344v1

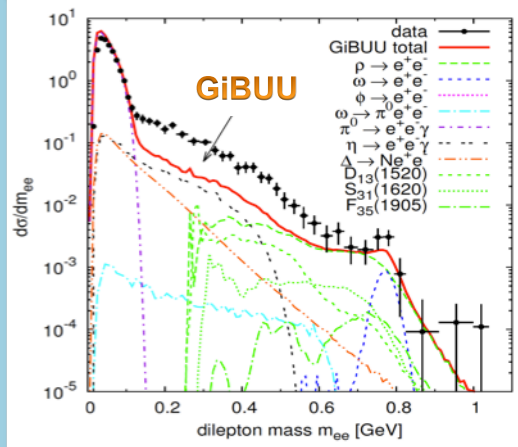


E.L. Bratkovskaya, NPA 807 (2008) 214

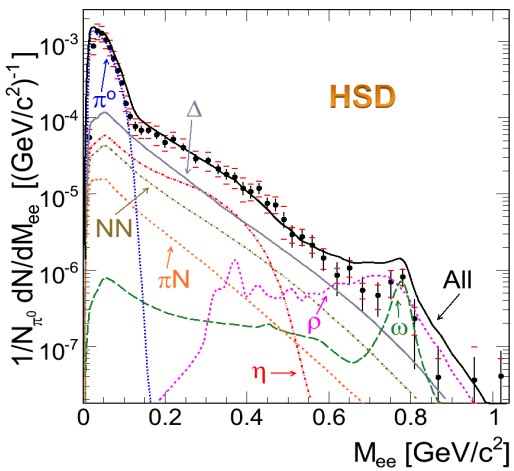


J. Aichelin et al, in preparation

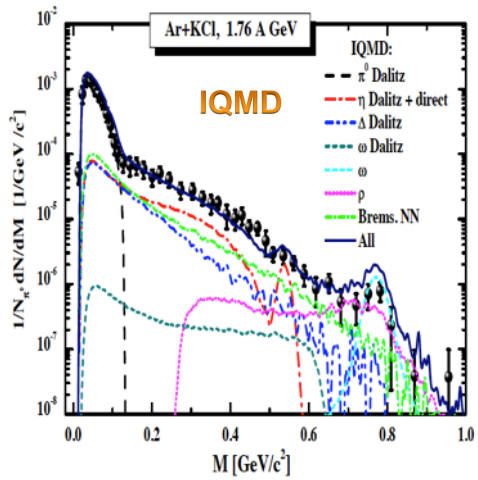


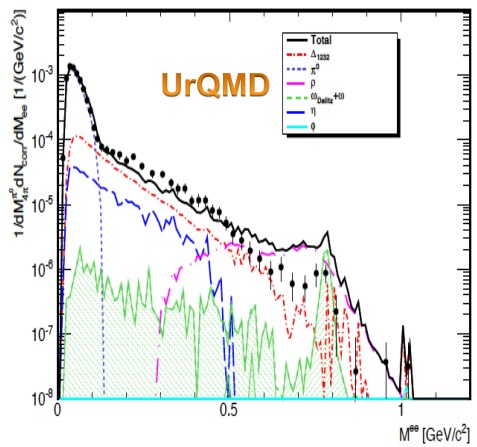


## No consistent picture yet:

- don't describe (yet) QF n+p data
- „excess" region dominated by Δ but with different contributions
- Treatment of NN, πN bremsstrahlung?
- $M_{e+e-}$>0.6 GeV/c$^2$ dominates by ρ with complicated vacuum structure

# Hot and dense matter



## Time-evolution of the hot and dense QCD medium in T - $\mu$ space from model calculation

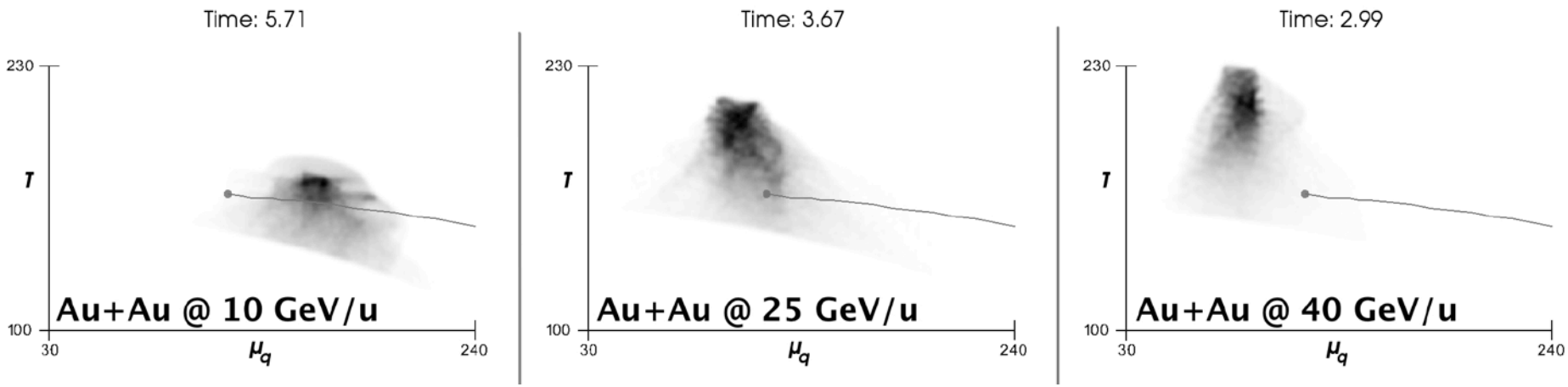


MADAI WORKBENCH

an incident beam energy of 25 GeV/u seems to provide the best opportunity for creating and probing QCD matter in the vicinity of the CEP.

*H. Petersen et al. , arXiv:1202.0076v1 [nucl-th]*

# Connections between dilepton data and chiral symmetry restoration

Paul Hohler
Texas A&M University

Thermal Radiation Workshop
Brookhaven National Lab
December 6, 2012

# Chiral symmetry restoration

- Observing chiral symmetry restoration experimentally may be the most important outstanding problem in heavy-ion physics.

- Ideally, one would measure a chiral order parameter, such as the quark condensate.

On the lattice:

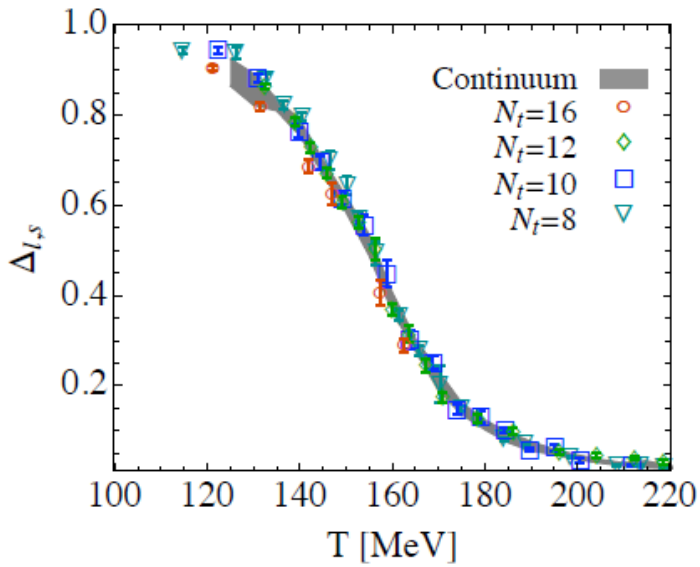


Wuppental-Budapest Collaboration

However, the chiral condensate is not directly measureable.

Need a probe: chiral partners

- Chiral partners
  - Hadronic states which transform into one another through chiral transformations (s wave pion).
  - Iso-vector vector and axial-vector states (ρ and $a_1$) $a_1 \leftrightarrow \rho + \pi$
  - The relative differences between chiral partners are sensitive to chiral order parameters.
- Determine the in-medium properties of ρ and $a_1$ mesons.
  - Vector: Thermal dileptons in heavy ion collisions $\rho \to \gamma \to e^+e^-$
  - Axial-vector: Background too large $a_1 \to \gamma\pi$

Couple the $a_1$ spectral function to the rho spectral function and quark condensate within one framework.

Then measure the rho spectral function and infer the $a_1$ spectral function and probe chiral symmetry restoration.

## Techniques to connect vector and axial-vector channels

- Sum Rules
  - Relate spectral functions to operator product expansion (OPE)
- Hadronic effective field theories
  - ρ, a1, and π are dynamical degrees of freedom.
  - Couple in-medium resonances

## Outline for systematic study

1. Vacuum
2. Rigorous low temperature predictions
3. Extend to higher temperatures
4. Effective field theory

# Sum rules

- Weinberg type sum rules:
  - Moments of the difference between vector and axial-vector SFs
  - Directly related to chiral symmetry breaking.

$$\int ds(\rho_V - \rho_A)s^n = f_n$$

$$f_{-2} = \frac{1}{3}f_\pi^2\langle r_\pi^2\rangle - F_A, f_{-1} = f_\pi^2, f_0 = -m_q\langle\bar{q}q\rangle, f_1 = -2\pi\alpha_s\langle\mathcal{O}_4^{\chi SB}\rangle$$

Weinberg, 1967; Das, Mathur, and Okubo, 1967; Kapusta and Shuryak 1994

- QCD sum rules (with Borel transform):
  - Constrains vector or axial-vector SFs individually.

Shiffman, Vainshtein, Zakharov, 1979

$$\frac{1}{M^2}\int ds\frac{\rho_V(s)}{s}e^{-s/M^2} = \frac{1}{8\pi^2}\left(1+\frac{\alpha_s}{\pi}\right) + \frac{m_q\langle\bar{q}q\rangle}{M^4} + \frac{1}{24M^4}\langle\frac{\alpha_s}{\pi}G_{\mu\nu}^2\rangle - \frac{56\pi\alpha_s}{81M^6}\langle\mathcal{O}_4^V\rangle$$

$$\frac{1}{M^2}\int ds\frac{\bar{\rho}_A(s)}{s}e^{-s/M^2} = \frac{1}{8\pi^2}\left(1+\frac{\alpha_s}{\pi}\right) + \frac{m_q\langle\bar{q}q\rangle}{M^4} + \frac{1}{24M^4}\langle\frac{\alpha_s}{\pi}G_{\mu\nu}^2\rangle + \frac{88\pi\alpha_s}{81M^6}\langle\mathcal{O}_4^A\rangle$$

# Step 1: Vacuum

- Consider a phenomenological model of the spectral functions for both the vector and axial-vector mesons.
  - Constrain the parameters by the ALEPH data (τ decay) and the Weinberg sum rules (0-2).

- Key and novel features:
  - Rho: microscopic calculation Rapp and Wambach (1999)
  - Identical continuum in both channels
    - Smooth continuum pushes "threshold" to energies higher than previous considered
  - Include the ρ' resonance.

  - Agreement with Weinberg sum rules <u>requires</u> an excited axial vector resonance state.

# Spectral functions in vacuum

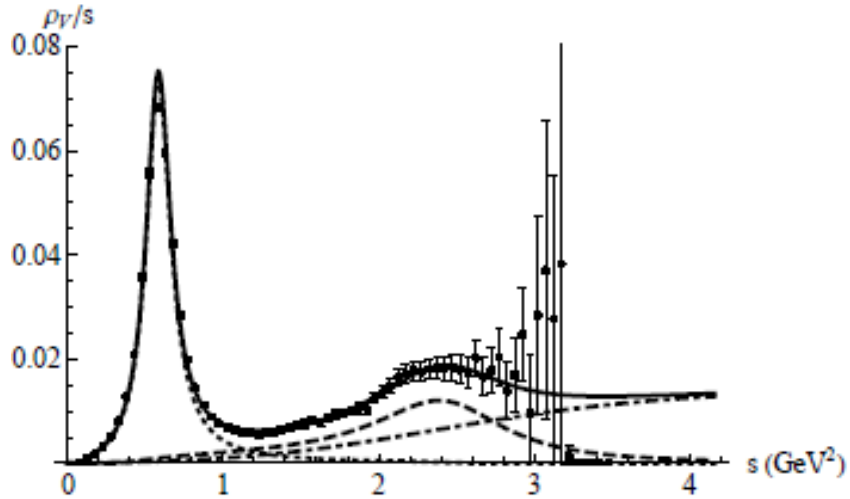


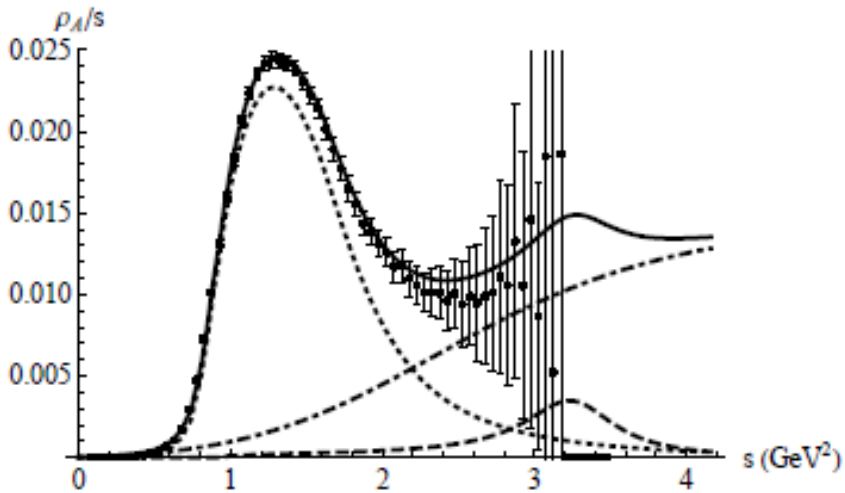


PMH and Rapp, 2012

Data from ALEPH (Barate et al. 1998)

Some parameters of interest

| | Mass (GeV) | Width (GeV) |
|---|---|---|
| ρ’ | 1.56 | 0.32 |
| a1 | 1.24 | 0.61 |
| a1’ | 1.80 | 0.2 |

# How well are the sum rules satisfied?

Weinberg-type sum rules

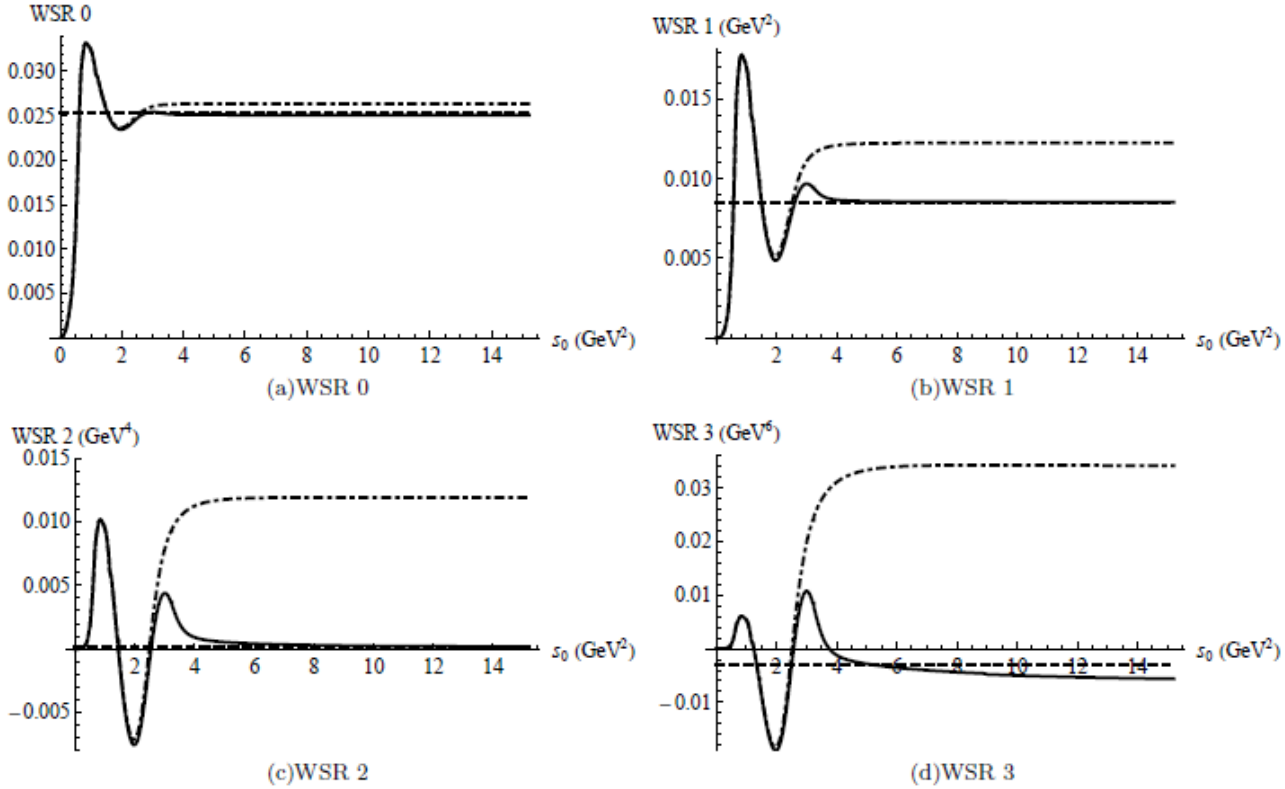


| WSR 0 | WSR 1 | WSR 2 | WSR 3 |
|---|---|---|---|
| 1.28% | ~0% | ~0% | -96% |

QCD sum rules

Chose the values for κ and the gluon condensate so that sum rules are satisfied.

$$\langle \mathcal{O}_4^V \rangle_0 = \langle \mathcal{O}_4^A \rangle_0 = \kappa \langle \bar{q}q \rangle_0^2 \qquad \kappa = 2.1^{+.3}_{-.2} \qquad \langle \tfrac{\alpha_s}{\pi} G^2 \rangle = .022 \pm .002 \mathrm{GeV}^4$$

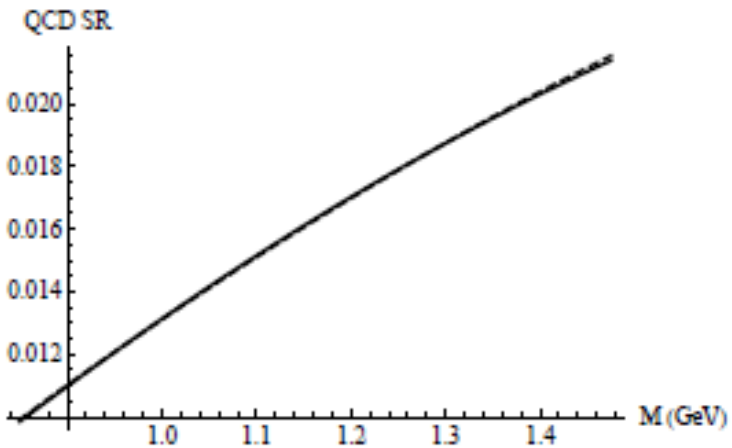

(a)Vector Channel

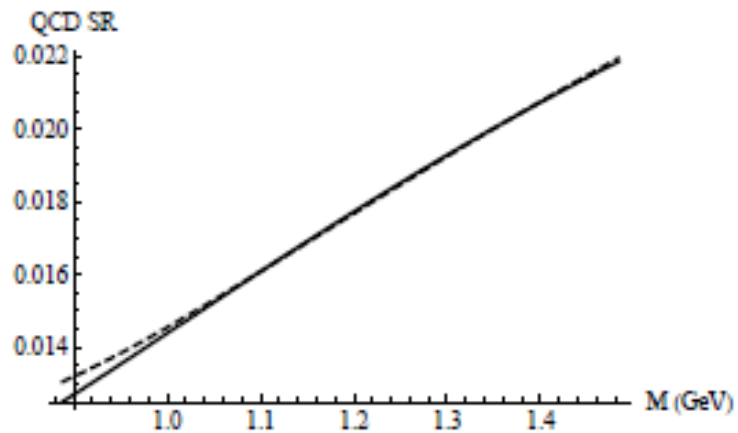

(b)Axial-Vector Channel

$$d_V = 0.24\% \qquad d_A = 0.56\%$$

# In-medium

- Condensates develop a temperature dependence and new non-scalar operators become available for the OPE.
  - Input needed for analysis
- The sum rules then translate these changes of the condensates into modifications of the spectral function.

$$\frac{1}{M^2}\int ds \frac{\rho_V(s)}{s} e^{-s/M^2} = \frac{1}{8\pi^2}\left(1+\frac{\alpha_s}{\pi}\right) + \frac{m_q\langle\bar{q}q\rangle}{M^4} + \frac{1}{24M^4}\langle\frac{\alpha_s}{\pi}G^2_{\mu\nu}\rangle - \frac{56\pi\alpha_s}{81M^6}\langle\mathcal{O}_4^V\rangle$$

$$\frac{1}{M^2}\int ds \frac{\bar{\rho}_A(s)}{s} e^{-s/M^2} = \frac{1}{8\pi^2}\left(1+\frac{\alpha_s}{\pi}\right) + \frac{m_q\langle\bar{q}q\rangle}{M^4} + \frac{1}{24M^4}\langle\frac{\alpha_s}{\pi}G^2_{\mu\nu}\rangle + \frac{88\pi\alpha_s}{81M^6}\langle\mathcal{O}_4^A\rangle$$

Reduction of condensates produces a need for more lower energy spectral strength.

# Step 2: Rigorous low temperature prediction

- At low temperatures, in-medium effects are dominated by interaction with thermal pions.

$$\rho_V(T) = \rho_V(T=0)(1-\epsilon) + \rho_A(T=0)\epsilon$$

$$\rho_A(T) = \rho_A(T=0)(1-\epsilon) + \rho_V(T=0)\epsilon$$

Dey, Eletsky, Ioffe, 1990

$$\epsilon = \frac{2}{f_\pi^2}\int \frac{d^3p}{(2\pi)^3 E_p} n_B(E_p)$$

- Temperature dependence of condensates also govern by pions.

$$\langle \bar{q}q\rangle(T) = \langle \bar{q}q\rangle(0)\left(1 - \frac{3}{4}\epsilon\right)$$

Hatsuda, Koike, Lee, 1993; Steele, Yamagishi, Zahed, 1996; Chanfrey, Delorme, Erison, 1998; Krippa 1998; Marco, Hoffman, Weise, 2002; Kwon, Sasaki, Weise, 2010;Etc.

How does one implement chiral mixing with different continuum thresholds?

What effect does a finite pion mass have on analysis?

With smooth continuum, no ambiguity in mixing.

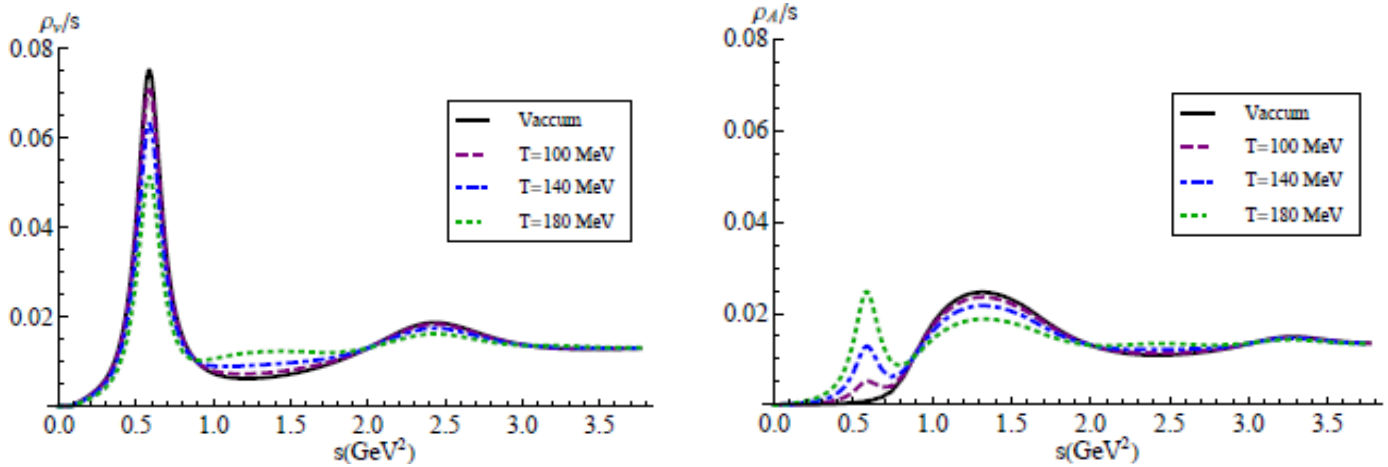


Holt, PMH, Rapp, 2012

- Flattening
- Trend to one-another

# How high in T can analysis be taken?

- $m_\pi = 0$

Marco, Hoffman, Weise, 2002

  - Both WSR and QCDSR are exactly satisfied to order ε
  - Low temperature prescription persists to high (all) temperatures.

- $m_\pi \neq 0$
  - WSR is still satisfied
  - Numerical evaluation is need for QCDSR

| T (MeV) | 0 | 100 | 120 | 140 | 160 |
|---|---|---|---|---|---|
| ε | 0 | .06 | .1 | .16 | .23 |
| dV (%) | .24 | .32 | .48 | .85 | 1.43 |
| dA (%) | .56 | .65 | .78 | 1.05 | 1.6 |

QCDSRs self-limiting

Need additional physics beyond $T \sim m_\pi$

# Step 3: Beyond low temperatures

- Low temperature study revealed a need for more resonances
  - Model the temperature dependence of condensates on a modified Hadron Resonance Gas
    - All established resonances with mass less than 2 GeV included.

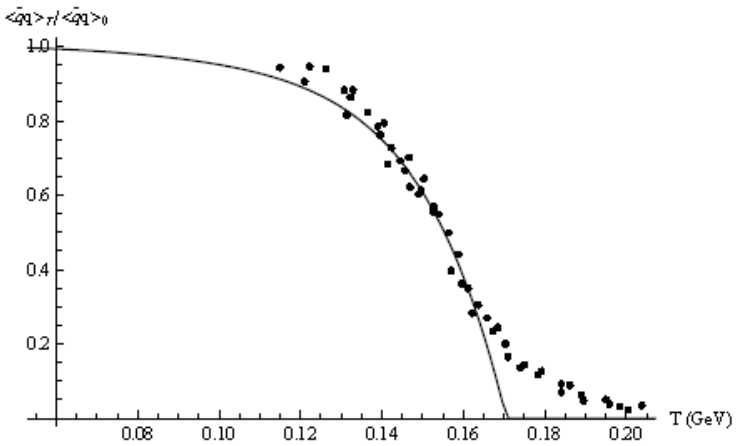


Quark condensate

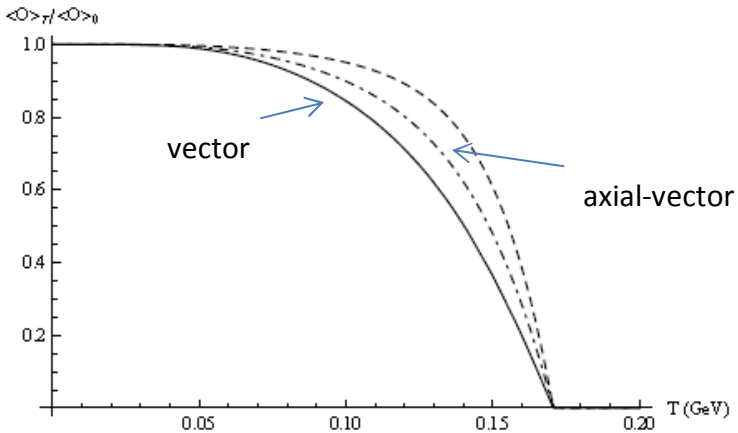


4-quark condensate

"modified HRG" = HRG + $T^{10}$ term

# Reduction in condensates induce changes in SFs

- Vector Channel
  - ρ spectral function. Rapp and Wambach, 1999
    - Provides a handle to base the rest of the study.
    - THESE SFS ARE CONSISTENT WITH DILEPTON MEASUREMENTS.
    - Spectral strength is allowed to vary slightly (deviations to VMD)
  - ρ' spectral function
    - Adjust mass, width, spectral strength
  - Continuum has no temperature dependence.
  - QCDSR determine temperature dependence

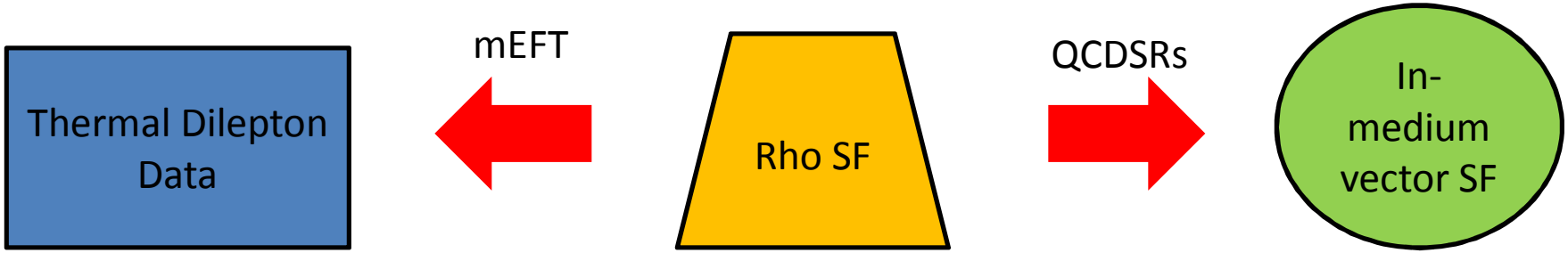

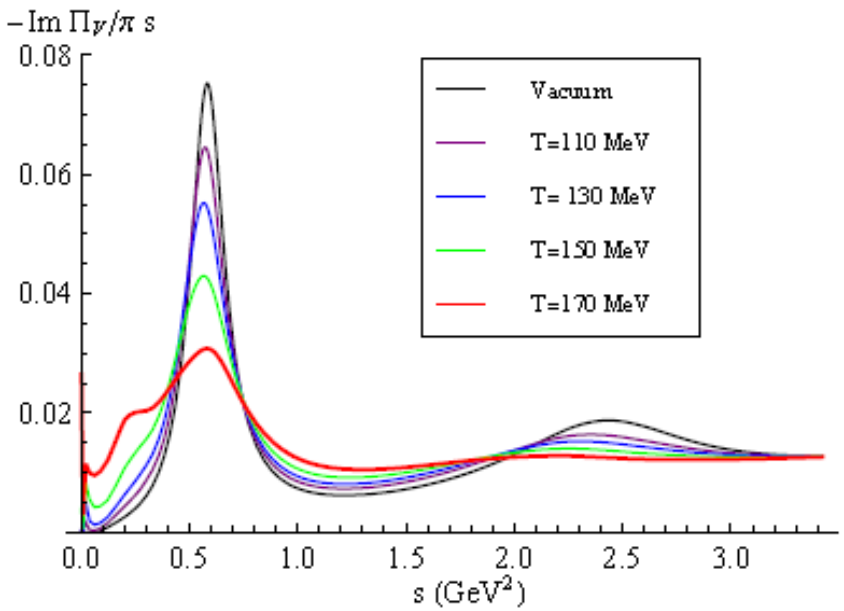


ρ peak develops a low energy shoulder and a reduction in strength

ρ’ peak is reduced and flattens out.

Correction to VMD needed range from <1% to 6%.

QCDSR are satisfied with deviations ranging from 0.44% to 0.75%.

- Axial-Vector Channel
  - a1' peak:
    - Adjust the mass, width, and spectral strength.
  - a1 peak:
    - Adjust mass, width, and spectral strength
    - Additional width component at low energies. (Needed for axial-vector "conductivity" and broadening below threshhold.)
    - Additional low energy peak – "a-sobar"
  - Pion pole:
    - Assume that pion does not develop a width.
    - Temperature dependence of pion mass is chosen from XPT.
    - Temperature dependence of $f_\pi$ taken from quark condensate and GOR.

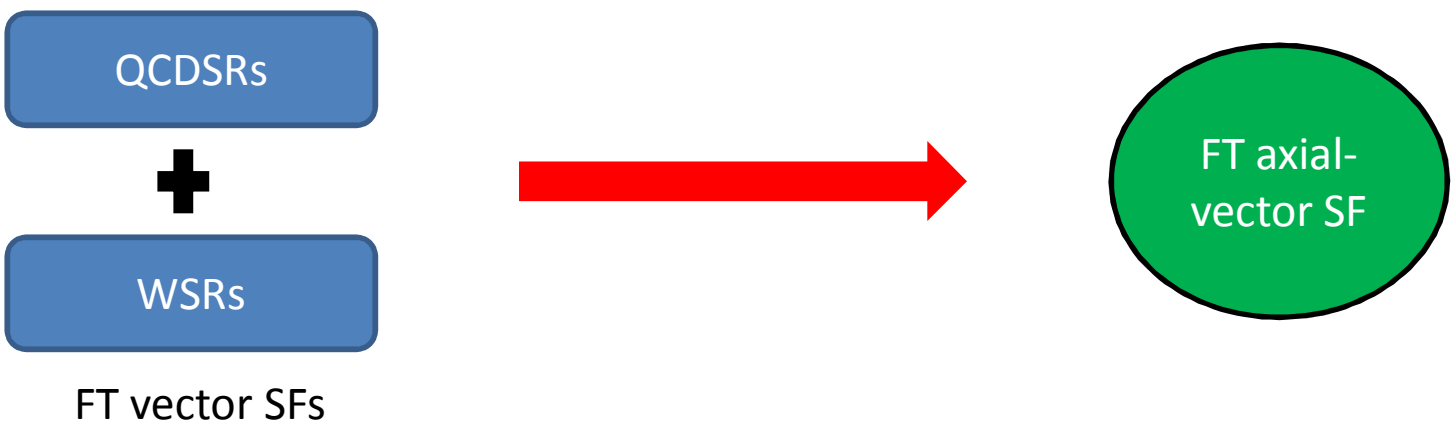

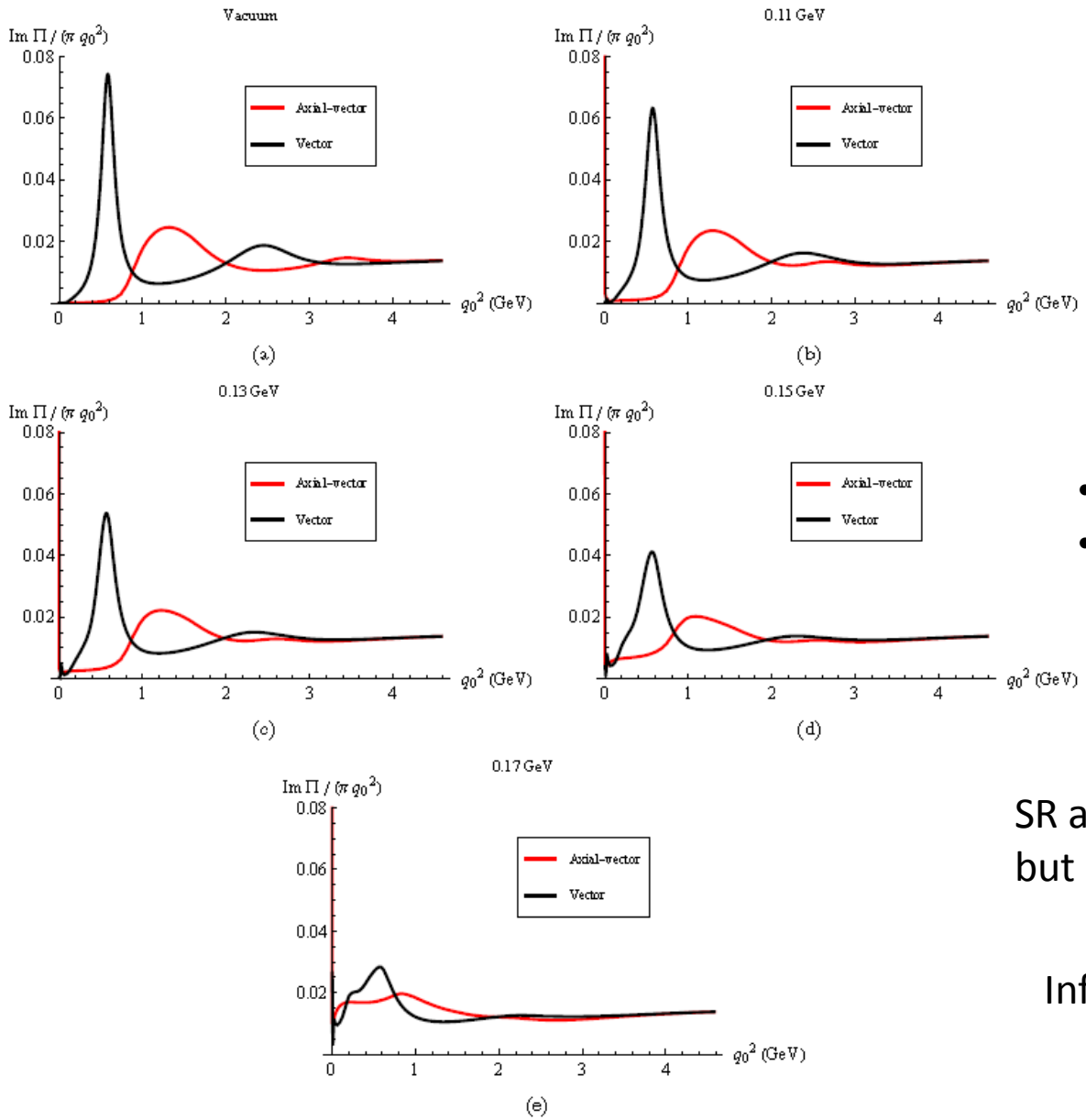


- Peaks shift and broaden
- New low energy structure
- Trend towards agreement

- WSR 1-2 satisfied <1%
- QCDSR satisified 0.45% -0.95%

SR analysis can give precise SF, but some ambiguity remains.

Info beyond SRs is needed

# Step 4: Hadronic effective field theory

- Massive Yang-Mills

Gomm, Kaymakcalan, and Schecter, 1984; Ko and Rudaz, 1994, etc.

  - Vector and axial-vector SFs and quark condensate can all be calculated simultaneously within this framework.

  - Pions are implemented by a non-linear sigma model
  - Gauge theory with two local chiral gauge symmetries.
    - Perserves chiral symmetry

$$SU_L(2) \times SU_R(2)$$

  - Vector and axial-vector mesons are represented by the corresponding gauge bosons.
  - Gauge symmetry is broken by an explicit mass term for the mesons.

  - Lagrangian has 4 free parameters: m0, g, σ, and ξ.
    - Will use $m_\rho$, $m_a$, $g_{\rho\pi\pi 1}$, $g_{\rho\pi\pi 3}$

Vector self energy diagrams

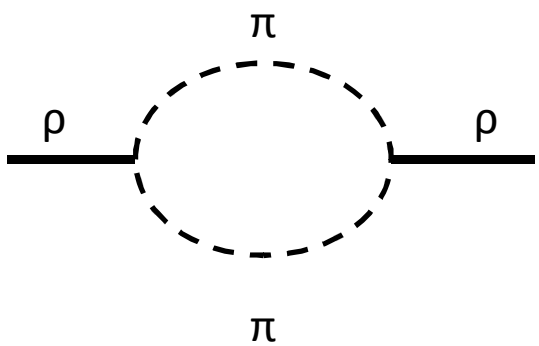


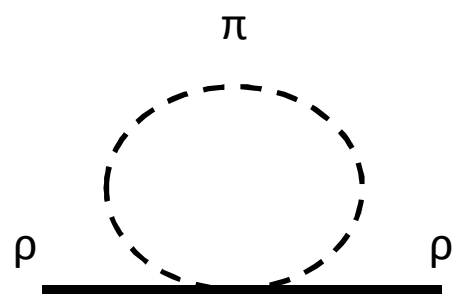


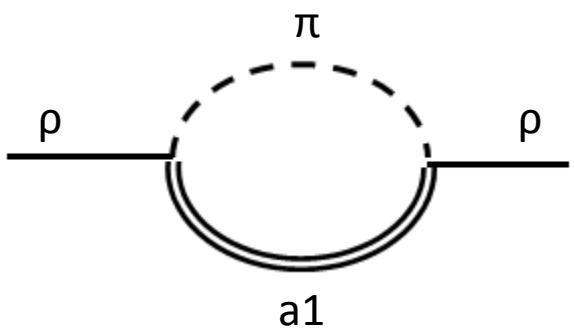


Axial-vector self energy diagrams

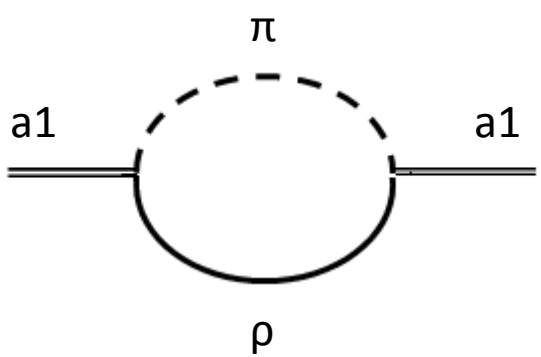


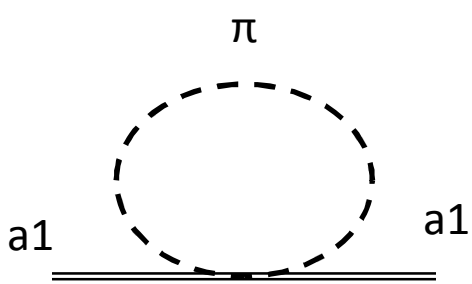


Calculate 1-loop diagrams and then resum.

# Vacuum Spectral functions

Data from ALEPH (Barate et al. 1998)

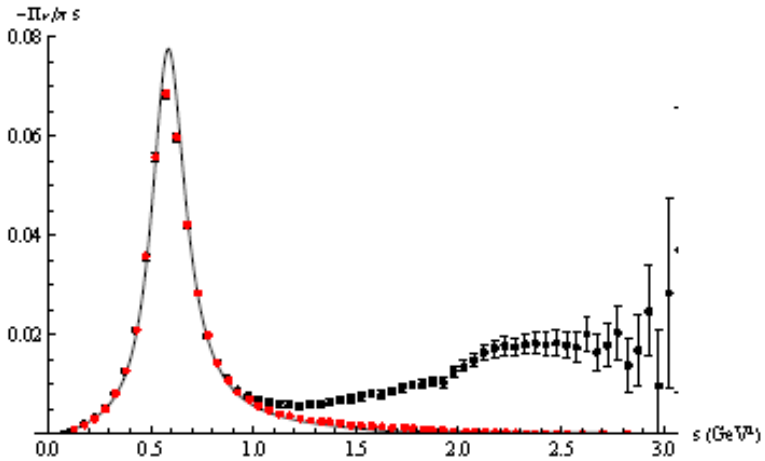


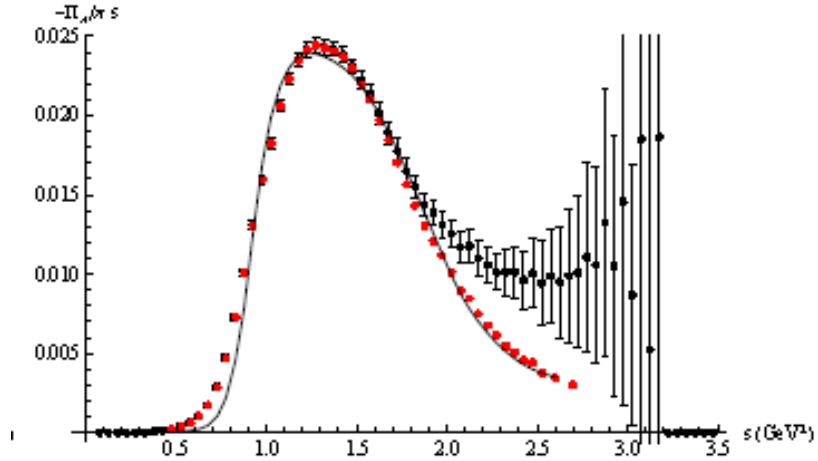


| | Calc. | Expt. |
|---|---|---|
| $\Gamma(a_1 \to \gamma\pi)$ | 828 keV | 640±246 keV |
| D/S | -0.084 | -0.09±.03 |

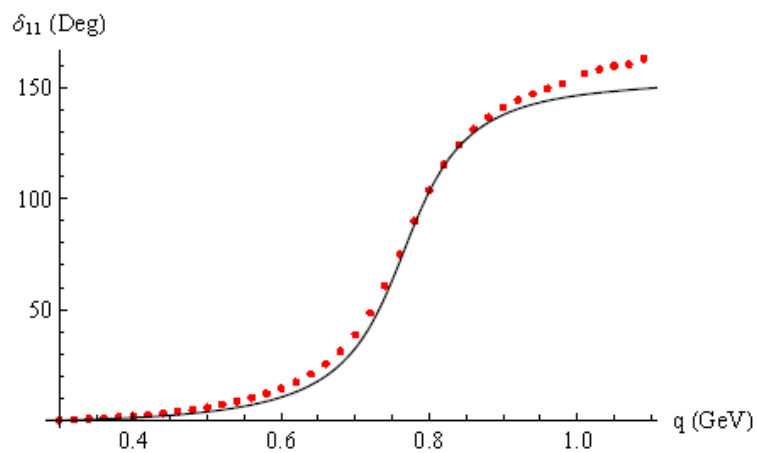


Data from Froggatt and Petersen, 1977

In-medium calculation on the way.

# Summary

- Explored the connection between vector and axial-vector SFs in order to probe chiral symmetry restoration.

- Vacuum
  - Spectral functions were constructed which agreed with SRs
  - Sum rules indicate a need for excited axial-vector state
- Low temperatures
  - SF constructed in a rigorous low temperature prescription
  - QCDSR along with finite pion mass indicate that analysis is limited in T
- Beyond low temperatures
  - Rho SF used from microscopic model which agrees with dilepton data
  - Constructed axial-vector SF from sum rule analysis
  - SF exhibit a shift of spectral strength to lower energies
  - SRs give precise SFs but there remains some ambiguity
- Hadronic effective theory
  - Constructed vacuum fits
  - More work is need for in-medium study.

# Di-electron spectra in p+p and Au+Au at 200 GeV from STAR

**Bingchu Huang** *(for the STAR Collaboration)*
*Brookhaven National Laboratory*

BROOKHAVEN NATIONAL LABORATORY

# Outline

- Motivation
- Analysis
- Di-electron production in p+p and Au+Au at 200 GeV
- Summary

# Motivation

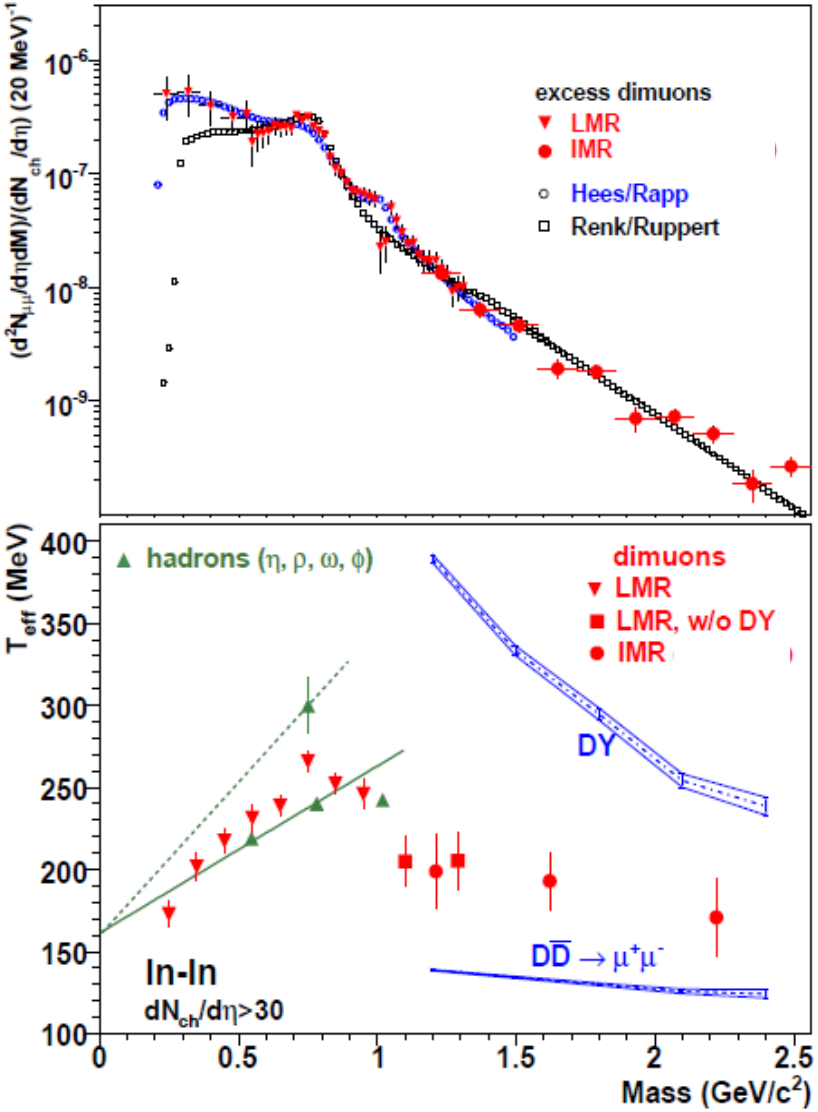


*NA60:* ***Eur.Phys.J.C59:607-623,2009***

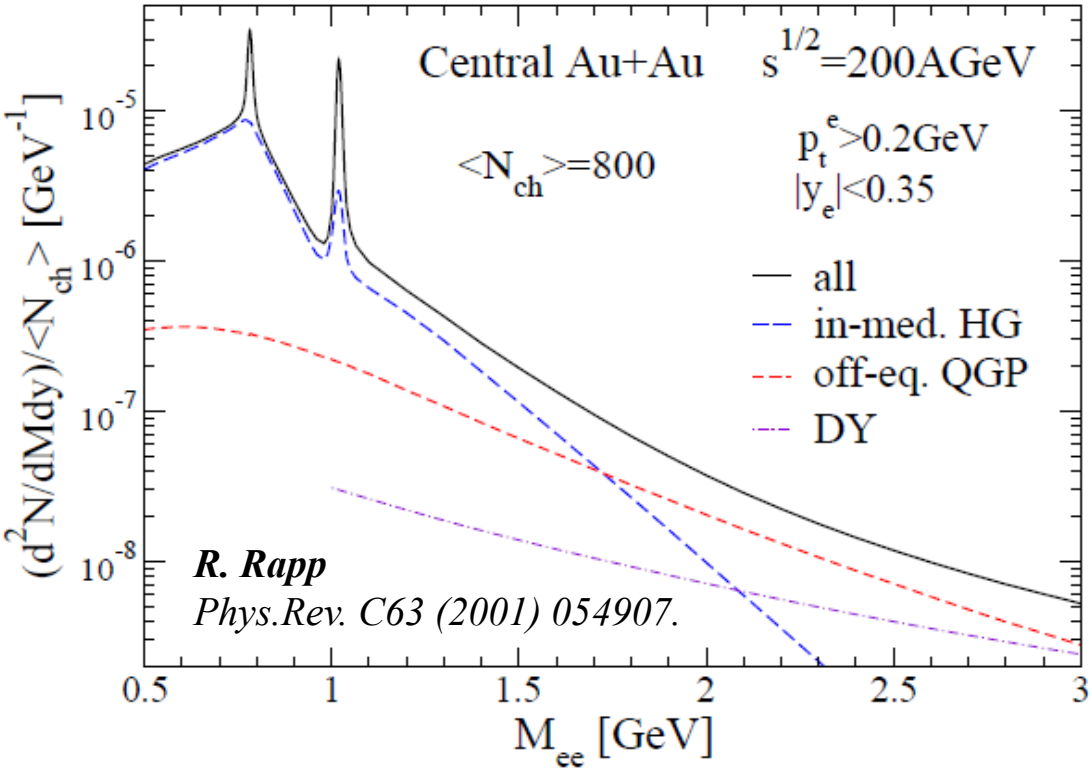


**Low mass range (LMR):**

In-medium modifications of vector mesons.

Possible link to chiral symmetry restoration.

**Intermediate mass range (IMR):**

QGP thermal radiation.

Heavy flavor modification.

# Electron identification

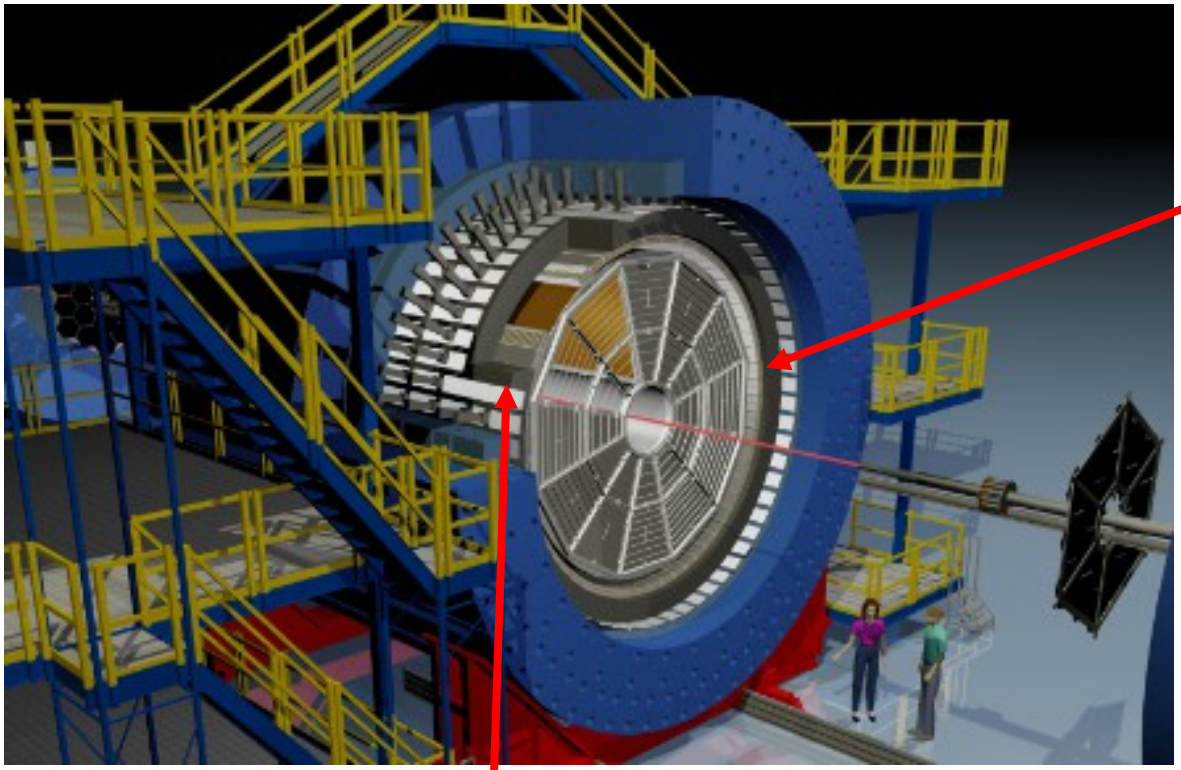

**Tracking: TPC**

Time Projection Chamber
1. Tracking
2. Ionization energy loss (dE/dx PID)
3. Coverage -1<η<1

**Particle ID: TOF**

Time Of Flight ----
1. Timing resolution (<100ps)
2. Coverage: -0.9<η<0.9
3. Completed in 2010 (72% in 2009)

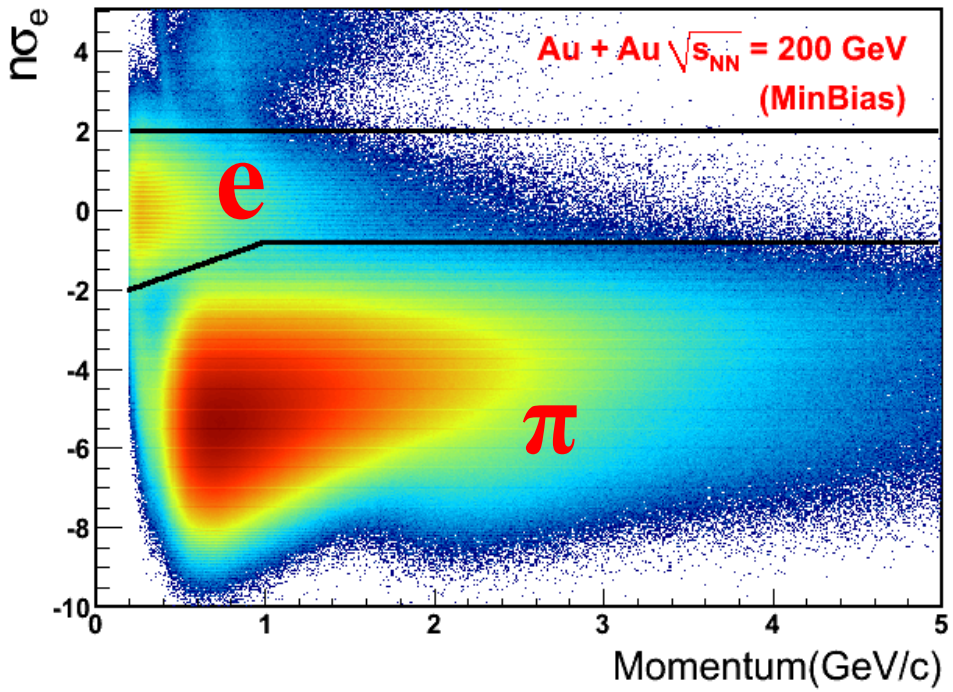

# Background subtraction

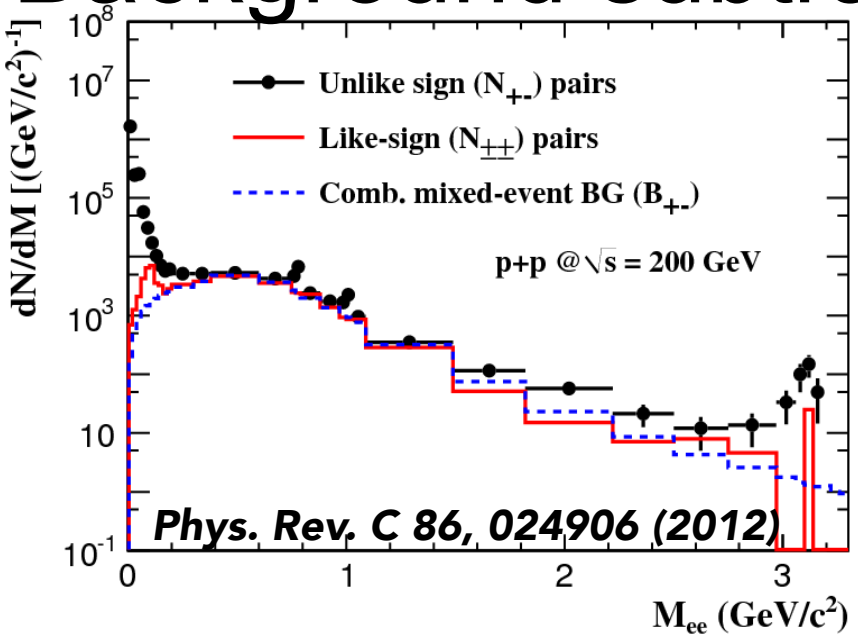


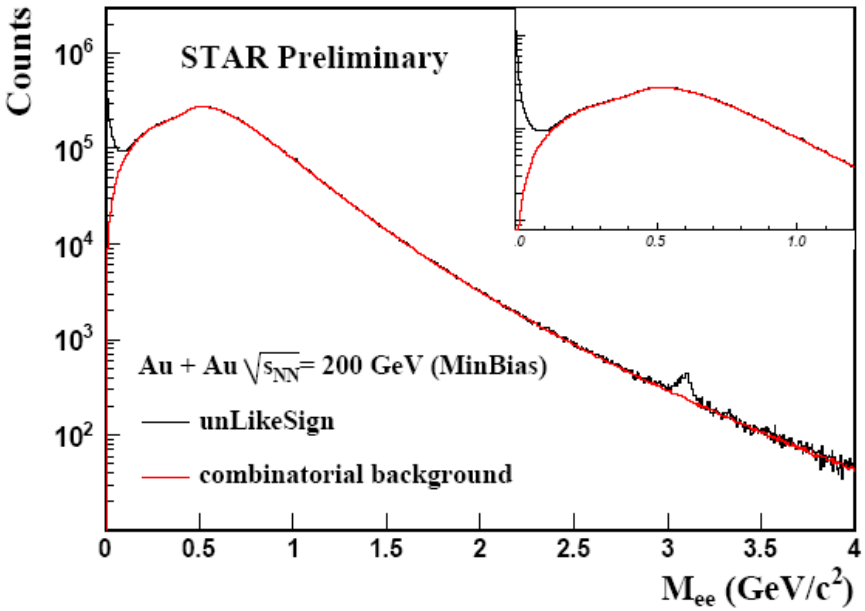


Like-sign background has been corrected by acceptance factor:

$$\frac{B_{+-}^{Mix}}{2\sqrt{B_{++}^{Mix}B_{--}^{Mix}}}$$

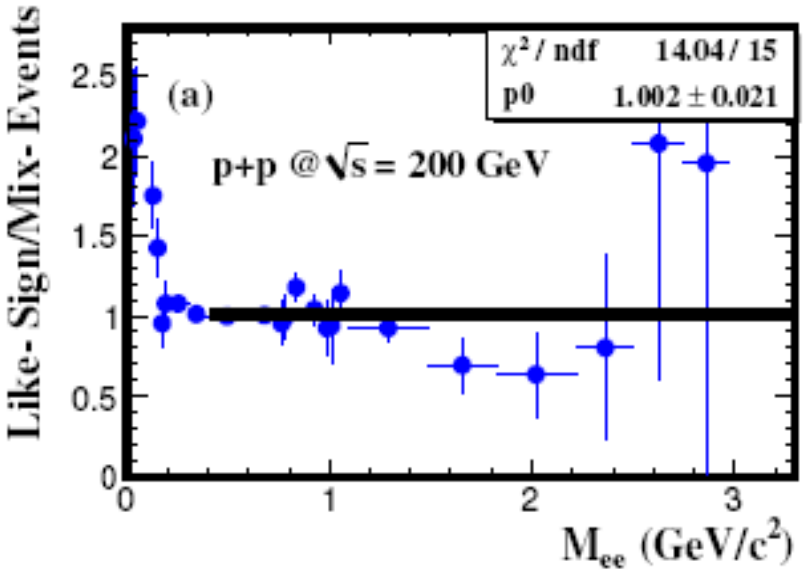


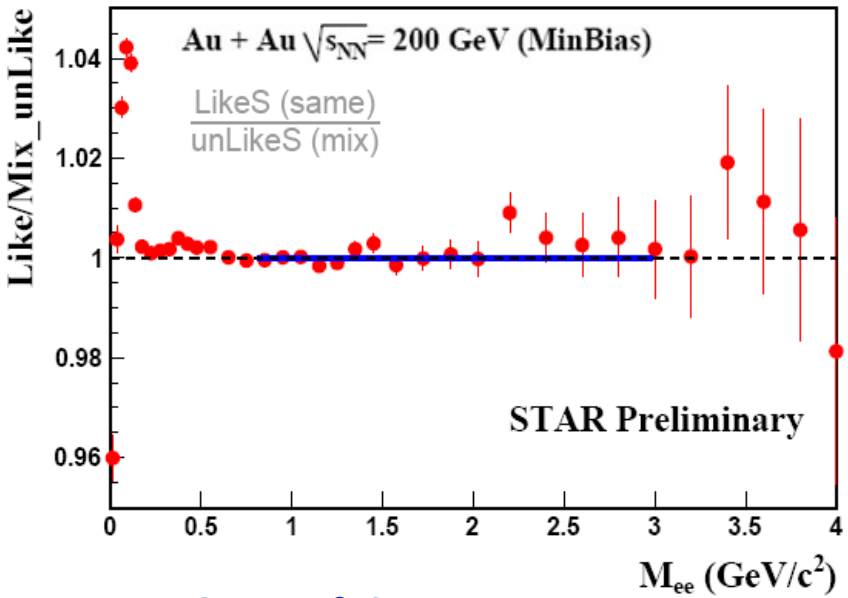


Normalization range of Mee:
p+p : (0.4,1.5) GeV/c²
Au+Au: (0.7,3) GeV/c²

Mixed-event BG subtraction range: $M_{ee}$>0.4 GeV/c² for p+p and $M_{ee}$>0.75 GeV/c² for Au+Au 200 GeV.

# Signal/background

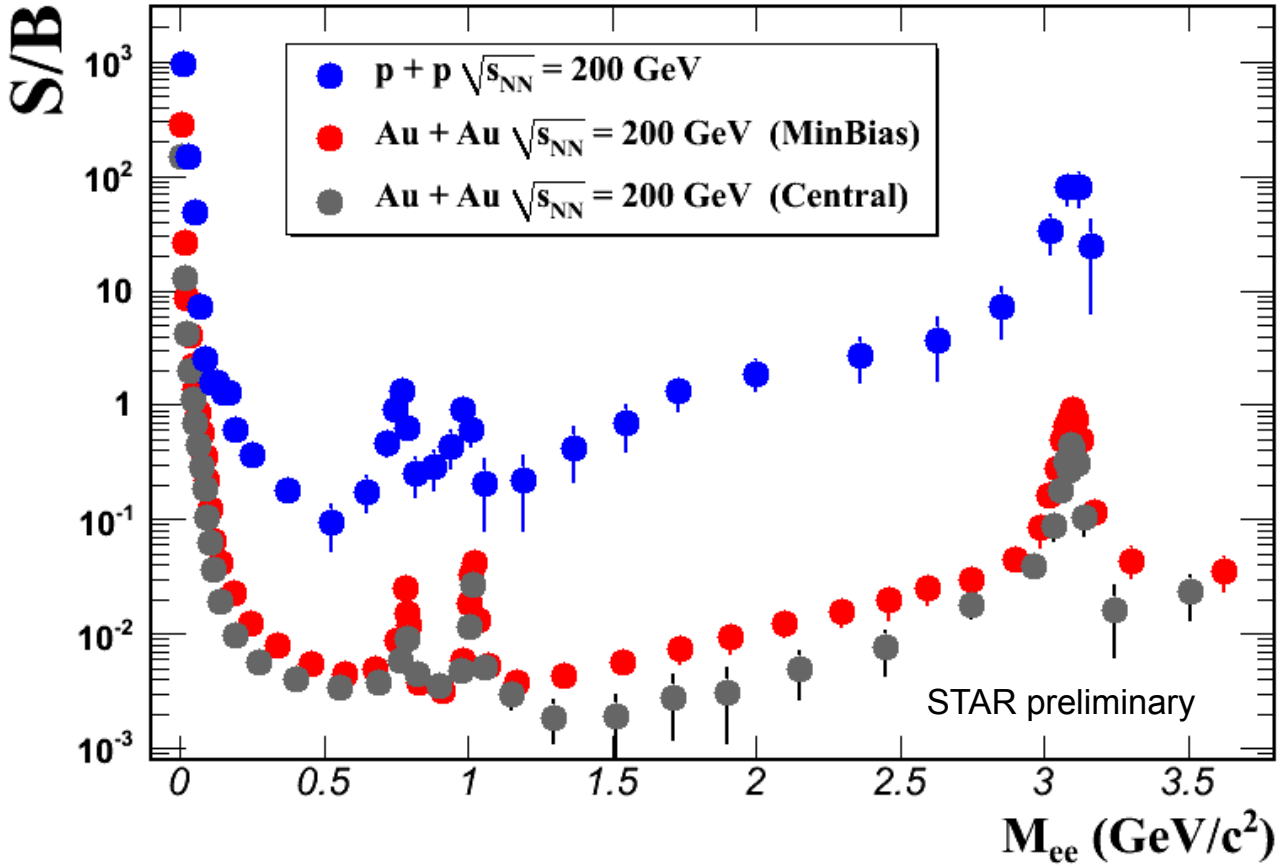


- **Signal/background ratio: $M_{ee}$ ~ 0.5 GeV/$c^2$**

  *~ 1:10 for p + p collisions*

  *~ 1:200 for Au + Au minbias collisions*

  *~ 1:250 for Au + Au central collisions*

# Efficiency of single electron

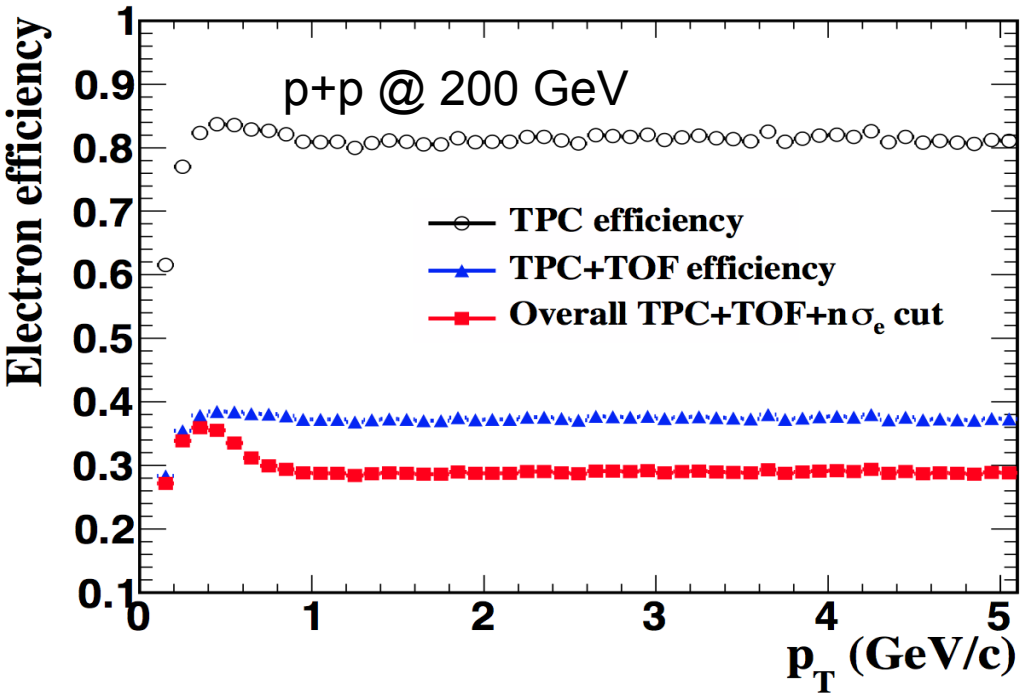


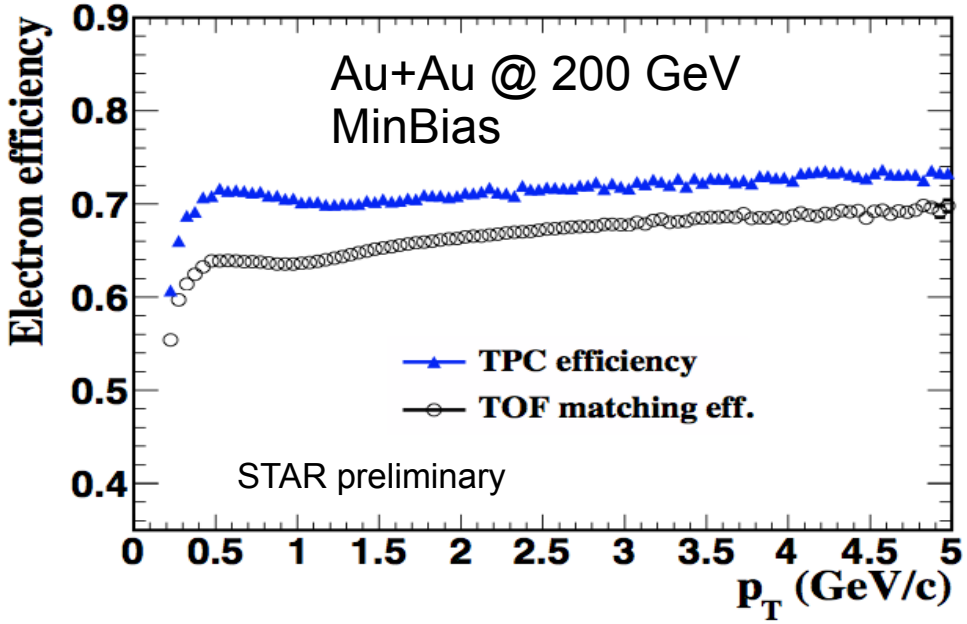


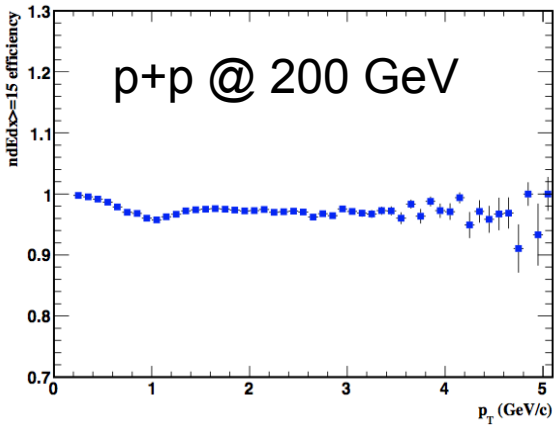


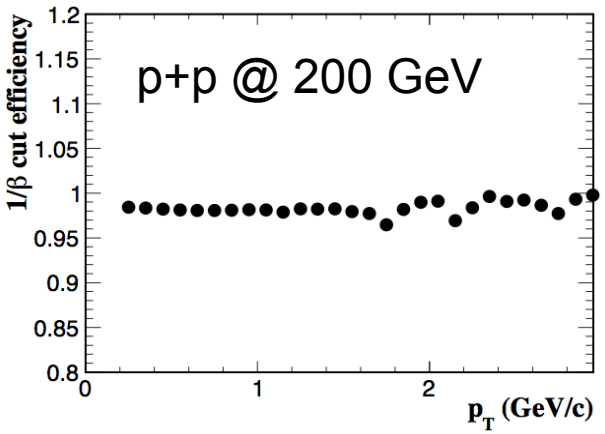


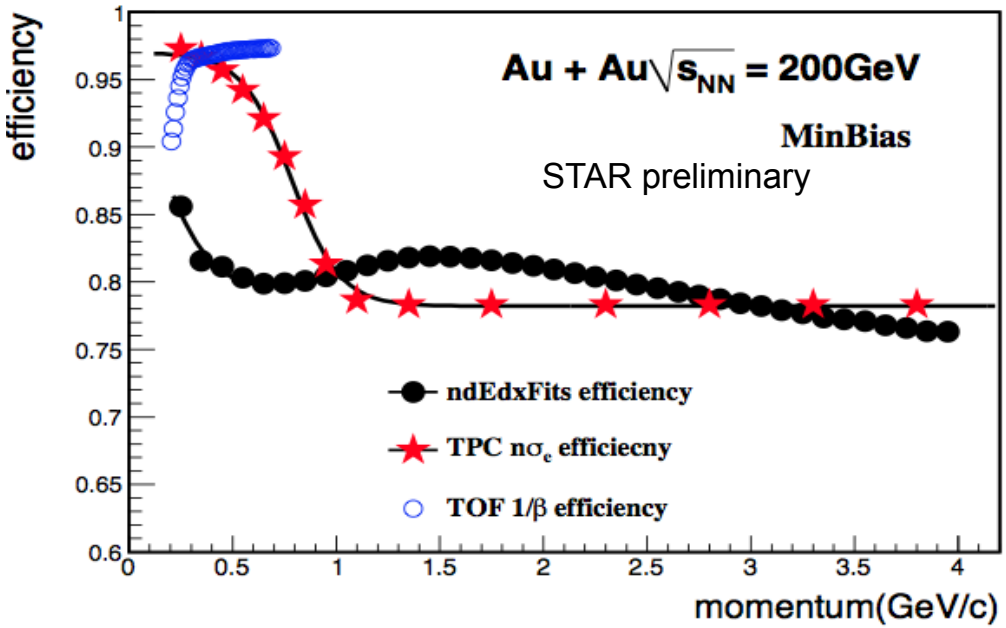

# Simulation

**Inputs:**

- **Kinetics: flat rapidity (-1,1) , flat Φ (0, 2π), $p_T$ Tsallis function fit for all measured particles.**
- **Hadrons decay: using Kroll-Wada formula, form factors are from measurements.**
- **Heavy flavor sources: line shapes from PYTHIA, scaled by STAR measured cross-section.**

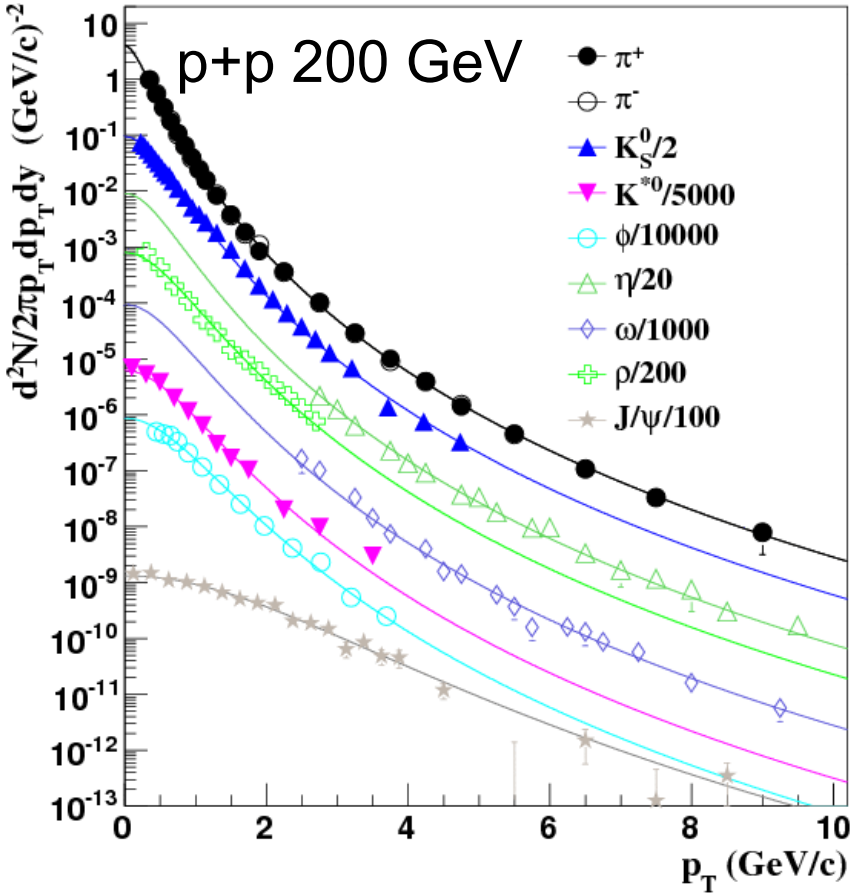


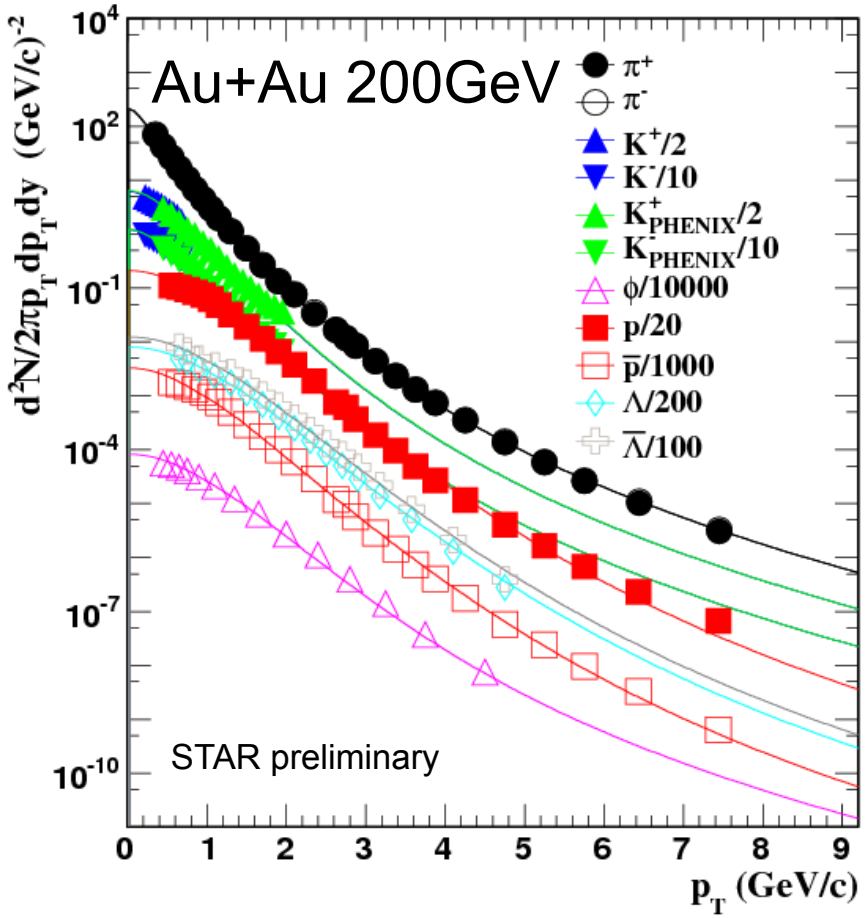


η and J/ψ are fitted separately in Au+Au.

Zebo Tang et al, PRC 79, 051901(R) (2009)

# Meson decay

Kroll-Wada Formula:

$$\frac{dN}{dm_{ee}} \propto \sqrt{1-\frac{4m_e^2}{m_{ee}^2}} \cdot \left(1+\frac{2m_e^2}{m_{ee}^2}\right) \cdot \frac{1}{m_{ee}} \cdot \left(1-\frac{m_{ee}^2}{M_h^2}\right)^3 |F(m_{ee}^2)|^2$$

QED | Phase Space | Form Factor

*N.M. Kroll, et al., Phys Rev, 98 (1955) 5.*

Twobody: Breit-Wigner

Dalitz: Kroll-Wada

FF: parameterized from measurement.

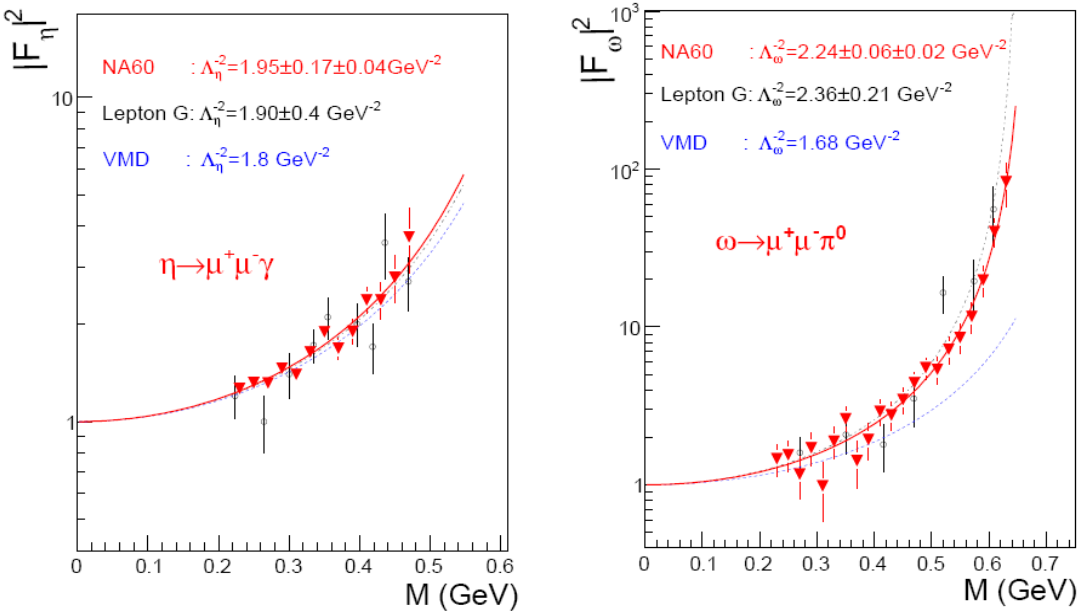


NA60: PLB677 (2009) 260.

$$|F(m_{ee}^2)|^2 = \frac{1}{(1-m_{ee}^2\cdot\Lambda^{-2})^2+\Gamma_0^2\cdot\Lambda^{-2}}$$

Phase Space term for omega, phi:

$$(1-\frac{m_{ee}^2}{m_h^2})^3 \Rightarrow ((1+\frac{m_{ee}^2}{m_\omega^2-m_{\pi^0}^2})^2-\frac{4m_\omega^2 m_{ee}^2}{(m_\omega^2-m_{\pi^0}^2)^2})^{\frac{3}{2}}$$

$$\frac{dN}{dm_{ee}dp_T} \propto \frac{m_{ee}M_\rho\Gamma_{ee}}{(M_\rho^2-m_{ee}^2)^2+M_\rho^2(\Gamma_{\pi\pi}+\Gamma_{ee}\Gamma_2)^2} \times PS,$$

Rho meson:

P-wave of ππ channel: $\Gamma_{\pi\pi} = \Gamma_0\frac{M_\rho}{m_{ee}}(\frac{m_{ee}^2-4M_\pi^2}{M_\rho^2-4M_\pi^2})^{3/2},$

S-wave of ee channel: $\Gamma_{ee} = \Gamma_0\frac{M_\rho}{m_{ee}}(\frac{m_{ee}^2-4m_e^2}{M_\rho^2-4m_e^2})^{1/2},$

$$PS = \frac{m_{ee}}{\sqrt{m_{ee}^2+p_T^2}}e^{-\frac{\sqrt{m_{ee}^2+p_T^2}}{T}}.$$

*PRC 78, 044906 (2008)*

# Pair efficiency

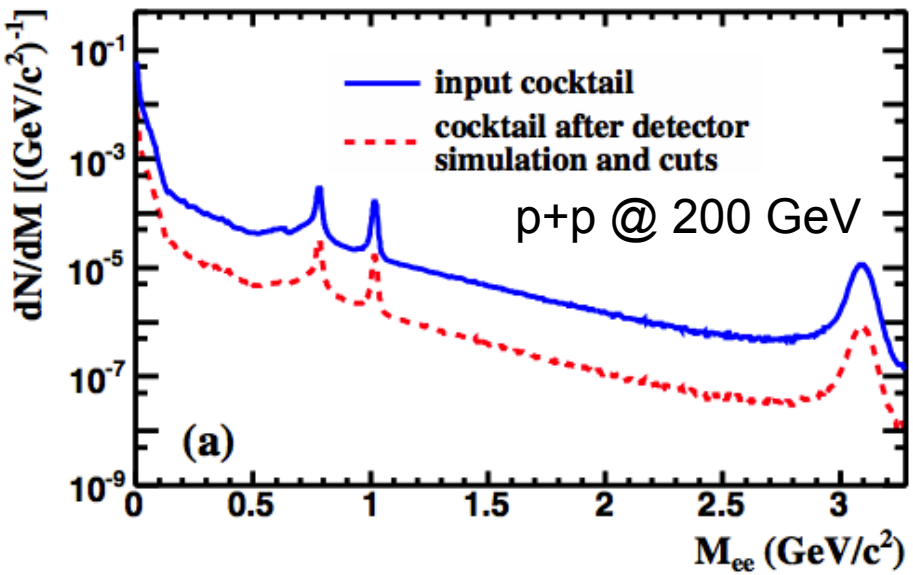


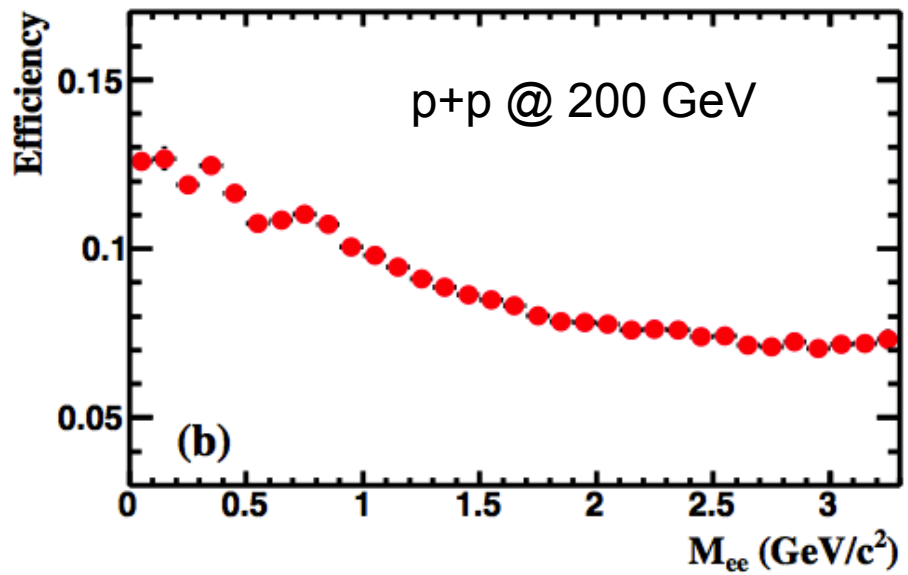


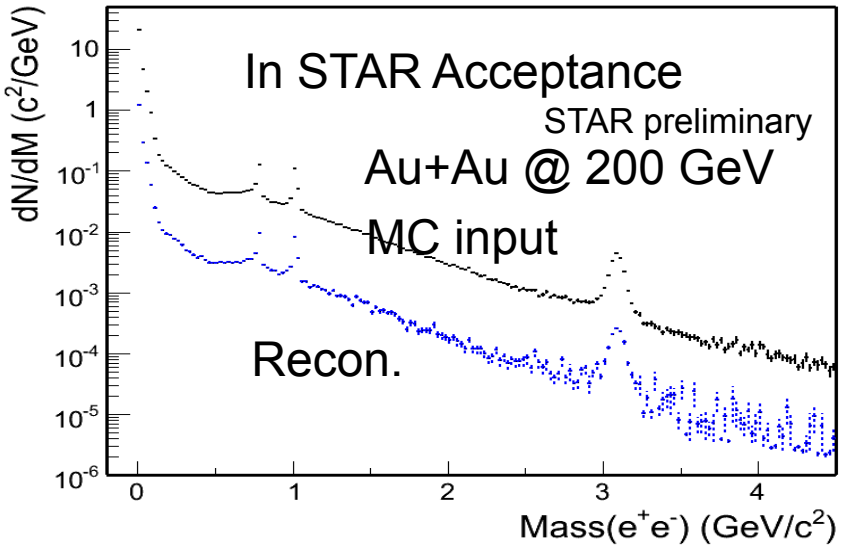


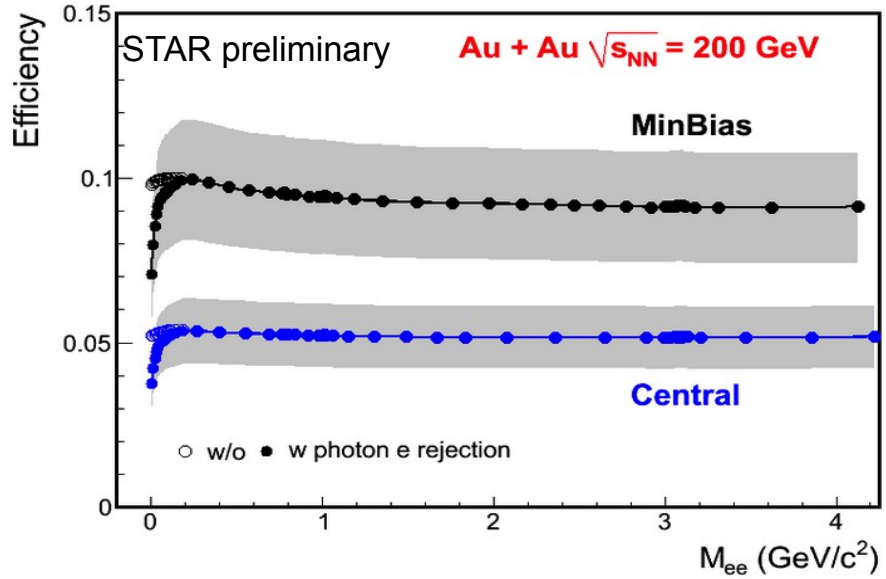


$$pair\ eff. = \frac{(cocktail\ sampled\ single\ electron\ eff.)}{(input\ cocktail)}$$

# Di-electron results in p+p 200 GeV

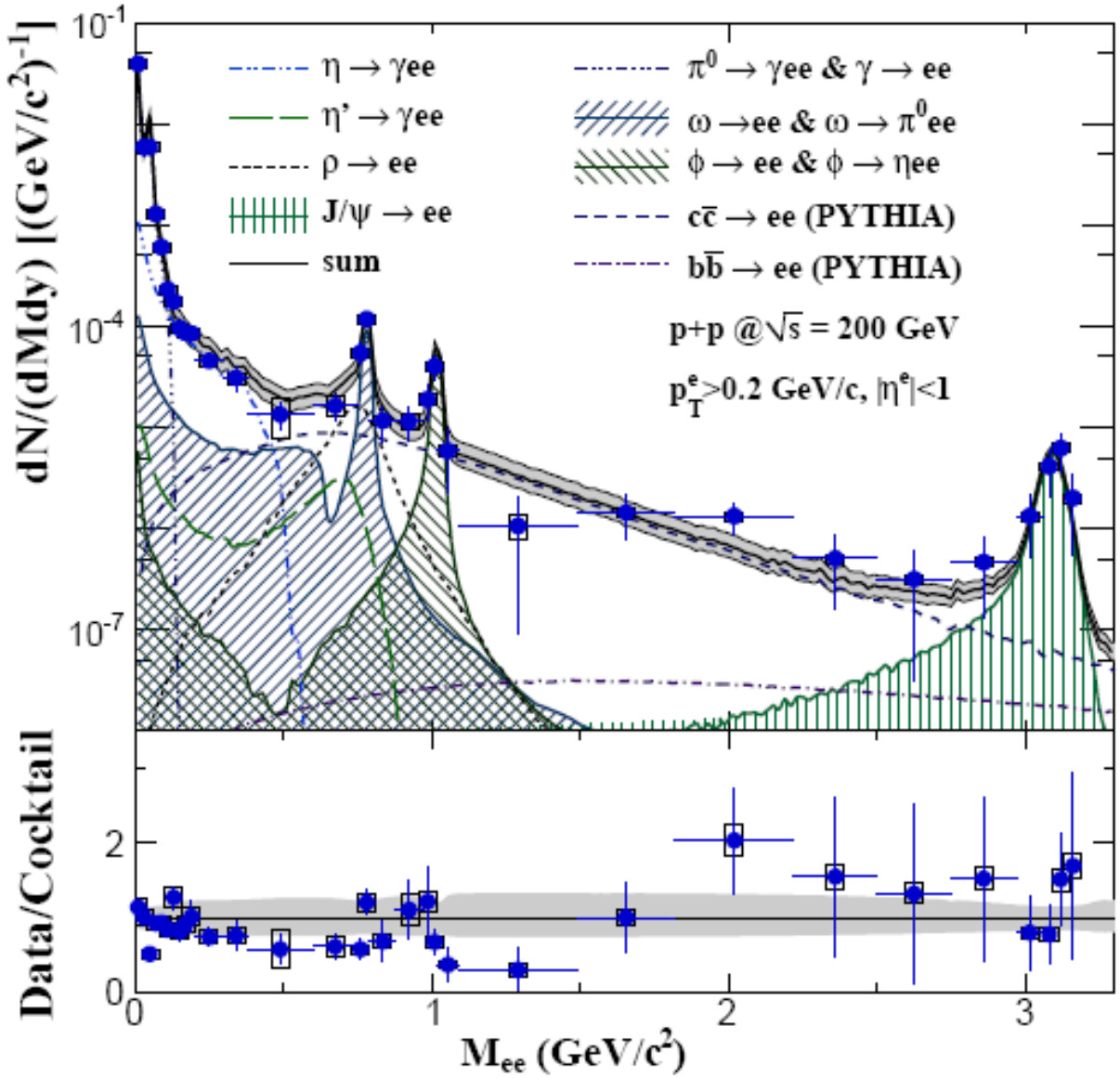


**Phys. Rev. C 86, 024906 (2012)**

- Cocktail simulation is consistent with di-electron spectrum within quoted uncertainties.
- Intermediate mass region is dominated by charm correlation contribution.

# Di-electron results in Au+Au 200 GeV

*STAR QM2011:J. Phys. G:38 124134*

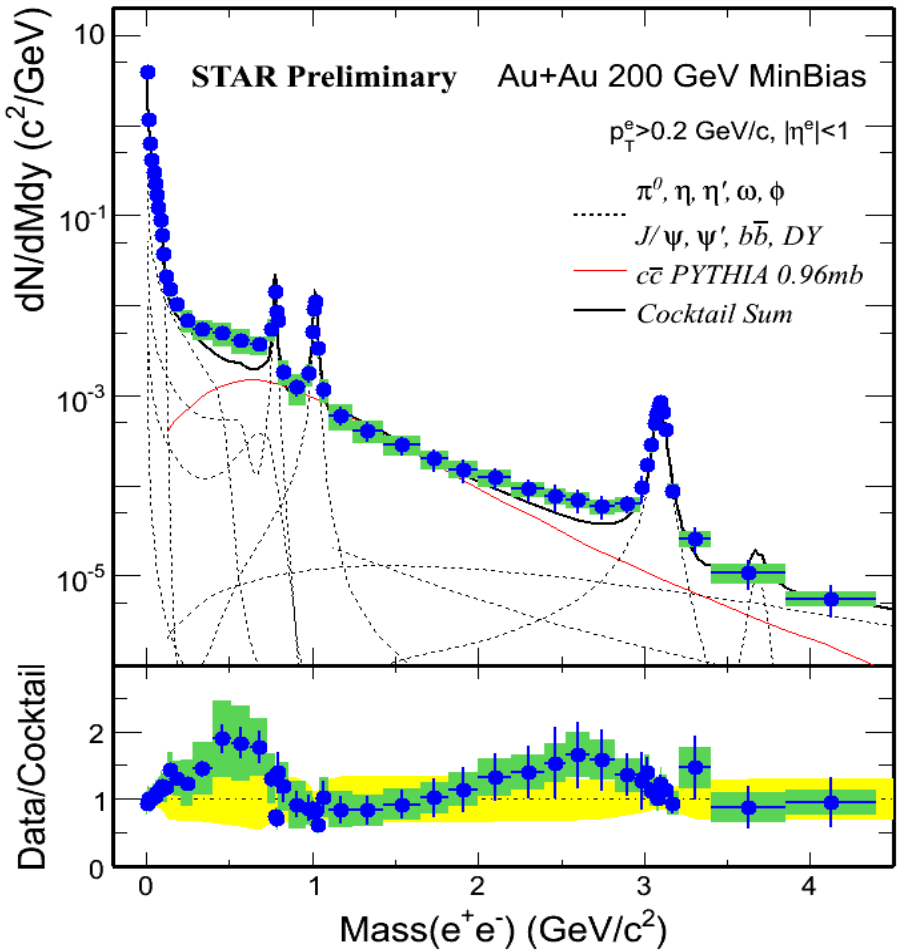


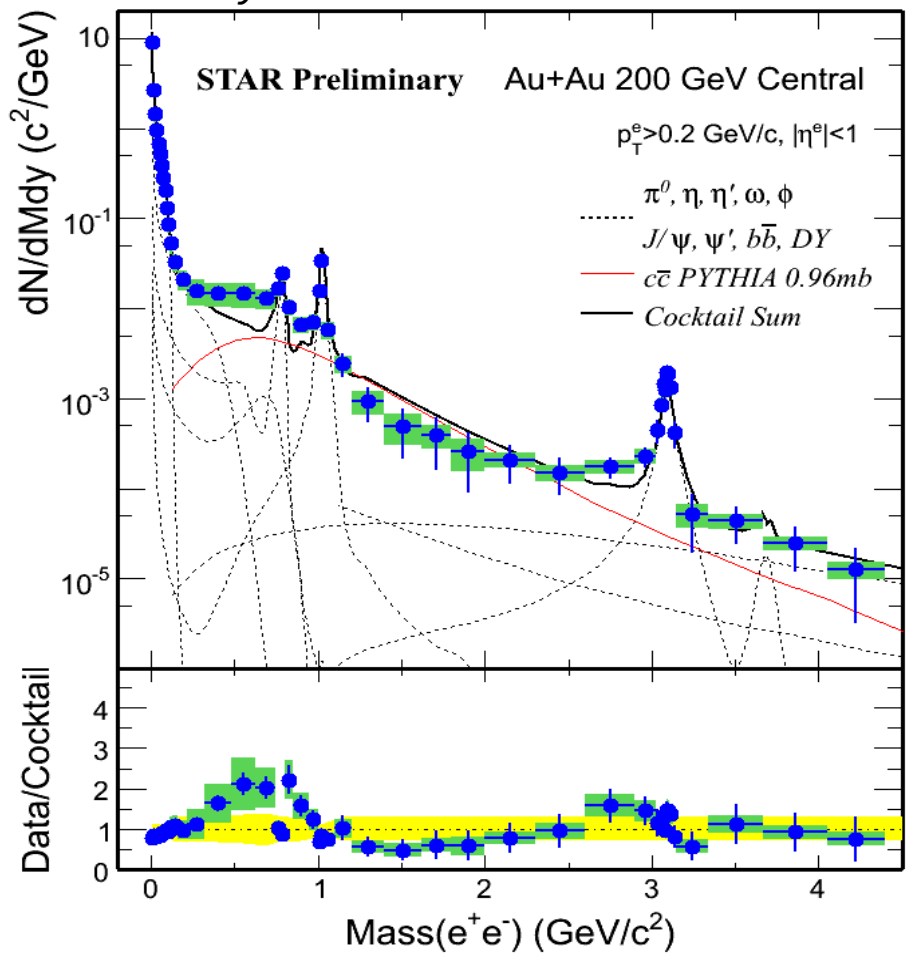


**Enhancement factor in 0.15<Mee<0.75 Gev/c2**

| | Minbias (value ± stat ± sys) | Central (value ± stat ± sys) |
|---|---|---|
| STAR | 1.53 ± 0.07 ± 0.41 (w/o ρ)<br>1.40 ± 0.06 ± 0.38 (w/ ρ) | 1.72 ± 0.10 ± 0.50 (w/o ρ)<br>1.54 ± 0.09 ± 0.45 (w/ ρ) |
| PHENIX | 4.7 ± 0.4 ± 1.5 | 7.6 ± 0.5 ± 1.3 |
| Difference | 2.0 σ | 4.2 σ |

**PHENIX** *Phys.Rev. C81 (2010) 034911*

# Centrality dependence in Au+Au 200 GeV

By Jie Zhao

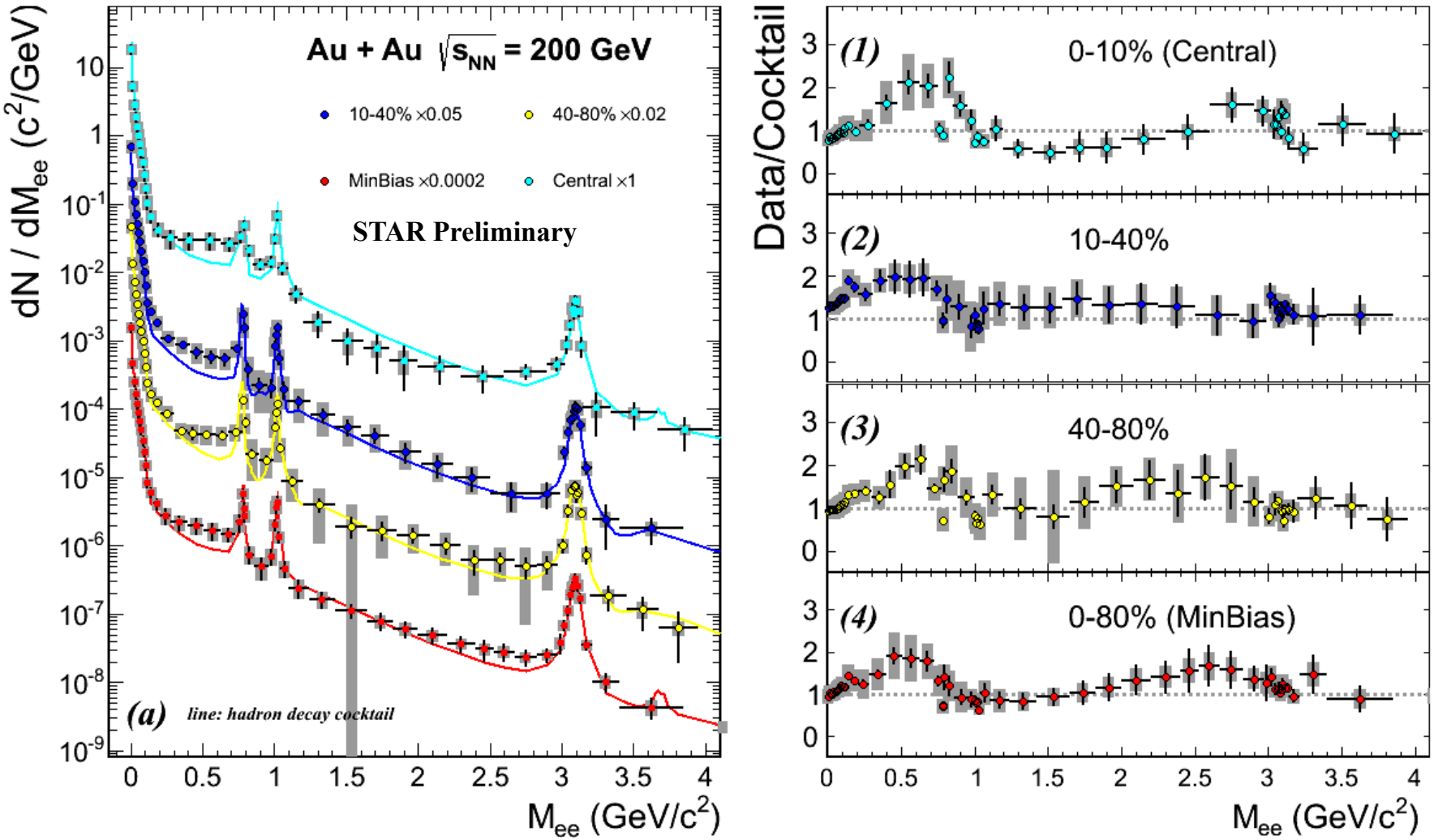

# LMR yields in Au+Au

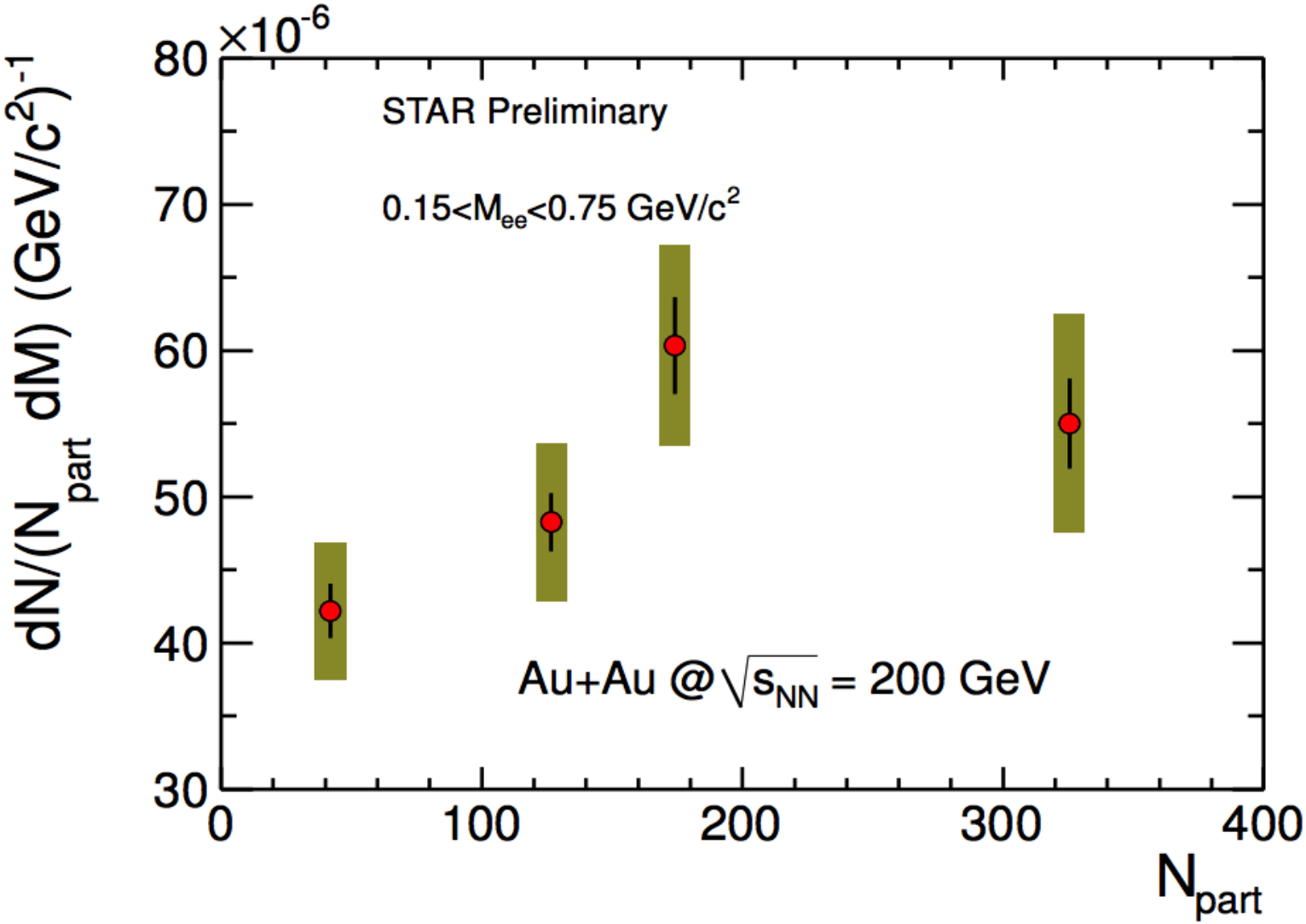


LMR enhancement scaled by Npart vs. centrality.

# Comparison to theoretical calculation

**Theoretical calculation**:
*Blue: Hadron gas contribution in medium(HG) with a broadened ρ spectral function.*
*Pink: QGP.*
*R. Rapp*(private communication).
*R. Rapp, Phys.Rev. C 63 (2001) 054907*
*R. Rapp & J. Wambach, EPJ A 6 (1999) 415*

Solid lines: *cocktail + HG+QGP*
*Black : cocktail*

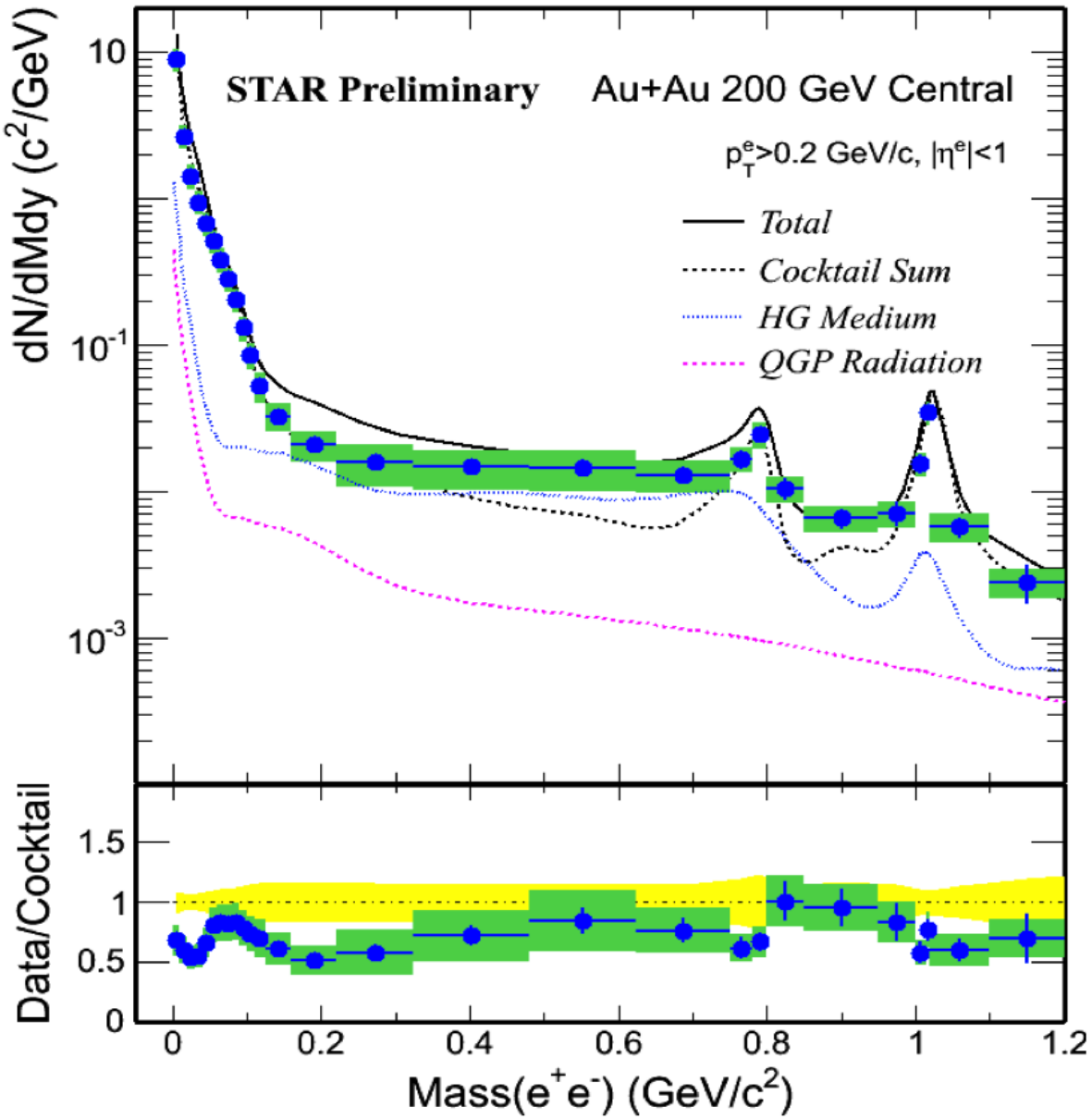


A sum of cocktail+HG+QGP agree with data within uncertainty. It satisfies with a broadened rho spectral function. Indicates the rho emission rate is dominated by hadron gas phase.

# Comparison to theoretical calculation

O. Linnyk et al., Phys. Rev. C 85 024910 (2012)
H. Xu et al., Phys. Rev. C 85 024906 (2012)

Parton-Hadron-String Dynamics (PHSD)

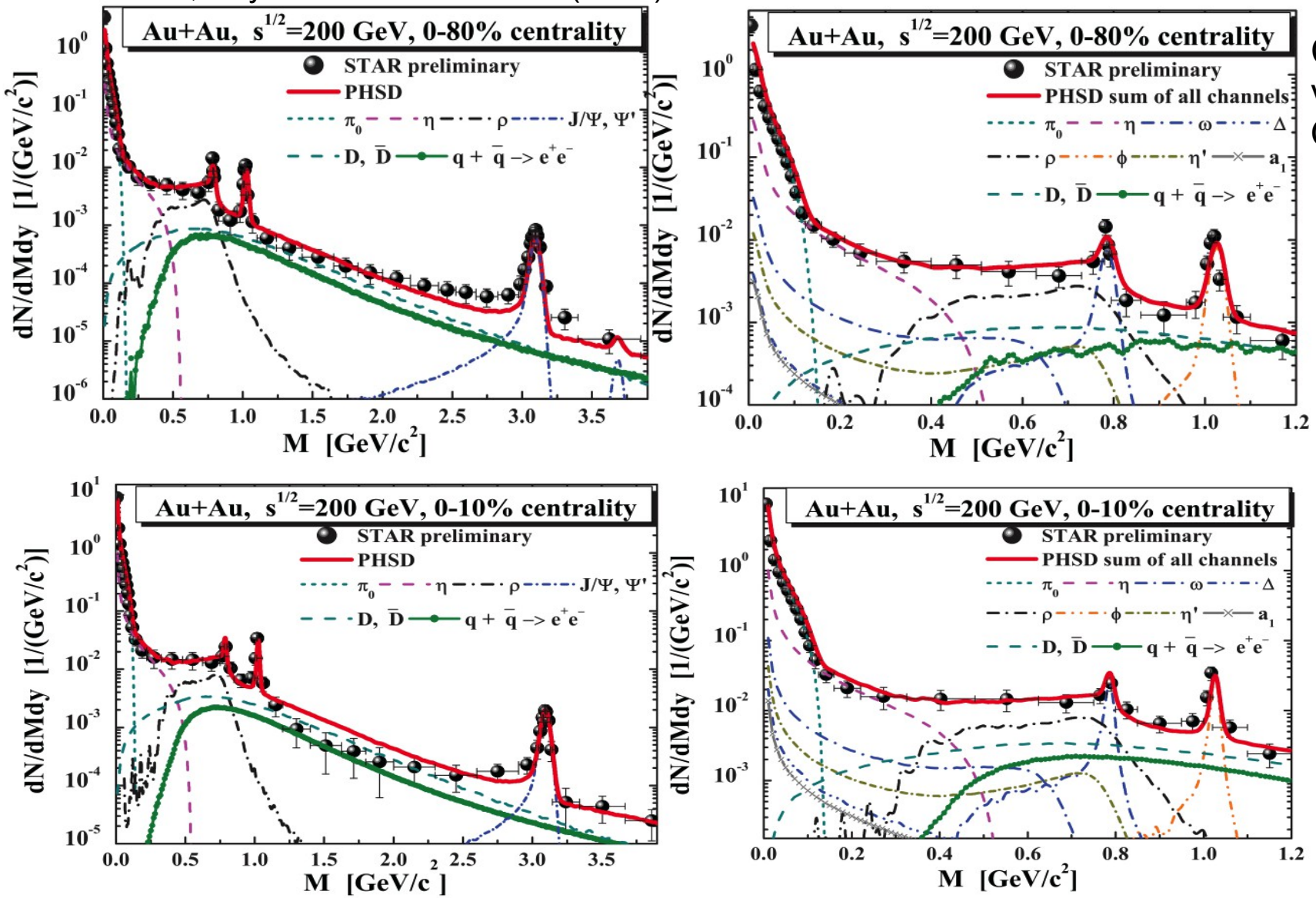


Consists of broadened vector mesons and QGP thermal radiation.

Agreements show in enhancement region (0.3-0.7 GeV/$c^2$) in minbias and central.

# Transverse mass spectra

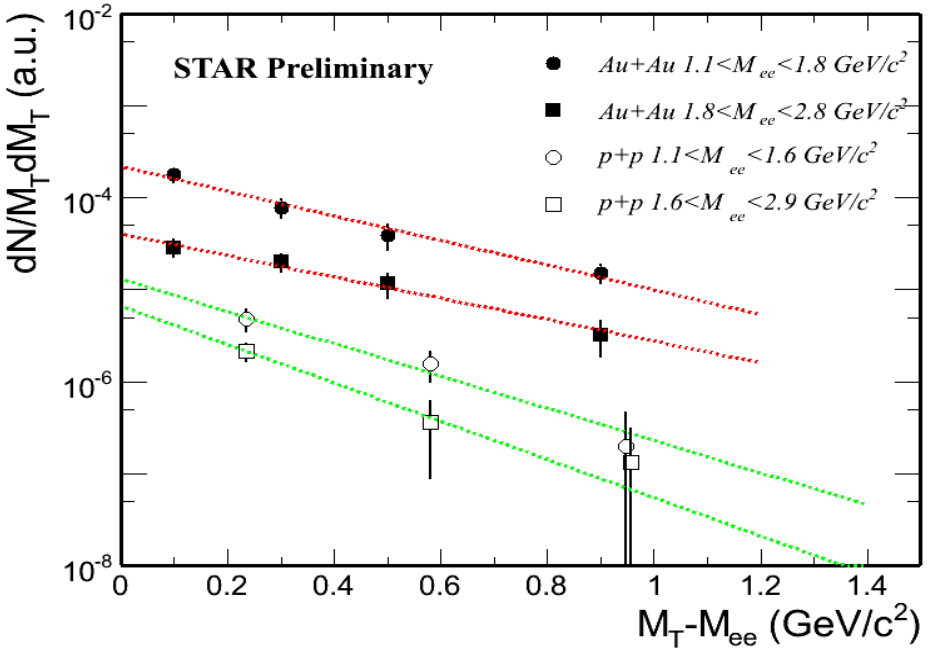


**A + A: Minbias collisions**

RHIC Au + Au 200 GeV / SPS In + In 17.2 GeV

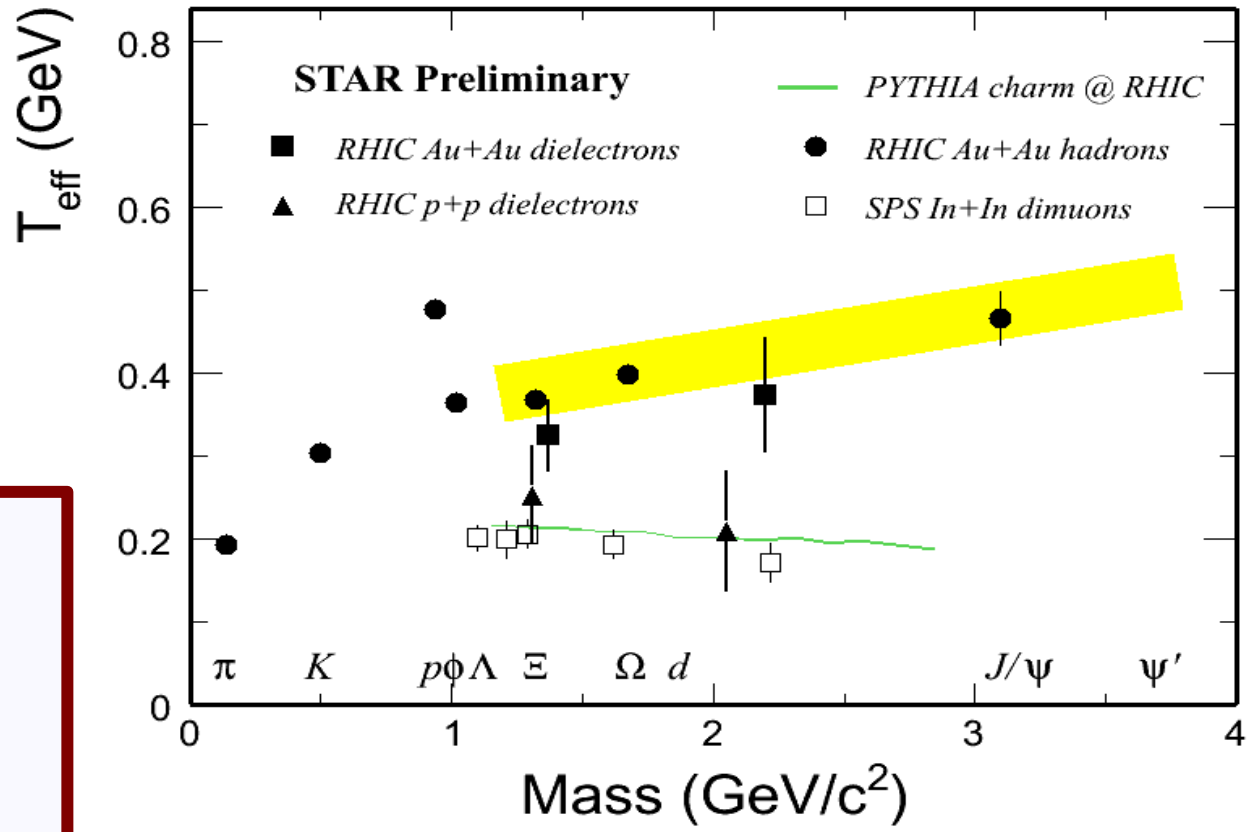


- **p + p result consistent with PYTHIA charm**
- **$m_T$ slope parameter in Au+Au is higher than that in p + p**

  *hint of thermal di-lepton production and/or charm modification*
- **Inclusive di-lepton slope in Au+Au at RHIC is also higher than that (charm/DY subtracted) from SPS**

**SPS data: charm/DY subtracted - PRL 100, 022302 (2008)**
**STAR data: inclusive di-electron, statistical error only**
**Yellow band indicates the sys. uncertanties at STAR.**

# Summary

- Di-electron productions have been measured in p+p and Au+Au at 200 GeV.
  - Di-electron measurement in p+p is consistent with the expected yields within uncertainties.
  - Observed an enhancement at low mass region in Au+Au at 200 GeV.
  - Slope parameter in Au+Au is higher than that in p+p.
- A broadened $\rho$ spectral function scenario can describe the low mass enhancement observed in Au+Au central collisions at 200 GeV.

**Thank you !**

# Backup

# Check with acceptance difference

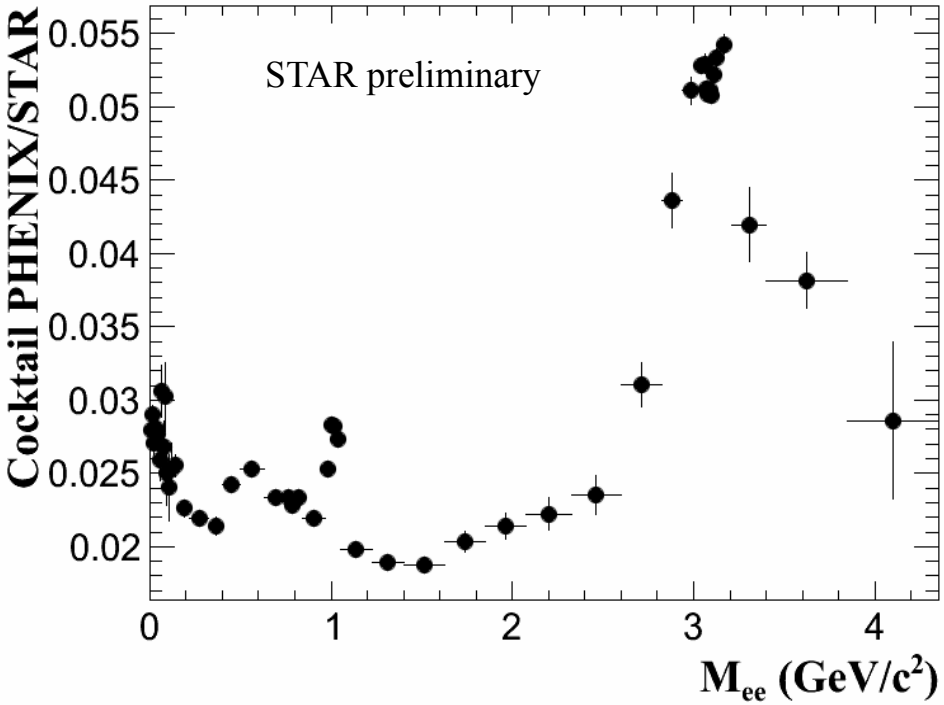


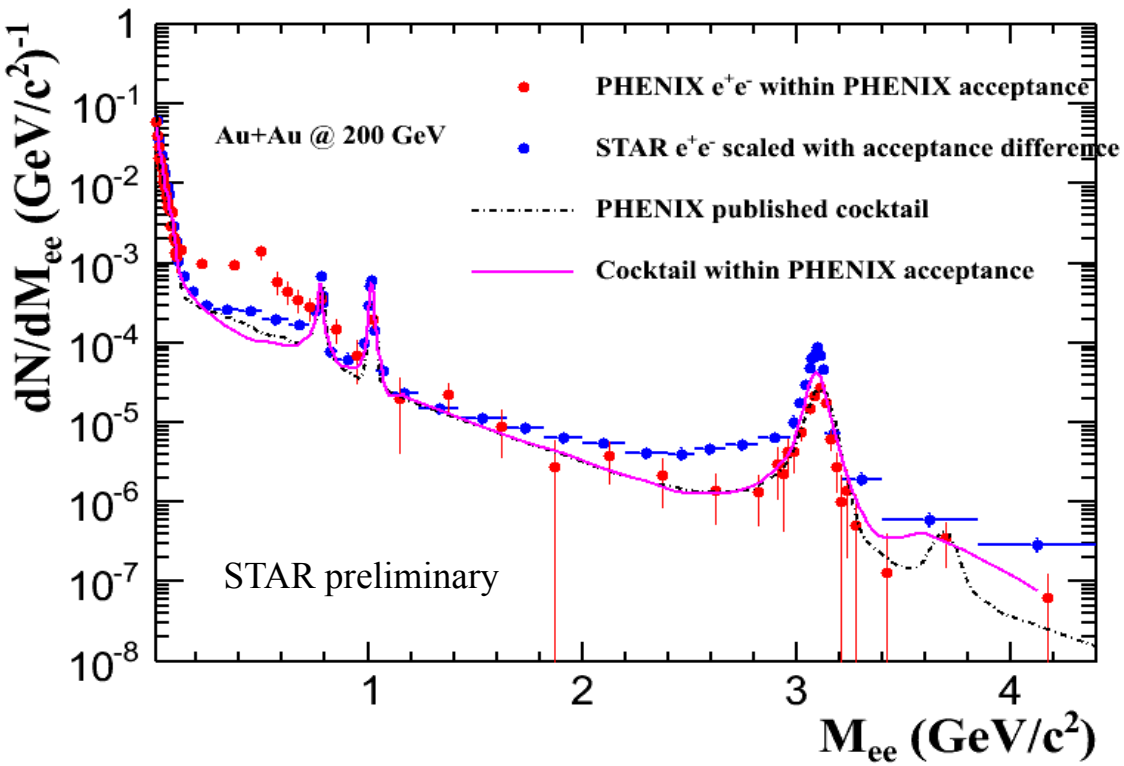


Scaled by the acceptance difference

Acceptance difference:

$$\frac{\text{Cocktail in PHENIX acceptance}}{\text{Cocktail in STAR acceptance}}$$

Scaled by same meson and charm yields.

Difference at low mass is not from the simulation but from the measurements.

# STAR with PHENIX Φ acceptance

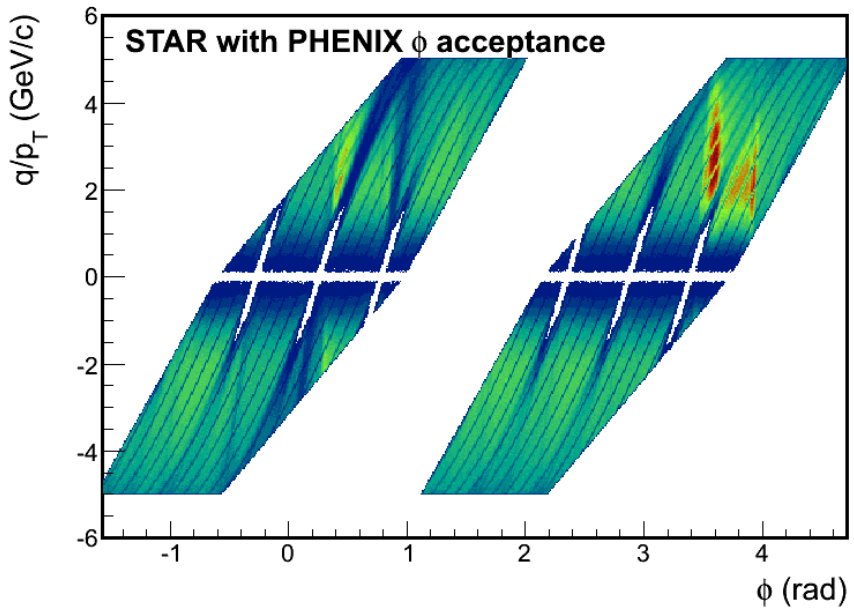


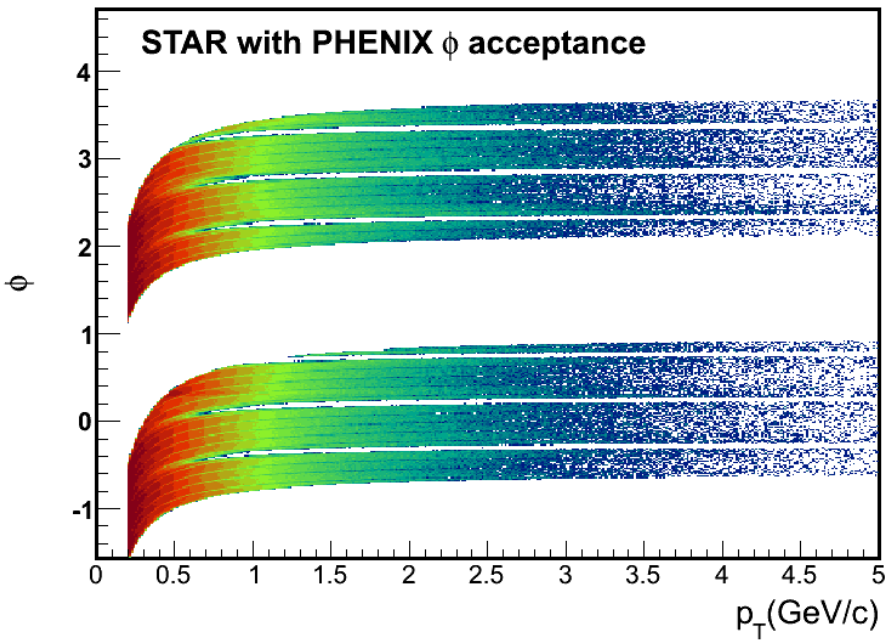


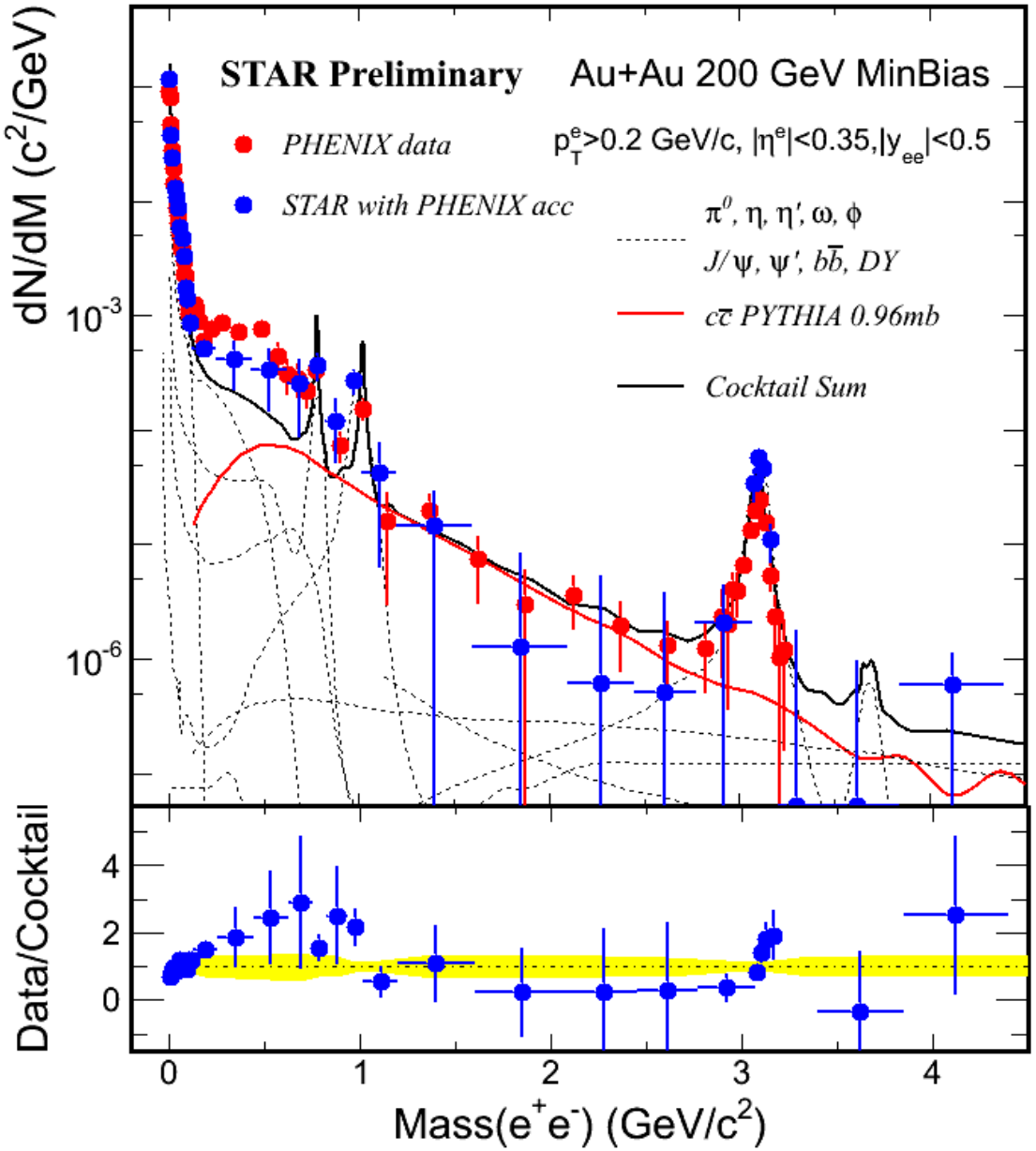

# Simulation in PHENIX acceptance

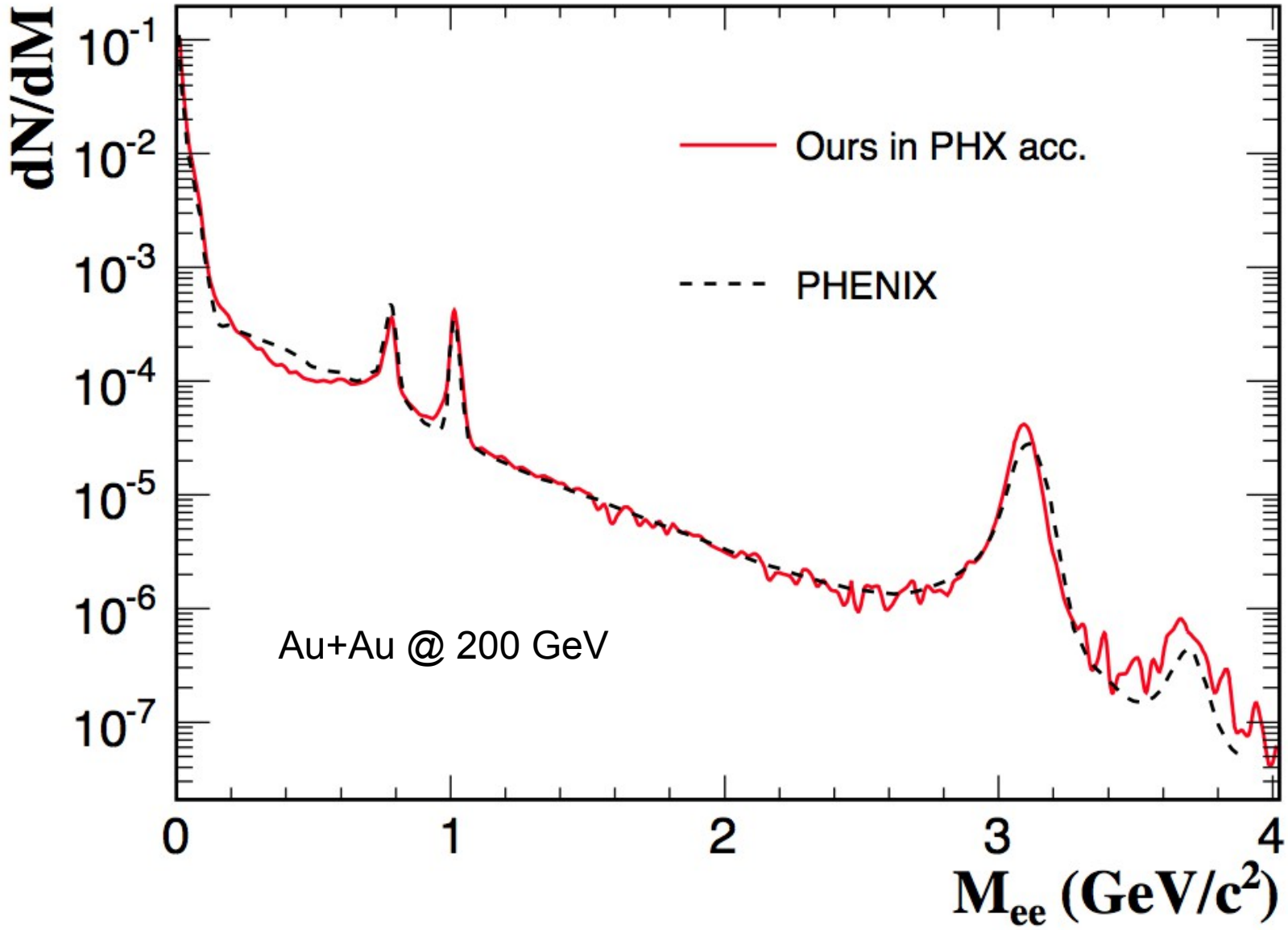


Red line: STAR simulation method applied to PHENIX acceptance. All components scaled by the yields and B.R.s PHENIX used.

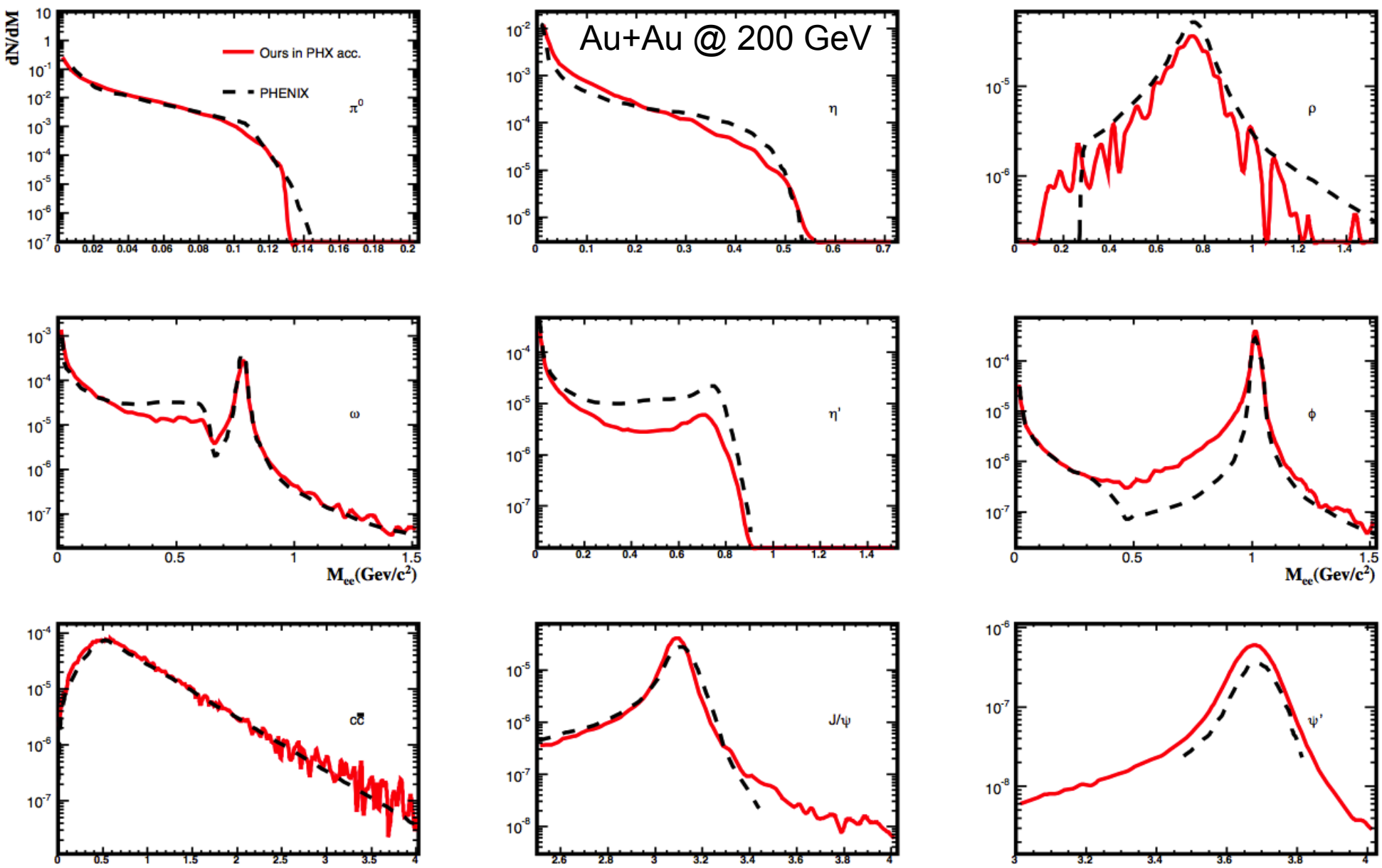
Au+Au @ 200 GeV
dN/dM
Ours in PHX acc.
PHENIX
π0
η
ρ
ω
η'
φ
cc̄
J/ψ
ψ'
Mee(Gev/c2)
Mee(Gev/c2)

# Ratio to PHENIX

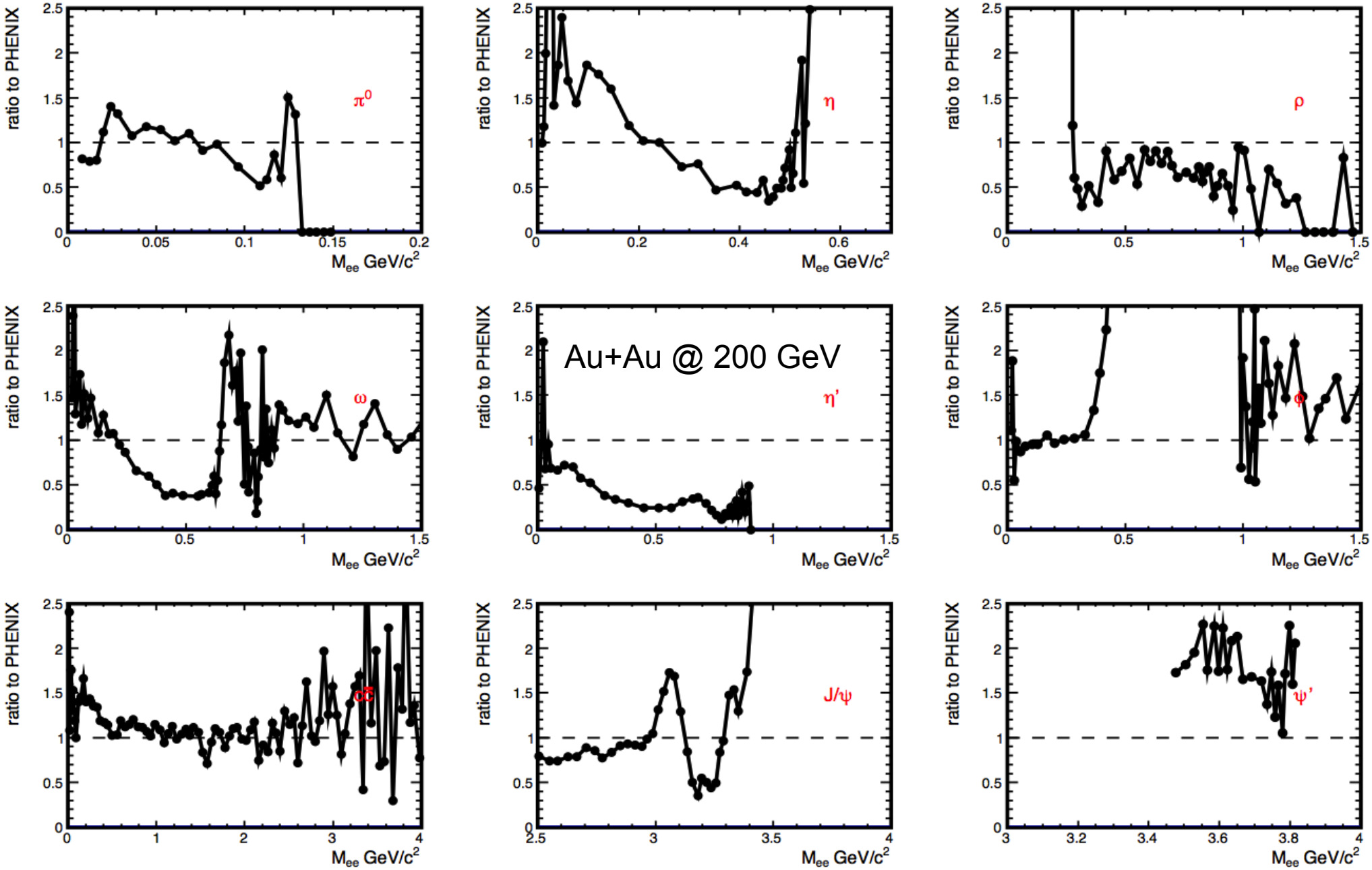

# Simulation in PHENIX acceptance

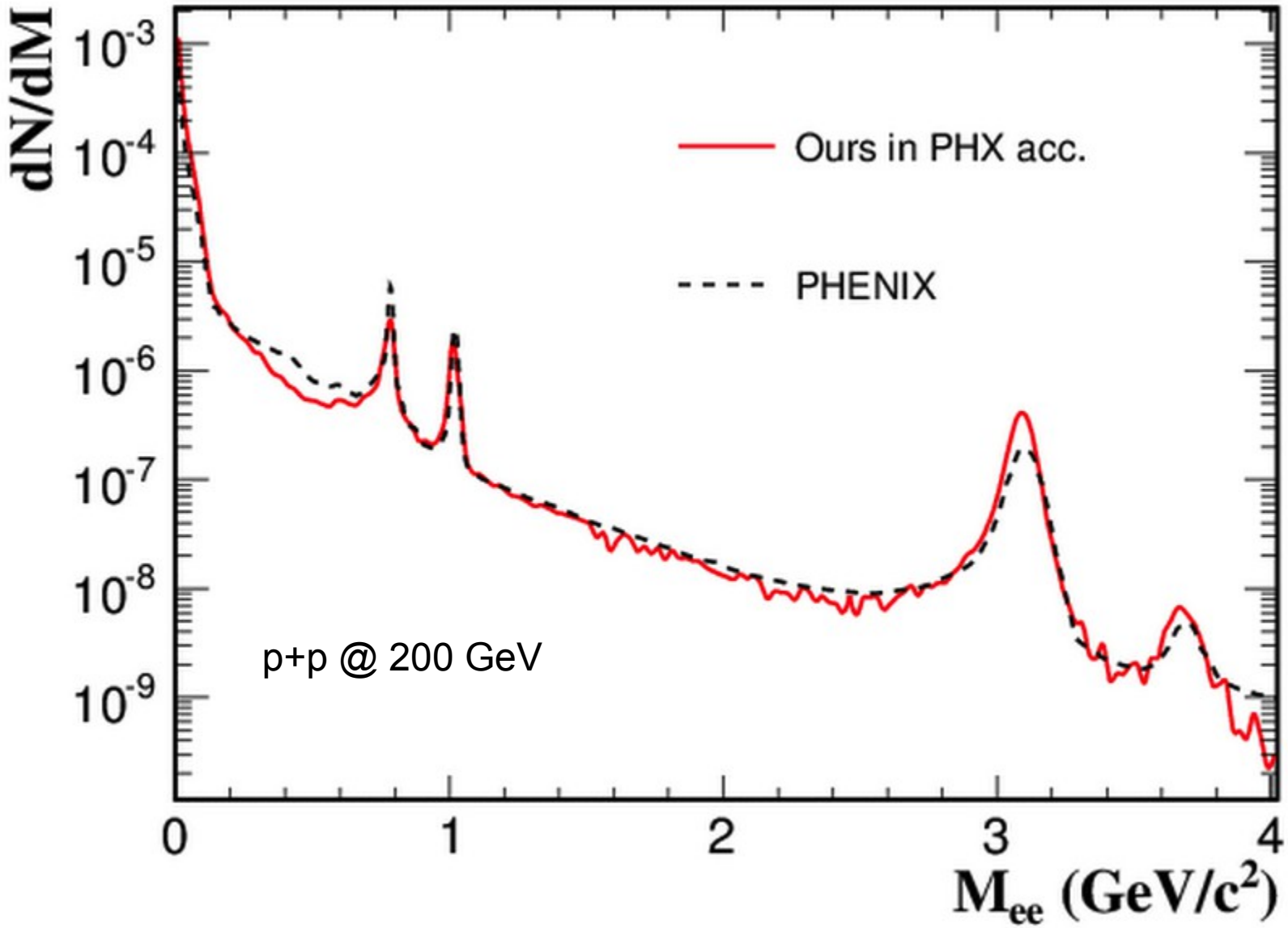

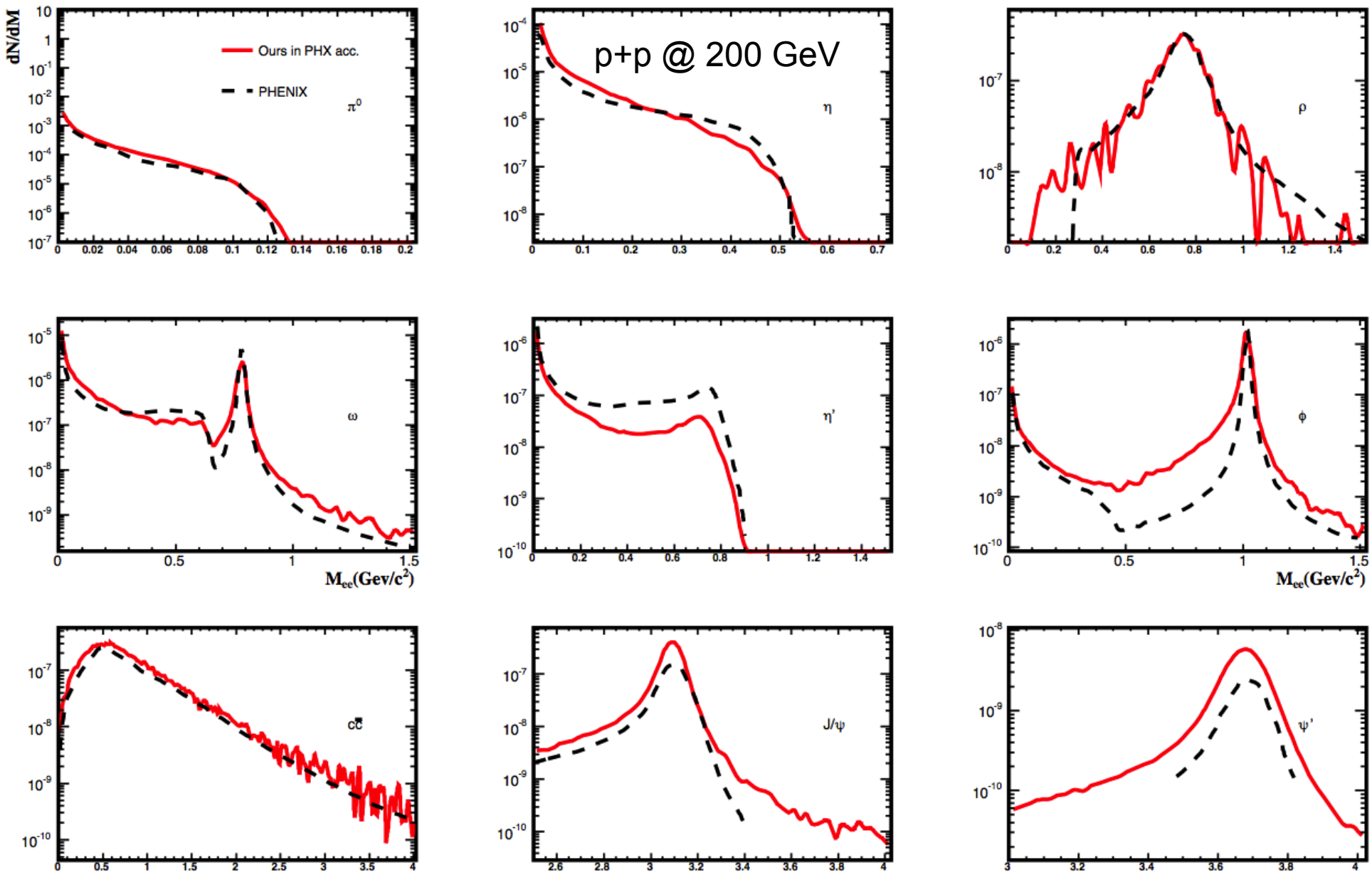
p+p @ 200 GeV
dN/dM
Ours in PHX acc.
PHENIX
π0
η
ρ
ω
η'
φ
cc̄
J/ψ
ψ'
Mee(Gev/c2)
Mee(Gev/c2)

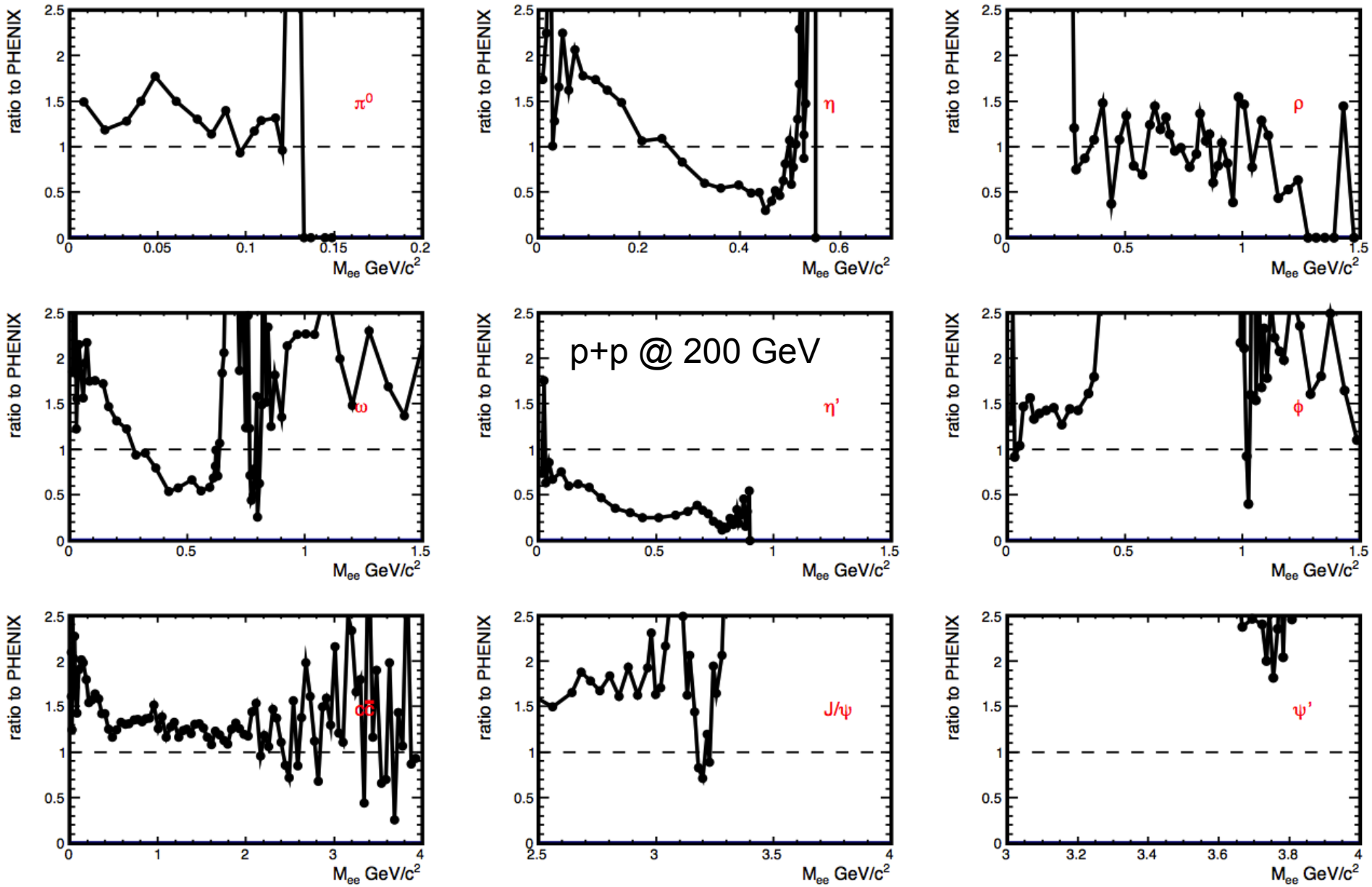
ratio to PHENIX
$M_{ee}$ GeV/$c^2$
$\pi^0$
$\eta$
$\rho$
$\omega$
p+p @ 200 GeV
$\eta'$
$\phi$
$c\bar{c}$
J/$\psi$
$\psi'$

# Dielectron Production in Au+Au Collisions at BES Energies

## and its energy dependence from SPS to top RHIC energies

**Patrick Huck for the STAR Collaboration**

RBRC Thermal Radiation Workshop, BNL

12/06/2012

*Table of Contents*


- Motivation
- Data Analysis
- Results & Conclusions
- Summary


Lawrence Berkeley National Laboratory

Central China Normal University

Goethe Universität Frankfurt am Main

DAAD Deutscher Akademischer Austausch Dienst German Academic Exchange Service

# Study the QCD Phase Diagram

## Fundamental Questions for HIC's

1) thermally equilibrated matter produced through sufficient rescattering?
   magnitude of collective expansion indicates $\tau$ < 1-2 fm/c
   characterize medium by bulk thermodynamic variables

2) distinctive footprint of individual partons?
   $v_2$ NCQ scaling: collectively expanding partonic source

3) deconfinement? chiral restoration?
   spectroscopy via short-lived resonances due to inaccessible order parameter

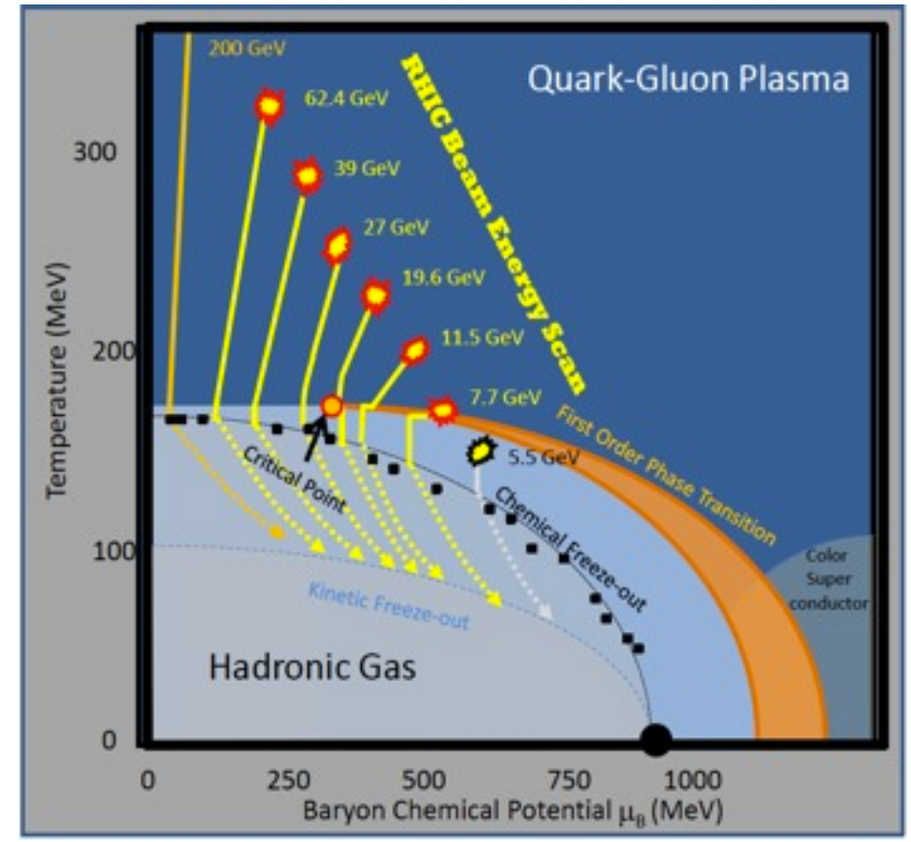


## Bulk Penetrating EM Probes

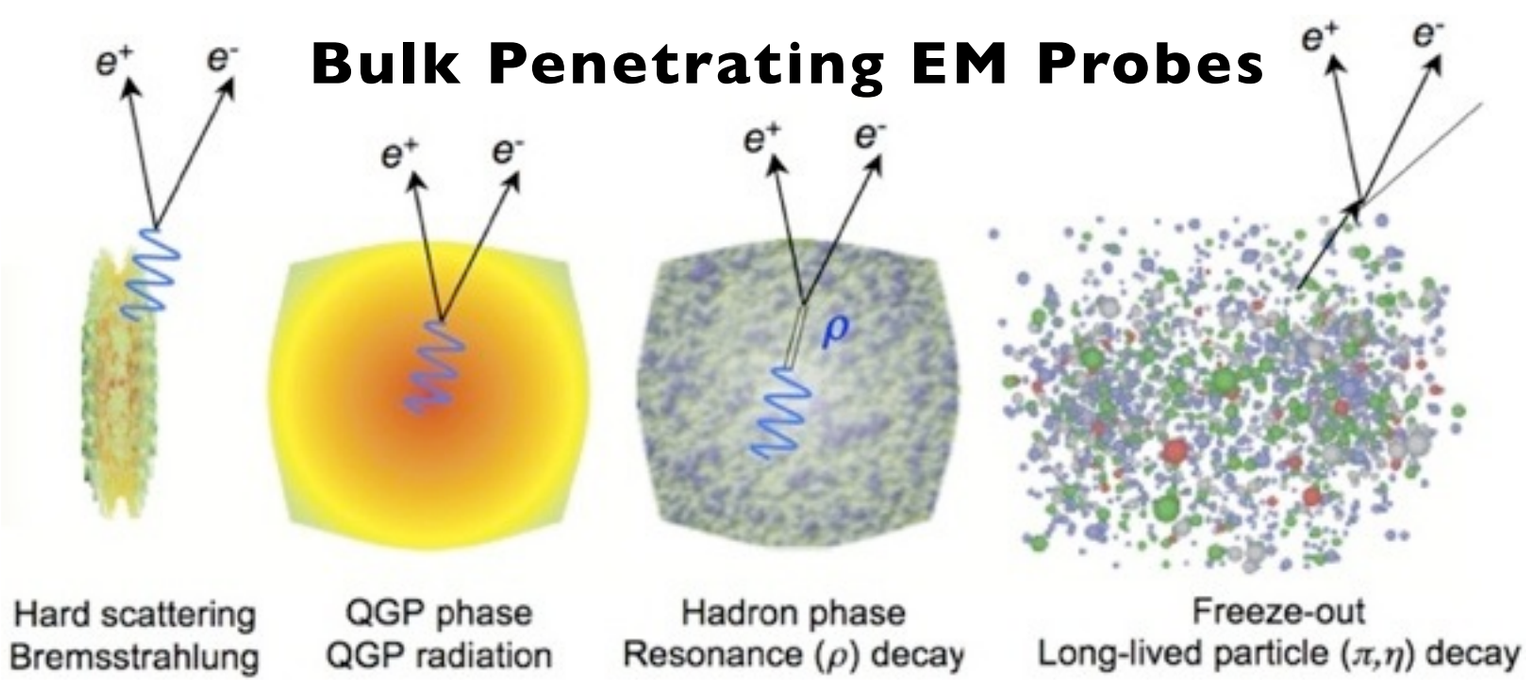


## Beam Energy Scan Program

consistently combine various signatures over a wide range of beam energies

- access hadronic spectral functions via EM probes ($\gamma$ / $l^+l^-$)
  negligible FS interactions due to $\lambda_{mfp} >> \tau_{FB}$
- additional dynamic information about HIC stages encoded in invariant mass

# Dielectron Physics @ STAR

## Low-Mass-Region ($M_{ee}$ < 1.1 GeV/$c^2$)

- distinct features of fireball radiation from hadronic phase hidden by direct decays
- ~50% reduction in $\rho/\omega$ region
- factor 2 enhancement at ~0.5 GeV/$c^2$
- $\omega/\phi$ less susceptible to in-med. modifications
- possibly connected to $\chi$SR through analogy with reduced duality threshold

R. Rapp, arXiV:0901.3289 & PRC 63 054907

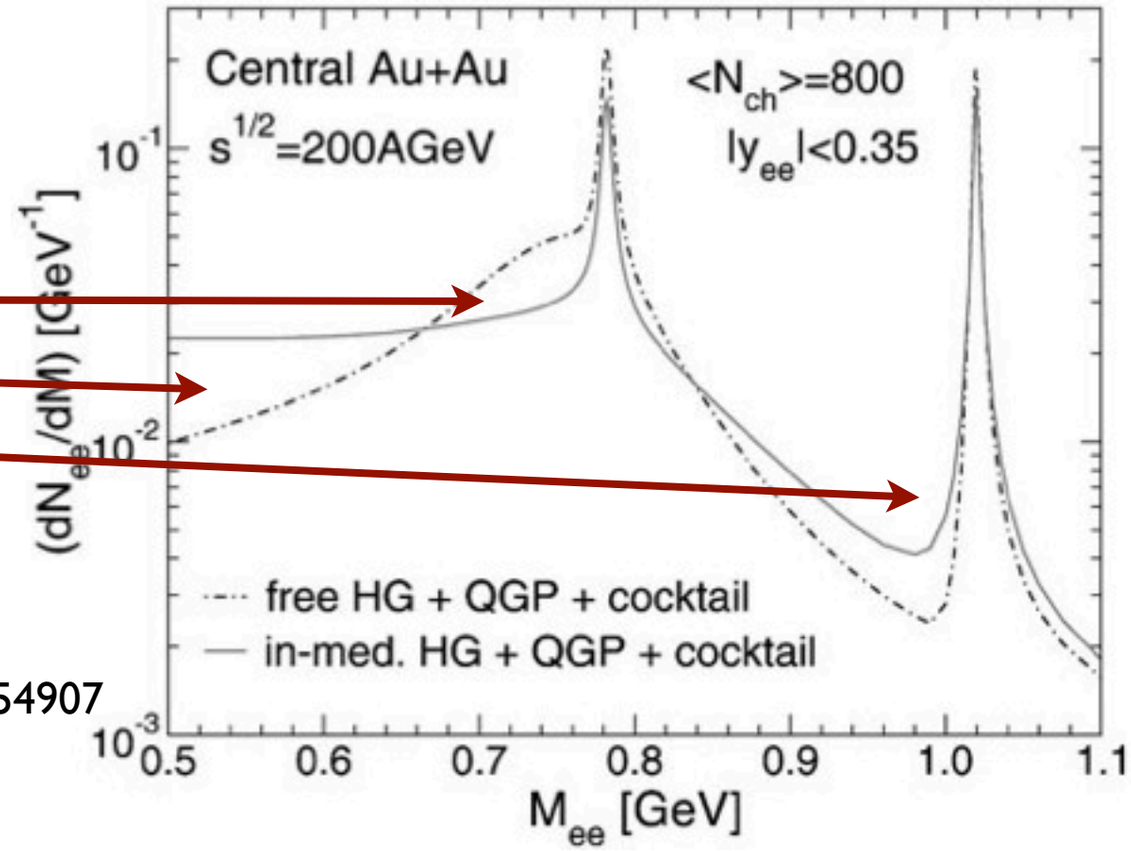


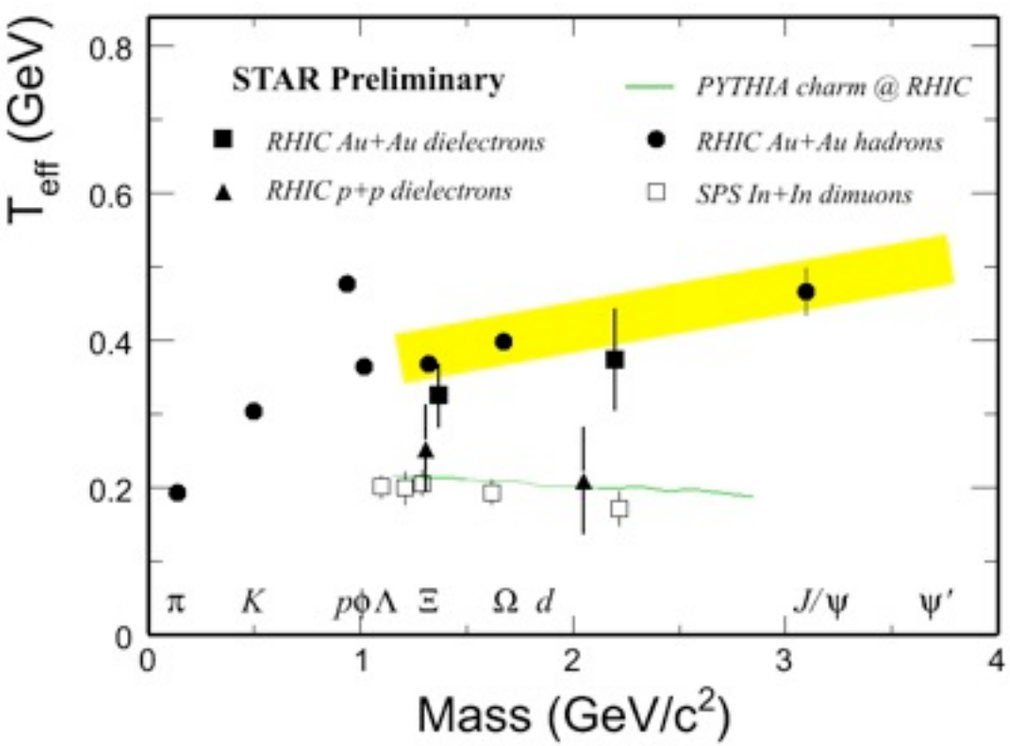


## Intermediate-Mass-Region (1.1 < $M_{ee}$ < 3 GeV/$c^2$)

- measure initial QGP temperature from IMR $m_T$ spectra
  - however, with contributions from correlated charmed decays unknown, large systematic uncertainties arise even at 200 GeV.
  - thus, BES analyses presented here concentrate on LMR physics

STAR in unique position to study energy dependent dielectron production and study/confirm medium consequences on spectra w.r.t to their energy dependence

# Datasets, Electron-ID & Conversion Rejection

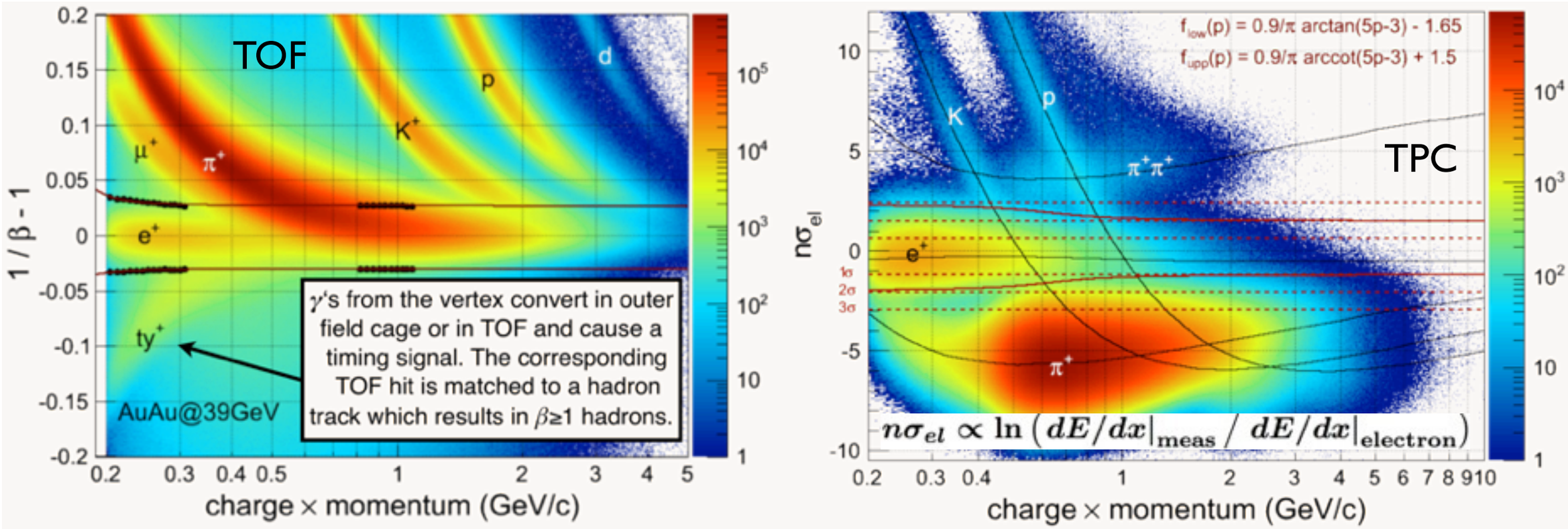


| Energy | 19.6 GeV | 39 GeV | 62.4 GeV | 200 GeV |
|---|---|---|---|---|
| used MB Evts | 35.8 M | 99.4 M | 54.6 M | 240 M |

- installation of TOF completed in 2010 enables pure elD combined with energy loss in TPC
- photon conversion sources: beam pipe, SVT support cones and inner TPC field cage
- >98% conversion rejection via $\phi_V$ cut

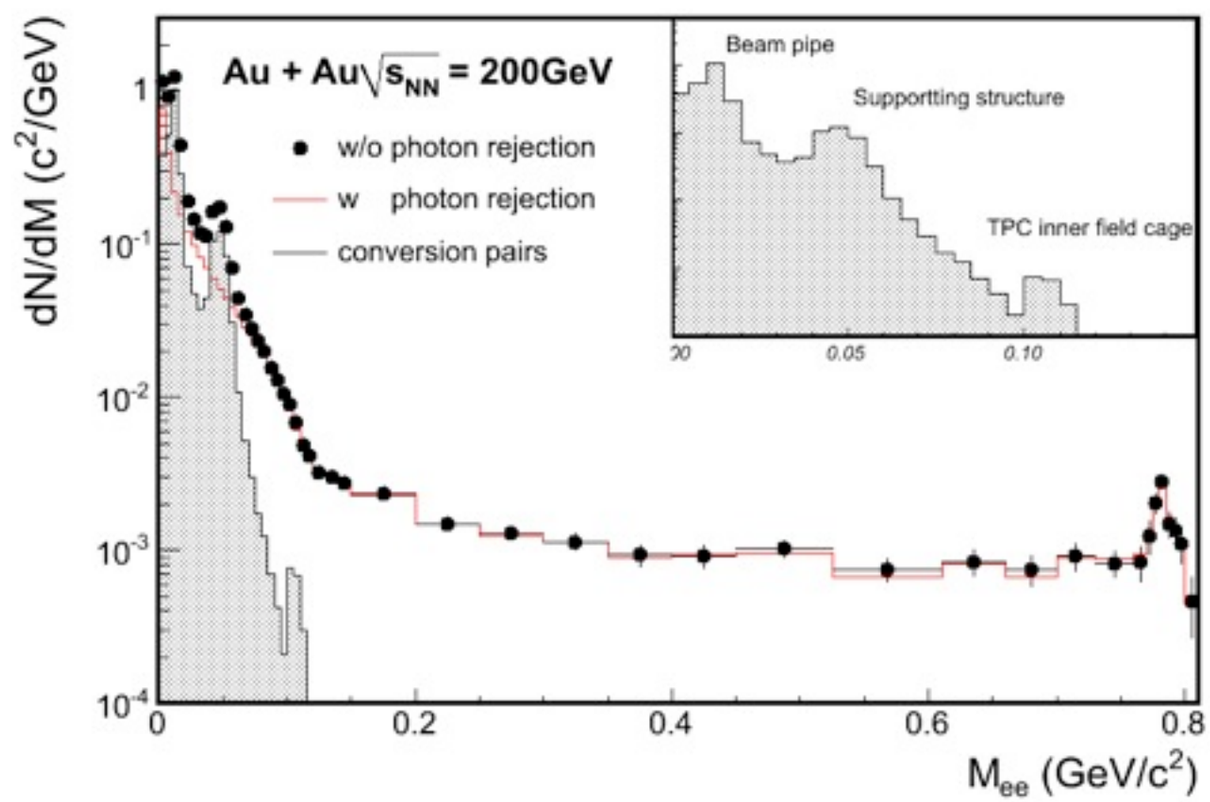

# Background Subtraction Methods

*$e^+/e^-$ created in pairs*
⇒ unlike-sign BG is *geometric mean* of the like-sign BGs independent of primary probability/multiplicity distribution

$$\langle BG_{+-}\rangle = 2\sqrt{\langle BG_{++}\rangle\langle BG_{--}\rangle}$$

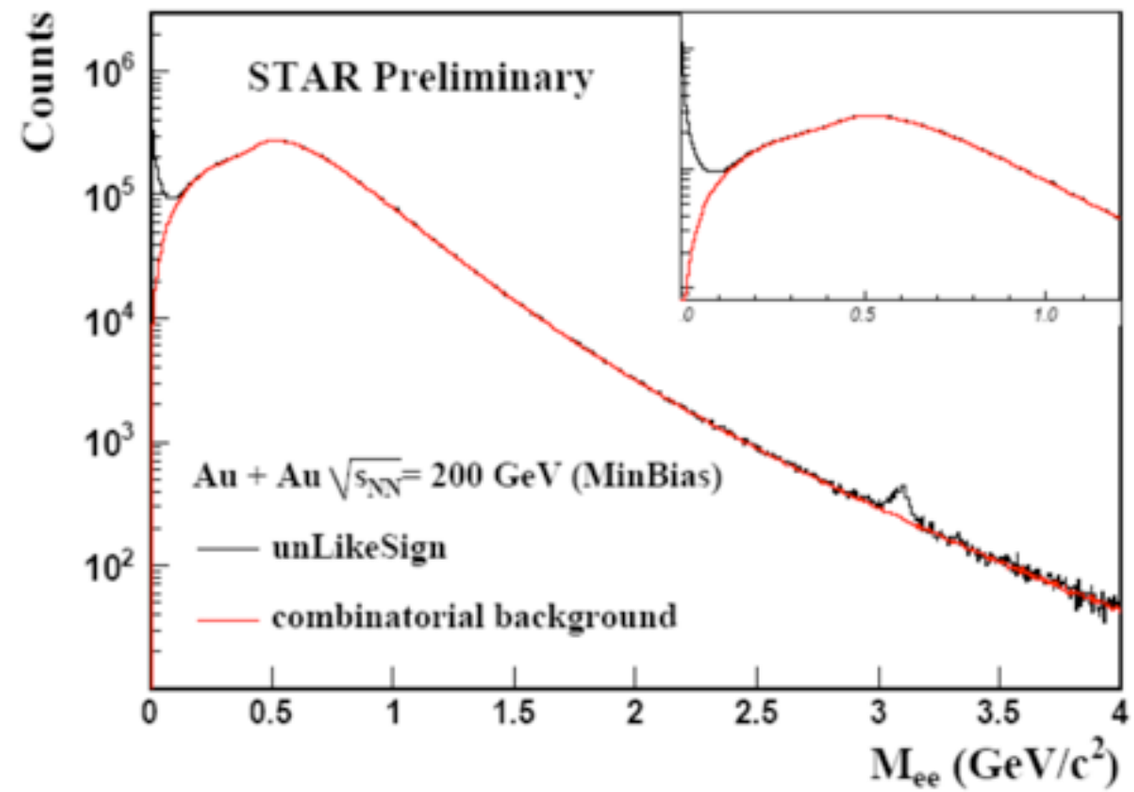


## 1) Like-Sign Same Event Method

- All like-sign pairs of one event are combined and averaged.
- Method reproduces the background from all correlated sources.
- Acceptance difference of like-sign to unlike-sign pairs is corrected using the ME Technique.

## 2) Unlike-Sign Mixed Event Method

- Charges from two different events within same event class are combined (event vertex, reference multiplicity & event plane).
- Method describes uncorrelated BG only.

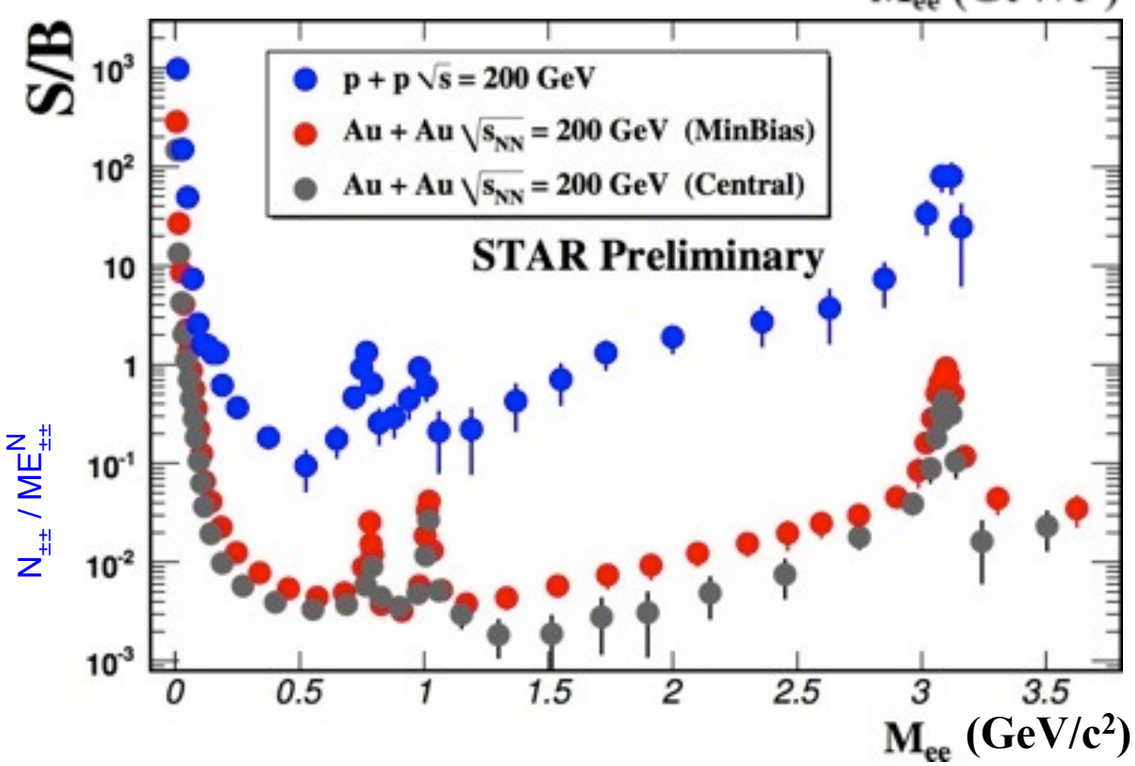


### Pair-Acceptance Correction & Mixed Event Normalization

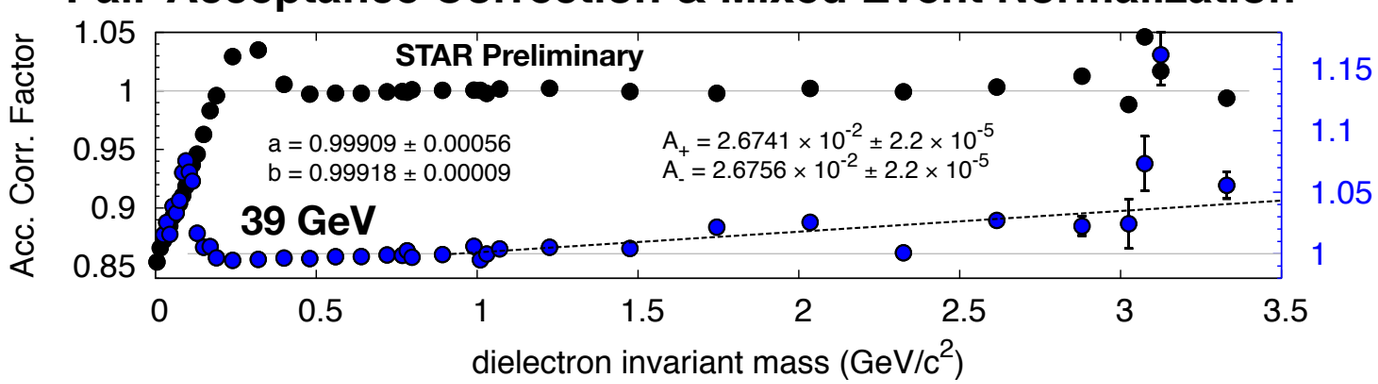

# Efficiency Correction

## TPC Selection Efficiency & Purity

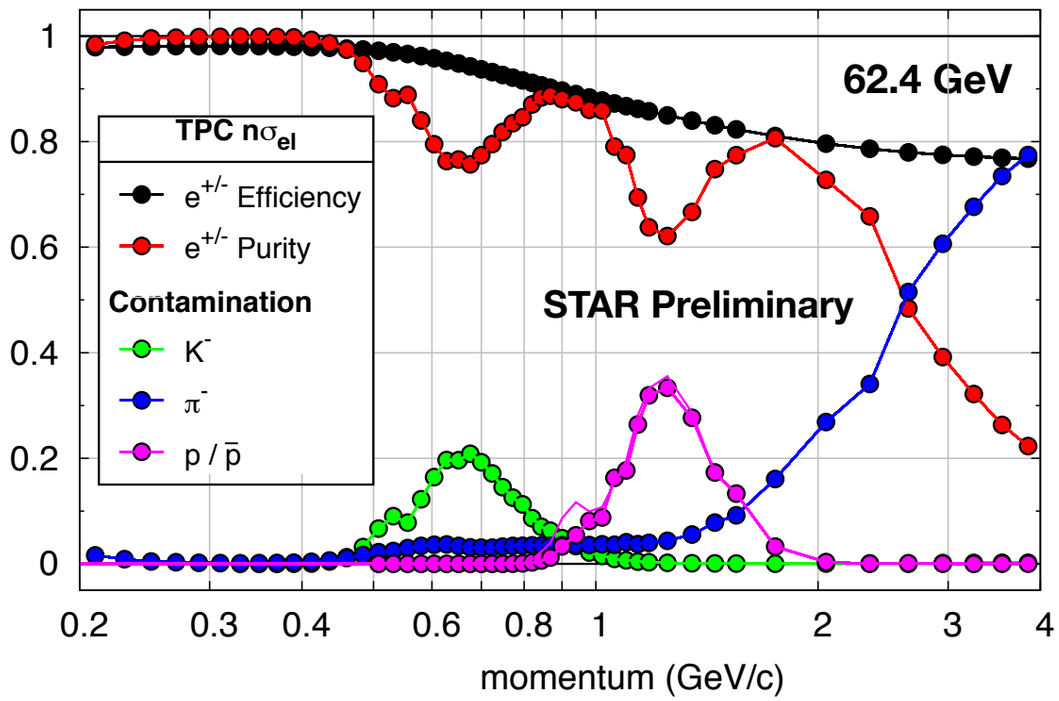


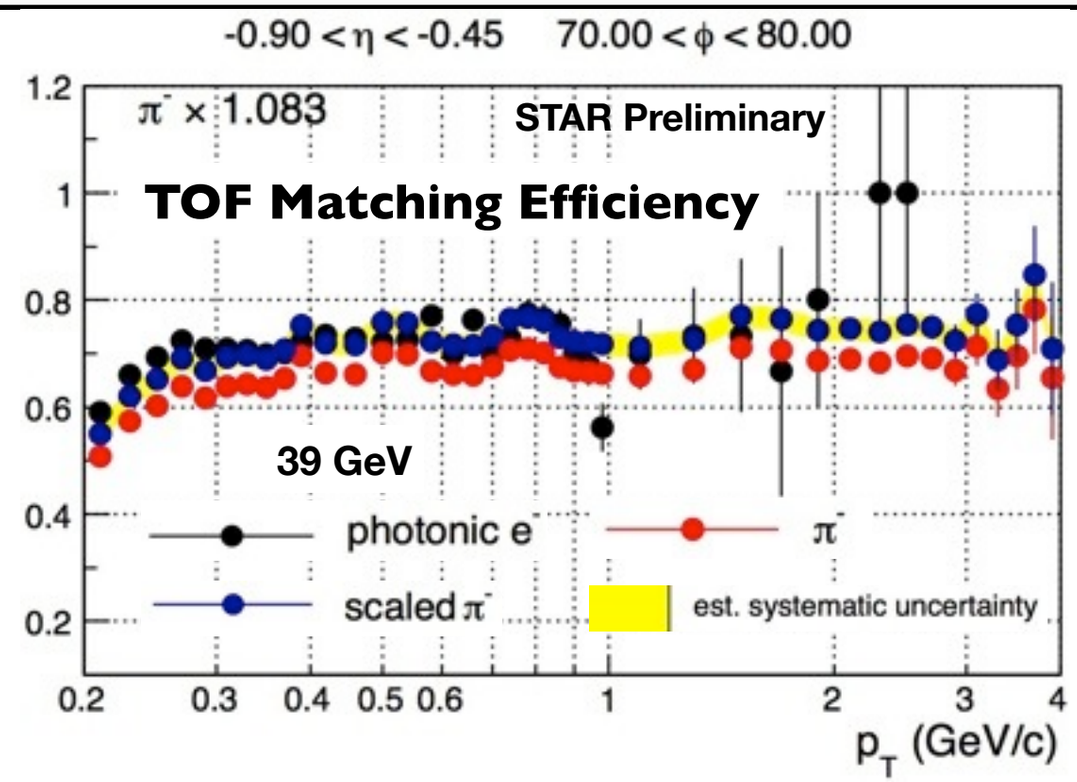


## Systematic Uncertainty of Track Quality Cuts

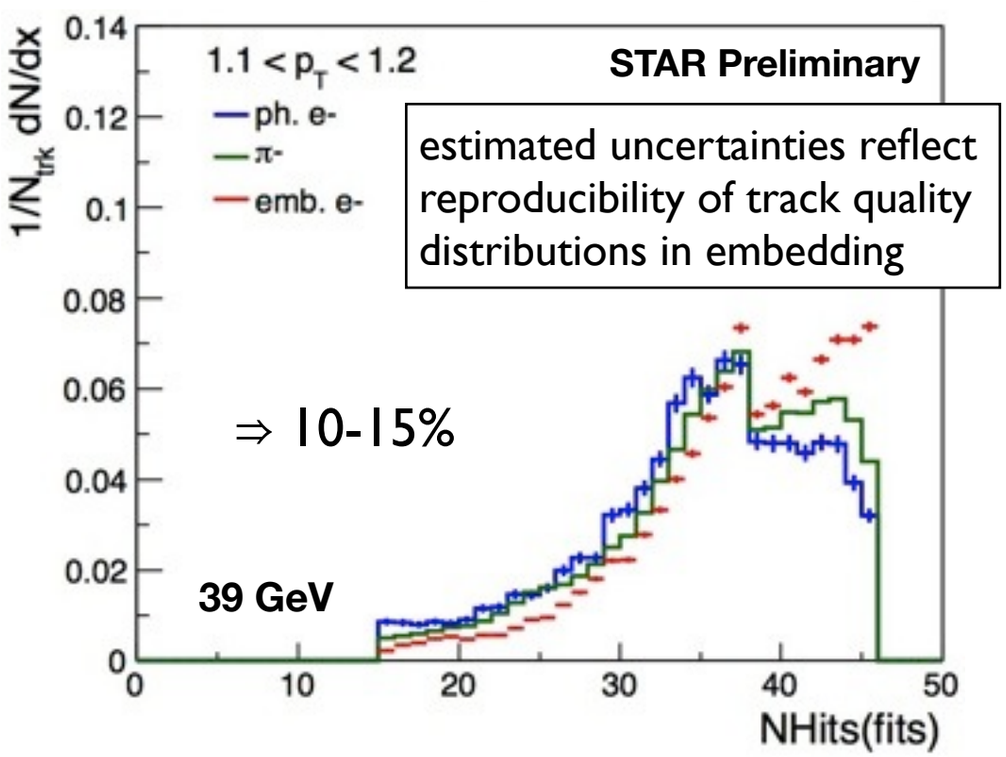


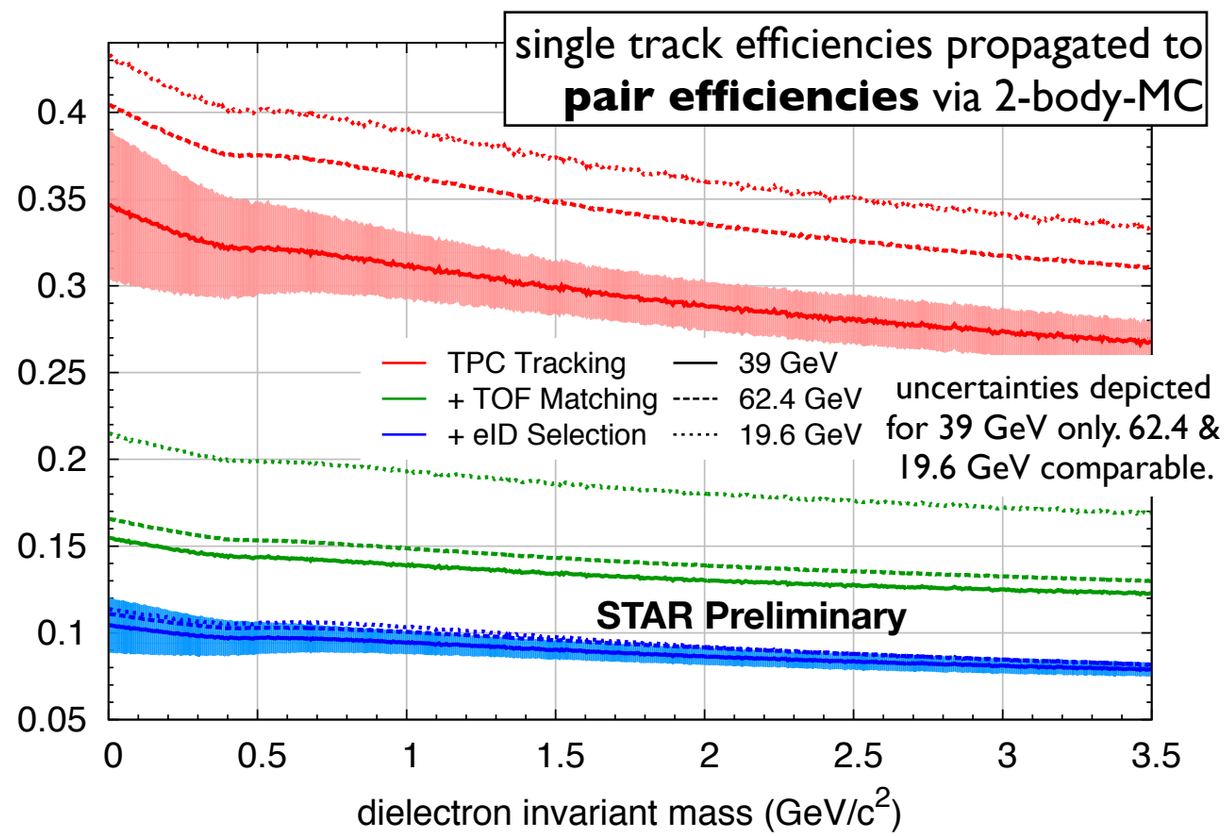

# Cocktail Simulation

- flat η [-1,1] & $\phi$ [0,2π], Kroll-Wada for Dalitz decays & according form-factors from measurements (PDG)
- *AuAu@19.6 GeV:*
  - Tsallis fits to meson spectra from SPS PbPb@17.3GeV
  - meson/$\pi^0$ ratio from SPS & $\pi^0$ yield from STAR
  - Conversion included via full STAR GEANT simulation
- *AuAu@39 & 62.4 GeV:*
  - $\pi^0$ $p_T$ spectra from $\pi^{+/-}$ @STAR, K spectra used for η
  - Unknown $p_T$ distributions taken from AMPT
  - According yields extrapolated from 200 GeV based on AMPT's √s-dependence
  - conversion rejected via $\phi_V$ cut
- Contributions due to correlated charmed decays simulated using PYTHIA and scaled to Au+Au by $N_{bin}$

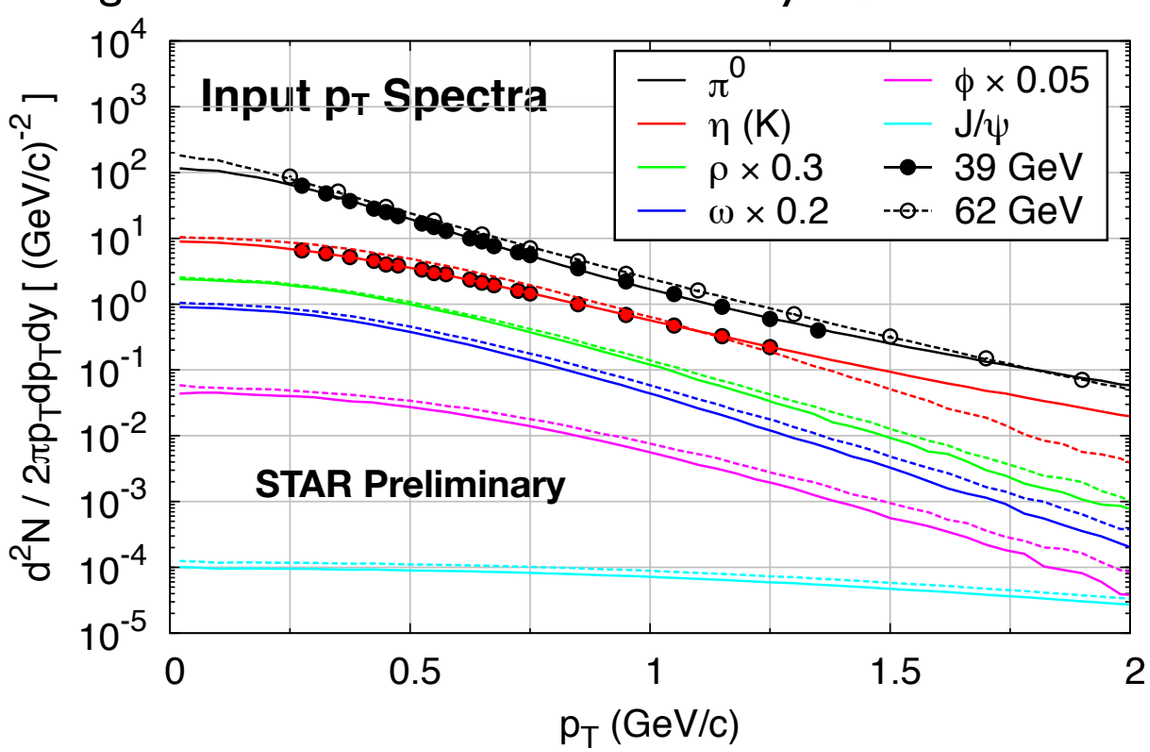


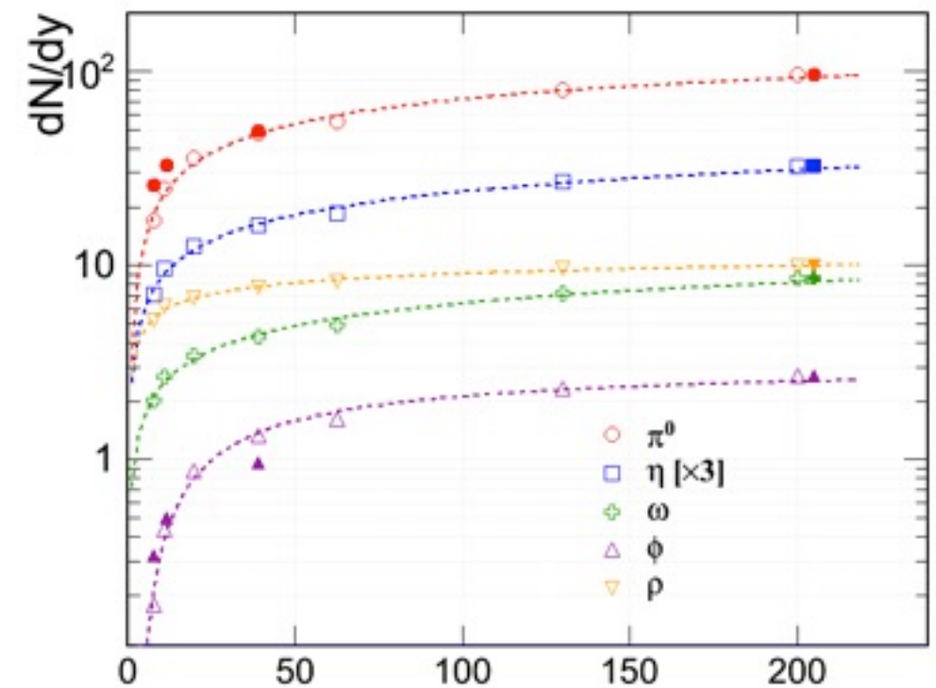


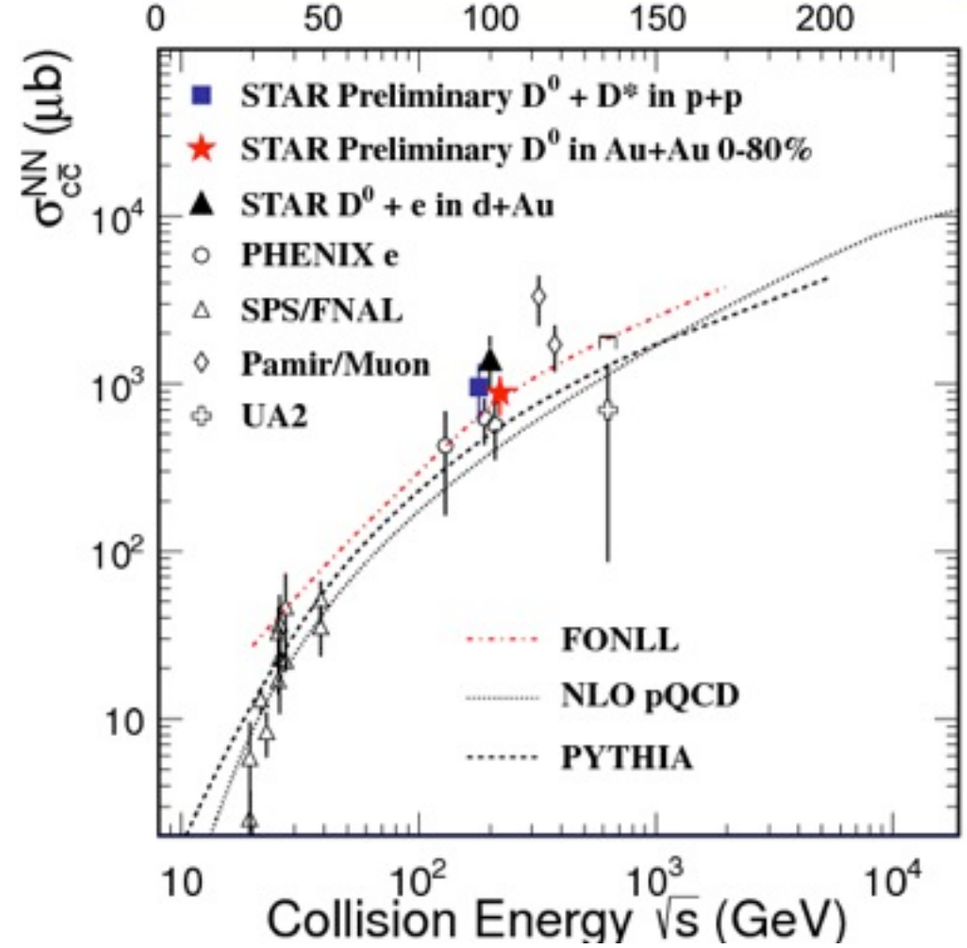

# BES Dielectron Spectra

QM 2012

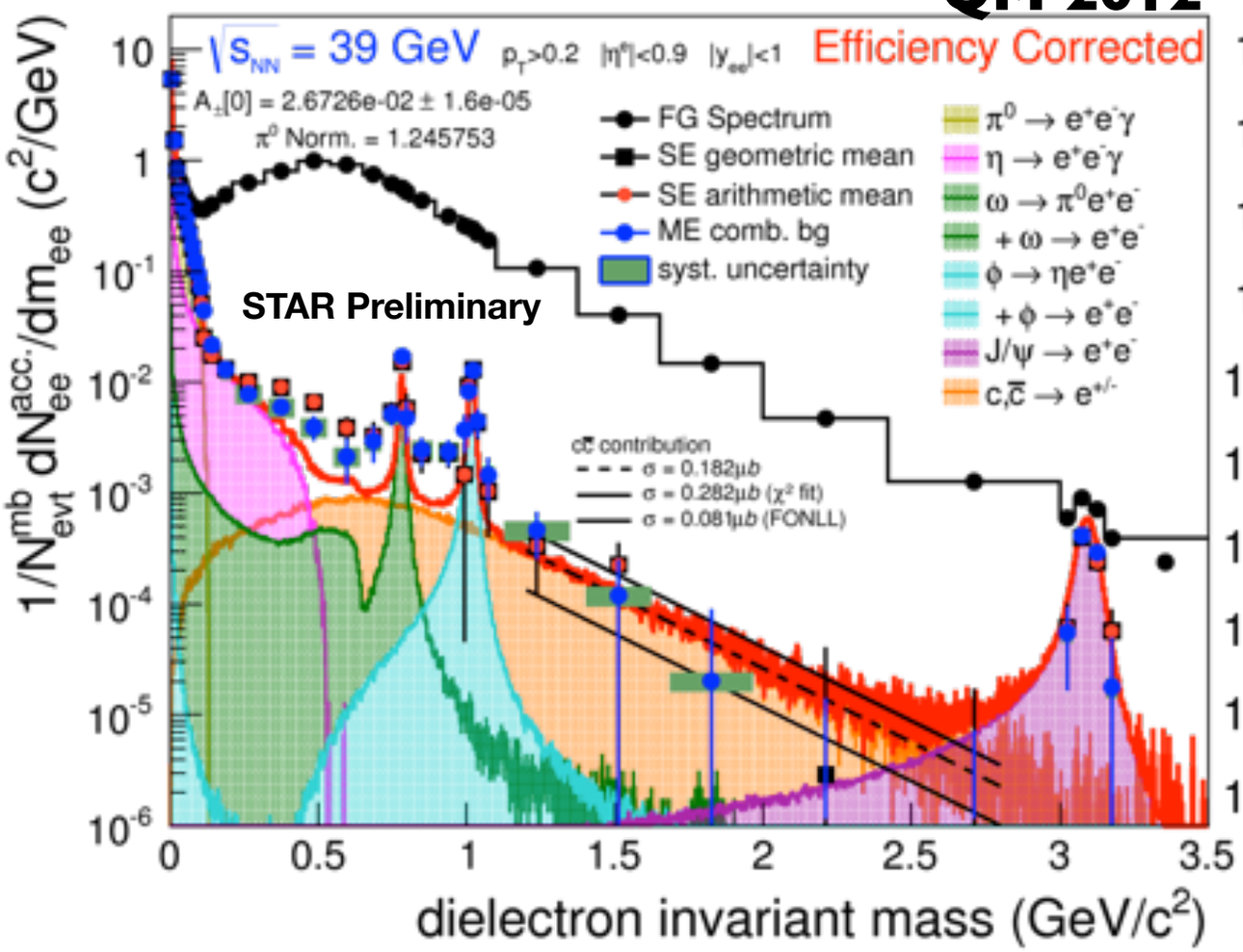


QM 2012

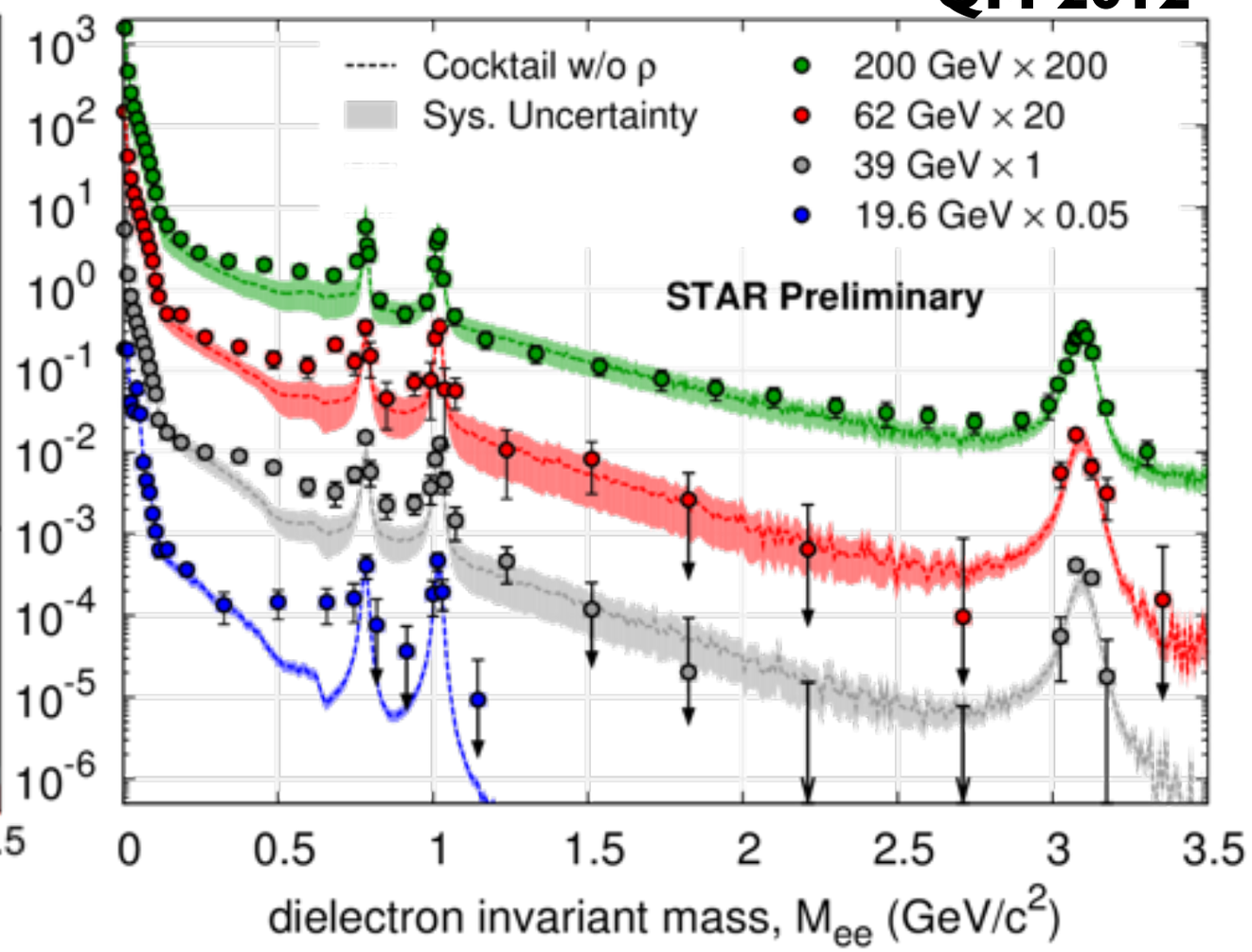


- $e^+e^-$ production below 3.5 GeV/$c^2$ systematically studied in STAR from $\sqrt{s_{NN}}$ = 19.6 GeV up to top RHIC energy.
- correlated charm adjusted to observed dielectron yield
  FONLL predictions are used as lower and
  $\chi^2$ fits to the IMR data as upper limits
- vacuum-ρ does not account for the excess yield in the LMR

# LMR Enhancement

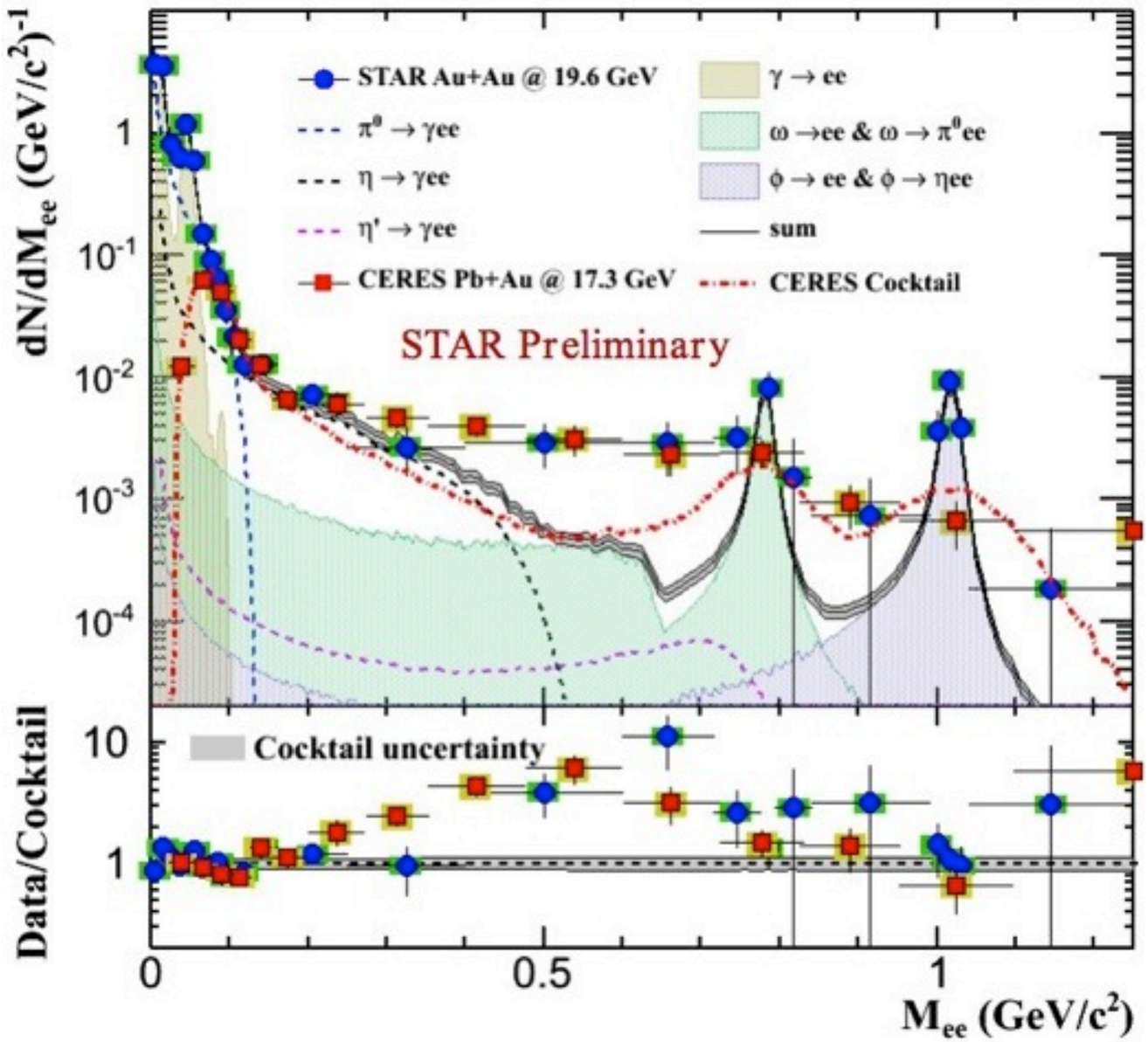


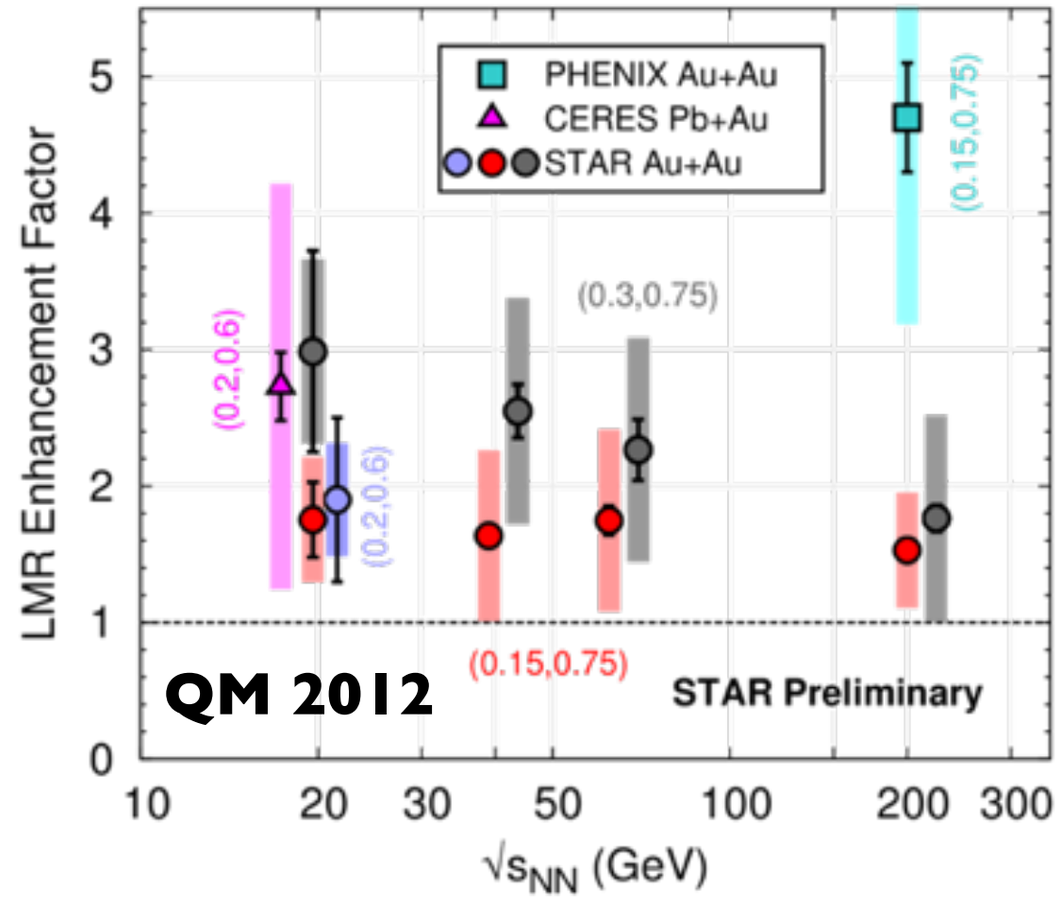


- visible LMR excess over hadronic cocktail observed for all energies. (excl. $\rho \to e^+e^-$)
- systematic measurement of the LMR enhancement factor (agreement with CERES result)
  [ $M_{ee}$-dep. energy overlay see backup ]

- LMR enhancement at 19.6 GeV comparable with CERES at 17.3 GeV
  (note: different experimental acceptances)
- increasing enhancement with decreasing energy w.r.t. the cocktail?
  "any energy dep. in X-Factor might be physics directly related to dielectrons from earlier creation times due to $\rho_B^{tot}$~const" Z. Xu

# Energy Dependence of In-Medium Mods

Rapp & Wambach, Adv. Nucl.Phys. 25, 1 (2000) Phys. Rept. 363, 85 (2002) displayed energies through priv. comm.

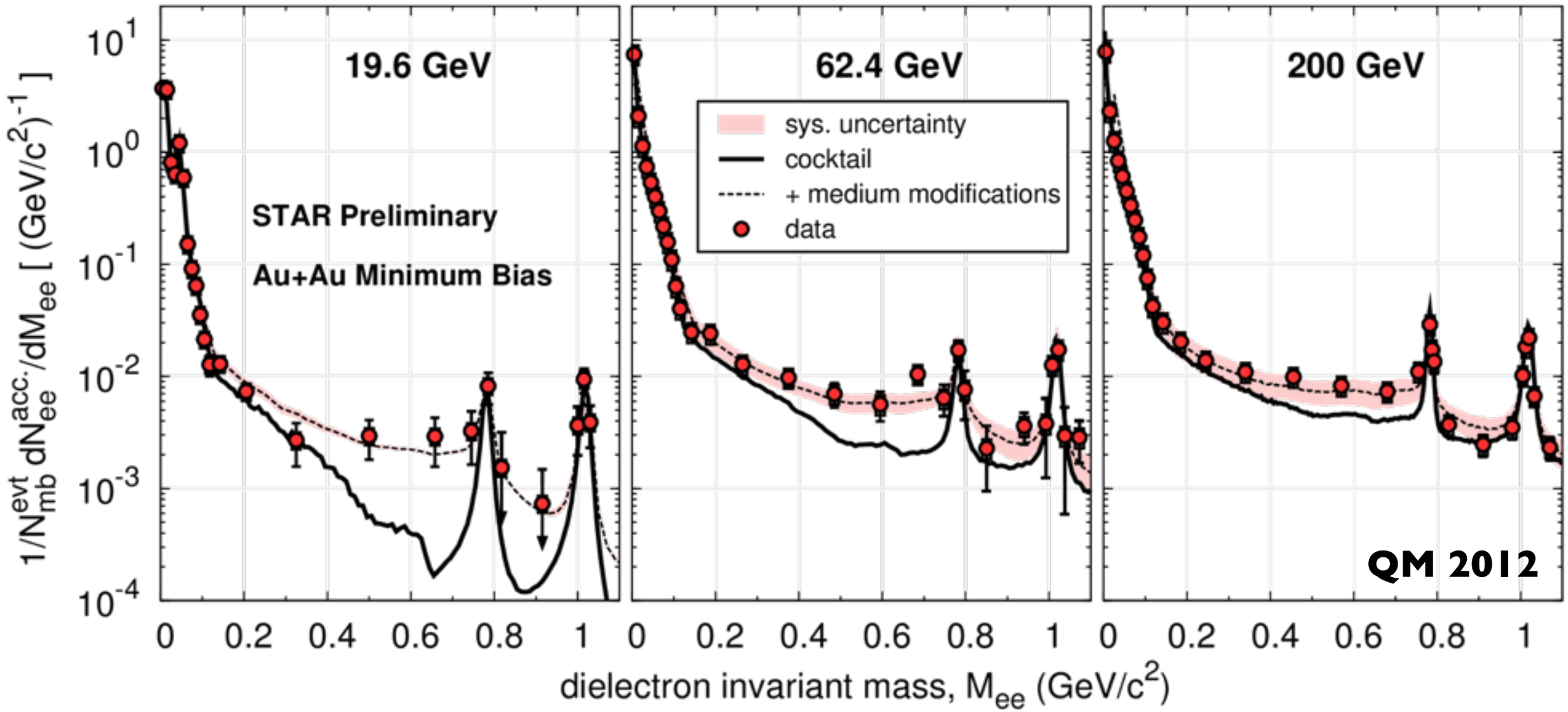


- Within systematic uncertainties, in-medium modifications of the ρ spectral function consistently describe the LMR enhancement from SPS to top RHIC energies.

# Summary , Outlook & Work in Progress

- Dielectron spectra from Au+Au collisions measured in STAR at $\sqrt{s_{NN}}$ = 19.6, 39, 62.4 & 200 GeV and compared to cocktail calculations.
- LMR excess yield can be accounted for by in-medium modifications to the ρ spectral function across a wide range of energies.
- enhancement increasing with decreasing energy w.r.t. the cocktail?
- measurements will provide comprehensive data for the better understanding of the LMR enhancement ($p_T$, centrality and energy dependence)

**work in progress**

- complete BES data set
- $p_T$ spectra for $M_{ee}$ regions
- detailed systematic uncertainty studies
- cocktail improvements

**outlook**

- IMR: Charm continuum contribution and its possible in-medium modification need better understanding in Au+Au to possibly access QGP radiation in the future
  ⇒ study energy dependence of initial temperature
  ⇒ STAR HFT & MTD upgrades

## Thank you for your attention

# BACKUP SLIDES

- absence of baryonic resonances with $\phi$N decay channels due to OZI-rule *

  * $\bar{s}$ annihilation into excitation energy strongly suppressed

| $\sqrt{s_{NN}}$ (GeV) | Vector Meson Yields (30% uncertainty assigned) | | | | | $\sigma_{pp}^{c\bar{c}}$ (mb) ± sys. | $N_{bin}^{coll}$ |
|---|---|---|---|---|---|---|---|
| | $\pi^0$ † | $\eta$ † | $\omega$ | $\phi$ | J/$\psi$ | | |
| 39 | 57 | 9.37 | 4.42 | 1.39 | $4.8 \times 10^{-4}$ | 0.19 ± 0.11 | 243 |
| 62.4 | 72.9 | 11.4 | 5.38 | 1.79 | $1.2 \times 10^{-3}$ | 0.40 ± 0.25 | 253 |

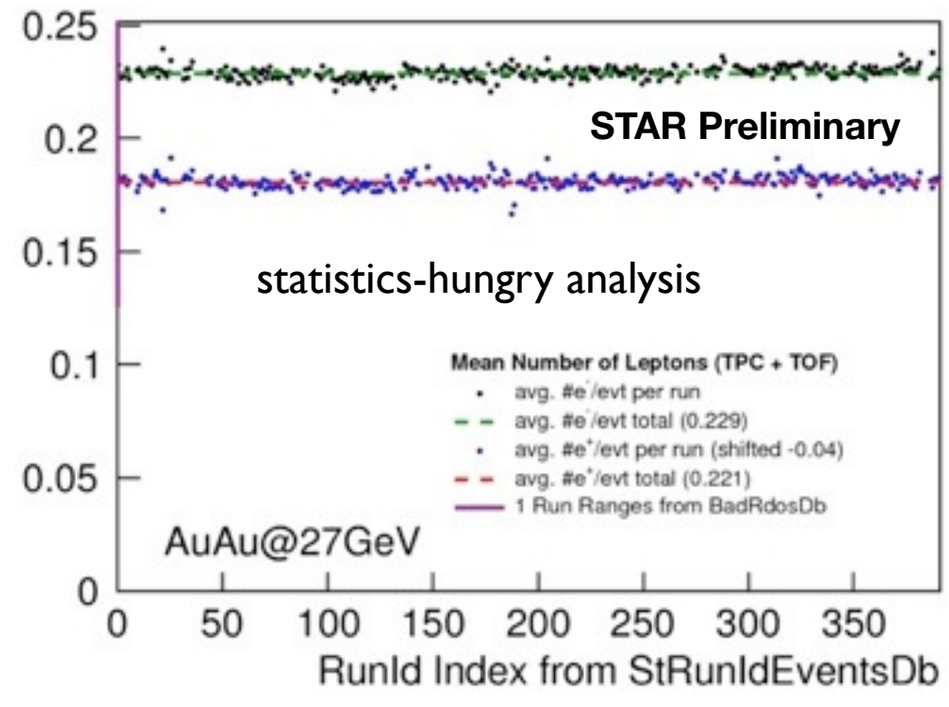


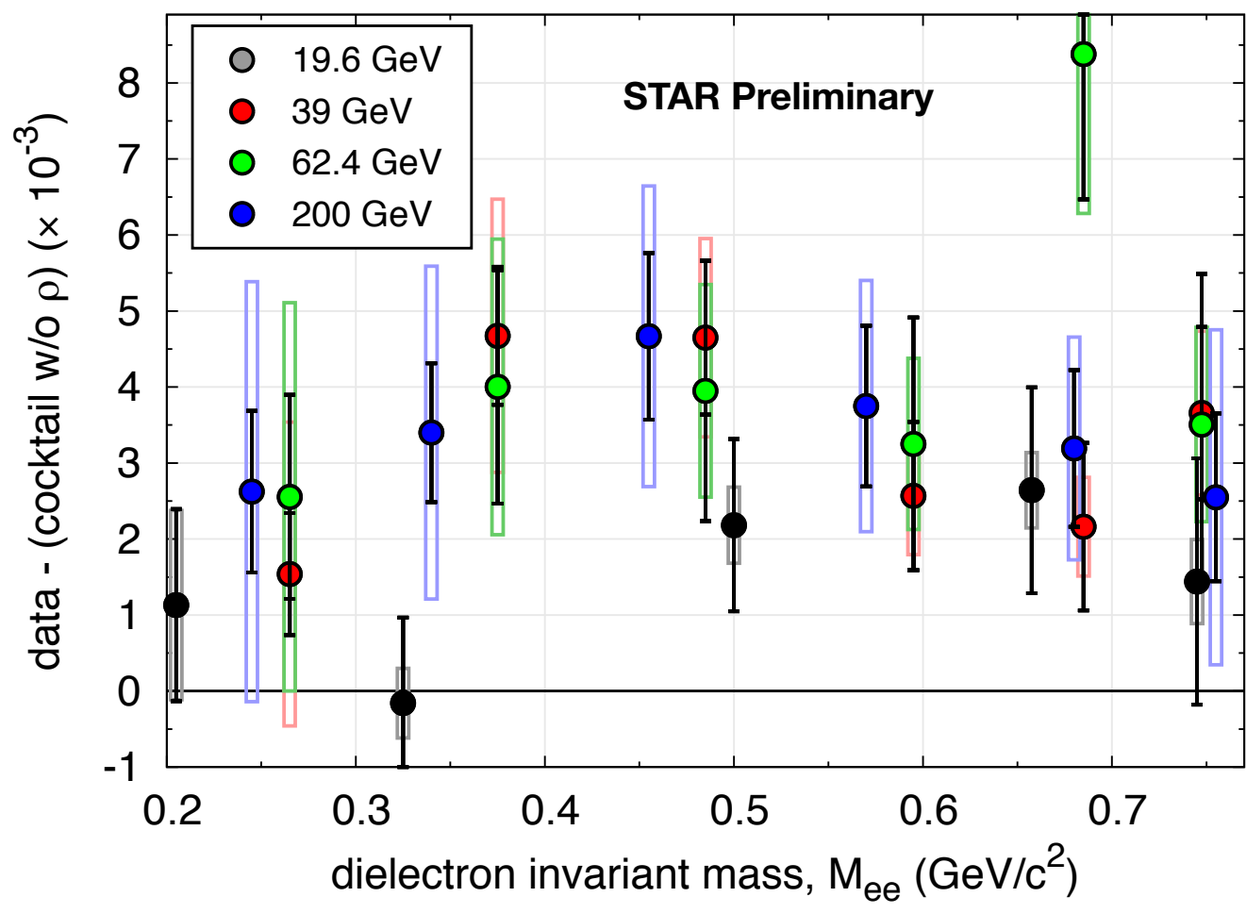


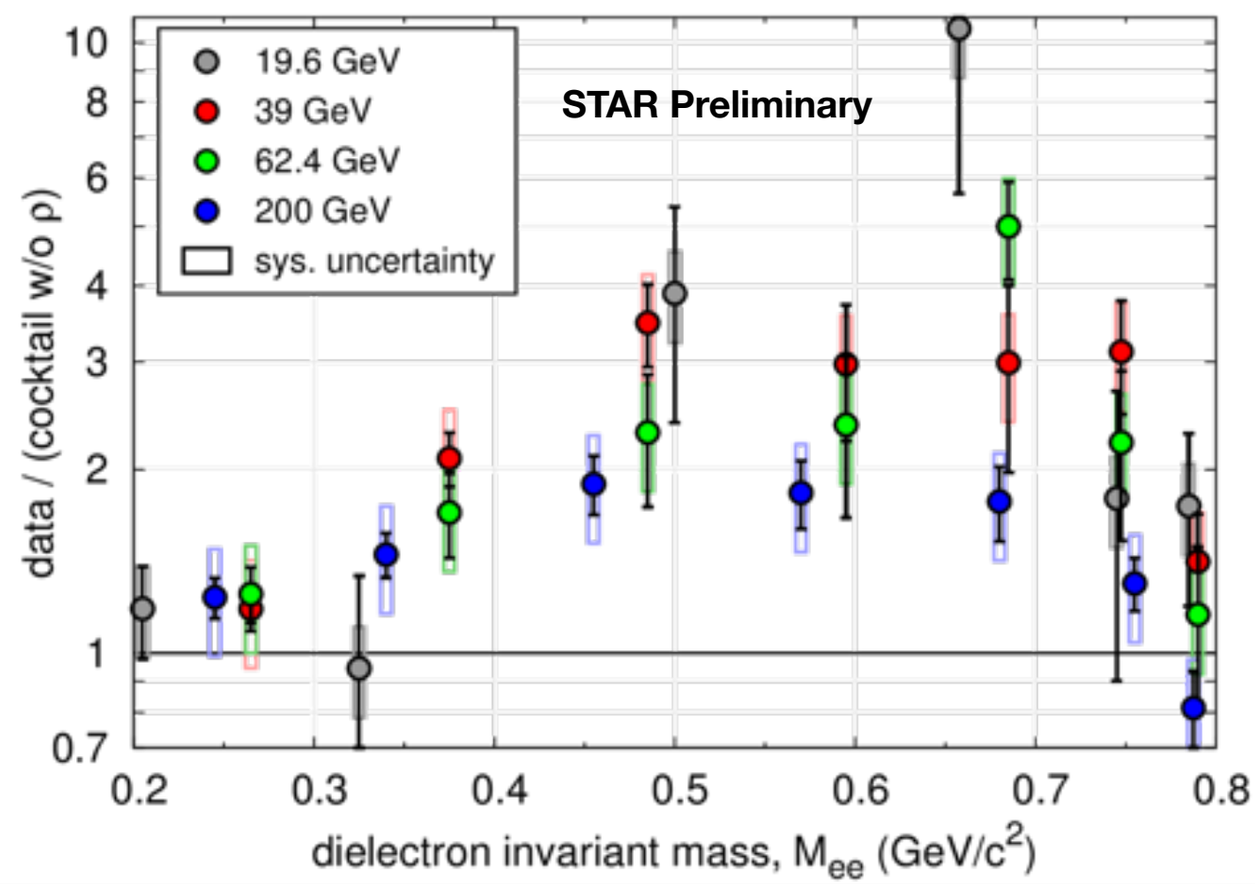

# Vector Meson Signals & S/N

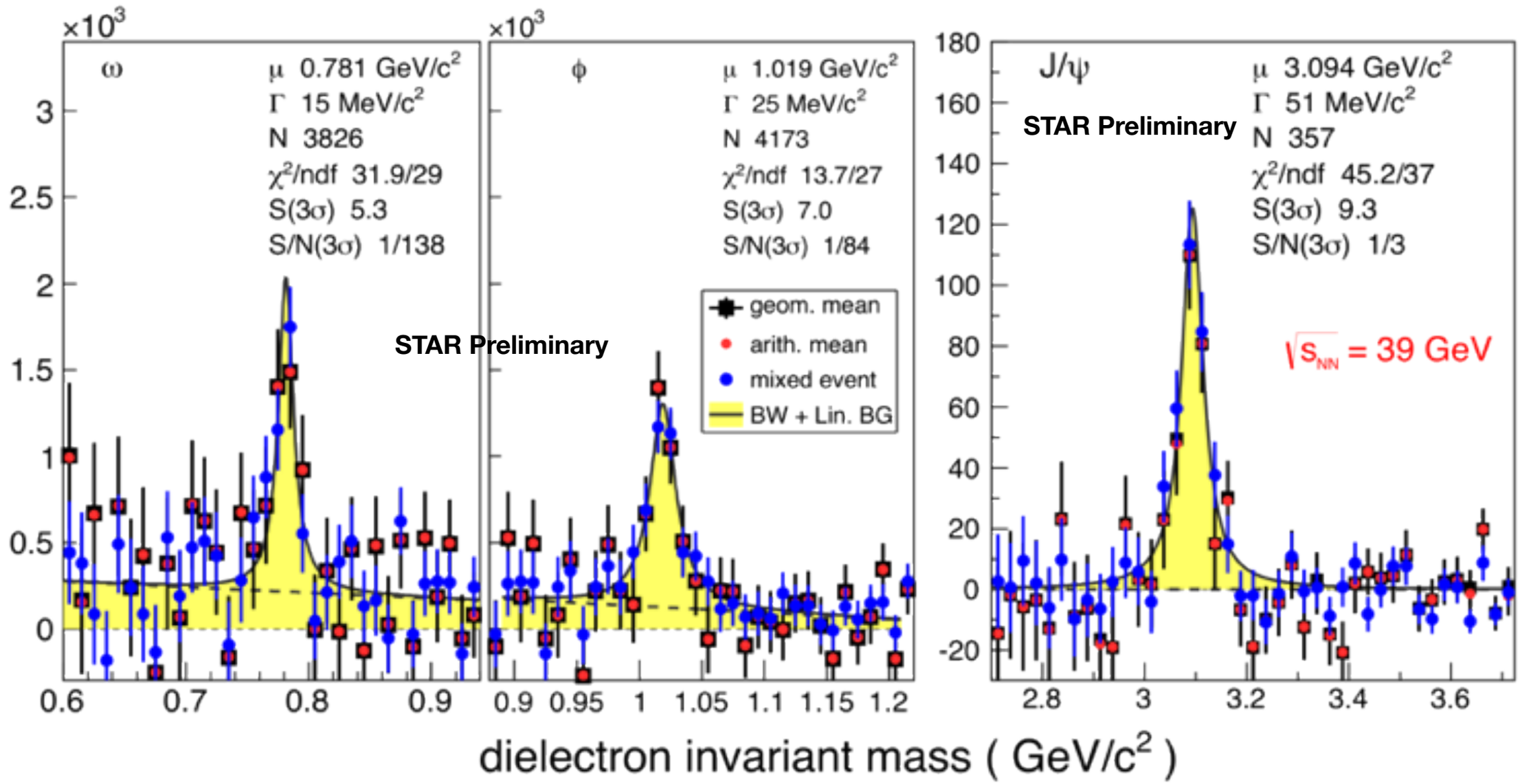


- ρ/ω region exhibiting a S/N ratio of ~1/100 - 1/250
- background subtraction crucial
- prominent vector meson signals after background subtraction

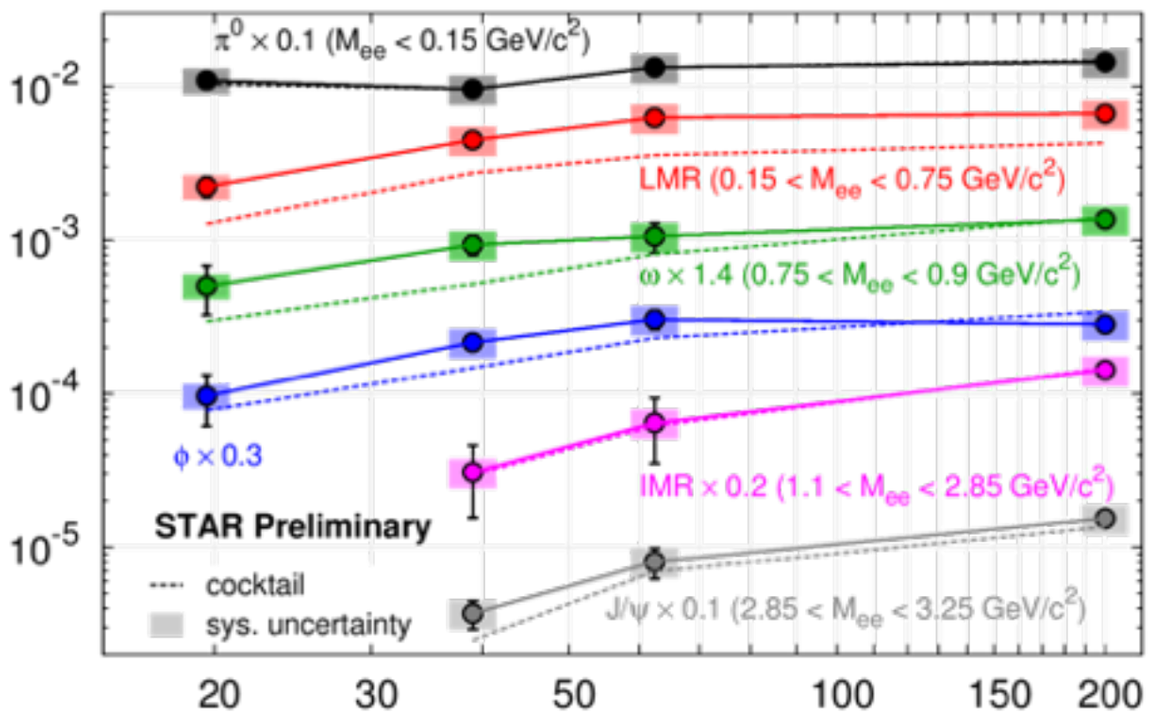


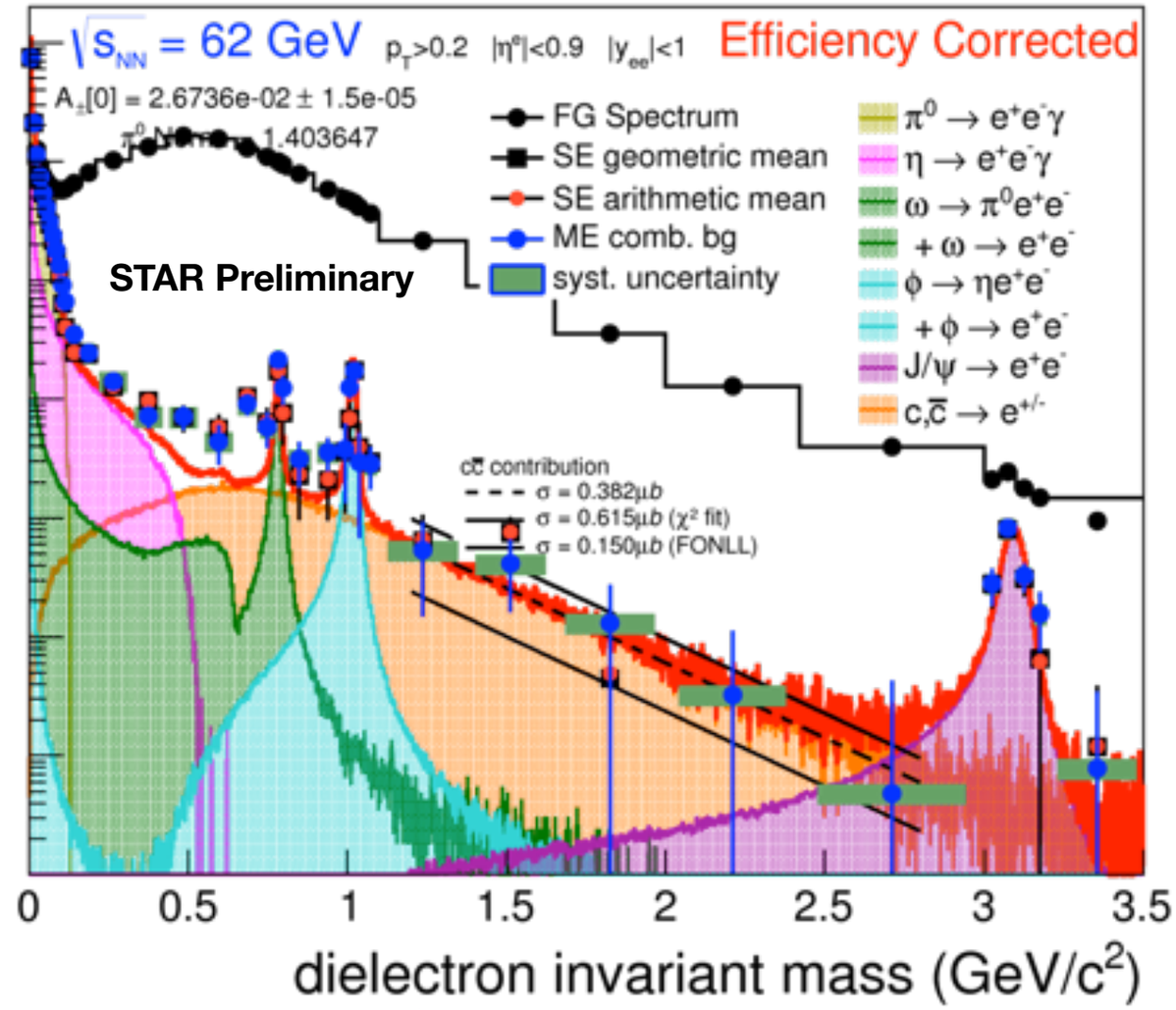


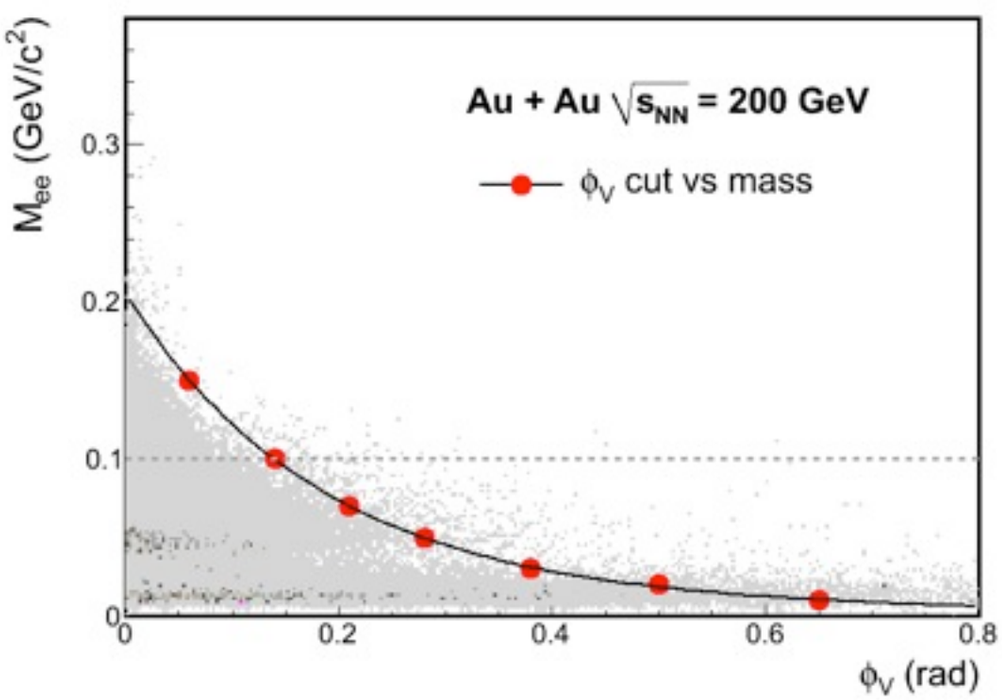


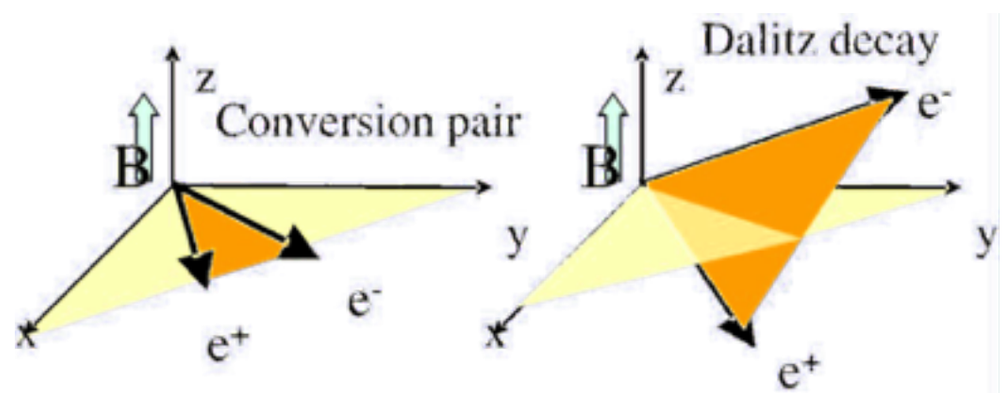


define phiV as the orientation of the dilepton plane w.r.t the magnetic field

# Cocktail w/ Vacuum-Rho

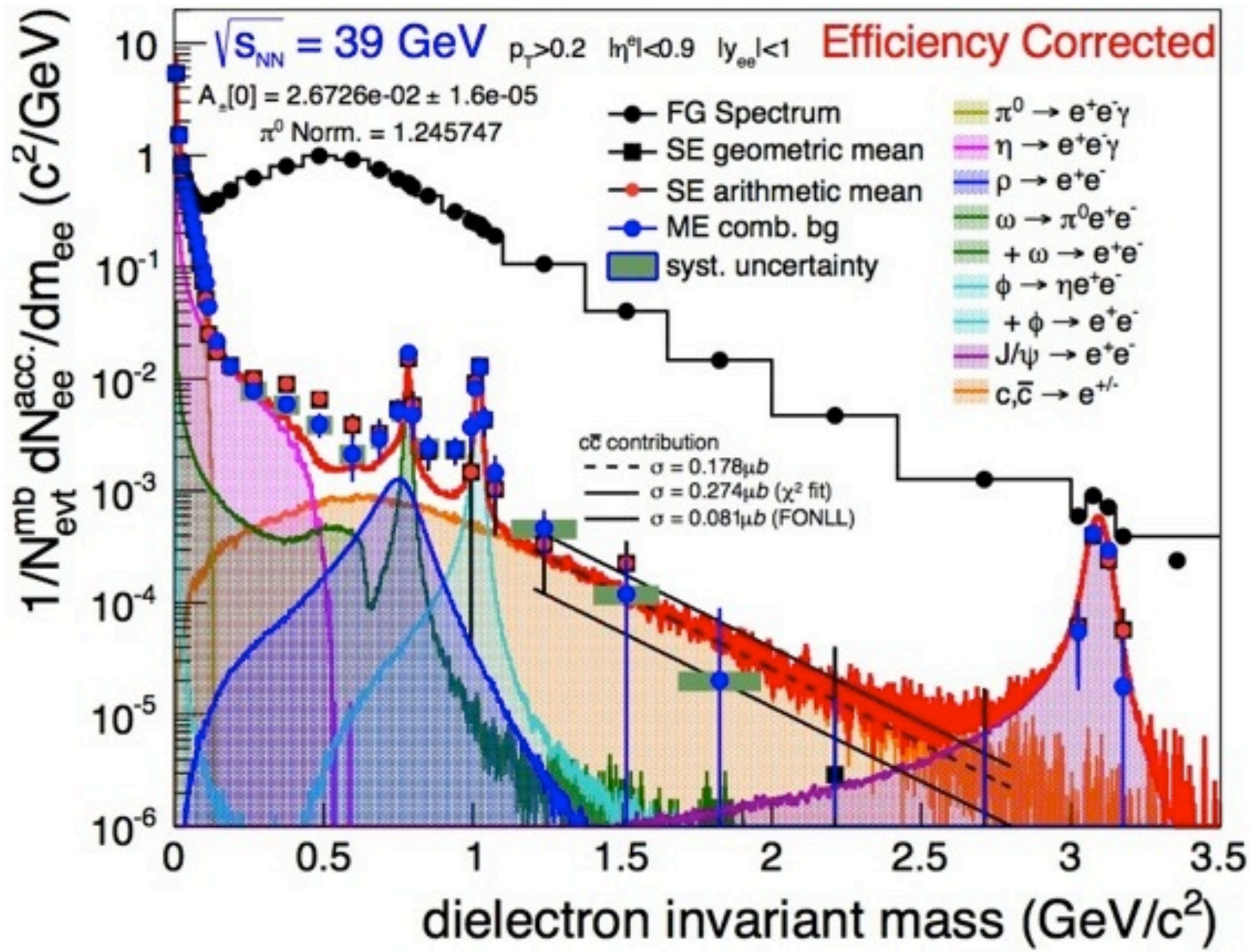

# Cold nuclear matter effects on dilepton and photon production

*Zhong-Bo Kang*
*Los Alamos National Laboratory*

Thermal Radiation Workshop
RBRC, Brookhaven National Laboratory
December 5-7, 2012

# Outline

- Introduction
  - Nuclear PDFs
  - Color Glass Condensate (MS-bar)
- Our approach on cold nuclear matter effects
  - Isospin
  - Nuclear shadowing
  - Cronin effect
  - Parton energy loss
- Power corrections at low mass (and low pt)
- Summary

# Interesting experimental result - I

- A modest nuclear modification in d+Au

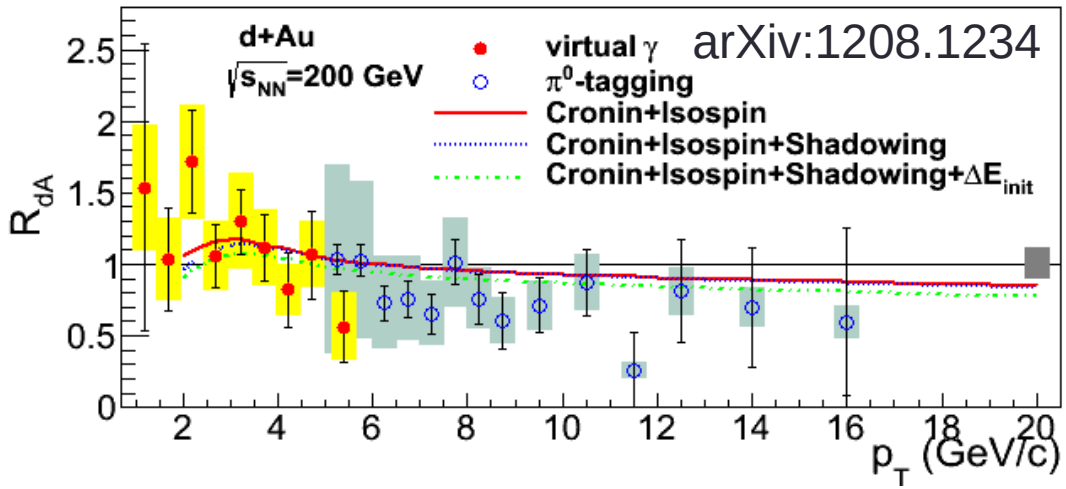


- Similar modest nuclear modification in Au+Au (at high pt)

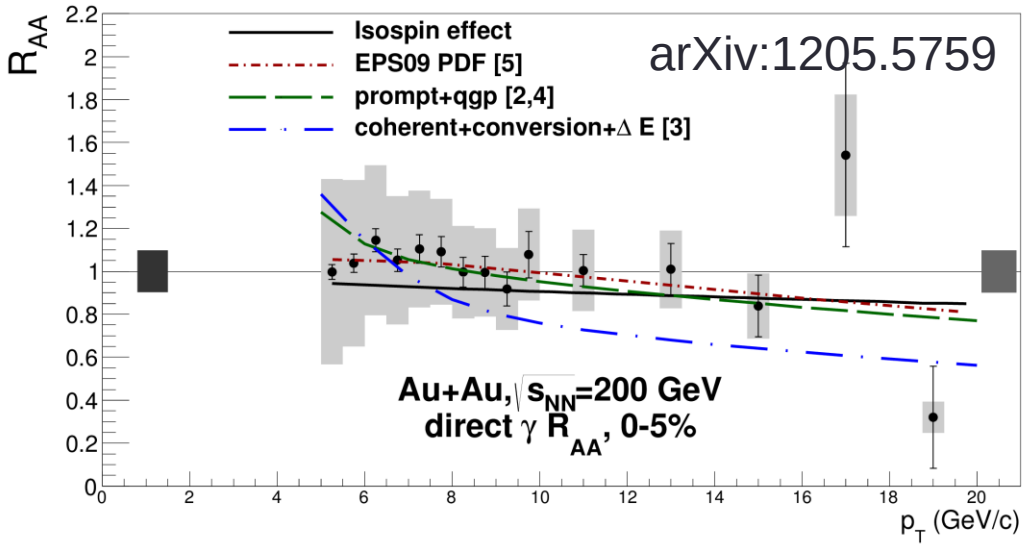

# Interesting experimental results - II

- However, large excess at low pt in Au+Au

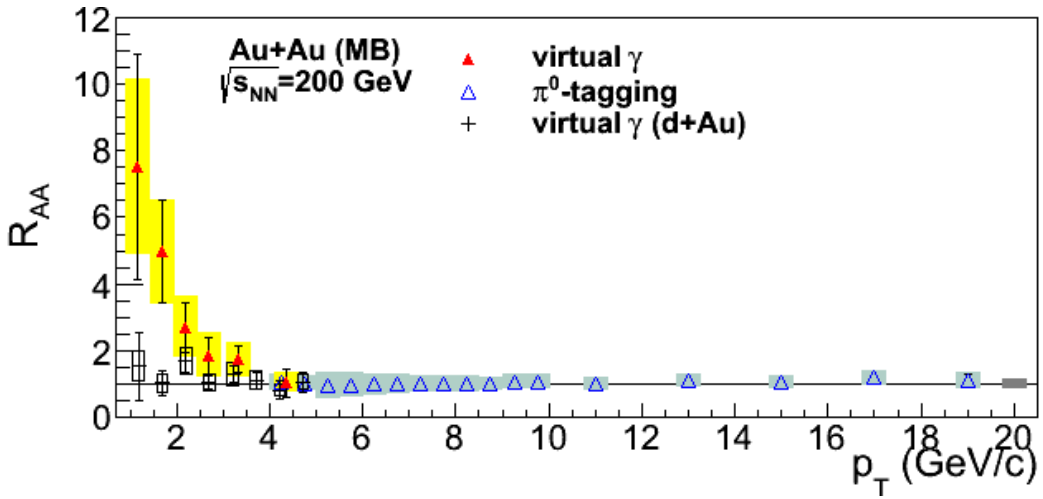


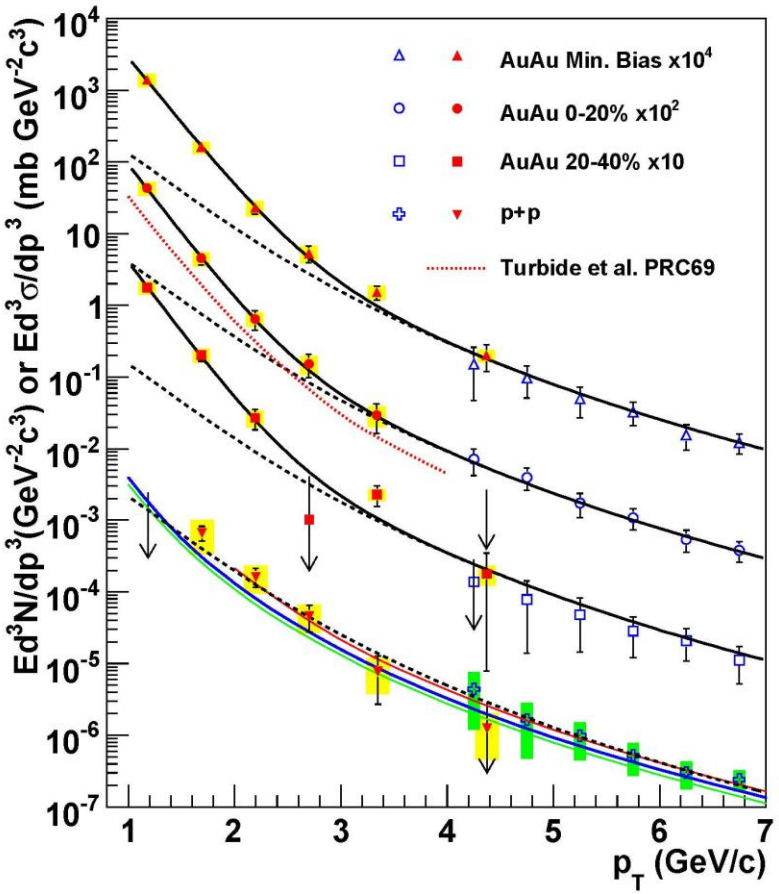

# Interesting experimental results - III

- Large excess at low mass (0.2 < M < 0.7 GeV)

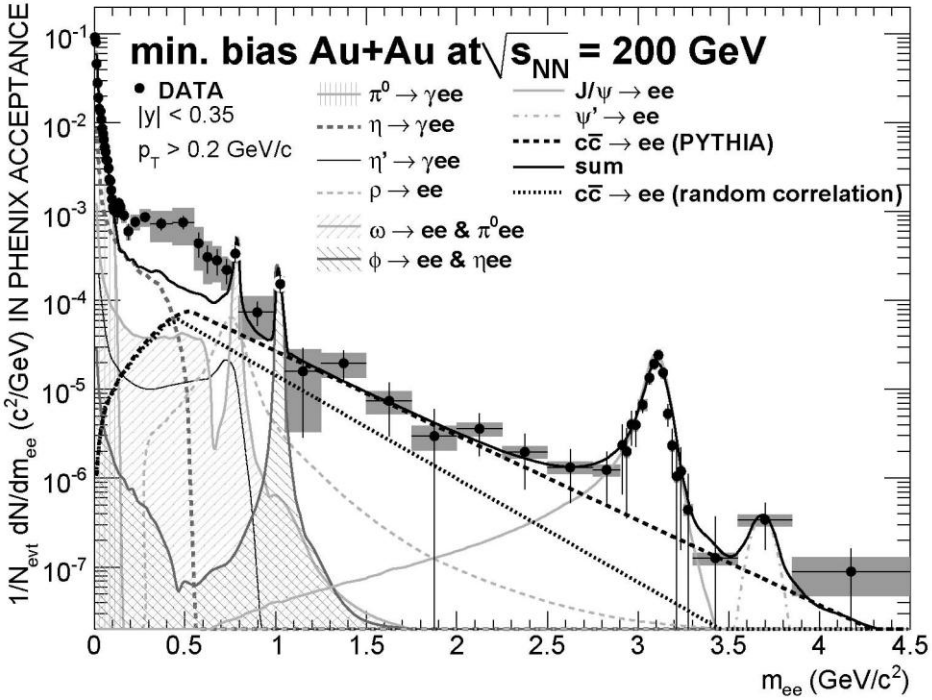


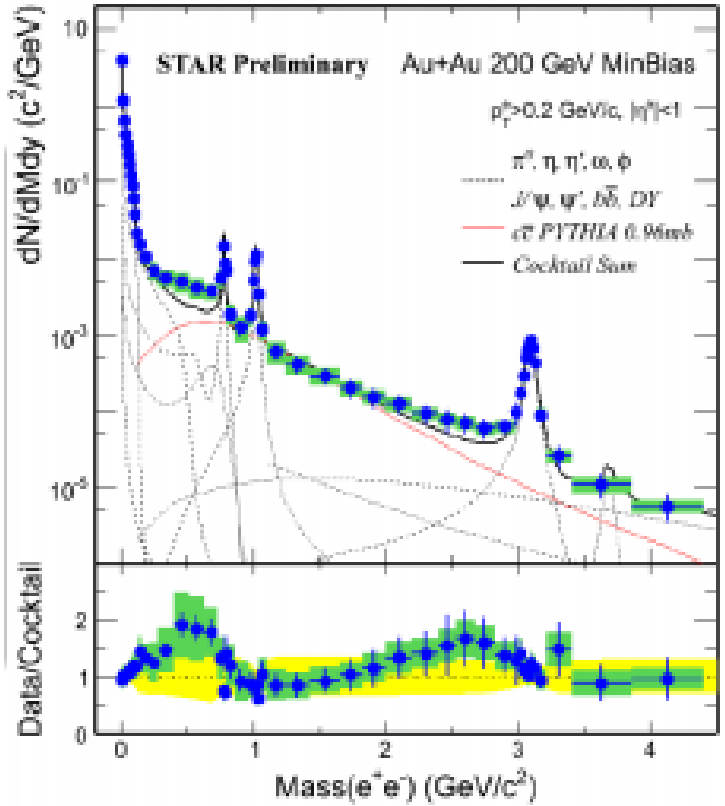


- Similar results at SPS

# Hadron production in usual pQCD factorization

- Usual hadron production

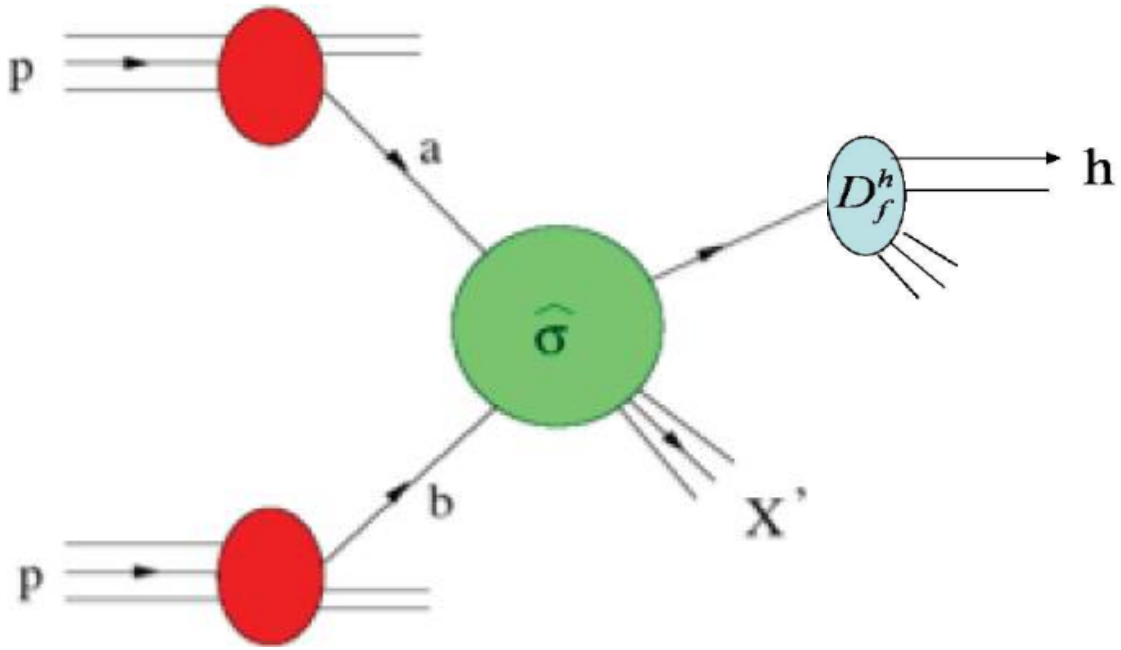

# Prompt photon production in p+p collisions

$$\frac{d\sigma}{dyd^2p_T} = \frac{d\sigma^{\rm dir.}}{dyd^2p_T} + \frac{d\sigma^{\rm frag.}}{dyd^2p_T}$$

- Direct production

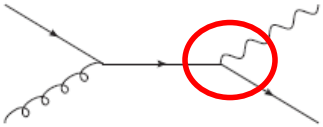

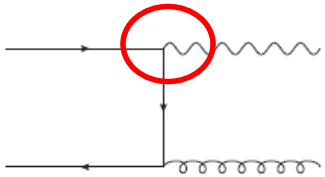

$$\frac{d\sigma^{\rm dir.}}{dyd^2p_T} = K\frac{\alpha_{\rm em}\alpha_s}{s}\sum_{a,b}\int\frac{dx_a}{x_a}d^2k_{aT}\,f_{a/N}(x_a,k_{aT}^2)\int\frac{dx_b}{x_b}d^2k_{bT}\,f_{b/N}(x_b,k_{bT}^2)\,H_{ab\to\gamma}(\hat{s},\hat{t},\hat{u})\delta\left(\hat{s}+\hat{t}+\hat{u}\right)$$

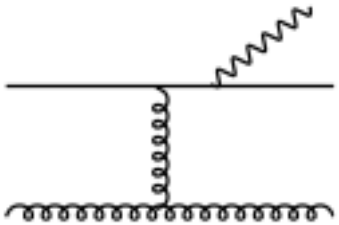

- Fragmentation component

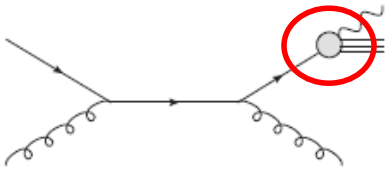

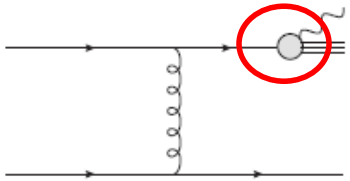

$$\frac{d\sigma^{\rm frag.}}{dyd^2p_T} = K\frac{\alpha_s^2}{s}\sum_{a,b,c}\int\frac{dx_a}{x_a}d^2k_{aT}\,f_{a/N}(x_a,k_{aT}^2)\int\frac{dx_b}{x_b}d^2k_{bT}\,f_{b/N}(x_b,k_{bT}^2)\int\frac{dz_c}{z_c^2}\,D_{\gamma/c}(z_c)H_{ab\to c}(\hat{s},\hat{t},\hat{u})\delta(\hat{s}+\hat{t}+\hat{u})$$

# Baseline: works perfect fine with p+p collisions

- Comparing to RHIC and LHC experiments

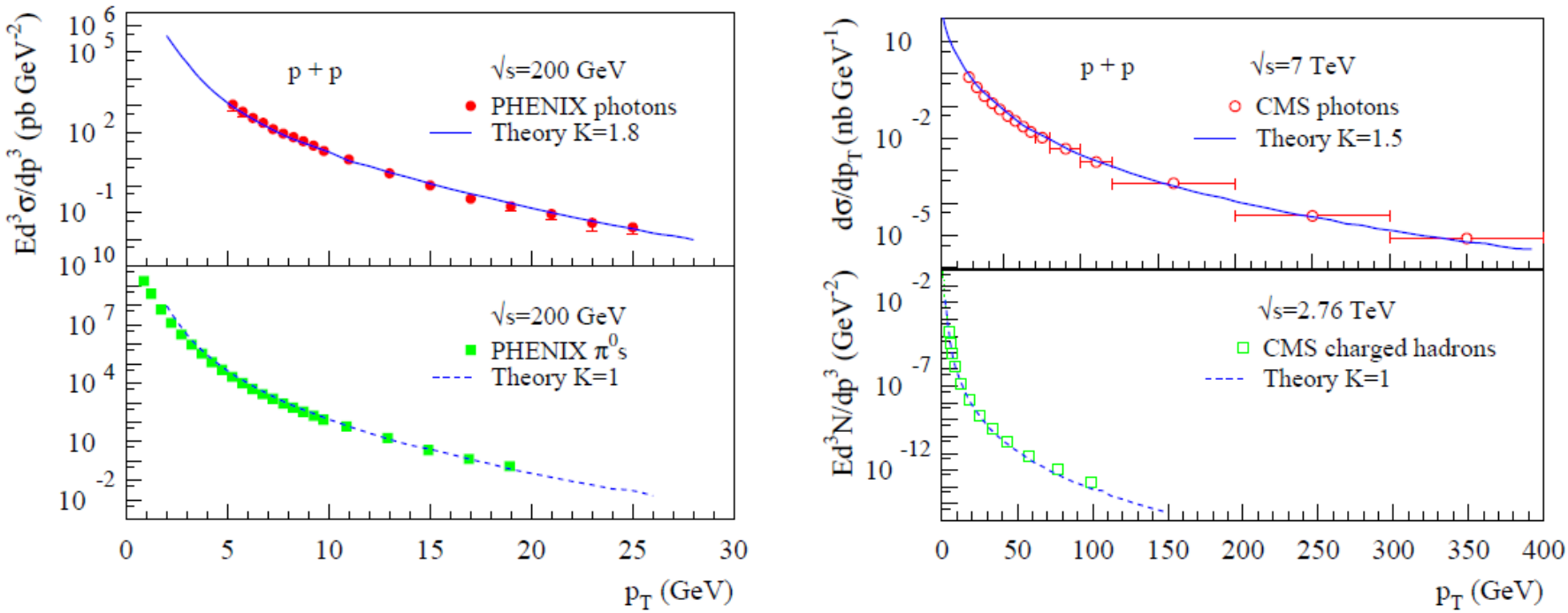

# How to understand these interesting nuclear modification

- Different approaches to incorporate nuclear effects
  - Nuclear parton distribution functions (nPDFs)

$$f_i^A(x,Q^2) \equiv R_i^A(x,Q^2) f_i^{\mathrm{CTEQ6.1M}}(x,Q^2)$$

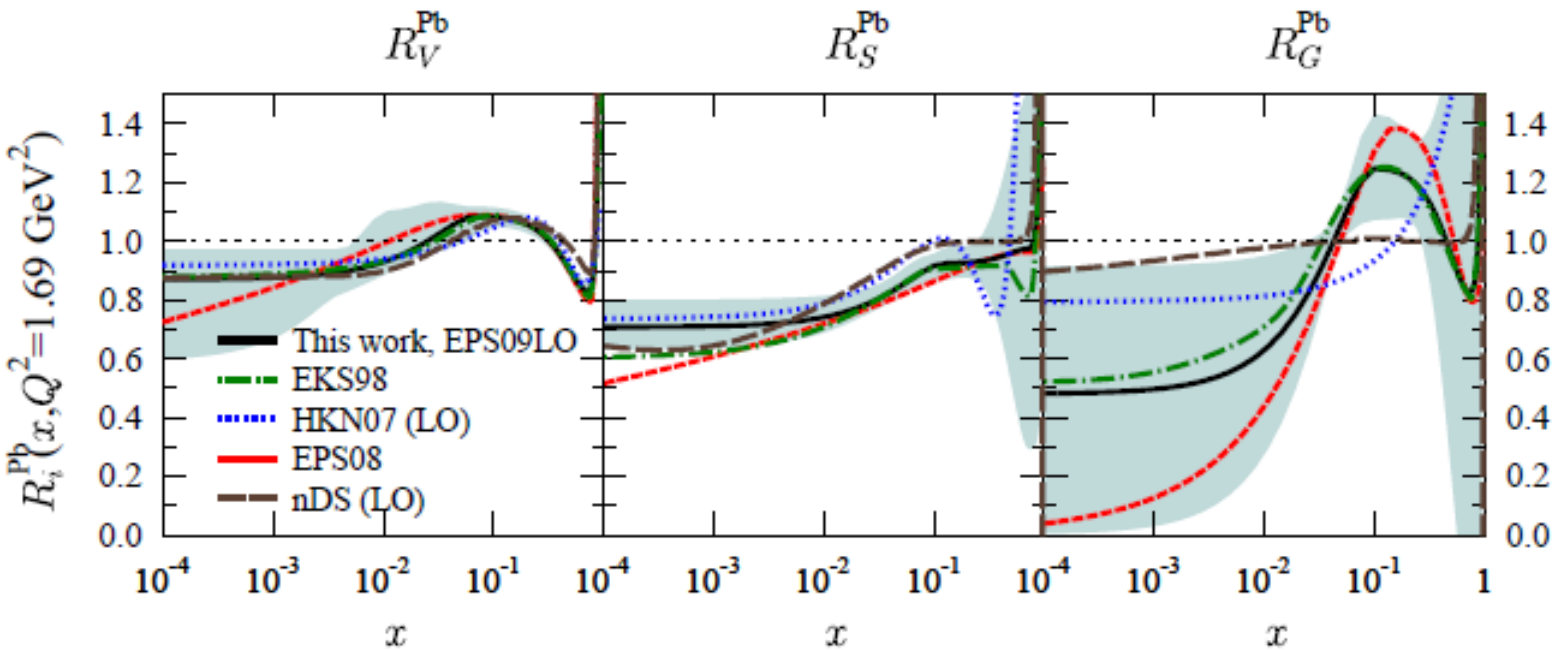

# Predictions based on nPDFs

- Predictions for prompt photon production arXiv: 1211.2130

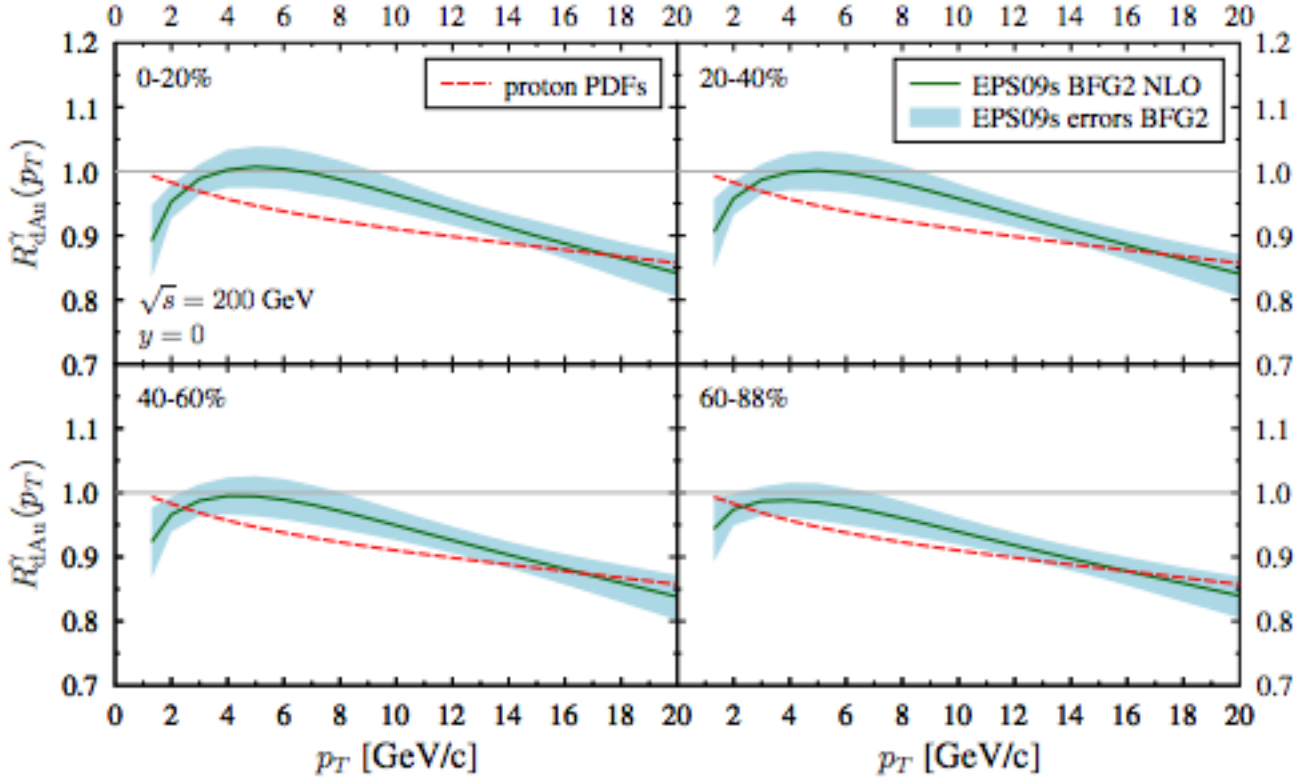


- in d+Au collisions, isospin effect dominates at high pt
- roughly consistent with the data

# Color glass condensate approach

- At small-x region, Color Glass Condensate approach takes care of gluon saturation effect
  - An incoming quark scatters with the classical gluon field of the target nucleus and then radiate a photon

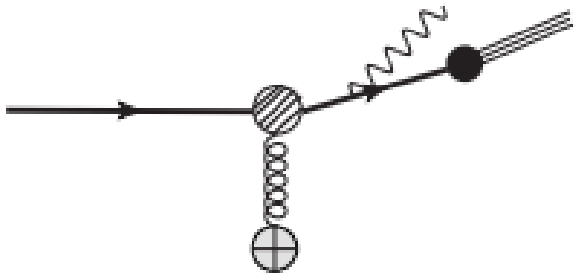

  - Calculation is straightfoward

$$\frac{d\sigma^{pA\to\gamma X}}{dy_\gamma d^2p_\perp} = \frac{\alpha_{\rm e.m.}e_q^2}{2\pi^2}\int_\tau^1 \frac{d\xi}{\xi} xq(x)\left[1+(1-\xi)^2\right]\int d^2q_\perp \mathcal{F}(q_\perp)\frac{\xi^2 q_\perp^2}{p_\perp^2(p_\perp-\xi q_\perp)^2}$$

$$\mathcal{F}(k_\perp) = \int \frac{d^2x_\perp d^2y_\perp}{(2\pi)^2} e^{-ik_\perp\cdot(x_\perp-y_\perp)}\frac{1}{N_c}\left\langle {\rm Tr}U(x_\perp)U^\dagger(y_\perp)\right\rangle_Y$$

# Structure of divergence

- There is a divergence in this naïve formalism
  - coming from the phase space when photon is radiated collinearly to the parent quark: collinear divergence
  - Jalilian-Marian, Rezaeian regularize this divergence by a cut-off: if radiated collinearly, then it is absorbed into a quark-to-photon fragmentation function; if photon is well separated from the quark, it remains as a direct contribution

arXiv: 1204.1319

$$\frac{d\sigma^{q(p)\,T\to\gamma(k)\,X}}{d^2\vec{b}_t d^2\vec{k}_t d\eta_\gamma} = \frac{d\sigma^{\text{Fragmentation}}}{d^2\vec{b}_t d^2\vec{k}_t d\eta_\gamma} + \frac{d\sigma^{\text{Direct}}}{d^2\vec{b}_t d^2\vec{k}_t d\eta_\gamma}$$

$$= \frac{1}{(2\pi)^2}\frac{1}{z} D_{\gamma/q}(z,k_t^2)\, N_F(x_g,b_t,k_t/z) + \frac{e_q^2\alpha_{em}}{\pi(2\pi)^3} z^2[1+(1-z)^2]\frac{1}{k_t^4}\int^{k_t^2} d^2\vec{l}_t\, l_t^2\, N_F(\bar{x}_g,b_t,l_t)$$

  - It is okay, it will lead to mismatch if one wants to use the standard PDFs, which is usually extracted based on MS-bar scheme

# Prompt photon production in MS-bar schme

- Use dimensional regularization to regular and separate the divergence
  - Expression with divergence explicit

$$c_0 = 2e^{-\gamma_E}$$

$$\frac{d\sigma^{pA\to\gamma X}}{dy_\gamma d^2p_\perp} = \frac{\alpha_{\rm e.m.}e_q^2}{2\pi^2}\int_\tau^1 \frac{d\xi}{\xi^2} xq(x,\mu)\frac{1}{\xi}\left[1+(1-\xi)^2\right]\int \frac{d^2x_\perp d^2y_\perp}{(2\pi)^2} S_Y^{(2)}(x_\perp,y_\perp)$$
$$\times\left[\pi\left(-\frac{1}{\hat\epsilon}+\ln\frac{c_0^2}{\mu^2 r_\perp^2}\right)e^{-ik_\perp\cdot r_\perp}+\frac{(2\pi)^2\delta^2(r_\perp)}{k_\perp^2}-\int d^2b_\perp e^{-ik_\perp\cdot(r_\perp-b_\perp)}\frac{2r_\perp\cdot b_\perp}{r_\perp^2 b_\perp^2}\right]$$

  - Then one sees to avoid large logarithms, it is better to choose factorization scale $\mu = c_0/r_\perp$

$$\frac{d^3\sigma_{\rm dir}^{p+A\to\gamma+X}}{dyd^2p_\perp} = \int_\tau^1 \frac{d\xi}{\xi^2} xq(x,\mu)\frac{1}{\xi}\left[1+(1-\xi)^2\right] S_{q\gamma}$$

$$S_{q\gamma} = \frac{\alpha_{\rm e.m.}e_q^2}{2\pi}\int \frac{d^2x_\perp d^2y_\perp}{(2\pi)^2} S_Y^{(2)}(x_\perp,y_\perp)(4\pi)\left[\frac{\delta^2(r_\perp)}{k_\perp^2}-\int\frac{d^2b_\perp}{(2\pi)^2}e^{-ik_\perp\cdot(r_\perp-b_\perp)}\frac{2r_\perp\cdot b_\perp}{r_\perp^2 b_\perp^2}\right]$$

  - A main feature: factorization scale depends on r, the PDFs need to change accordingly when we integrate over all the coordiates

# Some predictions based on CGC

- CGC predictions for RHIC kinematics at forward rapidity

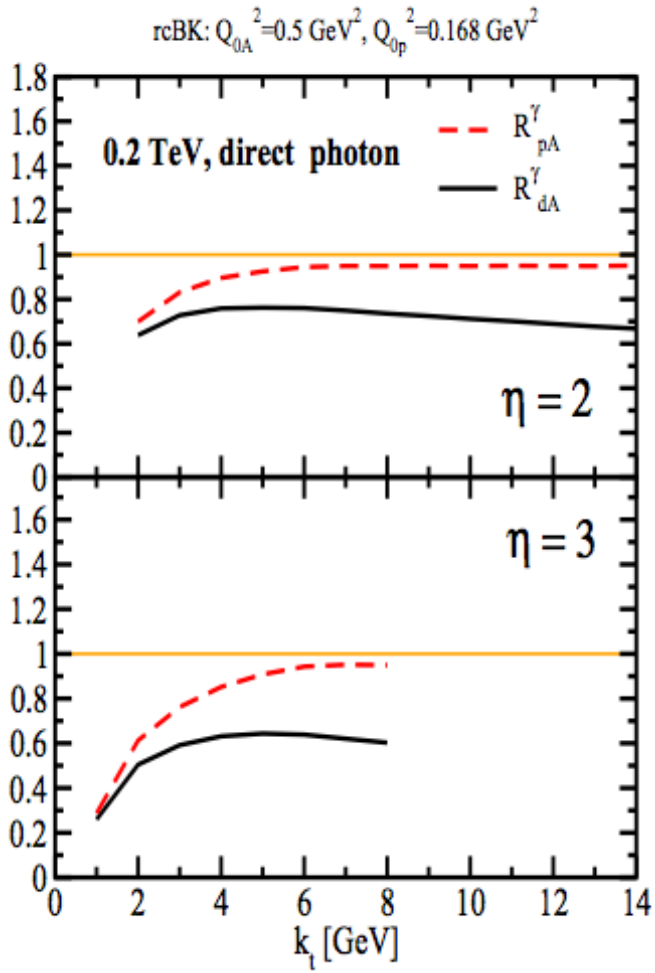


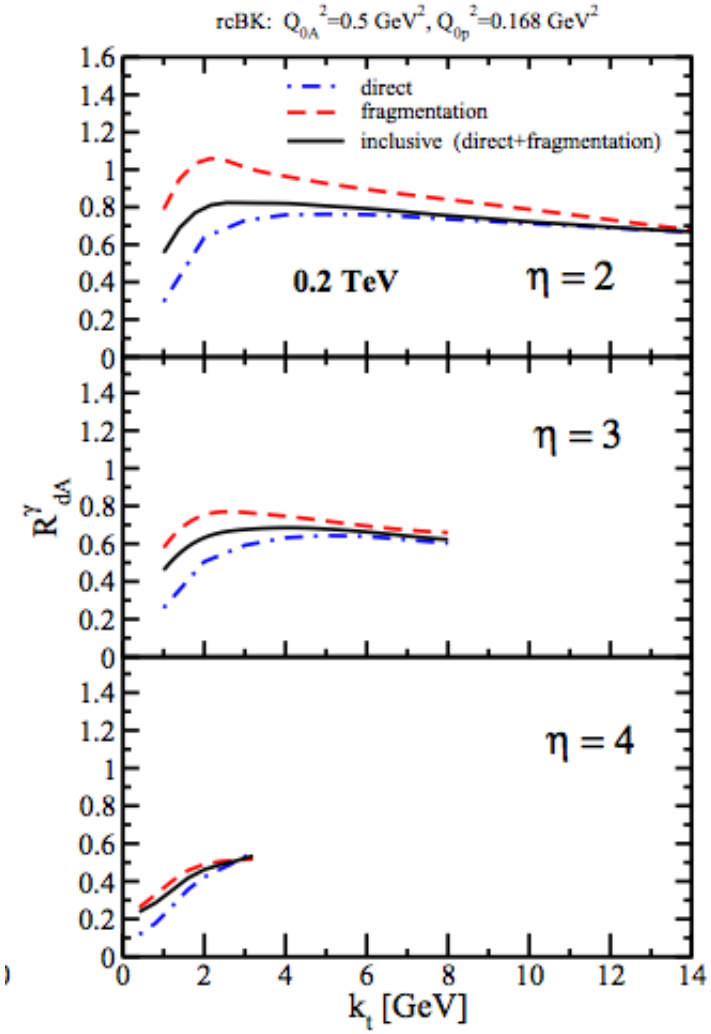


arXiv: 1204.1319

# Our approach: all kinds of nuclear effects

Z. Kang, I. Vitev and H. Xing, 2012

- Cronin effect

J. Cronin, 1975

Cronin ratio:

$$R(p_T) = \frac{B}{A}\frac{d\sigma_{pA}/d^2p_T}{d\sigma_{pB}/d^2p_T}$$

- Smaller than one in small pT
- Larger than one in moderate pT
- Approach to one in large pT

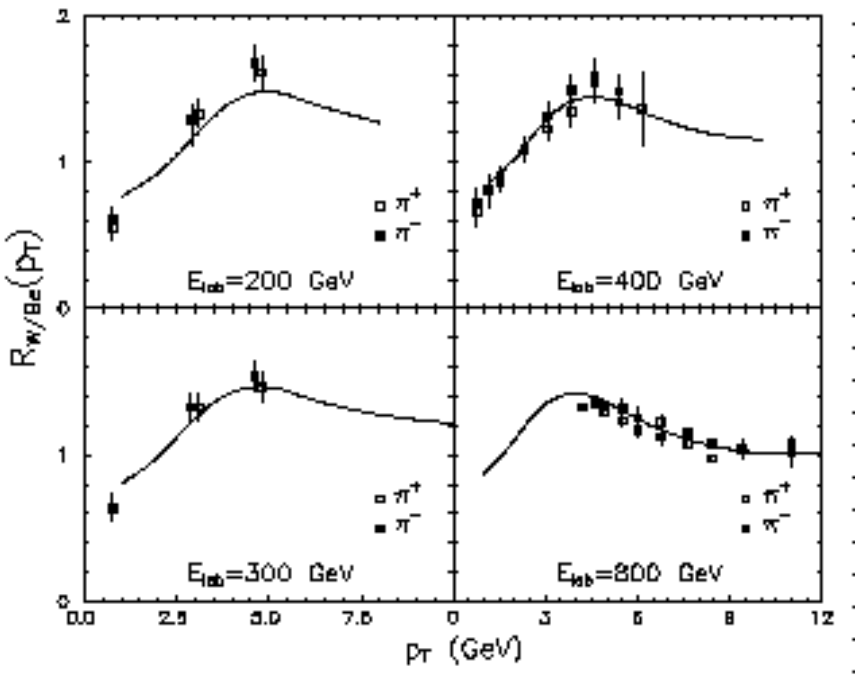


$$p + A \to \text{hadron(p)} + X$$

# Incorporate Cronin effect

- Initial-state multiple scattering

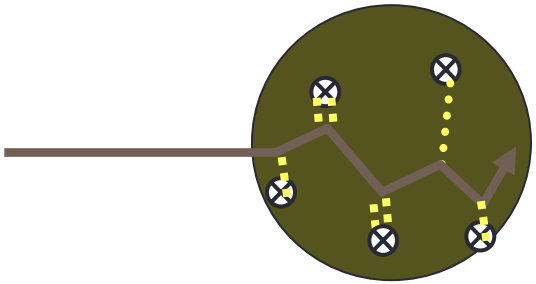

Z. Kang, I. Vitev and H. Xing, 1209.6030

- Total momentum = pp baseline + nuclear broadening

$$\langle k_{a,T}^2 \rangle_{pA} = \langle k_{a,T}^2 \rangle_{pp} + \left\langle \frac{2\mu^2 L}{\lambda_{q,g}} \right\rangle \xi \qquad \zeta = \ln(1+\delta p_T^2)$$

$$\delta = 0.14\ \mathrm{GeV}^{-2},\ \mu^2 = 0.12\ \mathrm{GeV}^2,\ \lambda_g = C_F/C_A \lambda_q = 1\ \mathrm{fm}$$

# Nuclear shadowing effect

- Dynamic shadowing from power correction

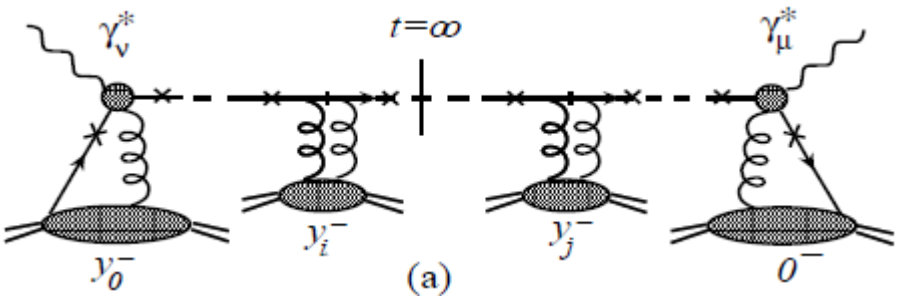


$$F_T^A(x,Q^2) \approx \sum_{n=0}^{N} \frac{A}{n!}\left[\frac{\xi^2(A^{1/3}-1)}{Q^2}\right]^n x^n \frac{d^n F_T^{(\mathrm{LT})}(x,Q^2)}{d^n x}$$

$$\approx A\, F_T^{(\mathrm{LT})}\left(x + \boxed{\frac{x\xi^2(A^{1/3}-1)}{Q^2}}\, Q^2\right), \qquad (10)$$

$$\xi^2 = \frac{3\pi\alpha_s(Q^2)}{8\, r_0^2}\langle p|\, \hat{F}^2(\lambda_i)\, |p\rangle$$

$$= 0.09 - 0.12\ \mathrm{GeV}^2$$

Qiu, Vitev , PRL, 2004

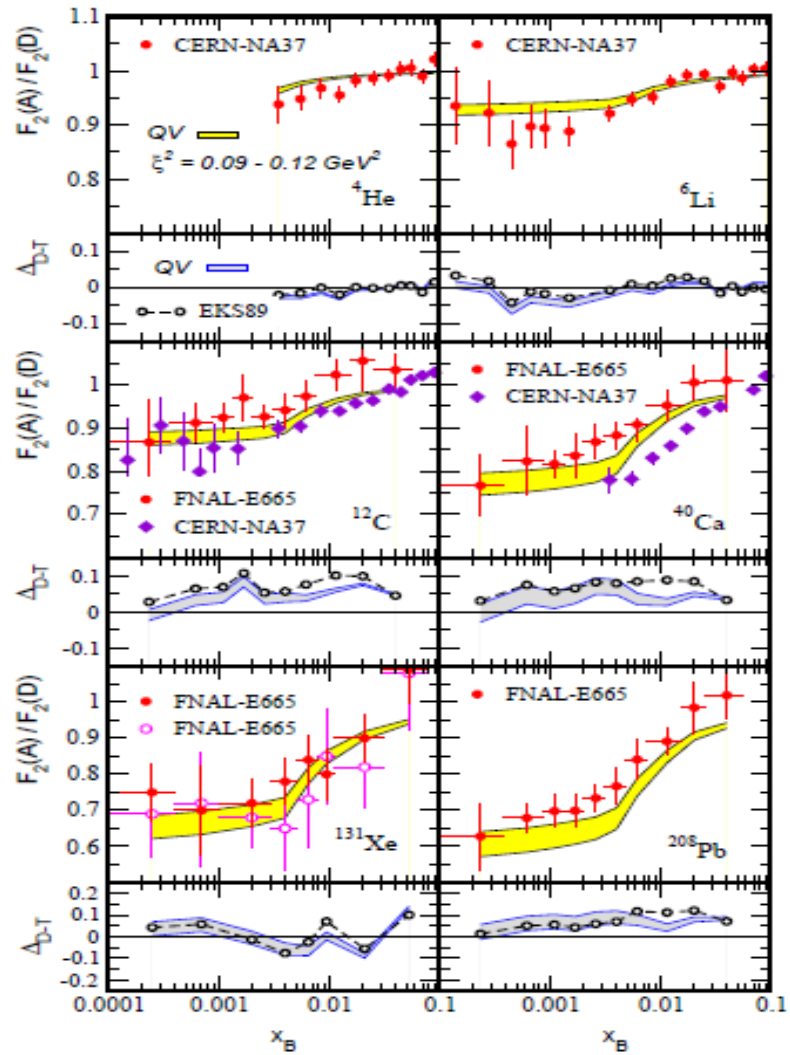

# Generalize to p+A collisions

- Power corrections in p+A collisions

Qiu, Vitev, PLB, 2006

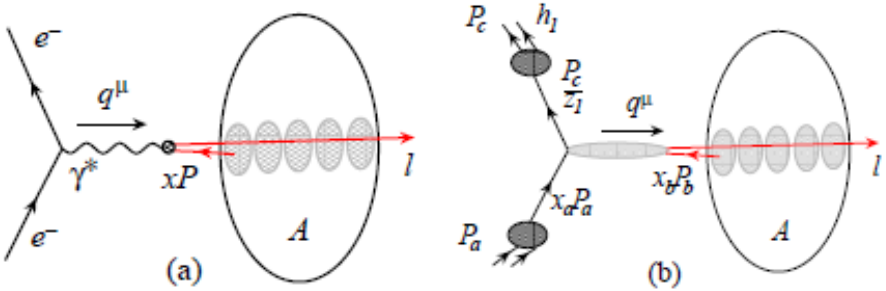


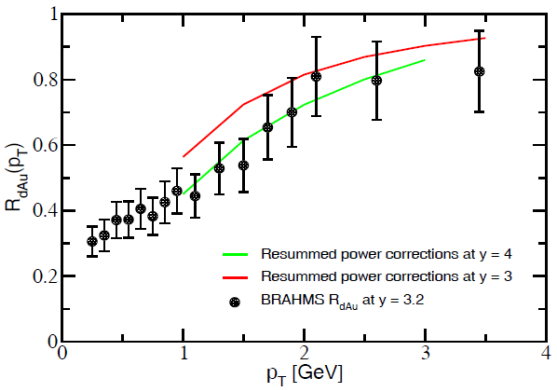


- At forward rapidity region t-channel dominates (t is small)

$$x_b \to x_b \left(1 + \frac{C_d \xi^2 (A^{1/3} - 1)}{(-\hat{t})}\right)$$

# Parton energy loss in cold nuclear matter

- This has been computed in both a GLV-type and higher-twist type formalisms

Xing, Wang, et.al., NPA,2012; Ivan, 2007

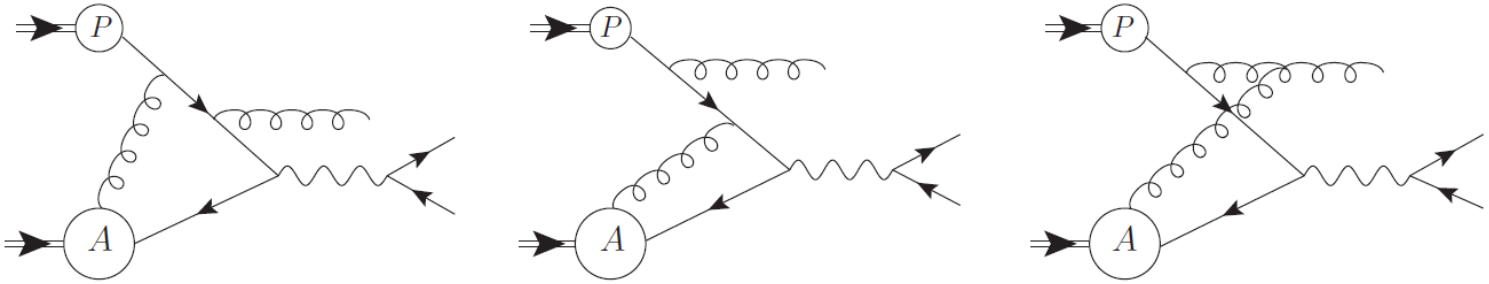


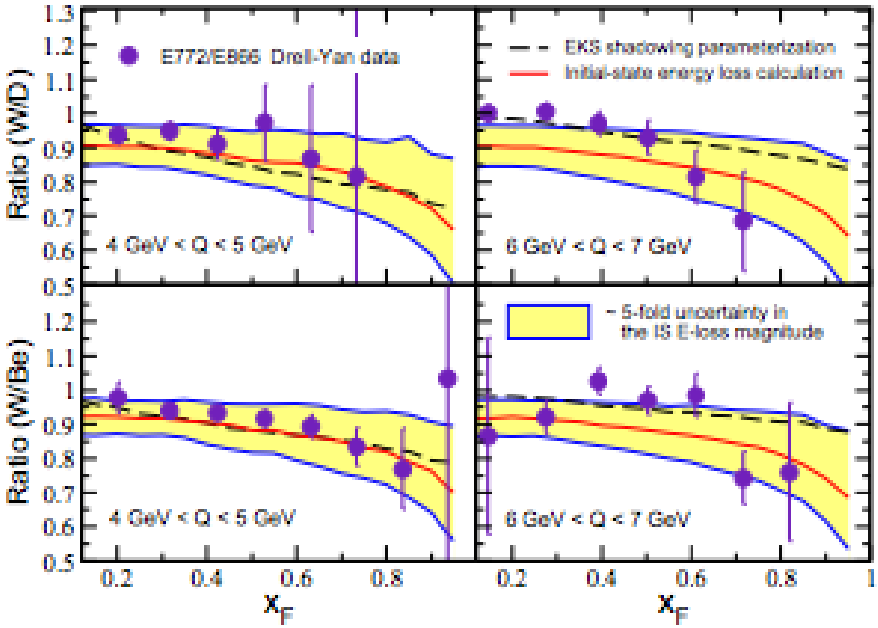

# Recap: all the cold nuclear matter effects

- All cold nuclear matter effects are centered around the idea of multiple parton scattering
  - Parton energy loss
  - Cronin effect
  - Dynamic shadowing
- Take a lood again at the p+p baseline

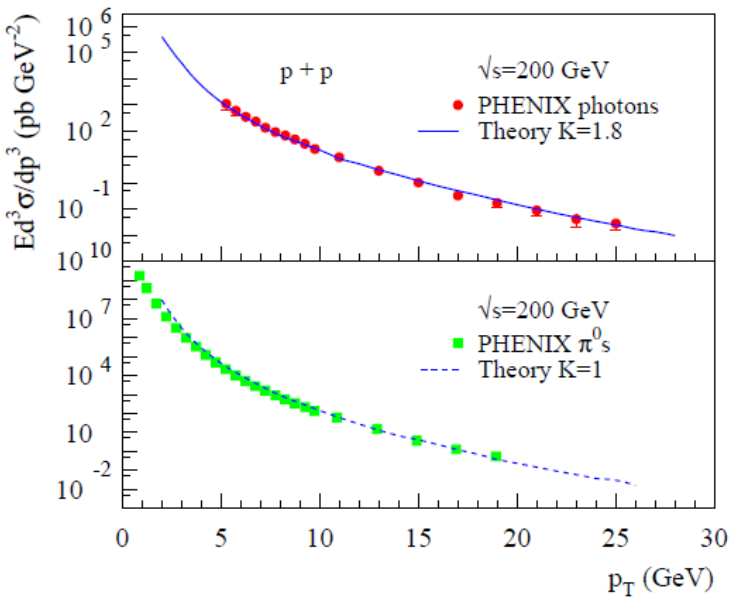


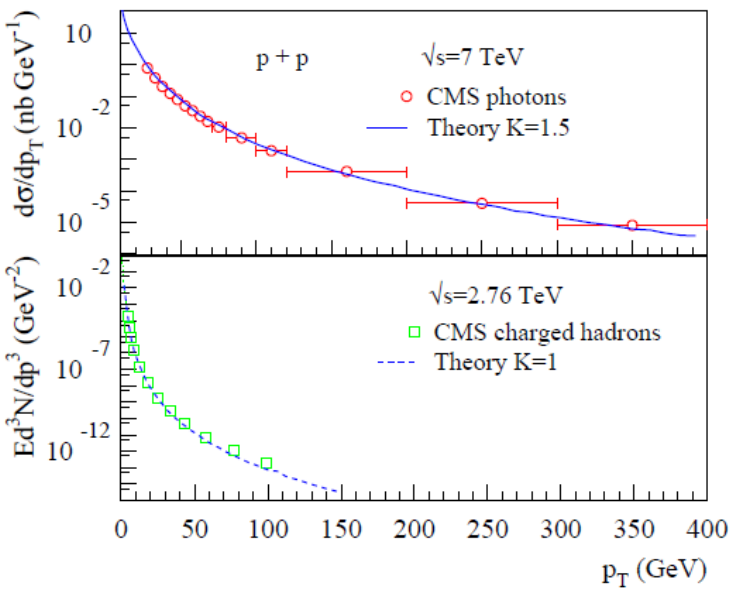


$$g(\vec{k}_T) = \frac{1}{\pi\langle k_T^2\rangle}\exp[-k_T^2/\langle k_T^2\rangle]$$

$$\langle k_T^2\rangle = 1.8\ \mathrm{GeV}^2$$

# Incorporate all the cold nuclear matter effects - I

- Incorporate these cold nuclear matter effects

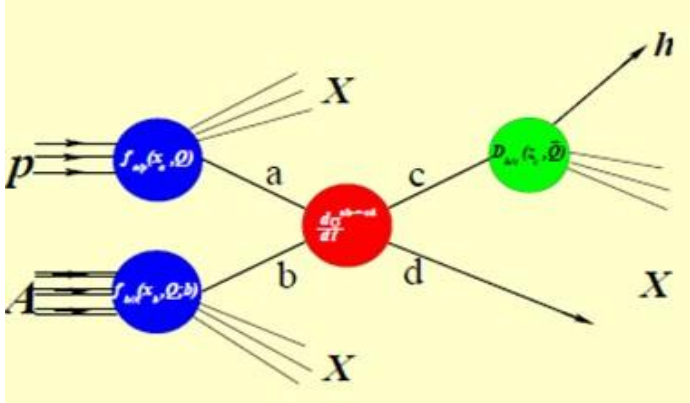


$$E_h \frac{d\sigma_h^{pA}}{d^3p} = K \sum_{abcd} \int dx_a dx_b d^2k_{aT} d^2k_{bT} \boxed{g_A(k_{aT}, Q^2)} g_p(k_{bT}, Q^2) f_{a/p}(x_a, Q^2) \boxed{f_{b/A}(x_b, Q^2)} \frac{d\sigma}{d\hat{t}} \frac{D_{h/c}(z_c, Q^2)}{\pi z_c^2} \hat{s}\delta(\hat{s} + \hat{t} + \hat{u})$$

- Cronin effect: $g(\vec{k}_T) = \frac{1}{\pi \langle k_T^2 \rangle} \exp[-k_T^2/\langle k_T^2 \rangle]$ $\quad \langle k_{a,T}^2 \rangle_{pA} = \langle k_{a,T}^2 \rangle_{pp} + \left\langle \frac{2\mu^2 L}{\lambda_{q,g}} \right\rangle \xi$

- Shadowing effect: $x_b \to x_b \left(1 + \boxed{C_d \frac{\xi^2 (A^{1/3} - 1)}{-\hat{t}}}\right)$

# Incorporate all the cold nuclear matter effects - II

- Continue …

$$E_h \frac{d\sigma_h^{pA}}{d^3p} = K \sum_{abcd} \int dx_a dx_b d^2k_{aT} d^2k_{bT} g_A(k_{aT}, Q^2) g_p(k_{bT}, Q^2) \boxed{f_{a/p}(x_a, Q^2)} \boxed{f_{b/A}(x_b, Q^2)} \frac{d\sigma}{d\hat{t}} \frac{D_{h/c}(z_c, Q^2)}{\pi z_c^2} \hat{s}\delta(\hat{s} + \hat{t} + \hat{u})$$

Energy loss: $f_{q/p}(x_a) \to f_{q/p}\left(\frac{x_a}{1-\epsilon_{\text{eff.}}}\right), \quad f_{g/p}(x_a) \to f_{g/p}\left(\frac{x_a}{1-\epsilon_{\text{eff.}}}\right)$

$$\epsilon_{eff} = \frac{\Delta E}{E}$$

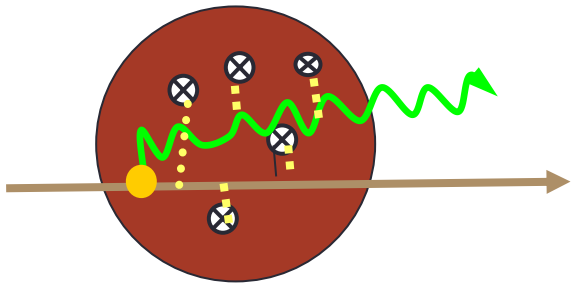

Isospin: $f_{a/A}(x) = \frac{Z}{A} f_{a/p}(x) + \left(1 - \frac{Z}{A}\right) f_{a/n}(x)$

# CNM effect: isospin

$$R_{pA} = \frac{1}{\langle N_{\rm coll}\rangle}\frac{d\sigma_{pA}}{dyd^2p_T}\Big/\frac{d\sigma_{pp}}{dyd^2p_T}$$

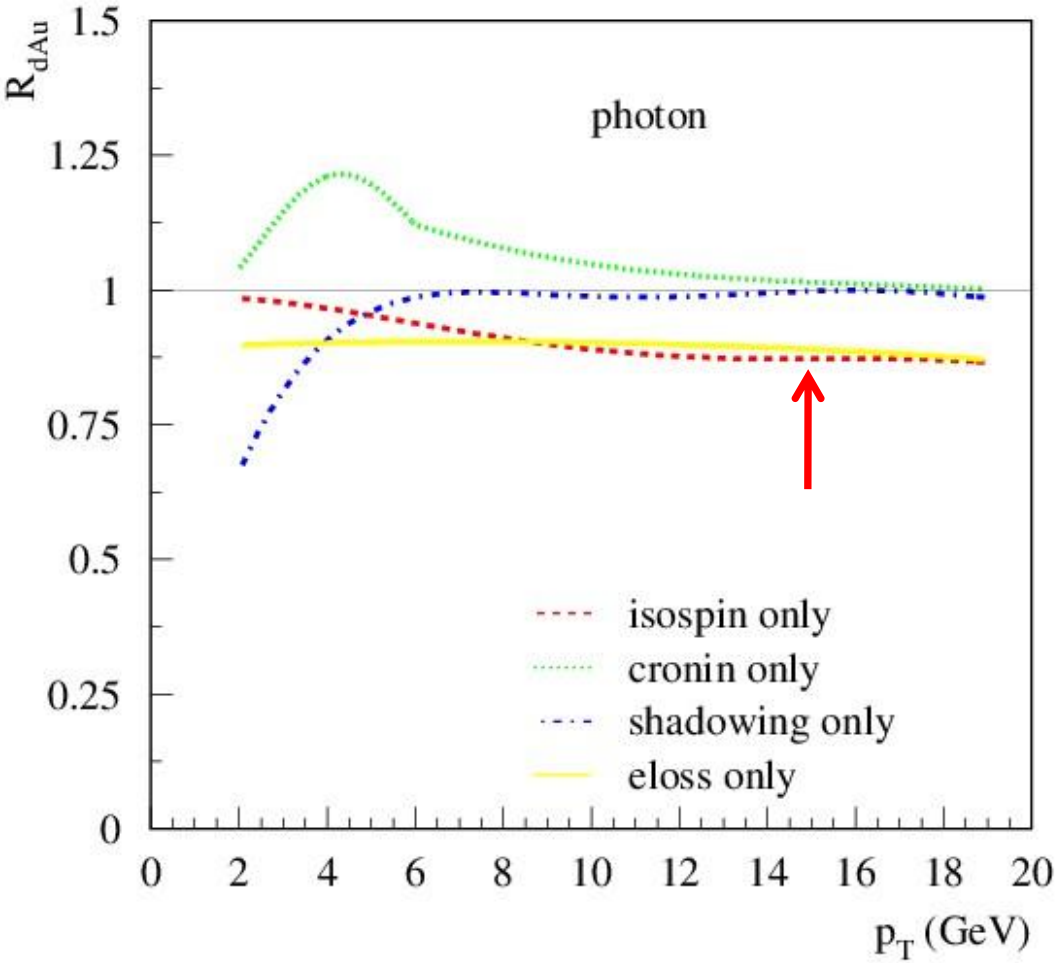


Strong isospin effect

$$f_i^p(x,Q^2) \to [Z\cdot f_i^p + (A-Z)\cdot f_i^n]/A$$

$$\sigma_{qg} \propto \frac{4}{9}f_u^n + \frac{1}{9}f_d^n = \frac{4}{9}f_d^p + \frac{1}{9}f_u^p$$

$$f_u^p > f_d^p$$

$$\sigma^{np} < \sigma^{pp}$$

# CNM effect: Cronin

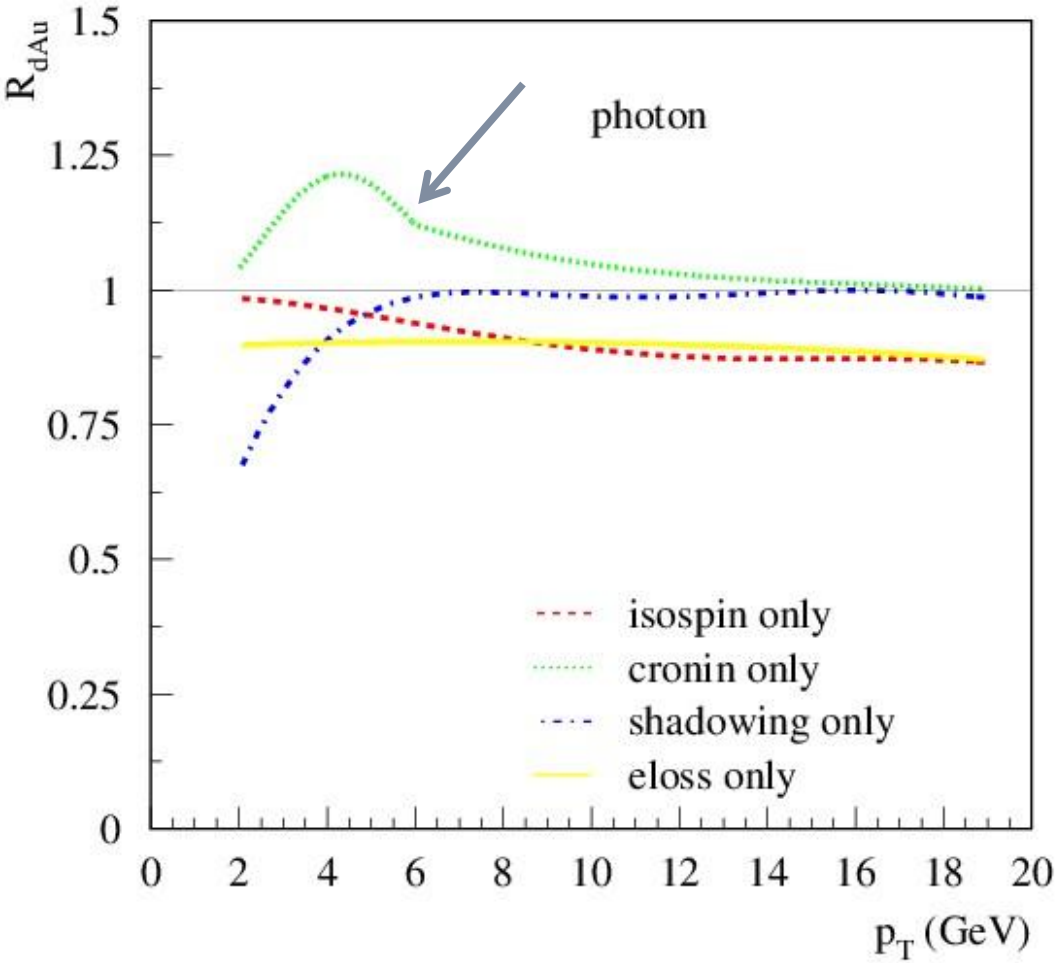


Cronin enhancement

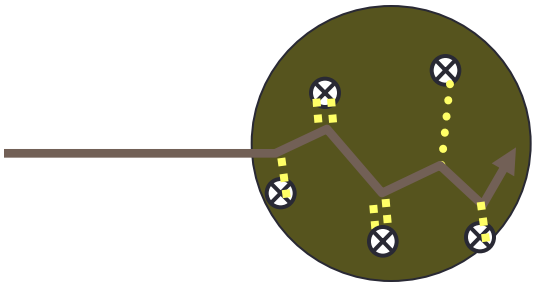

# CNM effect: shadowing

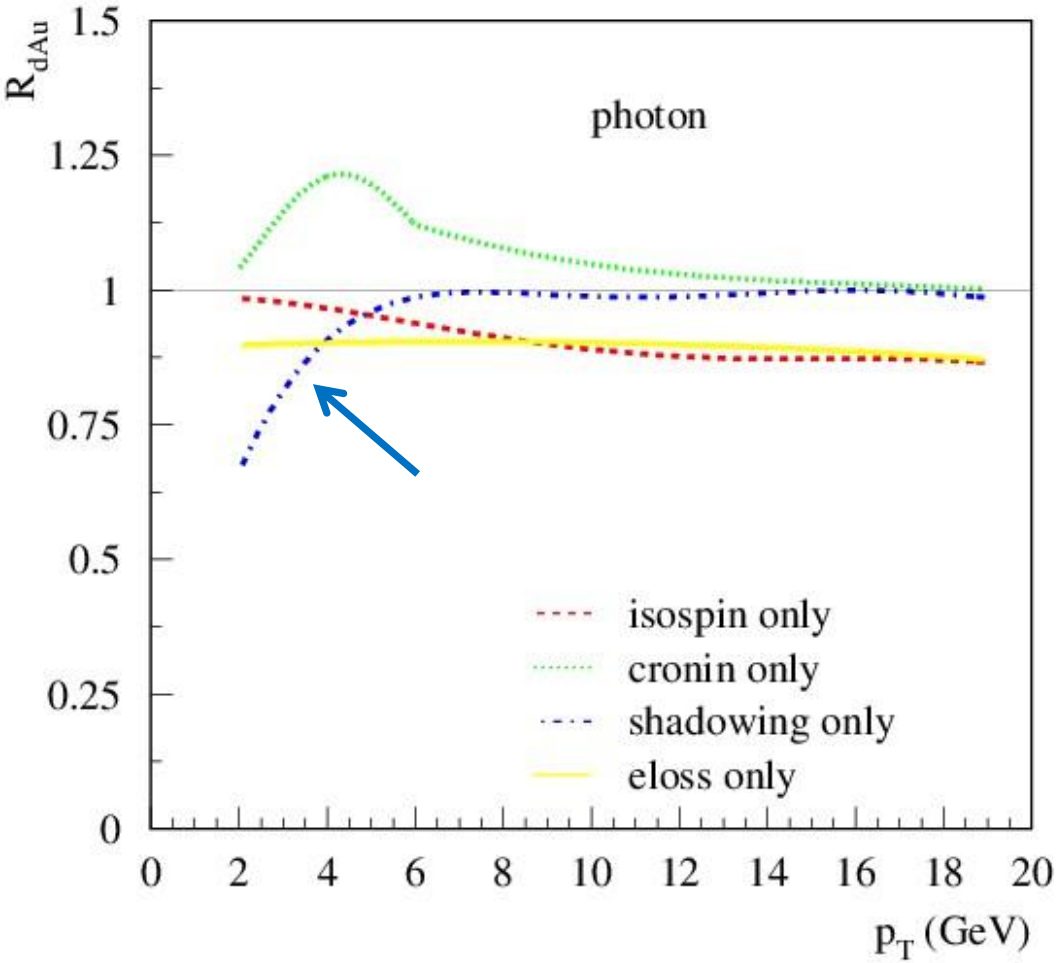


Shadowing suppression

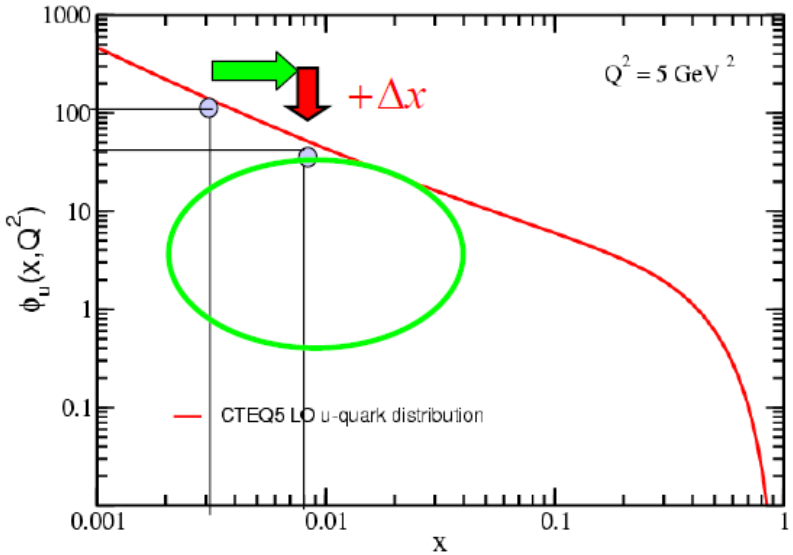

# CNM effect: energy loss

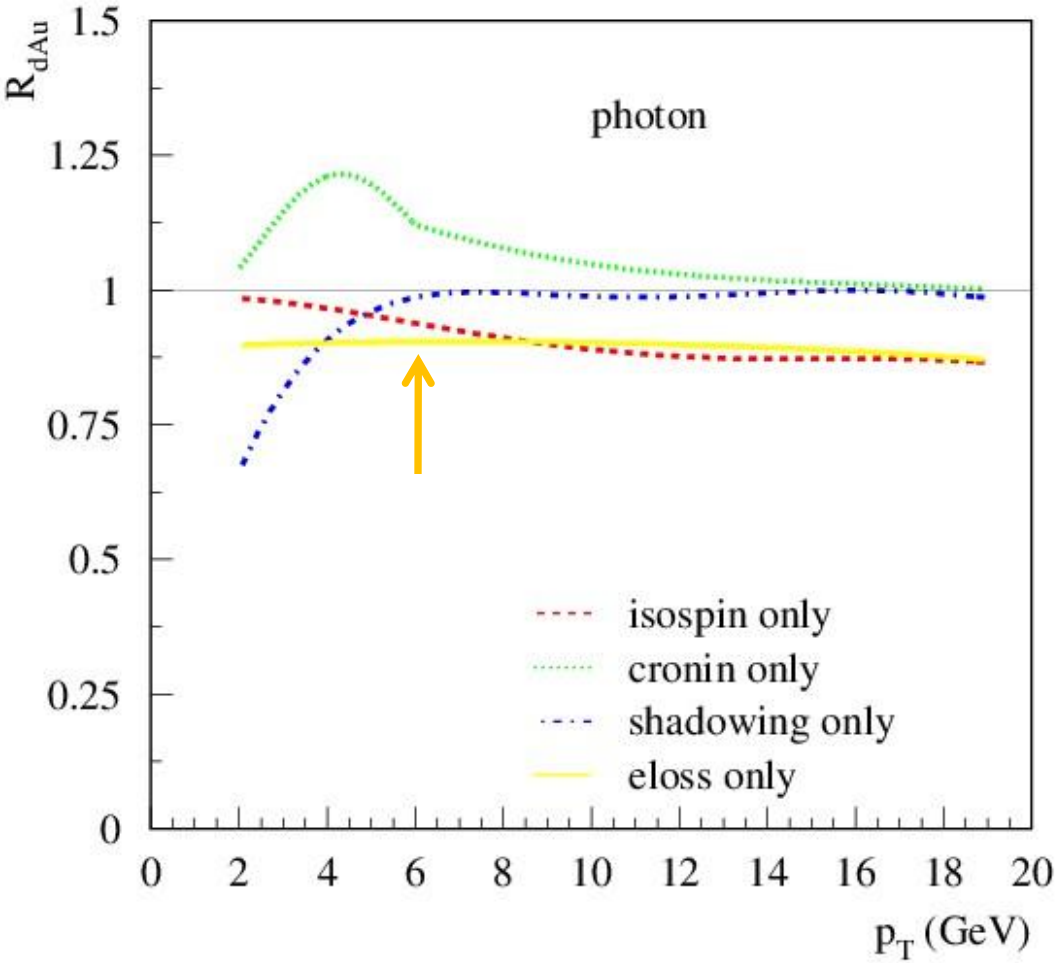


energy loss suppression

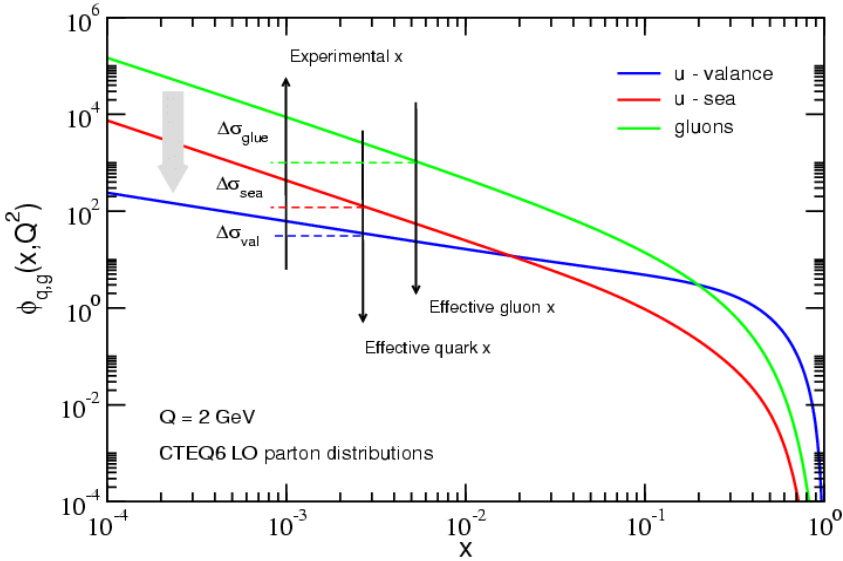

# Nuclear modification at RHIC

Z. Kang, I. Vitev and H. Xing, 2012

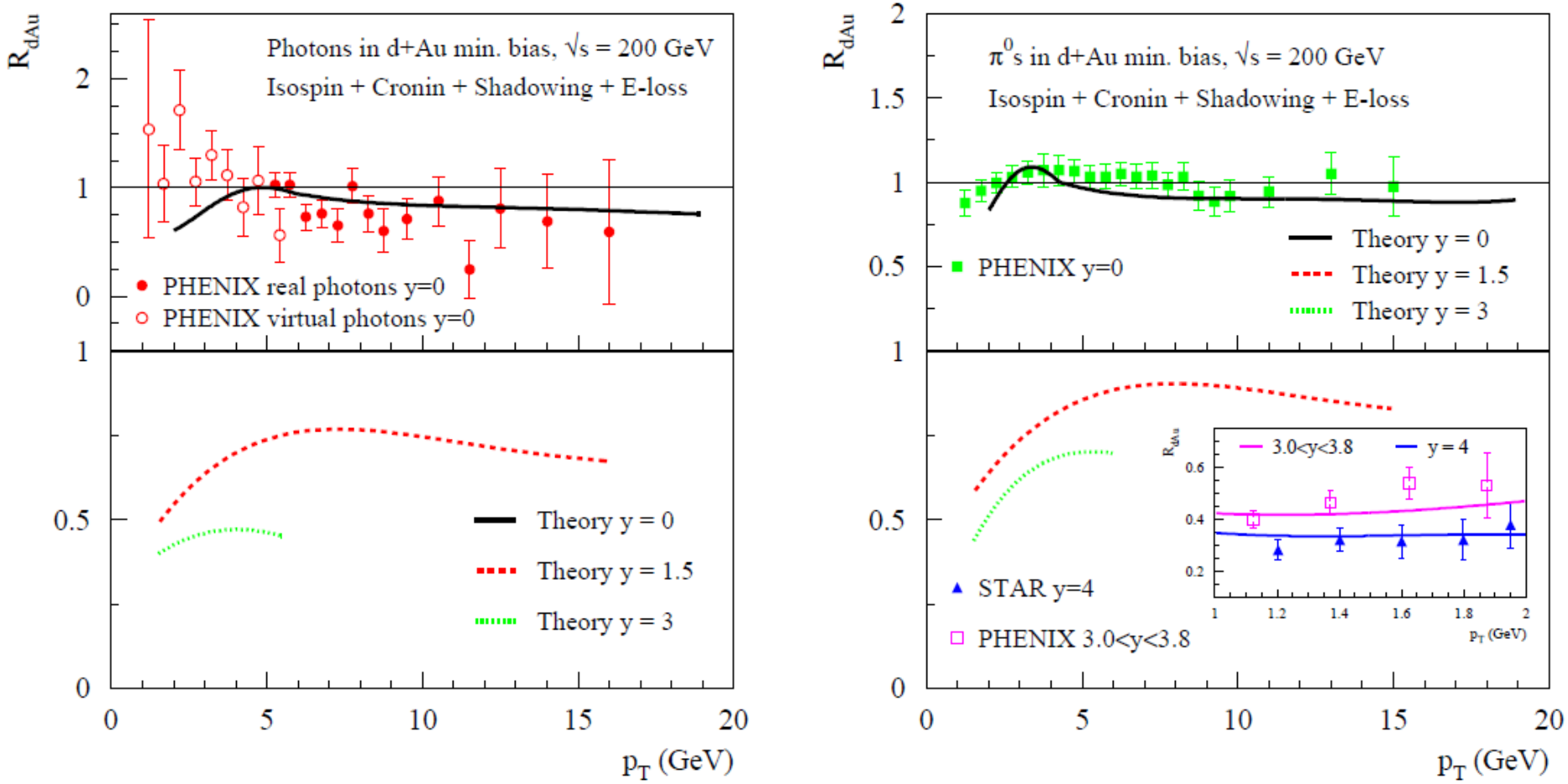


Work well at central and forward rapidities for both photon and hadron.

# Nuclear modification at LHC

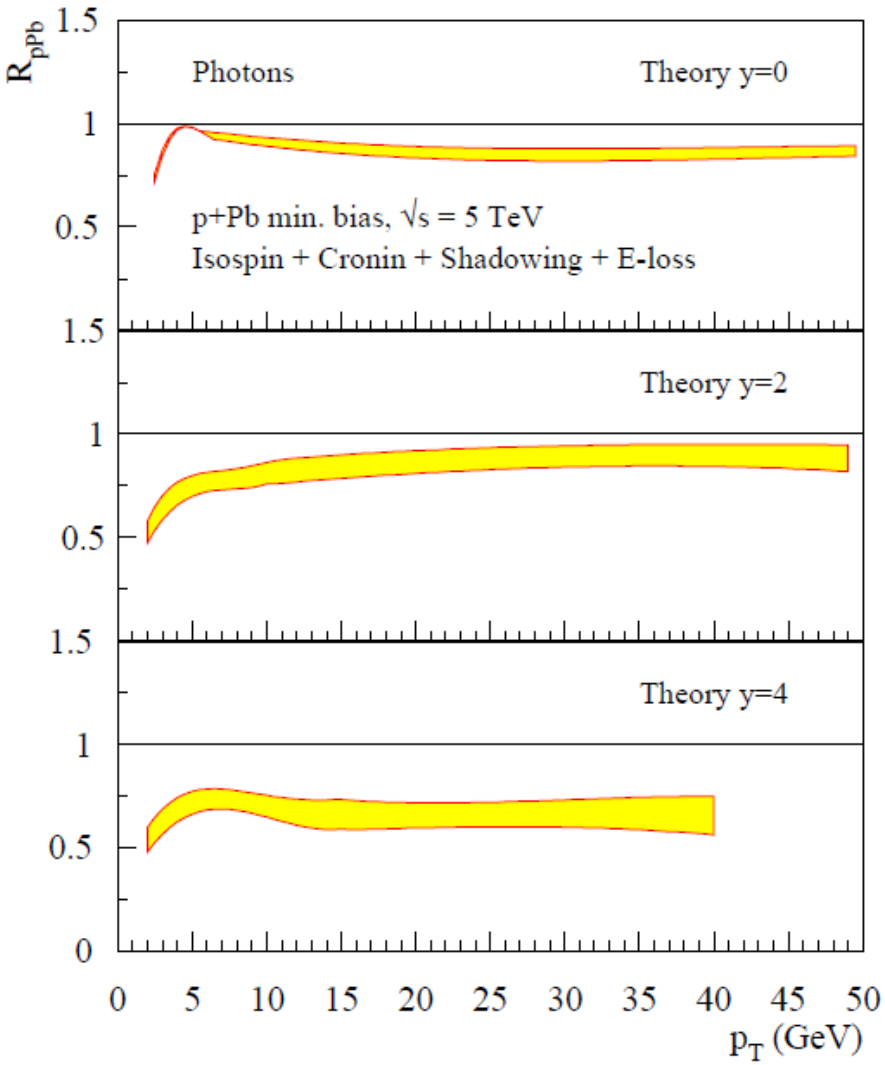


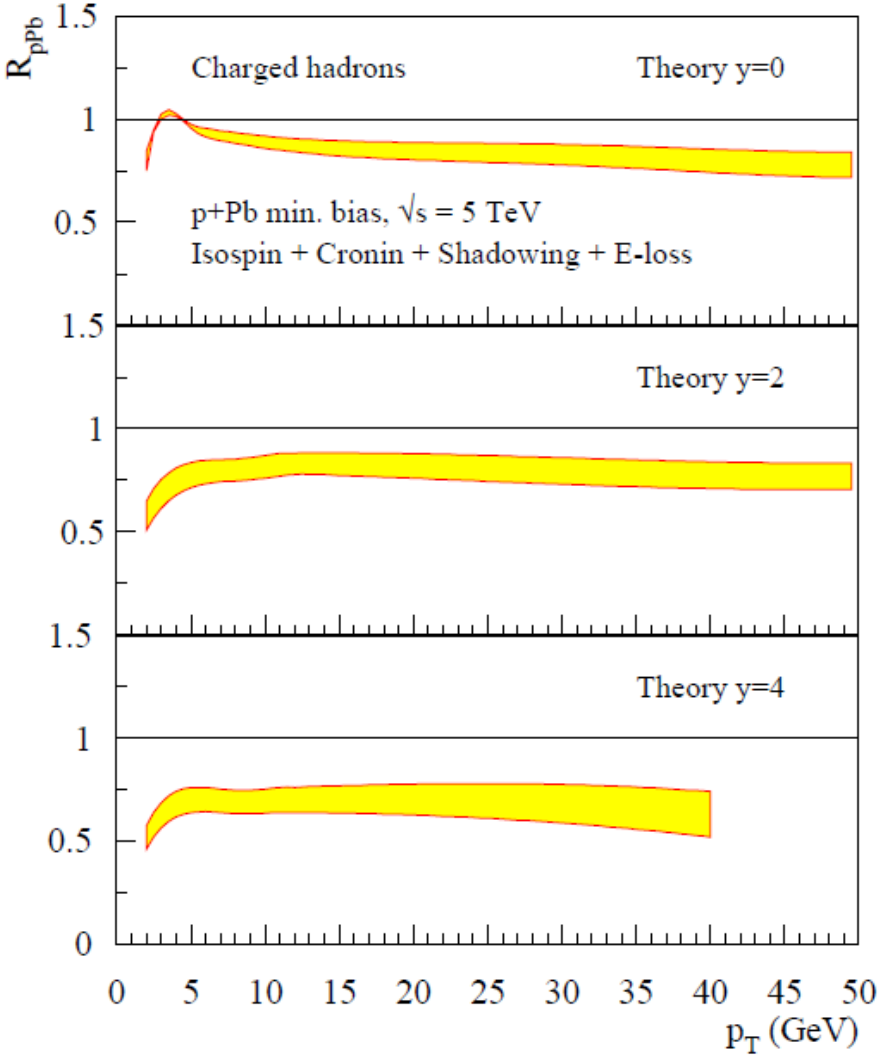

# Comparison with the latest ALICE data

- reasonable agreement: larger energy loss effect at high pt

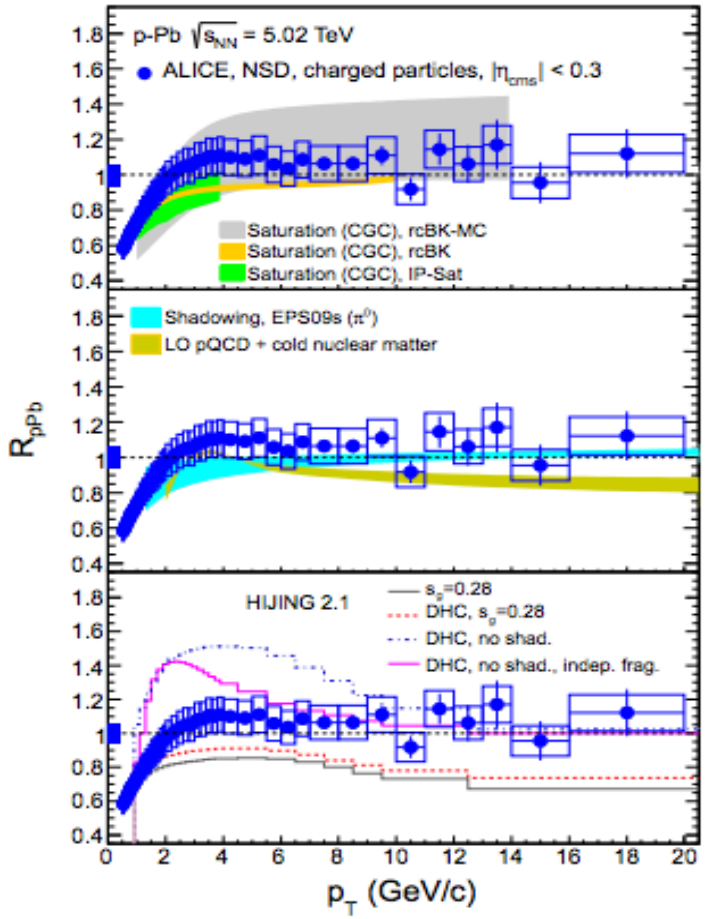


- So far we are the only model with energy loss: these new data help us to constrain energy loss much better

# Several final comments

- What about the low pt and low mass dilepton (photon) data? Is it possible to understand (at least partially) the large excess?
  - Initial state multiple scattering leads to enhancement for low mass dilepton

Qiu, Zhang, PLB, 2002

$$R_{AB}(Q) \approx \frac{4\pi^2\alpha_s}{3Q^2}\lambda^2 \times \frac{\sum_q e_q^2 \int dy \left\{A^{1/3}\left[2\,\phi_{q/N}(x) - x\frac{\partial}{\partial x}\phi_{q/N}(x)\right]\phi_{\bar{q}/N}(x') + B^{1/3}[x \leftrightarrow x']\right\}}{\sum_q e_q^2 \int dy\, \phi_{q/N}(x)\,\phi_{\bar{q}/N}(x')}$$

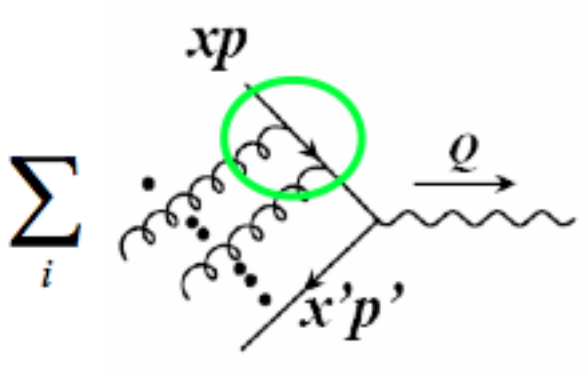


$$\lambda^2 = 0.01\mathrm{GeV}^2$$

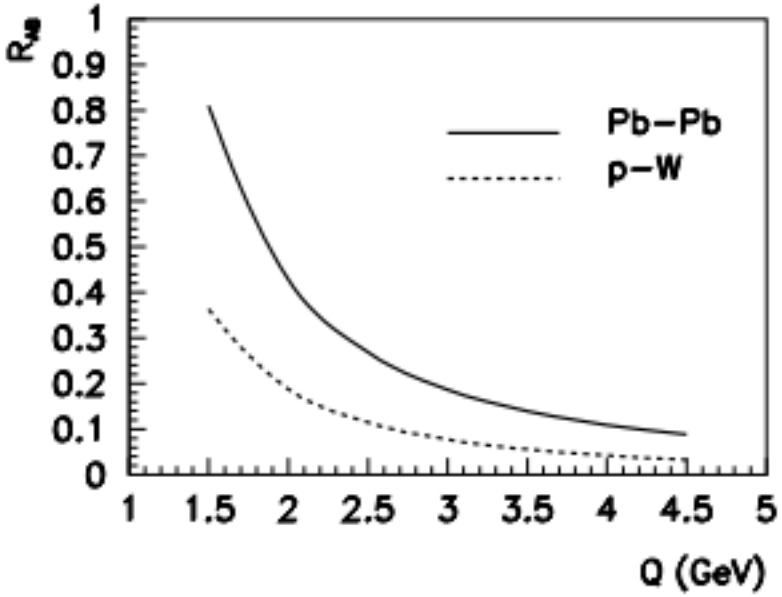

# Also an enhancement for low pt photon

- Initial state multiple scattering to direct photon production also leads to an enhancement at low pt (70-90%)

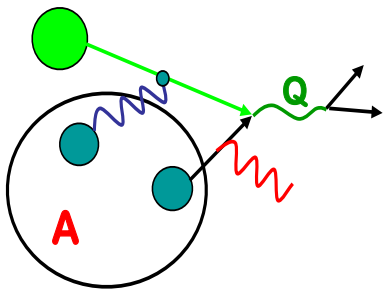


Kang-Qiu-Vogelsang, PRD, NPA, 2009

$$\lambda^2 = 0.01\mathrm{GeV}^2$$

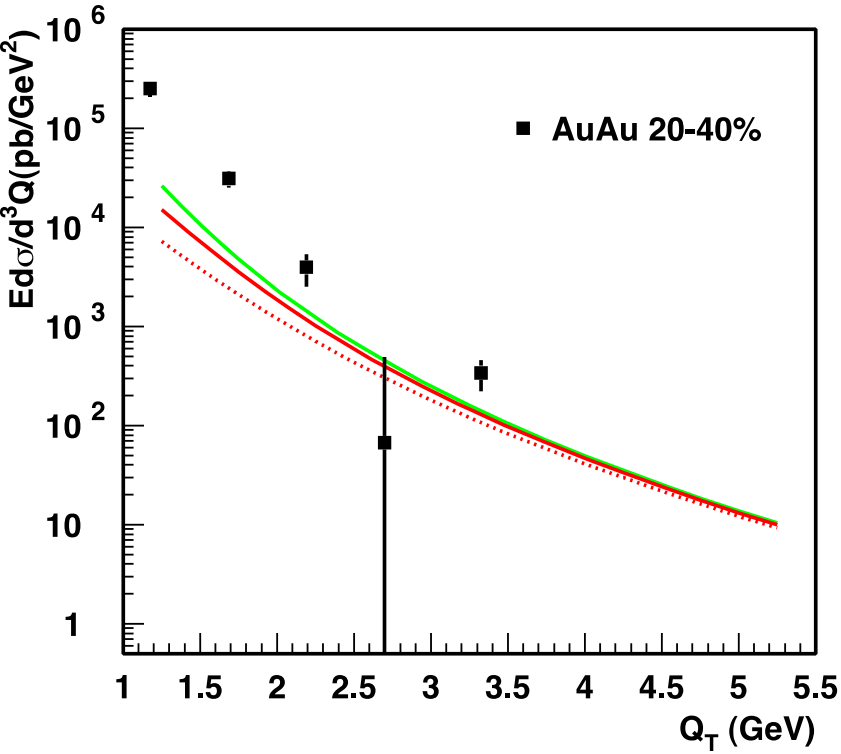


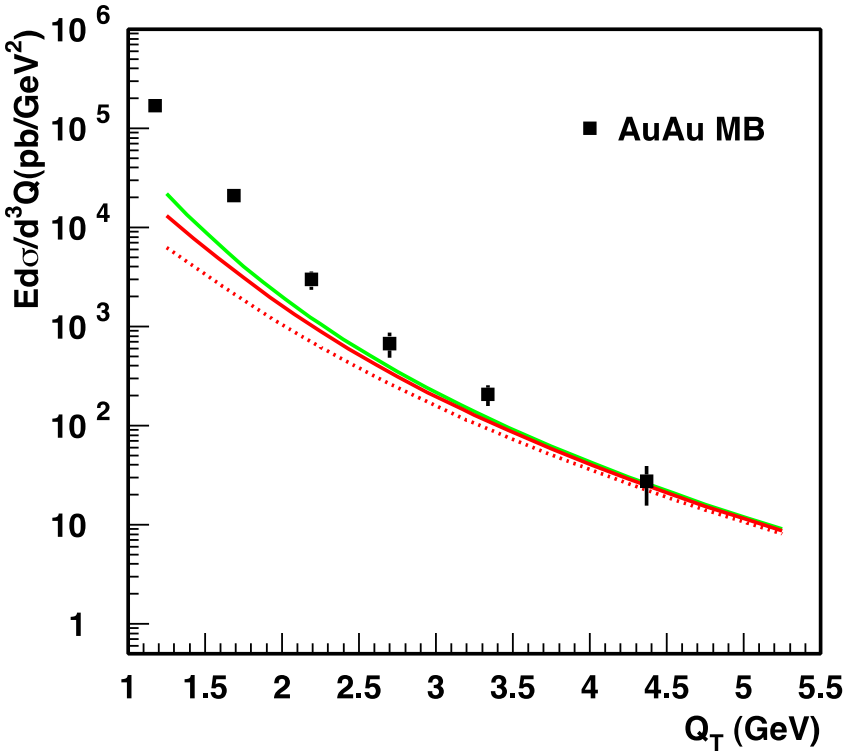

# Comments

- The old $\lambda^2 = 0.01\mathrm{GeV}^2$ was extracted from transverse momentum broadening Drell-Yan data at Fermilab (very old data, also low energy). This parameter is much smaller than those constrained from RHIC data by 3-4 times $\xi^2 = 0.12\mathrm{GeV}^2$

$$\xi^2 = \frac{4\pi^2}{N_c}\lambda^2$$

- If add this new contribution to the A+A cross section, it leads to about 3 times enhancement at A+A collisions. Certainly not be able to describe the PHENIX data (~30 times enhancement)
  - The remaining is thermal photons?

# Summary

- There are different approaches to incorporate various cold nuclear matter effects
- We clarified a mis-match in a usual widely used CGC formalism for photon production, by providing a formalism in MS-bar scheme
- Based on a pQCD formalism, we incorporate so far the Cronin, shadowing, parton energy loss, which give a good description of RHIC and LHC data: parton energy loss should be further constrained
- Initial-state multiple scattering could indeed lead to enhancement at low mass and low pt. This might not be enough to explain the observed ~30 times enhancement
- Looking forward to the LHC data on both p+A and A+A for low mass lepton pair

THERMAL RADIATION WORKSHOP (2012)

RIKEN BNL Research Center Workshop
December 5-7, 2012 at Brookhaven National Laboratory

# Probing hot QCD matter with dileptons using PHSD aproach

Olena Linnyk

HIC for FAIR

JUSTUS-LIEBIG-UNIVERSITÄT GIESSEN

PHSD

# Big Bang vs. Little Bang

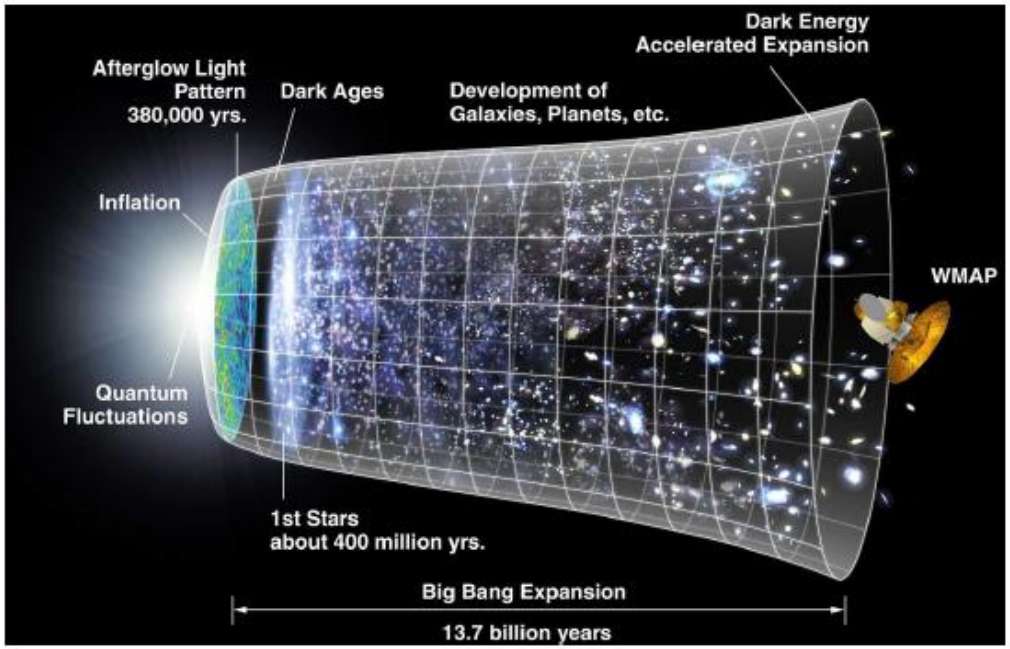


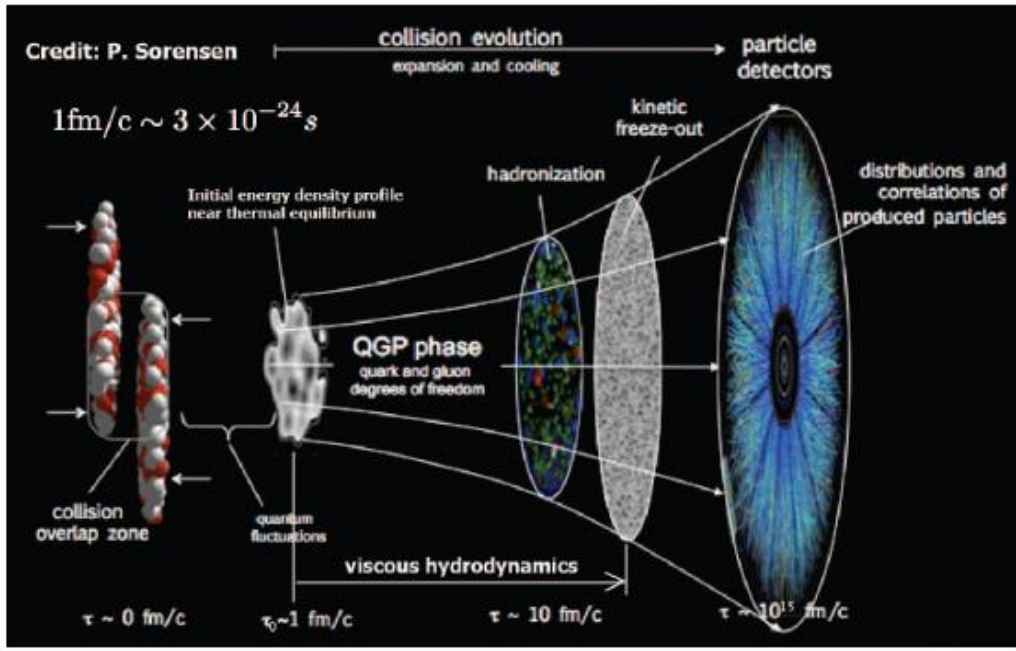


**Similarities:** Hubble-like expansion, expansion-driven dynamical freeze-out
chemical freeze-out (nucleo-/hadrosynthesis) before thermal freeze-out (CMB, hadron $p_T$-spectra)
initial-state quantum fluctuations imprinted on final state

**Can we go back in time ?**

**Differences:** Expansion rates differ by 18 orders of magnitude
Expansion in 3d, not 4d; driven by pressure gradients, not gravity
Time scales measured in fm/$c$ rather than billions of years
Distances measured in fm rather than light years

# ‚Little Bangs' in the Laboratory

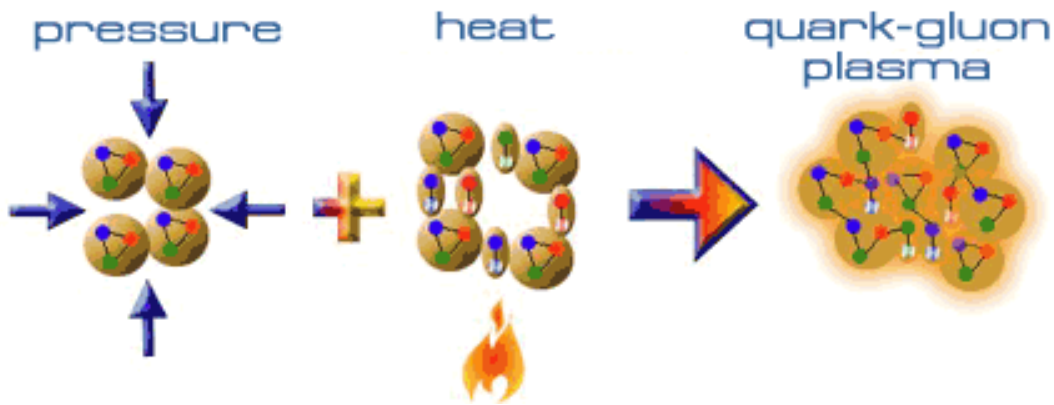


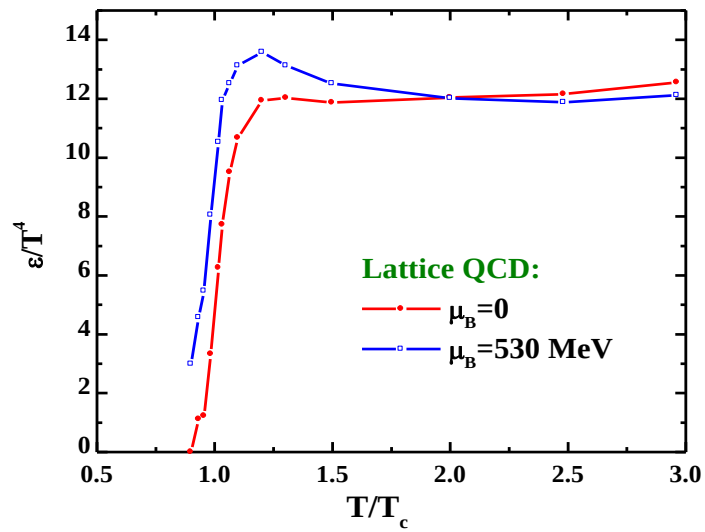


Z. Fodor et al., PLB 568 (2003) 73

Initial State

Hadronization

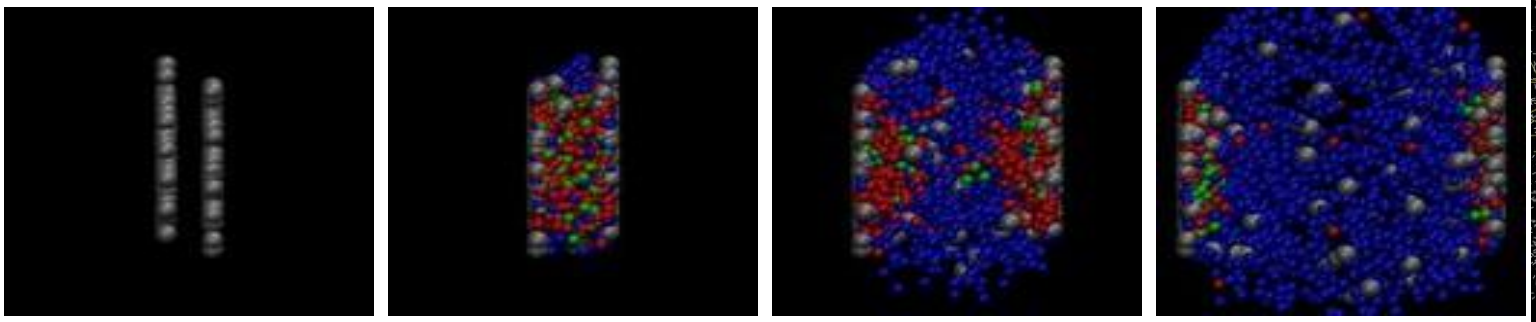

Au Au

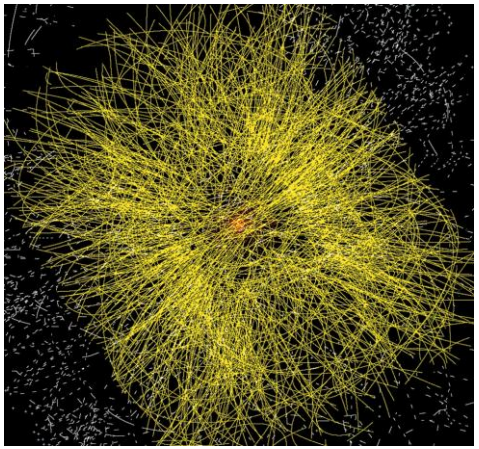

Equilibrium QGP?

hadrons → quarks and gluons → hadrons

# Dileptons in heavy ions

- Direct dilepton radiation from QGP

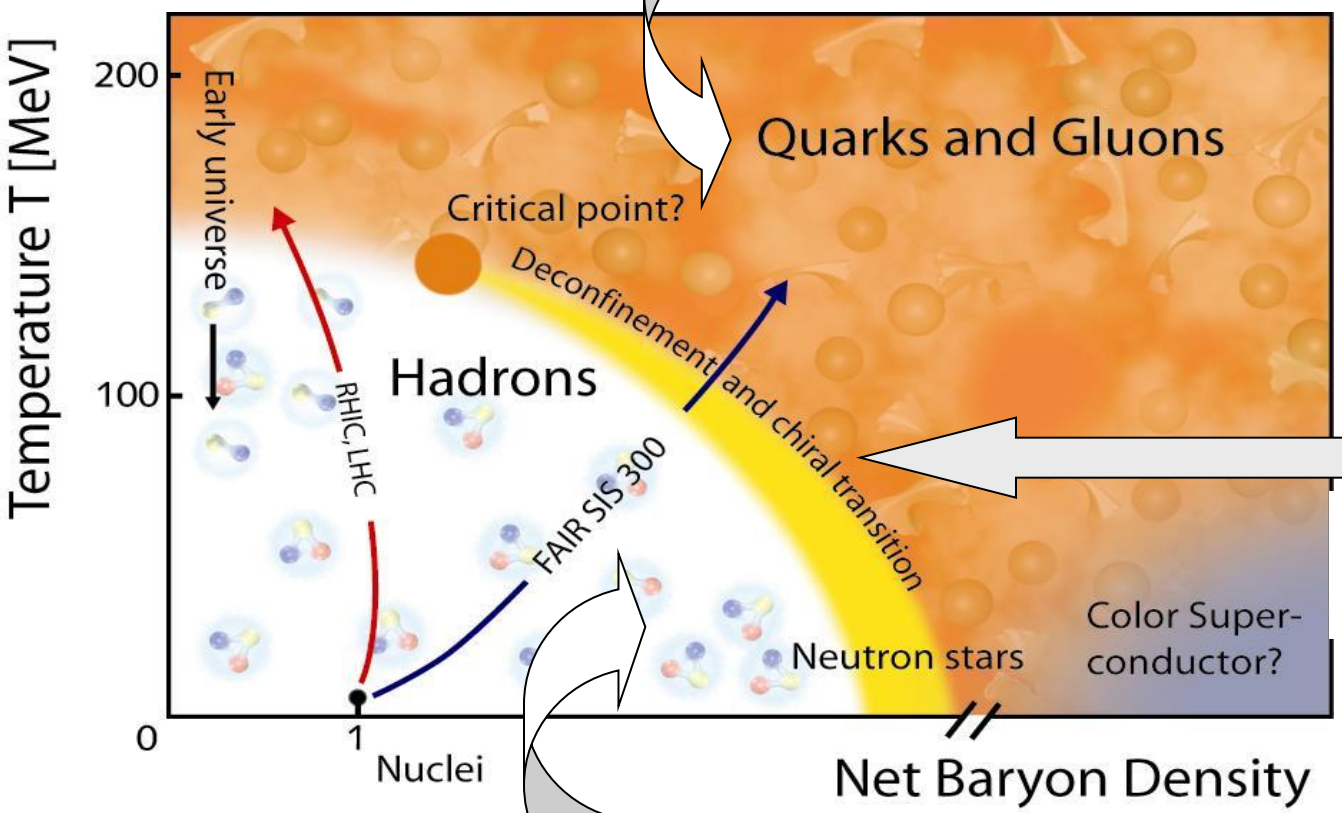


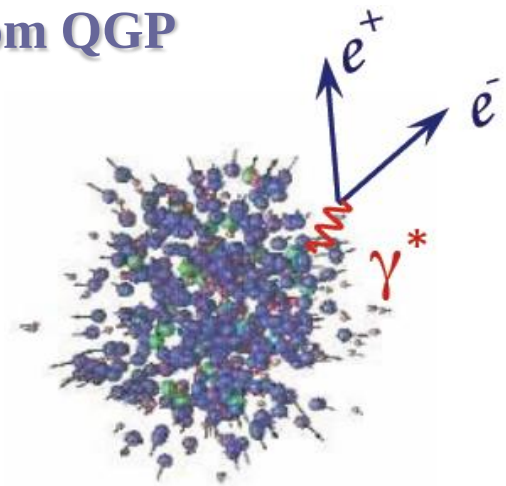


- In-medium modification of meson properties

- Secondary hadronic sources (meson-meson and multi-meson interactions)

# Parton-Hadron-String Dynamics

**Main goal – description of heavy-ion collisions and properties of matter at high temperature and density as well as of p+p and p(d)+A reactions.**

- ✓ **Unified description of collisions at all energies from AGS to LHC.**
- ✓ **Non-equilibrium: applicable to far from equilibrium configurations as explosion-like heavy-ion collisions as well as to equilibrated matter („in the box“).**
- ✓ **Universal: dileptons, charm, flow (v1, v2, v3, v4), chiral magnetic effect, spin, …**
- ✓ **Dynamics: mean fields (hadronic and partonic), scattering (elastic, inelastic, 2<–>2, 2<–>n), resonance decays, retarded electro-magnetic fields.**
- ✓ **Microscopic phase transition (cross over) according to the lattice QCD equation of state, hadronic and partonic degrees of freedom, spacial co-existance, dynamical hadronisation.**
- ✓ **Off-shell transport: takes into account 2-particle correlations beyond the one-particle distributions.**

# Goal: microscopic transport description of the partonic and hadronic phase

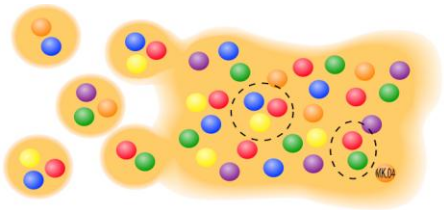

**Problems:**

- **How to model a QGP phase in line with lQCD data?**
- **How to solve the hadronization problem?**

**Ways to go:**

**pQCD based models:**

- **QGP phase: pQCD cascade**
- **hadronization: quark coalescence**

➔ **BAMPS, AMPT, HIJING**

**‚Hybrid' models:**

- **QGP phase: hydro with QGP EoS**
- **hadronic freeze-out: after burner**

**- hadron-string transport model**

➔ **Hybrid-UrQMD**

- **microscopic transport description of the partonic and hadronic phase in terms of strongly interacting dynamical quasi-particles and off-shell hadrons**

➔ **PHSD**

# DQPM Lattice QCD –> The Dynamical QuasiParticle Model (DQPM)

**Quasiparticle properties:**

- **large width and mass for gluons and quarks**

**Lorentzian spectral function, HTL limit at high T**

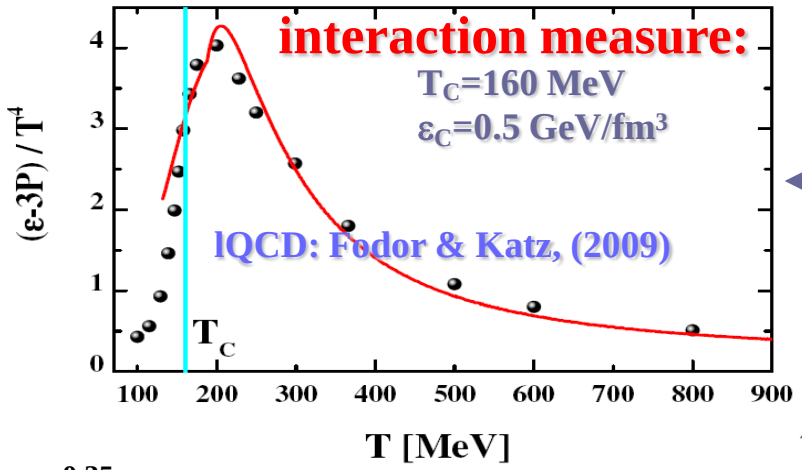


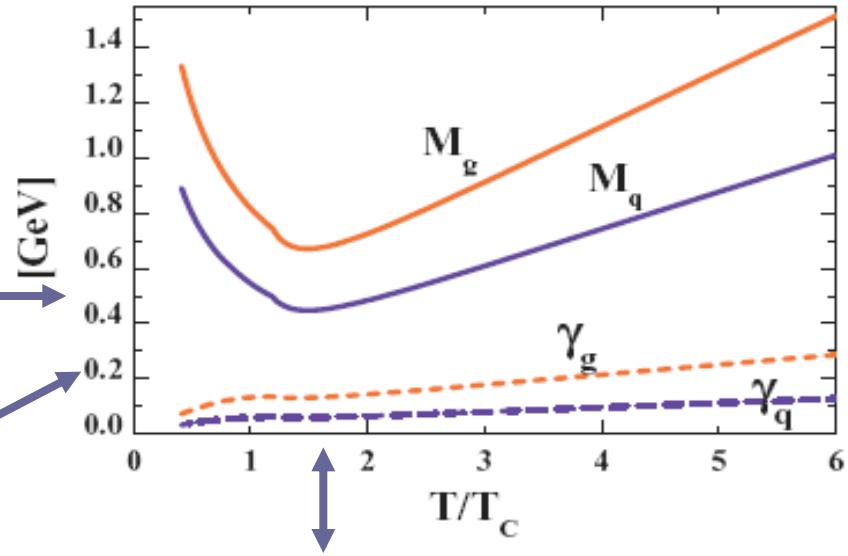


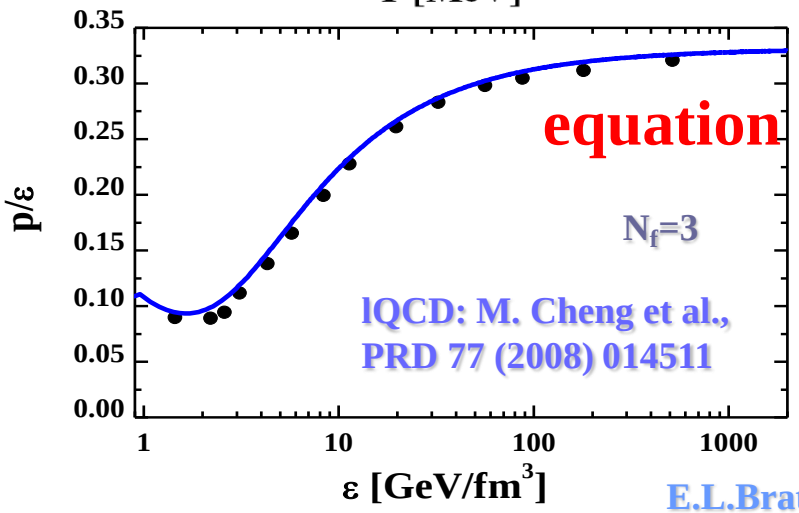


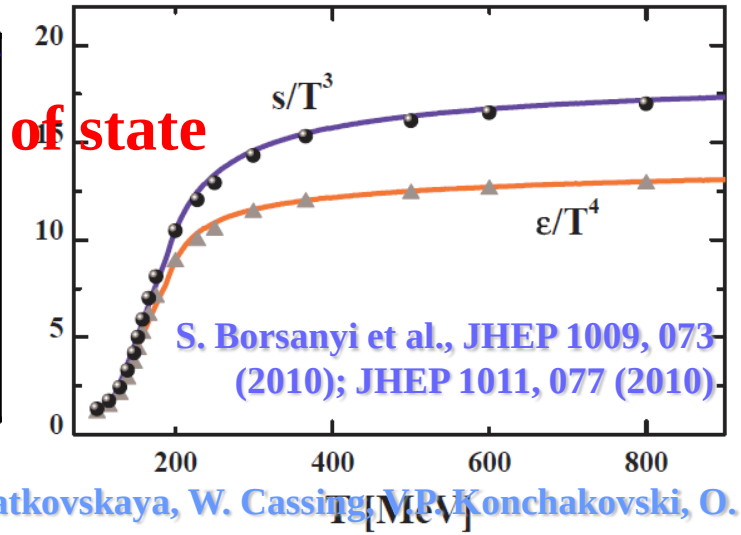


E.L.Bratkovskaya, W. Cassing, V.P.Konchakovski, O. Linnyk, NPA856 (2011) 162

# Boltzmann equation –> off-shell transport

$$\left(\frac{\partial}{\partial t} + \vec{v}_1 \cdot \nabla_{\vec{r}} + \frac{\vec{K}}{m} \cdot \nabla_{\vec{v}_1}\right) f_1 = \int d\Omega \int d\vec{v}_2\, \sigma(\Omega) |\vec{v}_1 - \vec{v}_2| \left(f_1' f_2' - f_1 f_2\right)$$

**GENERALIZATION**

**(First order gradient expansion of the Wigner-transformed Kadanoff-Baym equations)**

drift term — Vlasov term — backflow term — collision term = ‚loss' term - ‚gain' term

$$\diamond\{P^2 - M_0^2 - Re\Sigma^{ret}_{XP}\}\{S^<_{XP}\} - \diamond\{\Sigma^<_{XP}\}\{ReS^{ret}_{XP}\} = \frac{i}{2}\left[\Sigma^>_{XP} S^<_{XP} - \Sigma^<_{XP} S^>_{XP}\right]$$

**Backflow term incorporates the off-shell behavior in the particle propagation**
**! vanishes in the quasiparticle limit $A_{XP} = 2\pi\,\delta(p^2-M^2)$**

**Propagation of the Green's function $iS^<_{XP}=A_{XP}N_{XP}$, which carries information not only on the number of particles, but also on their properties, interactions and correlations**

$$A_{XP} = \frac{\Gamma_{XP}}{(P^2 - M_0^2 - Re\Sigma^{ret}_{XP})^2 + \Gamma^2_{XP}/4}$$

$$\diamond\{F_1\}\{F_2\} := \frac{1}{2}\left(\frac{\partial F_1}{\partial X_\mu}\frac{\partial F_2}{\partial P^\mu} - \frac{\partial F_1}{\partial P_\mu}\frac{\partial F_2}{\partial X^\mu}\right)$$

$\Gamma_{XP}$ – **width of spectral function = reaction rate of a particle (at phase-space position XP)**

W. Cassing , S. Juchem, NPA 665 (2000) 377; 672 (2000) 417; 677 (2000) 4451

# Off-shell propagation

**The off-shell spectral function becomes on-shell in the vacuum dynamically!**

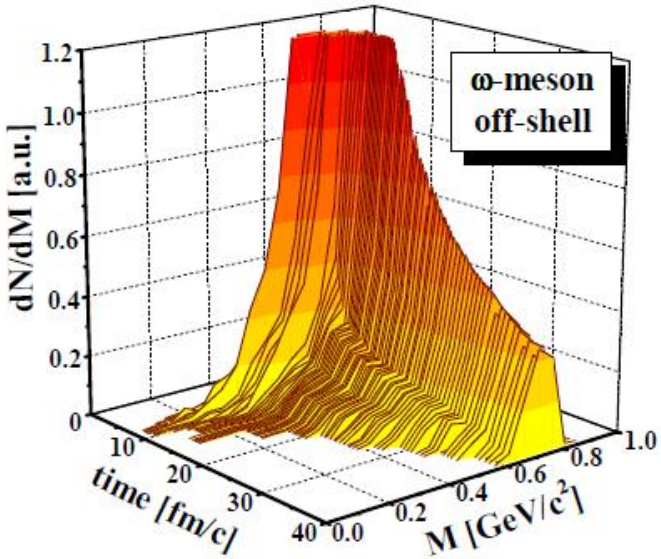


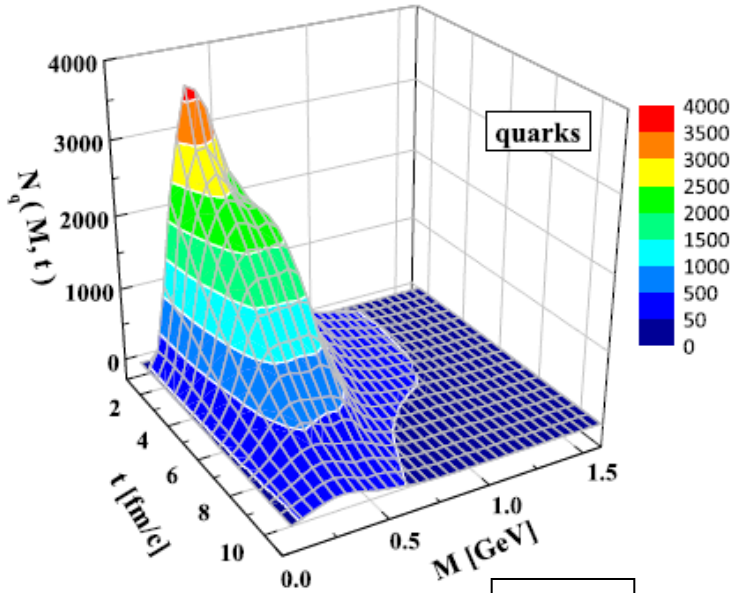


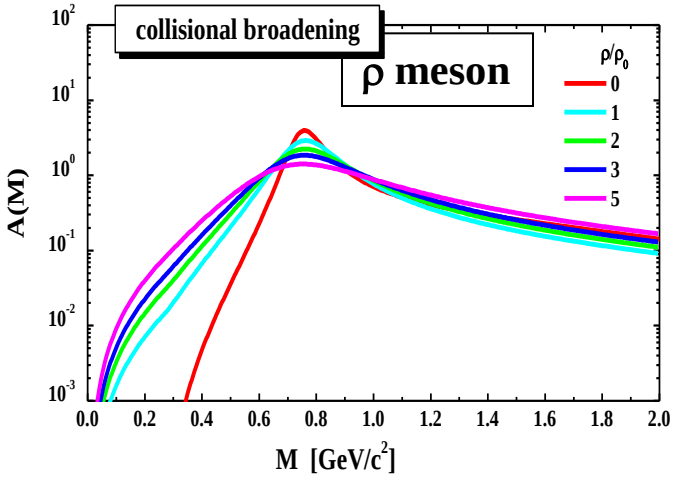


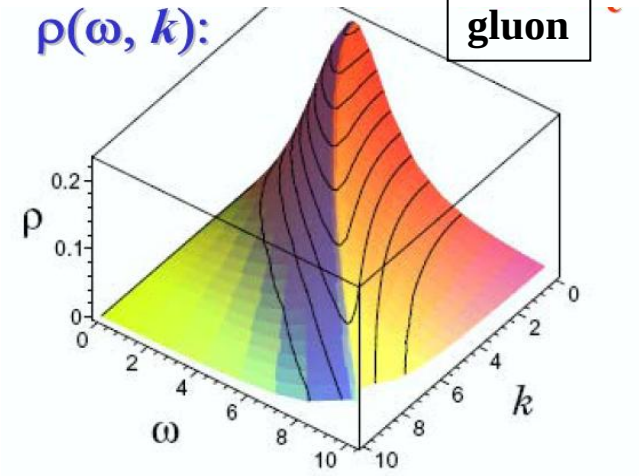


E.L. Bratkovskaya, W. Cassing, V. P. Konchakovski, O. Linnyk, NPA856(2011) 162; E.L. Bratkovskaya, W. Cassing, NPA 807 (2008) 214;

# Off-shell equations of motion

**Employ testparticle Ansatz for the real valued quantity *i* $S^{<}_{XP}$ -**

$$F_{XP} = A_{XP} N_{XP} = i\, S^{<}_{XP} \sim \sum_{i=1}^{N} \delta^{(3)}(\vec{X} - \vec{X}_i(t))\ \delta^{(3)}(\vec{P} - \vec{P}_i(t))\ \delta(P_0 - \epsilon_i(t))$$

**insert in generalized transport equations and determine equations of motion !**

**General testparticle off-shell equations of motion:**

$$\frac{d\vec{X}_i}{dt} = \frac{1}{1-C_{(i)}} \frac{1}{2\epsilon_i} \left[ 2\,\vec{P}_i + \vec{\nabla}_{P_i} Re\Sigma^{ret}_{(i)} + \frac{\epsilon_i^2 - \vec{P}_i^2 - M_0^2 - Re\Sigma^{ret}_{(i)}}{\Gamma_{(i)}} \vec{\nabla}_{P_i} \Gamma_{(i)} \right],$$

$$\frac{d\vec{P}_i}{dt} = -\frac{1}{1-C_{(i)}} \frac{1}{2\epsilon_i} \left[ \vec{\nabla}_{X_i} Re\Sigma^{ret}_{i} + \frac{\epsilon_i^2 - \vec{P}_i^2 - M_0^2 - Re\Sigma^{ret}_{(i)}}{\Gamma_{(i)}} \vec{\nabla}_{X_i} \Gamma_{(i)} \right],$$

$$\frac{d\epsilon_i}{dt} = \frac{1}{1-C_{(i)}} \frac{1}{2\epsilon_i} \left[ \frac{\partial Re\Sigma^{ret}_{(i)}}{\partial t} + \frac{\epsilon_i^2 - \vec{P}_i^2 - M_0^2 - Re\Sigma^{ret}_{(i)}}{\Gamma_{(i)}} \frac{\partial \Gamma_{(i)}}{\partial t} \right],$$

with $F_{(i)} \equiv F(t, \vec{X}_i(t), \vec{P}_i(t), \epsilon_i(t))$

$$C_{(i)} = \frac{1}{2\epsilon_i} \left[ \frac{\partial}{\partial \epsilon_i} Re\Sigma^{ret}_{(i)} + \frac{\epsilon_i^2 - \vec{P}_i^2 - M_0^2 - Re\Sigma^{ret}_{(i)}}{\Gamma_{(i)}} \frac{\partial}{\partial \epsilon_i} \Gamma_{(i)} \right]$$

W. Cassing , S. Juchem, NPA 665 (2000) 377; 672 (2000) 417; 677 (2000) 445

# PHSD: hadronization

**Based on DQPM; massive, off-shell quarks and gluons with broad spectral functions hadronize to off-shell mesons and baryons:**

| | |
|---|---|
| gluons → q + qbar | q + qbar → meson |
| | q + q +q → baryon |

**Parton-parton recombination rate =**

$$\frac{dN_m(x,p)}{d^4x d^4p} = Tr_q Tr_{\bar{q}}\ \delta^4(p - p_q - p_{\bar{q}})\ \delta^4\left(\frac{x_q + x_{\bar{q}}}{2} - x\right)$$
$$\times \omega_q\ \rho_q(p_q)\ \omega_{\bar{q}}\ \rho_{\bar{q}}(p_{\bar{q}})\ |v_{q\bar{q}}|^2\ W_m(x_q - x_{\bar{q}}, p_q - p_{\bar{q}})$$
$$\times N_q(x_q, p_q)\ N_{\bar{q}}(x_{\bar{q}}, p_{\bar{q}})\ \delta(\text{flavor, color}). \qquad (7)$$

**$W_m$ - Gaussian in phase space with** $\sqrt{< r^2 >} = 0.66$ fm

**Hadronization happens when the effective interactions |v| become attractive, approx. for parton densities $1 < \rho_P < 2.2$ fm$^{-3}$ <= from DQPM**

W. Cassing, E.L. Bratkovskaya, PRC 78 (2008) 034919; W. Cassing, EPJ ST 168 (2009) 3

# Transport model simulation

- **Transport theory is the general basis for an understanding of nuclear dynamics on a microscopic level**

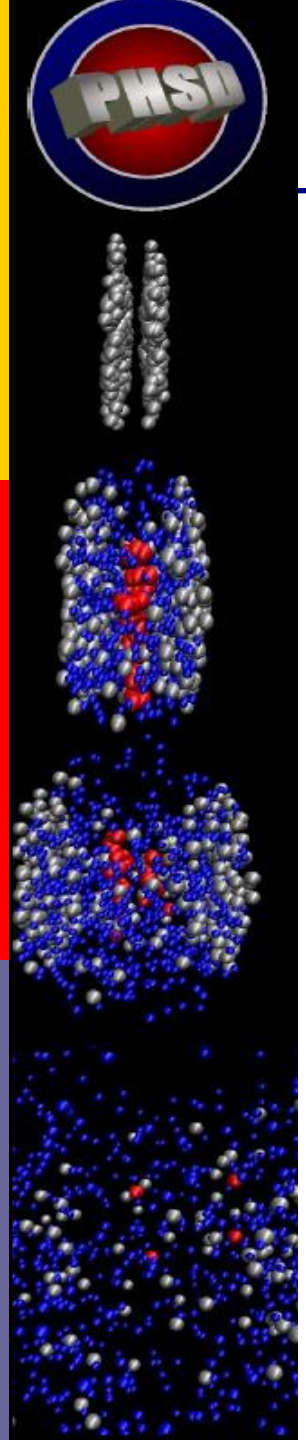

# Heavy-ion collision

**Initial A+A collisions:** string formation and decay to pre-hadrons

**Fragmentation** of pre-hadrons into quarks using the quark spectral functions from the Dynamical Quasi-Particle Model

**Partonic phase:** quarks and gluons with constituent mass and broad spectral functions defined by DQPM. **Elastic and inelastic parton-parton interactions**

- ✓ q + qbar <=> gluon <=> s + sbar
- ✓ gluon + gluon <=> gluon
- ✓ q + qbar (color neutral) <=> hadron resonances

**Hadronization:** massive, off-shell quarks and gluons with broad spectral functions hadronize to off-shell hadrons:

- ✓ gluons → q + qbar; q + qbar → off-shell meson or ‚string';
- ✓ q + q +q → baryon or ‚string';

**Hadronic phase:** hadron-hadron interaction, propagation and decays

W. Cassing, E. Bratkovskaya, PRC 78 (2008) 034919; NPA831 (2009) 215; EPJ ST 168 (2009) 3; NPA856 (2011) 162

# Dileptons

# Dileptons - an ideal probe to study the properties of the hot and dense medium

**Dilepton sources:**

**1) from the QGP via partonic (q,qbar, g) interactions:**

**2) from hadronic sources:**

- **direct decay of vector mesons (ρ,ω,ϕ,J/Ψ,Ψ‘)**
- **Dalitz decay of mesons and baryons ($\pi^0$,η, Δ,…)**
- **radiation from secondary meson interaction: p + p, p + r, p + w, r + r, p + a1**
- **correlated semi-leptonic decays of D- and B-mesons**

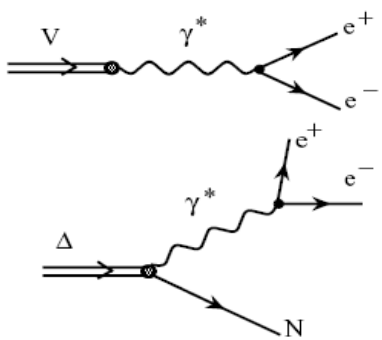


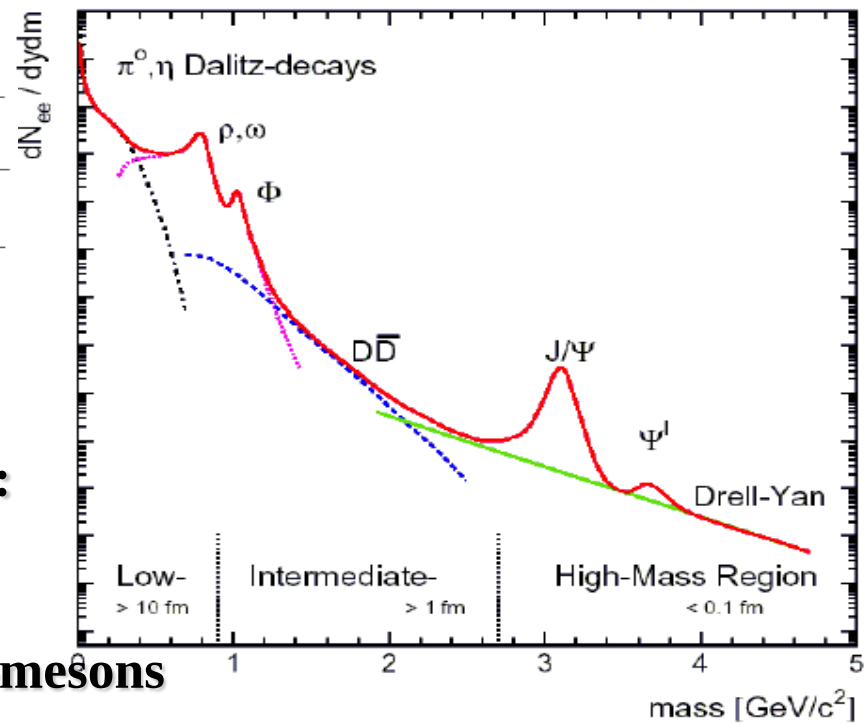

# Thermal rates in lattice QCD

**Dilepton sources:**

**partonic (q,qbar, g) interactions:**

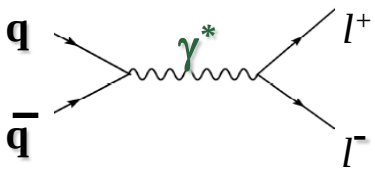


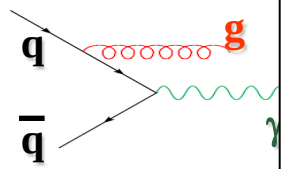


**Qualitative agreement between dynamical quasiparticels, lQCD, HTL**

**Quantitative comparison – work in progress (calculations ‚in the box‘)**

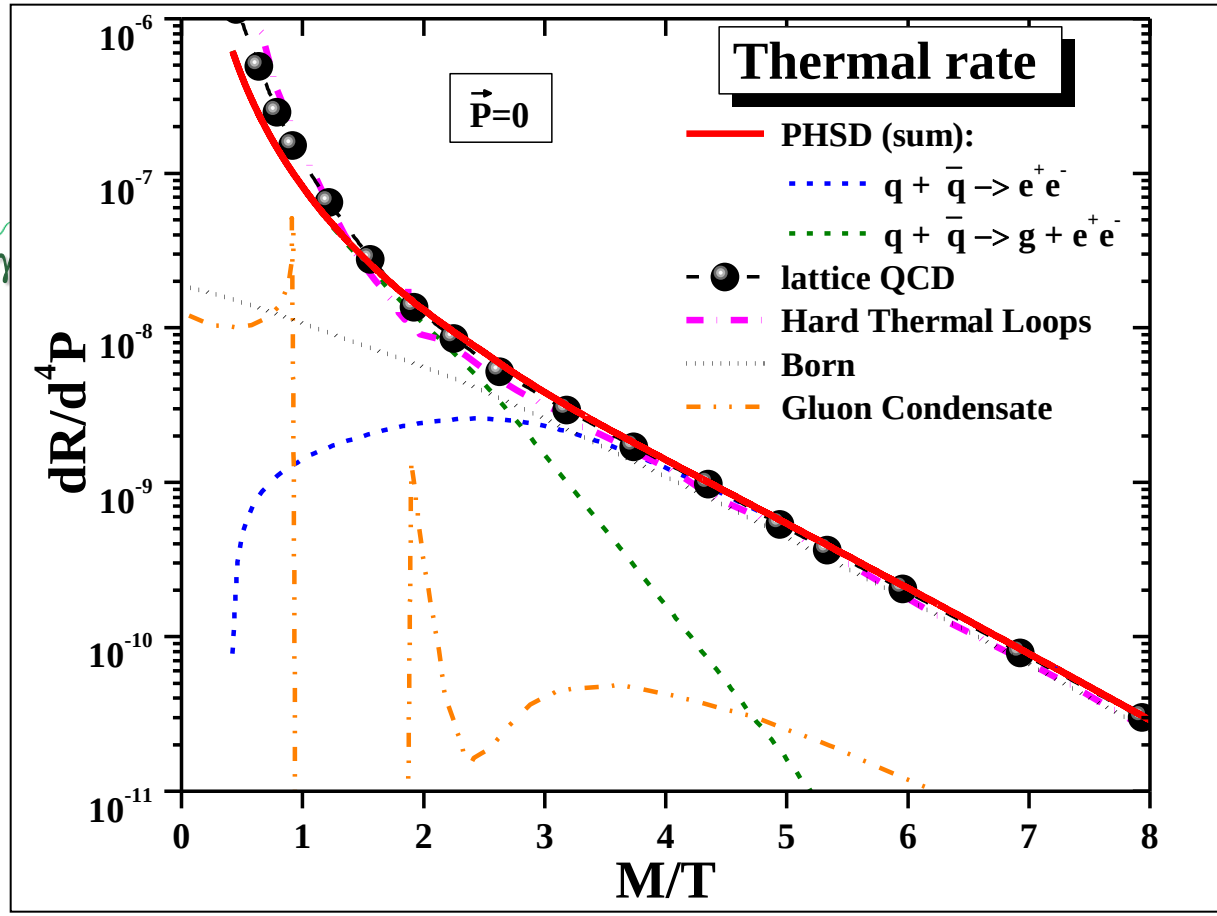

# NA60: sQGP shines already at SPS

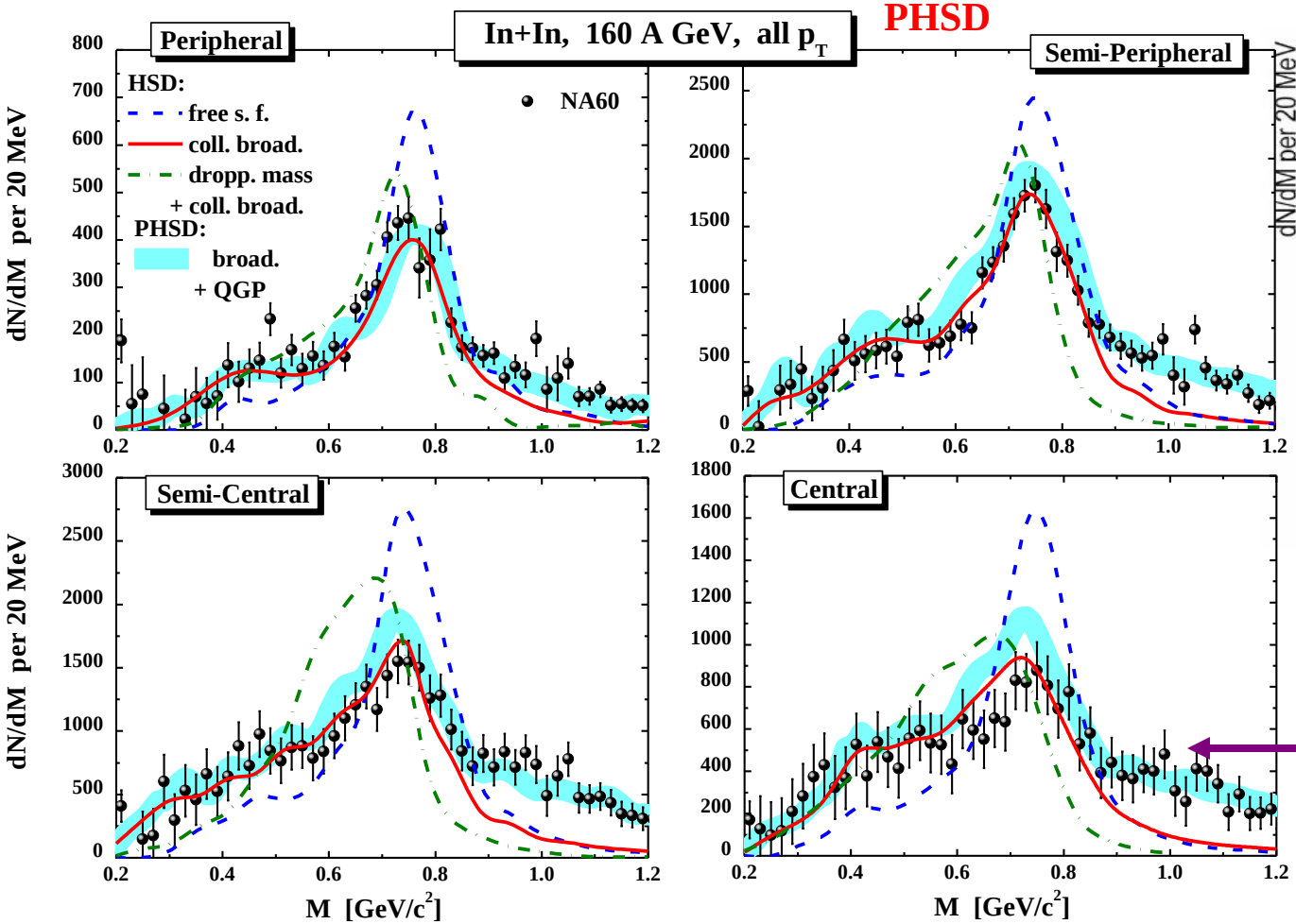


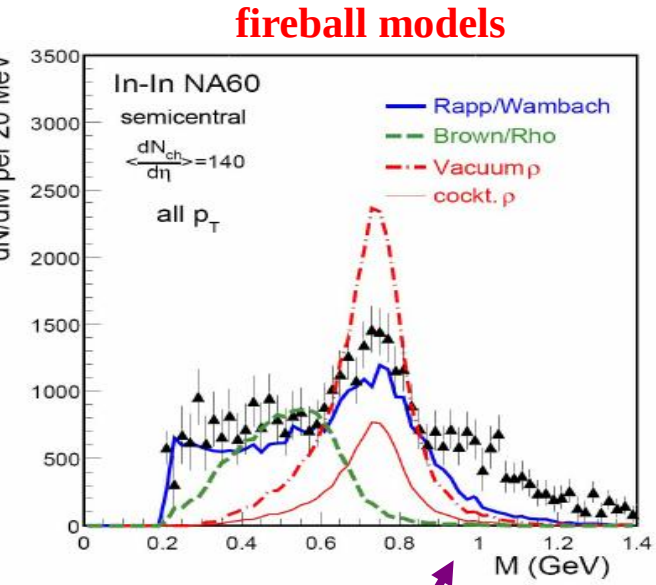


**M>1 GeV dominated by QGP**

**NA60 data at low M are well described by an in-medium scenario with collisional broadening**

**Dilepton spectra at low energies (CERES, HELIOS-3, DLS and HADES) show similar in-medium modification of vector mesons**

E. Bratkovskaya, W. Cassing, O. Linnyk, PLB 670 (2009) 428

# Dileptons at SPS: NA60

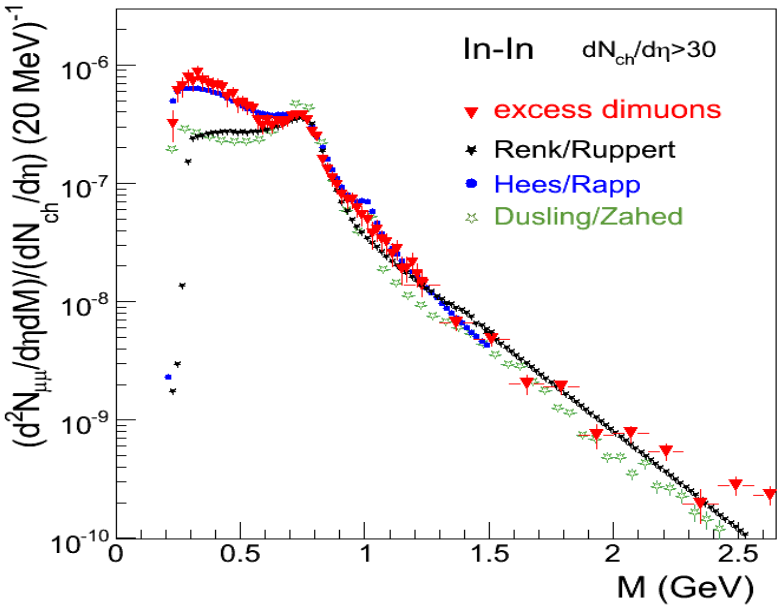


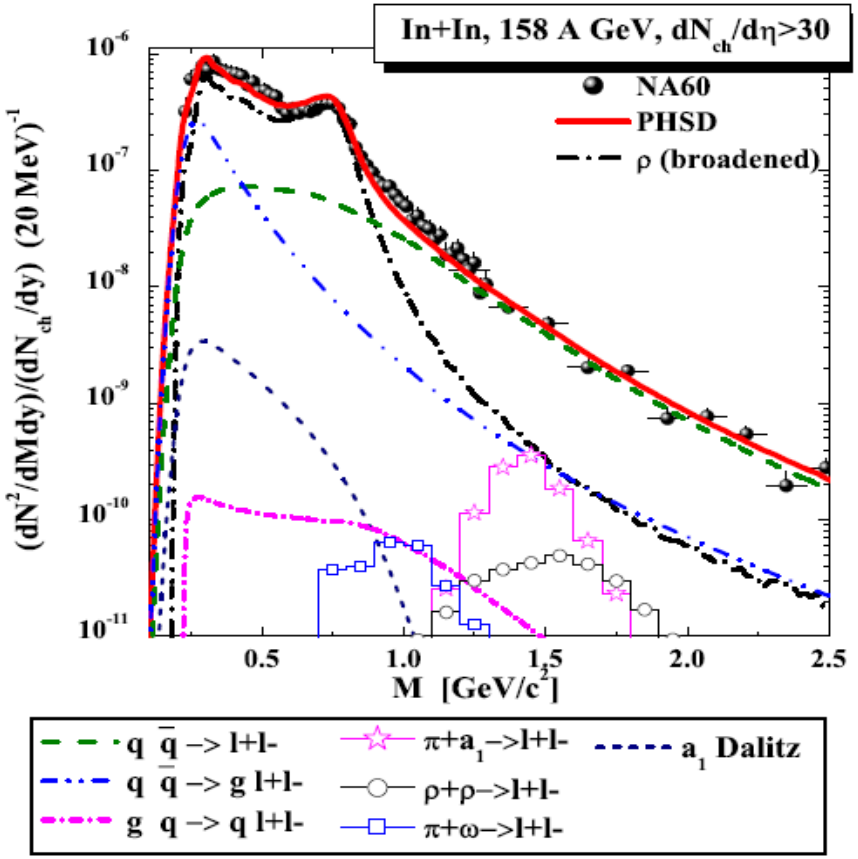


**Fireball model – Renk/Ruppert**

**Fireball model – Rapp/vanHees**

**Hydro model – Dusling/Zahed**

**Parton-Hadron-String-Dynamics microscopic transport model - PHSD**

**➔ good agreement with data in shape and absolute yield**

- **Mass region above 1 GeV is dominated by partonic radiation**
- **Contributions of "4π" channels (radiation from multi-meson reactions) are small**

O. Linnyk, E. Bratkovskaya, V. Ozvenchuk, W. Cassing and C.M. Ko, PRC 84 (2011) 054917, O. Linnyk, J.Phys.G38 (2011) 025105, NA60 Collaboration, Eur. Phys. J. C 59 (2009) 607; CERN Courier 11/2009

# Teff for M>1GeV: theoretical models

**Hadronic sources** $(2\pi+4\pi+a_1\pi)$

- continuous rise of $T_{eff}$ ;
- no discontinuity at M=1 GeV or at any other mass

→**Partonic dominance** at M>1 GeV

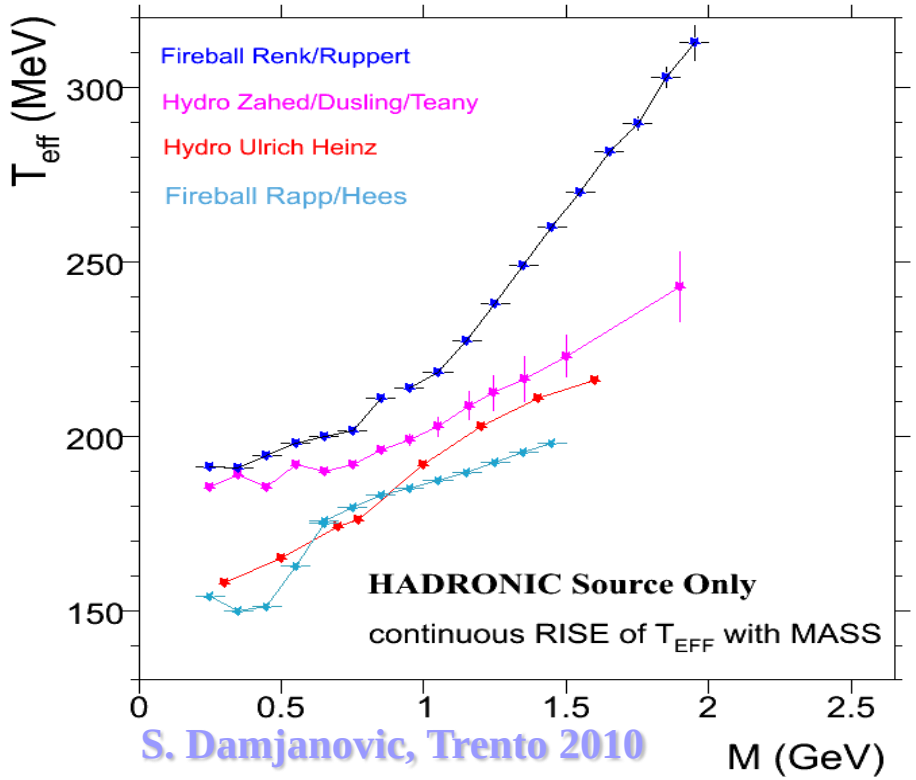


S. Damjanovic, Trento 2010

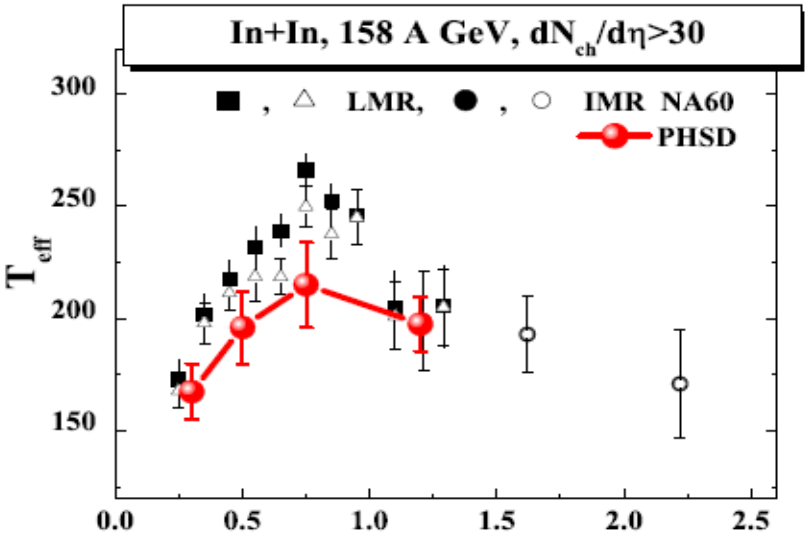


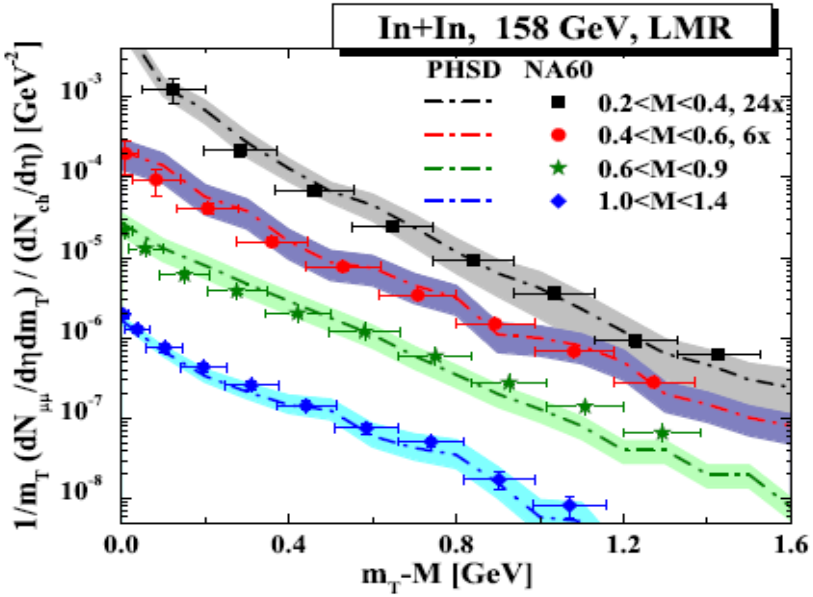


O. Linnyk, E. Bratkovskaya, V. Ozvenchuk, W. Cassing and C.M. Ko, PRC 84 (2011) 054917

# NA60: differential spectrum

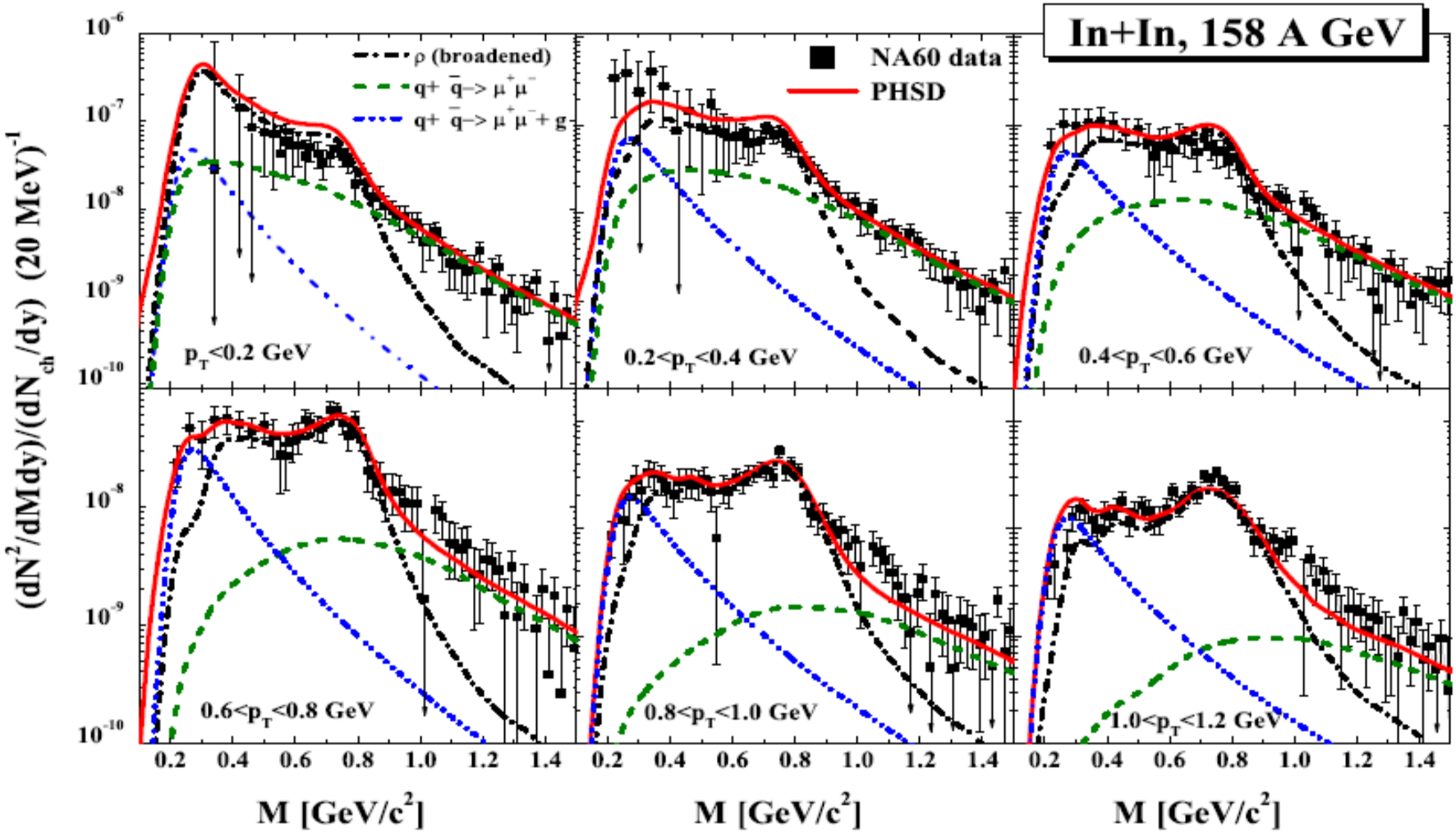


**Parton dominance at M>1 GeV and rho broadening confirmed by the differencial data**

O. Linnyk, E.Bratkovskaya, V. Ozvenchuk, W. Cassing and C.M. Ko, PRC 84 (2011) 054917

# NA60: differential spectrum

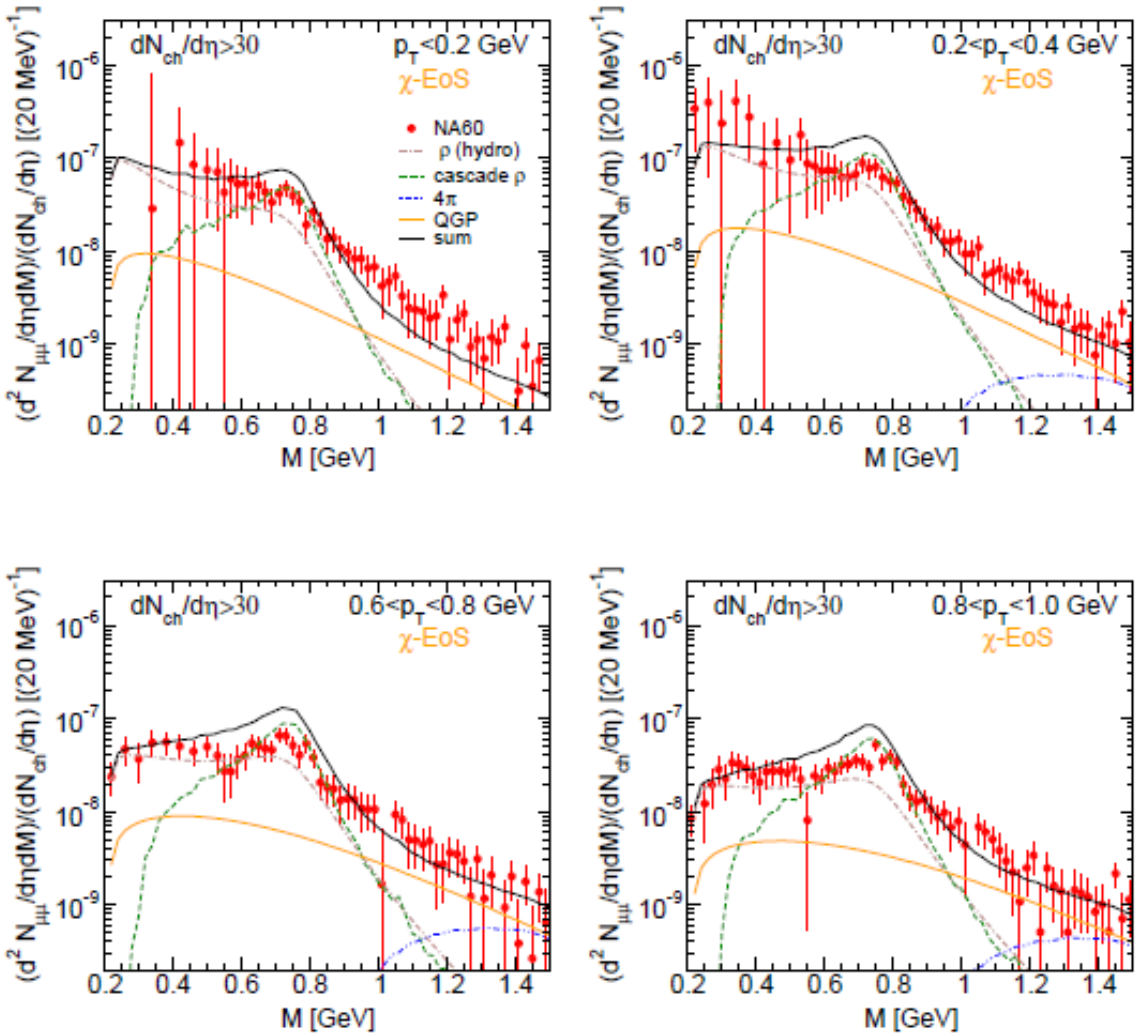


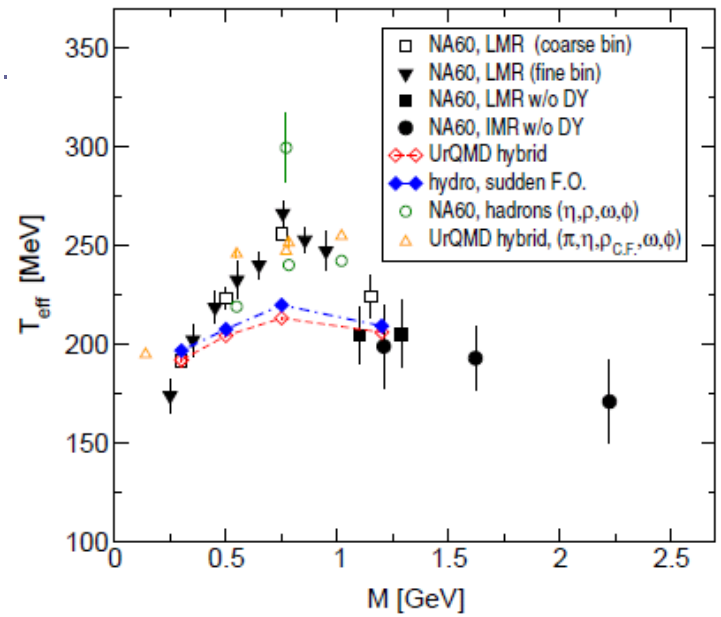


**Analogous conclusions in the hybrid hydro+UrQMD model**

E. Santini et al. Phys.Rev. C84 (2011) 014901

# Centrality dependent NA60 data

**PHSD predictions versus preliminary data**

**Dominant rho-channel at low and quark annihilation at intermediate masses !**

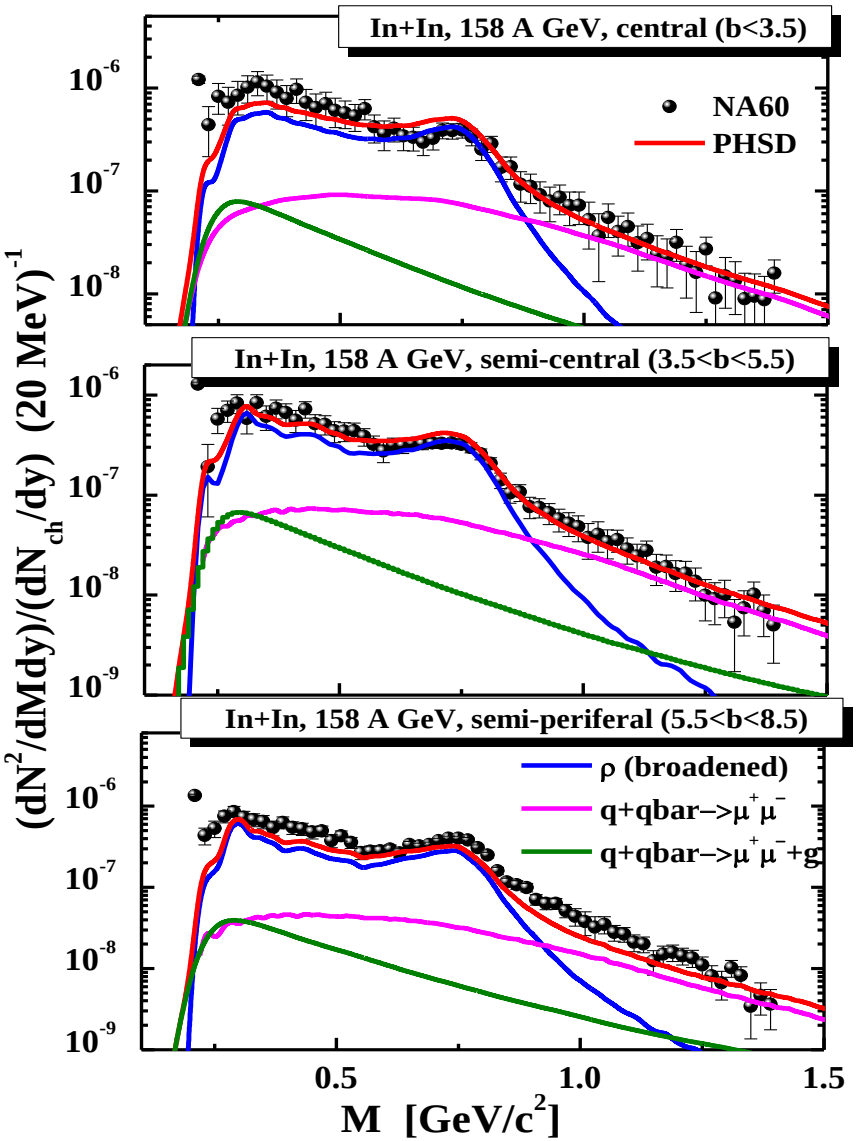


O. Linnyk, E. Bratkovskaya, V. Ozvenchuk, W. Cassing and C.M. Ko, PRC 84 (2011) 054917

# RHIC:Dileptons in pp and in heavy ions

**PHENIX: pp**

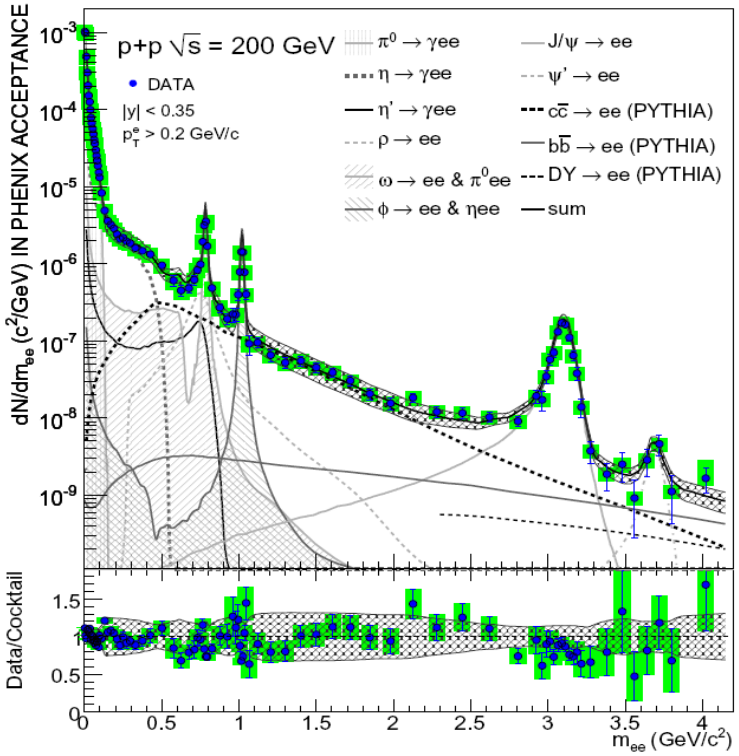


**PHENIX: Au+Au**

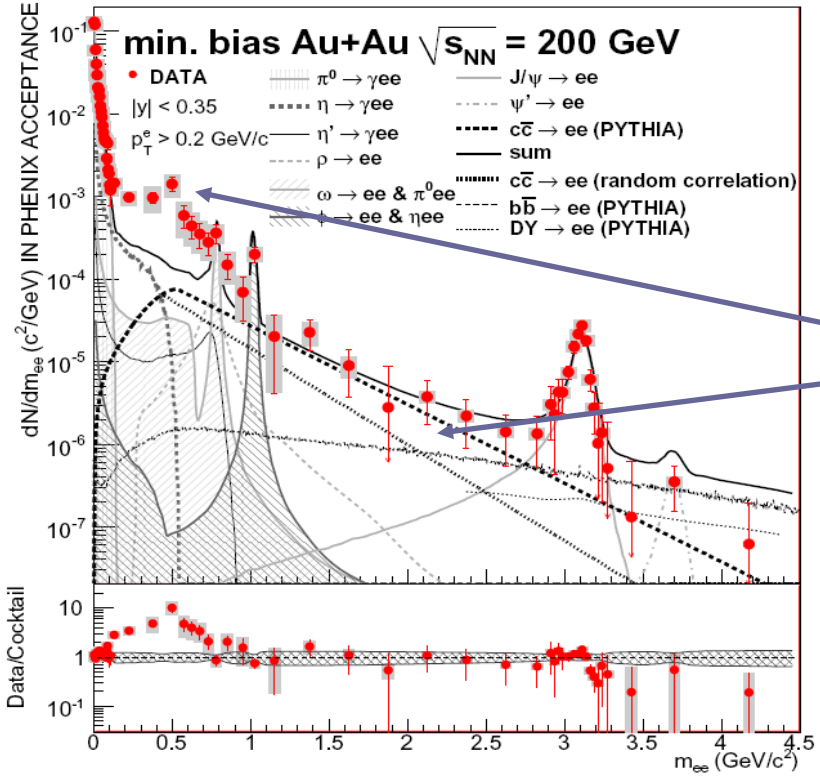


**‚excess'**

**Dilepton cocktail provides a good description of pp data as well as peripheral Au+Au data, however, fails in describing the central bins!**

Phys.Rev.C81 (2010) 034911

# Data vs. models

‚Cocktail‘

Fireball model – Rapp/Hees

Hydro model – Dusling/ Zahed

PHSD model, in-medium effects: coll. broadening

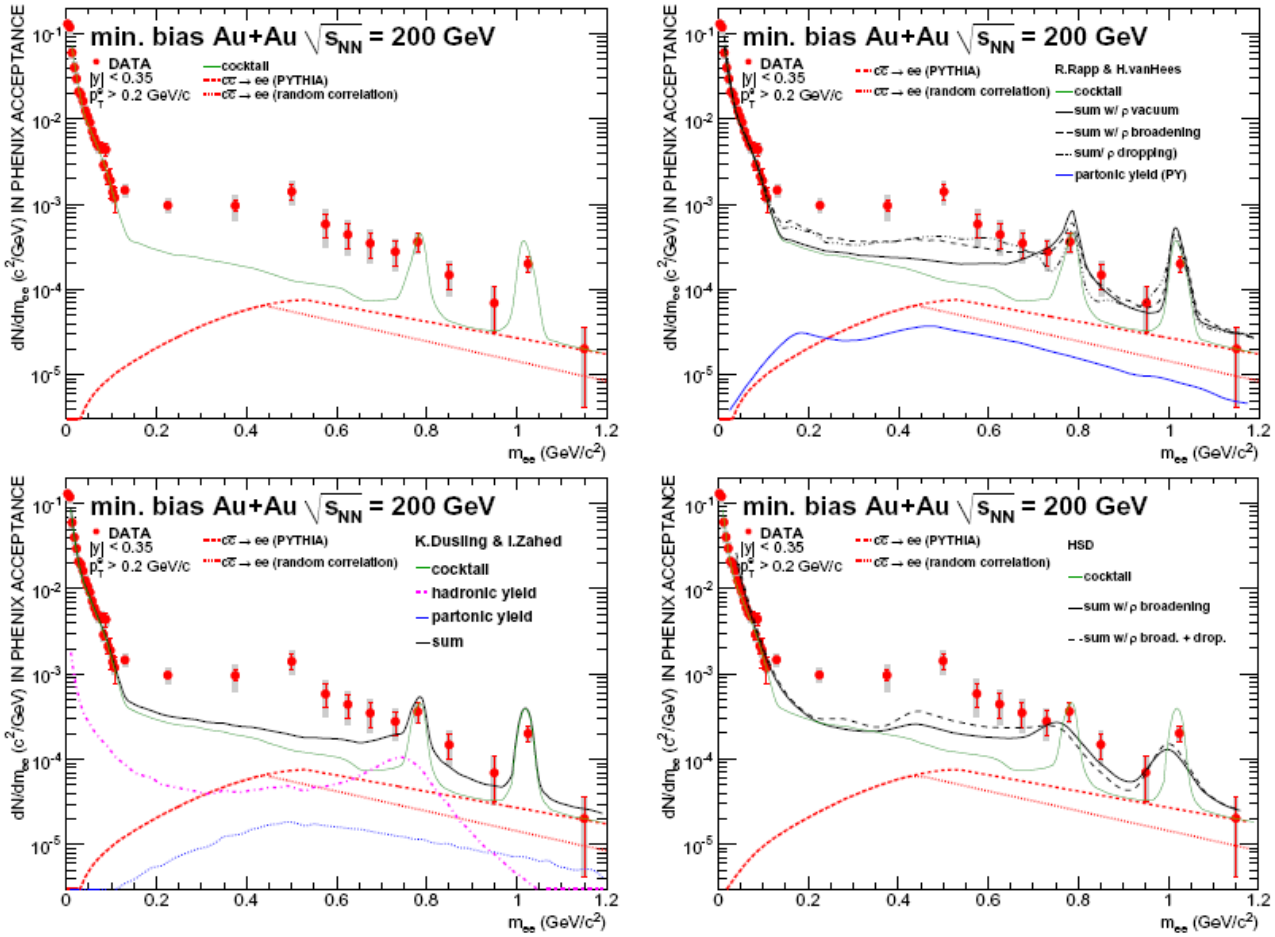


**Large discrepances between the models and PHENIX data in the invariant mass region from 0.2 to 0.7 GeV in central Au+Au collisions.**
**–> PHENIX dilepton puzzle?**

Phys.Rev.C81 (2010) 034911

# PHENIX: dileptons from QGP

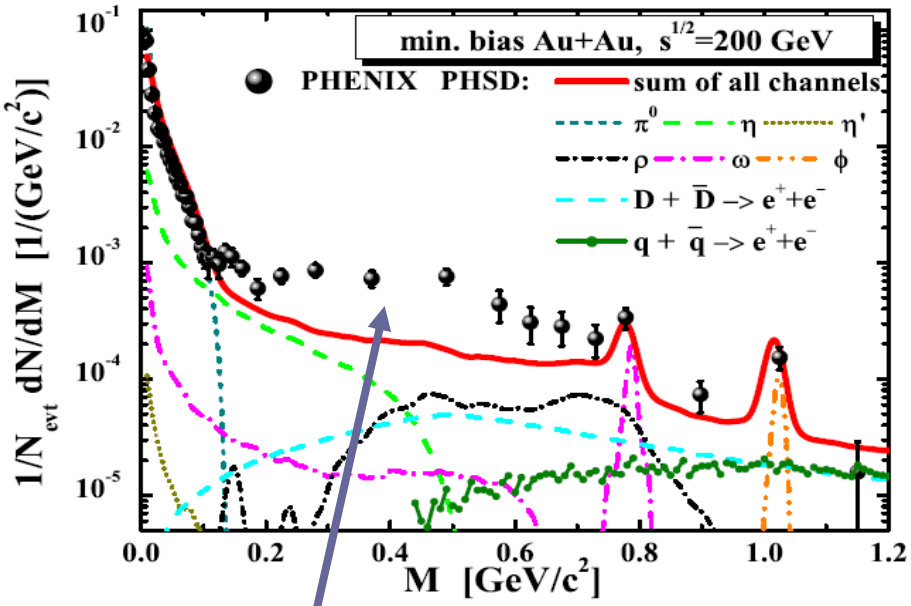


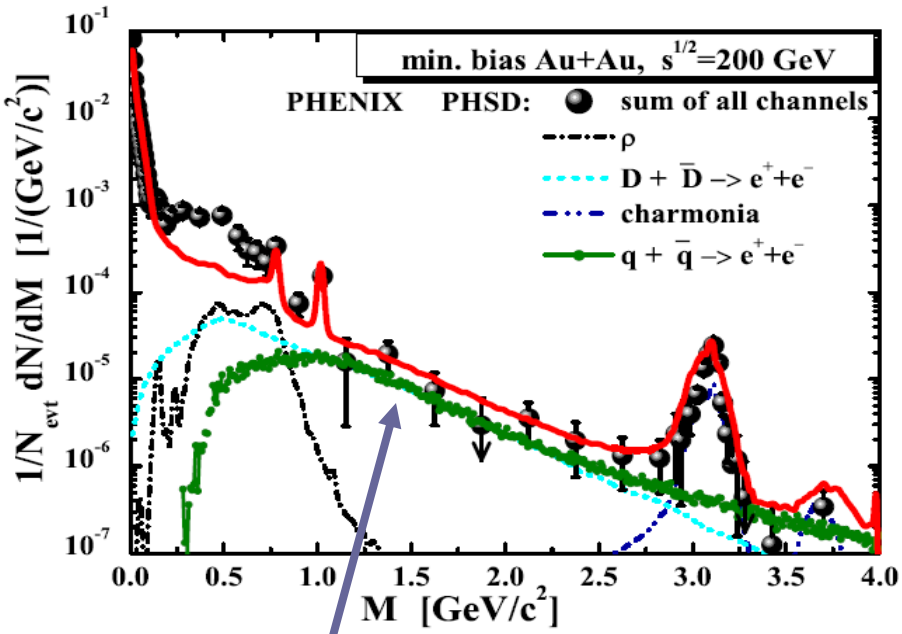


- The excess over the considered mesonic sources for M=0.15-0.6 GeV is not explained by the QGP radiation as incorporated presently in PHSD

- The partonic channels fill up the discrepancy between the hadronic contributions and the data for M>1 GeV

O. Linnyk, W. Cassing, J. Manninen, E.Bratkovskaya and C.M. Ko, PRC 85 (2012) 024910

# PHENIX: $p_T$ spectra

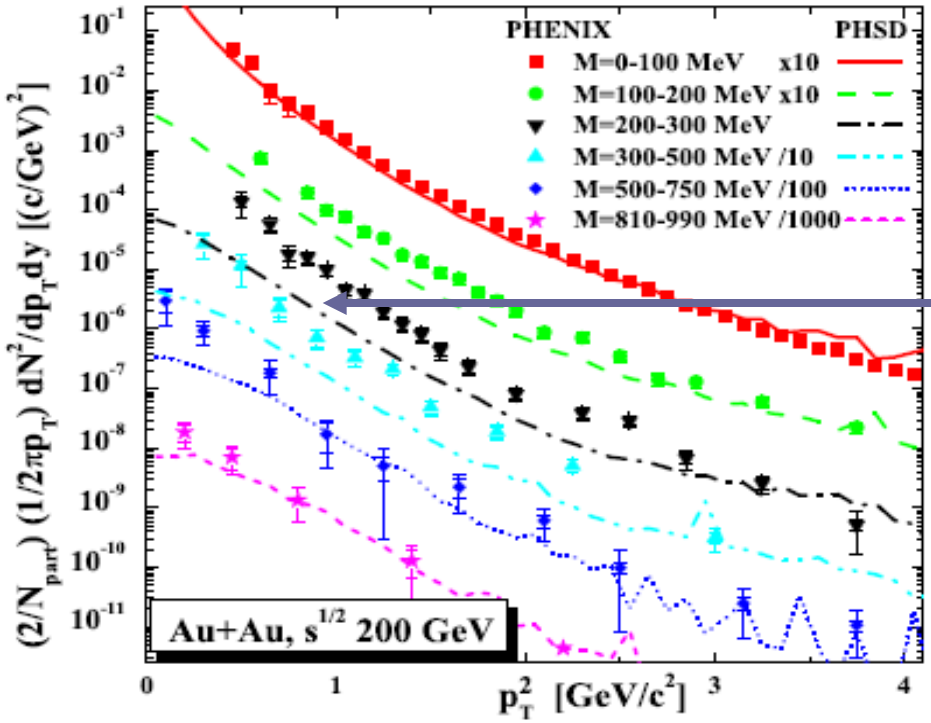


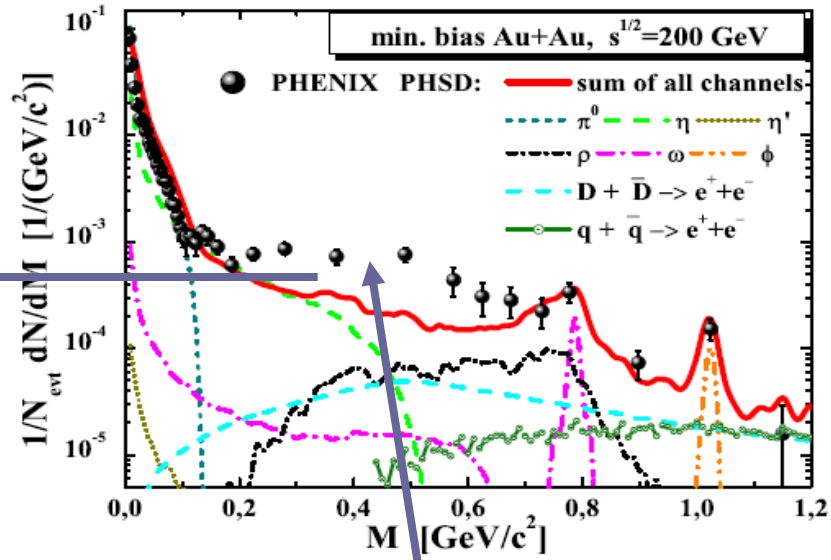


- The lowest and highest mass bins are described very well
- Underestimation of $p_T$ data for 100<M<750 MeV bins consistent with dN/dM
- The 'missing source'(?) is located at low $p_T$ !

O. Linnyk, W. Cassing, J. Manninen, E.B. and C.-M. Ko, PRC 85 (2012) 024910

# PHENIX: mass spectra

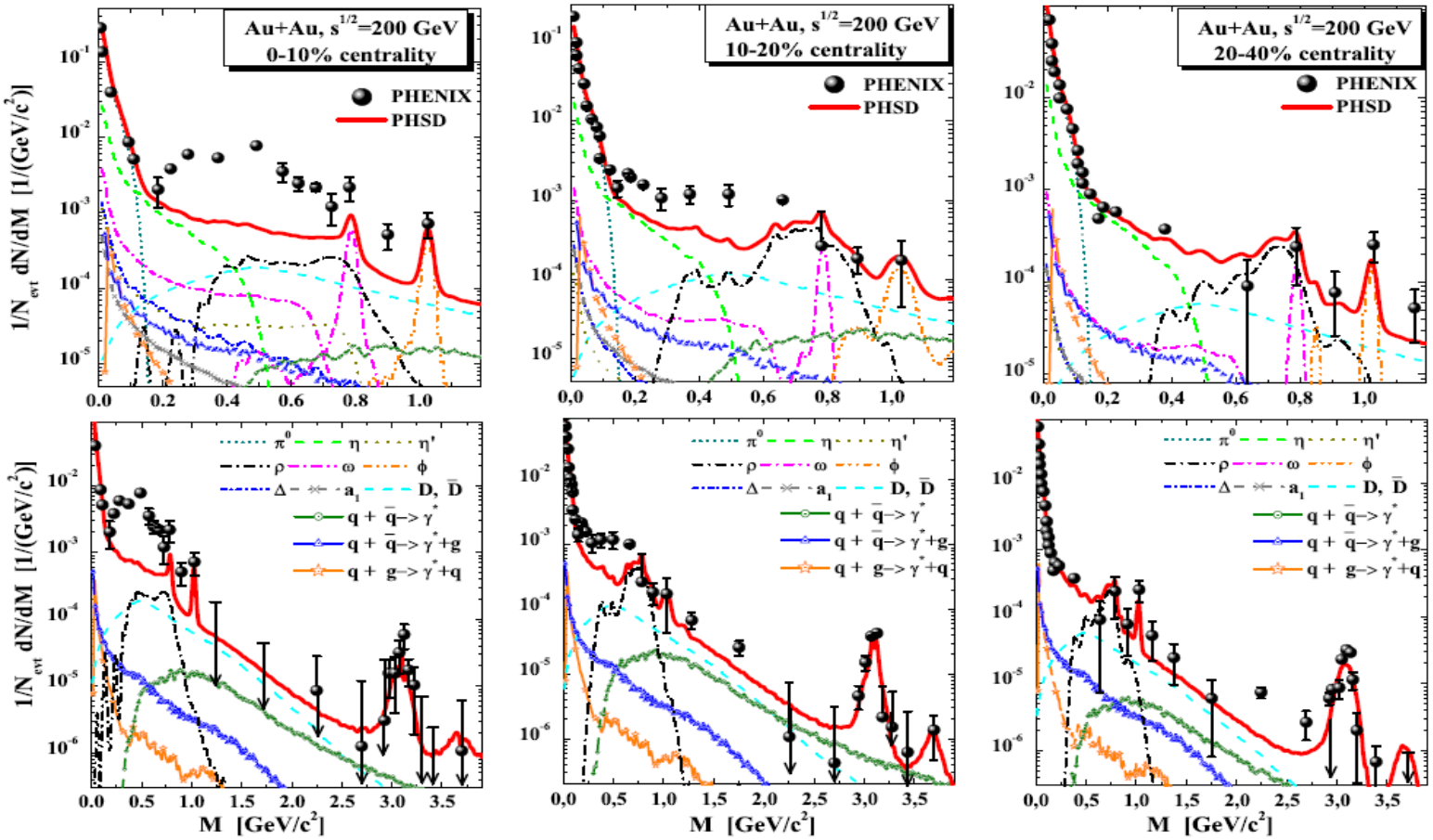


(a)0-10% centrality (b)10-20% centrality (c)20-40% centrality

- **Peripheral collisions (and pp) are well described, however, central fail!**

O. Linnyk, W. Cassing, J. Manninen, E.B. and C.-M. Ko, PRC 85 (2012) 024910

# STAR: dilepton mass spectra

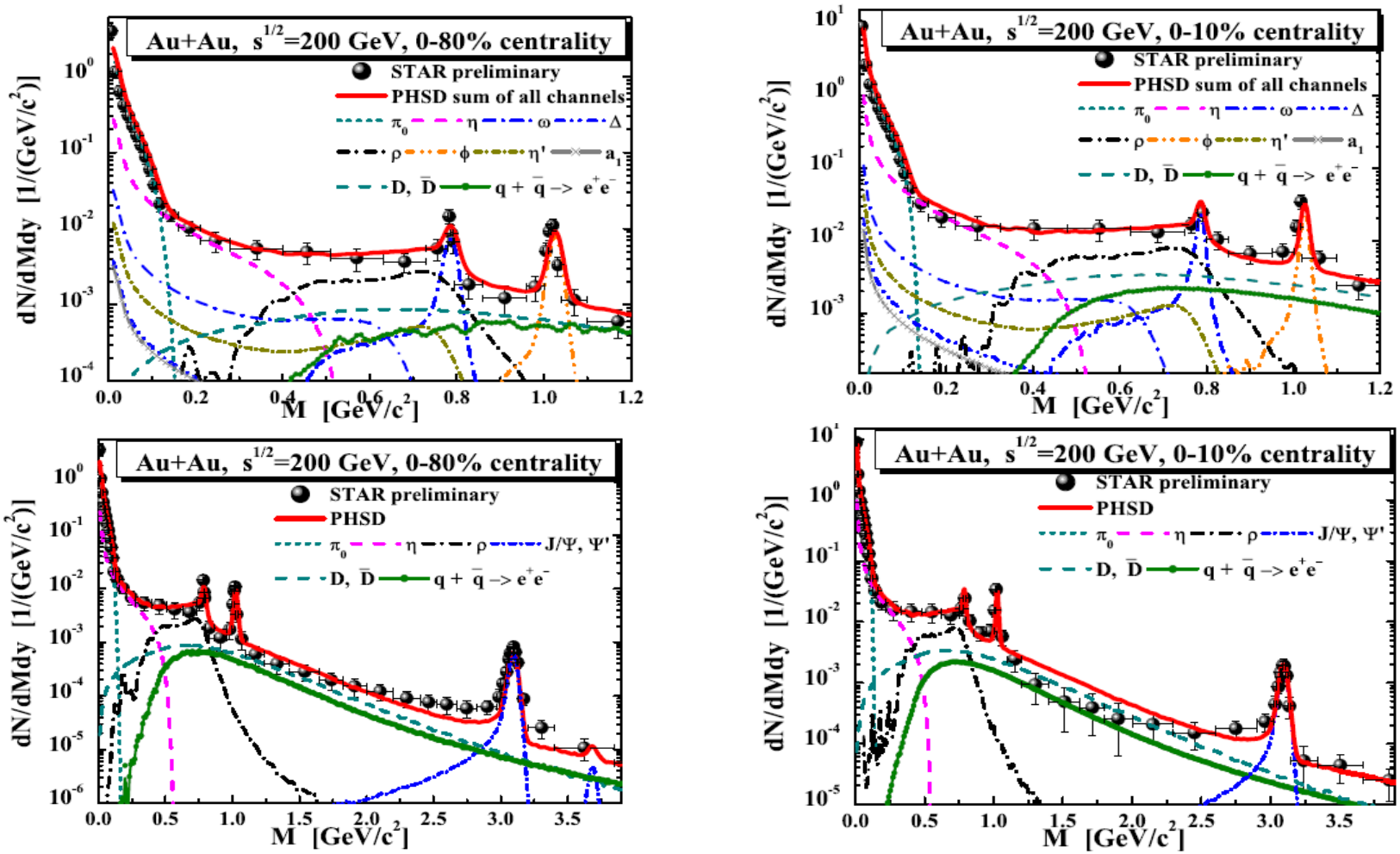


- **STAR data are well described by the PHSD predictions**
- **Confirmed by the extended data set at QM2012**

O. Linnyk, W. Cassing, J. Manninen, E.Bratkovskaya and C.M. Ko, PRC 85 (2012) 024910

# PHENIX: mass spectra with HBD

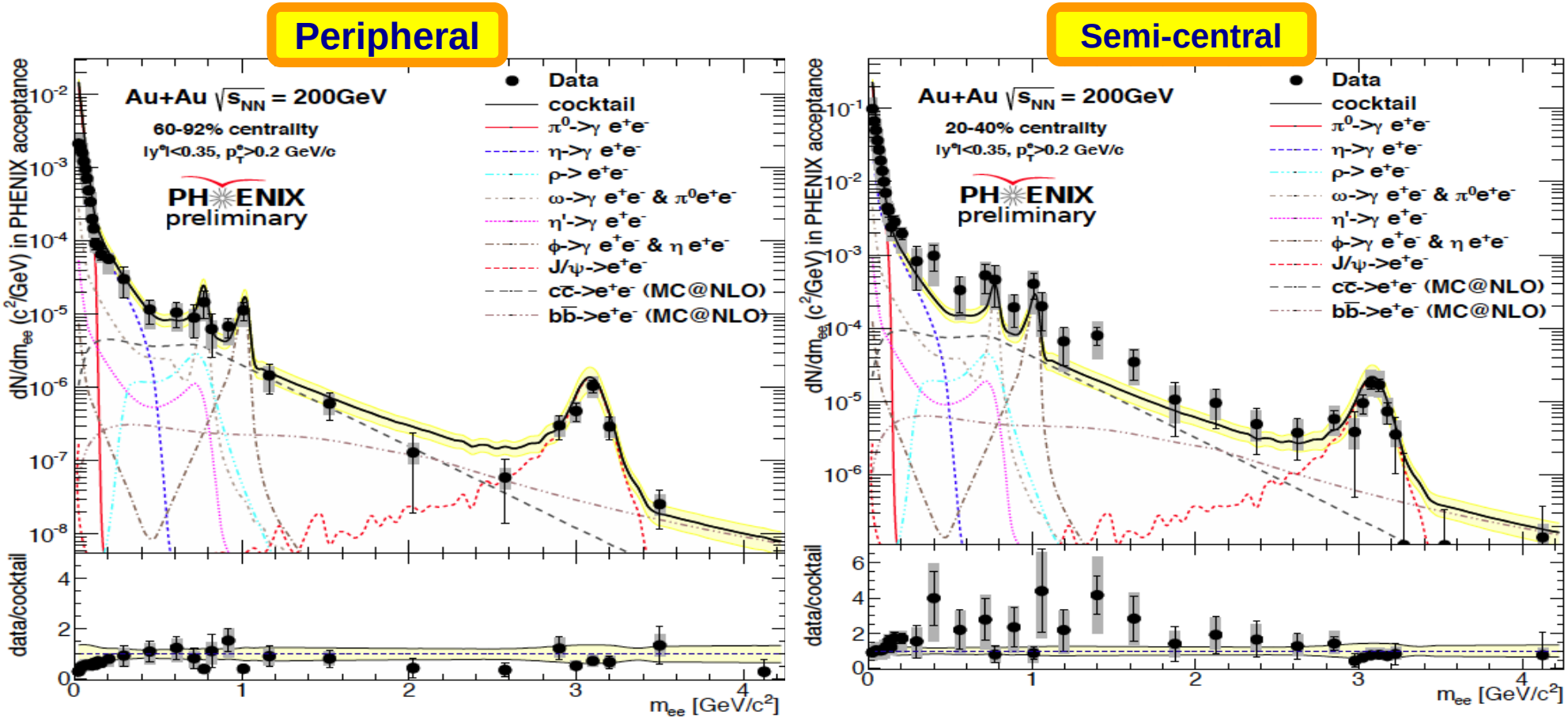


- **Preliminary PHENIX data with Hadron-Blind Detector (HBD) presented at QM 2012**
- **The "PHENIX-puzzle" will be solved soon**

I. Tserruya for PHENIX Collaboration, Quark Matter 2012

# Predictions for LHC

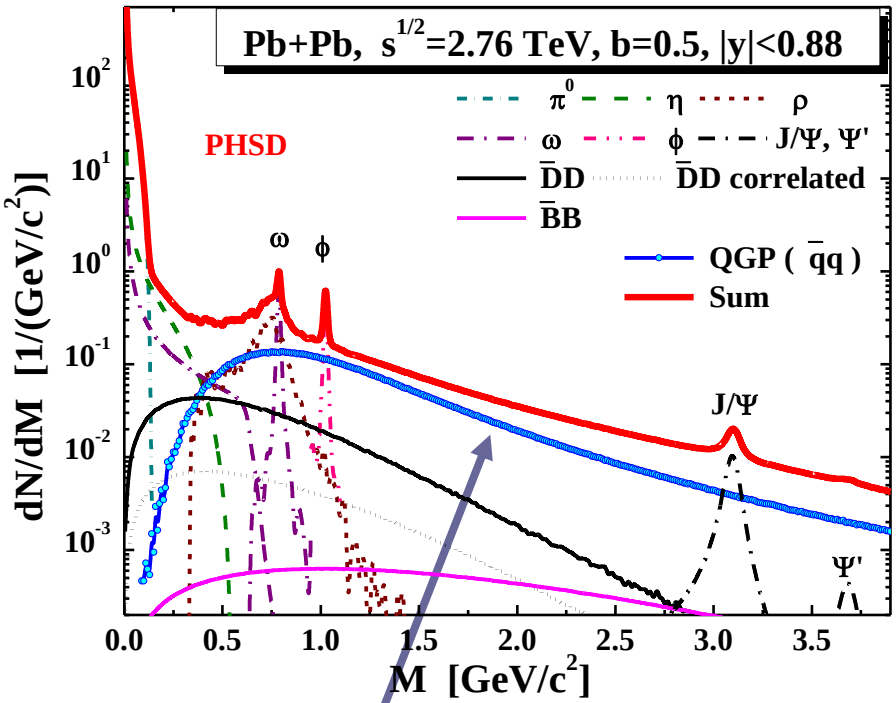


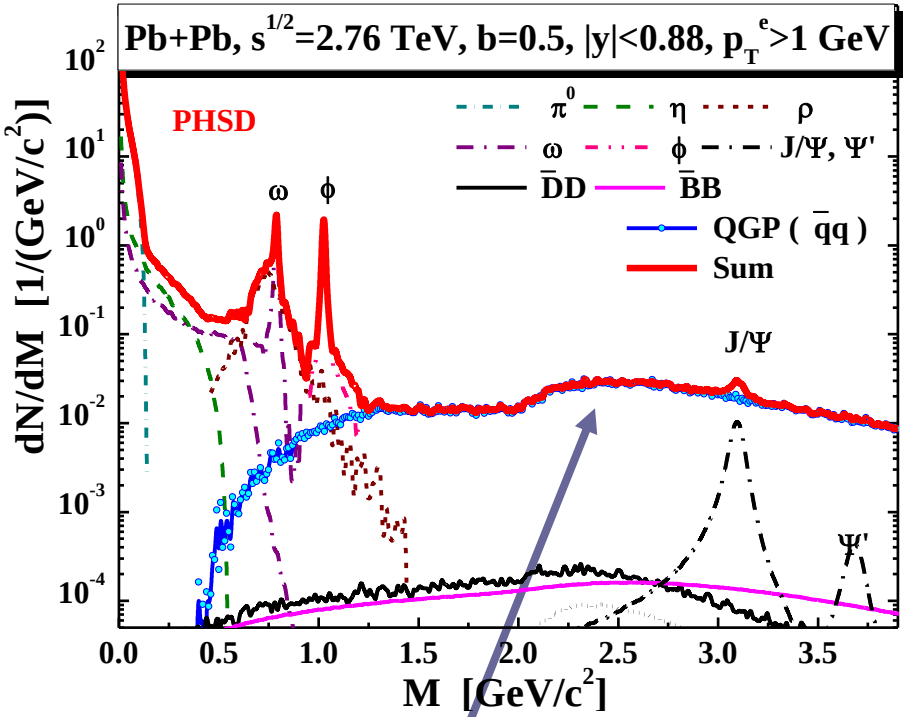


**QGP(qbar-q) dominates at M>1.2 GeV**

**$p_T$ cut enhances the signal of QGP(qbar-q)**

**D-, B-mesons energy loss from Pol-Bernard Gossiaux and Jörg Aichelin**

**JPsi and Psi' nuclear modification from Che-Ming Ko and Taesoo Song**

O. Linnyk et al. arXiv:1208.1279 (2012)

# Equilibration

**Initialize the system in a finite box with periodic boundary conditions with some energy density ε and chemical potential $\mu_q$**

**Evolve the system in time until equilibrium is achieved**

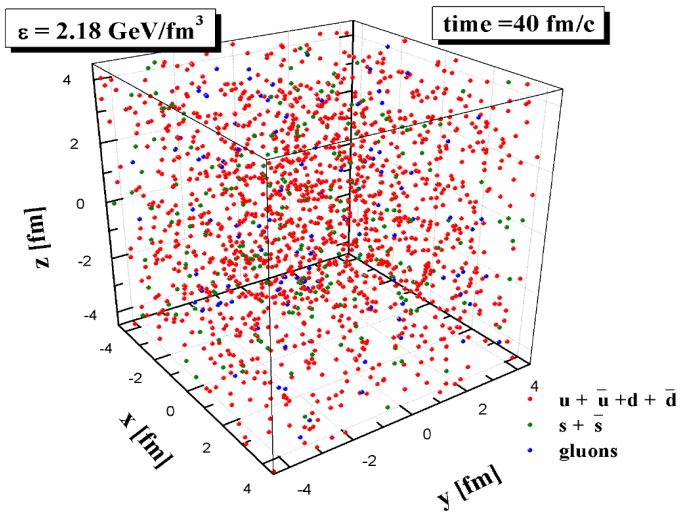


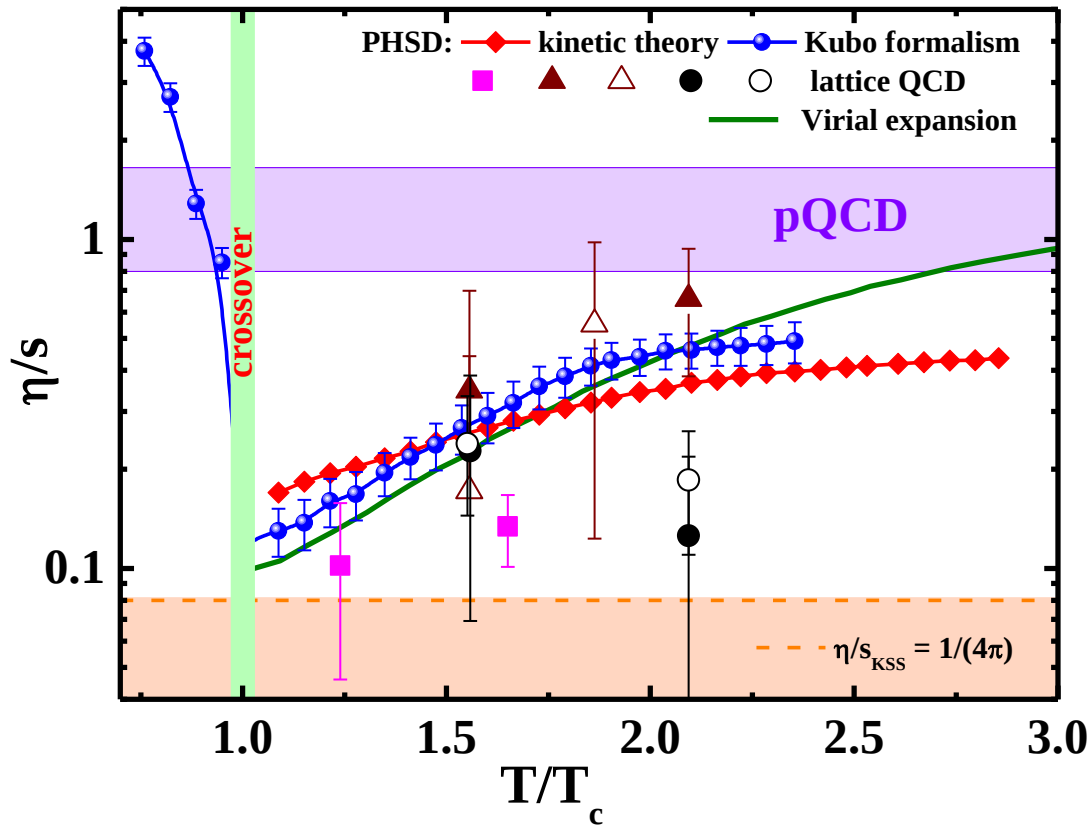


V. Ozvenchuk et al., arXiv:1203.4734

# Electro-magnetic fields

## PHSD - transport model with electromagnetic fields.

**Generalized transport equations:**

$$\dot{\vec{r}} \rightarrow \frac{\vec{p}}{p_0} + \vec{\nabla}_p U \ ,$$

$$\dot{\vec{p}} \rightarrow -\vec{\nabla}_r U + e\vec{E} + e\vec{v} \times \vec{B}$$

$$\vec{A}(\vec{r},t) = \frac{1}{4\pi} \int \frac{\vec{j}(\vec{r'},t')\ \delta(t - t' - |\vec{r} - \vec{r'}|/c)}{|\vec{r} - \vec{r'}|}\ d^3r'dt'$$

$$\Phi(\vec{r},t) = \frac{1}{4\pi} \int \frac{\rho(\vec{r'},t')\ \delta(t - t' - |\vec{r} - \vec{r'}|/c)}{|\vec{r} - \vec{r'}|}\ d^3r'dt'$$

**Magnetic field evolution in HSD/PHSD :**

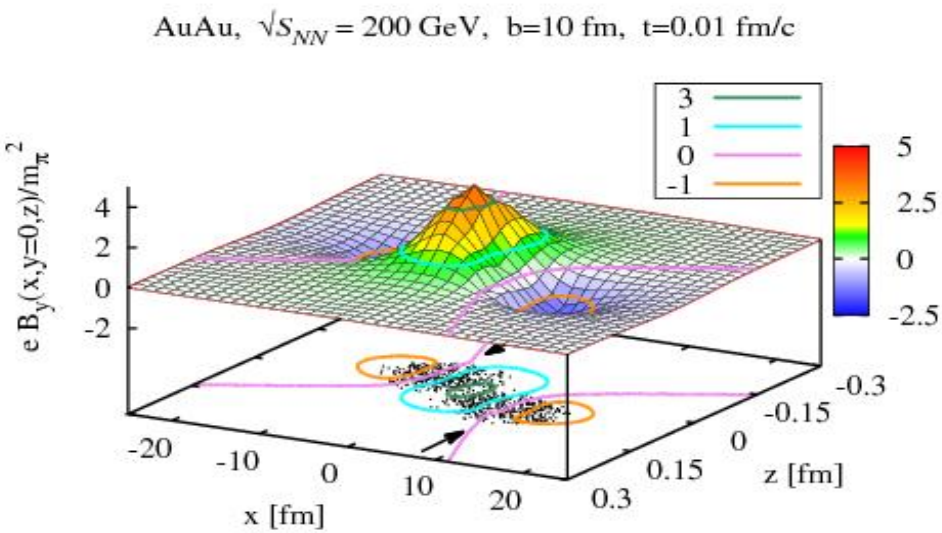


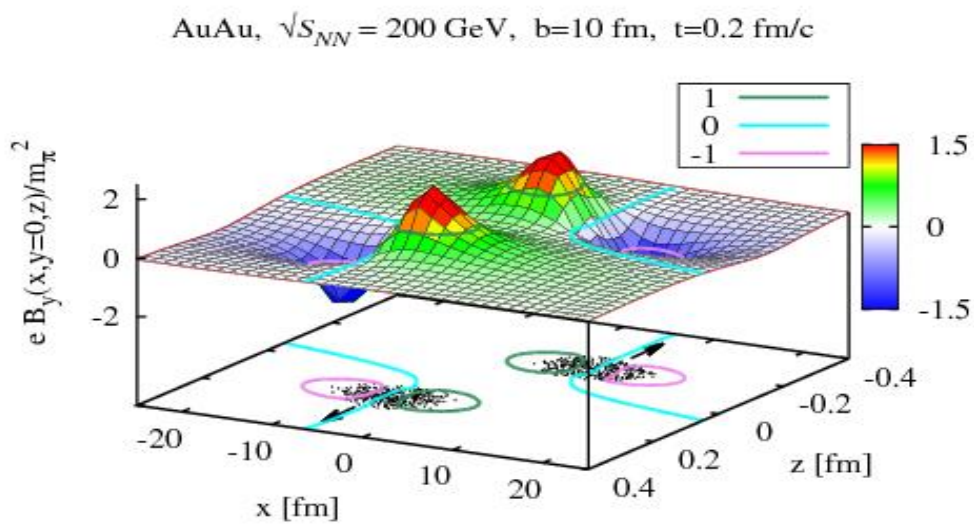


V. Voronyuk et al., Phys.Rev. C83 (2011) 054911

# Conclusions

- **Parton-Hadron-String-Dynamics (PHSD) model provides a consistent description of the phase transition to the QGP in heavy-ion collisions. The dynamical quasiparticle model (DQPM) defines the input for the partonic phase in the PHSD transport in line with lattice QCD.**

- **The dilepton data provide evidence for off-shell dynamics of vector mesons and partons.**

- **Yield of dilepton pairs at masses above 1 GeV indicates the presence of the strongly interacting QGP and is described by the q+q interaction.**

- **Neither the incorporated hadronic no partonic sources account for the enhancement observed by PHENIX in the invariant mass from 0.2 to 0.5 GeV in central Au+Au collisions at $s^{1/2}$=200 (relative to the p+p).**

- **Outlook: first order phase transition (RHIC low energy scan, FAIR/NICA)**

# Thank you!

HIC for FAIR

**Wolfgang Cassing**
**Elena Bratkovskaya**

Volodya Konchakovski
Jaakko Manninen
Vitalii Ozvenchuk
Rudy Marty

PHSD Team

Che-Ming Ko
Taesoo Song
Jörg Aichelin
Pol Bernard Gossiaux
Mark I. Gorenstein
Viatcheslav D. Toneev
Vadym Voronyuk

Collaboration

JUSTUS-LIEBIG-UNIVERSITÄT GIESSEN

GOETHE UNIVERSITÄT FRANKFURT AM MAIN

Subatech

TEXAS A&M UNIVERSITY

# Back up slides

# Flow harmonics ($v_1$, $v_2$, $v_3$, $v_4$)

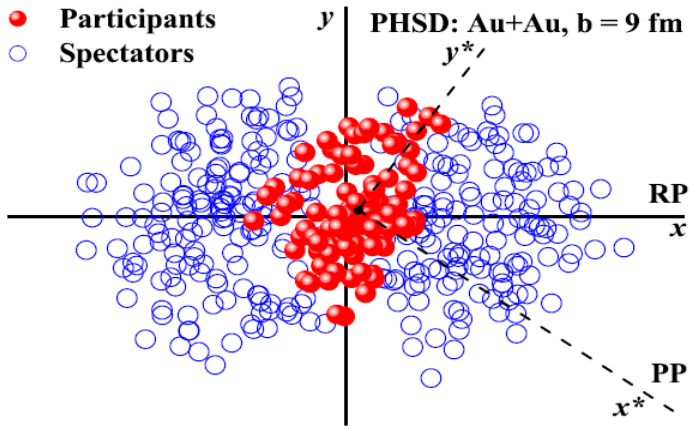


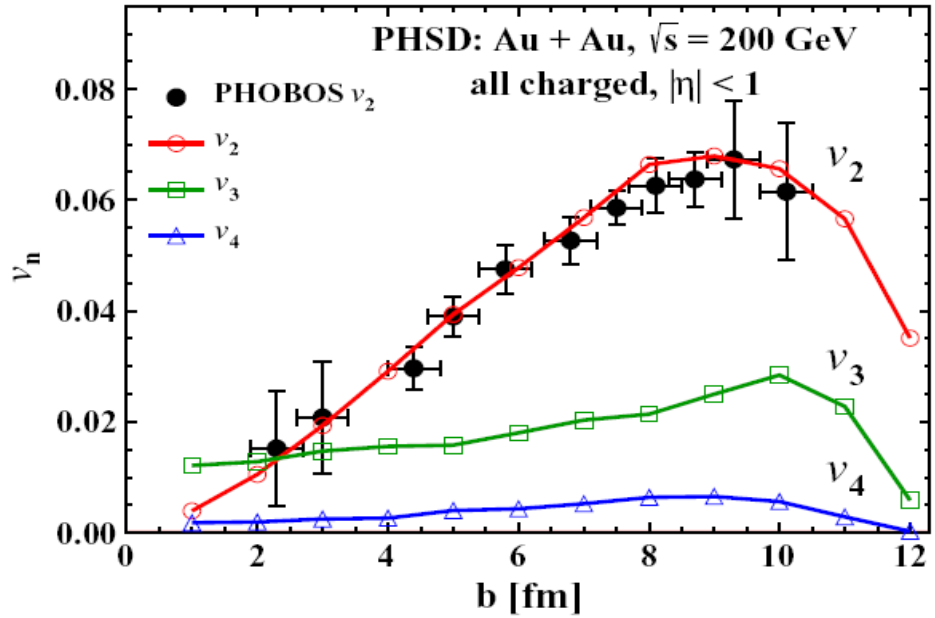


**Increase of $v_2$ with impact parameter but flat $v_3$ and $v_4$**

**$v_2/\varepsilon$ = const, indicates near ideal hydrodynamic flow !**

**Expected since η/s is very small in the DQPM and PHSD.**

E. Bratkovskaya, W. Cassing, V. Konchakovski, O. Linnyk, NPA856 (2011) 162;
V. P. Konchakovski et al., PRC 85 (2012) 044922

# Hadron abundances

- very good description of particle production in pp, pA reactions with HSD
- unique description of nuclear dynamics from low (~100 MeV) to ultrarelativistic (~20 TeV) energies

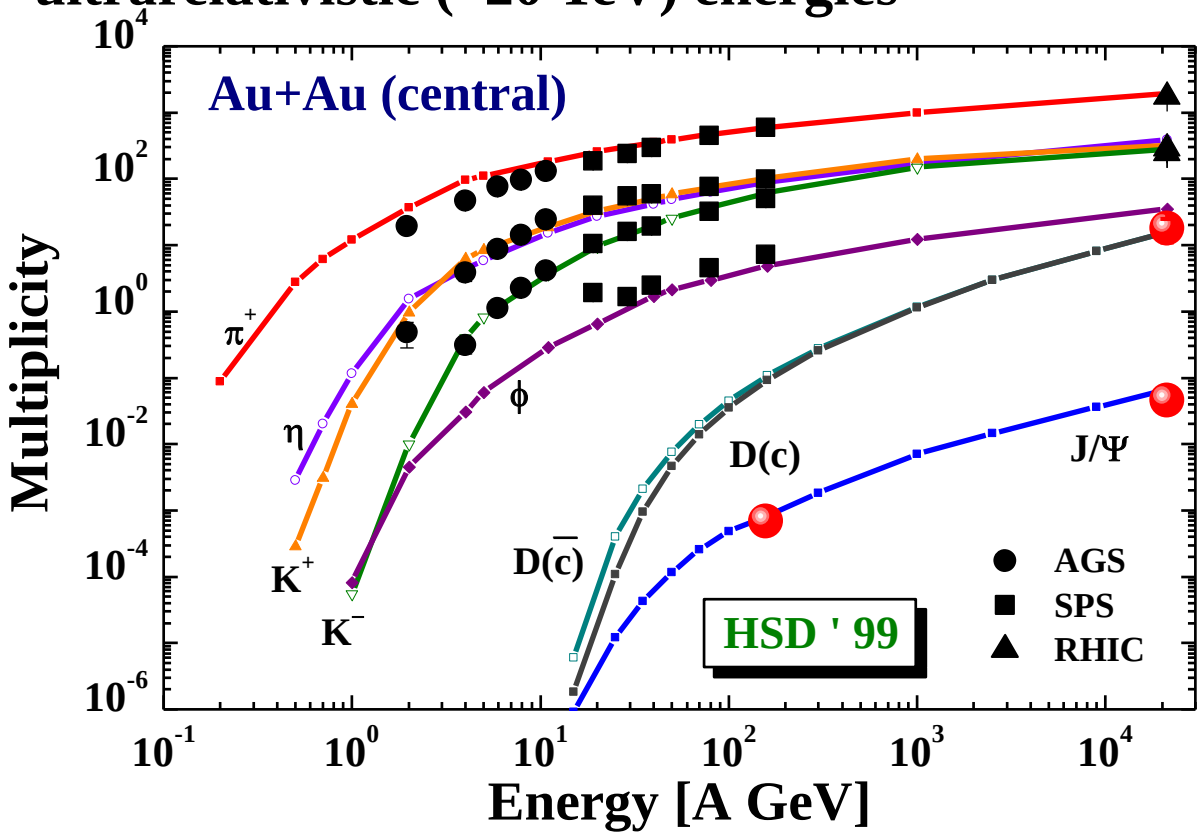


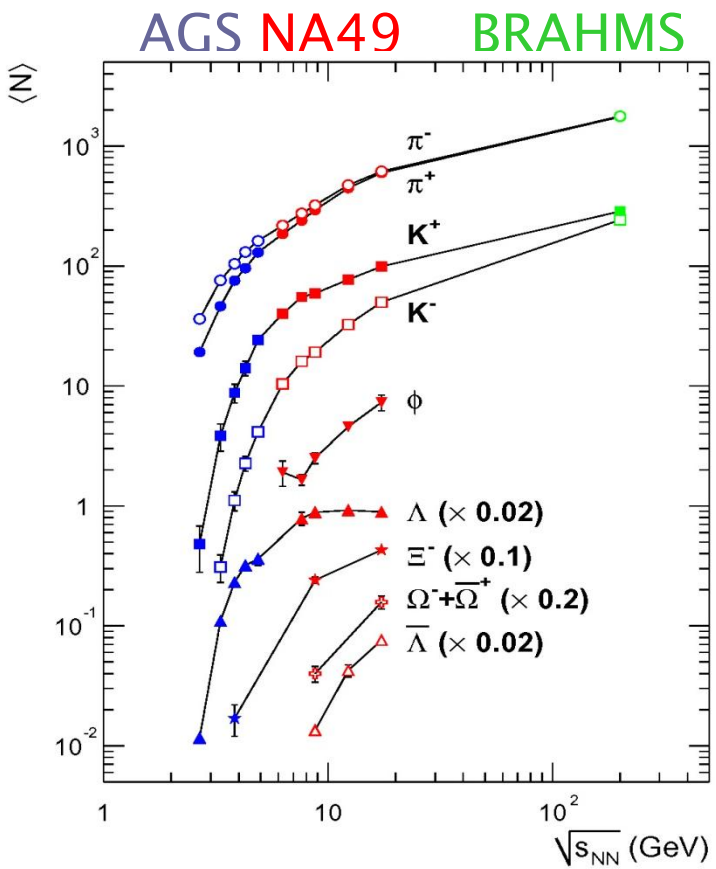


**HSD predictions from 1999; data from the new millenium!**

# PHSD: Transverse mass spectra at top SPS

Central Pb + Pb at top SPS energies

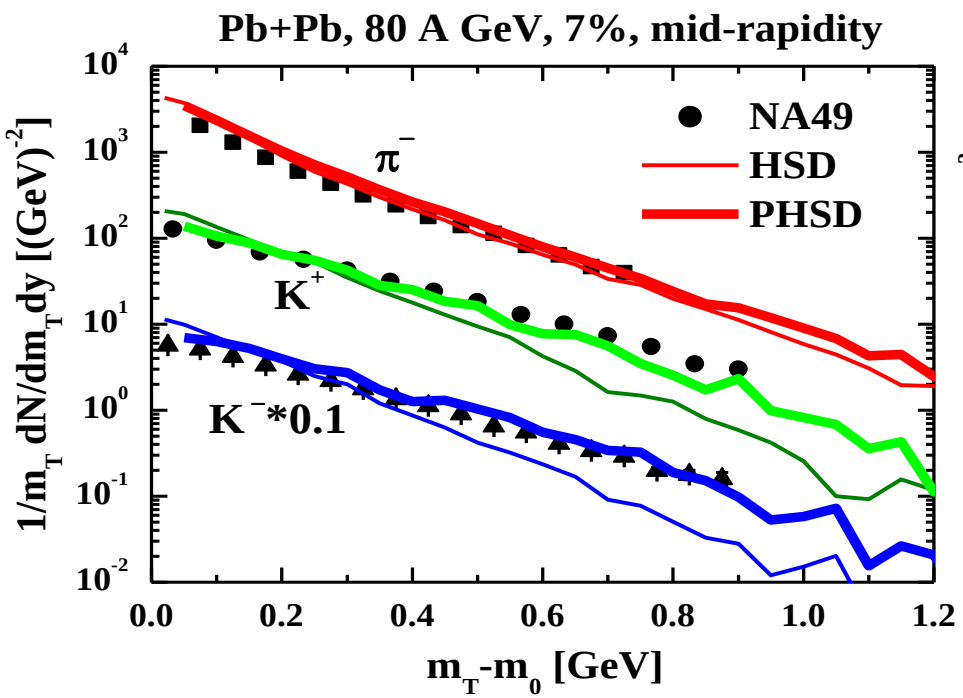


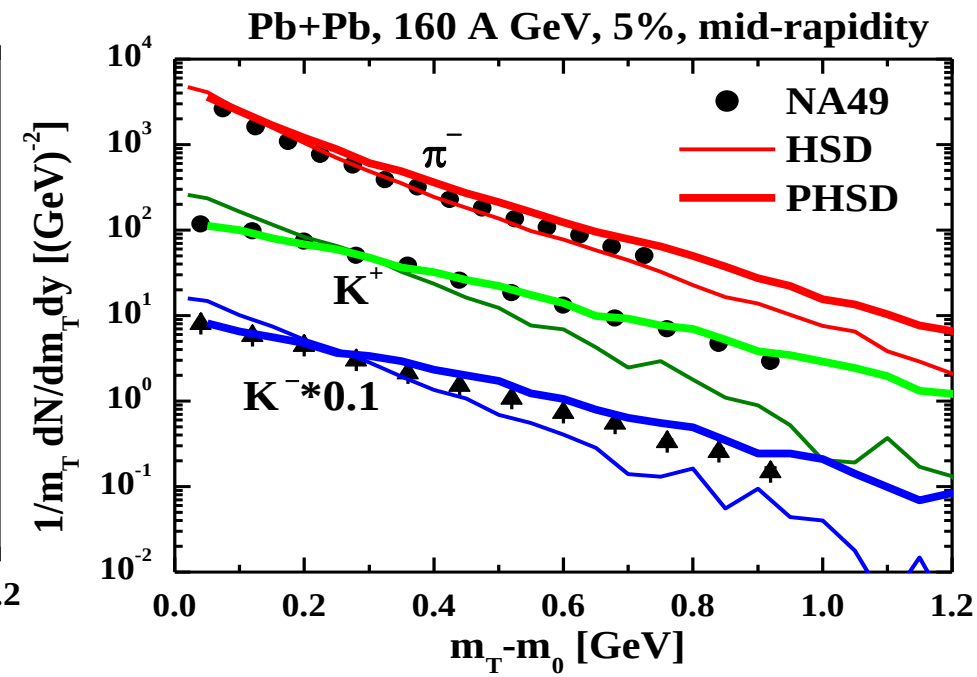


☺ PHSD gives harder spectra and works better than HSD at top SPS energies

# Rapidity distributions of p, $K^+$, $K^-$ at SPS

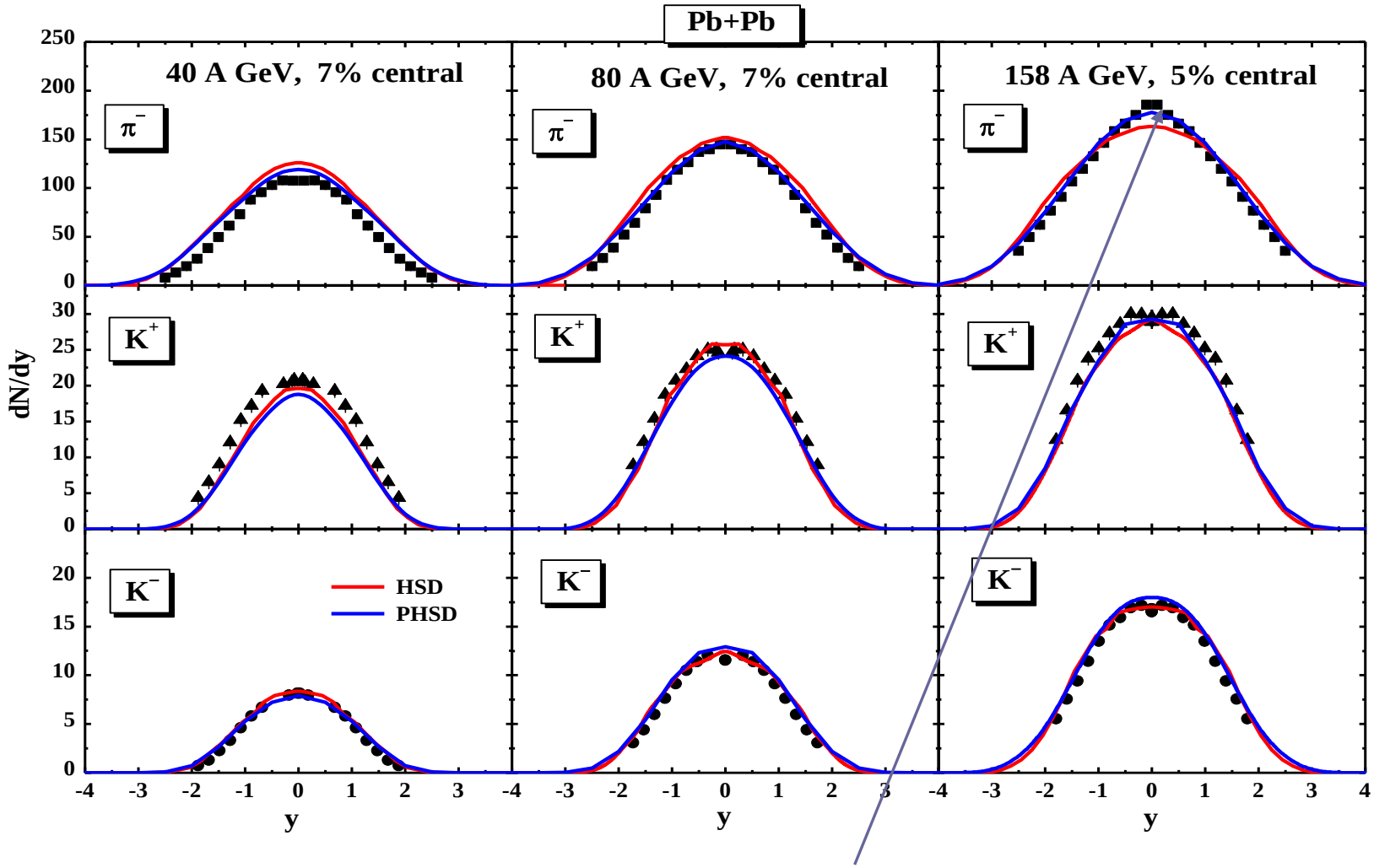


➔ pion and kaon rapidity distributions become slightly narrower

W. Cassing, E.L. Bratkovskaya, NPA 831 (2009) 215

# Transverse mass spectra at SPS

## Central Pb + Pb at SPS energies

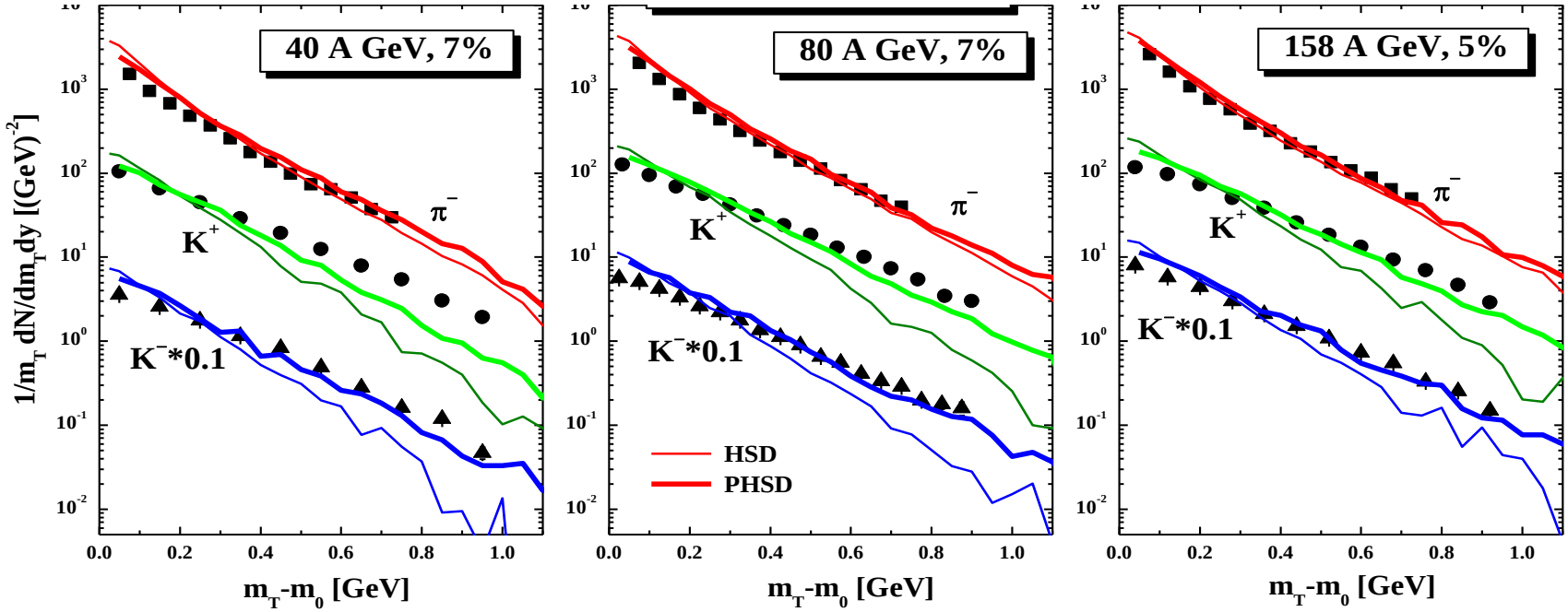


☺ PHSD gives harder spectra and works better than HSD at SPS (and top FAIR) energies

☹ However, at low SPS (and low FAIR) energies the effect of the partonic phase is NOT seen in rapidity distributions and $m_T$ spectra

W. Cassing, E.L. Bratkovskaya, NPA 831 (2009) 215

# Rapidity distributions in central Au+Au at RHIC

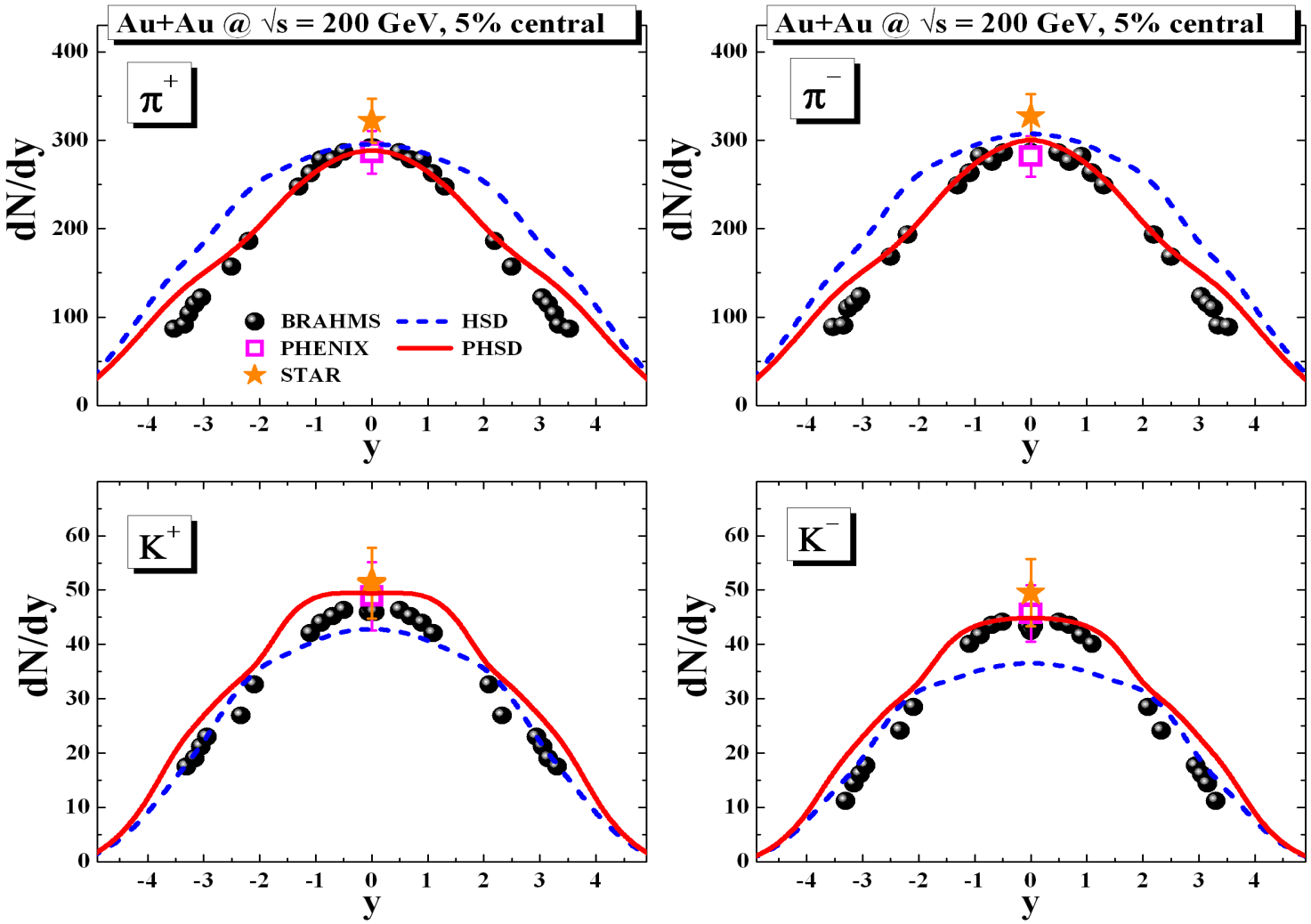


➔ **reasonable description of the data from BRAHMS, STAR, PHENIX!**

E. Bratkovskaya, W. Cassing, V. Konchakovski, O. Linnyk, NPA 856 (2011) 162

# Transverse mass distributions at RHIC

**Au+Au at midrapidity |y| < 0.5**

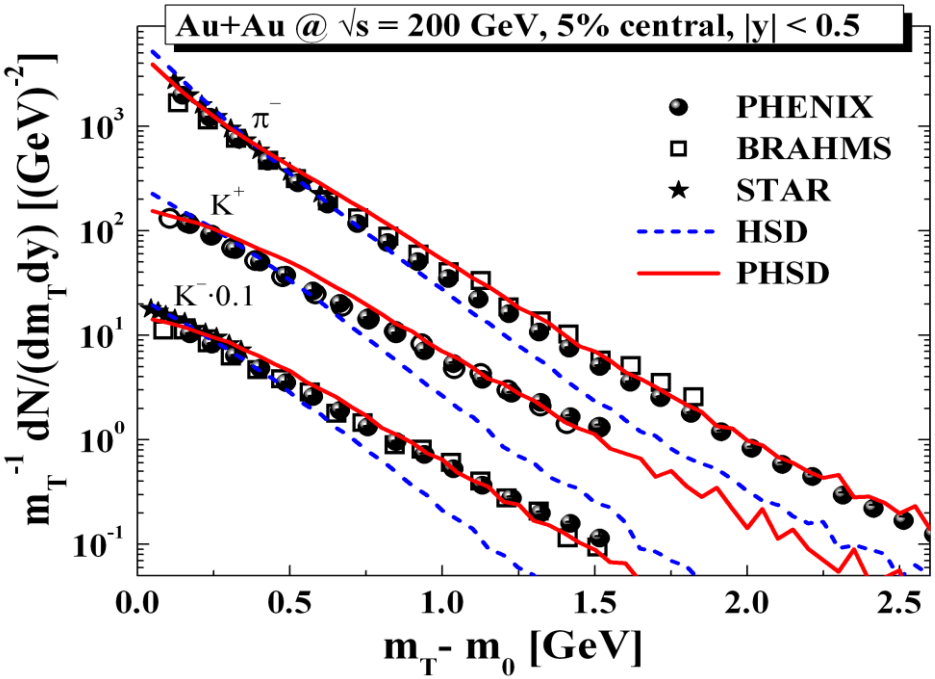


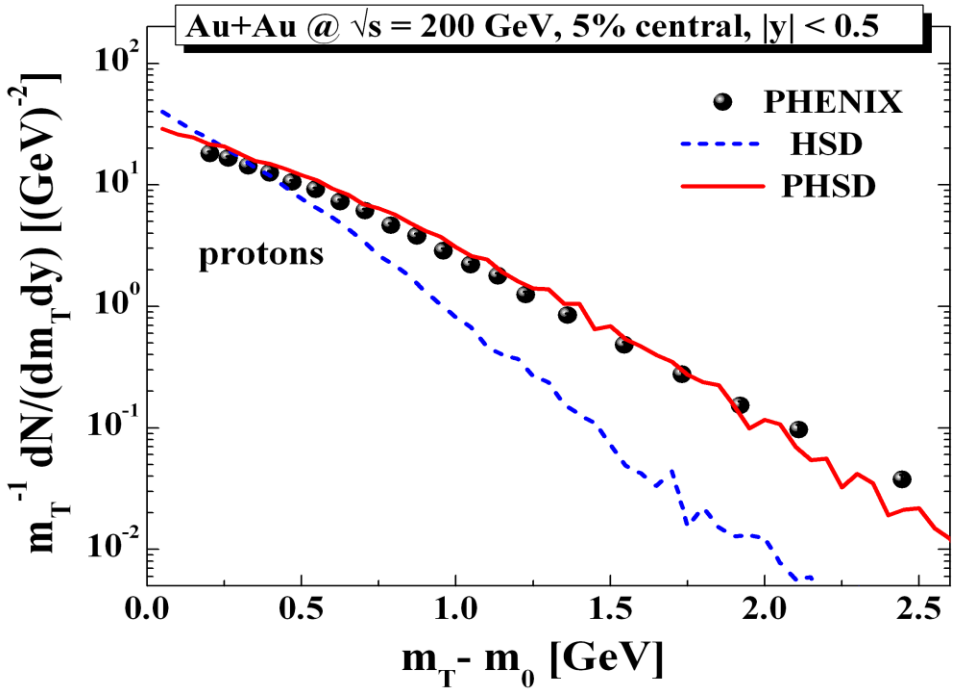


➔ **PHSD gives harder spectra and works better than HSD at RHIC**

**Note: In PHSD the protons at midrapidity stem from hadronization of quarks.**

E. Bratkovskaya, W. Cassing, V. Konchakovski, O. Linnyk, NPA 856 (2011) 162

# Parton-Hadron-String Dynamics (PHSD)

**Description of heavy-ion collisions as well as p+p, p+A, d+A, π+A reactions.**

**Features:**

- ✓ **Unified description of collisions at all energies from AGS to LHC.**
- ✓ **Non-equilibrium approach: applicable to far from equilibrium configurations as explosion-like heavy-ion collisions as well as to equilibrated matter („in the box“).**
- ✓ **Dynamics: mean fields (hadronic and partonic), scattering (elastic, inelastic, 2<–>2, 2<–>n), resonance decays, retarded electro-magnetic fields.**
- ✓ **Phase transition (cross over) according to the lattice QCD equation of state, hadronic and partonic degrees of freedom, spacial co-existance, dynamical hadronisation.**
- ✓ **Off-shell transport: takes into account 2-particle correlations beyond the one-particle distributions.**

# The baseline concepts of HSD

## HSD – Hadron-String-Dynamics transport approach:

- for each particle species *i* (*i* = *N*, *R*, *Y*, π, ρ, K, …) the phase-space density $f_i$ follows the generalized transport equations

  with collision terms $I_{coll}$ describing:

  - elastic and inelastic hadronic reactions:

    baryon-baryon, meson-baryon, meson-meson

    BB <–> B´B´, BB <–> B´B´m

    mB <–> m´B´, mB <–> B´

  - formation and decay of

    baryonic and mesonic resonances

    and strings - excited color singlet states *(qq - q)* or *(q – qbar)* -

    (for inclusive particle production: BB –> X , mB –>X, X =many particles)

    Baryons:

    B=(p, n, Δ(1232), N(1440), N(1535), ...)

    Mesons:

    m=(π, η, ρ, ω, ϕ, ...)

- implementation of detailed balance on the level of 1<–>2 and 2<–>2 reactions (+ 2<–>n multi-particle reactions in HSD !)

- off-shell dynamics for short-lived states

HSD is an open code: http://www.th.physik.uni-frankfurt.de/~brat/hsd.html

# (Collision term) Description of elementary reactions in HSD

**Low energy collisions:**

- binary 2<–>2 and 2<–>3 reactions
- formation and decay of baryonic and mesonic resonances

BB <–> B´B´
BB <–> B´B´m
mB <–> m´B´
mB <–> B´
mm <–> m´m´
mm <–> m´
. . .

**Baryons:**
B=(p, n, Δ(1232), N(1440), N(1535), ...)
**Mesons:**
m=(π, η, ρ, ω, ϕ, ...)

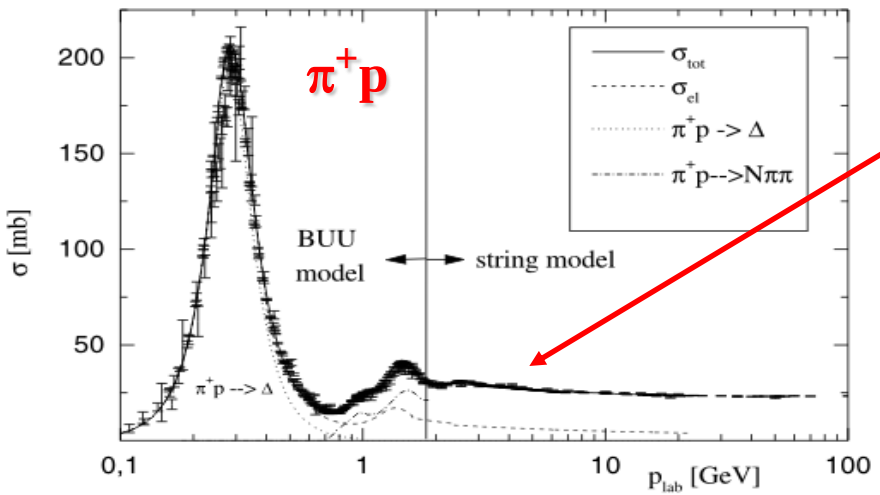


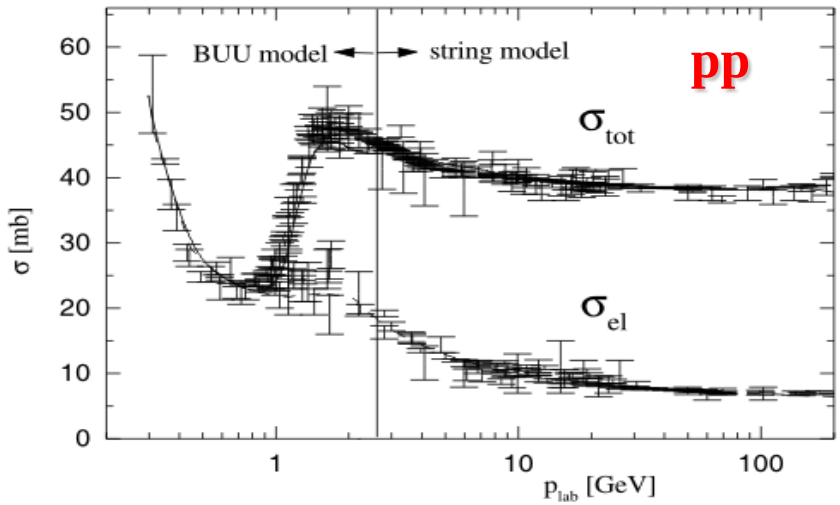


**High energy collisions:**
(above $s^{1/2}$~2.5 GeV)

**Inclusive particle production:**
BB –> X , mB –>X
X =many particles described by **strings** (= excited color singlet states *q-qq*, *q-qbar*) **formation and decay**

# Remarks on IMR: partonic vs. hadronic

**Modeling of ‚hadronic' high mass dileptons in the fireball model by Rapp/vanHees:**

**1) Spectral function: M>1 GeV → ‚4π' contribution: $\pi + a_1(\omega) \rightarrow e^+e^-$**

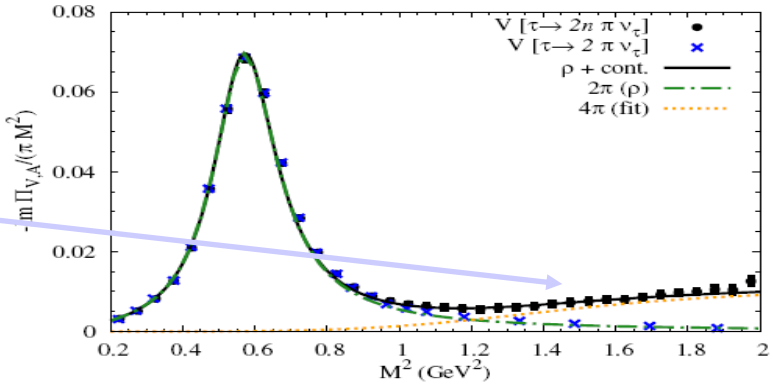


**2) Modeling of the time evolution of the fireball:**

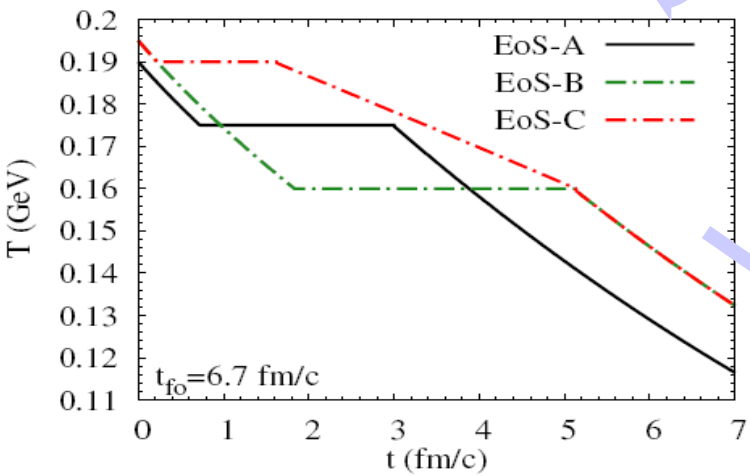


- EoS-A: $T_c = T_{\rm chem} = 175$ MeV
- EoS-B: $T_c = T_{\rm chem} = 160$ MeV
- EoS-C: $T_c = 190$ MeV, $T_{\rm chem} = 160$ MeV
  - $T_c \geq T \geq T_{\rm chem}$: hadron gas in chemical equilibrium

**! Warnings:**

- **EoS: T=const for a long time:**

**R/H: 1st order phase transition vs. LQCD:crossover**

- **Hadronic yield at high M (‚4π') enhanced by the long ‚mixed' phase according to T(t):**

$$dN_{ll}/dMdT \propto \mathrm{Im}\,\Pi_{\rm em}(M,T)\ \exp(-M/T)\ T^{-5.5}$$

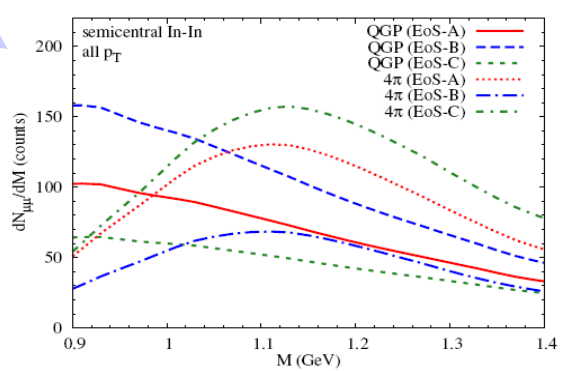


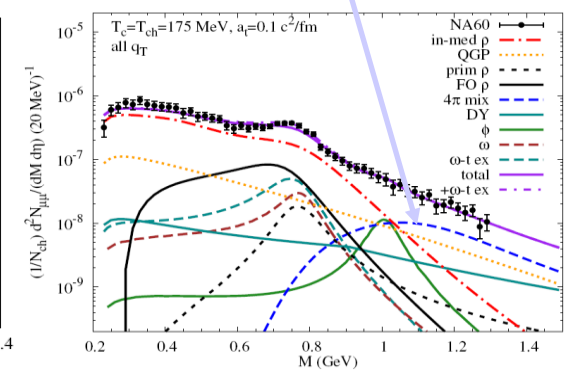


**→Importance of REALISTIC dynamical evolution of heavy-ion collisions**

# Remarks on ‚4π' contribution

**History: Importance of ‚4π' contribution has been indicated already by C. Song, C.M. Ko and C. Gale *[PRD50 (1994)R1827]* and calculated by G.Q. Li & C. Gale *[PRC58 (1998) 2914]* within the microscopical transport model (AMPT) for S+W at 200 AGeV**

We carry out a study of intermediate-mass (between 1 and 2.5 GeV) dilepton spectra from hadronic interactions in heavy-ion collisions. The processes considered are $\pi\pi \to l\bar{l}$, $\pi\rho \to l\bar{l}$, $\pi a_1 \to l\bar{l}$, $\pi\omega \to l\bar{l}$, $K\bar{K} \to l\bar{l}$, and $K\bar{K}^* + \text{c.c.} \to l\bar{l}$. The elementary cross sections for those are obtained from chiral Lagrangians involving pseudoscalar, vector, and axial-vector mesons. The respective electromagnetic form factors are determined by fitting to experimental data for the reverse processes of $e^+e^- \to$ hadrons. Based on this input we calculate cross sections and thermal dilepton emission rates and compare our results with those from other approaches. Finally we use these elementary cross sections with a relativistic transport model and calculate dilepton spectra in $S+W$ collisions at SPS energies. The comparison of our results with experimental data from the HELIOS-3 Collaboration indicates the importance of the secondary hadronic contributions to the intermediate-mass dilepton spectra. [S0556-2813(98)01411-3]

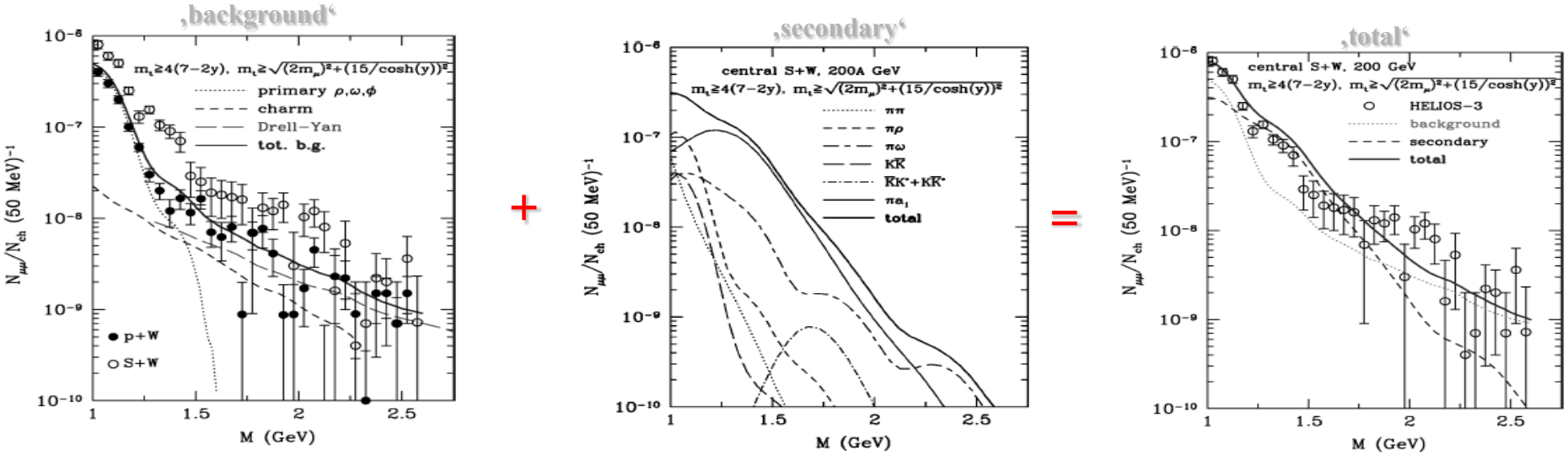


**! Problems:** * **uncertainties in $\pi a_1 \to e^+e^-$ cross section (dominant channel);**

* **accounting for the in-medium effects for broad resonances ($a_1$,ρ)**

# Thermal Radiation (?) Workshop

based on work with M. Chiu T. Hemmick, A. Leonidov, J. Liao, V. Khachatryan

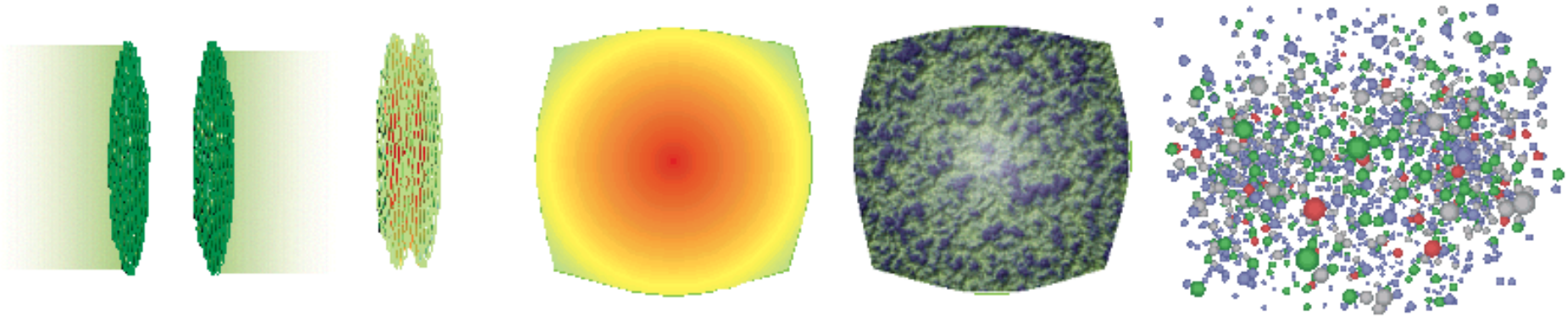

CGC | Initial Singularity | Glasma | Thermalized sQGP | Hadron Gas

<----------sQGP ---------->

The Space-Time Evolution of Heavy Ion Collisions

RIKEN BNL Research Center · RIKEN · RUPRECHT-KARLS-UNIVERSITÄT HEIDELBERG · HUAZHONG UNIVERSITY

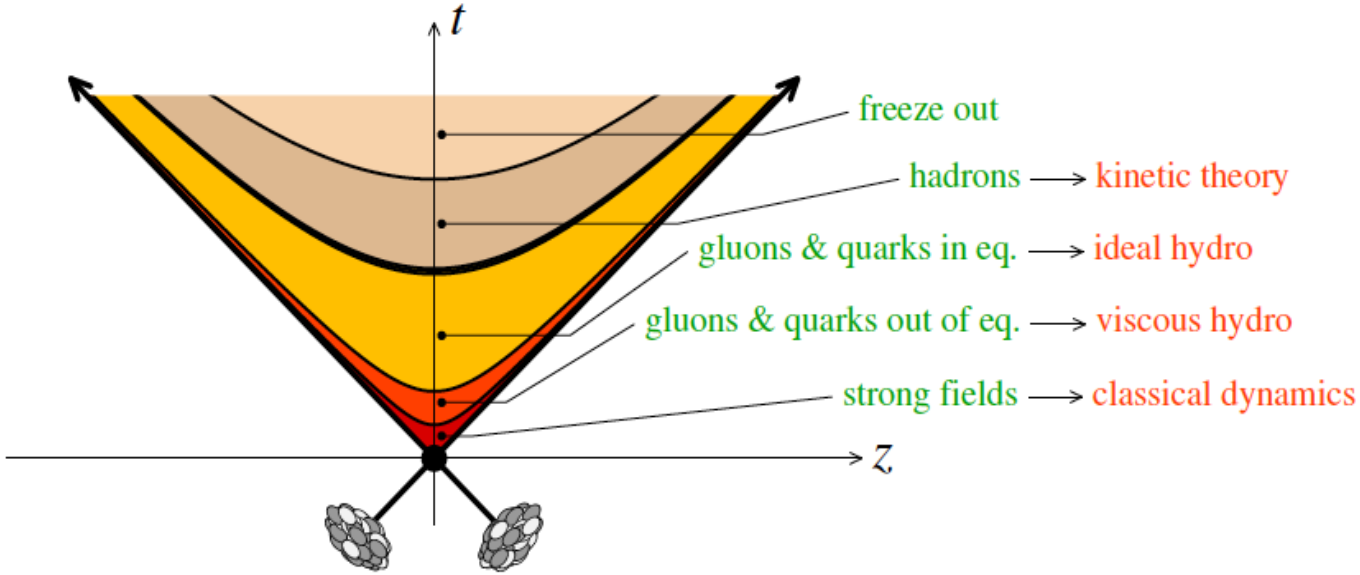


Color Glass Condensate:
The High Density Gluonic States of a high energy hadron that dominate high energy scattering.

Glasma:
Highly coherent gluon fields arising from the Glasma that turbulently evolve into the thermalized sQGP while making quarks

Thermalized sQGP:
Largely incoherent quark and gluons that are reasonably well thermalized

# The Glasma

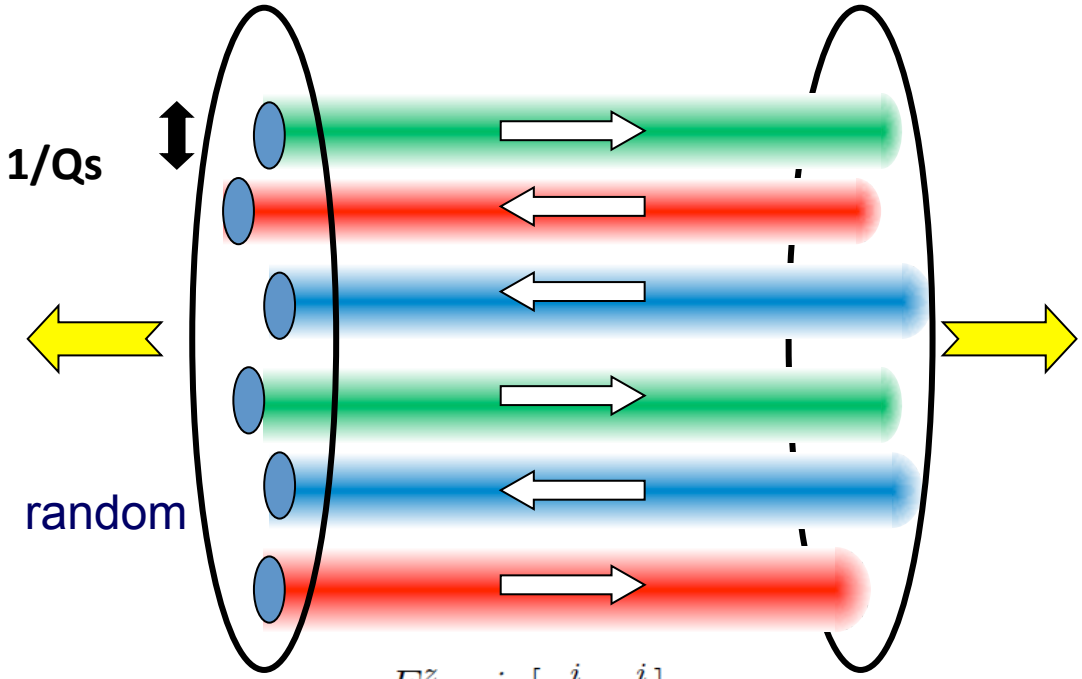


$$E^z = ig[\alpha_1^i, \alpha_2^i]$$
$$B^z = ig\epsilon^{ij}[\alpha_1^i, \alpha_2^j].$$

Typical configuration of a single event just after the collision

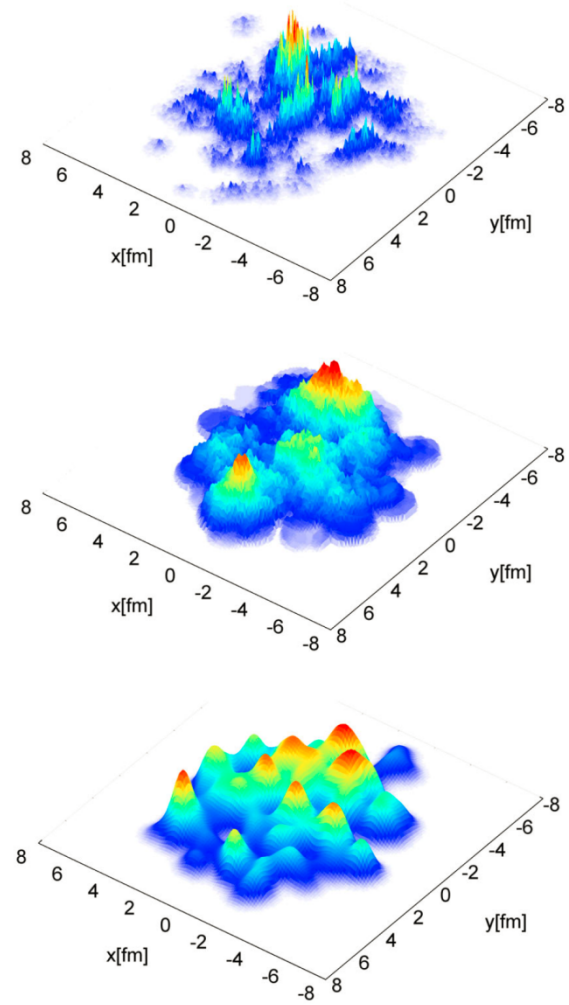


Highly coherent colored fields:
Stringlike in longitudinal direction
Stochastic on scale of inverse saturation momentum in transverse direction
Multiplicity fluctuates as negative binomial distribution

# The Glasma:

Weak coupling but strongly interacting due to coherence of the fields
In transport or classical equations, the coupling disappears!
Two scales

$$\Lambda_{coh}(t_{in}) \sim \Lambda_{UV}(t_{in}) \sim Q_{sat}$$

But it takes time to separate the scales and make a thermal distribution

$$\Lambda_{coh}(t_{therm}) \sim \alpha_s \Lambda_{UV}(t_{therm}) \sim \alpha_s T_{init}$$

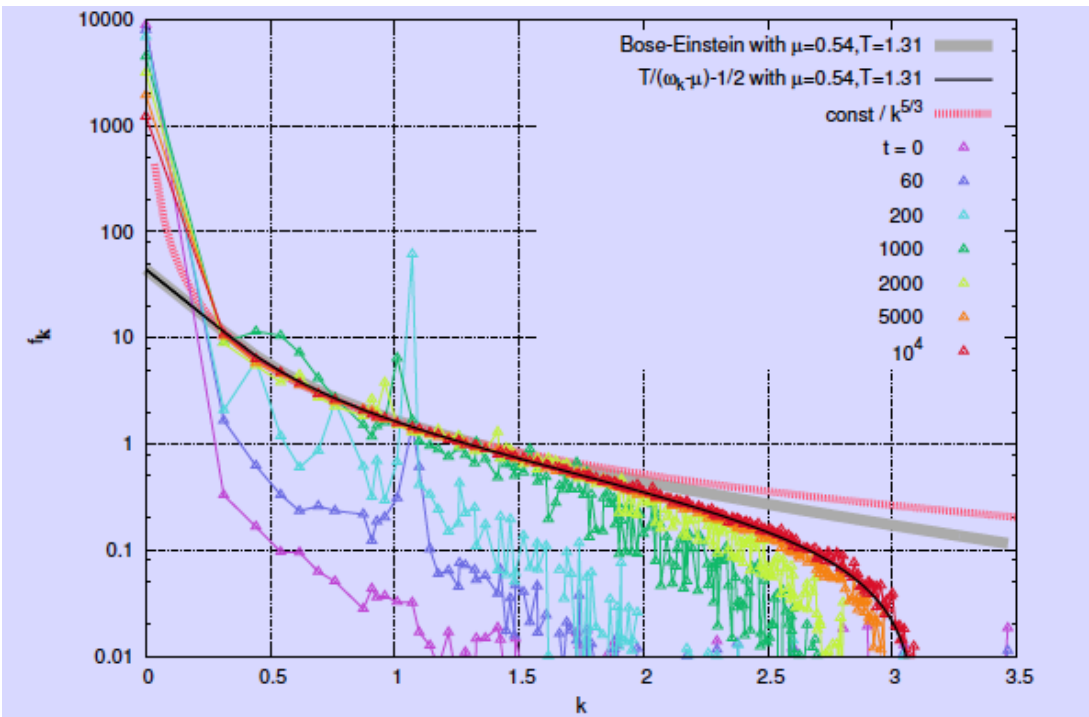


How long does it take to thermalize?

Are there Bose-Einstein Condensates formed?

For how long is the system in homogeneous with longitudinal pressure not equal to transverse?

Can we measure a difference between longitudinal and transverse pressure?

Gelis: Scalar field

Order parameters: Electric and magnetic confinement

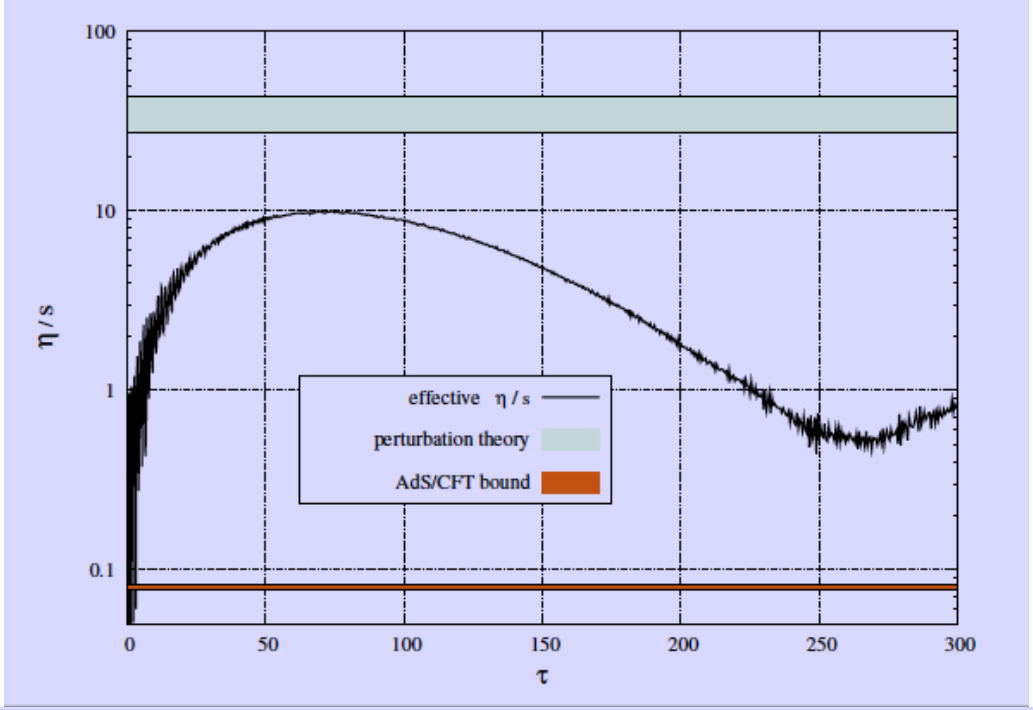


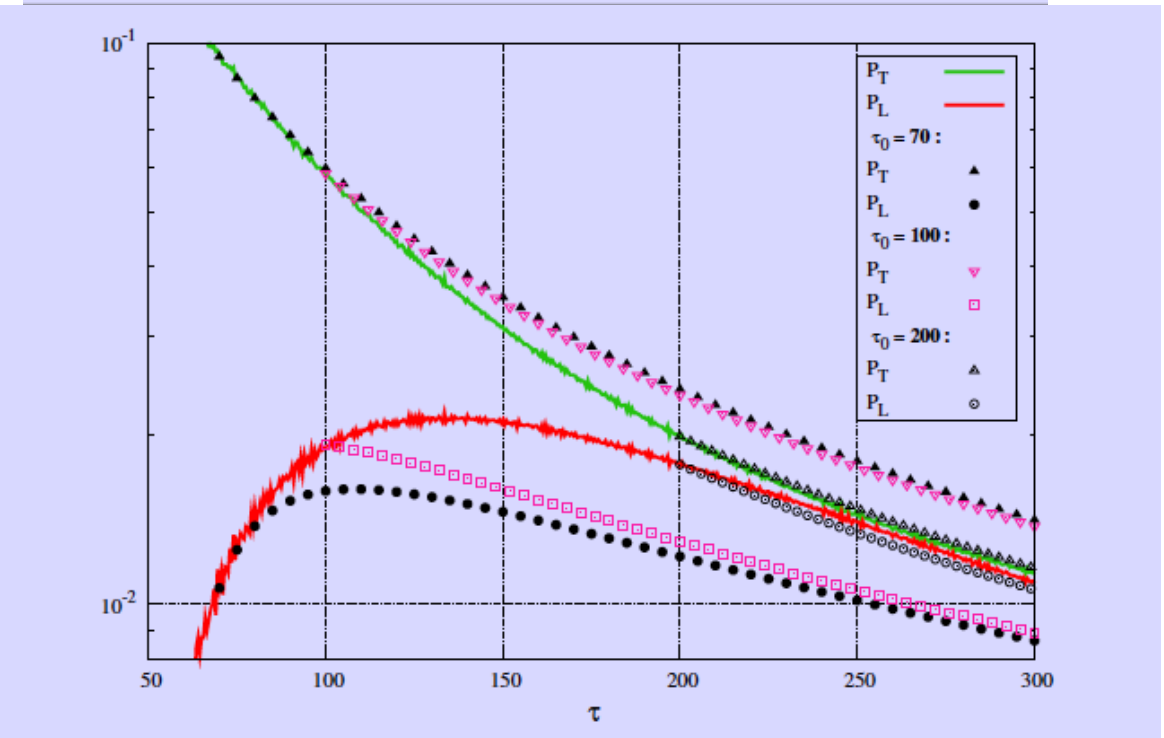


In scalar field theory:

Smallish viscosity

Eventual equilibration of longitudinal and transverse pressure

Longish time for thermalization

Yang Mills theory with realistic numbers?

What condenses?

The Glasma and turbulent coherent fields is generically a new type of matter:

There may be genuinely new phenomenon associated with electric and magnetic confinement and perhaps superfluidity

Vacuum ~ Turbulent Fluctuations?

# Holographic description of a boost invariant plasma

(Heller, Janik, Witaszczyk, 2011)

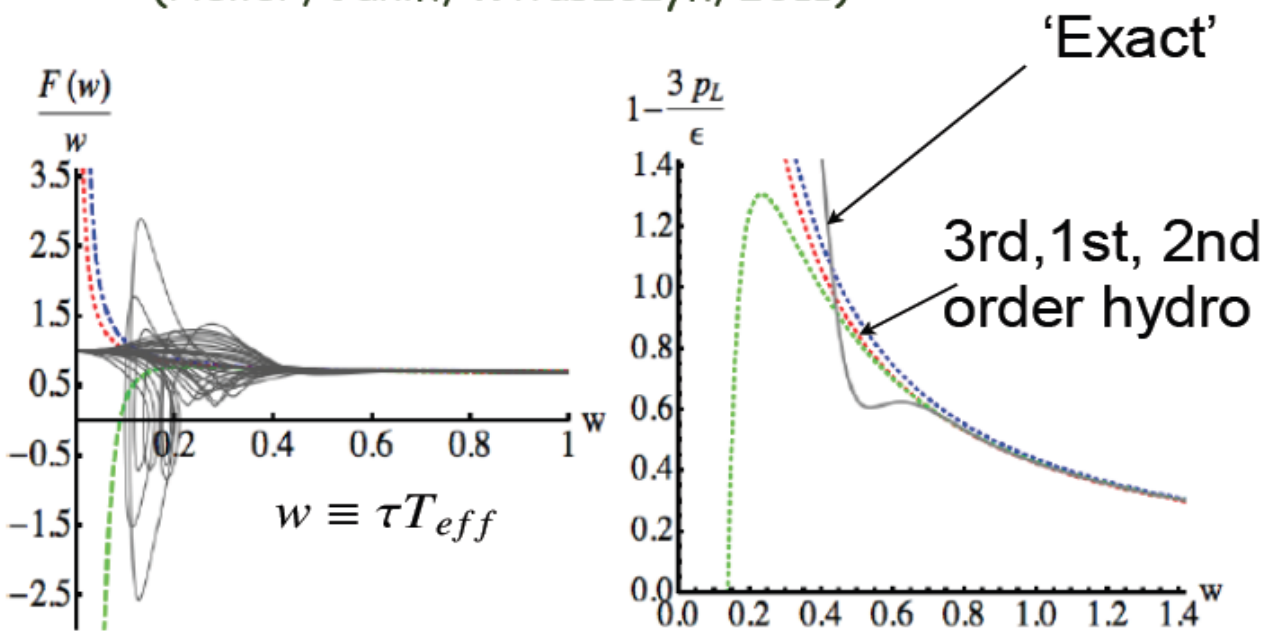


Viscous hydro can cope with partial thermalization, and large differences between longitudinal and transverse pressures

In fact, there is little experimental evidence that complete local equilibrium is reached in nuclear collisions

---

The Glasma may be a nearly perfect fluid, even though it is not a thermalized sQGP. It is certainly a sQGP

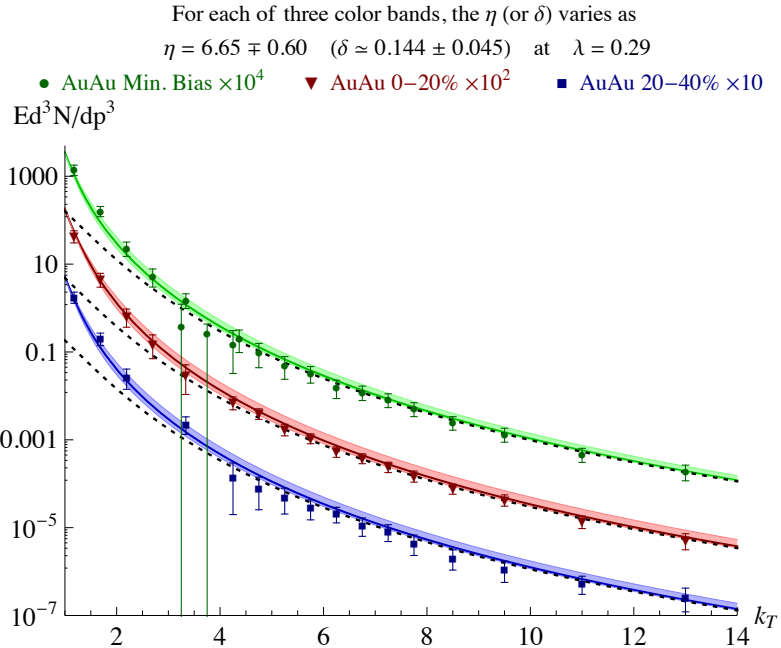


Photon excess in Phenix as function of centrality and pT

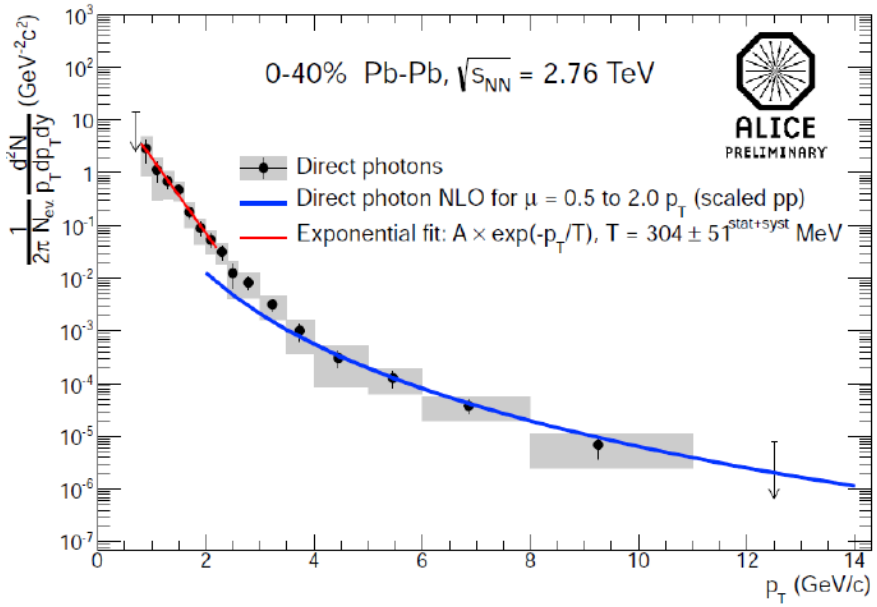


Similar photon excess seen in Pb-Pb at Alice

Confirmed
High pT suggests photons comes from early time
V2
and
geometric scaling of multiplicity dependence seen in Phenix
suggest photons did not arise from a very hot thermalized QGP

Large Flow seen in both Phenix and Alice

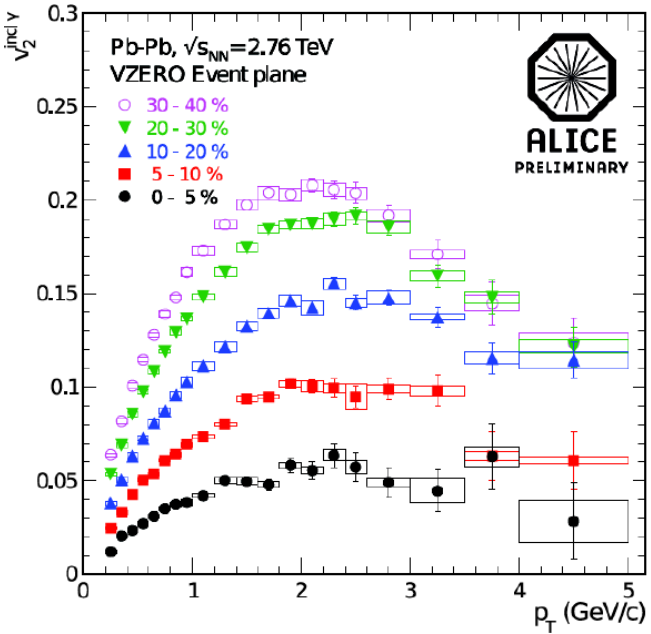

Geometric scaling of photon distributions:

$$\frac{1}{\sigma}\frac{dN}{d^2p_T} = F(Q_{sat}/p_T)$$

$\sigma$ Is the geometrical overlap area $\sim N_{part}^{2/3}$

$$Q_{sat} \sim N_{part}^{1/3}\,(\Lambda_{QCD}/p_T)^{\lambda} \qquad \lambda \sim .3$$

Power law fit to pT spectrum give a power of about 8, and therefore roughly a N_{part}^2 dependence on centrality
Fit is shown on previous figure

Rate for Glasma emission is

$$\frac{dN}{d^4x dy d^2k_T} = \frac{\alpha}{\pi}\Lambda_s \Lambda g(E/\Lambda)$$

Can fold together with expected power law evolution of ultraviolet and infrared scales, and power law found in data is not unreasonable, given current uncertainty in Glasma evolution, Find a power law behaviour

In the Glasma,

$$N_{gl} \sim \Lambda_s \Lambda^2 / \alpha_s$$

$$N_{quark} \sim \Lambda^3$$

At thermalization

$$\alpha_s \Lambda = \Lambda_s$$

Initially, gluons dominate but at thermalization the number of quarks is of the order of the number of gluons

Some enhancement of flow but probably not enough

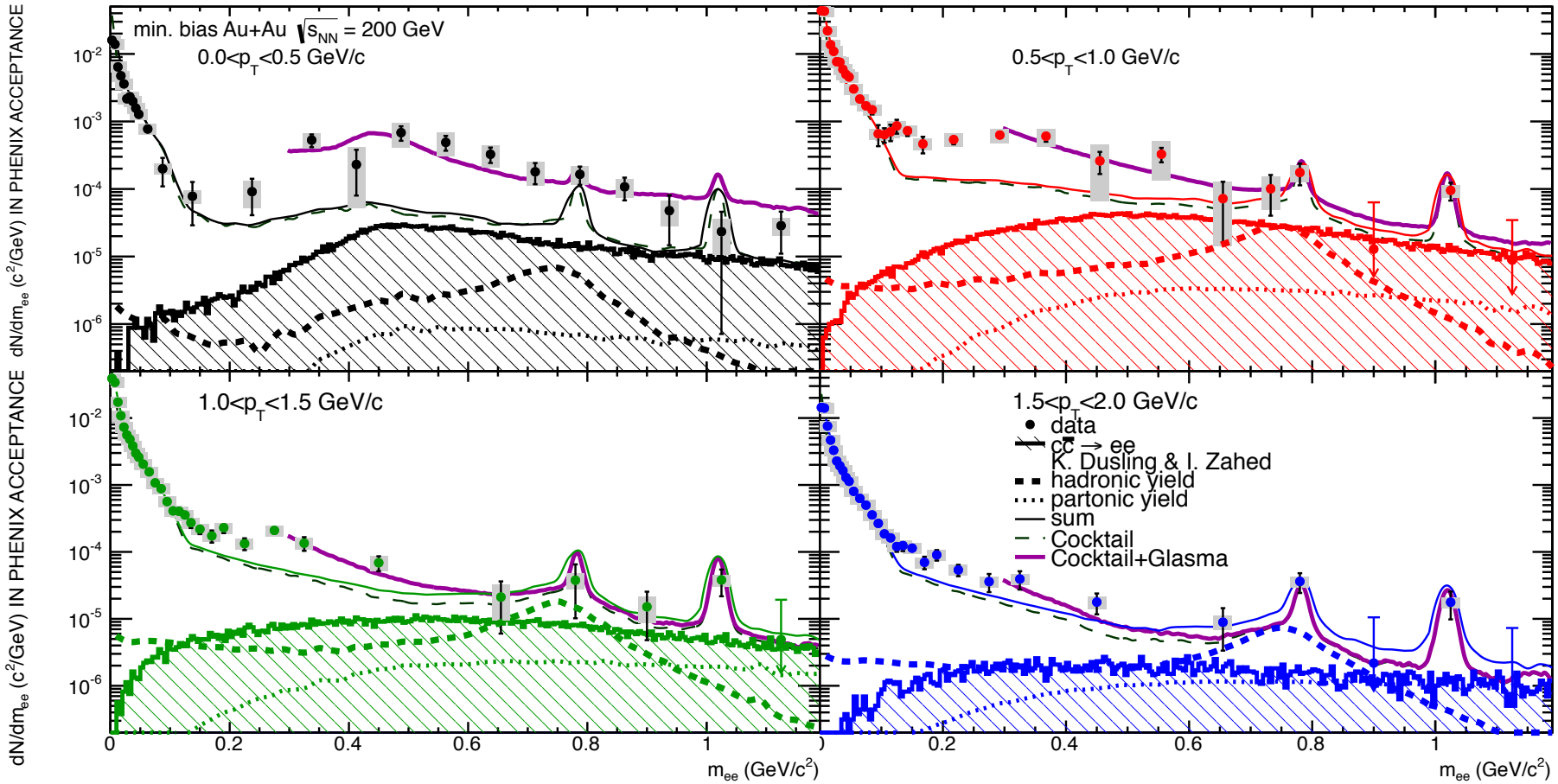


Phenix measures a large enhancement at small p_T in intermediate mass range

Star has small enhancement, not greatly enhanced for small pT. Star result probably can be explained by oridnary emission processes from either a Glasma or thermalized QGP

What would we need to do in order to get an enhancement at low p_t from the Glasma

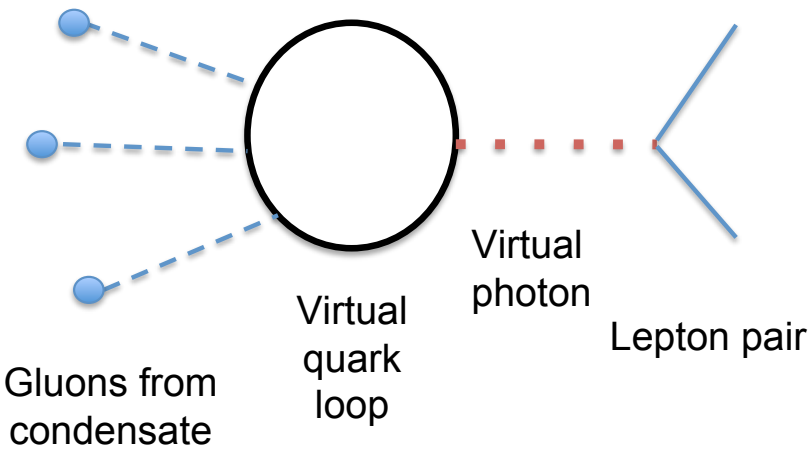


Decay from a gluon condensate?

Low pT is naturally enhanced

(Could also be any condensate as well)

Naturally get the power law mass dependence needed to fit the dilepton data

Centrality dependence?

Summary:

The photon date is inconsistent with a thermal explanation
Glasma is natural candidate at high pT of photons, and naturally explains features of the data, but photon flow is a common problem

Star vs Phenix for dileptons must be sorted out. If Phenix is correct and dileptons have a strong enhancement at low pT, some sort of condensation phenomenon is suggested opf which the Glasma provides candidate

# Hydrogen-like Atoms
## from Ultrarelativistic Nuclear Collisions

Ágnes Mócsy
Pratt Institute, BNL

Thermal Radiation Workshop, BNL
December 5-7 2012

amocsy@pratt.edu

# H-like Atoms

- Coulomb bound-sates: hadron π, K, p nucleus captured a lepton e, μ

- πμ observed in $K_L$ decays at BNL 1976 and Fermilab 1982

M. Schwartz et al. PRL37(1976)249

S.H. Aronson et al. PRL 48(1982)1078

- pμ used as precision tool for fundamental physics: proton size 2010

Pohl et al. Nature 466 (8 July 2010) 09250

# H-like Atoms in HIC

## Discovering Exotics: Antimatter Muonic Hydrogen ?!

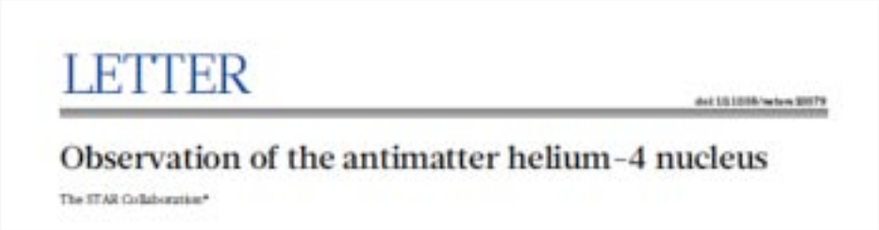
LETTER

Observation of the antimatter helium-4 nucleus

The STAR Collaboration*

# H-like Atoms in HIC

## Discovering Exotics: Antimatter Muonic Hydrogen ?!

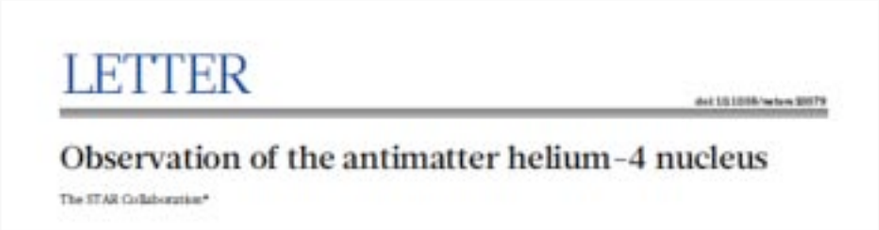
LETTER

Observation of the antimatter helium-4 nucleus

The STAR Collaboration*

## Direct Measurement of Single Lepton Spectrum

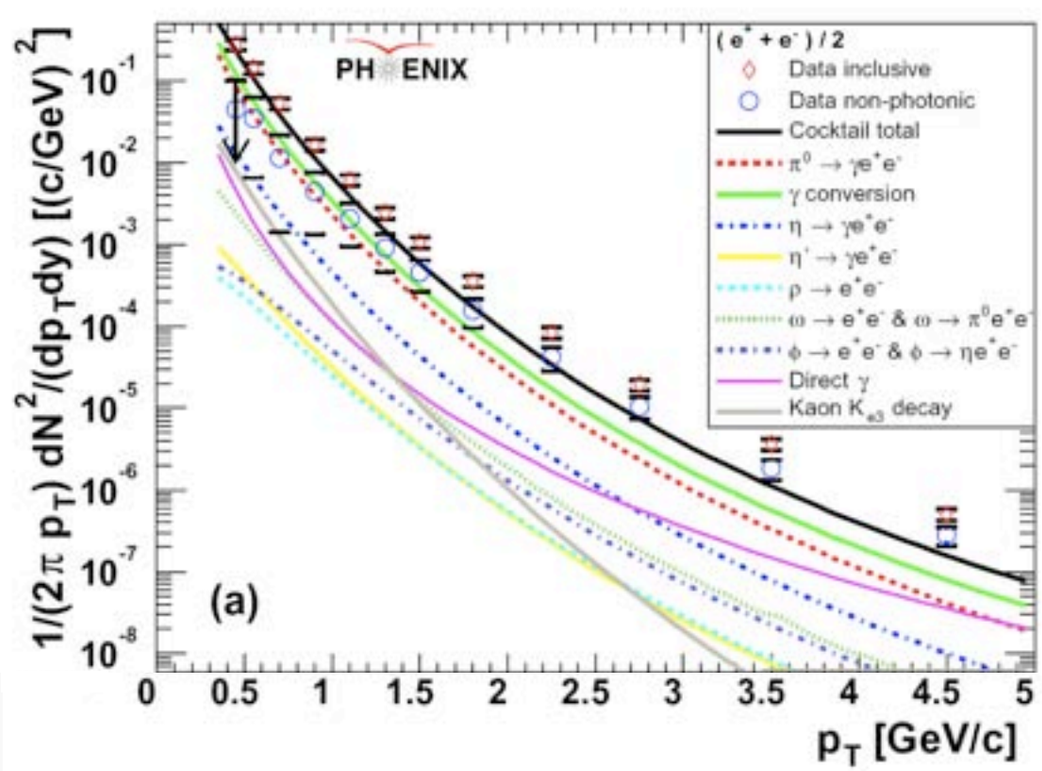


The shine of the QGP is buried in the background

Measure the distribution of atoms formed by the binding of directly produced leptons to charged hadrons emerging from the final state of a nuclear collision

PHENIX.Phys. Rev. Lett. 96, 032301 (2006)

M. Schwartz (early 1990's, unpublished)

amocsy@pratt.edu

# Ångstrom-Scale Muon Detectors

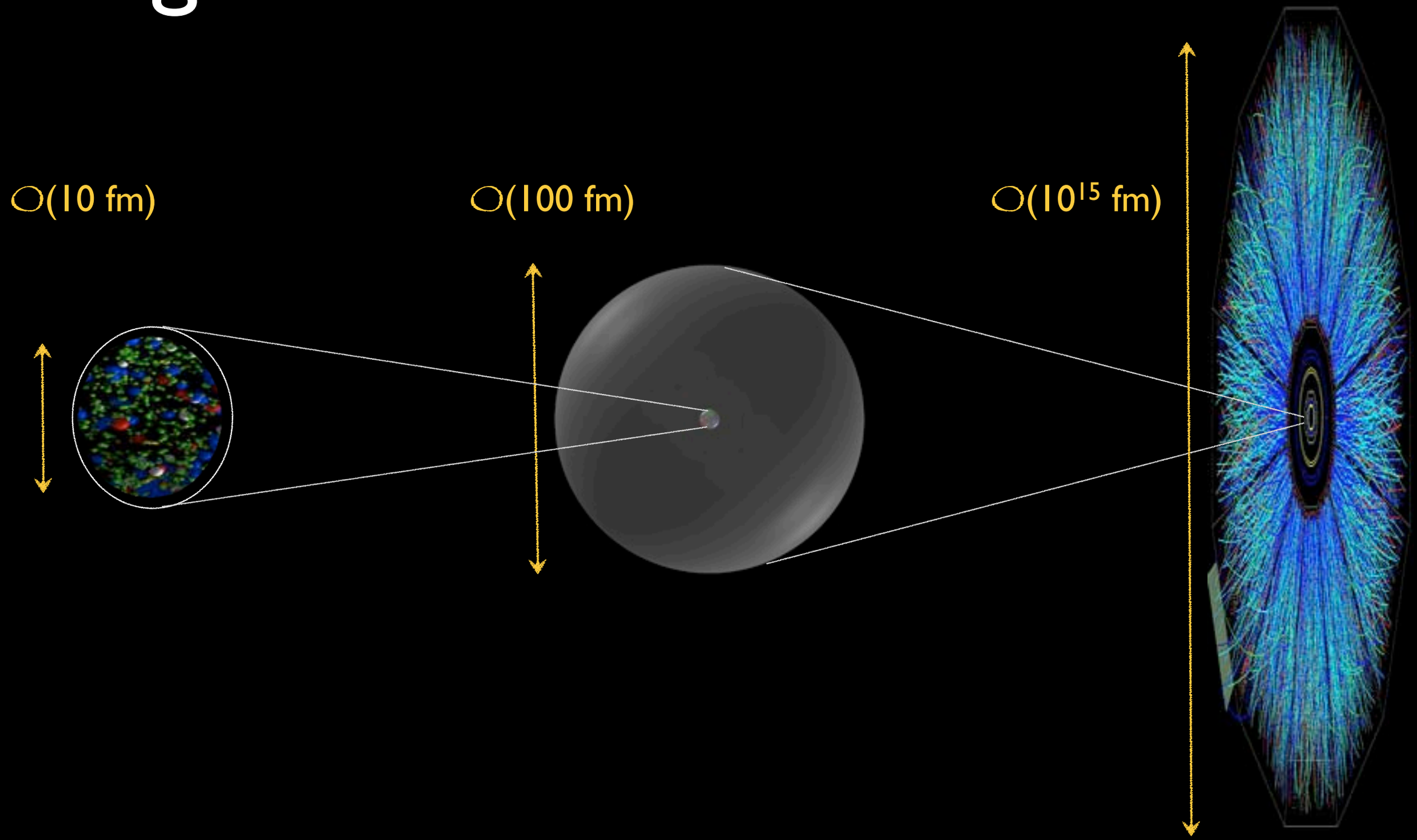


Atoms form after freeze-out

Background produced far from collision zone

amocsy@pratt.edu

# Production Rate

$$\frac{dN_{\text{atom}}}{dy d^2 p_{\perp,\text{atom}}} = 8\pi^2 \zeta(3) \alpha^3 m_{\text{red}}^2 \frac{dN_h}{dy d^2 p_{\perp,h}} \frac{dN_l}{dy d^2 p_{\perp,l}}$$

G. Baym et al. PRD 48 (1993) R3957

- Atom yield depends strongly on the shape of lepton and hadron spectra
- Atoms form only if lepton and hadron are close in phase-space:

$$\frac{p_t^{atom}}{m_{atom}} = \frac{p_t^{lepton}}{m_{lepton}} = \frac{p_t^{hadron}}{m_{hadron}}$$

- Atom production estimated

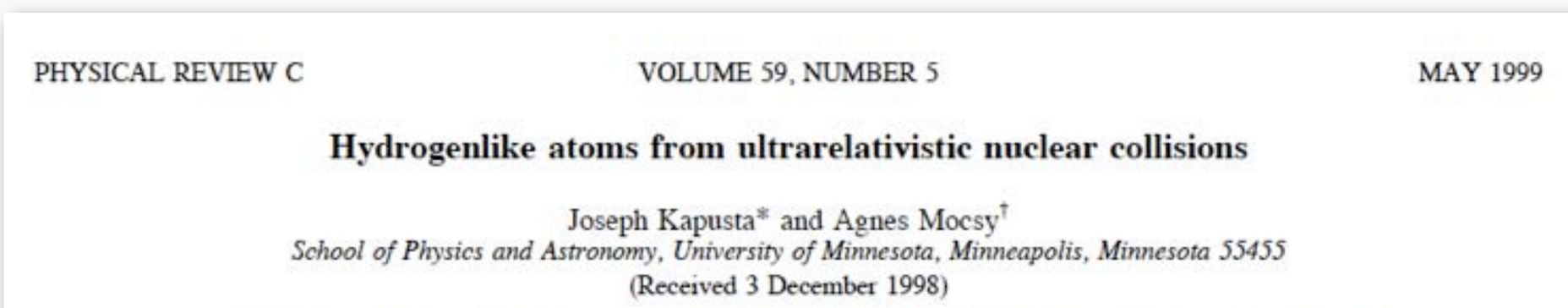
PHYSICAL REVIEW C VOLUME 59, NUMBER 5 MAY 1999

**Hydrogenlike atoms from ultrarelativistic nuclear collisions**

Joseph Kapusta* and Agnes Mocsy†

*School of Physics and Astronomy, University of Minnesota, Minneapolis, Minnesota 55455*

(Received 3 December 1998)

# Spectra & Yield estimates from 1998

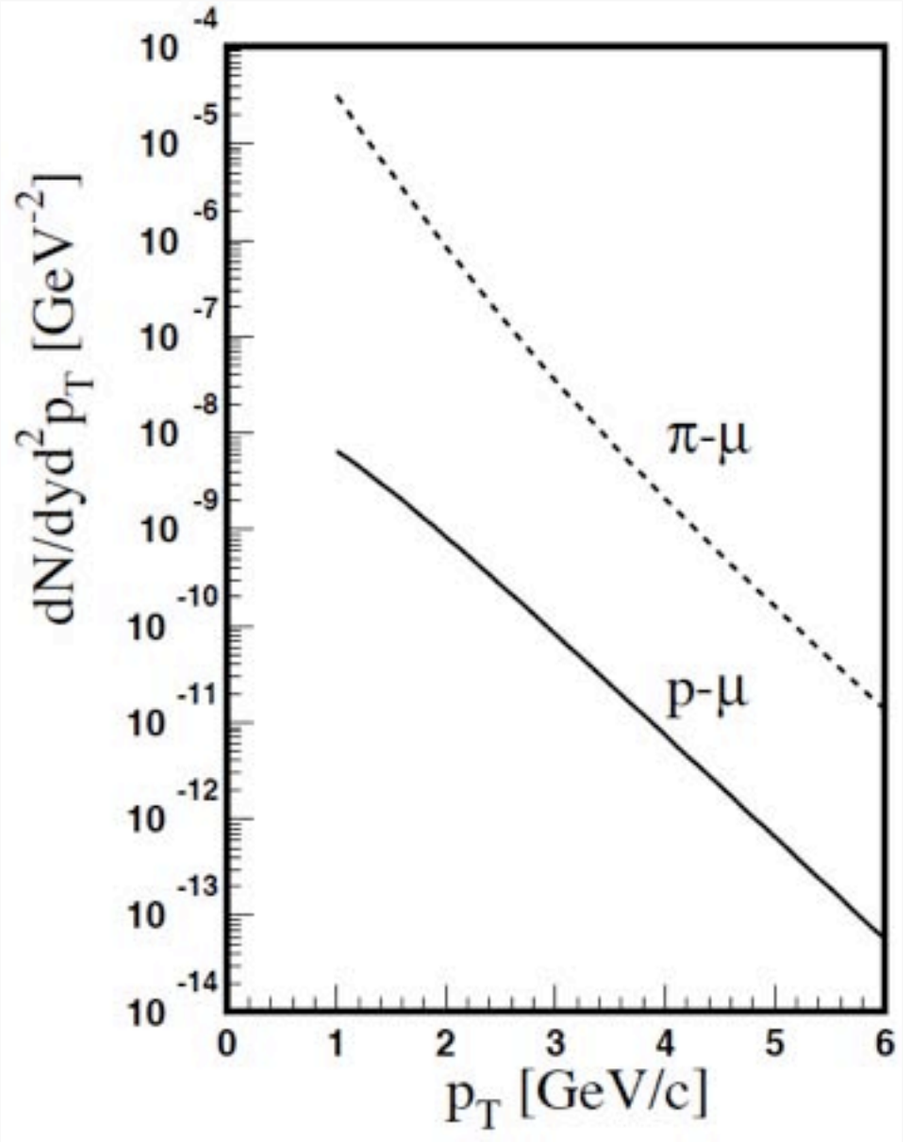


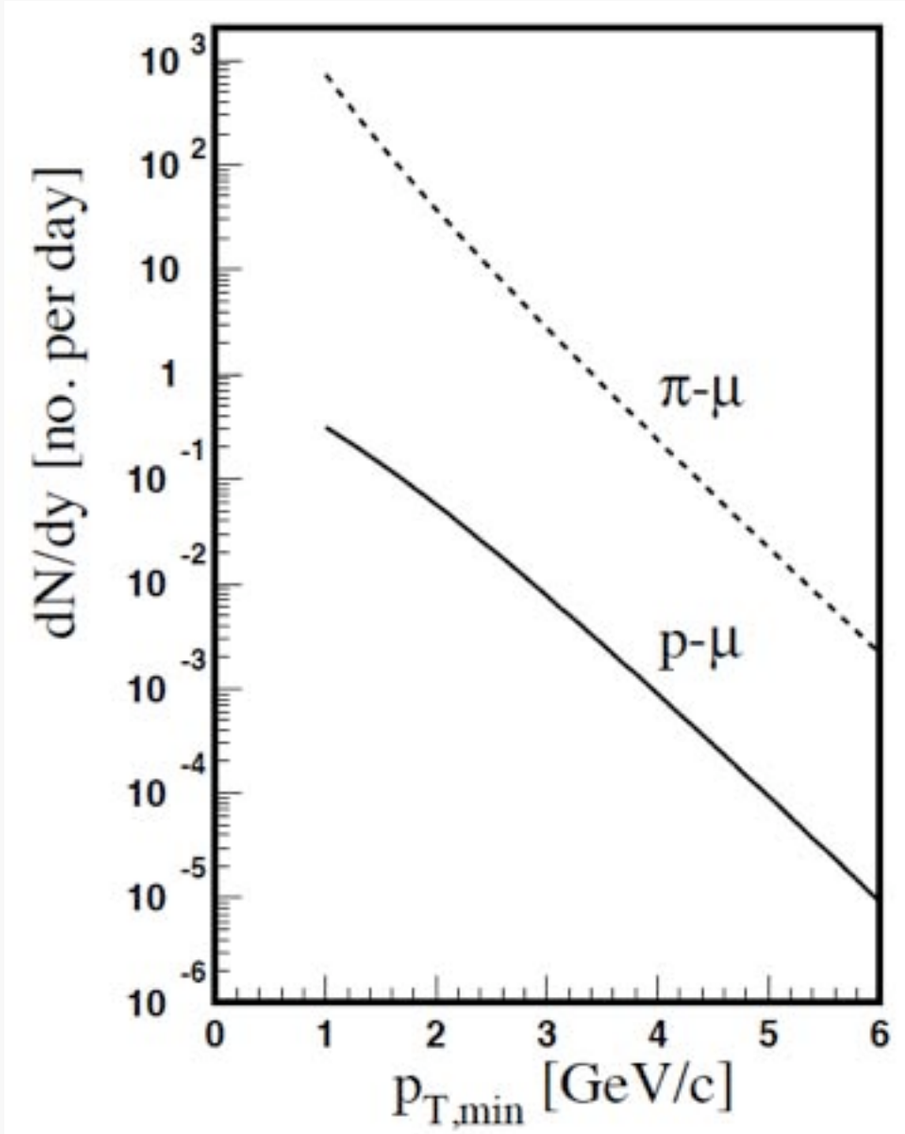


J.Kapusta, A.Mocsy PRC 59 (1998) 2937

Based on estimated luminosity of $2 \times 10^{26}$ $cm^{-2}s^{-1}$

~ 1000 $\pi\mu$ per unit rapidity per day with $p_T > 1$GeV/c

# Updates

estimates from 2011

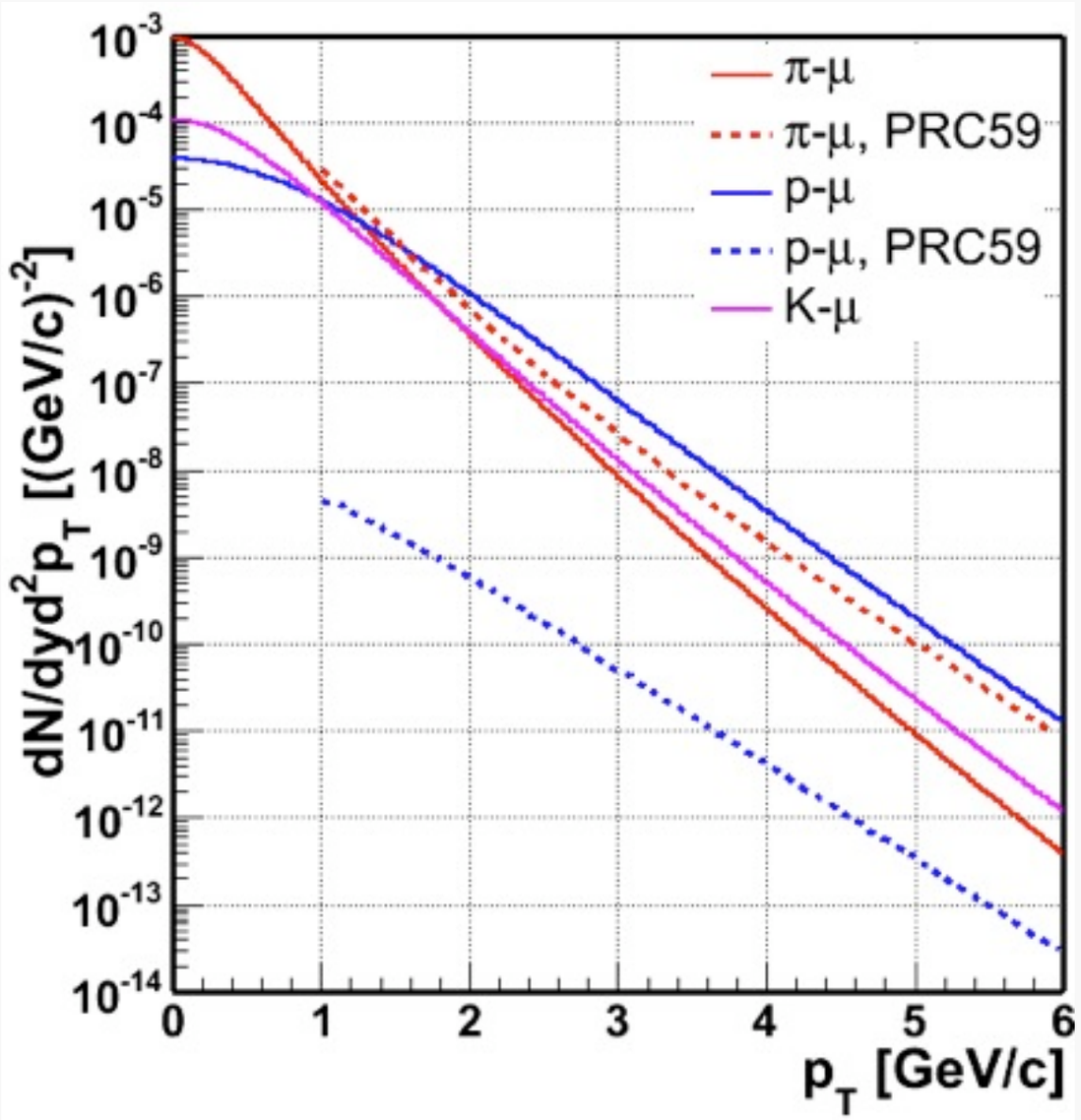


New estimates using
- measured hadron spectra
- μ spectra from π spectra scaled by $(\alpha/\alpha_s)^2$

πμ shows good agreement

Old pμ estimates are well below the new ones

Zhangbu Xu et al 2011

# Feasibility in STAR

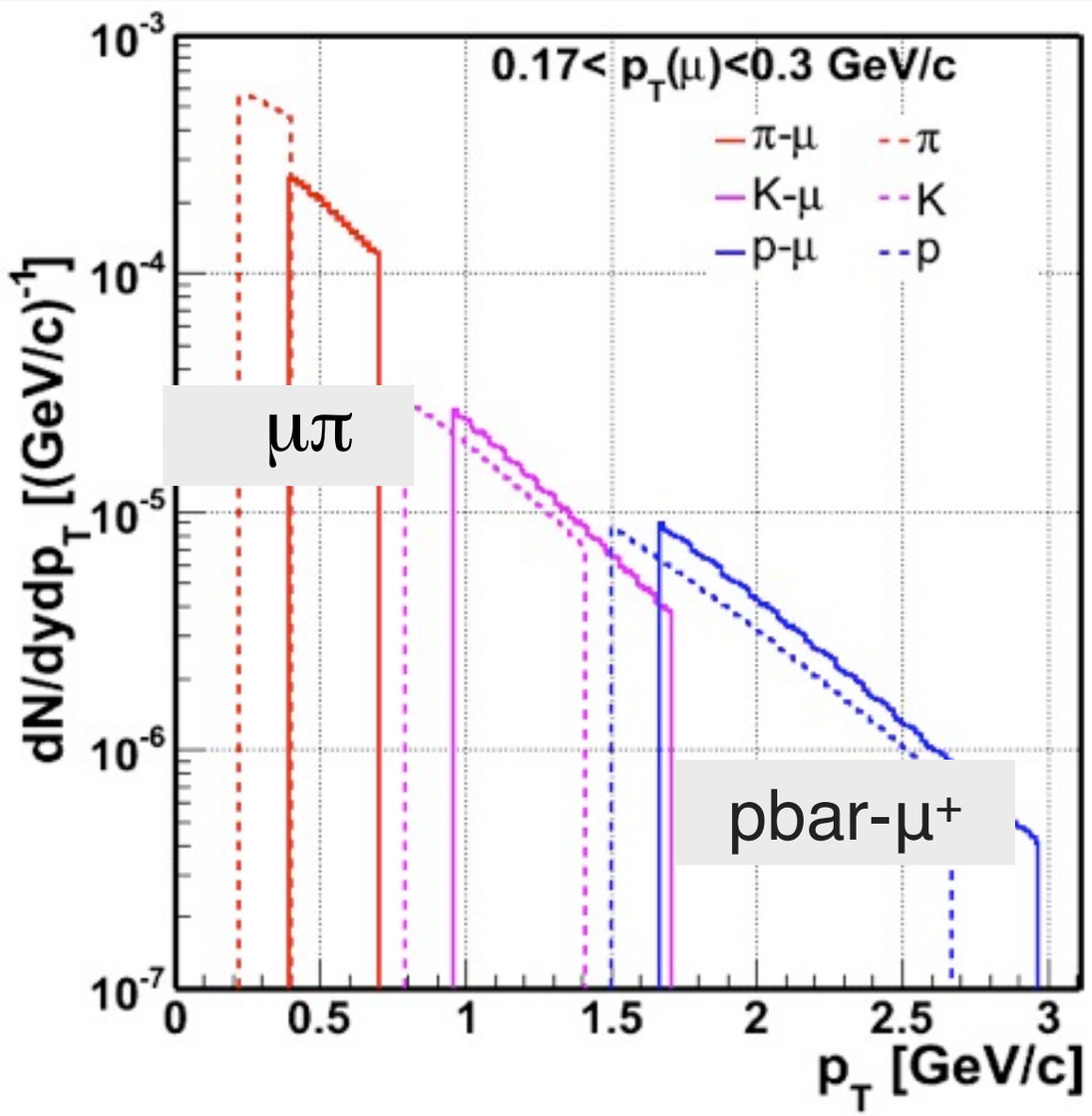


Muons can be identified at low $p_T$

$$0.17 < p_T < 0.3 \text{ GeV/c}$$

In 500M central events (one run):

500 never before observed anti-muonic-hydrogen

22k $\pi\mu$ atoms

Zhangbu Xu et al 2011

$$\mathbf{p}_{\perp,\text{atom}}/m_{\text{atom}} = \mathbf{p}_{\perp,h}/m_h = \mathbf{p}_{\perp,l}/m_l$$

# Feasibility in STAR

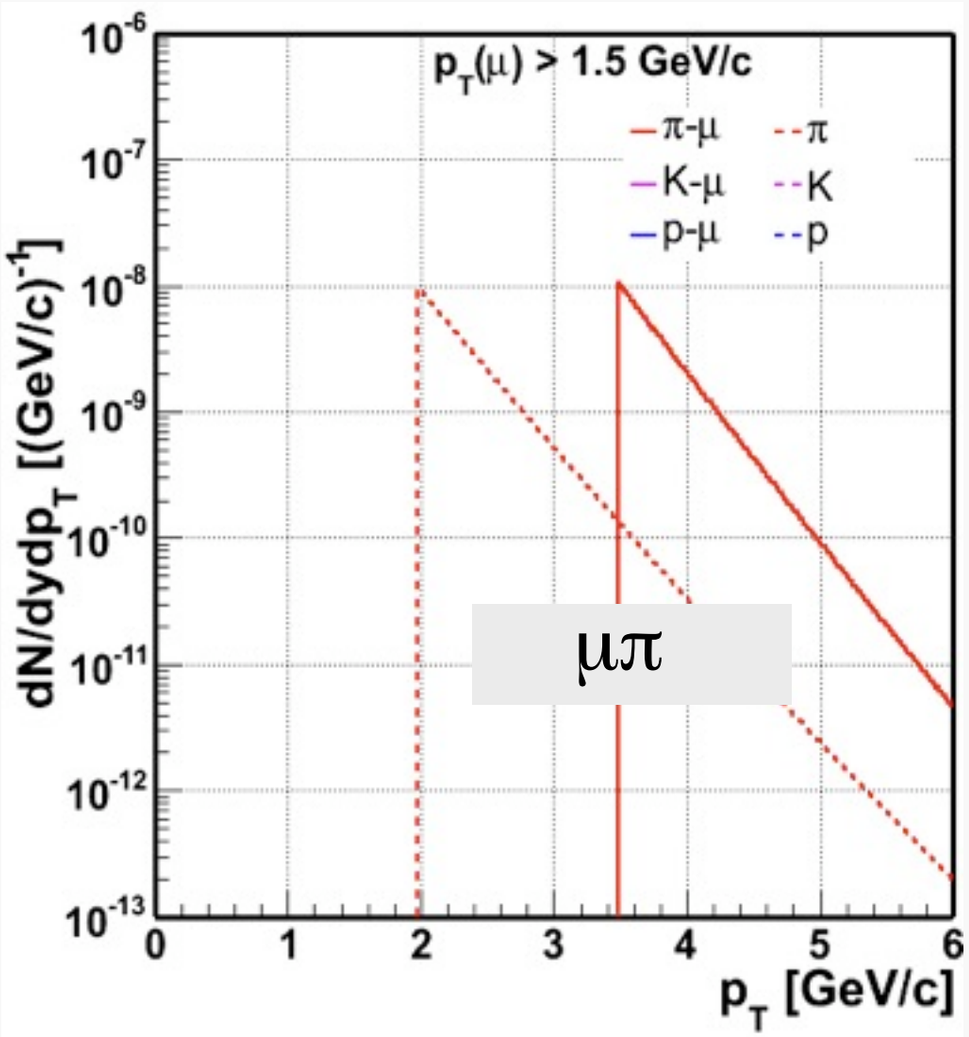


Zhangbu Xu et al 2011

Detector upgrades MTD will be used to trigger on high $p_T$ muons

With RHICII Luminosity in a 12 week run:

~200 $\pi\mu$ atoms w $p_{T,\mu} > 1.5$ GeV

Rates are accessible!

In conclusion, we have reinvestigated the rates for the production of hydrogenlike atoms at RHIC. The results are quite promising for their experimental detection. It remains to be seen whether an efficient detector can be designed to observe them.

J. Kapusta, A. Mocsy PRC 59 (1998) 2937

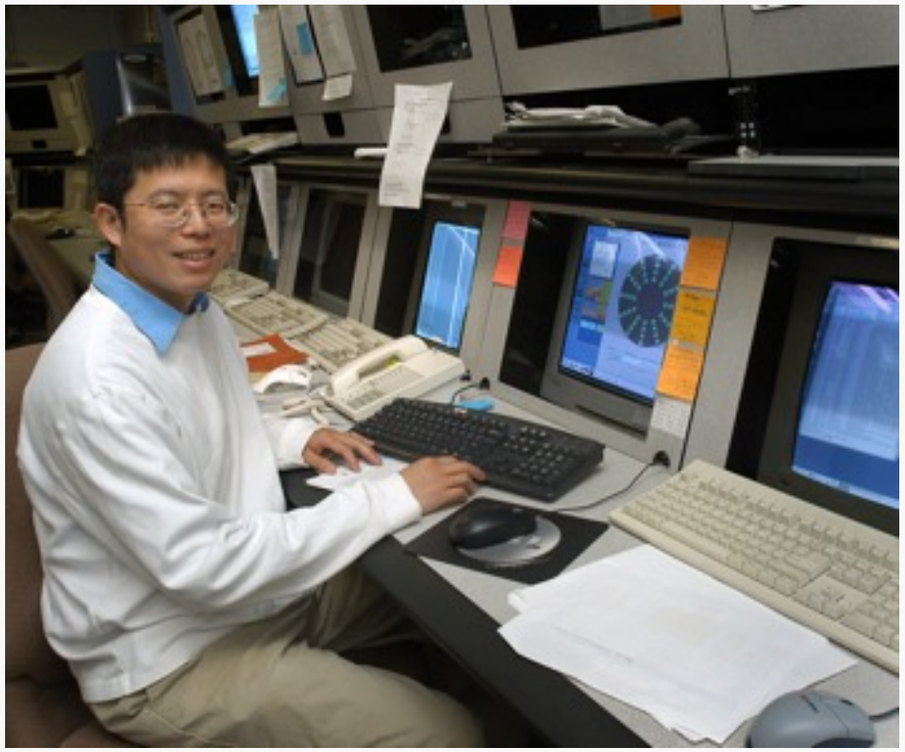

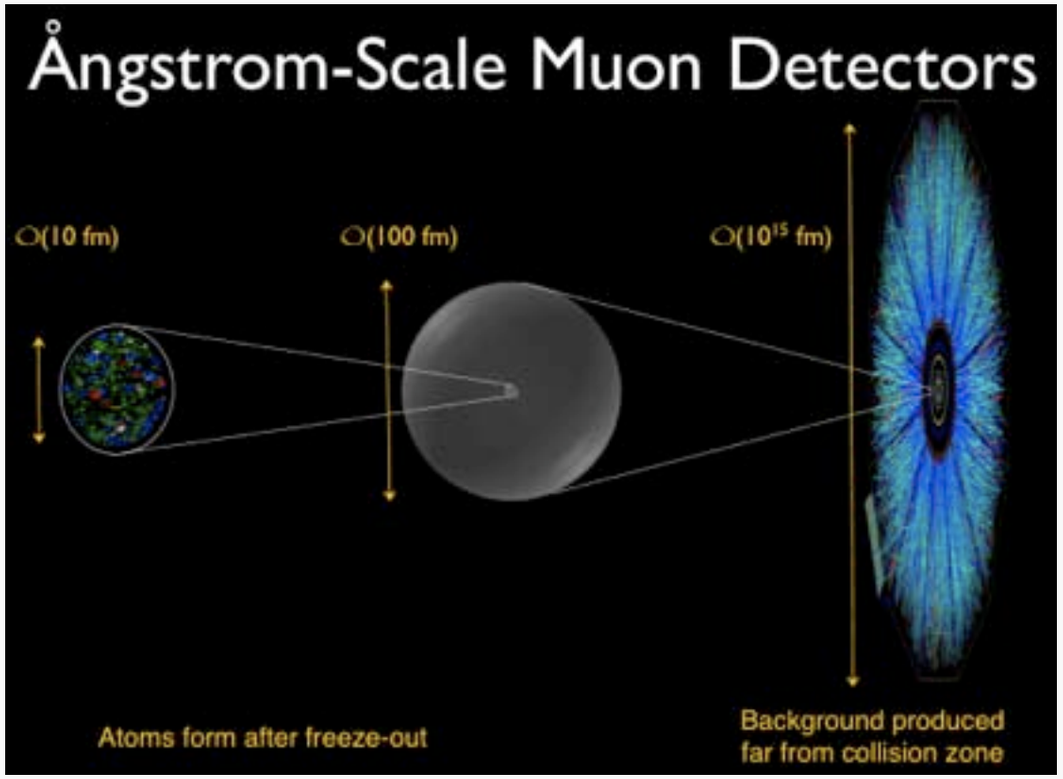


- STAR: they can be measured
  - provides information on the direct lepton spectrum
  - possible discovery of new particle: anti-matter muonic hydrogen!
- What about at the LHC?
- Theory revisited in collaboration with Mauricio Martinez & Liliana Apolinario (Santiago de Compostella)

# The End

# Thermal Photon Yield and Elliptic Flow in 200 GeV Au+Au Collisions from PHENIX

Richard Petti for the PHENIX Collaboration
Stony Brook University

Thermal Radiation Workshop

Brookhaven National Lab

12/6/2012

PHENIX

Stony Brook University

# Talk Overview

- Motivation for study
- Experimental Techniques at PHENIX
- Observation of Direct Photons
  - Direct Photon Elliptic Flow
  - Direct Photon Invariant Yield
- Summary and Future Outlook



PHENIX

Stony Brook University

# Motivation for Study

- Important global properties of the collision can be characterized by thermal photons
  - temperature
    - thermal photon $p_T$ spectra
  - $\tau_0$
    - thermal photon $v_2$
- A thermal photon puzzle
  - thermal photons expected to dominate at low $p_T$
  - direct photon spectra indicate thermal photons are emitted early
  - large direct photon $v_2$ indicate thermal photon emission is late
  - difficult to reconcile both with the current understanding of the evolution
  - possibly another source of low $p_T$ photons other than thermal?



PHENIX

Stony Brook University

# Experimental Techniques at PHENIX

- Large background from hadron decays makes analysis difficult
- 3 techniques at PHENIX
  - photons deposit energy into emcal
    - best at high momentum
  - external photon conversions
    - measure real photons
    - greatly reduce hadron contamination
  - internal photon conversions
    - measure virtual photons
    - reduce background from $\pi^0$ Dalitz decays

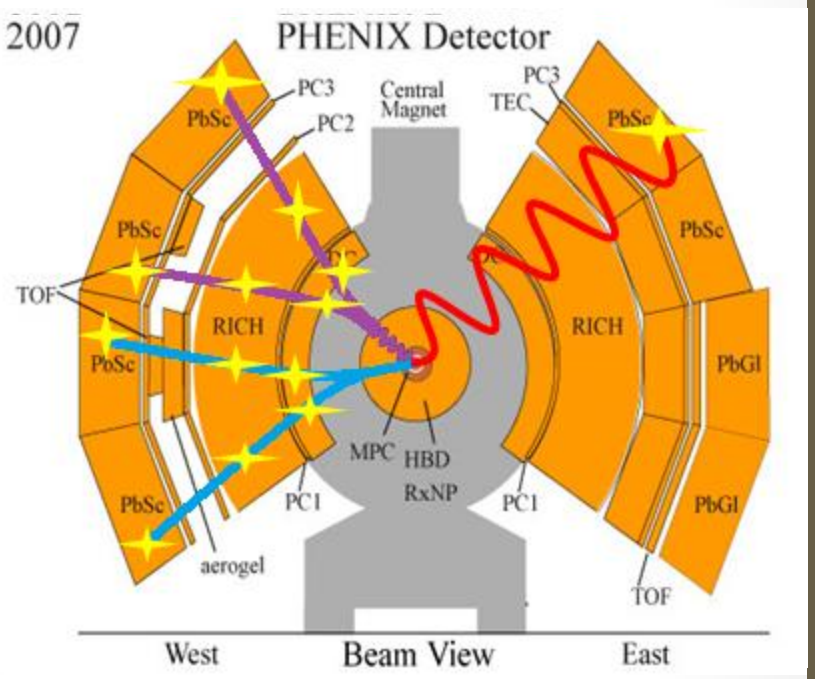

# We See Direct Photons in Collisions at RHIC: $R_\gamma$ Via External and Internal Conversions

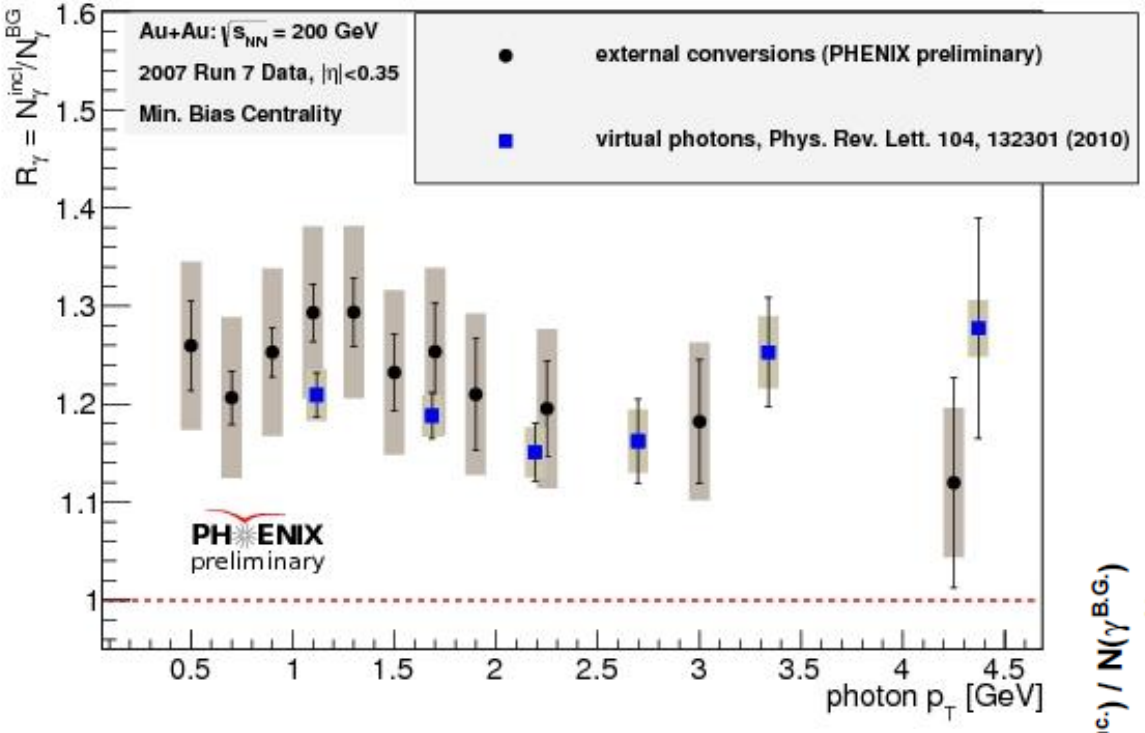


$$R_\gamma = N^{incl}/N^{BG}$$

Phys. Rev. Lett. 109, 122302 (2012)

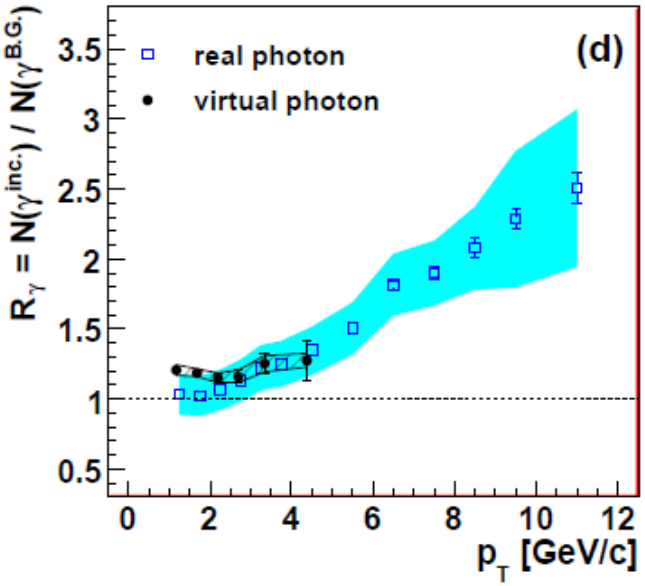

# Direct Photons In Different Systems

- PHENIX has measured low $p_T$ direct photon ratio in various collision systems, showing clear enhancement in A+A
- From virtual photon (internal conversion) analysis

$$r = 1 - 1/R_\gamma$$

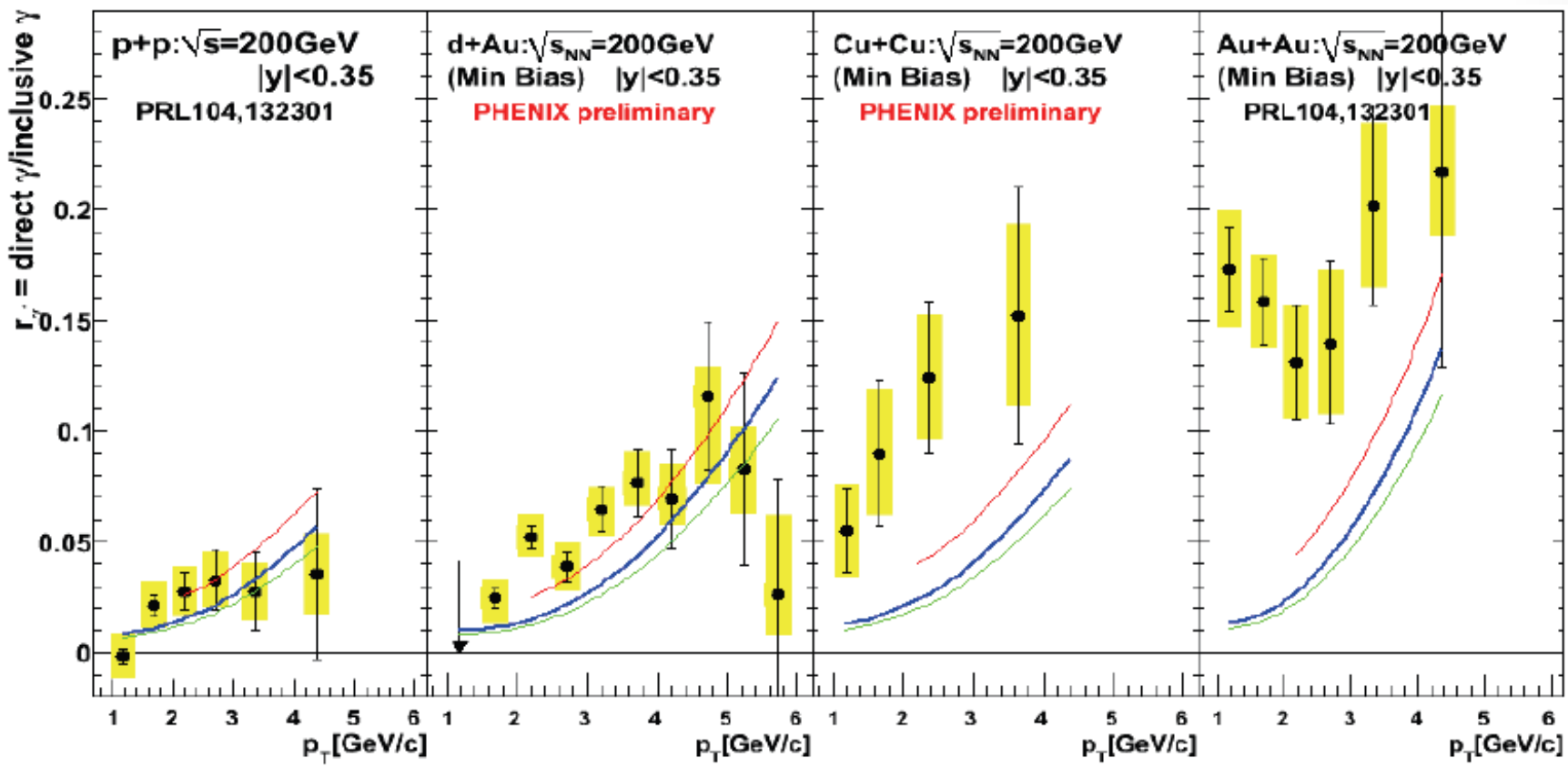

# $R_\gamma$ From Dilepton Techniques

- **External Conversions**
  - measure through a double ratio

$$R_\gamma = \frac{\gamma^{incl}(p_T)}{\gamma^{hadr}(p_T)} = \frac{\varepsilon_\gamma(p_T) f(p_T) \cdot \left( \frac{N_\gamma^{incl}(p_T)}{N_\gamma^{\pi^0 tag}(p_T)} \right)_{Data}}{\left( \frac{N_\gamma^{hadr}(p_T)}{N_\gamma^{\pi^0}(p_T)} \right)_{Sim}}$$

  - tag photons as coming from $\pi^0$ decays
  - other decays accounted for with a cocktail (as in the internal analysis)

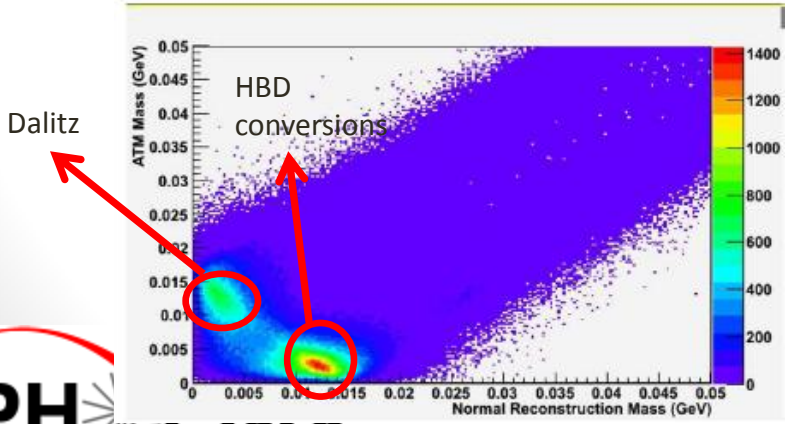


- **Internal Conversions**
  - observed excess in dilepton mass distribution attributed to virtual photons (at $p_T \gg m_{ee}$)
  - fit mass distribution with a two component fit
    - r is a floating fit parameter

$$f(m_{ee}; r) = (1 - r) f_c(m_{ee}) + r f_{dir}(m_{ee})$$

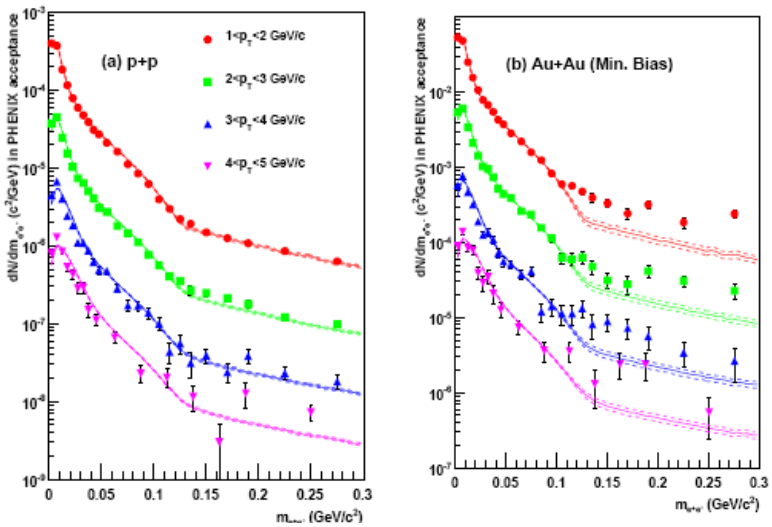


Phys. Rev. Lett. 104, 132301 (2010)

# Direct Photon Elliptic Flow

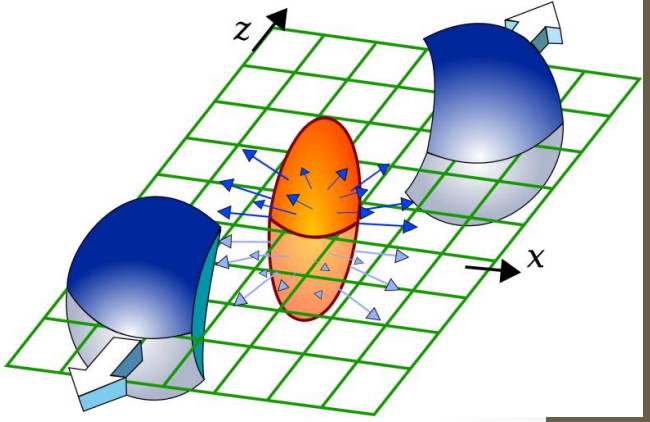


- PHENIX has measured the elliptic flow of direct photons using combinations of all three techniques

$$v_2^{dir.} = \frac{R_\gamma v_2^{inc.} - v_2^{BG}}{R_\gamma - 1}$$

- $R_\gamma$ is the fraction of direct photon, $\gamma^{incl}/\gamma^{hadron}$
- $v_2^{BG}$ is the $v_2$ of photons from hadron decays
- $v_2^{inc}$ is the measured $v_2$ of all photons

# Inclusive photon $v_2$

$$v_2^{dir.} = \frac{R_\gamma \boxed{v_2^{inc.}} - v_2^{BG}}{R_\gamma - 1}$$

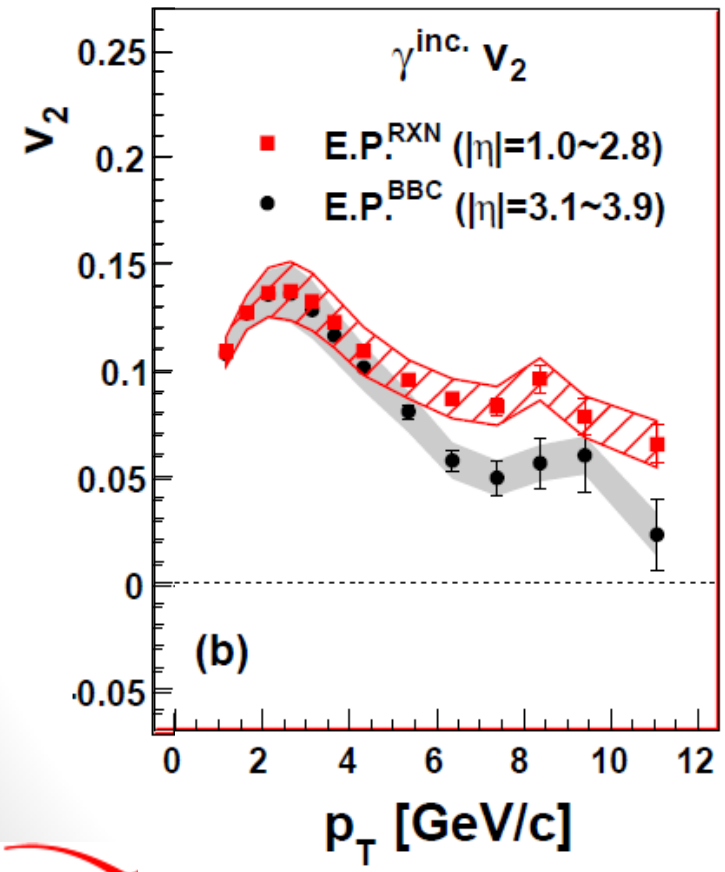


- Photons measured in the EMCal
- PID consists of
  - Shower shape cut
  - Charged track veto with PC
- Significant number of hadrons pass cuts below 6 GeV
  - up to 20% below 2 GeV deposited energy
  - Correct for this with GEANT sim

$$v_2^{\gamma,\mathrm{obs}} = \frac{v_2^{\gamma,\mathrm{meas}} - (N^{\mathrm{hadr}}/N^{\mathrm{meas}})v_2^{\mathrm{hadr}}}{1 - N^{\mathrm{hadr}}/N^{\mathrm{meas}}}$$

Phys. Rev. Lett. 109, 122302 (2012)

# Hadron contamination check

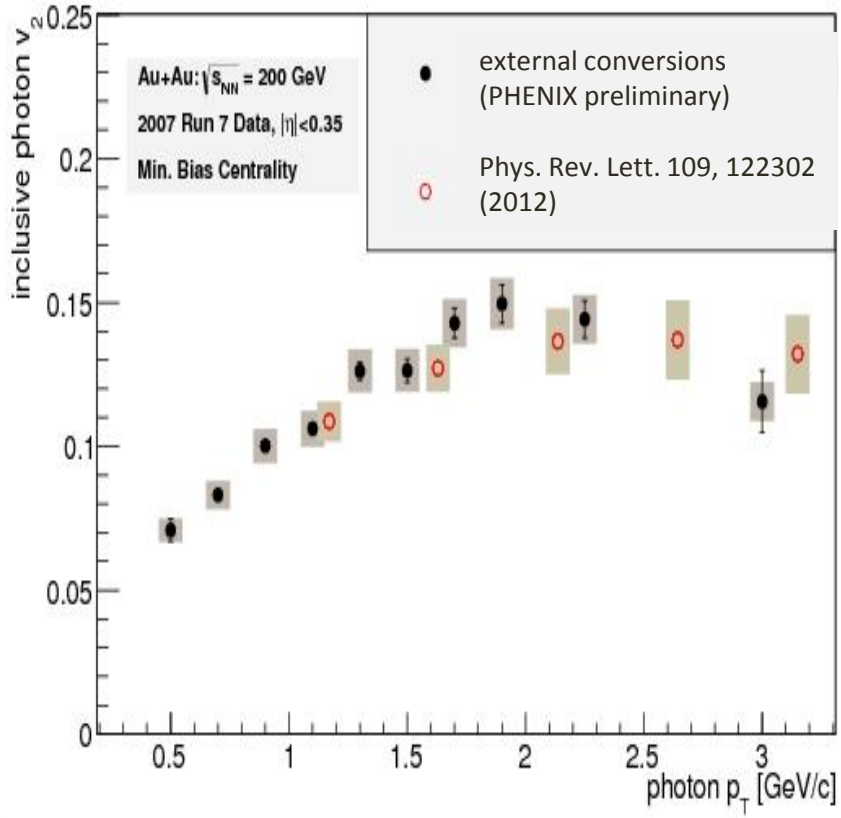


- Hadron contamination can be significant
- Check with an external conversion analysis
  - Identify photons via external conversions
  - No hadron contamination
- Two measurements are consistent
- Hadron contamination in the real photon (EMCal) measurement well understood

# Hadron Decay Photon $v_2$

- We only measure $\pi^0$ $v_2$
  - about 80% of BG
- Assume $v_2$ of other hadrons from $KE_T$ scaling
- $v_2$ modulation put into cocktail
- cocktail gives the total BG $v_2$ from decay photons

$$v_2^{dir.} = \frac{R_\gamma v_2^{inc.} - v_2^{BG}}{R_\gamma - 1}$$

Phys.Rev.Lett.98:162301,2007

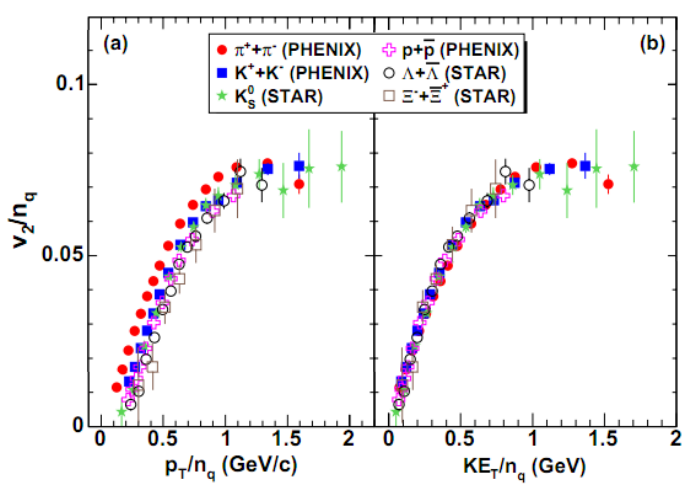


Phys. Rev. Lett. 109, 122302 (2012)

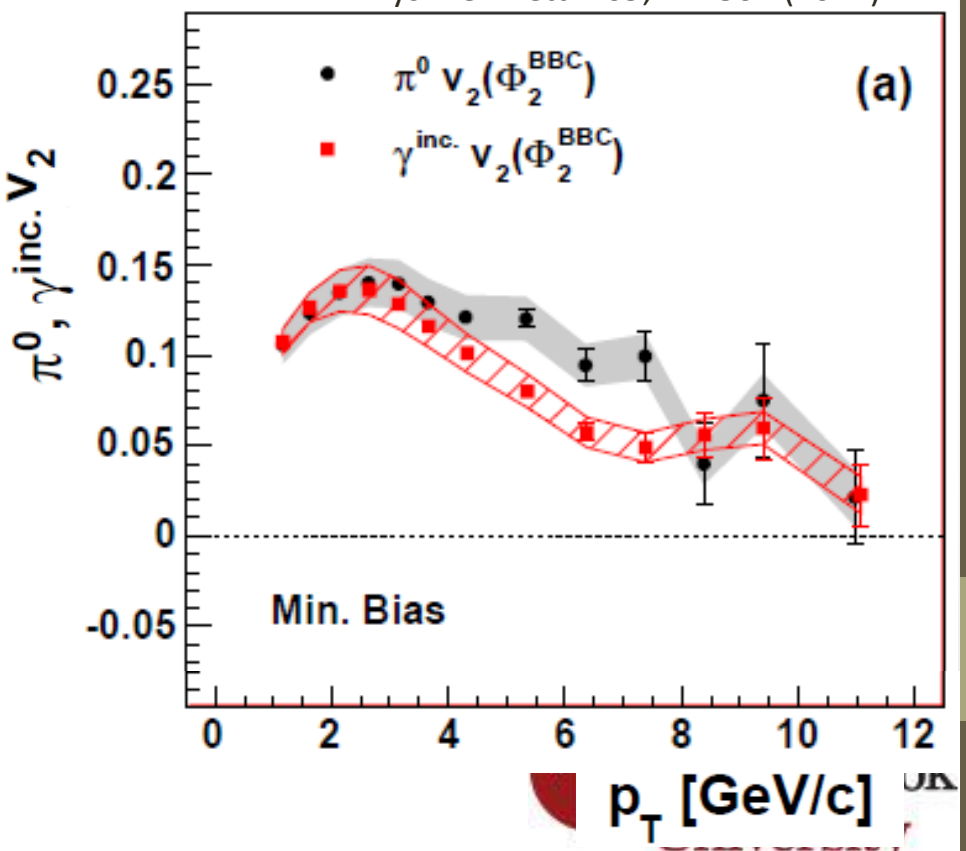

# Direct Photon Flow

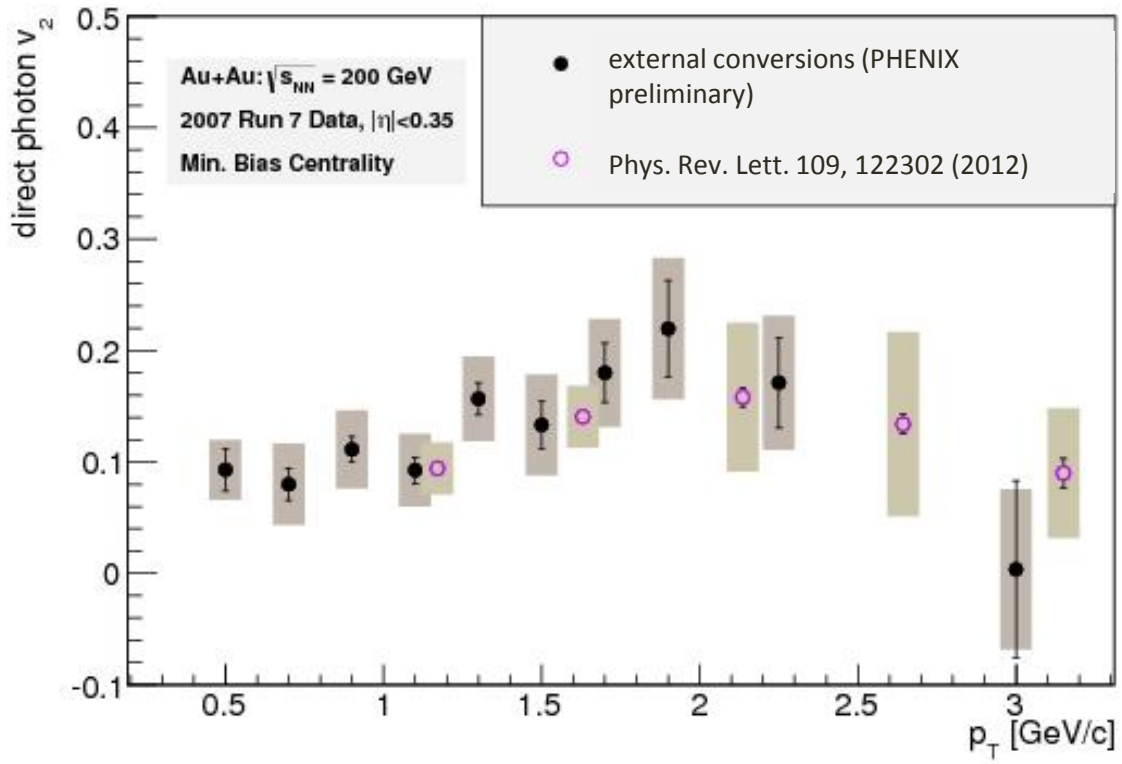


$$v_2^{dir.} = \frac{R_\gamma v_2^{inc.} - v_2^{BG}}{R_\gamma - 1}$$

# Direct Photon Invariant Yield

$$\gamma^{direct} = r\gamma^{incl}$$

- significant excess in low pT region compared to pQCD
- shape consistent with thermal emission
- fit yield with a two component function
  - pQCD power law
  - exponential
- Extract inverse slope parameter which is related to the temperature
  - T = 233±14±19 MeV in MB

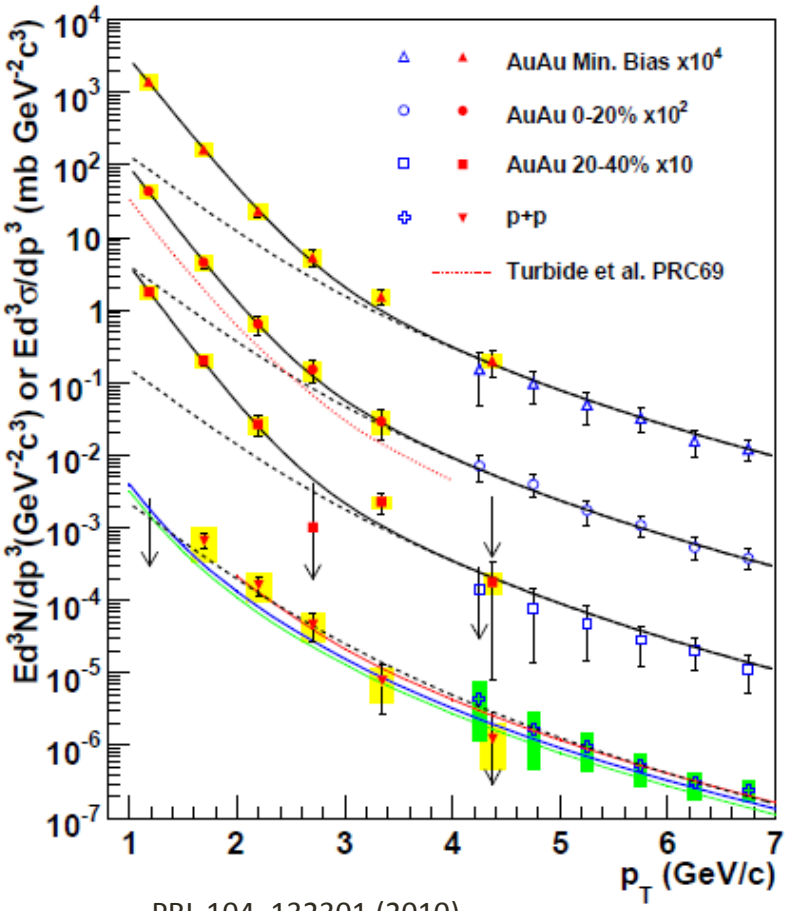


PRL 104, 132301 (2010)

# Comparing the Yield to Theory

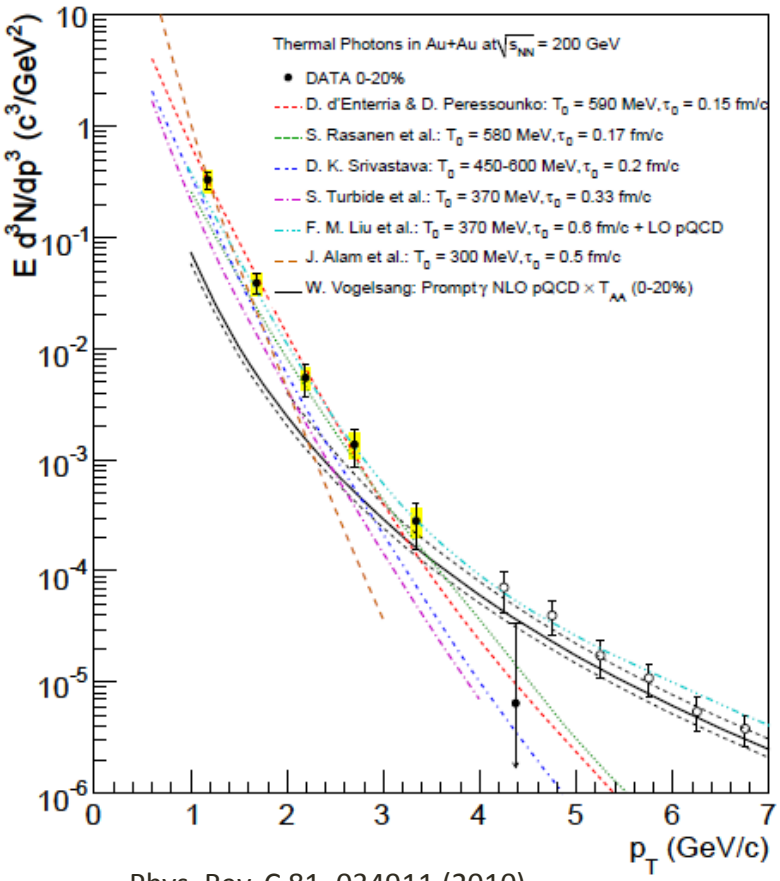


Phys. Rev. C 81, 034911 (2010)

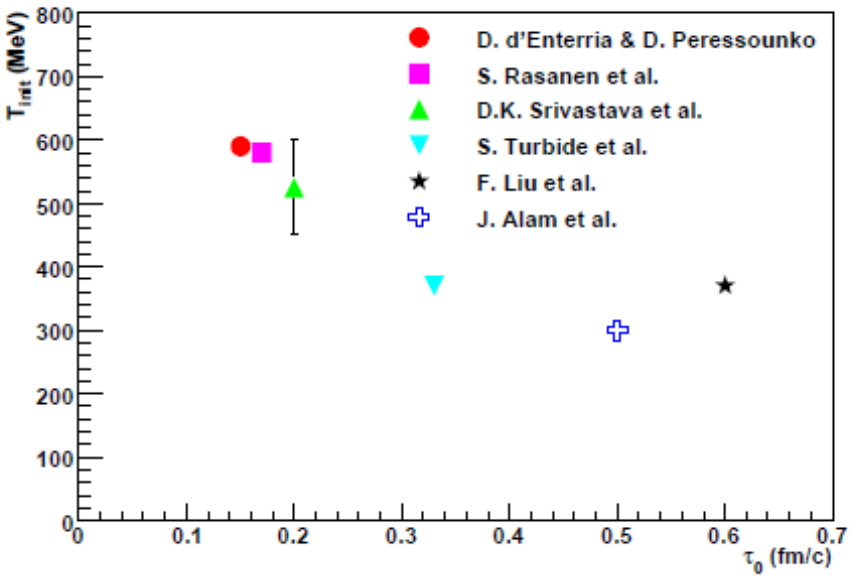


- model range in initial T is 300 to 600 MeV
- thermalization time range from about 0.6 to 0.15 fm/c



PHENIX

Stony Brook University

# Comparison To Theory for 0-20% Centrality $v_2$

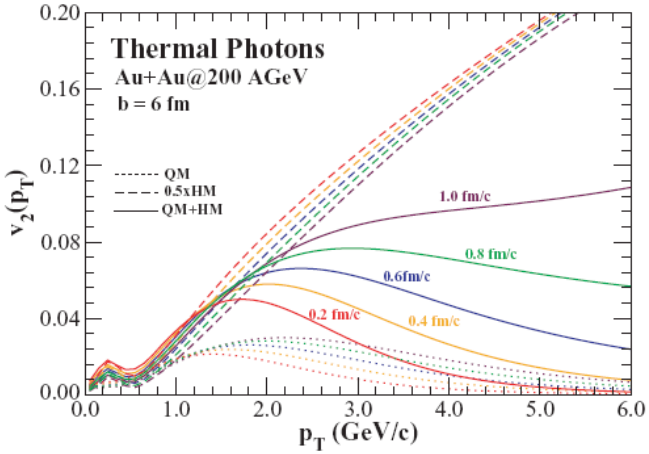


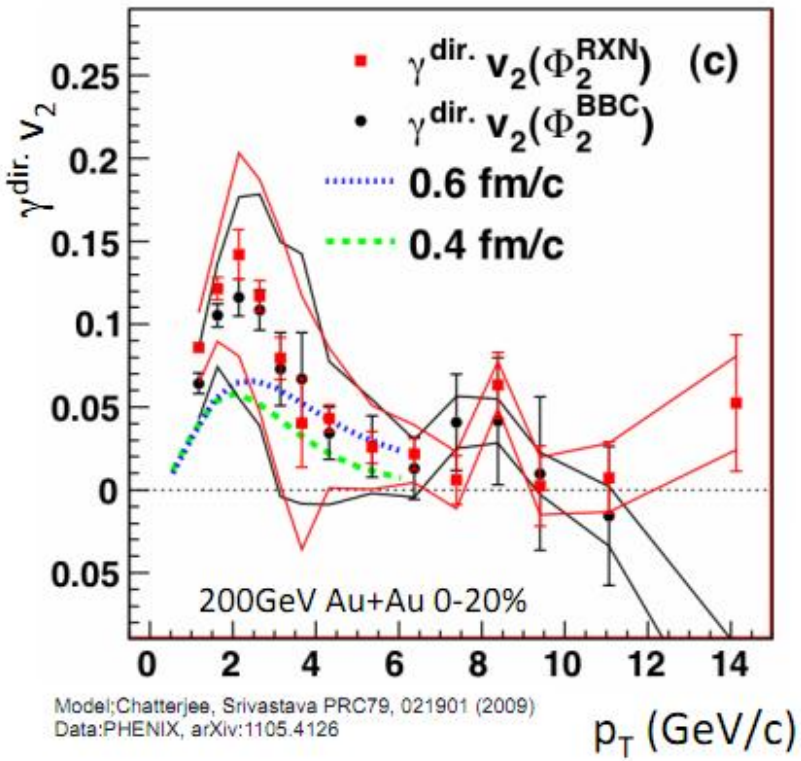


Model:Chatterjee, Srivastava PRC79, 021901 (2009)
Data:PHENIX, arXiv:1105.4126

H. van Hees, C. Gale, R. Rapp
Phys. Rev. C 84, 054906 (2011)

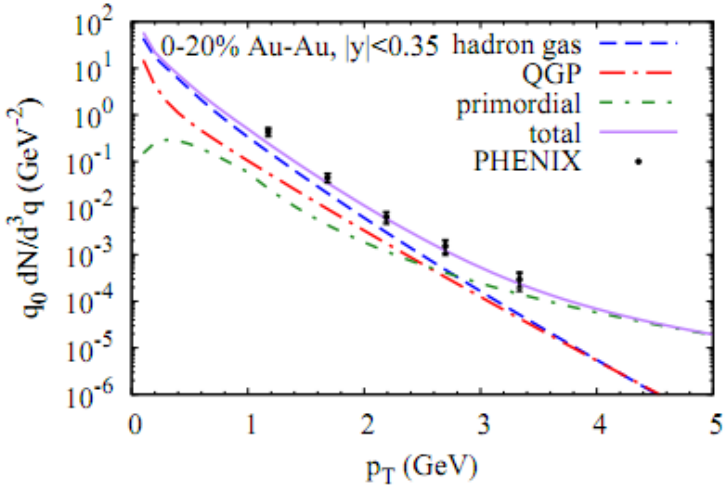


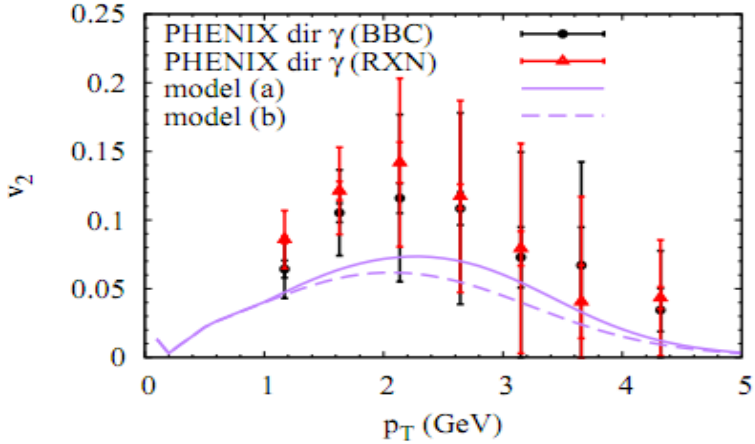




Stony Brook University

# Summary

- Direct photons have a $v_2$ similar to that of hadrons at low $p_T$
- An excess of direct photons is found at low $p_T$ and is unique to heavy ion collisions
  - This excess is thermal in shape and indicates a high temperature
- These two results are seemingly at odds with our standard picture of the heavy ion collision at RHIC

# Outlook

- Improved data on the direct photon invariant yield a la external conversions
  - more points at low $p_T$
  - lower $p_T$ reach



PHENIX

Stony Brook University

# References

**Theory curves on direct photon yield:**


- D. d'Enterria and D. Peressounko, Eur. Phy. J. C46, 451 (2006).
- S. Turbide, R. Rapp, and C. Gale, Phys. Rev. C 69, 014903 (2004).
- P. Huovinen, P. V. Ruuskanen, and S. S. Rasanen, Phys. Lett. B535, 109 (2002).
- D. K. Srivastava and B. Sinha, Phys. Rev. C 64, 034902 (2001).
- Jan-e Alam, S. Sarkar, T. Hatsuda, T.K. Nayak, and B. Sinha Phys. Rev. C 63, 021901(R) (2001).
- F. M. Liu, T. Hirano, K.Werner, and Y. Zhu, Phys. Rev. C 79, 014905 (2009).


**All other references written directly on the slide**



PHENIX

Stony Brook University

# Backups

# Measuring External Photon Conversions: Identification

- PHENIX tracks outside magnetic field
  - Need to assume the origin
  - Assume particles come from event vertex
- We are interested in conversions in the HBD backplane (radius ≈ 60cm)
  - Now our assumption is incorrect
  - Gives pairs an artificial opening angle
  - Leads to an apparent mass

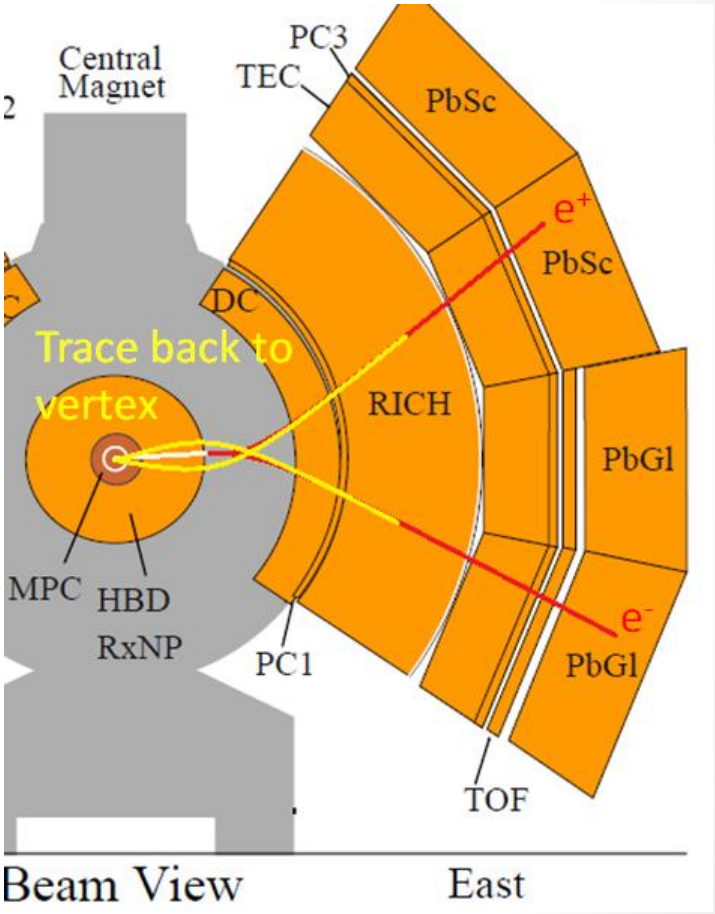




PHENIX

Stony Brook University

# Some Simulations of Conversions

- Full GEANT simulation of photon conversions
- Assume all particles come from a radius of 60cm (ATM)

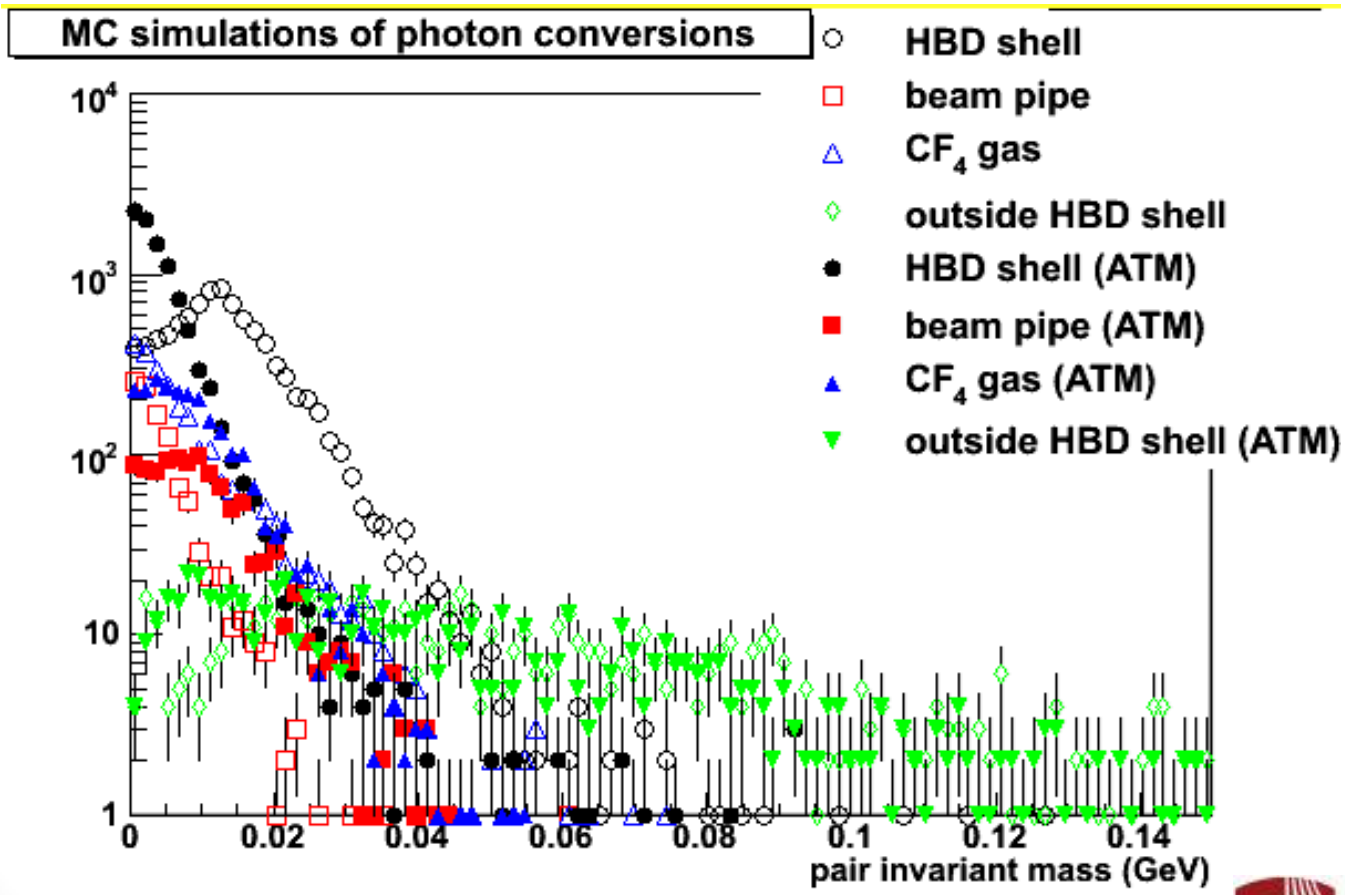




PHENIX

Stony Brook University

# The di-electron spectrum

region of virtual photons

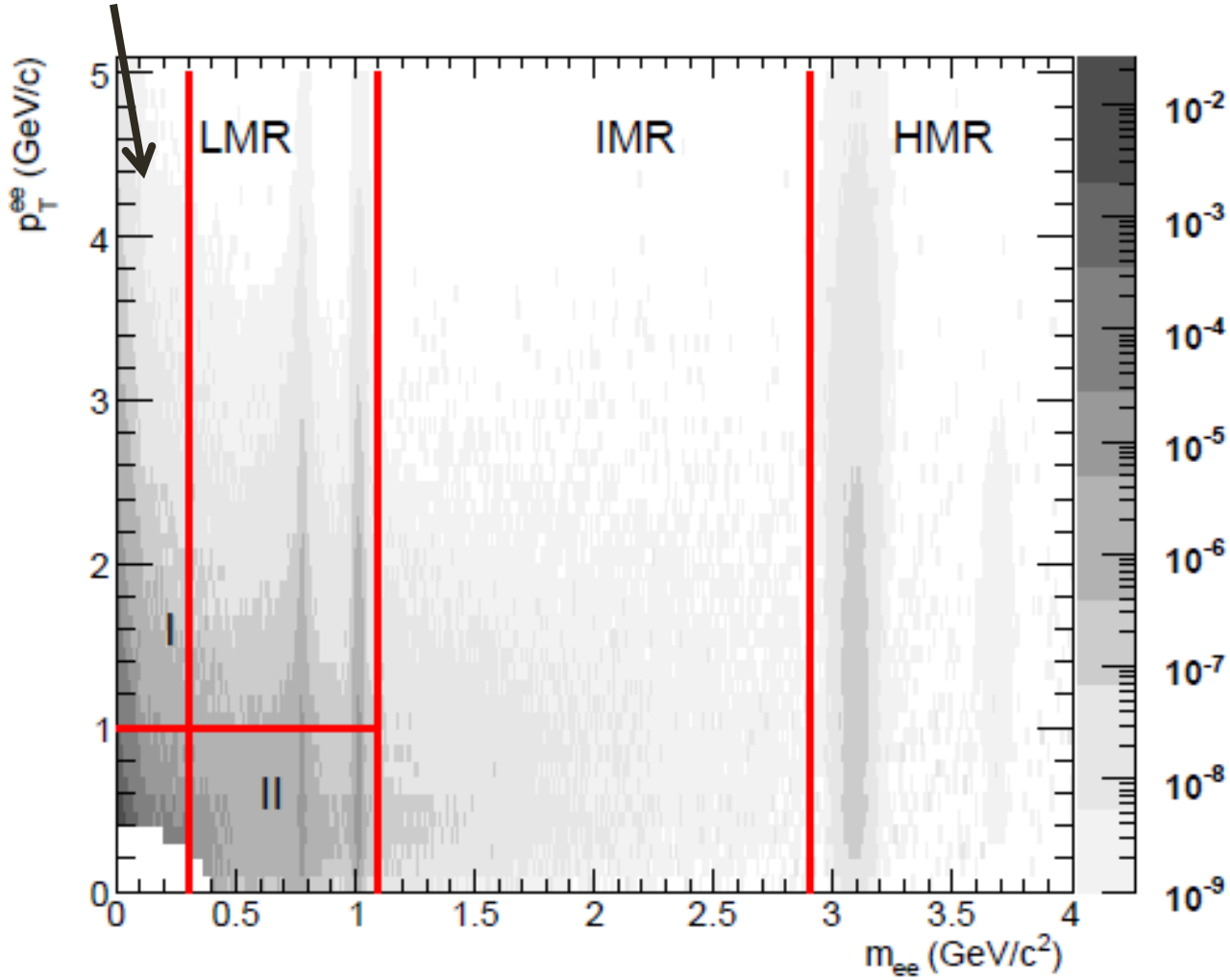


Phys. Rev. C 81, 034911 (2010)

# Measuring Virtual Photons

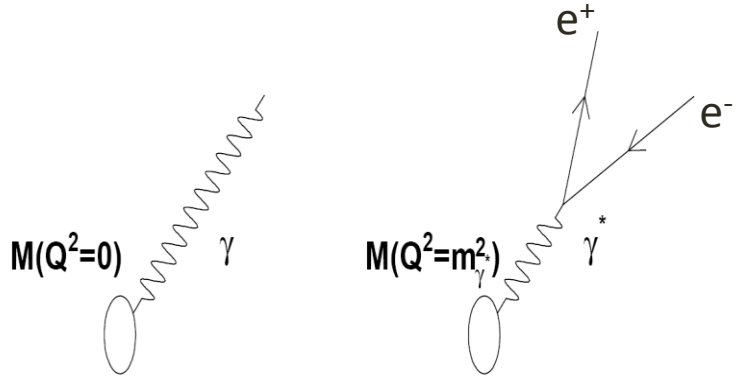


- Processes which produce photons can also produce virtual photons
  - Decay into low-mass $e^+e^-$ pairs
  - The relation between photon and pair production can be written as

$$\frac{d^2 n_{ee}}{dm_{ee}} = \frac{2\alpha}{3\pi}\frac{1}{m_{ee}}\sqrt{1-\frac{4m_e^2}{m_{ee}^2}}\left(1+\frac{2m_e^2}{m_{ee}^2}\right)S dn_\gamma$$

- Measure low mass, high momentum dileptons
  - Correspond to nearly real photons
  - Extrapolate back to zero mass
- Analyze above $\pi^0$ mass to remove 90% of hadron background

Phys. Rev. C 81, 034911 (2010)

# Virtual Photons

- excess seems to be consistent with the assumption of originating from virtual photons
- S(m, $p_T$) is constant

$$R(m,p_T) \simeq \frac{dN_{\gamma^*}^{\text{excess}}(m,p_T)}{dp_T} \Big/ \frac{dN_{\gamma}^{\text{incl}}(p_T)}{dp_T}$$
$$= S(m,p_T) dN_{\gamma}^{direct}(p_T) / dN_{\gamma}^{\text{incl}}(p_T)$$

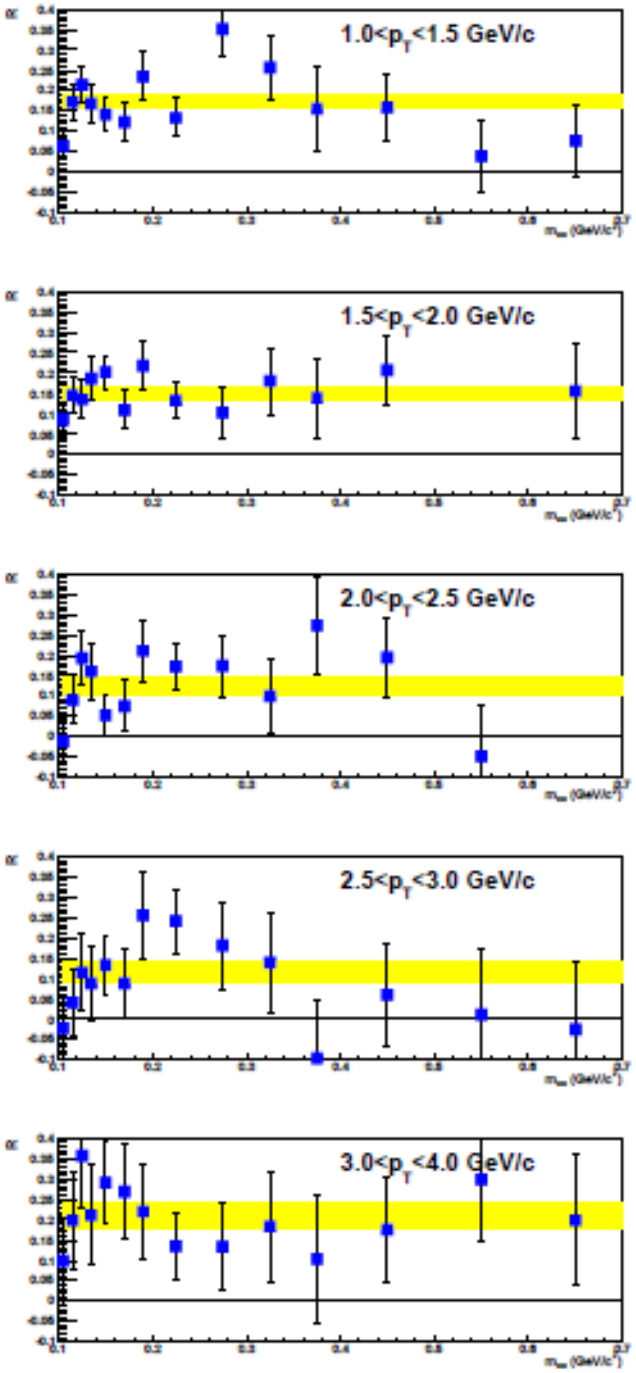


Phys. Rev. C 81, 034911 (2010)

# Theory Comparison (III)

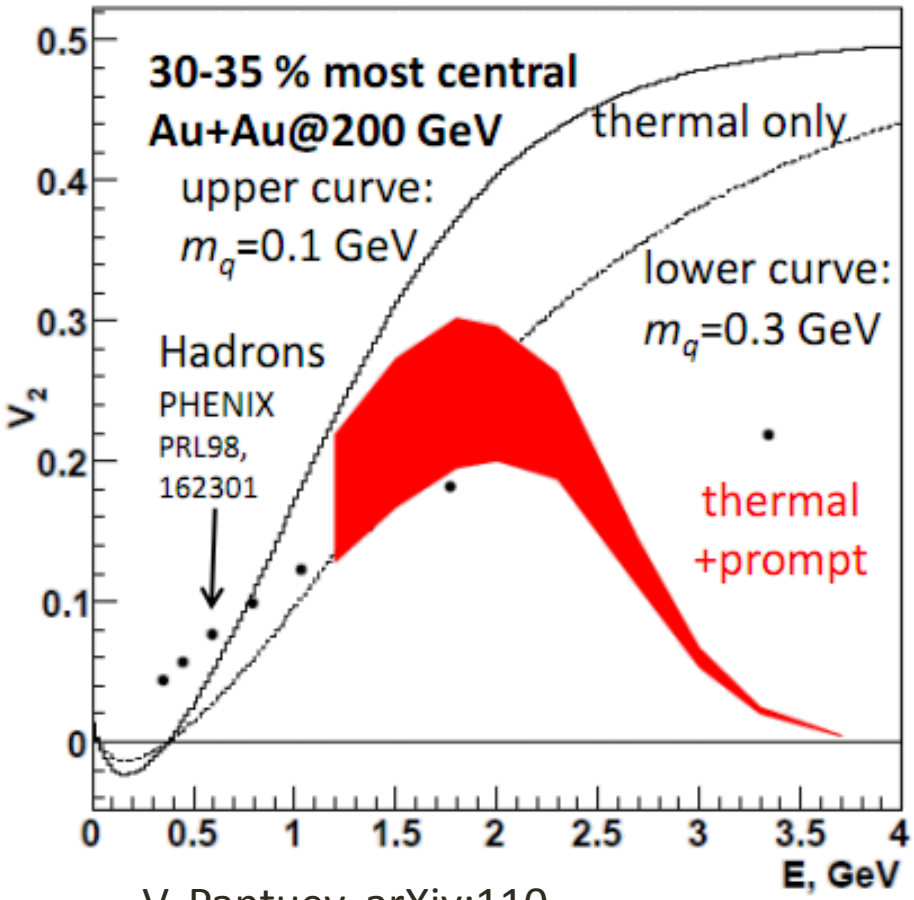


V. Pantuev, arXiv:110

- Nothing about photon production included in model
  - Assume thermal shape and normalize to data
  - Describes effect of Doppler shift

$$dN/d\omega_0 = exp(-\omega_0/T),$$

$$\omega = \omega_0 \frac{\sqrt{1-\beta^2}}{1-\beta cos\theta}.$$

$$dN/dE = \frac{1-\beta_T cos\theta}{\sqrt{1-\beta^2}} exp(-\frac{E(1-\beta_T cos\theta)}{T\sqrt{1-\beta^2}}).$$

- Cylindrical expanding fireball

# Experimental Techniques at PHENIX (I)

- Beam Beam Counter (BBC)
  - Centrality
  - Z vertex
  - Reaction plane
- Reaction Plane Detector (RxNP)
  - Reaction plane

- Electromagnetic Calorimeter (EMCal)
  - Photon energy and id
- Pad Chamber (PC)
  - Veto charged tracks
- Drift Chamber (DC)
  - Charged tracking
- Ring Imaging Cherenkov detector (RICH)
  - Electron id

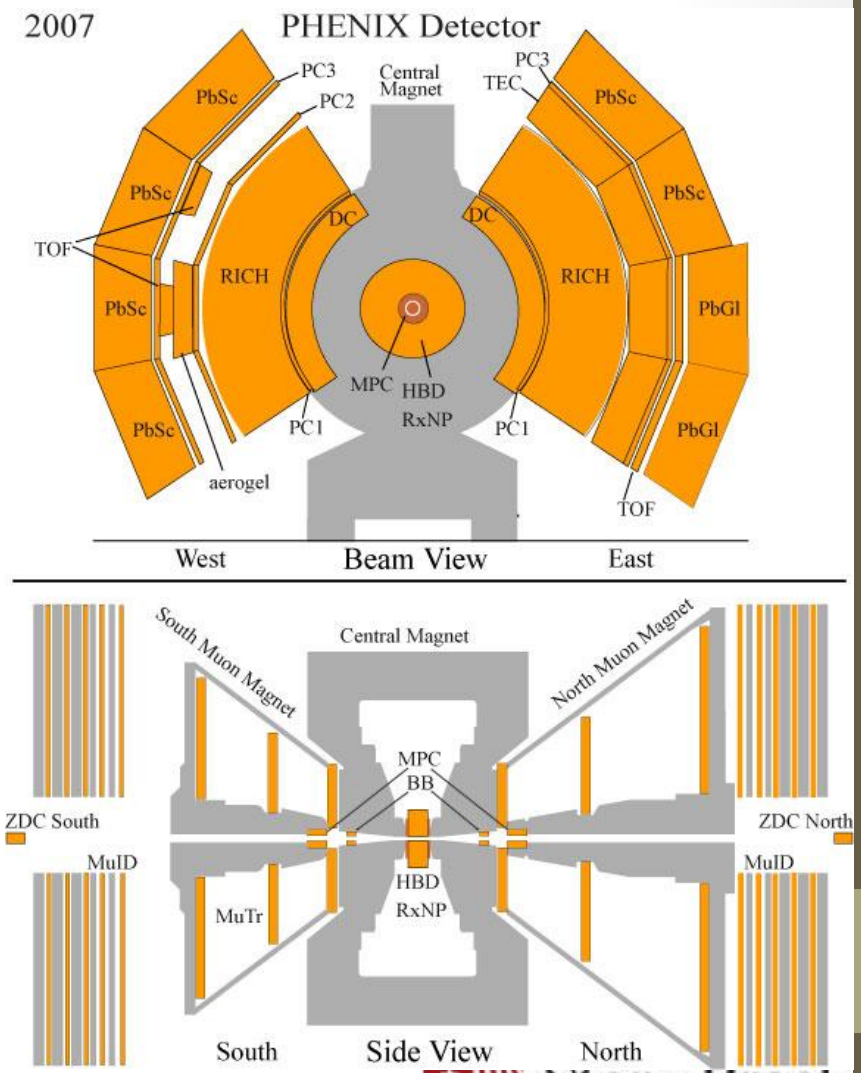

# Published Direct Photon Flow

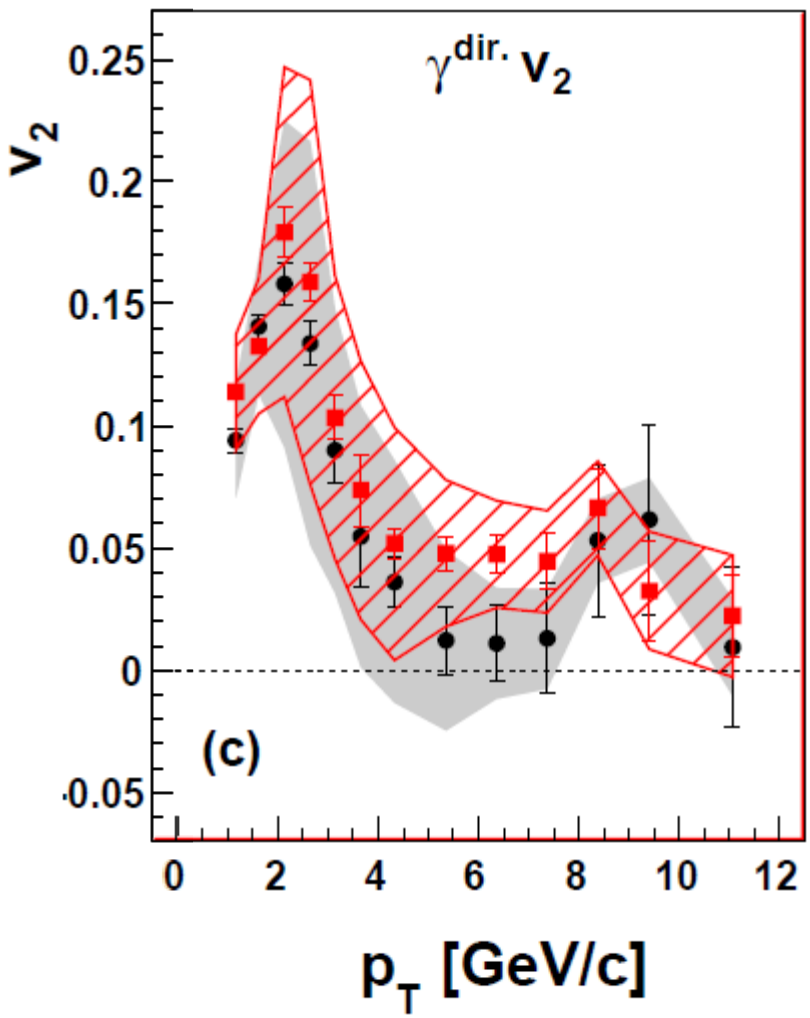


- E.P.$^{RXN}$ ($|\eta|$=1.0~2.8)
- E.P.$^{BBC}$ ($|\eta|$=3.1~3.9)

Phys. Rev. Lett. 109, 122302 (2012)

# Direct Photons in HIC

- Initial collision
- QGP
- Hadron gas

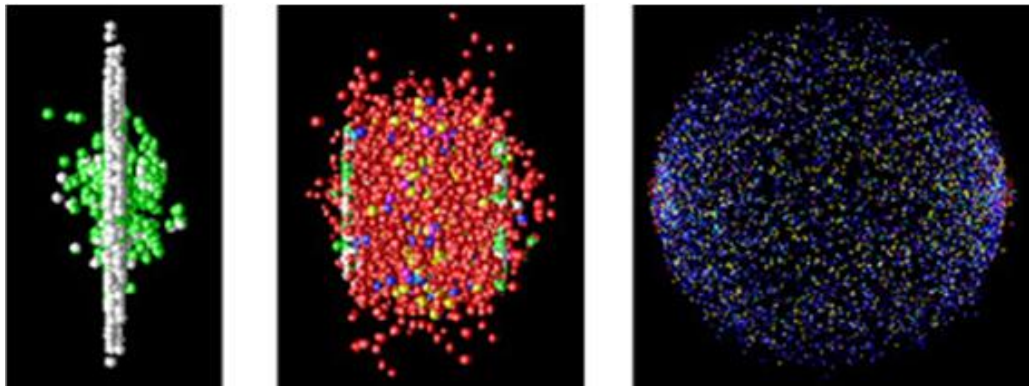

- Direct photons = (inclusive photons) – (hadron decay photons)
  - Initial collision
    - Hard scattering of partons $v_2 = 0$
    - Pre-thermalized radiation $v_2 = ?$
  - QGP
    - Thermal radiation $v_2 > 0$
    - Jet Fragmentation $v_2 > 0$
    - Bremsstrahlung $v_2 < 0$
    - Jet conversions $v_2 < 0$

    High $p_T$ phenom. Reflective of geometry, not dynamics
  - Hadron Gas
    - Thermal radiation $v_2 > 0$

# Thermal Dileptons + Photons: Baseline Approach

Ralf Rapp
Cyclotron Institute +
Dept of Phys & Astro
Texas A&M University
College Station, USA

RIKEN/BNL Workshop on
"Thermal Radiation" in Heavy-Ion Reactions
BNL (Upton, NY), 05.-07.12.12

# 1.) Intro: EM Spectral Function + Fate of Resonances

$$\frac{dN_{ee}}{d^4x\,d^4q} = \frac{-\alpha_{em}^2}{\pi^3 M^2} f^B(q_0,T)\ \mathrm{Im}\,\Pi_{em}(M,q;\mu_B,T)$$

**Im $\Pi_{em}$(M) in Vacuum**

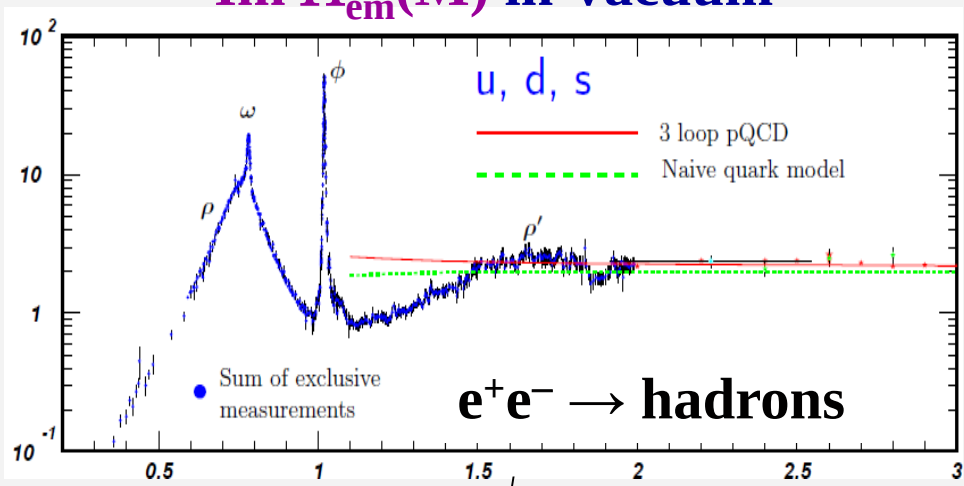


- **Electromagnetic spectral function**
  - **$\sqrt{s}$ < 2 GeV** : non-perturbative
  - **$\sqrt{s}$ > 2 GeV** : perturbative ("dual")

- **Vector resonances "prototypes"**
  - representative for bulk hadrons: neither Goldstone nor heavy flavor

- **Medium modifications of resonances**
  - QCD phase structure
  - HICs: correlate ($\mu_N$,T) ↔ spectral shape

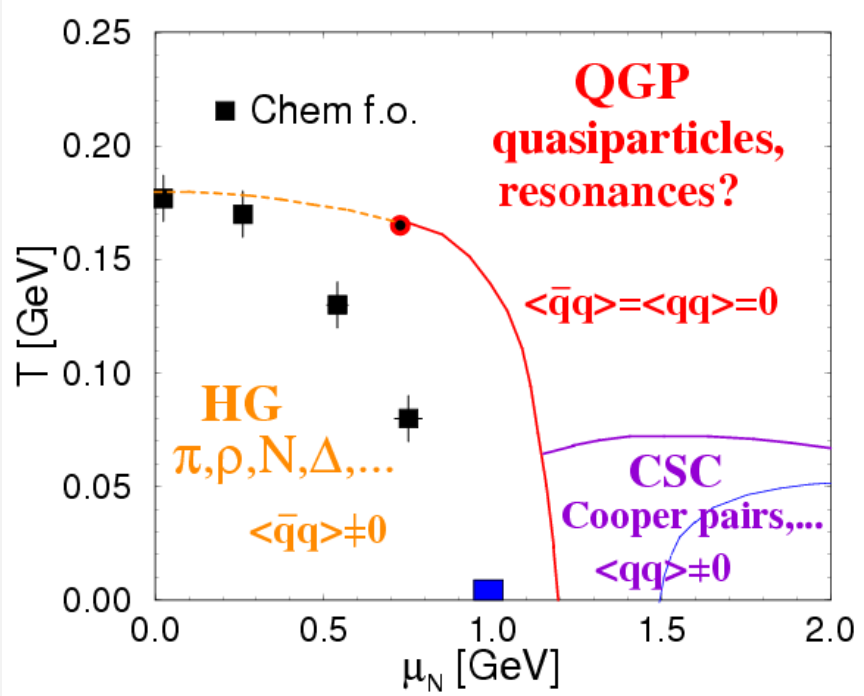

# 1.2 Chiral Restoration in Lattice QCD

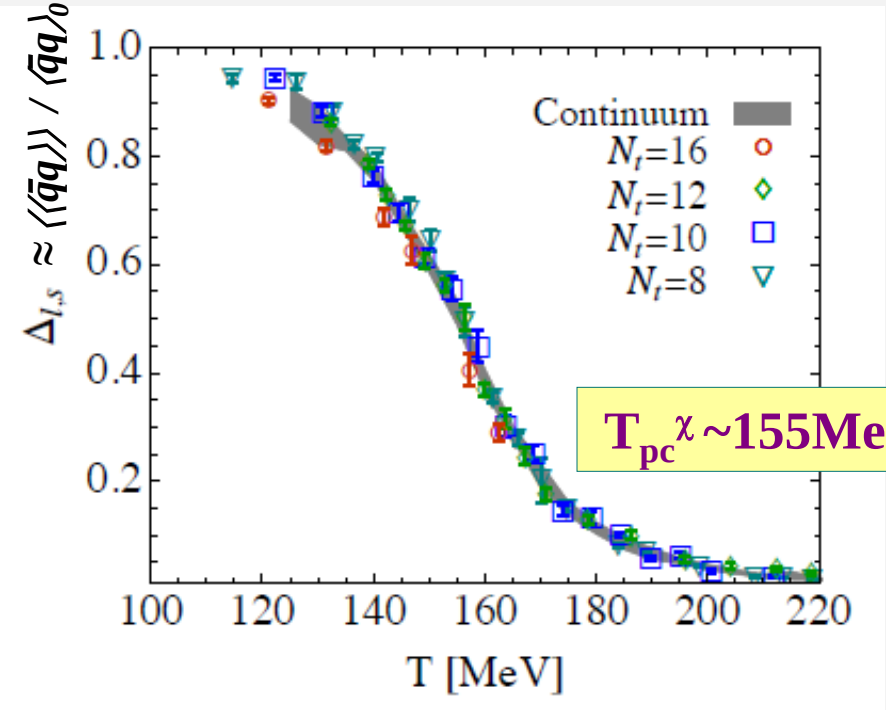


$T_{pc}^{\chi}$~155MeV

[Fodor et al '10]

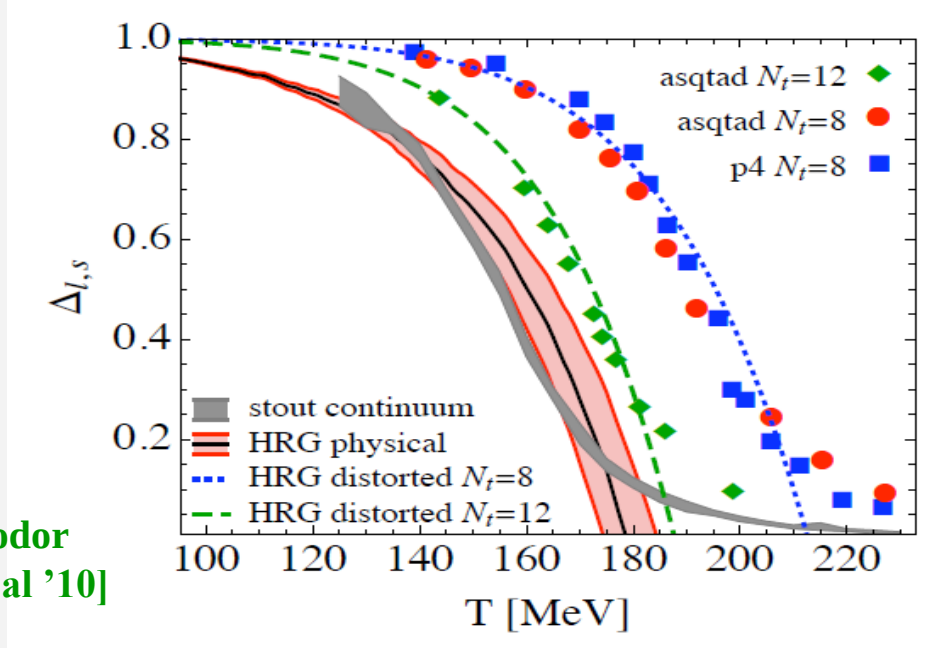


- compatible with hadron resonance gas (also for thermodynamics!)
- chiral restoration in "hadronic phase"? (low-mass dileptons!)
- cross-over ↔ smooth EM emission rates across $T_{pc}$

# Outline

2.) **Spectral Function in Medium**

- Effective Hadronic Theory in Medium
- QGP Emission and Lattice QCD
- Chiral Restoration

3.) **Dilepton Spectra in Heavy-Ion Collisions**

- Nature of Emission Source from SPS to RHIC
- Spectral Shapes and Temperatures
- Radial and Elliptic Collectivity

4.) **Conclusions**

# 2.1 Baseline I: ρ Meson in Hadronic Matter

[Pisarski, Chanfray et al, Herrmann et al, Asakawa et al, RR et al, Koch et al, Steele et al, Post et al, Eletsky et al, Harada et al …]

**ρ-Propagator:**

$$D_\rho(M,q;\mu_B,T) = [M^2 - m_\rho^2 - \Sigma_{\rho\pi\pi} - \Sigma_{\rho B} - \Sigma_{\rho M}]^{-1}$$

**Selfenergies:** $\Sigma_{\rho\pi\pi} =$

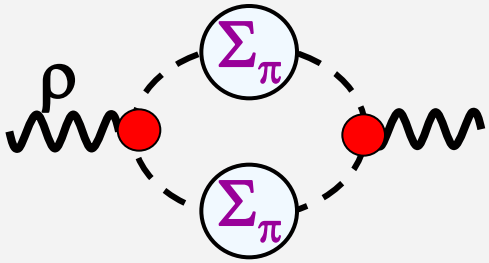


$\Sigma_{\rho B,\rho M} =$

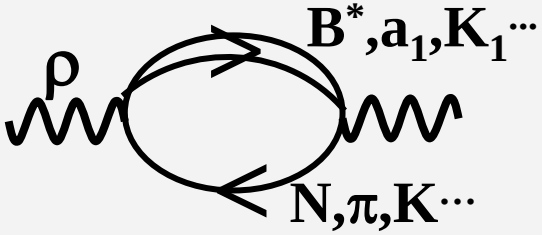


**Constraints:** decays: **B,M→ ρN, ρπ, … ;** scattering: **πN→ρN, γA, …**

**SPS**

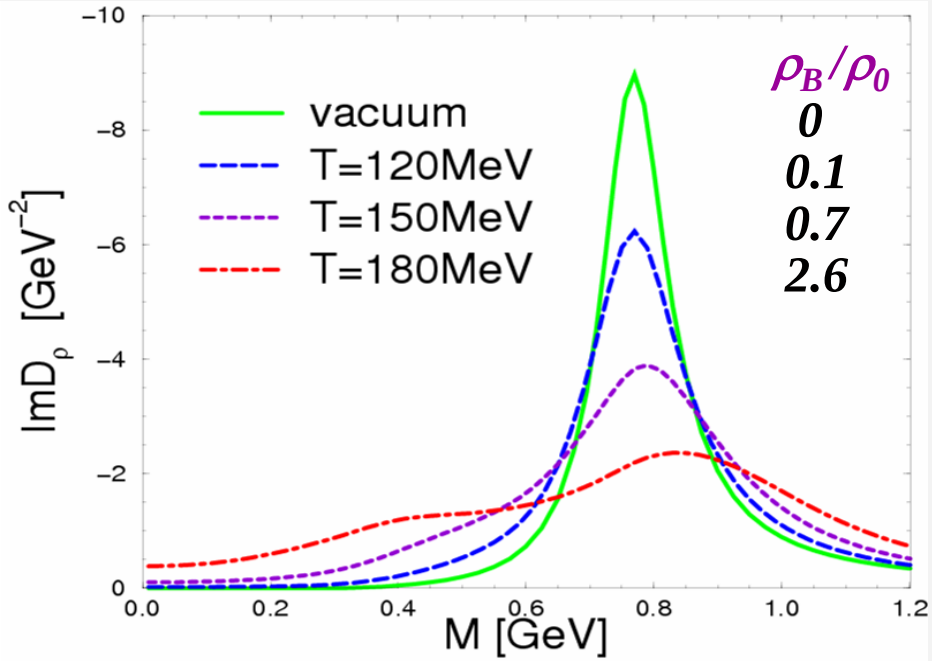


**RHIC / LHC**

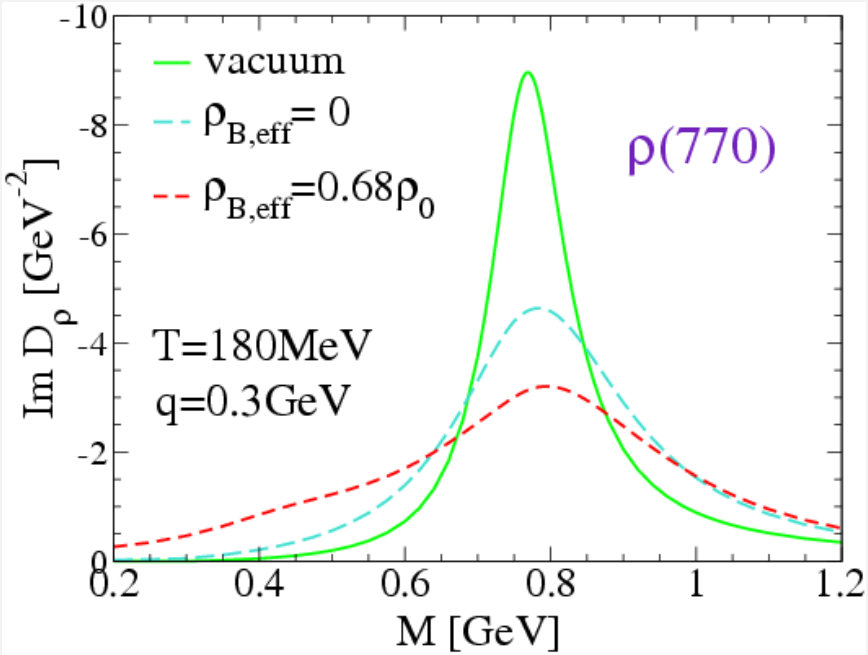

# 2.2 Chiral Condensate + ρ-Meson Broadening

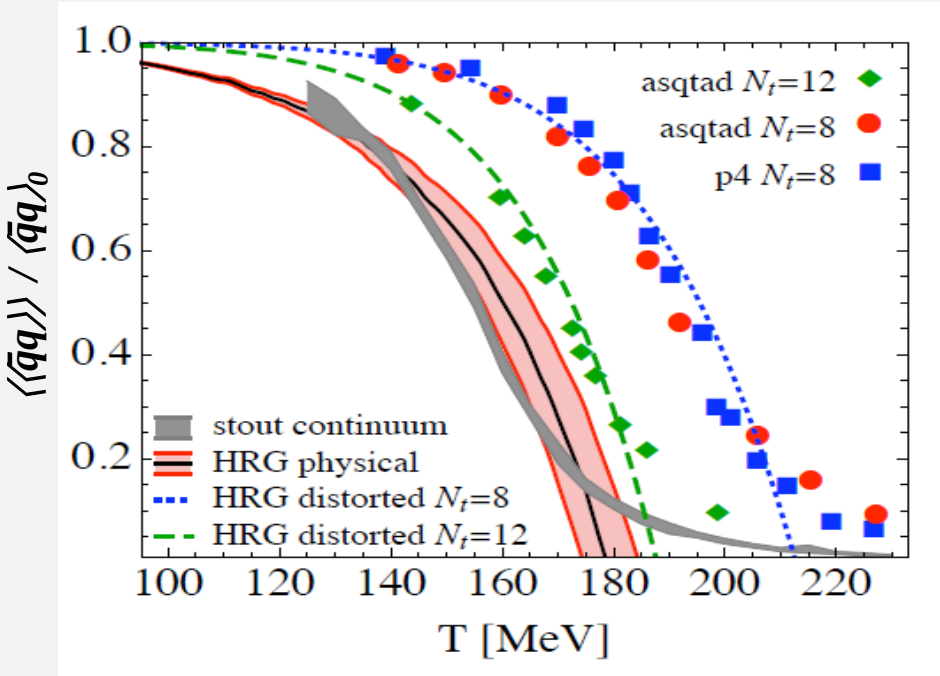


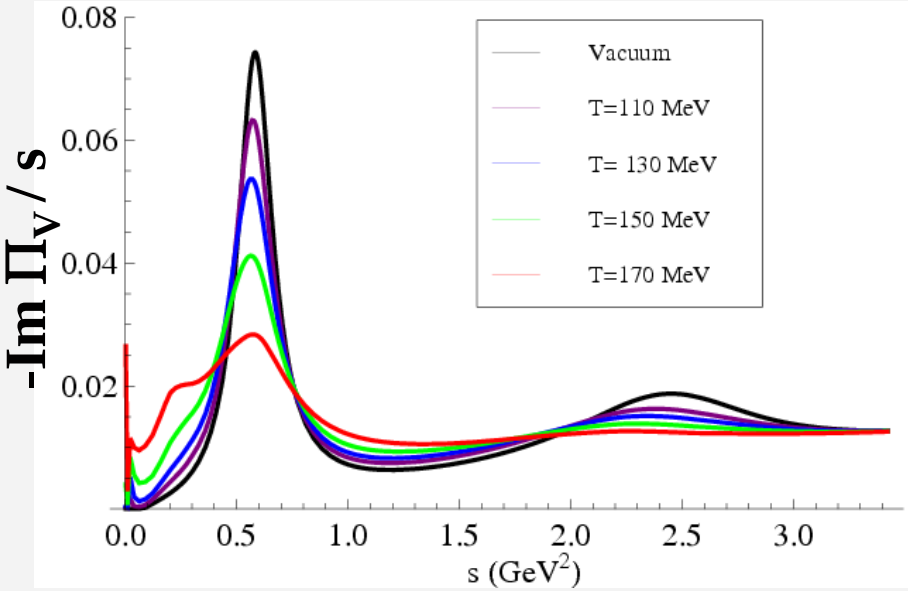


$$\frac{\langle\langle\bar{q}q\rangle\rangle(T,\mu_B)}{\langle\bar{q}q\rangle} = 1 - \sum_h \frac{\varrho_h^s \Sigma_h}{m_\pi^2 f_\pi^2}$$

⟺ effective hadronic theory

- $\Sigma_h = m_q \langle h|\bar{q}q|h\rangle > 0$ contains quark core + pion cloud

$= \Sigma_h^{core} + \Sigma_h^{cloud} \sim$

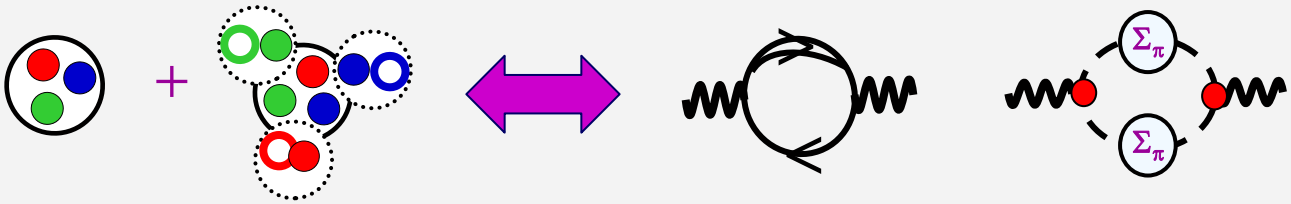


- **matches spectral medium effects: resonances + pion cloud**
- **resonances + "chiral mixing" drive ρ-SF toward chiral restoration**

# 2.3 Baseline II: Perturbative + Lattice QGP Rates

$dR_{ee}/dM^2 \sim \int d^3q \;\; f^B(q_0;T)\; \mathrm{Im}\,\Pi_{em}$

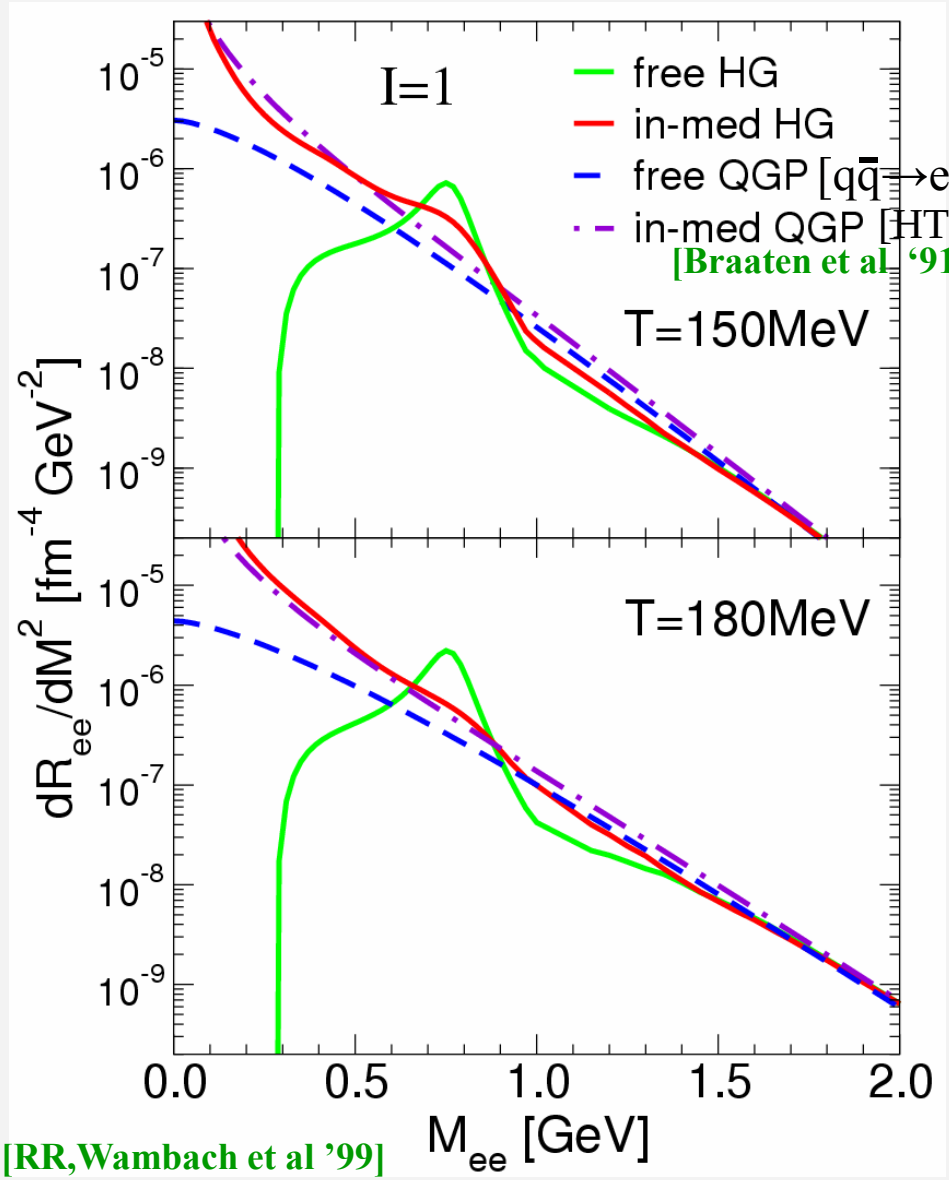


- **rates smoothly match around $T_{pc}$:**
  - **compatible with cross-over**
  - **3-fold "degeneracy"**

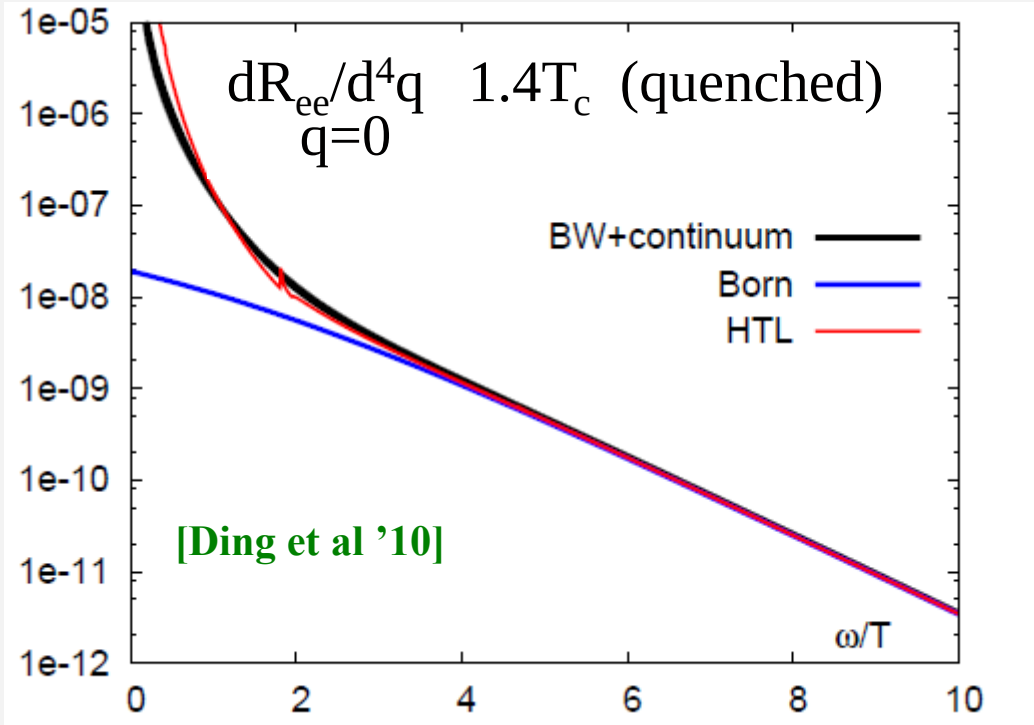

# 2.4 Vector Correlator in Thermal Lattice QCD

- Euclidean Correlation fct.

$$\Pi_{em}(\tau,q;T) = \int_0^\infty \frac{dq_0}{2\pi}\, \rho_{em}(q_0,q;T)\, \frac{\cosh[q_0(\tau - 1/2T)]}{\sinh[q_0/2T]}$$

**Lattice (quenched)** [Ding et al '10]

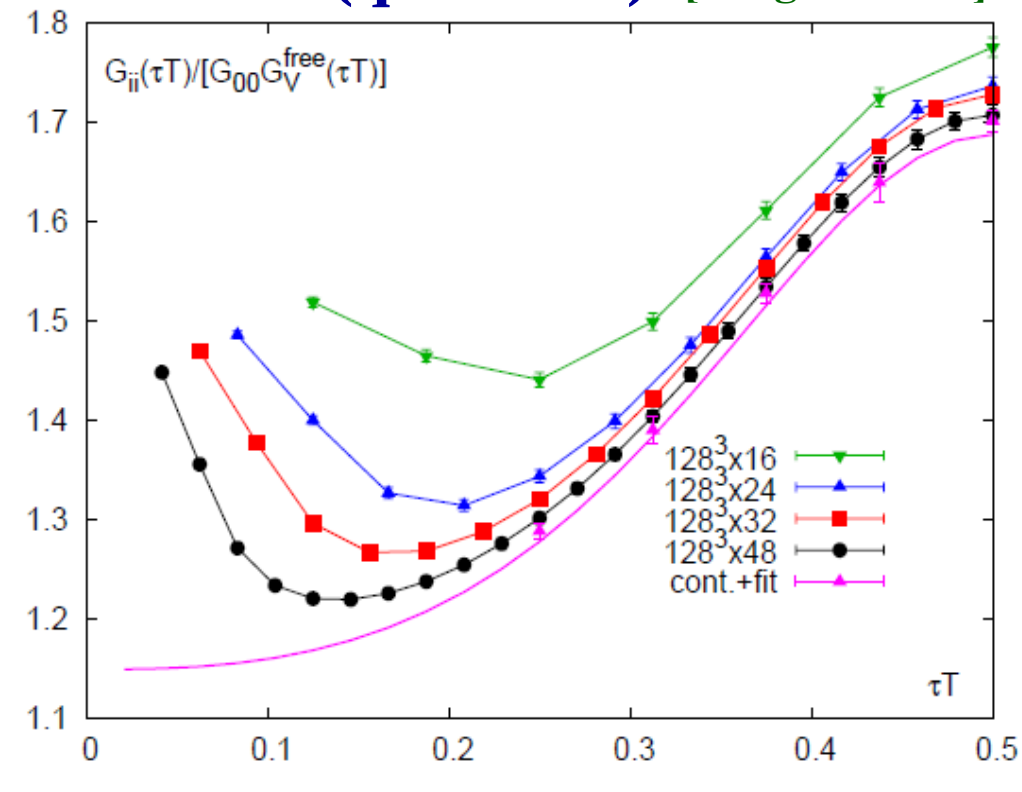


**Hadronic Many-Body** [RR '02]

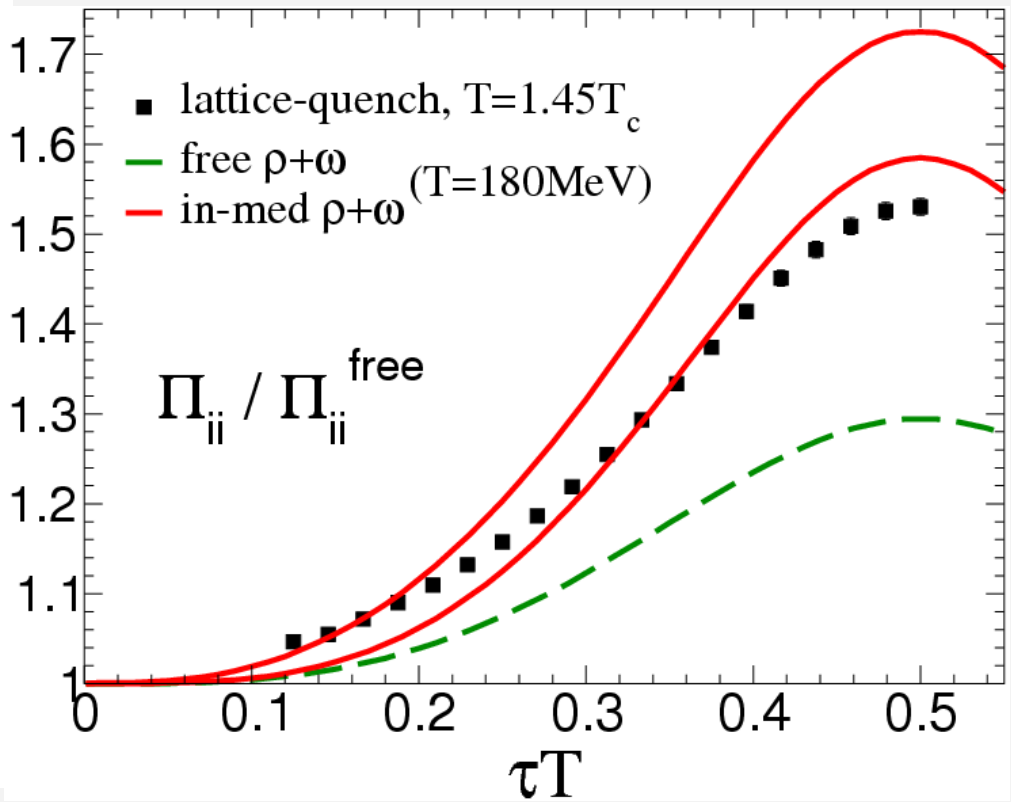


- "Parton-Hadron Duality" of finite-T lattice + in-medium hadronic?

# 2.5 Criteria for Chiral Restoration

- **Vector (ρ) – Axialvector ($a_1$) degenerate**

$$I_n = -\int \frac{ds}{\pi} s^n \left(\mathrm{Im}\,\Pi_V - \mathrm{Im}\,\Pi_A\right)$$

[Weinberg '67, Das et al '67, Kapusta+ Shuryak '94]

$$I_{-1} = f_\pi^2, \quad I_0 = 0, \quad I_1 = c\alpha_s \langle (\bar{q}q)^2 \rangle$$

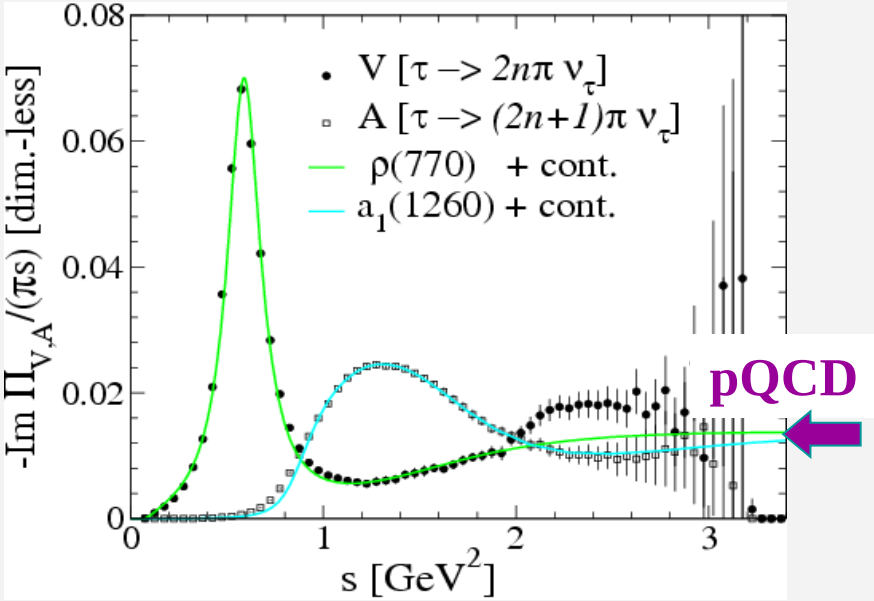


→ Talk by Hohler

- **QCD sum rules:**

  **medium modifications ↔ vanishing of condensates**

- **Degeneracy with thermal lattice-QCD**

- **Approach to perturbative rate (QGP)**

# Outline

2.) **Spectral Function in Medium**

- Effective Hadronic Theory in Medium
- QGP Emission and Lattice QCD
- Chiral Restoration

3.) **Dilepton Spectra in Heavy-Ion Collisions**

- Nature of Emission Source from SPS to RHIC
- Spectral Shapes and Temperatures
- Radial and Elliptic Collectivity

4.) **Conclusions**

# 3.1 Thermal Dilepton + Photon Emission Rates

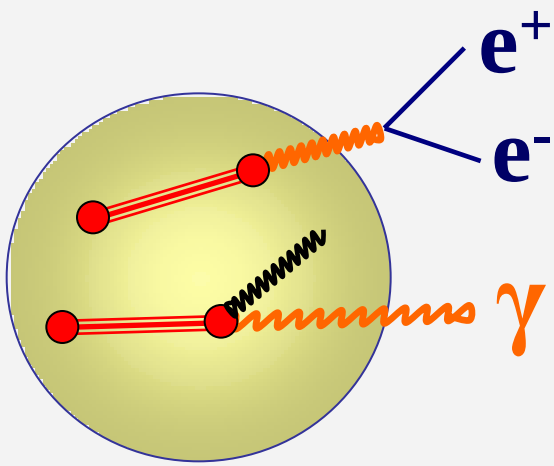


$$\frac{dR_{ee}}{d^4q} = \frac{-\alpha_{em}^2}{\pi^3 M^2} f^B(T)\ \mathrm{Im}\,\Pi_{em}(M,q;\mu_B,T)$$

$$q_0 \frac{dR_\gamma}{d^3q} = \frac{-\alpha_{em}}{\pi^2} f^B(T)\ \mathrm{Im}\,\Pi_{em}(q_0=q;\mu_B,T)$$

- determined by the same spectral function
- finite photon rate ↔ divergent dilepton rate for **M → 0**
- low mass: $\mathrm{Im}\Pi_{em} \sim [\mathrm{Im}D_\rho + \mathrm{Im}D_\omega/10 + \mathrm{Im}D_\phi/5]$ **$\rho$-meson dominated**

# 3.2 SPS I: Dielectrons with CERES/NA45

- **Evolve rates over fireball expansion:**

$$\frac{dN^{therm}_{\mu\mu}}{dM} = \int_{\tau_0}^{\tau_{fo}} d\tau V_{FB}(\tau) \int \frac{M\, d^3q}{q_0} \frac{dR^{therm}_{\mu\mu}}{d^4q}$$

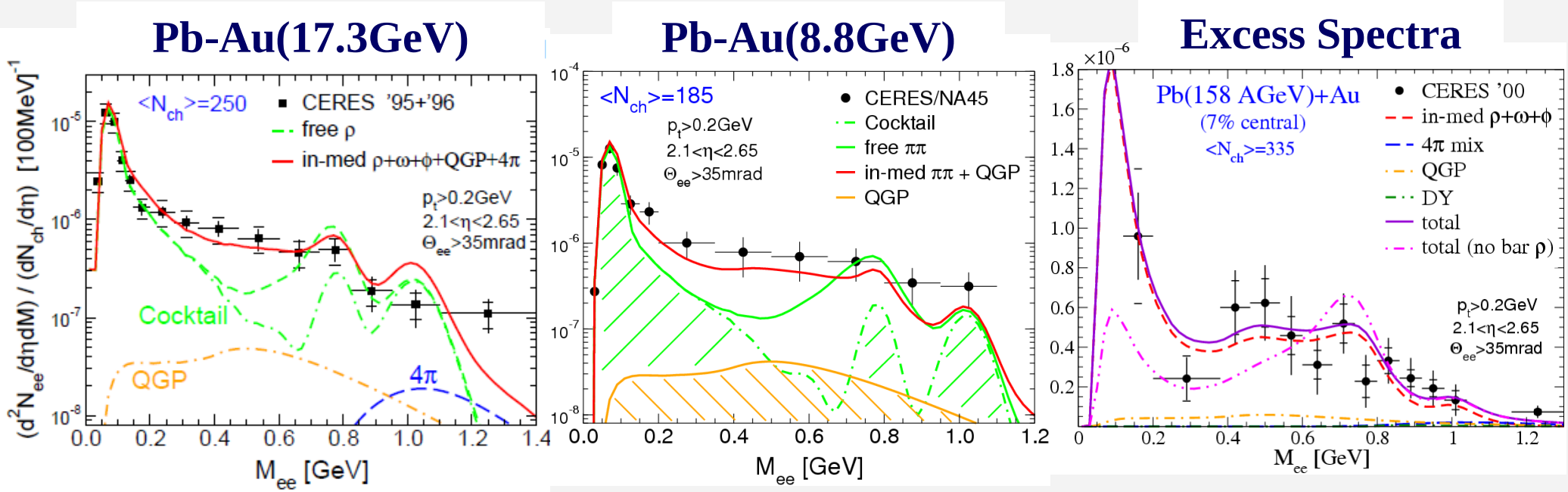


- established large enhancement
- consistent with a "**ρ-melting**" around $\mathbf{T_{pc}}$
- large effects at lower beam energy: baryons!
- **M→0**: photon point!

# 3.3 SPS II: Precision with $\mu^+\mu^-$ at NA60

**Acc.-corrected Excess Spectra vs. Theoretical Input Rates**

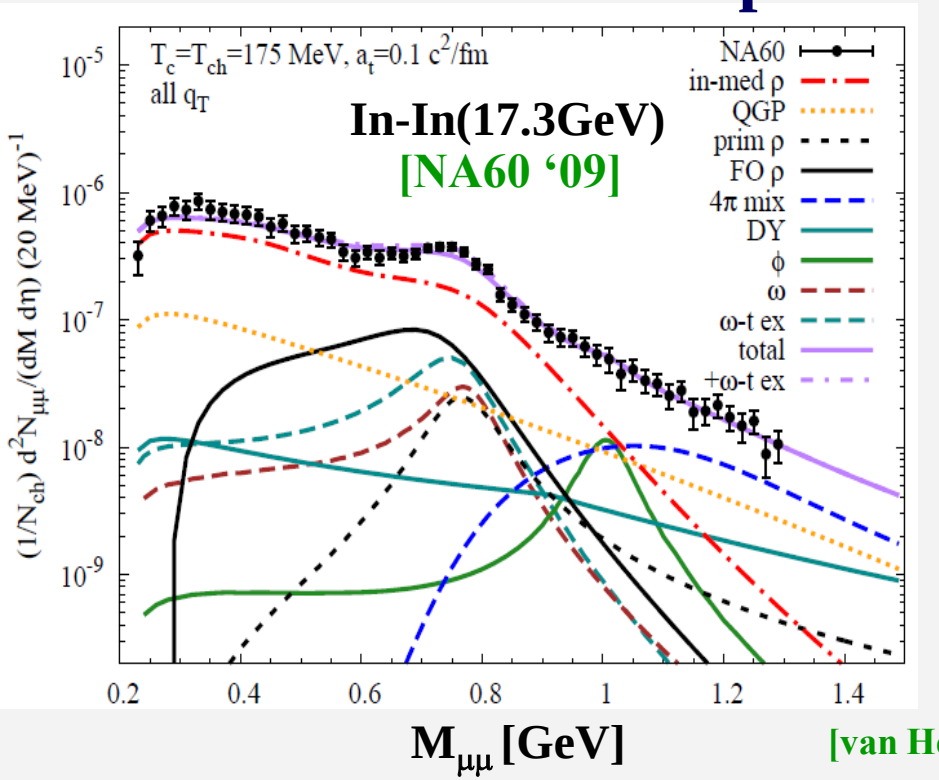


[van Hees+RR '08]

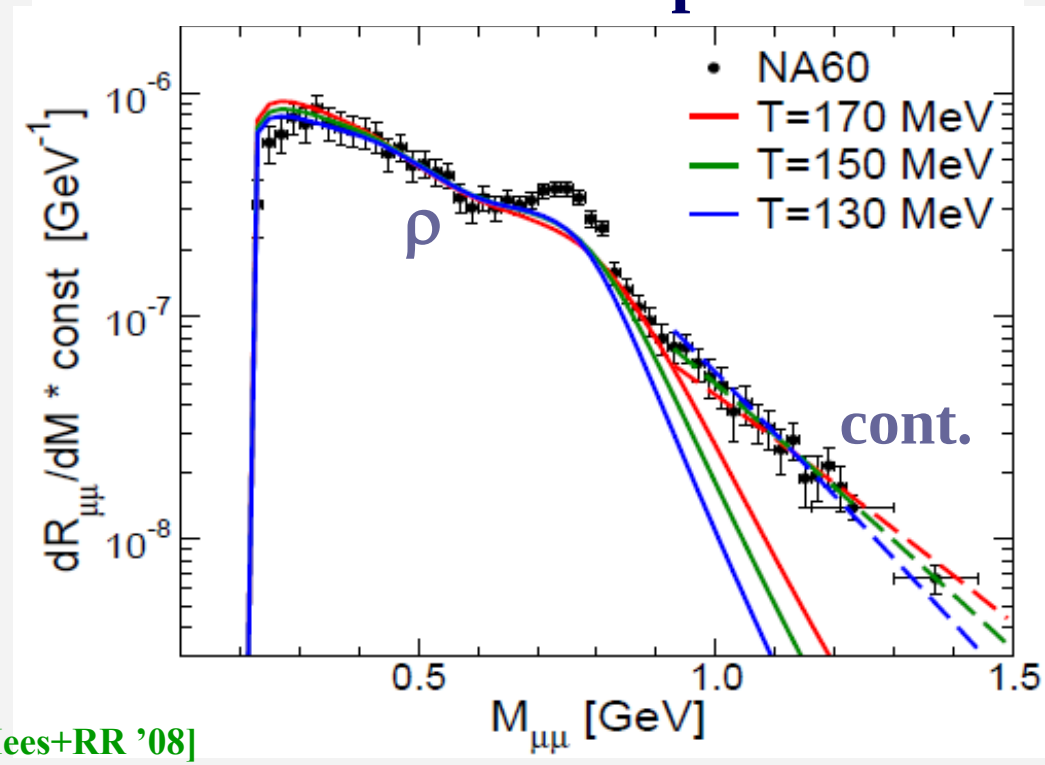


- broadened ρ spectral function quantitatively confirmed
- **invariant-mass** spectrum directly reflects thermal emission **rate**!
- mass slope reveals emission temperature around $T_{pc}^{\chi} \sim 150$ **MeV**

# 3.4 Low-Mass $e^+e^-$ Excitation Function at RHIC

**PHENIX**

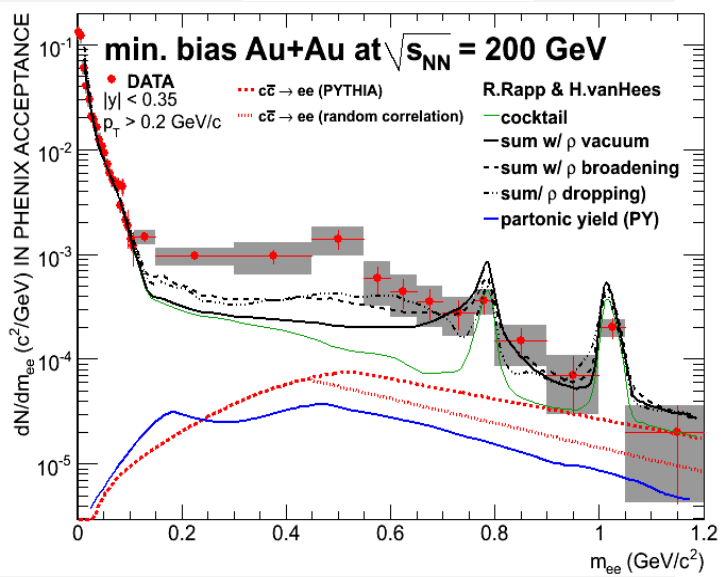


**STAR**

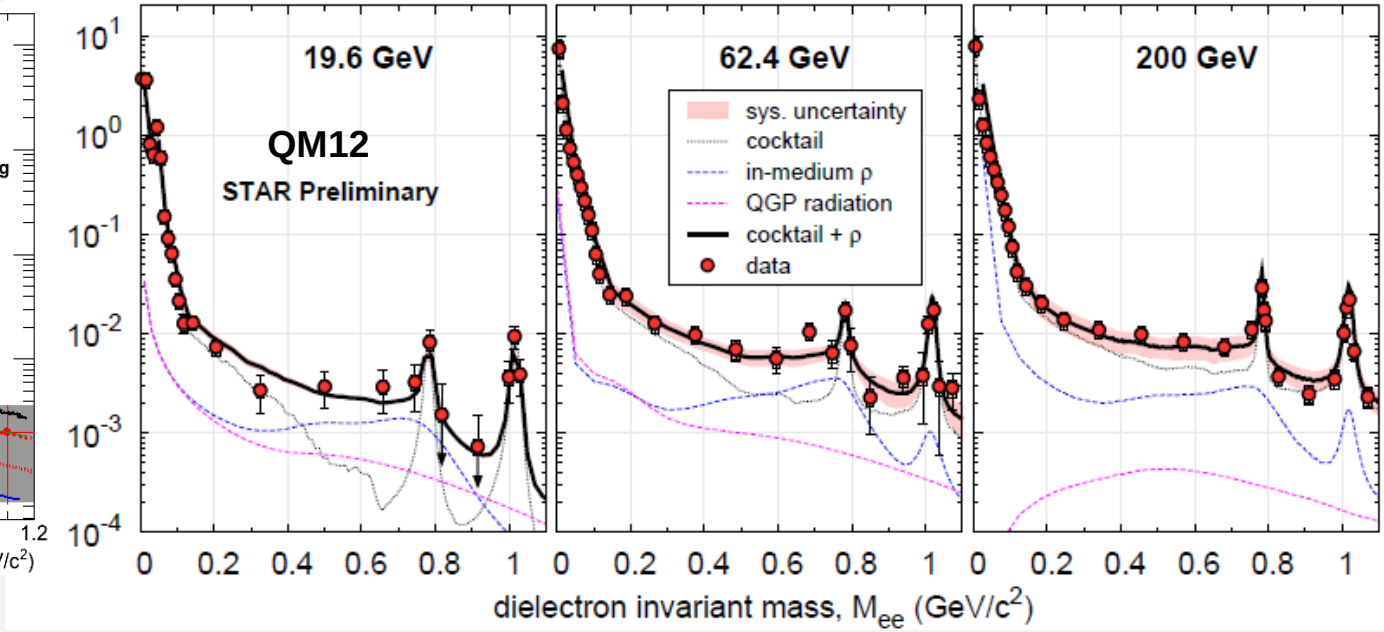


- tension between **PHENIX** and **STAR** (central **Au-Au**)
- non-central **Au-Au** consistent with **"universal" source** around $T_{pc}$
- partition hadronic/QGP depends on EoS

**→ Talks by Wang, Vujanovic, Linnyk**

# 3.4.2 Hadronic vs. QGP Emission at RHIC

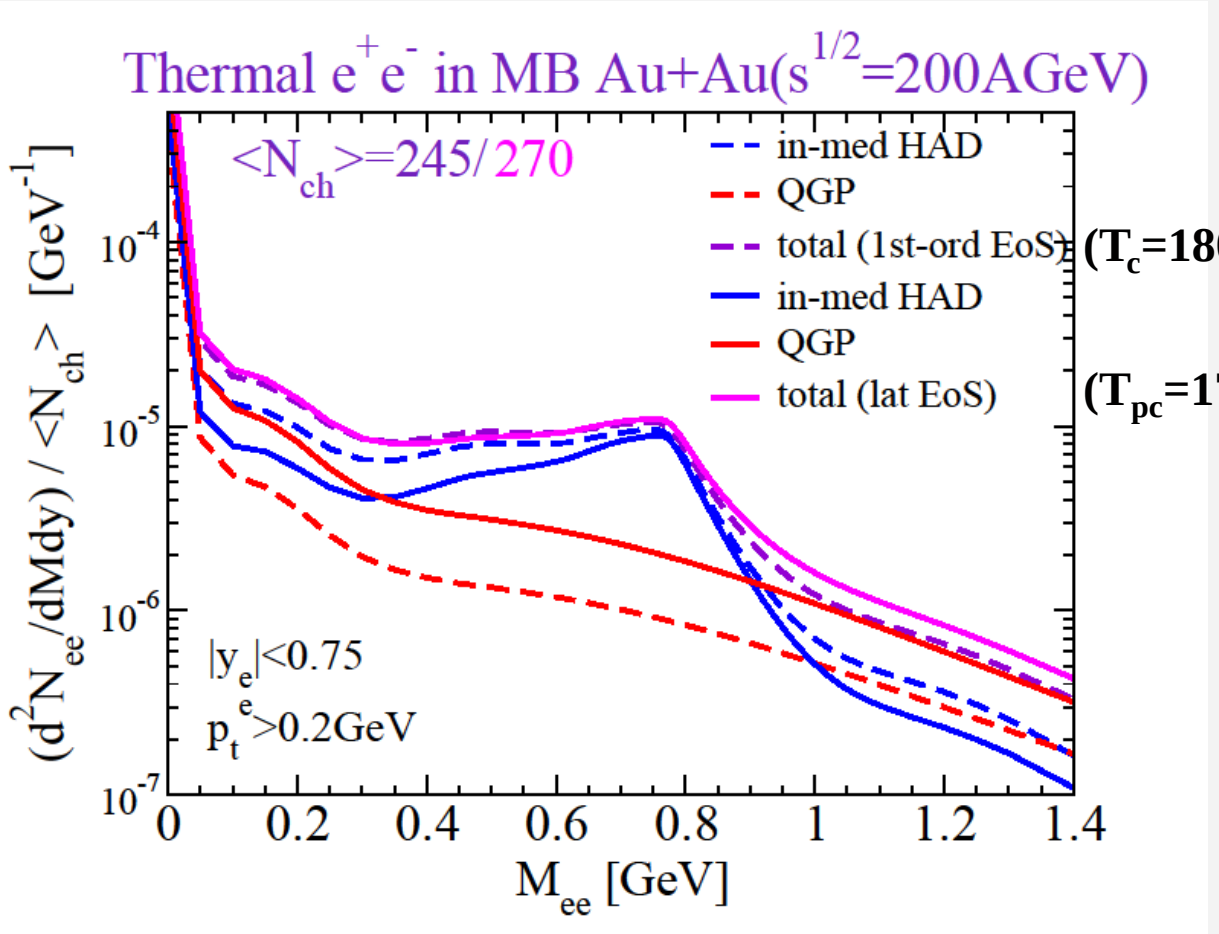


- smaller $T_{pc}$ + lattice EoS enhance QGP + deplete hadronic yield
- corroborates prevalent emission source around $T_{pc}$

# 3.5 Direct Photons at RHIC

## Spectra

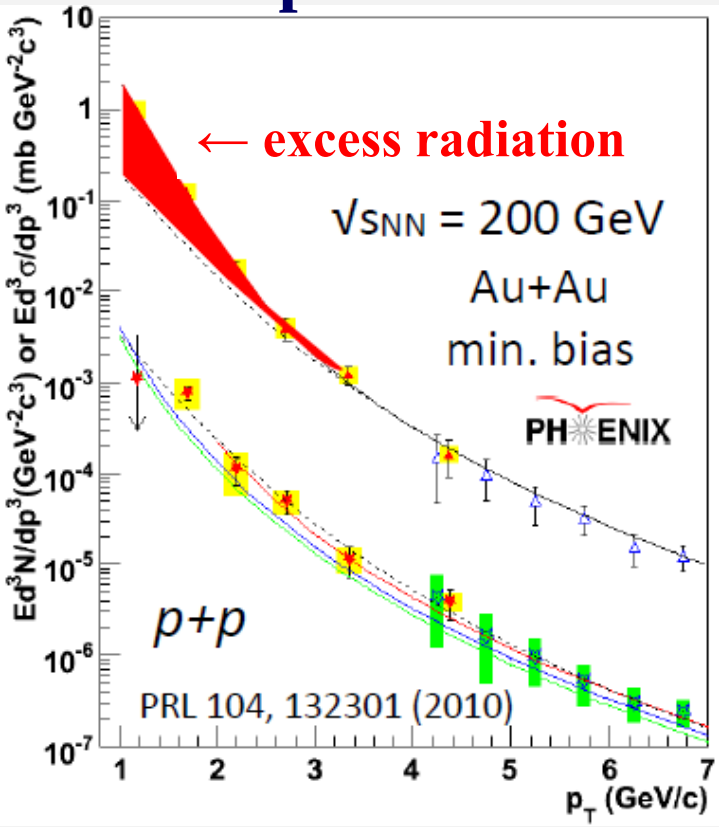


## Elliptic Flow

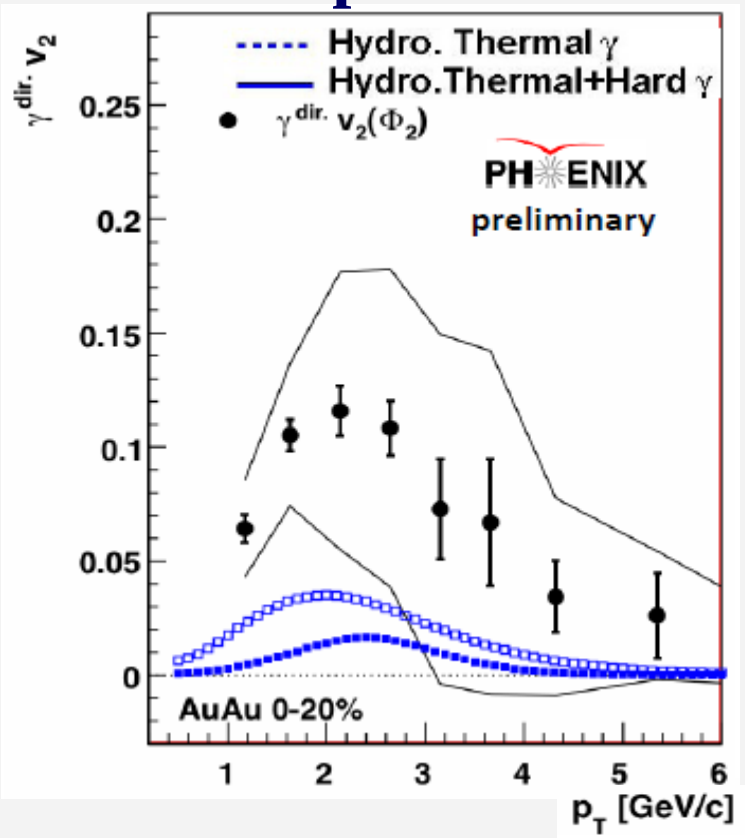


- $T_{eff}^{excess}$ = (220 25) MeV "moderate"

  ~ $\langle T \sqrt{(1+\beta)/(1-\beta)} \rangle$ suggests $\langle T \rangle < 200$ MeV

- **large $v_2$** also suggests "later" emission (aka ~$T_{pc}$)

# 3.5.2 Thermal Photon Spectra + $v_2$

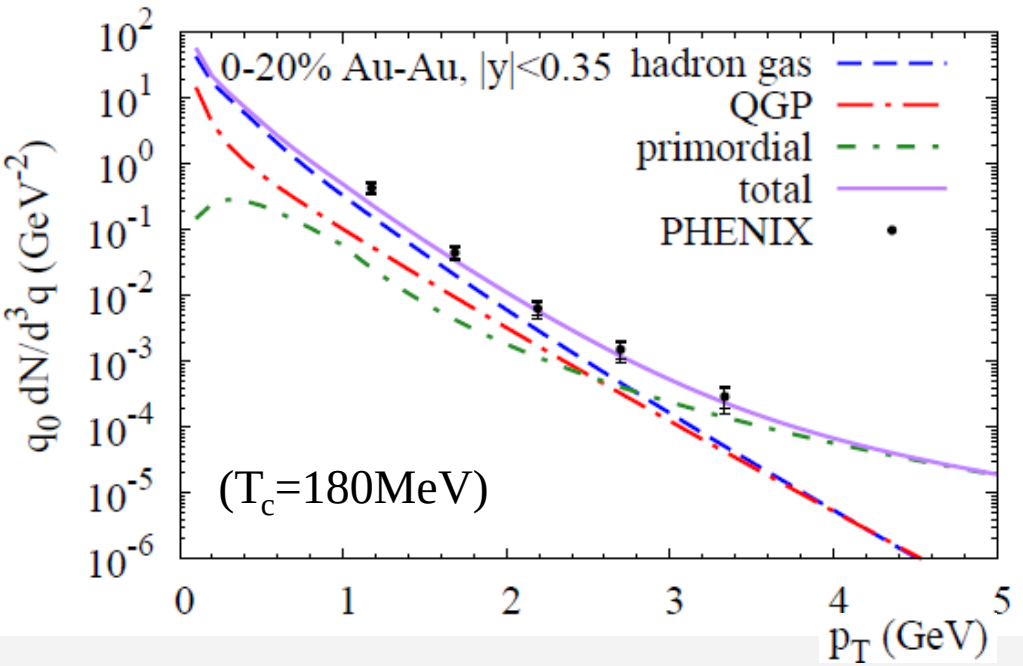


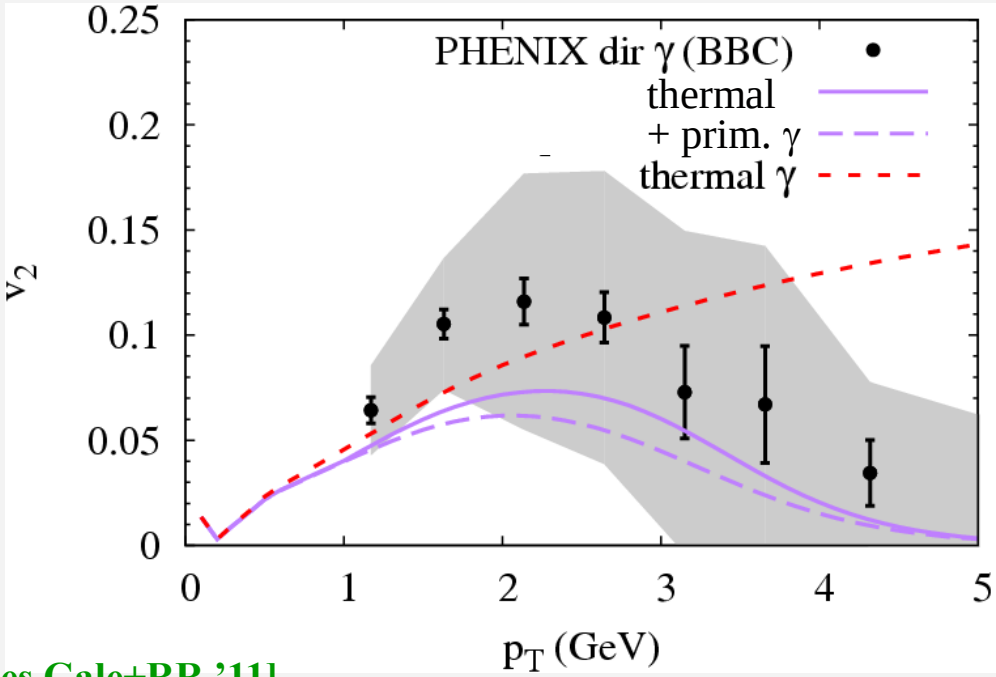


[van Hees,Gale+RR '11]

- **M → 0** limit of dilepton rates (continuous across $T_c$!)
- flow blue-shift, e.g. **β=0.3**: **⟨T⟩ ~ 220MeV / 1.35 ~ 160 MeV**
- confirms **bulk emission around $T_{pc}$**
- compatible with hydro evolution if bulk-$v_2$ saturates at $T_{pc}$ [He at al in prep.]

→ Talks by Skokov, Tuchin, Dusling

# 3.6 Elliptic Flow of Dileptons at RHIC

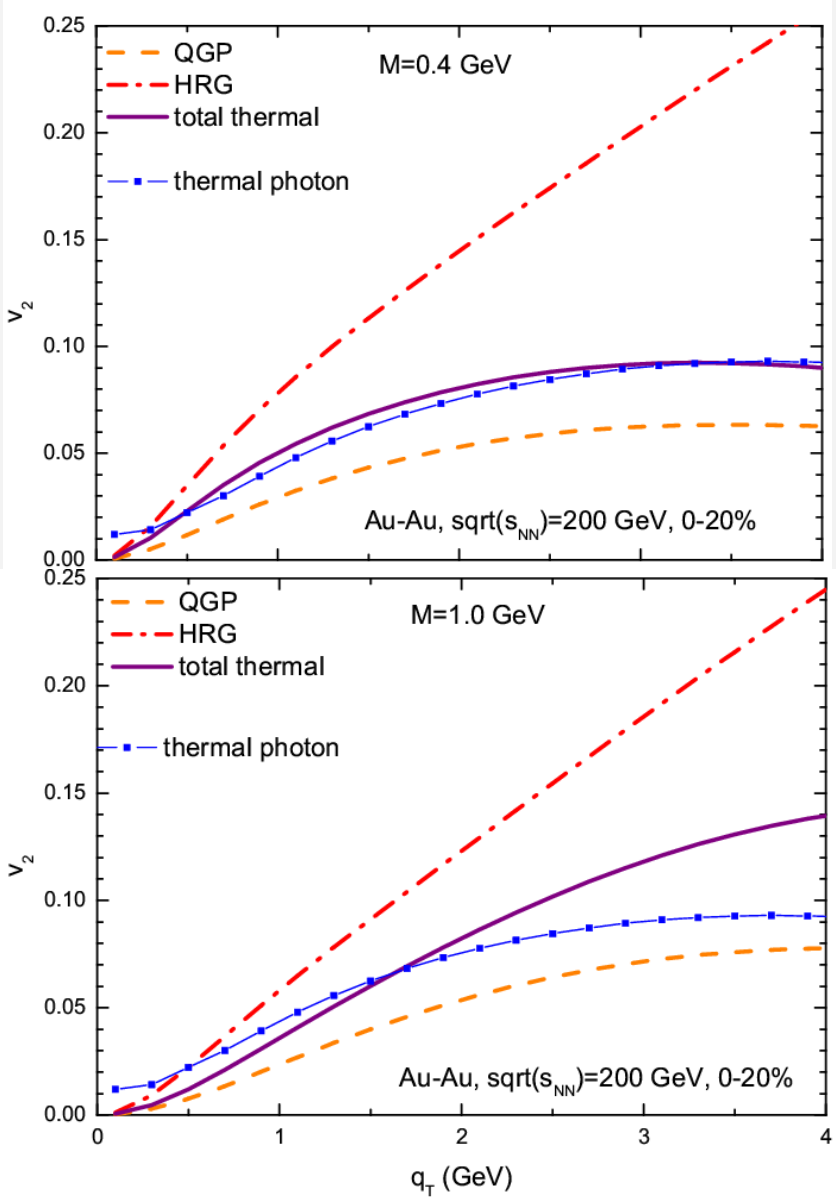


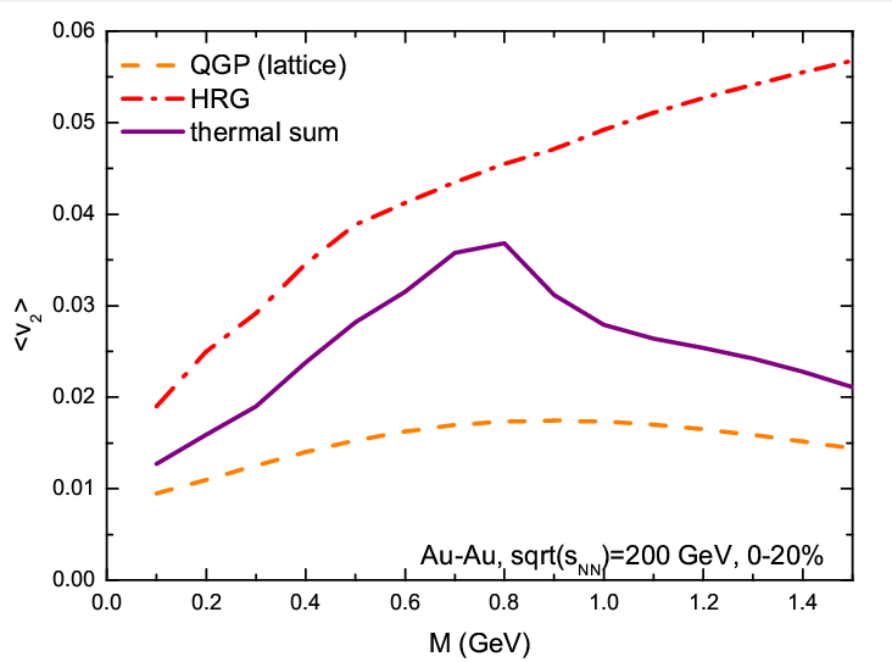


- maximum structure due to late ρ decays **[He et al in prep.]**

**[Chatterjee et al '07, Zhuang et al '09]**

# 4.) Conclusions

- Low-mass dileptons at SPS+RHIC point at universal source, avg. emission temperatures **$T \sim 150\text{MeV} \sim T_{pc}^{\chi}$** (slopes, $v_2$)
- ρ-meson smoothly melts into QGP continuum radiation
- Mechanisms underlying ρ-melting (π cloud + resonances) find counterparts in hadronic **Σ**-terms, restoring chiral symmetry
- Quantitative studies relating ρ-SF to chiral order parameters with QCD and Weinberg-type sum rules ongoing
- Need conditions under which medium effects turn off
- Future precise characterization of EM emission source at **RHIC, LHC** + **CBM/NICA/SIS** holds rich info on QCD phase structure (spectral shape + disp. rel., source collectivity + lifetime)

# 4.1 How to Turn off Medium Effects

- **pp** collisions: cocktail - seems to work (but: **no** medium effect)
- Peripheral collisions - challenging: dense hadronic phase persists
- **d-A** collisions: forward vs. backward **y** (formation time effects?)
- High(er) $\mathbf{p_T}$
  - seems to work: **NA60** $\mu^+\mu^-$

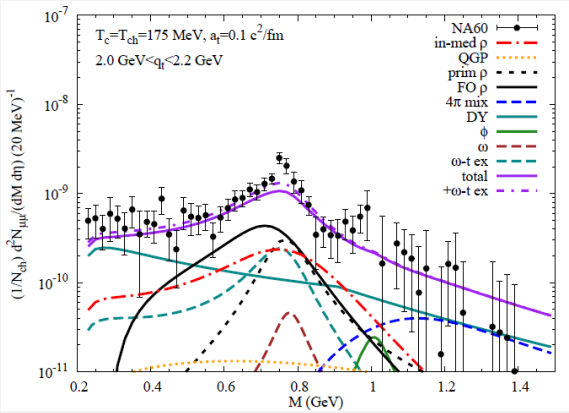


- Elementary projectiles on cold nuclei
  - seems to work: **CLAS** $\gamma A \rightarrow e^+e^- X$

$(\Gamma_\rho \approx 220$ **MeV**$)$

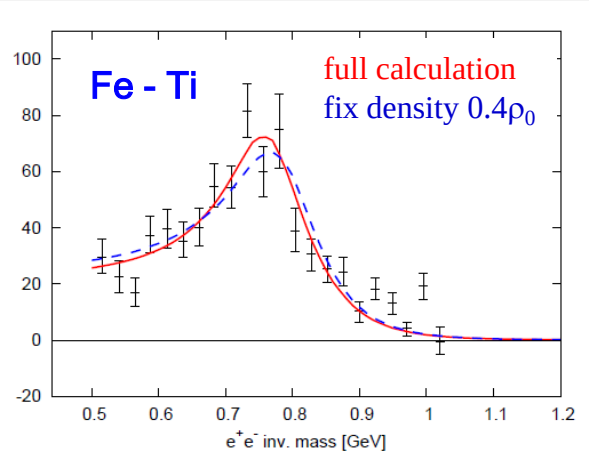

# 2.3.2 NA60 Mass Spectra: $p_t$ Dependence

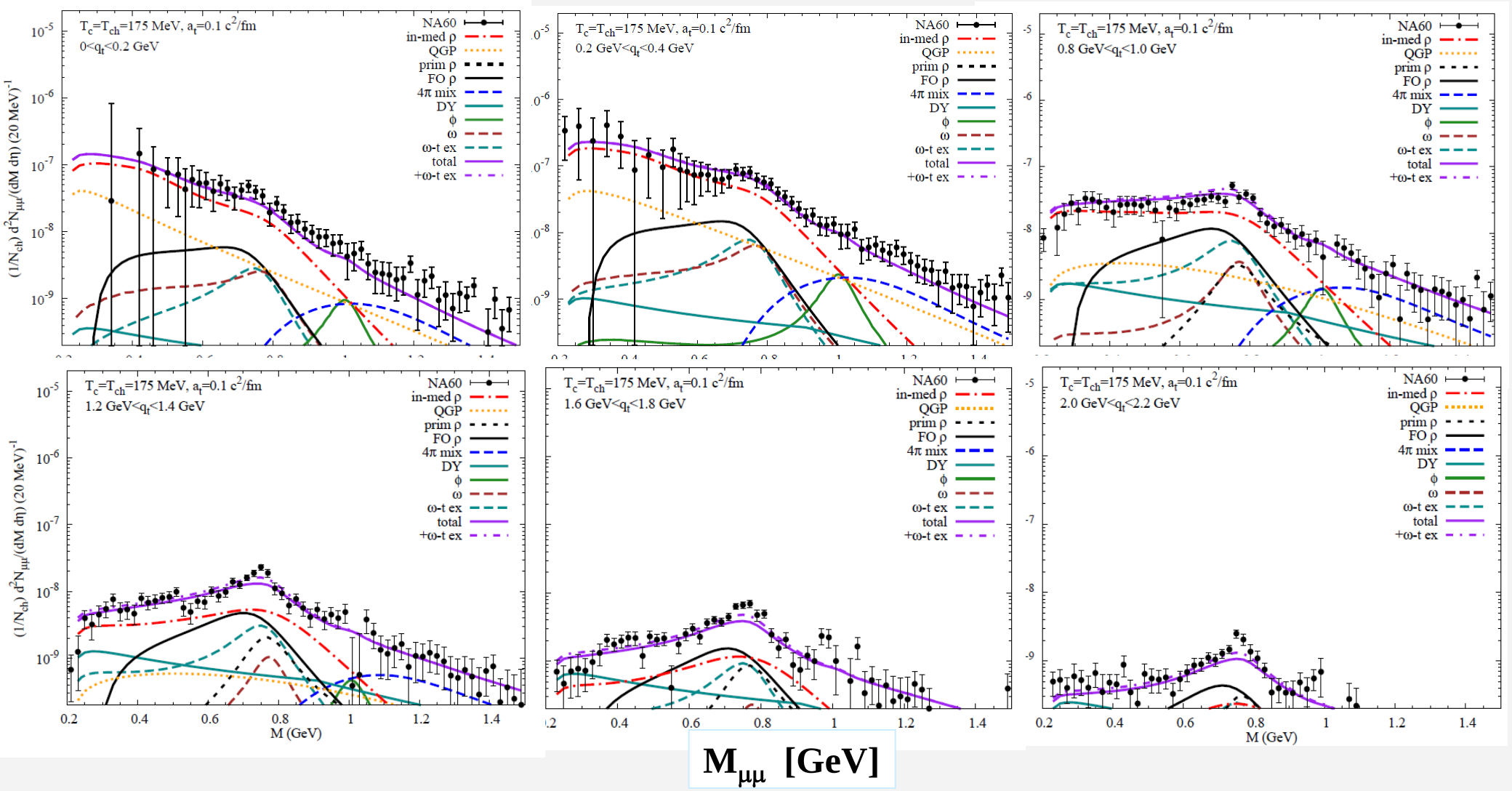


$M_{\mu\mu}$ [GeV]

- rather involved at $p_T$>1.5GeV: Drell-Yan, primordial/freezeout ρ , …

# 3.4.3 Hadronic vs. QGP Photons at RHIC

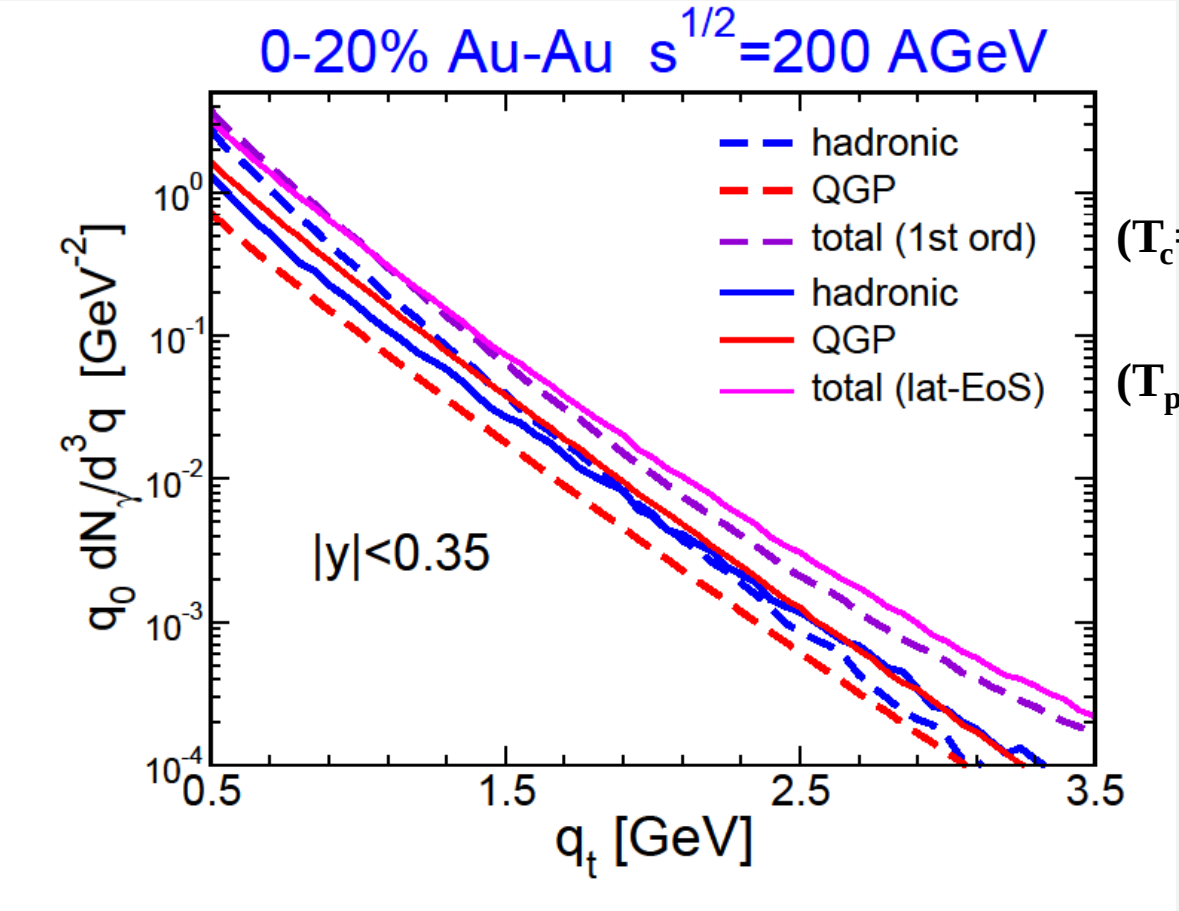


**($T_c$=180MeV)**

**($T_{pc}$=170MeV)**

- smaller $\mathbf{T_{pc}}$ + lattice EoS enhance QGP + deplete hadronic yield
- corroborates prevalent emission source around $\mathbf{T_{pc}}$

# 3.6 QGP Barometer: Blue Shift vs. Temperature

**SPS**

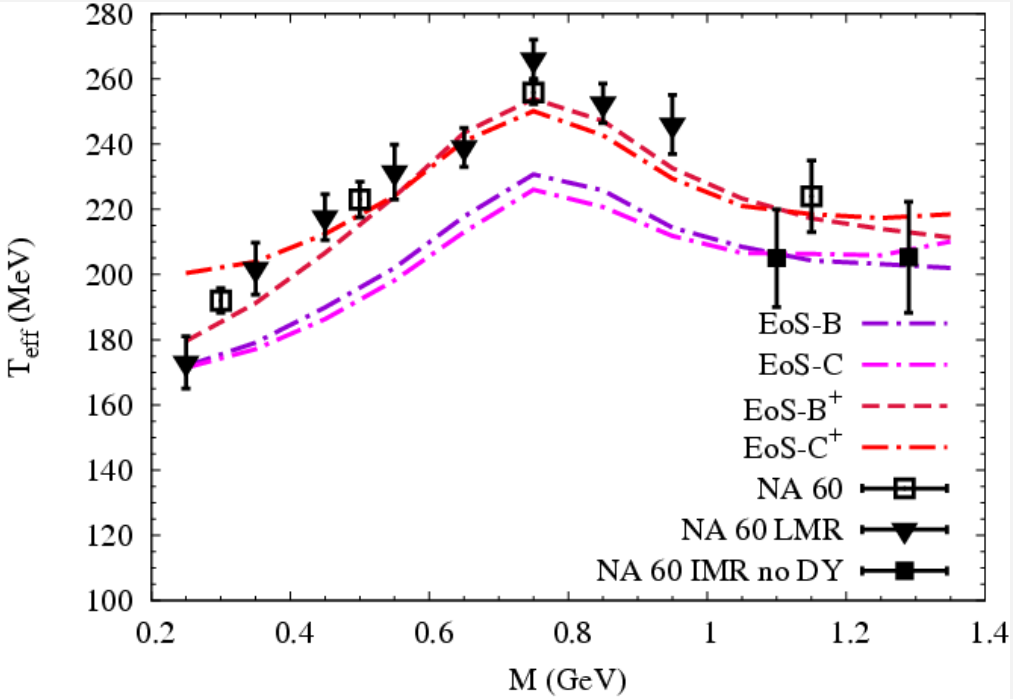


**RHIC**

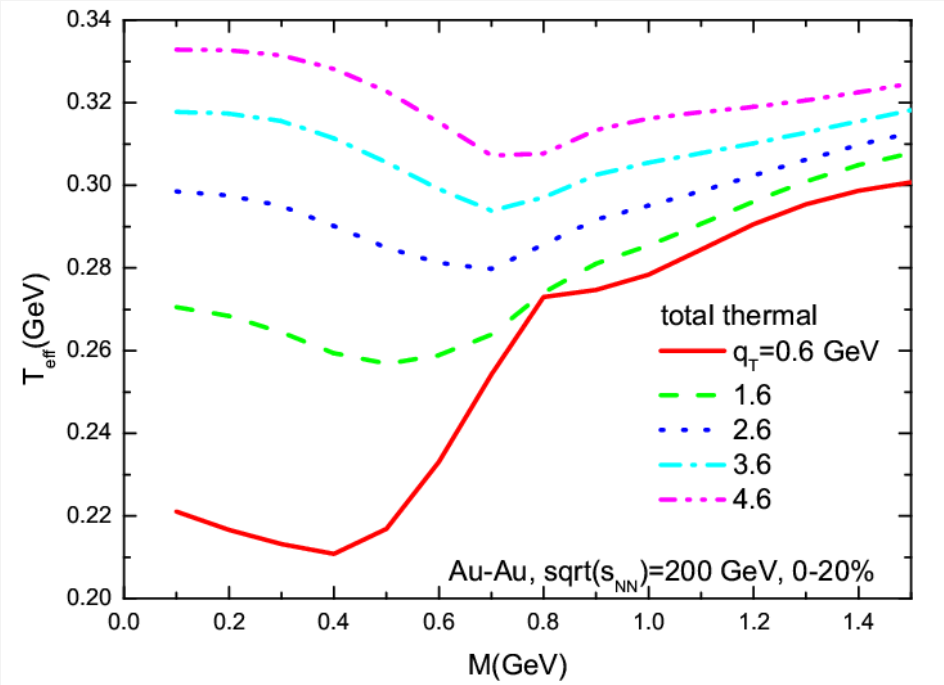


- QGP-flow driven increase of $T_{eff} \sim T + M\,(\beta_{flow})^2$ at **RHIC**
- high $p_t$: high **T** wins over high-flow ρ's → minimum (opposite to **SPS**!)
- saturates at "true" early temperature $T_0$ (no flow)

# 4.1.2 Sensitivity to Spectral Function

## In-Medium ρ-Meson Width

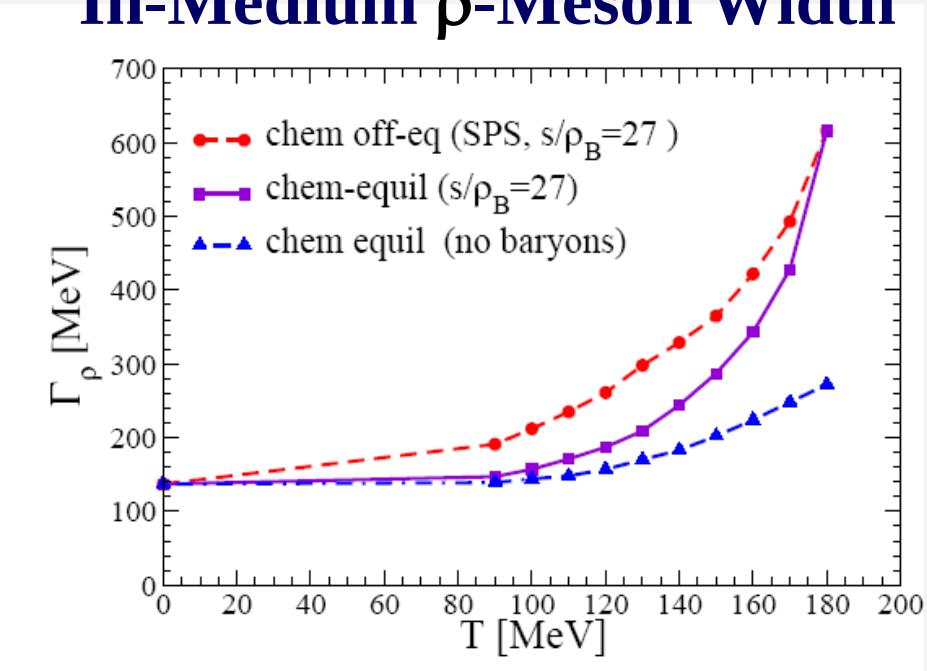


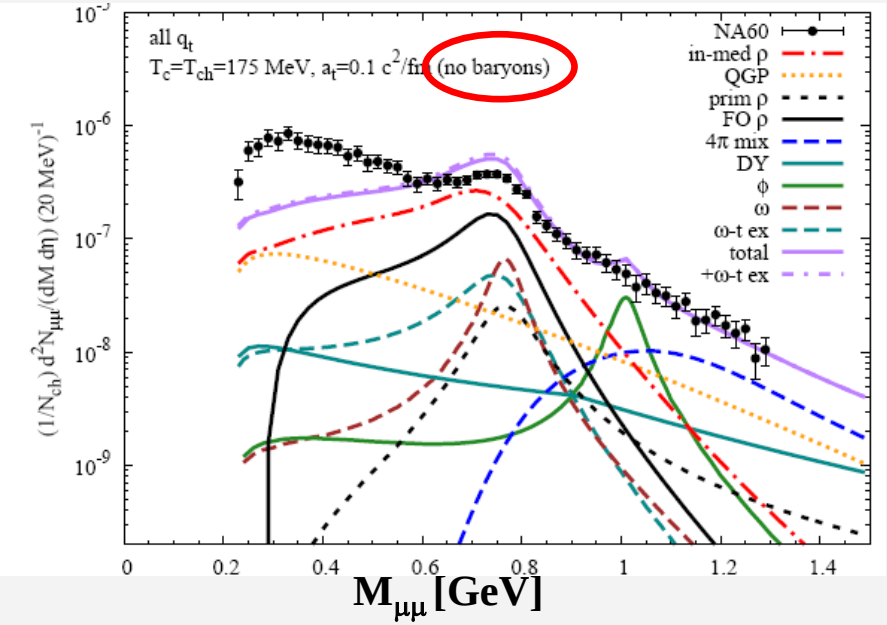


- avg. $\Gamma_\rho(T\sim150\,\text{MeV})\sim370\,\text{MeV} \Rightarrow \Gamma_\rho(T\sim T_c)\approx600\,\text{MeV} \rightarrow m_\rho$
- driven by (anti-) baryons

# 4.1.3 Mass Spectra as Thermometer

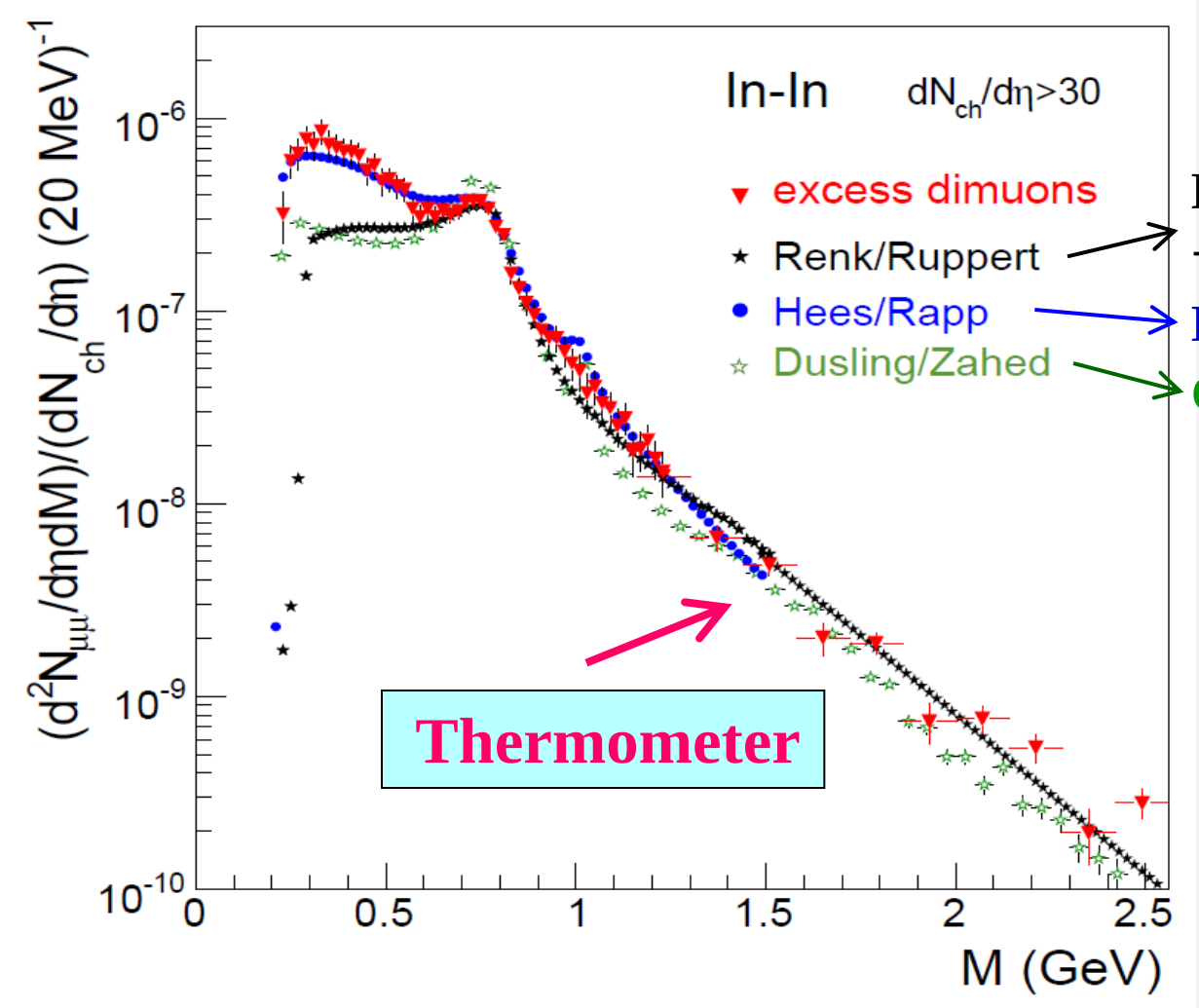


Emp. scatt. ampl. + T-ρ approximation

Hadronic many-body

Chiral virial expansion

[NA60, CERN Courier Nov. 2009]

- Overall slope T~150-200MeV (true T, no blue shift!)

# 3.2 Spectral Functions + Weinberg Sum Rules

- Quantify chiral symmetry breaking via observable spectral functions
- Vector **(ρ)** - Axialvector **($a_1$)** spectral splitting

$$I_n = -\int \frac{ds}{\pi} s^n (\rho_V - \rho_A)$$

[Weinberg '67, Das et al '67; Kapusta+Shuryak '93]

$$I_{-2} = \frac{1}{3} f_\pi^2 r_\pi^2 - F_A, \qquad I_{-1} = f_\pi^2,$$

$$I_0 = -2m_q \langle 0|\bar{q}q|0\rangle, \quad I_1 = c\alpha_s \langle 0|(\bar{q}q)^2|0\rangle$$

$\tau \to (2n)\pi$ [ALEPH '98,OPAL '99] $\tau \to (2n+1)\pi$

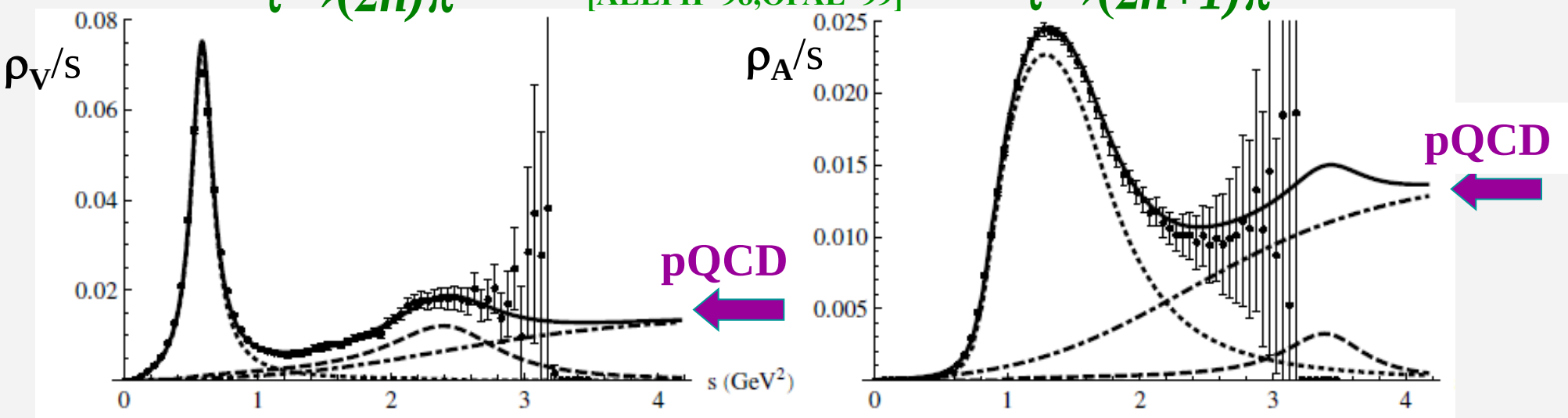


- Updated "fit": [Hohler+RR '12]

ρ + $a_1$ resonance, excited states (ρ'+ $a_1$'), universal continuum (pQCD!)

# 3.2.2 Evaluation of Chiral Sum Rules in Vacuum

- **pion decay constants**

- **chiral quark condensates**

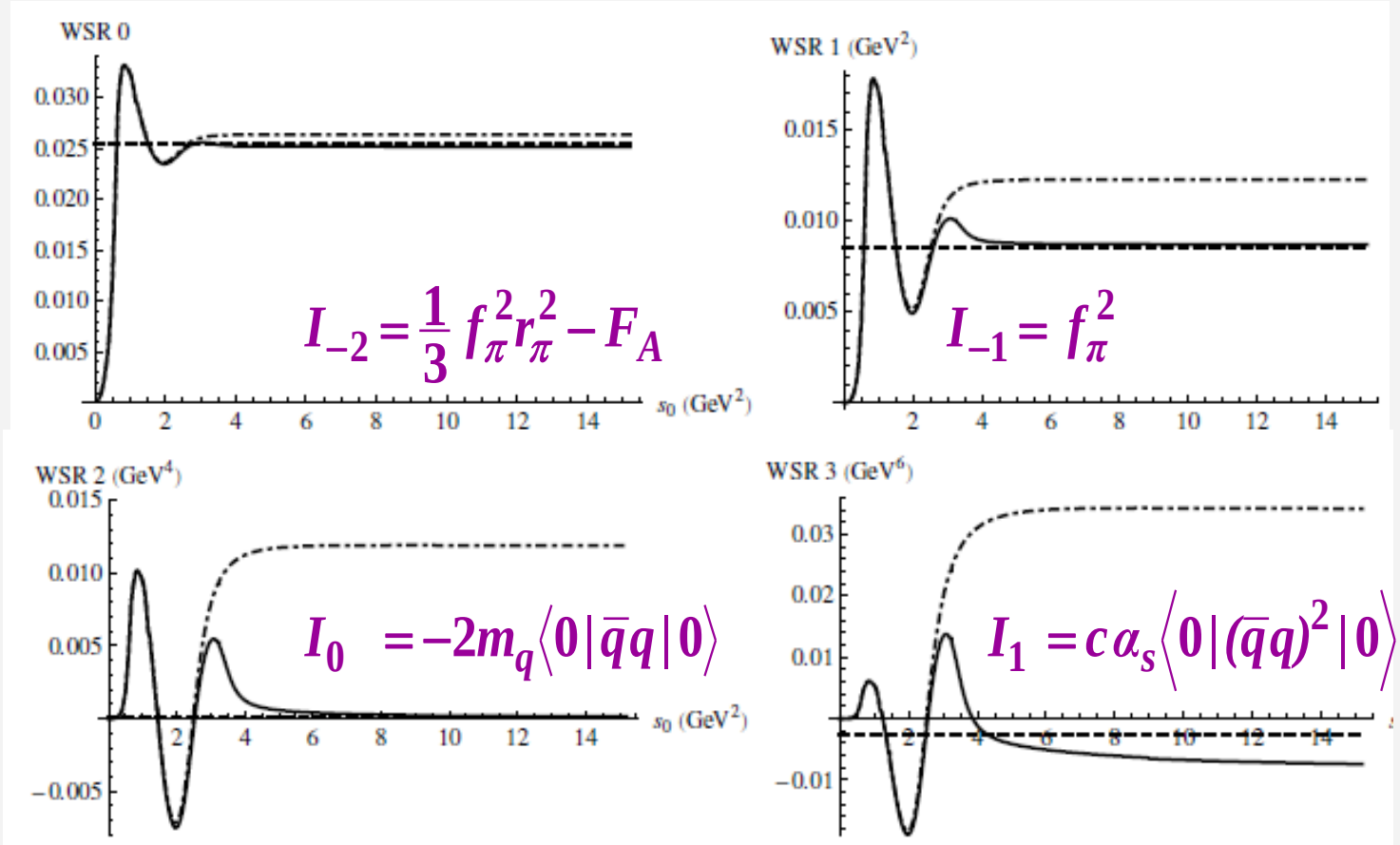


- vector-axialvector splitting quantitative observable of spontaneous chiral symmetry breaking
- **promising starting point to analyze chiral restoration**

# 2.3 QCD Sum Rules: ρ and $a_1$ in Vacuum

- dispersion relation: $$\int_0^\infty \frac{ds}{s}\,\frac{\mathrm{Im}\,\Pi_\alpha(s)}{Q^2+s} = \frac{\Pi_\alpha(Q^2)}{Q^2}$$ [Shifman,Vainshtein+Zakharov '79]

- ***lhs:*** hadronic spectral fct.
- ***rhs:*** operator product expansion

$$\frac{1}{M^2}\int_0^\infty ds\frac{\rho_V(s)}{s}e^{-s/M^2} = \frac{1}{8\pi^2}\left(1+\frac{\alpha_s}{\pi}\right) + \frac{m_q\langle\bar{q}q\rangle}{M^4} + \frac{1}{24M^4}\langle\frac{\alpha_s}{\pi}G^2_{\mu\nu}\rangle - \frac{56\pi\alpha_s}{81M^6}\langle\mathcal{O}_4^V\rangle\ldots$$

$$\frac{1}{M^2}\int_0^\infty ds\frac{\bar{\rho}_A(s)}{s}e^{-s/M^2} = \frac{1}{8\pi^2}\left(1+\frac{\alpha_s}{\pi}\right) + \frac{m_q\langle\bar{q}q\rangle}{M^4} + \frac{1}{24M^4}\langle\frac{\alpha_s}{\pi}G^2_{\mu\nu}\rangle + \frac{88\pi\alpha_s}{81M^6}\langle\mathcal{O}_4^A\rangle\ldots$$

- 4-quark + gluon **condensate** dominant

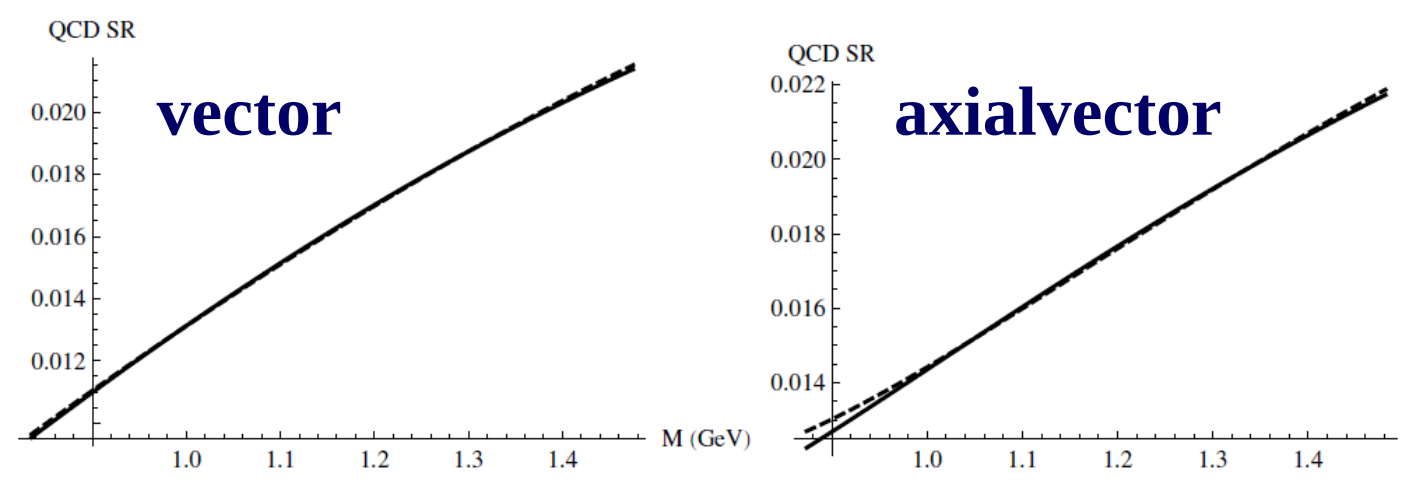

# 3.3 QCD Sum Rules at Finite Temperature

$$\frac{1}{M^2}\int_0^\infty ds\frac{\rho_V(s)}{s}e^{-s/M^2} = \frac{1}{8\pi^2}\left(1+\frac{\alpha_s}{\pi}\right) + \frac{m_q\langle\bar{q}q\rangle}{M^4} + \frac{1}{24M^4}\langle\frac{\alpha_s}{\pi}G^2_{\mu\nu}\rangle - \frac{56\pi\alpha_s}{81M^6}\langle\mathcal{O}_4^V\rangle\ldots$$

[Hatsuda+Lee'91, Asakawa+Ko '93, Klingl et al '97, Leupold et al '98, Kämpfer et al '03, Ruppert et al '05]

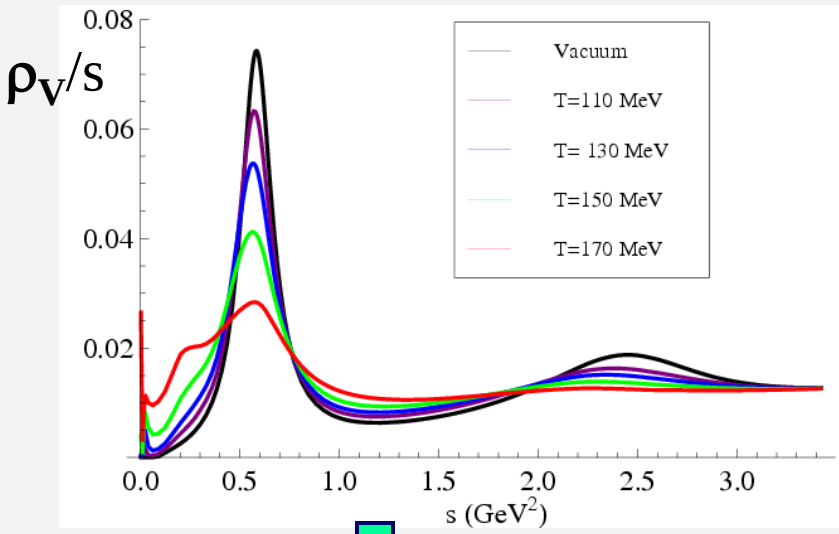


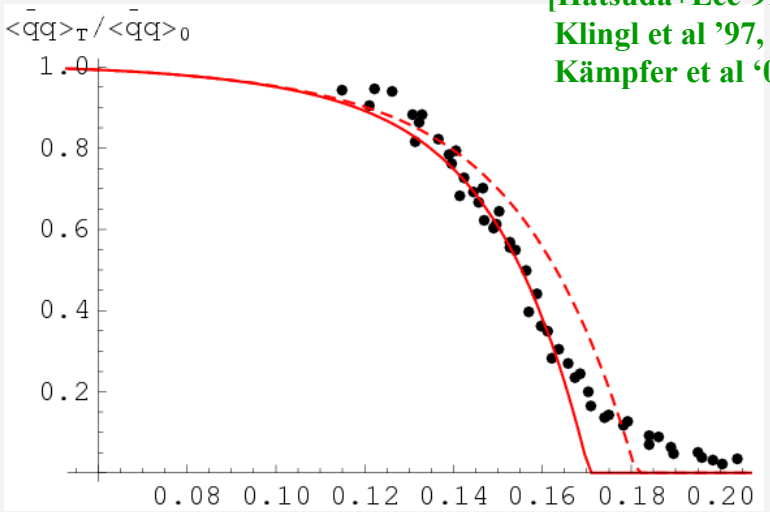


T [GeV]

**Percentage Deviation**

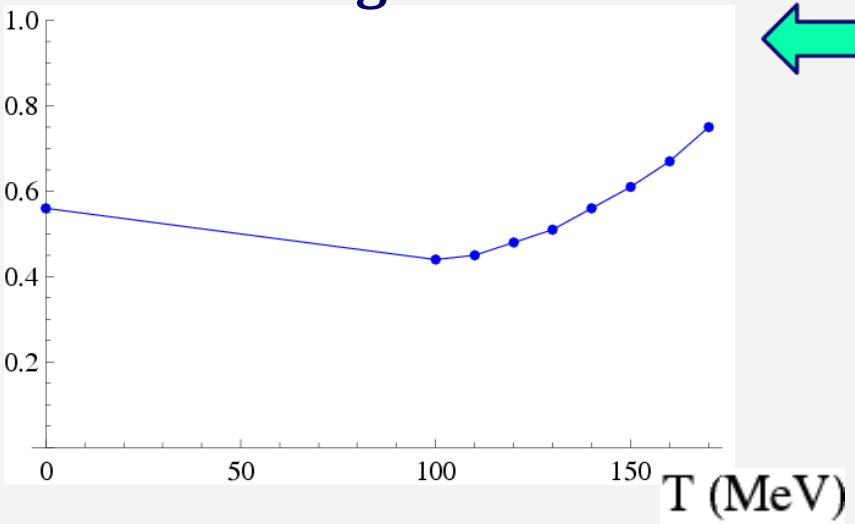


- **ρ and ρ' melting compatible with chiral restoration**

[Hohler +RR '12]

# 2.4 Dilepton Thermometer: Slope Parameters

## Invariant Rate vs. M-Spectra

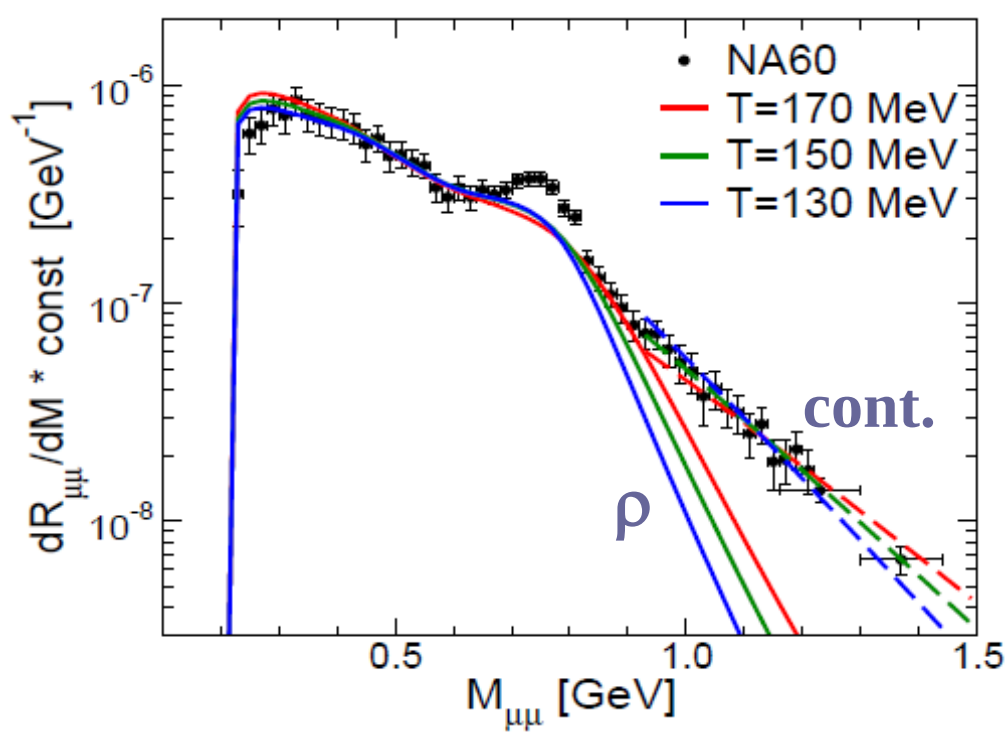


## Transverse-Momentum Spectra

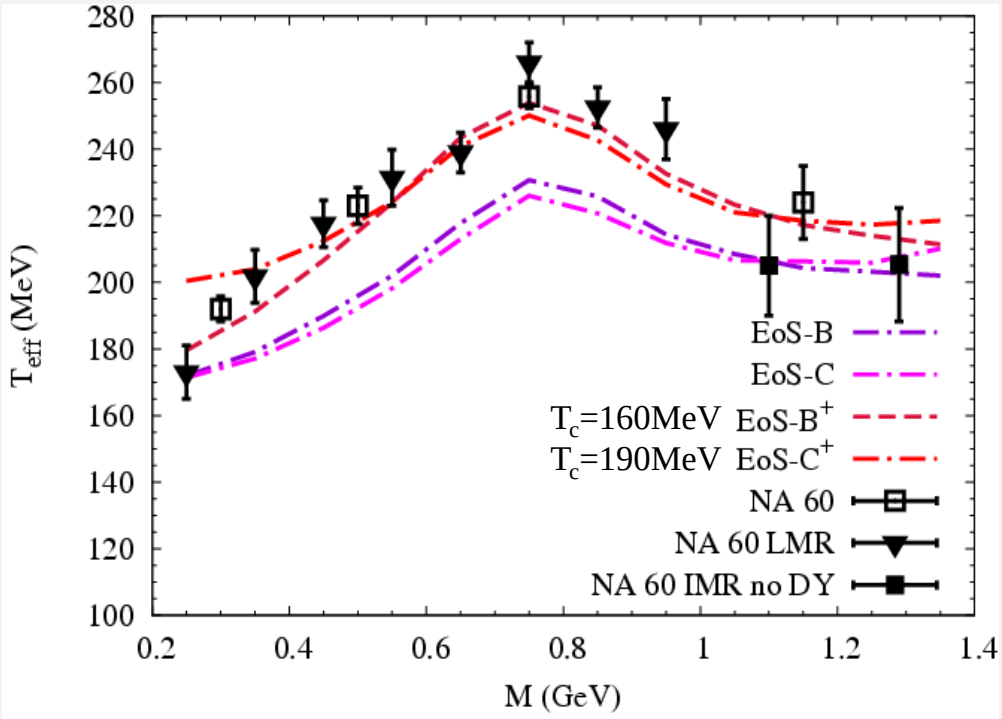


- Low mass: radiation from around **$T \sim T_{pc}\chi \sim 150$MeV**
- Intermediate mass: **$T \sim 170$ MeV** and above
- Consistent with **$p_T$** slopes incl. flow: **$T_{eff} \sim T + M\,(\beta_{flow})^2$**

# 4.3.2 Revisit Ingredients

## Emission Rates

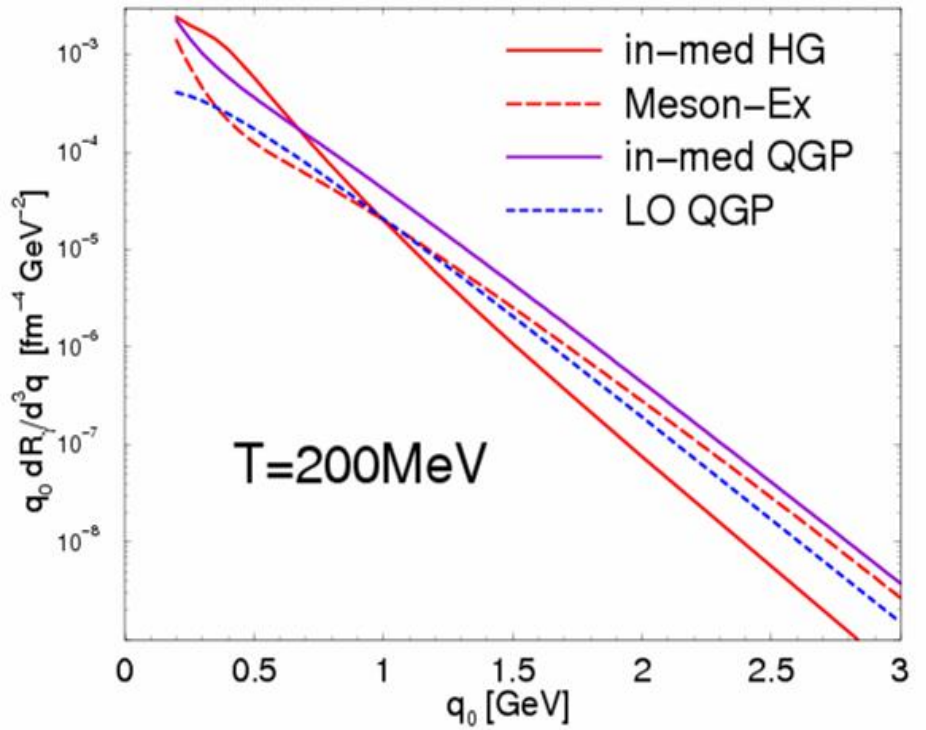


## Fireball Evolution

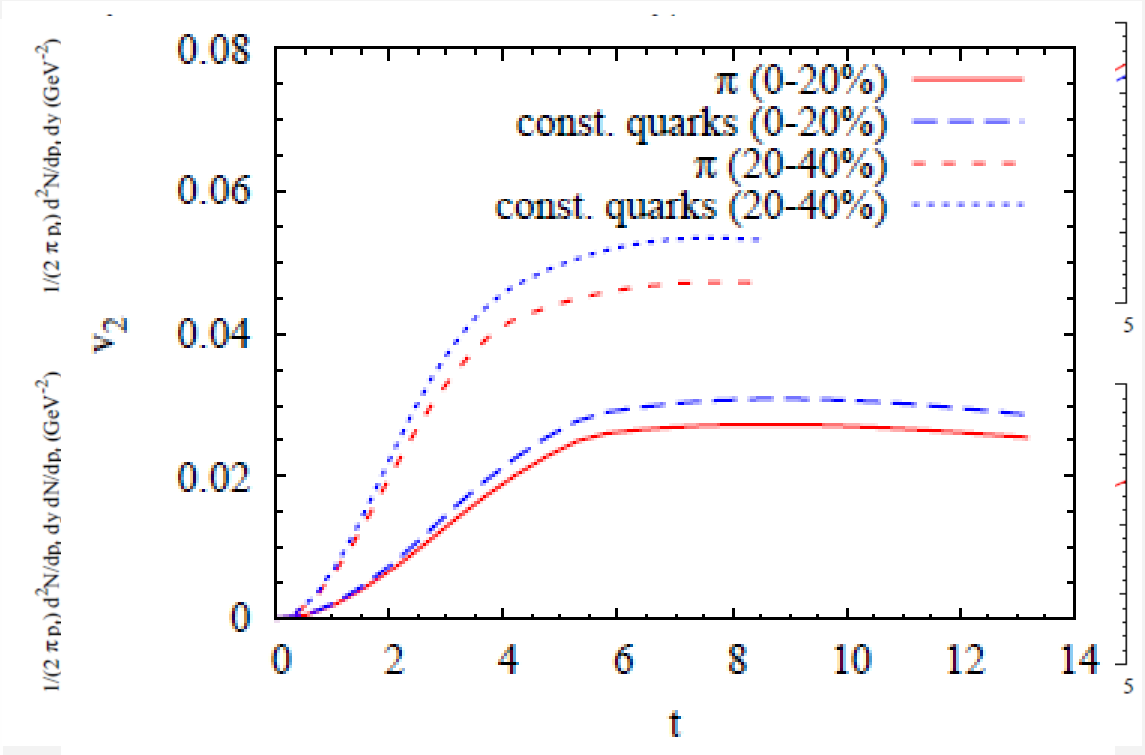


- Hadron - QGP continuity!
- conservative estimates…

[Turbide et al '04]

- multi-strange hadrons at "$T_c$"
- $v_2^{bulk}$ fully built up at hadronization
- chemical potentials for **π, K, …**

[van Hees et al '11]

# 5.1 Thermal Dileptons at LHC

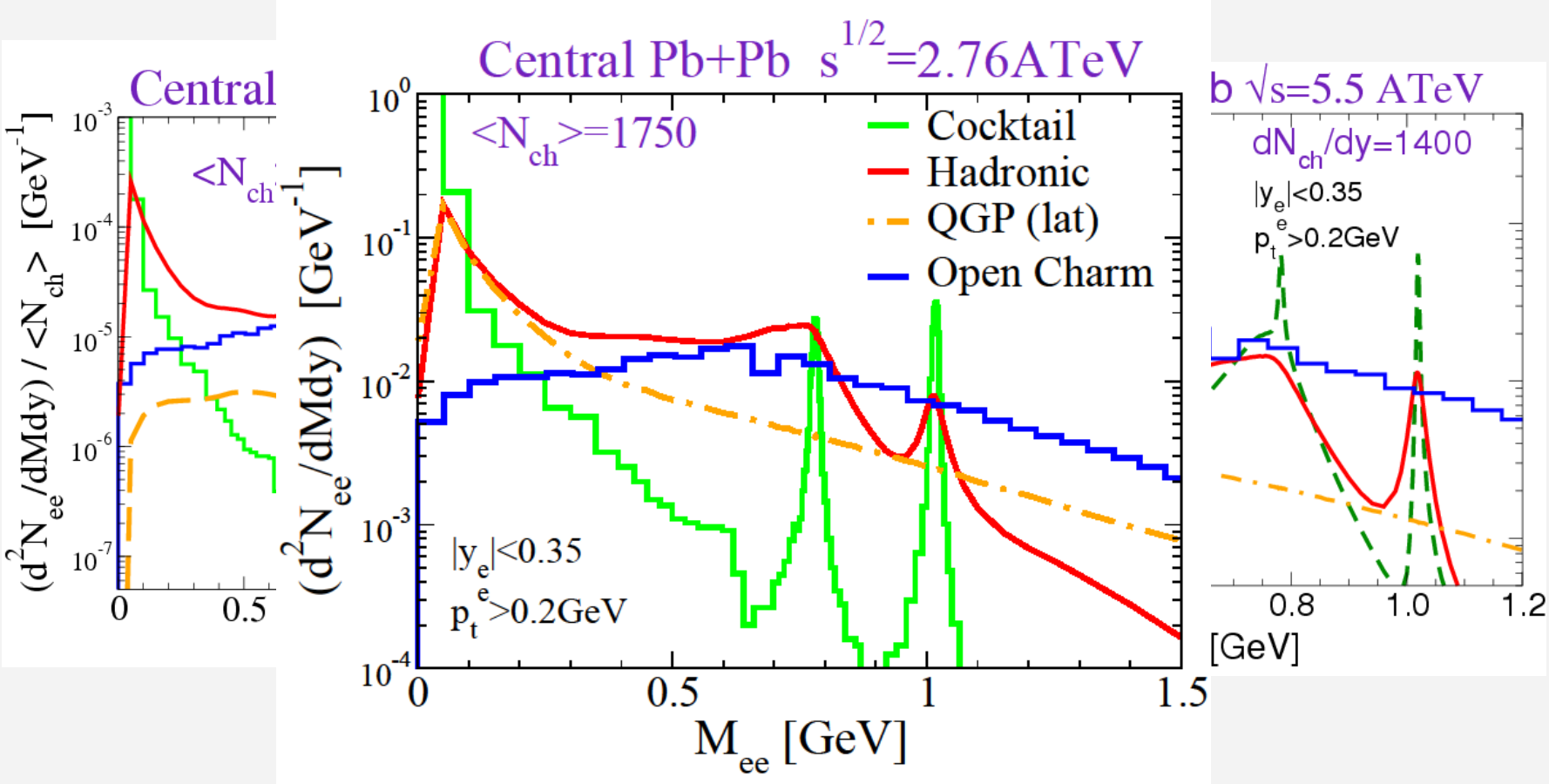


- charm comparable, accurate (in-medium) measurement critical
- low-mass spectral shape in chiral restoration window

# 5.2 Chiral Restoration Window at LHC

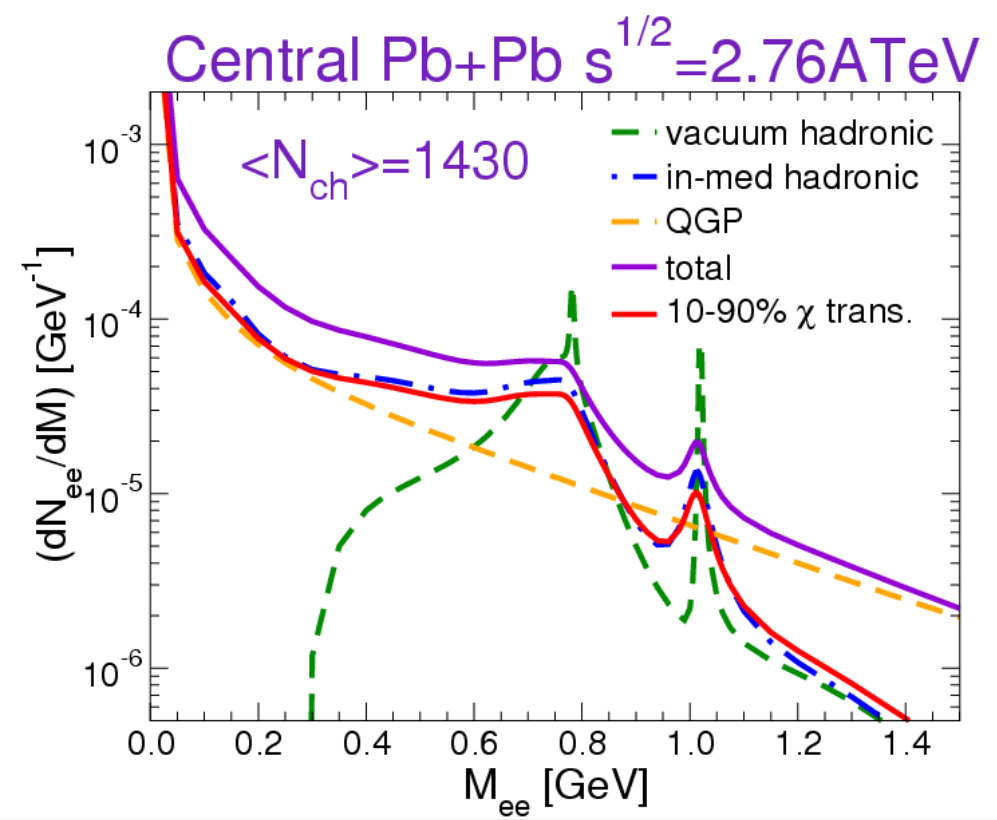


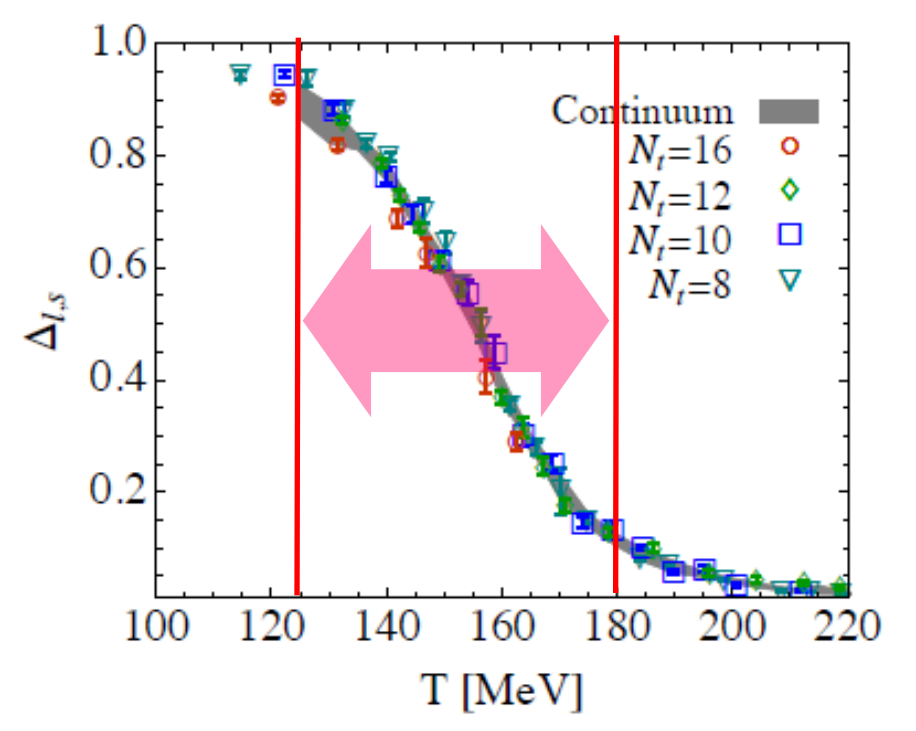


- low-mass spectral shape in chiral restoration window:

  **~60%** of thermal low-mass yield in "chiral transition region"

  **(T=125-180MeV)**

- enrich with (low-) $\mathbf{p_t}$ cuts

# 4.3 Dimuon $p_t$-Spectra and Slopes: Barometer

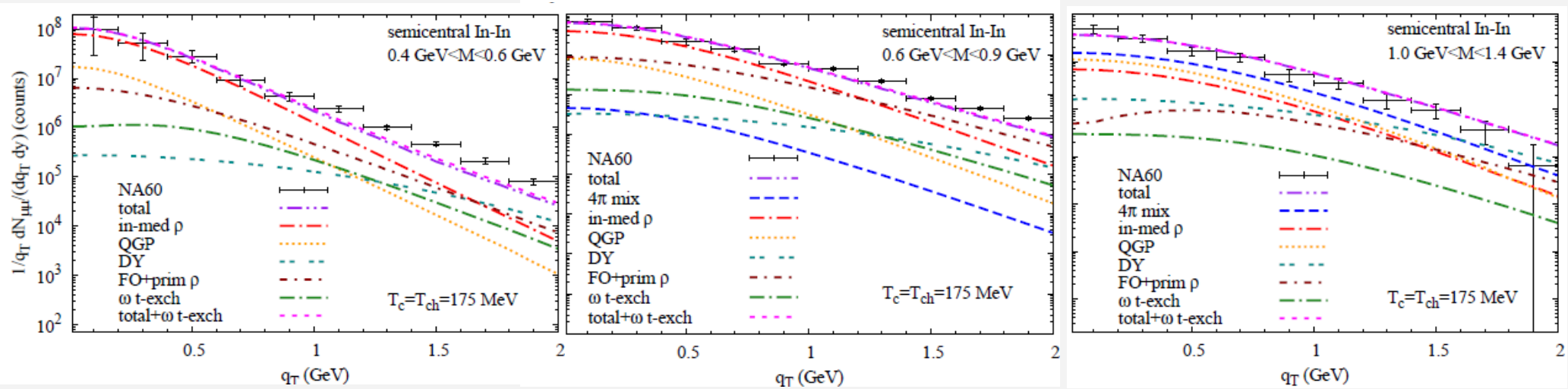


## Effective Slopes $T_{eff}$

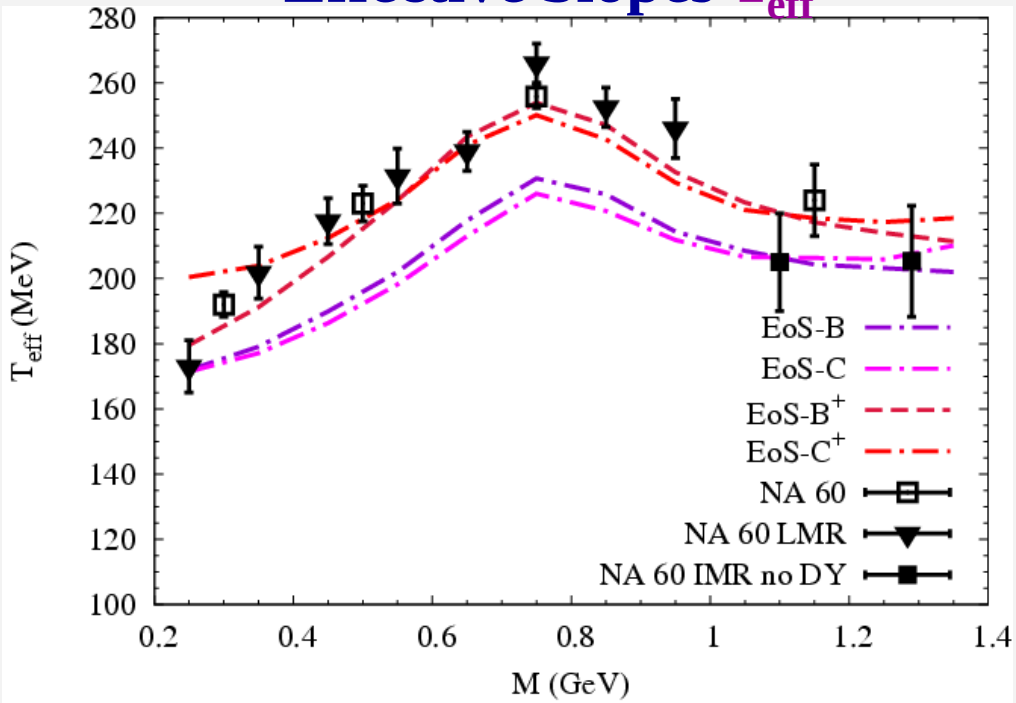


- theo. slopes originally too soft
- increase fireball acceleration, e.g. $a_\perp = 0.085/\text{fm} \rightarrow 0.1/\text{fm}$
- insensitive to $T_c$=160-190MeV

# 3.4.2 Back to Spectral Function

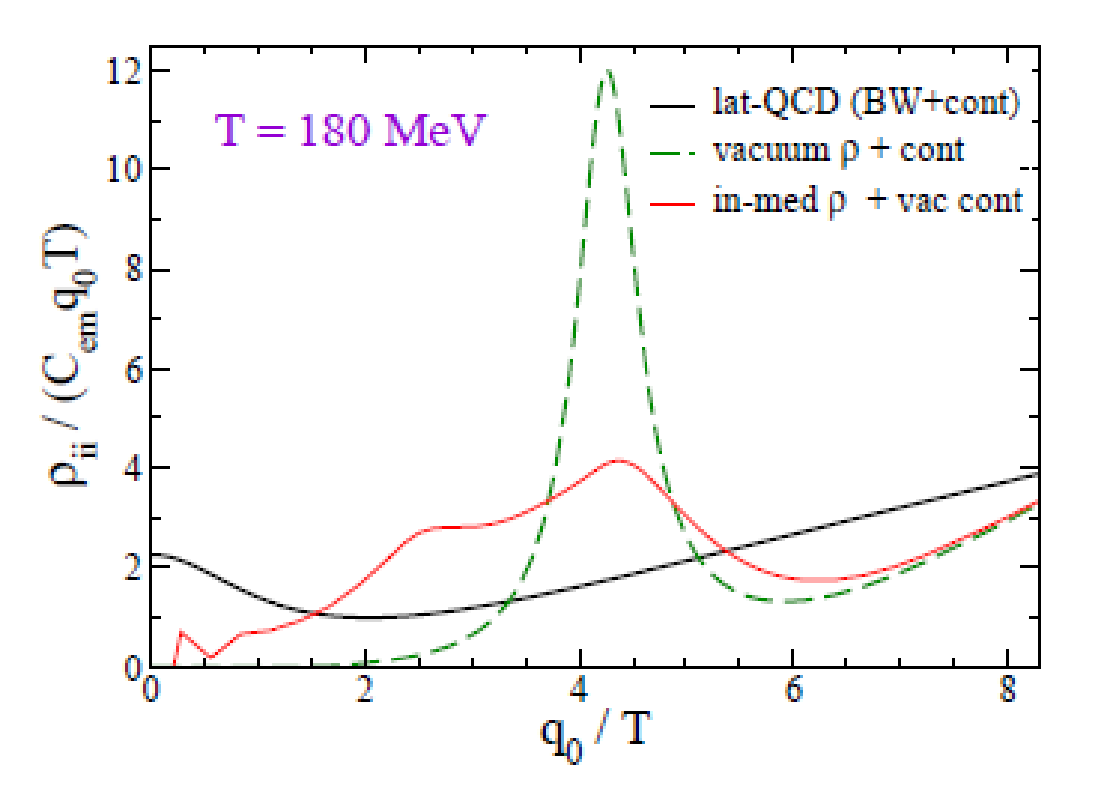


- **suggests approach to chiral restoration + deconfinement**

# 4.2 Improved Low-Mass QGP Emission

$$\frac{dR_{ee}}{d^4q} = \frac{\alpha_{em}^2}{6\pi^3 M^2} f^B(q_0;T)\rho_V(q_0,q)$$

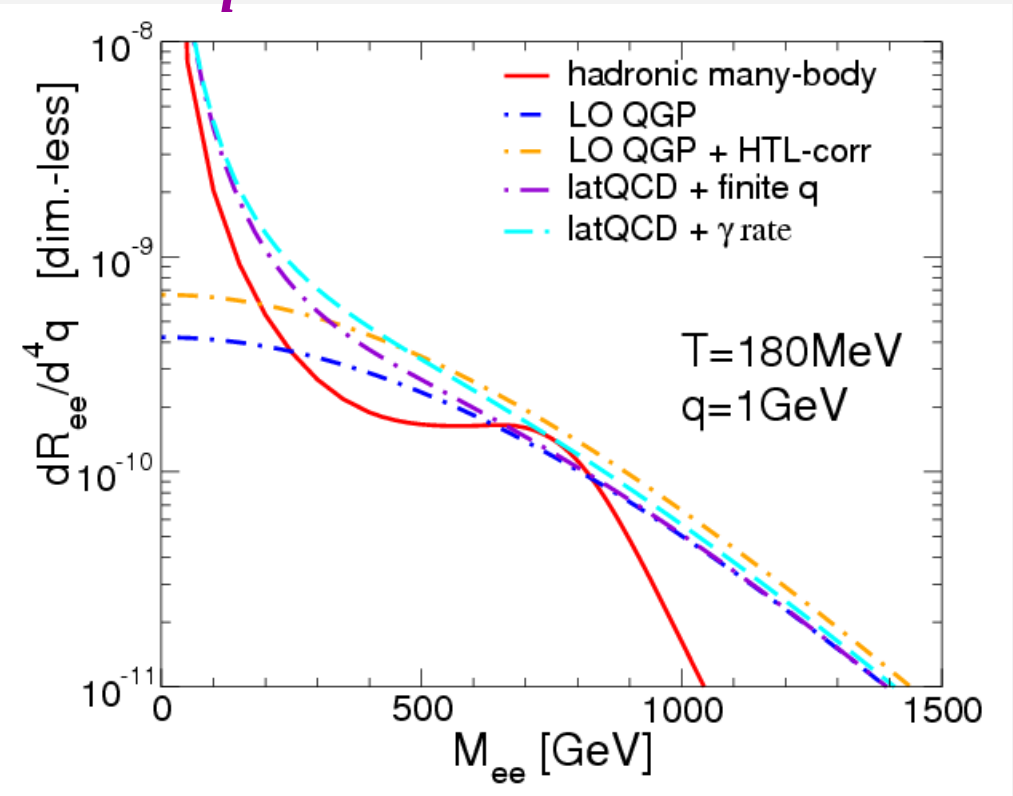


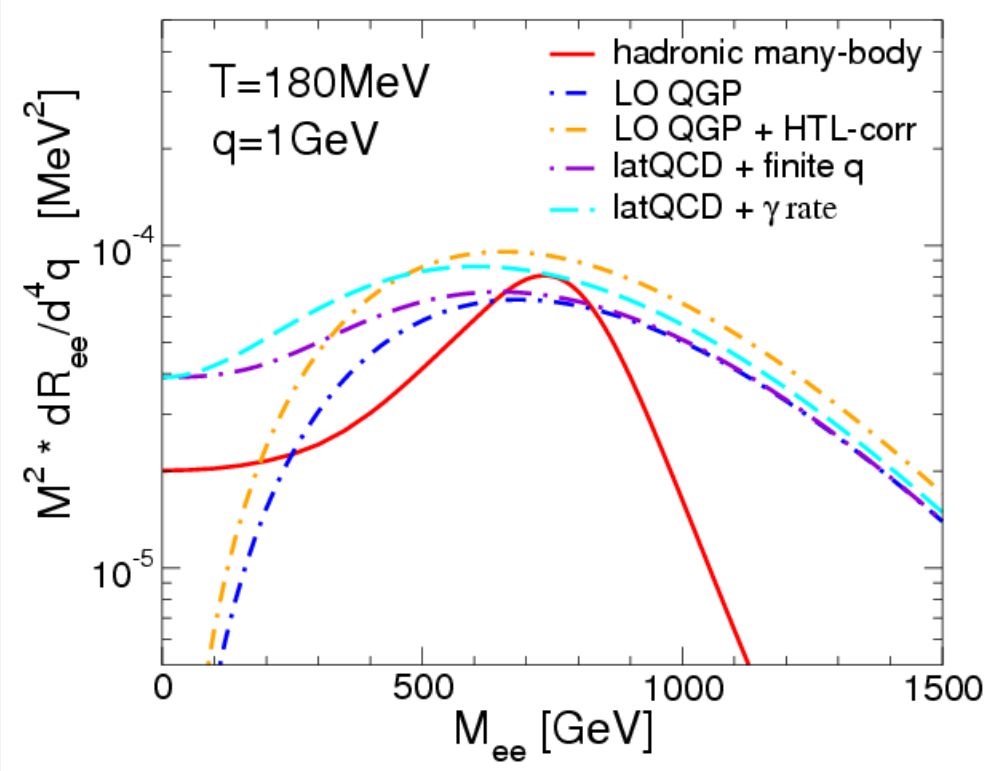


- LO pQCD spectral function: $\rho_V(q_0,q) = {}^6\!/_9\, 3M^2/2\pi\, [1+Q_{HTL}(q_0)]$
- augment lat-QCD rate with finite 3-momentum (γ rate)

$$\rho_V^{fit}(q_0,q) = \rho_{q\bar{q}}^{pert}(M)\left[1+\bar{C}\alpha_s\frac{T^2}{M^2}\ln\left(1+\frac{Cq_0}{\alpha_s T}\right)\right]$$

# 4.2 Low-Mass $e^+e^-$ at RHIC: PHENIX vs. STAR

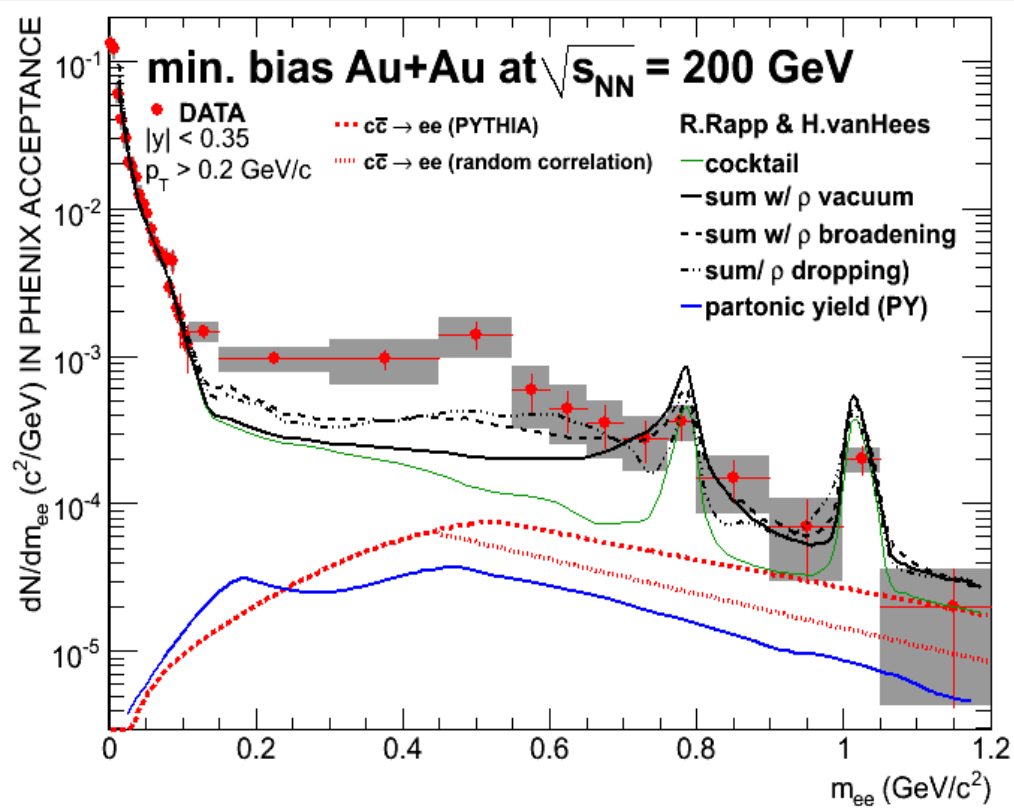


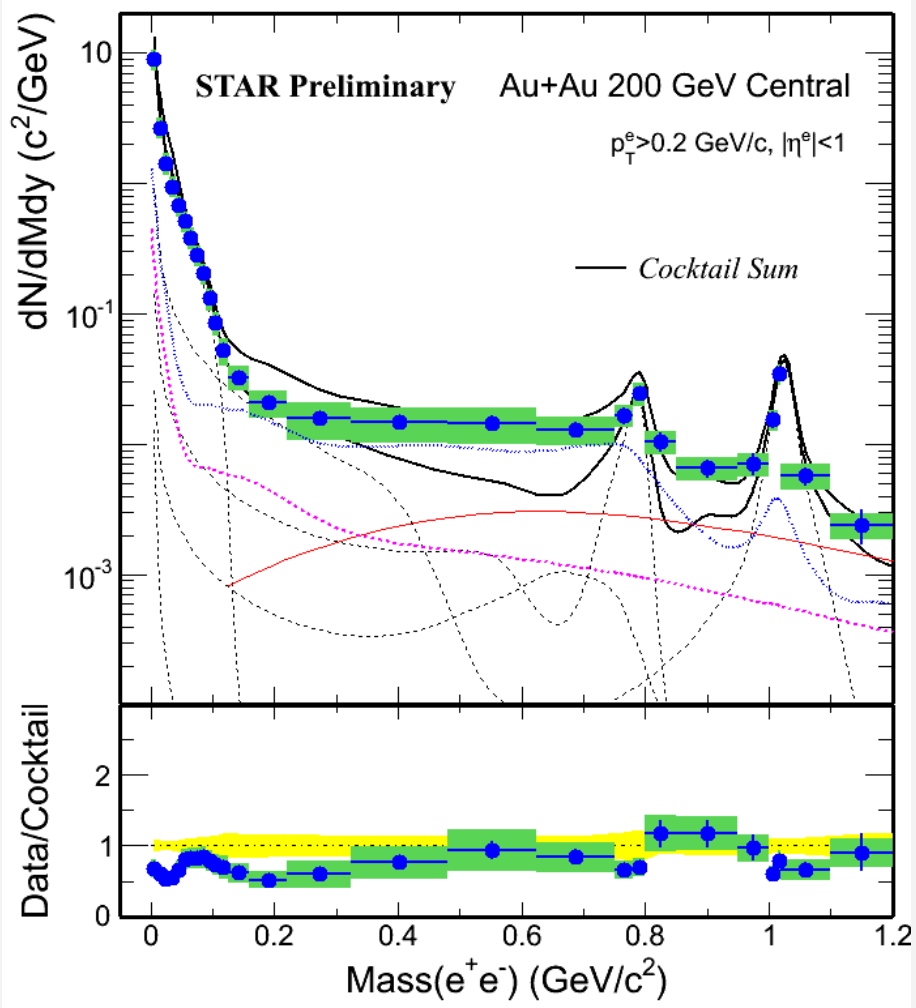


- large enhancement not accounted for by theory
- cannot be filled by QGP radiation…

- (very) low-mass region overpredicted… (**SPS**?!)

# 4.2 Low-Mass Dileptons: Chronometer

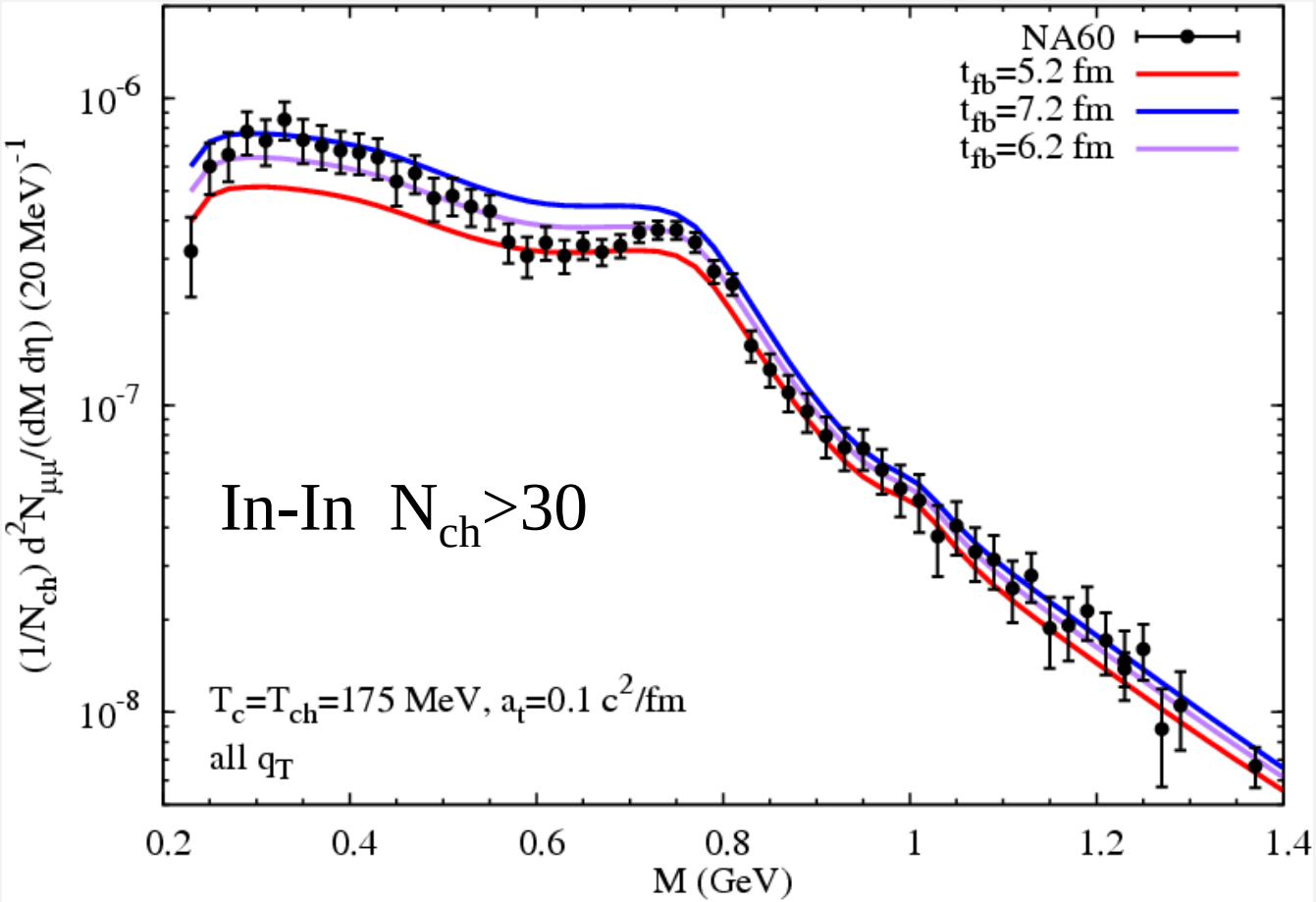


- first "explicit" measurement of interacting-fireball **lifetime**:

  $\tau_{FB} \approx (6 \quad 1)$ **fm/c**

# 3.2 Axialvector in Nucl. Matter: Dynamical $a_1(1260)$

**Vacuum:**

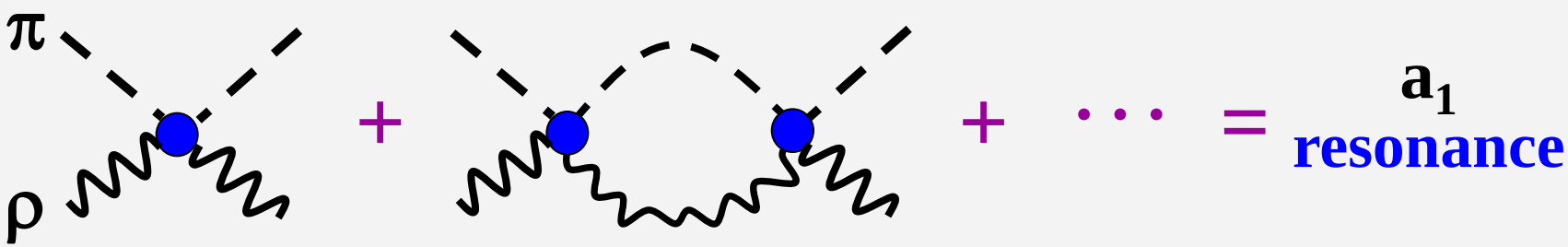


**In Medium:**

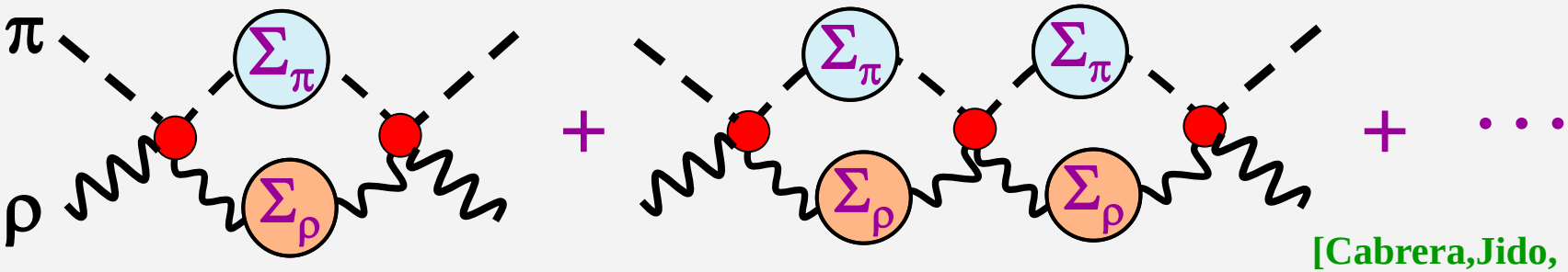


[Cabrera,Jido, Roca+RR '09]

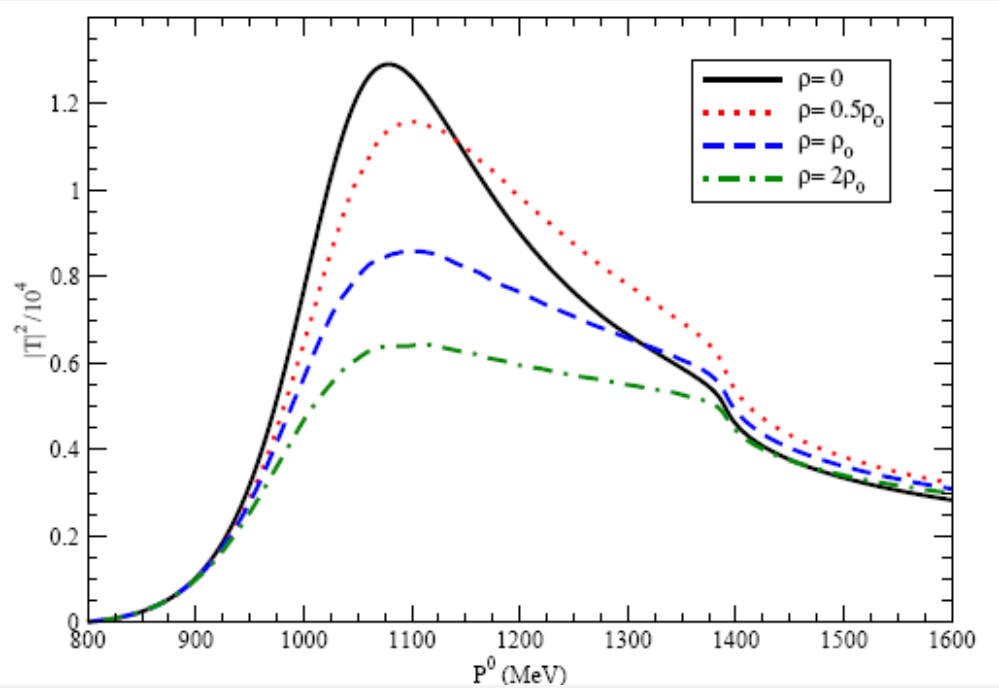


- in-medium π + ρ propagators
- broadening of π-ρ scatt. Amplitude
- pion decay constant in medium:

| $\rho/\rho_0$ | present work ($\pi$-selfenergy A) | present work ($\pi$-selfenergy B) |
|---|---|---|
| 0 | 93 | 93 |
| 1/2 | 100-108 | 91-101 |
| 1 | 65-86 | 66-93 |

# 3.6 Strategies to Test For Chiral Restoration

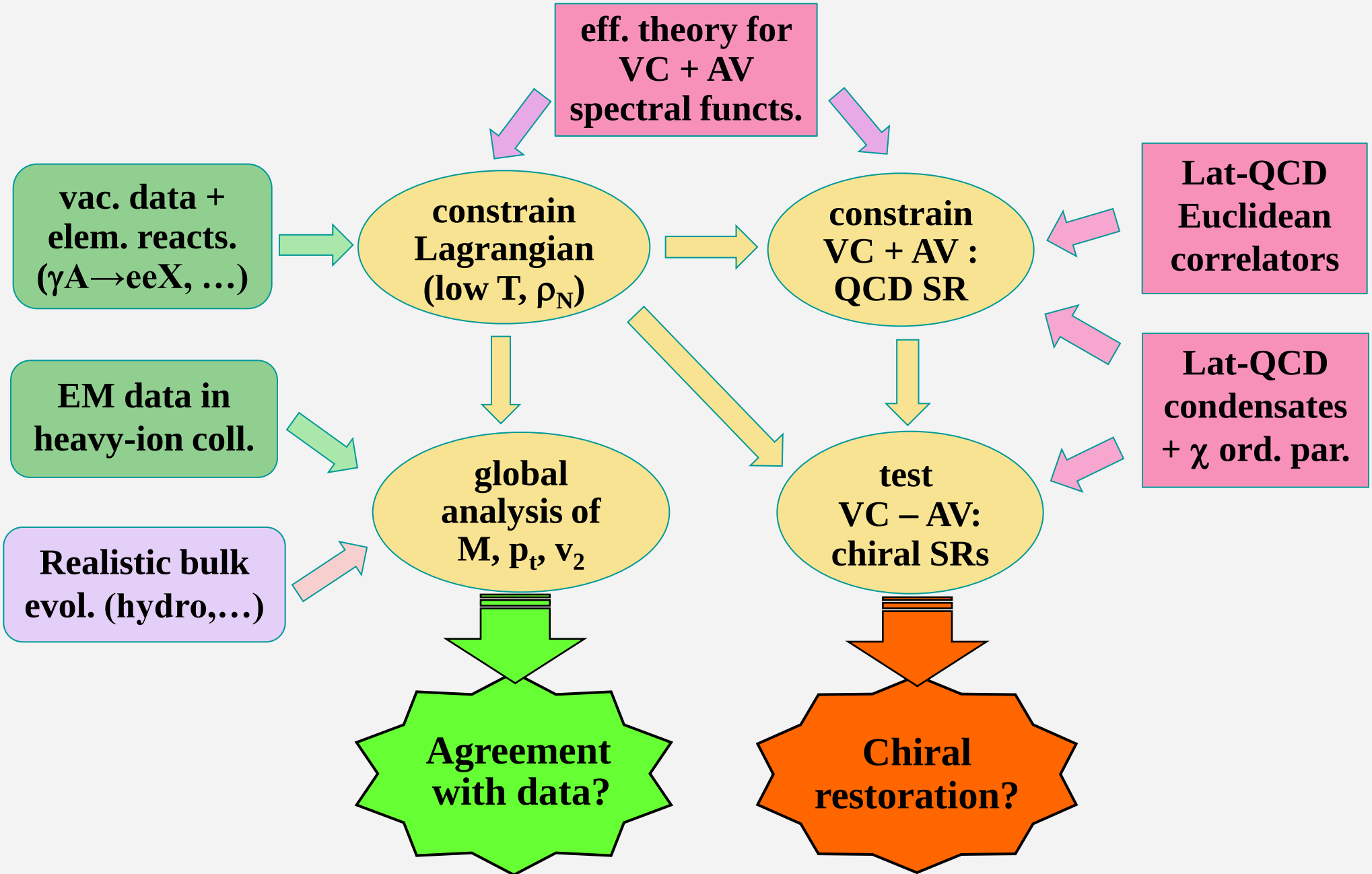

# 4.1 Quantitative Bulk-Medium Evolution

- initial conditions (compact, initial flow?)
- EoS: lattice (QGP, $T_c$~170MeV) + chemically frozen hadronic phase
- spectra + elliptic flow: multistrange at $T_{ch}$ ~ 160MeV

  π, K, p, Λ, … at $T_{fo}$ ~ 110MeV

[He et al '11]

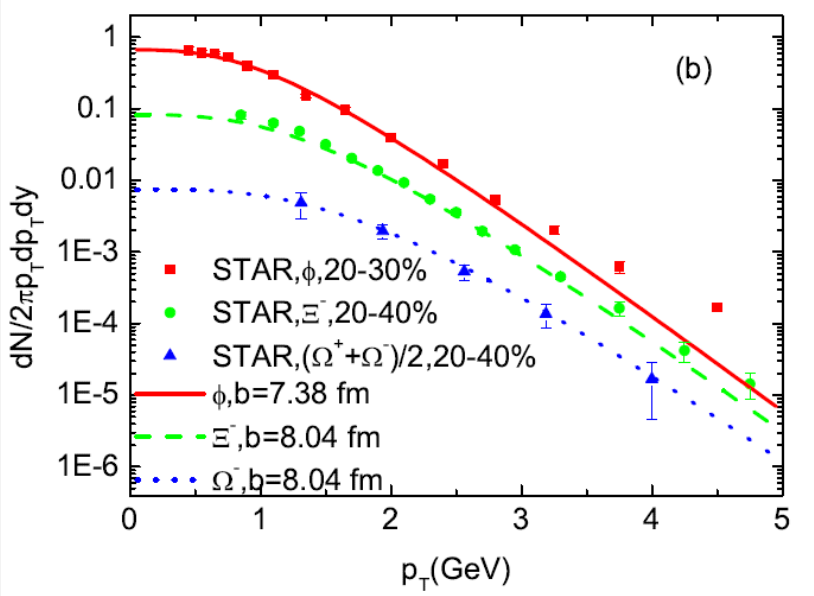


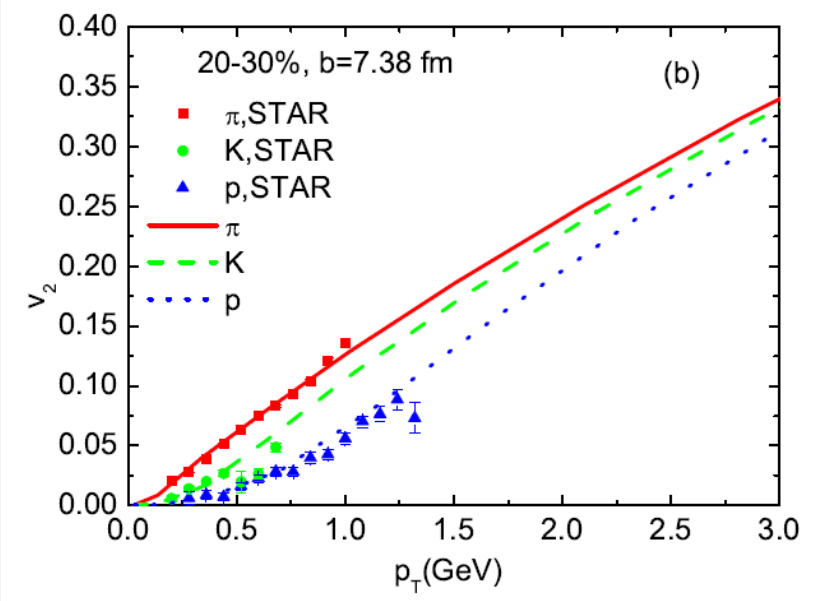


- $v_2$ saturates at $T_{ch}$, good light-/strange-hadron phenomenology

# 2.1 Chiral Symmetry + QCD Vacuum

$\mathcal{L}_{\mathrm{QCD}}(m_{u,d} \approx 0)$ : flavor + "chiral" (left/right) invariant

## "Higgs" Mechanism in Strong Interactions:

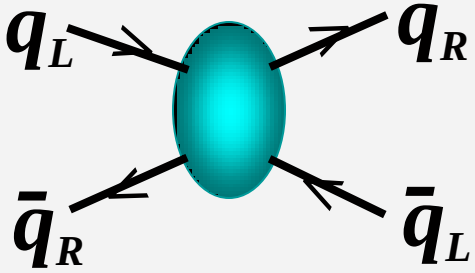


- $\bar{q}q$ attraction $\Rightarrow$ condensate fills QCD vacuum!

$$\langle 0|\bar{q}q|0\rangle = \langle 0|\bar{q}_L q_R + \bar{q}_R q_L|0\rangle \approx -5\, fm^{-3}$$

**Spontaneous Chiral Symmetry Breaking**

## Profound Consequences:

- effective quark mass: $m_q^* \propto \langle 0|\bar{q}q|0\rangle$

  $\leftrightarrow$ **mass generation!**

- near-massless Goldstone bosons $\pi^0$,

- "chiral partners" split: $\Delta M \approx 0.5\mathrm{GeV}$

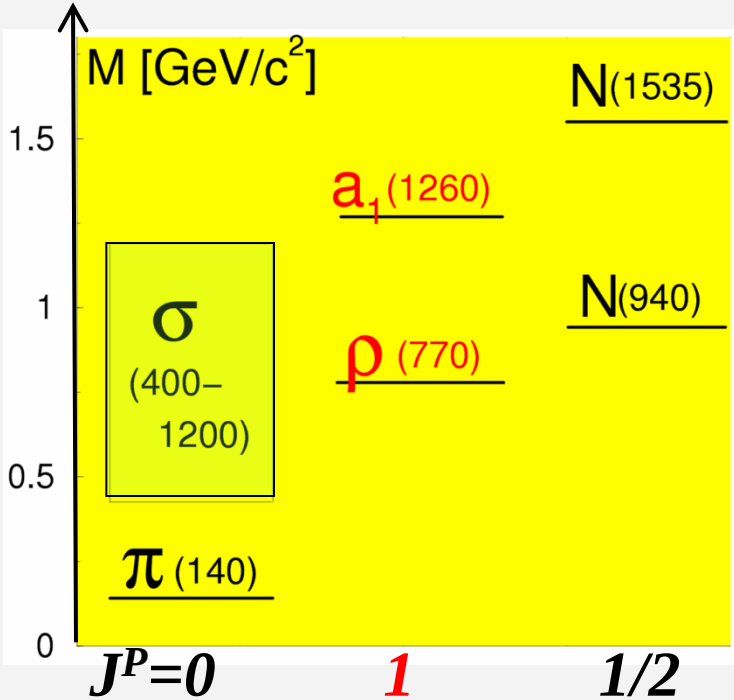

# 4.4.3 Origin of the Low-Mass Excess in PHENIX?

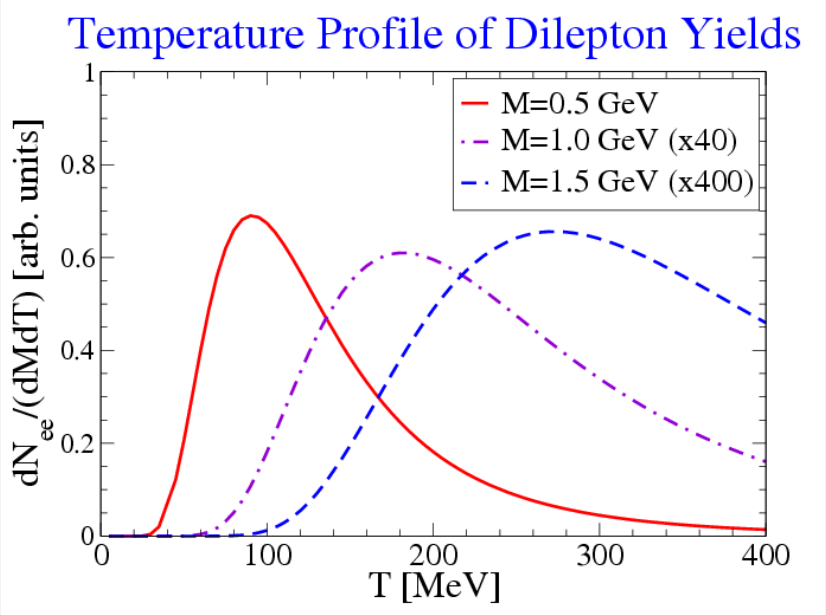


- **QGP radiation insufficient:**

  space-time , lattice QGP rate + resum. pert. rates **too small**

- **must be of long-lived hadronic origin**

- **Disoriented Chiral Condensate (DCC)?** **[Bjorken et al '93, Rajagopal+Wilczek '93]**
  - "baked Alaska" ↔ small **T**
  - rapid quench+large domains ↔ central **A-A**
  - $\pi_{therm} + \pi_{DCC} \rightarrow e^+ e^-$ ↔ **M~0.3GeV**, small $p_t$

  **[Z.Huang+X.N.Wang '96 Kluger,Koch,Randrup '98]**

- **Lumps of self-bound pion liquid?**

- **Challenge: consistency with hadronic data, NA60 spectra!**

# 2.2 EM Probes at SPS

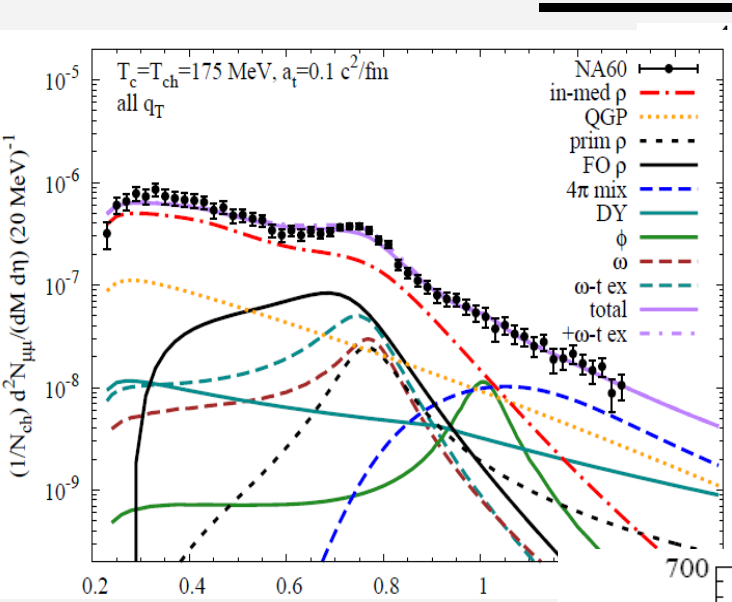


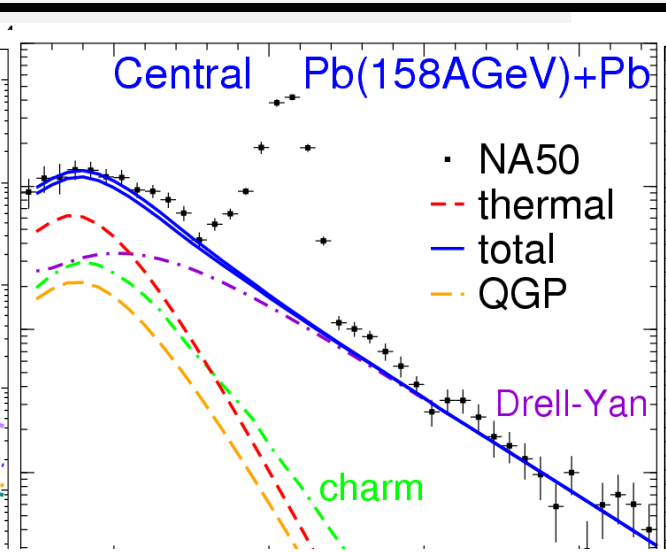


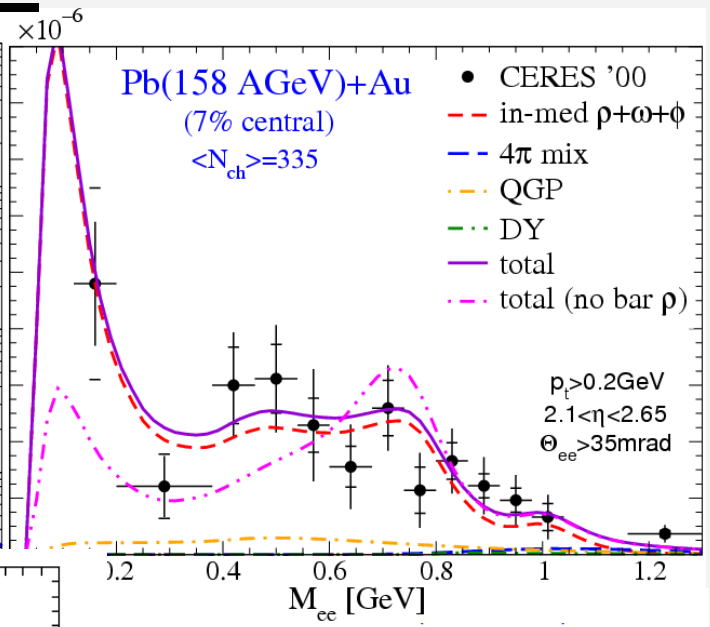


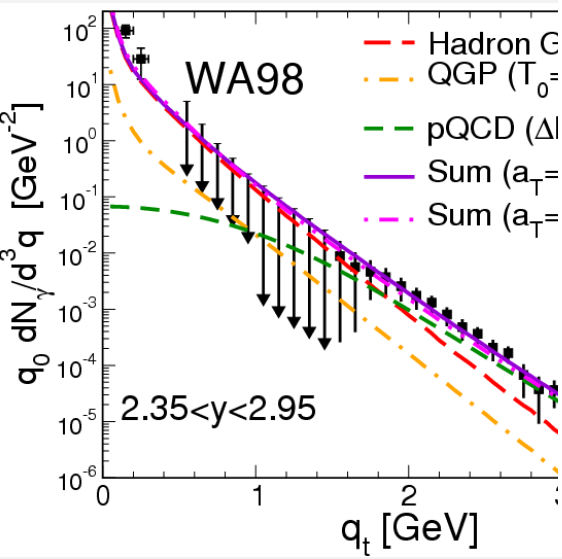


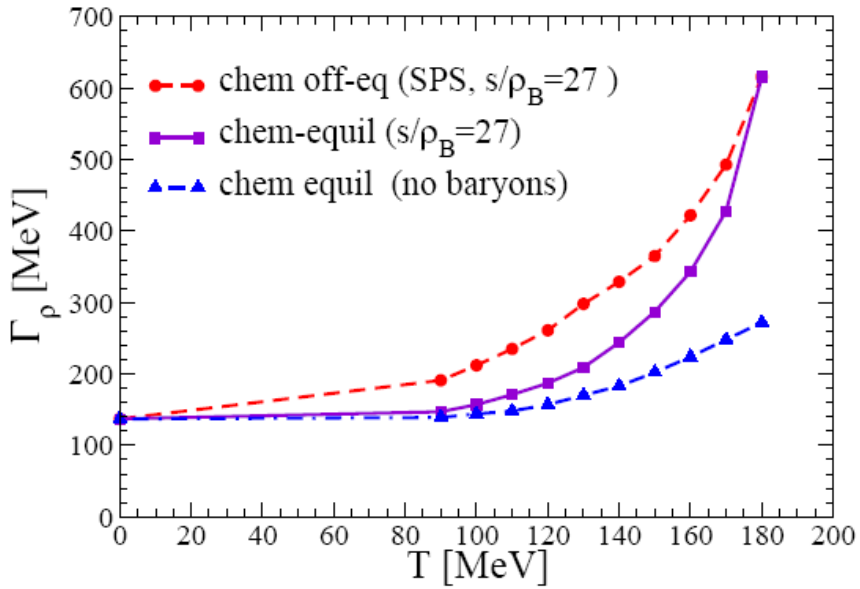


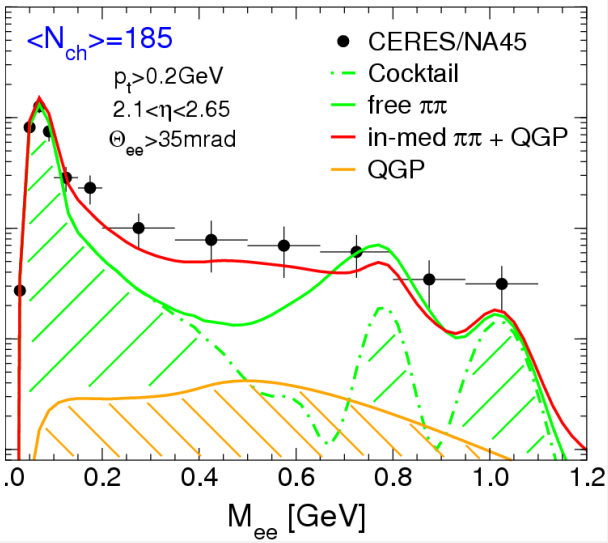


- all calculated with the **same e.m. spectral function**!
- thermal source: **$T_i$≈210MeV**, HG-dominated, **ρ-meson melting**!

# 5.2 Intermediate-Mass Dileptons: Thermometer

- use **invariant** continuum radiation (**M>1GeV**): no blue shift, $T_{slope} = T$ !

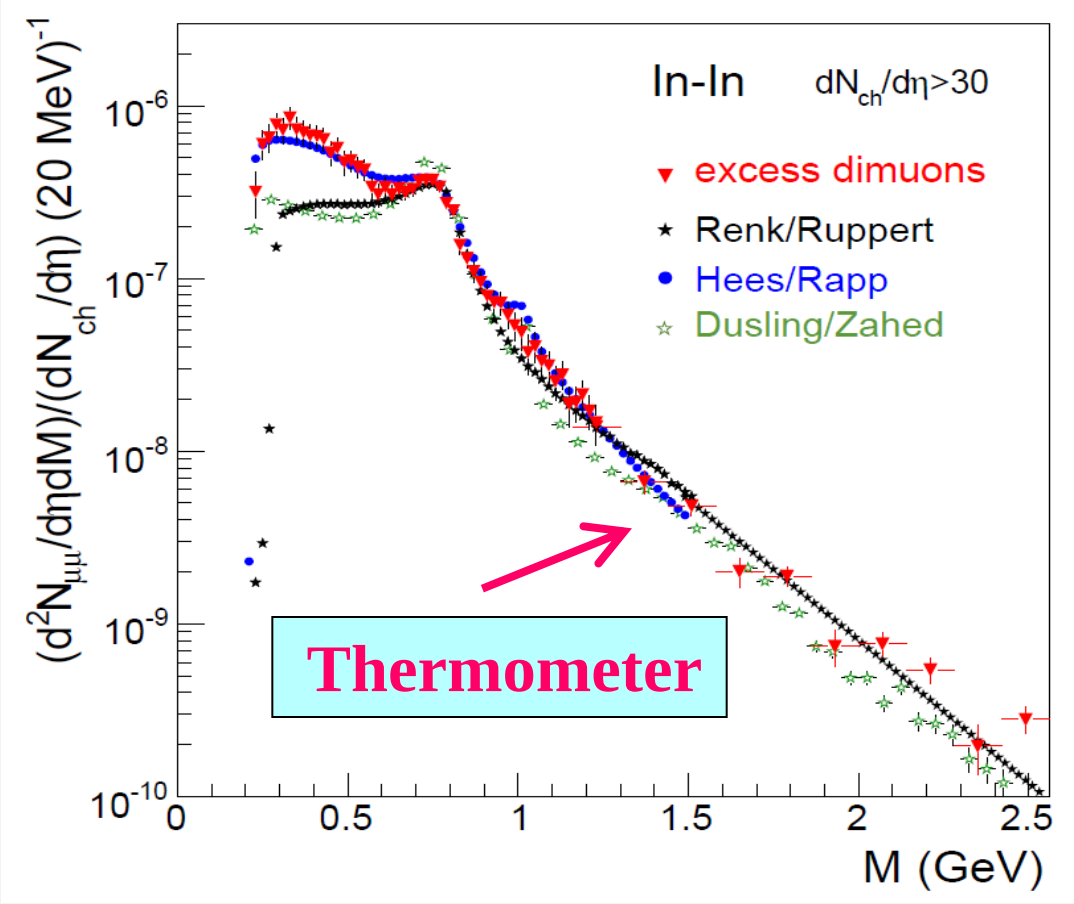


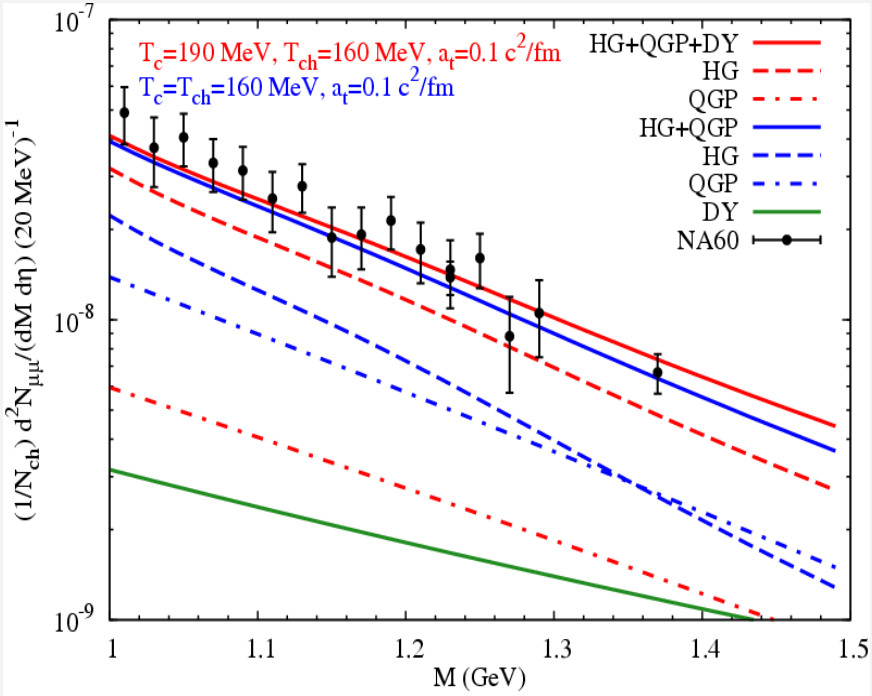


- independent of partition HG vs QGP (dilepton rate continuous/dual)
- initial temperature $T_i$ ~ **190-220 MeV** at **CERN-SPS**

# 4.7.2 Light Vector Mesons at RHIC + LHC

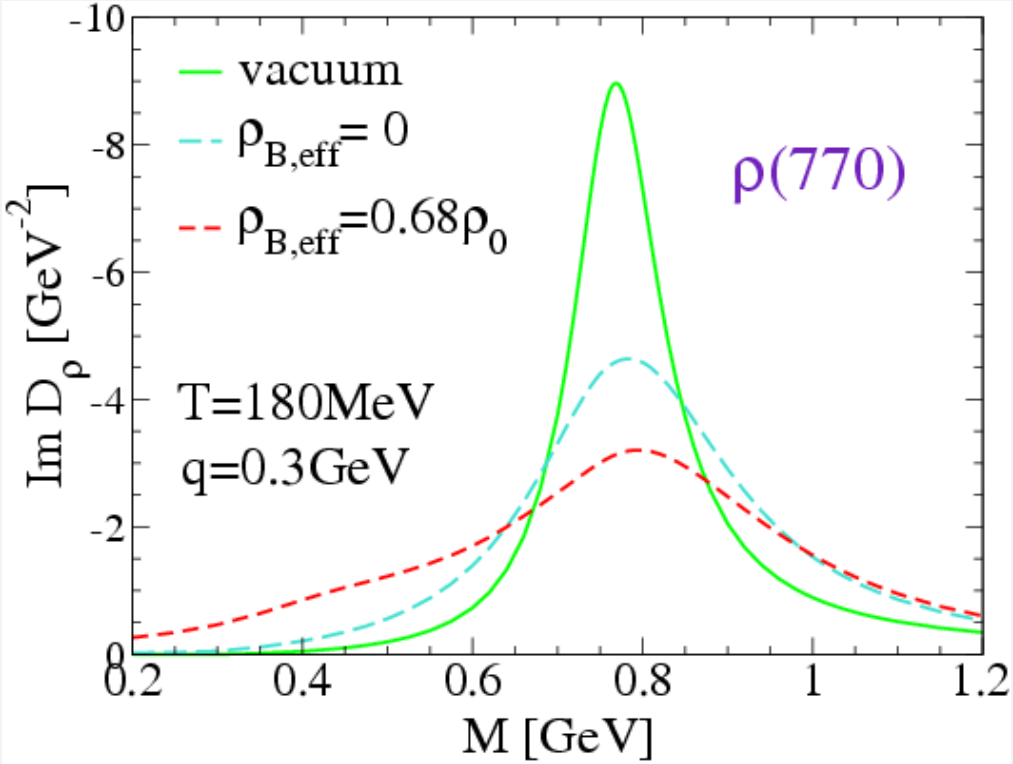


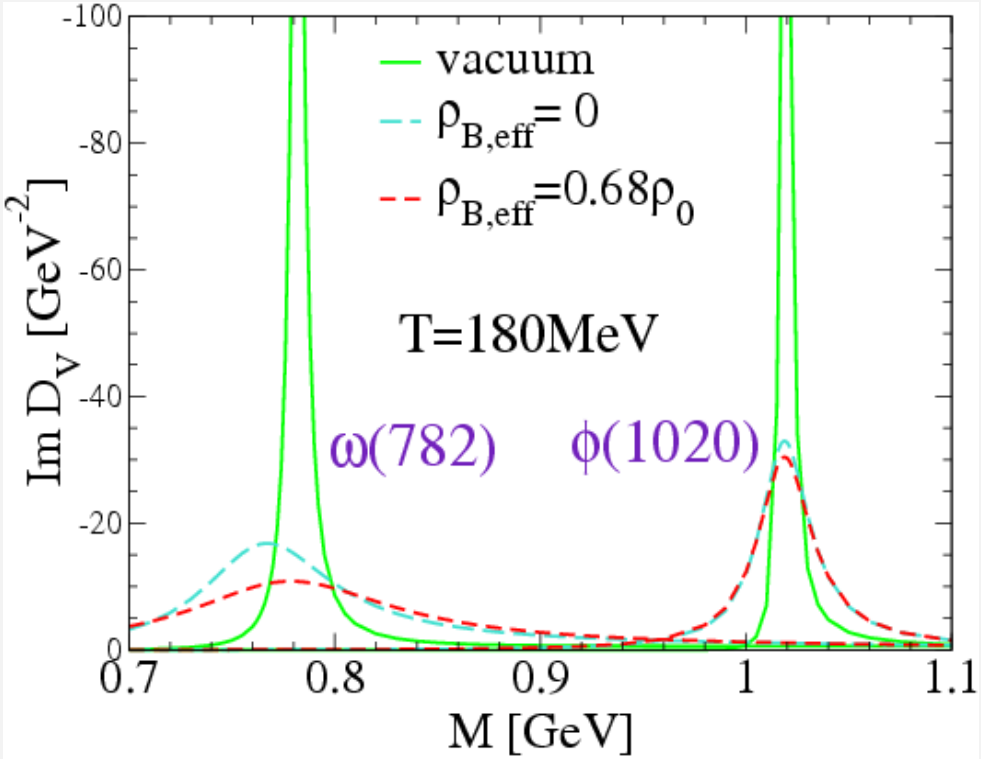


- **baryon effects important even at $\rho_{B,tot}$= 0 :**
  **sensitive to $\rho_{Btot}$= $\rho_B$ + $\rho_{\bar{B}}$ (ρ-N and ρ-$\bar{N}$ interactions identical)**
- **ω also melts, ϕ more robust ↔ OZI**

# 5.3 Intermediate Mass Emission: "Chiral Mixing"

[Dey, Eletsky +Ioffe '90]

- low-energy pion interactions fixed by chiral symmetry

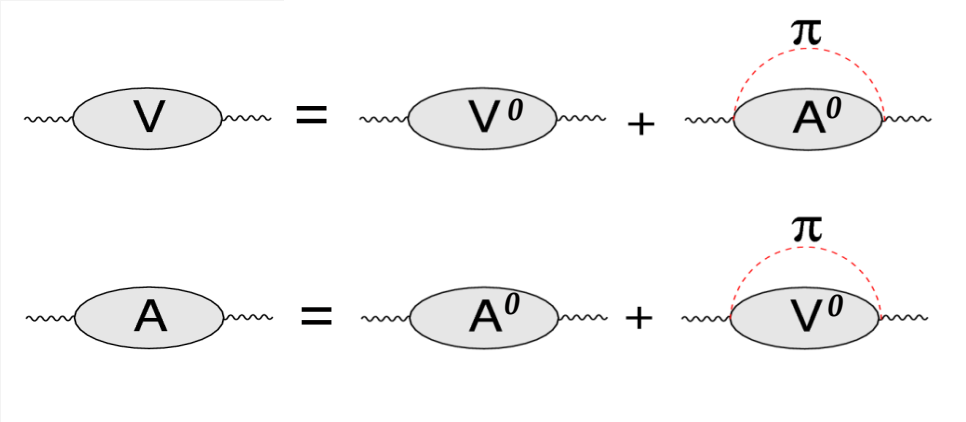


$$\Pi_V^{\mu\nu}(q) = (1-\varepsilon)\Pi_V^{0,\mu\nu}(q) + \varepsilon\Pi_A^{0,\mu\nu}(q)$$

$$\Pi_A^{\mu\nu}(q) = (1-\varepsilon)\Pi_A^{0,\mu\nu}(q) + \varepsilon\Pi_V^{0,\mu\nu}(q)$$

- mixing parameter

$$\varepsilon = \frac{4}{f_\pi^2}\int \frac{d^3k}{(2\pi)^3 2\omega_k} f^\pi(\omega_k) \approx \frac{T^2}{6 f_\pi^2}$$

- **degeneracy with perturbative spectral fct. down to M~1GeV**
- physical processes at **M≥ 1GeV:**

**$\pi a_1 \rightarrow e^+e^-$ etc. ("4π annihilation")**

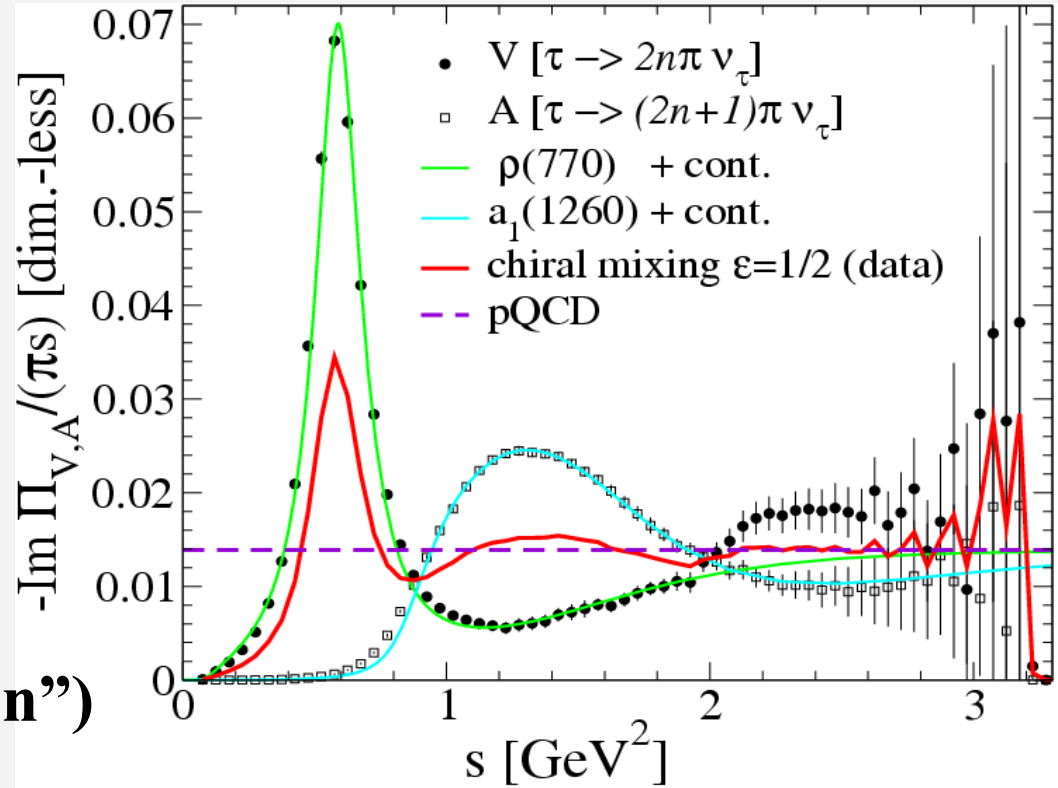

# 3.2 Dimuon $p_t$-Spectra and Slopes: Barometer

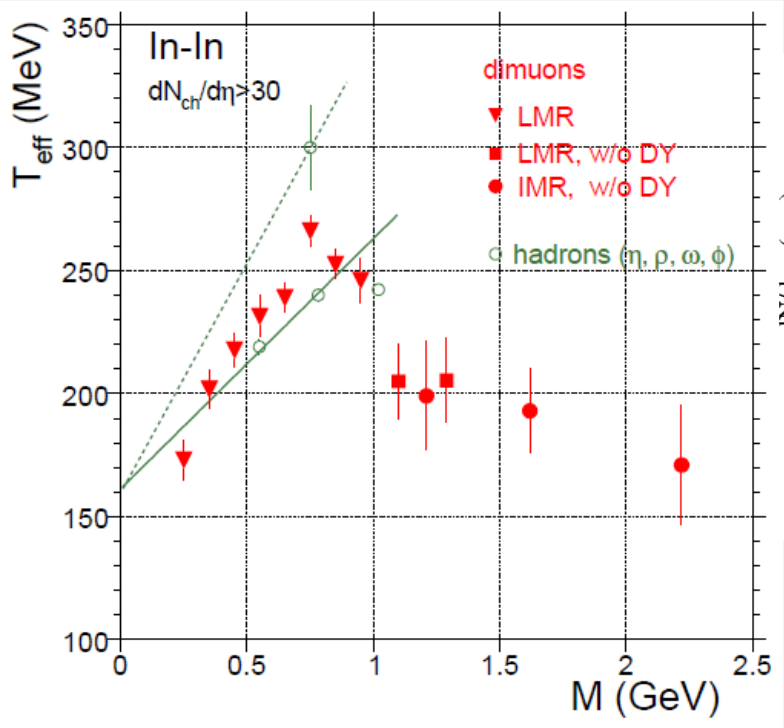


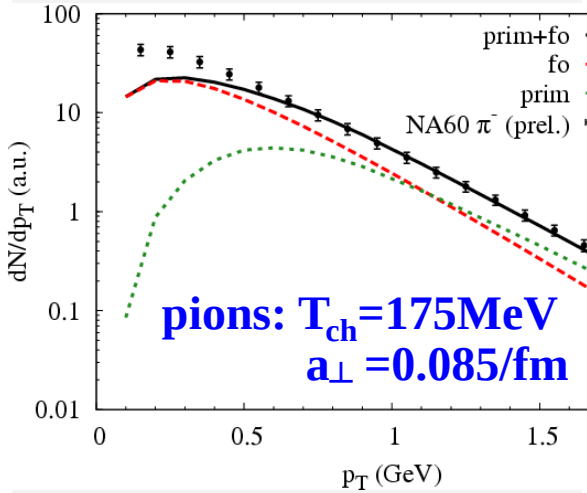


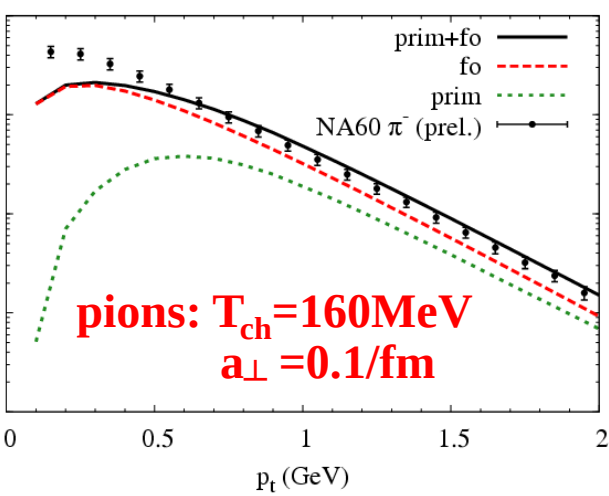


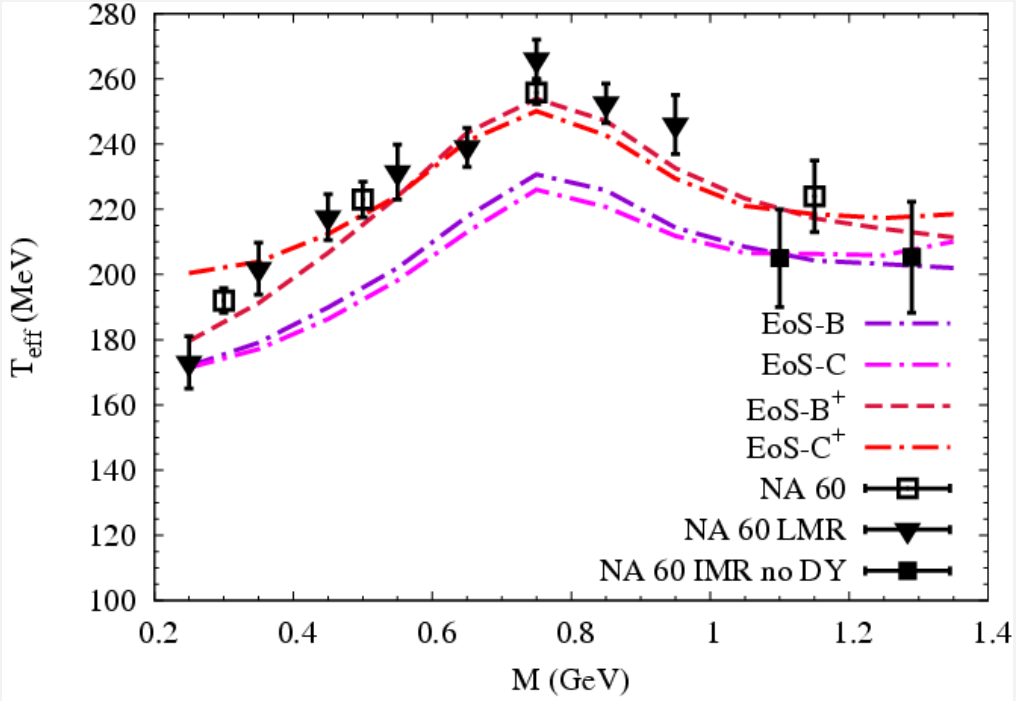


- modify fireball evolution:
  e.g. $a_\perp = 0.085/\text{fm} \rightarrow 0.1/\text{fm}$
- both large and small $T_c$ compatible with excess dilepton slopes

# 2.3.3 Spectrometer III: Before Acceptance Correction

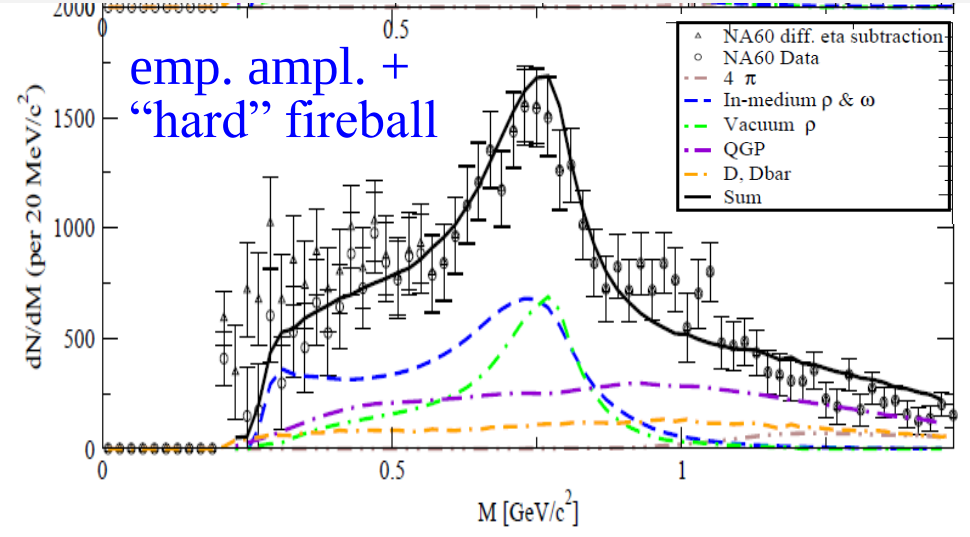


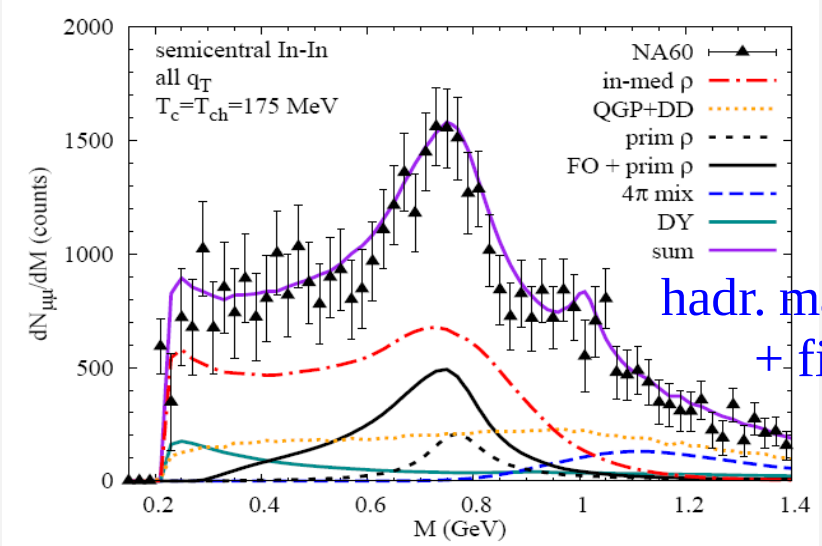


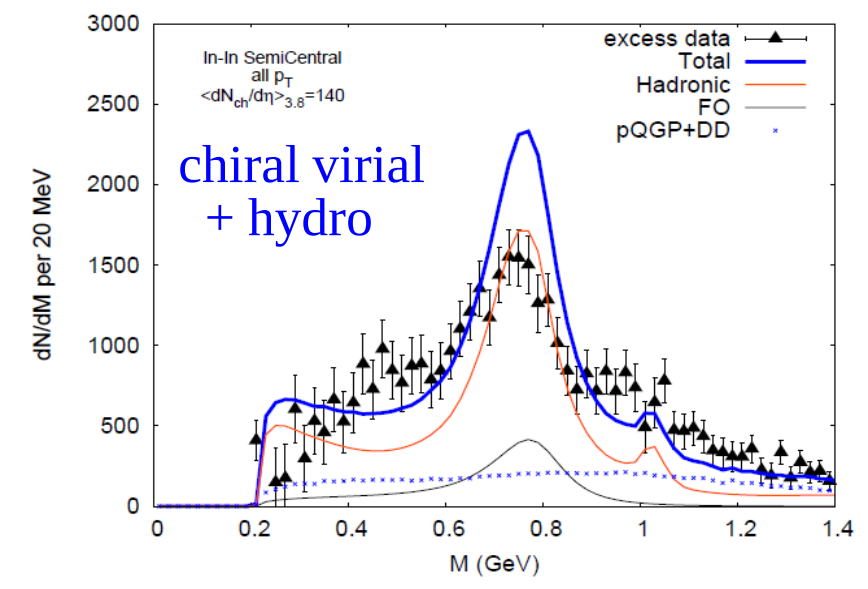


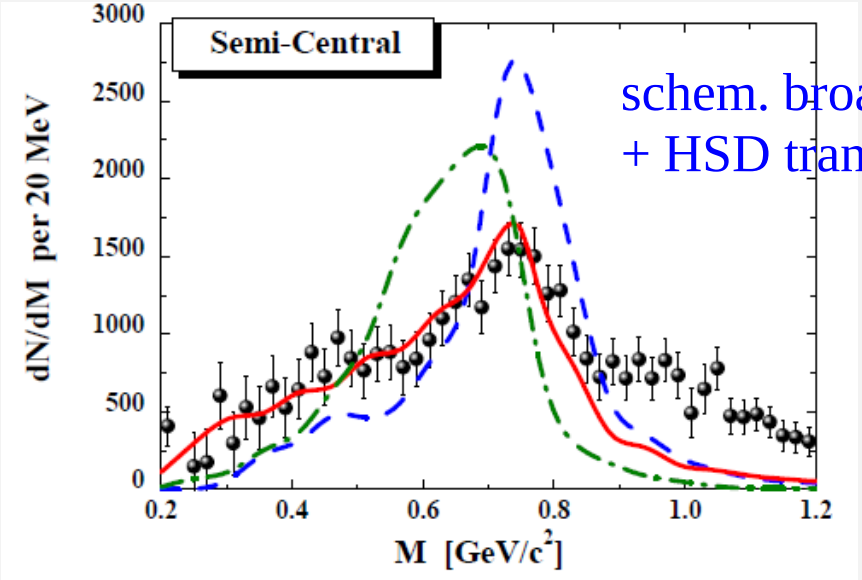


- **Discrimination power much reduced**
- can compensate spectral "deficit" by larger flow: lift pairs into acceptance

# 4.1 Nuclear Photoproduction: ρ Meson in Cold Matter

$\gamma + A \rightarrow e^+e^- X$

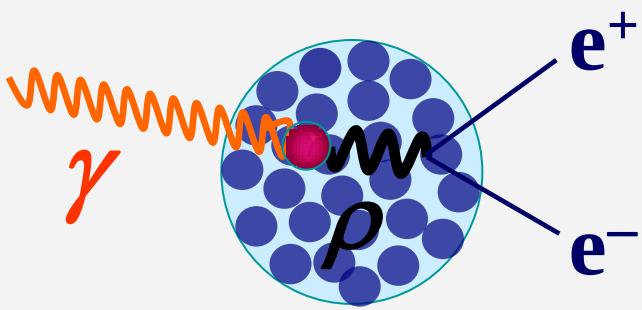


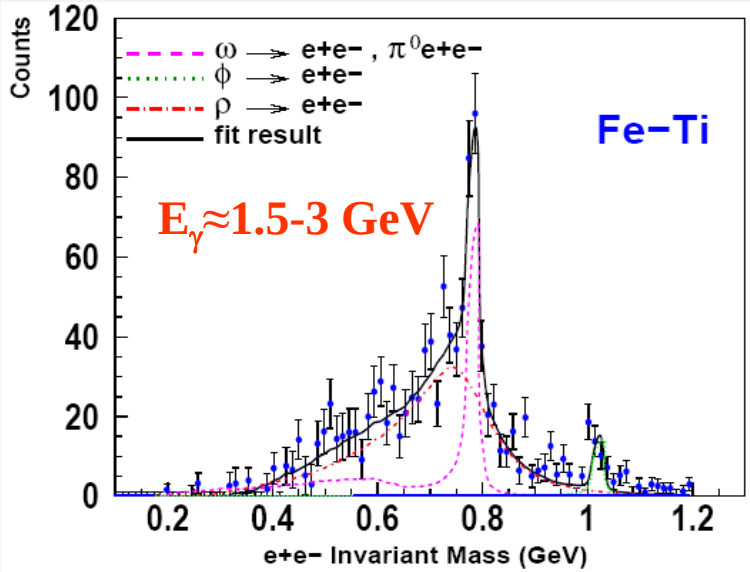


- extracted "in-med" ρ-width $\Gamma_\rho \approx 220$ MeV

[CLAS '08]

- **Microscopic Approach:**

production amplitude + in-med. ρ spectral fct.

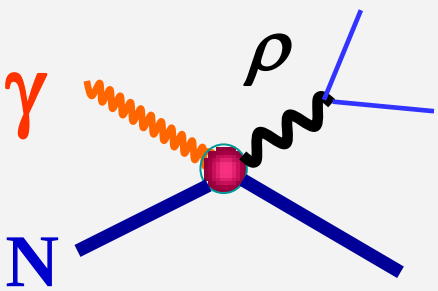


[Riek et al '08, '10]

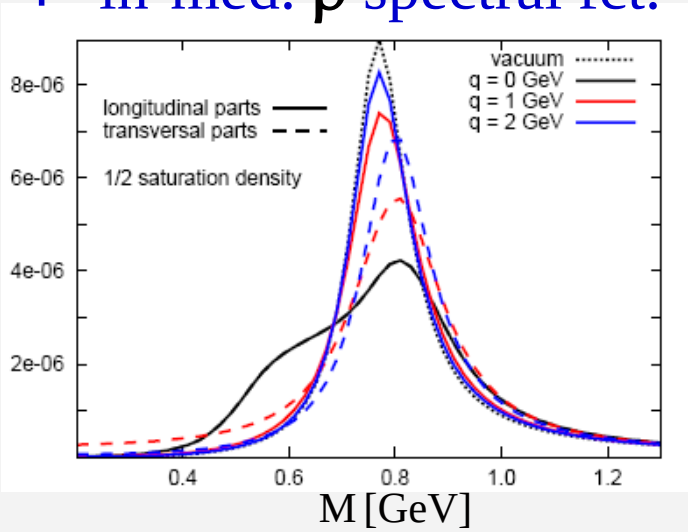


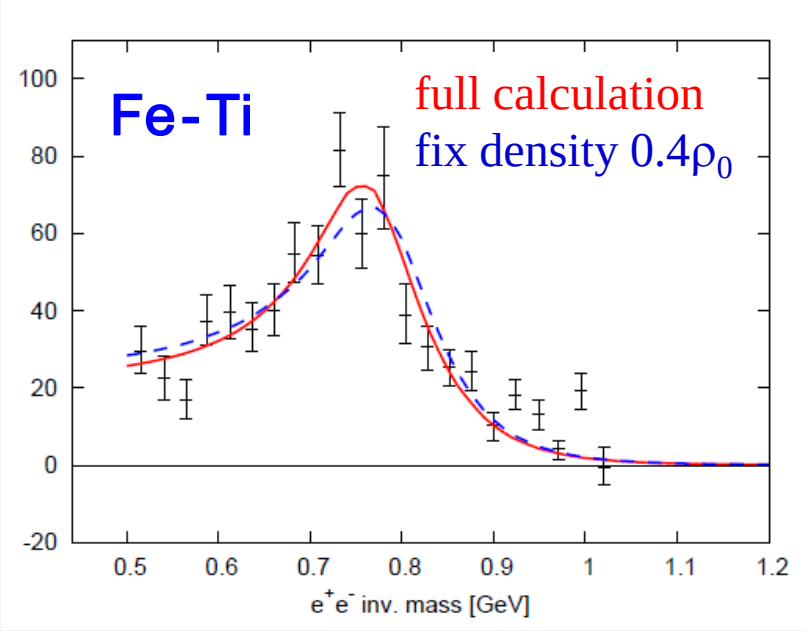


- ρ-broadening reduced at high 3-momentum; **need low momentum cut!**

# 2.3.6 Hydrodynamics vs. Fireball Expansion

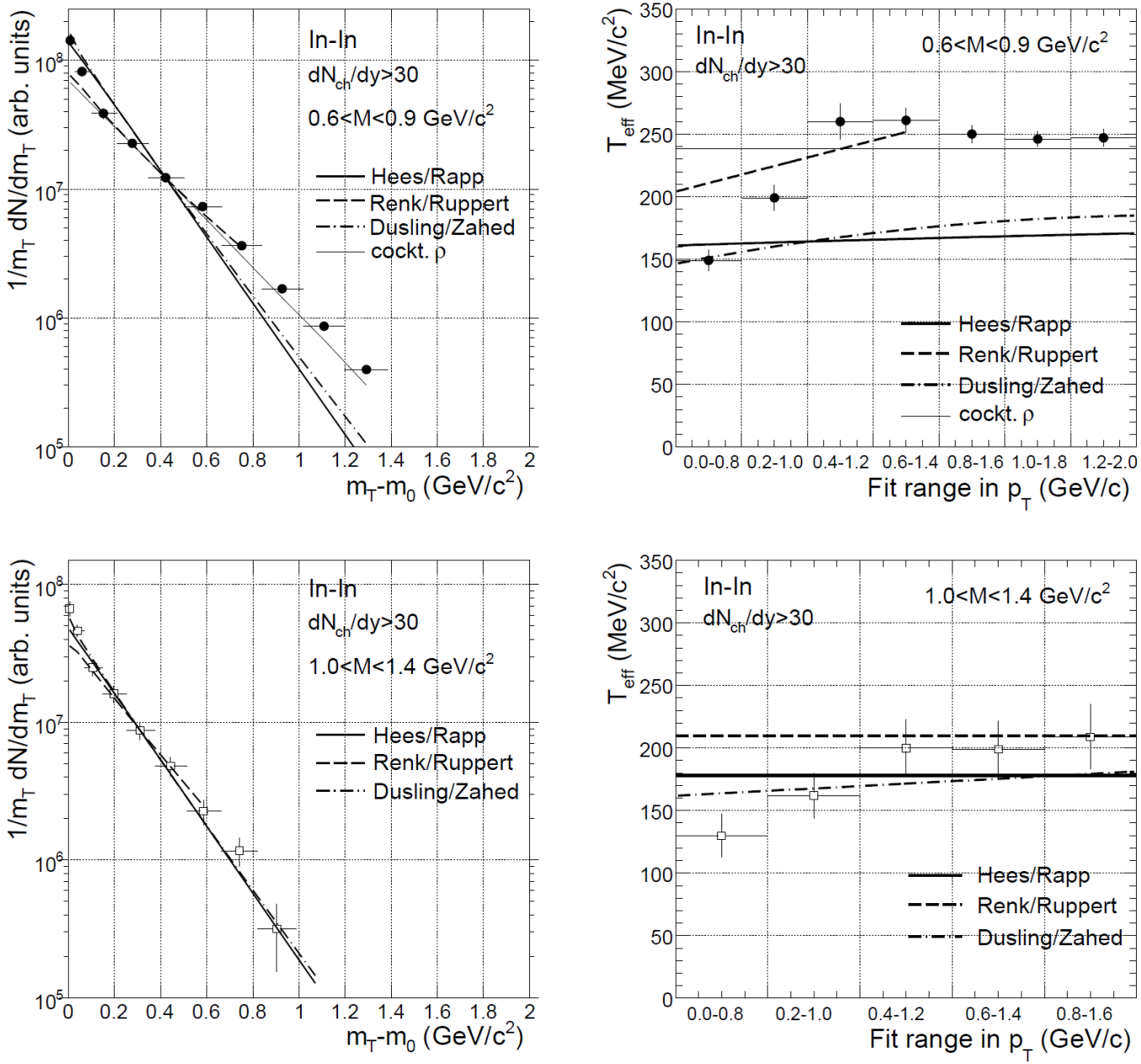


- very good agreement between original hydro [Dusling/Zahed] and fireball [Hees/Rapp]

# Di-electron spectra from 200 GeV p+p and Au+Au with the HBD from PHENIX

Ilia Ravinovich
for the PHENIX Collaboration
Weizmann Institute of Science

Thermal Radiation Workshop, BNL, December 5-7, 2012

# Outline

- Published PHENIX results
- Hadron Blind Detector (HBD)
- Preliminary results with the HBD
- Comparison to published results w/o HBD
- Summary

# PHENIX dilepton program

- PHENIX has measured the dielectron continuum over a wide range of mass and transverse momentum
- The program includes a variety of collision systems:
  - p+p, with and without HBD;
  - d+Au without HBD;
  - Cu+Cu without HBD;
  - Au+Au, with and without HBD;

# Dilepton continuum in p+p collisions

- Data and cocktail of known sources represent pairs with $e^+$ and $e^-$ in PHENIX acceptance
- Data are efficiency corrected

Excellent agreement of data and hadron decay contributions within systematic uncertainties

Phys. Lett. B 670, 313 (2009)

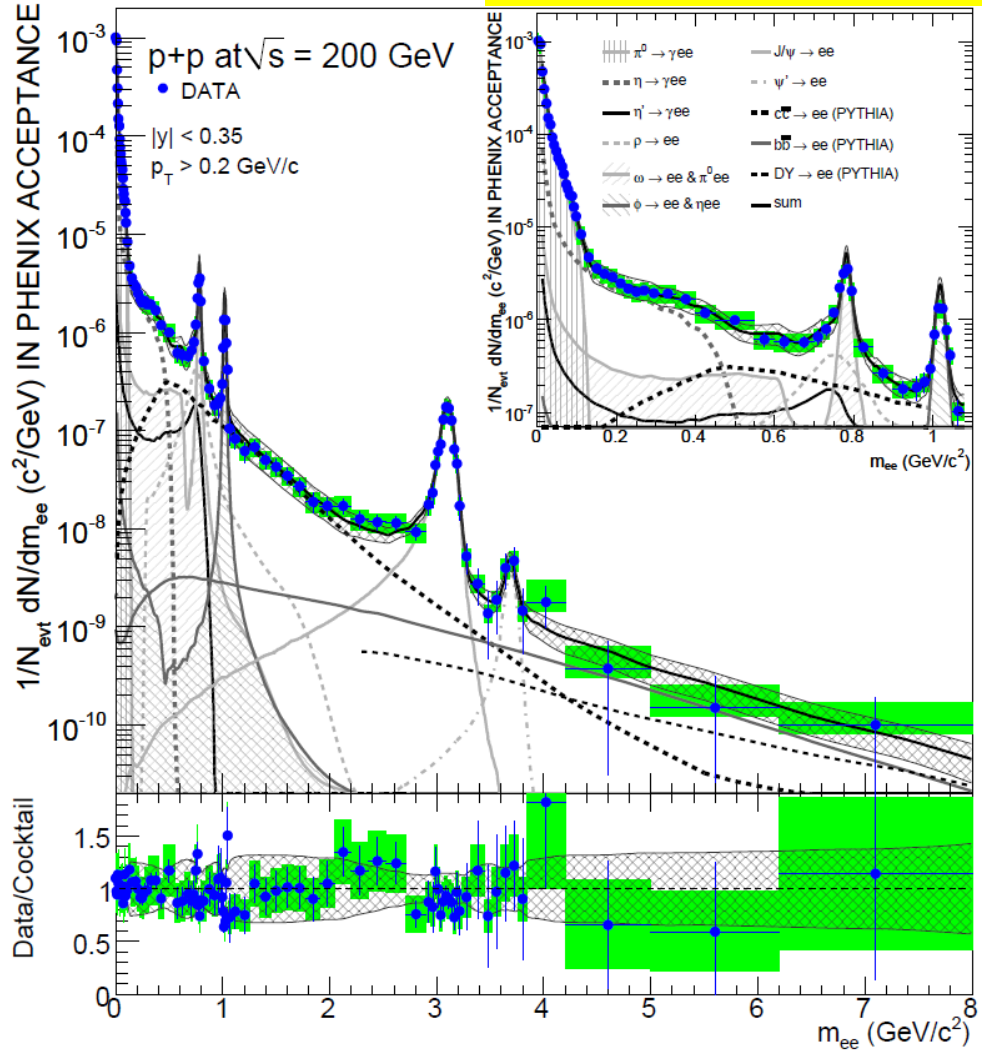

# Estimate of expected sources, "Cocktail"

- Hadron decays:
  - Fit $\pi^0$ and $\pi^\pm$ data p+p or Au+Au

$$E\frac{d^3\sigma}{d^3p} = \frac{A}{\left(\exp(-ap_T - bp_T^2) + p_T/p_0\right)^n}$$

  - for other mesons η, ω, ρ, ϕ, J/Ψ etc. replace $p_T \rightarrow m_T$ and fit normalization to existing data where available

Hadron data follows "$m_T$ scaling"

- Heavy flavor production:
  - $s_c = N_{coll} \times 567 \pm 57 \pm 193$ mb from single electron measurement

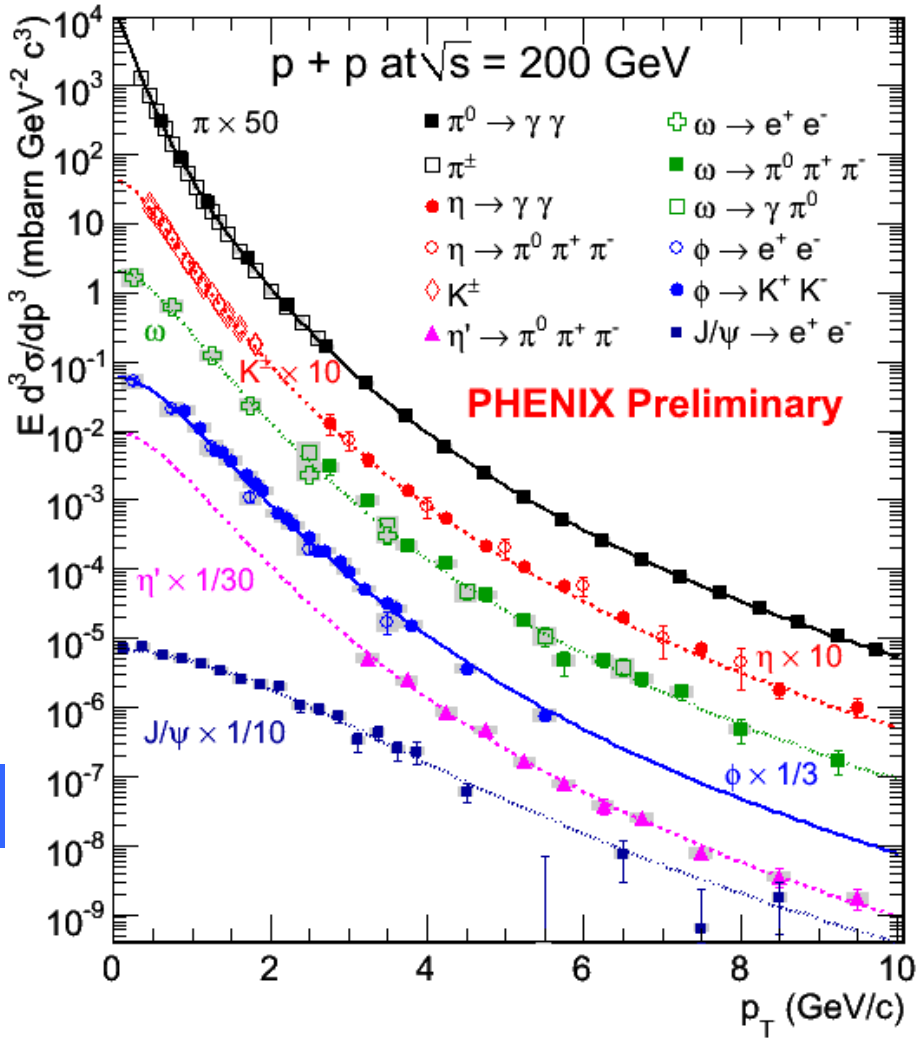


Predict cocktail of known pair sources

# Au+Au dilepton continuum

PRC 81, 034911 (2010

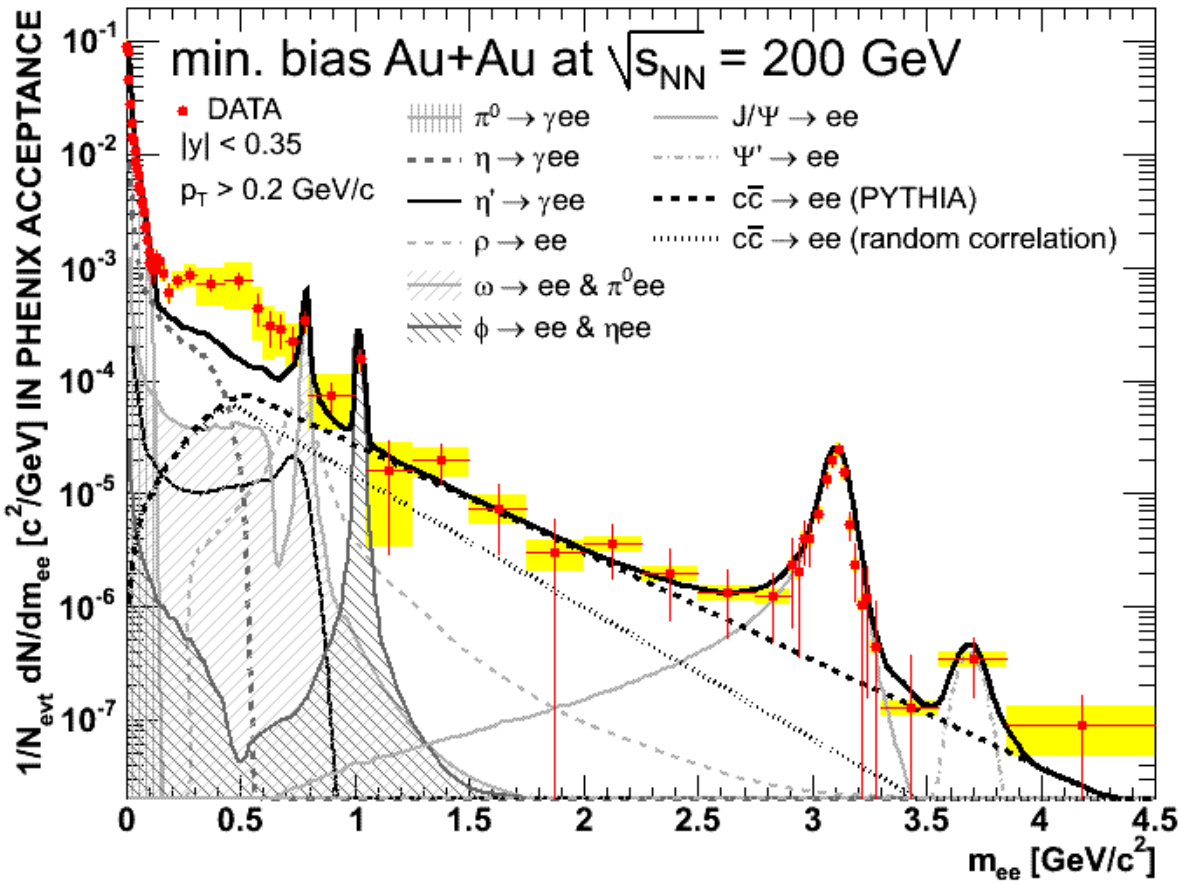


- Strong excess of dielectron pairs at low masses:
  4.7 +/- 0.4 (stat) +/- 1.5 (syst) +/- 0.9 (model)

# Centrality dependence of the enhancement

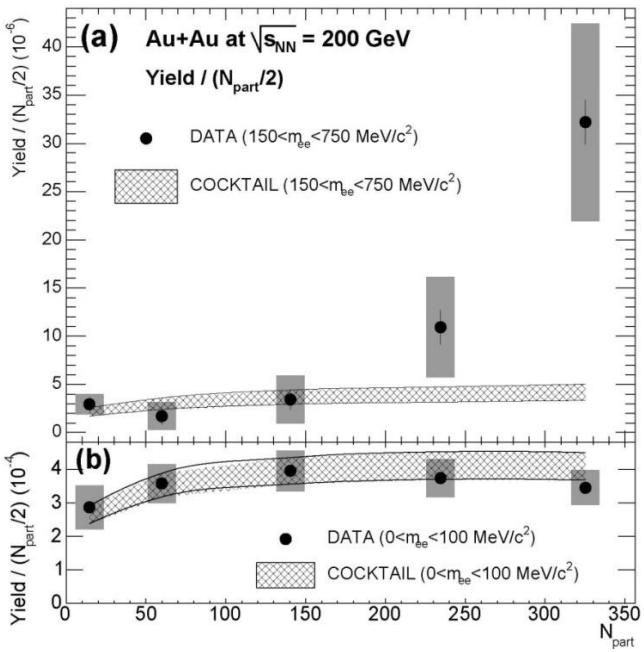


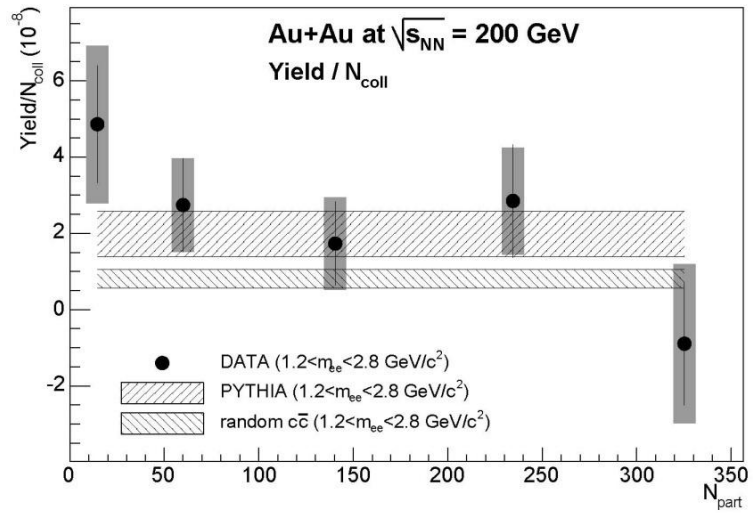


In the LMR the integrated yield increases faster with the centrality of the collisions than the number of participating nucleons

In the IMR the normalized yield shows no significant centrality dependence

# $p_T$ dependence of low mass enhancement

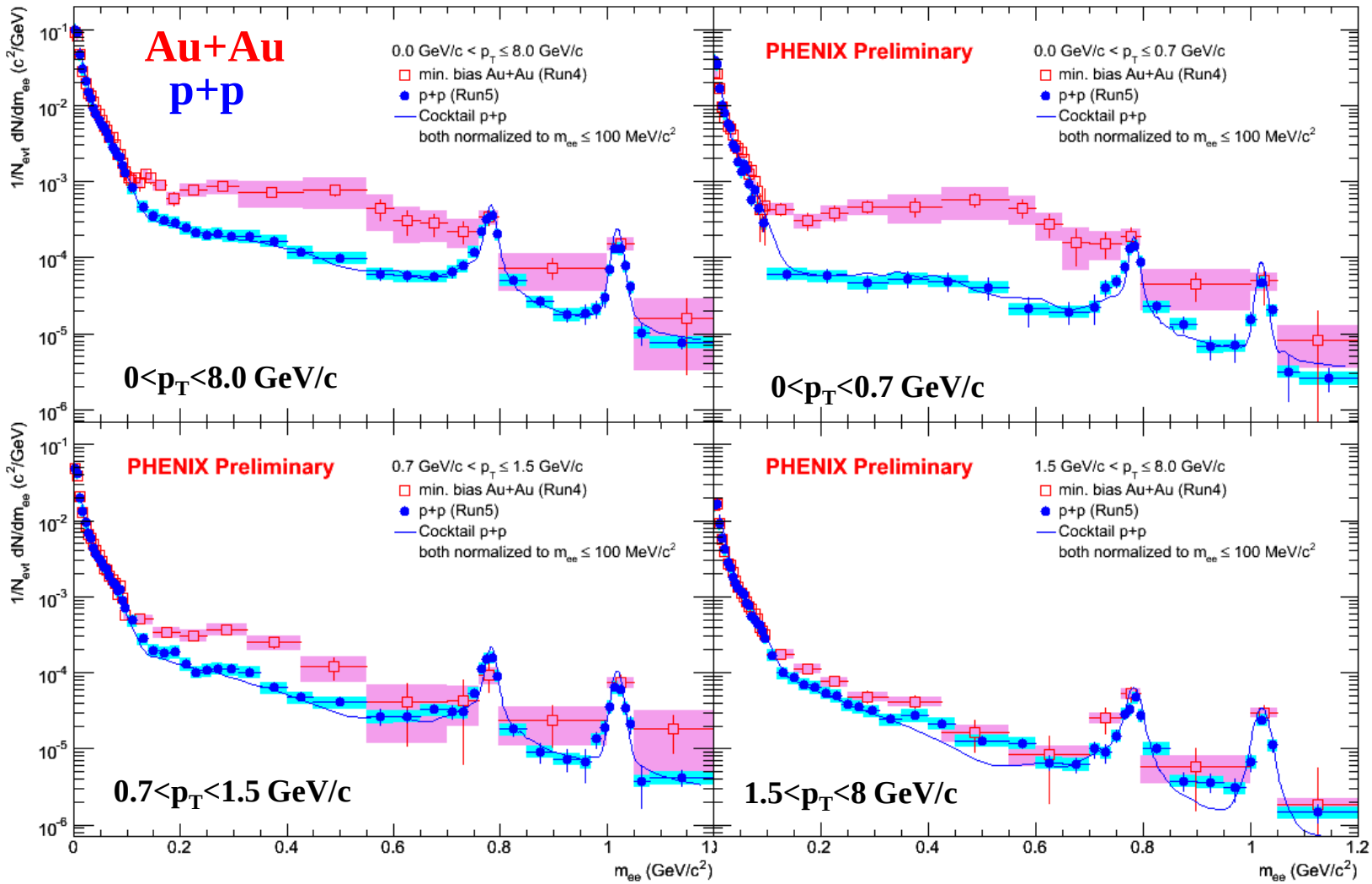


Low mass excess in Au-Au concentrated at low $p_T$!

# $m_T$ distribution of low-mass excess

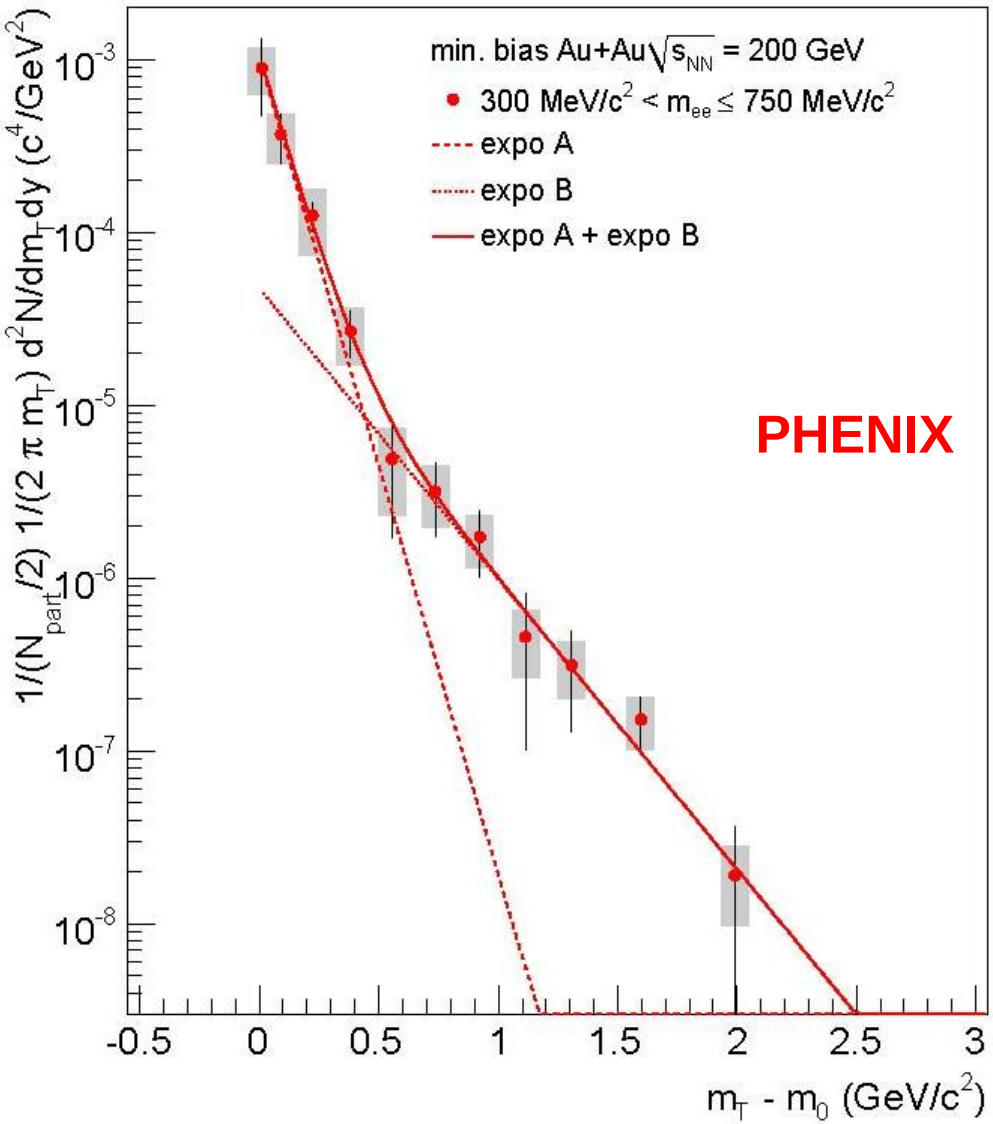


- Excess present at all pair $p_T$ but is more pronounced at low pair $p_T$
- The excess $m_T$ distribution exhibits two clear components
- It can be described by the sum of two exponential distributions with inverse slope parameters:
- $T_1 = 92 \pm 11.4^{stat} \pm 8.4^{syst}$ MeV
- $T_2 = 258.3 \pm 37.3^{stat} \pm 9.6^{syst}$ MeV

# Comparison to theoretical models

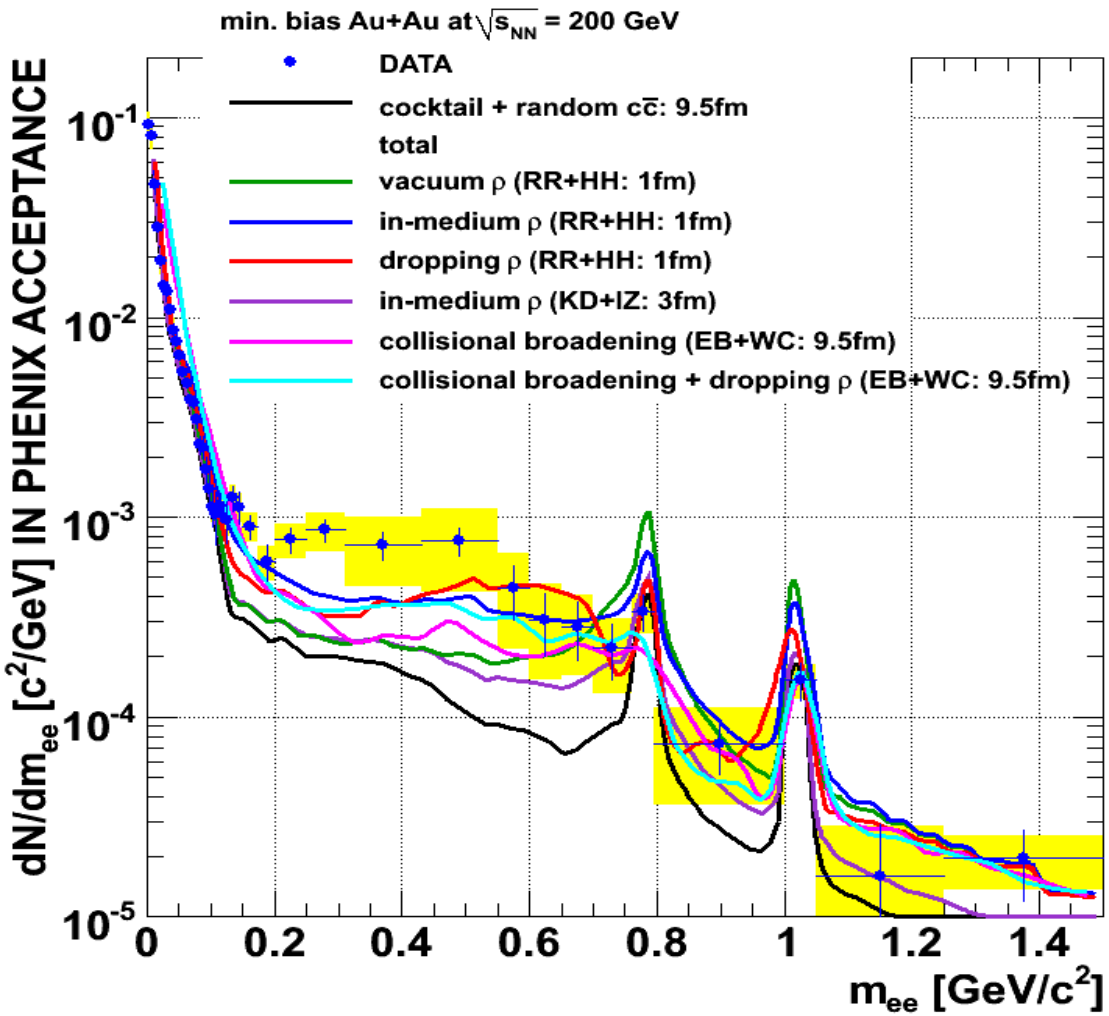


All models and groups that successfully described the SPS data fail in describing the PHENIX results

# Motivation

- The excess at masses 0.2-0.7 GeV/$c^2$ is

4.7 +/- 0.4 (stat) +/- 1.5 (syst) +/- 0.9 (model)

- It is mainly concentrated in the central collisions.
- But in this low mass range we have a very poor S/B ratio (~1/200), especially in the central collisions.
- So, the results are limited by this large uncertainty due to the huge combinatorial background.

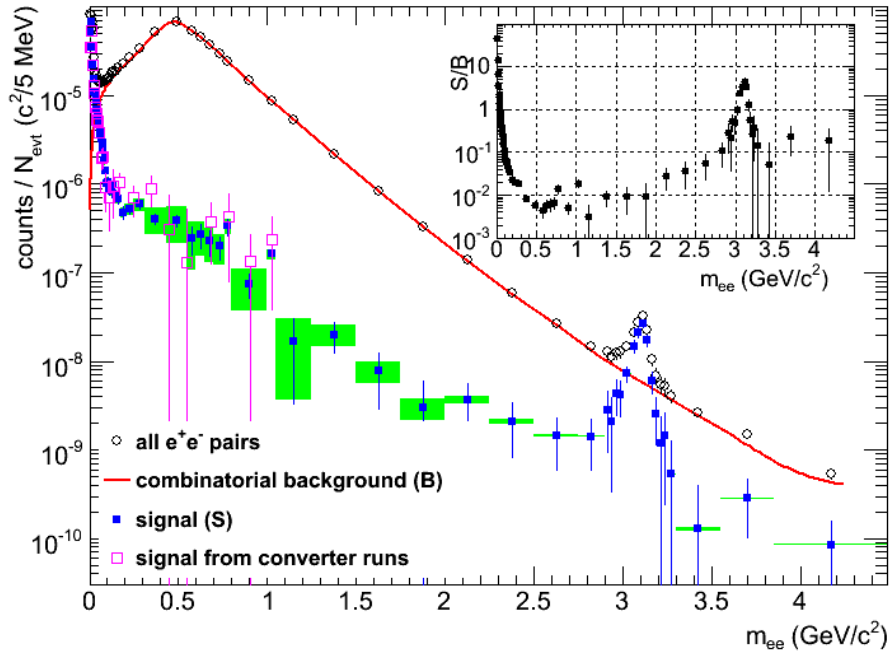


**The goal of the HBD is to improve the signal significance!**

# Key Challenge for PHENIX: Pair Background

- No background rejection → Signal/Background ≥ 1/100 in Au-Au
- Combinatorial background: $e^+$ and $e^-$ from different uncorrelated source

$$\pi^0 \rightarrow e^+ e^- \gamma \qquad\qquad \gamma \rightarrow e^+ e^-$$

- unphysical correlated background:
  - track overlaps in detectors
- Correlated background: $e^+$ and $e^-$ from same source but not "signal"
  - "Cross" pairs

$$\pi^0 \rightarrow \gamma\gamma$$

$$e^+ e^- \quad \times \quad e^+ e^-$$

"Jet" pairs

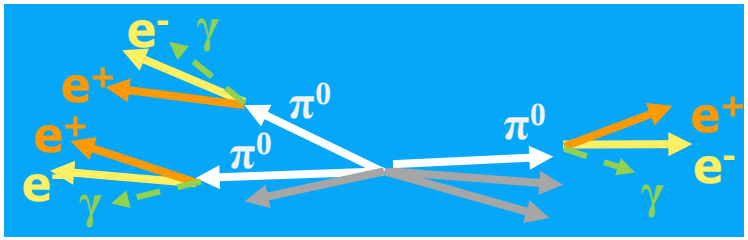

# How can we spot the background?

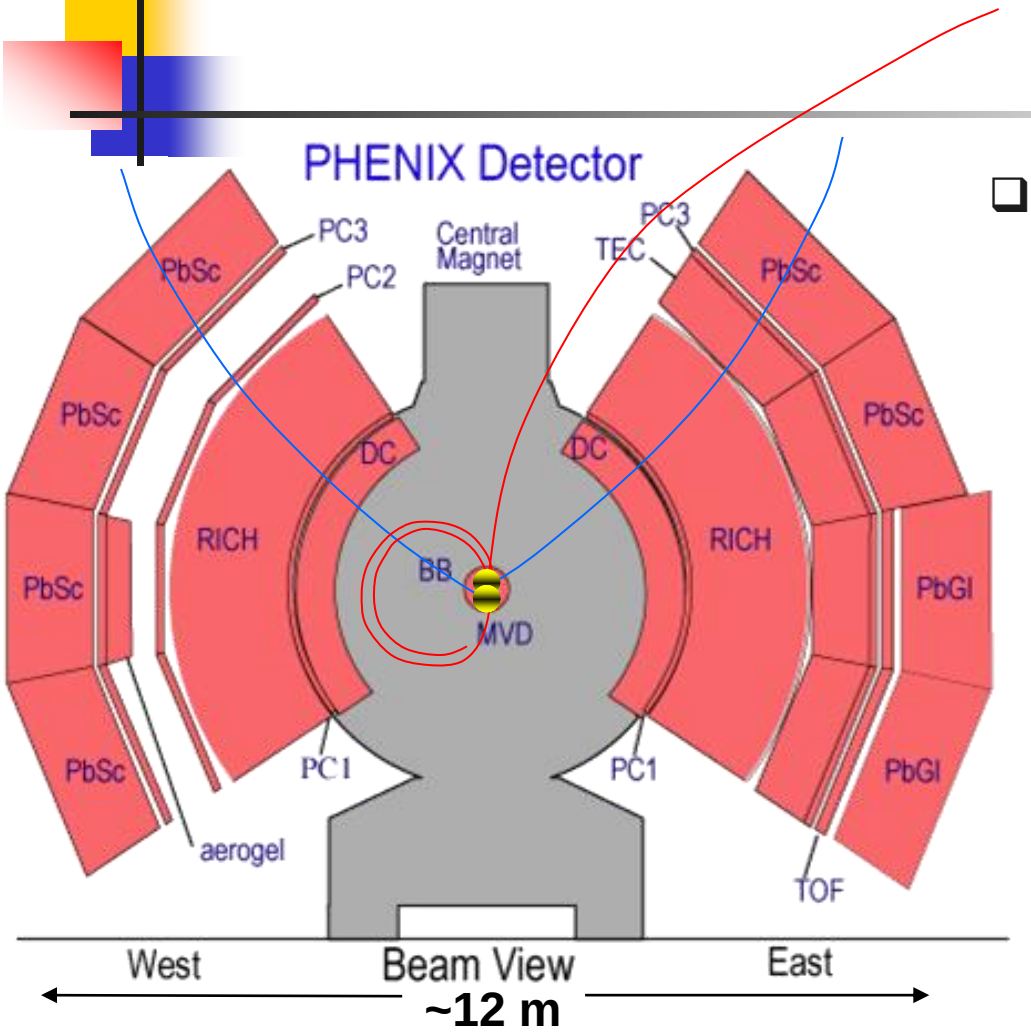


- Typically only 1 electron from a pair falls within the PHENIX acceptance:
  - the magnetic field bends the pair in opposite directions.
  - some spiral in the magnetic field and never reach tracking detectors.
- To eliminate these problems:
  - detect electrons in field-free region
  - need >90% efficiency

# Separating signal from background

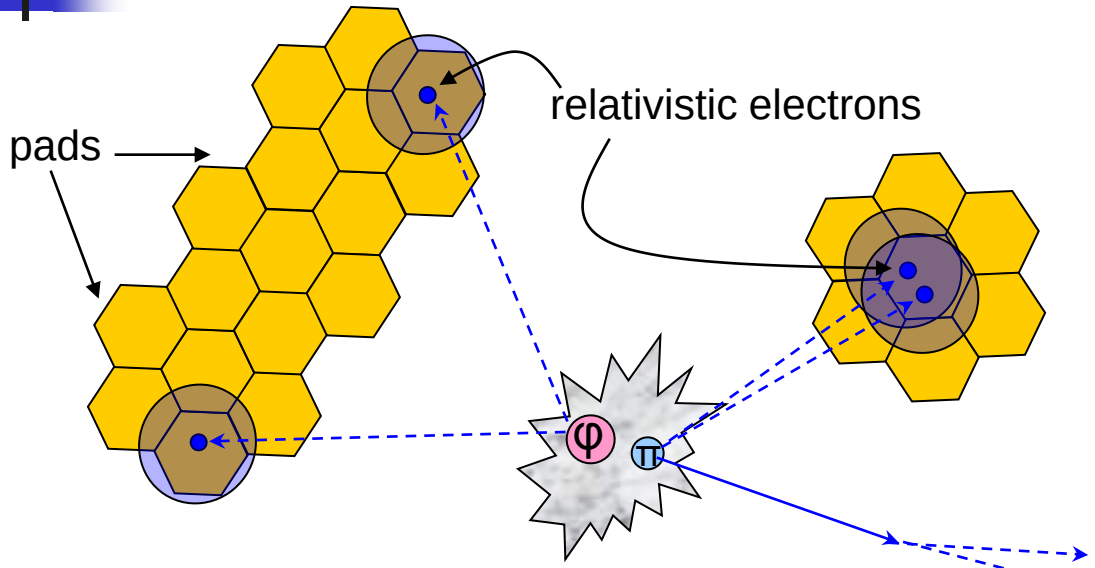


Mass spectrum from pion Dalitz decays peaked around $2m_e$

Spectrum from photon conversion tightly peaked around $2m_e$

Heavier meson decays have large opening angles

- Opening angle can be used to cut out photon conversion and Dalitz decays
  - must be able to distinguish single hits ("interesting" electrons) from double hits (Dalitz and photon conversion).

# HBD design and performance

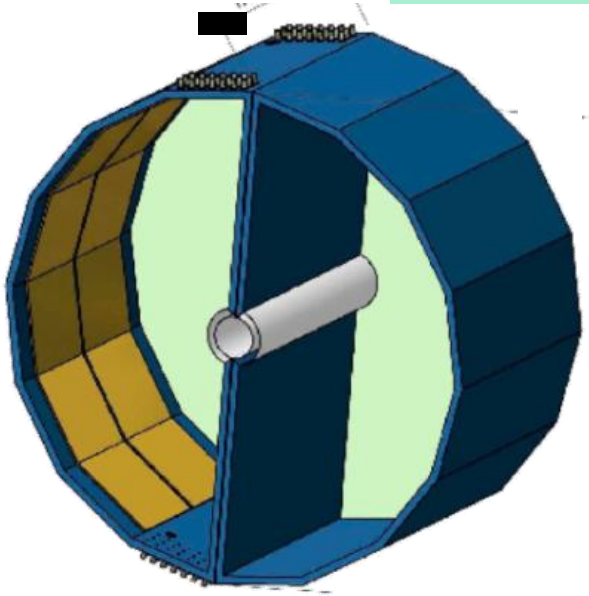

NIM A646, 35 (2011)

Windowless $CF_4$ Cherenkov detector
GEM/CSI photo-cathode readout
Operated in B-field free region

Goal: improve S/B by rejecting conversions and $\pi^0$ Dalitz decays

- Successfully operated:
  2009 p+p data
  2010 Au+Au data

**Single electron**

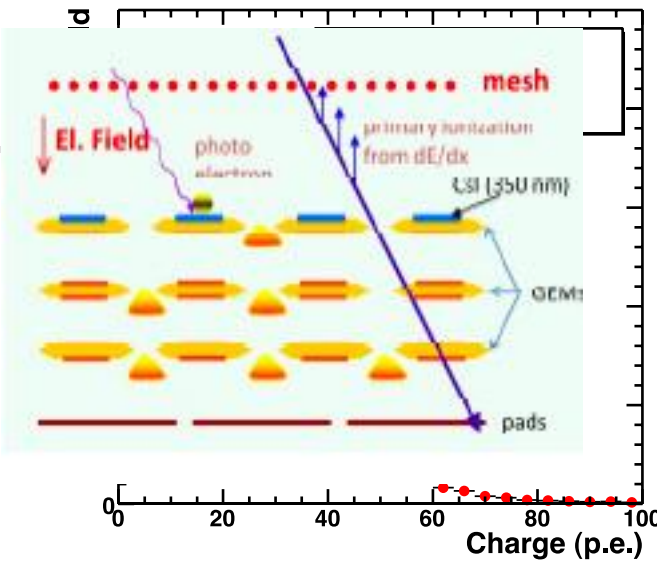


**Hadron blindness e-h separation**

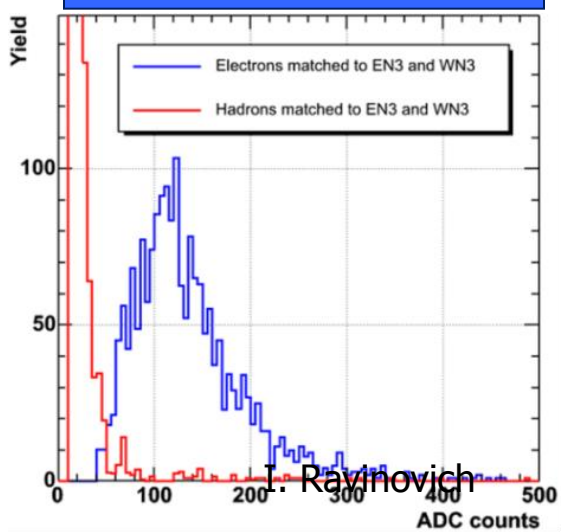


- Figure of merit: $N_0$ = 322 $cm^{-1}$
- 20 p.e. for a single electron
- Preliminary results:
  S/B improvement of ~5 wrt previous results w/o HBD

**Double electron**

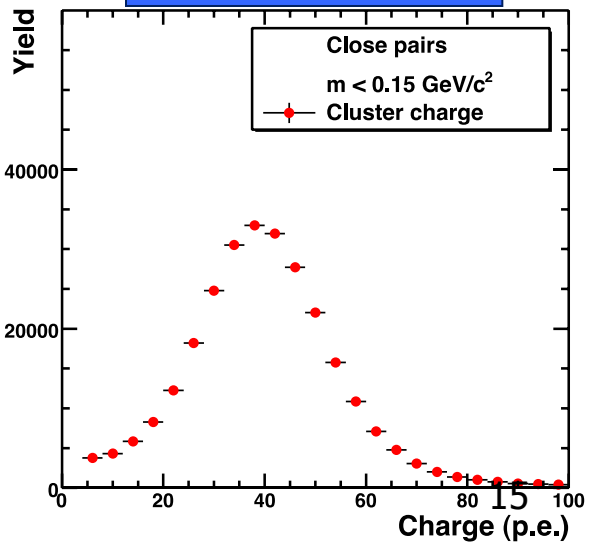

# HBD installed in PHENIX IR

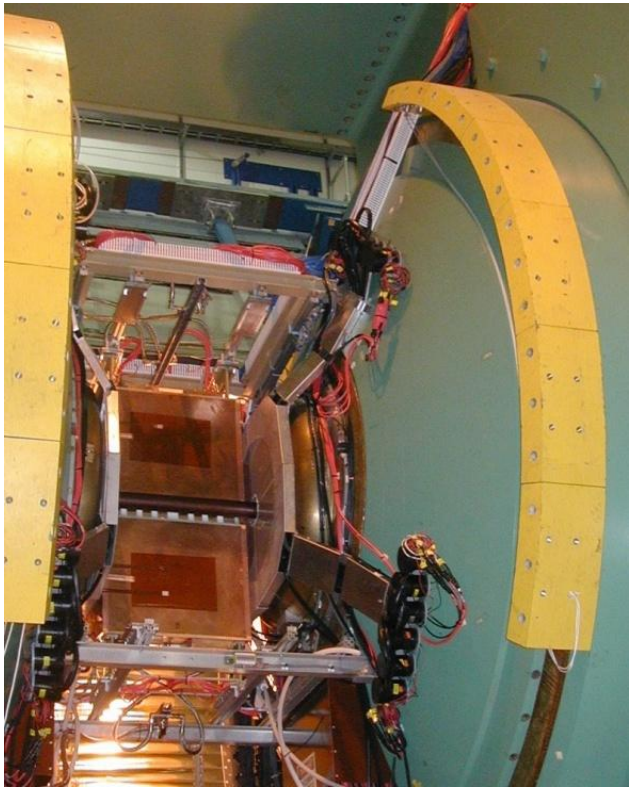

HBD West

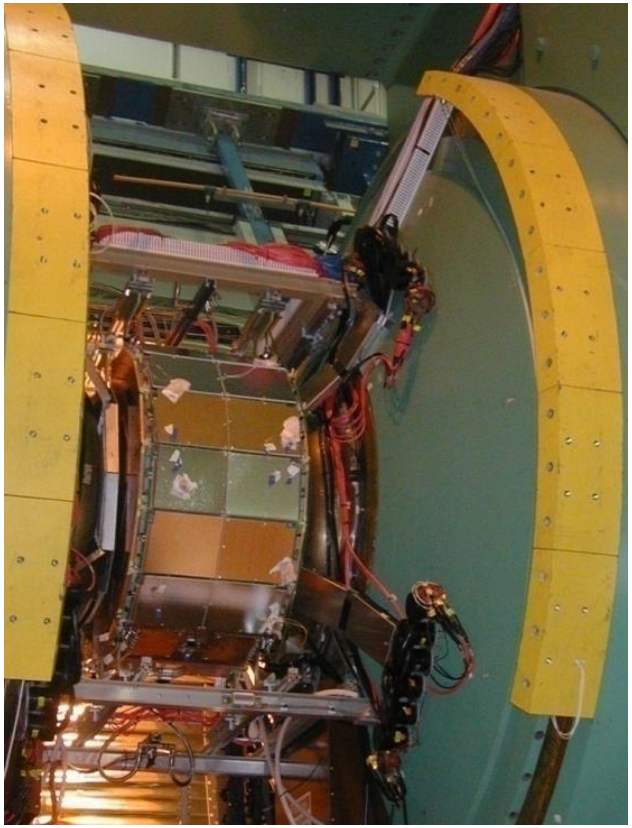

HBD East

# Analysis details of Au+Au with HBD

- Strong run QA and strong fiducial cuts to homogenize response of the central arm detectors over time
  - large price in statistics and pair efficiency
- Two parallel and independent analysis streams: provide crucial consistency check

| Stream A | Stream B |
|---|---|
| HBD: underlying event subtraction using average charge per pad | HBD: underlying event subtraction using average charge in track projection neighborhood |
| Neural network for eid and for single/double electron separation | Standard 1d cuts for both eid and for single/double electron separation |
| Correlated background (cross pairs and jets) subtracted using acceptance corrected like-sign spectra | Correlated background subtracted using MC for the cross pairs and jet pairs |

Results shown here are from stream A

# Run-9 p+p dileptons with the HBD

- Factor of 5-10 improvement in S/B ratio
  - this improvement is achieved using HBD only as an additional eID detector
  - more should be possible by using a double rejection cut
- Fully consistent with published result
- Provide crucial proof of principle and testing ground for understanding the HBD

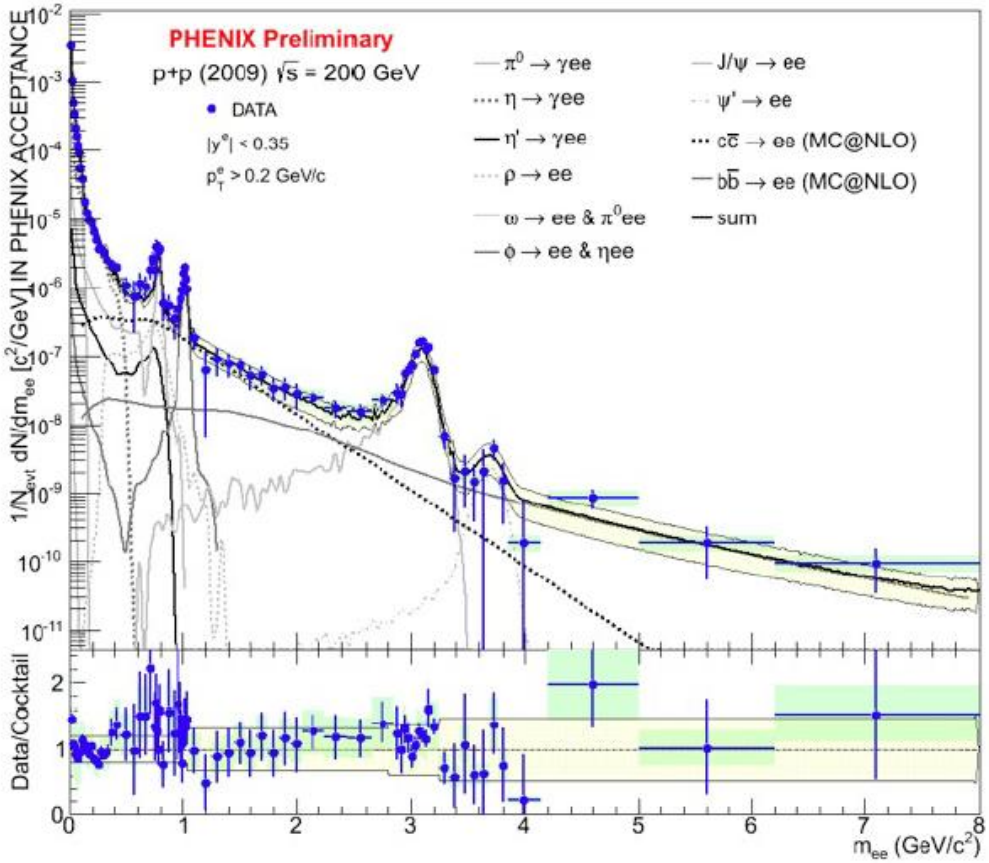

# Run-10 Au+Au dileptons with the HBD

**Peripheral**

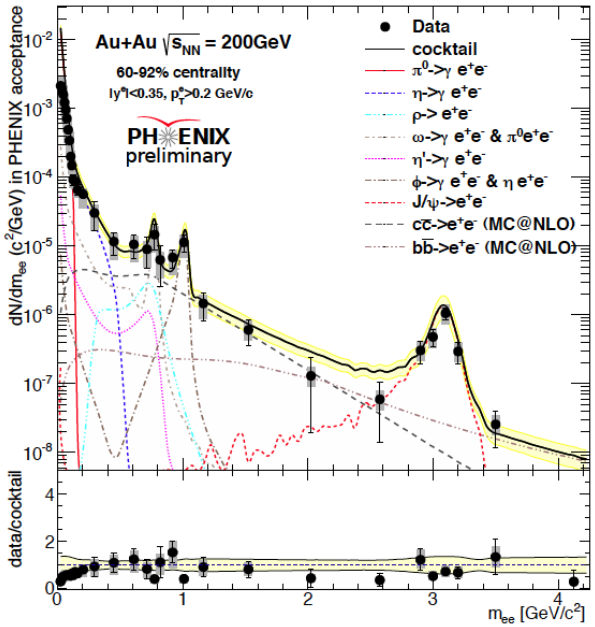


**Semi-peripheral**

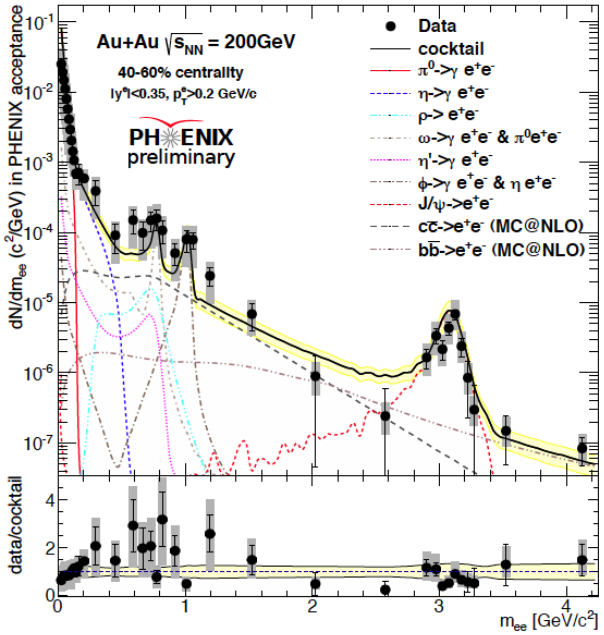


**Semi-central**

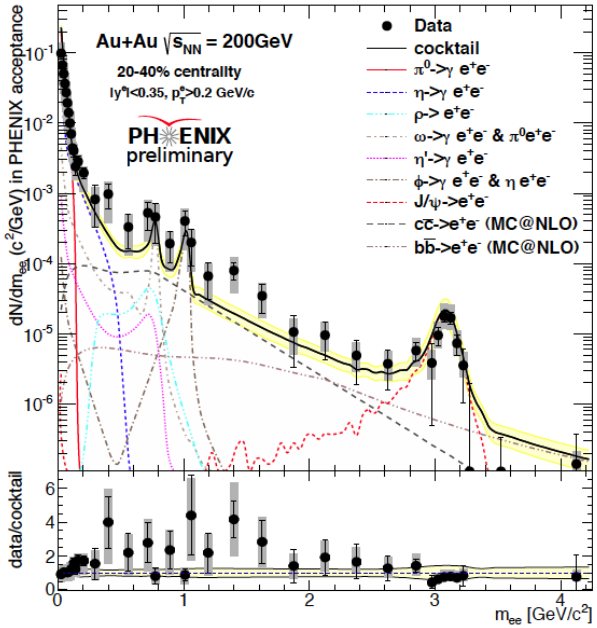

# Run-10 data with HBD: data/cocktail

- Hint of enhancement for more central collisions
- Not conclusive given the present level of uncertainties

**LMR (m = 0.15 – 0.75 GeV/c²)**

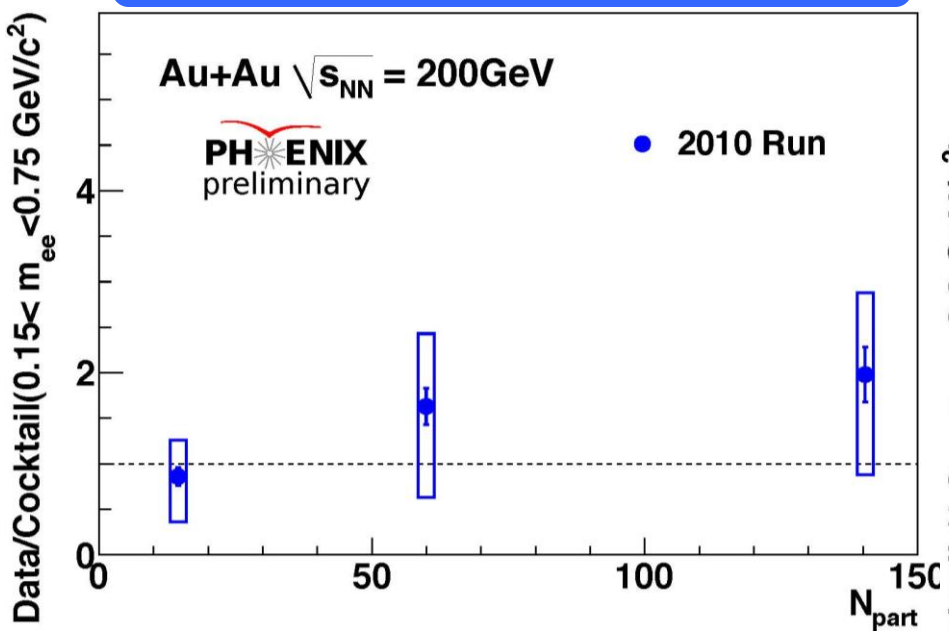


**IMR (m = 1.2 – 2.8 GeV/c²)**

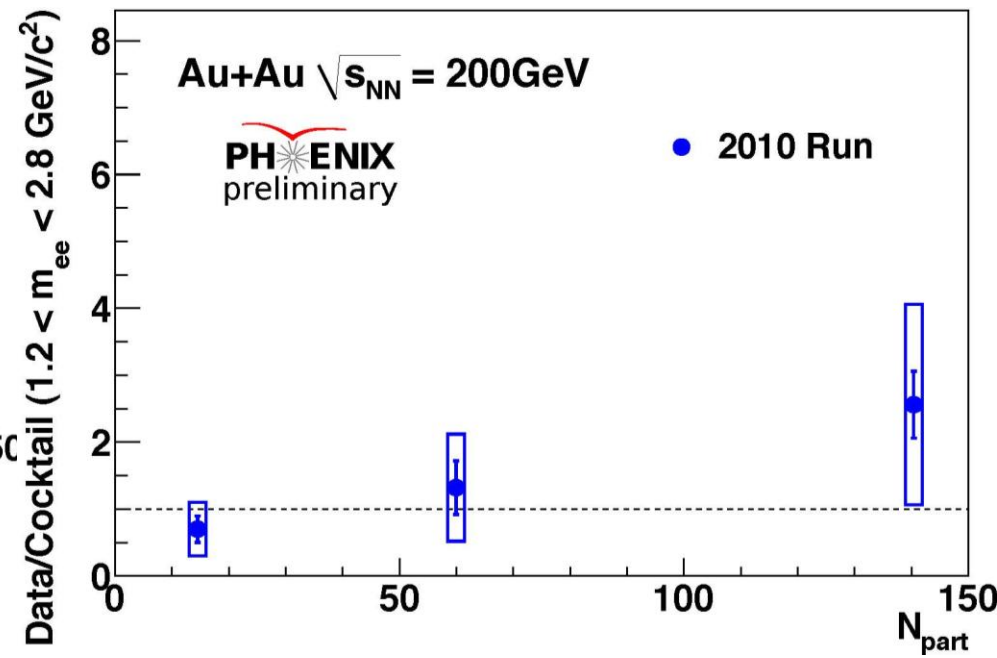


- Similar conclusions for the IMR

# Differences in runs with and without HBD

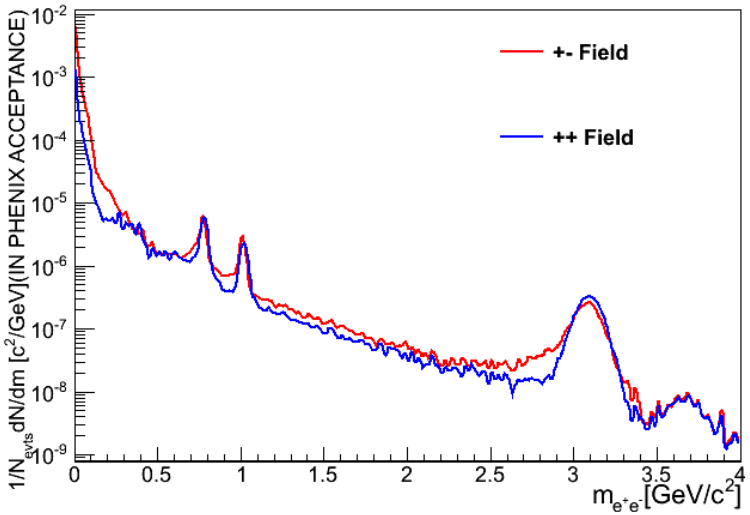


Data:

- Different magnetic field configuration:
  - Run-9 (p+p) and Run-10 (Au+Au) with HBD: +- field configuration
  - all other runs: ++ field configuration
  - larger acceptance of low $p_T$ tracks in +- field
- More material due to HBD:
  - more J/Ψ radiative tail

- We can compare results in three centrality bins: 20-40%, 40-60% and 60-92%

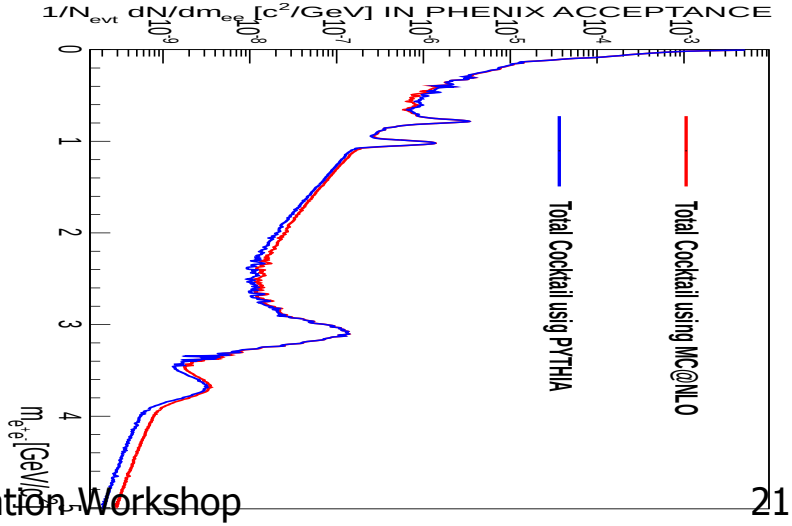


Cocktail:

- MC@NLO for open heavy flavor (c,b) contribution instead of PYTHIA
- MC@NLO**(1.2-2.8) =** PYTHIA**(1.2-2.8) * 1.16**

# Comparison of run-10 to published run-4 results

**LMR (m = 0.15 – 0.75 GeV/c²)**

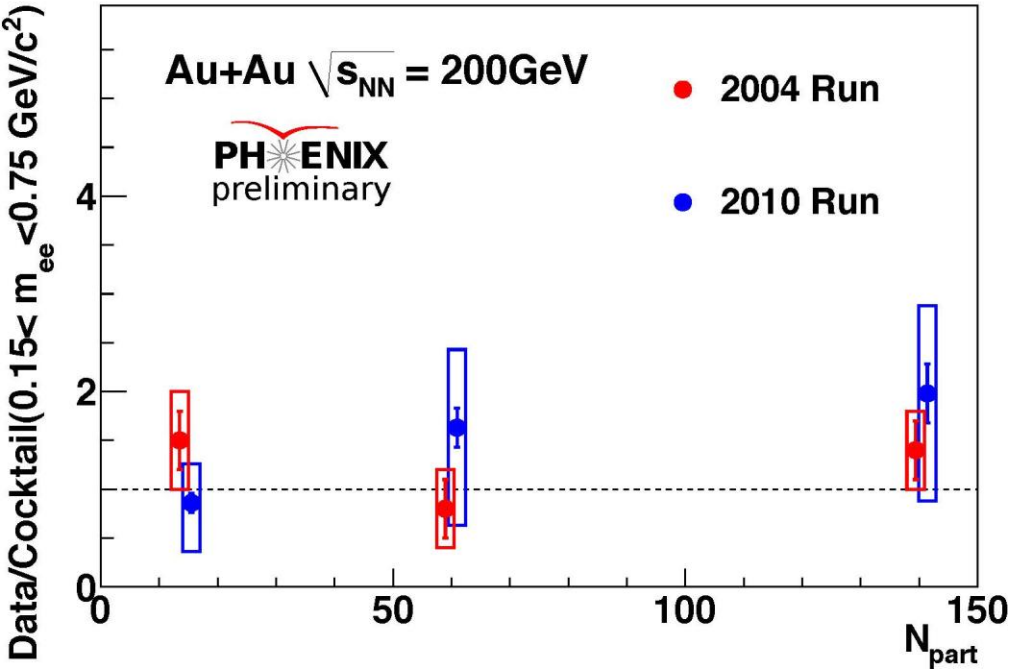


Run 10 – Data/ cocktail

| Centrality | Value | Stat | Syst(up) | Syst(dwn) |
|---|---|---|---|---|
| 20-40% | 1.98 | 0.3 | 0.9 | 1.1 |
| 40-60% | 1.63 | 0.2 | 0.8 | 1.0 |
| 60-92% | 0.86 | 0.1 | 0.4 | 0.5 |

Run 4 – Data/ cocktail

Phys Rev C81, 034911 (2010)

| Centrality | Value | Stat | Syst | model |
|---|---|---|---|---|
| 20-40% | 1.4 | 0.3 | 0.4 | 0.3 |
| 40-60% | 0.8 | 0.3 | 0.4 | 0.2 |
| 60-92% | 1.5 | 0.3 | 0.5 | 0.3 |

**Consistent results**

# Comparison of run-10 to published run-4 results

**IMR (m = 1.2 – 2.8 GeV/c²)**

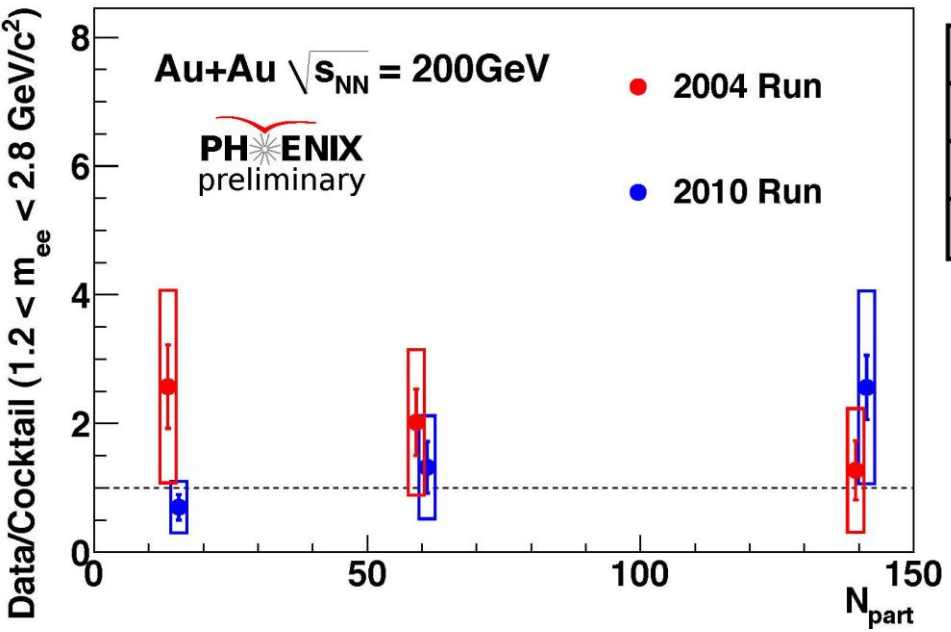


Run 10 – Data/ cocktail

| Centrality | Value | Stat | Syst(up) | Syst(dwn) |
|---|---|---|---|---|
| 20-40% | 2.56 | 0.5 | 1.5 | 1.5 |
| 40-60% | 1.32 | 0.4 | 0.8 | 0.8 |
| 60-92% | 0.70 | 0.2 | 0.4 | 0.4 |

Run 4 – Data/ cocktail
c,b yields based on MC@NLO
MC@NLO = PYTHIA * 1.16

| Centrality | Value | Stat | Syst |
|---|---|---|---|
| 20-40% | 1.3 | 0.5 | 1.0 |
| 40-60% | 2.0 | 0.5 | 1.1 |
| 60-92% | 2.6 | 0.6 | 1.5 |

**Consistent results**

# Summary

- Preliminary results on dielectrons in p+p and Au+Au collisions at 200 GeV in three centrality bins with Hadron Blind Detector in PHENIX.
- These results are consistent with previously published PHENIX results.
- The next step should be to complete the analysis relaxing the QA and fiducial cuts and providing most central bins.

# Initial State Fluctuations and Hydrodynamics

Björn Schenke
Physics Department, Brookhaven National Laboratory, Upton, NY

December 7 2012

*in collaboration with C. Gale, S. Jeon, P. Tribedy, R. Venugopalan*

Thermal Radiation Workshop 2012
Brookhaven National Laboratory

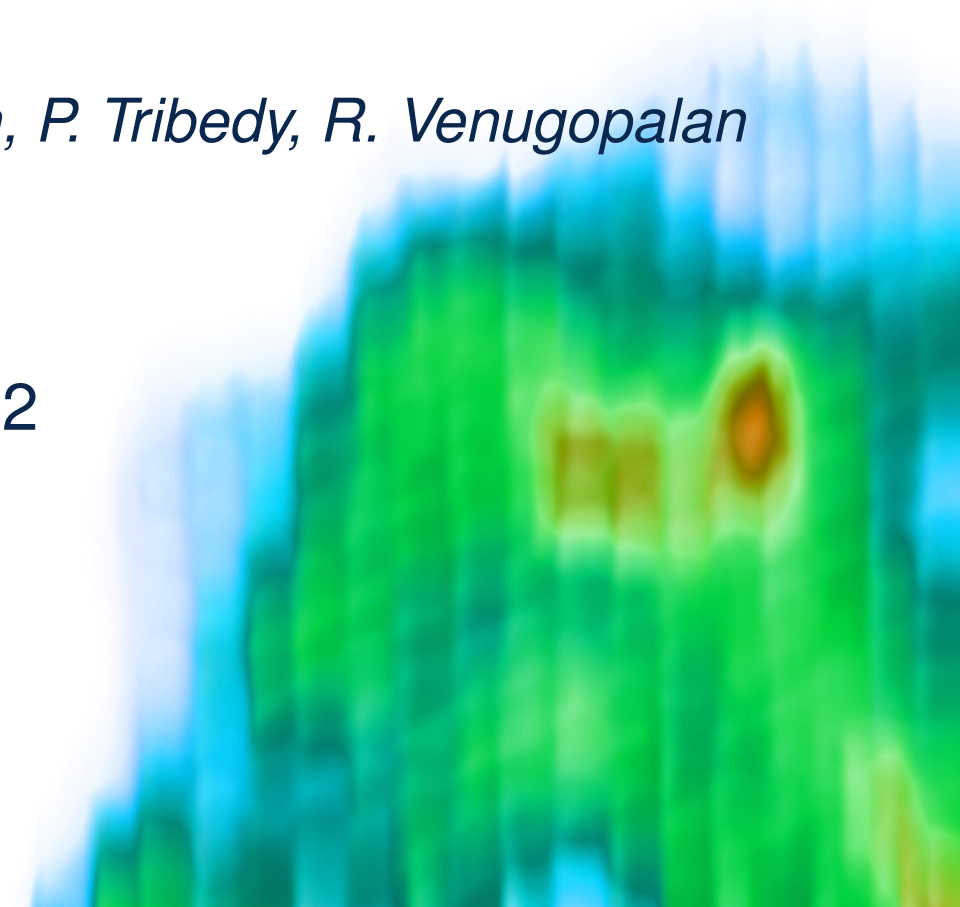

BROOKHAVEN
NATIONAL LABORATORY

# Introduction - Flow and Fluctuations

- Large elliptic flow has indicated fluid behavior of matter created at RHIC in early 2000's BNL announces "perfect liquid" in 2005 press release
- The importance of fluctuations was realized later and analysis of odd flow harmonics began in 2010
  since B. Alver, G. Roland, Phys.Rev. C81, 054905
- The knowledge of the (fluid dynamic) evolution of the system is necessary for the calculation of thermal photon and dilepton production
- I will
  - give an overview of recent developments
  - concentrate on a new QCD based model for the initial state including geometric and color charge fluctuations
  - present comparisons of theory and experimental data
  - present first photon flow calculations with the new initial state model

# Initial state fluctuations: MC-Glauber model

Positions of nucleons fluctuate; so does energy density in every event

Simple way to implement this: Monte-Carlo(MC)-Glauber model:

- Sample Woods-Saxon distributions to determine all nucleon positions (green and red circles)
- Sample impact parameter $b$ and overlap nuclei

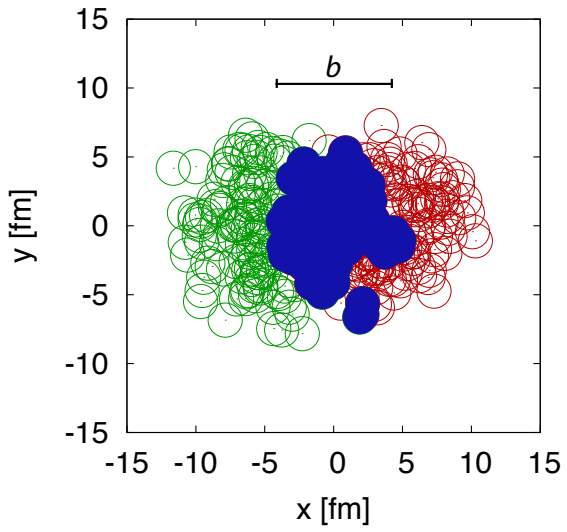


- Nucleon-nucleon collision occurs if distance is $< \sqrt{\sigma_{NN}/\pi}$
- At position of collision (blue blobs) add 2D-Gaussian energy density distribution with width $\sigma_0$
  $\sigma_0$ (e.g. $0.4\,\mathrm{fm}$) is a model parameter

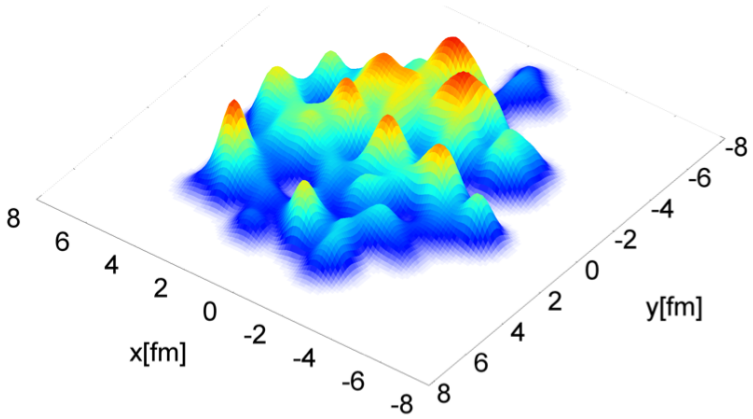

# Nearly perfect fluid $\leftrightarrow$ Hydrodynamic evolution

The system evolves from the initial energy density distribution according to energy and momentum conservation:

$$\partial_\mu T^{\mu\nu} = 0$$

$$T^{\mu\nu} = (\epsilon + P)u^\mu u^\nu - P g^{\mu\nu} + \pi^{\mu\nu}$$

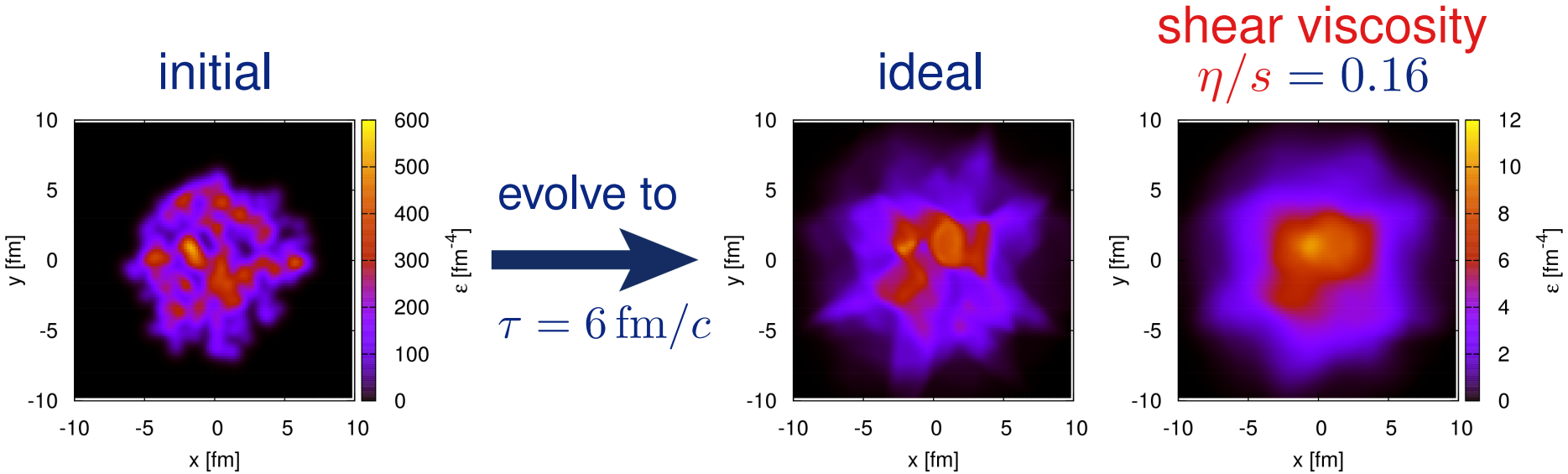


MUSIC B. Schenke, S. Jeon, C. Gale, Phys. Rev. C82, 014903 (2010); Phys.Rev.Lett.106, 042301 (2011)

3+1D event-by-event relativistic viscous hydrodynamic simulation

# Flow analysis

System expands, becomes dilute, freezes out

Spatial anisotropy is transformed into momentum anisotropy

Compute particle spectra at freeze-out using the Cooper-Frye formula:

$$E\frac{dN}{d^3p} = \int_\Sigma d\Sigma_\mu p^\mu f(T, p_\mu u^\mu, \pi^{\mu\nu})$$

$\Sigma =$ freeze-out surface, $f =$ particle distribution Cooper and Frye, Phys.Rev.D10, 186 (1974)

Analyze azimuthal distribution of particles in terms of Fourier series:

$$\frac{dN}{d\phi} = \frac{N}{2\pi}\left(1 + \sum_n (2v_n \cos(n(\phi - \psi_n)))\right)$$

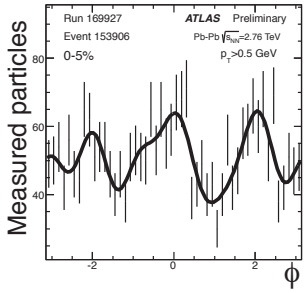


ATLAS

so

$$v_n = \langle \cos[n(\phi - \psi_n)] \rangle$$

with the event-plane angle $\psi_n = \frac{1}{n} \arctan \frac{\langle \sin(n\phi) \rangle}{\langle \cos(n\phi) \rangle}$

# Why the study of fluctuations is so powerful

Analysis analogous to that of the cosmic microwave background (CMB)

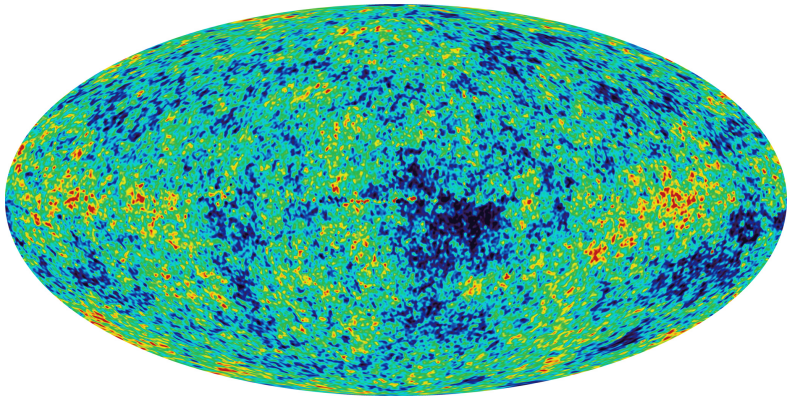

CMB Credit: WMAP Science Team, NASA

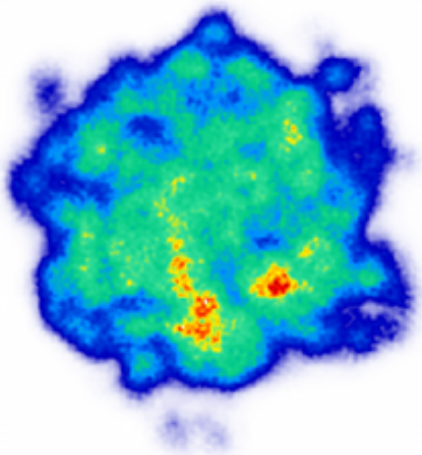

Heavy-Ion Collision

# Why the study of fluctuations is so powerful

Analysis analogous to that of the cosmic microwave background (CMB)

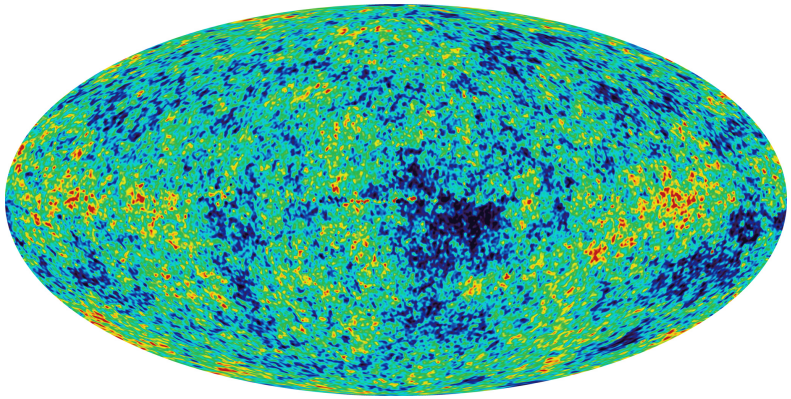

CMB Credit: WMAP Science Team, NASA

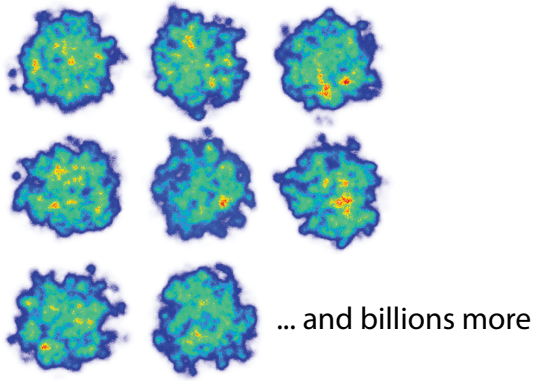


Heavy-Ion Collision

# Why the study of fluctuations is so powerful

Analysis analogous to that of the cosmic microwave background (CMB)

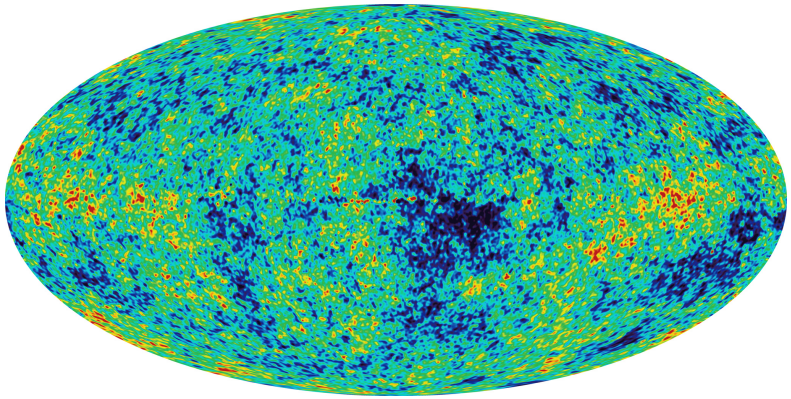

CMB Credit: WMAP Science Team, NASA

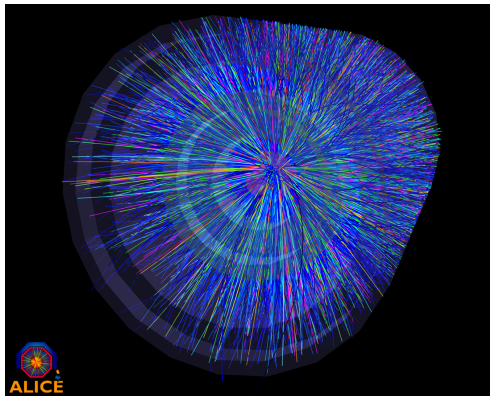


ALICE

Heavy-Ion Collision

# Why the study of fluctuations is so powerful

Analysis analogous to that of the cosmic microwave background (CMB)

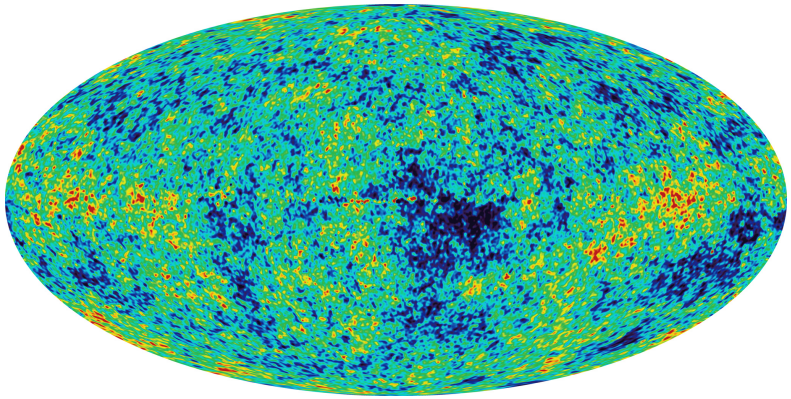

CMB Credit: WMAP Science Team, NASA

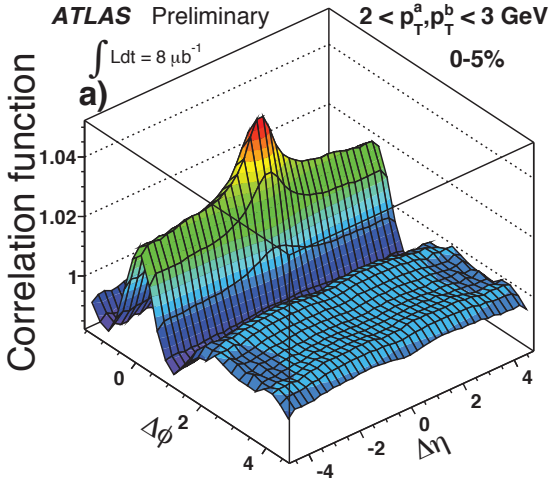


Heavy-Ion Collision

# Why the study of fluctuations is so powerful

Analysis analogous to that of the cosmic microwave background (CMB)

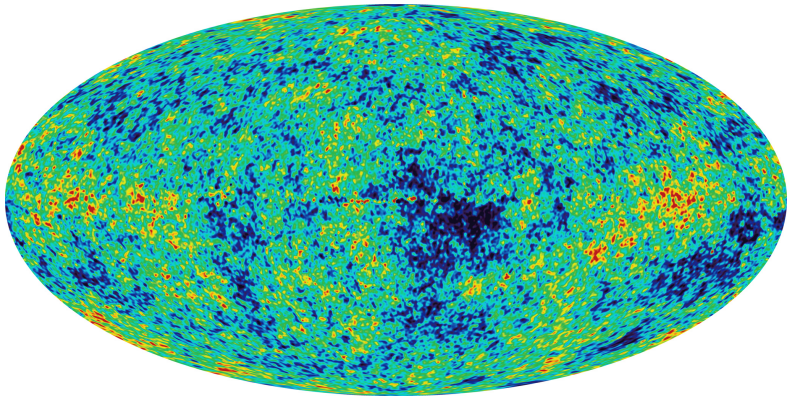

CMB Credit: WMAP Science Team, NASA

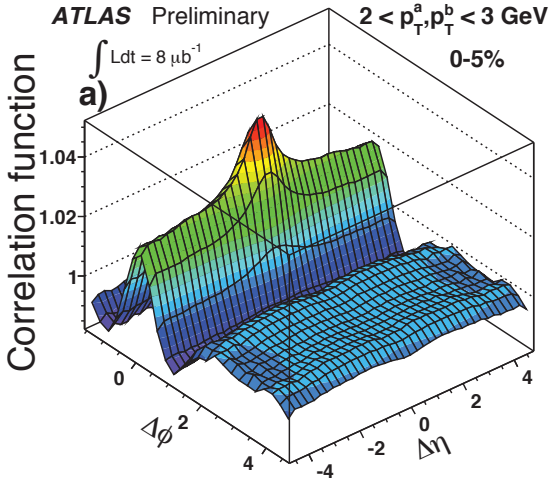


Heavy-Ion Collision

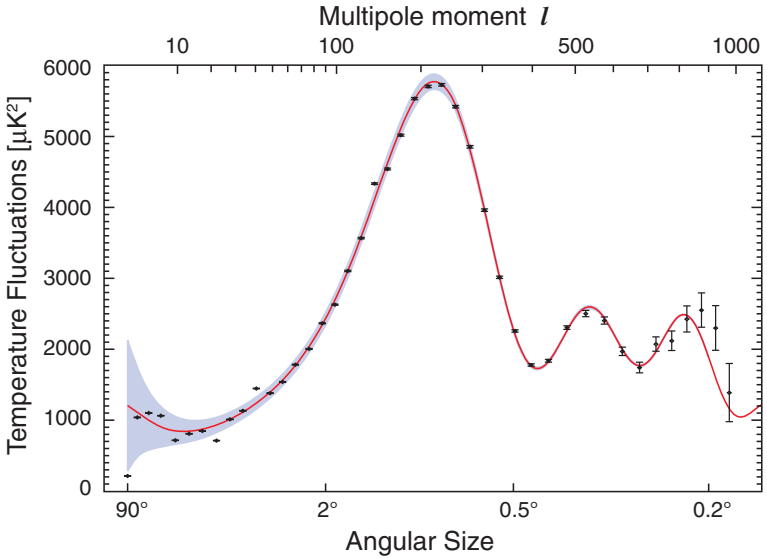


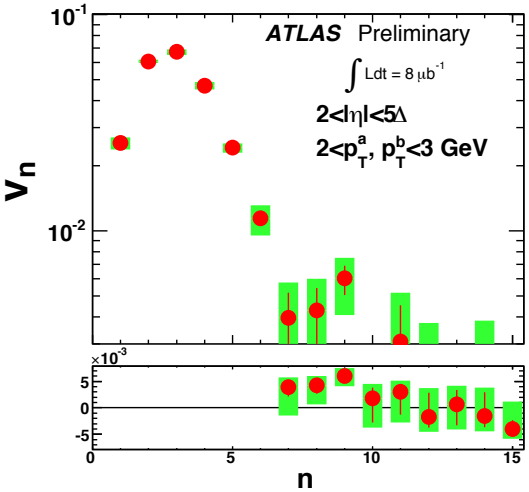

# Flow analysis B. Schenke, S. Jeon, C. Gale, Phys. Rev. C85, 024901 (2012)

## Sensitivity of event averaged $v_n$ on

viscosity

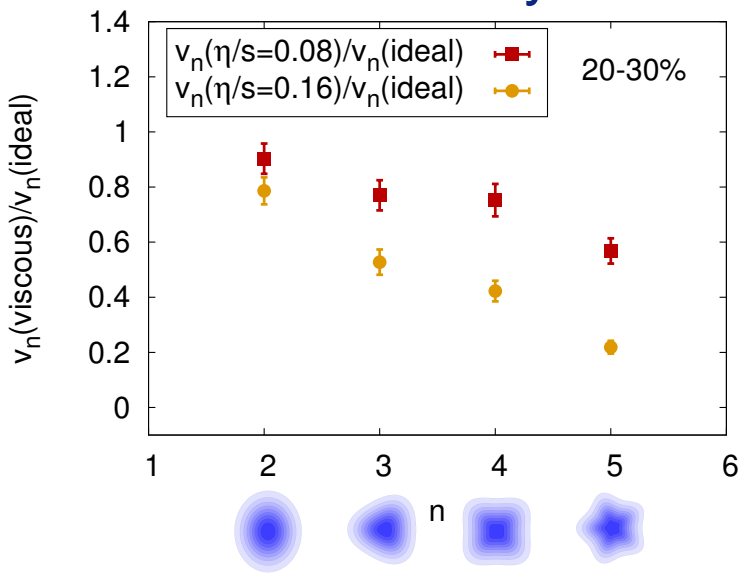


initial state granularity

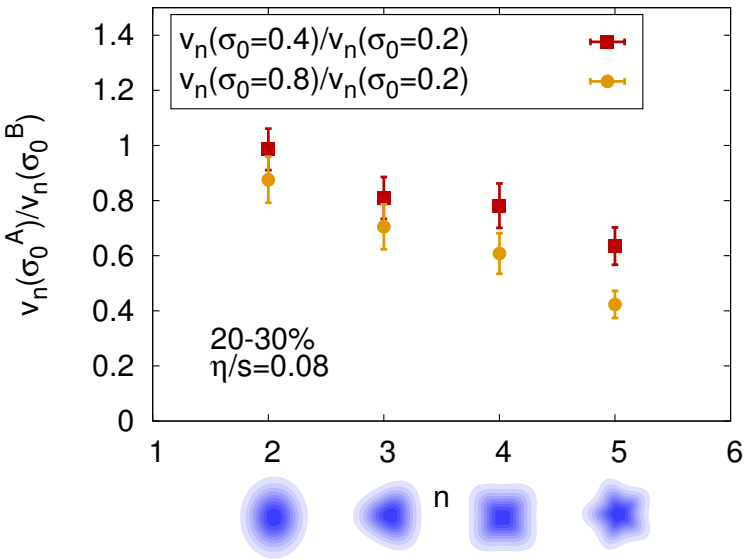


Shown are ratios of

viscous to ideal results

smoother to more granular results

Sensitivity to viscosity and initial state structure increases with $n$

# New model for the initial state

To make use of $v_n$ measurements we need a more rigorous understanding of the initial state and its fluctuations

Simple billard balls with a geometric cross section: not realistic

**QCD** should tell us what the incoming nuclei look like and what the fluctuations are

Color Glass Condensate (CGC) effective theory of QCD and Yang-Mills calculation of two colliding CGCs

# Gluon saturation

$x$ = longitudinal momentum fraction of partons in a hadron or nucleus

as we go to higher energy / smaller $x$, gluons split, number increases:

BFKL (Balitsky,Fadin,Kuraev,Lipatov) equation describes $x$-evolution
but violates unitarity: cross-sections grow without bound

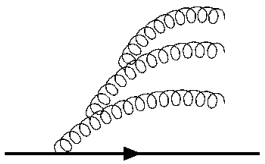

JIMWLK (Jalilian-Marian, Iancu, McLerran, Weigert, Leonidov, Kovner) and BK (Balitsky, Kovchegov)
equations include saturation

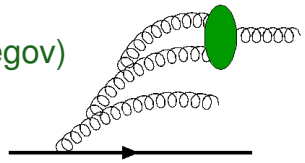

small $x$: the hadron/nucleus wavefunction is characterized by
the saturation scale $Q_s \gg \Lambda_{\rm QCD}$

$\mathbf{p}_T \lesssim Q_s$: strong fields $A_\mu \sim 1/g$:

- occupation numbers $\sim 1/\alpha_s$
- classical field approximation
- small $\alpha_s$, but non-perturbative

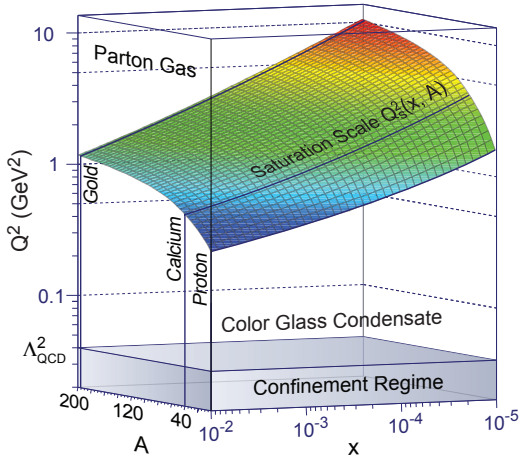

# Modeling $x$ and $b$ dependence: IP-Sat model

Want to determine color charge distribution in a nucleus. Proton first:
We use the IP-Sat model to parametrize

- $x$-dependence
- Impact parameter dependence (IP)

  Kowalski, Teaney, Phys.Rev. D68 (2003) 114005

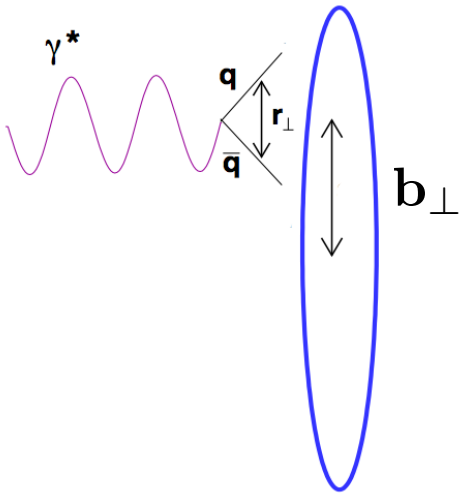


$x$-evolution can be computed using JIMWLK,
but parametrization is easier for now

Proton dipole cross section in DIS:

$$\frac{\mathrm{d}\sigma^{\mathrm{p}}_{\mathrm{dip}}}{\mathrm{d}^2\mathbf{b}_\perp}(\mathbf{r}_\perp, x, \mathbf{b}_\perp) = 2\mathcal{N}(\mathbf{r}_\perp, x, \mathbf{b}_\perp) = 2\left[1 - \exp\left(-\frac{\pi^2}{2N_c}\mathbf{r}_\perp{}^2\alpha_s(\tilde{\mu}^2)xg(x,\tilde{\mu}^2)T_p(\mathbf{b}_\perp)\right)\right]$$

with $\tilde{\mu}^2$ an energy scale related to the dipole radius $\mathbf{r}_\perp$ and $xg(x,\tilde{\mu}^2)$ is the gluon density
$T_p$ is a Gaussian with width fit to HERA diffractive data

$Q_s$ is defined by the value of $r$ at which $\mathcal{N}$ reaches the saturated regime

$\mathcal{N}(R_s, x, \mathbf{b}_\perp) = 1 - e^{-1/2}, \;\; \text{with } Q_s^2 = \frac{2}{R_s^2}$

# Color charge densities of incoming nuclei

- Sample nucleon positions from Woods-Saxon distributions.
- Use IP-Sat model fit to HERA data to get $Q_s^2(x, \mathbf{b}_\perp)$ for each nucleon. The color charge density squared $g^2\mu^2$ is proportional to $Q_s^2$.
- Add all $g^2\mu^2(\mathbf{x}_\perp)$ in each nucleus to obtain $g^2\mu_1^2(\mathbf{x}_\perp)$ and $g^2\mu_2^2(\mathbf{x}_\perp)$.

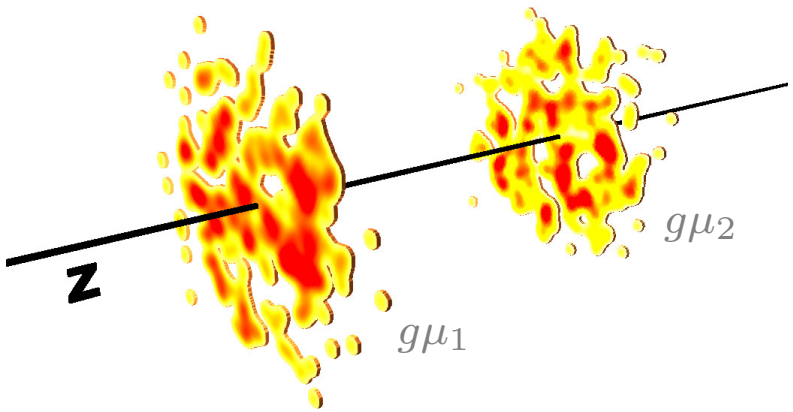


- Sample $\rho^a$ from local Gaussian distribution for each nucleus

$$\langle \rho^a(\mathbf{x}_\perp)\rho^b(\mathbf{y}_\perp)\rangle = \delta^{ab}\delta^2(\mathbf{x}_\perp - \mathbf{y}_\perp)g^2\mu^2(\mathbf{x}_\perp)$$

# Gauge fields before the collision

Color currents:

$$J_1^\nu = \delta^{\mu+}\rho_1(x^-, \mathbf{x}_\perp)$$
$$[D_\mu, F^{\mu\nu}] = J_1^\nu$$

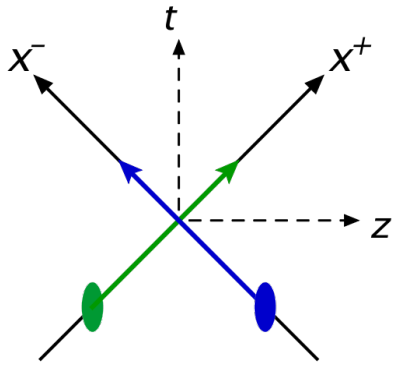


$$J_2^\nu = \delta^{\mu-}\rho_2(x^+, \mathbf{x}_\perp)$$
$$[D_\mu, F^{\mu\nu}] = J_2^\nu$$

Correlations and fluctuations in the gluon fields:

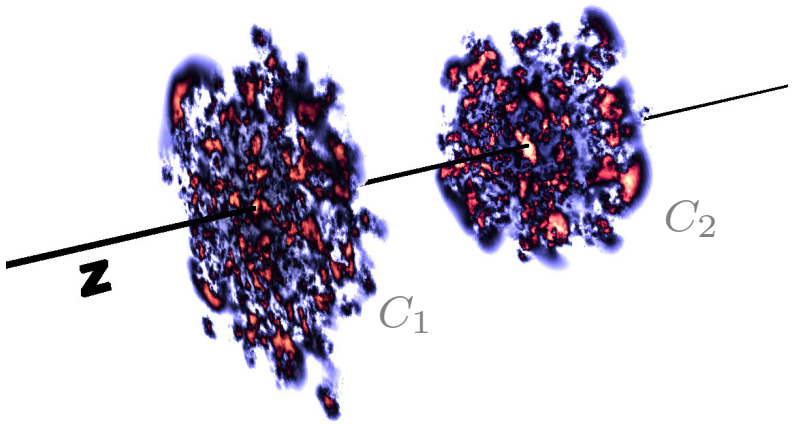


Shown is the correlator of the Wilson lines

$$C_{(1,2)}(\mathbf{x}_\perp) = \frac{1}{N_c}\mathrm{Re}[\mathrm{tr}(V(1,2)^\dagger(0,0)V(1,2)(x,y))]$$

The length scale of fluctuations is $1/Q_s$ - not the nucleon size

# Energy density B.Schenke, P.Tribedy, R.Venugopalan, Phys.Rev.Lett. 108, 252301 (2012)

Solve for gauge fields after the collision in the forward lightcone
Compute energy density in the fields at $\tau = 0$ and later times with CYM evolution
Lattice: Krasnitz, Venugopalan, Nucl.Phys. B557 (1999) 237

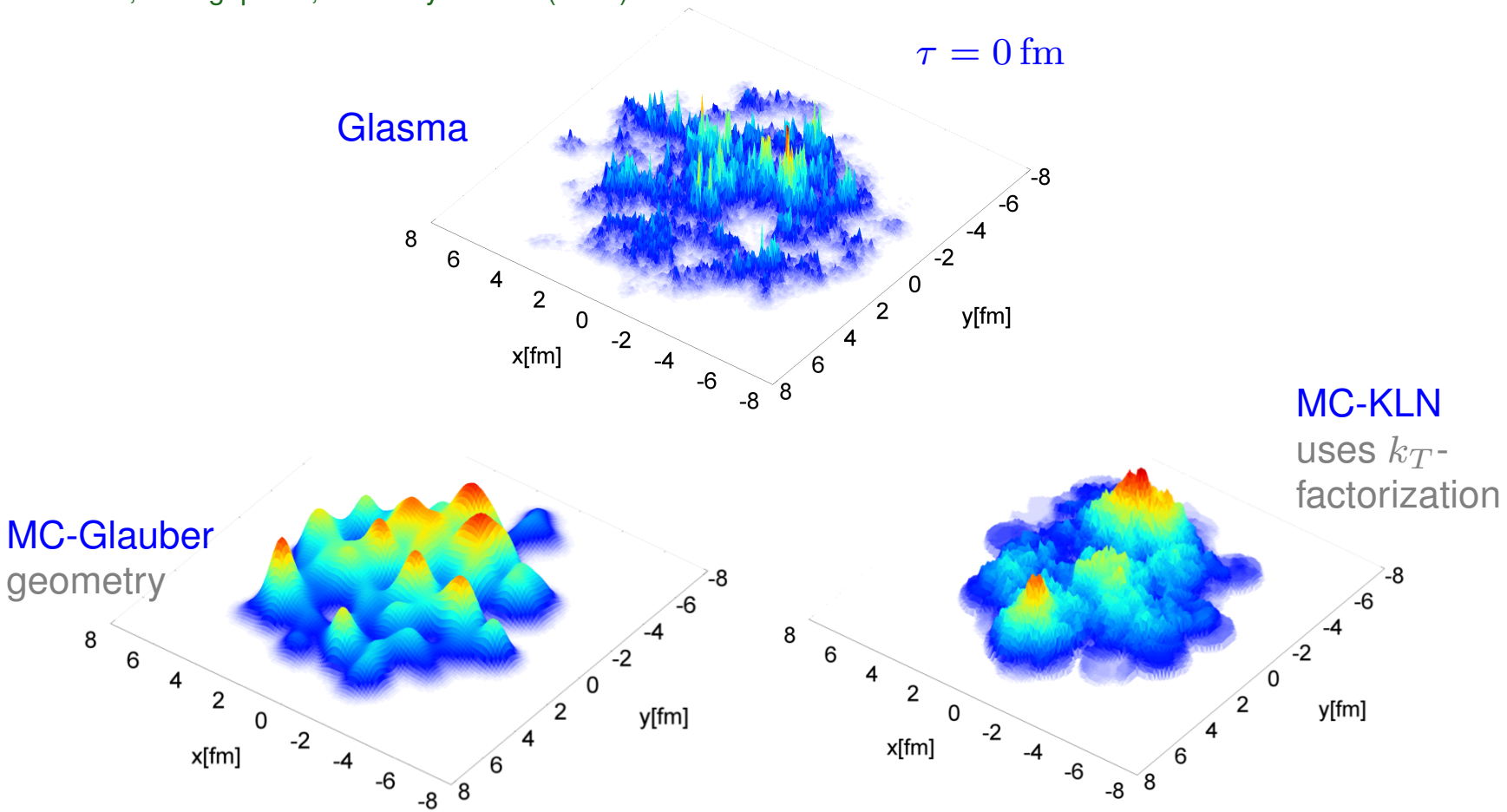


Very different initial energy density distributions in the models

MC-KLN: Drescher, Nara, nucl-th/0611017
mckln-3.52 from `http://physics.baruch.cuny.edu/files/CGC/CGC_IC.html` with defaults, energy density scaling

# Energy density B.Schenke, P.Tribedy, R.Venugopalan, Phys.Rev.Lett. 108, 252301 (2012)

Solve for gauge fields after the collision in the forward lightcone
Compute energy density in the fields at $\tau = 0$ and later times with CYM evolution
Lattice: Krasnitz, Venugopalan, Nucl.Phys. B557 (1999) 237

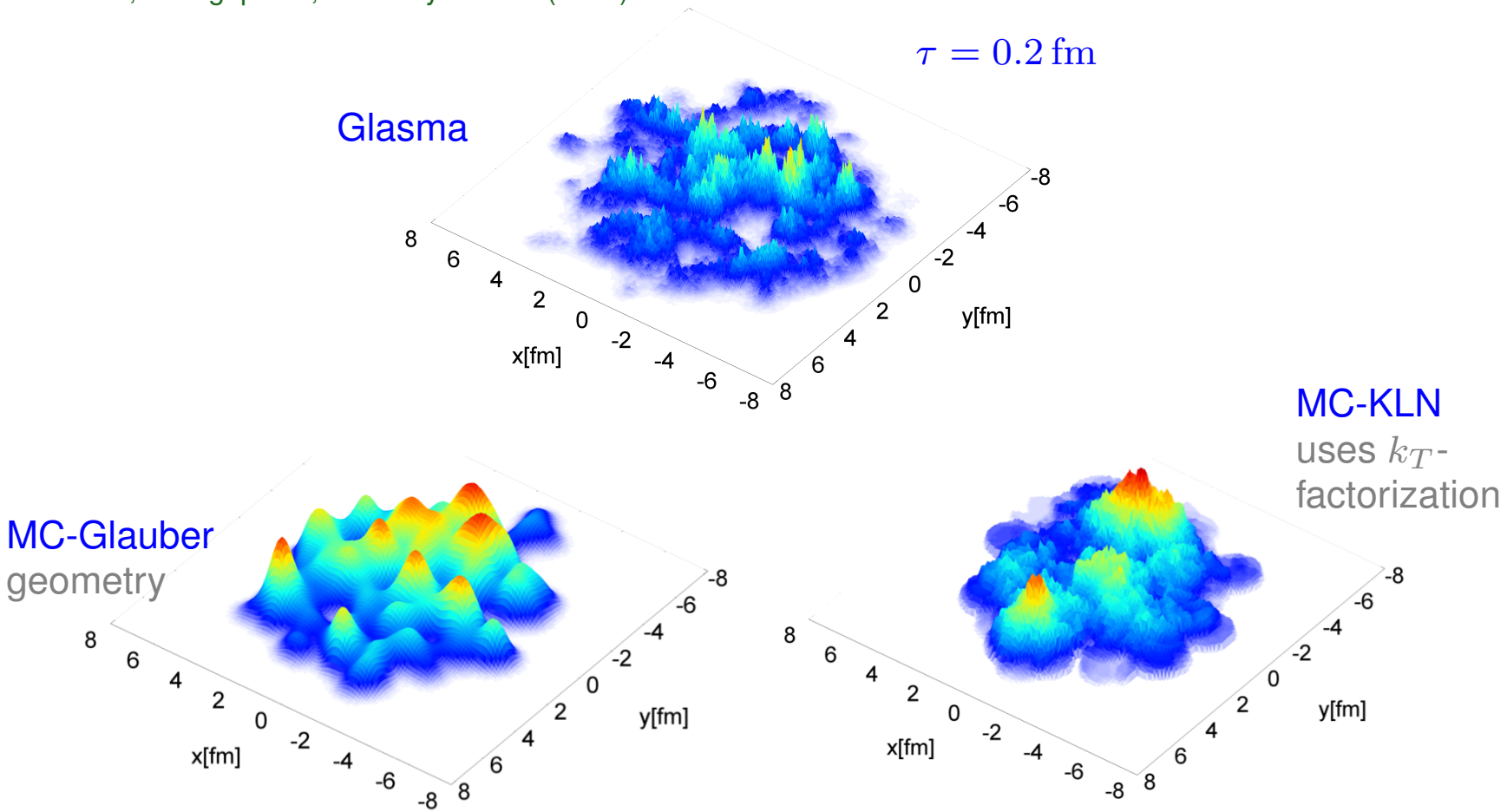


Very different initial energy density distributions in the models

MC-KLN: Drescher, Nara, nucl-th/0611017
mckln-3.52 from `http://physics.baruch.cuny.edu/files/CGC/CGC_IC.html` with defaults, energy density scaling

# Multiplicity B.Schenke, P.Tribedy, R.Venugopalan, Phys. Rev. C86, 034908 (2012)

$dN_{\mathrm{g}}/dy$ in transverse Coulomb gauge $\partial_i A^i = 0$
$N_{\mathrm{part}}$ from MC-Glauber with $\sigma_{NN} = 42\,\mathrm{mb}$ and $64\,\mathrm{mb}$ respectively

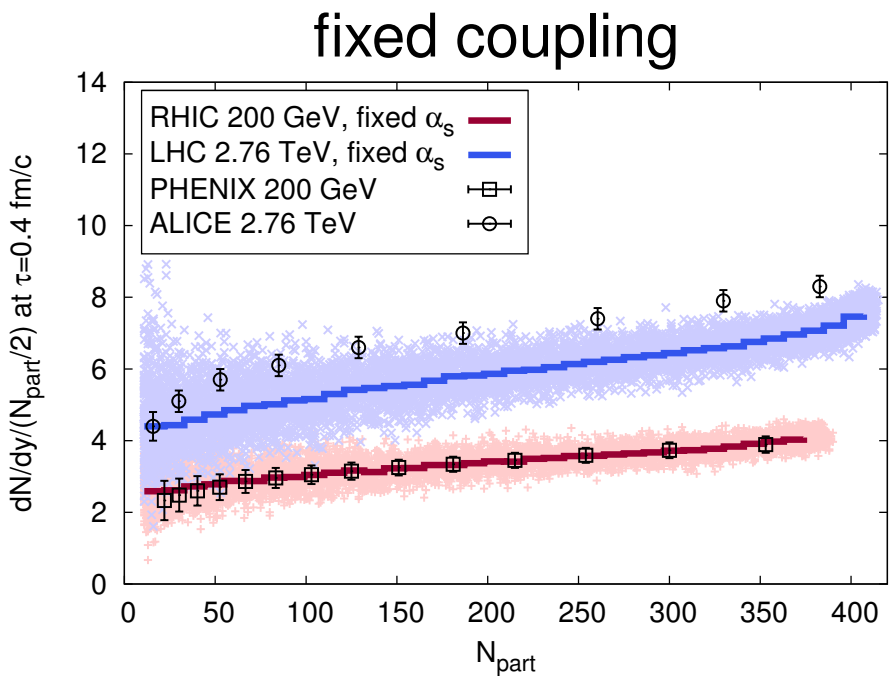


Experimental data: PHENIX, Phys.Rev.C71 034908 (2004) and ALICE, Phys.Rev.Lett. 106, 032301 (2011)

Scaled by $2/3$ to compare to charged particles.

Some freedom in normalization - will need to account for entropy production.

# Multiplicity B.Schenke, P.Tribedy, R.Venugopalan, Phys. Rev. C86, 034908 (2012)

$dN_{\mathrm{g}}/dy$ in transverse Coulomb gauge $\partial_i A^i = 0$
$N_{\mathrm{part}}$ from MC-Glauber with $\sigma_{NN} = 42\,\mathrm{mb}$ and $64\,\mathrm{mb}$ respectively

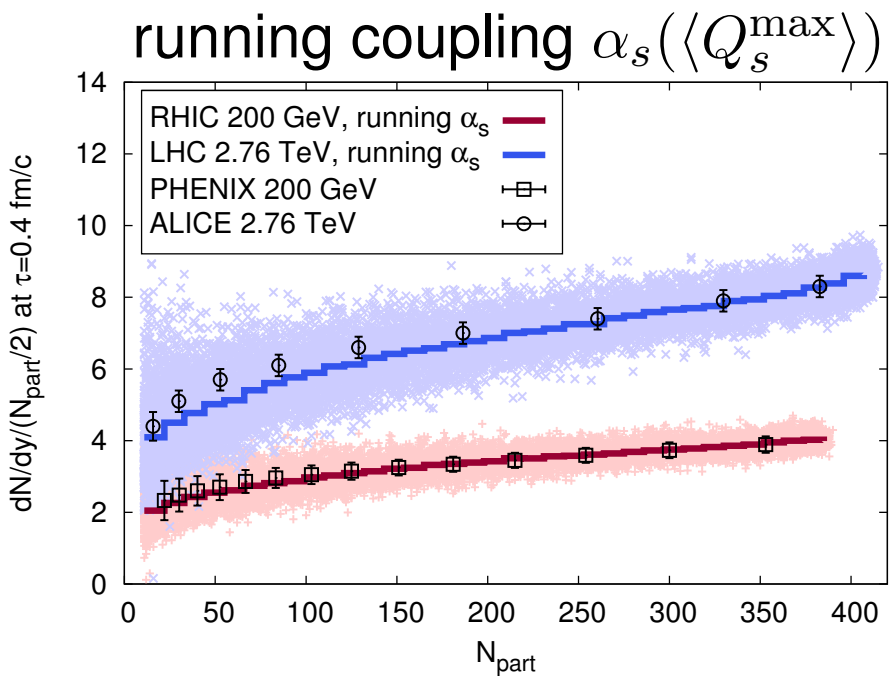


Experimental data: PHENIX, Phys.Rev.C71 034908 (2004) and ALICE, Phys.Rev.Lett. 106, 032301 (2011)

Scaled by $2/3$ to compare to charged particles.

Some freedom in normalization - will need to account for entropy production.

# Multiplicity B.Schenke, P.Tribedy, R.Venugopalan, Phys. Rev. C86, 034908 (2012)

$P(dN_g/dy)$ at time $\tau = 0.4\,\mathrm{fm}$ with $P(b)$ from a Glauber model

Experimental data: STAR, Phys. Rev. C79, 034909 (2009)

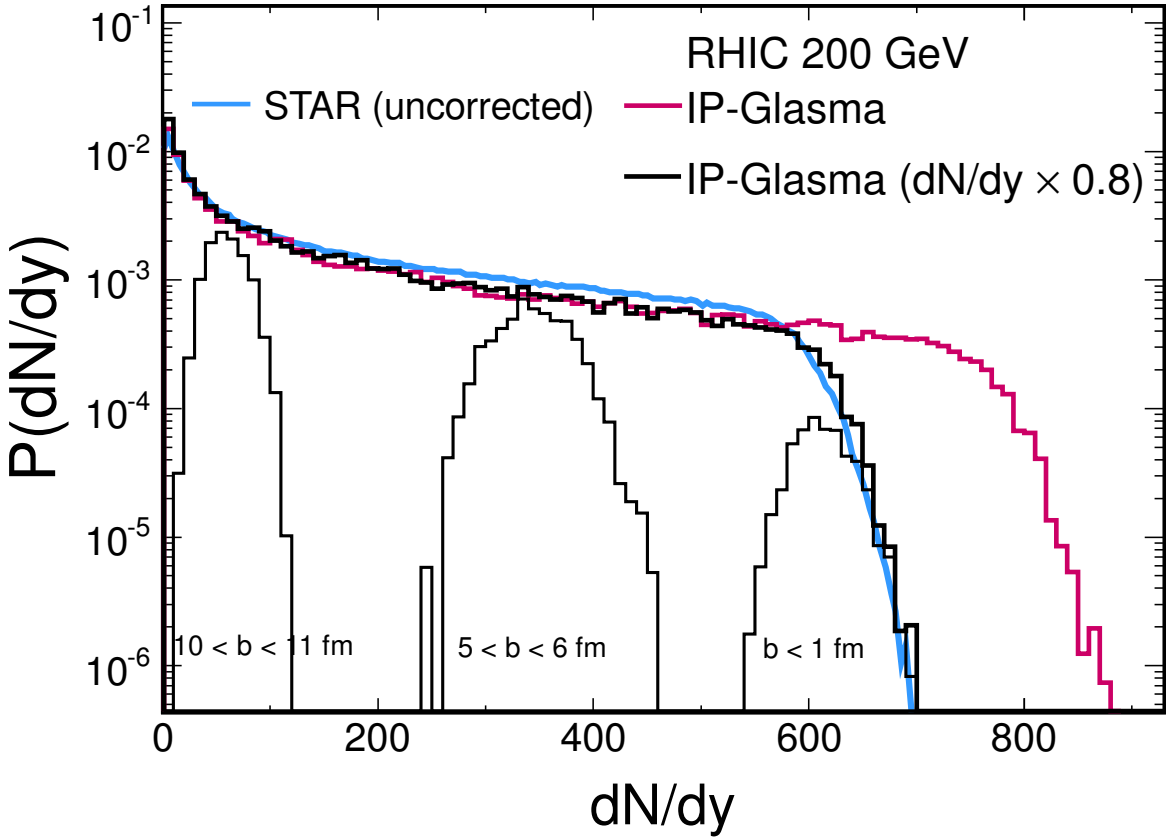


Glasma model gives a convolution of negative binomial distributions

No need to put them in by hand

# Eccentricities B.Schenke, P.Tribedy, R.Venugopalan, Phys. Rev. C86, 034908 (2012)

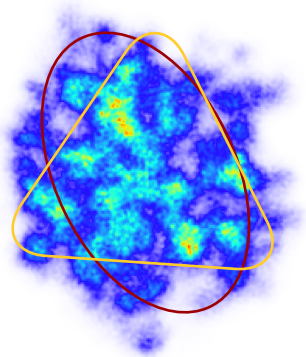

Characterize the initial distribution by its ellipticity, triangularity, etc...

$$\varepsilon_n = \sqrt{\langle r^n \cos(n\phi)\rangle^2 + \langle r^n \sin(n\phi)\rangle^2}/\langle r^n\rangle$$

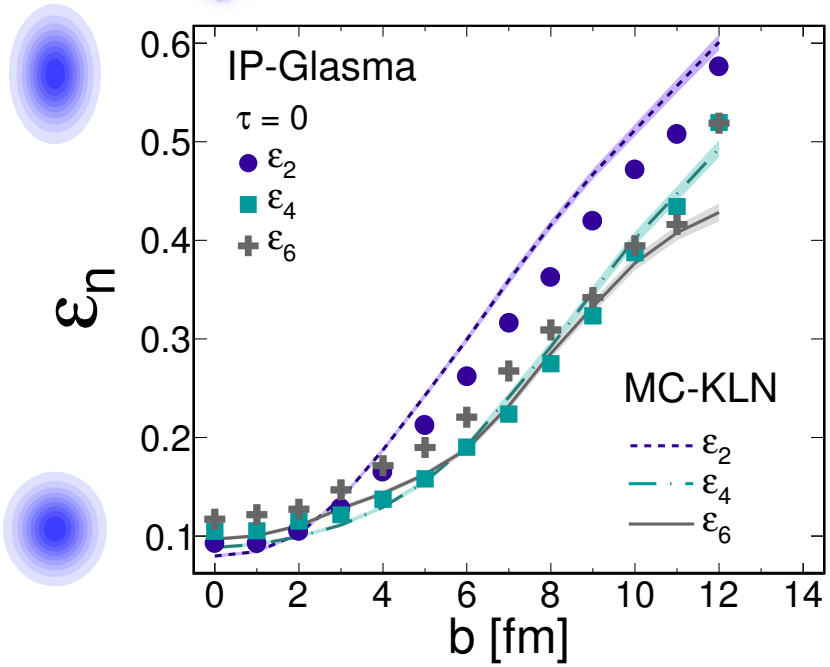


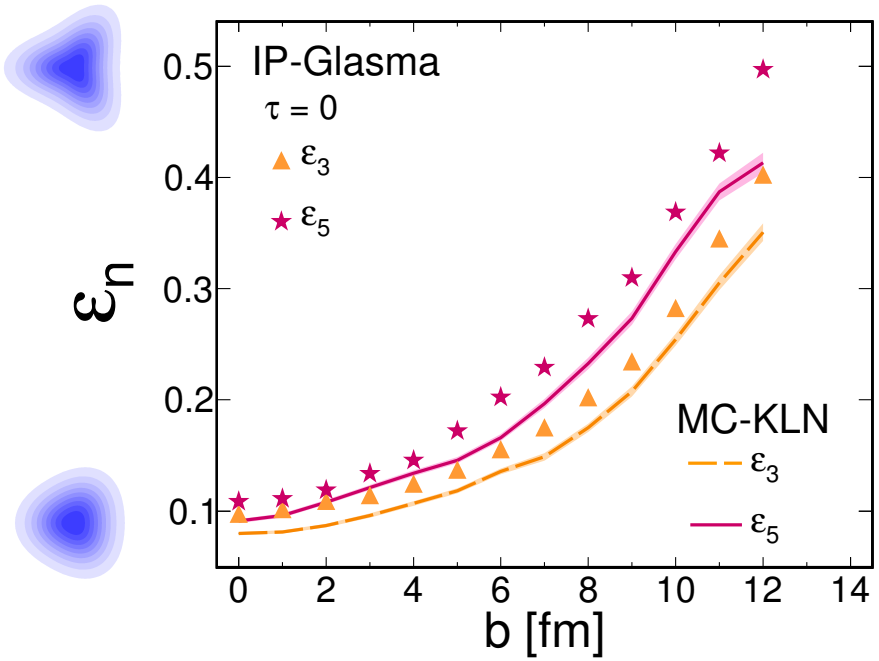


- $\varepsilon_n$ larger in Glasma model for odd $n$
- $\varepsilon_n$ smaller in Glasma model for $n = 2$ (for $b > 3\,\mathrm{fm}$) about equal for $n = 4$, larger for $n = 6$

# Matching to hydro: $T^{\mu\nu}$ and flow velocities

Compute all components of $T^{\mu\nu}$
Determine energy density and $(u^x, u^y)$ at $\tau > 0\,\mathrm{fm}$ from $u_\mu T^{\mu\nu} = \varepsilon u^\nu$
as input for hydrodynamic simulations

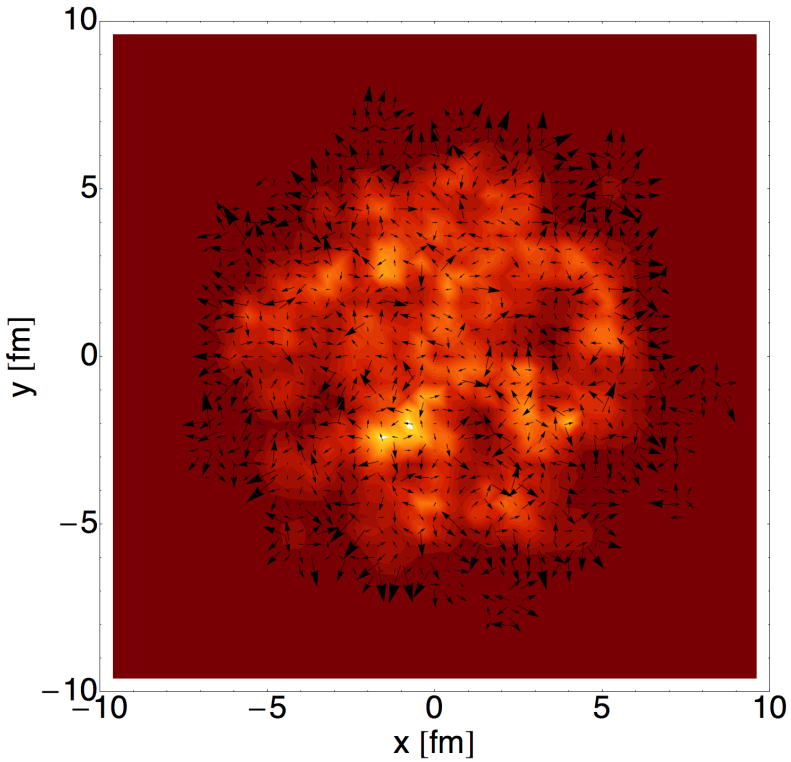


Energy density
and $(u_x, u_y)$
at $\tau = 0.4\,\mathrm{fm}/c$

No instabilities (need full 3+1D Yang-Mills for that):
system is far from equilibrium - cannot yet match $\Pi^{\mu\nu}$

# Centrality selection and flow

C. Gale, S. Jeon, B.Schenke,
P.Tribedy, R.Venugopalan, arXiv:1210.5144 (2012)

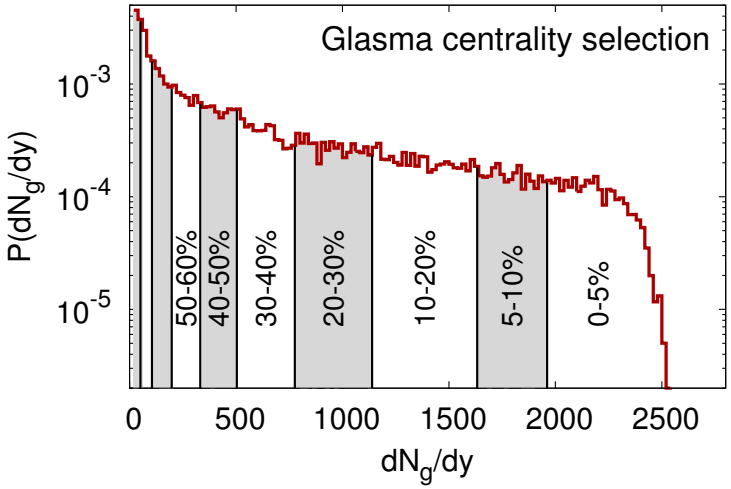

# Centrality selection and flow

C. Gale, S. Jeon, B.Schenke,
P.Tribedy, R.Venugopalan, arXiv:1210.5144 (2012)

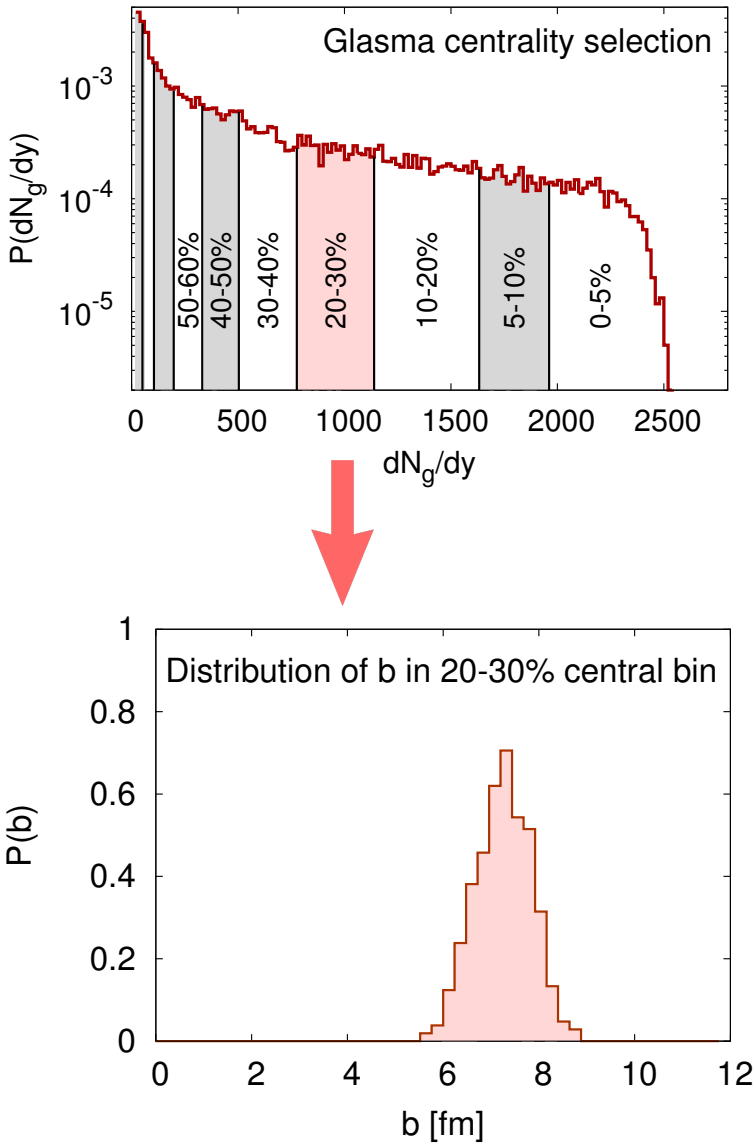

# Centrality selection and flow

C. Gale, S. Jeon, B.Schenke,
P.Tribedy, R.Venugopalan, arXiv:1210.5144 (2012)

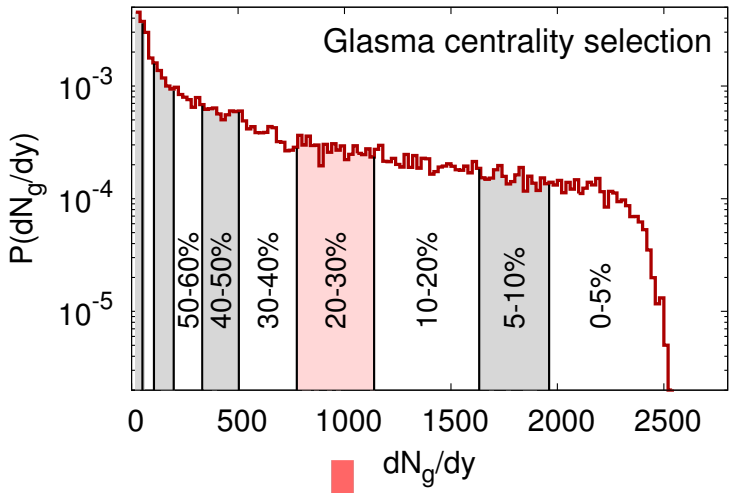


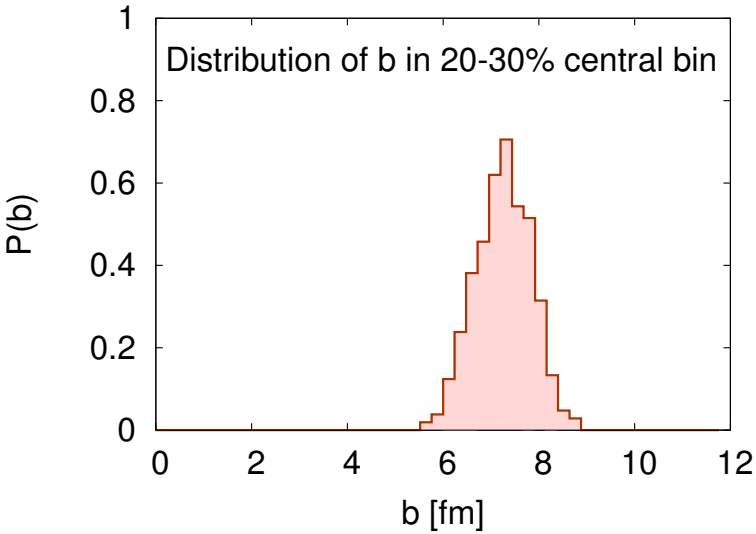


Hydro evolution

MUSIC

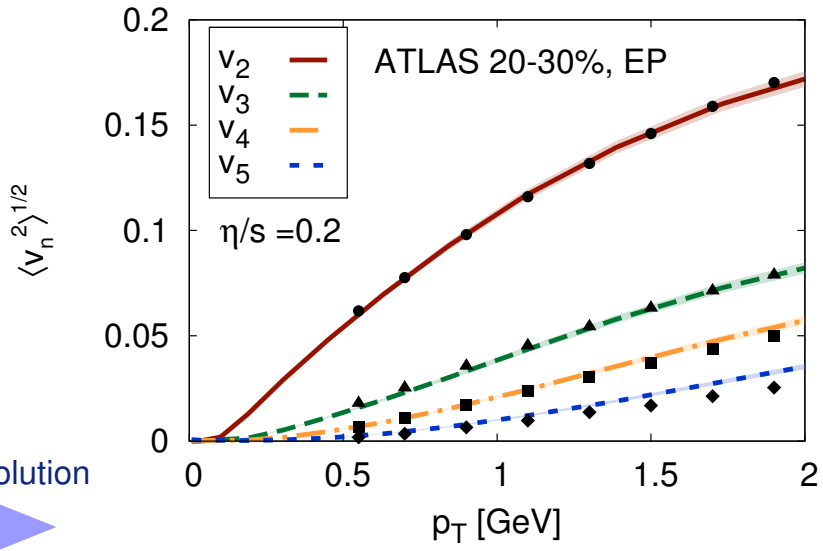

# Centrality selection and flow

C. Gale, S. Jeon, B.Schenke,
P.Tribedy, R.Venugopalan, arXiv:1210.5144 (2012)

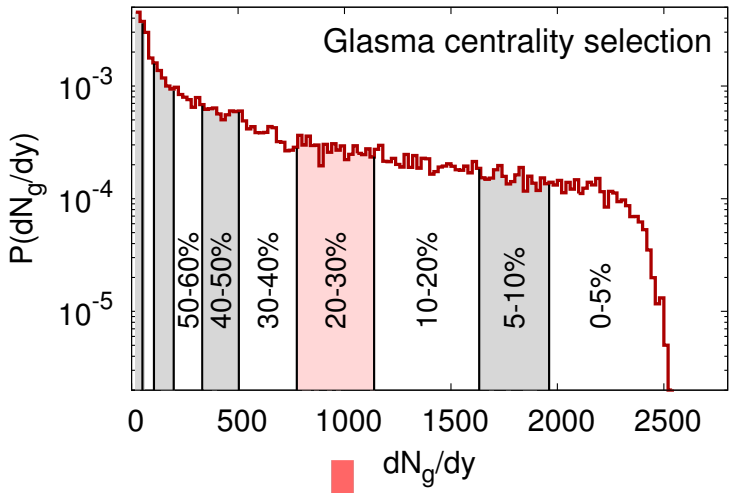


Hydro evolution

MUSIC

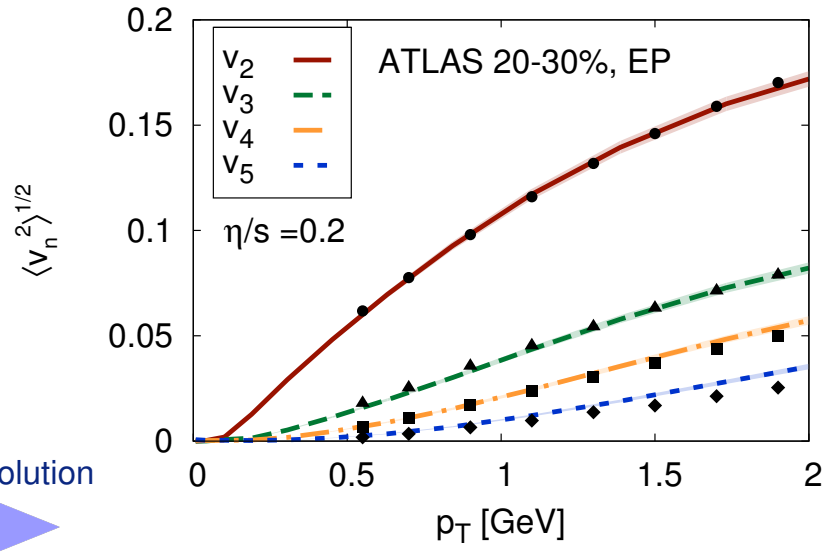


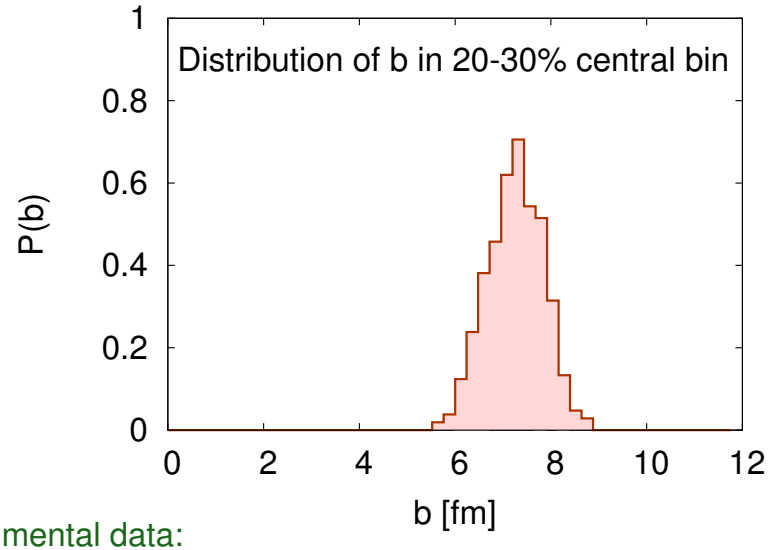


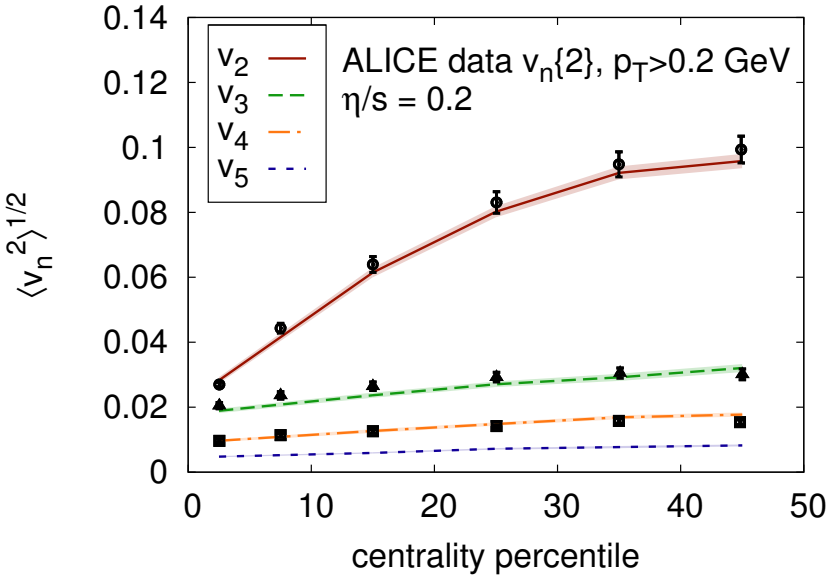


Experimental data:
ATLAS collaboration, Phys. Rev. C 86, 014907 (2012)
ALICE collaboration, Phys. Rev. Lett. 107, 032301 (2011)

# Temperature dependent $\eta/s$

Use $\eta/s(T)$ as in Niemi et al., Phys.Rev.Lett. 106 (2011) 212302 and arXiv:1203.2452

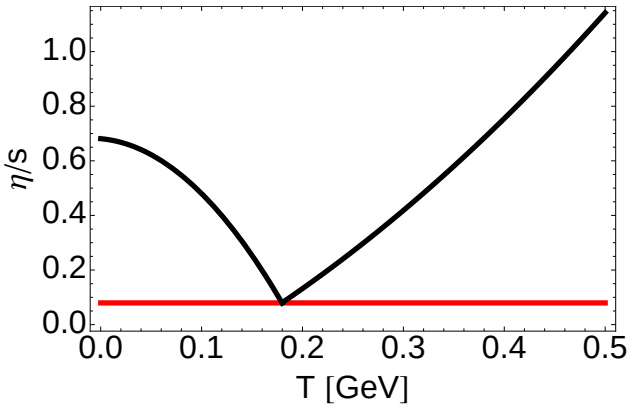


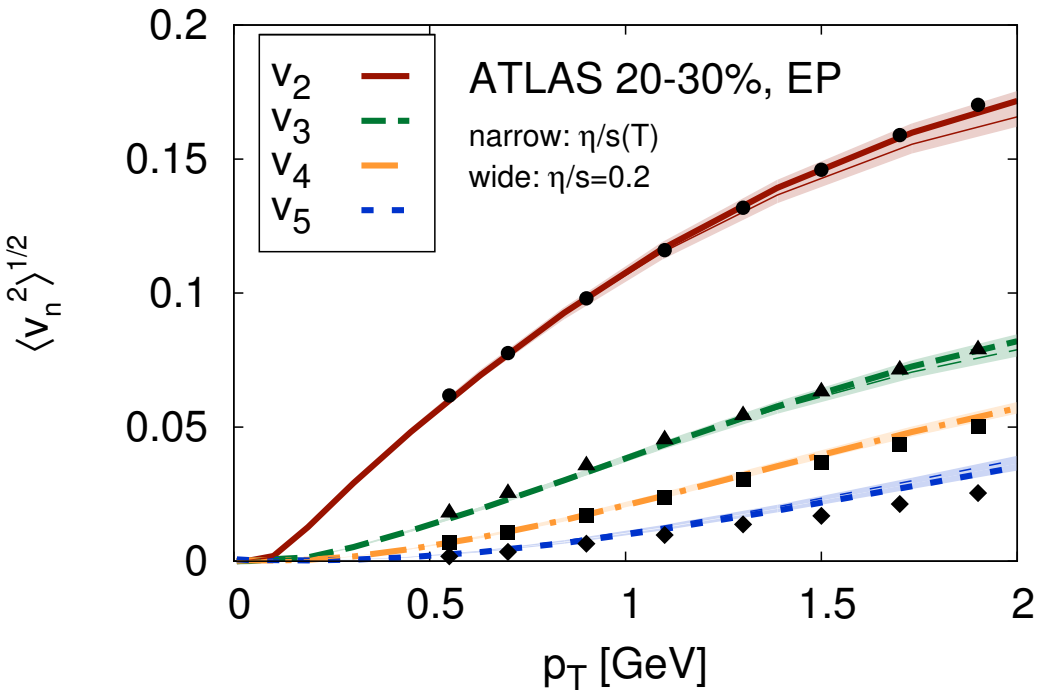


$v_n(p_T)$ for given $\eta/s(T)$ indistinguishable from constant $\eta/s = 0.2$

More detailed study needed - include different RHIC energies and LHC

Experimental data:
ATLAS collaboration, Phys. Rev. C 86, 014907 (2012)

# Comparison to RHIC data

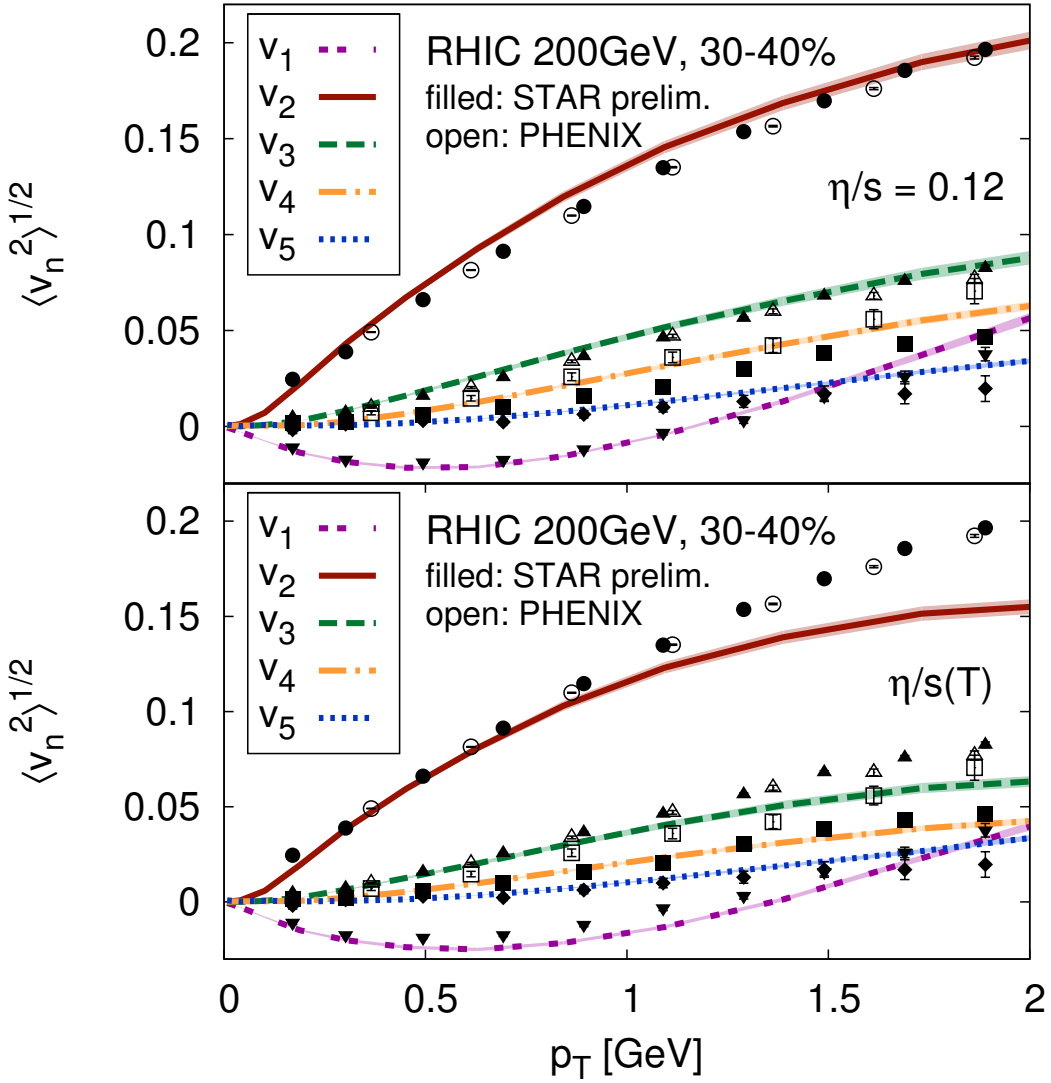


Lower effective $\eta/s$ than at LHC needed to describe data

Hints at increasing $\eta/s$ at high temperature

Can be used to gain information on $(\eta/s)(T)$

Experimental data:
A. Adare et al. (PHENIX Collaboration), Phys.Rev.Lett. 107, 252301 (2011)
Y. Pandit [for the STAR collaboration], Quark Matter 2012, (2012)

# New measurements of single event $v_n$

The ATLAS collaboration presented first measurements of $v_n$ in single events at Quark Matter 2012

https://atlas.web.cern.ch/Atlas/GROUPS/PHYSICS/CONFNOTES/ATLAS-CONF-2012-114/

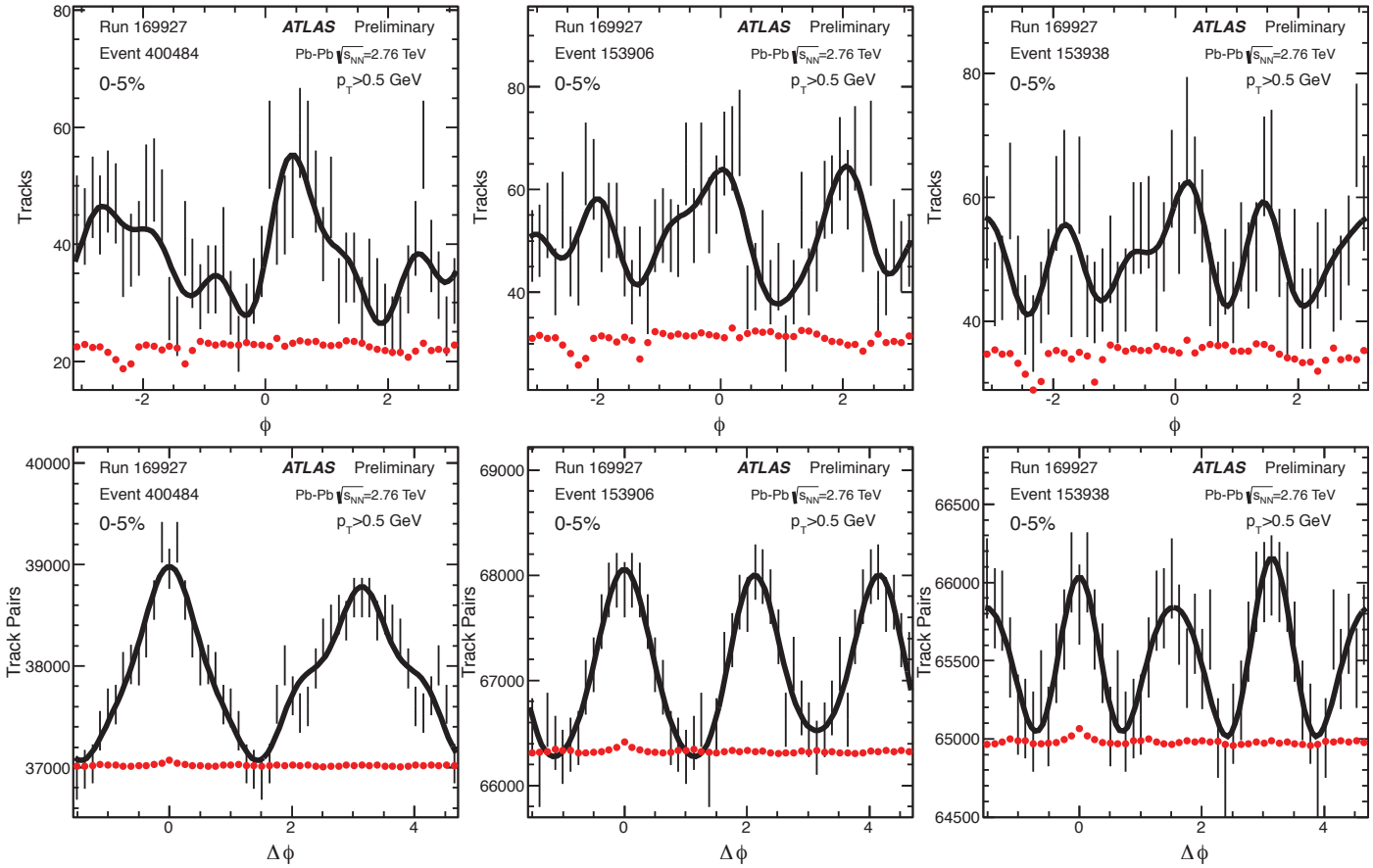


$\phi$-distribution of particles(upper) or pairs(lower).
Black lines: Fourier expansion, $v_n$ fit.

# Event-by-event distributions of $v_n$

So now we can compare event-by-event distributions of $v_n$.

https://atlas.web.cern.ch/Atlas/GROUPS/PHYSICS/CONFNOTES/ATLAS-CONF-2012-114/

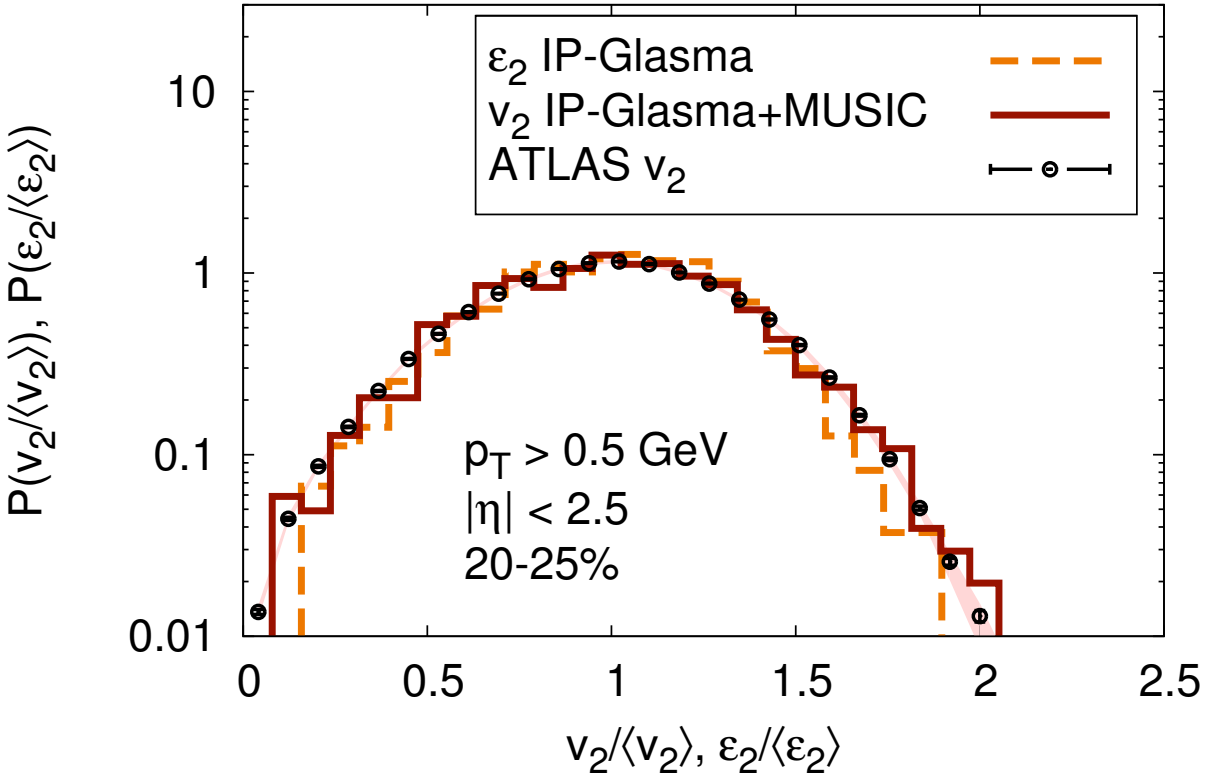


C. Gale, S. Jeon, B.Schenke, P.Tribedy, R.Venugopalan, arXiv:1210.5144 (2012)

# Event-by-event distributions of $v_n$

So now we can compare event-by-event distributions of $v_n$.

https://atlas.web.cern.ch/Atlas/GROUPS/PHYSICS/CONFNOTES/ATLAS-CONF-2012-114/

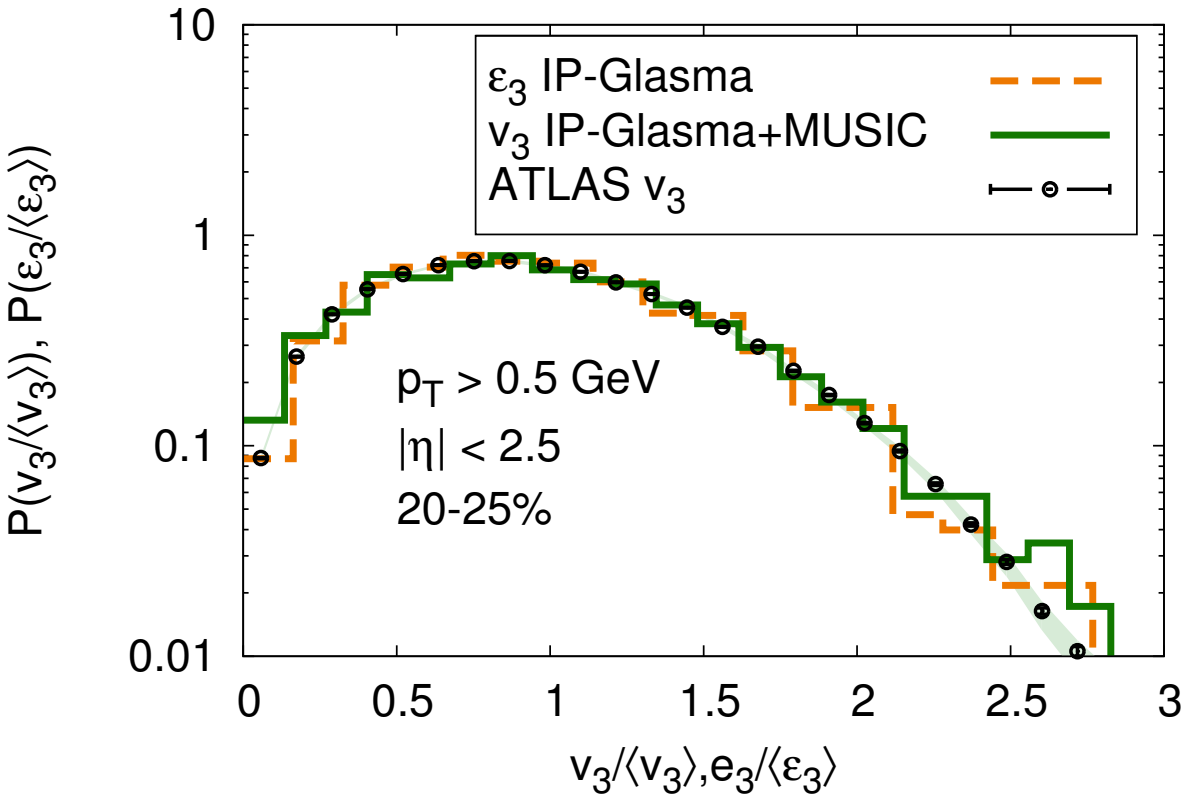


C. Gale, S. Jeon, B.Schenke, P.Tribedy, R.Venugopalan, arXiv:1210.5144 (2012)

# Event-by-event distributions of $v_n$

So now we can compare event-by-event distributions of $v_n$.

https://atlas.web.cern.ch/Atlas/GROUPS/PHYSICS/CONFNOTES/ATLAS-CONF-2012-114/

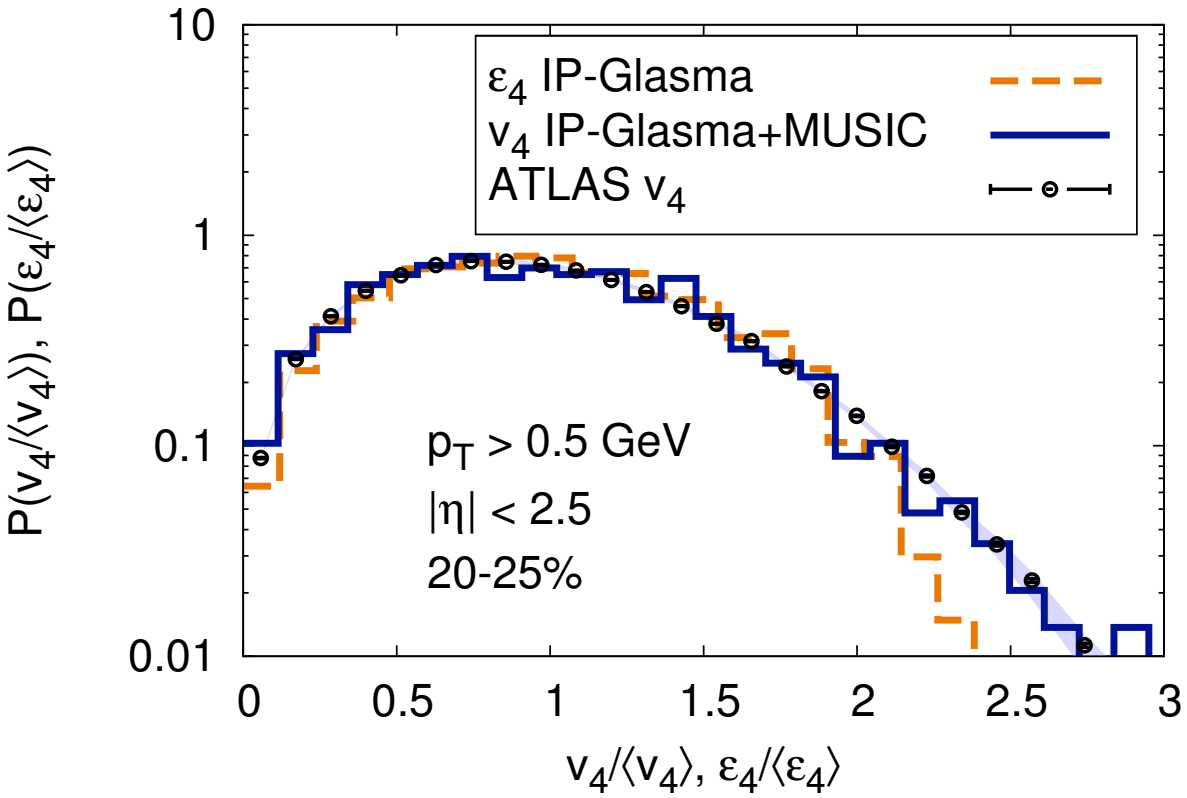


C. Gale, S. Jeon, B.Schenke, P.Tribedy, R.Venugopalan, arXiv:1210.5144 (2012)

# Event-by-event distributions of $v_n$ - other models

Showing eccentricity distributions (yellow on the right)

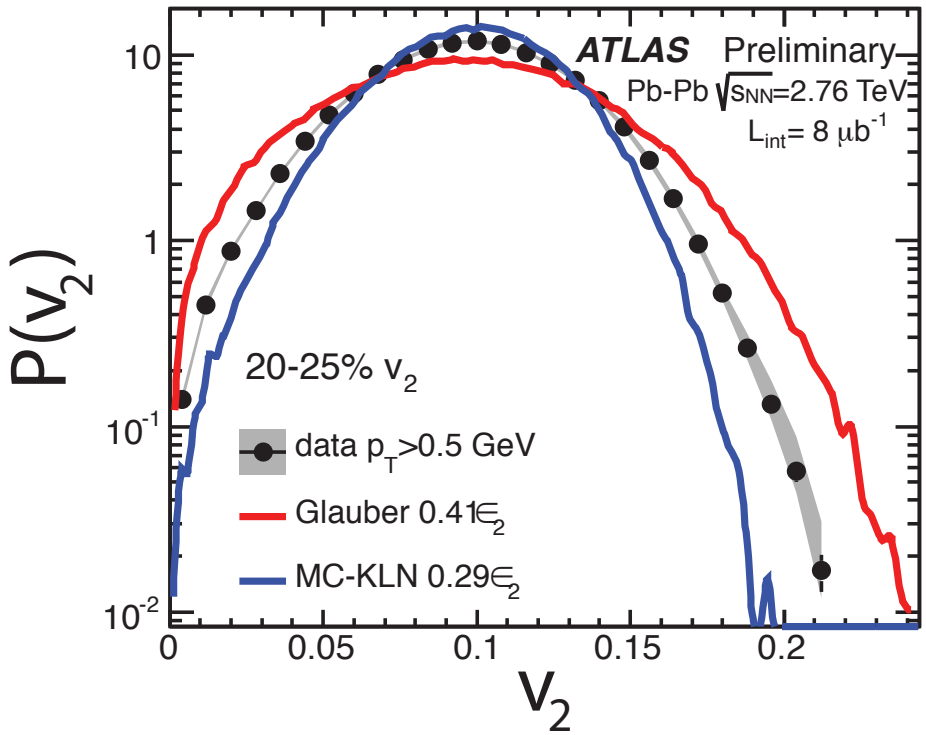


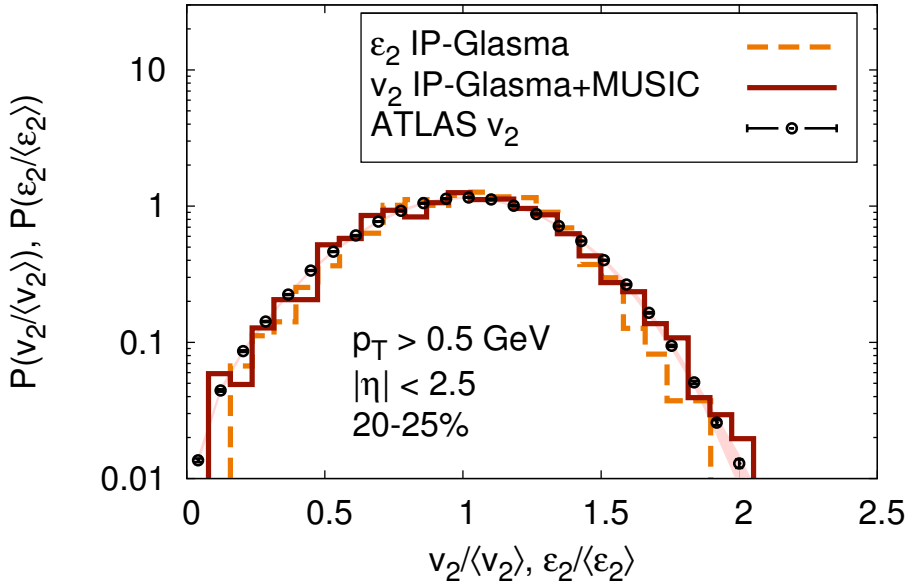


Event-by-event distributions can distinguish between different initial state models

Experimental data: `https://atlas.web.cern.ch/Atlas/GROUPS/PHYSICS/CONFNOTES/ATLAS-CONF-2012-114/`

# Photon elliptic flow at LHC

Kozlov, Paquet, Schenke, Jeon, Gale, in preparation

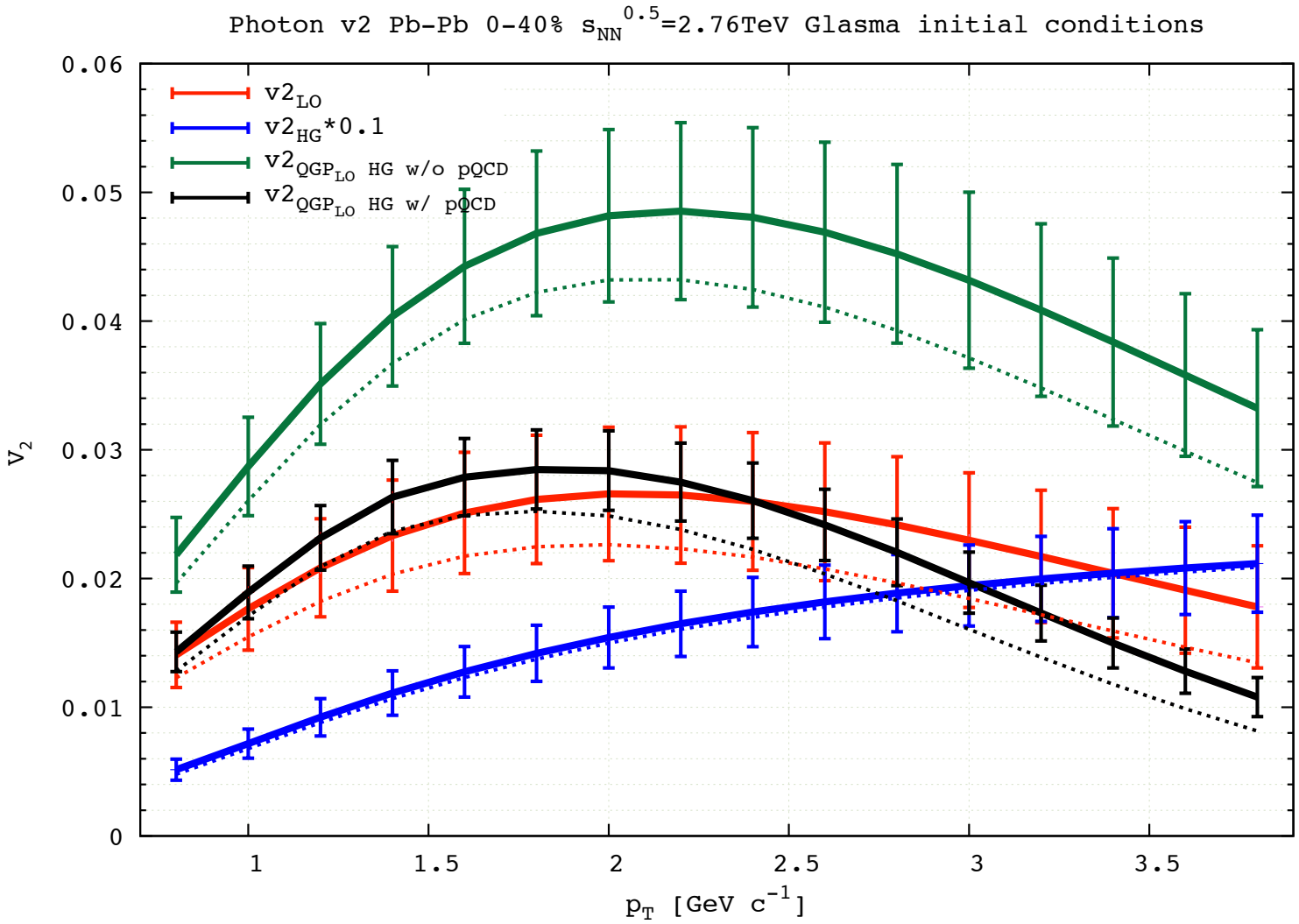


Effect of initial flow (solid vs. dashed) not large enough to explain data

# Photon triangular flow at LHC

Kozlov, Paquet, Schenke, Jeon, Gale, in preparation

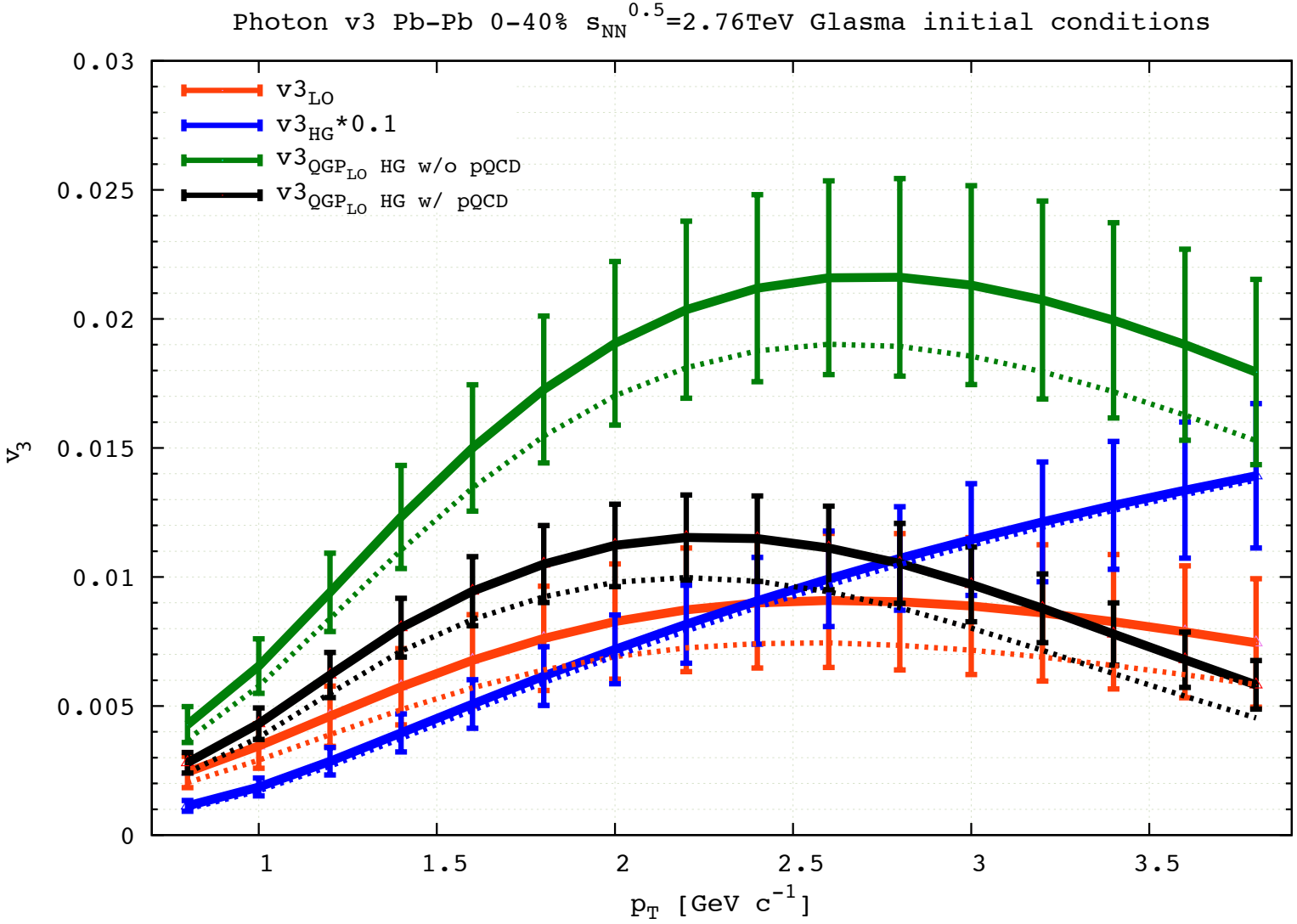

# Summary and conclusions

- Knowledge of initial state and hydrodynamic evolution important for thermal radiation
- Different initial state models exist
  Yield rather different initial energy density distributions
- IP-Glasma model
  - includes geometric and color charge fluctuations
  - produces negative binomial fluctuations
  - has different eccentricities than previous CGC based models
  - provides initial flow profile from the non-equilibrium stage
  - describes flow coefficients up to at least $v_5$
  - describes $v_n$ distributions where others fail
  - does not (yet) include instabilities and (possible) isotropization
- Outlook: study different collision energies, learn about $(\eta/s)(T)$, more on em-probes, study instabilities/isotropization, combine IP-Glasma and anisotropic hydro

# BACKUP

# KLN, fKLN, MC-KLN, ...

- original KLN:
  - uses $k_T$-factorization
  - $(Q_s^A)^2(\mathbf{x}_\perp) \propto N_{\mathrm{part,A}}(\mathbf{x}_\perp)$.
  - Saturation scales are not universal: $N_{\mathrm{part,A}}(\mathbf{x}_\perp)$ depends on nucleus B.
  - The energy density ($\epsilon \propto Q_{s,\mathrm{larger}} Q^2_{s,\mathrm{smaller}}$) is suppressed in the edge region along the impact parameter direction $\rightarrow$ larger eccentricity.
- fKLN:
  - uses $k_T$-factorization
  - Different definition of unintegrated gluon distribution (correct limit: where there is one nulceon at the edge the uGDF is that of one nucleon - not so in KLN)
  - Universal saturation scales in nucleus A and B. (Important at the edges of the nuclei)
- MC-KLN: Monte-Carlo implementation of fKLN with fluctuating positions of the nucleons
- IP-Glasma (CYM):
  - Does not use $k_T$-factorization (because it is strictly not valid in A+A collisions - at least one source has to be dilute)
  - $Q_s(\mathbf{x}_\perp)$ universal and constrained by HERA data.
  - No utilization of the nucleon-nucleon cross section.
  - Takes into account non-linearities.
  - Includes fluctuations of color charges within a nucleon.

# Comparison with other models: “MC-Glauber”

- Sample nucleon positions in nucleus $A$ and $B$, then overlap the two distributions.
- An interaction happens when the distance $d$ between a nucleon from nucleus A and one from nucleus B fulfills:

$$d \leq \sqrt{\sigma_{\text{inel}}^{NN}/\pi}$$

- Add Gaussian energy density with width $\sigma_0$ for every wounded nucleon, binary collision, or combination.

Result for $\sigma_0 = 0.4\,\text{fm}$

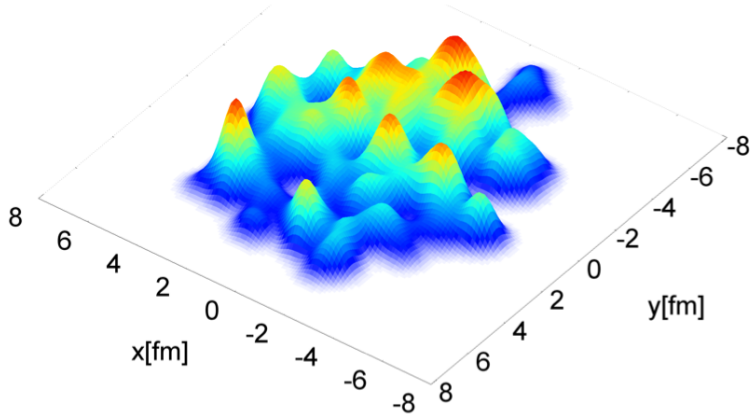

# Comparison with other models: “MC-KLN”

- Determine gluon production using $k_T$-factorization:

$$\frac{dN}{dr_\perp^2\, dy} \sim \int \frac{d^2 p_\perp}{p_\perp^2} \int d^2 k_\perp \alpha_s \phi_A(x_1, k_\perp^2) \phi_B(x_2, (p_\perp - k_\perp)^2)$$

- Energy density analogously.
- Kharzeev-Levin-Nardi (KLN) model for $\phi$:

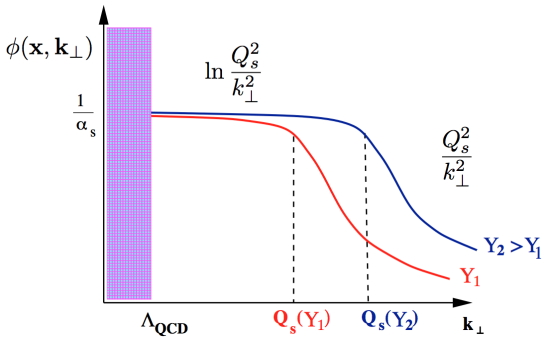


$$\phi_{A,B}(x, k_\perp^2, \mathbf{r}_\perp) \sim \frac{1}{\alpha_s(Q_s^2)} \frac{Q_s^2}{\max(Q_s^2, k_\perp^2)}$$

with $Q_{s,A}^2(x, \mathbf{r}_\perp) = 2\,\mathrm{GeV}^2 \frac{T_A(\mathbf{x}_\perp)}{1.53\,\mathrm{fm}^{-2}} \left(\frac{0.01}{x}\right)^\lambda, \lambda = 0.28$

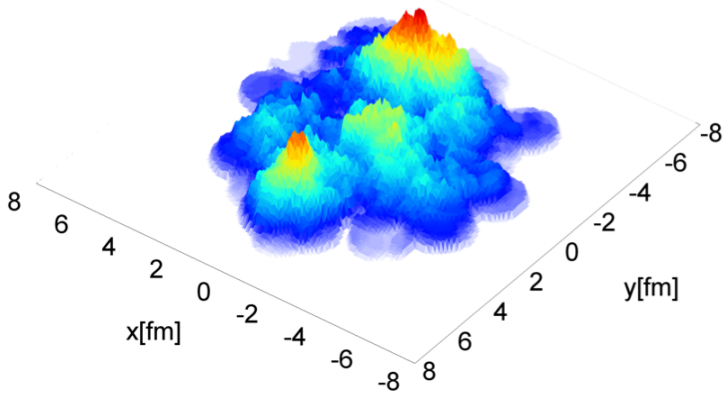

# $T^{\mu\nu}$ and flow velocities

Compute all components of $T^{\mu\nu}$
Determine energy density and $(u^x, u^y)$ at $\tau > 0\,\mathrm{fm}$ from $u_\mu T^{\mu\nu} = \varepsilon u^\nu$
as input for hydrodynamic simulations

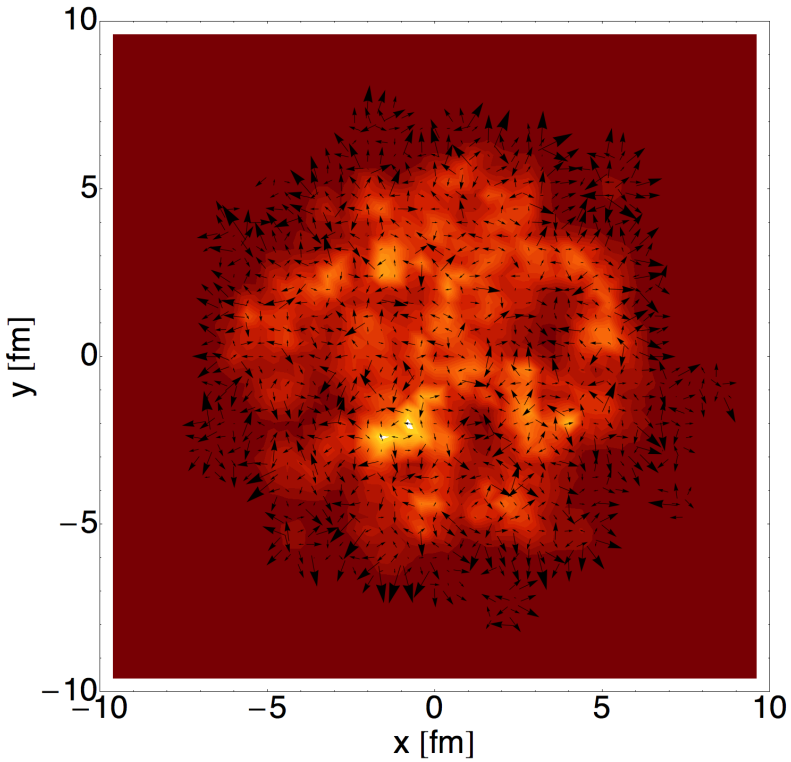


Energy density
and $(u_x, u_y)$
at $\tau = 0.4\,\mathrm{fm}/c$

No instabilities (need full 3+1D Yang-Mills for that):
system is far from equilibrium - cannot yet match $\Pi^{\mu\nu}$

# Effect of initial flow

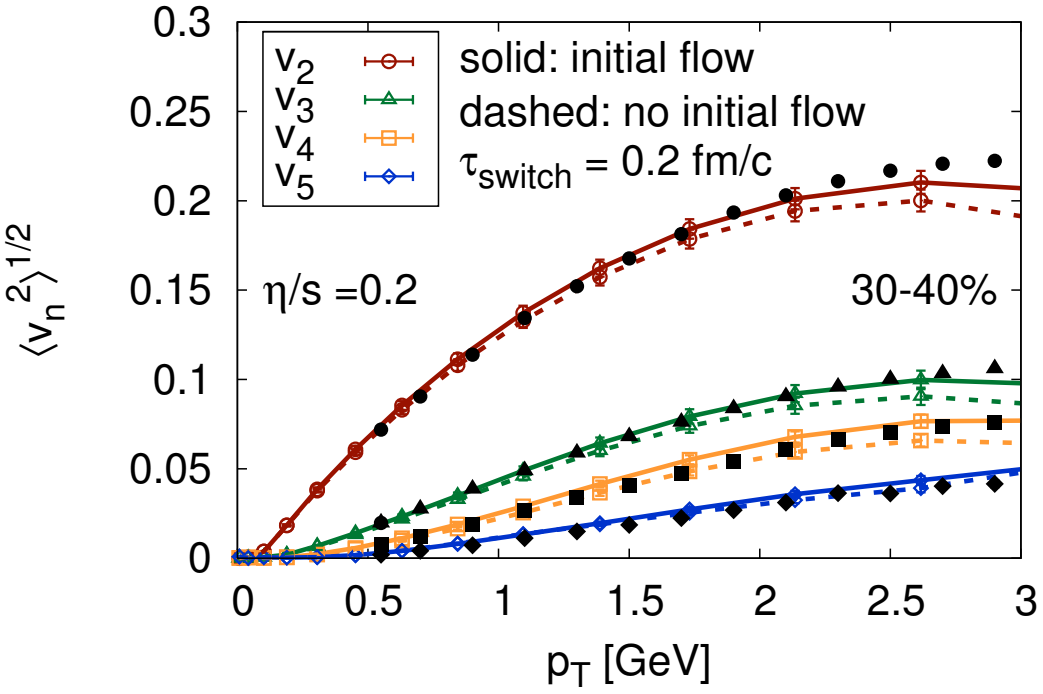


Weak effect of initial flow on hadron $v_n(p_T)$

Expect stronger effect for photon $v_n$:
Photons are mostly produced early at high temperatures

Effect of different switching time $0.4\,\mathrm{fm}/c$ is very weak

Experimental data:
ATLAS collaboration, Phys. Rev. C 86, 014907 (2012)

# Directed flow $v_1$

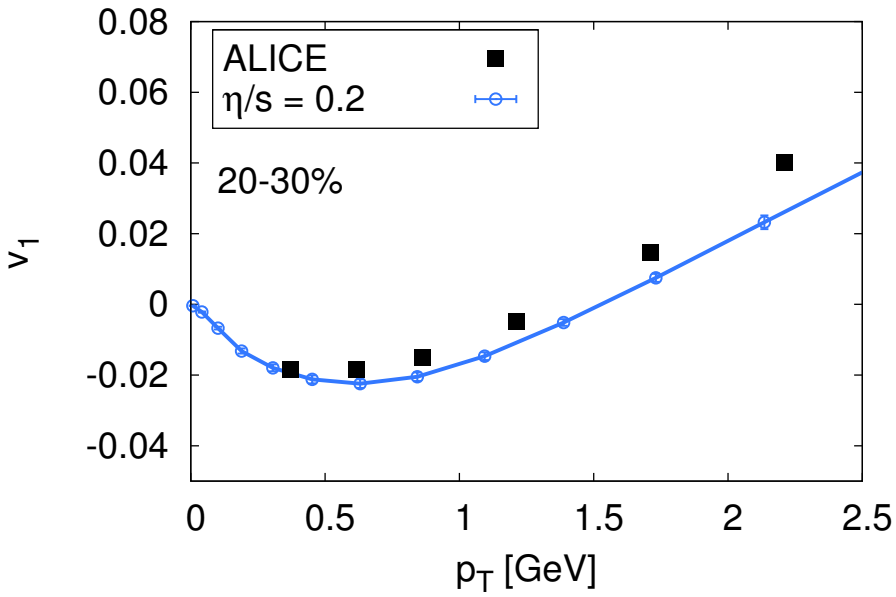


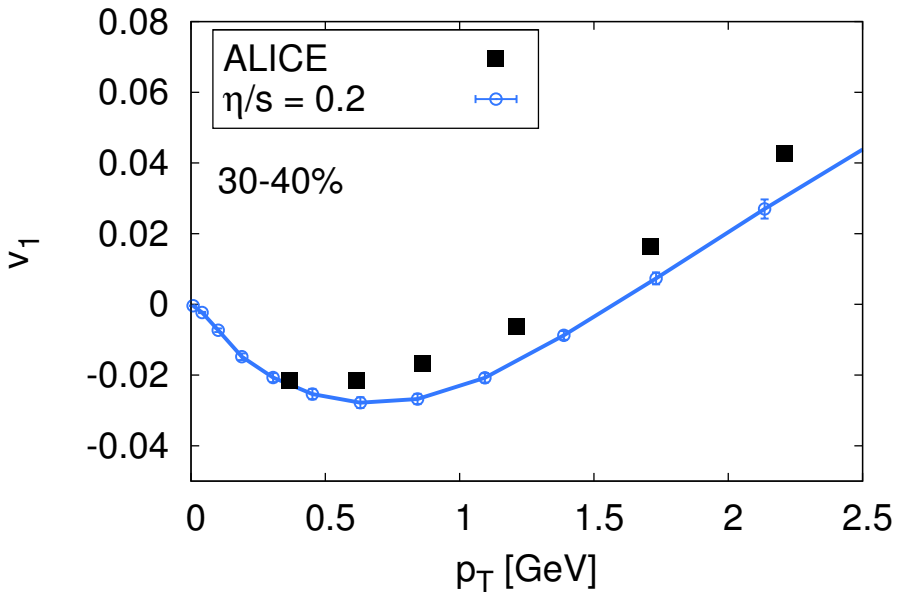


Experimental data:

extracted in Retinskaya et al., Phys.Rev.Lett. 108 (2012) 252302

from ALICE data in K. Aamodt et al., Phys. Lett. B 708, 249 (2012)

# Gauge fields before the collision

Color currents:

$$J_1^\nu = \delta^{\mu+}\rho_1(x^-, \mathbf{x}_\perp)$$
$$[D_\mu, F^{\mu\nu}] = J_1^\nu$$

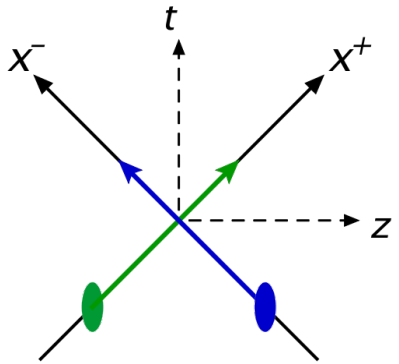


$$J_2^\nu = \delta^{\mu-}\rho_2(x^+, \mathbf{x}_\perp)$$
$$[D_\mu, F^{\mu\nu}] = J_2^\nu$$

Solution in covariant gauge:

$$A^+_{\mathrm{cov}(1,2)}(x^-, \mathbf{x}_\perp) = -\frac{g\rho_{(1,2)}(x^-, \mathbf{x}_\perp)}{\nabla_\perp^2 + m^2}$$

with infrared cutoff $m$ of order $\Lambda_{\mathrm{QCD}}$.

Solution in light cone gauge:

$$A^+_{(1,2)}(\mathbf{x}_\perp) = A^-_{(1,2)}(\mathbf{x}_\perp) = 0$$
$$A^i_{(1,2)}(\mathbf{x}_\perp) = \frac{i}{g} V_{(1,2)}(\mathbf{x}_\perp)\partial_i V^\dagger_{(1,2)}(\mathbf{x}_\perp)$$

$V$ is the path-ordered exponetial of $A^+_{\mathrm{cov}(1,2)}$

# Gauge fields before the collision

The correlator of the Wilson lines

$$C_{(1,2)}(\mathbf{x}_\perp) = \frac{1}{N_c}\mathrm{Re}[\mathrm{tr}(V(1,2)^\dagger(0,0)V(1,2)(x,y))]$$

with

$$V_{(1,2)}(\mathbf{x}_\perp) = P\exp\left(-ig\int dx^- \frac{\rho_{(1,2)}(x^-,\mathbf{x}_\perp)}{\nabla_\perp^2 + m^2}\right)$$

shows the degree of correlations and fluctuations in the gluon fields.

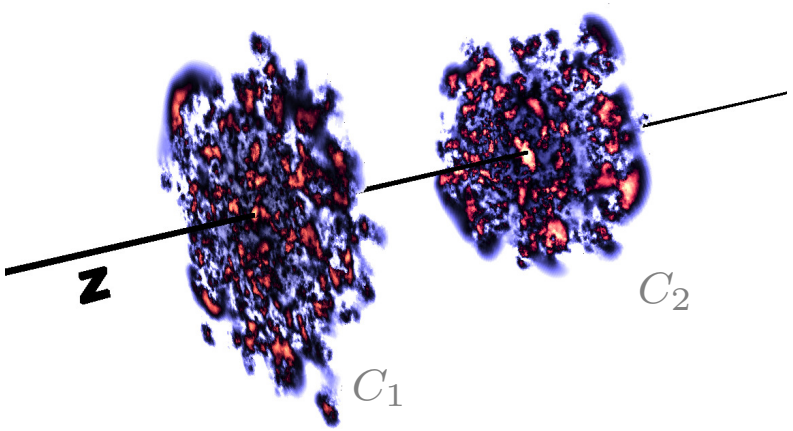


The length scale of fluctuations is $1/Q_s$. Not the nucleon size.

# Gauge fields after the collision (Glasma)

Initial condition on the lightcone: require that fields match smoothly on the lightcone.

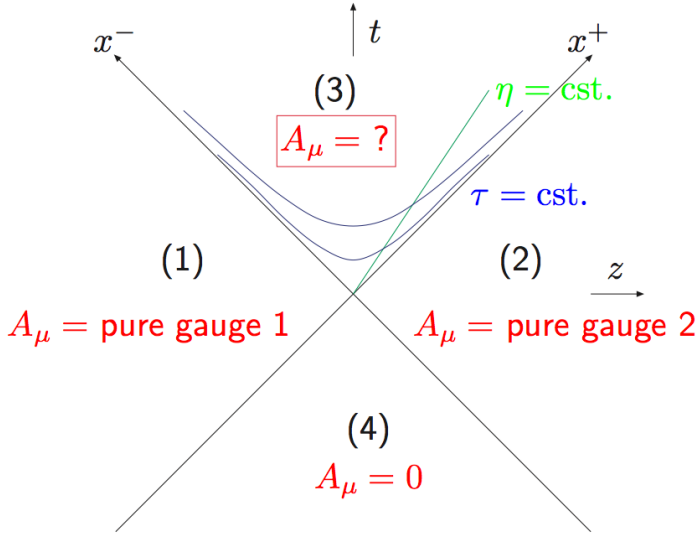


figure from Lappi, arXiv:1003.1852

Solution:

$$A^i_{(3)}|_{\tau=0} = A^i_{(1)} + A^i_{(2)}$$

$$A^\eta_{(3)}|_{\tau=0} = \frac{ig}{2}[A^i_{(1)}, A^i_{(2)}]$$

On the lattice the Wilson lines in the future lightcone are obtained from the condition:

$$\mathrm{tr}\left\{t^a\left[\left(U^i_{(1)} + U^i_{(2)}\right)(1 + U^{i\dagger}_{(3)}) - (1 + U^i_{(3)})\left(U^{i\dagger}_{(1)} + U^{i\dagger}_{(2)}\right)\right]\right\} = 0$$

where $t^a$ are the generators of $SU(N_c)$ in the fundamental representation. Solve iteratively.

Krasnitz, Venugopalan, Nucl.Phys. B557 (1999) 237

$$U^i_{(1,2),j} = V_{(1,2),j} V^\dagger_{(1,2),j+\hat{e}_i}$$ (gauge transform of $\mathbf{1}$: pure gauge)

# Negative binomial fluctuations

Fluctuations in the total energy per unit rapidity produce negative binomial distribution (NBD).

B.Schenke, P.Tribedy, R.Venugopalan, arXiv:1202.6646, Phys.Rev.Lett. 108, 252301 (2012)

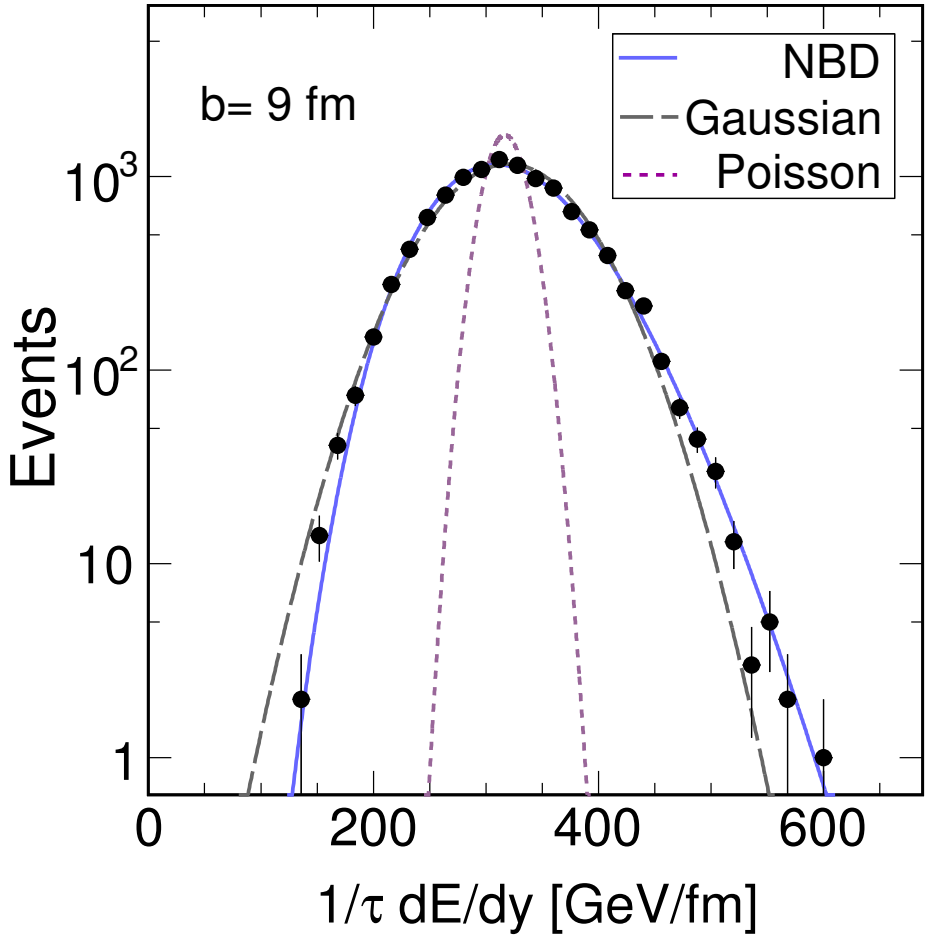


$$P(n) = \frac{\Gamma(k+n)}{\Gamma(k)\Gamma(n+1)} \frac{\bar{n}^n k^k}{(\bar{n}+k)^{n+k}}$$

Good, since multiplicity in pp collisions can be described well with NBD.

In AA, convolution of NBDs at all impact parameters describes data well too.

P. Tribedy and R. Venugopalan
Nucl.Phys. A850 (2011) 136-156

MC-KLN does not do that - these fluctuations need to be put in by hand.

see Dumitru and Nara arXiv:1201.6382

# Negative binomial fluctuations

Extract $k$ and $\bar{n}$ using a fit with

$$P(n) = \frac{\Gamma(k+n)}{\Gamma(k)\Gamma(n+1)} \frac{\bar{n}^n k^k}{(\bar{n}+k)^{n+k}}$$

at fixed impact parameters.

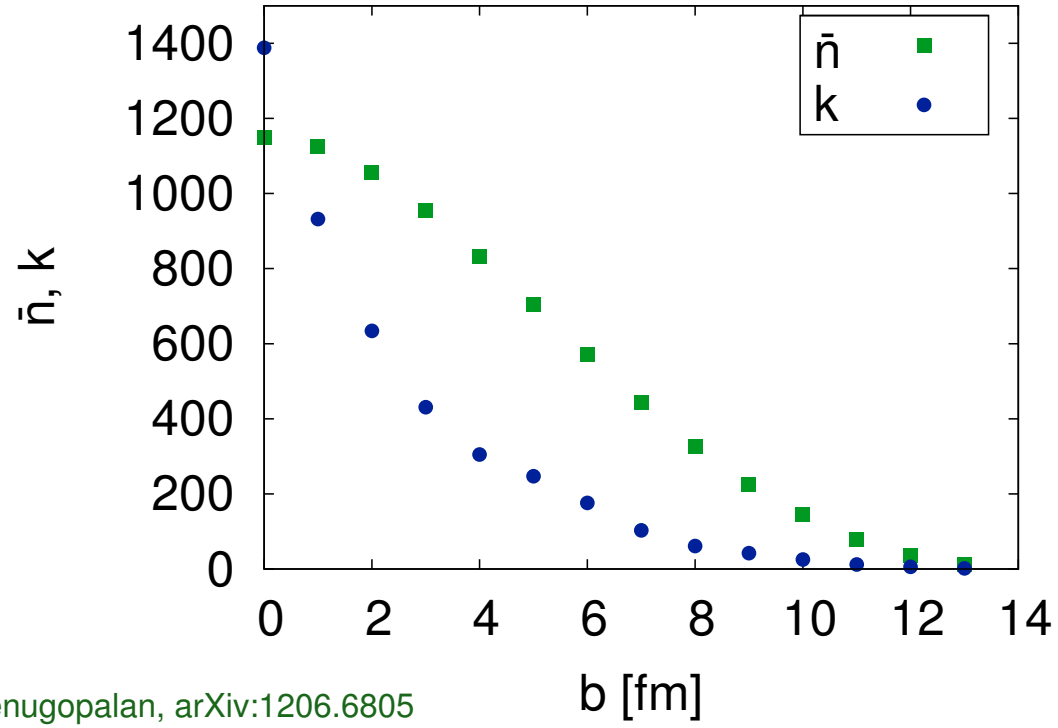


B.Schenke, P.Tribedy, R.Venugopalan, arXiv:1206.6805

Ratio of $k/\bar{n}$ is $> 1$ for small $b$ and becomes small $\sim 0.14$ for large $b$.
That is close to the value extracted for $p+p$ collisions: Dumitru and Nara arXiv:1201.6382

# NBDs and Glasma flux tubes

Glasma flux tube picture:

$$k = \zeta \frac{N_c^2 - 1}{2\pi} Q_s^2 S_\perp$$

Gelis, Lappi, Mclerran, arXiv:0905.3234.

Width of NBD is inversely proportional to the number of flux tubes $Q_s^2 S_\perp$.
$S_\perp =$ interaction area.

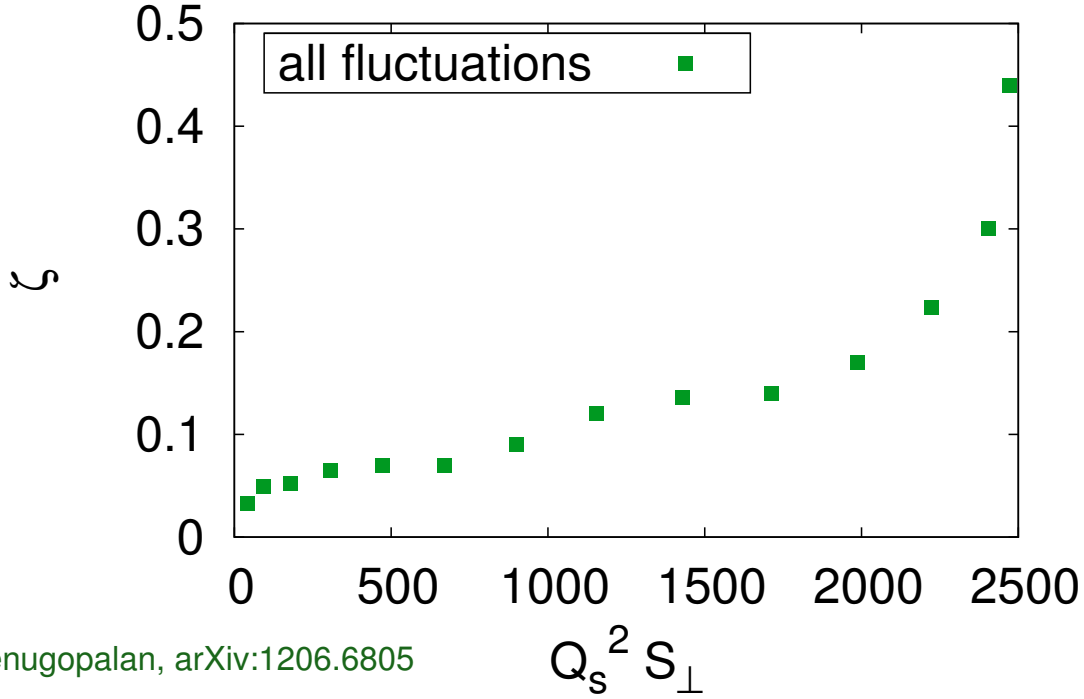


B.Schenke, P.Tribedy, R.Venugopalan, arXiv:1206.6805

$\zeta$ should be close to constant in the flux tube picture.

# NBDs and Glasma flux tubes

$\zeta$ is not constant because geometric fluctuations are very important. Were not considered in the derivation of

$$k = \zeta \frac{N_c^2 - 1}{2\pi} Q_s^2 S_\perp$$

Eliminate by using smooth nucleon distributions:

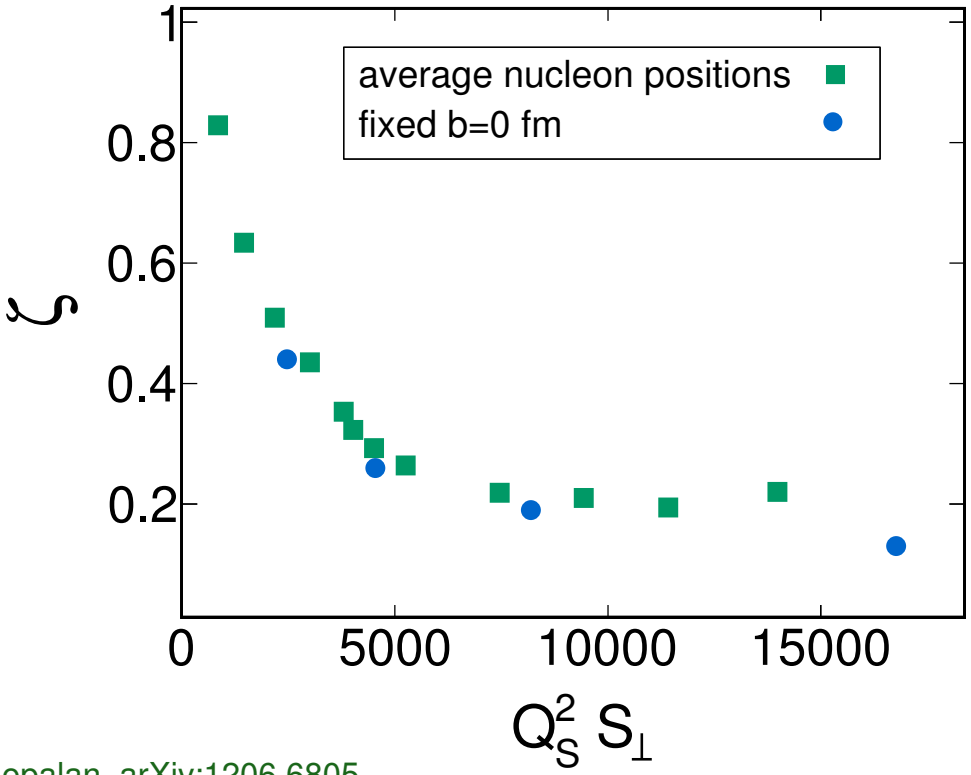


B.Schenke, P.Tribedy, R.Venugopalan, arXiv:1206.6805

# More centrality classes: IP-Glasma + MUSIC

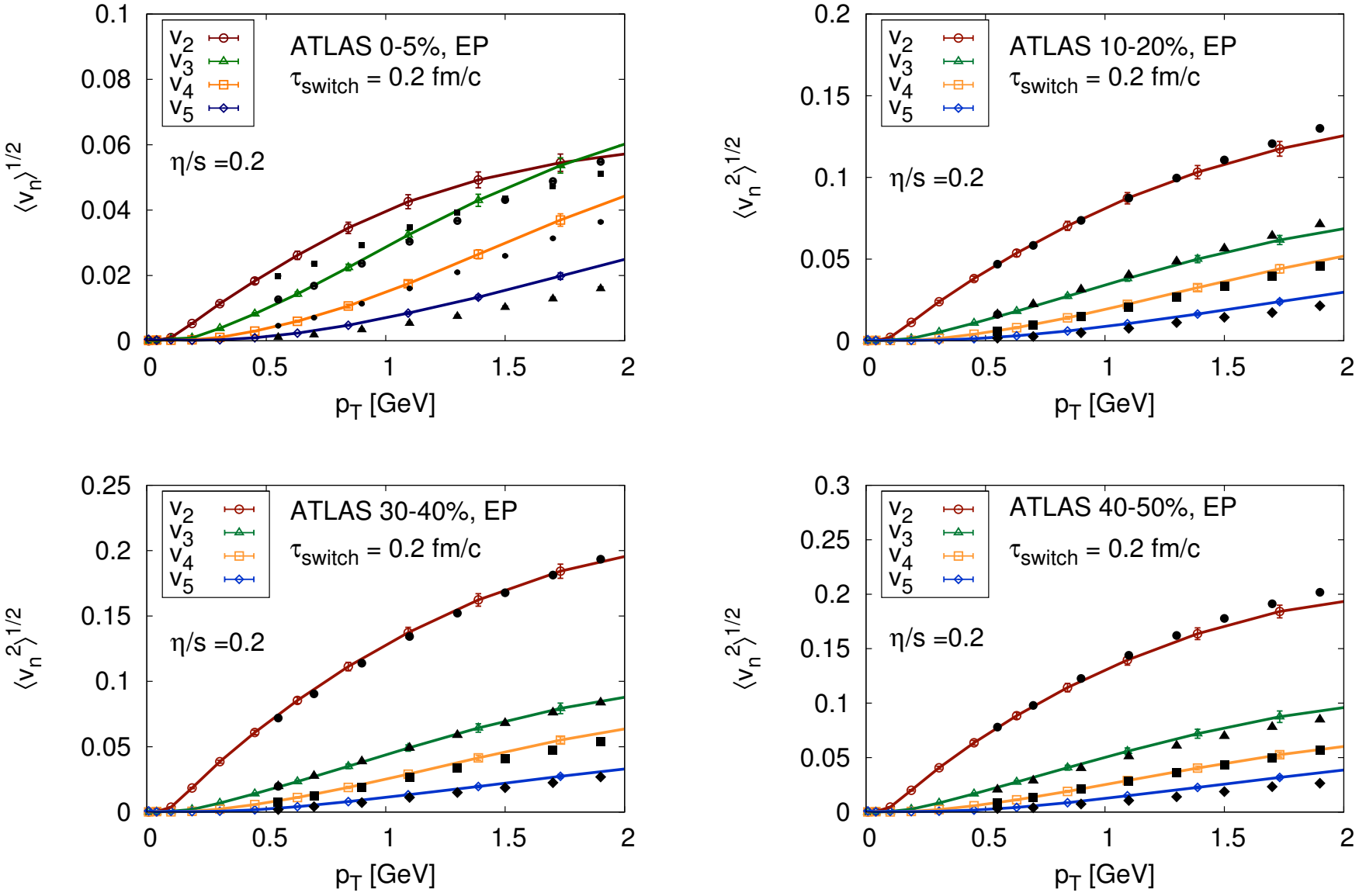

# Smaller average $\eta/s$

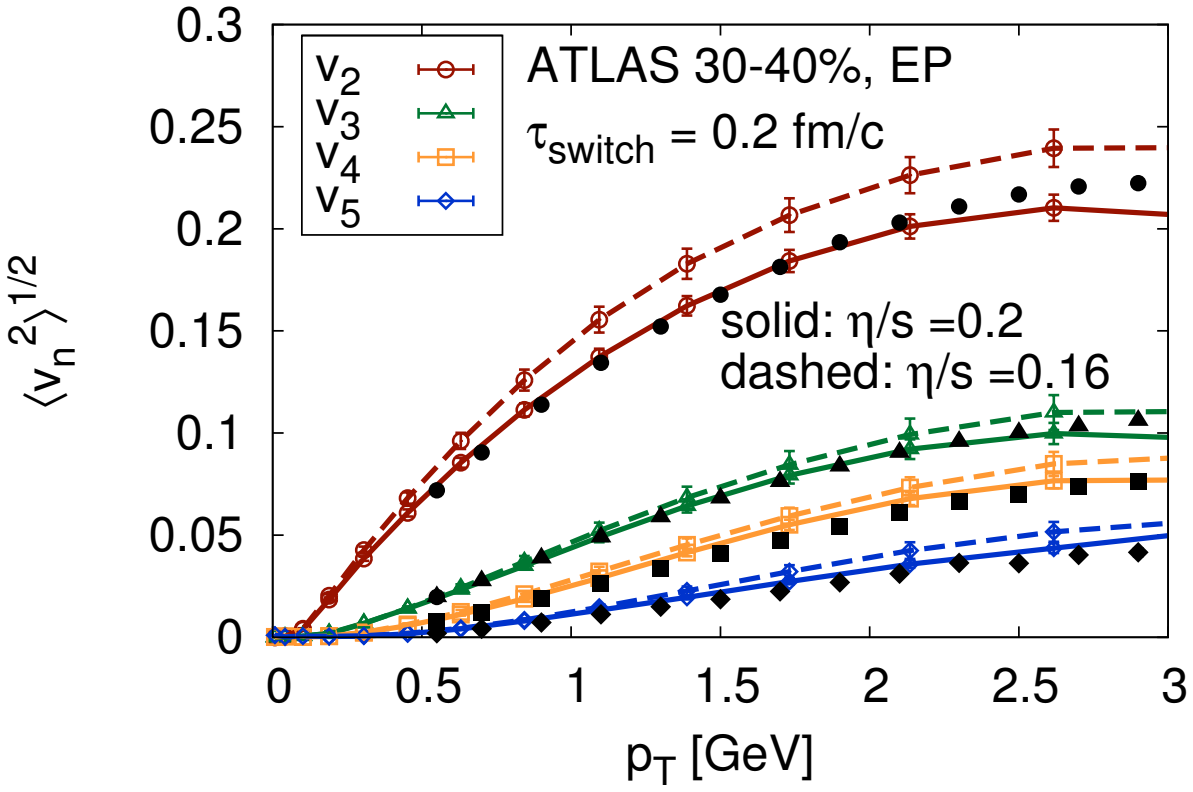


Using $\eta/s = 0.16$ overestimates all $v_n$

Experimental data:
ATLAS collaboration, Phys. Rev. C 86, 014907 (2012)

# *Dielectron Spectrum in $d + Au$ Collsions at $\sqrt{s_{NN}}$=200 GeV*

Deepali Sharma

PHENIX Collaboration

*Stony Brook University*

6th December, 2012

# Outline

1. *Motivation*
2. *PHENIX experimental set-up*
3. $d + Au$ *Dielectron Spectrum*
   - Analysis Details
   - Comparison to the Cocktail
     - $p_T$ Dependence
     - Centrality Dependence
   - Comparison to other collision systems
     - Comparison to $p + p$
     - Comparison to Heavy Ions
4. *Heavy Flavor Extraction using the* $d + Au$ *data*

## *Dilepton mass spectrum*

**Diverse physics signal**

- Sources "long" after collision:
  - $\pi^0$, $\eta$, $\omega$ Dalitz decays
  - $\rho$, $\omega$, $\phi$, $J/\psi$, $\psi'$ decays
- Early in collision (hard probes):
  - Heavy flavor production
  - Drell Yan, direct radiation
- Baseline from $p + p$
- Thermal (black body) radiation:
  - in dileptons and photons
  - temperature evolution
- Medium modifications of mesons
  - $\pi^+\pi^- \rightarrow \rho \rightarrow e^+e^-$
  - Chiral symmetry restoration
- Medium effects on hard probes
  - Heavy flavor energy loss

**Modifications to the dilepton spectrum due to the QCD phase transition**

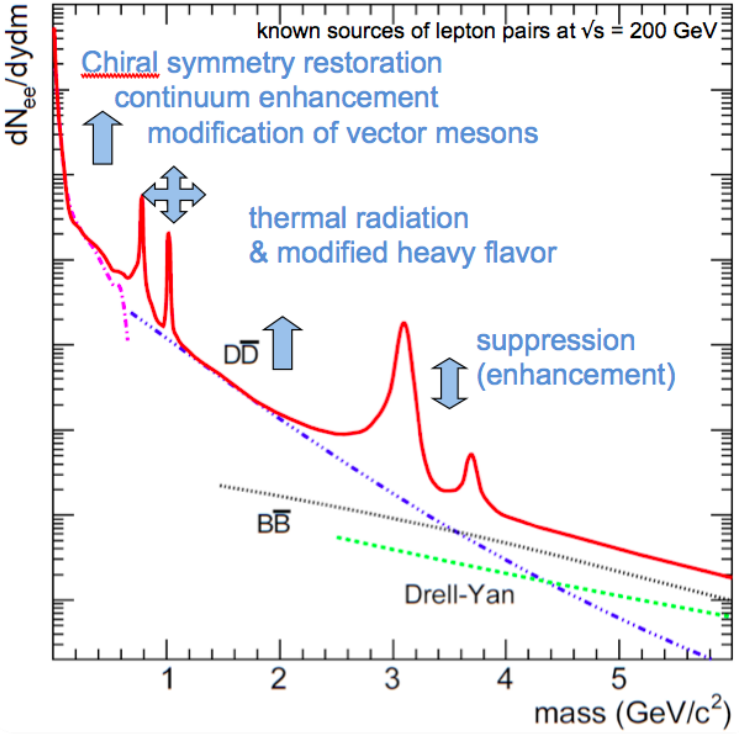

# The PHENIX Detector

# PHENIX Experimental set-up

**PHENIX Central arms Acceptance: -0.35$<\eta<$0.35, 2$\times$90$^\circ$ in $\varphi$**

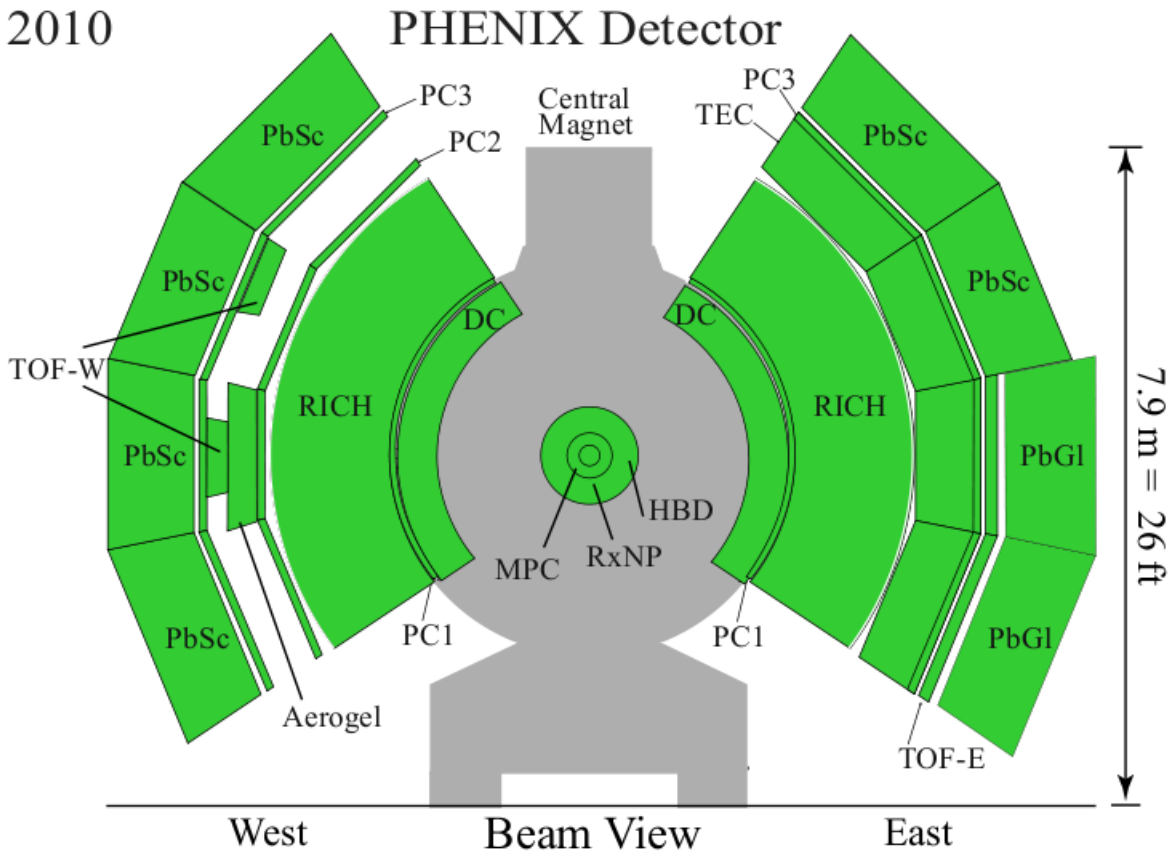


Measure rare probes in different collision systems: **p+p, d+Au, Cu+Cu, Au+Au**

- Vertex: **BBC**
- Tracking: **DC/PC1**
- $p_e > 0.2$ GeV/c;

Electron identification based on:

- **RICH** (Ring Imaging Čerenkov detector) ($e/\pi$ rejection >1000)
- **EMCal** (Electromagnetic Calorimeter) (E-p matching, $e/\pi$ rejection $\sim 10$)

# *Dielectrons in $p + p$ collisions*

*fundamental baseline for heavy-ion*

- Inclusive mass spectrum of $e^+e^-$ measured from $0 < m < 8$ GeV/$c^2$.
- Very well understood in terms of
  - hadron cocktail at low masses.
  - heavy Flavor + DY at high masses
- **Charm: integration after cocktail subtraction;** $\sigma_{c\bar{c}} = 544 \pm 39(stat) \pm 142(sys) \pm 200(model)\mu b$ (*consistent with PHENIX single electron measurement*)
- **Simultaneous fit of charm and bottom;**
  - $\sigma_{c\bar{c}} = 518 \pm 47(stat) \pm 135(sys) \pm 190(model)\mu b$
  - $\sigma_{b\bar{b}} = 3.9 \pm 2.4(stat) \pm^{3}_{2}(sys)\mu b$

**PLB 670, 313 (2009)**

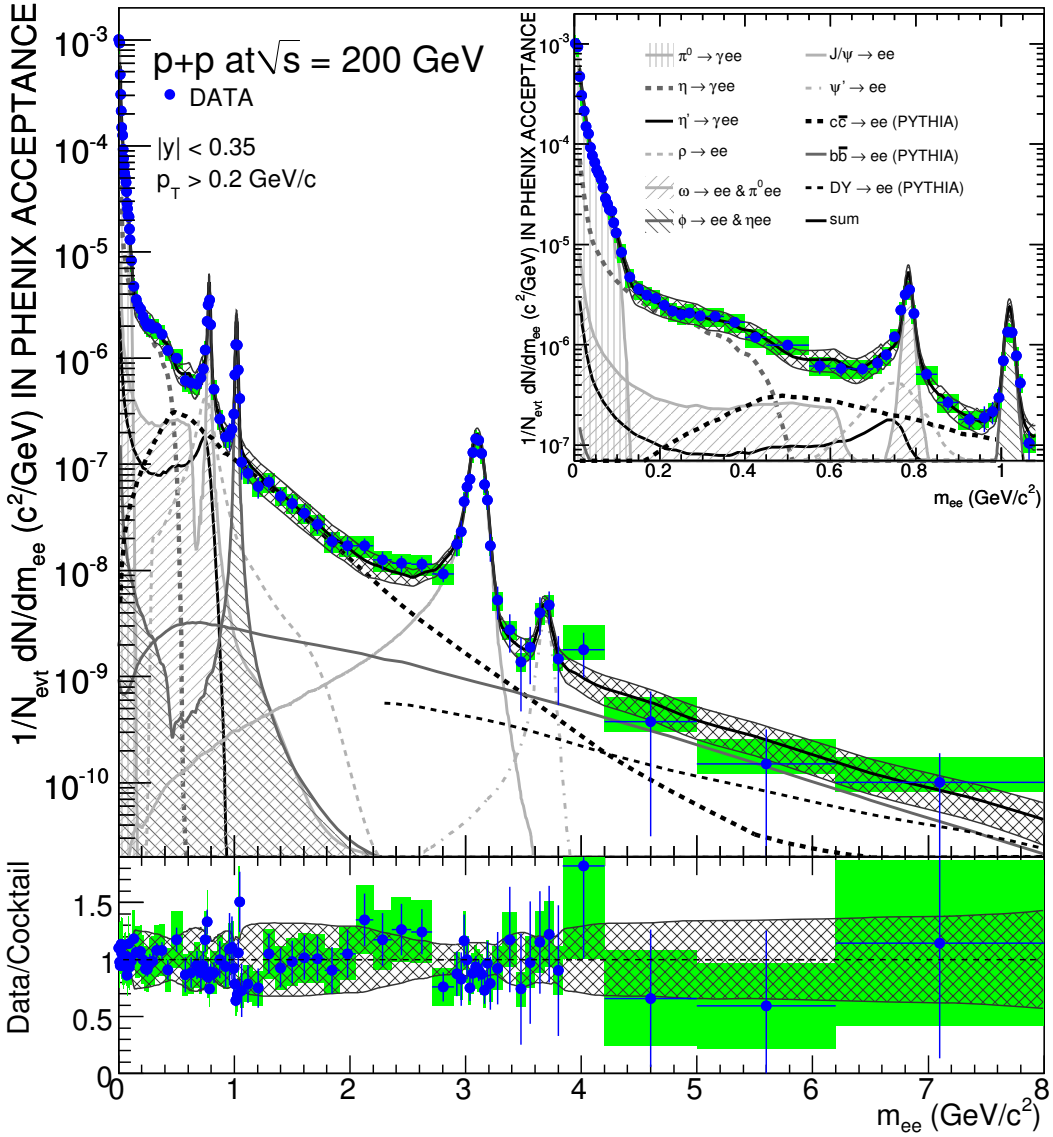

# *Heavy Ion Dielectrons*

*Au + Au and Cu + Cu*

## $Au + Au$ (PRC 79, 81 034911(2010))

$N_{part}$ = 109

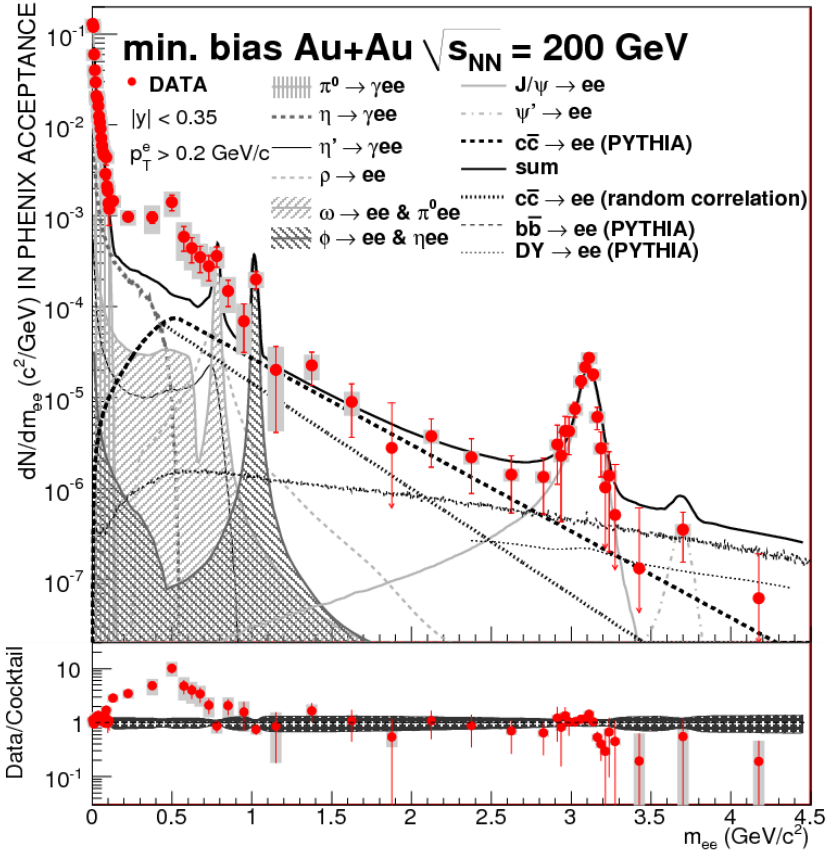


- Minimum Bias $Au + Au$ compared to Cocktail.
- Striking enhancement in LMR (150 - 750 MeV/$c^2$).
- No enhancement in the IMR !!

## $Cu + Cu$ (0-10%)

$N_{part}$ = 98

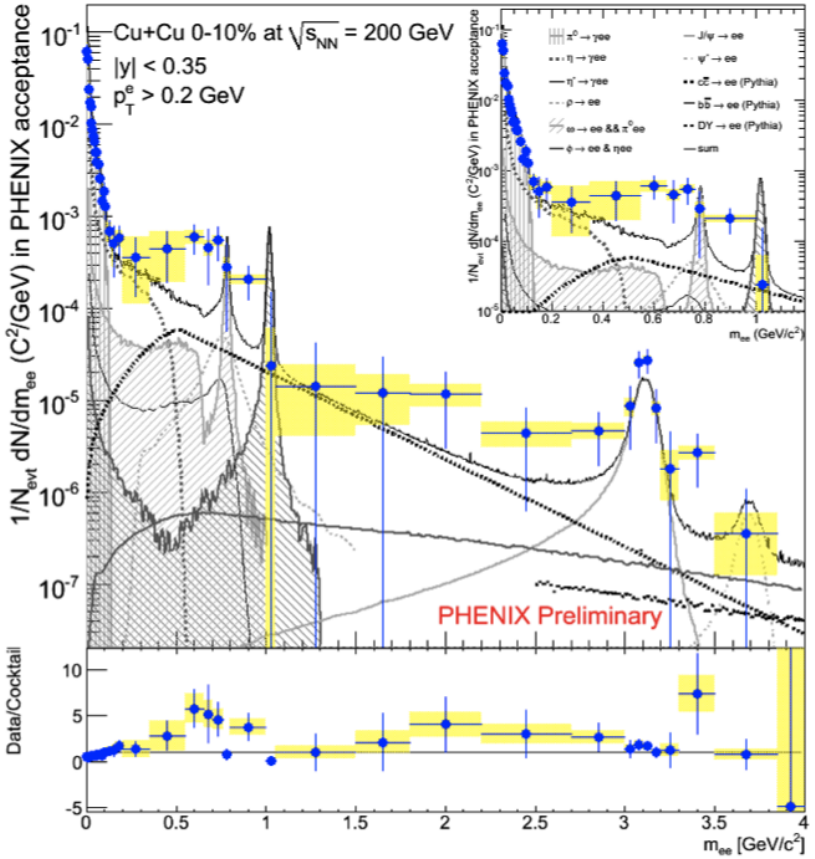


- Central $Cu + Cu$ compared to Cocktail.
- Some enhancement seen in LMR.
- Hints of enhancement in IMR ?

Stony Brook University

PHENIX

# $d + Au$ Dielectron Spectrum

# $d + Au$ Data Analysis Details

- Background Estimation
  - Like-sign technique is used for the signal extraction, after the like-sign pairs are corrected for the acceptance difference for $++$ and $--$ pairs. The relative accceptance correction $\alpha$ is derived from the mixed events and is defined as follows:

$$\alpha = \frac{BG_{+-}}{BG_{++} + BG_{--}}$$

- Signal to Background in $d + Au$

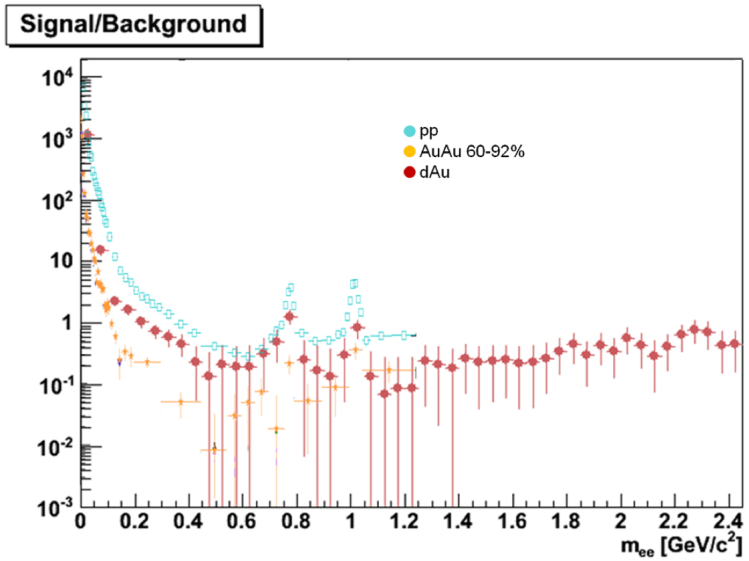


- Like-sign heavy quark correlations

## Origin of Like-sign correlated pairs

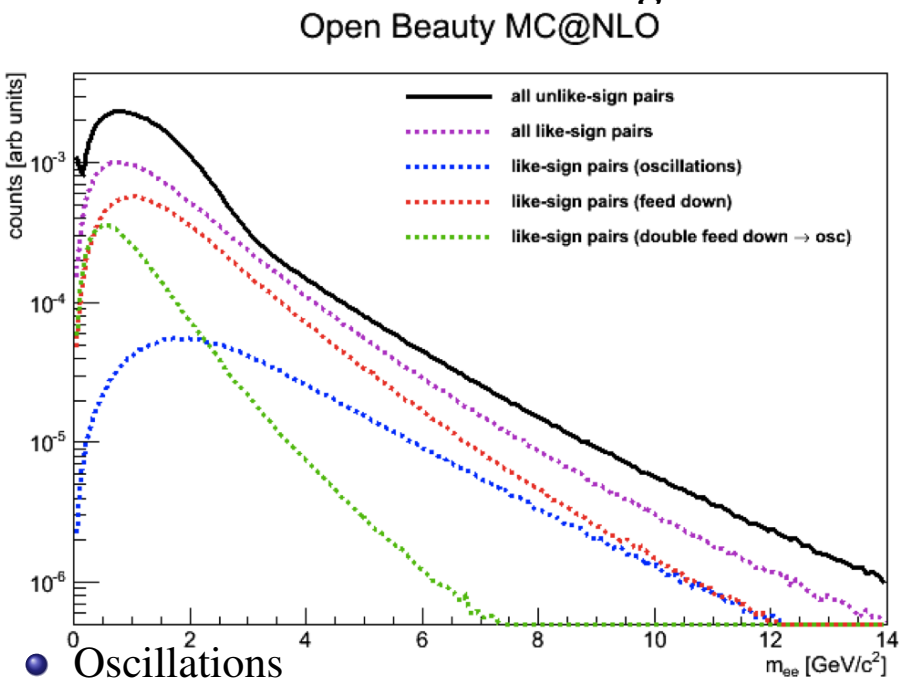


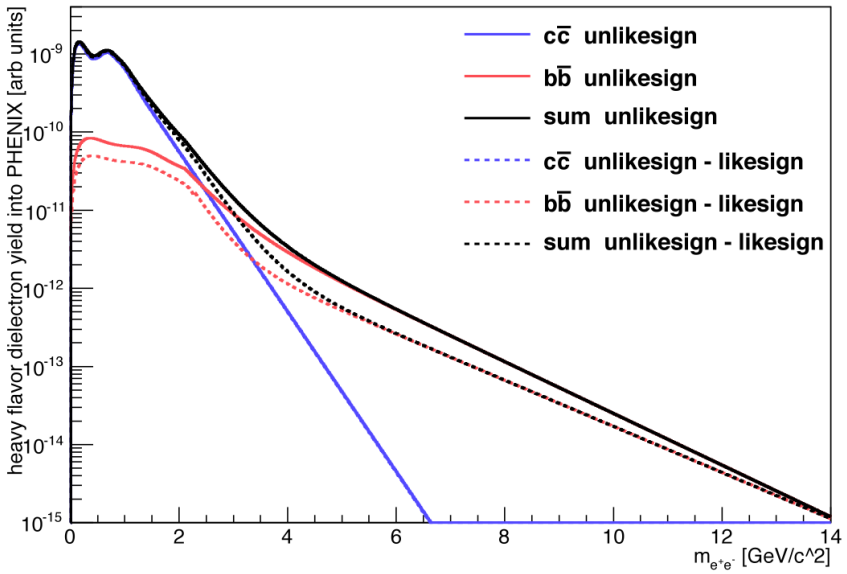


- Oscillations
  - $B^0\bar{B}^0$ mixing. This leads to $\sim 60\%$ unlike-sign pairs and $\sim 40\%$ like-sign pairs.
- Feed Down
  - BR for $B \to e \sim 10\%$, BR for $B \to D \sim 10\%$,
- Nearly half the bottom yield is like-sign!. However this is less extreme for charm ($<1\%$ within PHENIX acceptance).

- So if one uses like-sign subtraction in data, this should be accounted for in the simulations also.
- makes an appreciable difference in mass spectrum.

# *Minimum Bias $d + Au$ Dielectrons*

## *PYTHIA for heavy flavor*

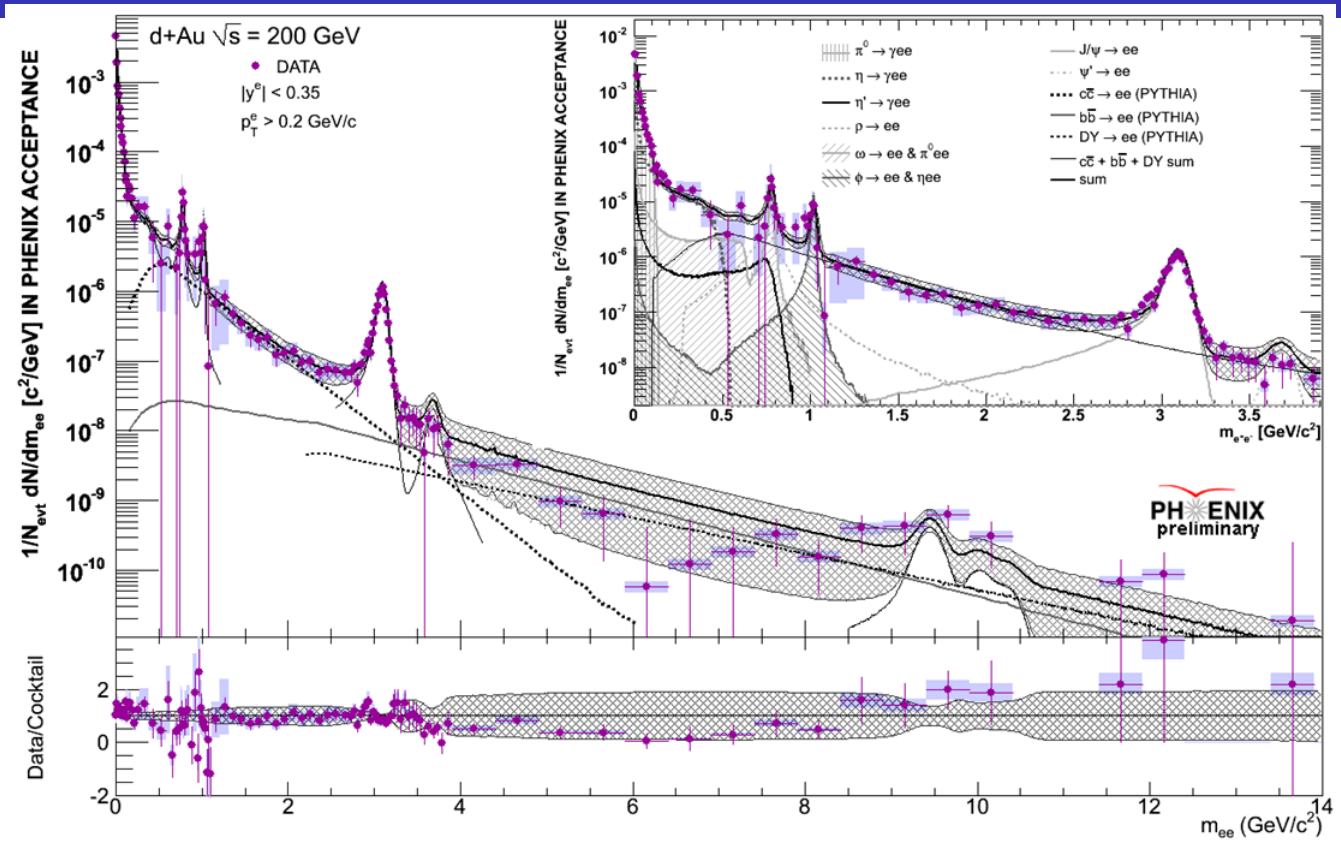


- Consistent with the expected cocktail of known sources
- Large mass range coverage $0 - 14\ GeV/c^2$.
- Open heavy flavor is $N_{coll}$ scaled PYTHIA
- $\sigma_{cc}$ and $\sigma_{bb}$ consistent with $p + p$
  **-like-sign heavy quark correlations not taken into account !**

# *Transverse Momentum Dependence of $d + Au$ Dielectron Spectrum*

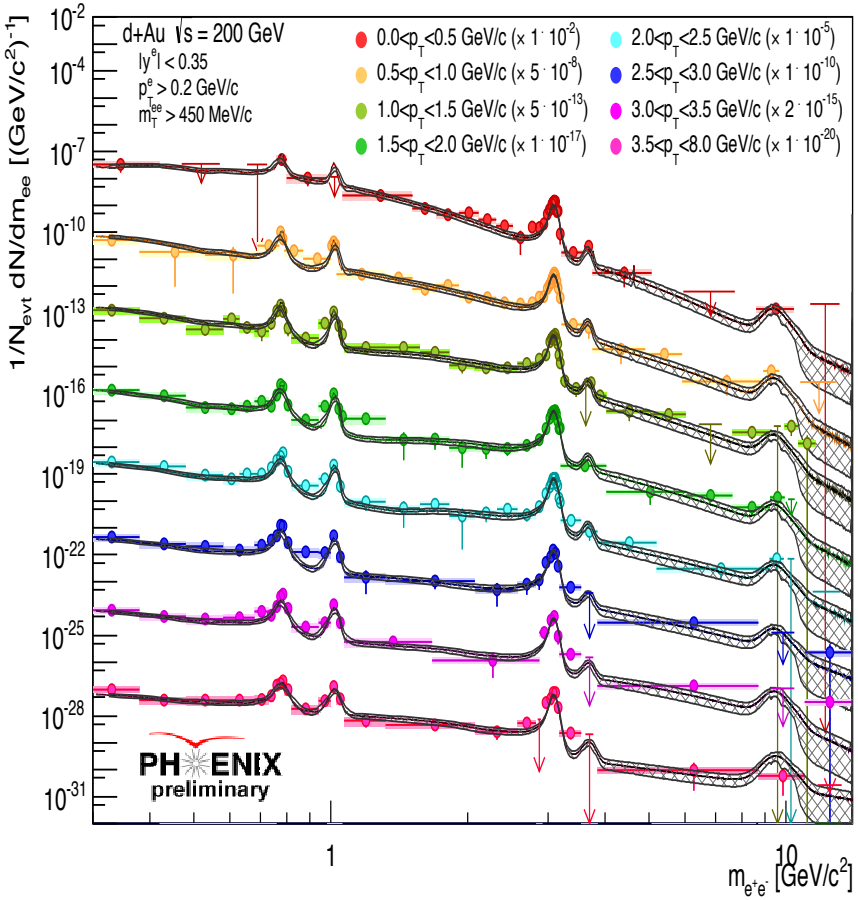


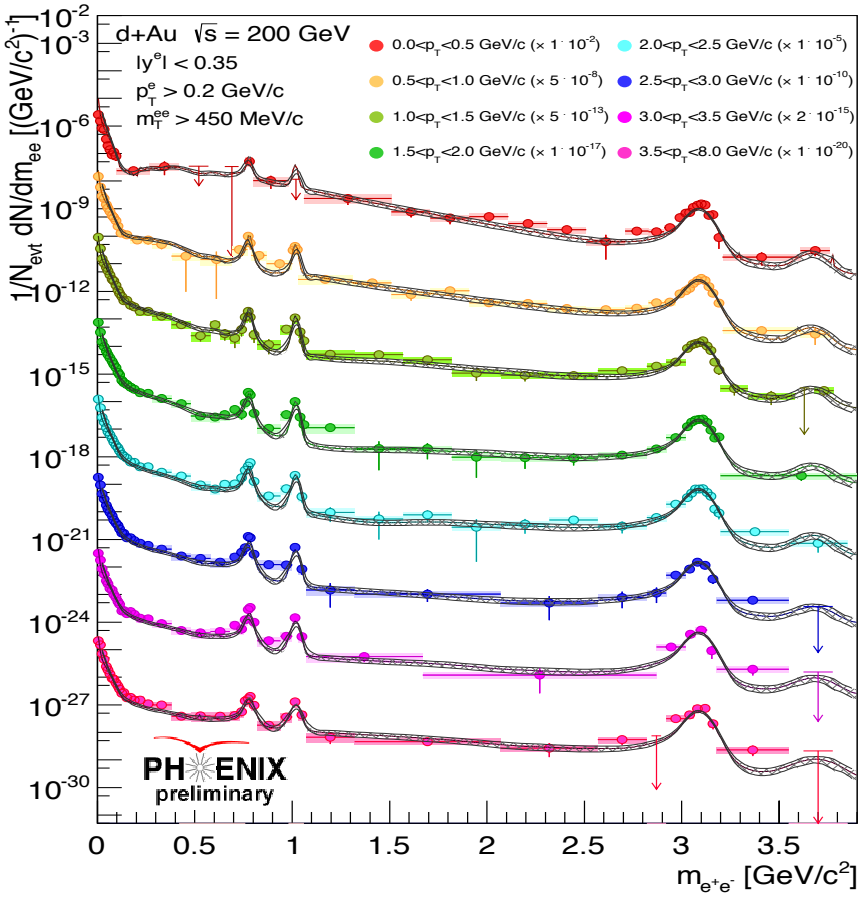


- Very good agreement with the cocktail over the entire $p_T$ range, demonstrates a good control over the cocktail.

# *Centrality Dependence of $d + Au$ Dielectron Spectrum*

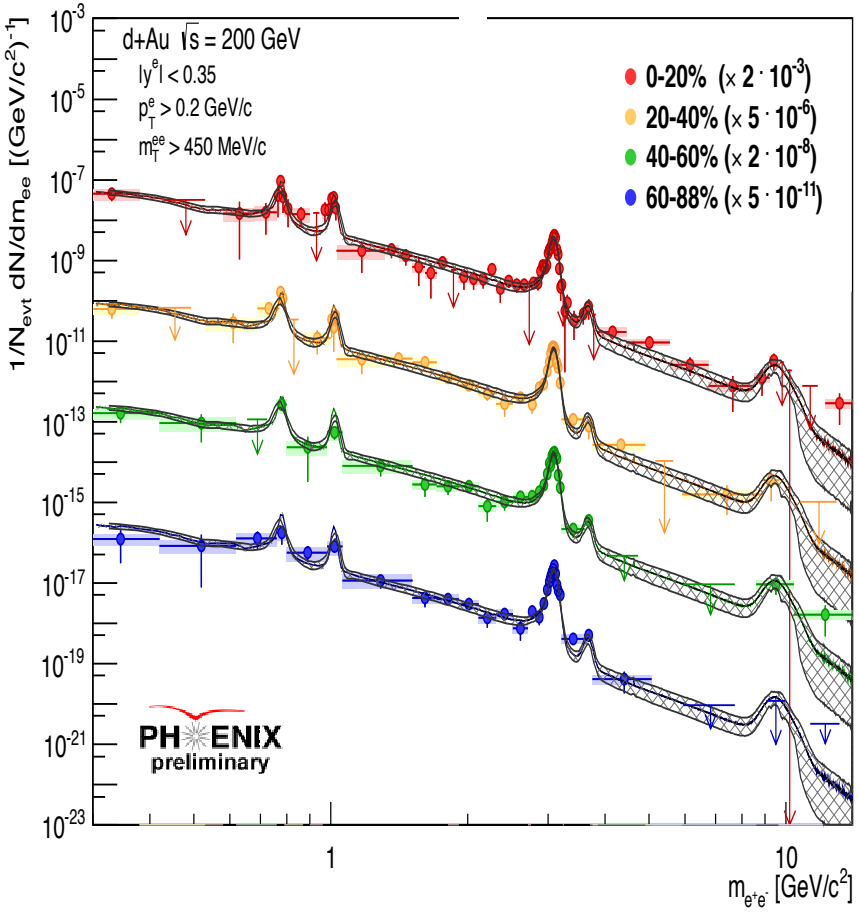


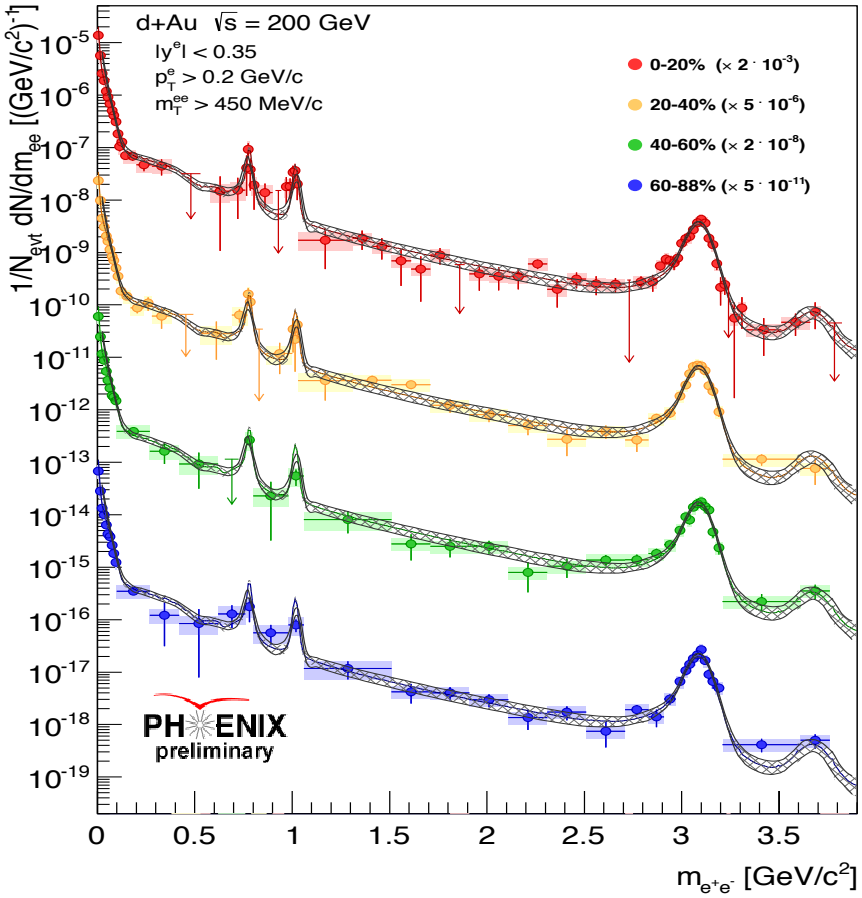


- For a given centrality the open heavy flavor is scaled by $N_{coll}$
- The centrality dependence is also very well described by the cocktail.

# Comparison of $d + Au$ to Scaled $p + p$

# *Comparison of $d + Au$ to scaled $p + p$ data*

**Low mass region**

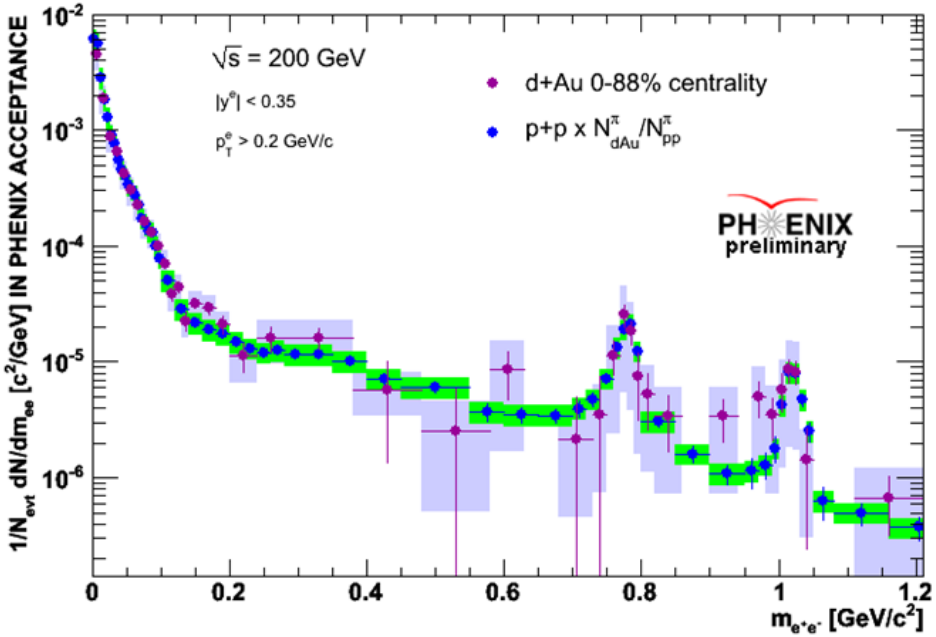


- No excess in LMR.
- $d + Au$ consistent with scaled $p + p$.

**Intermediate mass region**

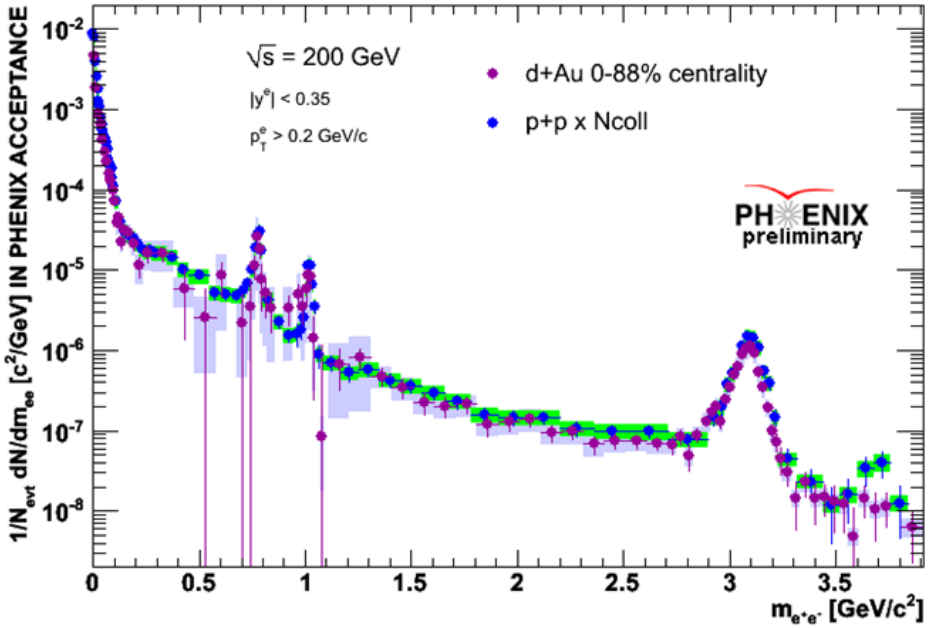


- No excess in IMR.
- $d + Au$ consistent with scaled $p + p$.
- $J/\psi$ suprresion $\sim 0.75$ observed.

# Comparison of $d + Au$ to $Au + Au$ and $Cu + Cu$

# *Centrality Dependence of Yields across Different Systems*

***ordered by $N_{coll}$***

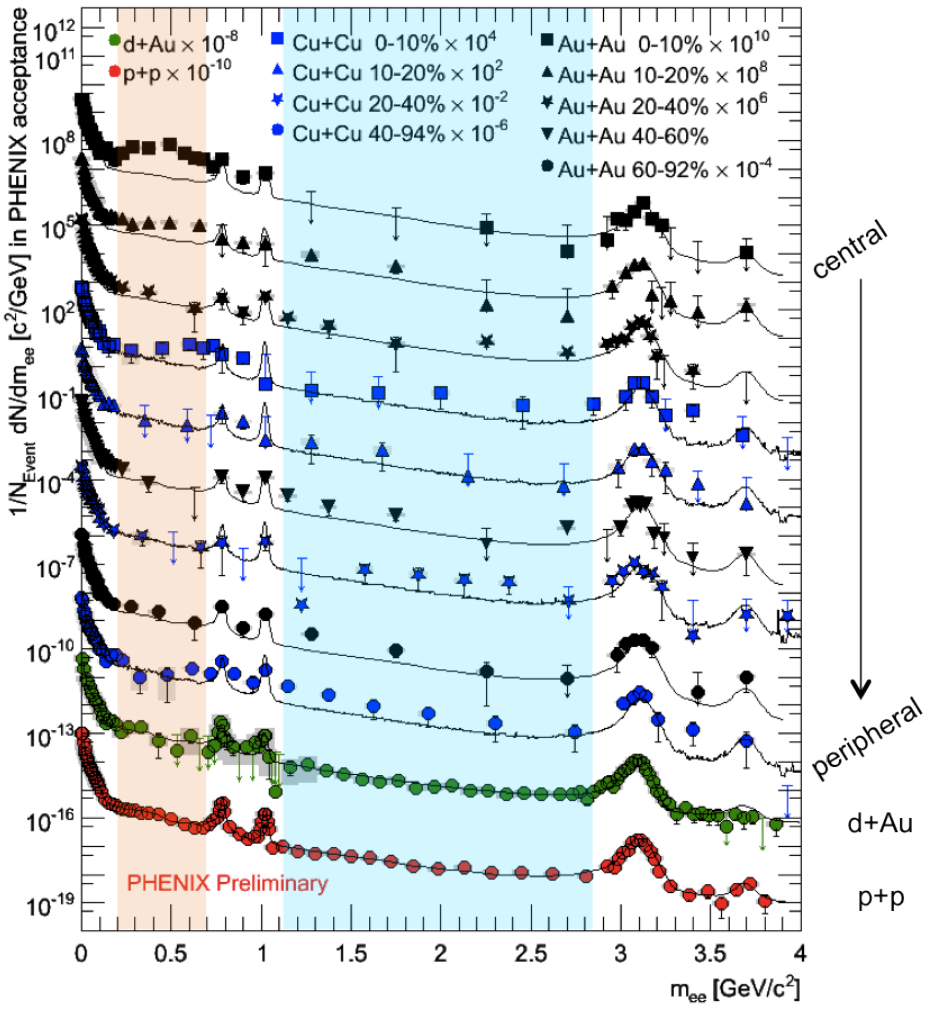


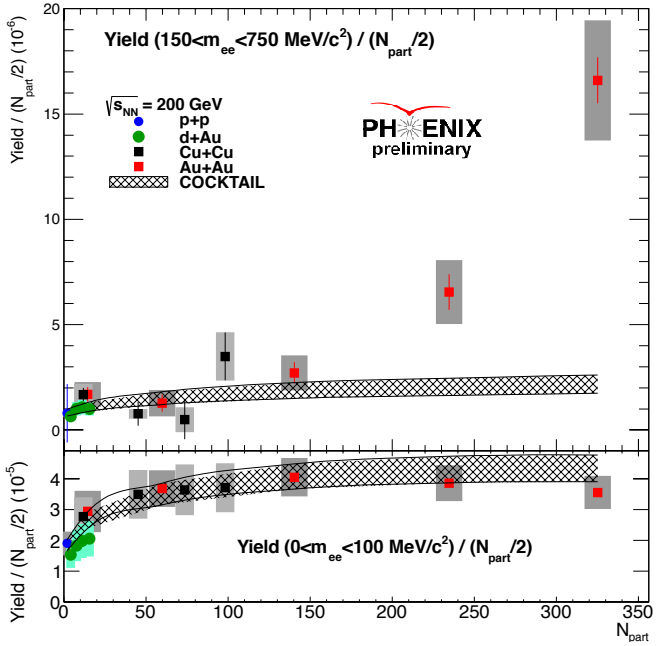


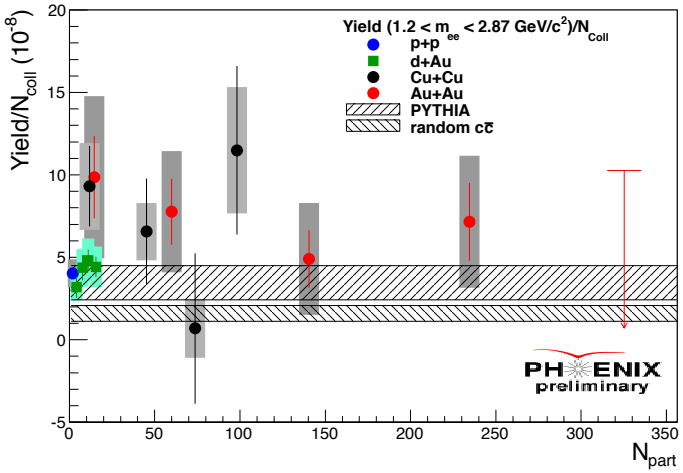

# *Centrality Dependence of Yields across Different Systems*

***ordered by $N_{coll}$***

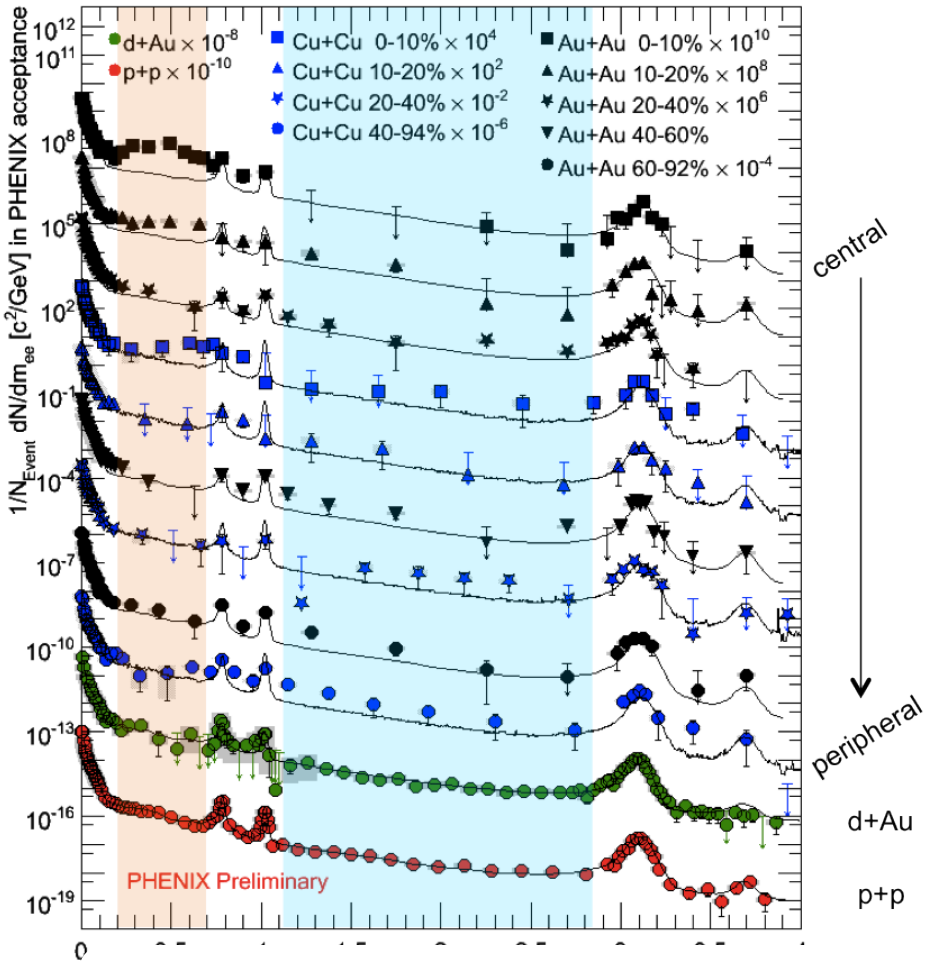


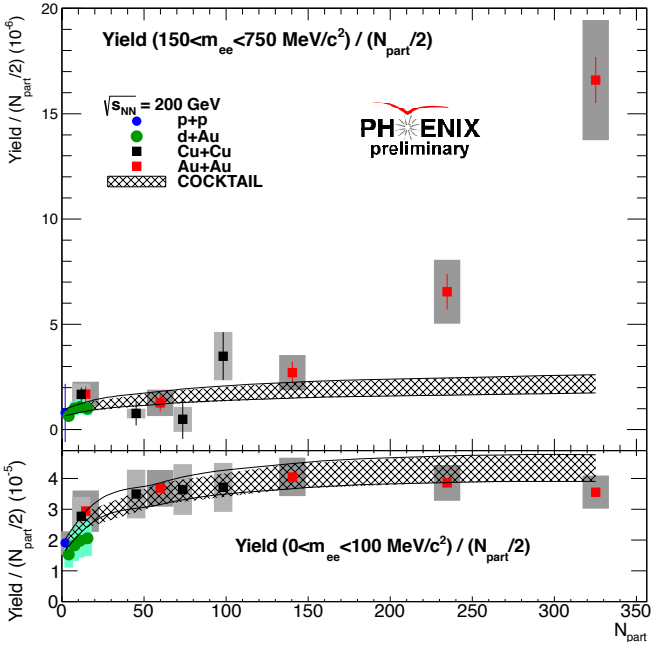


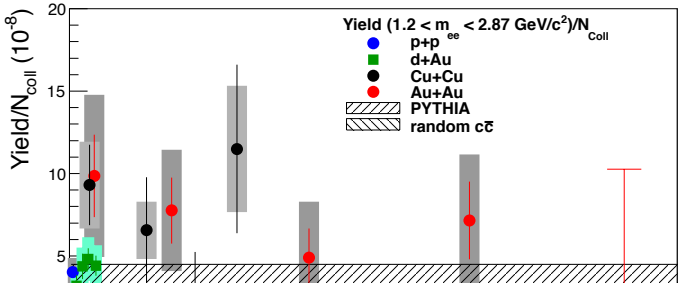


- Enhancement in low mass region is a strong function of centrality.
- Enhancement seen in both $Cu + Cu$ and $Au + Au$ systems.
- No excess is seen in $d + Au$

# Heavy Flavor Extraction using the $d + Au$ data

# *Mass Spectrum of Heavy Flavor in $d + Au$*

## *MC@NLO*

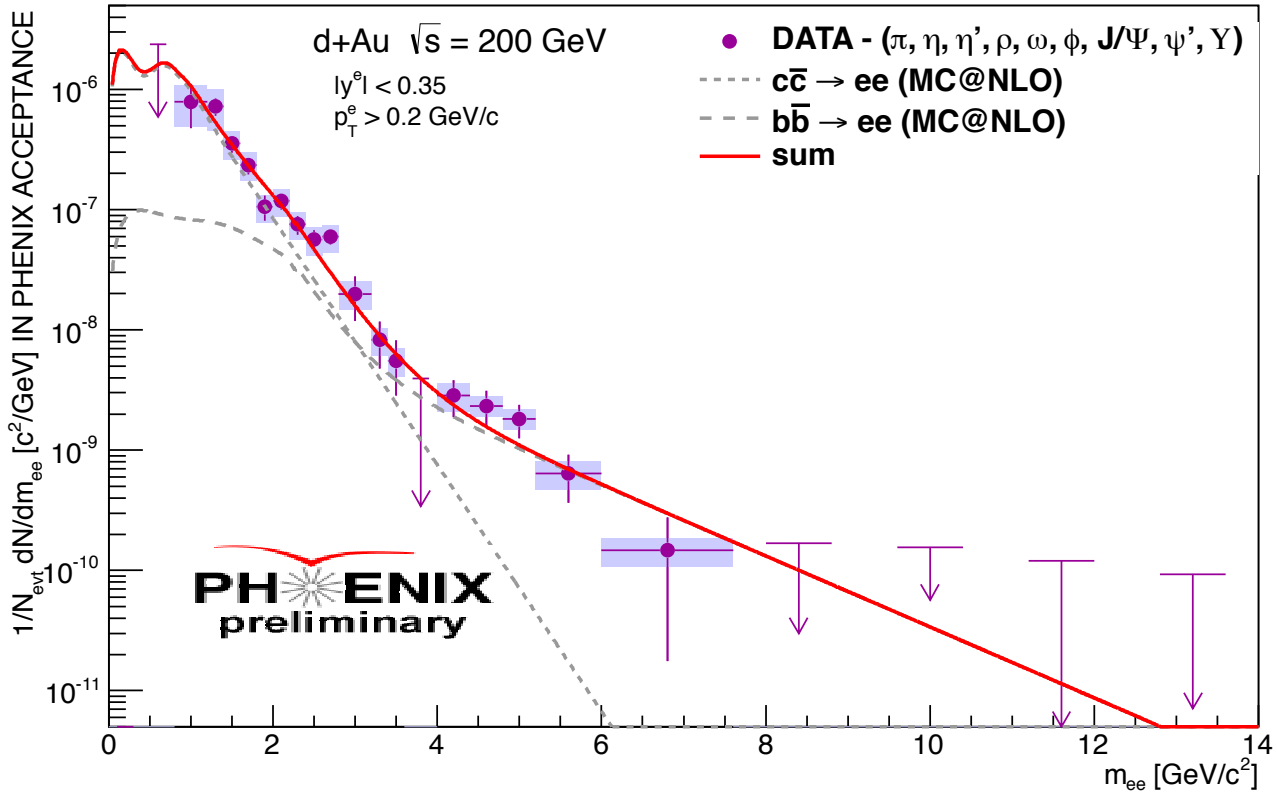


- All hadronic components subtracted from the data
- Like-sign HQ correlations subtracted in simulation.
- MC@NLO normalization fit to data 2D differentially (mass vs $p_T$).
- Extrapolated heavy flavor cross-sections:
  - $\sigma_{cc} = 711 \pm 62$ (stat) $\pm 183$ (syst) $\pm 80$ (model) $\mu$b.
  - $\sigma_{bb} = 4.46 \pm 0.70$ (stat) $\pm 1.08$ (syst) $\pm 0.22$ (model) $\mu$b.

# $p_T$ Dependence of Heavy Flavor Spectrum

## MC@NLO calculations

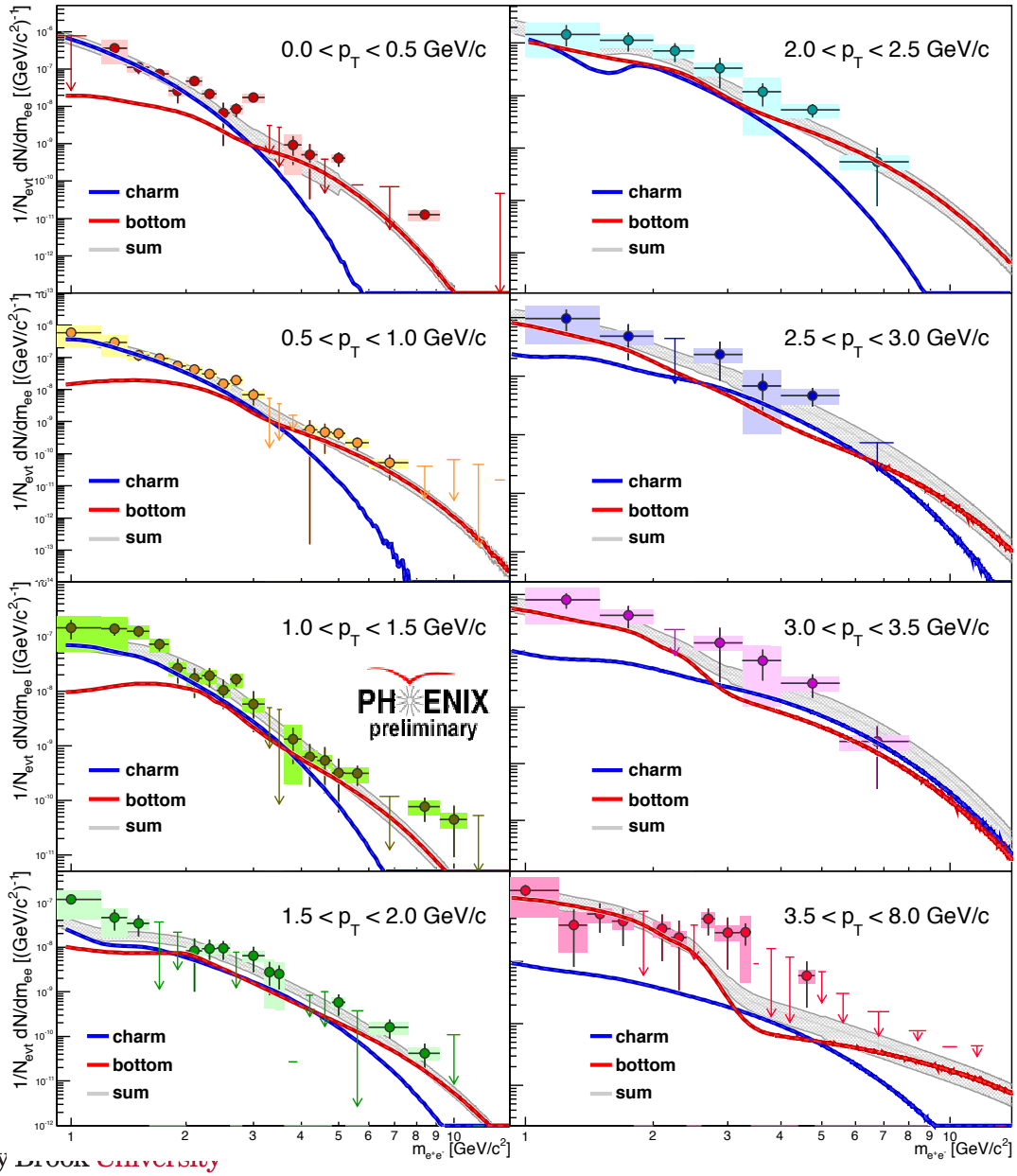


- MC@NLO predicts a complex interplay between charm and beauty
- Low $p_T$:
  - IMR -charm
  - HMR -beauty
- Intermediate $p_T$:
  - charm and beauty similar
- High $p_T$:
  - IMR -beauty
  - HMR -charm
- MC@NLO predicts the data !!
- A powerful confirmation of NLO data.

# LO vs NLO

## PYTHIA vs MC@NLO

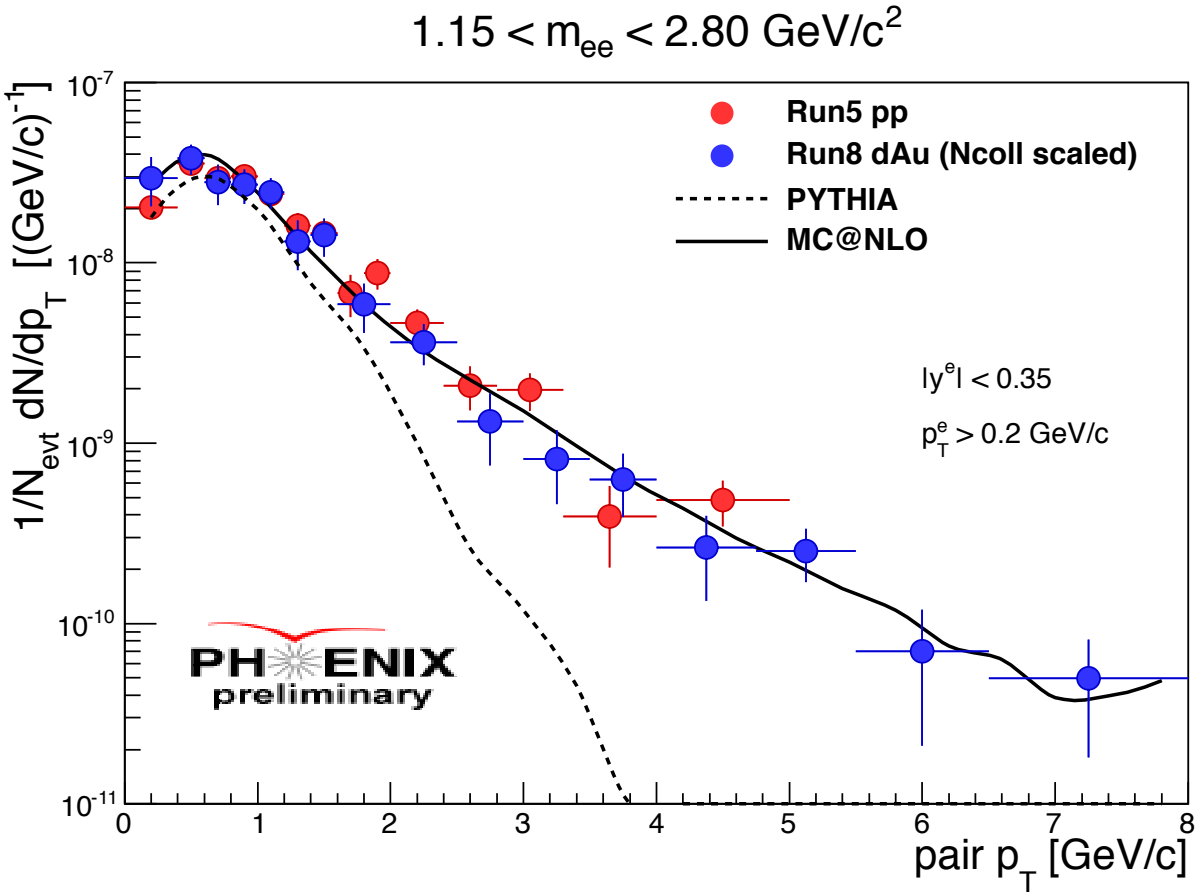


- $p_T$ dependence of integrated yield in IMR.
- PYTHIA normalized by fitting to $p+p$ data and MC@NLO normalized uding the $d+Au$ data.
- MC@NLO does a better job of describing the data while PYTHIA underestimates the data above $\sim 2$ GeV/c.

# Global Perspective

## Charm X-section

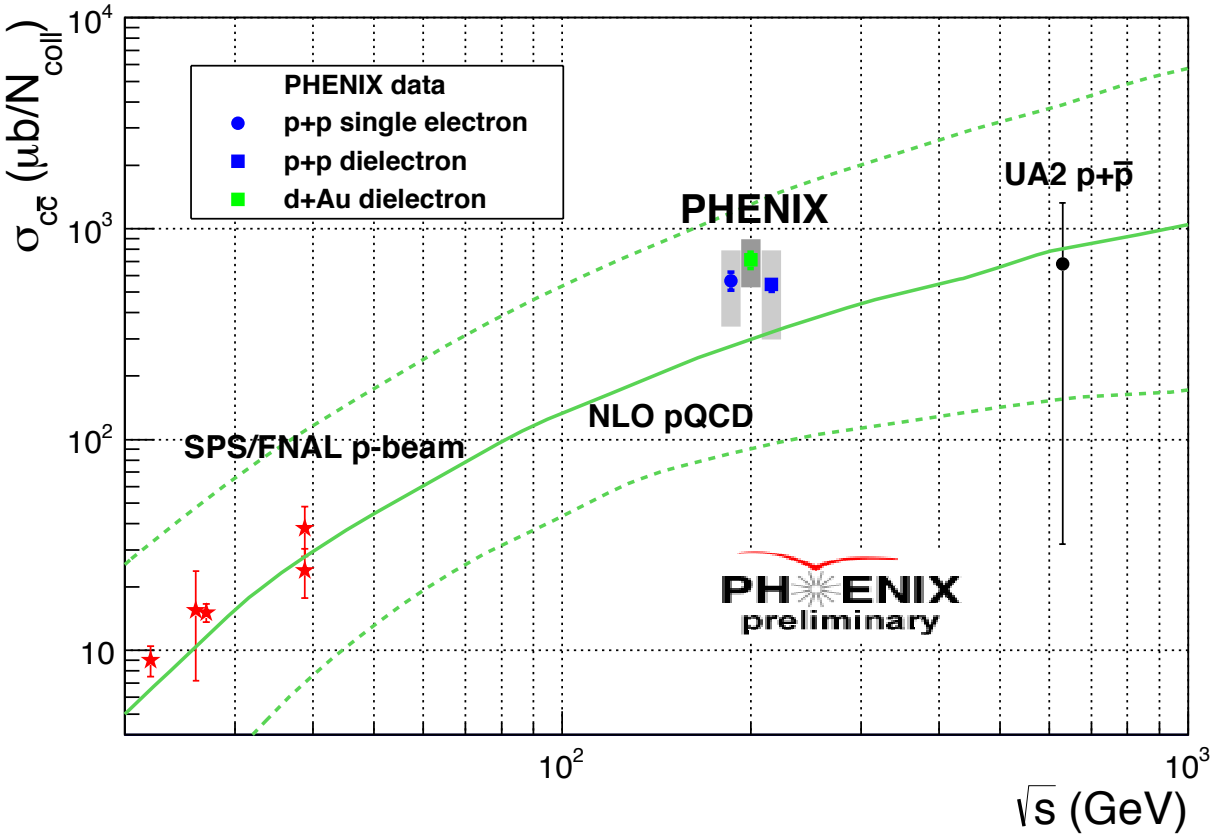


- PHENIX has 3 electron measurements of extrapolated cross-setion
  - All are in agreement with each other.
  - All fall within pQCD NLO.

# Global Perspective

## Beauty X-section

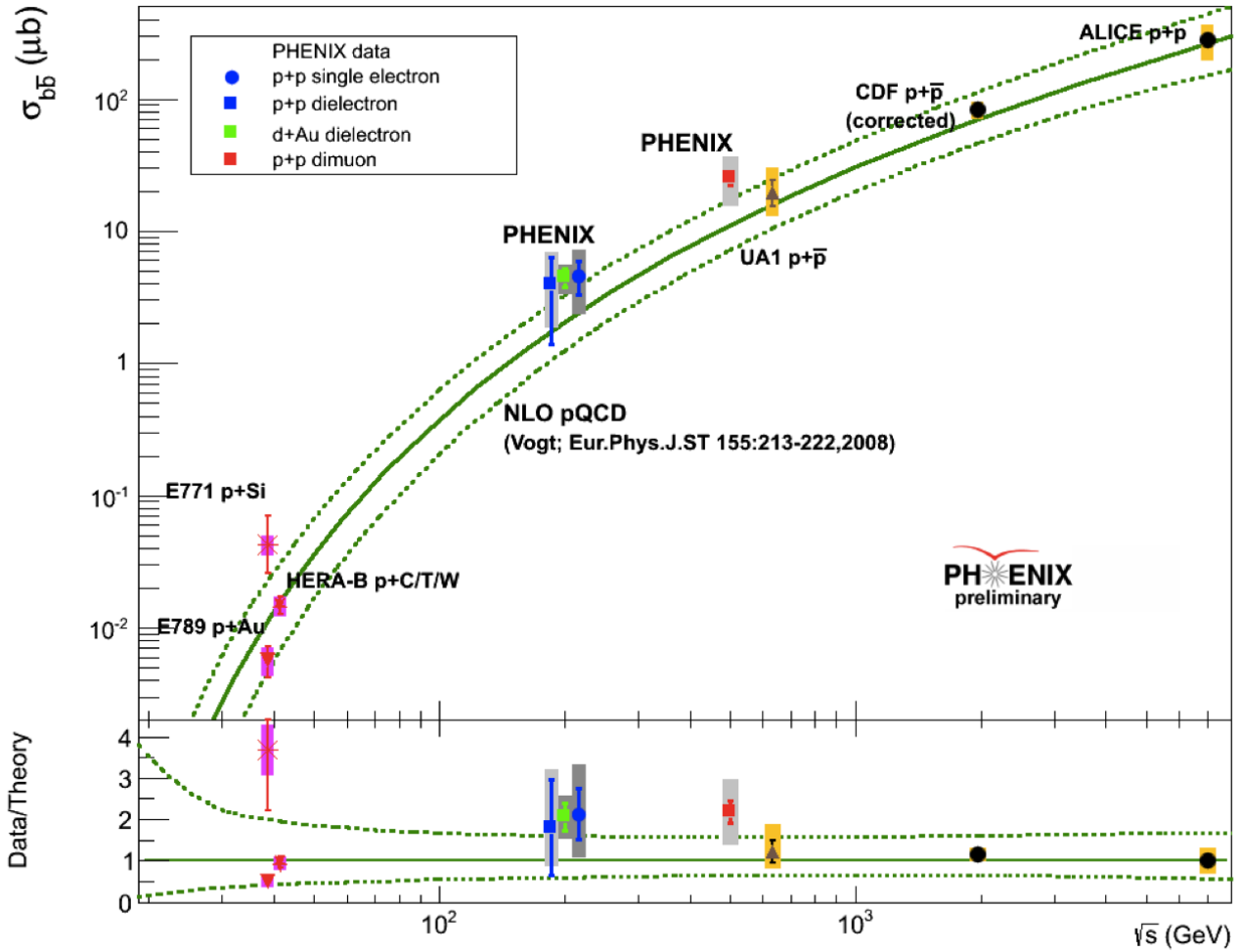


- PHENIX has 4 lepton measurements of extrapolated cross-setion
  - All are in agreement with each other.
  - All fall within pQCD NLO.

# Summary

- The d+Au data dielectron spectrum is consistent with the expected cocktail of known sources and, to the scaled $p + p$ results.
- Any enhancement seen in the HI collisions is not due to any cold nuclear matter effects.
- Dielectron like-sign correlations are useful and should be taken into account.
- The $d + Au$ dielectrons data provides a new independent measurement for the heavy flavor that are consistent with the already published results.
- The next-to-leading order calculations (MC@NLO) describe the data very nicely as compared to the leading order calculation (PYTHIA).
- PHENIX dielectron heavy flavor cross-sections are in good agreement with pQCD predictions.

# Back-ups

# Cocktail of Expected Sources

# Estimate of Expected Sources

## Cocktail

- Hadron decays
  - Fit the $\pi^{\pm}$ and $\pi^0$ data for a given collision system

$$E\frac{d^3\sigma}{dp^3} = \frac{A}{(e^{-(ap_T+bp_T^2)} + p_T/p_0)^n}$$

  - Use $m_T$ scaling for shape of other hadrons: $p_T \rightarrow \sqrt{p_T^2 - m_{\pi^0}^2 + m_{hadron}^2}$ and fix normalization using the existing data where available.
  - Fits are done independently for each particle and each centrality.
- Open heavy flavor (c, b) contributions determined using MC@NLO.
  - For a given collision system use $N_{coll} \times \sigma_{cc} = 567 \pm 57 \pm 193$ measured in $p+p$ from single electrons.
- Put the ideal PHENIX acceptance filter.
- $R_{dAu}$ of $J/\psi$ included in the Cocktail.

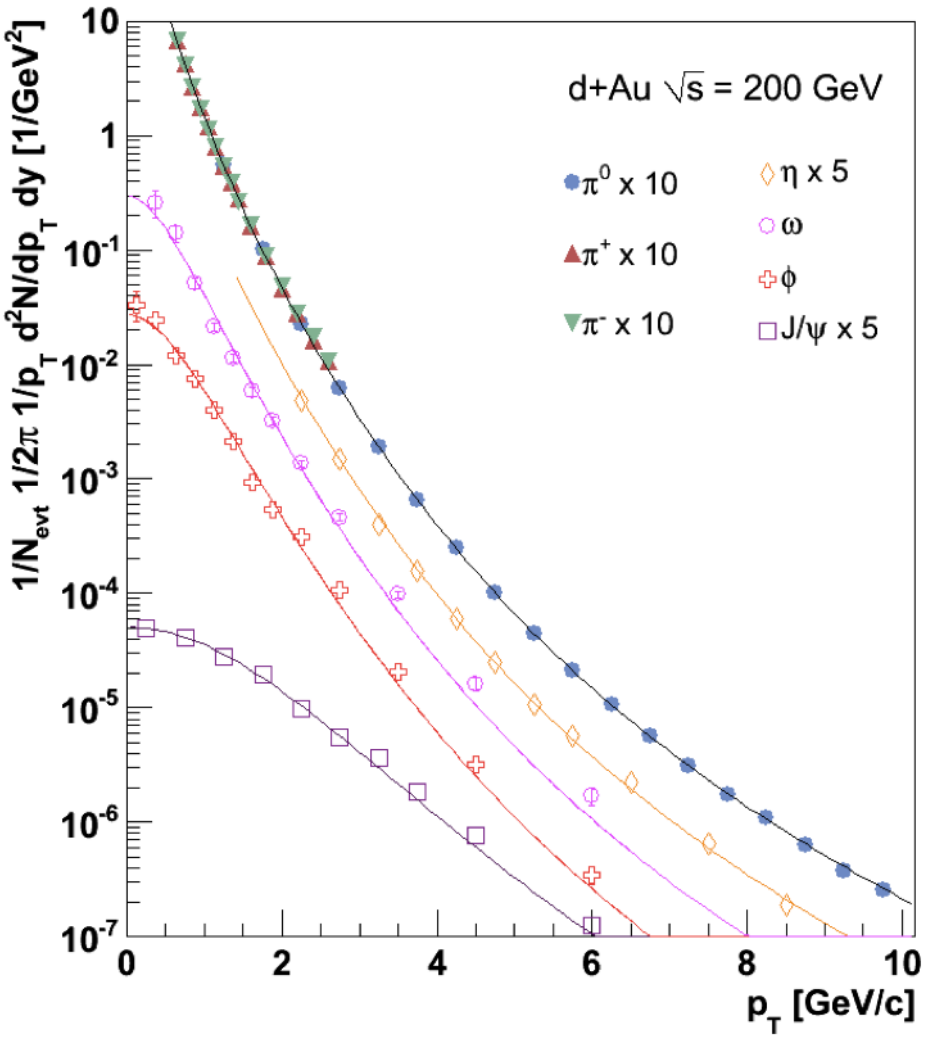


Compilation of meson invariant yields in $d+Au$ collisions. The data are compared to the parameterization based on $m_T$ scaling.

# *Centrality Dependence across Various Collision Systems*

***ordered by $N_{coll}$***

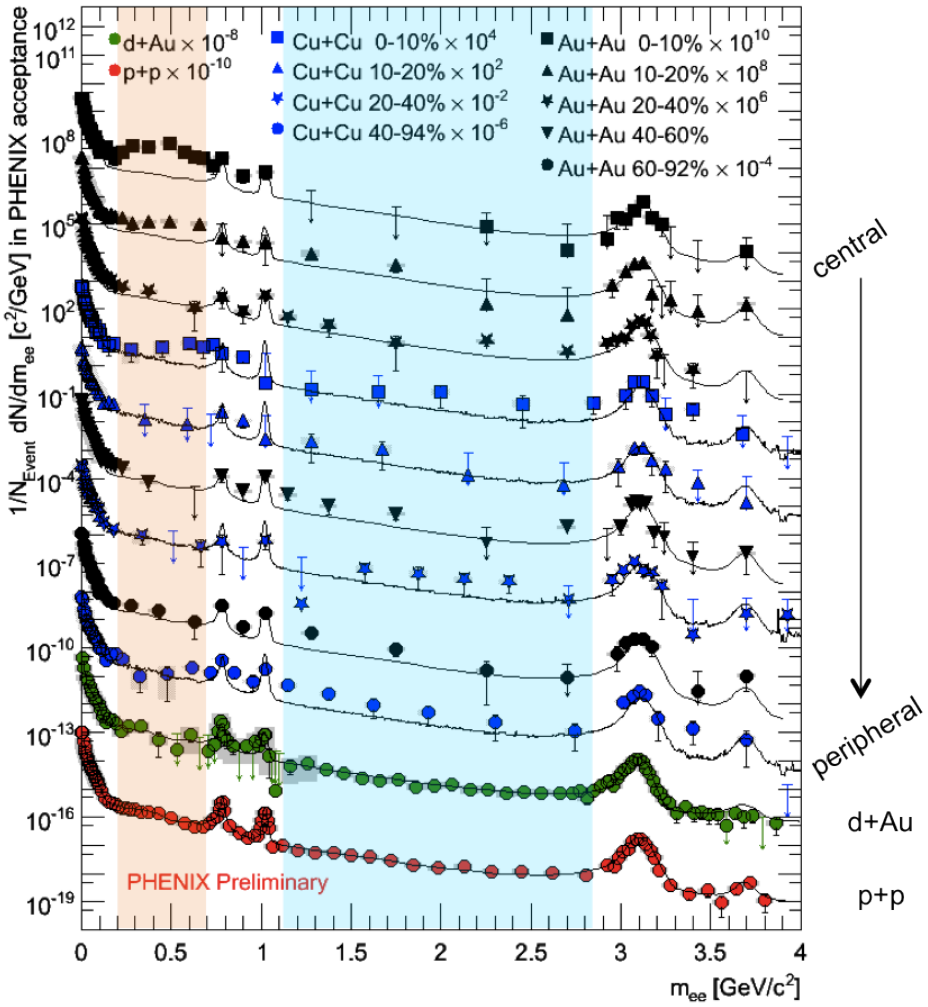


**All PHENIX dielctron data**

- Heavy Ions, $p+p$ and $d+Au$
  - $Au+Au$ by Centrality.
  - $Cu+Cu$ also plotted into centrality.
- $d+Au$ and $p+p$ are at the bottom
- Black line correspond to the respective cocktail for the given system.

**Centrality Dependence**

- LMR excess in more central.
- Slight IMR excess in peripheral heavy-ion collisions.
- $d+Au$ and $p+p$ are consistent with the Cocktail.

# Low Mass Region (LMR) Scaling of Yields

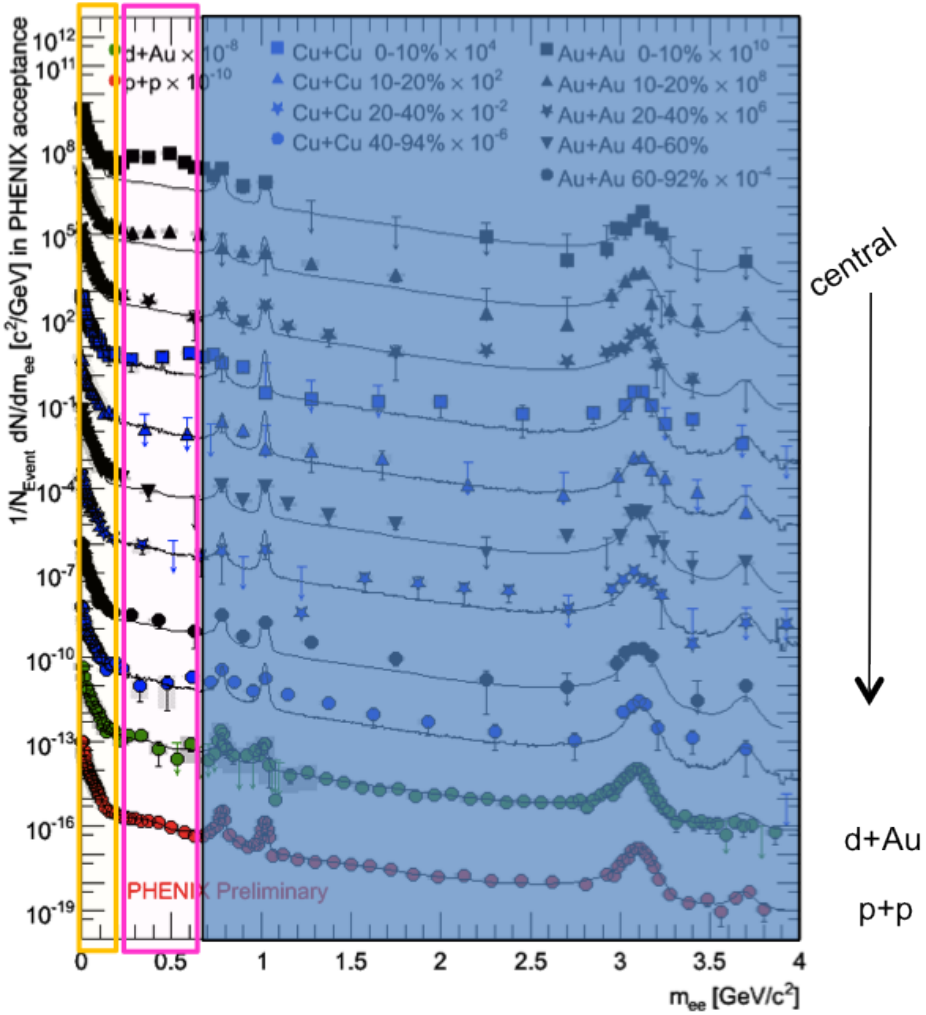


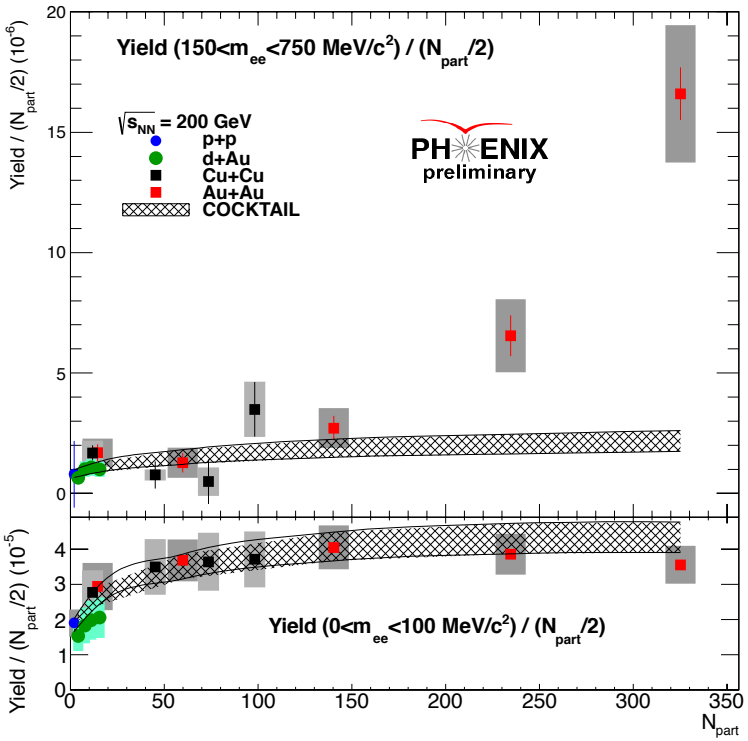


- Yield in the $\pi^0$ region scales approximately with $N_{part}$.
- Enhancement in the LMR (0.15 - 0.75 GeV/c$^2$) is a strong function of the Centrality.
- Excess seen in both $Au + Au$ and $Cu + Cu$
- No excess in $p + p$ or $d + Au$.

# *Intermediate Mass Region (IMR) Scaling of Yields*

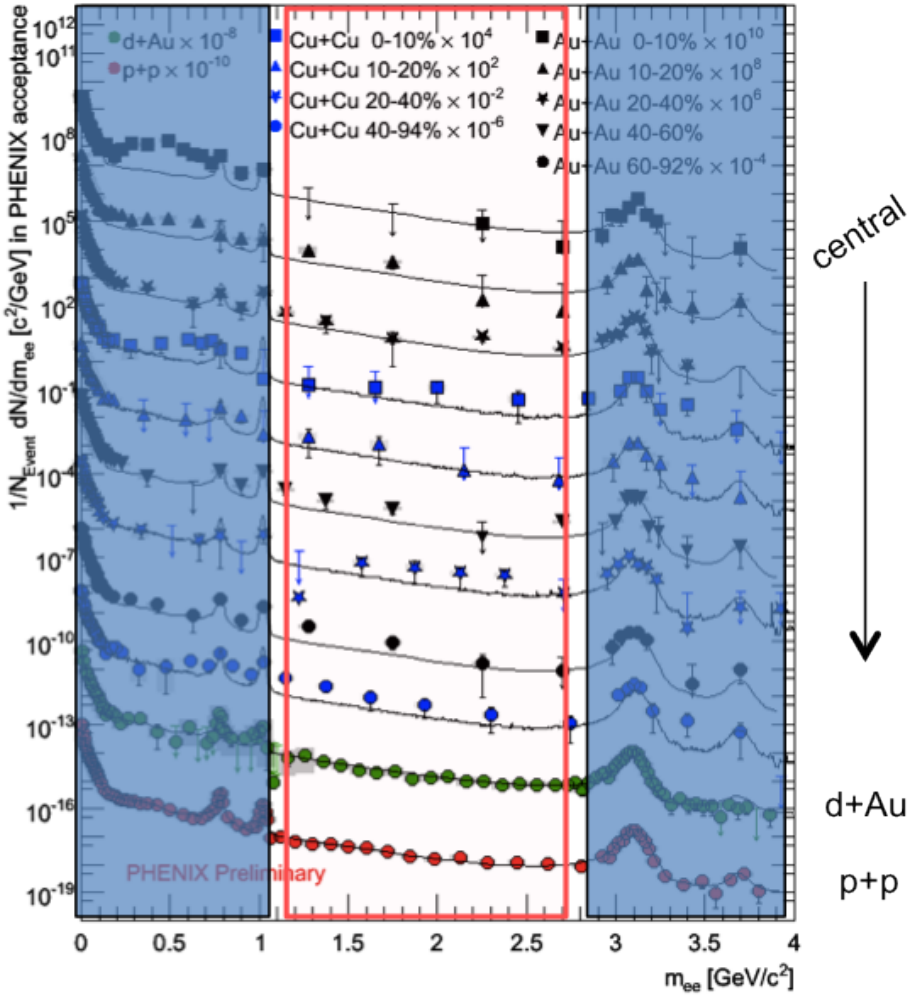


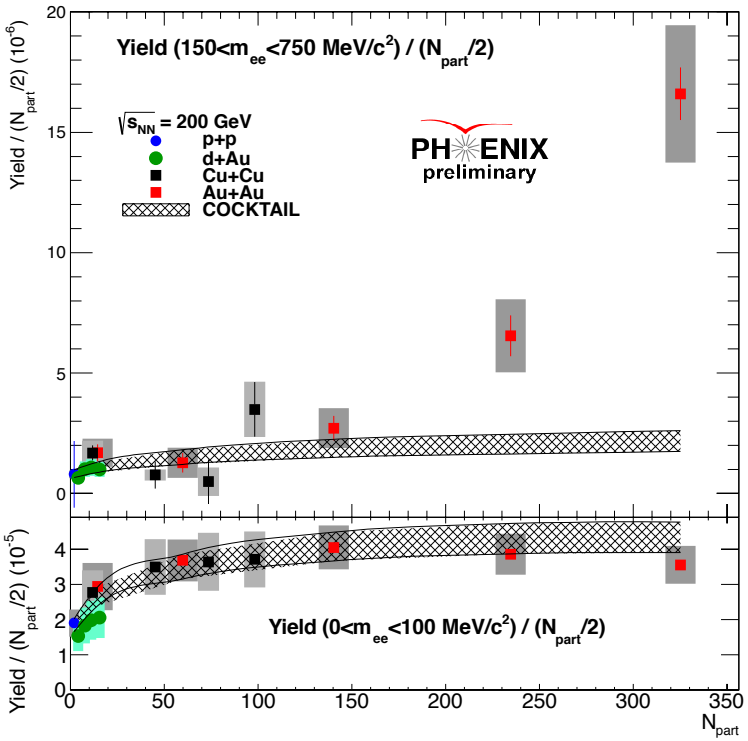


- Very little or no enhancement seen within the large systematic uncertainties of $Au + Au$ and $Cu + Cu$ as compared to the cocktail.

BNL workshop on
E/M probes. Dec.2012

Stony Brook University

# New ideas on the Penetrating Probes

Edward Shuryak
Stony Brook University

# outline

# outline

- **"hot glue scenario"** **(ES,1992) + comment on anisotropy vs dilepton polarization**
  **(ES .2012)**

# outline

- **"hot glue scenario"** **(ES,1992) + comment on anisotropy vs dilepton polarization**
  **(ES .2012)**

- **coherent effective photon+ hard photon => e+e-** **(Staig,ES,2009)**
  **coherent photon+q => q + real photon**
  **(Liao,ES,in progress)**

# outline

- **"hot glue scenario"** **(ES,1992) + comment on anisotropy vs dilepton polarization**
  **(ES .2012)**

- **coherent effective photon+ hard photon => e+e-** **(Staig,ES,2009)**
  **coherent photon+q => q + real photon**
  **(Liao,ES,in progress)**

- **B+photon <=> $O^+$ glue (scale anomaly) inchannel and $G^2BA$ interaction**
  **(Basar,Kharzeev,Skokov 2012)**

# outline

- **"hot glue scenario"** (ES,1992) + **comment on anisotropy vs dilepton polarization** (ES .2012)

- **coherent effective photon+ hard photon => e+e-** (Staig,ES,2009)
  **coherent photon+q => q + real photon** (Liao,ES,in progress)

- **B+photon <=> $O^+$ glue (scale anomaly) inchannel and $G^2BA$ interaction** (Basar,Kharzeev,Skokov 2012)

- **(DIS on GLASMA) or (hydro stress tensor coupled to 2 photons) B A <=> $2^+$, $0^+$ glue $O(T_{\mu\nu}AA)$** (Basar,Kharzeev,ES in

# outline, page 2

QGP

**near Tc**

- photon radiation rates <= quarks and gluons are not the only quasiparticles, **monopoles appear in large number and help to explain large scattering rates** (small viscosity). We need to include those collisions in photon rates

hadronic time

- news on chiral symmetry restoration

# Two-Stage Equilibration in High Energy Heavy Ion Collisions

E. Shuryak
*Department of Physics, State University of New York at Stony Brook, Stony Brook, New York 11794*
(Received 9 March 1992)

Using the (lowest-order) perturbative QCD, we argue that high energy heavy ion collisions proceed via two stages: *equilibration of gluons* takes time $\tau_g \sim \frac{1}{2}$ fm/$c$, while *production and equilibration of quarks* needs time at least $\tau_q \sim 2$ fm/$c$. If so, the initial gluon plasma is much hotter than usually estimated, $T_g \sim 400$ MeV, which leads to enhanced charm production and significant modifications of other proposed signals.

fined by $d\sigma/dt = (\pi\alpha_s^2/s^2)M^2$] are

$$M^2_{gg\to gg} = \frac{9}{2}\left[3 - \frac{ut}{s^2} - \frac{us}{t^2} - \frac{st}{u^2}\right],$$

$$M^2_{gg\to \bar{q}q} = \frac{1}{6}\frac{(u^2+t^2)}{ut} - \frac{3}{8}\frac{u^2+t^2}{s^2},$$

$$M^2_{qg\to qg} = -\frac{4}{9}\frac{u^2+s^2}{us} + \frac{u^2+s^2}{t^2},$$

$$M^2_{q_1q_2\to q_1q_2} = \frac{4}{9}\frac{s^2+u^2}{t^2}.$$

Spectra of the produced *photons and dileptons* should also be significantly modified in this scenario: During the "transitory period" ($\tau_g < \tau < \tau_q$) one has *smaller* number of quarks, but those are *hotter*. The reason is again that $gg \to \bar{q}q$ is dominated by *small angles*, so the produced quarks have the same momentum distribution as gluons. As most photons and dileptons to be observed actually correspond to the *tails of the distribution functions*, it is important that their relaxation happens *from above*.

# Two-Stage Equilibration in High Energy Heavy Ion Collisions

E. Shuryak
*Department of Physics, State University of New York at Stony Brook, Stony Brook, New York 11794*
(Received 9 March 1992)

Using the (lowest-order) perturbative QCD, we argue that high energy heavy ion collisions proceed via two stages: *equilibration of gluons* takes time $\tau_g \sim \frac{1}{2}$ fm/$c$, while *production and equilibration of quarks* needs time at least $\tau_q \sim 2$ fm/$c$. If so, the initial gluon plasma is much hotter than usually estimated, $T_g \sim 400$ MeV, which leads to enhanced charm production and significant modifications of other proposed signals.

charm contribution needs to be subtracted to test early dileptons M=1..3 GeV

fined by $d\sigma/dt = (\pi\alpha_s^2/s^2)M^2$] are

$$M^2_{gg\to gg} = \frac{9}{2}\left[3 - \frac{ut}{s^2} - \frac{us}{t^2} - \frac{st}{u^2}\right],$$

$$M^2_{gg\to \bar{q}q} = \frac{1}{6}\frac{(u^2+t^2)}{ut} - \frac{3}{8}\frac{u^2+t^2}{s^2},$$

$$M^2_{qg\to qg} = -\frac{4}{9}\frac{u^2+s^2}{us} + \frac{u^2+s^2}{t^2},$$

$$M^2_{q_1q_2\to q_1q_2} = \frac{4}{9}\frac{s^2+u^2}{t^2}.$$

Spectra of the produced *photons and dileptons* should also be significantly modified in this scenario: During the "transitory period" ($\tau_g < \tau < \tau_q$) one has *smaller* number of quarks, but those are *hotter*. The reason is again that $gg \to \bar{q}q$ is dominated by *small angles*, so the produced quarks have the same momentum distribution as gluons. As most photons and dileptons to be observed actually correspond to the *tails of the distribution functions*, it is important that their relaxation happens *from above*.

M.Heller et al
arXiv:1103.3452

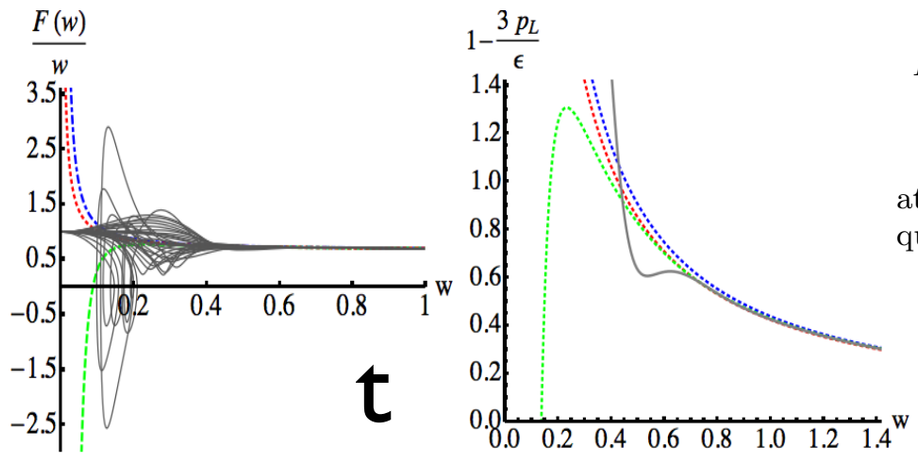


FIG. 1. a) $F(w)/w$ versus $w$ for all 29 initial data. b) Pressure anisotropy $1-\frac{3p_L}{\varepsilon}$ for a selected profile. Red, blue and green curves represent $1^{st}$, $2^{nd}$ and $3^{rd}$ order hydrodynamics fit.

**w=t $T_0$=t/(.5 fm) at LHC**

AdS/CFT collisions with various initial conditions converge to the same hydro, and they do so **when anisotropy is still large!**

**Monitoring parton equilibration in heavy ion collisions via dilepton polarization**


Edward Shuryak

*Department of Physics and Astronomy, State University of New York, Stony Brook, NY 11794*



(Dated: March 6, 2012)



In this note we discuss how angular distribution of the dileptons produced in heavy ion collisions at RHIC/LHC energies can provide an information about a degree of local equilibration of the quark-gluon plasma produced at different invariant mass regions.


$$\frac{d\sigma}{d\Omega} \sim (1 + acos^2\theta)$$

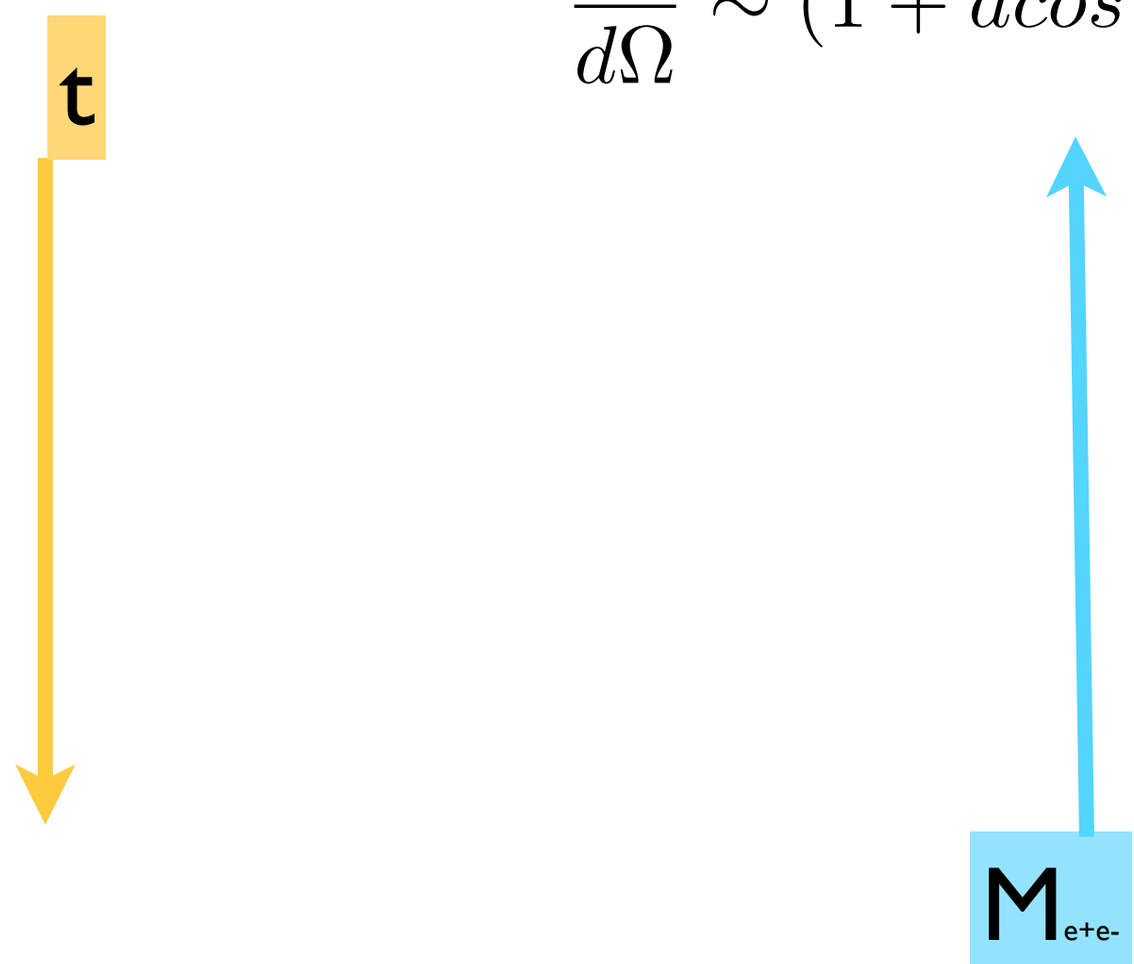



arXiv:1203.1012v1 [nucl-th] 5 Mar 2012

M.Heller et al
arXiv:1103.3452

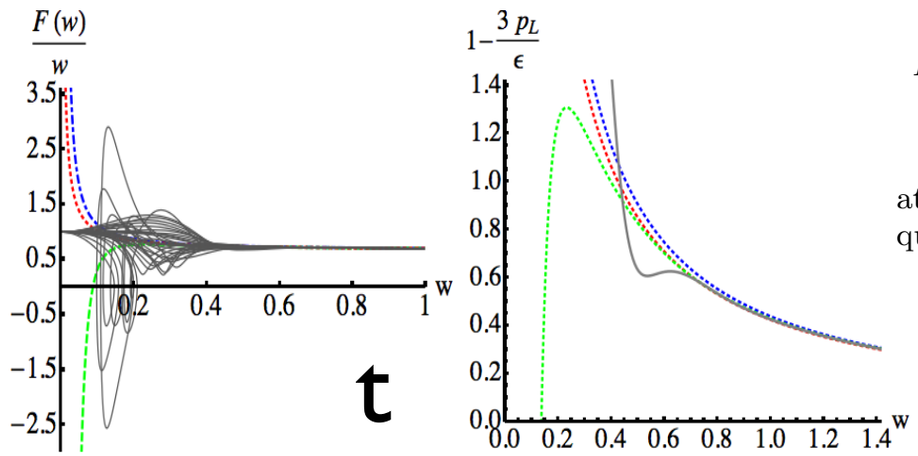


FIG. 1. a) $F(w)/w$ versus $w$ for all 29 initial data. b) Pressure anisotropy $1-\frac{3p_L}{\varepsilon}$ for a selected profile. Red, blue and green curves represent $1^{st}$, $2^{nd}$ and $3^{rd}$ order hydrodynamics fit.

**w=t $T_0$=t/(.5 fm) at LHC**

AdS/CFT collisions with various initial conditions converge to the same hydro, and they do so **when anisotropy is still large!**

<= series in higher gradients are very well convergent: Lublinsky,ES 2009

**Monitoring parton equilibration in heavy ion collisions via dilepton polarization**

Edward Shuryak

*Department of Physics and Astronomy, State University of New York, Stony Brook, NY 11794*
(Dated: March 6, 2012)

In this note we discuss how angular distribution of the dileptons produced in heavy ion collisions at RHIC/LHC energies can provide an information about a degree of local equilibration of the quark-gluon plasma produced at different invariant mass regions.

$$\frac{d\sigma}{d\Omega} \sim (1 + acos^2\theta)$$

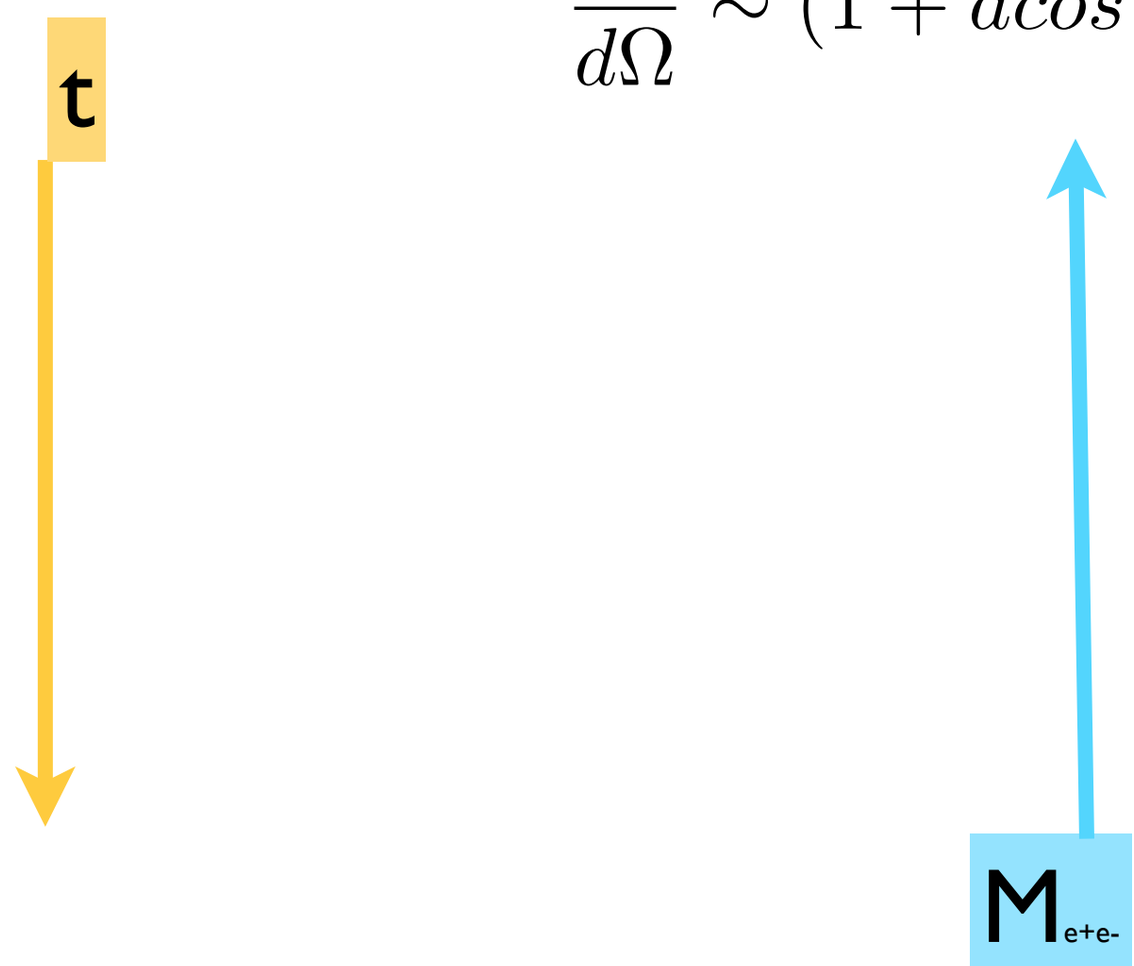


arXiv:1203.1012v1 [nucl-th] 5 Mar 2012

M.Heller et al
arXiv:1103.3452

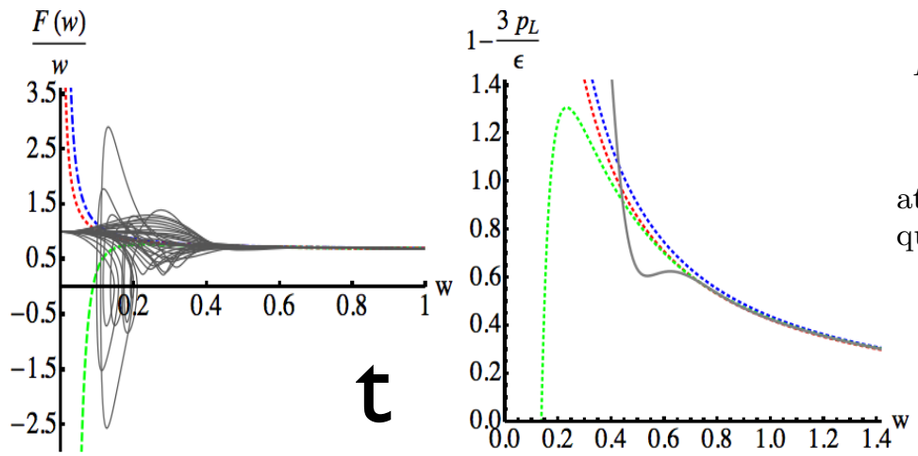


FIG. 1. a) $F(w)/w$ versus $w$ for all 29 initial data. b) Pressure anisotropy $1-\frac{3p_L}{\varepsilon}$ for a selected profile. Red, blue and green curves represent $1^{st}$, $2^{nd}$ and $3^{rd}$ order hydrodynamics fit.

**w=t $T_0$=t/(.5 fm) at LHC**

AdS/CFT collisions with various initial conditions converge to the same hydro, and they do so **when anisotropy is still large!**

<= series in higher gradients are very well convergent: Lublinsky,ES 2009

**Monitoring parton equilibration in heavy ion collisions via dilepton polarization**


Edward Shuryak

*Department of Physics and Astronomy, State University of New York, Stony Brook, NY 11794*



(Dated: March 6, 2012)



In this note we discuss how angular distribution of the dileptons produced in heavy ion collisions at RHIC/LHC energies can provide an information about a degree of local equilibration of the quark-gluon plasma produced at different invariant mass regions.



arXiv:1203.1012v1 [nucl-th] 5 Mar 2012


$$\frac{d\sigma}{d\Omega} \sim (1 + a cos^2\theta)$$

t

dilepton polarization

**a=1** for DY (partons come from the beam direction)

**a=-0.2** if elongated in transverse plane

a=0 in thermal case

$M_{e+e-}$

M.Heller et al
arXiv:1103.3452

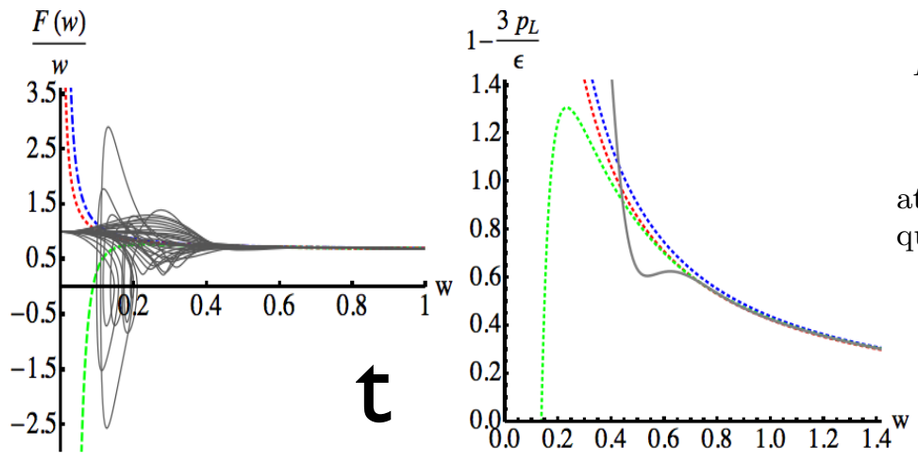


FIG. 1. a) $F(w)/w$ versus $w$ for all 29 initial data. b) Pressure anisotropy $1-\frac{3p_L}{\varepsilon}$ for a selected profile. Red, blue and green curves represent $1^{st}$, $2^{nd}$ and $3^{rd}$ order hydrodynamics fit.

**w=t $T_0$=t/(.5 fm) at LHC**

AdS/CFT collisions with various initial conditions converge to the same hydro, and they do so **when anisotropy is still large!**

<= series in higher gradients are very well convergent: Lublinsky,ES 2009

**Monitoring parton equilibration in heavy ion collisions via dilepton polarization**

Edward Shuryak

*Department of Physics and Astronomy, State University of New York, Stony Brook, NY 11794*
(Dated: March 6, 2012)

In this note we discuss how angular distribution of the dileptons produced in heavy ion collisions at RHIC/LHC energies can provide an information about a degree of local equilibration of the quark-gluon plasma produced at different invariant mass regions.

arXiv:1203.1012v1 [nucl-th] 5 Mar 2012

$$\frac{d\sigma}{d\Omega} \sim (1 + a cos^2\theta)$$

t

dilepton polarization
**a=1** for DY (partons come from the beam direction)
**a=-0.2** if elongated in transverse plane
a=0 in thermal case

Perhaps STAR/new PHENIX can catch out-of-equilibrium stage via a<0

# Production of soft $e^+e^-$ Pairs in Heavy Ion Collisions at RHIC by Semi-coherent Two Photon Processes

``exotic"

Pilar Staig and Edward Shuryak
Department of Physics and Astronomy
Stony Brook University, Stony Brook NY 11794 USA
(Dated: May 20, 2010)

We calculate the contribution of the two photon production process into $e^+e^-$ spectra, and c
pare the results with experimental data from the PHENIX detector at RHIC. We study the contr
tion given by "semi-coherent" kinematics, in which one photon is relatively hard and is incohere
emitted by participating protons, while another can be soft enough to be in a coherent domain

arXiv:1005.3531v1 [nucl-th] 19 May 2010

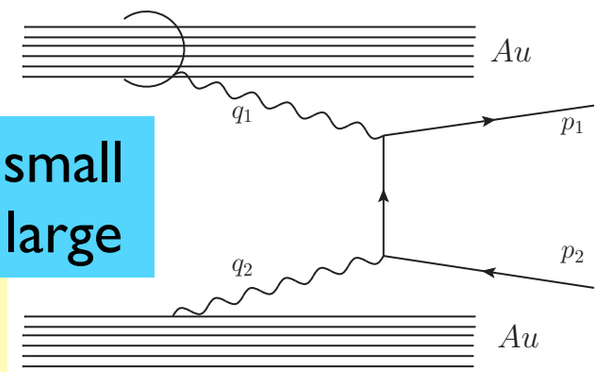


q1 small
q2 large

- ultra-peripheral is coherent-coherent
- parton processes are incoherent-incoherent
  gq=>gamma q
- semi-coherent has coherent field with small q1 and incoherent one with large q2 (resolving protons)

coherent Z^2

incoherent P's Z

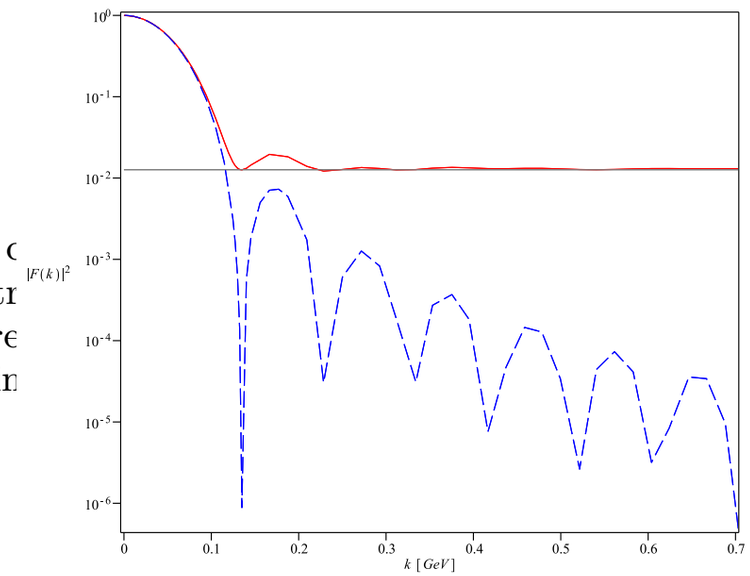


FIG. 3: (Color online)The square of the form factors plotted on a logarithmic scale. The (blue) dashed line corresponds to smooth Woods-Saxon charge distribution, the (red) continuous line corresponds to resolved discrete protons (but not quarks), as explained in the text.)

# Production of soft $e^+e^-$ Pairs in Heavy Ion Collisions at RHIC by Semi-coherent Two Photon Processes

``exotic"

Pilar Staig and Edward Shuryak
Department of Physics and Astronomy
Stony Brook University, Stony Brook NY 11794 USA
(Dated: May 20, 2010)

We calculate the contribution of the two photon production process into $e^+e^-$ spectra, and c
pare the results with experimental data from the PHENIX detector at RHIC. We study the contr
tion given by "semi-coherent" kinematics, in which one photon is relatively hard and is incohere
emitted by participating protons, while another can be soft enough to be in a coherent domain

arXiv:1005.3531v1 [nucl-th] 19 May 2010

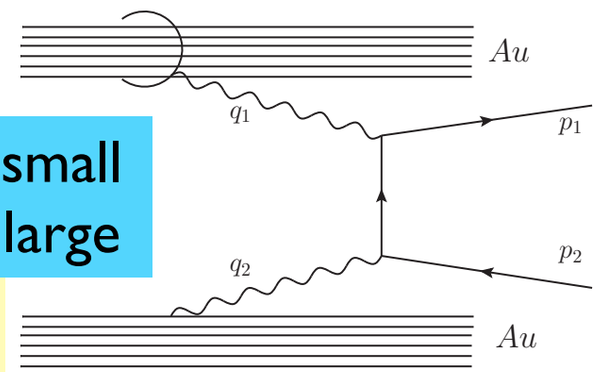


q1 small
q2 large

- ultra-peripheral is coherent-coherent

we did this calculation to explain the low-pt dilepton yield at PHENIX but the calculation showed that it gives dileptons outside of Phenix acceptance

coherent Z^2

incoherent P's Z

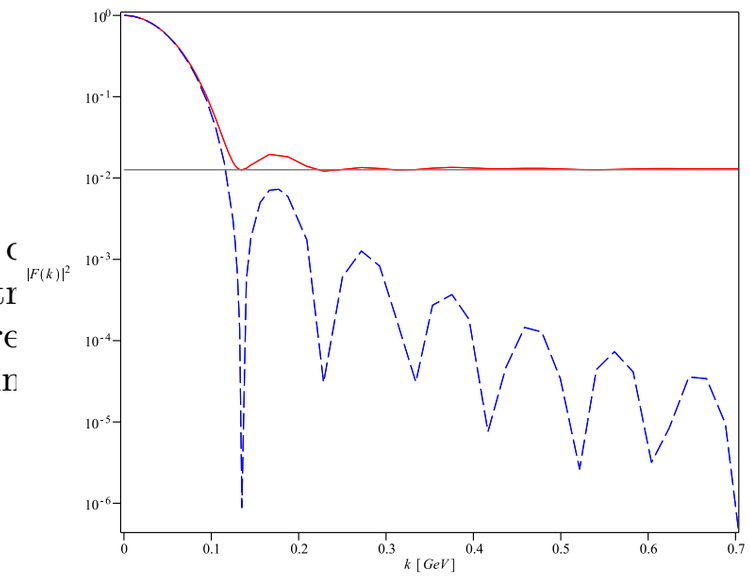


FIG. 3: (Color online)The square of the form factors plotted on a logarithmic scale. The (blue) dashed line corresponds to smooth Woods-Saxon charge distribution, the (red) continuous line corresponds to resolved discrete protons (but not quarks), as explained in the text.)

# Production of soft $e^+e^-$ Pairs in Heavy Ion Collisions at RHIC by Semi-coherent Two Photon Processes

``exotic"

Pilar Staig and Edward Shuryak
Department of Physics and Astronomy
Stony Brook University, Stony Brook NY 11794 USA
(Dated: May 20, 2010)

We calculate the contribution of the two photon production process into $e^+e^-$ spectra, and c
pare the results with experimental data from the PHENIX detector at RHIC. We study the contr
tion given by "semi-coherent" kinematics, in which one photon is relatively hard and is incohere
emitted by participating protons, while another can be soft enough to be in a coherent domain

arXiv:1005.3531v1 [nucl-th] 19 May 2010

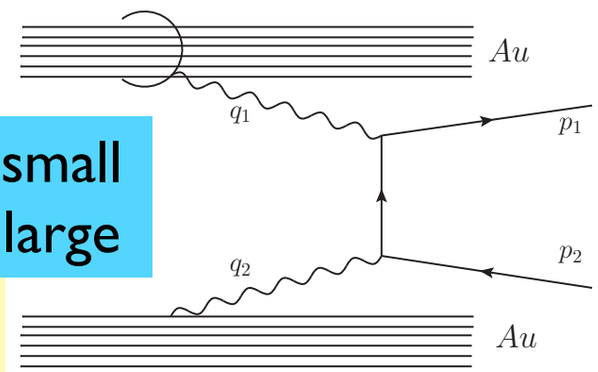


q1 small
q2 large

- ultra-peripheral is coherent-coherent

we did this calculation to explain the low-pt dilepton yield at PHENIX but the calculation showed that it gives dileptons outside of Phenix acceptance

coherent Z^2

incoherent P's Z

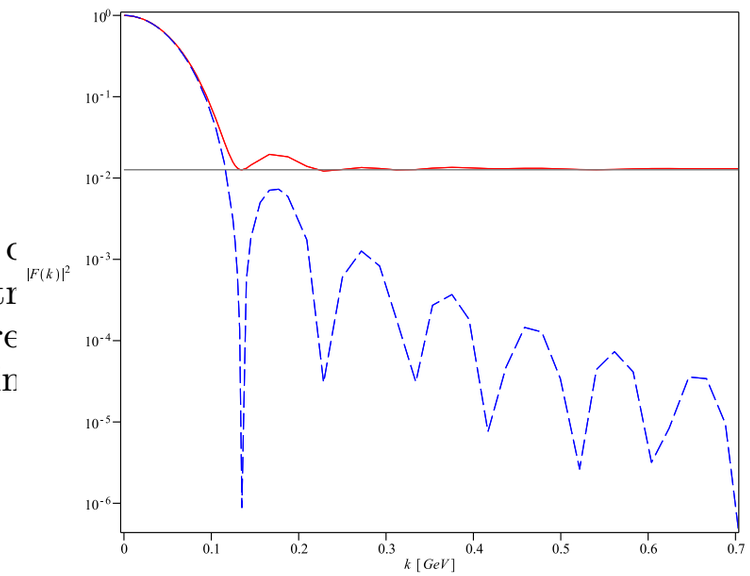


FIG. 3: (Color online)The square of the form factors plotted on a logarithmic scale. The (blue) dashed line corresponds to smooth Woods-Saxon charge distribution, the (red) continuous line corresponds to resolved discrete protons (but not quarks), as explained in the text.)

M=.5..0.75 GeV

# Production of soft $e^+e^-$ Pairs in Heavy Ion Collisions at RHIC by Semi-coherent Two Photon Processes

``exotic"

Pilar Staig and Edward Shuryak
Department of Physics and Astronomy
Stony Brook University, Stony Brook NY 11794 USA
(Dated: May 20, 2010)

We calculate the contribution of the two photon production process into $e^+e^-$ spectra, and c
pare the results with experimental data from the PHENIX detector at RHIC. We study the contr
tion given by "semi-coherent" kinematics, in which one photon is relatively hard and is incohere
emitted by participating protons, while another can be soft enough to be in a coherent domain

arXiv:1005.3531v1 [nucl-th] 19 May 2010

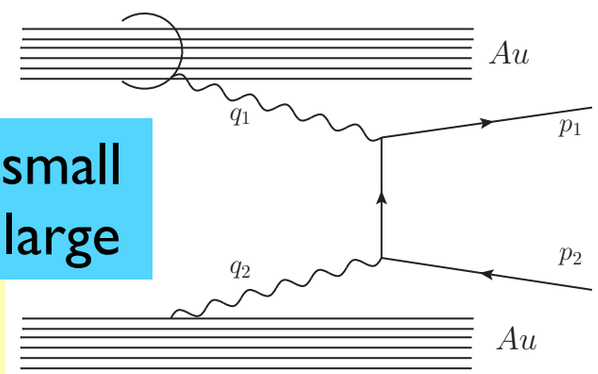


q1 small
q2 large

- ultra-peripheral is coherent-coherent

we did this calculation to explain the low-pt dilepton yield at PHENIX but the calculation showed that it gives dileptons outside of Phenix acceptance

coherent Z^2

incoherent P's Z

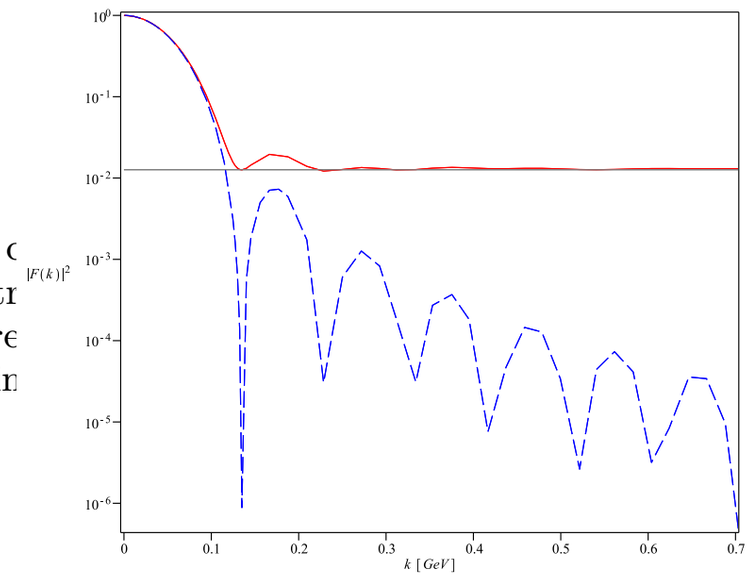


FIG. 3: (Color online)The square of the form factors plotted on a logarithmic scale. The (blue) dashed line corresponds to smooth Woods-Saxon charge distribution, the (red) continuous line corresponds to resolved discrete protons (but not quarks), as explained in the text.)

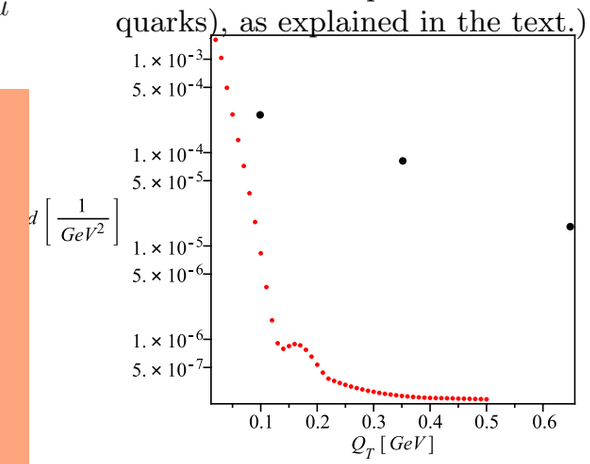


M=.5..0.75 GeV

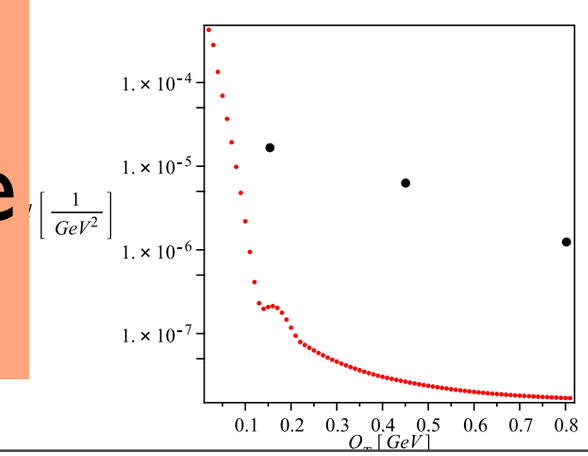

# Production of soft $e^+e^-$ Pairs in Heavy Ion Collisions at RHIC by Semi-coherent Two Photon Processes

``exotic"

Pilar Staig and Edward Shuryak
Department of Physics and Astronomy
Stony Brook University, Stony Brook NY 11794 USA
(Dated: May 20, 2010)

We calculate the contribution of the two photon production process into $e^+e^-$ spectra, and c
pare the results with experimental data from the PHENIX detector at RHIC. We study the contr
tion given by "semi-coherent" kinematics, in which one photon is relatively hard and is incohere
emitted by participating protons, while another can be soft enough to be in a coherent domain

arXiv:1005.3531v1 [nucl-th] 19 May 2010

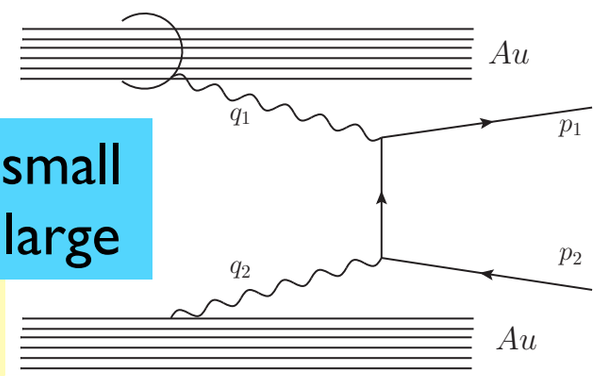


q1 small
q2 large

- ultra-peripheral is coherent-coherent

we did this calculation to explain the low-pt dilepton yield at PHENIX but the calculation showed that it gives dileptons outside of Phenix acceptance

coherent Z^2

incoherent P's Z

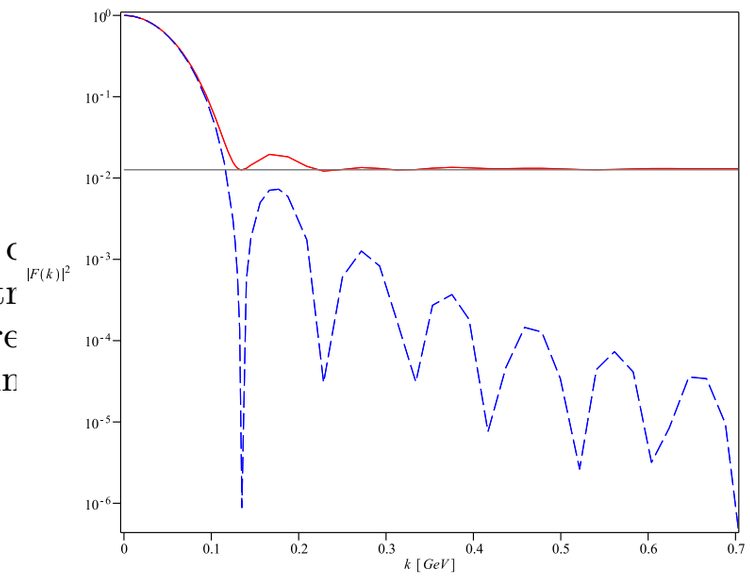


FIG. 3: (Color online)The square of the form factors plotted on a logarithmic scale. The (blue) dashed line corresponds to smooth Woods-Saxon charge distribution, the (red) continuous line corresponds to resolved discrete protons (but not quarks), as explained in the text.)

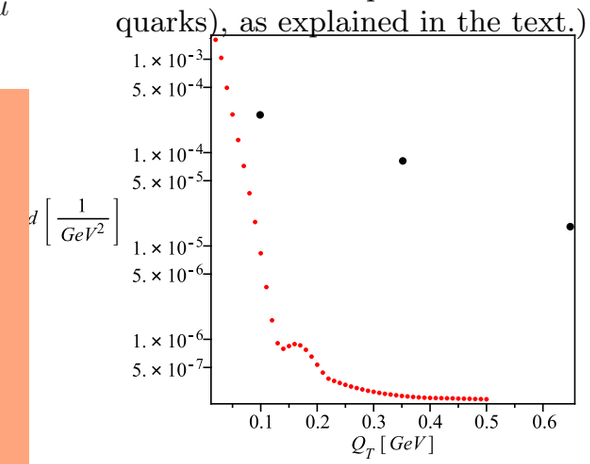


M=.5..0.75 GeV

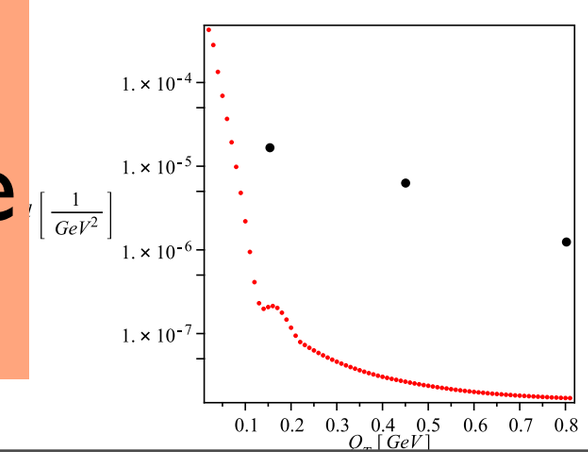


M=.81..0.99 GeV

# New puzzle: large v2 of photons (Phenix)

=> v2 is as large as that for hadrons
=> seems to persist even at large pt (?)
=> also seen by ALICE

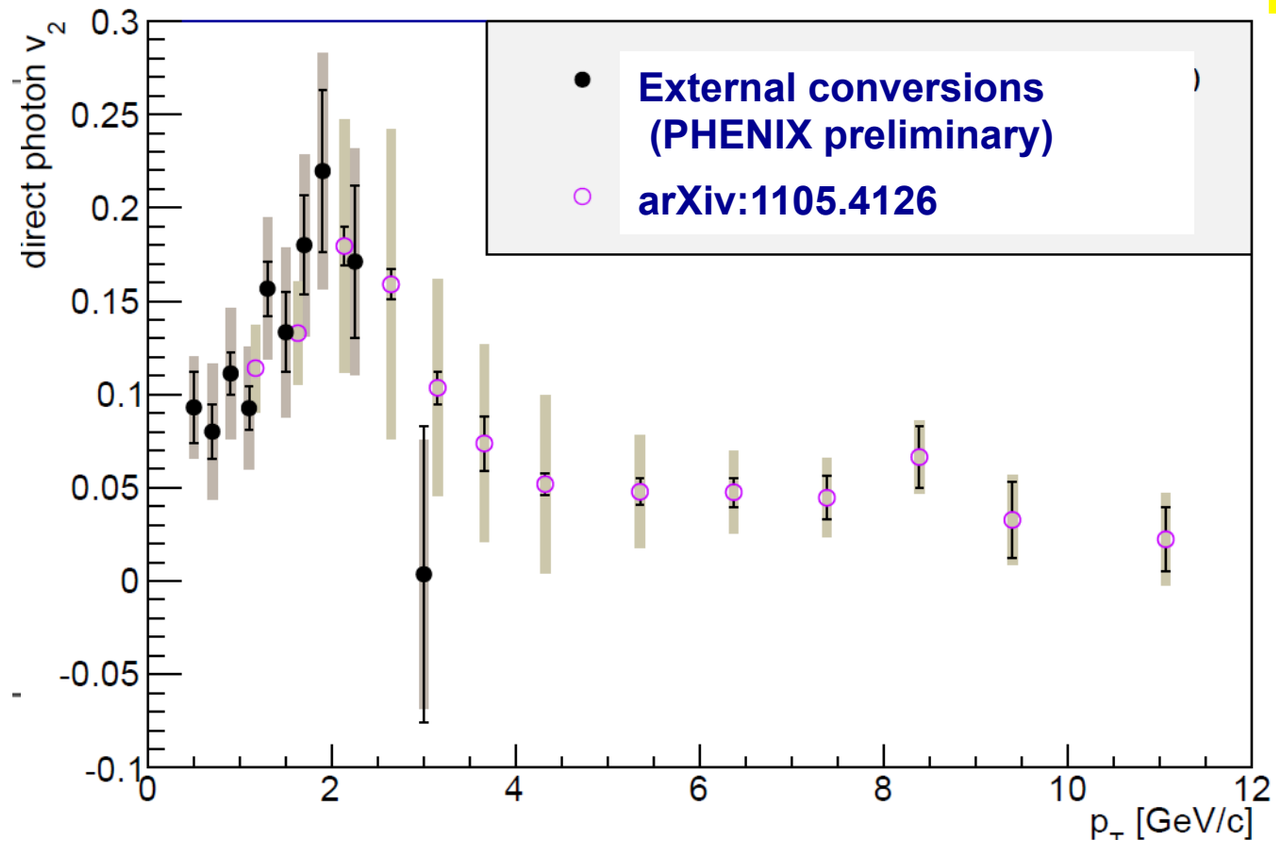

- q+**(semi-coherent eff.photon)**=>q+gamma

(with J-F. Liao) (WW approximation)

- q+ (B-correlated gluon) =>q+gamma

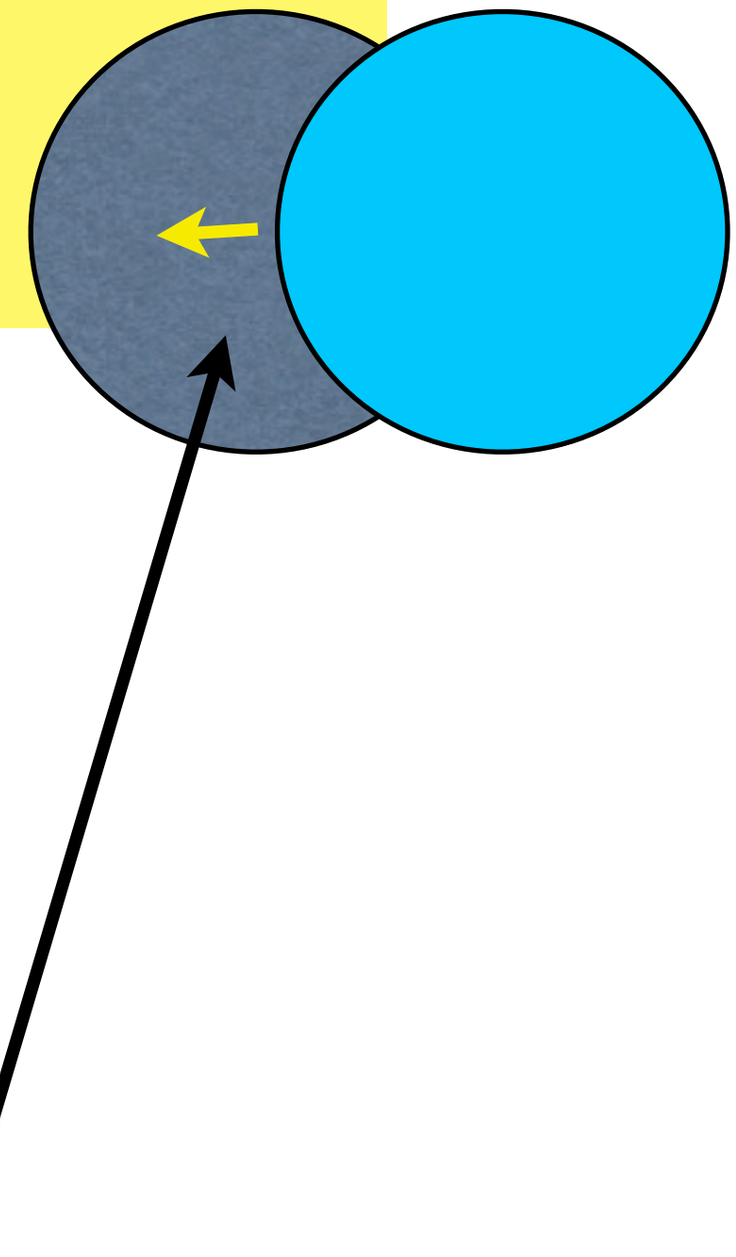

$$Z\alpha \sim \alpha_s$$

- q+**(semi-coherent eff.photon)**=>q+gamma

(with J-F. Liao) (WW approximation)

- q+ (B-correlated gluon) =>q+gamma

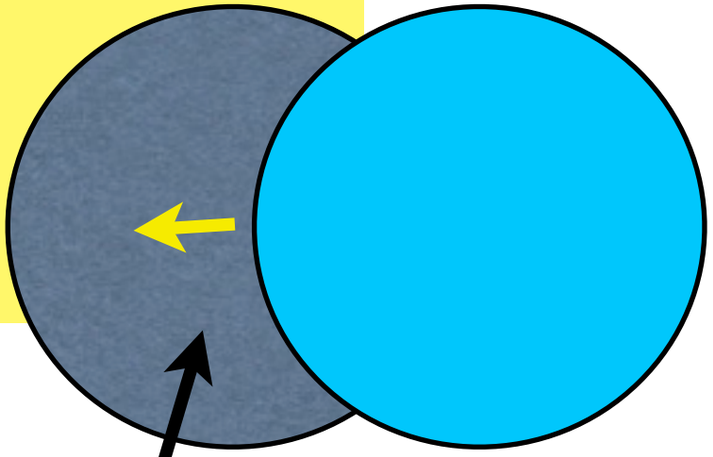

while $Z\alpha \sim \alpha_s$

effective gluon density is O(10) larger than equivalent photons,

but photon's momentum is **strongly correlated with the impact parameter b**

**coherent E/B field of the photon extends beyond the edge of the nuclei**

**even small effects need to be calculated!**

Basar,Kharzeev,Skokov arXiv:1206.1334

(1)virtual quark loop
(2)coherent magnetic field
(3)B+photon mix with scalar $G^2$
(4)Its correlators are related to bulk viscosity and correlators

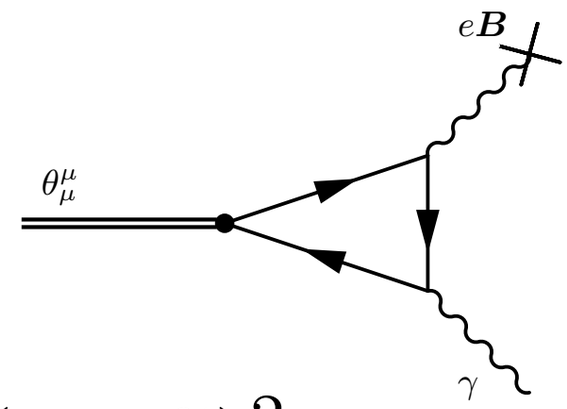


$$\sim (B_y q_x^\gamma)^2$$

**Spectral densities known from AdS/QCD models**

no effect along the B field!

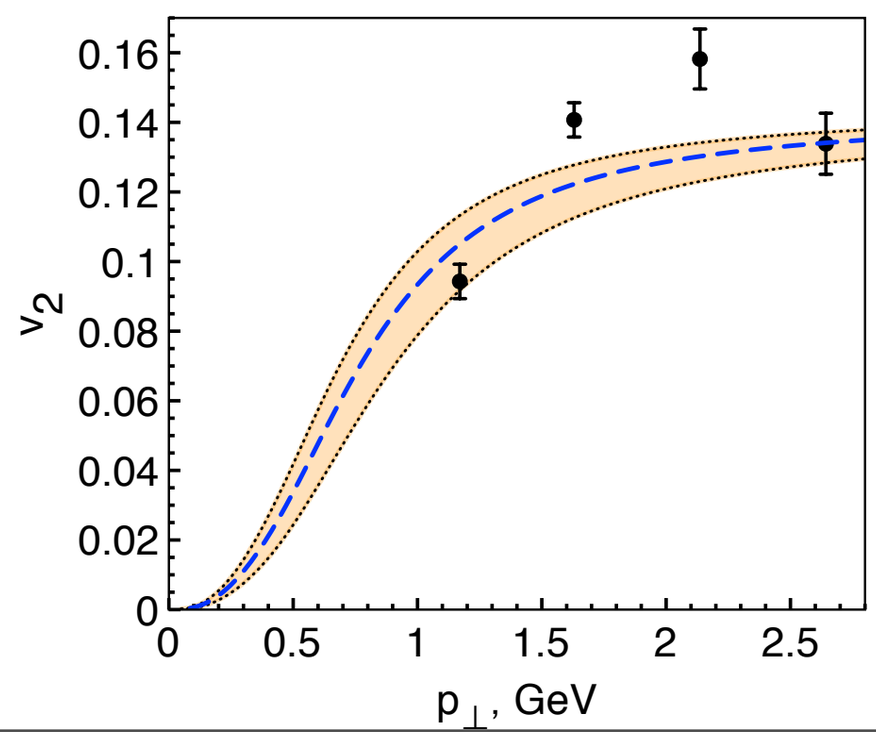


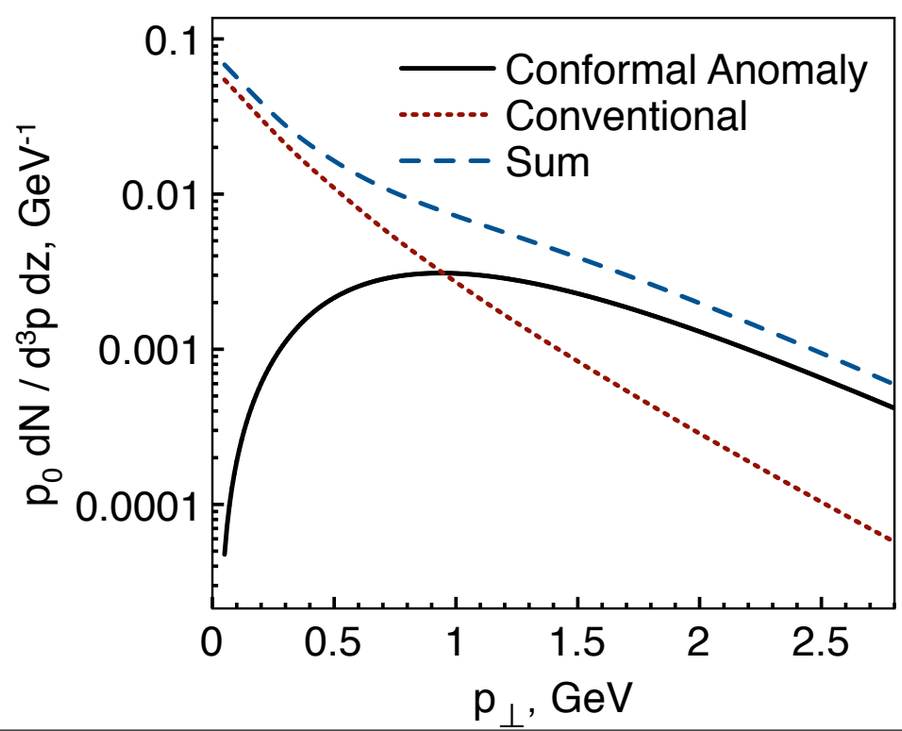

# DIS on GLASMA
# The tensor channel

Basar, Kharzeev, ES, in progress

$\vec{E}^2 - \vec{B}^2$ $\vec{E}^2 + \vec{B}^2$

# DIS on GLASMA
# The tensor channel

Basar, Kharzeev, ES, in progress

$\vec{E}^2 - \vec{B}^2$ $\vec{E}^2 + \vec{B}^2$

- Why $G^2$ and not $T_{\mu\nu}$? **Fermionic loop couples to both, and 2+ has more components**

# DIS on GLASMA
# The tensor channel

Basar, Kharzeev, ES, in progress

$\vec{E}^2 - \vec{B}^2$ $\vec{E}^2 + \vec{B}^2$

- Why $G^2$ and not $T_{\mu\nu}$? **Fermionic loop couples to both, and 2+ has more components**
- **Formfactors? B has energy $q^0$ of couple GeV, another photon can be virtual (=> dileptons)**

# DIS on GLASMA The tensor channel

Basar, Kharzeev, ES, in progress

$\vec{E}^2 - \vec{B}^2$ $\vec{E}^2 + \vec{B}^2$

- Why $G^2$ and not $T_{\mu\nu}$? **Fermionic loop couples to both, and 2+ has more components**
- **Formfactors? B has energy $q^0$ of couple GeV, another photon can be virtual (=> dileptons)**
- 2 OPE cases: (i) $\gamma\gamma$ hard, gg soft; (ii) $\gamma\gamma$ soft, gg hard. Calculation follows ES, Vainshtein **Nucl.Phys. B201 (1982) 141** and the result is not naive products of two stress tensors

$$L_{eff} = \Pi_{\mu\nu} A_\mu A_\nu$$

$$\Pi_{\mu\nu} = Tr(\gamma_\mu S(q,G)\gamma_\nu S^+(q,G))$$

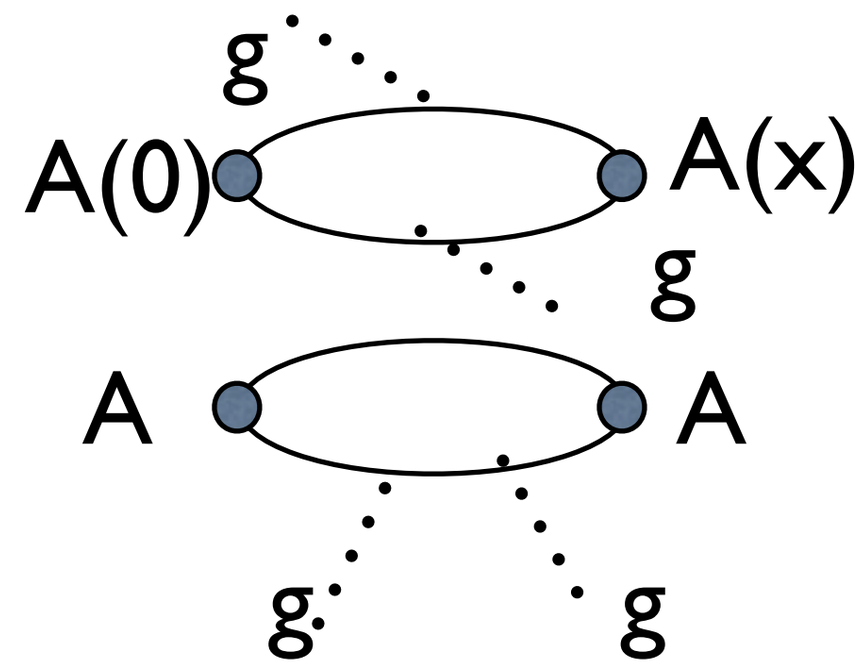

$$L_{eff} = \Pi_{\mu\nu} A_\mu A_\nu$$

$$\Pi_{\mu\nu} = Tr(\gamma_\mu S(q,G)\gamma_\nu S^+(q,G))$$

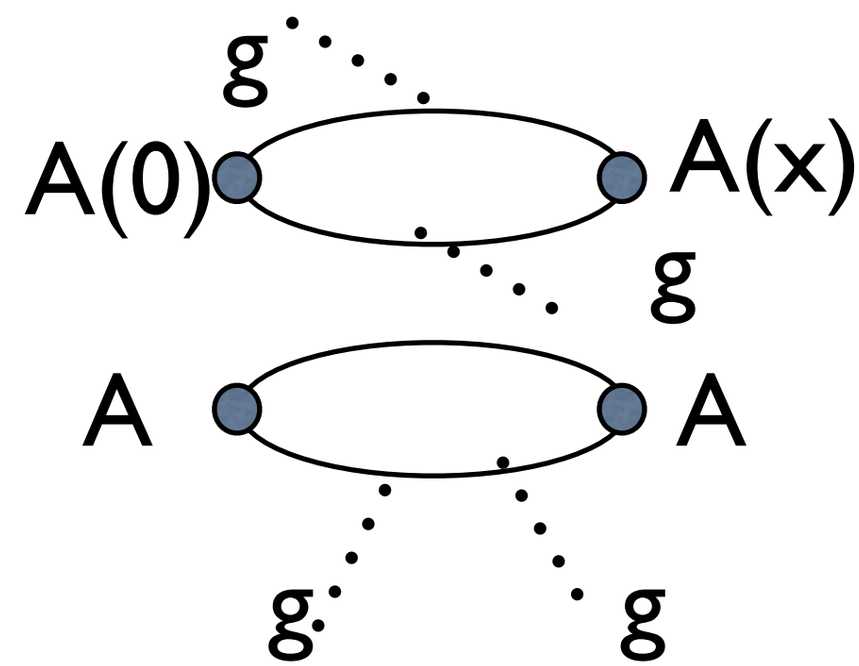


the usage of the so called fixed-point gauge

$$x_\mu A_\mu(x) = 0 \qquad (12)$$

invented by Fock, Schwinger and perhaps others. In this gauge $A_\mu(0) = 0$ and next order terms in $x$ expansion can be written as covariant derivatives of the field strength

$$A_\mu(x) = \sum_{k=0} \frac{1}{k!(k+2)} x_\nu x_{\alpha_1} \ldots x_{\alpha_k} (D_{\alpha_1} \ldots D_{\alpha_k} G_{\mu\nu}(0))$$

$$L_{eff} = \Pi_{\mu\nu} A_\mu A_\nu$$

$$\Pi_{\mu\nu} = Tr(\gamma_\mu S(q,G)\gamma_\nu S^+(q,G))$$

the usage of the so called fixed-point gauge

$$x_\mu A_\mu(x) = 0 \tag{12}$$

invented by Fock, Schwinger and perhaps others. In this gauge $A_\mu(0) = 0$ and next order terms in $x$ expansion can be written as covariant derivatives of the field strength

$$A_\mu(x) = \sum_{k=0} \frac{1}{k!(k+2)} x_\nu x_{\alpha_1} \dots x_{\alpha_k} (D_{\alpha_1} \dots D_{\alpha_k} G_{\mu\nu}(0))$$

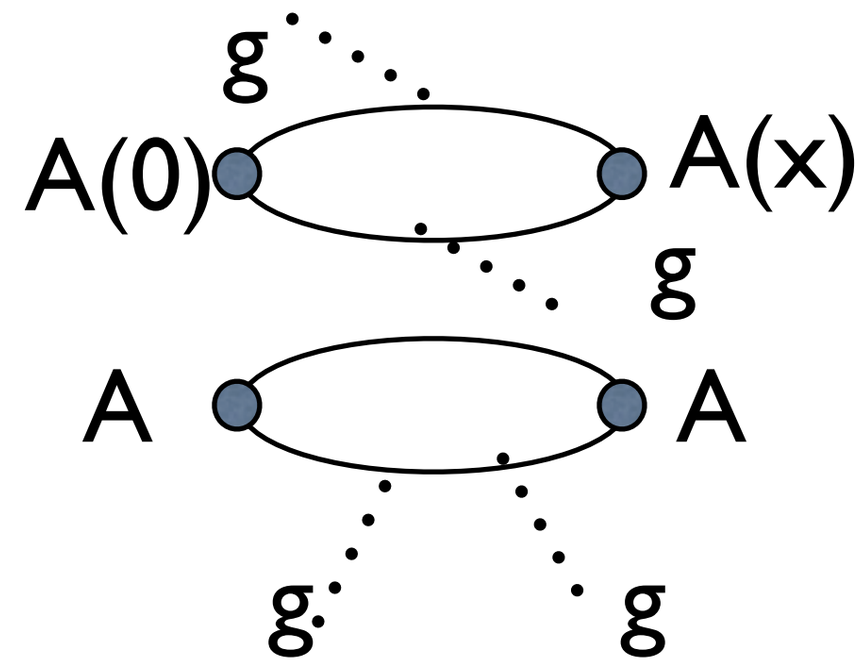


$$S(q) = \frac{1}{\hat{q}} - \frac{g}{2q^4} q_\alpha \tilde{G}_{\alpha\beta}\gamma_\beta\gamma_5$$

$$-\frac{g^2}{2q^8}\hat{q} q_\alpha G_{\alpha\beta} G_{\beta\gamma} q_\gamma + \frac{g^2}{4q^8} q^2 q_\alpha \{G_{\alpha\beta}, G_{\beta\gamma}\}_+ \gamma_\gamma$$

$$-\frac{g^2}{4q^8} q^2 q_\alpha [G_{\alpha\beta}, G_{\beta\gamma}]_- \gamma_\gamma + O(\frac{1}{q^6}) \tag{15}$$

$$L_{eff} = \Pi_{\mu\nu} A_\mu A_\nu$$

$$\Pi_{\mu\nu} = Tr(\gamma_\mu S(q,G)\gamma_\nu S^+(q,G))$$

the usage of the so called fixed-point gauge

$$x_\mu A_\mu(x) = 0 \tag{12}$$

invented by Fock, Schwinger and perhaps others. In this gauge $A_\mu(0) = 0$ and next order terms in $x$ expansion can be written as covariant derivatives of the field strength

$$A_\mu(x) = \sum_{k=0} \frac{1}{k!(k+2)} x_\nu x_{\alpha_1} \dots x_{\alpha_k} (D_{\alpha_1} \dots D_{\alpha_k} G_{\mu\nu}(0))$$

=> to x space
=> square (no integrals!)

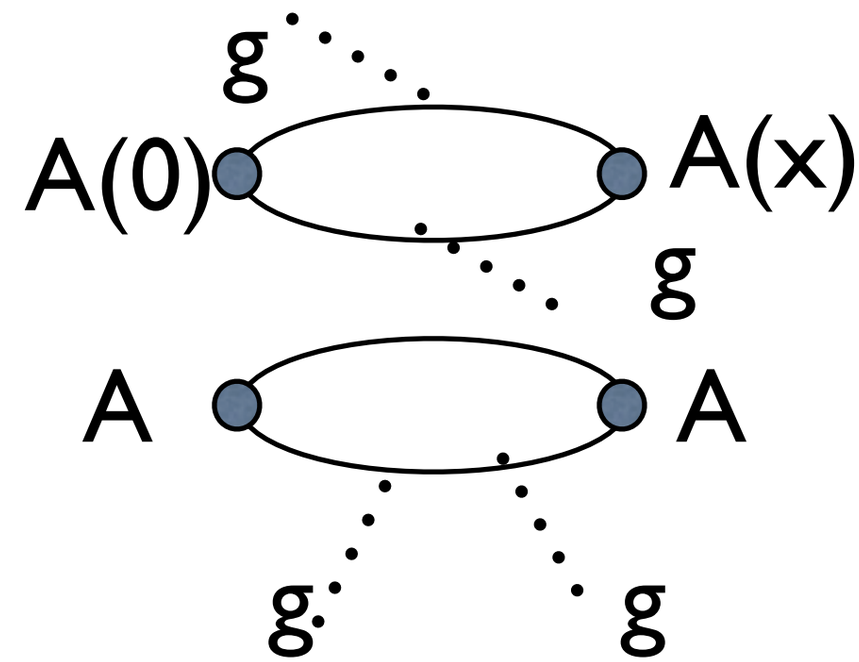


$$S(q) = \frac{1}{\hat{q}} - \frac{g}{2q^4} q_\alpha \tilde{G}_{\alpha\beta}\gamma_\beta\gamma_5$$

$$-\frac{g^2}{2q^8}\hat{q} q_\alpha G_{\alpha\beta} G_{\beta\gamma} q_\gamma + \frac{g^2}{4q^8} q^2 q_\alpha \{G_{\alpha\beta}, G_{\beta\gamma}\}_+ \gamma_\gamma$$

$$-\frac{g^2}{4q^8} q^2 q_\alpha [G_{\alpha\beta}, G_{\beta\gamma}]_- \gamma_\gamma + O(\frac{1}{q^6}) \tag{15}$$

$$L_{eff} = \Pi_{\mu\nu} A_\mu A_\nu$$

$$\Pi_{\mu\nu} = Tr(\gamma_\mu S(q,G)\gamma_\nu S^+(q,G))$$

the usage of the so called fixed-point gauge

$$x_\mu A_\mu(x) = 0 \tag{12}$$

invented by Fock, Schwinger and perhaps others. In this gauge $A_\mu(0) = 0$ and next order terms in $x$ expansion can be written as covariant derivatives of the field strength

$$A_\mu(x) = \sum_{k=0} \frac{1}{k!(k+2)} x_\nu x_{\alpha_1} \dots x_{\alpha_k} (D_{\alpha_1} \dots D_{\alpha_k} G_{\mu\nu}(0))$$

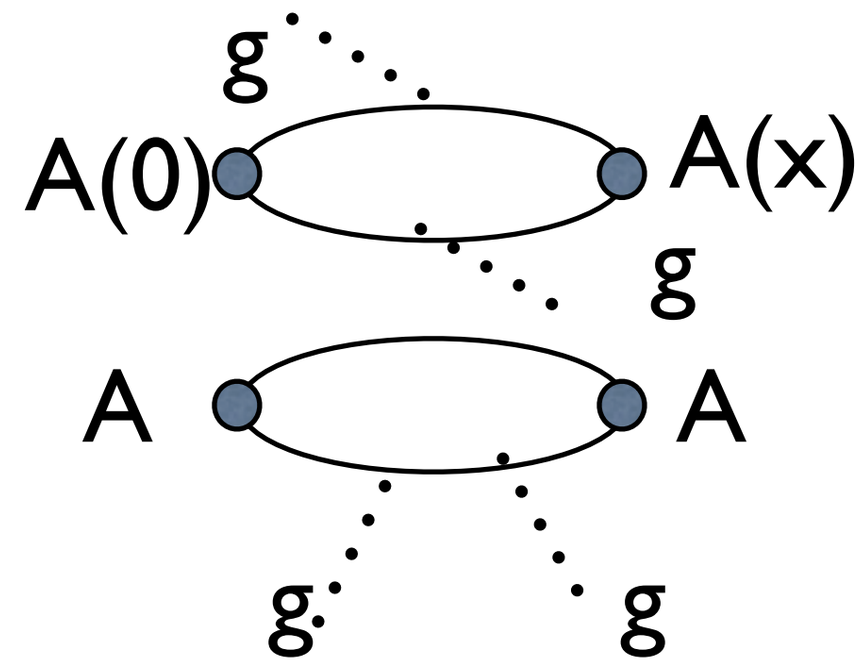


$$S(q) = \frac{1}{\hat{q}} - \frac{g}{2q^4} q_\alpha \tilde{G}_{\alpha\beta}\gamma_\beta\gamma_5$$

$$-\frac{g^2}{2q^8}\hat{q} q_\alpha G_{\alpha\beta} G_{\beta\gamma} q_\gamma + \frac{g^2}{4q^8} q^2 q_\alpha \{G_{\alpha\beta}, G_{\beta\gamma}\}_+ \gamma_\gamma$$

$$-\frac{g^2}{4q^8} q^2 q_\alpha [G_{\alpha\beta}, G_{\beta\gamma}]_- \gamma_\gamma + O(\frac{1}{q^6}) \tag{15}$$

=> to x space
=> square (no integrals!)

we have local effective interaction GG AA/q4 which of course preserve both gauge invariances

# PHENIX photons

pQCD describes the pp case

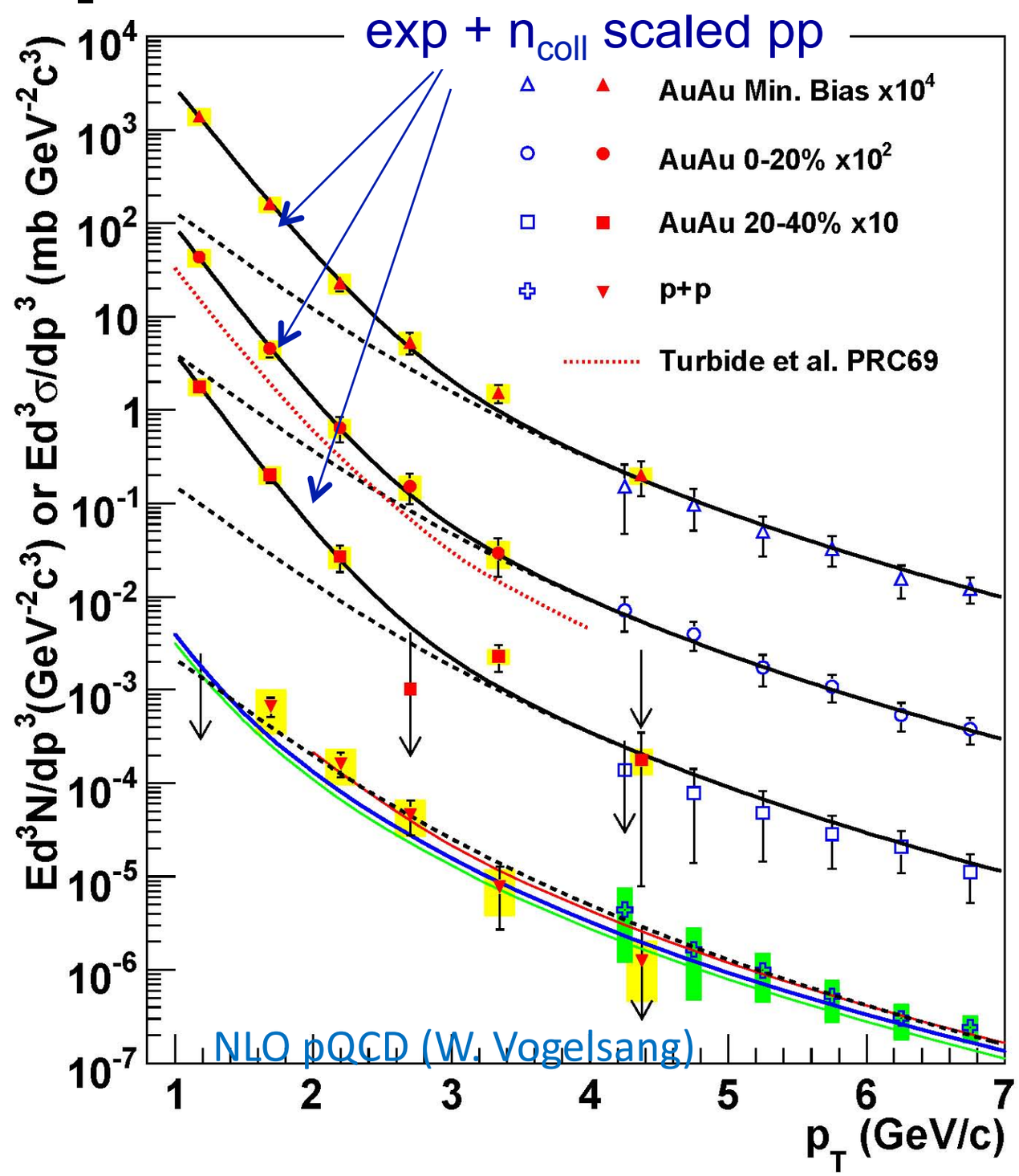

# PHENIX photons

pQCD describes the pp case

Note that Turbide et al miss a factor 2..3 in the rate.
Hadronic rate is calculated from a gas of pions,K,rho,K*, A1 plus baryons (rho-N resonances)
QGP rate is the HTL-corrected QCD Compton

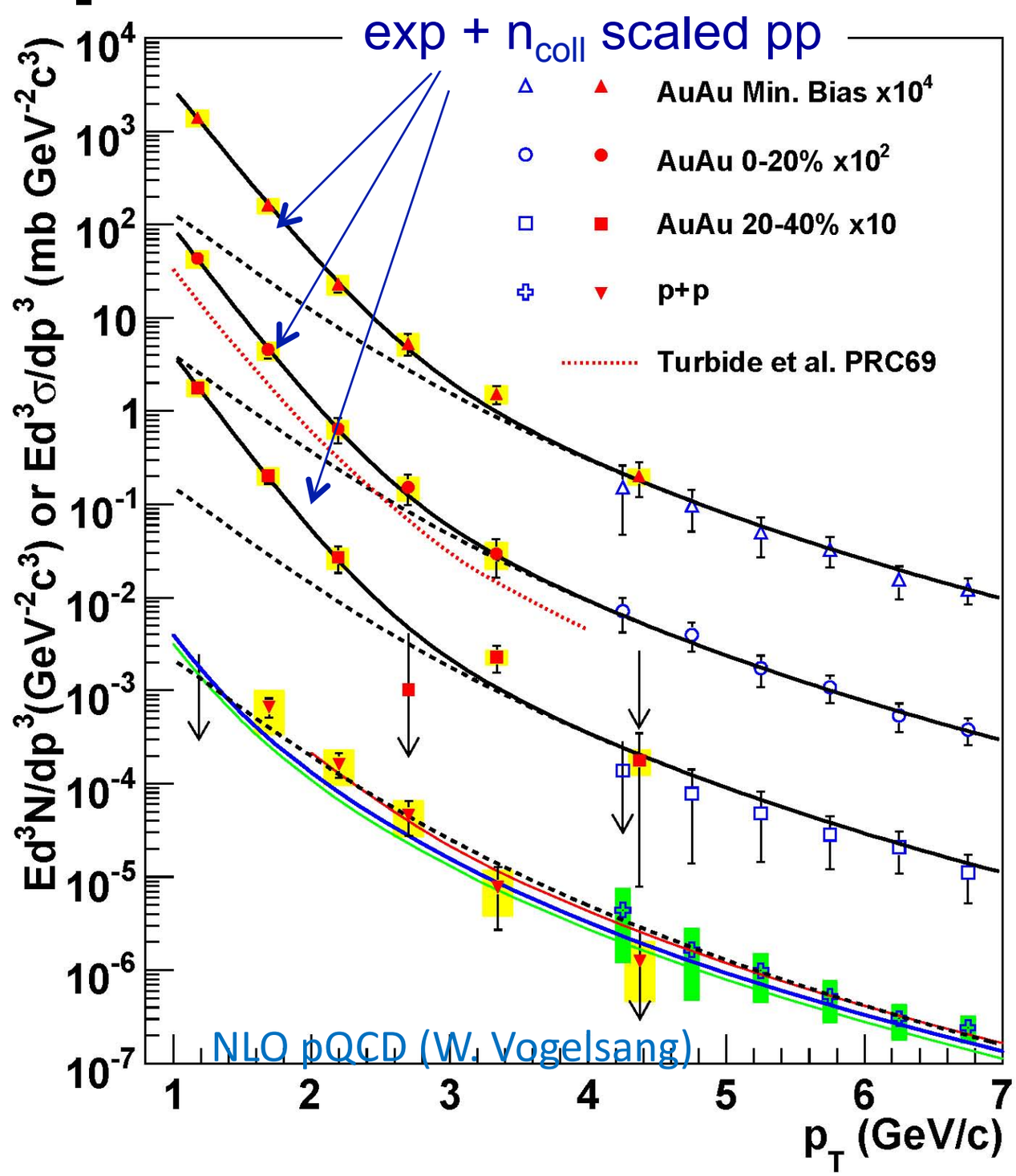

Kevin Dusling[a] and Ismail Zahed[b]

ArXiv: 0911.2426

# Are the rates too small?

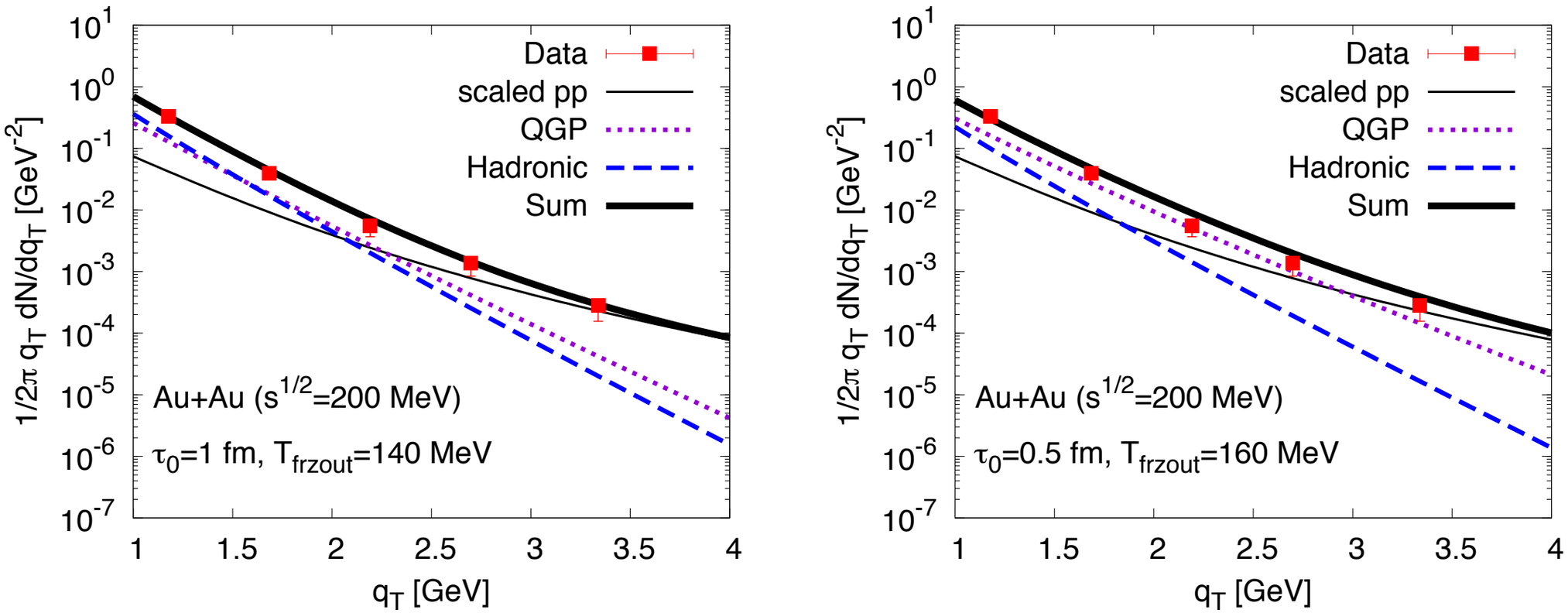


'IG. 9: Photon spectra at RHIC compared to the recent PHENIX data. The left plot is the volution set RHIC 1 and the right is for R

seems OK in this work, but this is for alpha_s=0.75!

# photons from QGP

(my original QGP paper, 1978) +HTL completion to it (Kapusta et al,PRD44,1991)

$$gq \to q\gamma, qq \to g\gamma \qquad q_0 \frac{dR_\gamma}{d^3q} = \frac{6}{9}\frac{\alpha\alpha_S}{2\pi^2}T^2 \mathrm{e}^{-q_0/T} \ln\left(1 + \frac{2.912}{4\pi\alpha_s}\frac{q_0}{T}\right) ,$$

# photons from QGP

(my original QGP paper, 1978) +HTL completion to it (Kapusta et al,PRD44,1991)

$$gq \to q\gamma, qq \to g\gamma \qquad q_0 \frac{dR_\gamma}{d^3q} = \frac{6}{9}\frac{\alpha\alpha_S}{2\pi^2}T^2 \mathrm{e}^{-q_0/T} \ln\left(1 + \frac{2.912}{4\pi\alpha_s}\frac{q_0}{T}\right) ,$$

- perturbative rescattering+LPM effect: Arnold, Moor, Yaffe arXiv: 0204343, roughly factor 2-3 smooth enhancement for pt>1 GeV, Teaney et al 2012 next order

# photons from QGP

(my original QGP paper, 1978) +HTL completion to it (Kapusta et al,PRD44,1991)

$$gq \to q\gamma, qq \to g\gamma \qquad q_0 \frac{dR_\gamma}{d^3q} = \frac{6}{9}\frac{\alpha\alpha_S}{2\pi^2}T^2 \mathrm{e}^{-q_0/T} \ln\left(1 + \frac{2.912}{4\pi\alpha_s}\frac{q_0}{T}\right) ,$$

- perturbative rescattering+LPM effect: Arnold, Moor, Yaffe arXiv: 0204343, roughly factor 2-3 smooth enhancement for pt>1 GeV, Teaney et al 2012 next order

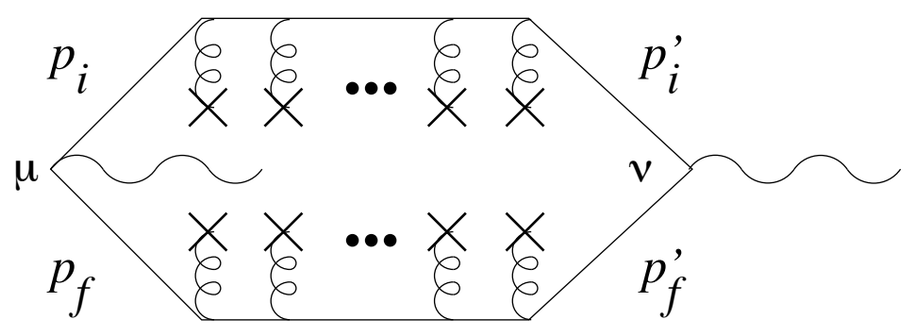

# photons from QGP

(my original QGP paper, 1978) +HTL completion to it (Kapusta et al,PRD44,1991)

$$gq \to q\gamma, qq \to g\gamma \qquad q_0 \frac{dR_\gamma}{d^3q} = \frac{6}{9}\frac{\alpha\alpha_S}{2\pi^2}T^2 \mathrm{e}^{-q_0/T} \ln\left(1 + \frac{2.912}{4\pi\alpha_s}\frac{q_0}{T}\right) ,$$

- perturbative rescattering+LPM effect: Arnold, Moor, Yaffe arXiv: 0204343, roughly factor 2-3 smooth enhancement for pt>1 GeV, Teaney et al 2012 next order

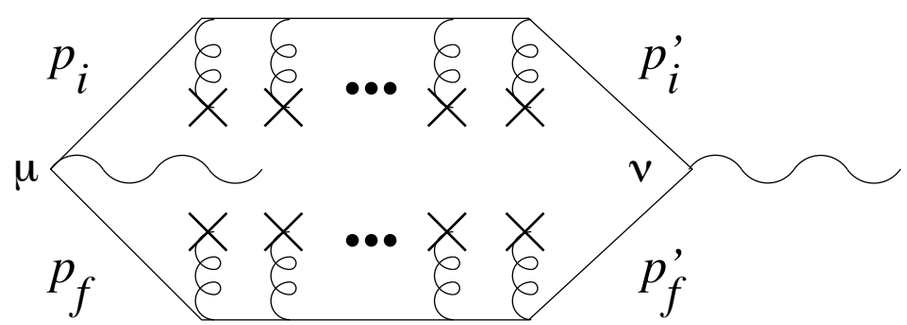


may work at large pt,
otherwise pQCD series does not converge
perhaps, strong coupling methods needed

# should there be extra contribution to the perturbative photon radiation rates?

(one expects it for e.g. **viscosities)**

# should there be extra contribution to the perturbative photon radiation rates?

(one expects it for e.g. **viscosities)**

- In QGP T> Tc large density of (color-magnetic) **monopoles** appear(which are not bose-condenced)

# should there be extra contribution to the perturbative photon radiation rates?

(one expects it for e.g. **viscosities)**

- In QGP T> Tc large density of (color-magnetic) **monopoles** appear(which are not bose-condenced)
- They are real quasiparticles and qM , gM scattering has been calculated and it needs to be included (Ratti,ES 2008)

# should there be extra contribution to the perturbative photon radiation rates?

(one expects it for e.g. **viscosities)**

- In QGP T> Tc large density of (color-magnetic) **monopoles** appear(which are not bose-condenced)
- They are real quasiparticles and qM , gM scattering has been calculated and it needs to be included (Ratti,ES 2008)
- Same with electomagnetic rates

# monopoles contribute to viscosities, via large angle scattering

$$\vec{B} = g\frac{\vec{r}}{r^3}.$$

$$m\frac{d^2\vec{r}}{dt^2} = e\vec{v}\times\vec{B} = \frac{eg}{r^3}\frac{d\vec{r}}{dt}\times\vec{r};$$

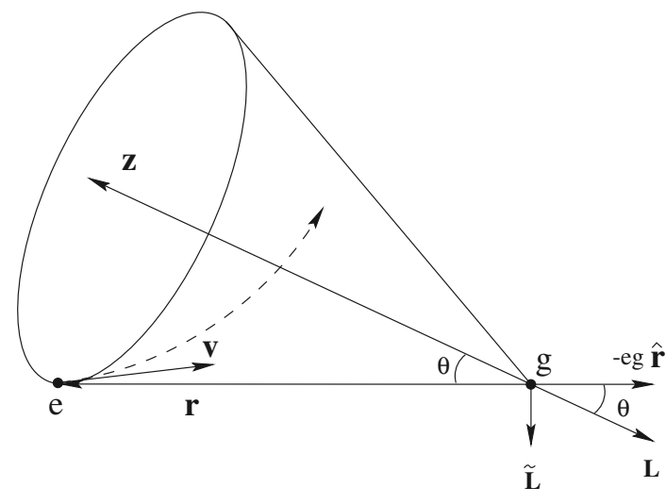


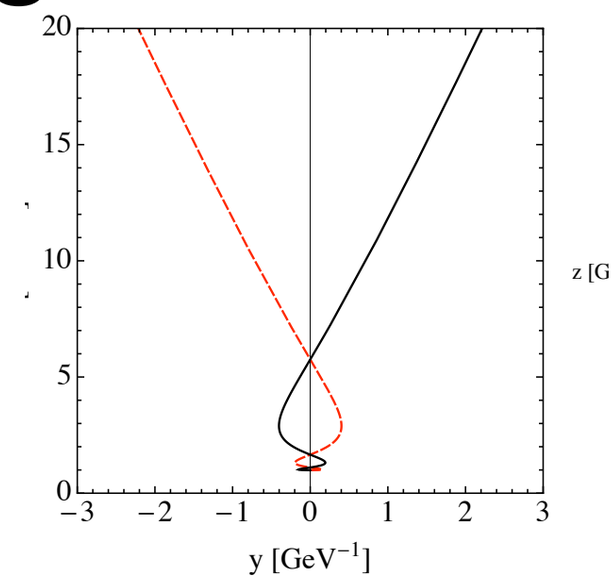


PHYSICAL REVIEW D **80,** 034004 (2009)

**Role of monopoles in a gluon plasma** The motion of an electric charge in the field of a magnetic monopole.

Claudia Ratti and Edward Shuryak*
*nomy, State University of New York at Stony Brook, Sto*
(Received 4 February 2009; published 5 August 2009)

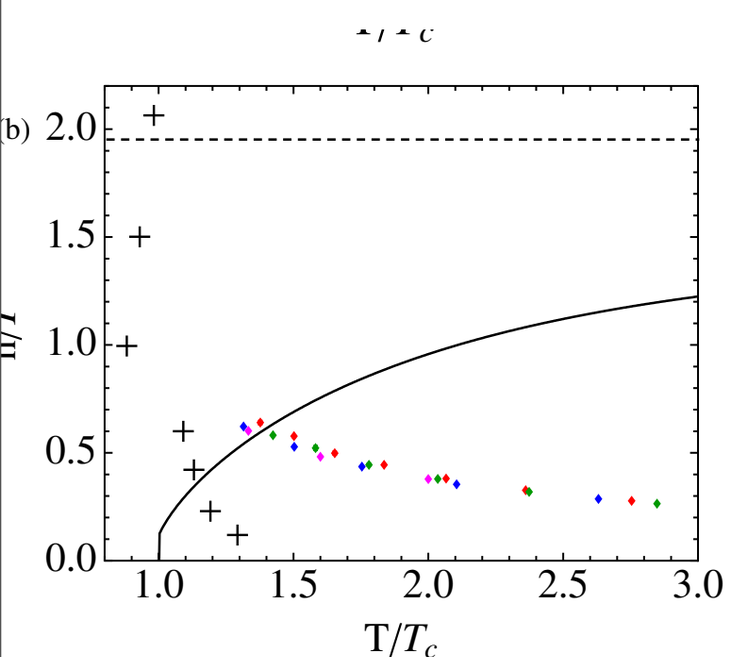


ROLE OF MONOPOLES IN A GLUON PLASMA PHYSICAL REVIEW D **80,** 034004 (2009)

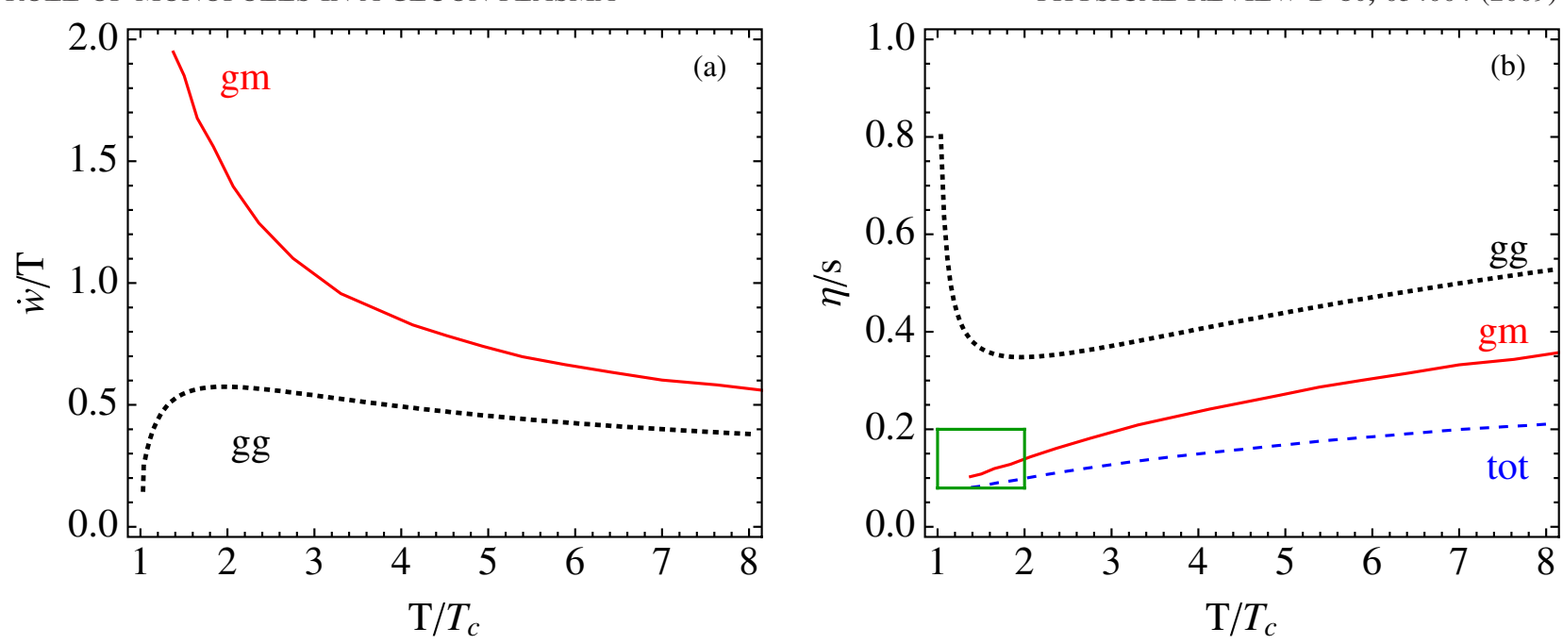


FIG. 15 (color online). (a) gluon-monopole and gluon-gluon scattering rates. (b) gluon-monopole and gluon-gluon viscosity over entropy ratio, $\eta/s$. The blue, dashed curve is the total $\eta/s$, which is evaluated from the $gg$ and $gm$ contributions. The green box represents the present estimate of $\eta/s$ in the RHIC temperature regime.

# monopoles contribute to the photon radiation:

arXiv:0910.1067v1 [hep-ph] 6 Oct 2009

Radiation of an electric charge in the field of a magnetic monopole

Michael Lublinsky[a,b], Claudia Ratti[a,c], Edward Shuryak[a]

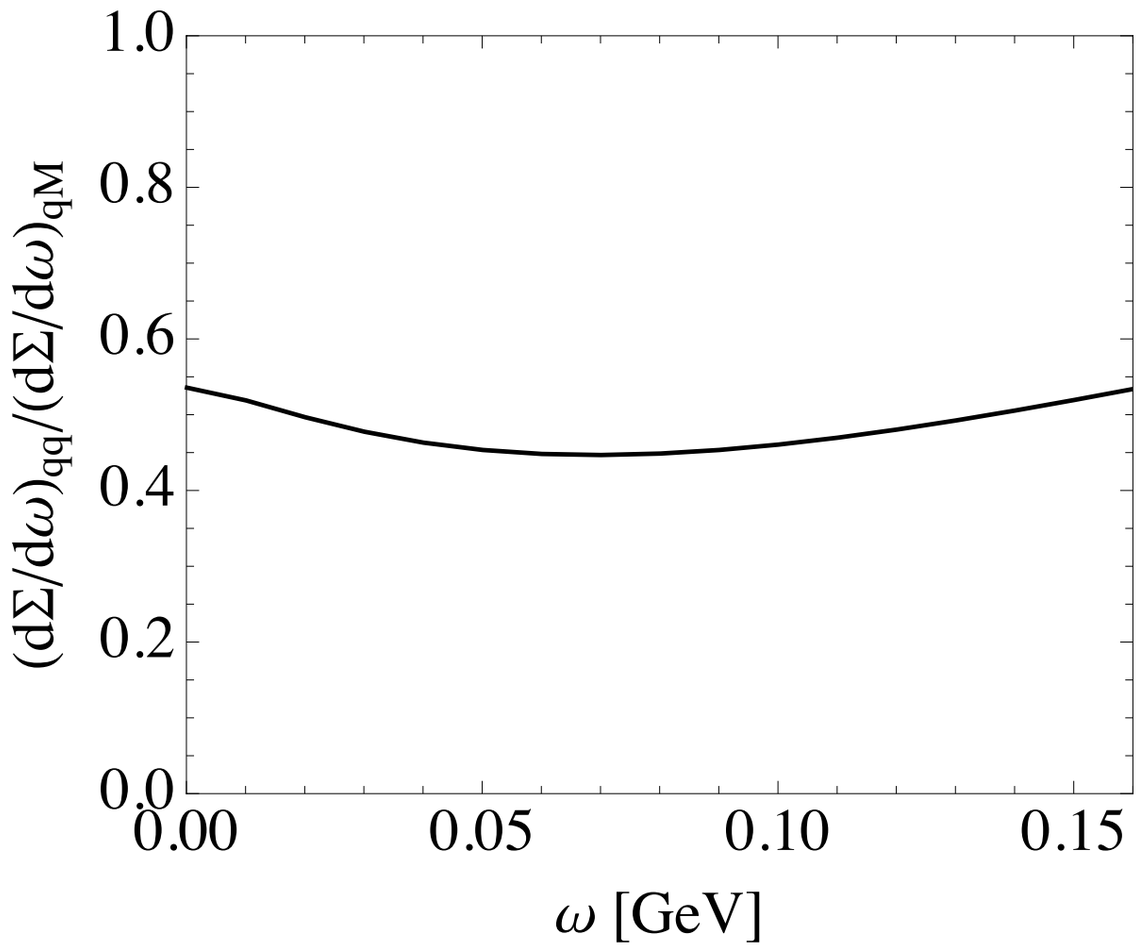


disclaimer:
only soft photons
calculated classically
from the trajectories

qM rate in RHIC condition
is about twice that for qq
(=> qq gamma)

# comments about chiral symmetry restoration

- Kapusta+ES, 1993 Weiberg-type sum rules for <VV-AA> correlator (Rapp revived recently)
- yet it was unclear how pion,rho,A1,rho' move as T grows (hard on the lattice as Matsubara box shrinks), e.g. rho=>pi, rho'=>A1 (Brown-Rho); or **no pion, rho=>A1**; or nobody moves and **all melt (???)**
- lattice thermodynamics, especially mu-derivatives suggest BARYONS get heavier. The **mass LR term disappears** but energy (LL+RR) appear and compensates

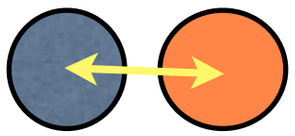

chiral breaking is due to small subset of states, ZMZ and its width is small (ES,1982)

given by the magnitude of the hopping from one instanton to the next

$$T_{I\bar{I}} \sim \frac{\rho^2}{R^3} \sim \frac{(0.3fm)^2}{(1fm)^3} \sim 20MeV$$

- people found it on the lattice and showed pions are completely described by ZMZ
- that is why quark mass dependence is nontrivial, and chiral perturbation

# recently the opposite exercise was done by the Graz group

**Symmetries of hadrons after unbreaking the chiral symmetry**

L. Ya. Glozman,* C. B. Lang,† and M. Schröck‡
*Institut für Physik, FB Theoretische Physik, Universität Graz, A–8010 Graz, Austria*

arXiv:1205.4887v3 [hep-lat] 19 Jul 2012

By eliminating narrow band of modes 1/10000 one finds that **A1 moves down while rho only slightly go up**

near-perfect chiral pairs are left, nearly the same in average => thus resonance gas works

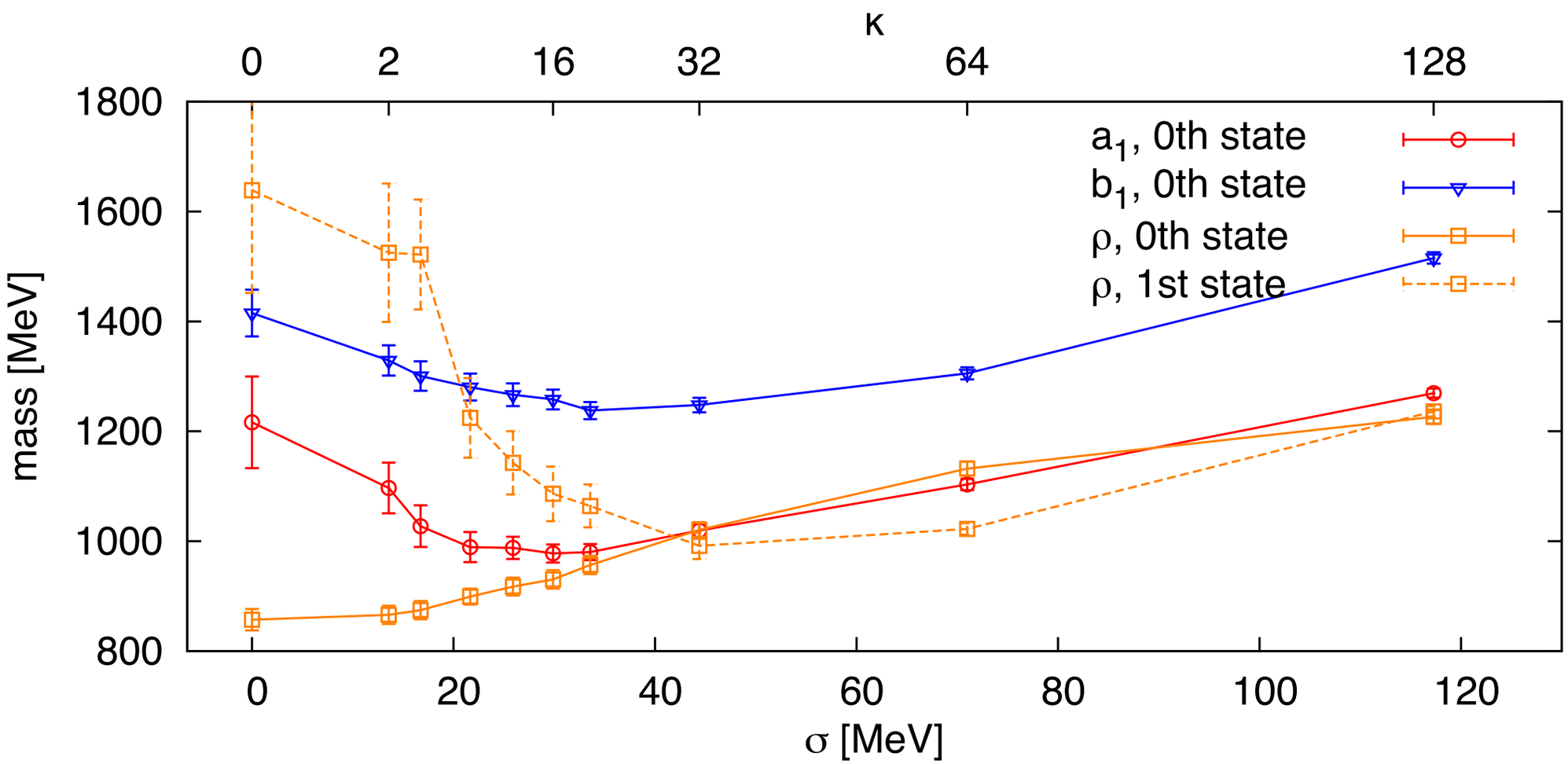

# summary

# summary

- penetrating probes remain on the front line of our field for 30 years. While basic QGP/hydro/rate scenario works, there is no shortage of experimental surprises and new ideas

# summary

- penetrating probes remain on the front line of our field for 30 years. While basic QGP/hydro/rate scenario works, there is no shortage of experimental surprises and new ideas

- dileptons: M is a clock, if 2-3 GeV early QGPif GLASMA perhaps suppression /higherT **polarization as measure of pressure isotropy**

# summary

- penetrating probes remain on the front line of our field for 30 years. While basic QGP/hydro/rate scenario works, there is no shortage of experimental surprises and new ideas

- dileptons: M is a clock, if 2-3 GeV early QGPif GLASMA perhaps suppression /higherT **polarization as measure of pressure isotropy**

- photons: small (nonpert) viscosity=> large (nonpert) gamma radiation rates.

# summary

- penetrating probes remain on the front line of our field for 30 years. While basic QGP/hydro/rate scenario works, there is no shortage of experimental surprises and new ideas
- dileptons: M is a clock, if 2-3 GeV early QGPif GLASMA perhaps suppression /higherT **polarization as measure of pressure isotropy**
- photons: small (nonpert) viscosity=> large (nonpert) gamma radiation rates.
- v2 <= need to calculate all fermion loop effects

# summary

- penetrating probes remain on the front line of our field for 30 years. While basic QGP/hydro/rate scenario works, there is no shortage of experimental surprises and new ideas
- dileptons: M is a clock, if 2-3 GeV early QGPif GLASMA perhaps suppression /higherT **polarization as measure of pressure isotropy**
- photons: small (nonpert) viscosity=> large (nonpert) gamma radiation rates.
- v2 <= need to calculate all fermion loop effects
- example: interplay of strong **coherent QED fields** with partonic reactions, including **virtual quark loops**

# Anisotropy of photon production in magnetic field

Vladimir Skokov

BROOKHAVEN NATIONAL LABORATORY

G. Basar, D. Kharzeev, V.S., arXiv:1206.1334
A. Bzdak, V.S., arXiv:1208.5502

Thermal radiation workshop; December 6, 2012

# Outline

- motivation: photon puzzle
  measurements vs expectations

- possible solutions:
  “hadronic”
  “partonic” + magnetic field

- magnetic field in heavy-ion collisions:
  essential properties: magnitude, lifetime, b-dependence
  natural source of anisotropy

- photon production and magnetic field:
  results & possible experimental signatures

# Experimental facts about γ

- transverse momentum spectrum

  $T_{ave}$ = 221 MeV ➙

  $T_{ini}$ = 300 to 600 MeV $\tau_0$ = 0.15 to 0.6 fm/c

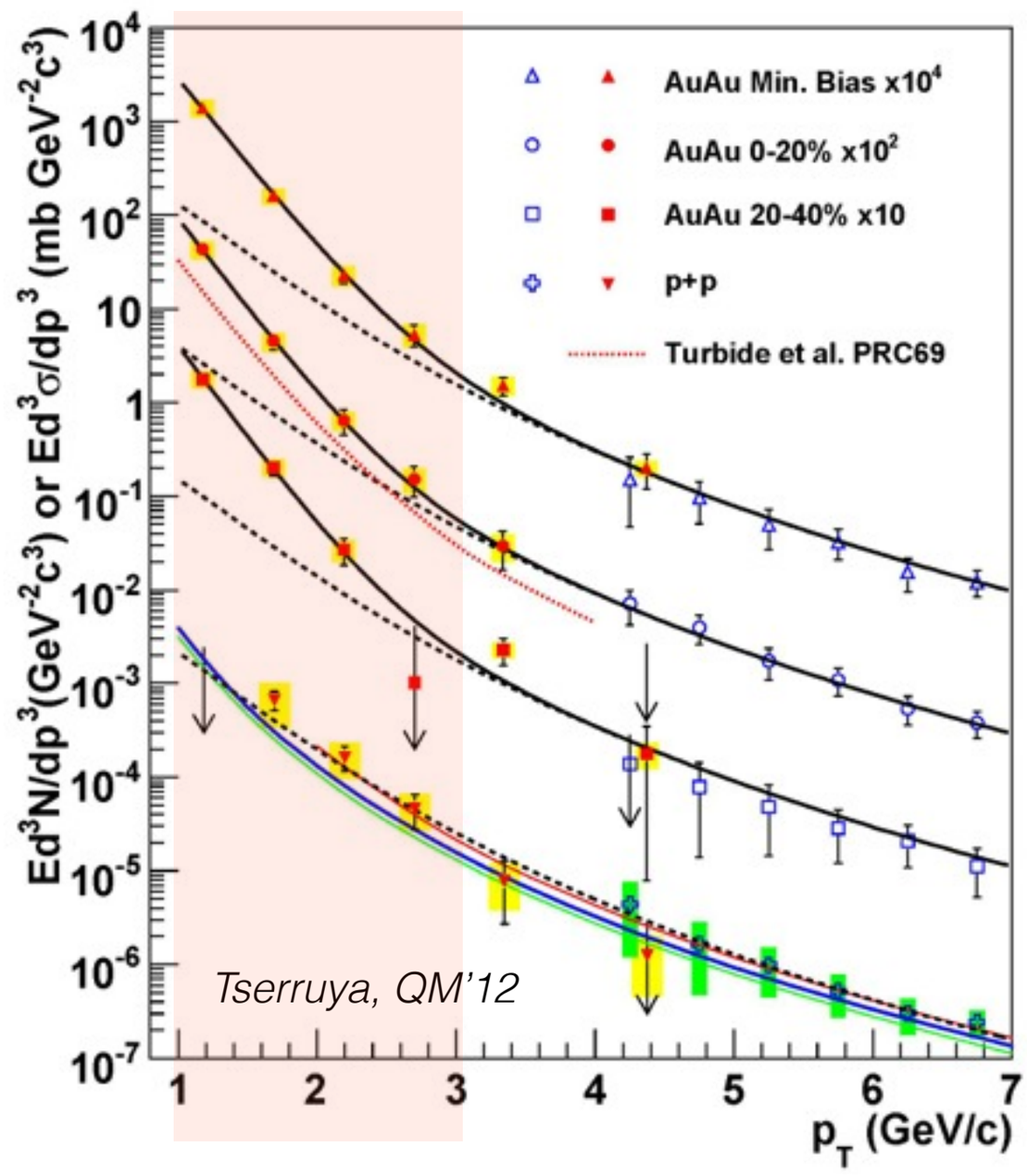

# Azimuthal anisotropy

- Direct photons:

*PHENIX*

- Hadrons:

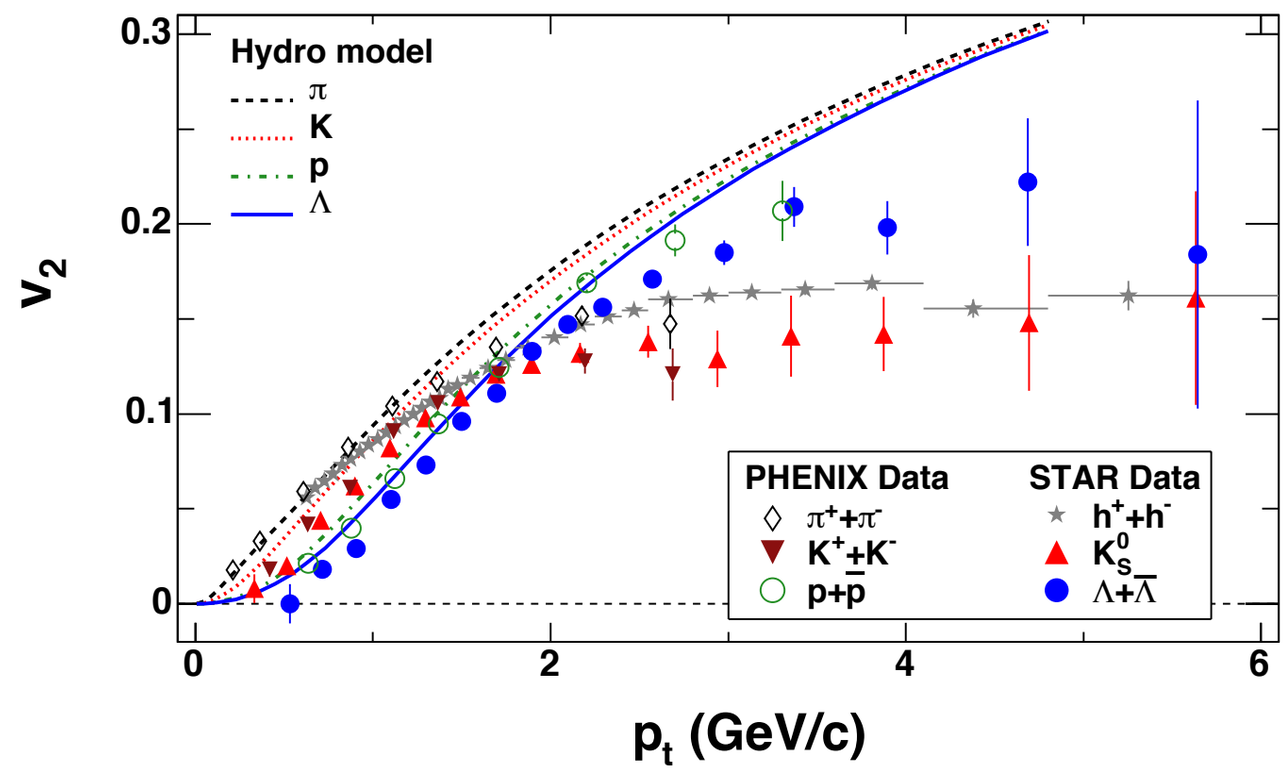

# Azimuthal anisotropy

- Direct photons:

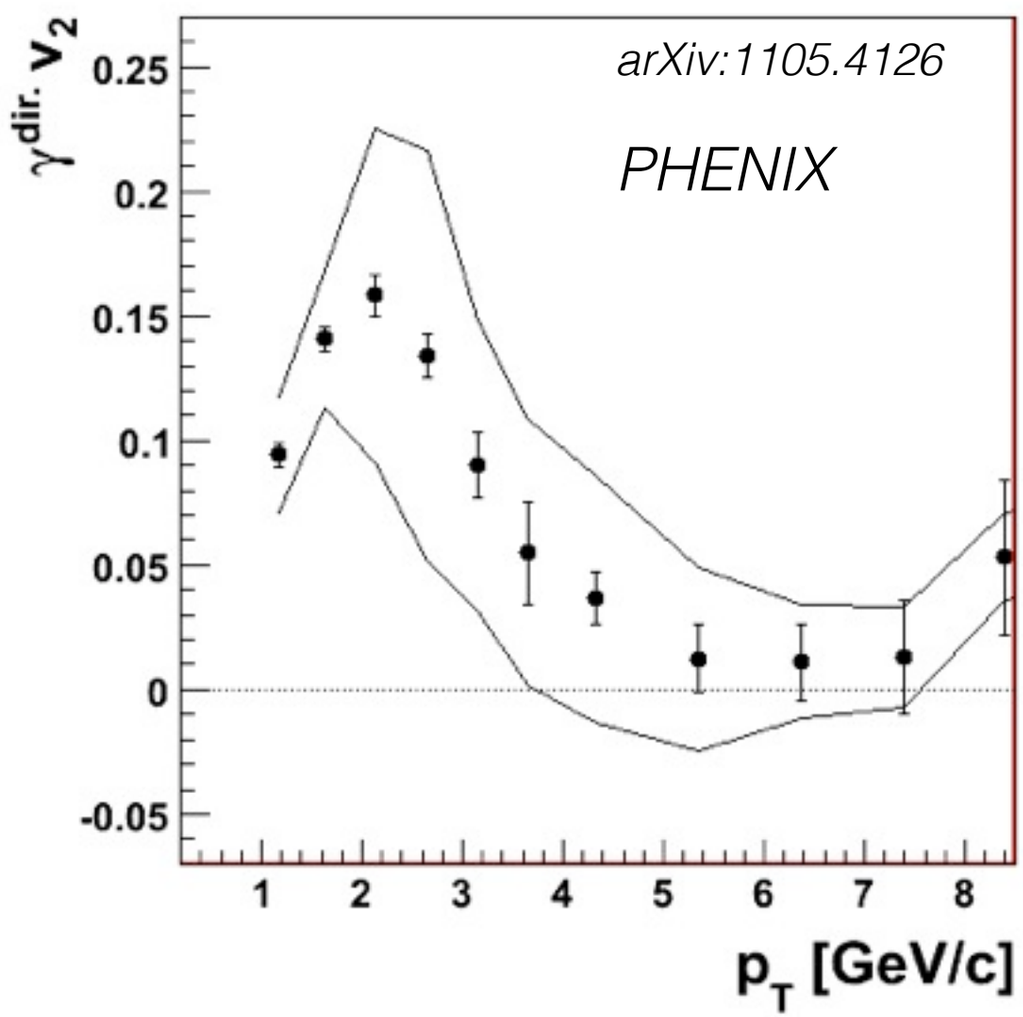


- Hadrons:

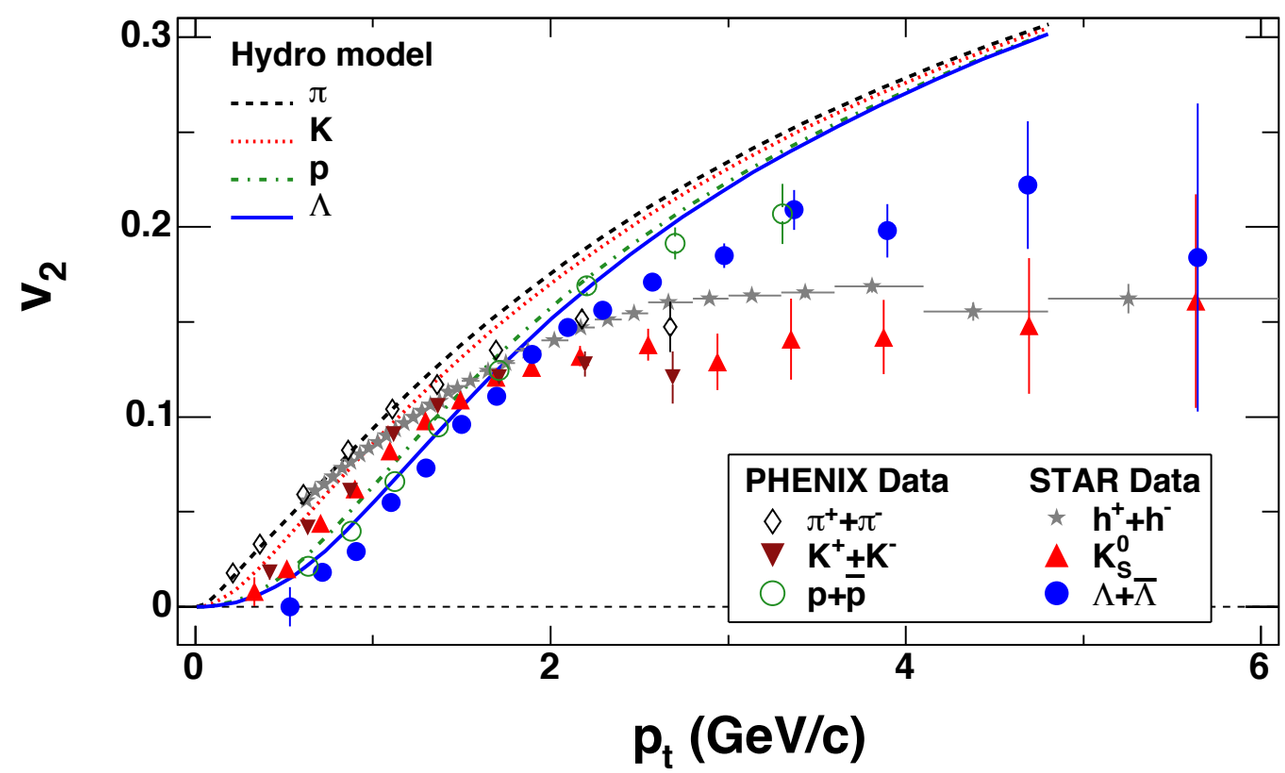

# Azimuthal anisotropy:LHC

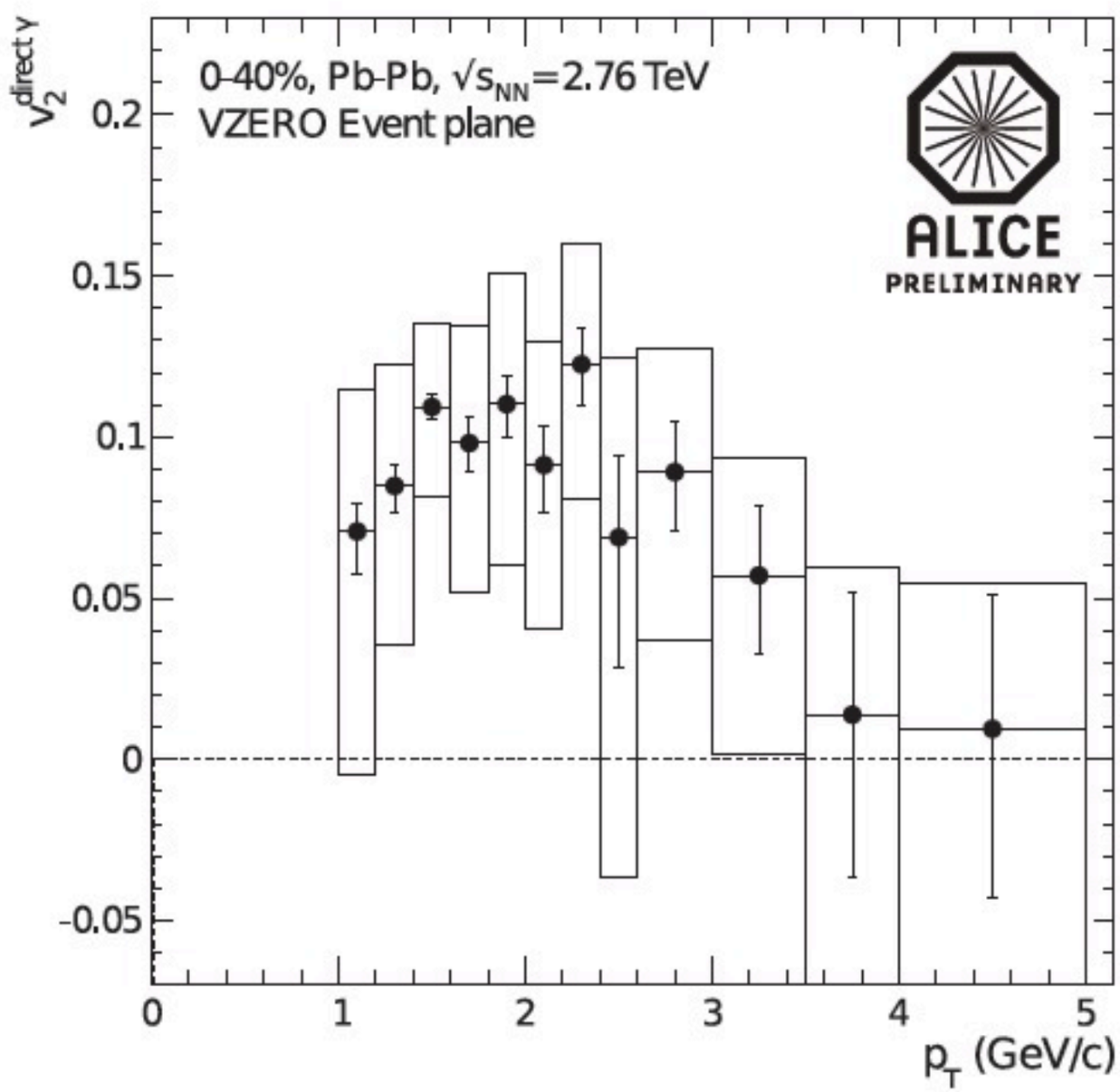


Daniel Lohner, Hot Quarks 2012

# Theory: Hydrodynamics

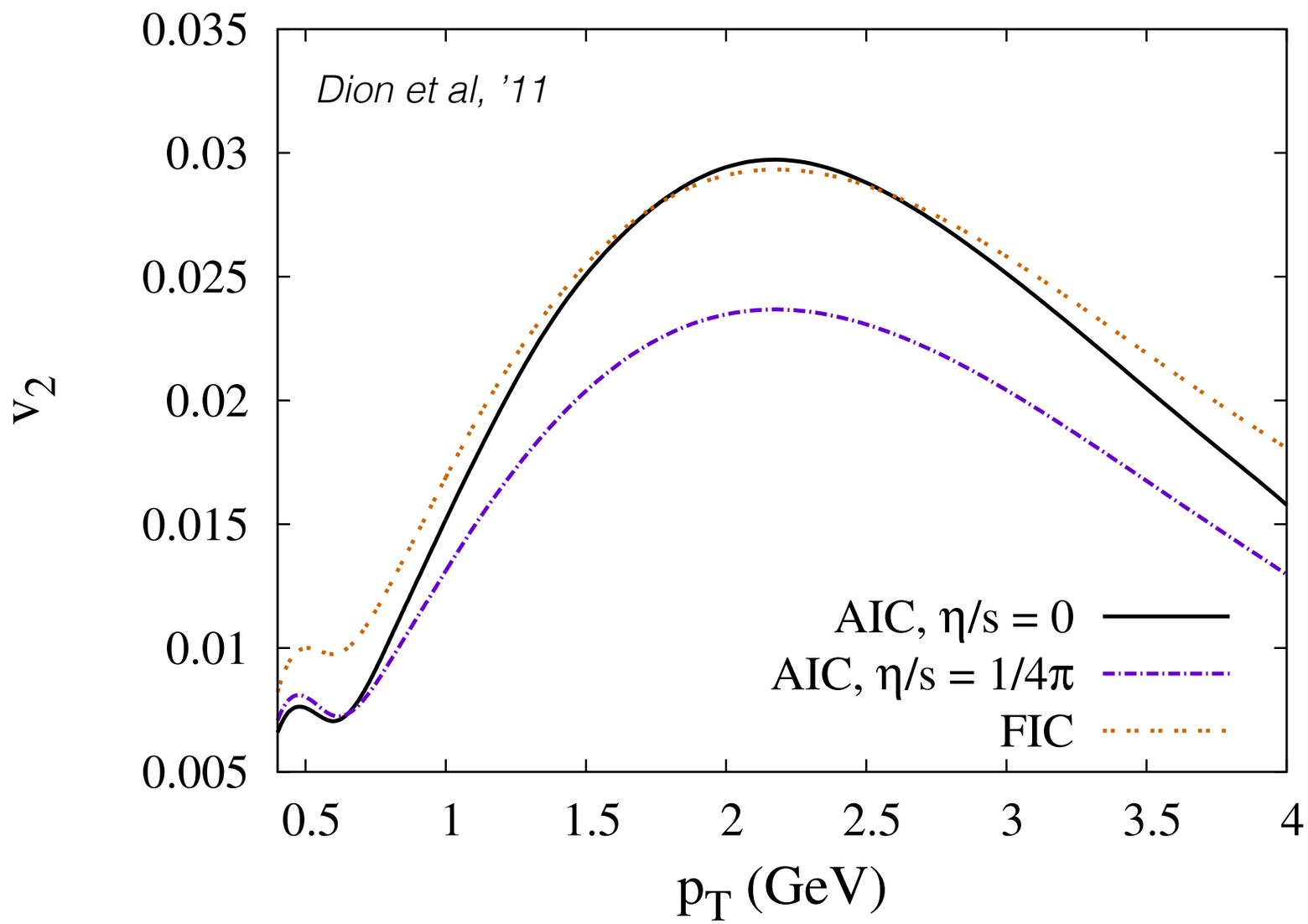


Hydro:
**5 times** smaller $v_2$
then in experiment

AIC: averaged initial conditions
FIC: fluctuating initial conditions

Large photon $v_2$ is difficult to explain with dominant QGP source

# Another source of anisotropy?

- anisotropy ≠ flow!
- other sources for anisotropy not related to flow?!
- magnetic field?! Perfect candidate for anisotropic photon production.

# Magnetic field in HIC I

- spectators form two currents

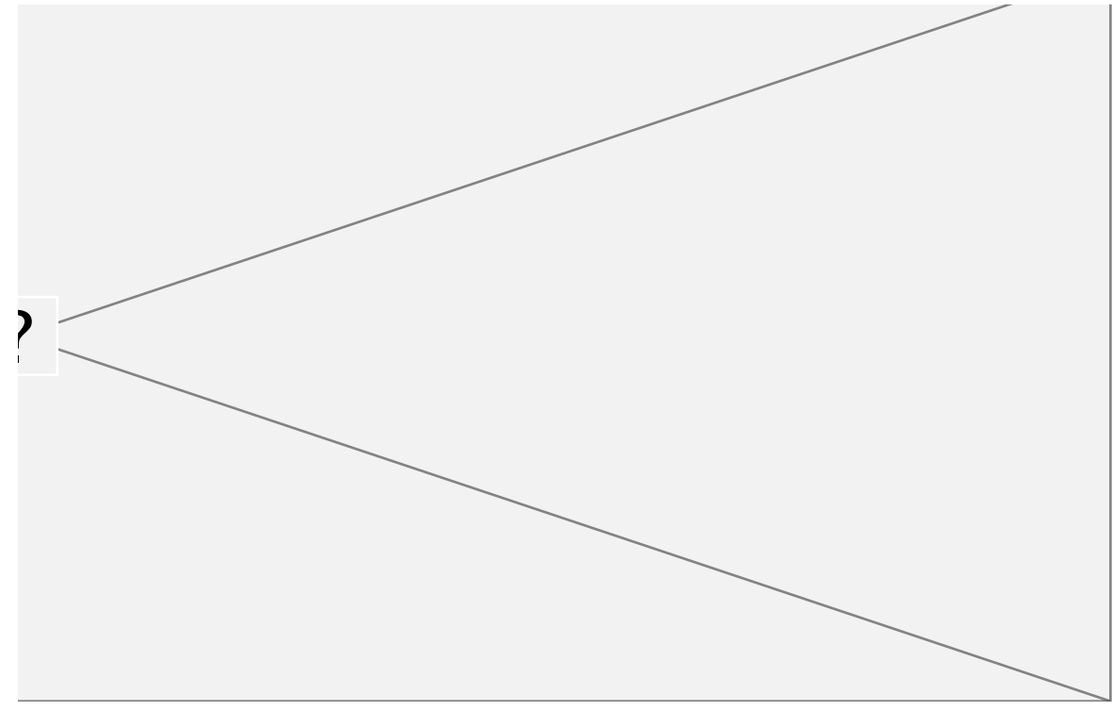

- resulting event average magnetic field
  $\langle eB_y \rangle \sim m_\pi^2$ (out-plane)
  $\langle eB_x \rangle \sim 0$ (in-plane)

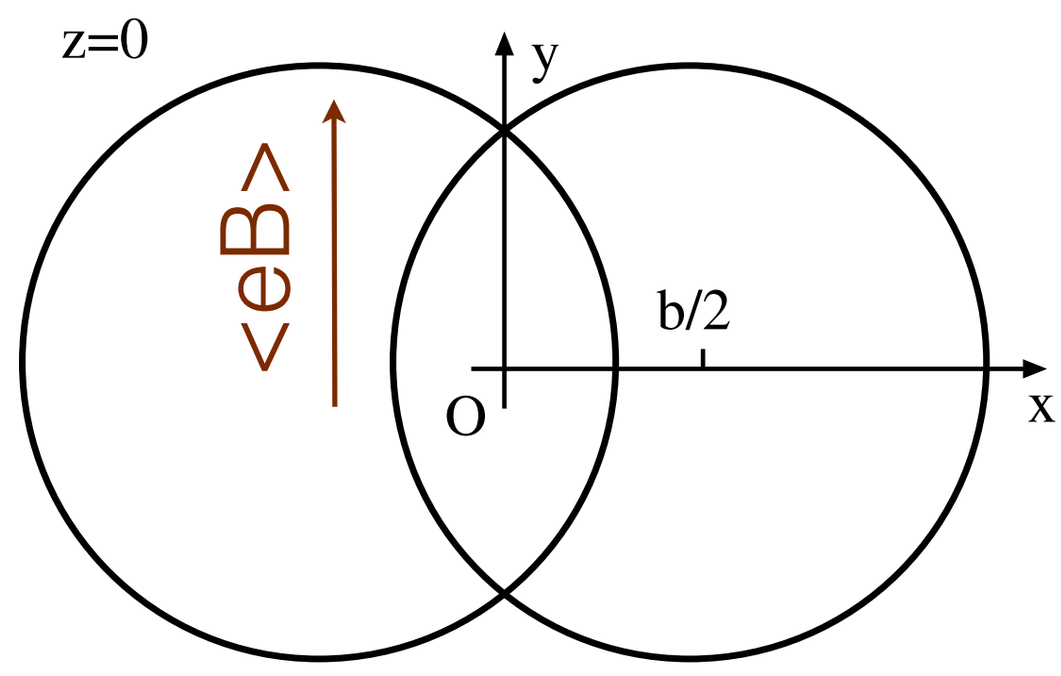

# Magnetic field in HIC II

- maximal eB ~ √s
- maximum at $t_M$ ~ 1/ √s
- life time $t_{lt}$ ~ 1/ √s
- integral ~ const

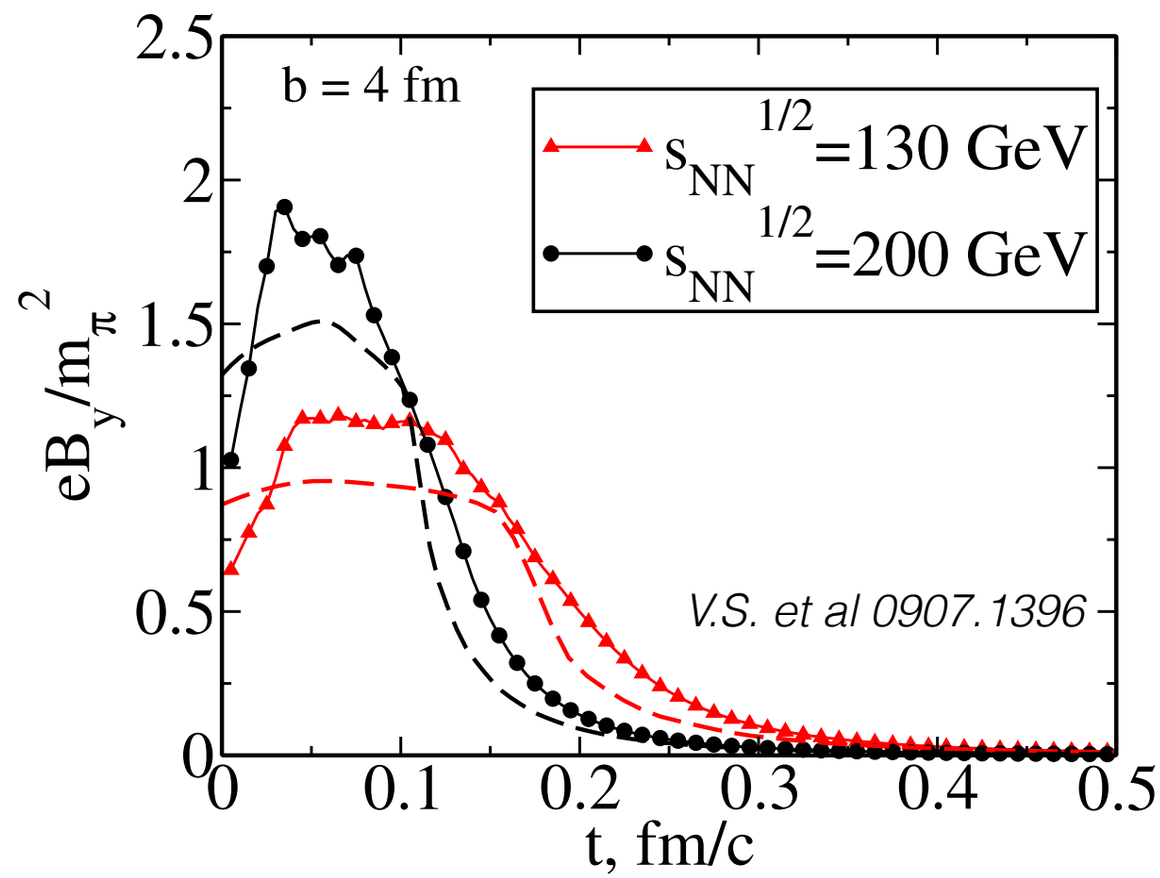


*D. Kharzeev, L. McLerran, H. Warringa, 0711.0950*
*V.S. et al, 0907.1396*

# Magnetic field in HIC III

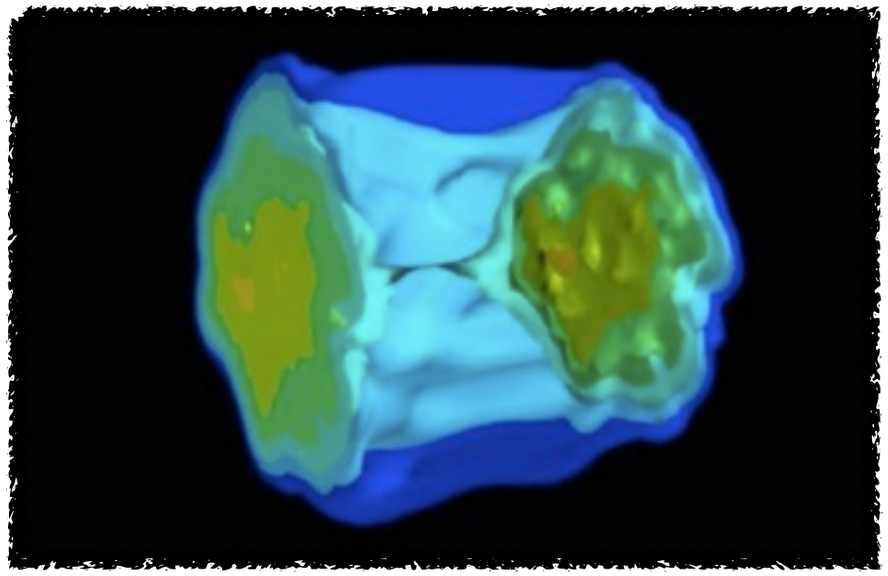

- fluctuations can play important role

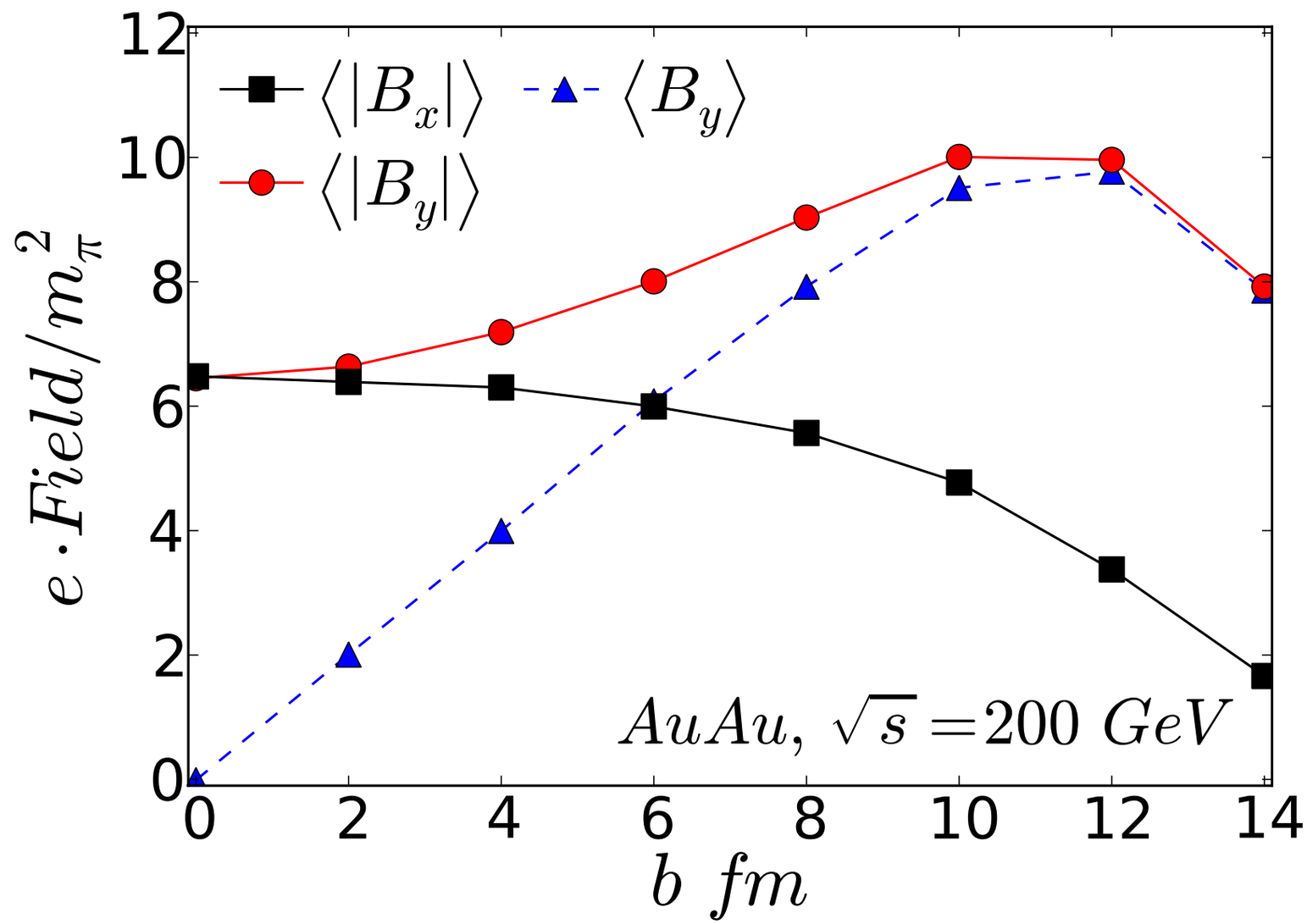


- lumpy distribution of electric charge in colliding nuclei results in nonzero randomly oriented magnetic field even in central collisions

*V.S. et al, 0907.1396;*
*A. Bzdak and V.S., 1111.1949*

# Magnetic field in HIC IV

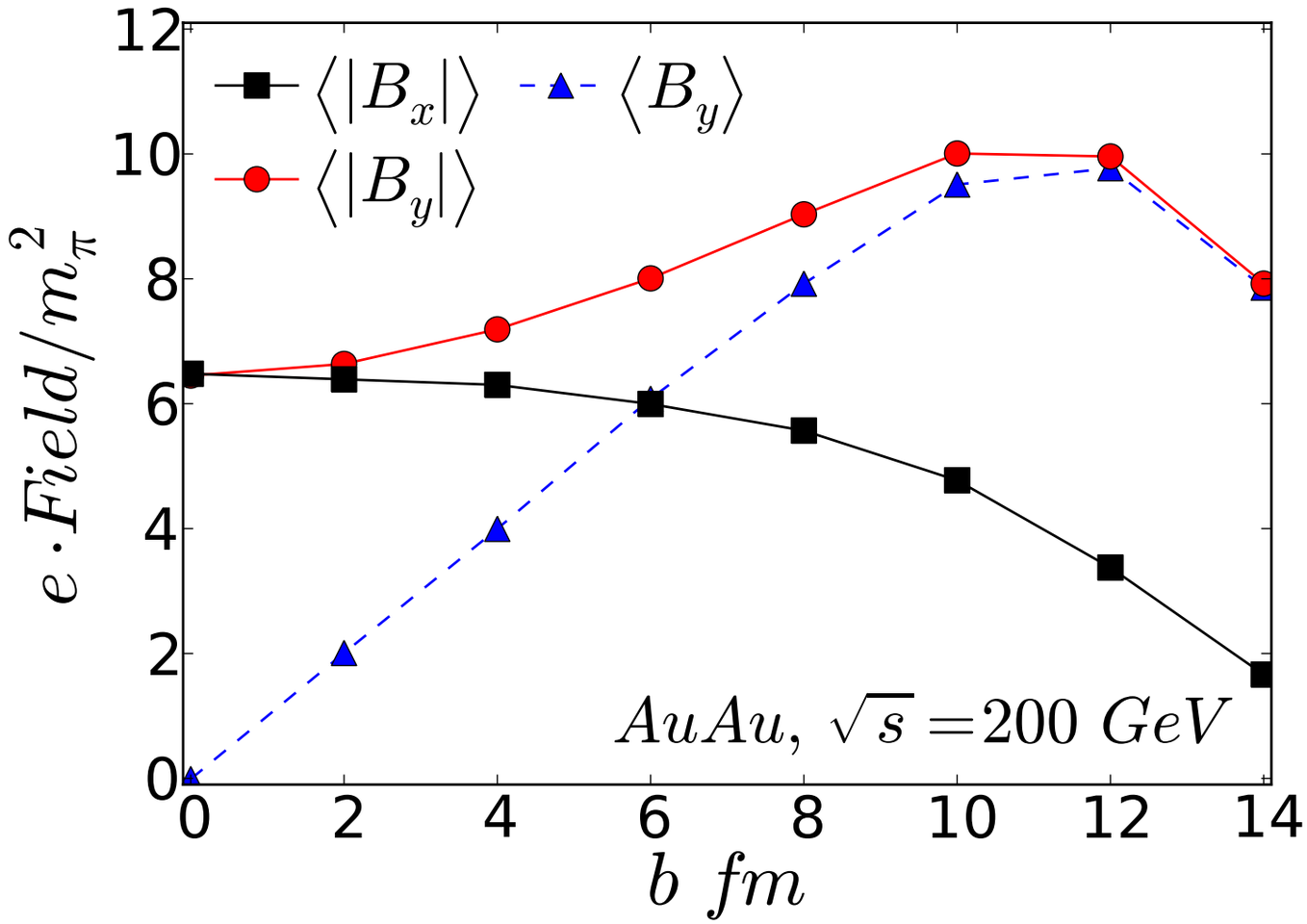


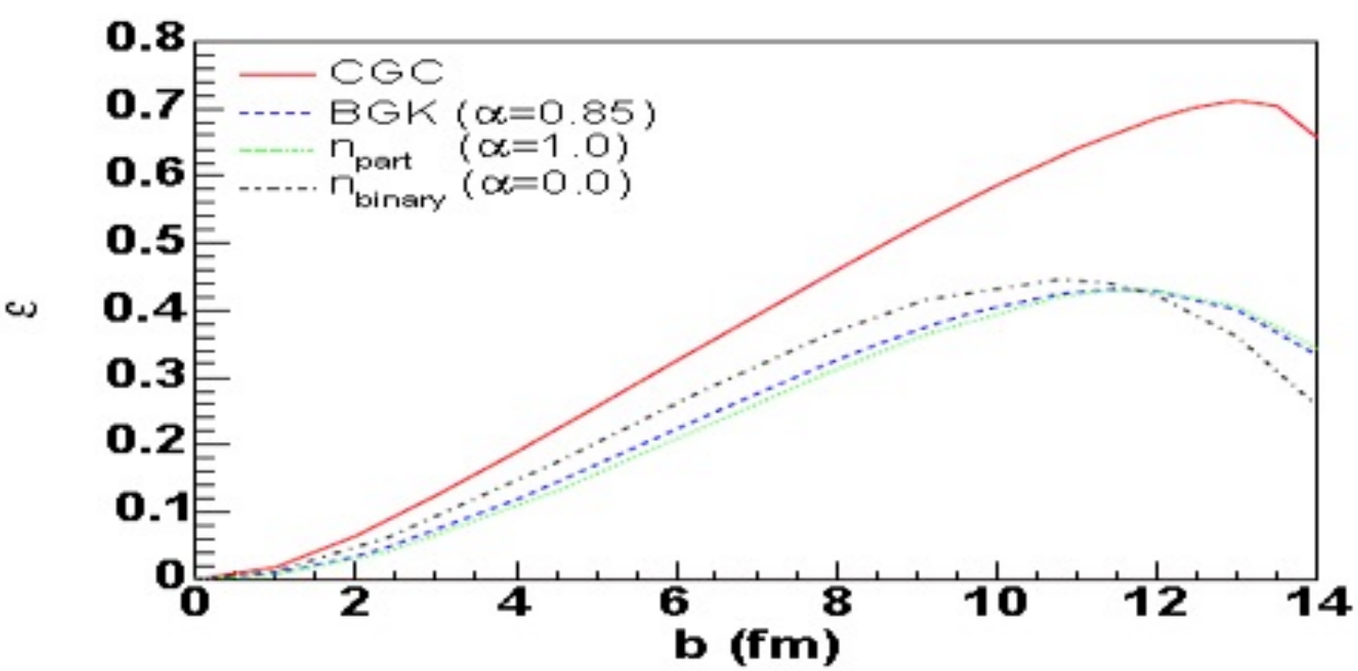


- <eB$_y$> is linear as a function of impact parameter
- this is common feature of <eB> and eccentricity $\boldsymbol{\varepsilon}_2$

# Magnetic field in HIC V

## eB in HIC compared to

- Hybrid magnet at

  National High Magnetic field Lab

  45 Tesla ~ $4.5\times10^{-13}\ m_\pi^2$

- Pulsed magnets:

  100 Tesla ~$10^{-12}\ m_\pi^2$

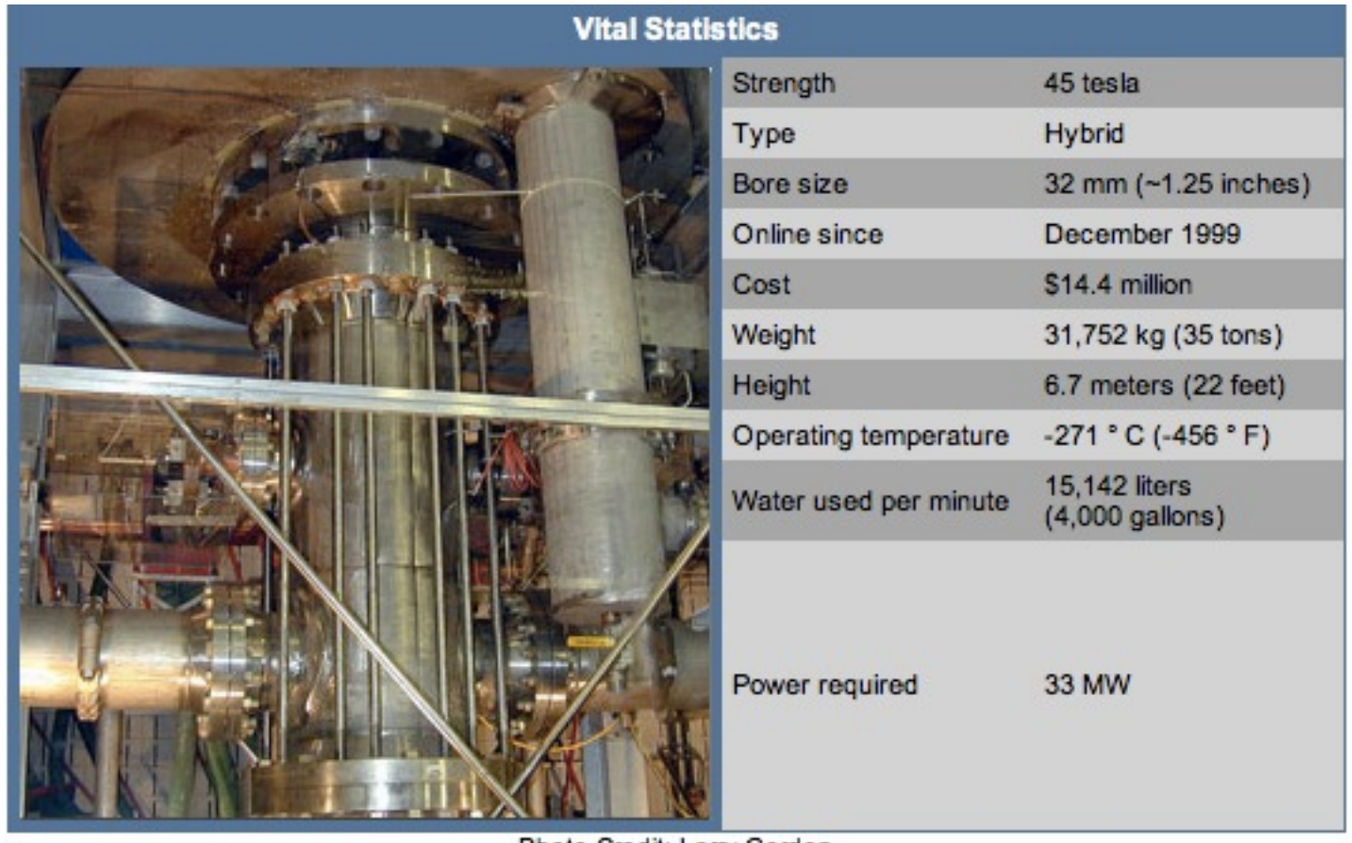

| Vital Statistics | |
|---|---|
| Strength | 45 tesla |
| Type | Hybrid |
| Bore size | 32 mm (~1.25 inches) |
| Online since | December 1999 |
| Cost | $14.4 million |
| Weight | 31,752 kg (35 tons) |
| Height | 6.7 meters (22 feet) |
| Operating temperature | -271 ° C (-456 ° F) |
| Water used per minute | 15,142 liters (4,000 gallons) |
| Power required | 33 MW |

Photo Credit: Larry Gordon

Watch an exploding pulsed magnet at work.

- Radio pulsars:

  $10^{-6}$-$10^{-5}\ m_\pi^2$

- Magnetars:

  $10^{-4}$-$10^{-3}\ m_\pi^2$

# High eB... So what?

Effects, that can be potentially observed:

- modification of QCD phase diagram
  (not really, short lifetime of B)

- chiral magnetic effect
  (sphaleron transition rate?!)

- chiral magnetic wave
  (life time for magnetic field ~ 4 fm/c)

- Photon splitting, and many other in the next talk

- **photon production!**

# Photon production from eB

Several mechanisms:

- synchrotron radiation of quarks in eB (K. Tuchin)
  unknown: density and distribution function of quarks in early stage

  *R. Venugopalan and V.S. Quark production in Glasma*

- axial anomaly (K. Fukushima)
  unknown: $\mu_5$ and spectral function of $G\tilde{G}$

  *G. Basar and D. Kharzeev*

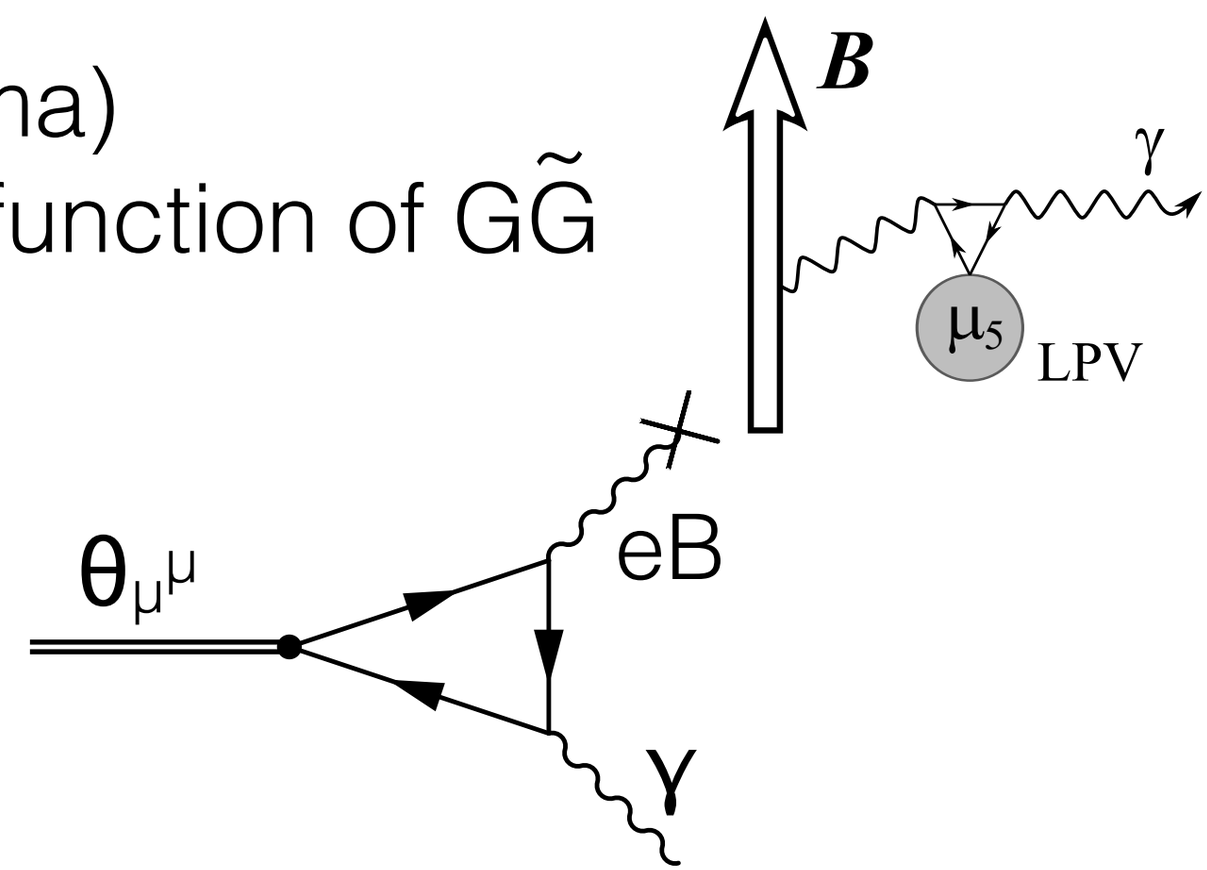


- **conformal anomaly**
  unknown?!: bulk viscosity

# Simple explanation

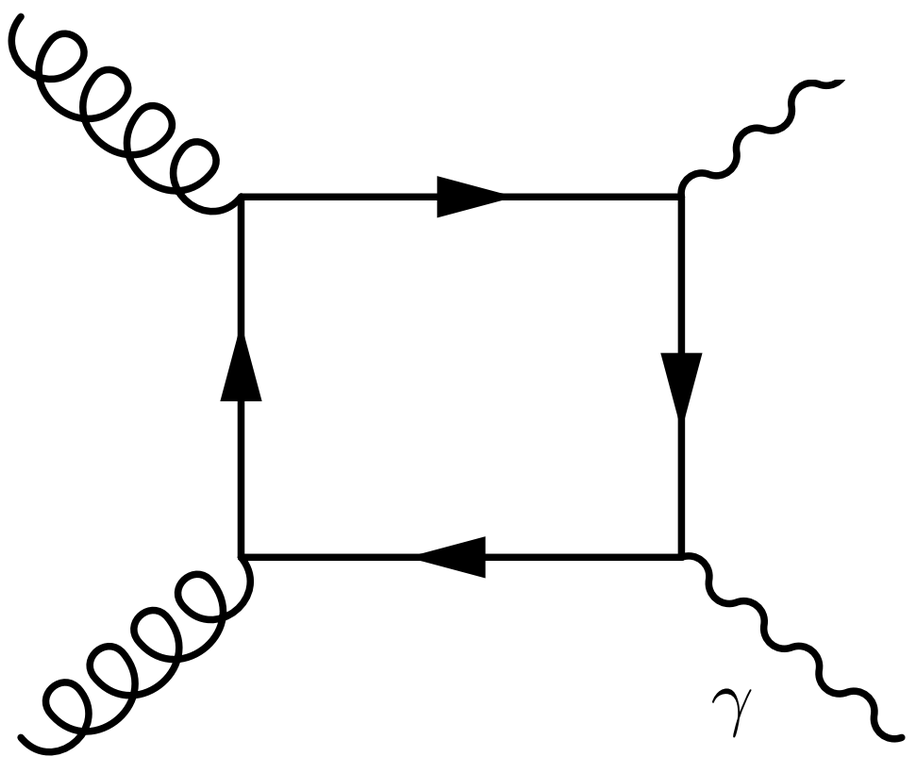

# Simple explanation

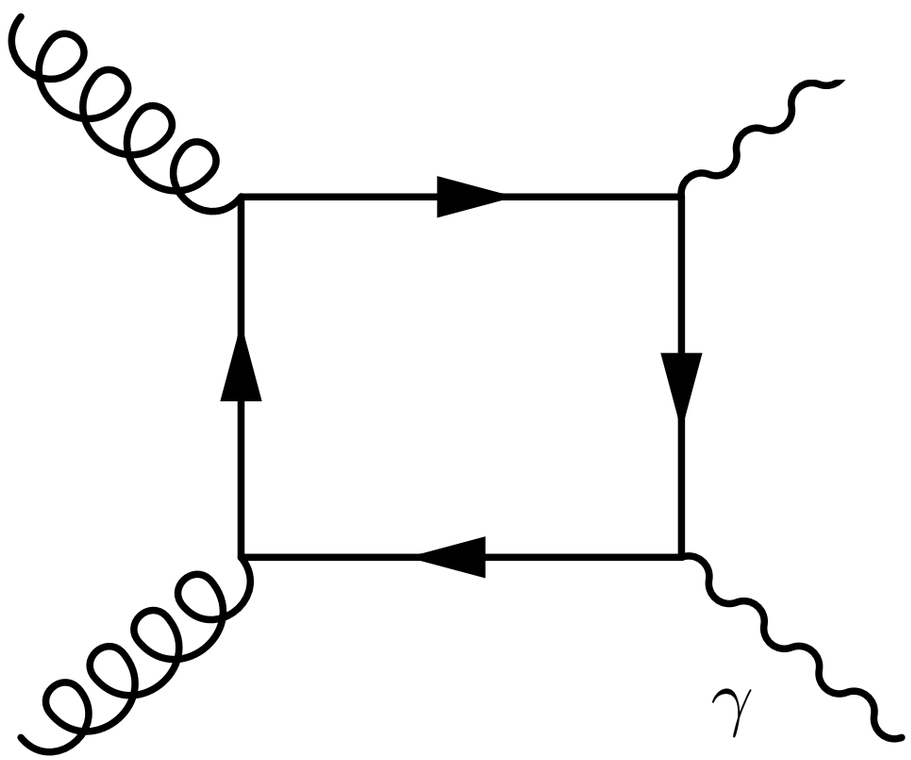


- Two photon production: $\alpha_s \alpha\ G^2 F^2$, $F^2 = F_{\mu\nu}F^{\mu\nu}$
  thus rate ~ $\alpha^2$

- Replace one photon with eB
  rate ~ $\alpha$

# Simple explanation

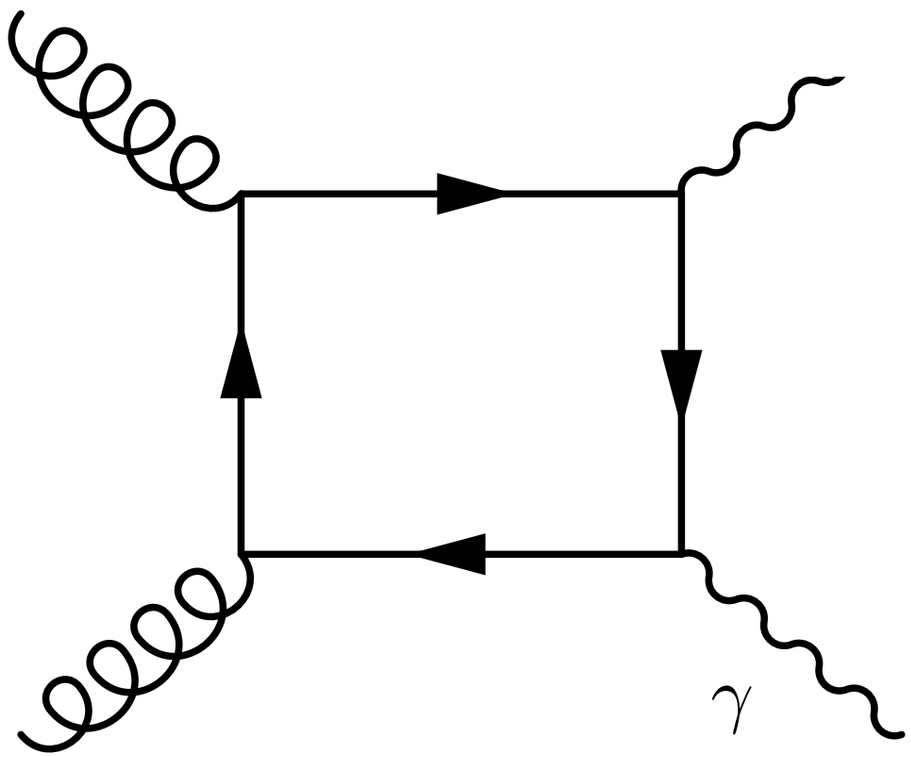


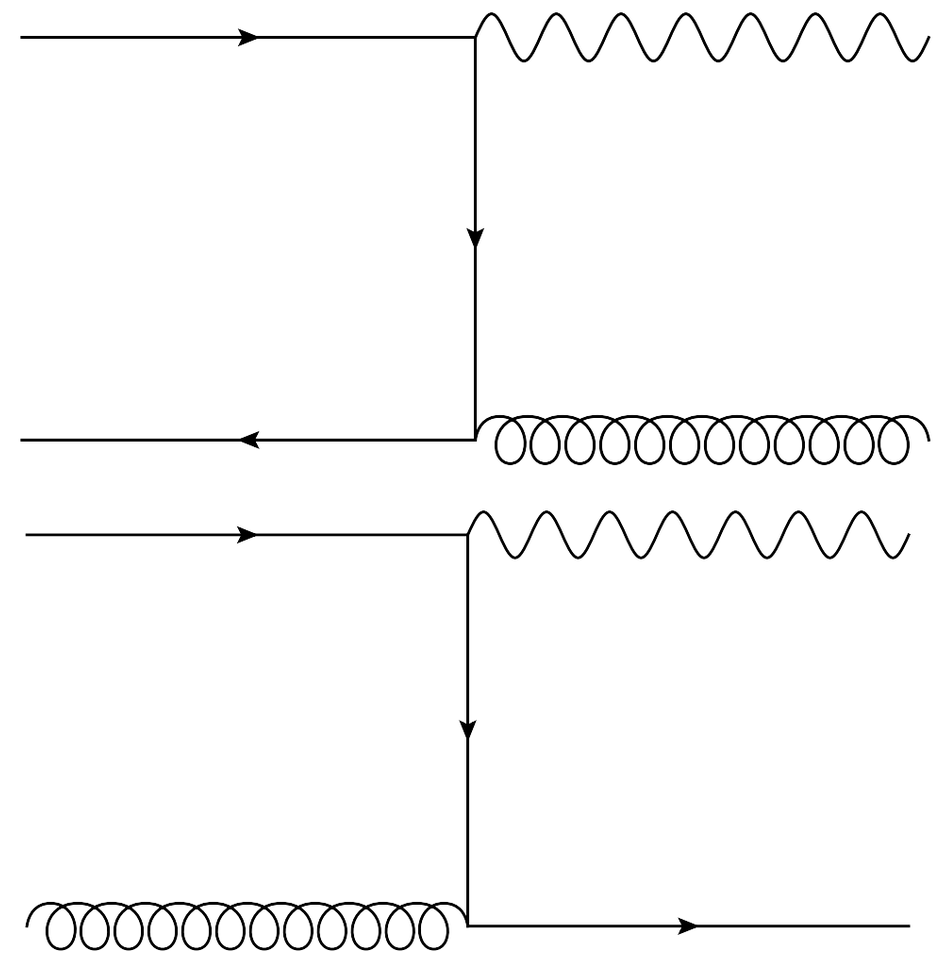

- Two photon production: $\alpha_s \alpha\, G^2 F^2$, $F^2 = F_{\mu\nu}F^{\mu\nu}$
  thus rate ~ $\alpha^2$

- Replace one photon with eB
  rate ~ $\alpha$

# Simple explanation

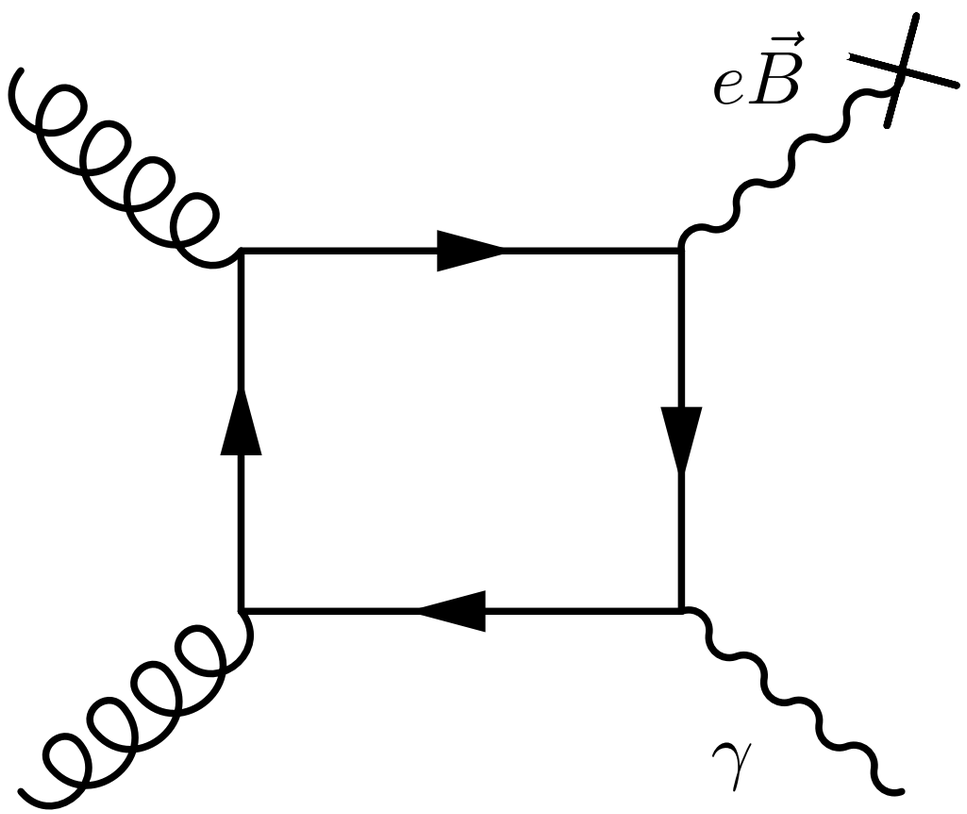


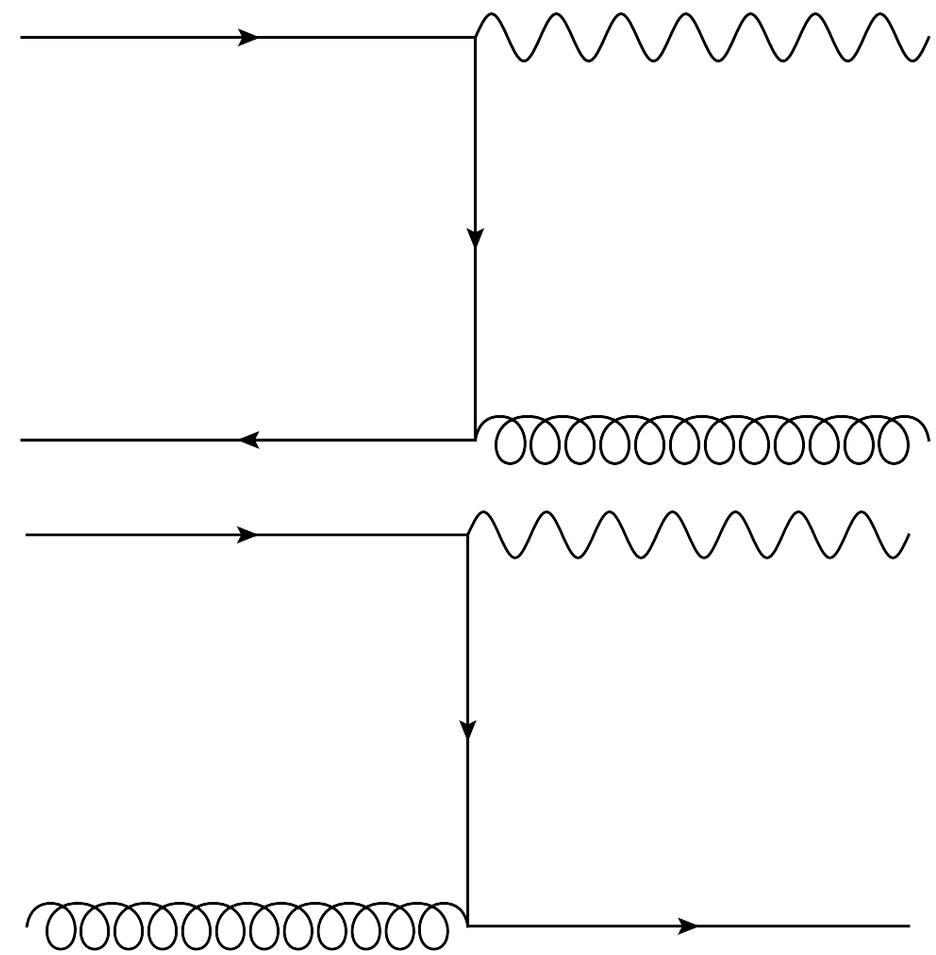

- Two photon production: $\alpha_s \alpha\, G^2 F^2$, $F^2 = F_{\mu\nu}F^{\mu\nu}$
  thus rate ~ $\alpha^2$

- Replace one photon with eB
  rate ~ $\alpha$

# Conformal anomaly

- divergence of dilatation current

$$\partial^\mu S_\mu = \theta^\mu_\mu = \frac{\beta(g)}{2g} G^{\mu\nu a} G_{\mu\nu a} + \sum_q m_q \left[1 + \gamma_m(g)\right] \bar{q} q$$

- color singlet states $\sigma \sim \theta_\mu{}^\mu$ *Migdal, Shifman*

$$\langle 0 | S^\mu | \sigma \rangle = i q^\mu f_\sigma; \quad \langle 0 | \partial_\mu S^\mu | \sigma \rangle = m_\sigma^2 \; f_\sigma$$

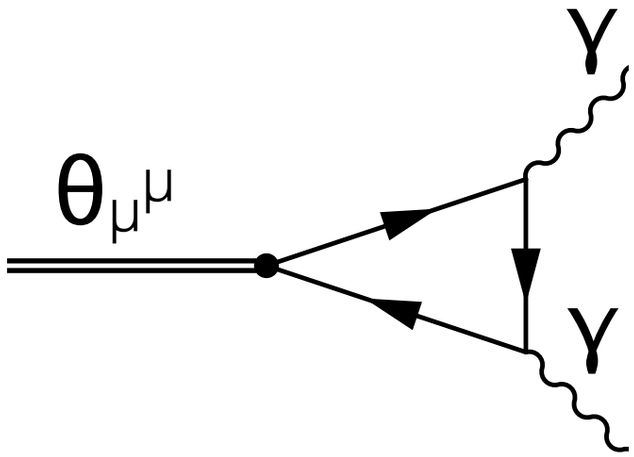


- effective Lagrangian

$$\mathcal{L}_{\sigma\gamma\gamma} = g_{\sigma\gamma\gamma} \; \sigma \; F_{\mu\nu} F^{\mu\nu}$$

- $g_{\sigma\gamma\gamma} \cong 0.02$ GeV$^{-1}$ *Ellis and Lanik; Crewther; Chanowitz*

# Photon production rate

- one of the photons: classical field eB

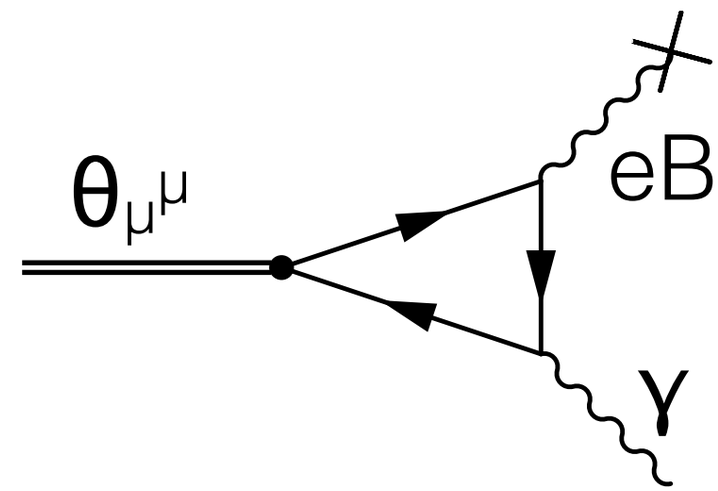


- production rate, as usual (β=1/T):

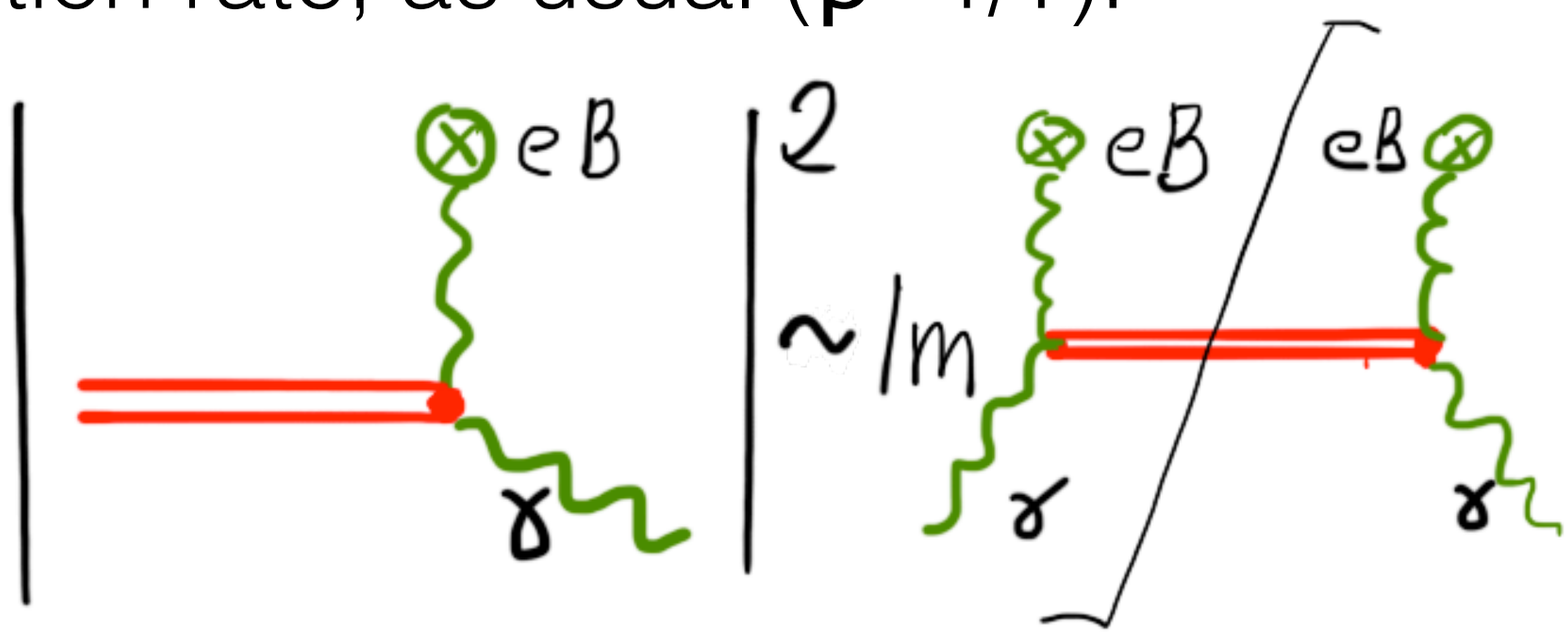


$$q_0 \frac{d\Gamma_B}{d^3q} = 2\left(\frac{g_{\sigma\gamma\gamma}}{\pi f_\sigma m_\sigma^2}\right)^2 \times \frac{(B_y^2 - B_x^2)q_x^2 + q_\perp^2 B_x^2}{\exp(\beta q_0) - 1}\rho_\theta(q_0 = |\vec{q}|).$$

# Final answer

$$q_0 \frac{d\Gamma_B}{d^3q} = 2\left(\frac{g_{\sigma\gamma\gamma}}{\pi f_\sigma m_\sigma^2}\right)^2 \times \frac{(B_y^2 - B_x^2)q_x^2 + q_\perp^2 B_x^2}{\exp(\beta q_0) - 1} \rho_\theta(q_0 = |\vec{q}|).$$

Numerical coefficient; constrained by hadronic observables

Momentum dependence; β=1/T; if e-b-e fluc. of magnetic field are neglected:

$$\frac{B_y^2 q_x^2}{\exp(\beta q_0) - 1}$$

Spectral function for $G^2$, or trace of energy momentum tensor

# Spectral function of $\theta_\mu{}^\mu$

- hydrodynamic approximation

$$\rho_\theta(q_0,\vec{q}) = \frac{1}{\pi}\mathcal{I}m[G_R^{\mu\mu,\nu\nu}(q_0,\vec{q})] = 9q_0\frac{\zeta}{\pi} + \frac{9}{\pi}(\epsilon+p)\left(\frac{1}{3}-c_s^2\right)^2 \frac{q_0\Gamma_s\,\vec{q}^4}{(q_0^2-c_s^2\,\vec{q}^2)^2+(q_0\Gamma_s\vec{q}^2)^2}$$

bulk viscosity

sound peak

- real photons, sound peak does not contribute:

$$\rho_\theta(q_0,\vec{q}) \approx 9q_0\frac{\zeta}{\pi}$$

# $G\tilde{G}$

- Similar calculations can be done for $F\tilde{F}$ $G\tilde{G}$

- Spectral function $G\tilde{G}$ in hydro approximation is defined by sphaleron transition rate and was calculated in pQCD and AdS/CFT.

# Bulk viscosity

- first principle Lattice QCD:
  H. Meyer SU(3) Yang Mills (YM)
  However, there are issues.

- approximations:

  $\zeta = C_\zeta\, \eta\, (1/3-c_s^2)^2$ (vs ADS/QCD $\zeta \geqq 2\, \eta\, (1/3-c_s^2)$)

  $C_\zeta$ = 15 in relaxation time appr. (S. Weinberg '71)
  $C_\zeta$ = 45 in NLO SU(3) YM (K. Dusling and T. Schafer '11)
  $C_\zeta$ = 2.5-5 phenomenological constraints
  in this talk: conservative $C_\zeta$ = 2.5-5

- also conservative $\eta/s=1/(4\pi)$. Entropy, s, from matrix model fitted to YM SU(3) (R. Pisarski)

# So one would expect...

$$q_0 \frac{d\Gamma_B}{d^3q} = 2\left(\frac{g_{\sigma\gamma\gamma}}{\pi f_\sigma m_\sigma^2}\right)^2 \times \frac{(B_y^2 - B_x^2)q_x^2 + q_\perp^2 B_x^2}{\exp(\beta q_0) - 1}\rho_\theta(q_0 = |\vec{q}|).$$

$$\rho_\theta(q_0, \vec{q}) \approx 9q_0 \frac{\zeta}{\pi}$$

$\zeta = C_\zeta\, \eta\, (1/3 - c_s^2)^2$

- negligible contribution from this mechanism?! eB is non-zero at early stage where $(1/3-c_s^2)^2$ is small

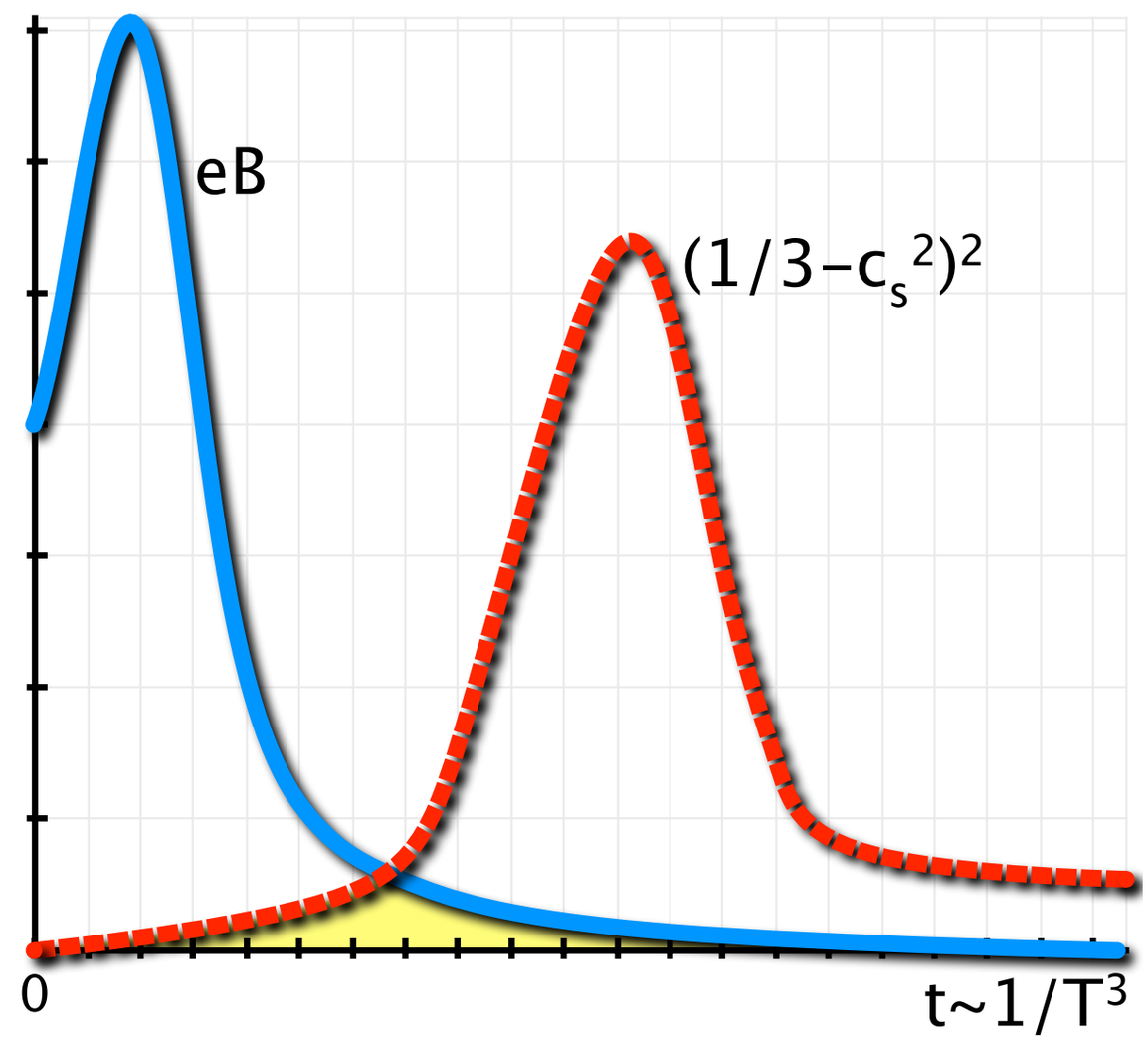

# However

- rate is proportional to $(1-c_s^2)^2\, T^3\, (eB)^2$

  rough estimate at early stage
  $(1-c_s^2)\sim(\varepsilon-3p)/T^4\sim$(from LQCD)$\sim$**1 / T^2** (talks by R. Pisarski)
  $(1-c_s^2)^2\, T^3 \sim$**1 / T**$\sim$(Bjorken expansion)$\sim t^{1/3}$
  while $eB\sim 1/(t^2+\text{const})$

  stringy?
  fuzzy bag?
  quasiparticles?
  monopoles?

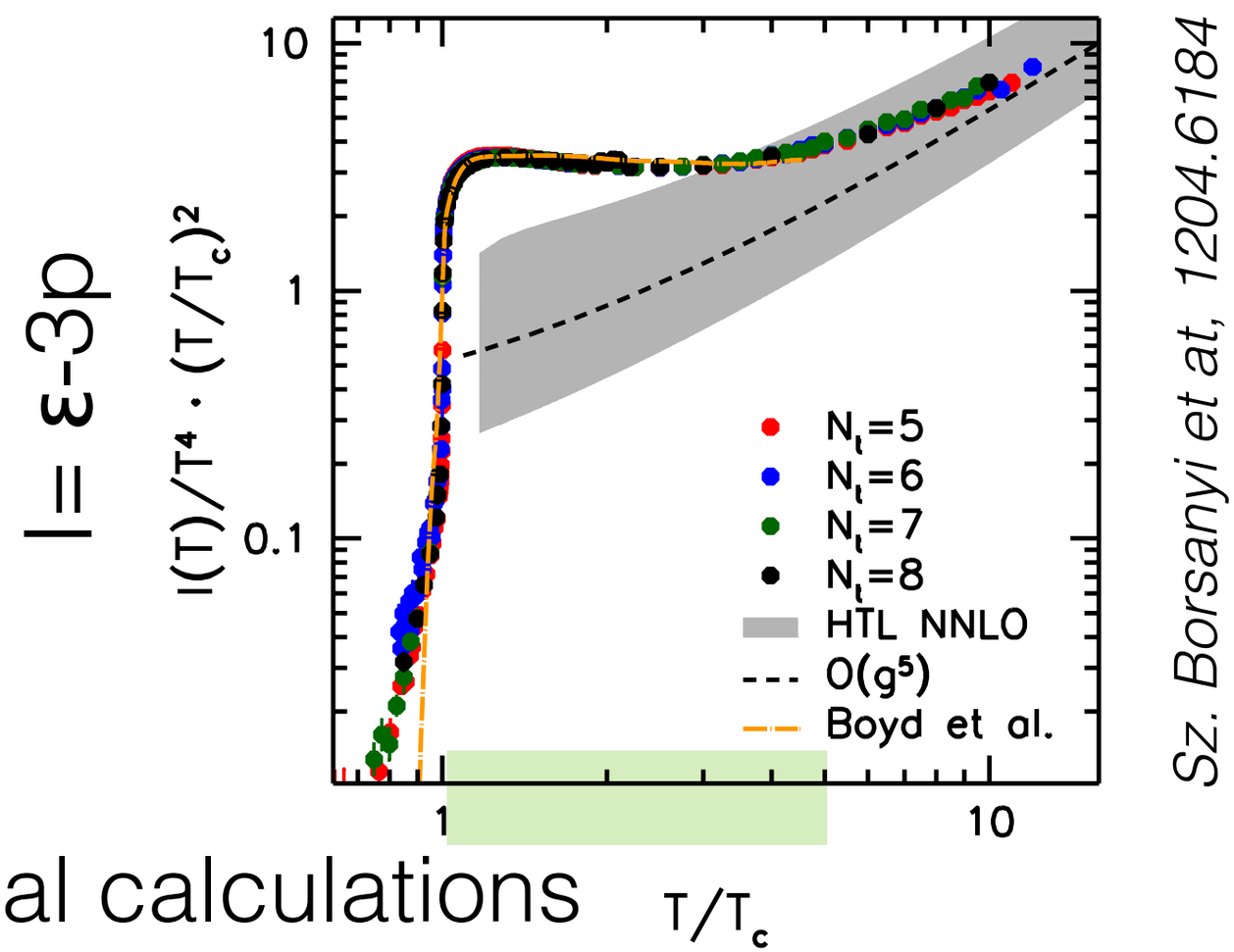


*Sz. Borsanyi et at, 1204.6184*

- rigorous answer: numerical calculations

# Anisotropy of production rate

- in this mechanism:

$dN/d\varphi \sim q_x^2 = q_T^2 \cos^2(\varphi) = q_T^2 [1+\cos(2\varphi)]/2$

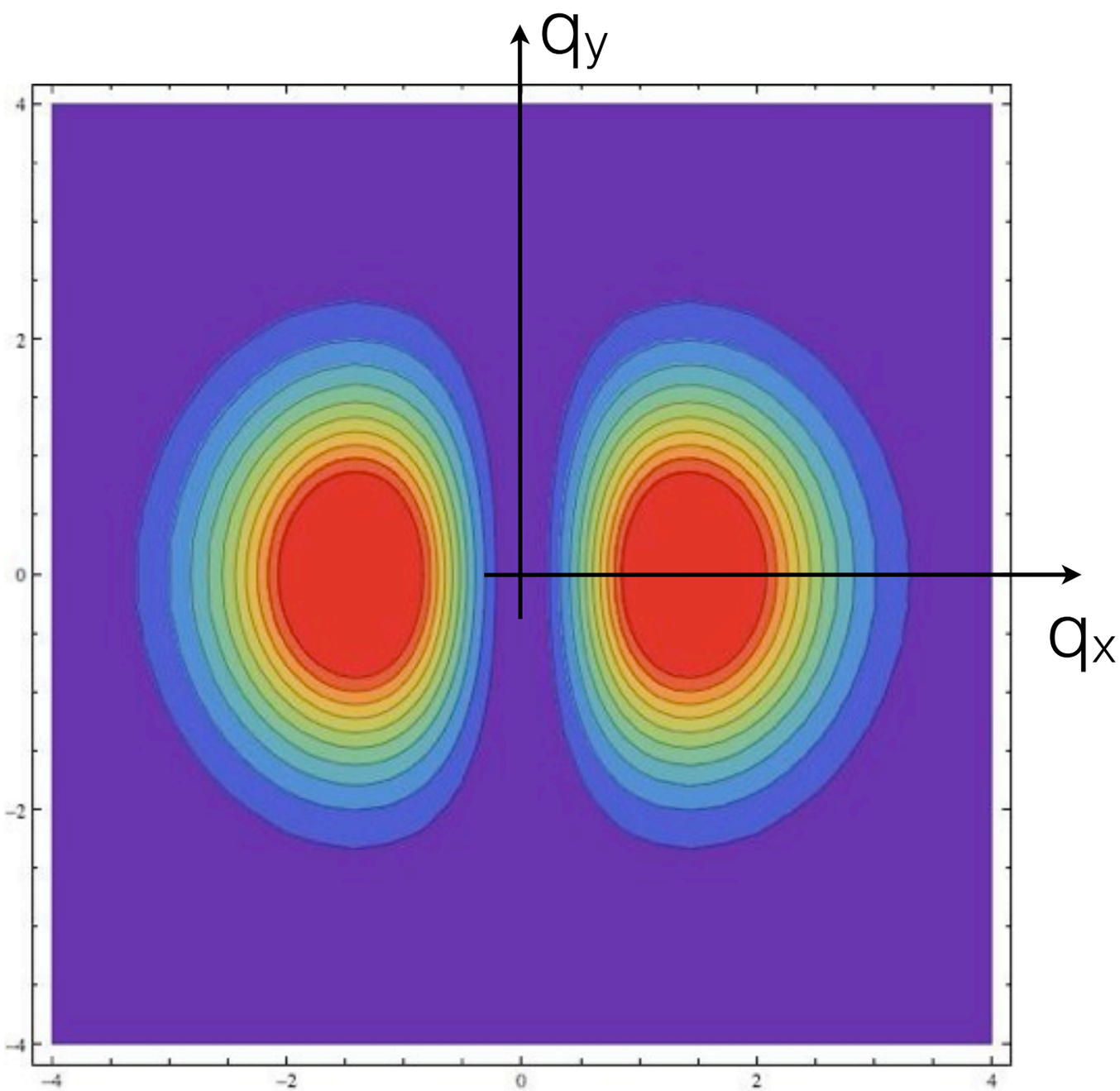


consequently:

- non-zero $v_2$
- small $v^\gamma_n$, n=4,...
  in contrast to hadronic $v_4$
  PHENIX: $v_4/v_2^2 \sim 1$

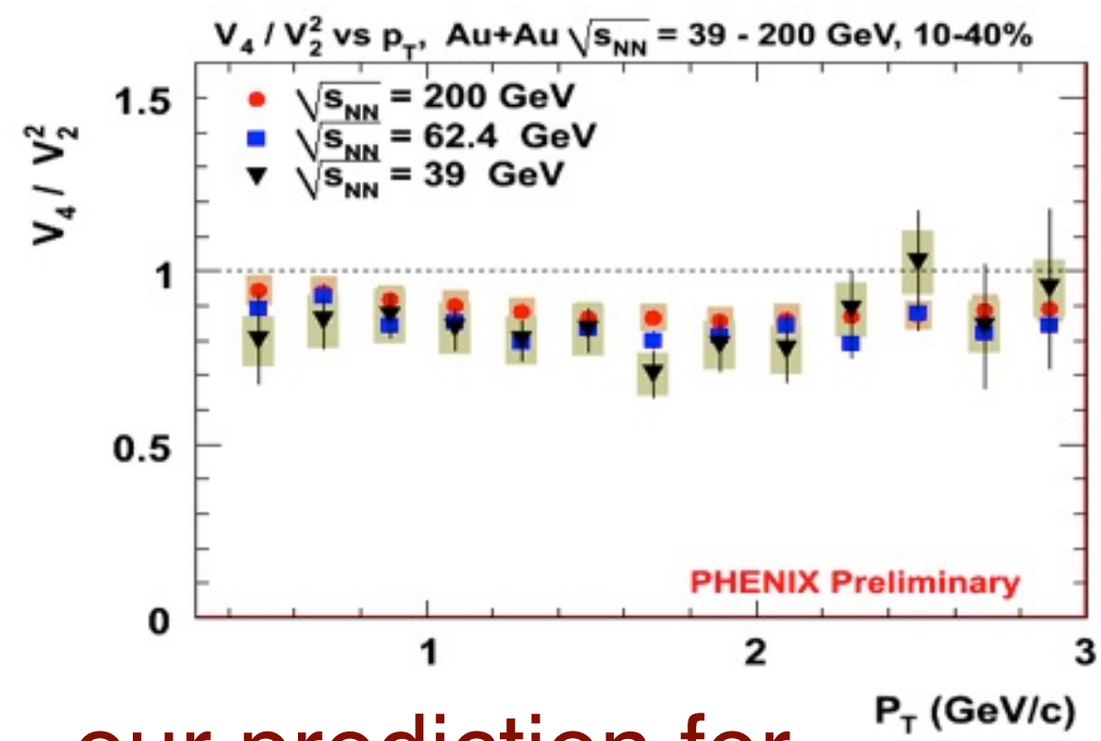


our prediction for photons: $v_4/v_2^2 \ll 1$

# Numerical calculations: $v_2$

- ingredients: thermal photons and photons from conformal anomaly +eB
- significant contribution to $v_2$
- higher $p_\perp$: prompt photons

*G. Basar, D. Kharzeev, V.S., arXiv:1206.1334*

# Numerical calculations: $v_2$

- ingredients: thermal photons and photons from conformal anomaly +eB
- significant contribution to $v_2$
- higher $p_\perp$: prompt photons

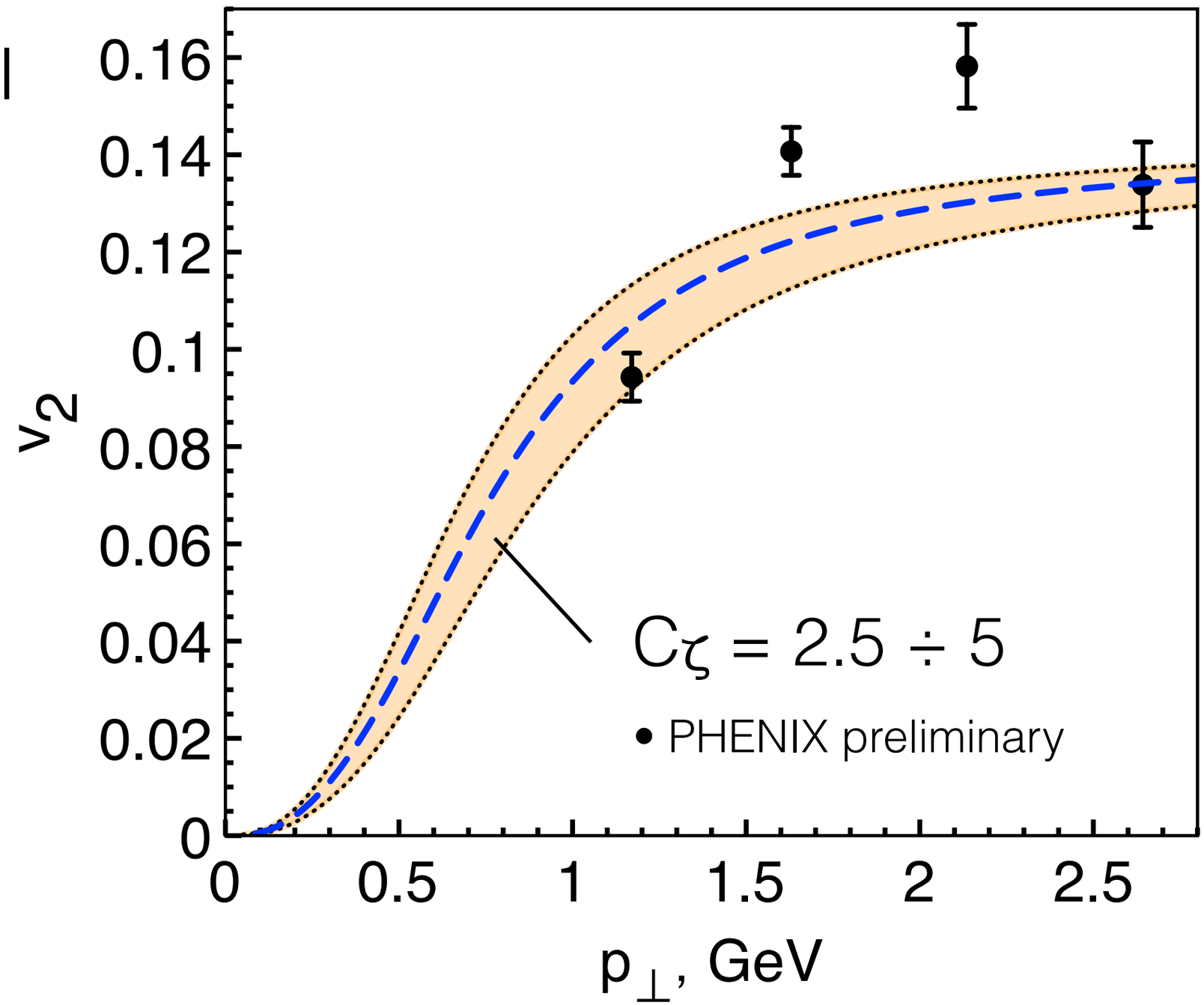


*G. Basar, D. Kharzeev, V.S., arXiv:1206.1334*

# Other parameters

- initial temperature T = 400 MeV
- initial time $\tau$=0.1 fm/c (no need for complete equilibrium, is to be discussed later)
- Bjorken expansion for T
- electromagnetic field from spectators only (with fluctuations taken into account). Possible induced magnetic field will only enhance production via this mechanism

# Transverse momentum spectra

- conformal anomaly:
  $dN/dp_\perp \sim \mathbf{p}_\perp^2 / [\exp(p_0/T)-1]$
  similar to effect of direct flow

- higher than thermal photons for $p_\perp > 1$ GeV

- higher $p_\perp$: prompt photons

*G. Basar, D. Kharzeev, V.S., arXiv:1206.1334*

# Transverse momentum spectra

- conformal anomaly:
  $dN/dp_\perp \sim \mathbf{p_\perp^2} / [\exp(p_0/T)-1]$
  similar to effect of direct flow

- higher than thermal photons for $p_\perp > 1$ GeV

- higher $p_\perp$: prompt photons

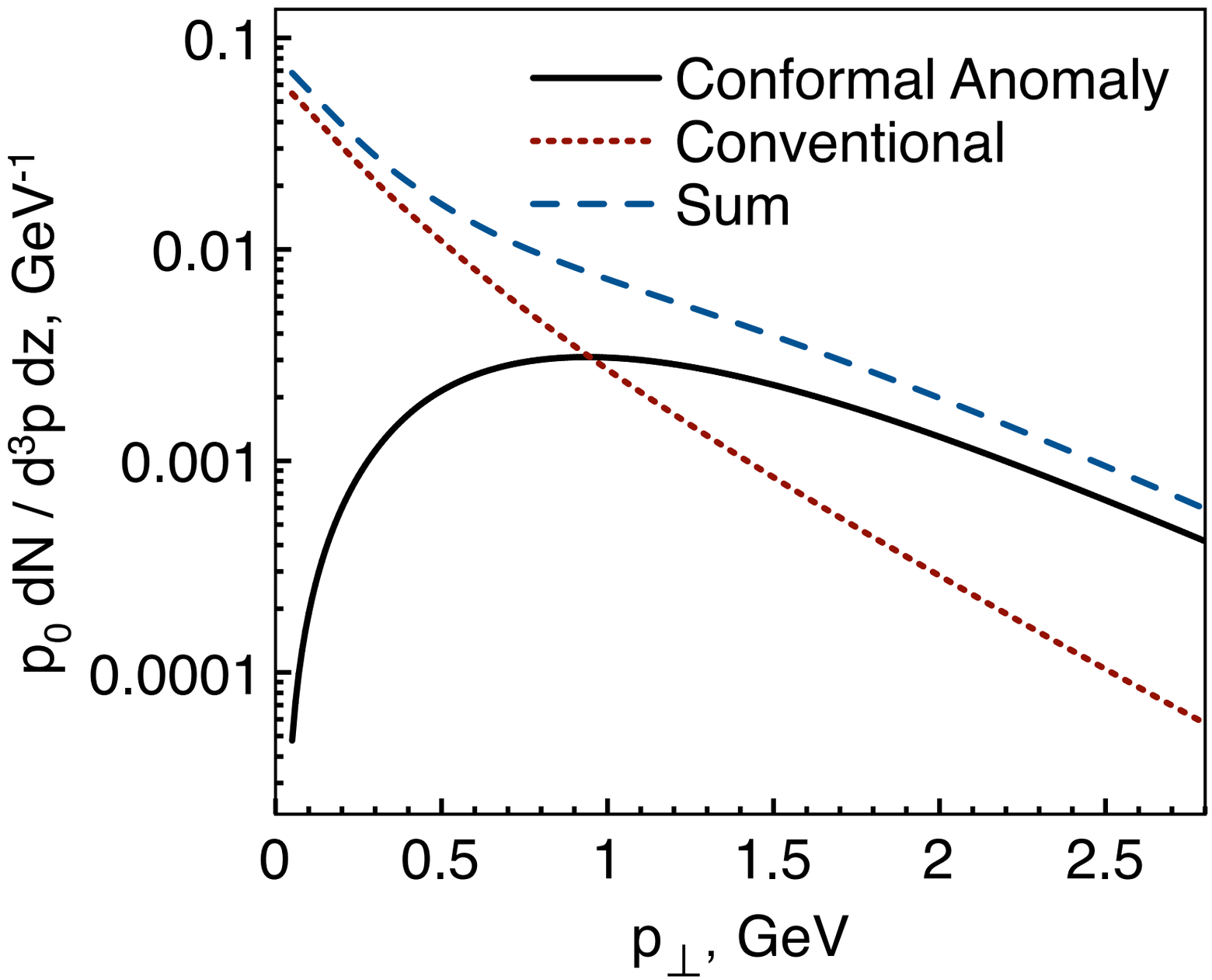


*G. Basar, D. Kharzeev, V.S., arXiv:1206.1334*

# Experimental tests I

- **1) magnetic field B** is generated mostly by spectators thus, B is defined by centrality (measured by ZDC), reaction plane

  **2) hadronic flow**: initial eccentricity **ε**
  **ε** depends on details of hadron interaction (Glauber fluctuations, fluctuations of energy deposition); participant plane

- so switch off either **1)** or **2)**

# Switching of B

- central U+U collisions
  U is deformed ion:
  events with (almost) no particles in ZDC: **B=0**, **ε≠0**;
  if photon $v_2$ is the same as the one of hadrons,
  our mechanism is ruled out

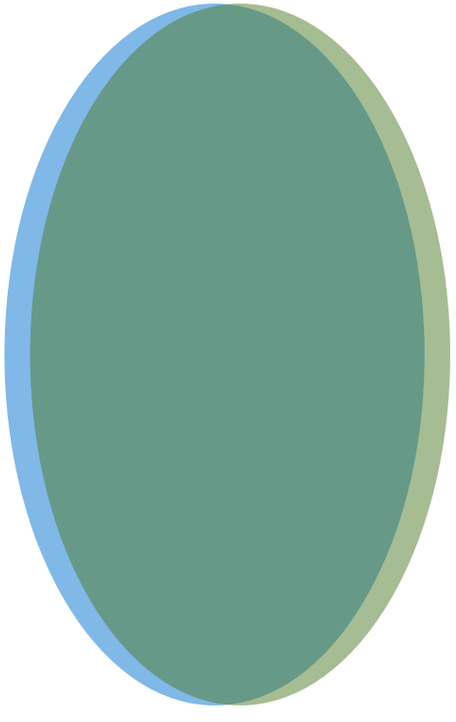

# Switching of ε

- non-central collisions: fluctuations of eccentricity

  in given centrality class (e.g. 45-50% defined by ZDC), **B = const**; while hadronic $v_2$ fluctuates because of initial eccentricity fluctuations.
  Limiting case:
  non-central collisions (➞ eB≠0) with zero $\mathbf{v_2}$.
  thus in such events anisotropy of photon production is due to eB.

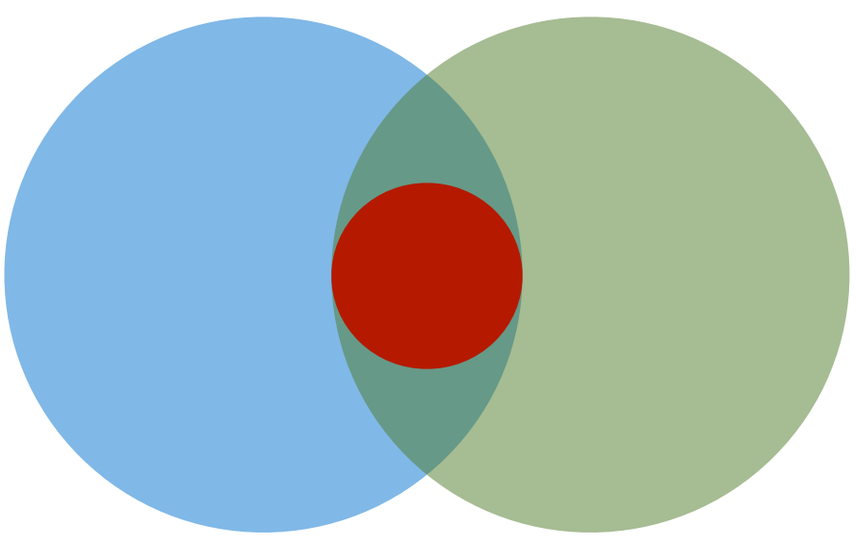

Our mechanism will be ruled out, if

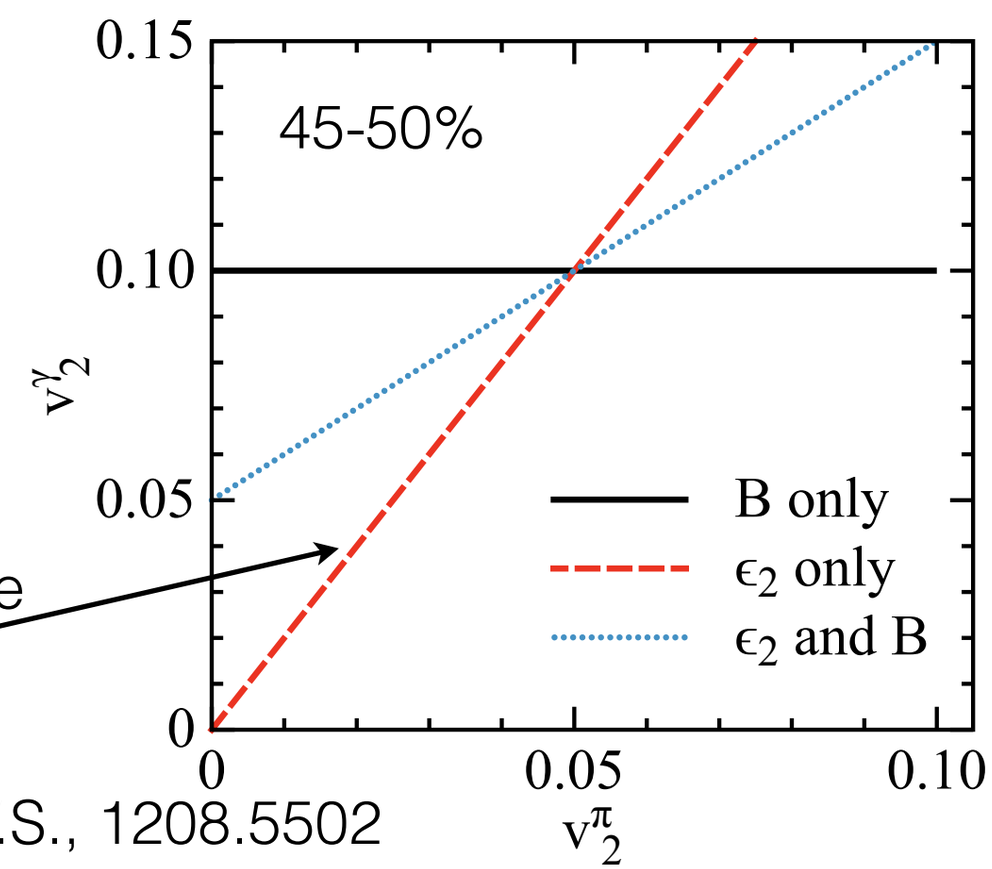


A. Bzdak and V.S., 1208.5502

# Experimental tests II

- small $v_4$; violation of scaling $v_4 \sim v_2^2$
- number of photons $N_{in\text{-}plane} > N_{out\text{-}plane}$
  $(N_{in\text{-}plane} - N_{out\text{-}plane}) \sim eB^2$ and thus is quadratic function of impact parameter
- in-plane polarization of photons

# Outlook:LHC energies

- Higher initial temperatures ➞ lower bulk viscosity
  $T_{ave}$ = 304 MeV

- Large $\gamma$ ➞ short time scales for non-zero magnetic field (modulo plasma response)
  $t_{LHC} = t_{RHIC}\, \Upsilon_{RHIC} / \Upsilon_{LHC}$ ➞ $t_{LHC} \propto 0.01$ fm/c vs $t_{RHIC} \propto 0.1$ fm/c

- LHC data can be described by:
  $T^{init}_{LHC} / T^{init}_{RHIC} = Q^{sat}_{LHC} / Q^{sat}_{RHIC}$ and $\tau_0^{LHC} / \tau_0^{RHIC} = Q^{sat}_{RHIC} / Q^{sat}_{LHC}$

- No need for equilibrium
  - production from Glasma:

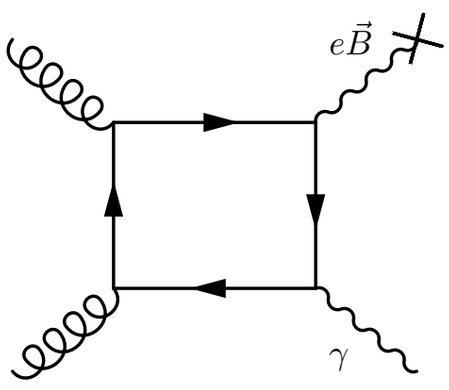


  - production from CGC:

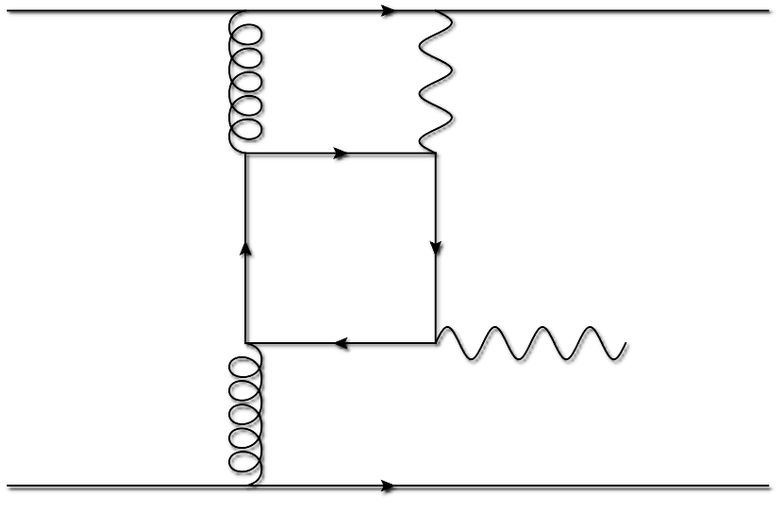

# Outlook:RHIC low energy scan

- lower energies -> lower eB, but longer time scales
- in equilibrium: bulk viscosity, $\zeta$, is divergent at critical point (CP)
- in reality (HIC): at CP $\zeta \sim \xi^{2.8}$ , $\xi$ is correlation length
- on O(4) line: $\zeta \sim \xi^2$ (while shear viscosity is finite)
  see *E. Nakano, V.S. and B. Friman, arXiv:1109.6822*
- rather speculative: small eB can compensate large $\zeta$

**MAGNETO-HYDRO**

# Summary

- photon $v_2$ puzzle:

  - hadronic physics?!

  - or effect of non-zero magnetic field?!

- there are ways to discriminate between hadronic and magnetic field related mechanisms of $v_2$!

- axial anomaly: similar effect, but unknown $\mu_5$ (similar to CME); synchrotron radiation: similar effect, but unknown quark distribution in initial state

# Backup

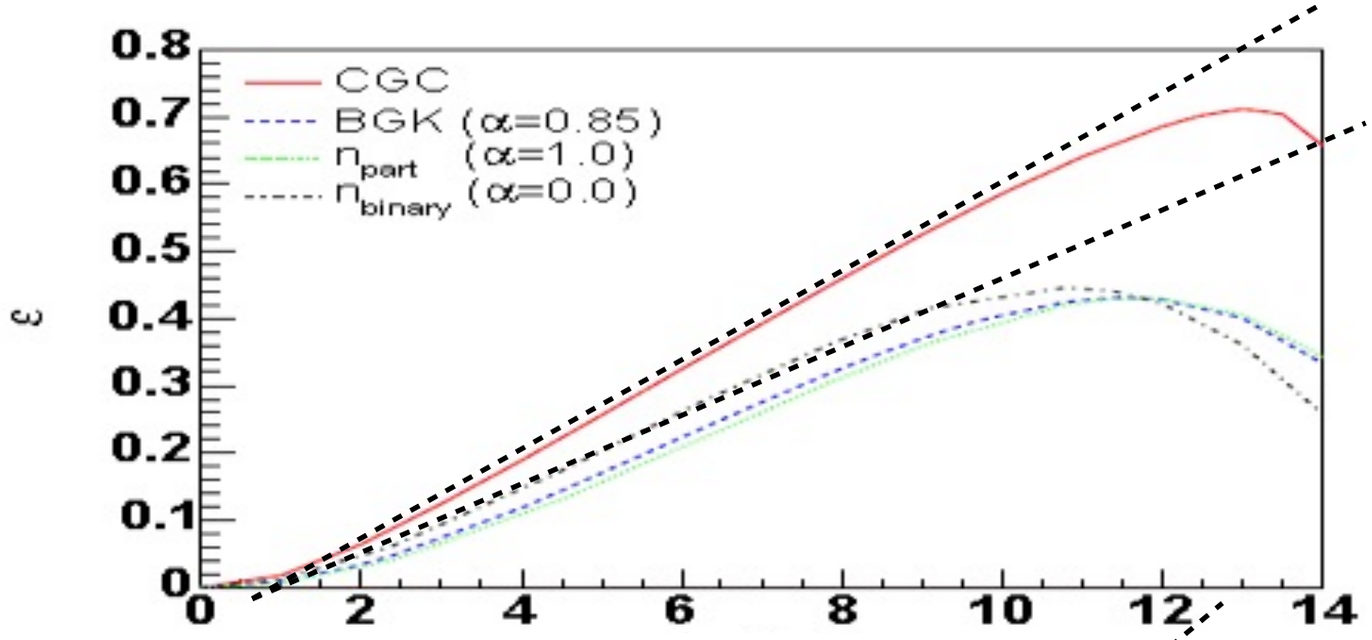


*Drescher Dumitru Hayashigaki Nara, nucl-th/0605012*

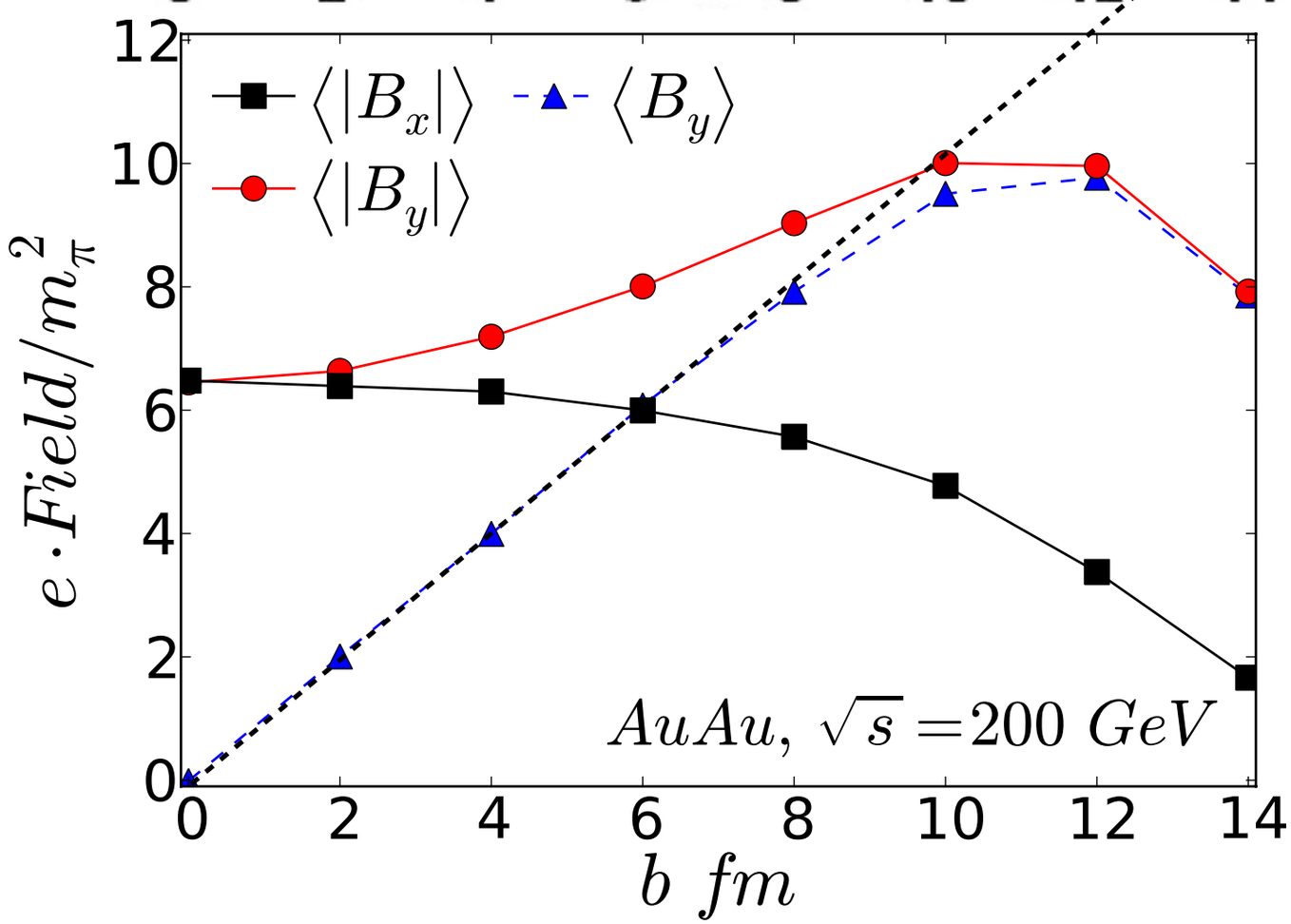


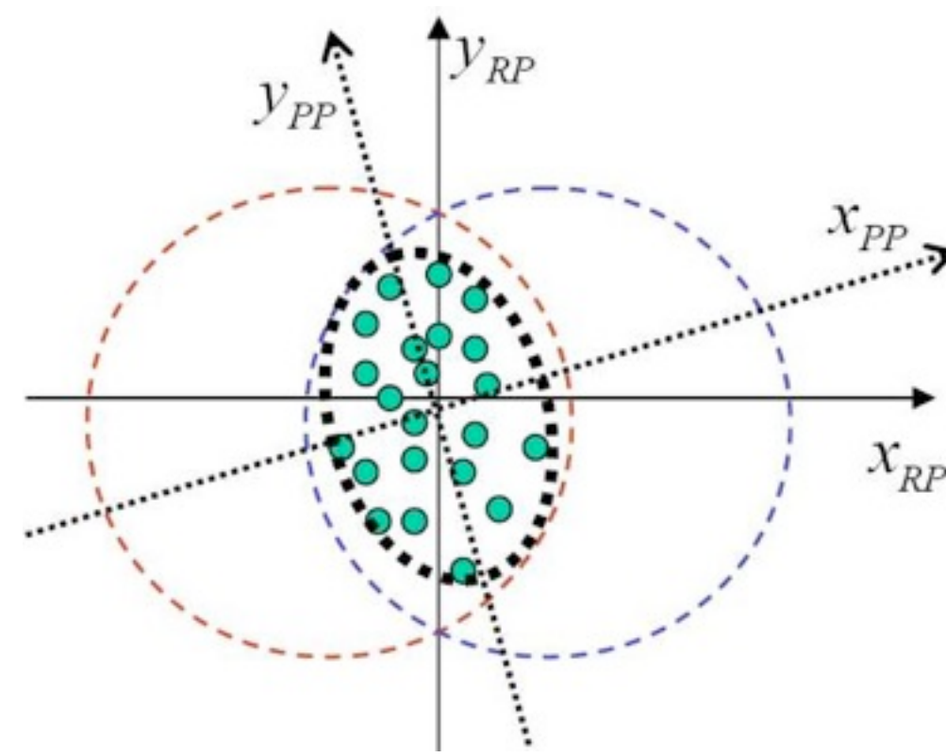

# Fluctuations of eB

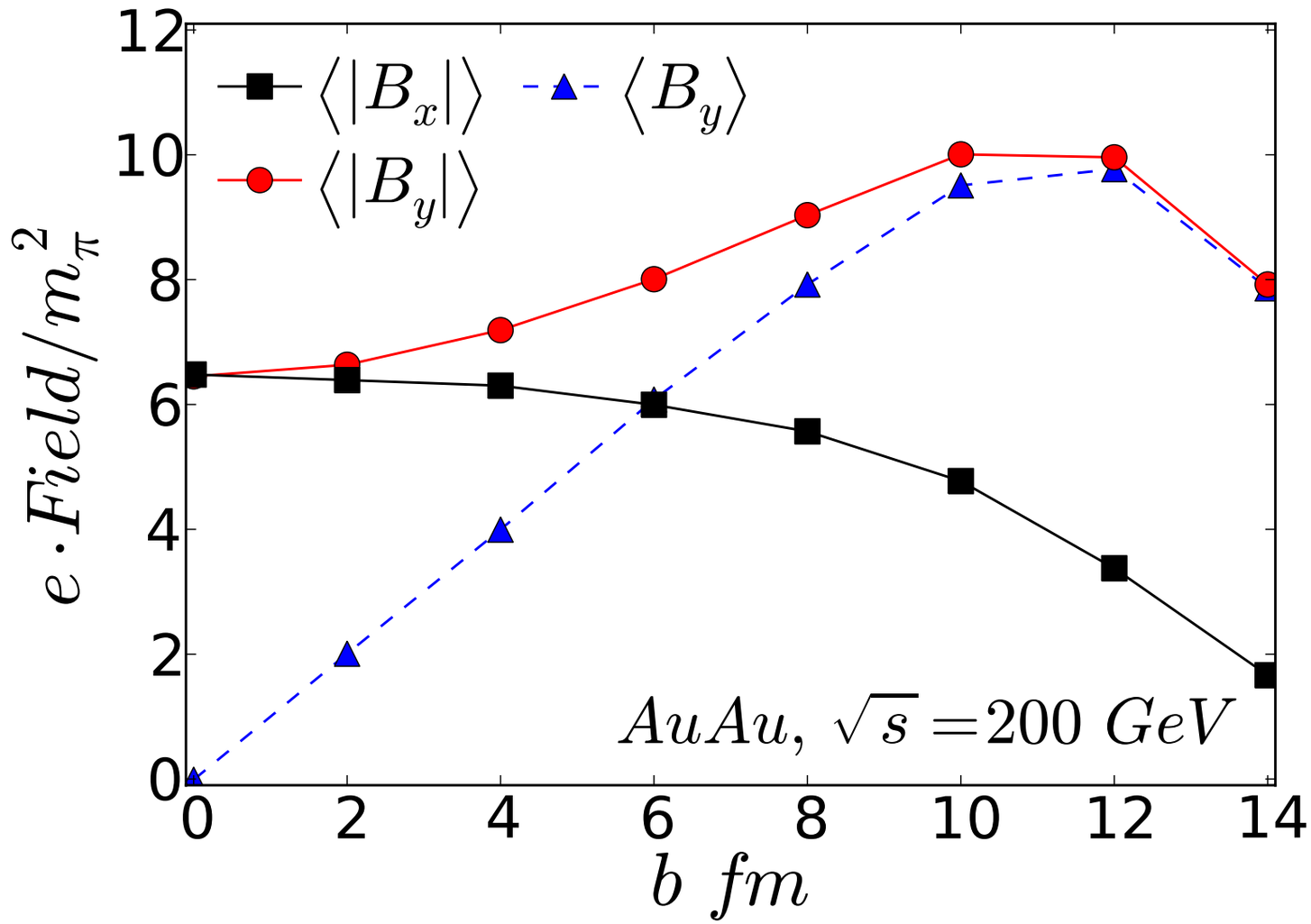


- for observables <eB> is not as significant as as <|$eB_y$ - $eB_x$|>

*A. Bzdak and V.S., 1111.1949*

- azimuthal fluctuations of eB relative to orientation of participant plane: J. Bloczynski et al1209.6594

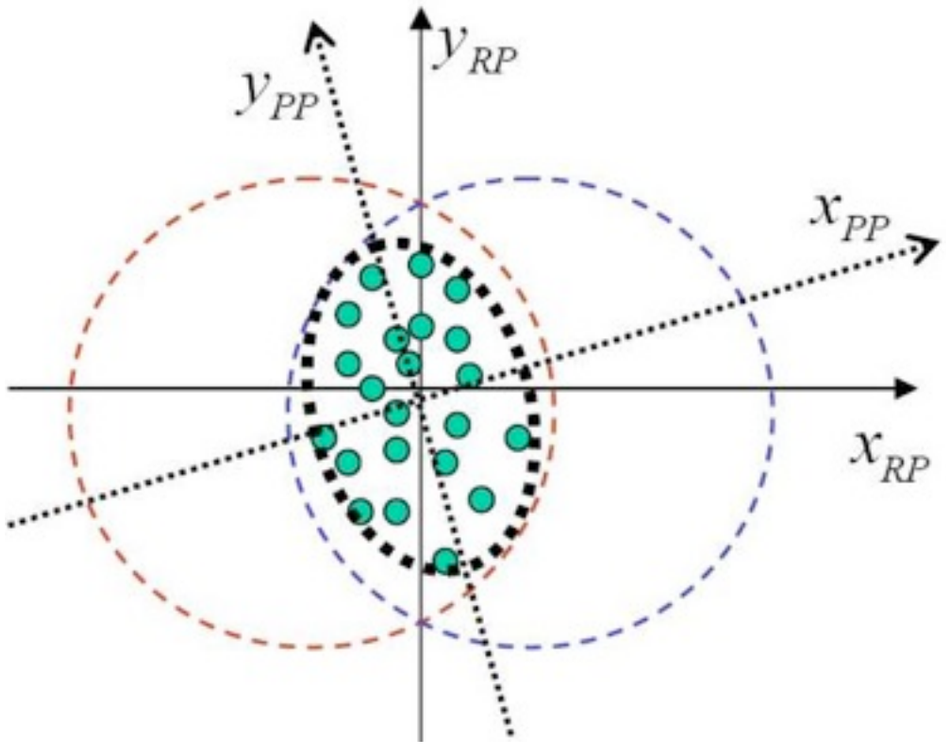

# Development of hadronic flow

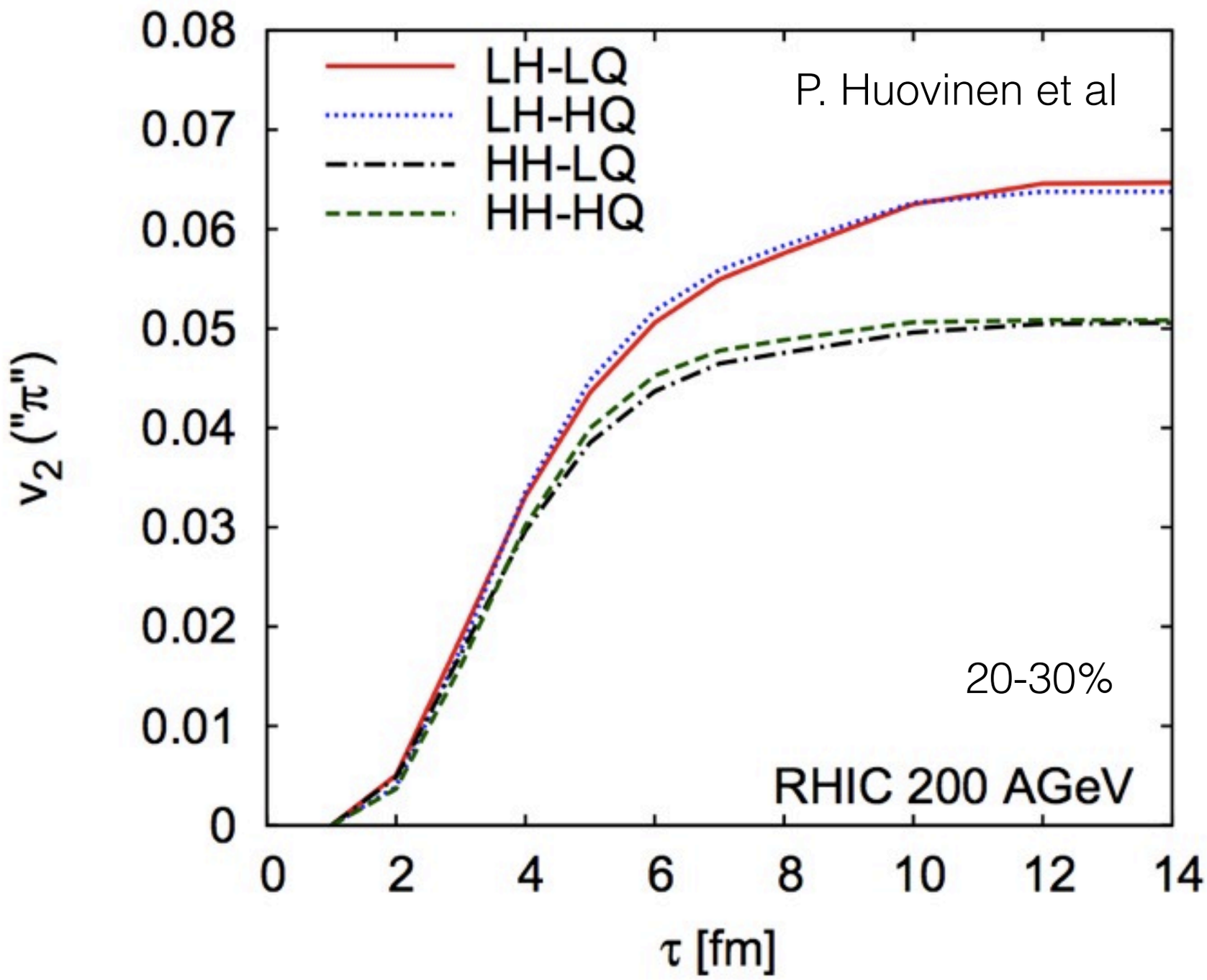

# Theory: Hydrodynamics II

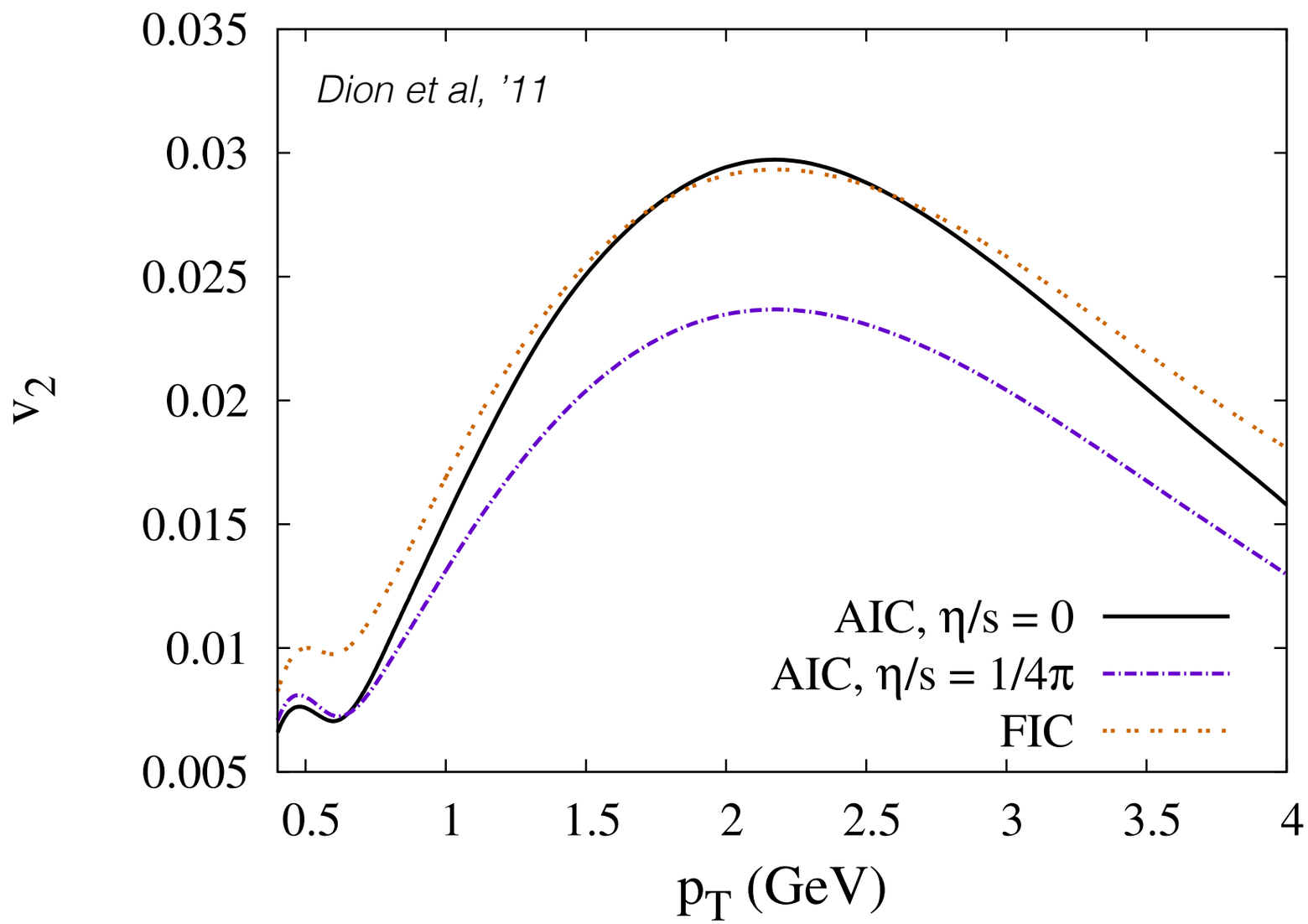


Hydro:
**5 times** smaller $v_2$
then in experiment

AIC: averaged initial conditions
FIC: fluctuating initial conditions

Large photon $v_2$ is difficult to explain with dominant QGP source

# Photon Production at NLO in Hot QCD

Derek Teaney

SUNY Stony Brook and RBRC Fellow

- Photons – In collaboration with Jacopo Ghiglieri, Juhee Hong, Aleksi Kurkela, Egang Lu, Guy Moore, arXiv:Almost.Done

Perturbation theory can work for thermodynamic quantities! Let's use it!

- HTLpt from Andersen, Su, Strickland. Dimensional Reduction/EQCD – the Finish Group

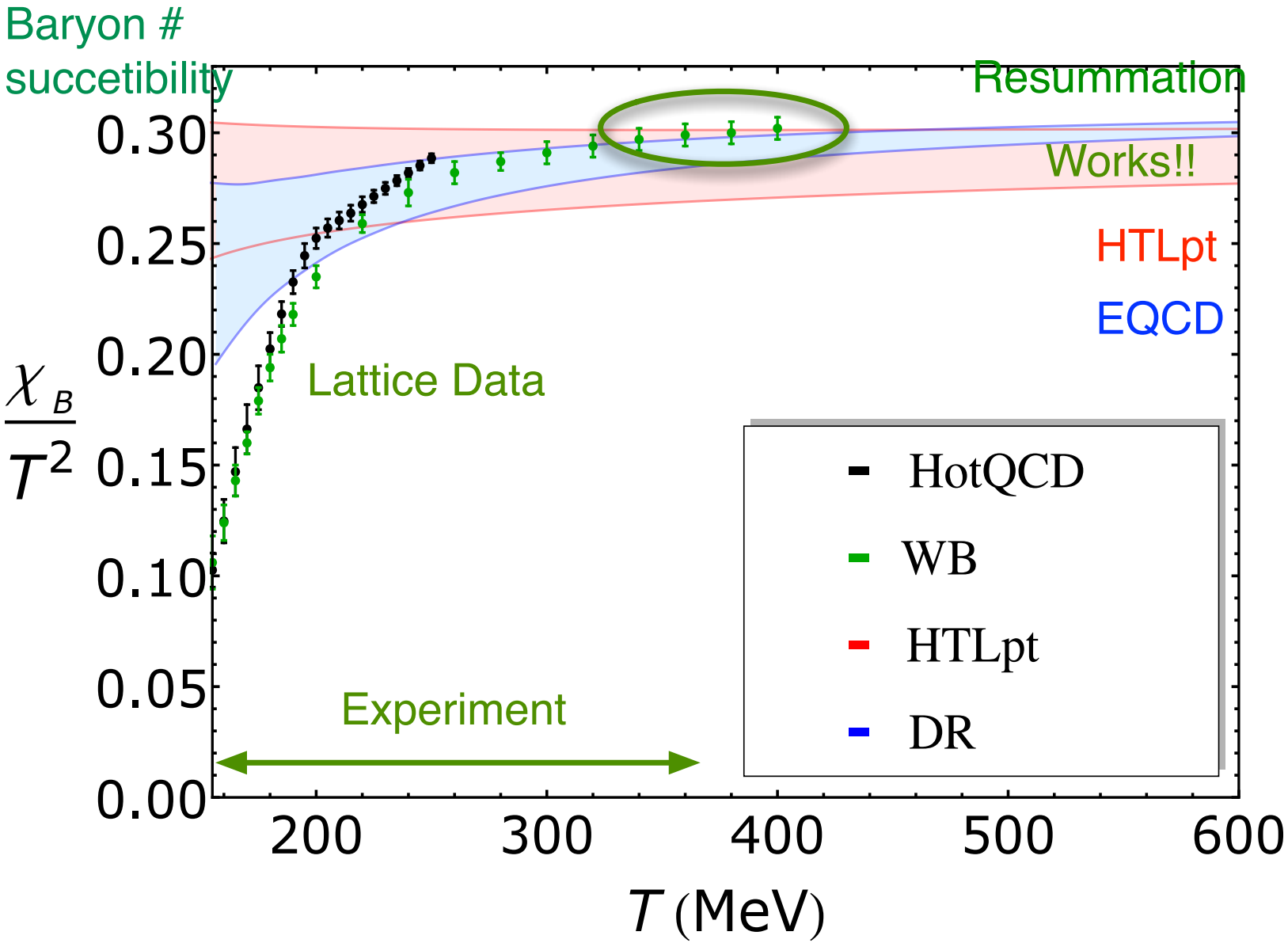


Want to compute transport with similar precision at high T

# Motivation

- This calculation uses LO order photon production rates (Turbide, Rapp, Gale)

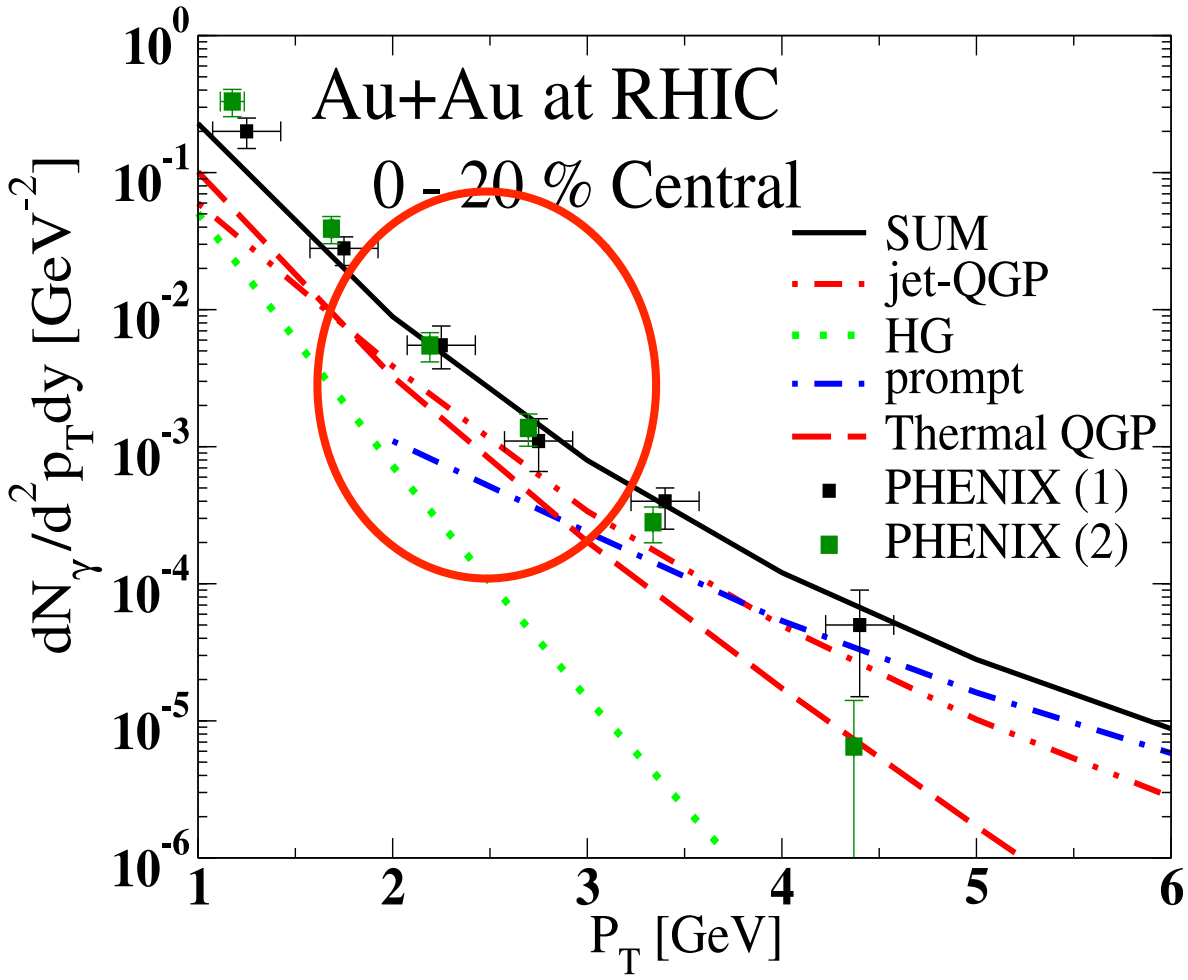


We want to compute this rate at NLO

Thermal rate is dominant for a certain momentum range

Direct photons are measured, but this is not my real motivation . . .

## My real motivations:

1. Energy loss.
2. The shear viscosity.

My real motivation. Energy loss at sub-asymptotic energies is important:

1. Kinematic constraints limit the agreement between energy loss formalisms
   - See the report of the Jet Collaboration: arXiv:1106.1106
2. Finite energy leads to large angle emission outside of radiative loss formalism

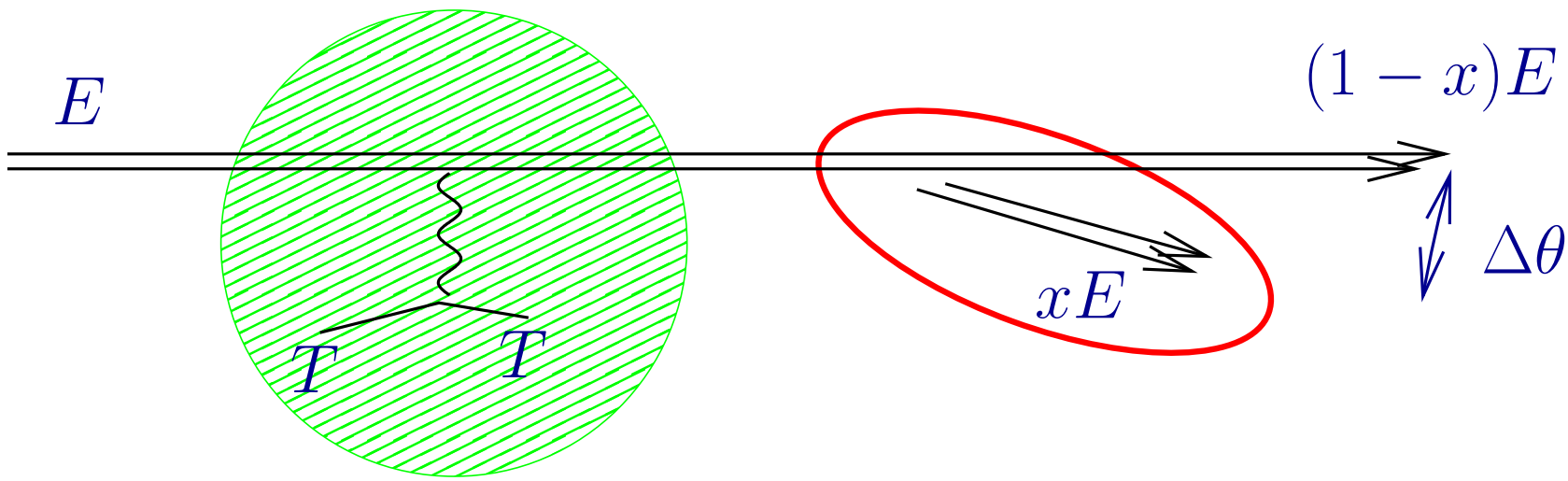


As the bremmed energy gets lower and lower, the angle $\Delta\theta$ gets larger and larger, limiting the agreement

My real motivations:

✓ Energy loss

2. The shear viscosity

## My real motivation. Shear viscosity and the kinetics of weakly coupled QGP

1. Hard Collisions: $2 \leftrightarrow 2$

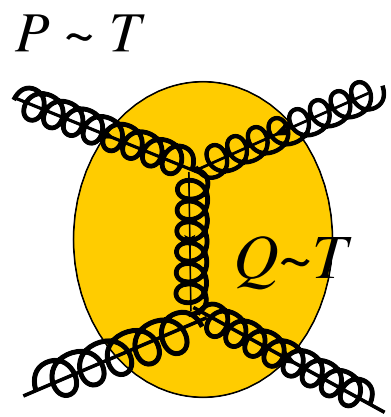


2. Diffusion: collisions with soft random classical field

soft fields have $p \sim gT$ and *large occupation numbers* $n_B \sim \frac{T}{p} \sim \frac{1}{g}$

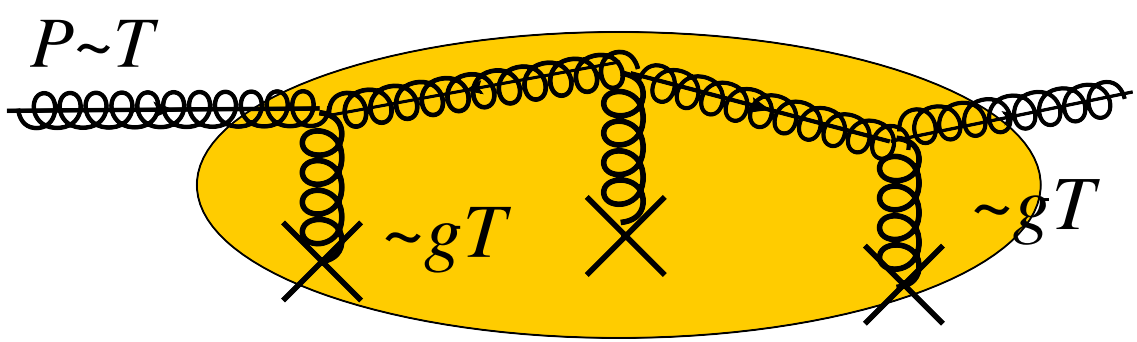

3. Brem: $1 \leftrightarrow 2$

- random walk induces collinear bremsstrhalung

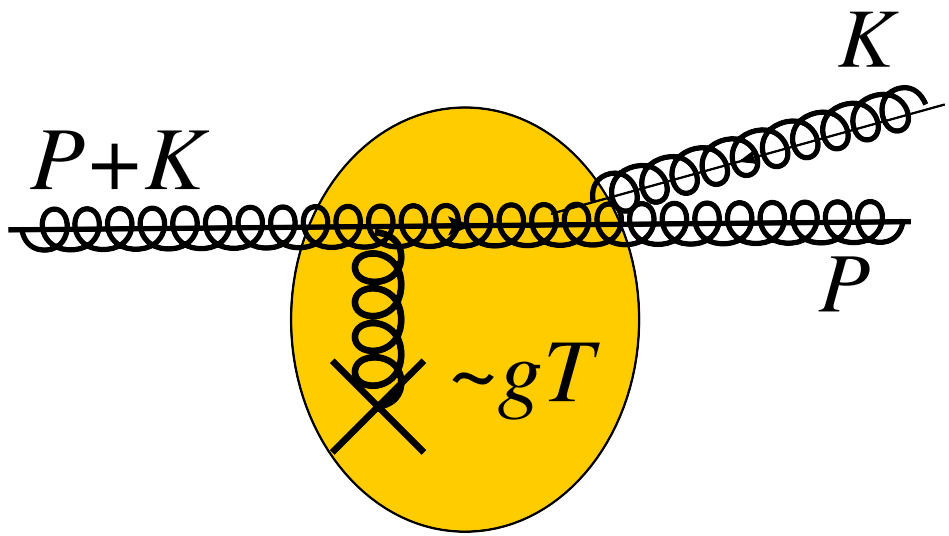


NLO involves corrections to these processes and the relation between them

But shear viscosity is too hard . . .

My real motivations:

- ✓ Energy loss
- ✓ The shear viscosity

Photon production at NLO is a good warm-up calculation.

Lets do it!

$$2k(2\pi)^3 \frac{\mathrm{d}\Gamma}{\mathrm{d}^3 k} = \text{Photon emission rate per phase-space}$$

The photon emission rate at weak coupling:

- The rate is function of the coupling coupling constant and $k/T$:

$$2k(2\pi)^3 \frac{\mathrm{d}\Gamma}{\mathrm{d}^3 k} \propto e^2 T^2 \Big[ \underbrace{O(g^2 \log) + O(g^2)}_{\text{LO AMY}} + \underbrace{O(g^3 \log) + O(g^3)}_{\text{From soft } gT \text{ gluons, } n_B \simeq \frac{T}{\omega} \simeq \frac{1}{g}} + \ldots$$

$O(g^3)$ is closely related to open issues in energy loss:

- At NLO must include drag, collisions, bremsstrhalung, and kinematic limits

## Three rates for photon production at Leading Order

Baier,Kapusta, AMY

1. Hard Collisions – a $2 \leftrightarrow 2$ processes

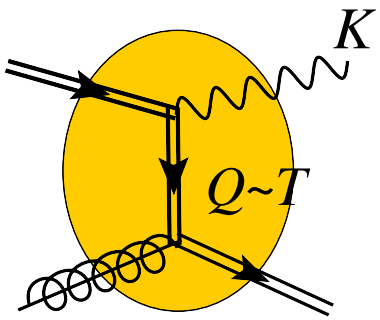


$$\sim e^2 \quad \underbrace{m_\infty^2}_{g^2 C_F T^2/4} \quad \times \quad \underbrace{n_F(k)}_{\text{fermi dist.}} \quad \times \left[ \log\left(T/\mu\right) + C_{2\text{to}2}(k) \right]$$

2. Collinear Bremsstrhalung – a $1 \leftrightarrow 2$ processes

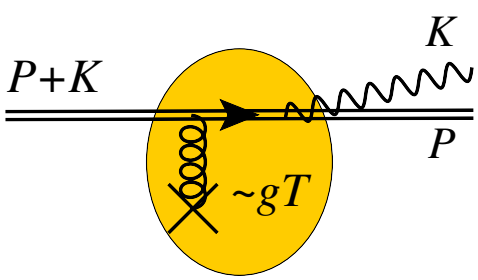


$$\sim e^2\, m_\infty^2 n_F \left[ \qquad \underbrace{C_{\text{brem}}(k)}_{\text{LPM + AMY and all that stuff!}} \qquad \right]$$

3. Quark Conversions – $1 \leftrightarrow 1$ processes (analogous to drag)

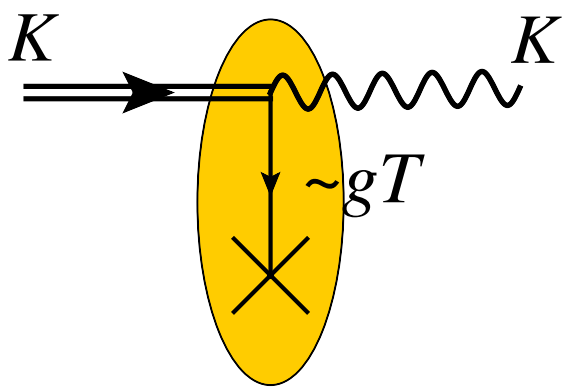


or

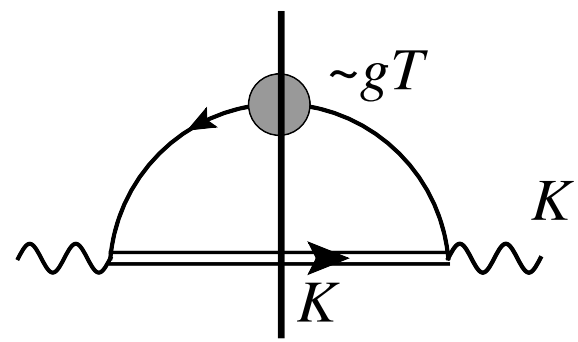


$$= \sim e^2 m_\infty^2 n_F \left[\log(\mu_\perp/m_\infty) + C_{\rm cnvrt}\right]$$

Full LO Rate is independent of scale $\mu_\perp$:

$$2k\frac{\mathrm{d}\Gamma}{\mathrm{d}^3k} \propto e^2 m_\infty^2 n_F \Big[\log\left(T/m_\infty\right) + \underbrace{C_{\rm cnvrt} + C_{\rm brem}(k) + C_{\rm 2to2}(k)}_{\equiv C_{LO}(k)}\Big]$$

## $O(g)$ Corrections to Hard Collisions, Brem, Conversions:

1. No corrections to Hard Collisions:

2. Corrections to Brem:

   (a) Small angle brem. Corrections to AMY coll. kernel. (Caron-Huot)

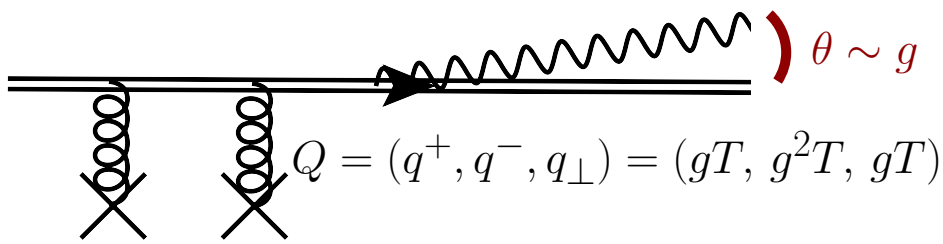


$$C_{LO}[q_\perp] = \frac{T g^2 m_D^2}{q_\perp^2 (q_\perp^2 + m_D^2)} \rightarrow \text{A complicated but analytic formula}$$

   (b) Larger angle brem. Include collisions with energy exchange, $q^- \sim gT$.

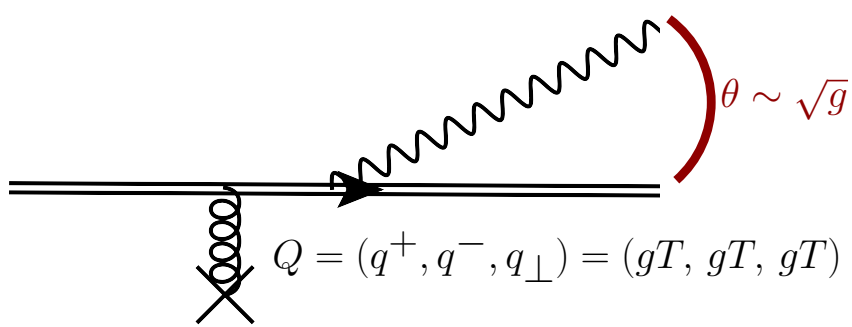

3. Corrections to Conversions:

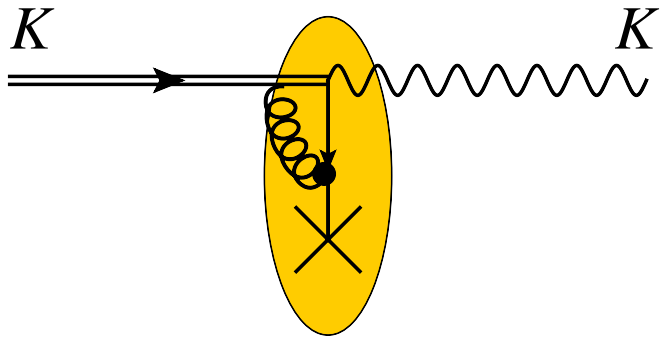


or

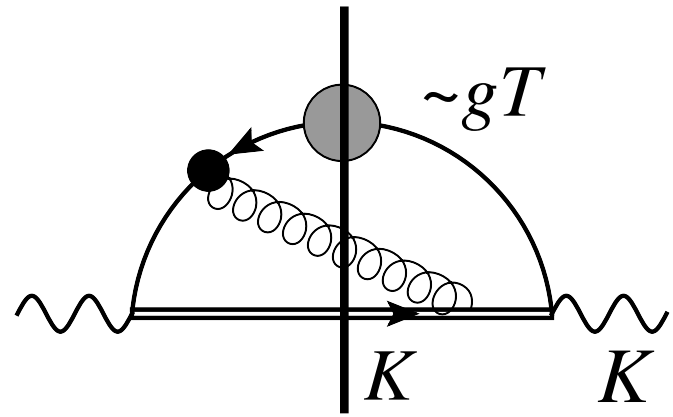


- Doable because of HTL sum rules (light cone causality)
- Gives a numerically small and momentum indep. contribution to the NLO rate

Simon Caron-Huot

Full results depend on all these corrections.

These rates smoothly match onto each other as the kinematics change.

# NLO Results: $\Gamma_{LO+NLO} \sim \mathrm{LO} + g^3 \log(1/g) + g^3$

$$2k\frac{\mathrm{d}\Delta\Gamma_{NLO}}{\mathrm{d}^3k} \propto e^2 m_\infty^2 n_F(k)\Big[\overbrace{\frac{\delta m_\infty^2}{m_\infty^2}\log\left(\frac{\sqrt{2Tm_D}}{m_\infty}\right)}^{\text{conversions}} + \overbrace{\frac{\delta m_\infty^2}{m_\infty^2}C_{\mathrm{large}-\theta}(k)}^{\text{large-}\theta\text{-brem}} + \overbrace{\frac{g^2C_AT}{m_D}C_{\mathrm{small}-\theta}(k)}^{\text{small-}\theta\text{-brem}}\Big]$$

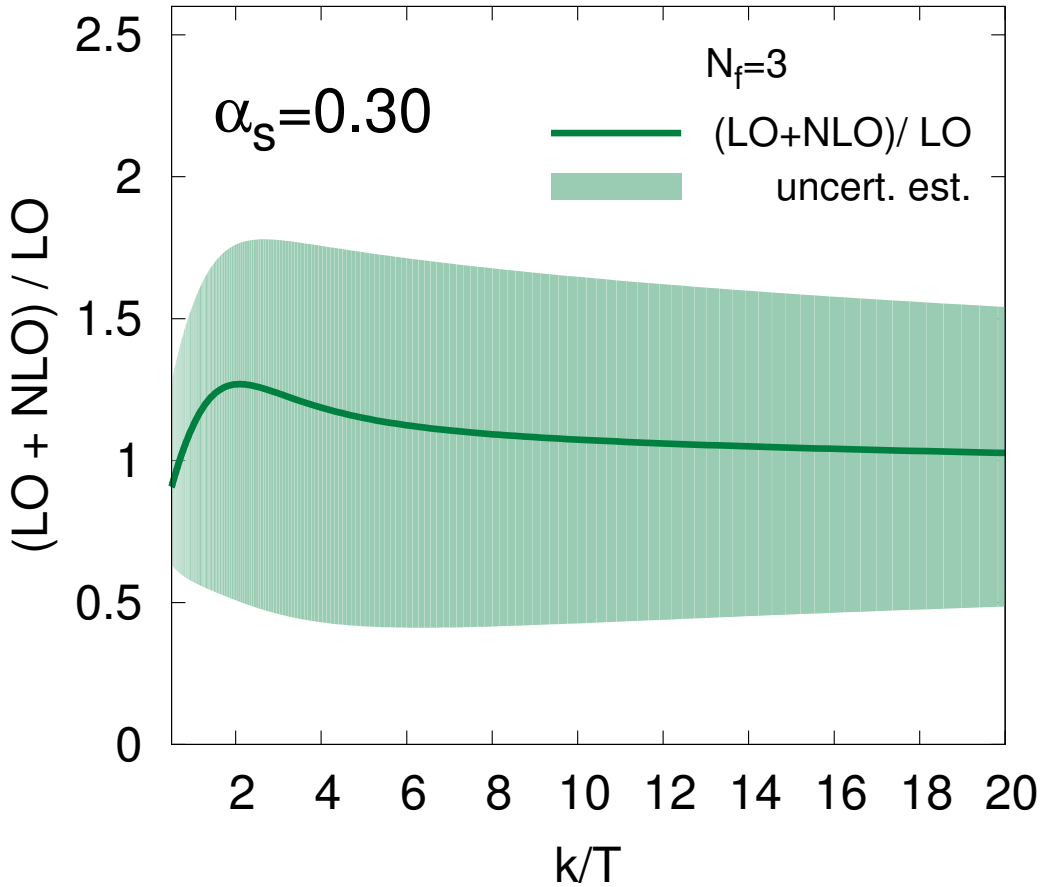


Corrections are small and $k$ independent

# NLO Results: $\Gamma_{LO+NLO} \sim \mathrm{LO} + g^3 \log(1/g) + g^3$

$$2k\frac{\mathrm{d}\Delta\Gamma_{NLO}}{\mathrm{d}^3k} \propto e^2 m_\infty^2 n_F(k)\Big[\overbrace{\frac{\delta m_\infty^2}{m_\infty^2}\log\left(\frac{\sqrt{2Tm_D}}{m_\infty}\right)}^{\text{conversions}} + \overbrace{\frac{\delta m_\infty^2}{m_\infty^2}C_{\mathrm{large}-\theta}(k)}^{\text{large-}\theta\text{-brem}} + \overbrace{\frac{g^2C_AT}{m_D}C_{\mathrm{small}-\theta}(k)}^{\text{small-}\theta\text{-brem}}\Big]$$

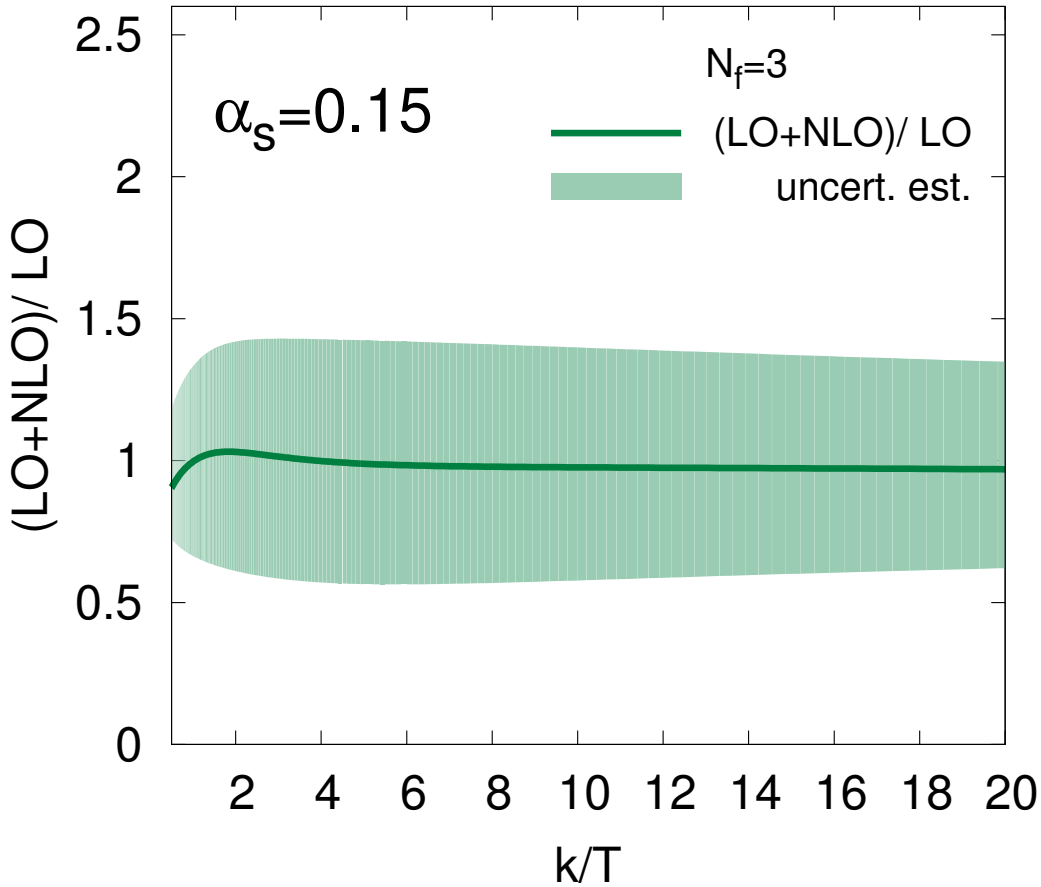


NLO Corrections are small and $k$ independent

The different contributions at NLO (conversions are not numerically important)

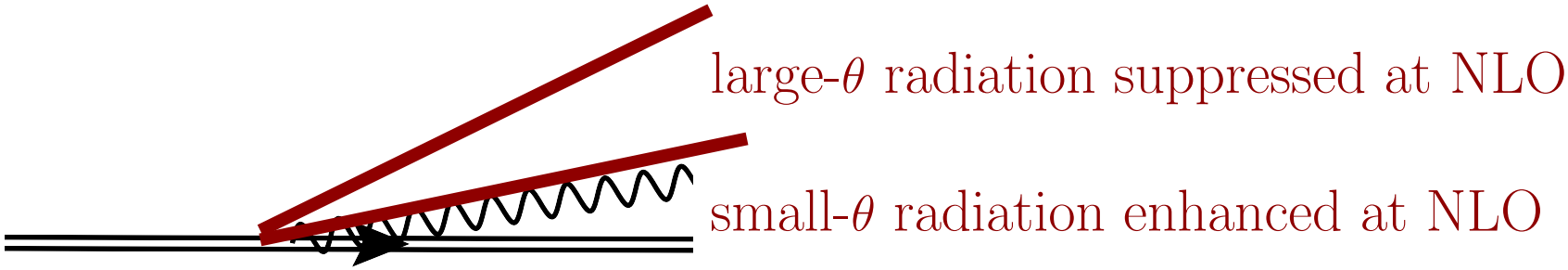


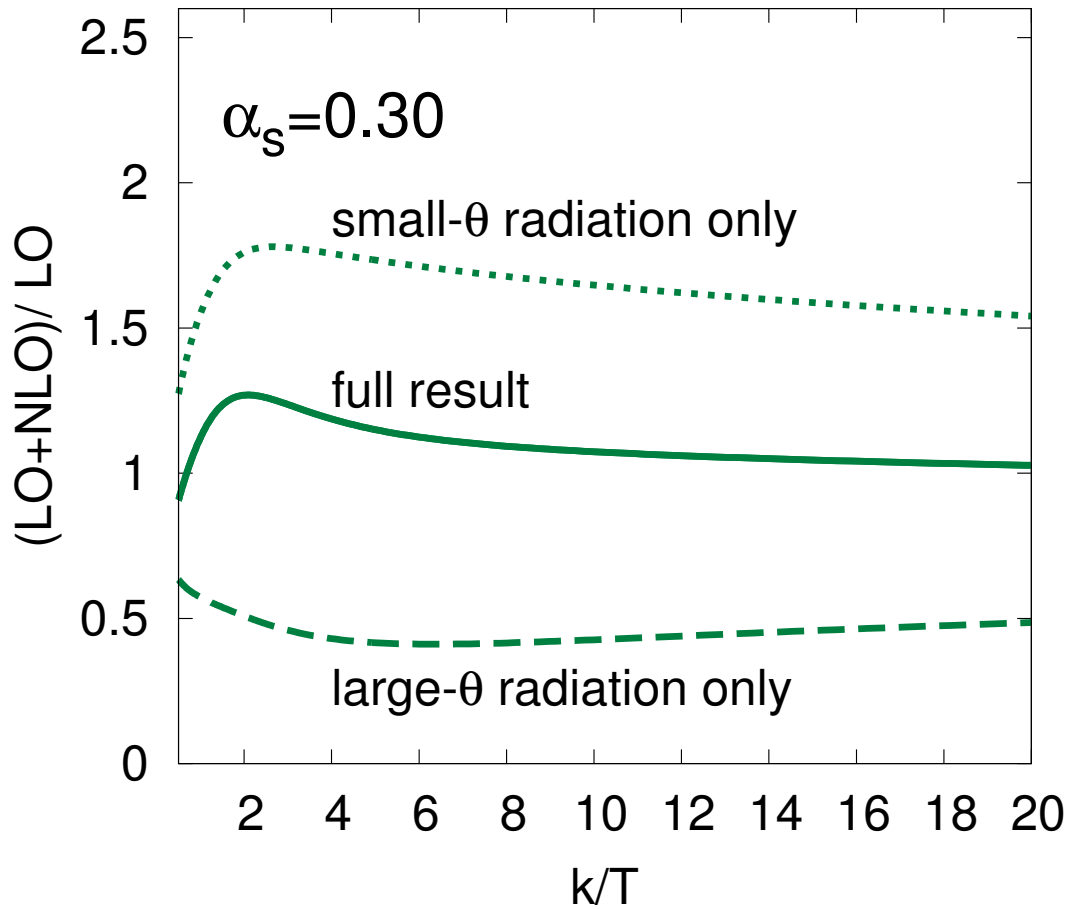

# The calculation

Semi-collinear radiation – a new kinematic window

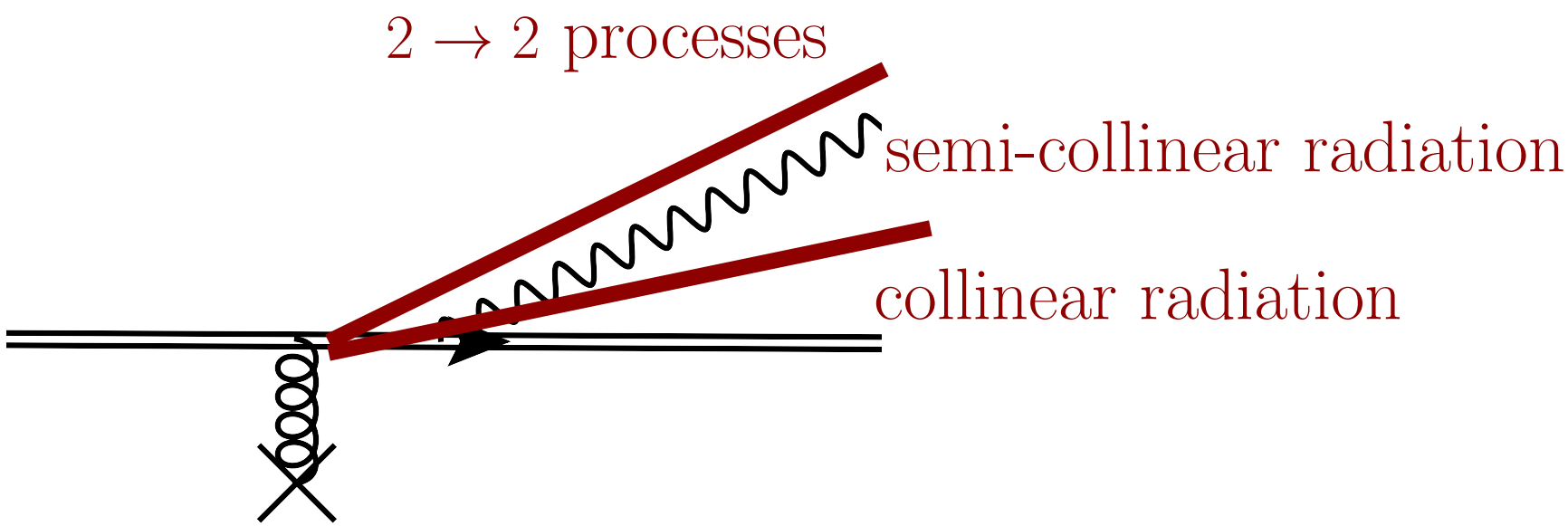


The semi-collinear regime interpolates between brem and collisions

## Matching collisions to brem

- When the gluon is hard the $2 \leftrightarrow 2$ collision:

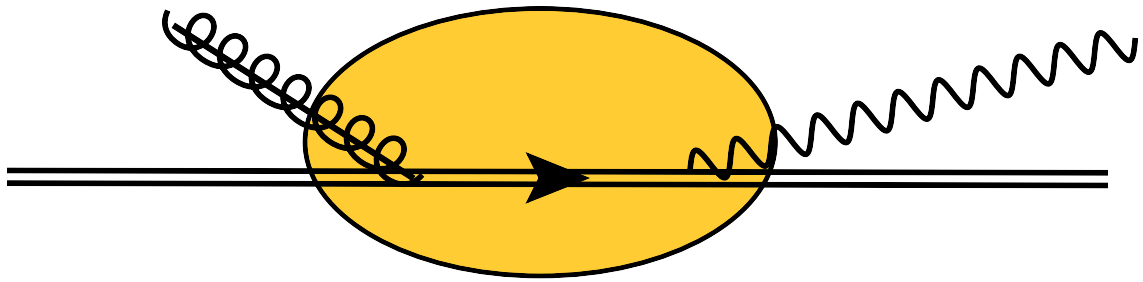

*is* physically distinct from the wide angle brem

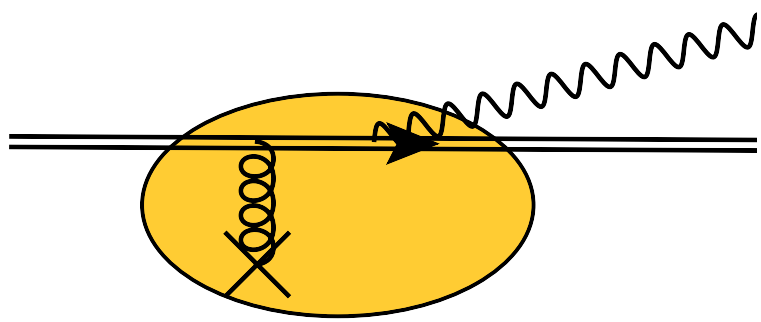

## Matching collisions to brem

- When the gluon becomes soft (a plasmon), the $2 \leftrightarrow 2$ collision:

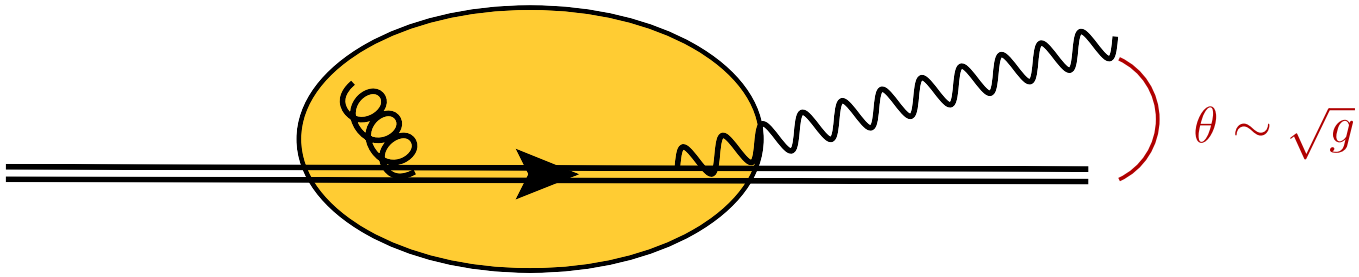


*is not* physically distinct from the wide angle brem

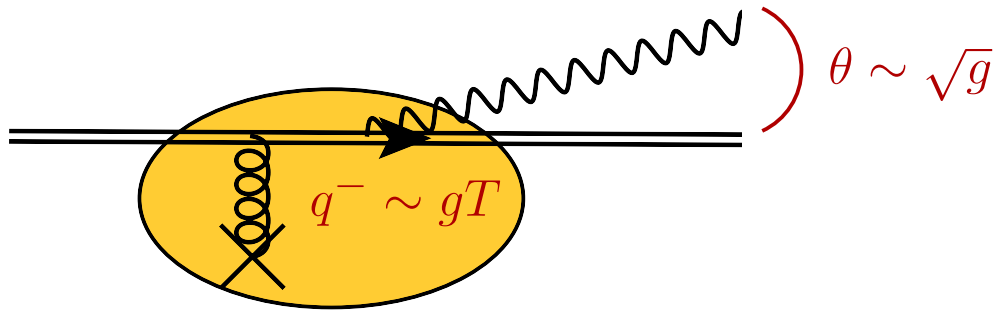


Need both processes

- For harder gluons, $q^- \to T$, this becomes a normal $2 \to 2$ process.
- For softer gluons, $q^- \to g^2 T$, this smoothly matches onto AMY.

## Matching collisions to brem

- When the gluon becomes soft (a plasmon), the $2 \leftrightarrow 2$ collision:

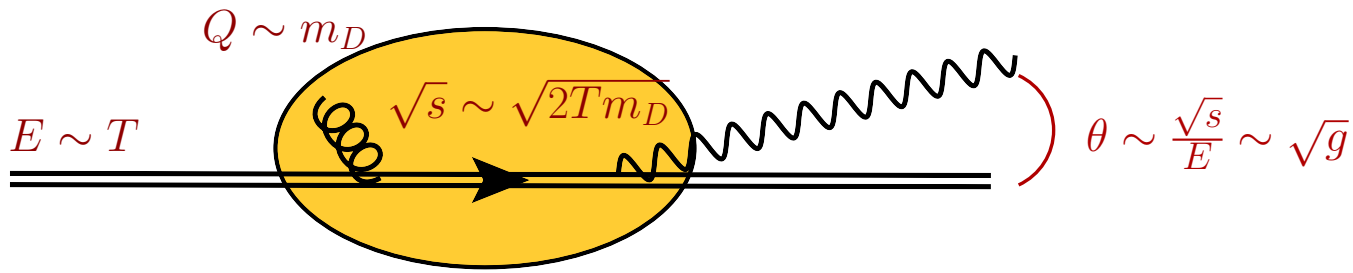


*is not* physically distinct from the wide angle brem

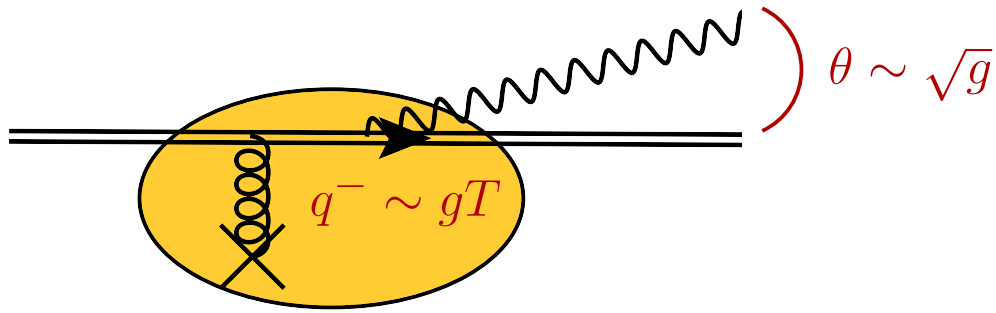


Need both processes

- For harder gluons, $q^- \to T$, this becomes a normal $2 \to 2$ process.
- For softer gluons, $q^- \to g^2T$, this smoothly matches onto AMY.

## Brem and collisions at wider angles (but still small!)

- Photon emission rate

$$2k\frac{\mathrm{d}\Gamma}{d^3k} \sim \int_{\mathrm{phase-space}} n_{\mathbf{p}}(1-n_{\mathbf{p}+\mathbf{k}})\,|\mathcal{M}|^2\,(2\pi)^4\delta^4(P_{\mathrm{tot}})$$

- The matrix element is

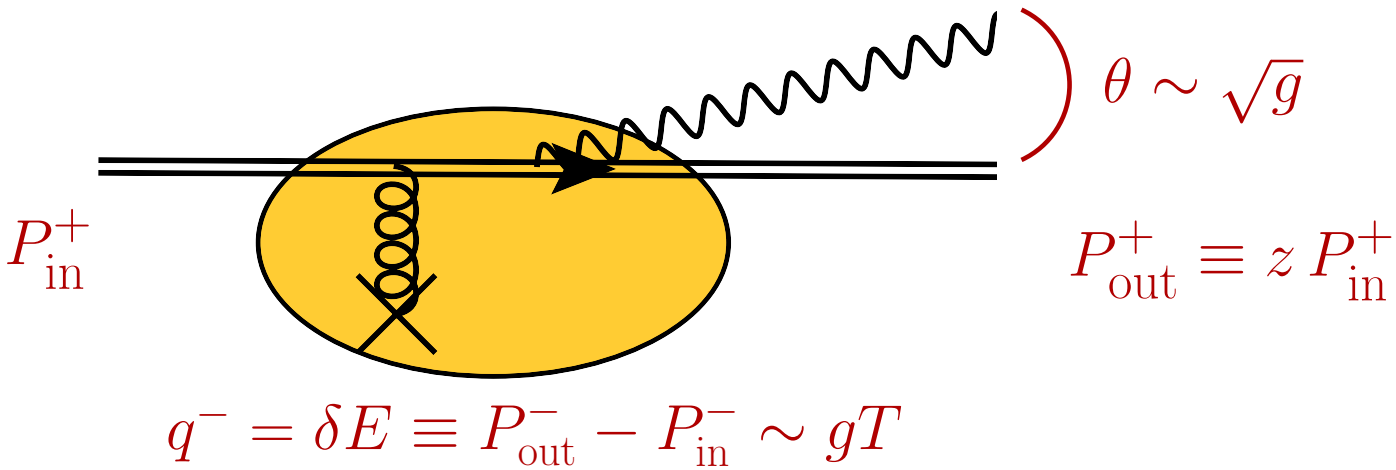


$$|\mathcal{M}|^2\,(2\pi)^4\delta^4(P_{\mathrm{tot}}) \propto \int_Q \underbrace{\frac{1+z^2}{z}}_{\text{QCD splitting fcn}} \frac{1}{(q^-)^2} \underbrace{\langle F_{i+}\,F_{i+}(Q)\rangle}_{\text{scattering-center}} 2\pi\delta(q^- - \delta E)$$

All of the dynamics of the scattering center in a single matrix element $\langle F_{i+}F_{i+}(Q)\rangle$

## Finite energy transfer sum-rule

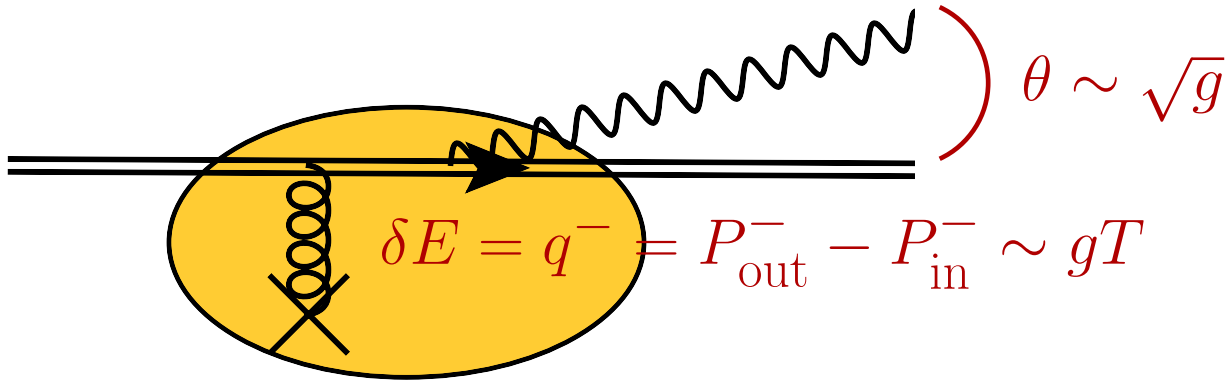


- The AMY collision kernel $C[q_\perp]$ involves

Aurenche, Gelis, Zakarat

$$q_\perp^2 C[q_\perp] = \int_{-\infty}^{\infty} \frac{\mathrm{d}q^+}{2\pi} \langle F_{i+} F_{i+}(Q) \rangle|_{q^-=0} = \frac{T m_D^2}{q_T^2 + m_D^2}$$

- We need a finite $q^- = \delta E$ generalization of the sum rule

$$\int_{-\infty}^{\infty} \frac{\mathrm{d}q^+}{2\pi} \langle F_{i+} F_{i+}(Q) \rangle|_{q^-=\delta E} = T \left[ \frac{2(\delta E)^2(\delta E^2 + q_\perp^2 + m_D^2) + m_D^2 q_\perp^2}{(\delta E^2 + q_\perp^2 + m_D^2)(\delta E^2 + q_\perp^2)} \right]$$

Wider angle emissions can be included by a “simple” modified collision kernel

Matching between brem and conversions

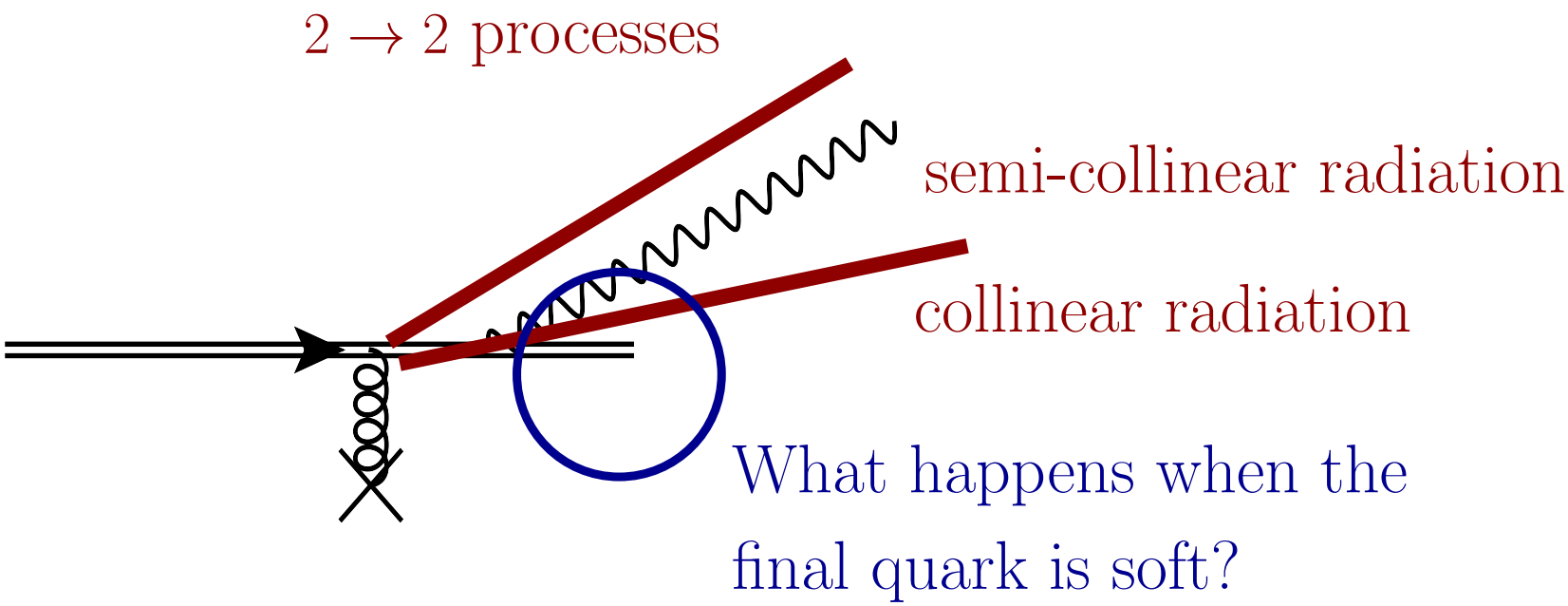


When the quark becomes soft need to worry about conversions.

## Matching between brem and conversions

- When the final quark line is hard, the brem process :

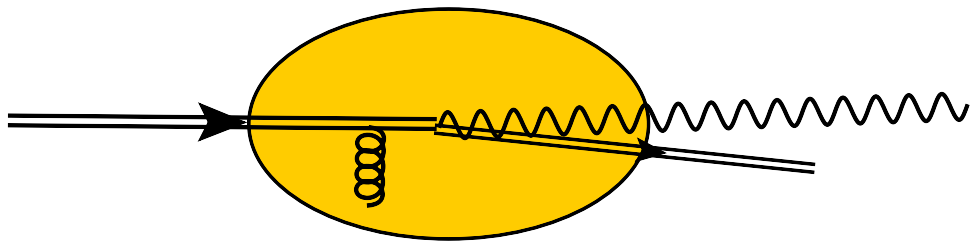

*is* physically distinct from the conversion process:

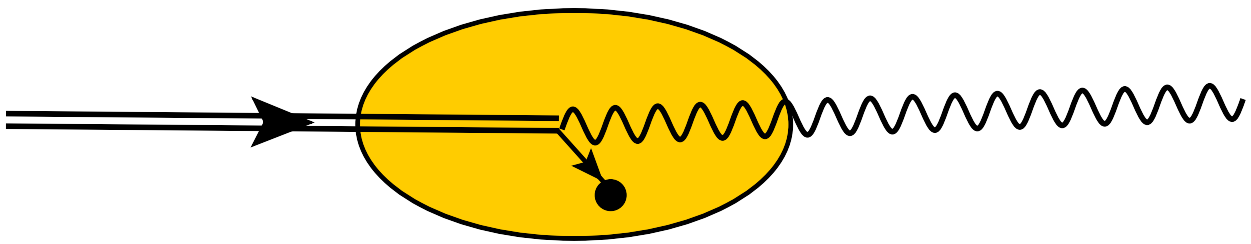

## Matching between brem and conversions

- When the final quark line becomes soft, the brem process :

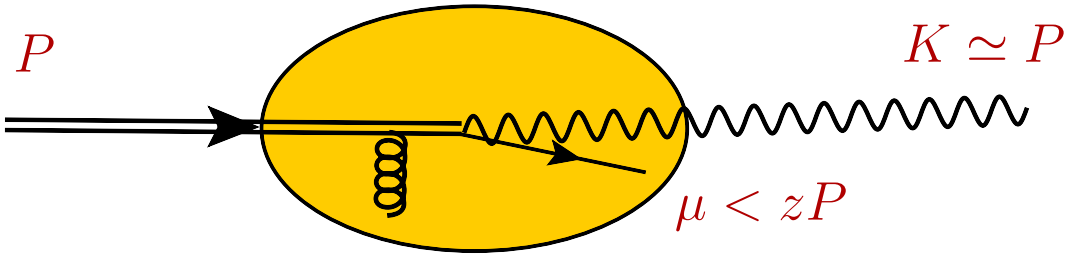


*is not* physically distinct from the conversion process

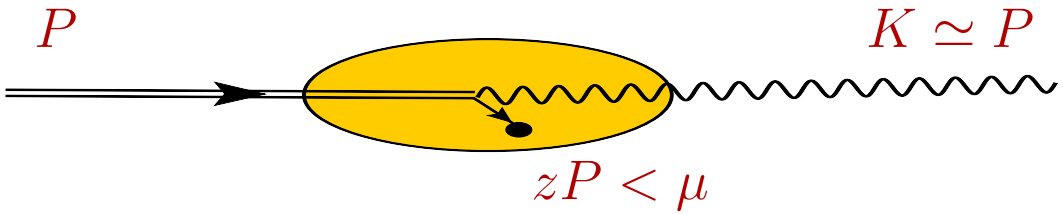


Separately both processes depend on the separation scale, $\mu \sim gT$, but . . .

the $\mu$ dep. cancels when both rates are included

- The LO small-$\theta$ and large-$\theta$ brem rates depend linearly and logarithmically on an infrared separation scale, $\mu$.

The NLO conversion rate will depend on a UV cutoff $\mu$ and cancels this dependence

## Brem rates with a soft quark

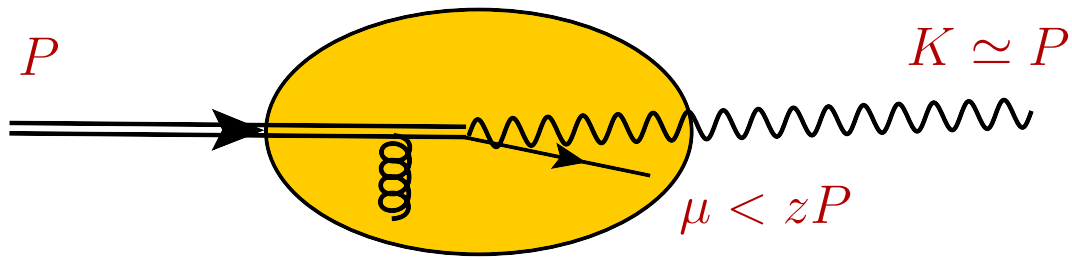


- Small angle brem

$$2k\frac{\mathrm{d}\Gamma}{d^3k}\bigg|_{zP>\mu} = \text{Leading Order Rate} \quad + \quad \text{Finite} \quad - \quad \underbrace{\#\, g^2\mu}_{\text{linear IR dependence } \mu}$$

- Wide angle brem

$$2k\frac{\mathrm{d}\Gamma}{d^3k}\bigg|_{zP>\mu} \propto \underbrace{\frac{\delta m_\infty^2}{4\pi}\log\frac{\sqrt{2Tm_D}}{\mu}}_{\text{Log IR dependence on } \mu} \quad + \quad \text{Finite}$$

The conversion rate should cancel this dependence on $\mu$

## Computing the conversion rate with sum-rules (LO):

(see also Bodeker)

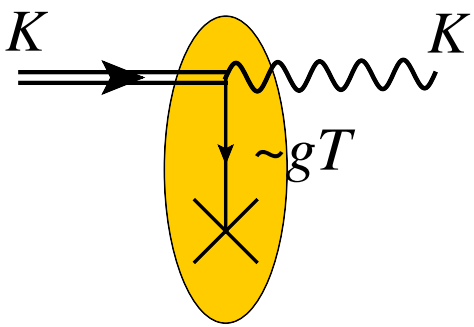


$$2k(2\pi)^3 \frac{\mathrm{d}\Gamma_{\mathrm{cnvrt}}}{\mathrm{d}^3 k} \propto e^2 n_F(k)\ \hat{q}_{\mathrm{cnvrt}}(\mu)$$

- $\hat{q}_{\mathrm{cnvrt}}$ is the quark version of $\hat{q}$

$$\hat{q}_{\mathrm{cnvrt}}(\mu_\perp) = \int^{\sim\mu} \frac{\mathrm{d}^2\mathbf{p}_T}{(2\pi)^2} \underbrace{\int_{-\mu}^{\mu} \frac{\mathrm{d}p^z}{2\pi}\, \mathrm{Tr}\left[\gamma_+ S^<(\omega,\mathbf{p})\right]_{\omega=p^z}}_{\text{evaluate with sum rule}}$$

$$= \int^{\mu} \frac{d^2\mathbf{p}_T}{(2\pi)^2} \frac{m_\infty^2}{p_T^2 + m_\infty^2}$$

where

$$S_R(X) = \left\langle \psi(X) e^{ig\int_0^X dx^\mu A_\mu} \bar{\psi}(0) \right\rangle$$

Computing the conversion rate at NLO with sum-rules:

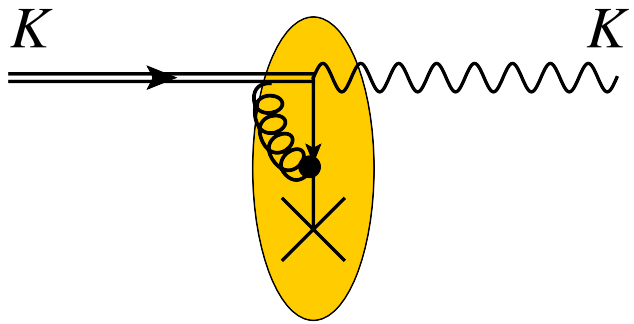


$$2k(2\pi)^3 \frac{\mathrm{d}\Gamma_{\mathrm{cnvrt}}}{\mathrm{d}^3 k} \propto e^2 \; n_F(k) \; \hat{q}_{\mathrm{cnvrt}}(\mu)$$

- At NLO we have only to replace $m_\infty^2 \to m_\infty^2 + \delta m_\infty^2$

$$\hat{q}_{\mathrm{cnvrt}} = \underbrace{\int^{\mu} \frac{d^2\mathbf{p}_\perp}{(2\pi)^2} \frac{m_\infty^2 + \delta m_\infty^2}{p_T^2 + m_\infty^2 + \delta m_\infty^2}}_{\text{finite + UV logarithmic divergence in } \mu} + \underbrace{\#g^2\mu}_{\text{linear UV divergence in } \mu}$$

The UV divergences of conversion rate match with the IR divergences of large and small angle brem giving a finite answer

Summary of the matching calculations at NLO

$$2k(2\pi)^3 \frac{\mathrm{d}\Delta\Gamma_{NLO}}{\mathrm{d}^3k} \propto \underbrace{\text{finite} \quad - \quad C_1 g^2 \mu}_{\text{collinear contribution}}$$

$$+ \underbrace{\text{finite} \quad + \quad C_2 \frac{\delta m_\infty^2}{4\pi} \log \frac{\sqrt{2Tm_D}}{\mu}}_{\text{semi-collinear contribution}}$$

$$+ \underbrace{\text{finite} \quad + \quad C_1 g^2 \mu \quad + \quad C_2 \frac{\delta m_\infty^2}{4\pi} \log \frac{\mu}{m_D}}_{\text{conversions}}$$

The $\mu$ dependence cancels between the different contributions

## Conclusion

- The result again

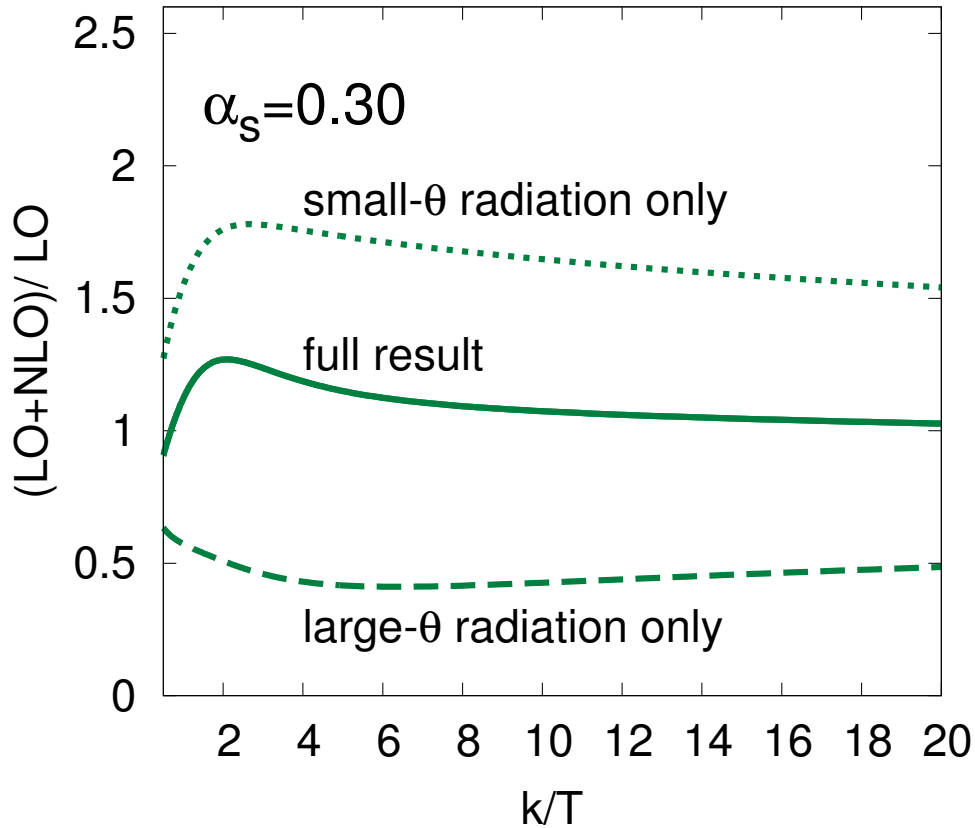


- All of the soft sector buried into a few coefficients, $\delta m_\infty^2$ and $\hat{q}_{\rm cnvrt}$
  - Can we compute these non-perturbatively ?

Many things can be computed next (e.g. shear viscosity and e-loss)

# Detecting quarkyonic matter via EM probes?

Based on ongoing work with Sascha Vogel
PRL107:152301,2011 , arXiv:1204.3272 with Stefano Lottini
Also , 1006.2471 (PRC ),with with Igor Mishustin ,1105.0188 (JHEP ) with Piero Nicolini

G. Torrieri
EMMI
HIC for FAIR
Helmholtz International Center
FIAS Frankfurt Institute for Advanced Studies

## Synopsis

**What is** quarkyonic matter. Definition from Nucl. Phys. A **796**, 83 (2007), by McLerran and Pisarski:
Coexistance of pQCD with confinement/baryonic degrees of freedom !
NOT confinement-chiral symmetry separation, chirally inhomogeneus phases etc!

**Does it exist?** An attempt at an estimate from percolation theory

**Towards a pheonomenolgy** of quarkyonic matter via electromagnetic signals

No conclusions as yet.

Lets get some insights in the large $N_c$ limit... $(N_c \simeq 3 \gg 1, N_c^{-1} \ll 1)$

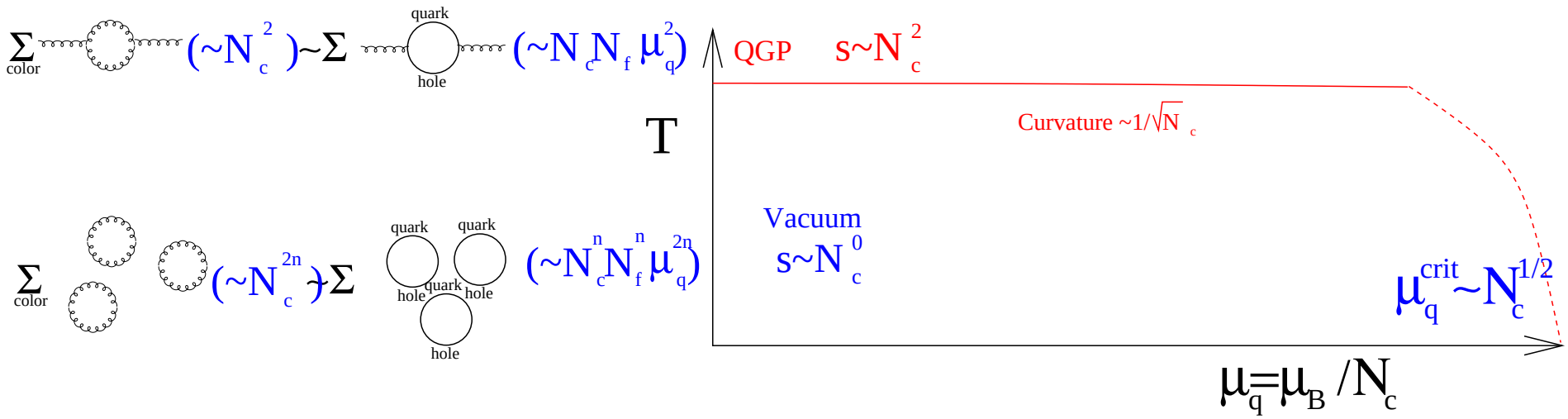


Deconfinement line flattens, since for deconfinement $\mu_Q \sim N_c^{1/2} N_f^{-1/2} m_B$ (also No critical point , $N_c \gg N_f$ means confined phase has $Z_N$ global symmetry, Deconfinement always a phase transition! )

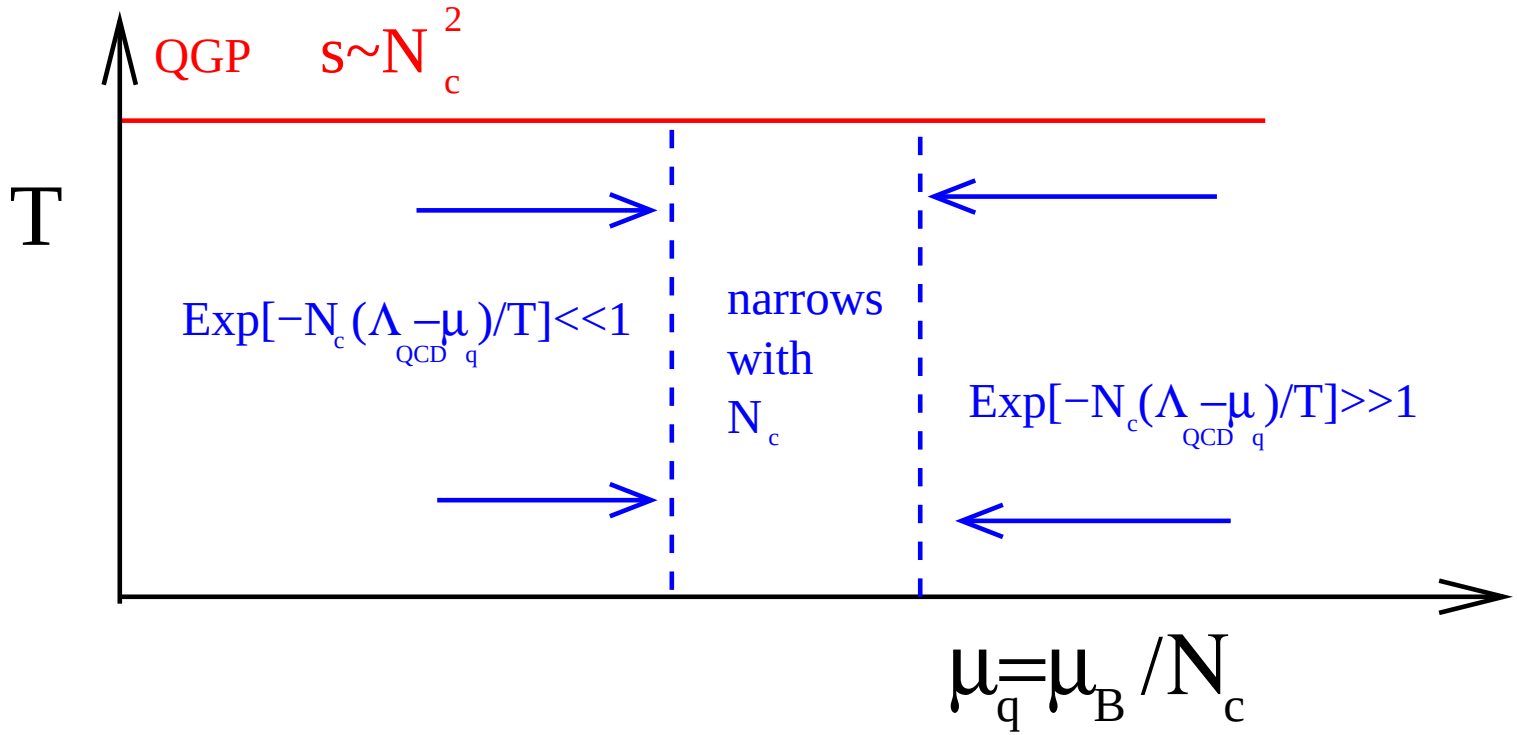


line separating "vacuum" from "dense nuclear matter" narrows
McLerran+Pisarski, arXiv:0706.2191: line defines new "quarkyonic" phase!

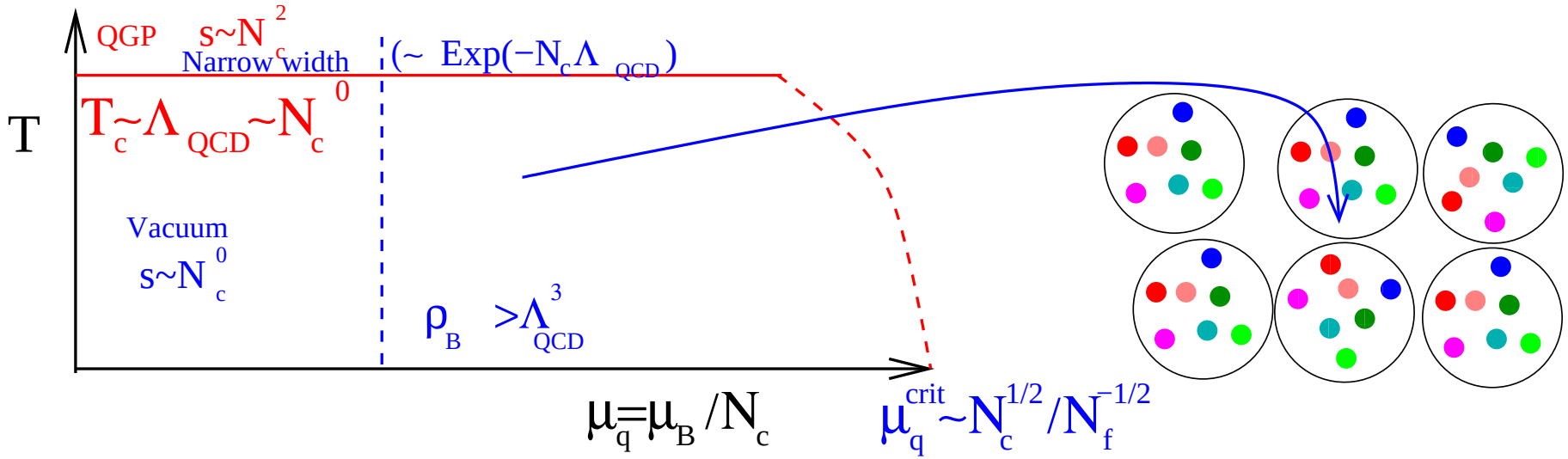


Inter-quark distance in this phase $\sim N_c^{-1/3} \to 0$ , asymptotic freedom in configuration space!
Confined but quasi-free quarks below fermi surface and $P \sim N_c$ (quark-hole?)

A totally new phase (FAIR,RHIC@low$\sqrt{s}$,Neutron stats,...) alternative to critical point, inaccessible to EFT! But...

How close are we to the $N_c \to \infty$ limit?

In vacuum many qualitative ($\sim \mathcal{O}(30\%)$) agreements (Skyrme,planar diagrams, OZI rule,... ). In-medium remarkable ($\sim \mathcal{O}(1000\%)$) failures

| Quantity | $N_c \to \infty$ | QCD |
|---|---|---|
| $E^{binding}_{Nucleus}$ | $N_c \Lambda_{QCD}$ | $\ll \Lambda_{QCD}, m_\pi$ |
| $\Delta E_{spin-flip}$ | $\sim \Lambda_{QCD}/N_c$ | $\sim \Lambda_{QCD}$ |
| Ground state | Crystal | Liquid |

Phase transitions in $N_c$ between $N_c = 3$ and $N_c = \infty$?
(Or is "quarkyonic matter" simply nuclear matter at large $N_c$?)

A conjecture: "in-medium" $N_c$ "not large" wrt <u>number of neigbhors</u>

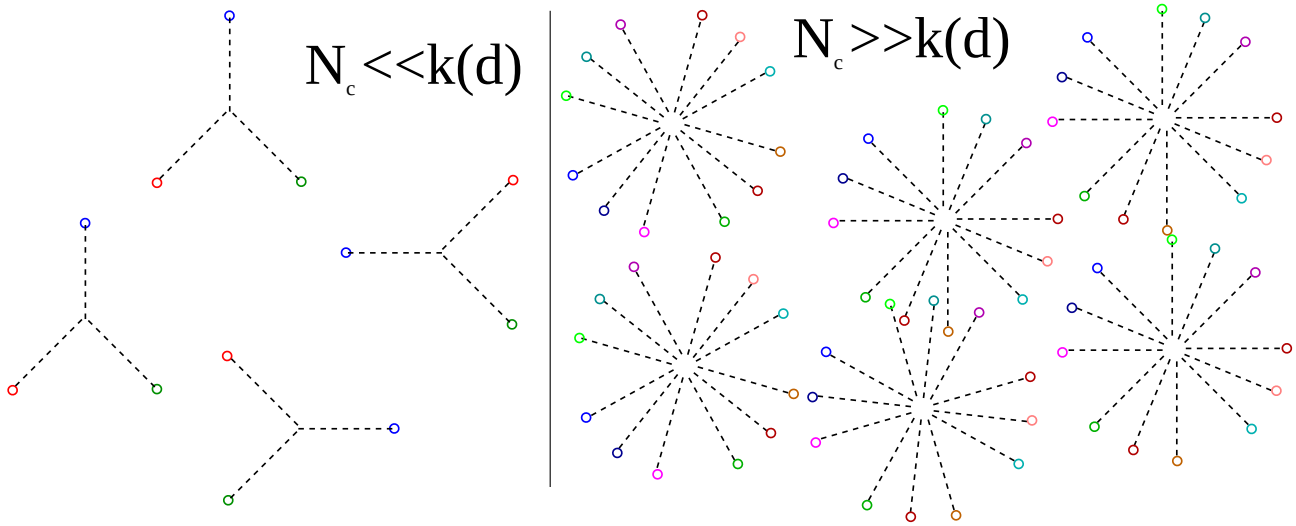


G.Torrieri,S.Lottini
Phys.Rev.Lett. 107 (2011) 152301

G.Torrieri,I.Mishustin
Phys.Rev. C82 (2010) 055202

**Pauli-blocking** of color wavefunctions in dense system ($\sim N_c/(N_f N_N)$ )

**Percolation** of any "perturbative" interactions ($\sim N_c/N_N$ )

Any "quarkyonic" phase-line will <u>curve</u> in $N_c - \rho_B$

## $N_c$ scaling and Percolation at $\mu_Q = \Lambda_{QCD}$

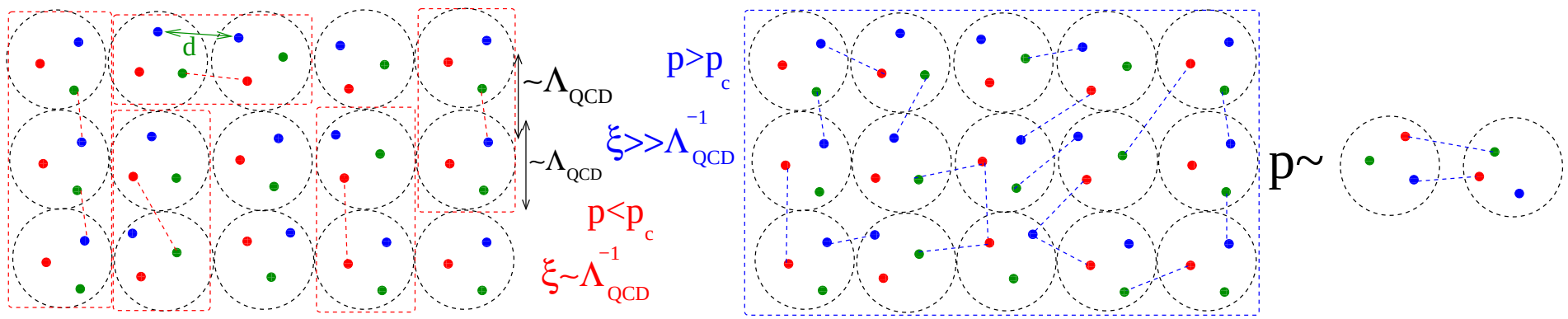


With $N_c$ colors, ways two baryons can interact with one another grows fast with $N_c$ . Correlation length diverges at percolation, existence of transition independent of microscopic details (percolation behavior universal! )

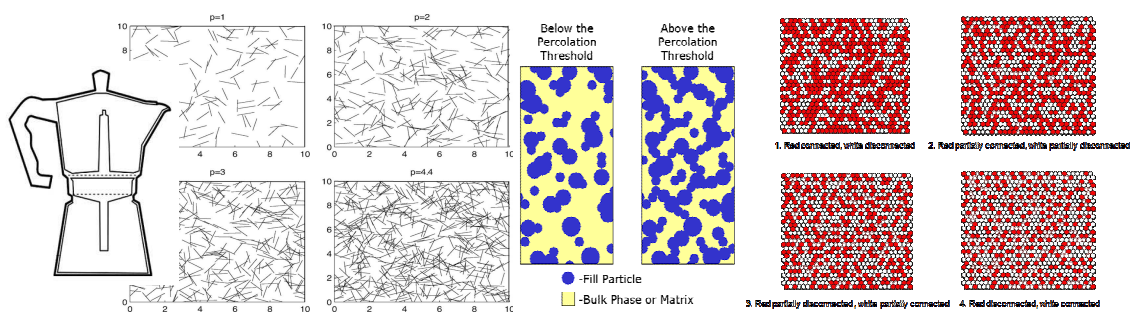

## An ansatz with confinement and correct $N_c$ scaling

$$p = 1 - \left(q_{(1),ij}\right)^{(N_c)^\alpha} \quad , \quad q_{(1),ij} = \int f_A(x_i)\mathrm{d}x_i \int f_B(x_j)\mathrm{d}x_j \left(1 - F(|x_i - x_j|)\right)$$

(Mathematically very similar to Glauber model) We assume a range of probability amplitudes for the exchange $i \leftrightarrow j$ with rapid fall-off at distances $\Lambda_{QCD}^{-1}$ ) (confinement) and right $N_c$ scaling ($\sim \lambda/N_c$ )

$$F(y) = \frac{\lambda}{N_c}\mathcal{N} \begin{cases} \theta(1 - \frac{y}{r_T}) \\ \exp\left(-\frac{3}{4}\frac{y^2}{r_T^2}\right) \\ \frac{2r_T^2}{\pi y^2}\sin^2\left(\frac{y}{r_T}\right) \end{cases}$$

(Generic phenomenological propagators including confinement, eg Gribov-Zwanziger )

A percolation transition in $N_c$ was found .

Keeping density fixed, Critical $N_c$ for $\Theta$-function $P_{i\leftrightarrow j}$ in position and momentum

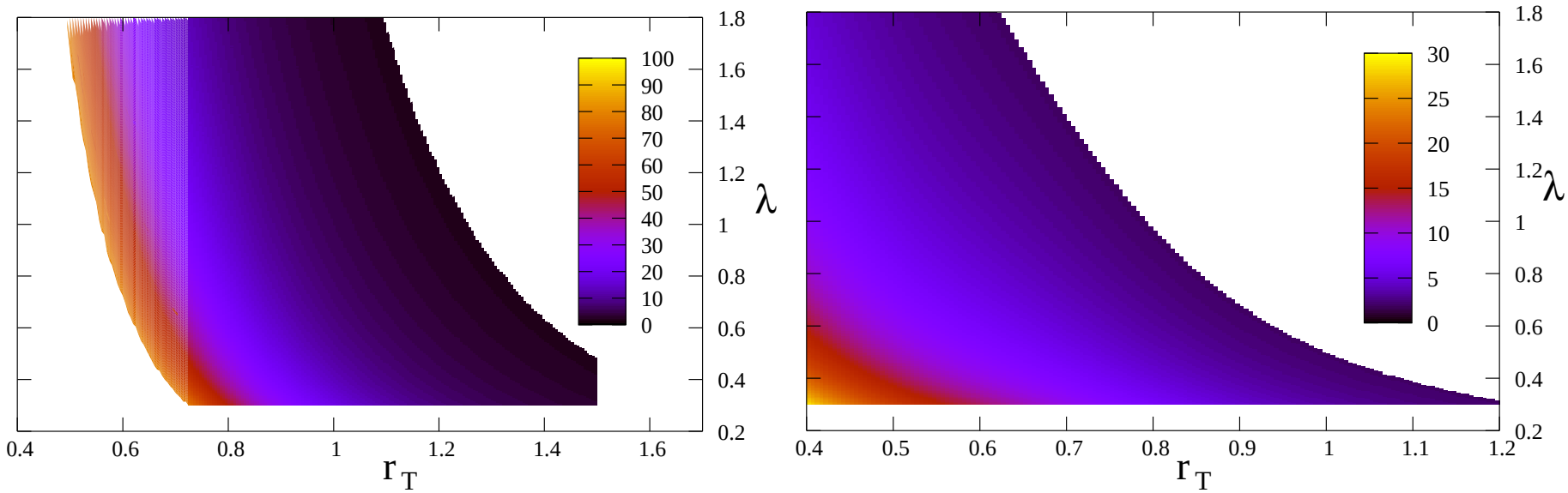


"typical" Parameters of order unity give a critical number of colors for percolation well above 3. These are lower limits, since we assume hexagonal lattice (Skyrme cubic and disordered $p_c$ higher).

## But lets vary $\mu_Q$:Percolation and deconfinement

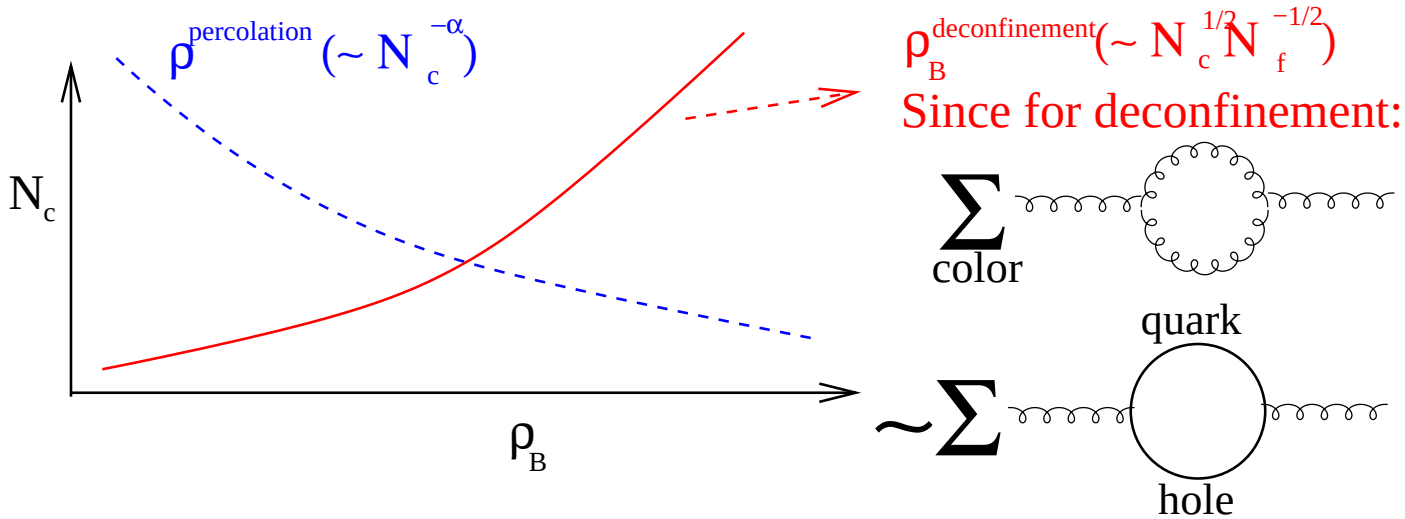


Percolation: $\rho - N_c$ anti correlated.
Deconfinement: $\rho - N_c$ correlated $\mu_B^{dec} \sim N_c^{1/2} N_f^{-1/2} m_B \sim N_c^{3/2} N_f^{-1/2} \mu_q$

$N_c \leq N_c^{crit}$ Deconfinement happens below percolation, ie percolation transition does not exist separately from deconfinement
$N_c \geq N_c^{crit}$ Percolation, deconfinement separate (Quarkyonic phase?)

What is this critical $N_c$? Percolation in a "glass": Conceptually similar, technically more involved

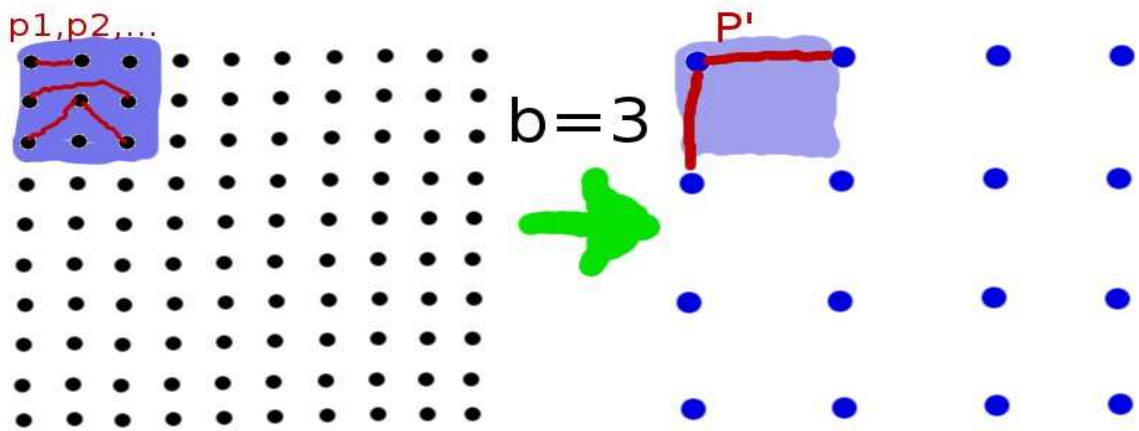


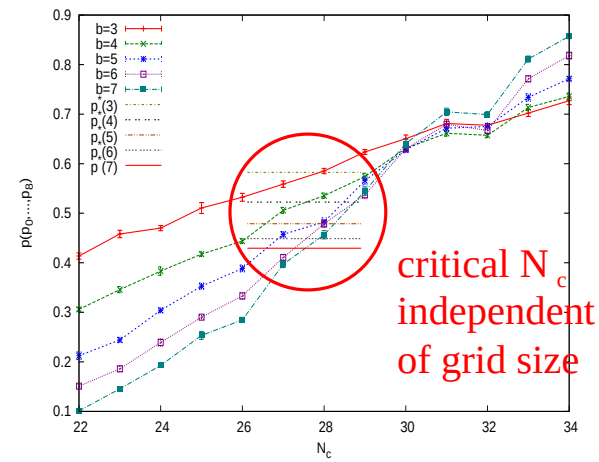


Gimel,Nicolai,Durand, J Phys A Math Gen 32 L515 (1999)

$$p^*\left(b, \Theta(x_T, \lambda, N_c)\right) = \Pi_{physical}\left(\Theta(x_T, \lambda, N_c)\right) + \beta b^{-y} \quad , \quad y = 0.81$$

Quarkyonic phase might exist at $\Lambda_{QCD} \leq \mu_Q \leq N_c N_f^{-1} \Lambda_{QCD}$

In PRL we neglected Density-$N_c$ curvature and fixed density to $\mu_B \sim \Lambda_{QCD}$

.

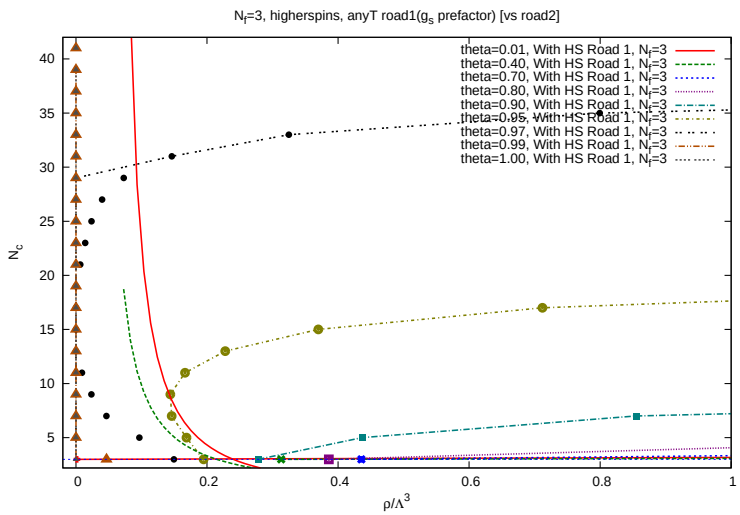


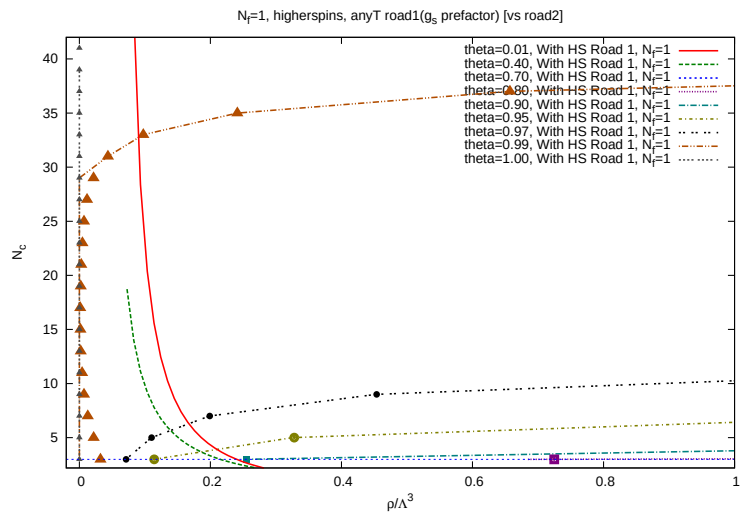


A sliver of $n - \rho - N_c = 3$ space which is percolating but confined seems to be there, but... Width depends a lot on whether $N_f = 2$ or $N_f = 3$ . "Systematic error too big . Need phenomenology (an experimental signature for quarkyonic matter)!

Observing such a percolating phase: What does it look like?

**Baryons** are heavy and immobile "background"

**Quarks** are <u>delocalized</u>, since $\rho_{baryon}^{-1/3} \leq R_{baryon}$ but color <u>confined</u> Color-Flavor-Spin separation could ensure "free" quarks while localizing color

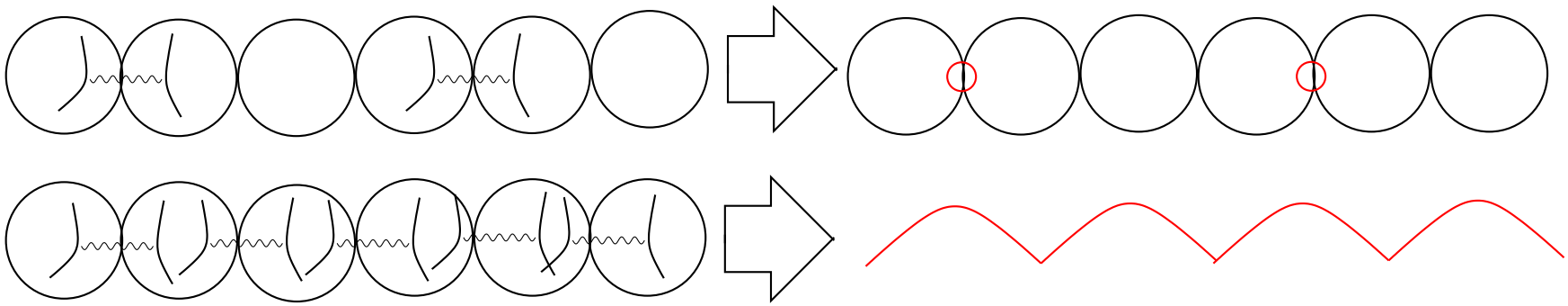

EoS similar to QGP. transport coefficients "non-trivial" (2-scale system)
An immediate physical analogy: conductor in QED, with baryons playing the role of <u>atoms</u>, percolation analogous to conductor-insulator transition

## pQCD but not quite: the role of baryons

Unlike pQCD, quarkyonic matter's "vacuum" is a classical dense baryon state. Treating baryons as mean fields will give a momentum-dependent form factor to all pQCD processes

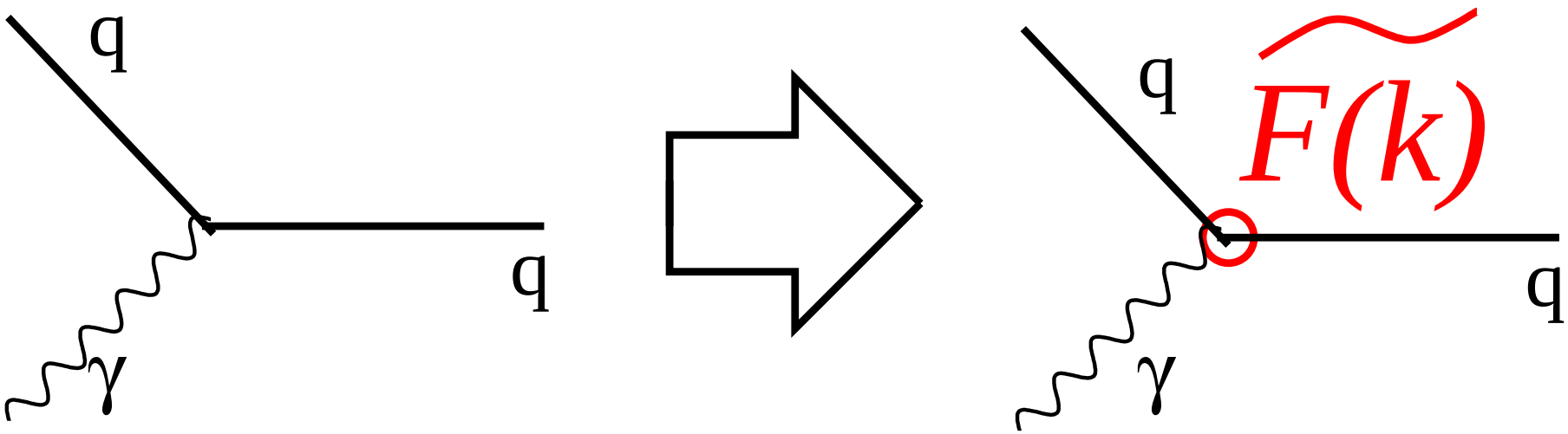


$F(k)$ gives the F.T. of the baryonic gluon content. For the equation of state, it should just be a $\mathcal{O}(1)$ normalization factor, but for scattering processes it is a qualitative difference from naive QCD.

# Modeling quarkyonic matter for FAIR/NICA/RHIC@low$\sqrt{s}$

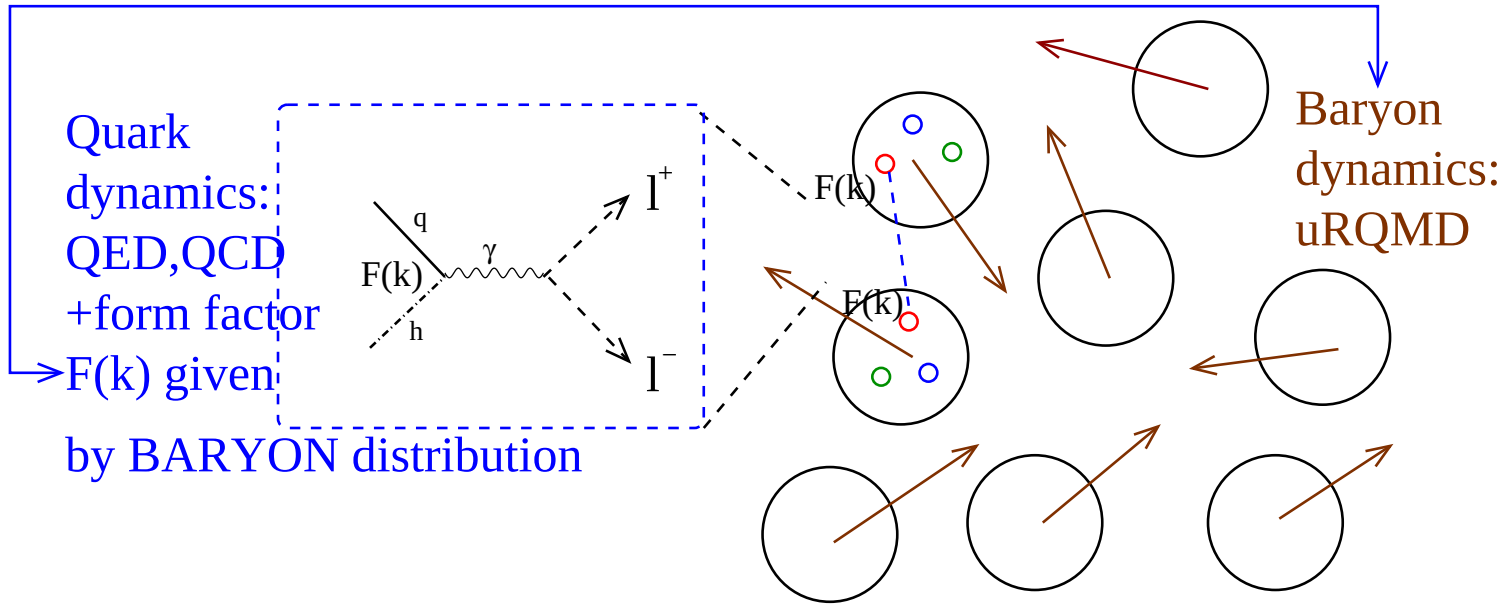


$$\Gamma \sim \left| \overbrace{\Psi(k_1)\Psi^*(k_2)}^{\hat{H}^{mf}_{baryons}|\psi>=E_k|\psi>} \underbrace{\mathcal{M}(k_{1,2,out})}_{pQCD} \right|^2 , \Psi(k) \sim \underbrace{e^{\left[-\frac{k^2}{\Lambda^2_{QCD}}\right]} \left( \sum_i^{baryons} \overbrace{\exp\left[i\vec{k_i}.\vec{x_{0i}}\right]}^{\vec{x_0} \leftarrow uRQMD} \right)^2}_{\text{FT baryon mean field}}$$

## Experimental implications: direct photon via quarkyonic Brehmsstrahlung

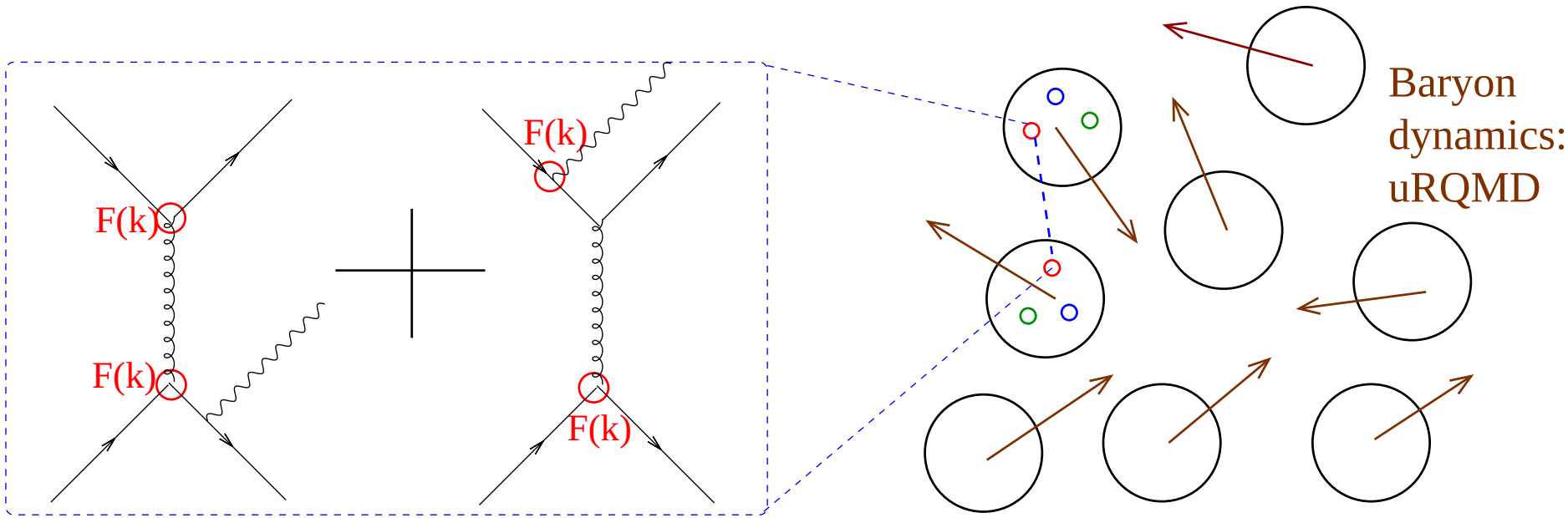


Calculation in progress: structures reflecting baryon radius,baryon flow expected

Experimental implications: dilepton production via quark-hole annihillation

Holes essential, so Initial state not enough, need

$$\ln Z_{quarks} \simeq \ln\left[\left(1+\exp\left[\frac{E_n-\mu_q}{T}\right]\right)\right], \left(\gamma_\mu\partial^\mu + m + V^{mf}_{baryons}\right)\psi = E_n\psi$$

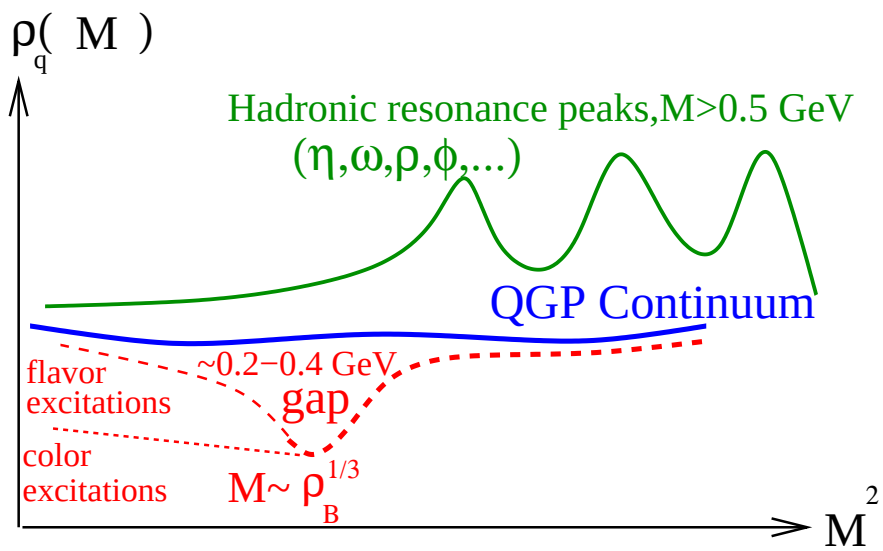


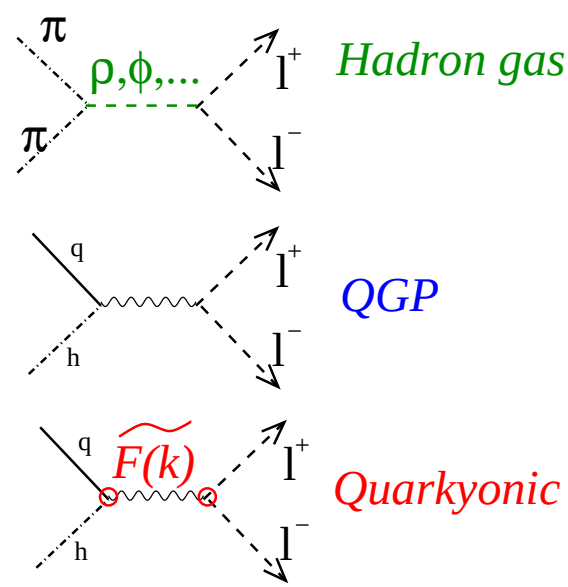


If baryons uniformly distributed, we have a qualitative signature: Analogue of energy gap in conductors due to Bloch-invariance of the quark wavefunction

but alas, at high density baryons might be highly irregular!

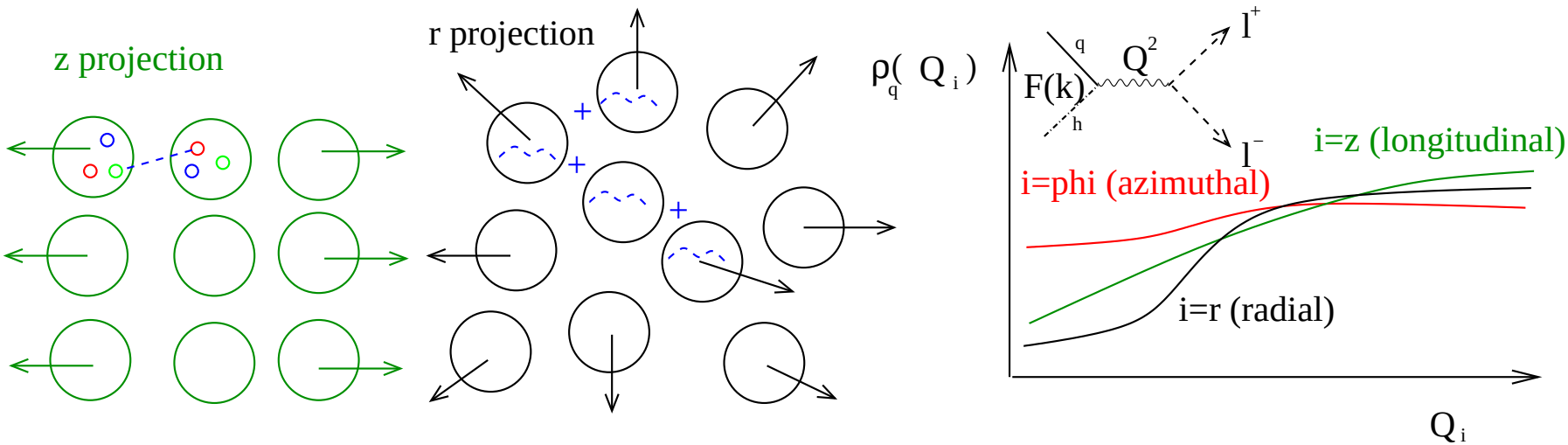


Event by event fireball structure <u>not regular</u>, but Collective structures exist in events flow profile (radial, longitudinal flow) and baryons have repulsive potential, soo structures in 3D dilepton spectral function $Q_{z,r,\phi}$ bound to exist!

## Conclusions

- Large $N_c$ expansion and asymptotic freedom imply quark degrees of freedom could appear even at confinement!

- On the other hand, not at all clear $N_c = 3 \simeq N_c \to \infty$
  Phase transition between the two likely to certain

- Percolation a natural model for quarkyonic matter, analogy with conductor in QED

- It is not clear whether percolating but confined phase possible at $N_c = 3$

- Phenomenology of quarkyonic matter needed. Electromagnetic probes best candidates

# Future Dilepton Experiments

Thermal Radiation Workshop
BNL, December 5-7, 2012

Itzhak Tserruya

WEIZMANN INSTITUTE OF SCIENCE

# Low-Mass Dileptons at a Glance:

## Energy Scale

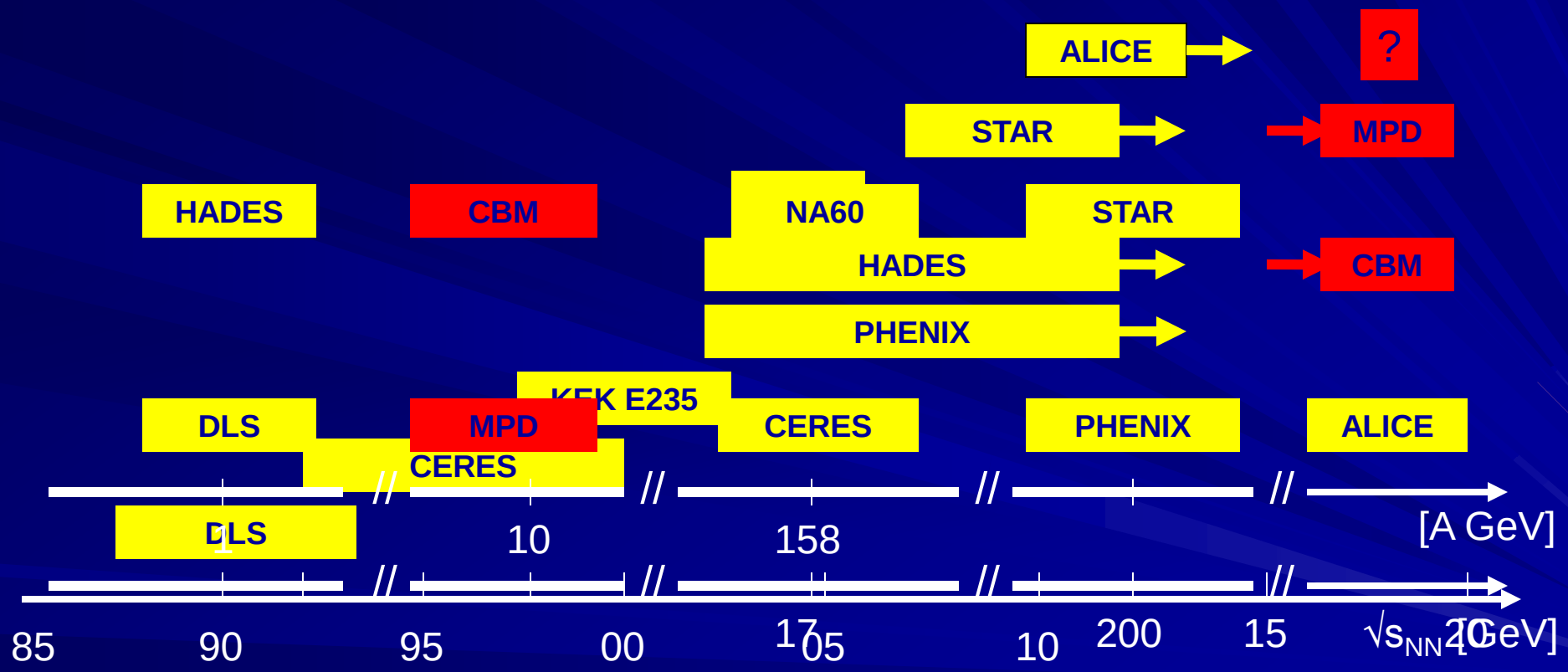


= Period of data taking

# Outline

- Top SPS energy
  - A well wrapped story - CERES, NA60
- Top RHIC energy
  - Challenging results PHENIX
  - PHENIX - STAR
- Low energies
  - FAIR, NICA, RHIC, SPS
- Elementary collisions?

# SPS

CERES – low masses

NA60 – low and intermediate masses

# CERES Pioneering Results (I)

**Strong enhancement of low-mass $e^+e^-$ pairs**
**(wrt to expected yield from known sources)**

First CERES result
PRL 75, (1995) 1272

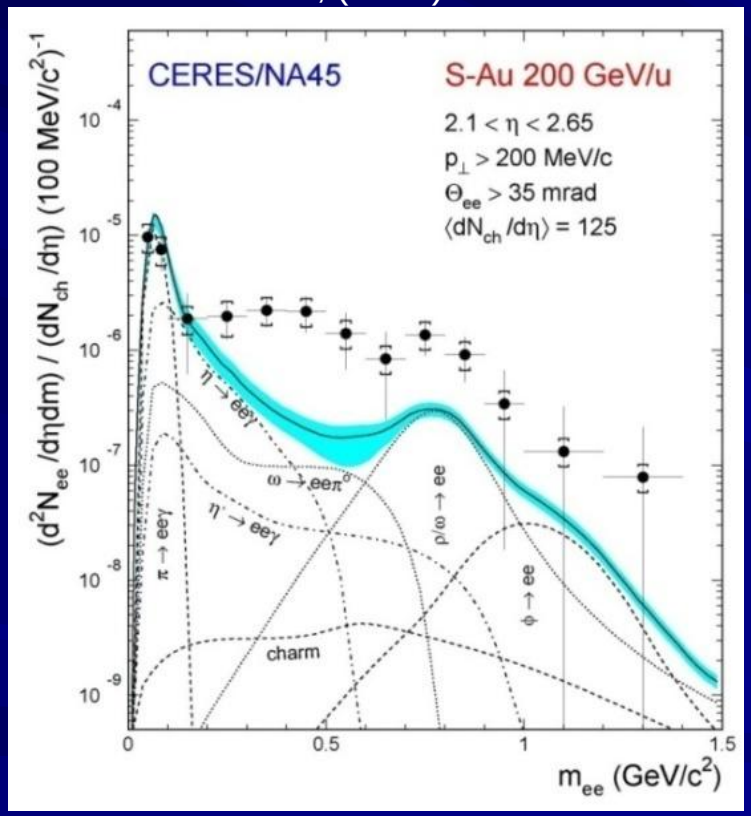


Last CERES result
2000 Pb run PLB 666(2008) 425

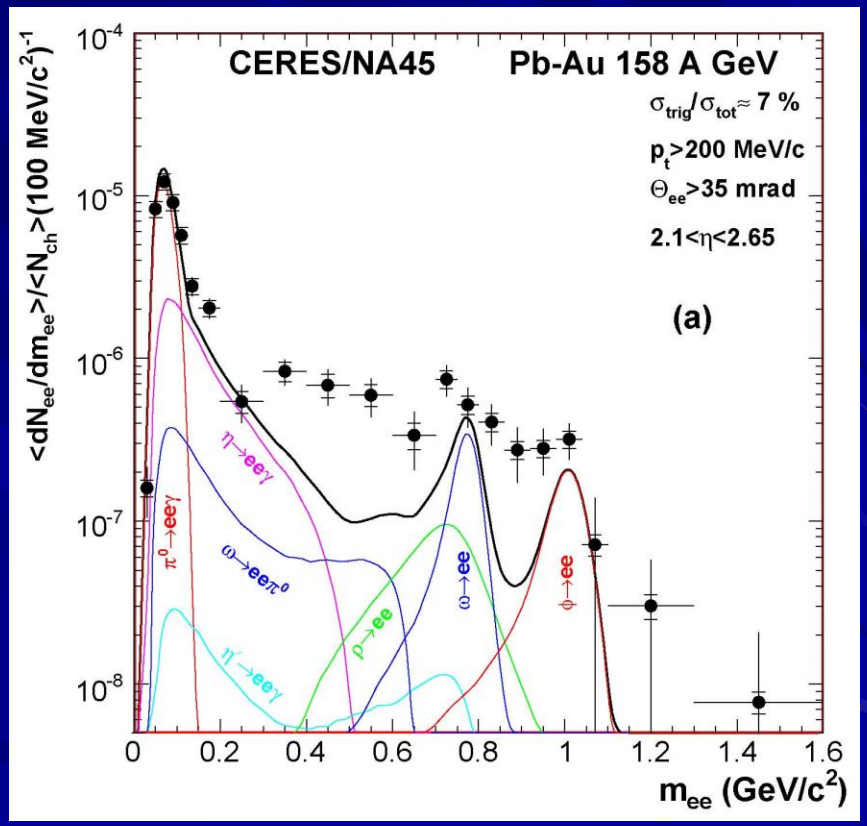


**Enhancement factor (0.2 <m < 1.1 GeV/c$^2$ ):**

**5.0 ± 0.7 (stat) ± 2.0 (syst)**

**2.45 ± 0.21 (stat) ± 0.35 (syst) ± 0.58 (decays)**

# Dropping Mass or Broadening (I) ?

* Interpretation:
  $\pi^+\pi^- \rightarrow \rho \rightarrow \gamma^* \rightarrow e^+e^-$

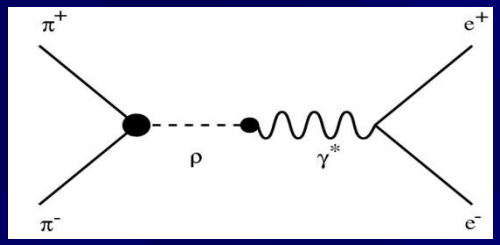


thermal radiation from HG

* vacuum ρ not enough to reproduce data

**CERES Pb-Au 158 A GeV 95/96 data**

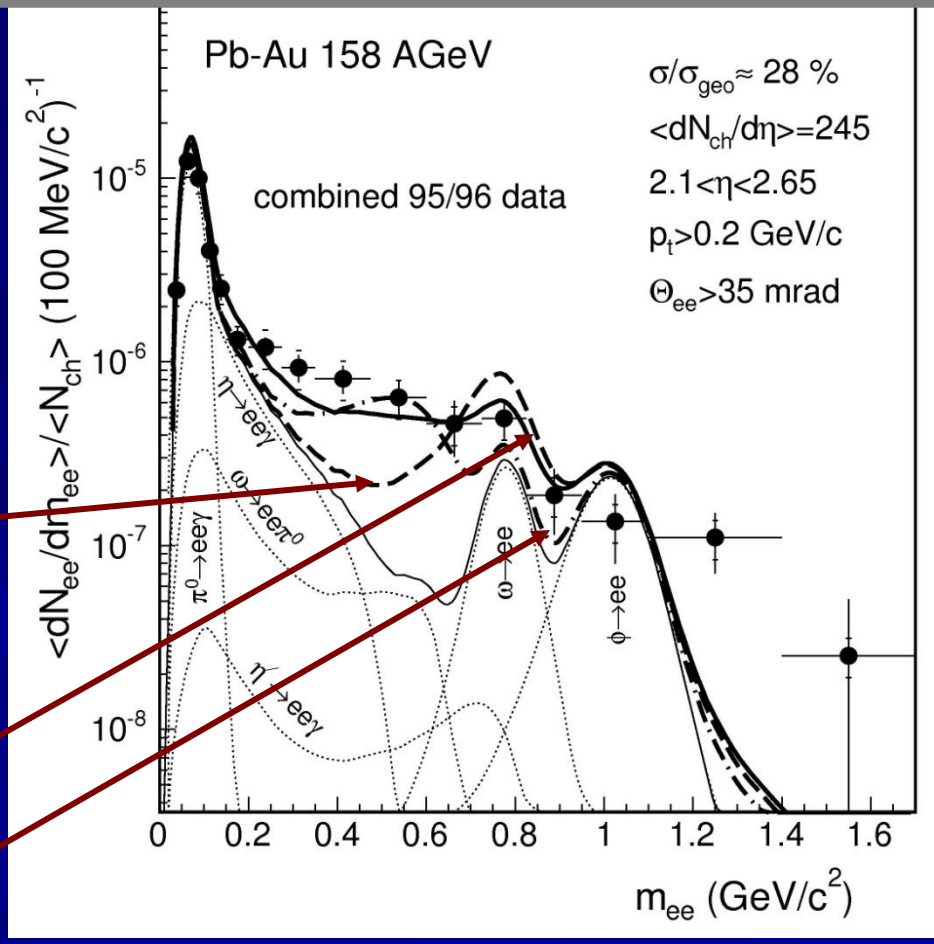


* in-medium modifications of ρ:

- broadening ρ spectral shape
  (Rapp and Wambach)
- dropping ρ meson mass
  (Brown et al)

# Dropping Mass or Broadening (II) ?

* Interpretation:

$\pi^+\pi^- \rightarrow \rho \rightarrow \gamma^* \rightarrow e^+e^-$

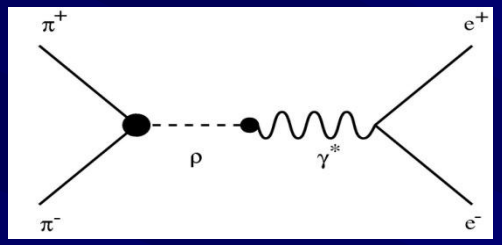


thermal radiation from HG

* vacuum ρ not enough to reproduce data

* in-medium modifications of ρ:

- broadening ρ spectral shape
  (Rapp and Wambach)
- dropping ρ meson mass
  (Brown et al)

**CERES Pb-A 158 A GeV 2000 data**

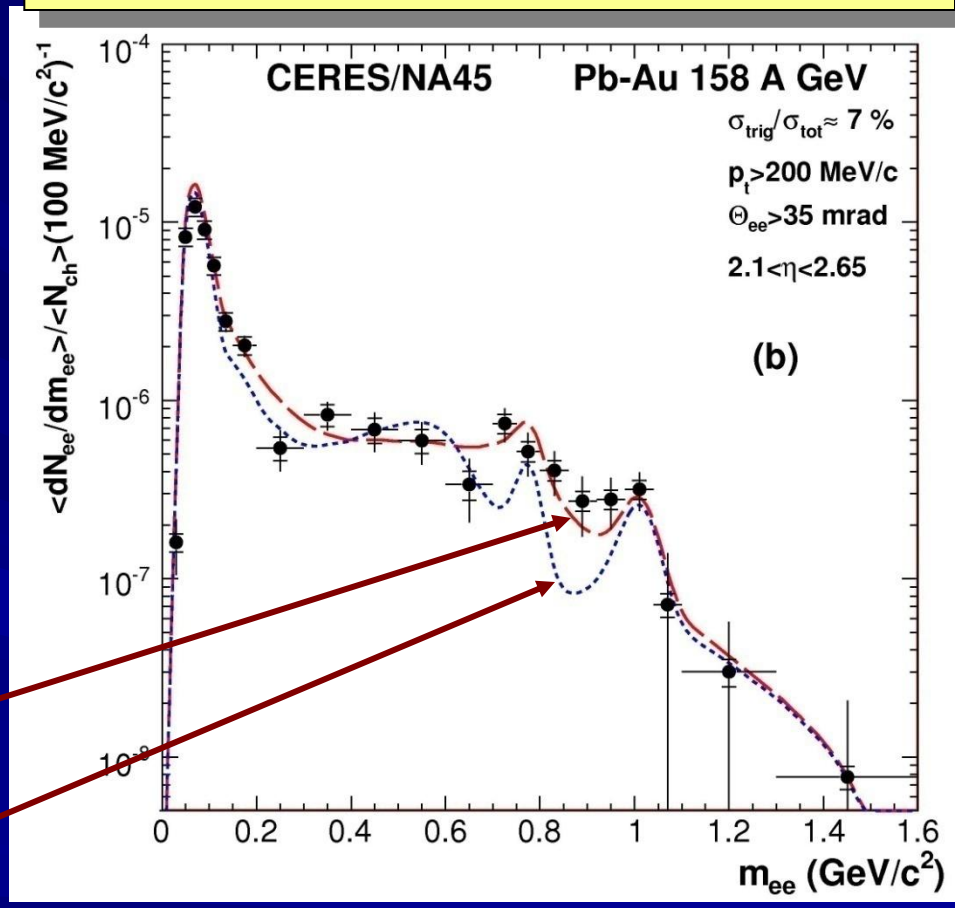


Data favor the broadening scenario.

# Quark – Hadron Duality

R. Rapp

In-medium $\pi^+ \pi^-$ ann. rates $\approx$ perturbative qbarq ann. rates
quark – hadron duality down to m ~ 0.5 GeV/$c^2$

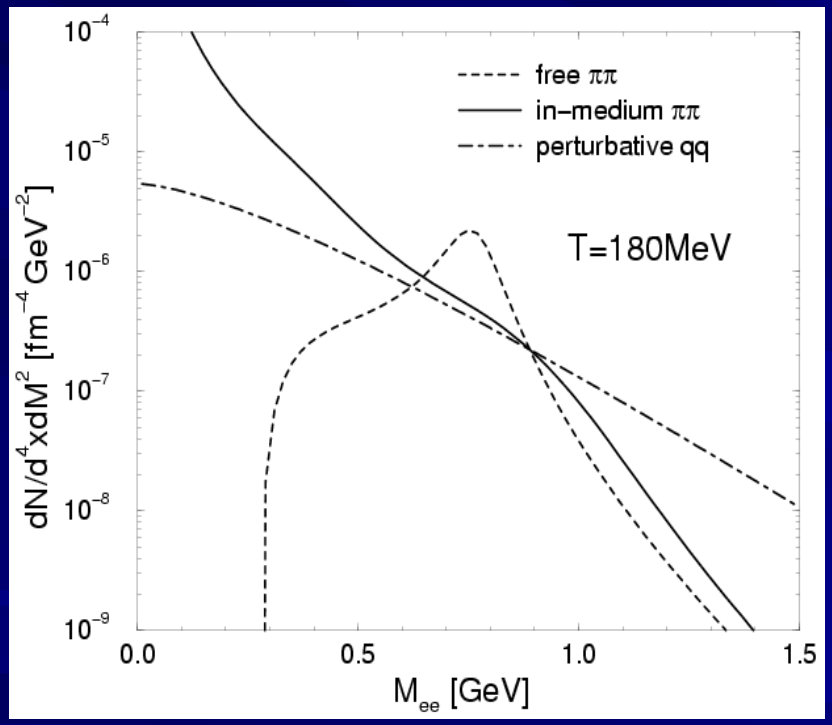


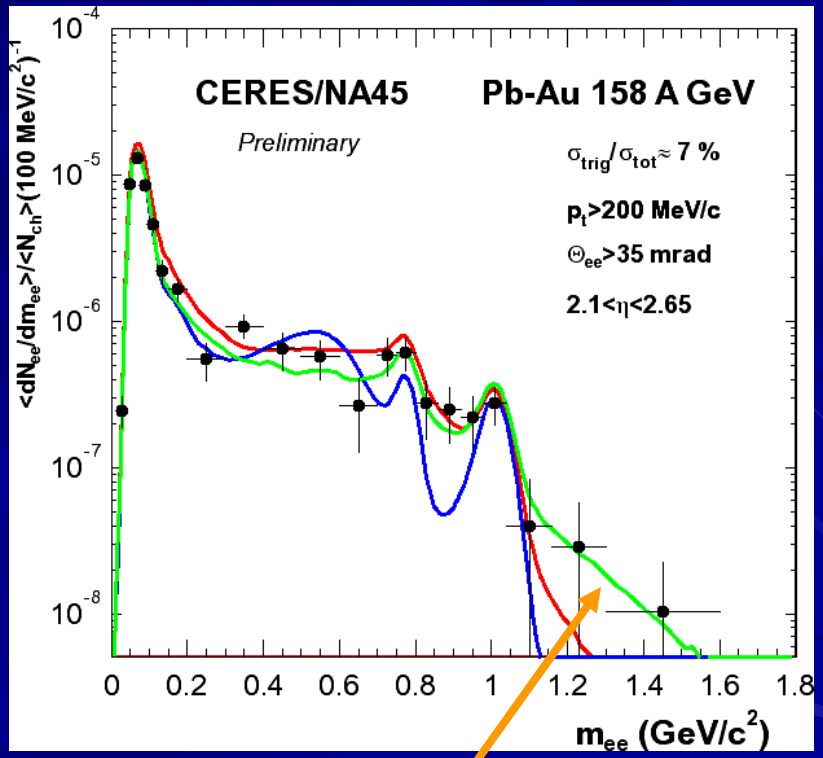


**Kämpfer calculations: Thermal radiation from the plasma or just a parametrization of the $e^+e^-$ yield inspired by quark-hadron duality?**

# NA60 Low-mass dimuons

**Superb data!!!**

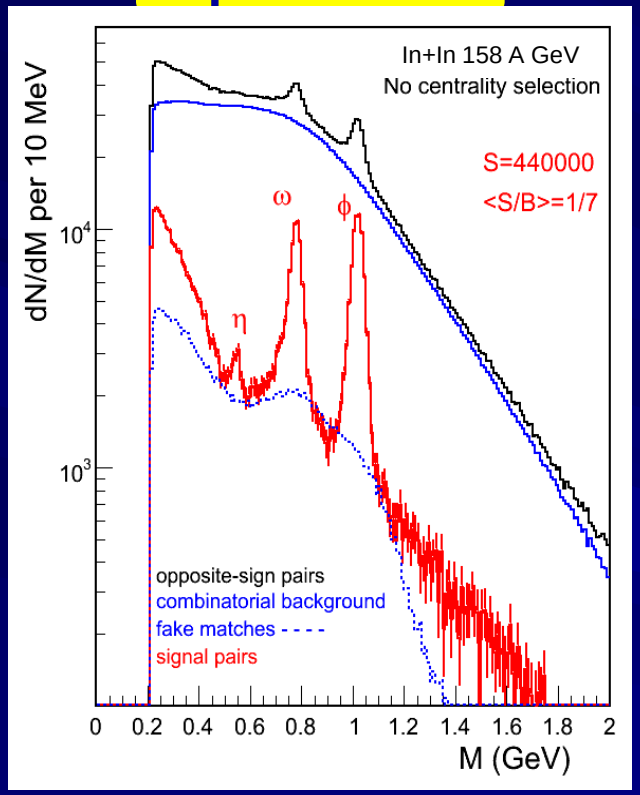


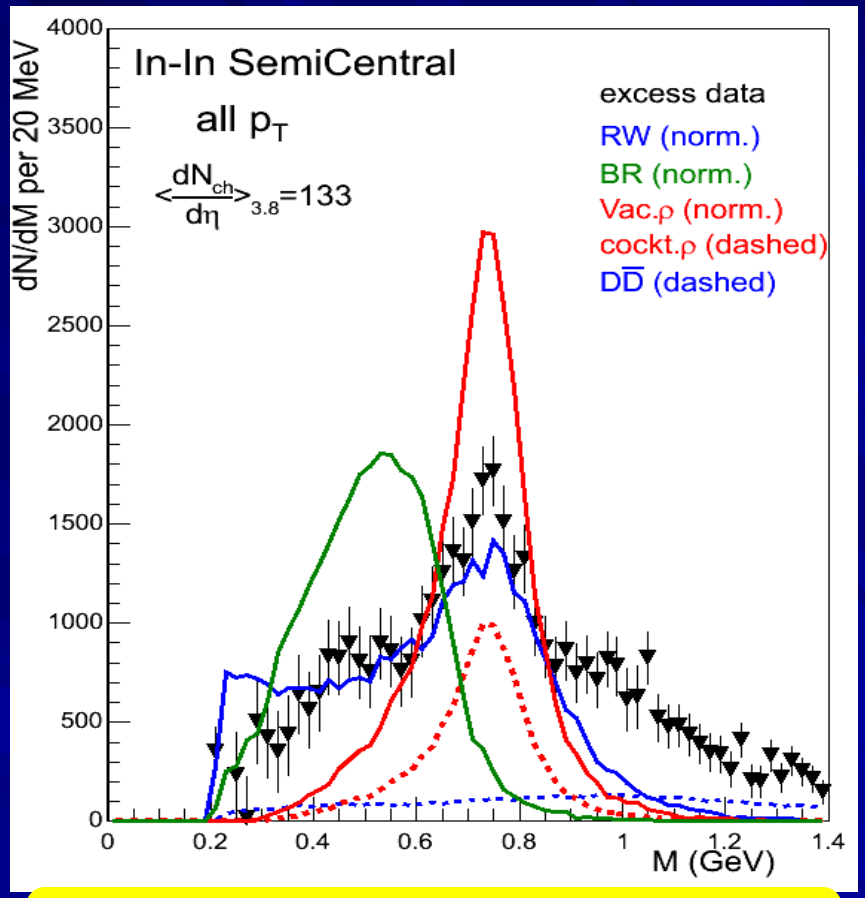


- Mass resolution:
23 MeV at the φ position

- S/B = 1/7

- **Excess shape in agreement with broadening of the ρ (Rapp-Wambach)**

- **Mass shift of the ρ (Brown-Rho) ruled out**

- **Melting of the ρ?**

# The IMR Excess

NA60 demonstrated that IMR excess is due to a prompt source.

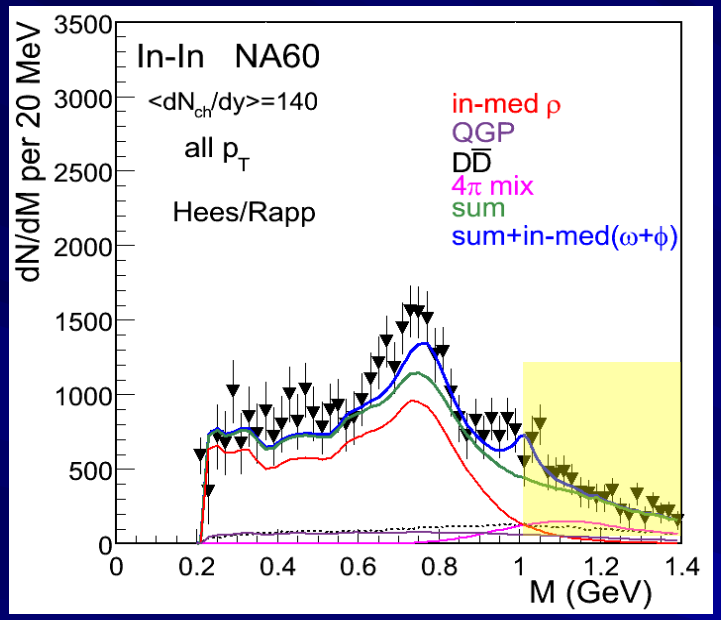


Hees/Rapp, PRL 97, 102301 (2006)

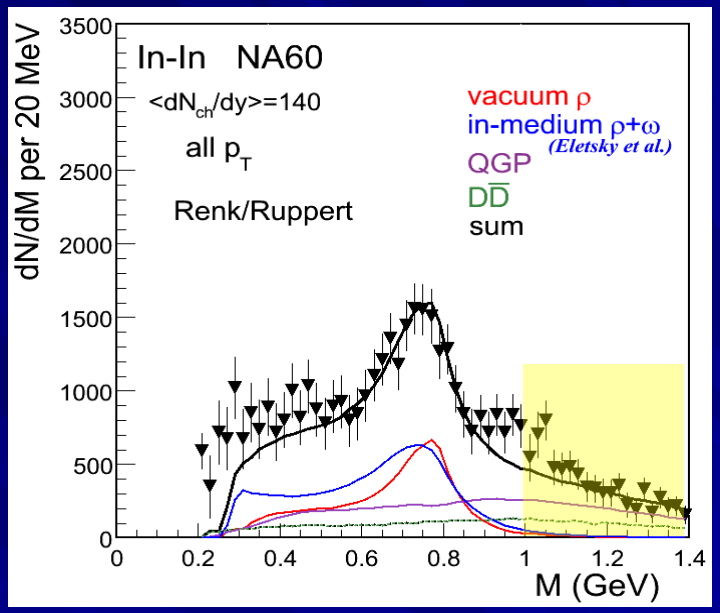


Renk/Ruppert, PRL 100,162301 (2008)

IMR excess can be explained by:

**hadronic processes, 4π …**

**partonic processes, qq annihilation**

**Quark-Hadron duality?**

# Acceptance corrected invariant mass spectrum

Eur. Phys. J. C 59 (2009) 607

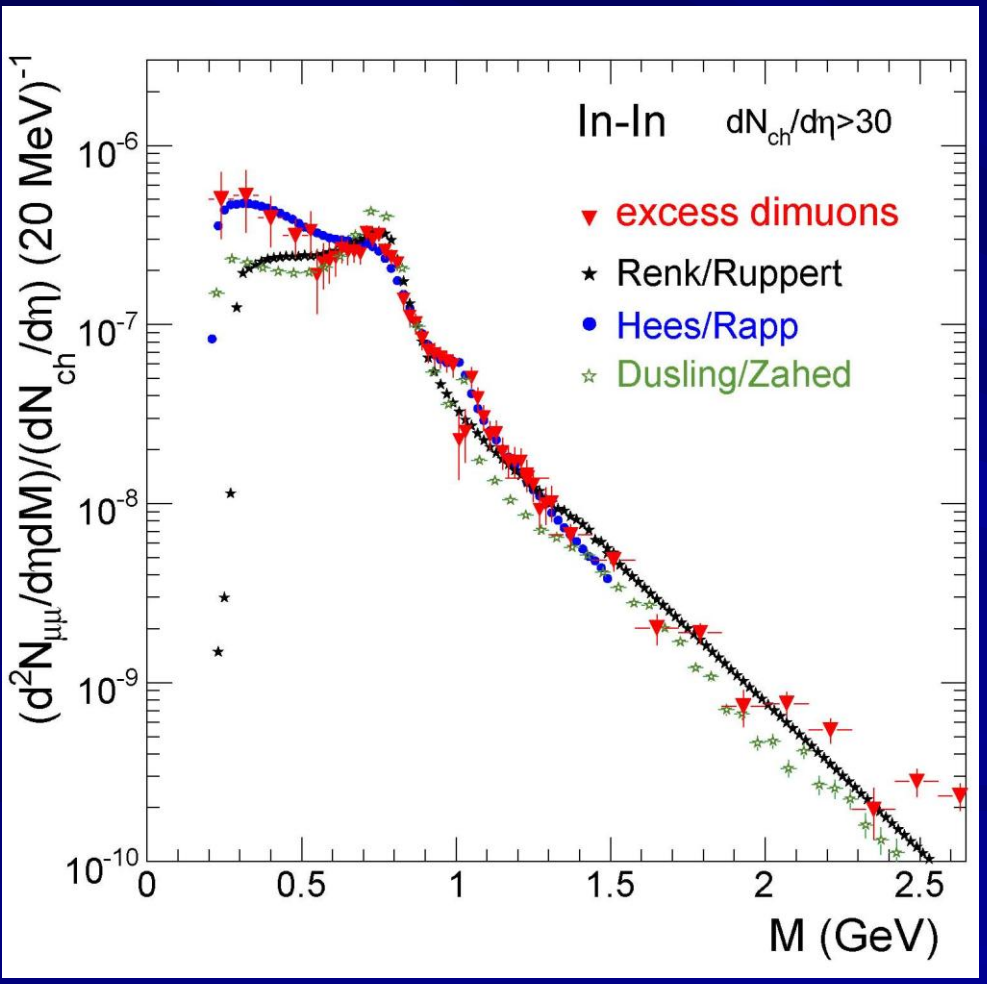


Mass spectrum corrected for acceptance in m - $p_T$

- LMR: thermal radiation from HG
  $\pi^+\pi^- \rightarrow \rho \rightarrow \mu^+\mu^-$
- IMR:

Thermal radiation from HG:
$\pi\ a_1 \rightarrow \mu^+\mu^-$ (Hees/Rapp)
Or
Thermal radiation from QGP
$qq \rightarrow \mu^+\mu^-$ (Renk/Ruppert)

*→Quark-Hadron duality?*

# $p_T$ distributions

Low-mass region

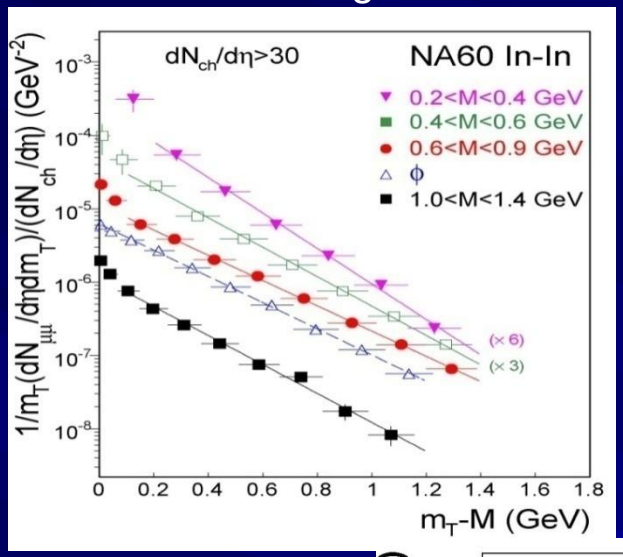


Intermediate mass region

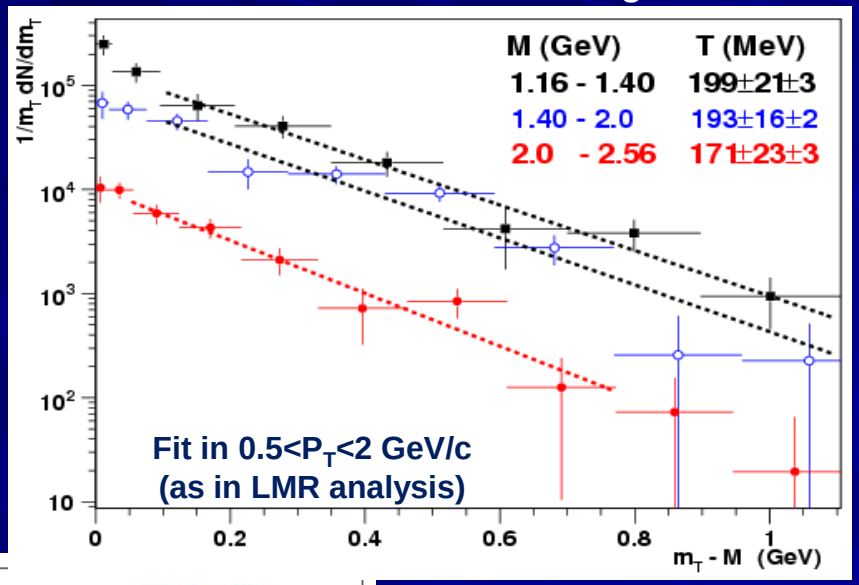


- $m_T$ spectra exponential
- inverse slopes depend on mass.
  → Radial Flow

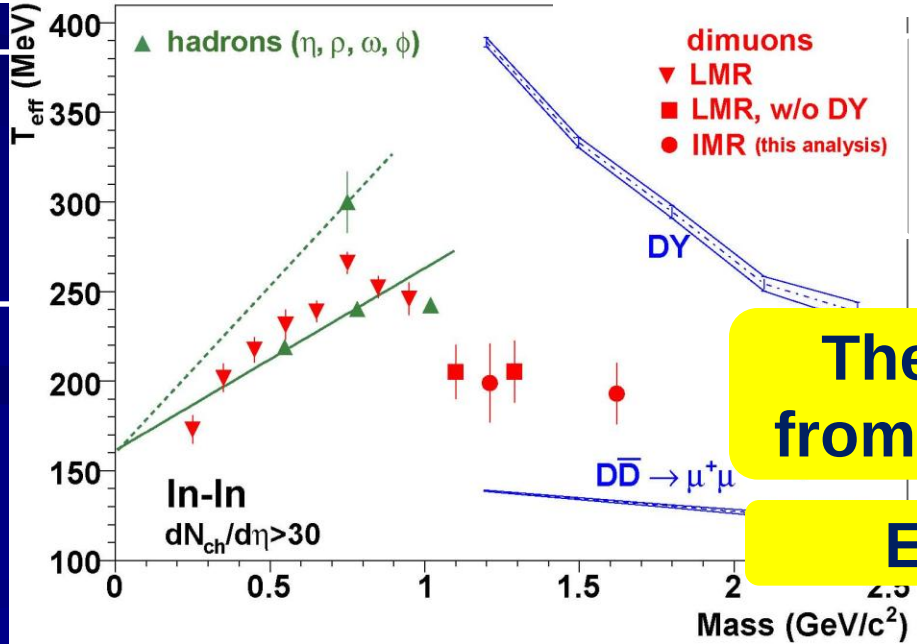


- $m_T$ spectra exponential
- inverse slopes do not depend on mass.

**Thermal radiation from partonic phase**

**Elliptic flow?**

# SPS top energy summary

Eur. Phys. J. C 59 (2009) 607

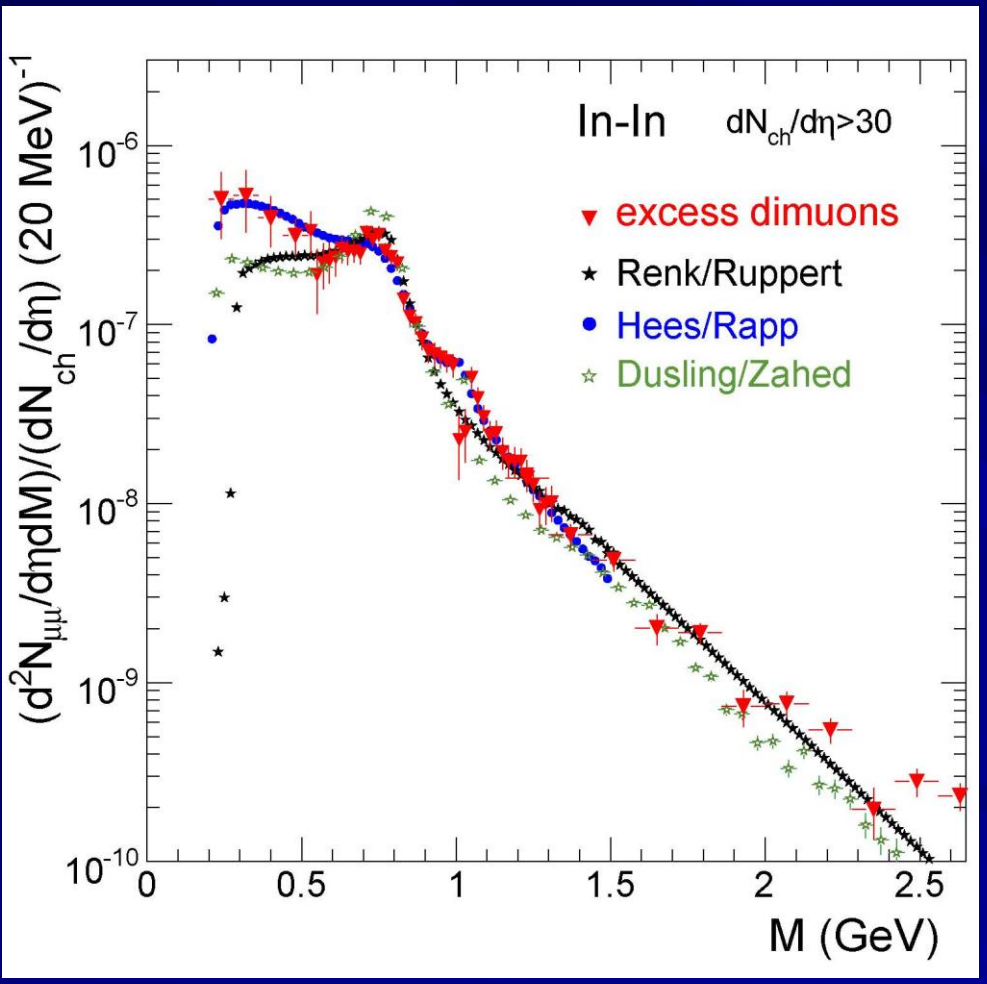


- LMR:
  - thermal radiation from HG
    $\pi^+\pi^- \rightarrow \rho \rightarrow \mu^+\mu^-$
  - Resonances melt as the system approaches CSR
- IMR:
  - Thermal radiation from QGP
    $qq \rightarrow \mu^+\mu^-$

# RHIC

# Low-mass $e^+e^-$ Pairs: Prospects at RHIC

- At SPS energies, the ρ-meson broadening, that explains both the CERES and NA60 data, relies on a high baryon density.
- What was expected at RHIC?

| | SPS (Pb-Pb) | RHIC (Au-Au) |
|---|---|---|
| dN( $\bar{p}$ ) / dy | 6.2 | 20.1 |
| Produced baryons ($\bar{p}$, p, $\bar{n}$, n ) | 24.8 | 80.4 |
| p – $\bar{p}$ | 33.5 | 8.6 |
| Participants nucleons ($\bar{p}$ – p )A/Z | 85 | 21.4 |
| Total baryon density | 110 | 102 |

- Baryon density is almost the same at RHIC and SPS

(the decrease in the participating nucleons transported to mid-rapidity is compensated by the copious production of nucleon-antinucleon pairs)

- **Strong enhancement of low-mass pairs predicted to persist at RHIC**

**R. Rapp nucl-th/0204003**

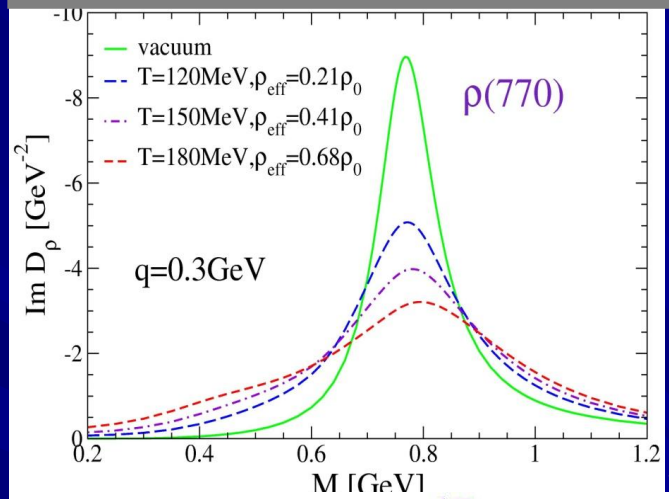


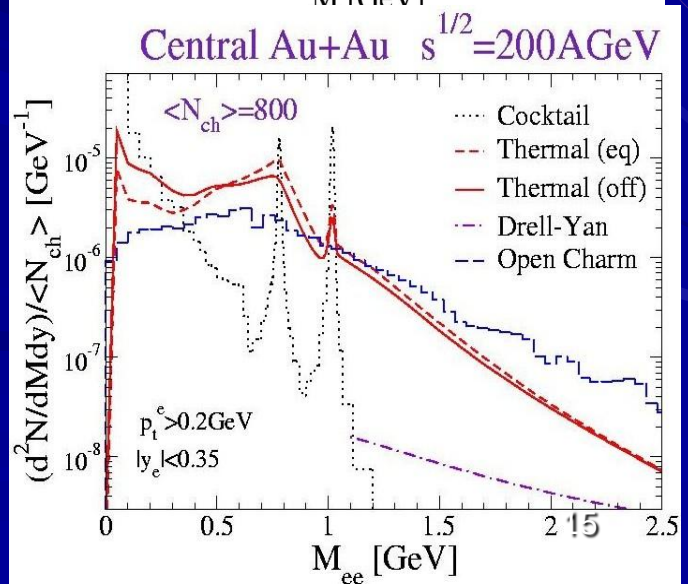

# Dileptons in PHENIX: Au+Au collisions

PRC 81, 034911 (2010)

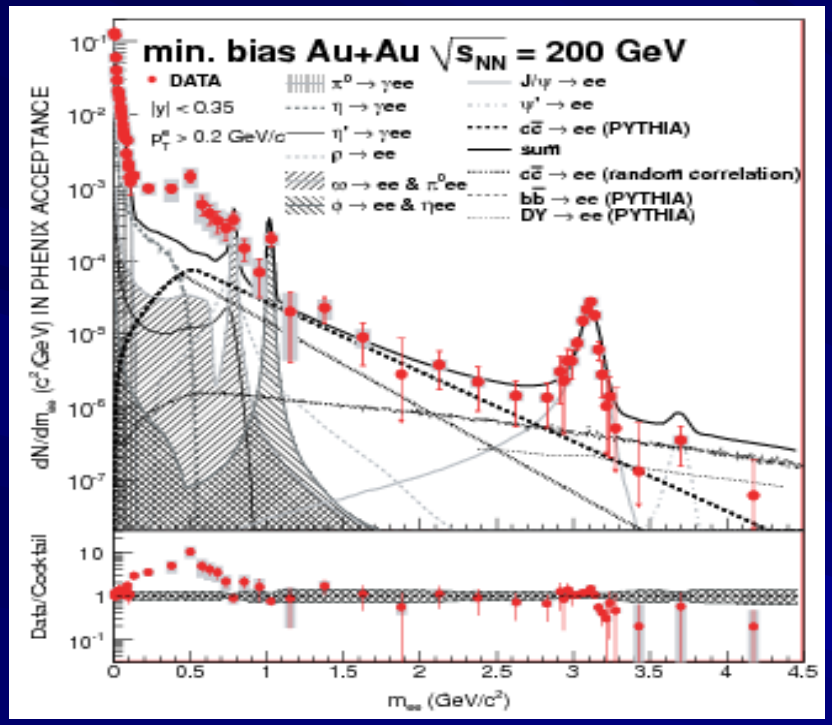


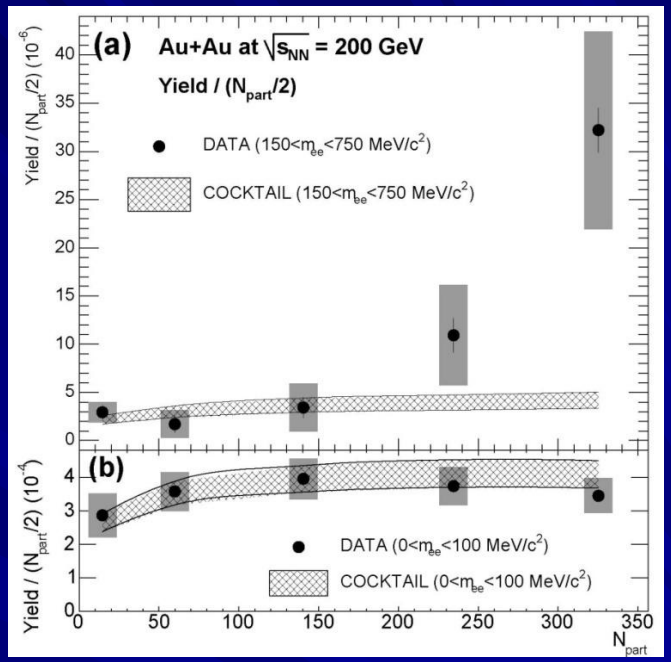


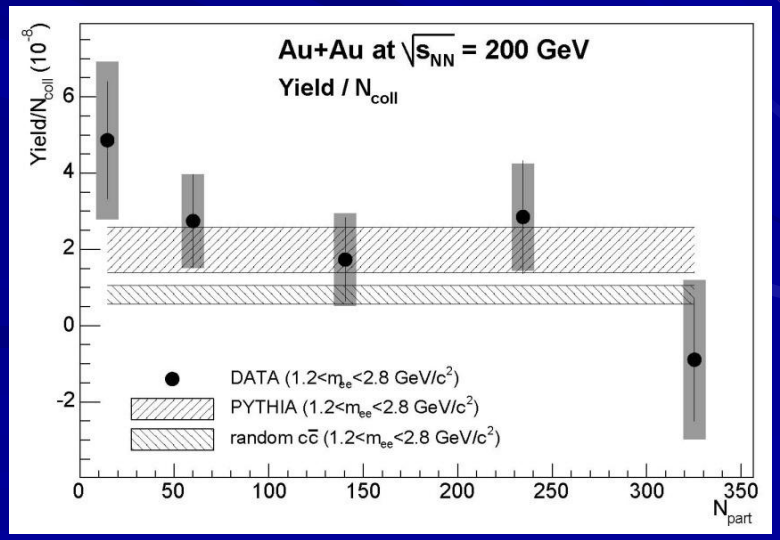


- LMR: Strong enhancement at m= 0.15 – 0.75 GeV/$c^2$.
  - min. bias 4.7 ± 0.4 (stat.) ±1.5 (syst.)
  - central collisions 7.6 ± 0.5 (stat.) ± 1.3 (syst.)
  - Enhancement down to very low masses
  - Enhancement concentrated in central collisions
- IMR: agreement with pp charm contribution scaled with $N_{coll}$

# Comparison to theoretical models

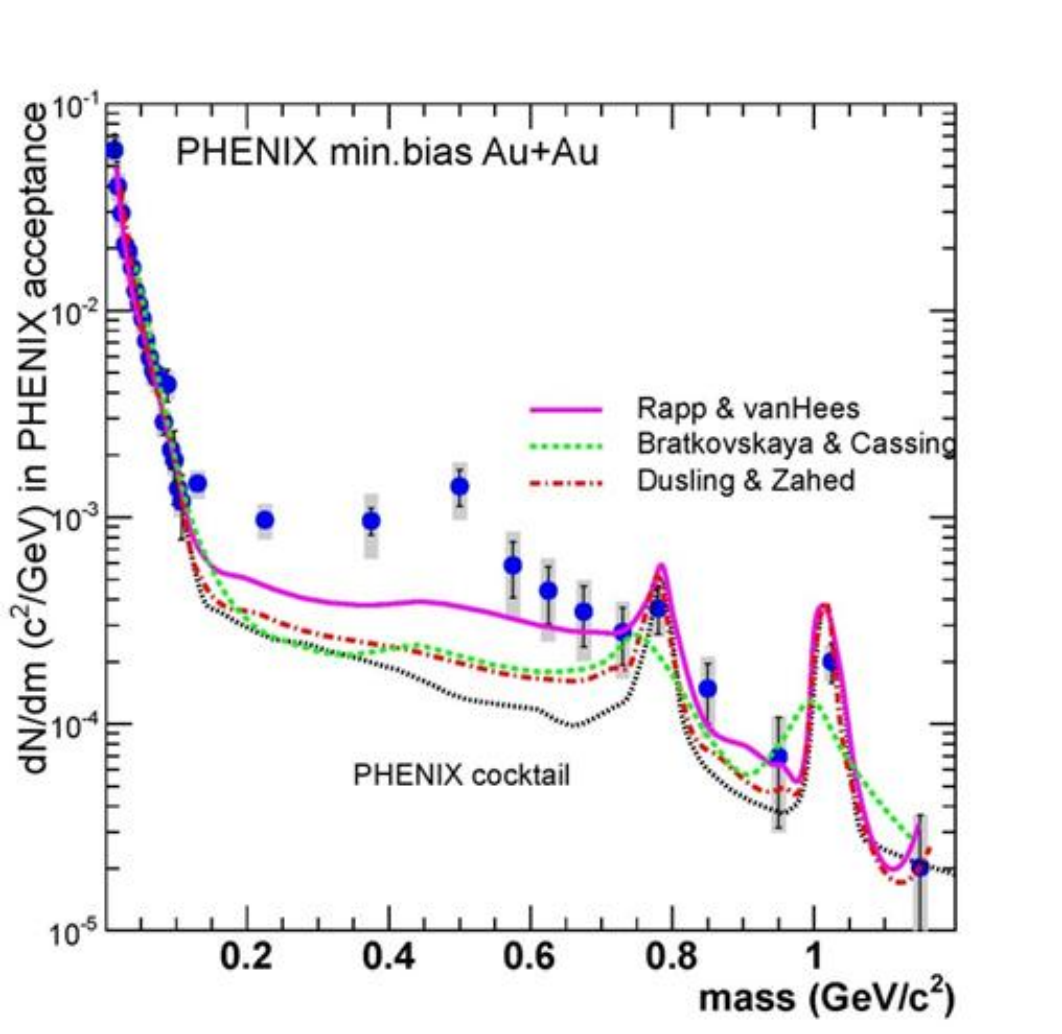


**Models that successfully described the SPS data fail in describing the PHENIX results**

# $m_T$ distribution of low-mass excess

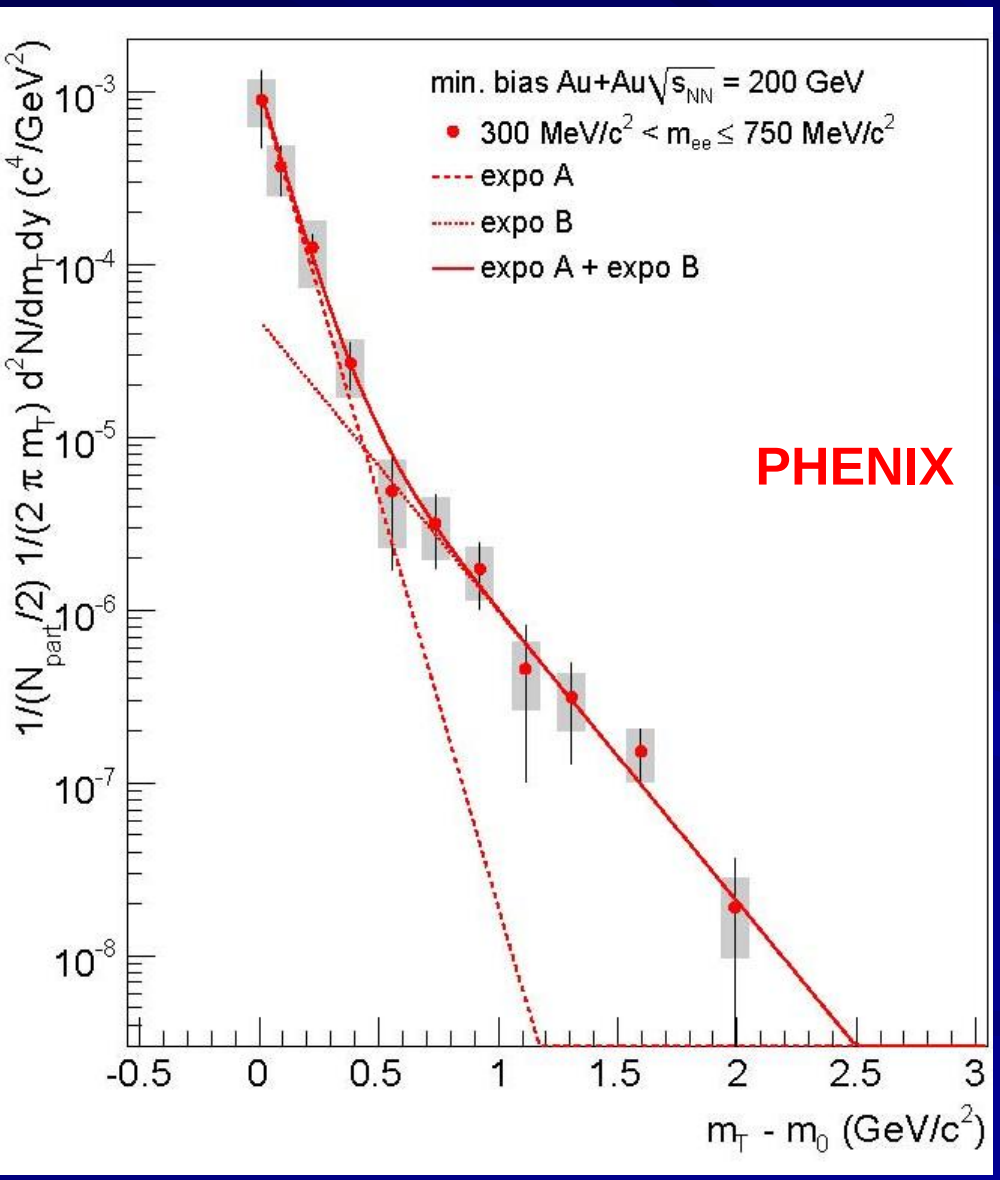


- Excess present at all pair $p_T$ but is more pronounced at low pair $p_T$
- The excess $m_T$ distribution exhibits two clear components
- It can be described by the sum of two exponential distributions with inverse slope parameters:

$T1 = 92 \pm 11.4^{stat} \pm 8.4^{syst}$ MeV

$T2 = 258.3 \pm 37.3^{stat} \pm 9.6^{syst}$ MeV

**All this is very different from the SPS results**
**New source?**

- Dileptons in STAR

# STAR Dileptons in Au+Au collisions

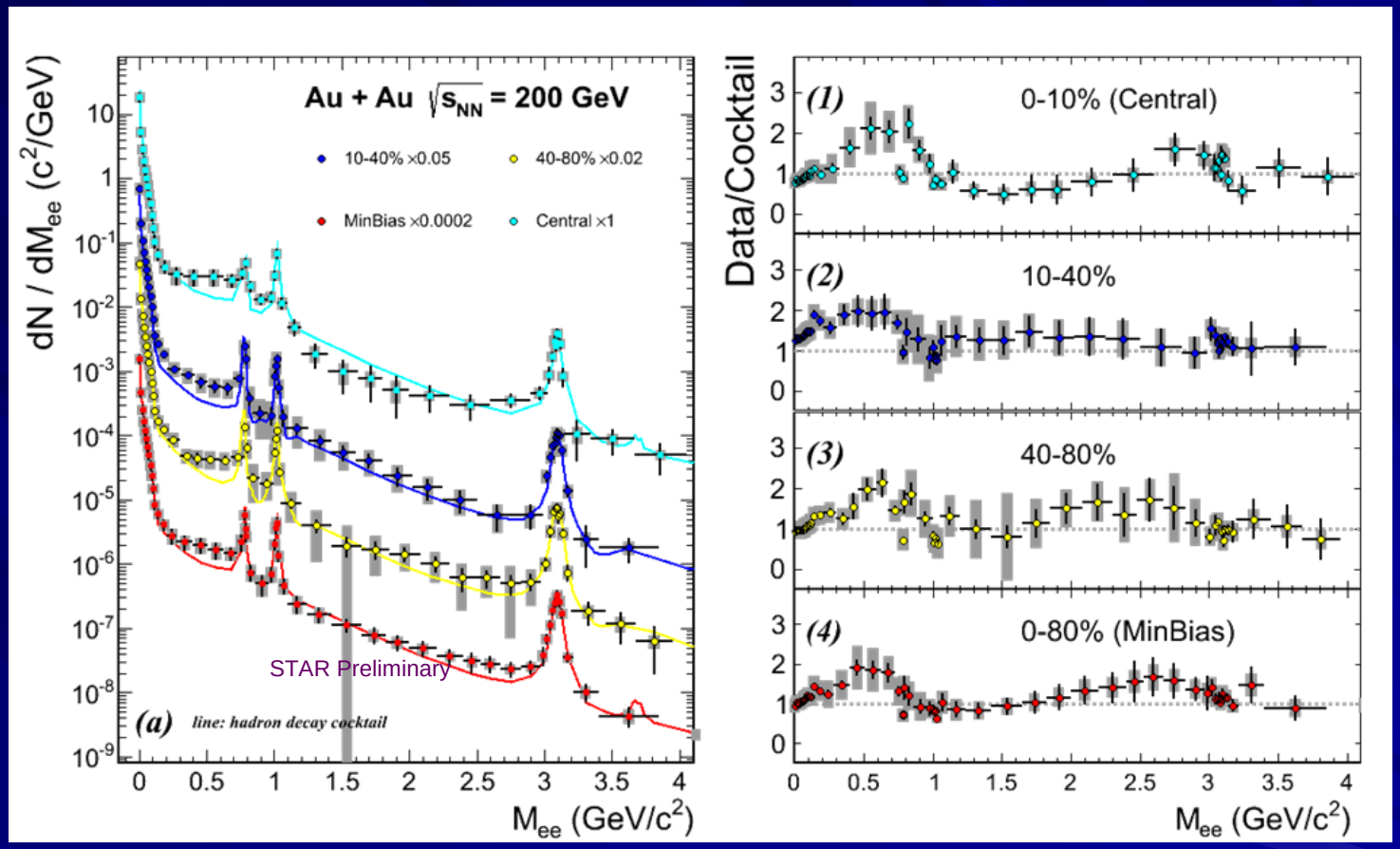


- LMR: clear enhancement wrt to cocktail
  little centrality dependence
- IMR: no clear picture

**LMR (MB): S/B = 1/200**

# PHENIX vs. STAR

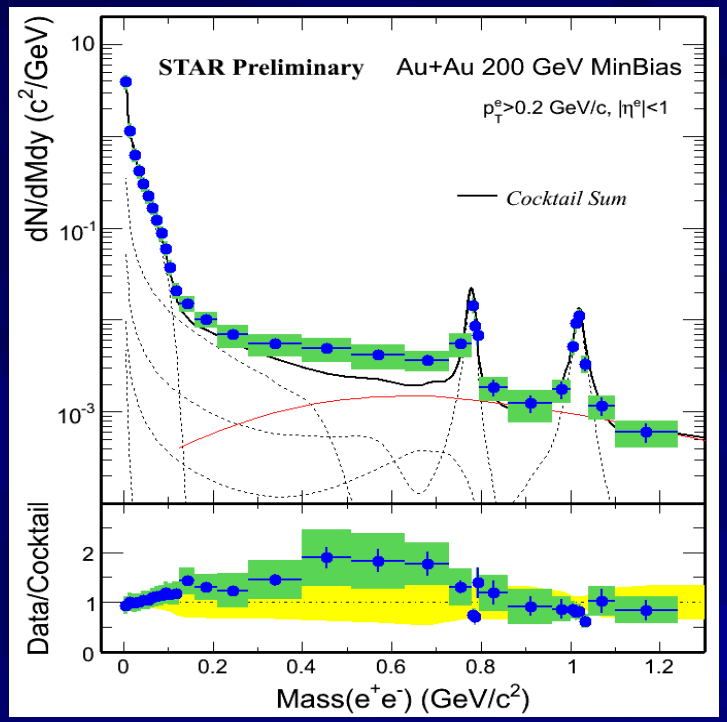


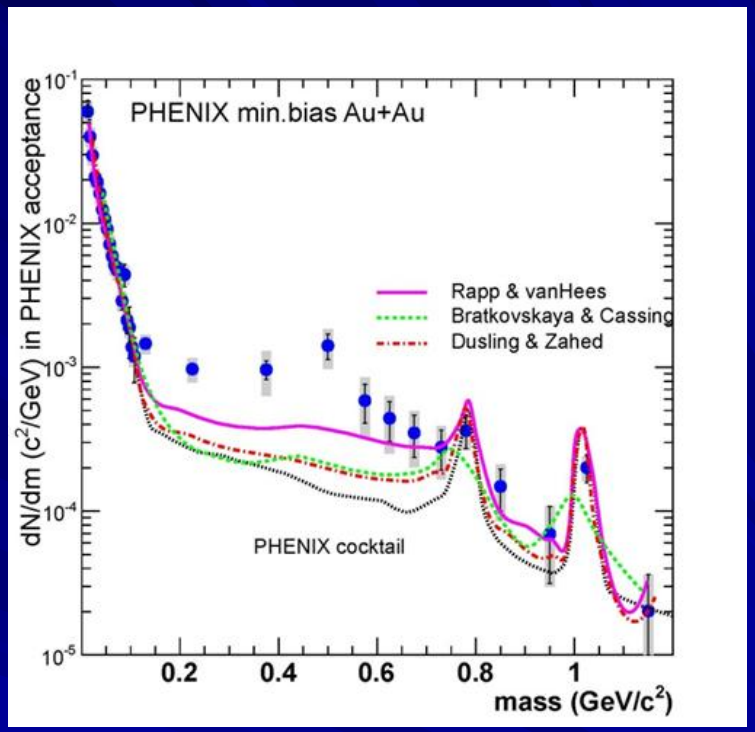


Enhancement factor in $0.15<M_{ee}<0.75$ Gev/$c^2$

| | Minimum Bias | Central collisions |
|---|---|---|
| PHENIX | 4.7 ± 0.4 ± 1.5 | 7.6 ± 0.5 ± 1.3 |
| STAR | 1.40 ± 0.06 ± 0.38 | 1.54 ± 0.09 ± 0.45 |

Large quantitative differences

# Compare to Rapp, Wambach, v. Hees

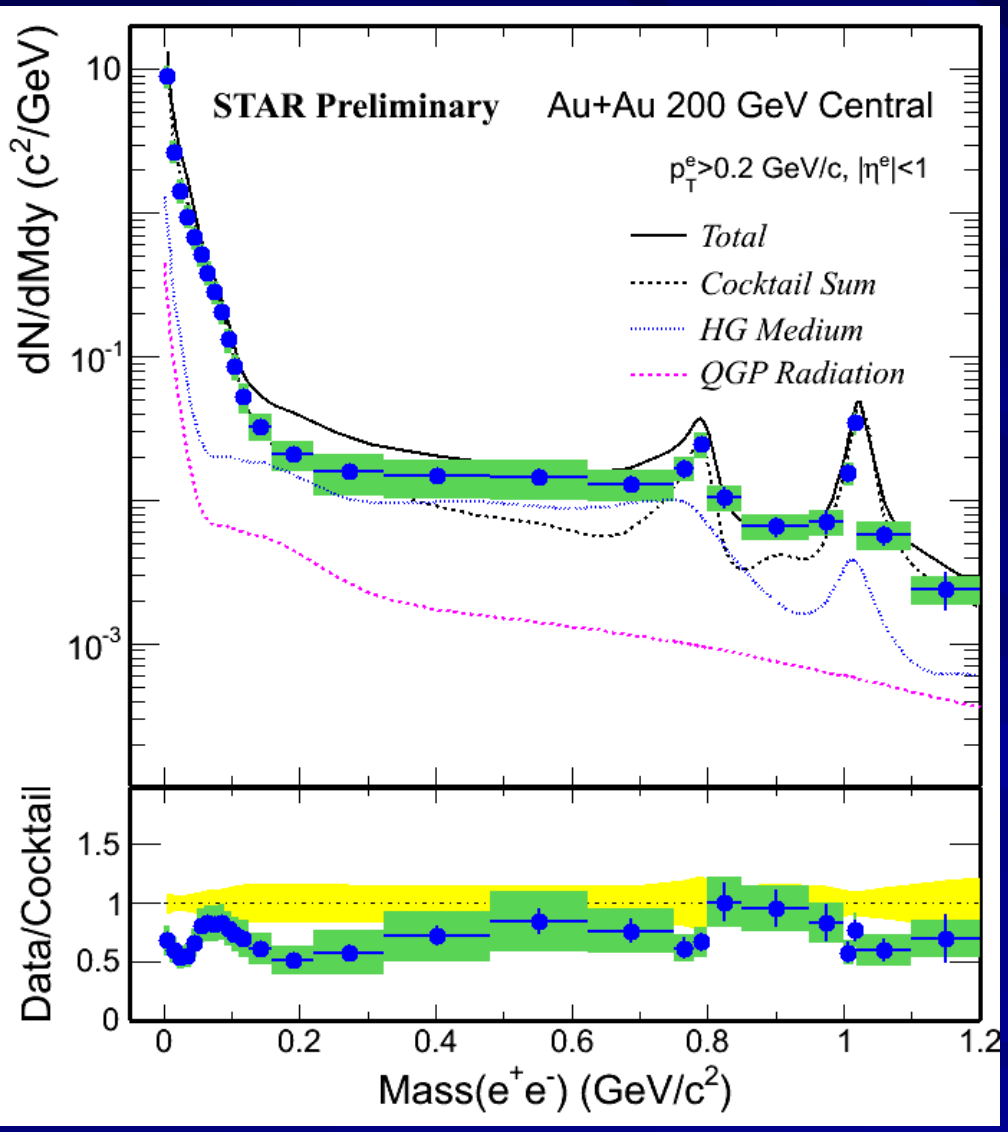


- STAR central 200 GeV Au+Au
- hadronic cocktail (STAR)
- Ralf Rapp (priv. comm. to STAR) Complete evolution (QGP+HG): cocktail + QGP + HG:
- Reasonable agreement with data

# Dileptons in PHENIX: Au+Au collisions

**Min bias Au+Au $\sqrt{s_{NN}}$ = 200 GeV**
**Phys. Rev. C81, 034911 (2010)**

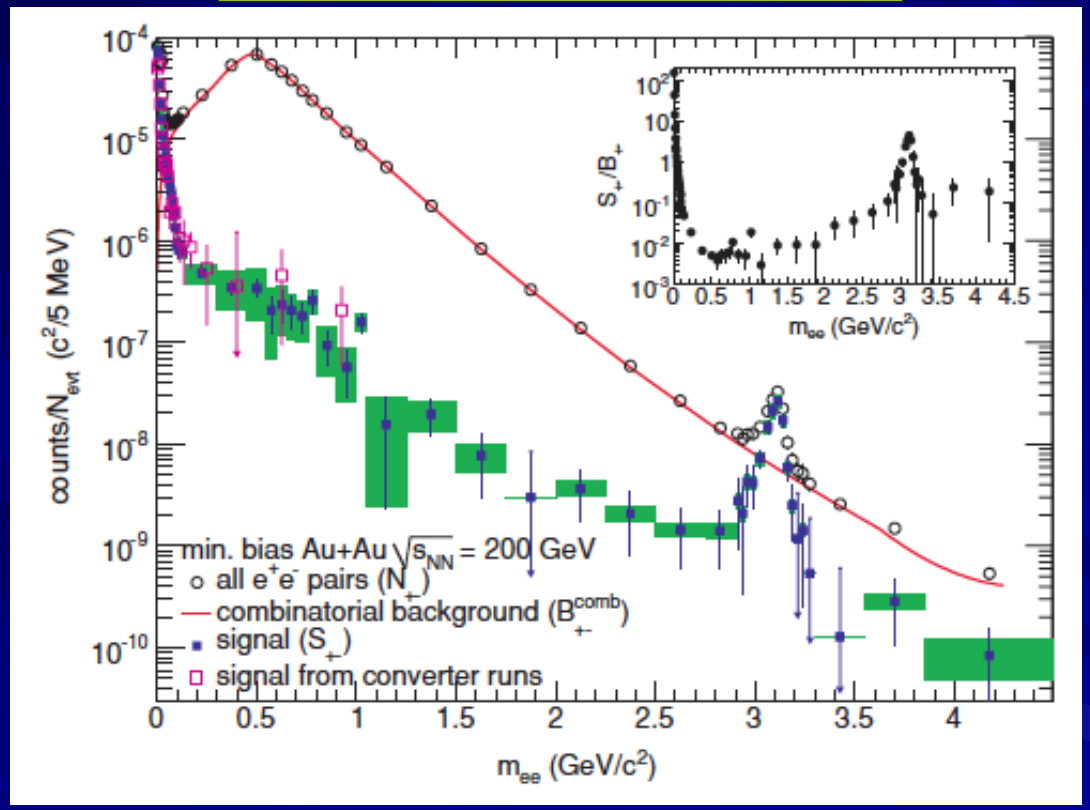


Integral: 180,000
above $\pi^0$: 15,000

S/B ≈ 1/200 → *large statistical and large systematic errors*

*Cocktail / B ≈ 1/1000*

*To improve the measurement PHENIX developed a Hadron Blind Detector*

# Run-9 p+p dileptons with the HBD

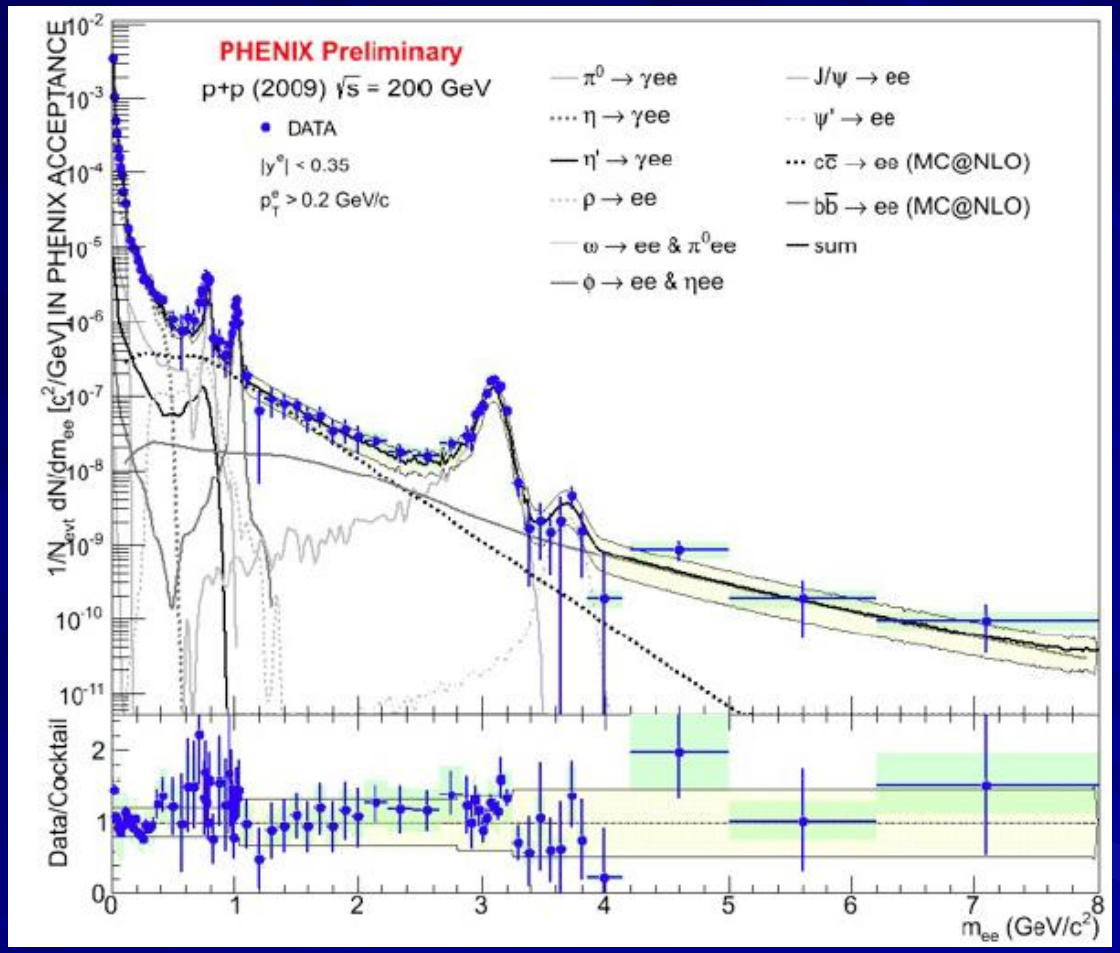


- Fully consistent with published result PR C81, 034911 (2010)
- Improvement in S/B by a factor of 5-10. Expected to do better in final analysis
- Provide crucial proof of principle and testing ground for understanding the HBD

# Run-10 Au+Au dileptons at $\sqrt{s_{NN}}$=200 GeV with the HBD

**Peripheral**

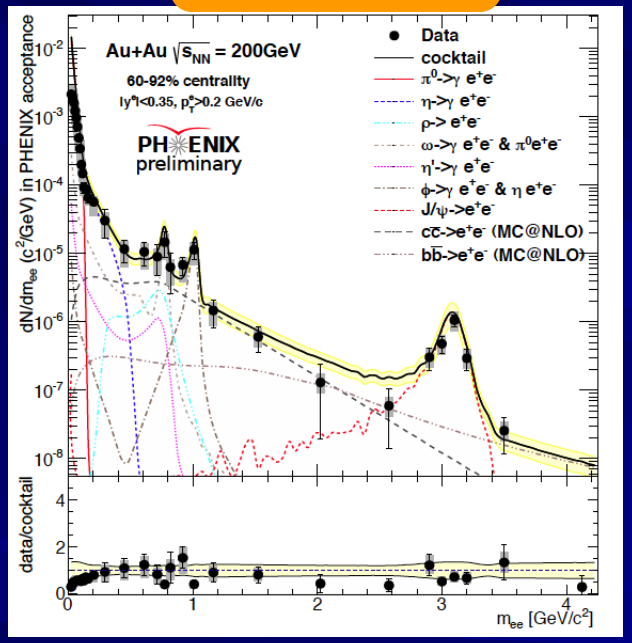


**Semi-peripheral**

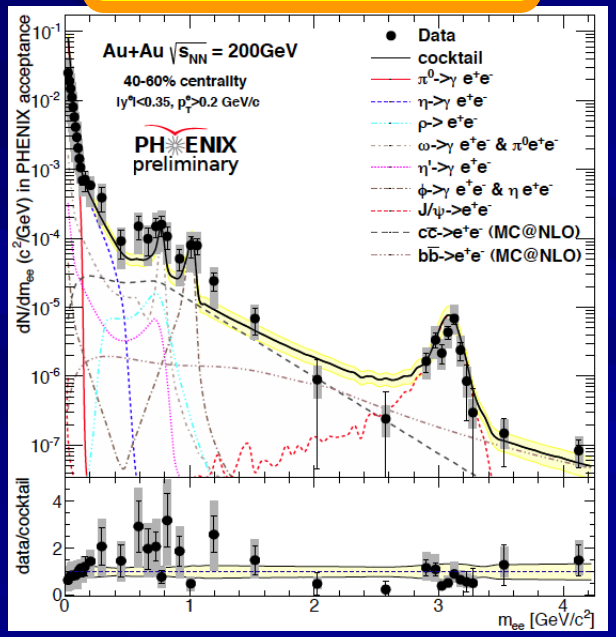


**Semi-central**

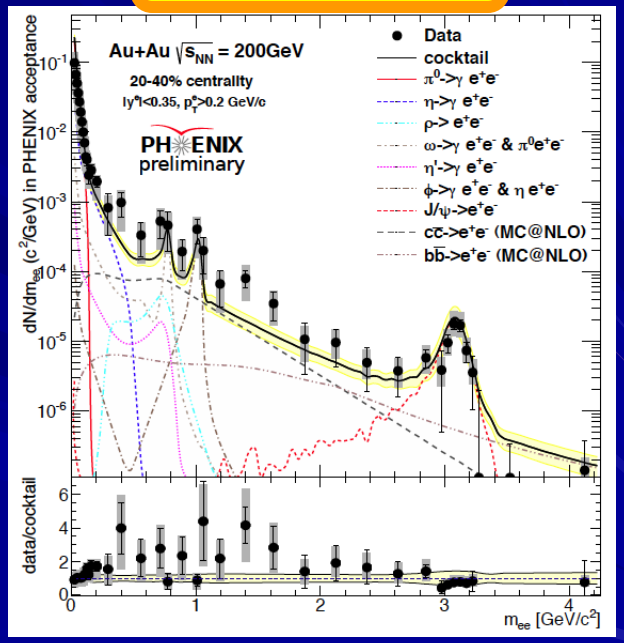

# Comparison Run10 – Run4

**LMR (m = 0.15 – 0.75 GeV/c²)**

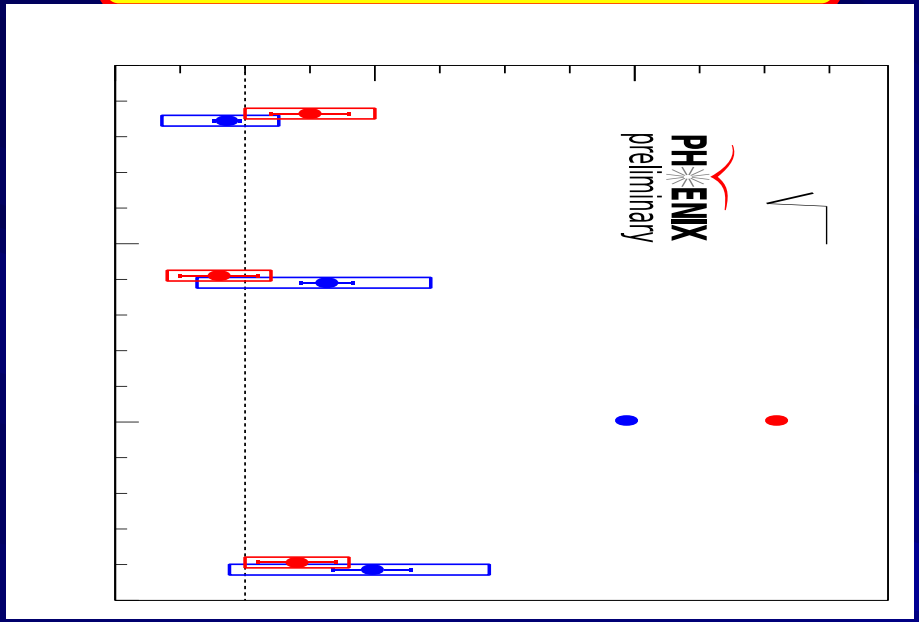


- Hint of enhancement for more central collisions
- Not conclusive given the present level of uncertainties

**IMR (m = 1.2 – 2.8 GeV/c²)**

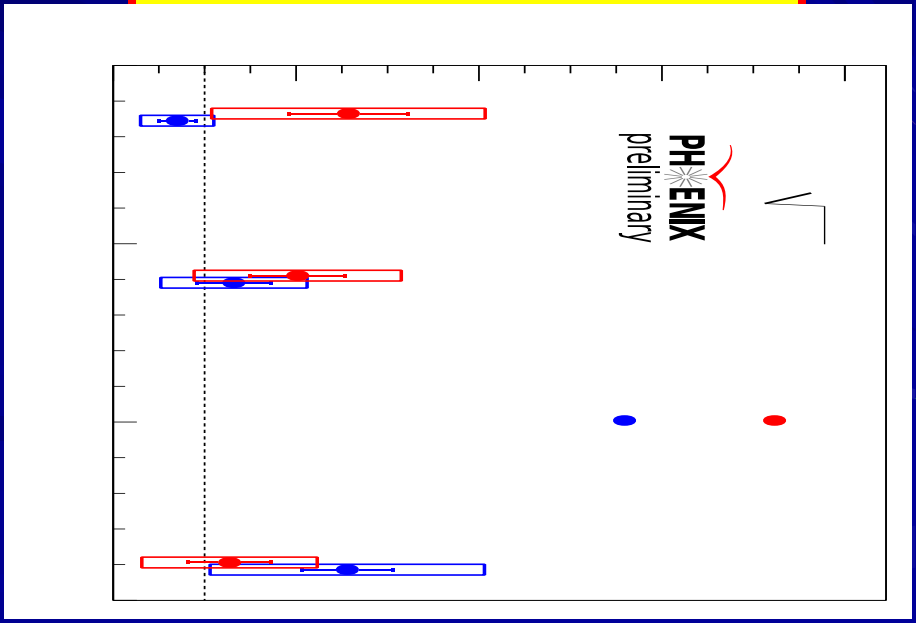


- Similar conclusions for the IMR
- Run 10 consistent with published Run4 results

# Future

- LMR: Solve the PHENIX - STAR discrepancy
  - HBD results in central Au+Au collisions
- IMR: higher precision data needed
  - Higher statistics and direct measurement of charm contribution

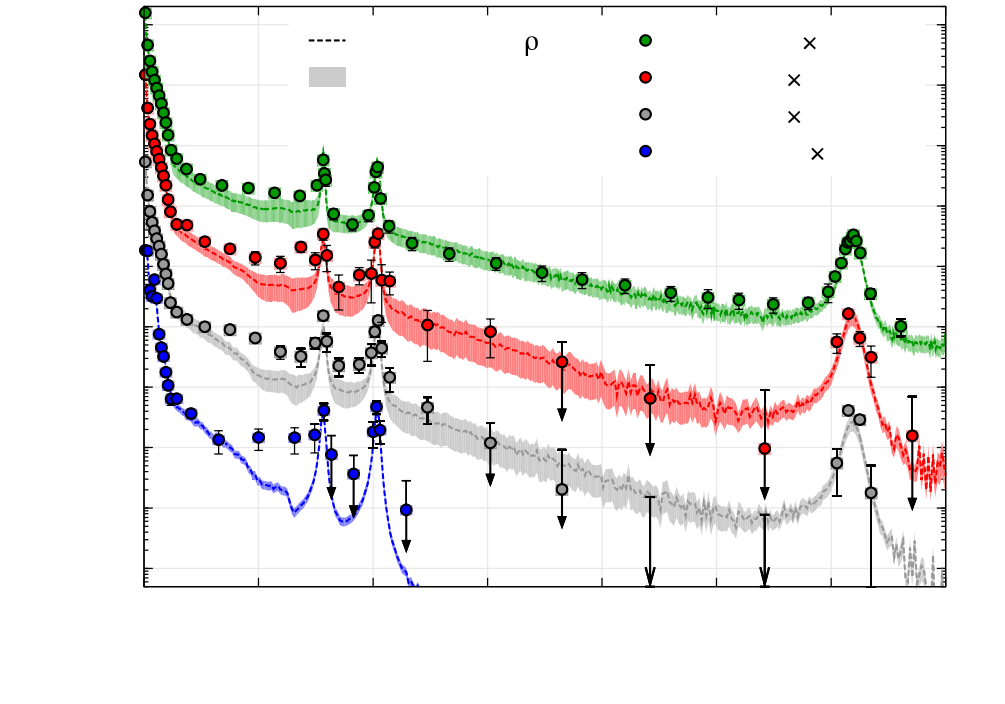


- Fill the gap between top SPS and top RHIC energy
  - Preliminary STAR results

# Dileptons with sPHENIX

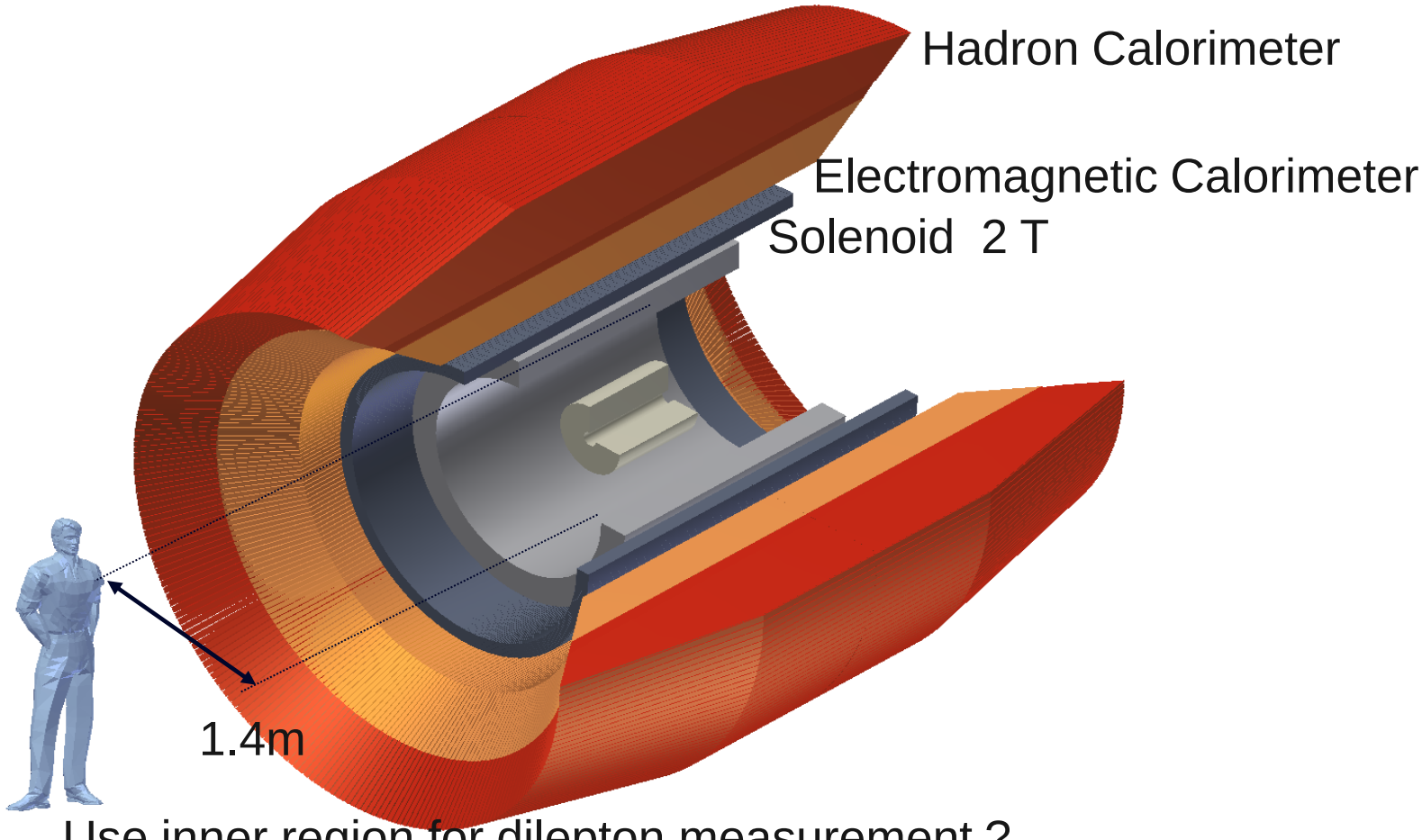


Use inner region for dilepton measurement ?

# TPC / HBD

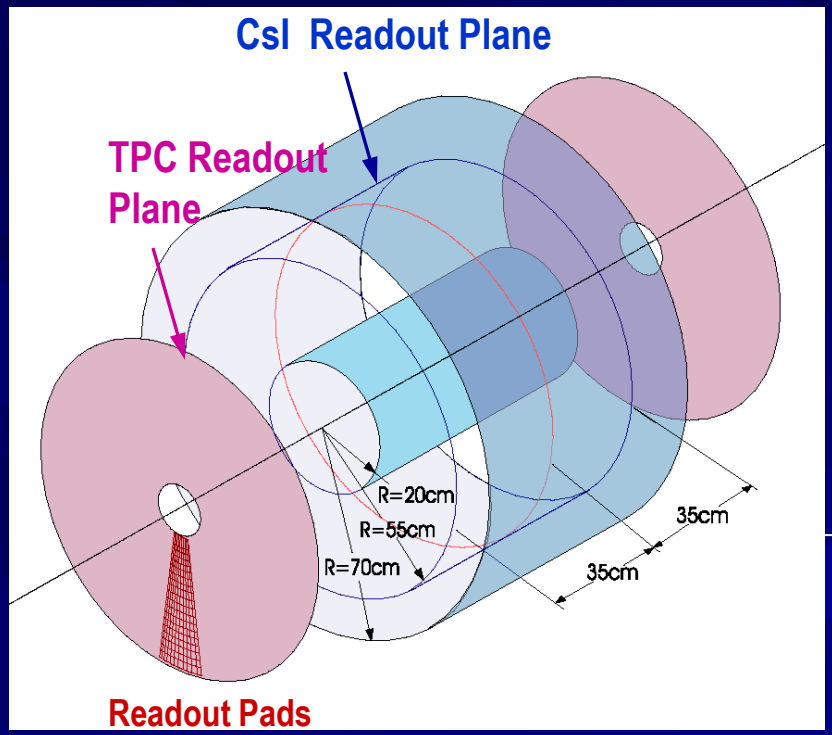


TPC provides tracking and eid by dE/dx
HBD provides eid
GEMs are used for both TPC and HBD

# Fast TPC + active beam pipe

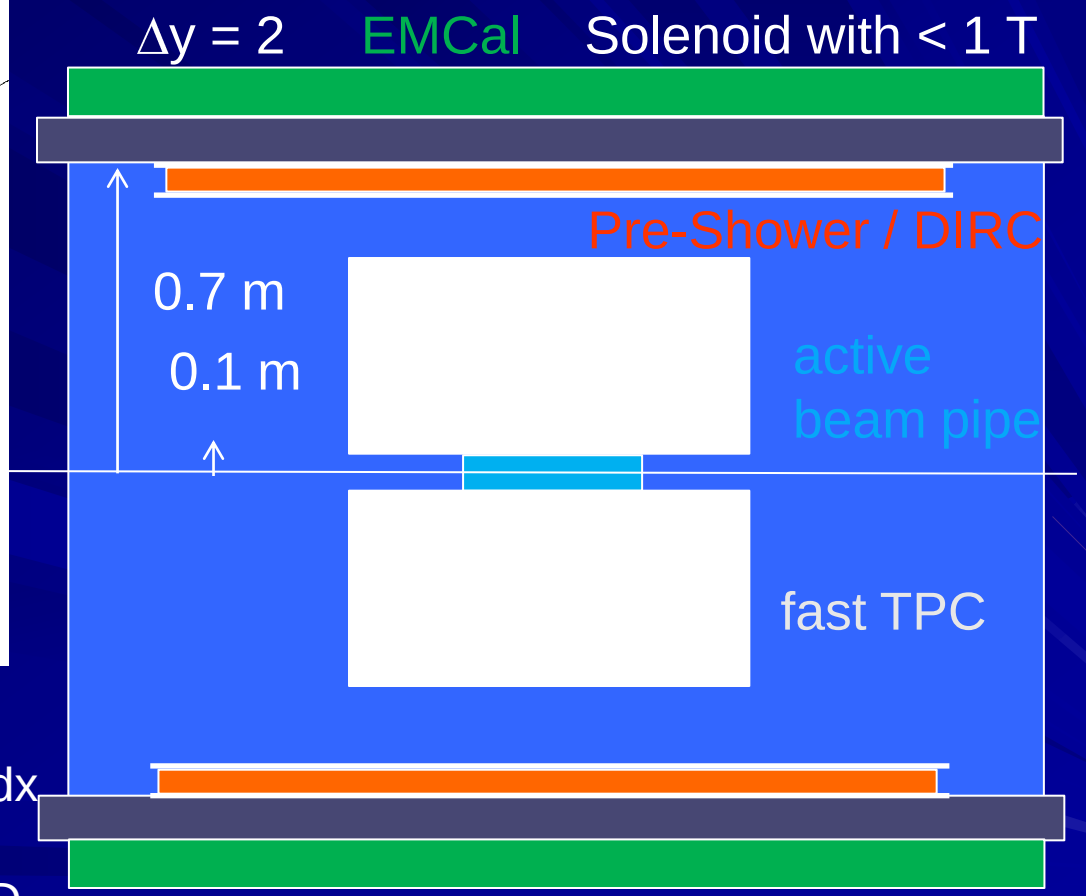


Silicon strip with $\sigma_\phi$ ~100 $\mu$m $\delta p/p$ << 1%p
Tracking with TPC

# Future

- LMR: Solve the PHENIX - STAR discrepancy
  - HBD results in central Au+Au collisions
- IMR: higher precision data needed
  - Higher statistics and direct measurement of charm contribution

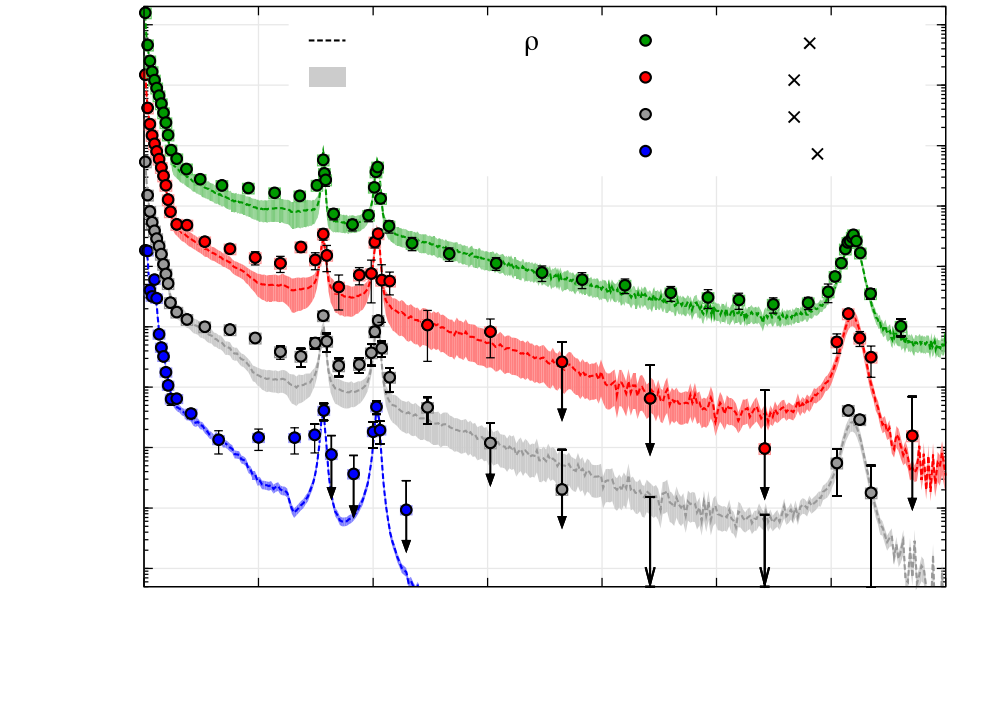


- Fill the gap between top SPS and top RHIC energy
  - Preliminary STAR results
- Dilepton $v_2$

# Dileptons $v_2$

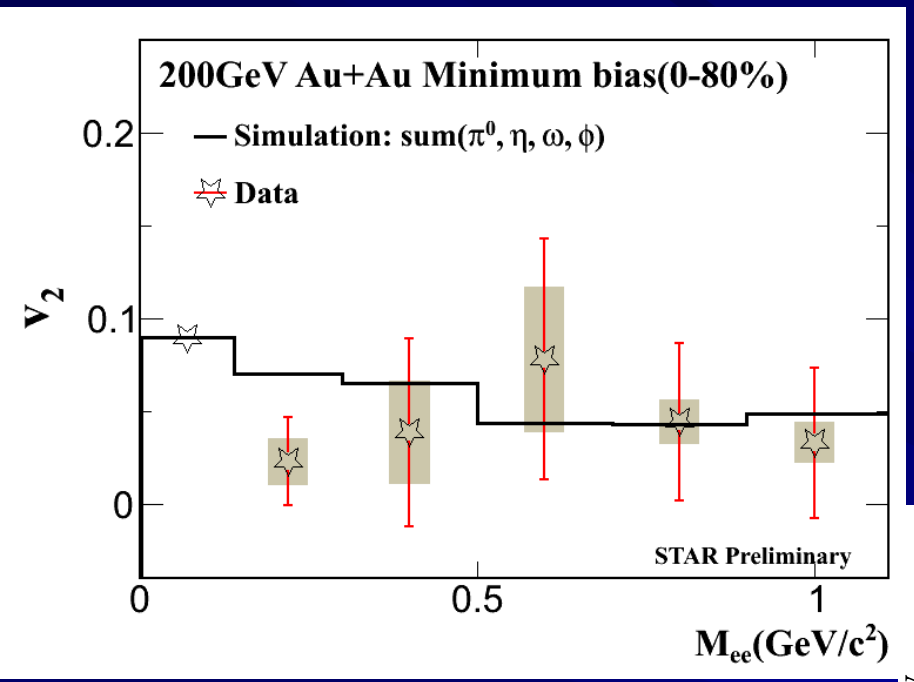


- First measurements by STAR

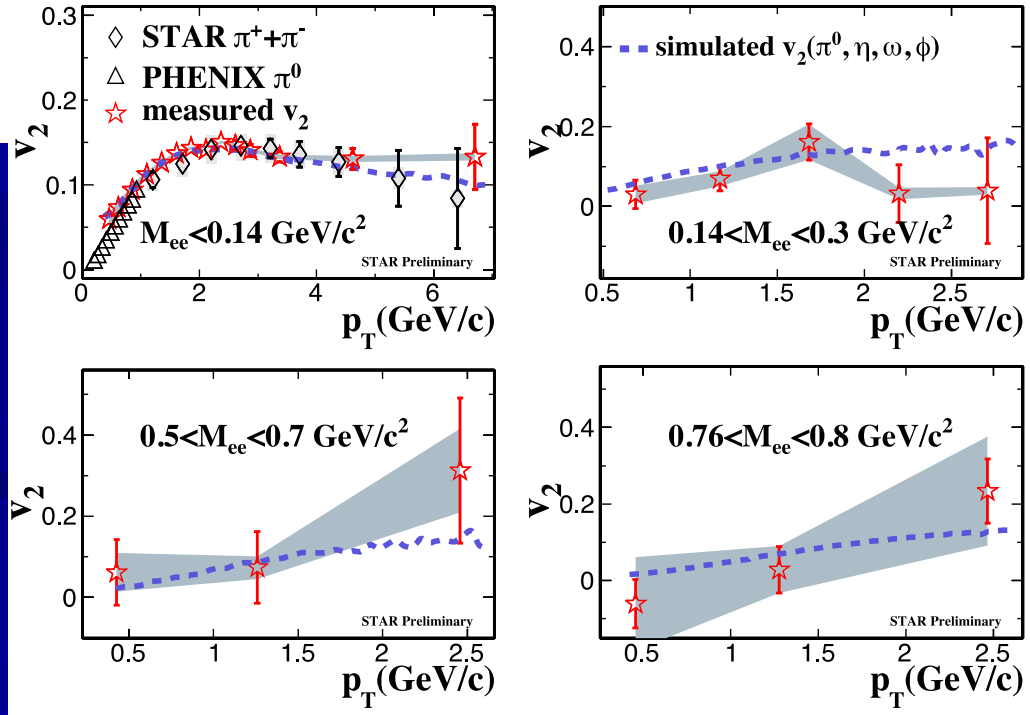


- Dilepton $v_2(m_{ee})$ and $v_2(p_T)$ results consistent with simulations based on hadronic sources

- Lower – energies:

# Low energies: testing the model

- Explanations of CERES and NA60 results rely on the high baryon density rather than the temperature of the system.
- Lower energies → controlled change of conditions: higher baryon density and lower temperature
- Only available test: CERES measurements at 40 AGeV.

Phys. Rev. Lett. 91, 042301 (2003)

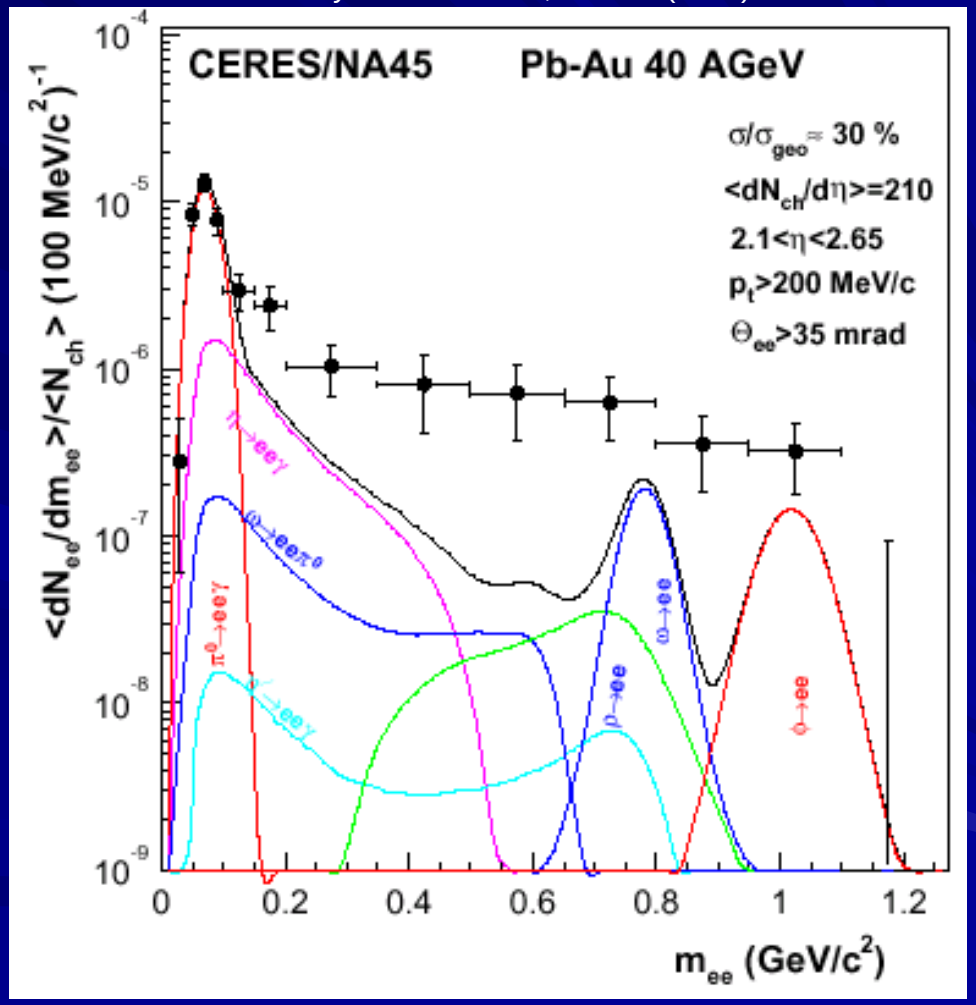


Enhancement factor:
5.9 ± 1.5 ± 1.2 ± 1.8 (cocktail)

# Highest baryon density

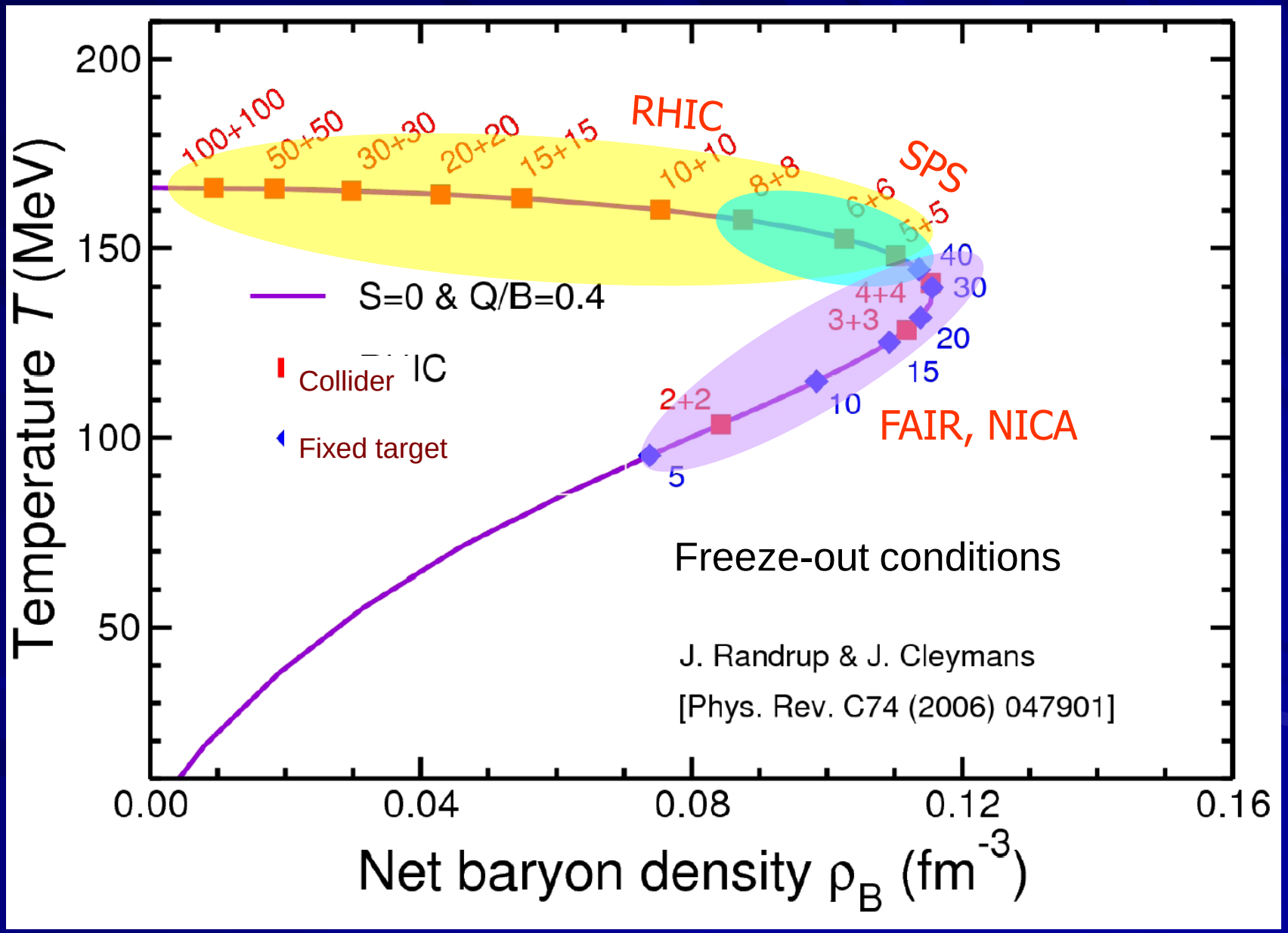

# Multi-Purpose Detector (MPD) at NICA

*3 stages of putting into operation.*
*First stage: 2017?*

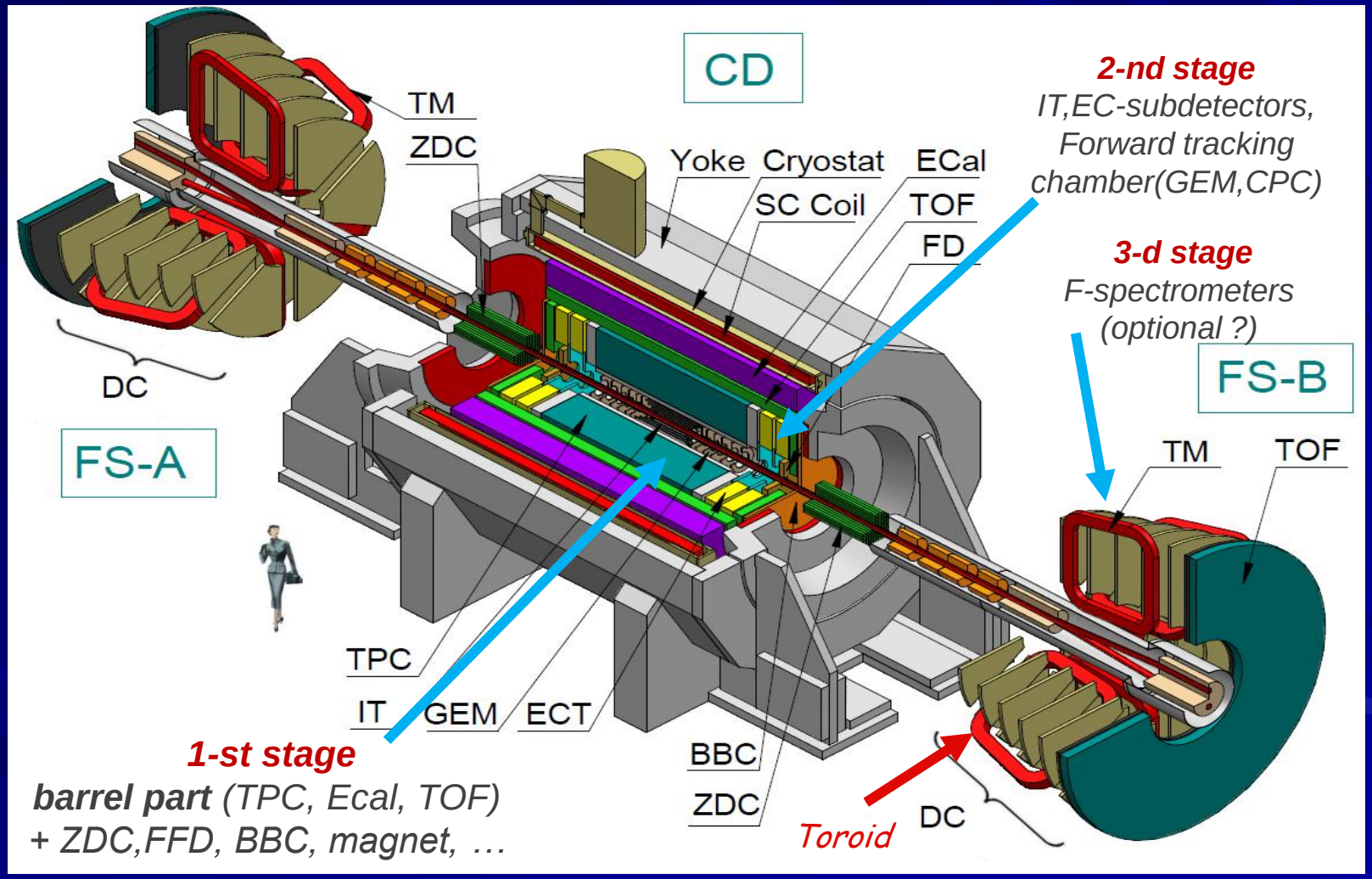

# Compressed Baryonic Matter (CBM) at FAIR

- tracking, momentum determination, vertex reconstruction: radiation hard silicon pixel/strip detectors (STS) in a magnetic dipole field

- hadron ID: TOF (& RICH)
- photons, $\pi^0$, $\eta$: ECAL
- PSD for event characterization
- high speed DAQ and trigger $\rightarrow$ rare probes!

- electron ID: RICH & TRD
  $\rightarrow \pi$ suppression $\geq 10^4$

- muon ID: absorber + detector layer sandwich
  $\rightarrow$ move out absorbers for hadron runs

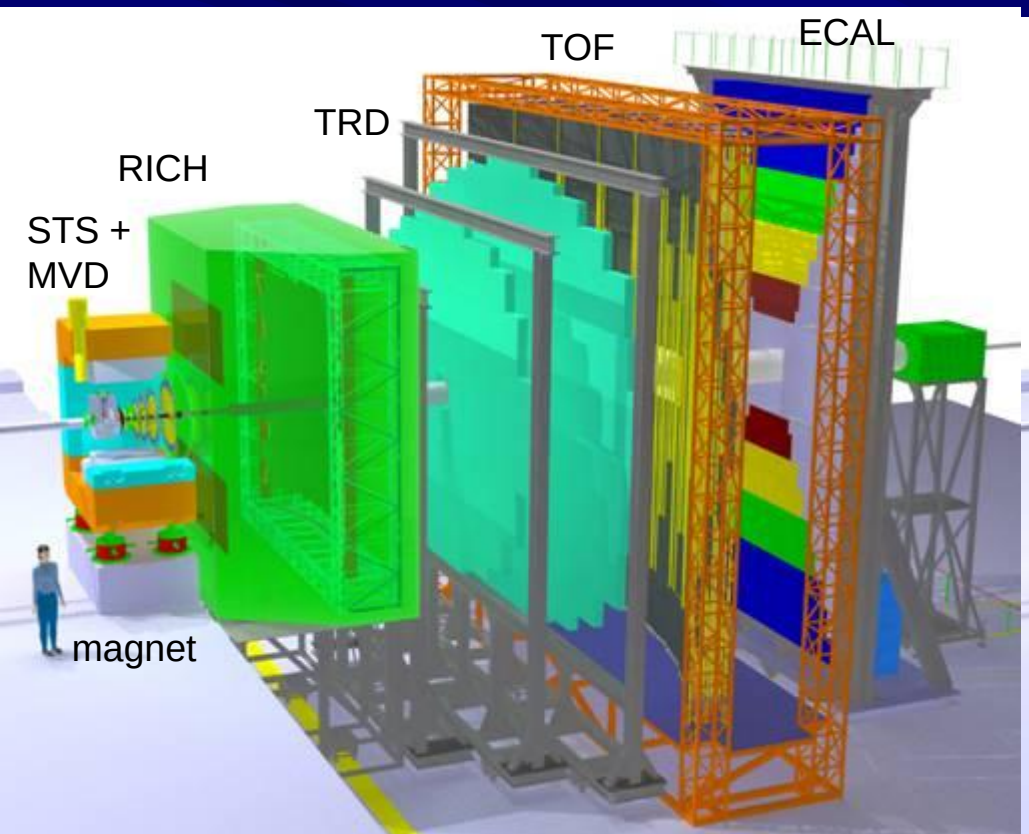


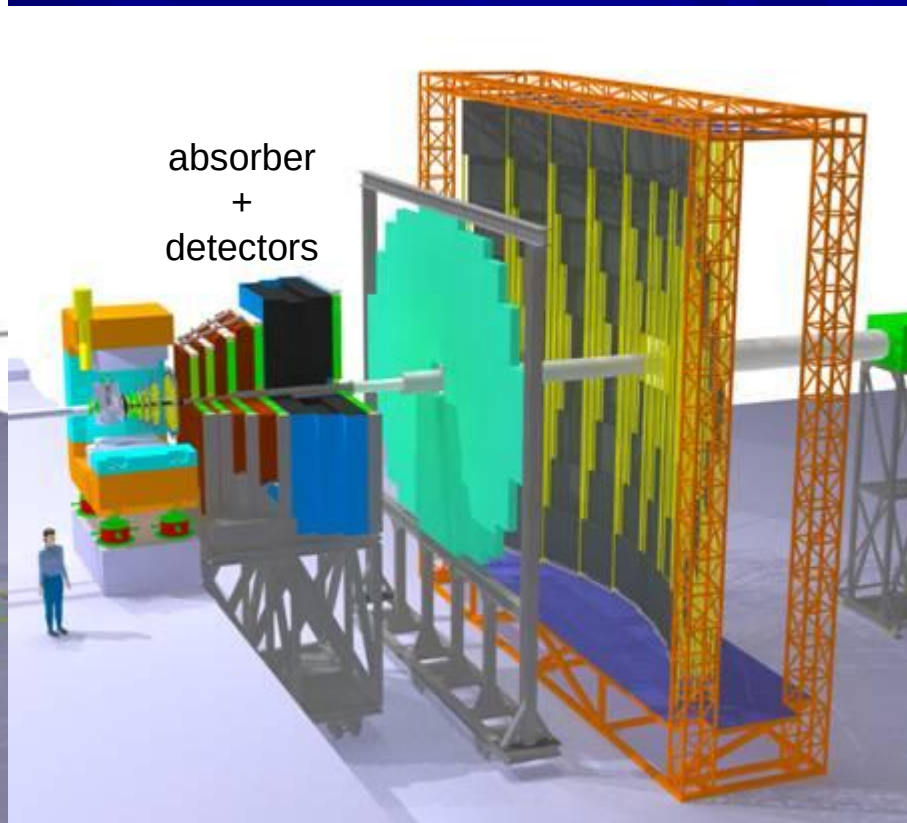

# LVM in pA Collisions

Cold nuclear matter at highest baryon density

Should broadening effects be visible?

# KEK E235 p+C, Cu @ 12 GeV

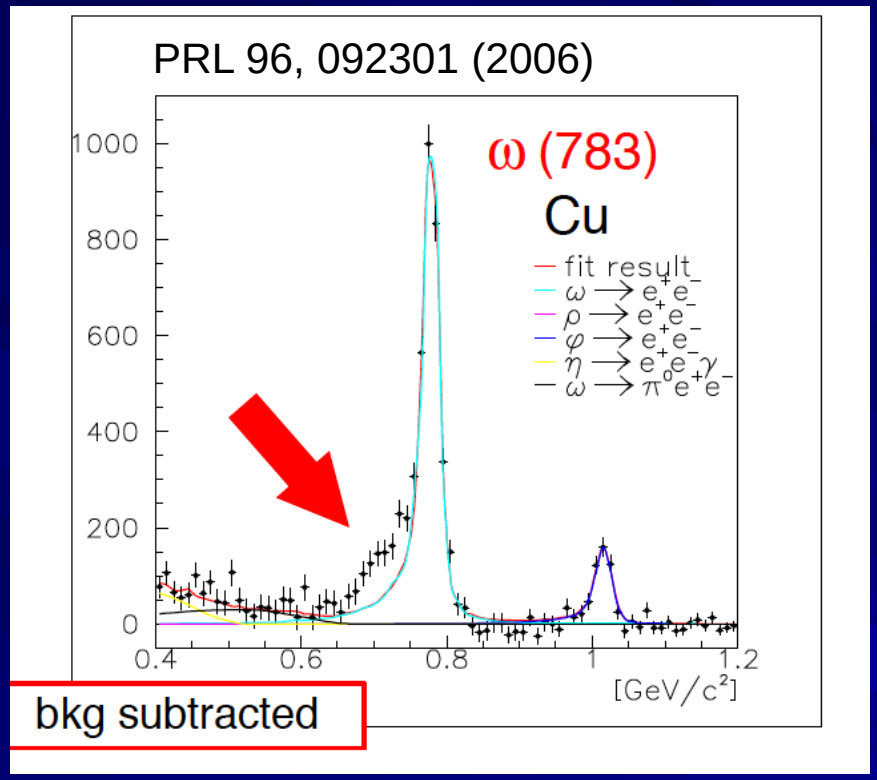


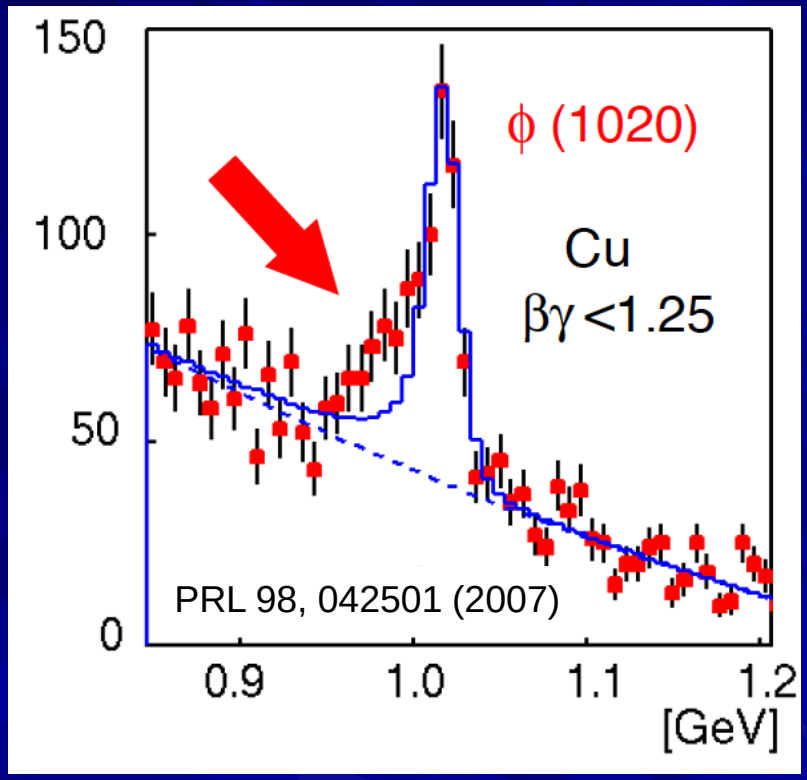


**Interpretation: masses drop by 9.2% (ρ,ω) and 3.4% (ϕ) at normal nuclear matter density**

CBELSA/TAPS: No mass shift. Shape consistent with ω in-medium broadening
CLAS: No effect. Results reproduced by transport model using vacuum mass values of ρ, ω and ϕ.

# Proposed experiment: JPARC – E16

30/50 GeV p beam on Cu, Pb targets

Tracking: GEM, eid: HBD, EMCal

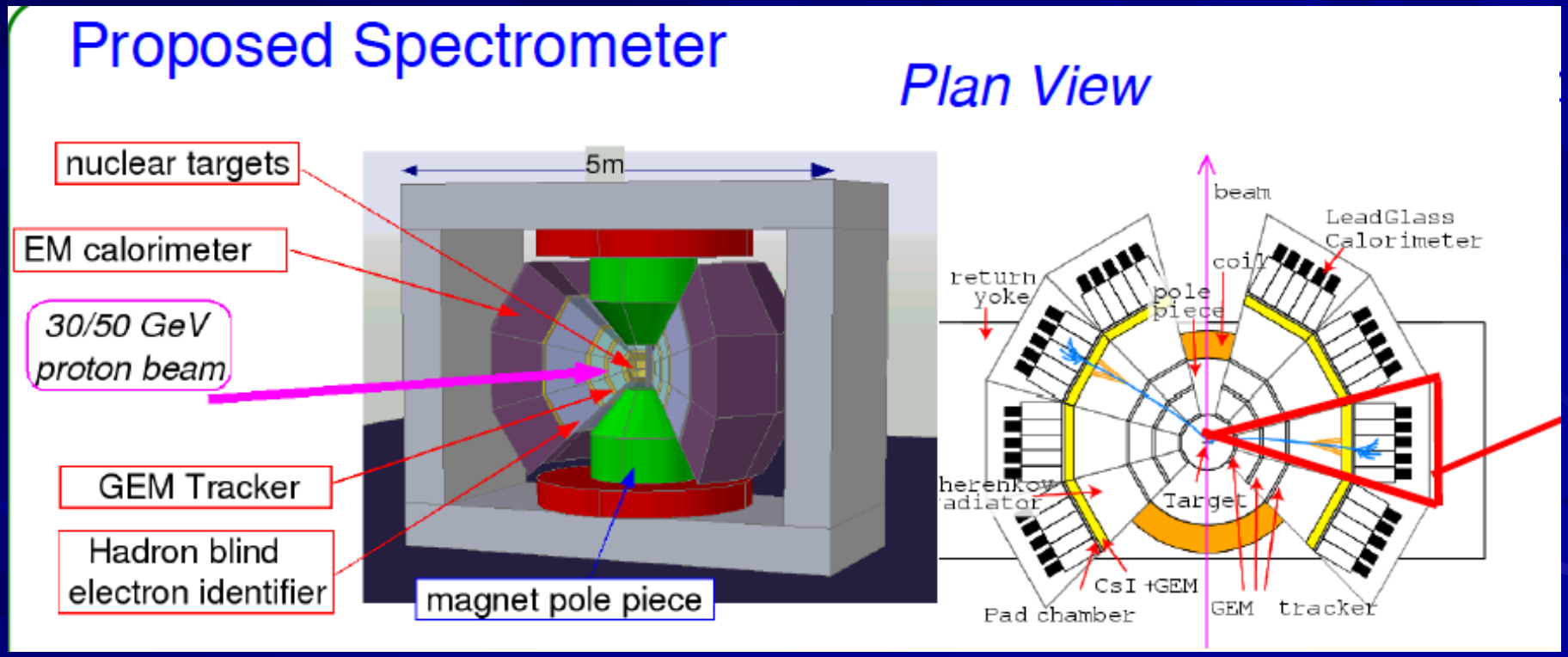

# Summary

- SPS energies: Consistent and coherent picture
  - Low-mass pair enhancement: thermal radiation from the HG
  - Approach to CSR proceeds through broadening (melting) of the resonances
  - IMR enhancement: thermal radiation from partonic phase
  - Missing: elliptic flow measurements
- Higher energies SPS → RHIC:
  - New source at top RHIC energies? Solve the PHENIX–STAR discrepancy - HBD results in central Au+Au collisions
  - IMR: need higher precision data: higher statistics and direct measurement of charm contribution
  - Fill the gap between top SPS and top RHIC energy – STAR, sPHENIX?
- Lower energies: explore the phase space of highest net baryon density
  - CBM at FAIR? MPD at NICA? SPS? RHIC?
- LVM in pA collisions: cold nuclear matter at the highest baryon density
  - JPARC E16 experiment

# Photons and di-leptons in strong magnetic field in heavy-ion collisions

Kirill Tuchin

IOWA STATE UNIVERSITY
OF SCIENCE AND TECHNOLOGY

RBRC Thermal radiation workshop, 12/06/2012

# OUTLINE

1. Time-dependence of magnetic field.
2. Synchrotron radiation.
3. Energy loss and polarization in magnetic field.

# MAGNETIC FIELD IN VACUUM

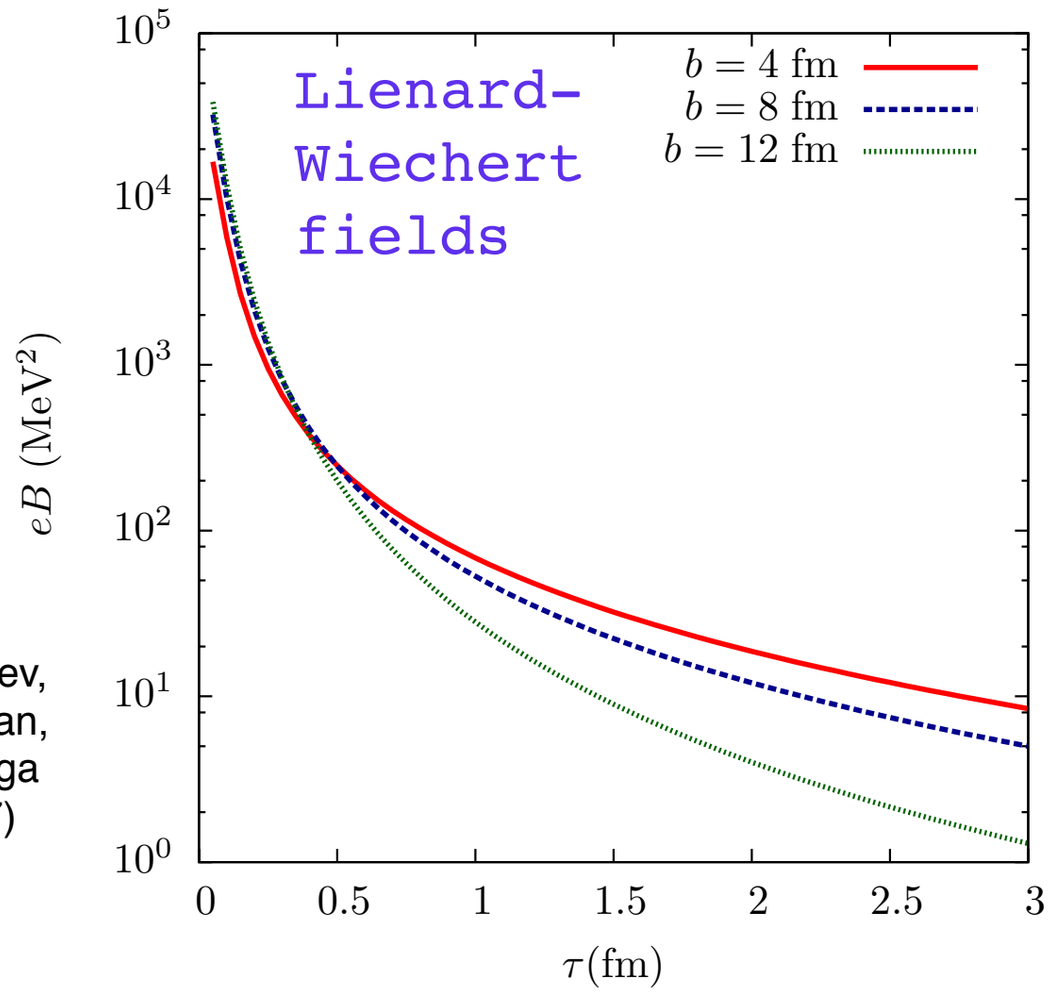


Kharzeev, McLerran, Warringa (2007)

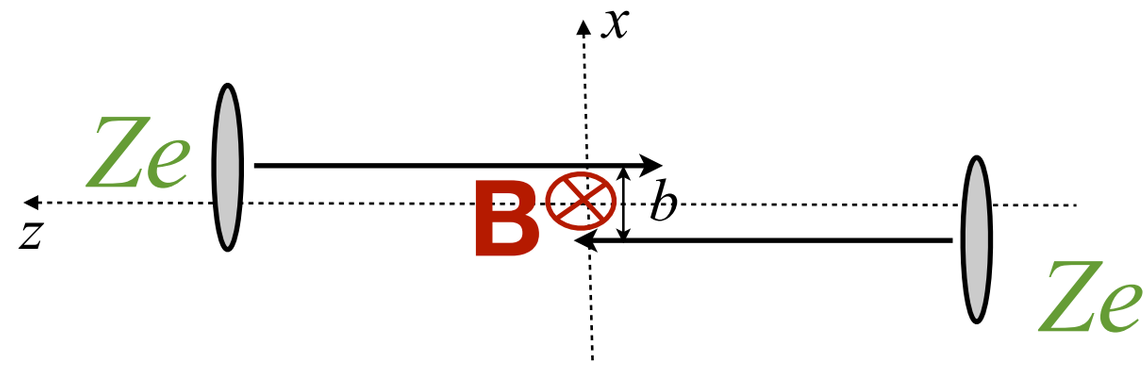


$$B \sim Ze\frac{b}{R^3}\gamma$$

For $Z=79$, $b=7$ fm, $\gamma=100$ we get $eB = (200\ \mathrm{MeV})^2 \approx m_\pi^2$

Similar results:

UrQMD based calculation: Skokov, Illarionov, Toneev (2009)

Hadron String Dynamic transport code: Voronyuk, Toneev, Cassing, Bratkovskaya, Konchakovski, Voloshin (2011)

# LEINARD-WIECHERT FILED IN DISPERSIVE MEDIUM

Medium is formed at a very early stage after a Heavy Ion Collision: Glasma (t~0.2 fm) gives way to Quark Gluon Plasma (t~0.5-2 fm). According to the state-of-the-art phenomenology it can be characterized by transport coefficients.

Magnetic field created by a single point charge *in medium:*

$$e\boldsymbol{B} = \frac{\alpha}{\pi}\,\hat{\boldsymbol{y}} \int_{-\infty}^{\infty} s(\omega)\, K_1(s(\omega)b)\, e^{i\omega(z/v-t)}\, d\omega \qquad s(\omega) = \omega\sqrt{\frac{1}{v^2} - \epsilon(\omega)}$$

At low frequencies dielectric constant has a pole due to a finite electric conductivity:

$$\epsilon(\omega) = 1 + \frac{i\sigma}{\omega}$$

The corresponding magnetic field in medium:

$$eB = \hat{\boldsymbol{y}}\,\frac{\alpha_{\rm em} b\,\sigma}{2(t-z)^2} e^{-\frac{b^2\sigma}{4(t-z)}}$$

Compared with the magnetic field in vacuum:

$$e\boldsymbol{B} = \hat{\boldsymbol{y}}\,\alpha_{\rm em}\frac{b\gamma}{(b^2+\gamma^2(t-z)^2)^{3/2}}$$

# MAGNETIC FIELD IN CONDUCTING PLASMA

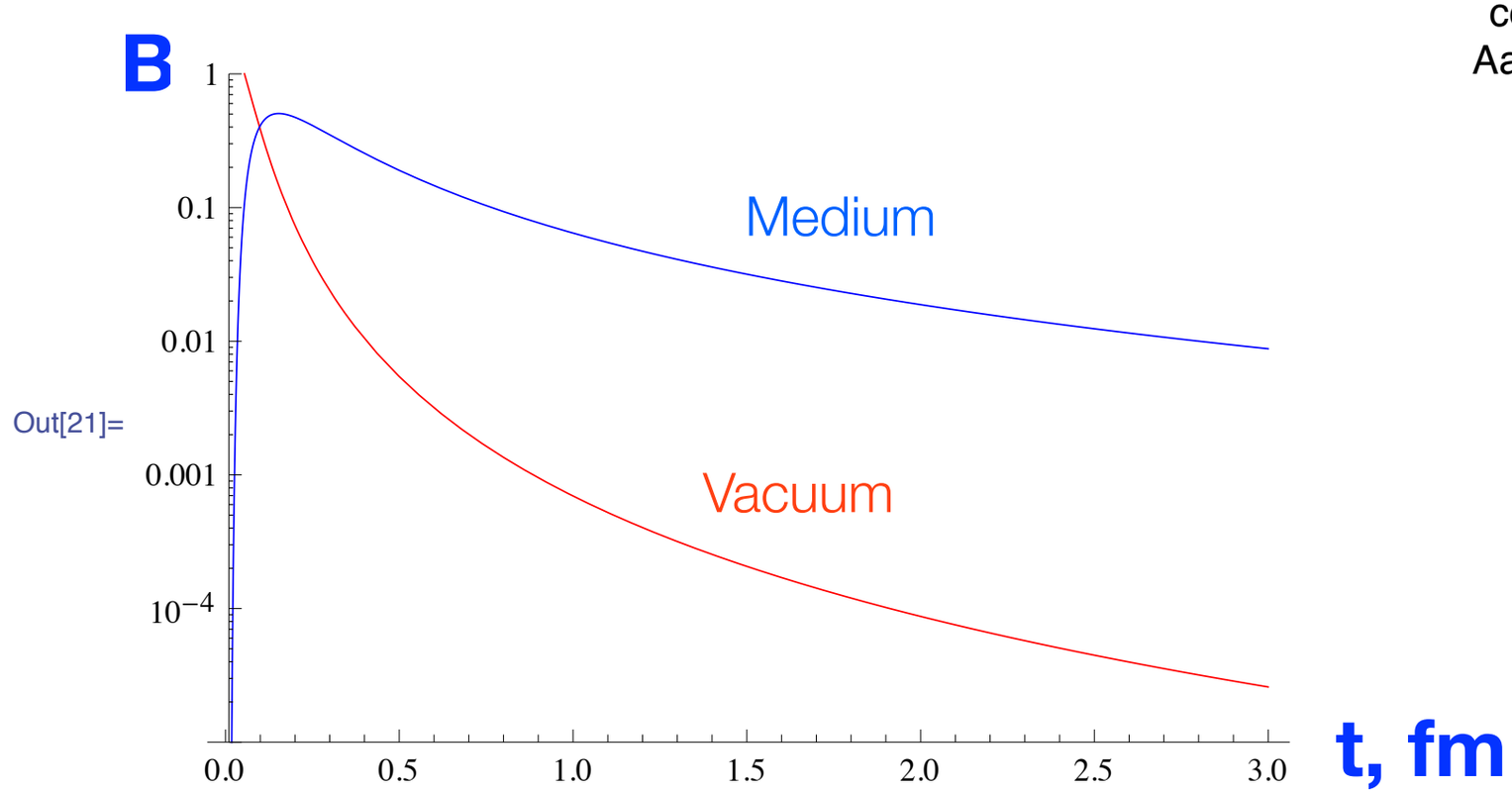


conductivity of QGP on the lattice:
Aarts at al (2007), Ding at al (2010):
only gluon contribution!

$$\sigma = 5\,\mathrm{MeV}$$

- This is magnetic field due to outgoing valence charges in infinite medium.

# MAGNETIC FIELD IN AN EXPANDING MEDIUM

K.T. 2010

$$\nabla \times \mathbf{E} = -\dot{\mathbf{B}}$$
$$\nabla \times \mathbf{B} = \mathbf{j} = \sigma \mathbf{E}$$

Lenz's law: induced B is parallel to the original B.

$$\nabla^2 \boldsymbol{B} = \sigma \dot{\boldsymbol{B}}$$

**j:** Foucault currents

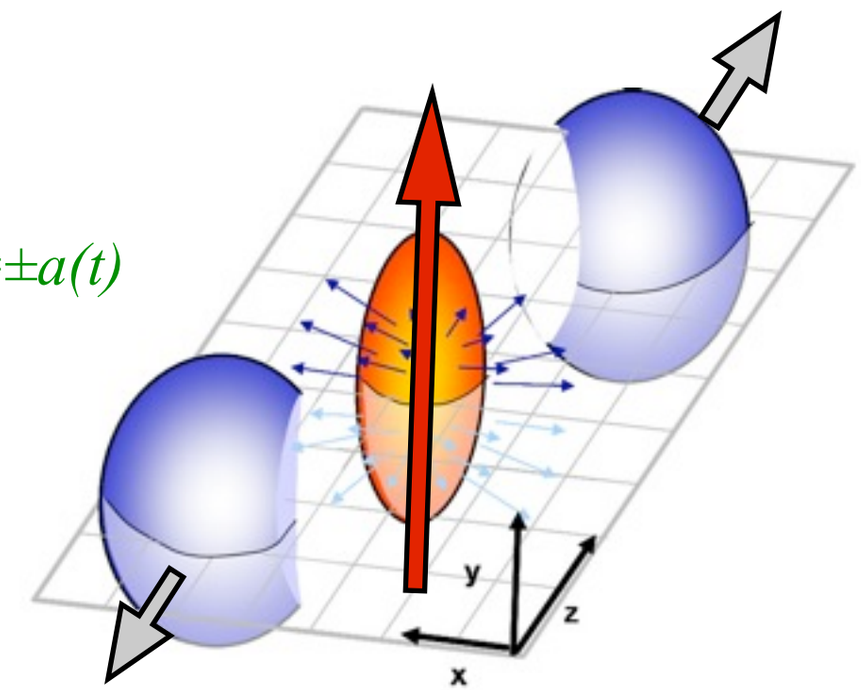


Problem: the boundary is time-dependent. It moves along $z=\pm a(t)$

Introduce rapidity $$\eta = \frac{1}{2} \ln \frac{a(t)+z}{a(t)-z}$$

Now the boundary is time-independent: $\eta=\pm\infty$

At $\eta \ll 1$ $$\nabla_\perp^2 \boldsymbol{B} + \frac{1}{a^2(t)} \frac{\partial^2 B}{\partial \eta^2} = \sigma \frac{\partial \boldsymbol{B}}{\partial t}$$

At early times $a(t) \ll R_A$, the transverse derivatives can be dropped, while at later times we can neglect the longitudinal derivatives.

# INDUCED MAGNETIC FIELD

The result of matching of the two solutions

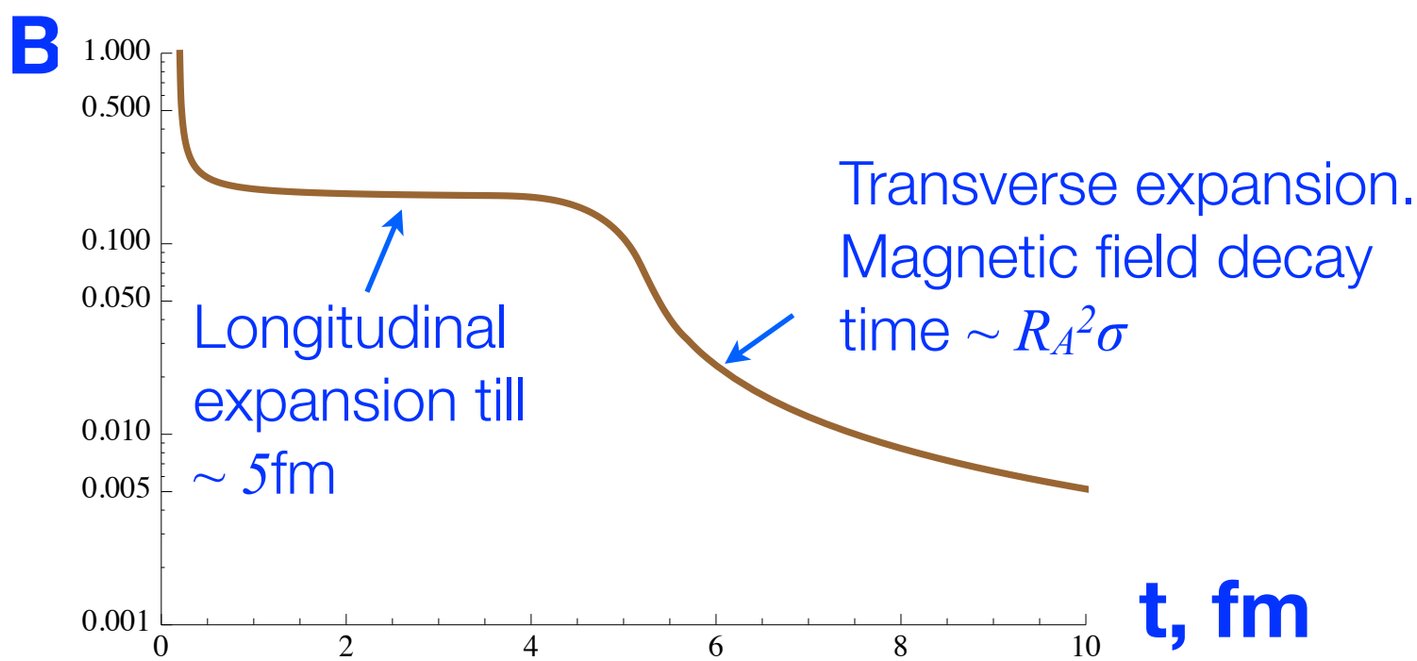


Not taken into account: dependence of conductivity on B.

see e.g. K.T. “On viscous flow and azimuthal anisotropy of quark-gluon plasma in strong magnetic field”, arXiv:1108.4394

# OUTLINE

1. Time-dependence of magnetic field.
2. Synchrotron radiation.
3. Energy loss and polarization in magnetic field.

# SYNCHROTRON RADIATION

KT (2010,2012)

Synchrotron radiation:

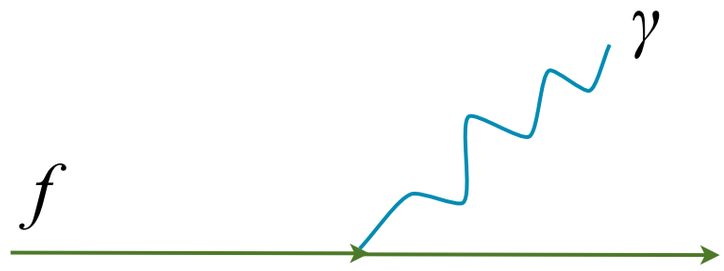


$$f(e_f, j, p) \to f(e_f, k, q) + \gamma(\boldsymbol{k})$$

QGP is transparent to the emitted electromagnetic radiation because its absorption coefficient is suppressed by $\boldsymbol{\alpha}^2$ (I'll show the precise calculation later).

Spacing between the Landau levels ~ $\boldsymbol{eB/\varepsilon}$, while their thermal width ~ $\boldsymbol{T}$. When $\boldsymbol{eB/\varepsilon \gtrsim T}$ it is essential to account for quantization of fermion spectra.

Fermion spectrum quantization is important not only for hard and electromagnetic probes but also for the bulk properties of QGP.

# KINEMATICS

$$\varepsilon_j = \sqrt{m^2 + p^2 + 2je_f B}\,, \quad \varepsilon_k = \sqrt{m^2 + q^2 + 2ke_f B}$$

$j$ $(k)$ is the quantum number of Landau orbit of *initial (final)* charged fermion.

$p$ $(q)$ is the projection of *initial (final)* fermion momentum on the direction of *B*

Magnetic field doesn't do work → energy is conserved. Magnetic Lorentz force has no component along the *B*-direction → momentum along B is conserved

$$\varepsilon_j = \omega + \varepsilon_k\,, \quad p = q + \omega\cos\theta$$

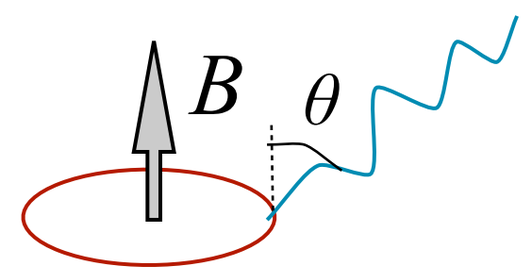


Angular distribution of the power spectrum:

$$\frac{dI^j}{d\omega d\Omega} = \sum_f \frac{z_f^2\alpha}{\pi}\omega^2 \sum_{k=0}^{j} \Gamma_{jk}\left\{|\mathcal{M}_\perp|^2 + |\mathcal{M}_\parallel|^2\right\}\delta(\omega - \varepsilon_j + \varepsilon_k)$$

## Matrix elements for synchrotron transitions corresponding to photon polarization perpendicular and parallel to *B*

Sokolov, Ternov (1968) and others

$$4\varepsilon_j\varepsilon_k|\mathcal{M}_\perp|^2 = (\varepsilon_j\varepsilon_k - pq - m^2)[I^2_{j,k-1} + I^2_{j-1,k}] + 2\sqrt{2je_fB}\sqrt{2ke_fB}[I_{j,k-1}I_{j-1,k}]\,.$$

$$\begin{aligned}4\varepsilon_j\varepsilon_k|\mathcal{M}_\parallel|^2 = {} & \cos^2\theta\big\{(\varepsilon_j\varepsilon_k - pq - m^2)[I^2_{j,k-1} + I^2_{j-1,k}] - 2\sqrt{2je_fB}\sqrt{2ke_fB}[I_{j,k-1}I_{j-1,k}]\big\} \\ & - 2\cos\theta\sin\theta\big\{p\sqrt{2ke_fB}[I_{j-1,k}I_{j-1,k-1} + I_{j,k-1}I_{j,k}] \\ & + q\sqrt{2je_fB}[I_{j,k}I_{j-1,k} + I_{j-1,k-1}I_{j,k-1}]\big\} \\ & + \sin^2\theta\big\{(\varepsilon_j\varepsilon_k + pq - m^2)[I^2_{j-1,k-1} + I^2_{j,k}] + 2\sqrt{2je_fB}\sqrt{2ke_fB}(I_{j-1,k-1}I_{j,k})\big\}\end{aligned}$$

$$I_{j,k} \equiv I_{j,k}(x) = (-1)^{j-k}\sqrt{\frac{k!}{j!}}e^{-\frac{x}{2}}x^{\frac{j-k}{2}}L_k^{j-k}(x).$$

Laguerre polynomials (recall Schrödinger equation for hydrogen)

$$x = \frac{\omega^2}{2e_fB}\sin^2\theta$$

# PHOTON NUMBER SPECTRUM

We are interested in the photon number spectrum radiated from QGP

$$\frac{dN^{\rm synch}}{dt d\Omega d\omega} = \sum_f \int_{-\infty}^{\infty} dp \frac{e_f B (2N_c) V}{2\pi^2} \sum_{j=0}^{\infty} \sum_{k=0}^{j} \frac{dI^j}{\omega d\omega d\Omega} (2-\delta_{j,0}) f(\varepsilon_j)[1-f(\varepsilon_k)]$$

$$f(\varepsilon) = \frac{1}{e^{\varepsilon/T}+1}$$

To take integral over p write

$$\delta(\omega - \varepsilon_j + \varepsilon_k) = \sum_{\pm} \frac{\delta(p - p^*_{\pm})}{\left|\frac{p}{\varepsilon_j} - \frac{q}{\varepsilon_k}\right|}$$

$$p^*_{\pm} = \Big\{ \cos\theta (m_j^2 - m_k^2 + \omega^2 \sin^2\theta) \pm \sqrt{[(m_j+m_k)^2 - \omega^2\sin^2\theta][(m_j-m_k)^2 - \omega^2 \sin^2\theta]} \Big\} / (2\omega \sin^2\theta)$$

$$m_j^2 = m^2 + 2je_f B\,, \quad m_k^2 = m^2 + 2ke_f B$$

$p_\pm$ is real in two cases:

$$\text{(i) } m_j - m_k \geq \omega \sin\theta\,, \quad \text{or} \quad \text{(ii) } m_j + m_k \leq \omega \sin\theta$$

synchrotron radiation

one-photon pair annihilation

In case (i) the $j \to k$ transition must satisfy

$$\omega \leq \omega_{s,jk} \equiv \frac{m_j - m_k}{\sin\theta} = \frac{\sqrt{m^2 + 2je_fB} - \sqrt{m^2 + 2ke_fB}}{\sin\theta}$$

in particular $j$=$k$ transition is forbidden.

Spectral distribution of the synchrotron radiation rate per unit volume:

$$\frac{dN^{\text{synch}}}{V dt d\Omega d\omega} = \sum_f \frac{2N_c z_f^2 \alpha}{\pi^3} e_f B \sum_{j=0}^{\infty} \sum_{k=0}^{j} \omega(1+\delta_{k0})\,\vartheta(\omega_{s,ij} - \omega) \int dp \sum_{\pm} \frac{\delta(p - p_\pm^*)}{\left|\frac{p}{\varepsilon_j} - \frac{q}{\varepsilon_k}\right|}$$

$$\times \left\{|\mathcal{M}_\perp|^2 + |\mathcal{M}_\parallel|^2\right\} f(\varepsilon_j)[1 - f(\varepsilon_k)]\,,$$

# HIGH-ENERGY REFERENCE FRAME

$$\boldsymbol{k} = \omega(\sin\alpha\cos\phi\hat{\boldsymbol{x}} + \sin\alpha\sin\phi\hat{\boldsymbol{y}} + \cos\alpha\hat{\boldsymbol{z}})$$

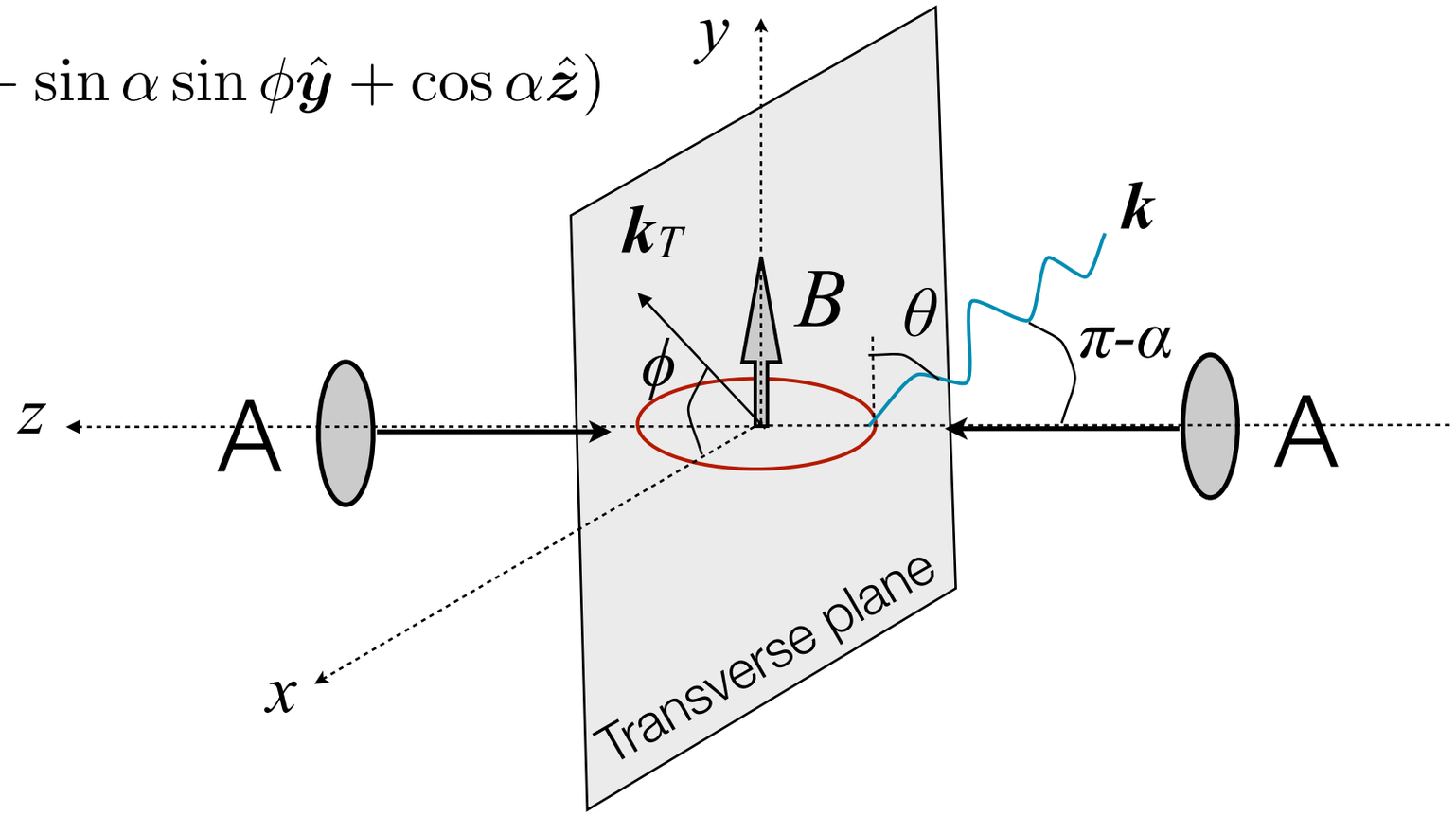


$$\hat{\boldsymbol{k}} \cdot \hat{\boldsymbol{y}} = \cos\theta \implies$$

$$\cos\theta = \sin\alpha\sin\phi$$

Thus, azimuthal dependence (ϕ) of the spectrum is an artifact of the frame choice!

$$k_\perp = \sqrt{k_x^2 + k_y^2} = \frac{\omega\cos\theta}{\sin\phi}\,, \quad y = -\ln\tan\frac{\alpha}{2}$$

$$\frac{dN^{\text{synch}}}{dV\,dt\,d^2k_\perp\,dy} = \omega\frac{dN^{\text{synch}}}{dV\,dt\,d^3k} = \frac{dN^{\text{synch}}}{dV\,dt\,\omega d\omega d\Omega}$$

# SYNCHROTRON SPECTRUM

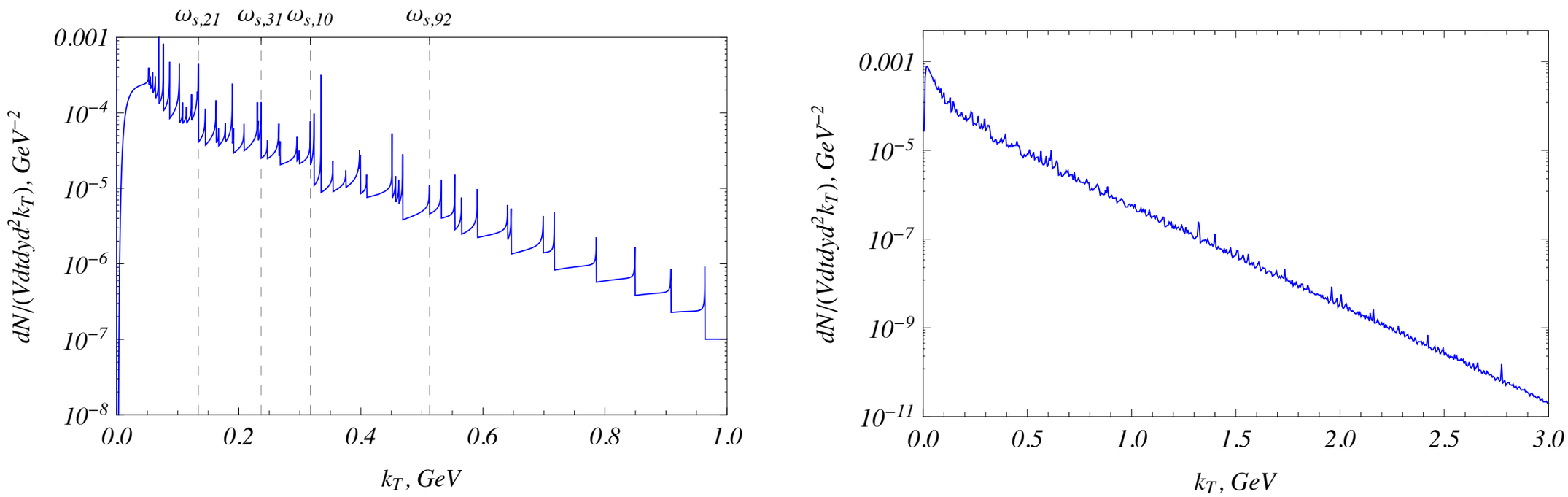


FIG. 1: Spectrum of synchrotron radiation by $u$ quarks at $eB = m_\pi^2$, $y = 0$, $\phi = \pi/3$: (a) contribution of 10 lowest Landau levels $j \leq 10$; several cutoff frequencies are indicated; (b) summed over all Landau levels. $m_u = 3$ MeV, $T = 200$ MeV.

# ANGULAR DISTRIBUTION OF SR

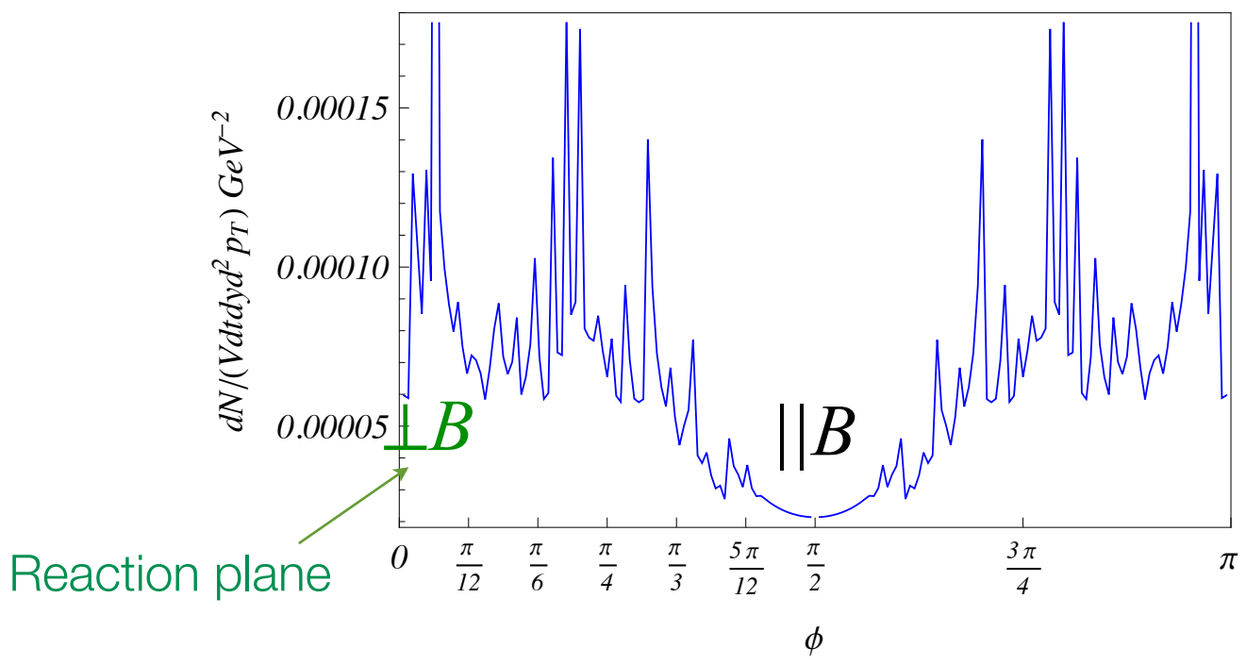


FIG. 2: Azimuthal distribution of synchrotron radiation by $u$-quarks at $k_\perp = 0.2$ GeV, $eB = m_\pi^2$, $y = 0$. $m_u = 3$ MeV.

This distribution implies that $v_2>0$ (to be calculated)

Since $\phi$ appears only in $\cos^2\phi$ term, there is clear symmetry $\phi\rightarrow\pi-\phi \Rightarrow$ only even harmonics survive. Odd harmonic arise from B fluctuations.

# SYNCHROTRON SPECTRUM

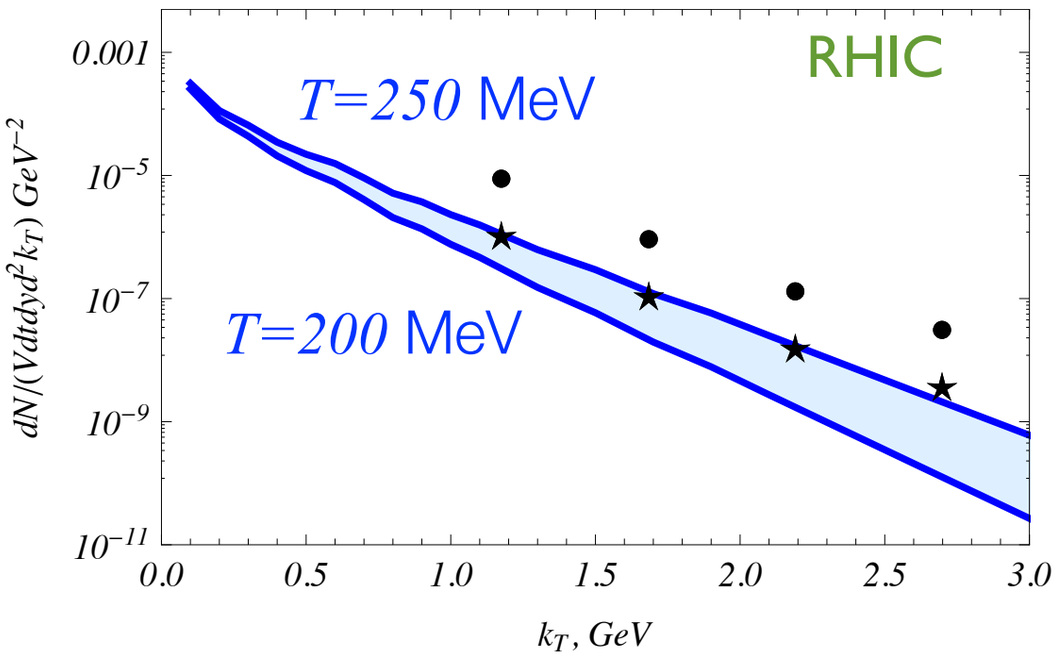


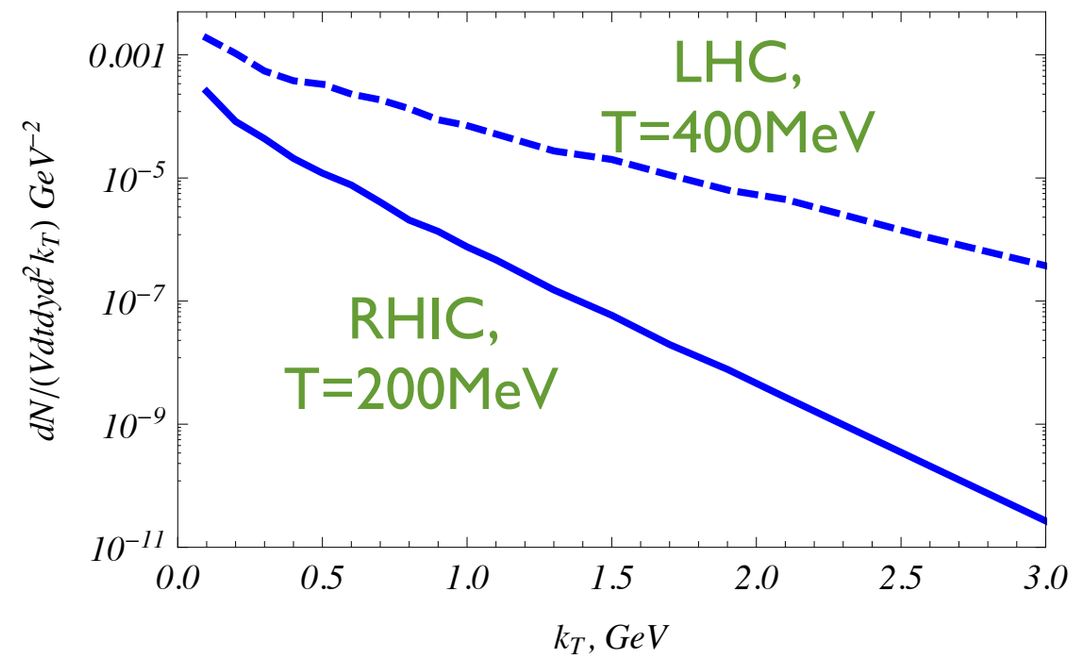


● $Vt=25\pi\ fm^4$

★ $Vt=9\times25\pi\ fm^4$

Photon spectrum is very sensitive to the QGP temperature.

# HOW MANY LANDAU LEVELS CONTRIBUTE?

$$\frac{dN^{\rm synch}}{dtd\Omega d\omega} = \sum_f \int_{-\infty}^{\infty} dp \frac{e_f B(2N_c)V}{2\pi^2} \sum_{j=0}^{j_{\rm max}} \sum_{k=0}^{j} \frac{dI^j}{\omega d\omega d\Omega}(2-\delta_{j,0}) f(\varepsilon_j)[1-f(\varepsilon_k)]$$

| $f$ | $u$ | $u$ | $u$ | $u$ | $u$ | $u$ | $s$ | $u$ | $u$ | $s$ |
|---|---|---|---|---|---|---|---|---|---|---|
| $eB/m_\pi^2$ | 1 | 1 | 1 | 1 | 1 | 1 | 1 | 15 | 15 | 15 |
| $T$, GeV | 0.2 | 0.2 | 0.2 | 0.2 | 0.2 | 0.2 | 0.2 | 0.4 | 0.4 | 0.4 |
| $\phi$ | $\frac{\pi}{3}$ | $\frac{\pi}{3}$ | $\frac{\pi}{3}$ | $\frac{\pi}{3}$ | $\frac{\pi}{6}$ | $\frac{\pi}{12}$ | $\frac{\pi}{3}$ | $\frac{\pi}{3}$ | $\frac{\pi}{3}$ | $\frac{\pi}{3}$ |
| $k_\perp$, GeV | 0.1 | 1 | 2 | 3 | 1 | 1 | 1 | 1 | 2 | 1 |
| $x$ | 0.096 | 9.6 | 38 | 86 | 29 | 35 | 19 | 0.64 | 2.6 | 1.3 |
| $j_{\rm max}$ | 30 | 40 | 90 | 150 | 120 | 200 | 90 | 8 | 12 | 16 |

TABLE I: The upper summation limit in (18) that yields the 5% accuracy. $j_{\rm max}$ is the highest Landau level of the initial quark that is taken into account at this accuracy. Throughout the table $y = 0$.

Large j,k correspond to quasi-classical limit.

# PAIR ANNIHILATION

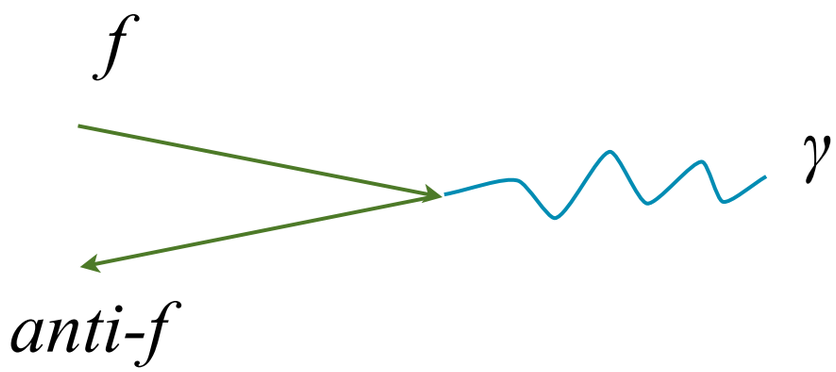


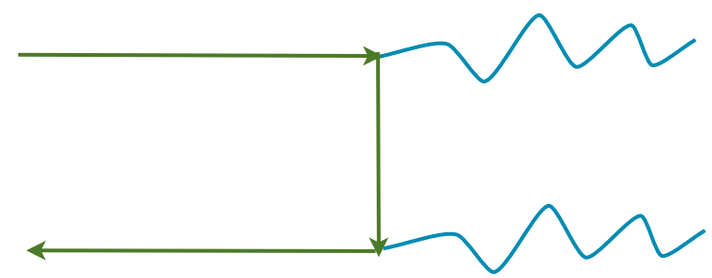

One and two-photon annihilation: At $eB \gg m^2$ one-photon annihilation dominates.

One-photon annihilation is a cross-channel of synchrotron radiation. The corresponding matrix elements are straightforward to calculate.

$$\frac{dN^{\rm annih}}{V dt d\omega d\Omega} = \sum_f \frac{\alpha z_f^2 \omega N_c}{4\pi e_f B} \sum_{j=0}^{\infty} \sum_{k=0}^{\infty} \int dp \, \frac{2 e_f B}{2\pi^2} f(\varepsilon_j) \int dq \, \frac{2 e_f B}{2\pi^2} f(\varepsilon_k)$$
$$\times \delta(p + q - \omega \cos\theta) \delta(\varepsilon_j + \varepsilon_k - \omega) \{ |\mathcal{T}_\perp|^2 + |\mathcal{T}_\parallel|^2 \}$$

# PAIR ANNIHILATION SPECTRUM

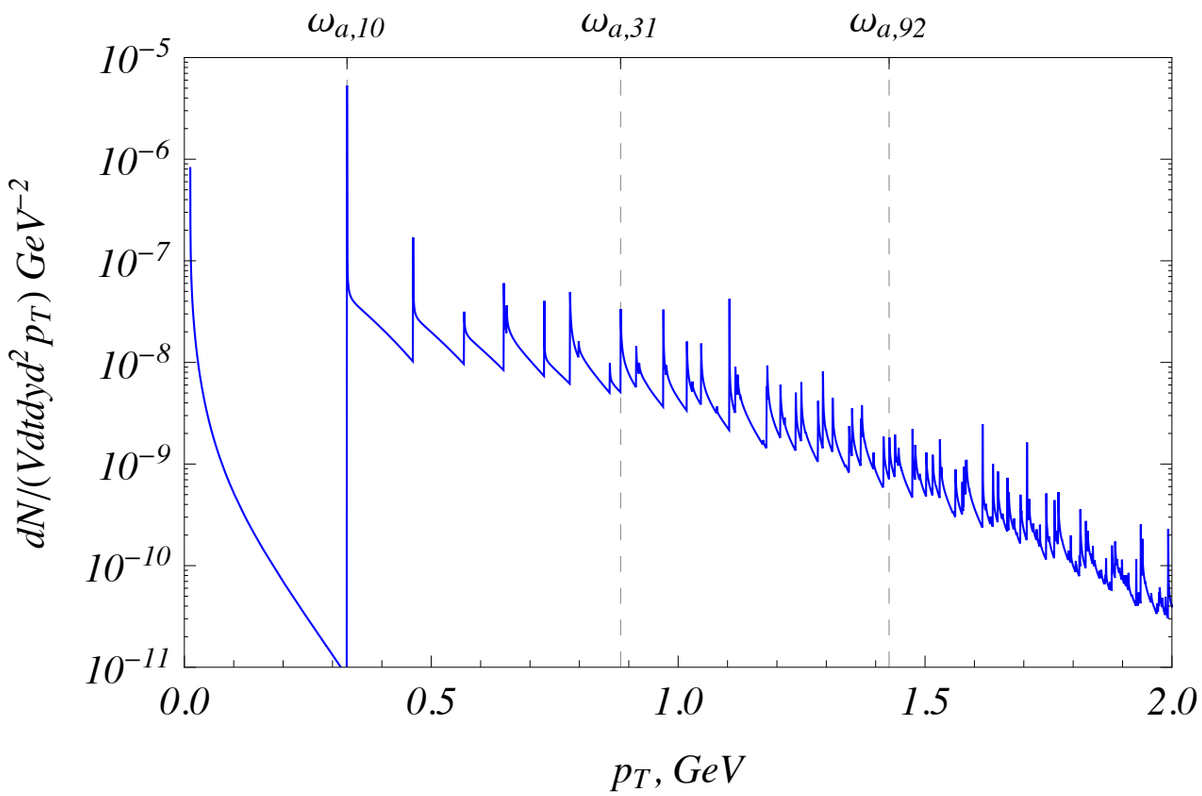


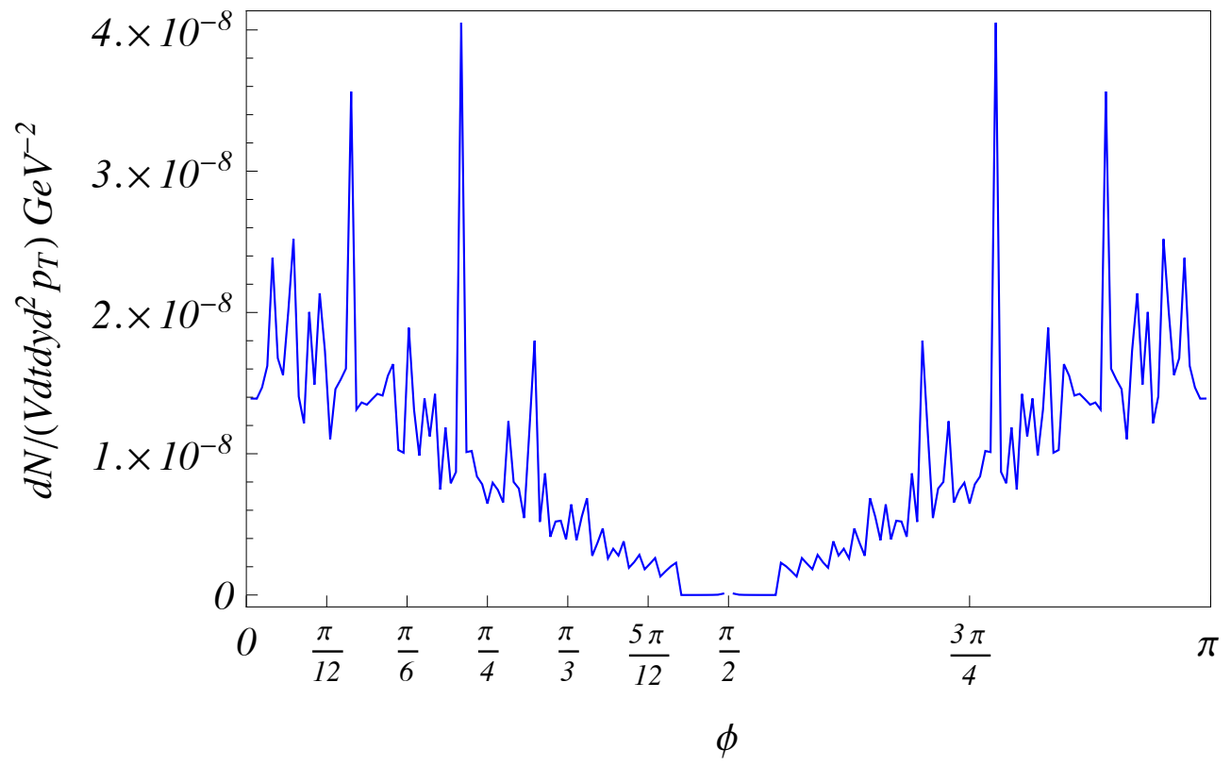


FIG. 5: Photon spectrum in one-photon annihilation of $u$ and $\bar{u}$ quarks. $eB = m_\pi^2$, $y = 0$. (a) $k_\perp$-spectrum at $\phi = \pi/3$, (b) azimuthal angule distribution at $k_\perp = 1$ GeV.

Pair annihilation is numerically much smaller than synchrotron radiation.

# CONCLUSIONS I

- Photon production by QGP due to its interaction with external magnetic field gives a considerable contribution to the total photon multiplicity in heavy-ion collisions.

- In the kinematic region relevant for the current high energy heavy-ion experiments, contribution of the synchrotron radiation is about two orders of magnitude larger than that of pair annihilation.

- One possible way to ascertain the contribution of electromagnetic radiation in external magnetic field is to isolate the azimuthally symmetric component with respect to the direction of the magnetic field by rotating the reference frame, so that z-axis coincides with B-direction.

# DILEPTON PRODUCTION VIA REAL PHOTON DECAY

KT (2010)

Photon decay is another cross-channel of the synchrotron radiation

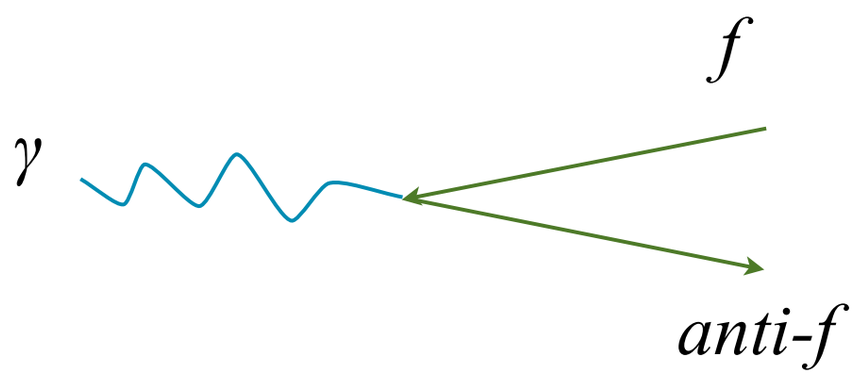


Rate in the quasi-classical ultra-relativistic approximation (discussed later):

$$w = -\sum_a \frac{\alpha_{\rm em}\, z_a^3\, eB}{m_a \varkappa_a} \int_{(4/\varkappa_a)^{2/3}}^{\infty} \frac{2(x^{3/2} + 1/\varkappa_a)\, {\rm Ai}'(x)}{x^{11/4}(x^{3/2} - 4/\varkappa_a)^{3/2}}$$

$$\varkappa_a^2 = -\frac{\alpha_{\rm em} z_a^2 \hbar^3}{m_a^6} \left(F_{\mu\nu} k^\nu\right)^2 = \frac{\alpha_{\rm em} z_a^2 \hbar^3}{m_a^6} (\boldsymbol{k} \times \boldsymbol{B})^2$$

# PHOTON DECAY RATE

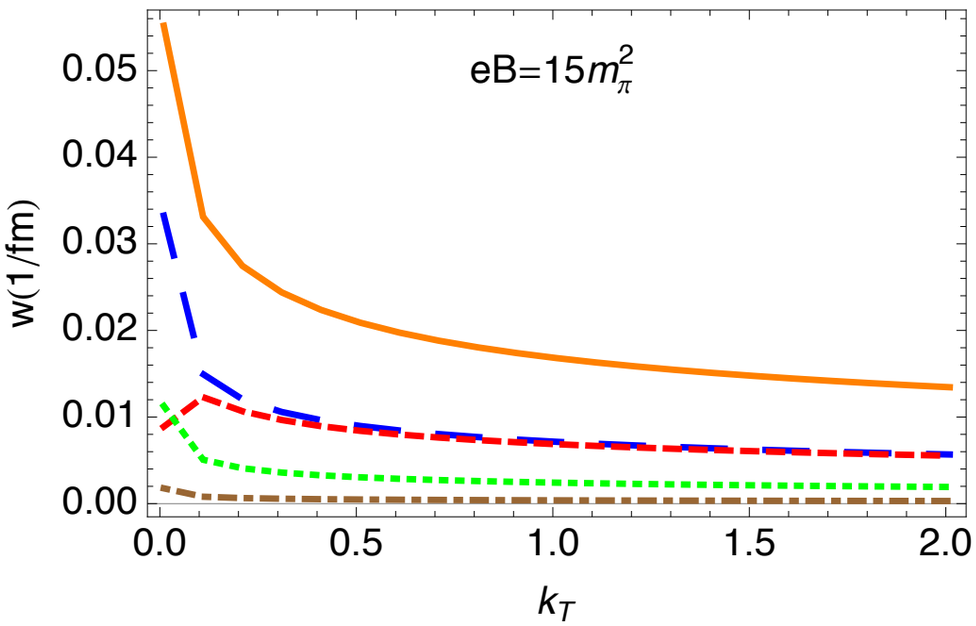


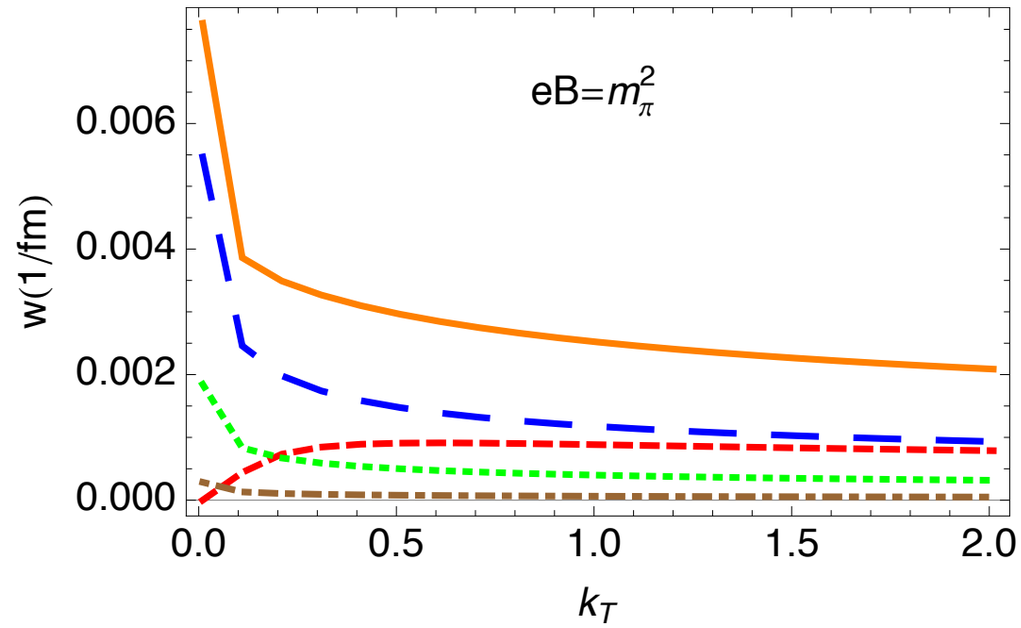


Survival probability: $P=1-w\Delta t$, where $\Delta t \approx 5fm \Rightarrow P$(RHIC)$=98.5\%$, $P$(LHC)$=90\%$

# AZIMUTHAL ASYMMETRY DUE TO PHOTON DECAY

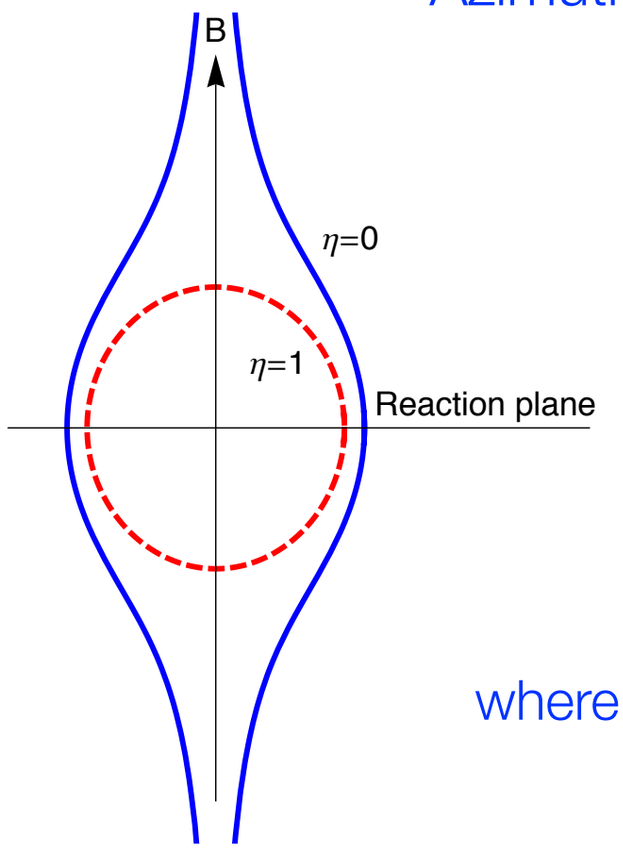


Azimuthal asymmetry of the decay rate $w$:

$$w = \frac{1}{2} w_0 \left[ 1 - \sum_{k=1}^{\infty} \frac{\sqrt{\pi}\Gamma\left(-\frac{1}{6}\right)}{2^{2/3} B\left(\frac{5}{6}+k, \frac{5}{6}-k\right)} \cos(2k\varphi) \right]$$

Azimuthal asymmetry of the survival probability P:

$$P = \bar{P}\left(1 + \sum_{k=1}^{\infty} v_{2k} \cos(2\varphi k)\right), \quad v_{2k} = -\frac{1-\bar{P}}{\bar{P}} \frac{2\, w_{2k}}{w_0}$$

where azimuthal average is $\bar{P} = \langle 1 - w\Delta t \rangle_\varphi = 1 - w_0 \Delta t \approx 1$

$$v_2 = \Delta t \, \frac{2\, 6^{2/3} \Gamma\left(\frac{2}{3}\right)}{7\pi} \sum_a \frac{\alpha_{\rm em} (eB)^{2/3} z_a^{8/3}}{(k_T)^{1/3}}$$

For $k_T = 1\,GeV$ and $\Delta t \approx 5$fm $\Rightarrow$ $v_2(RHIC) = 1\%$, $v_2(LHC) = 7\%$

Work in progress: $q \to q + \gamma \to q + \ell^+ + \ell^-$

# SYNCHROTRON RADIATION OF GLUON BY FAST QUARKS

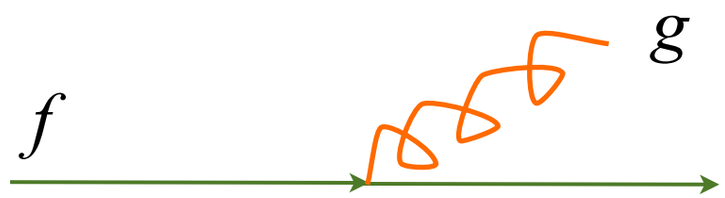


- General formulas for synchrotron radiation simplify if quark is **ultra-relativistic** $\varepsilon \gg m$ *before* and *after* gluon radiation.

  This is always true in week fields $eB \ll m^2$

  In strong fields $eB \gg m^2$ this approximation breaks down at the threshold $\omega \sim \varepsilon$, i.e. gluon carries away almost all quark energy ⇒ energy loss in this approximation must satisfy $\Delta\varepsilon \ll \varepsilon$

- Synchrotron radiation is **quasi-classical** if

  1. Spacing between Landau levels $eB/\varepsilon$ is much smaller than $\varepsilon$ $=> \varepsilon^2 \gg eB$
  2. Recoil due to gluon emission is small: $\omega \ll \varepsilon$ (i.e. far from the threshold)

# OUTLINE

1. Time-dependence of magnetic field.
2. Synchrotron radiation.
3. Energy loss and polarization in magnetic field.

# ULTRA-RELATIVISTIC + QUASI-CLASSICAL LIMIT

KT (2010,2012)

In the quasi-classical approximation $j \gg 1$, $k \gg 1$. Taking also the UR limit Laugerre polynomials reduce to Airy functions:

$$\frac{dI}{d\omega} = -\alpha_s C_F \frac{m^2\,\omega}{\varepsilon^2}\left\{\int_x^\infty \mathrm{Ai}(\xi)\,d\xi + \left(\frac{2}{x} + \frac{\omega}{\varepsilon}\,\chi\,x^{1/2}\right)\mathrm{Ai}'(x)\right\}$$

Invariant parameter $\chi^2 = -\dfrac{\alpha_{\mathrm{em}} Z_q^2 \hbar^3}{m^6}\,(F_{\mu\nu}p^\nu)^2 = \dfrac{\alpha_{\mathrm{em}} Z_q^2 \hbar^3}{m^6}(\mathbf{p}\times\mathbf{B})^2$

$$\chi^2 = \frac{\hbar^2 (eB)^2}{m^6}\,p_\perp^2\,(\sinh^2\eta + \cos^2\varphi)$$

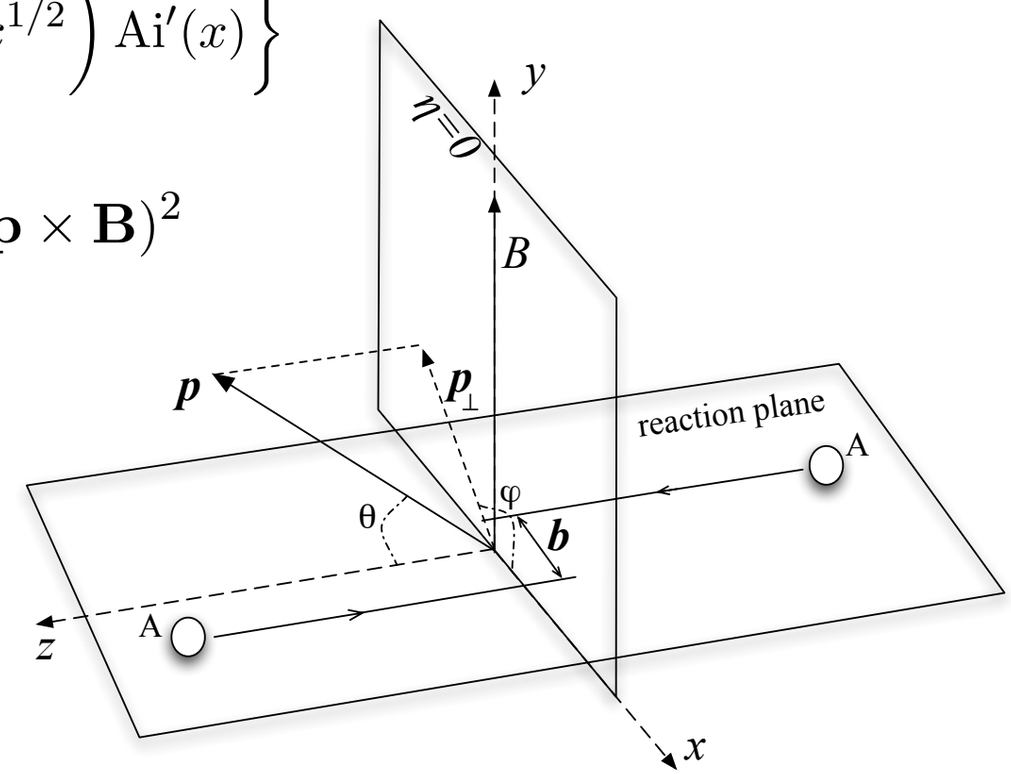


**Energy loss due to synchrotron radiation**

$$\frac{d\varepsilon}{dl} = -\int_0^\infty d\omega\,\frac{dI}{d\omega} = \alpha_s C_F\,\frac{m^2\,\chi^2}{2}\int_0^\infty \frac{4 + 5\chi\,x^{3/2} + 4\chi^2\,x^3}{(1+\chi\,x^{3/2})^4}\,\mathrm{Ai}'(x)\,x\,dx$$

$$\frac{d\varepsilon}{dl} = -\frac{2\,\alpha_s\,\hbar\,C_F\,(Z_q eB)^2\varepsilon^2}{3m^4}\,, \quad \chi \ll 1\,,$$ Weak fields

$$\frac{d\varepsilon}{dl} = -0.37\,\alpha_s\,\hbar^{-1/3}\,C_F\,(Z_q eB\,\varepsilon)^{2/3}\,, \quad \chi \gg 1$$ Strong fields

# Energy loss in magnetic field

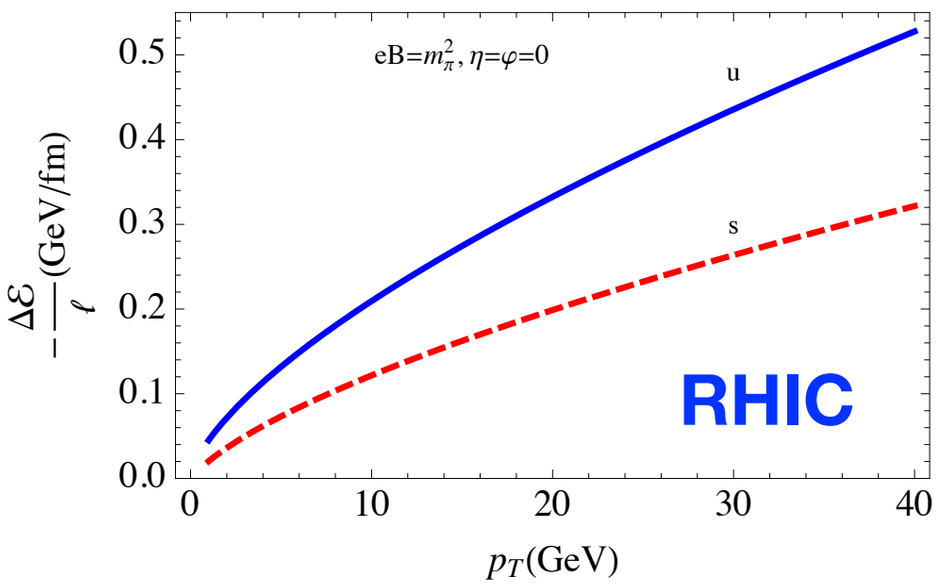


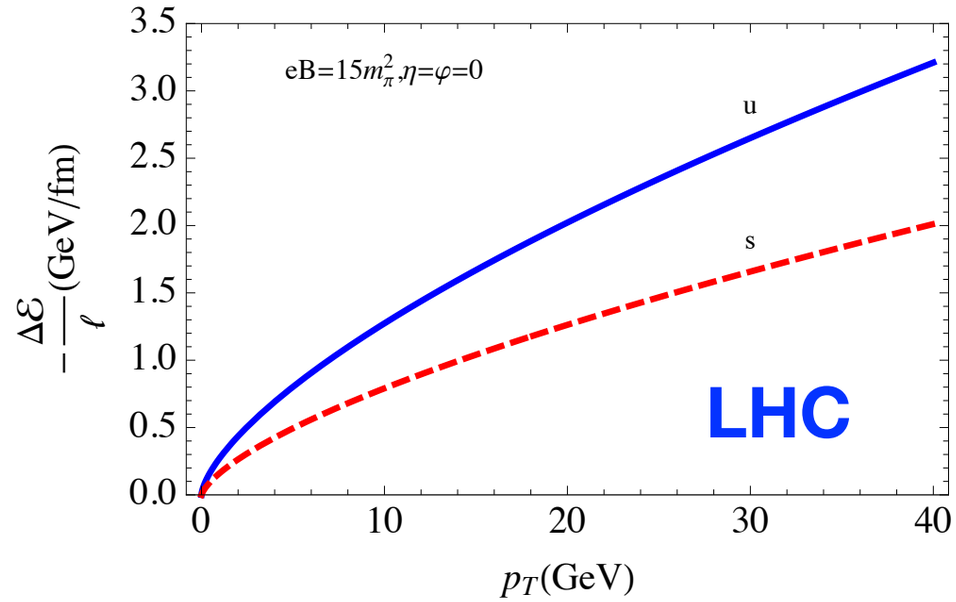


## Azimuthal asymmetry:

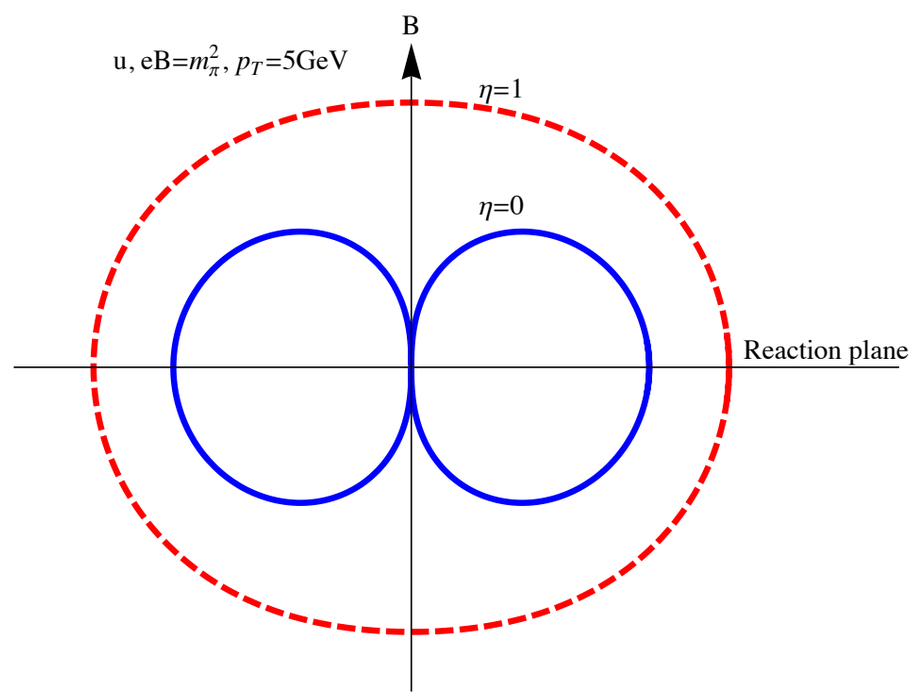

# POLARIZATION OF LEPTONS AND LIGHT QUARKS

Spin-flip probability per unit time

$$w = \frac{5\sqrt{3}\alpha_s C_F}{16}\frac{\hbar^2}{m^2}\left(\frac{\varepsilon}{m}\right)^5\left(\frac{Z_q e\,|\boldsymbol{v}\times\boldsymbol{B}|}{\varepsilon}\right)^3\left(1-\frac{2}{9}\left(\boldsymbol{\zeta}\cdot\boldsymbol{v}\right)^2-\frac{8\sqrt{3}}{15}\mathrm{sign}\left(e_q\right)\left(\boldsymbol{\zeta}\cdot\boldsymbol{b}\right)\right)$$

Sokolov, Ternov (1964)

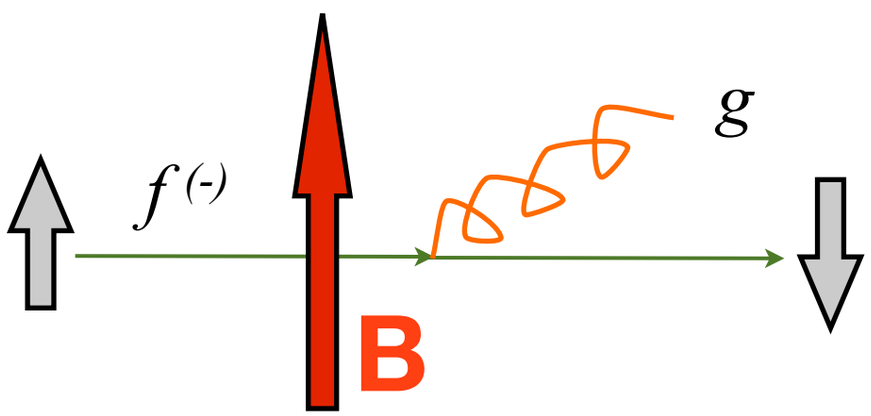


NR case: $H = -\boldsymbol{\mu}\cdot\boldsymbol{B} = -\left(\frac{geZ_q\hbar}{2m}\right)\boldsymbol{s}\cdot\boldsymbol{B}$

Spin-asymmetry: $A = \frac{n_\uparrow - n_\downarrow}{n_\uparrow + n_\downarrow}$ n(↑)/n(↓) be the number of fermions with given momentum and spin direction parallel /anti-parallel to the field in a given event.

$$A = \frac{8}{5\sqrt{3}} = 92\%$$

**A very strong polarization of quarks and leptons!**

# BEYOND THE QUASI-CLASSICAL APPROXIMATION

- **In strong fields $B \gg e/m^2$ near the threshold $\omega = \varepsilon$:**

  Quark looses almost all its energy due to synchrotron radiation and falls on one of the lowest Landau levels.

  This brakes both the quasi-classical and ultra-relativistic approximation.

- Transition to the ground state occurs with probability

$$w_{n0} = \frac{\alpha_s}{2} \frac{m^2}{\varepsilon} \frac{B}{B_c} e^{-B_c/B}$$

Sokolov, Borisov, Zhukovskii (1975)

where $B_c = e/m^2$

- In heavy-ion collisions $B$ is stronger than $B_c$, so such transitions must be taken into account.

  ☞ Future project.

# CONCLUSIONS II

- Synchrotron radiation of gluons contributes to the quark energy loss and is azimuthally asymmetric.

- Polarization of leptons escaping the QGP is a sensitive probe of magnetic field.

# SUMMARY

- Magnetic field in relativistic heavy-ion collisions is super-critical and slowly varying in time.

- Synchrotron photons maybe a significant part of the total photon spectrum at low $p_T$.

- Fast quarks and leptons loose a lot of energy and get polarized in magnetic field. **`Can the polarization be measured?`**

# Thermal dileptons at RHIC

Gojko Vujanovic

Thermal Radiation Workshop
Brookhaven National Laboratory

December 7th 2012

# Outline

- Overview of Dilepton sources

**Low Mass Dileptons**

- Thermal Sources of Dileptons

  1) QGP Rate (w/ viscous corrections)
  2) In-medium vector meson's Rate (w/ viscous corrections)

- 3+1D Viscous Hydrodynamics
- Thermal Dilepton Yields & $v_2$

**Intermediate Mass Dileptons**

- Charmed Hadrons: Yield & $v_2$
- Conclusion and outlook

# Evolution of a nuclear collision

## Space-time diagram

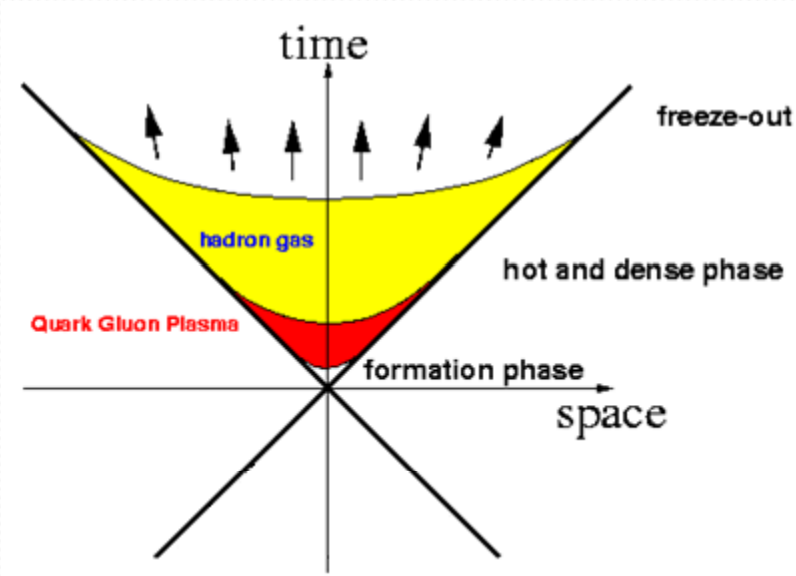


**Thermal** dilepton sources: HG+QGP

a) QGP: q+q-bar-> $\gamma^*$ -> $e^+e^-$

b) HG: In-medium vector mesons V=($\rho$, $\omega$, $\phi$)

V-> $\gamma^*$ -> $e^+e^-$

**Kinetic freeze-out:**

c) Cocktail Dalitz Decays ($\pi^0$, $\eta$, $\eta'$, etc.)

**Other** dilepton sources: Formation phase

d) Charmed hadrons: e.g. $D^{+/-}$-> $K^o$ + $e^{+/-}$ $\nu_e$

e) Beauty hadrons: e.g. $B^{+/-}$->$D^0$ + $e^{+/-}\nu_e$

f) Other vector mesons: Charmonium, Bottomonium

g) Drell-Yan Processes

} Sub-dominant the intermediate mass region

# Dilepton rates from the QGP

- An important source of dileptons in the QGP

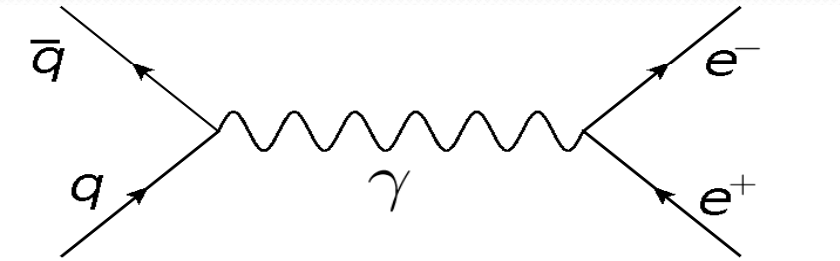


- The rate in kinetic theory (Born Approx)

$$\frac{d^4R}{d^4q} = \int \frac{d^3k_1}{(2\pi)^3}\frac{d^3k_2}{(2\pi)^3} n(E_1)n(E_2)v_{12}\sigma\delta^4(q-k_1-k_2)$$

$$v_{12} = \frac{M^2}{2E_1 2E_2} \qquad \sigma = \frac{16\,\pi^2\alpha^2 N_c \sum_q e_q^2}{3M^2}$$

$$\frac{d^4R}{d^4q} = \left(\frac{\alpha^2 N_c}{12\pi^4}\sum_q e_q^2\right)\frac{1}{\exp\left(\frac{q^0}{T}\right)-1}\left\{1-\frac{2T}{q}\ln\left[\frac{1+\exp\left(-\frac{q^0-q}{2T}\right)}{1+\exp\left(-\frac{q^0+q}{2T}\right)}\right]\right\}$$

- More complete approaches: HTL, Lattice QCD.

# Thermal Dilepton Rates from HG

- The dilepton production rate is :

$$\frac{d^4R}{d^4q} = \frac{\alpha^2}{\pi^3}\frac{L(M)}{M^2}\frac{m_V^4}{g_V^2}\left\{-\frac{1}{3}[Im\ D_V^R]_\mu^\mu\right\} n_{BE}(q^0)\ ;\ L(M) = \left(1+\frac{2m_l^2}{M^2}\right)\sqrt{1-\frac{4m_l^2}{M^2}}$$

- Where,

$$-Im\ \mathrm{D}_\mathrm{V}^\mathrm{R} = \frac{-Im\ \Pi}{(M^2 - m_V^2 - Re\ \Pi)^2 + (Im\ \Pi)^2}$$

- Model based on forward scattering amplitude [Eletsky, et al., Phys. Rev. C, 64, 035202 (2001)]

$$\Pi_V^{Total} = \Pi_V^{Vac}(M) + \sum_a \Pi_{Va}(q,T)$$

$\Pi_\mathrm{V}^\mathrm{Vac}(\mathrm{M})$ is described by effective Lagrangians

$$\Pi_{Va}(q,T) = -\int_{m_a}^{\infty} dk^0 \ln\left[\frac{1 \pm exp\left(-\frac{\omega_-}{T}\right)}{1 \pm exp\left(-\frac{\omega_+}{T}\right)}\right] f_{Va}\left(\frac{m_V}{m_a}k^0\right)$$

$$\omega_\pm = \frac{(q^0k^0 \pm qk)}{m_V}$$

# Vector meson self-energies (1)

- Vacuum part is described by the following Lagrangians
- For ρ:

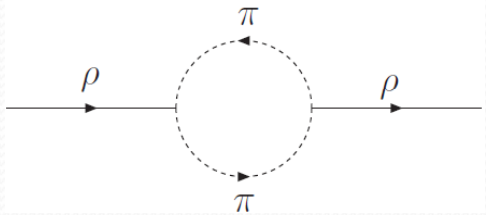


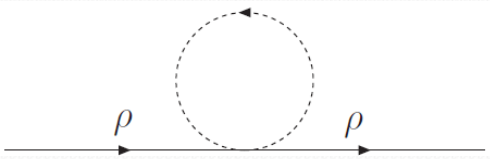


$$\mathcal{L}_{\rho\to\pi\pi} = \frac{1}{2}|D_\mu\pi|^2 - \frac{1}{2}m_\pi^2|\pi|^2 - \frac{1}{4}F^\rho_{\mu\nu}F^{\mu\nu}_\rho + \frac{1}{2}m_\rho^2\rho^\mu\rho_\mu$$

# Vector meson self-energies (2)

- Vacuum part is described by the following Lagrangians
- For ρ:

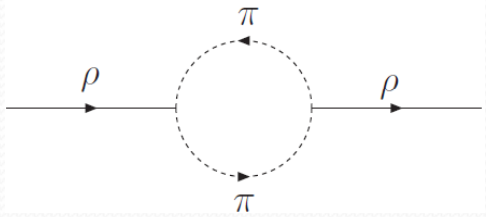


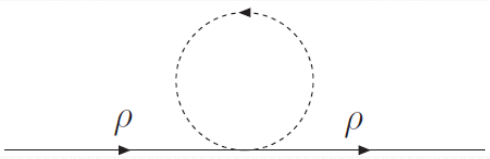


$$\mathcal{L}_{\rho\to\pi\pi} = \tfrac{1}{2}|D_\mu\pi|^2 - \tfrac{1}{2}m_\pi^2|\pi|^2 - \tfrac{1}{4}F^\rho_{\mu\nu}F^{\mu\nu}_\rho + \tfrac{1}{2}m_\rho^2\rho^\mu\rho_\mu$$

- Since ω has a small width and 3 body state in the self-energy, we model it as

$$\Pi = 0 + i\begin{bmatrix} M\Gamma_\omega\left(\dfrac{M^2 - 9m_\pi^2}{m_\omega^2 - 9m_\pi^2}\right)^2 & M \le m_\omega \\ M\Gamma_\omega & M > m_\omega \end{bmatrix}$$

# Vector meson self-energies (3)

- Vacuum part is described by the following Lagrangians
- For ϕ:

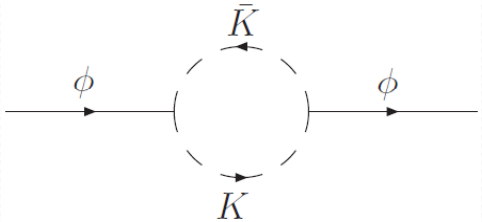


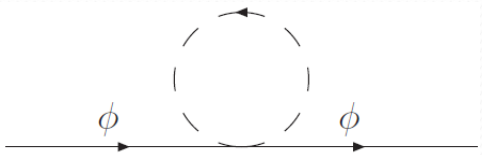


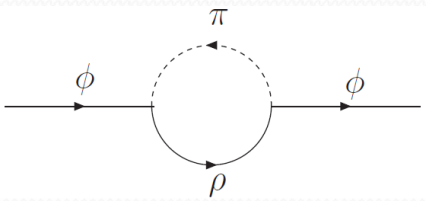


$$\mathcal{L}_{\phi\to K\bar{K}} = \tfrac{1}{2}|D_\mu K|^2 - \tfrac{1}{2}m_K^2|K|^2 - \tfrac{1}{4}F^\phi_{\mu\nu}F^{\mu\nu}_\phi + \tfrac{1}{2}m_\phi^2\phi^\mu\phi_\mu$$

$$\mathcal{L}_{(\omega,\phi)\rho\pi} = g\epsilon^{\alpha\beta\mu\nu}\partial_\alpha\rho_\beta\cdot\pi\left(\frac{\partial_\mu\omega^8_\nu + \sqrt{2}\partial_\mu\omega^s_\nu}{\sqrt{3}}\right)$$

$$\omega^8 = \phi\cos(\theta_V) + \omega\sin(\theta_V),$$
$$\omega^s = -\phi\sin(\theta_V) + \omega\cos(\theta_V)$$

- Since ω has a small width and 3 body state in the self-energy, we model it as

$$\Pi = 0 + i\begin{bmatrix} M\Gamma_\omega\left(\dfrac{M^2 - 9m_\pi^2}{m_\omega^2 - 9m_\pi^2}\right)^2 & M \le m_\omega \\ M\Gamma_\omega & M > m_\omega \end{bmatrix}$$

# Vector meson self-energies

- The Forward Scattering Amplitude
  - Low energies:

$$f_{Va}^{c.m.}(s) = \frac{1}{2q_{c.m.}} \sum_R \frac{W_{Va}^R \Gamma_{R\to Va}}{M_R - \sqrt{s} - \frac{1}{2} i\Gamma_R} - \frac{q_{c.m.}}{4\pi s} \frac{(1+\exp(-i\pi\alpha))}{\sin(\pi\alpha)} r_P^{Va} s^{\alpha_P}$$

$$W_{Va}^R = \frac{2s_R+1}{(2s_V+1)(2s_a+1)} \frac{2t_R+1}{(2t_V+1)(2t_a+1)}$$

$$q_{c.m.} = \frac{1}{2} \frac{\sqrt{([s-(m_V+m_a)^2][s-(m_V-m_a)^2])}}{\sqrt{s}}$$

Resonances [R] contributing to ρ's scatt. amp. & similarly for ω, ϕ

| | |
|---|---|
| $N(1700)$ | $\Delta(1905)$ |
| $N(1720)$ | $\Delta(1940)$ |
| $N(1900)$ | $\Delta(2000)$ |
| $N(2000)$ | $\phi(1020)$ |
| $N(2080)$ | $h_1(1170)$ |
| $N(2090)$ | $a_1(1260)$ |
| $N(2100)$ | $\pi(1300)$ |
| $N(2190)$ | $a_2(1320)$ |
| $\Delta(1700)$ | $\omega(1420)$ |
| $\Delta(1900)$ | |

  - High energies:

$$f_{Va}^{c.m.} = -\frac{q_{c.m.}}{4\pi s} \sum_i \frac{1+\exp(-i\pi\alpha_i)}{\sin(\pi\alpha_i)} r_{i,Va} s^{\alpha_i}$$

- Effective Lagrangian method by R. Rapp [Phys. Rev. C 63, 054907 (2001)]

# Imaginary part of the retarded propagator

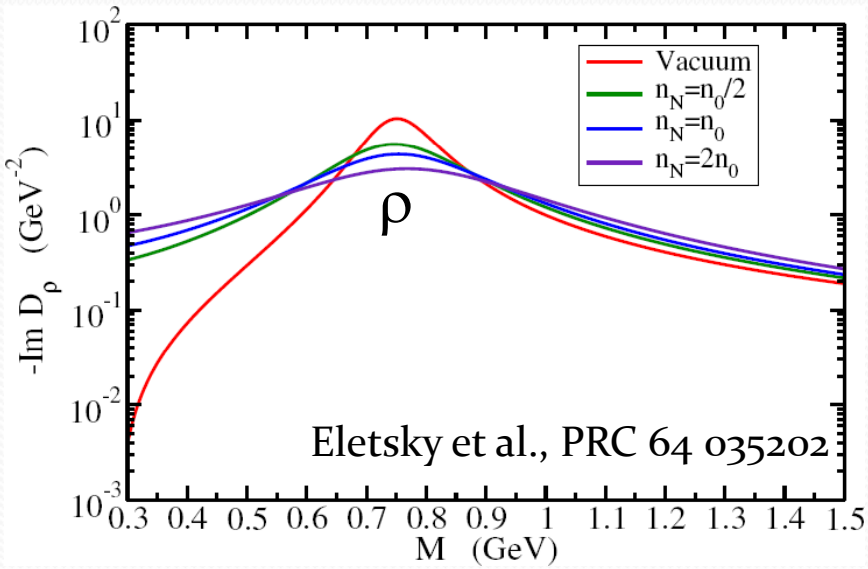


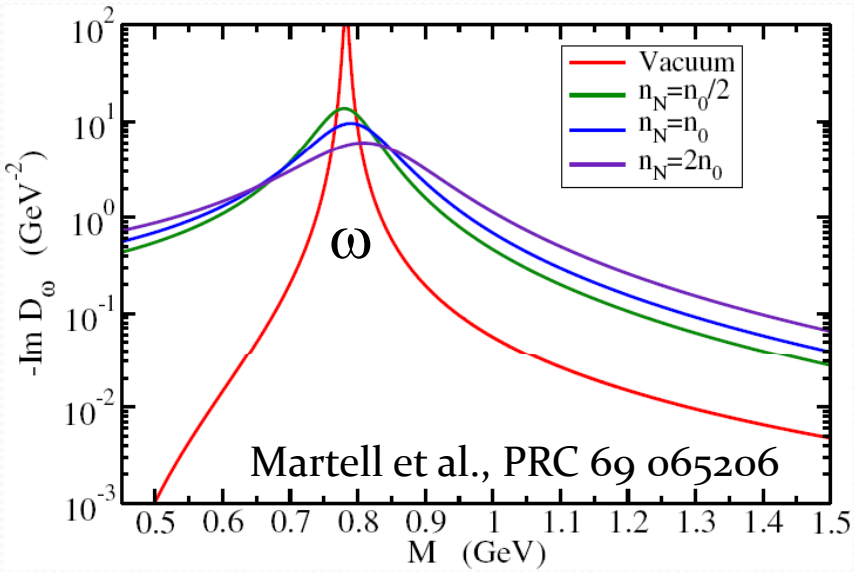


T=150MeV
$n_0=0.17/\mathrm{fm}^3$

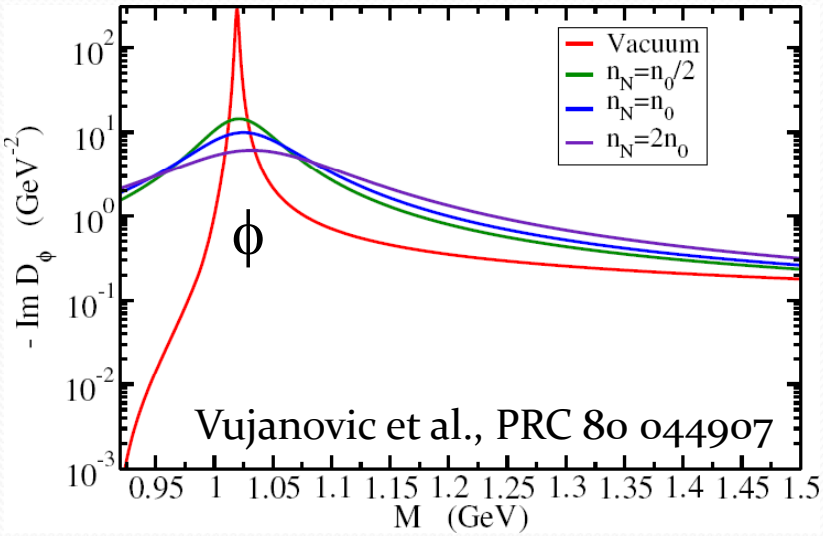

# 3+1D Hydrodynamics

- Viscous hydrodynamics equations for heavy ions:

$$\partial_\mu T^{\mu\nu} = 0$$ ← Energy-momentum conservation

$$T^{\mu\nu} = T_0^{\mu\nu} + \pi^{\mu\nu} \qquad T_0^{\mu\nu} = (\varepsilon + \mathcal{P})u^\mu u^\nu - \mathcal{P} g^{\mu\nu} \qquad \mathcal{P} = \mathcal{P}(\varepsilon)$$

$$\Delta^\mu_\alpha \Delta^\nu_\beta u^\sigma \partial_\sigma \pi^{\alpha\beta} = -\frac{1}{\tau_\pi}(\pi^{\mu\nu} - S^{\mu\nu}) - \frac{4}{3}\pi^{\mu\nu}(\partial_\alpha u^\alpha)$$

$\eta/s=1/4\pi$

$$S^{\mu\nu} = \eta\left(\nabla^\mu u^\nu + \nabla^\nu u^\mu - \tfrac{2}{3}\Delta^{\mu\nu}\nabla_\alpha u^\alpha\right) \qquad t = \tau \cosh \eta_s, \quad z = \tau \sinh \eta_s$$

- Initial conditions are set by the Glauber model.
- Solving the hydro equations numerically done via the Kurganov-Tadmor method using a Lattice QCD EoS [P. Huovinen and P. Petreczky, Nucl. Phys. A 837, 26 (2010).] (s95p-v1)
- The hydro evolution is run until the kinetic freeze-out. [For details: B. Schenke, et al., Phys. Rev. C 85, 024901 (2012)] ($T_f$=136 MeV)

# Viscous Corrections: QGP rates

- Viscous correction to the rate in kinetic theory rate

$$\frac{d^4R}{d^4q} = \int \frac{d^3k_1}{(2\pi)^3}\frac{d^3k_2}{(2\pi)^3} n(E_1)n(E_2)v_{12}\sigma\delta^4(q-k_1-k_2)$$

- Using the quadratic ansatz to modify F.-D. distribution

$$n_{FD}(k^0) \to n_{FD}(k^0) + \frac{\eta}{s}\frac{C_q}{2}\, n_{FD}(k^0)[1-n_{FD}(k^0)]\frac{k^\mu}{T}\frac{k^\nu}{T}\frac{\pi_{\mu\nu}}{\eta T}$$

$$\frac{d^4R}{d^4q} = \frac{d^4R_{ideal}}{d^4q} + \frac{d^4\delta R}{d^4q}\ ; \qquad \frac{d^4\delta R}{d^4q} = \frac{\eta}{s}\frac{C_q}{2}\, b_2(q^0,|\vec{q}|)\frac{q^\mu}{T}\frac{q^\nu}{T}\frac{\pi_{\mu\nu}}{\eta T}$$

$$b_2(q^0,|\vec{q}|) = \frac{1}{|\vec{q}|^5}\int_{E_-}^{E_+} n(E_1)n(q^0-E_1)\big(1-n(E_1)\big)\times\left[(3q_0^2-|\vec{q}|^2)E_1^2 - 3q^0E_1M^2 + \frac{3}{4}M^4\right]dE_1$$

- Dusling & Lin, Nucl. Phys. A 809, 246 (2008).

# Viscous corrections to HG rates?

- Two modifications are plausible: $\frac{d^4R}{d^4q} = \frac{\alpha^2}{\pi^3}\frac{L(M)}{M^2}\frac{m_V^4}{g_V^2}\left\{-\frac{1}{3}[Im\, D_V^R]^{\mu}_{\mu}\right\} n_{BE}(q^0)$

  1 2

- Self-Energy

$$\Pi_{Va}(p,T) = -\frac{m_a m_V T}{\pi p}\int \frac{d^3k}{(2\pi)^3}\frac{\sqrt{s}}{k^0} f_{Va}(s) n_a(k^0); \qquad \Pi_{Va}^{Total} = \Pi_{Va}^{Ideal} + \delta\Pi_{Va}$$

$$n_a(k^0) \to n_a(k^0) + \frac{\eta}{s}\frac{C_a}{2}\, n_a(k^0)[1 \pm n_a(k^0)]\frac{k^\mu}{T}\frac{k^\nu}{T}\frac{\pi_{\mu\nu}}{\eta T}; \quad \delta\Pi_{Va} = \frac{\eta}{s}\frac{C_a}{2}\, B_2(q^0,q)\frac{q^\mu}{T}\frac{q^\nu}{T}\frac{\pi_{\mu\nu}}{\eta T}$$

$$B_2(q^0,q) = -\frac{m_a}{2\pi q^2}\int_{m_a}^{\infty} dk^0 f_{Va}\left(\frac{m_V}{m_a}k^0\right)\left\{\begin{array}{c} -\frac{m_V T}{qk}\left[m_a^2 + \frac{3(q^0k+qk^0)^2-(q^0k^0+pk)^2}{m_V^2}\right]\frac{1}{\exp\left(\frac{\omega_+}{T}\right)\pm 1} \\ +\frac{m_V T}{qk}\left[m_a^2 + \frac{3(q^0k-qk^0)^2-(q^0k^0-pk)^2}{m_V^2}\right]\frac{1}{\exp\left(\frac{\omega_-}{T}\right)\pm 1} \\ \mp 2\left(\frac{m_V T}{qk}\right)^2\left[(3(q^0)^2-q^2)\frac{k^2}{m_V^2}+\frac{2q^0k^0qk}{m_V^2}\right]\ln\left(1\pm\exp\left(\frac{\omega_+}{T}\right)\right) \\ \mp 2\left(\frac{m_V T}{qk}\right)^2\left[(3(q^0)^2-q^2)\frac{k^2}{m_V^2}-\frac{2q^0k^0qk}{m_V^2}\right]\ln\left(1\pm\exp\left(\frac{\omega_-}{T}\right)\right) \\ \pm 2\left(\frac{m_V T}{qk}\right)^3\left[(3(q^0)^2-q^2)\frac{k^2}{m_V^2}\right]\left[Li_2\left(\mp\exp\left(\frac{\omega_+}{T}\right)\right)-Li_2\left(\mp\exp\left(\frac{\omega_-}{T}\right)\right)\right] \end{array}\right\}$$

- Performing the calculation => these corrections had no effect on the final yield result!

# Low Mass Dilepton Yields: HG+QGP

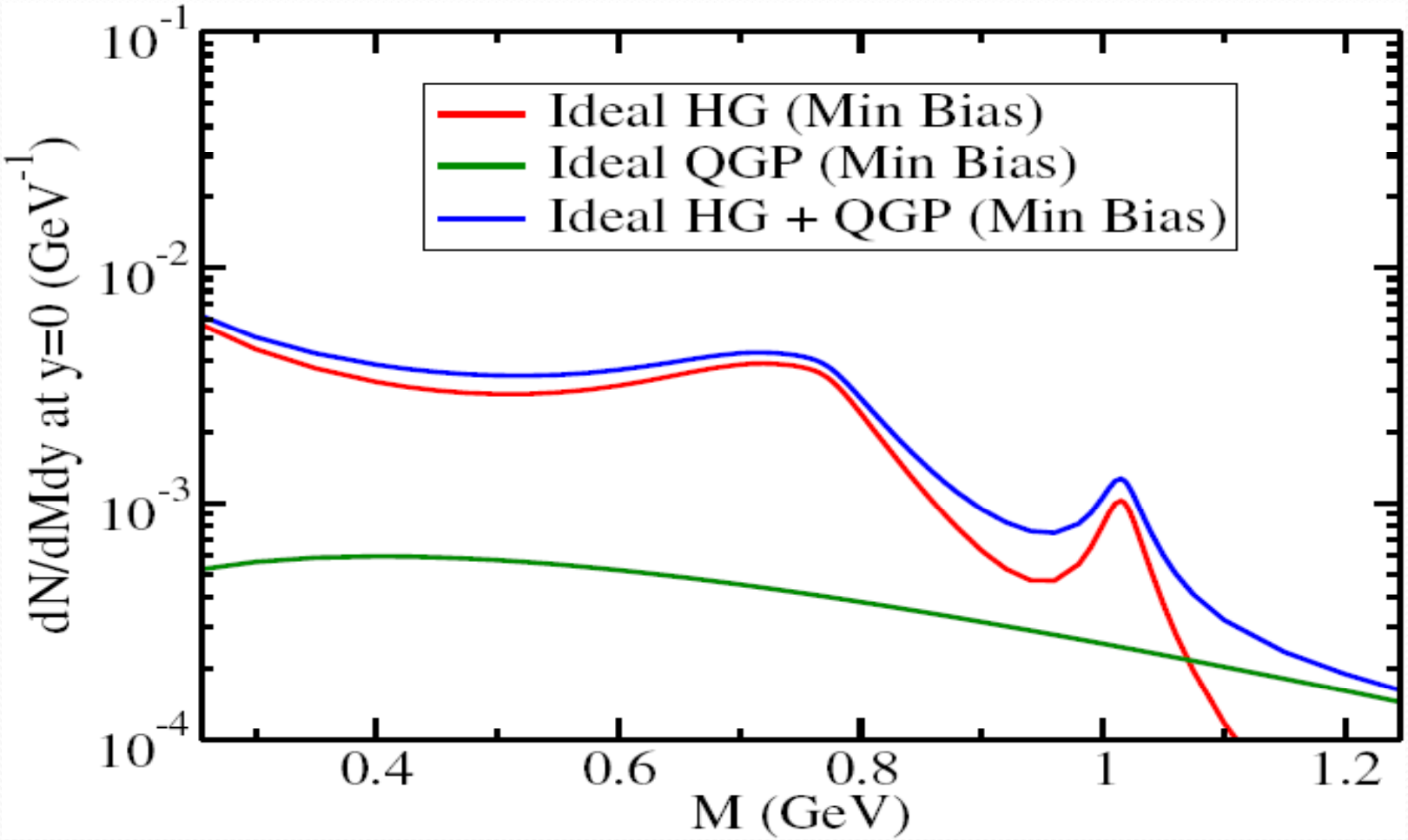


- For low M: ideal and viscous yields are almost identical and dominated by HG.
- These hadronic rates are consistent with NA60 data [Ruppert et al., Phys. Rev. Lett. 100, 162301 (2008)].

# How important are viscous corrections to HG rate?

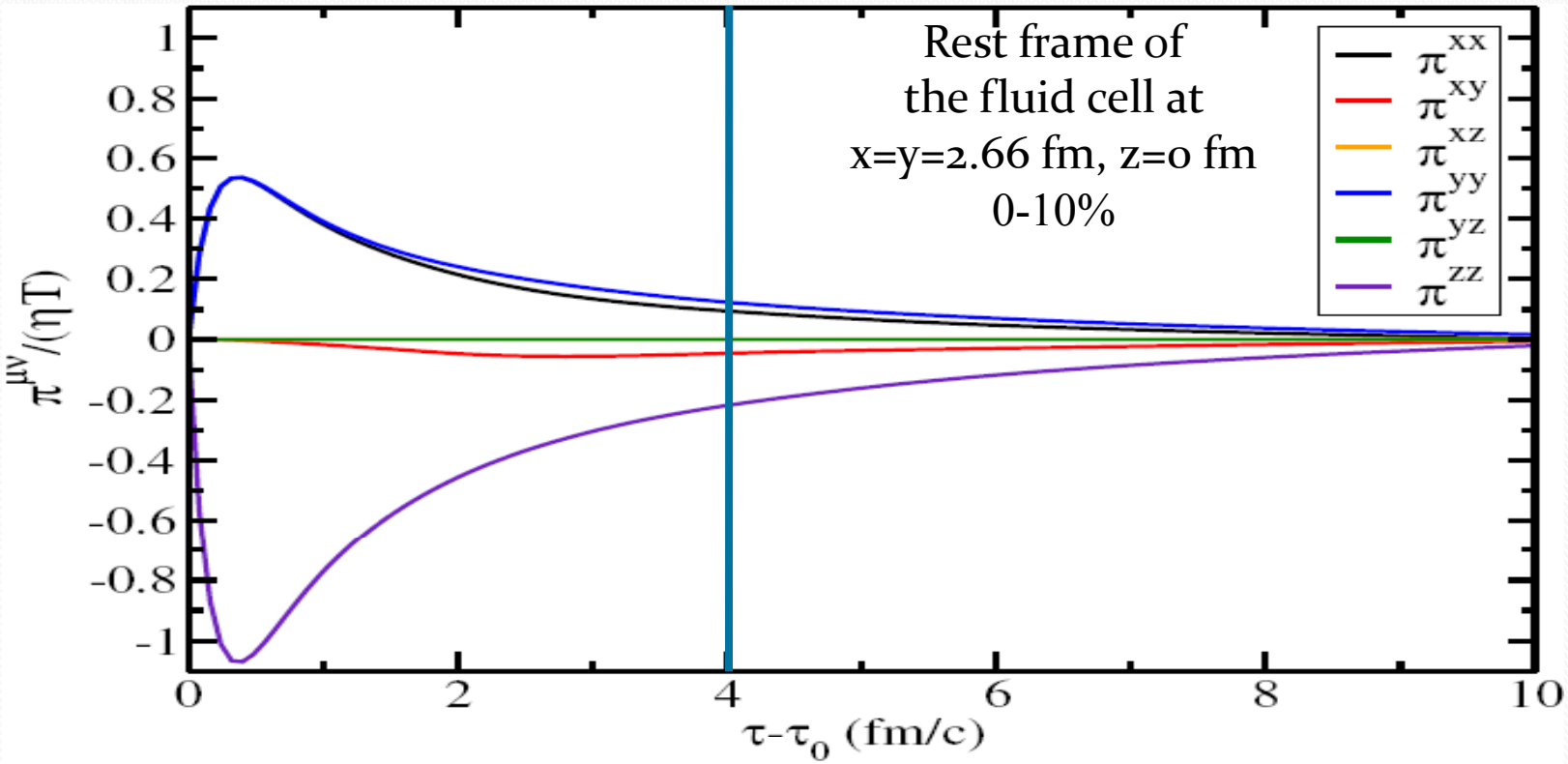


- Fluid rest frame, viscous corrections to HG rates: $\propto \frac{p_i}{T}\frac{p_j}{T}\frac{\pi^{ij}}{\eta T}$
- HG gas exists from $\tau$~4 fm/c => $\frac{\pi^{ij}}{\eta T}$ is small, so very small viscous corrections to the yields are expected.
- Direct computation shows this!

# Dilepton yields Ideal vs Viscous Hydro

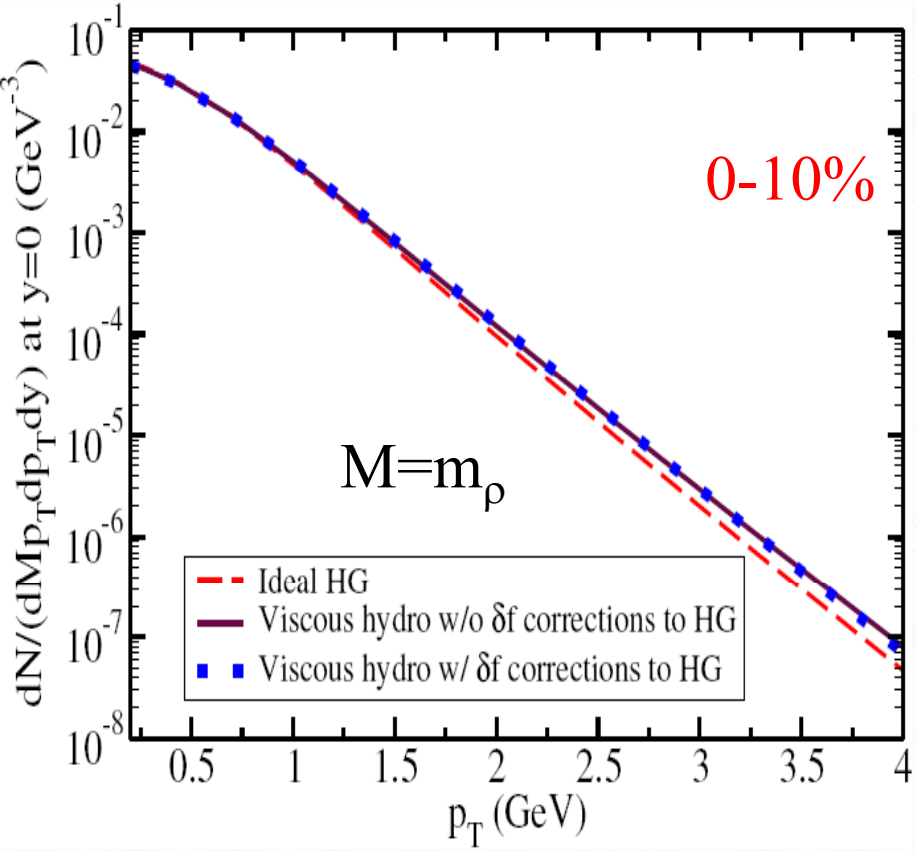


The presence of δf in the rates is not important per centrality class! This is not a Min Bias effect.

- Since viscous corrections to HG rates don't matter, only viscous flow is responsible for the modification of the $p_T$ distribution.
- Also observed viscous photons HG [M. Dion et al., Phys. Rev. C 84, 064901 (2011)]

# Dilepton yields Ideal vs Viscous Hydro

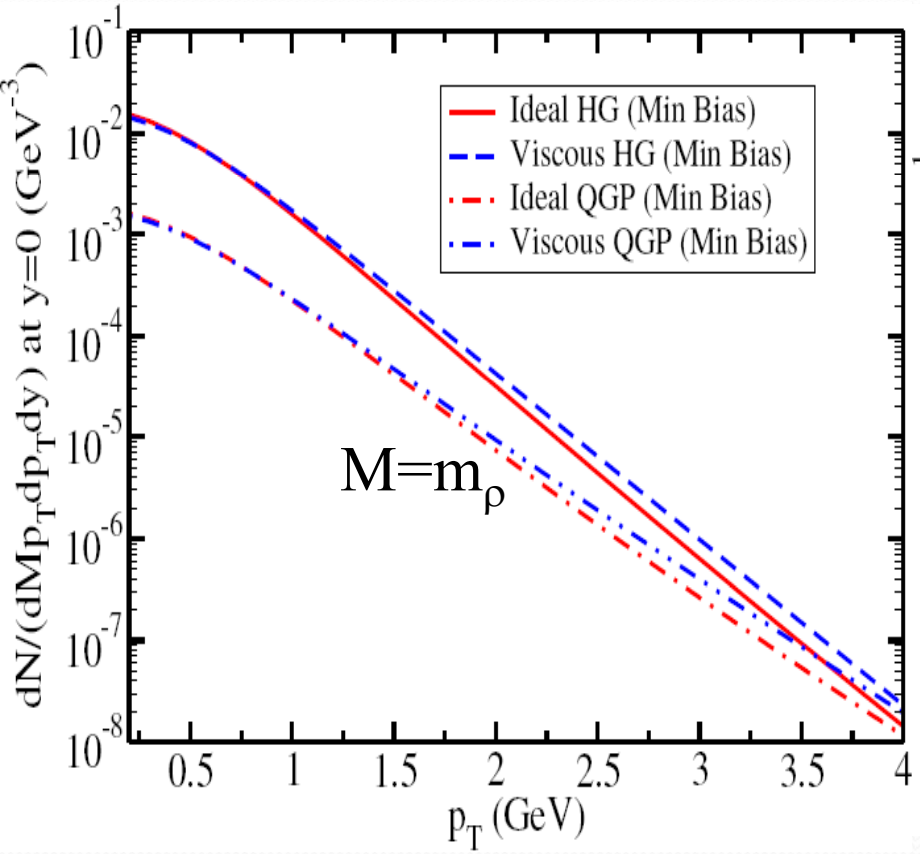


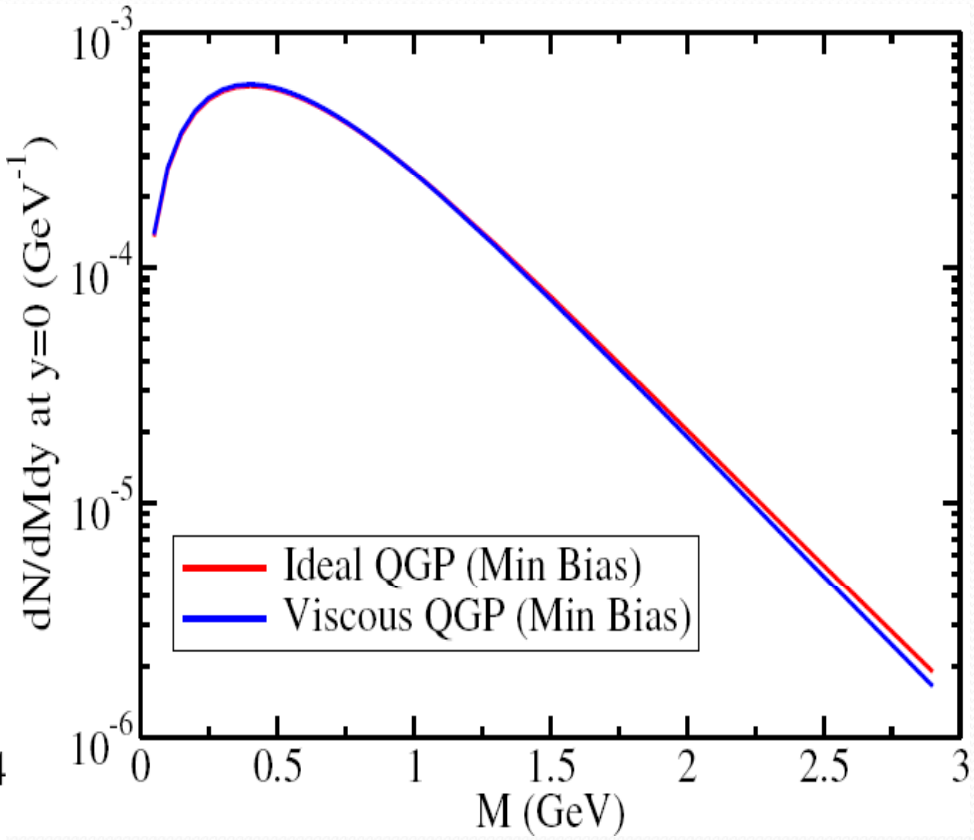


- For QGP yields, both corrections matter since the shear-stress tensor is larger.
- Integrating over $p_T$, notice that most of the yield comes from the low $p_T$ region.
- Hence, at low M there isn't a significant difference between ideal and viscous yields. One must go to high invariant masses.

# Dilepton yields Ideal vs Viscous Hydro

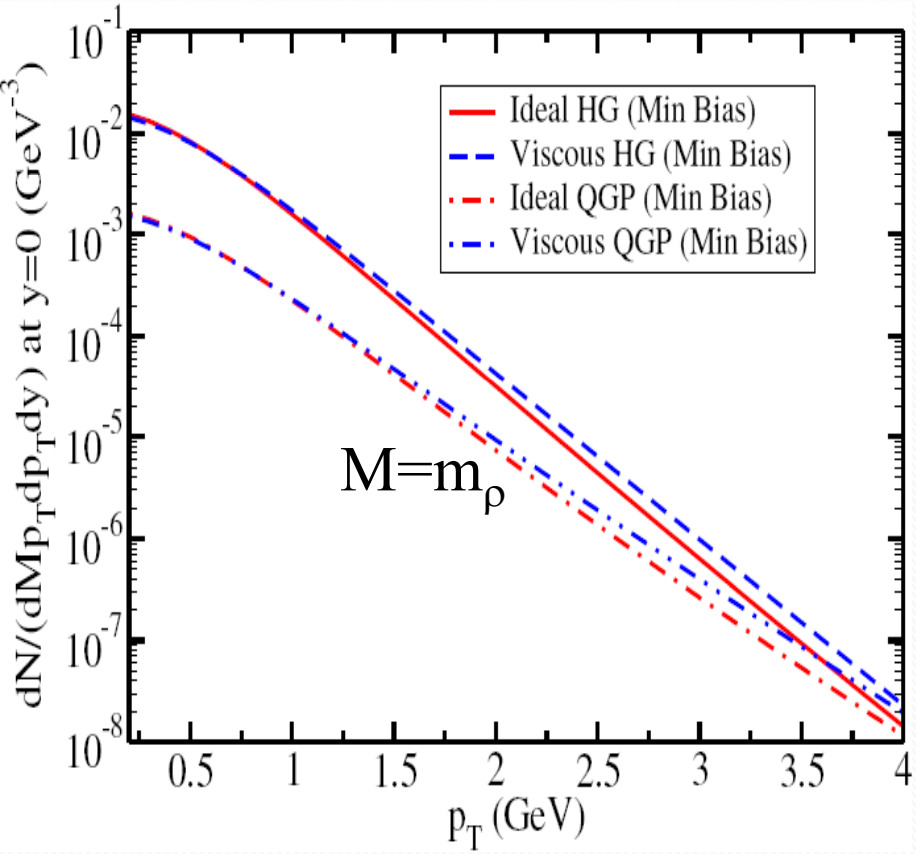


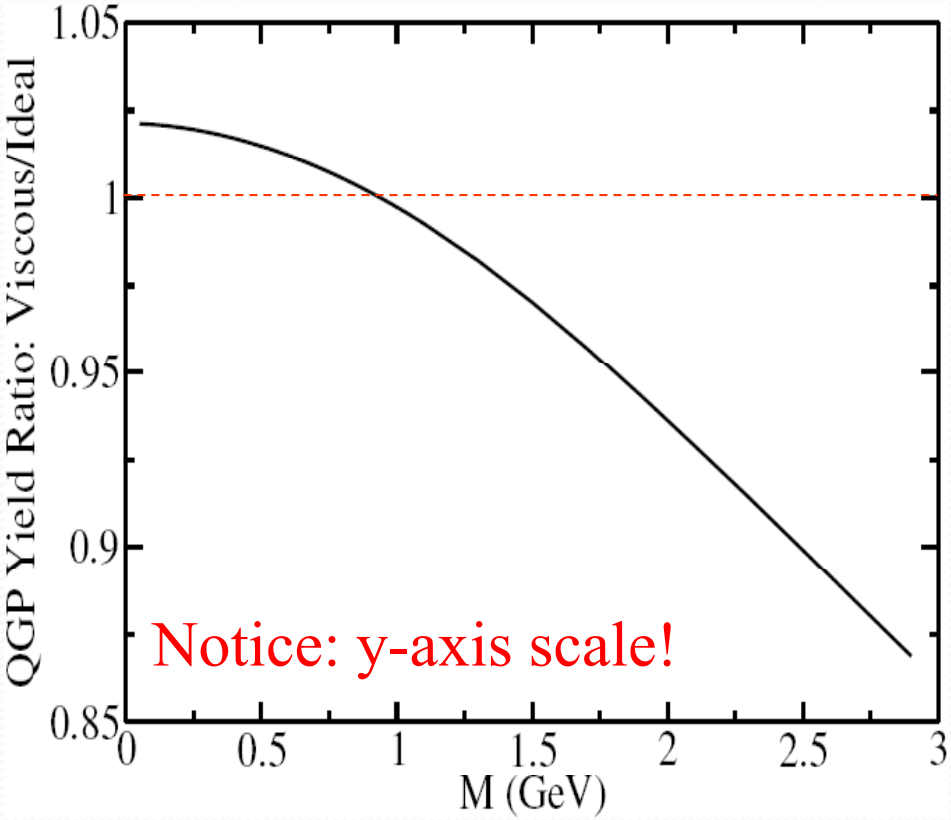


- For QGP yields, both corrections matter since the shear-stress tensor is large.
- Integrating over $p_T$, notice that most of the yield comes from the low $p_T$ region.
- Hence, at low M there isn't a significant difference between ideal and viscous yields. One must go to high invariant masses.

# A measure of elliptic flow ($v_2$)

- Elliptic Flow

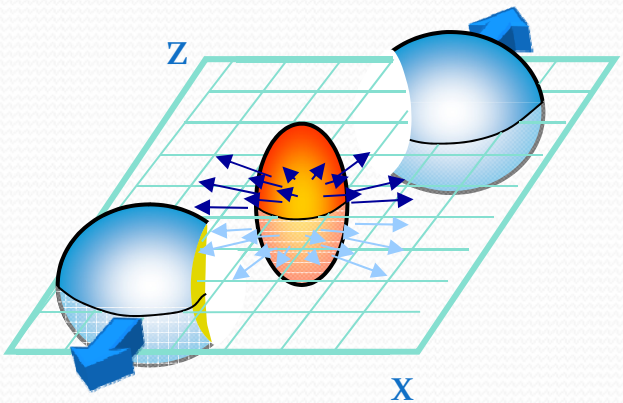


- A nucleus-nucleus collision is typically not head on; an almond-shape region of matter is created.
- This shape and its pressure profile gives rise to elliptic flow.

- To describe the evolution of the shape use a Fourier decomposition, i.e. flow coefficients $v_n$

$$\frac{dN}{dMp_T dp_T d\phi dy} = \frac{1}{2\pi}\frac{dN}{dMp_T dp_T dy}\left[1 + \sum_{n=1}^{\infty} 2v_n \cos\left(n\phi - n\psi_n\right)\right]$$

- Important note: when computing $v_n$'s from several sources, one must perform a yield weighted average.

# $v_2$ from ideal and viscous HG+QGP (1)

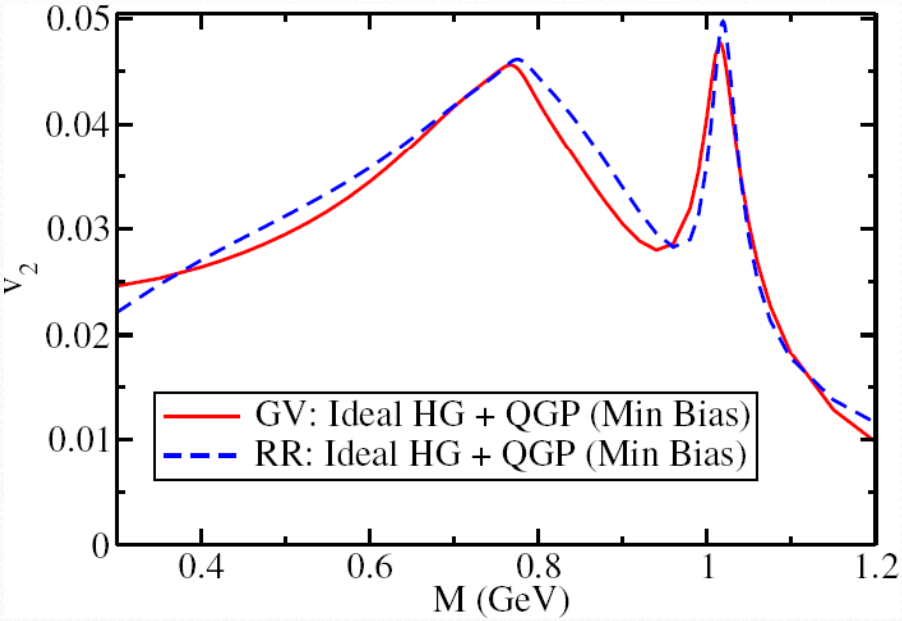


- Similar elliptic flow when comparing w/ R. Rapp's rates.

# $v_2$ from ideal and viscous HG+QGP (1)

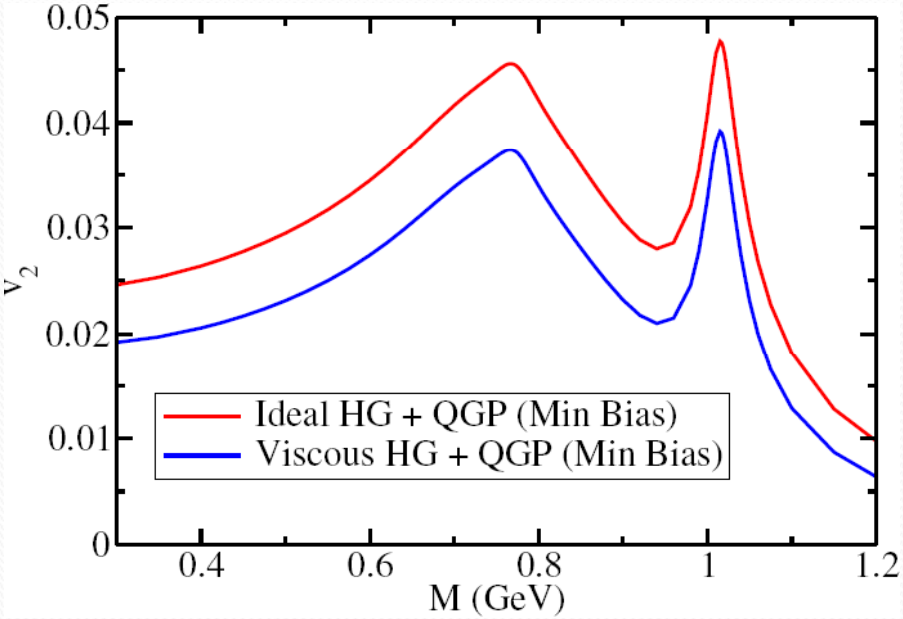


- Similar elliptic flow when comparing w/ R. Rapp's rates.
- Viscosity lowers elliptic flow.

# $v_2$ from ideal and viscous HG+QGP (1)

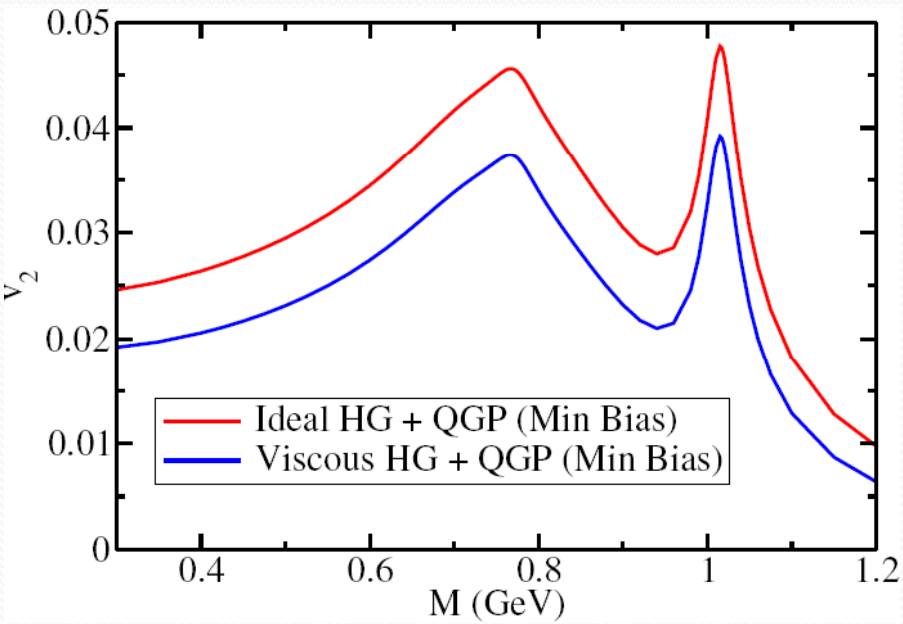


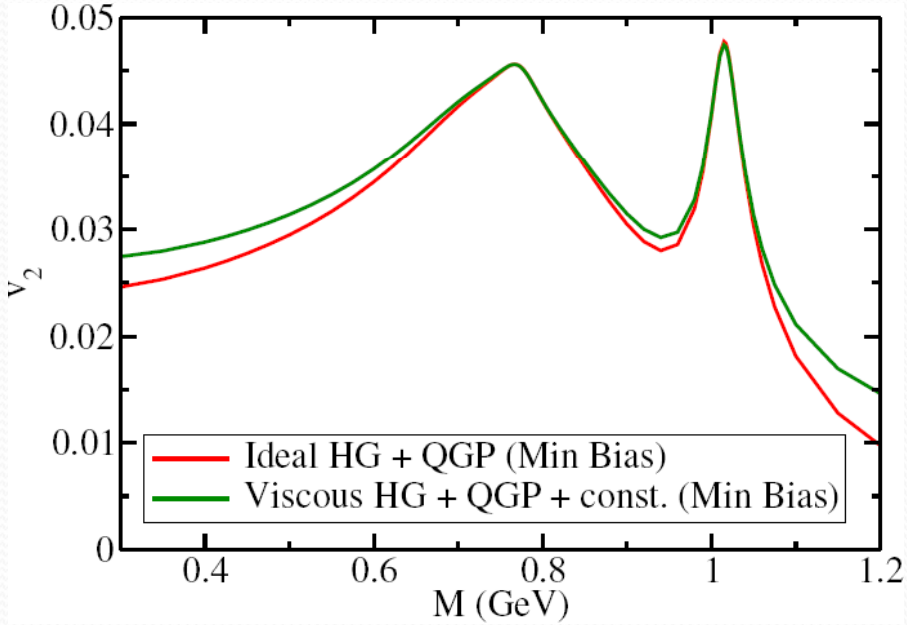


- Similar elliptic flow when comparing w/ R. Rapp's rates.
- Viscosity lowers elliptic flow.
- Viscosity slightly broadens the $v_2$ spectrum with M.

# $v_2(p_T)$ from ideal and viscous HG+QGP (2)

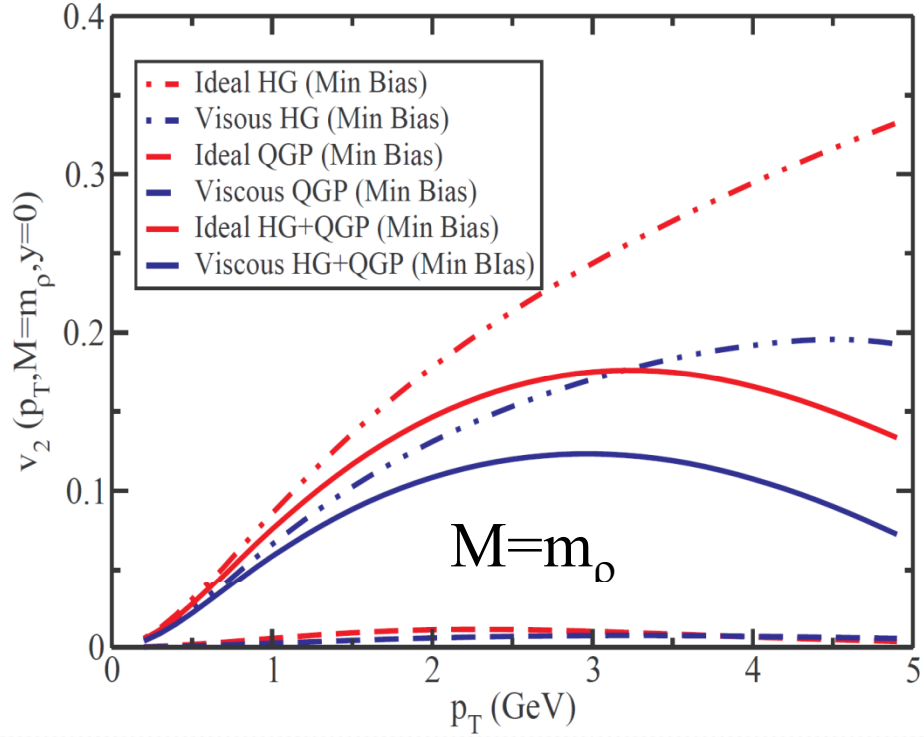


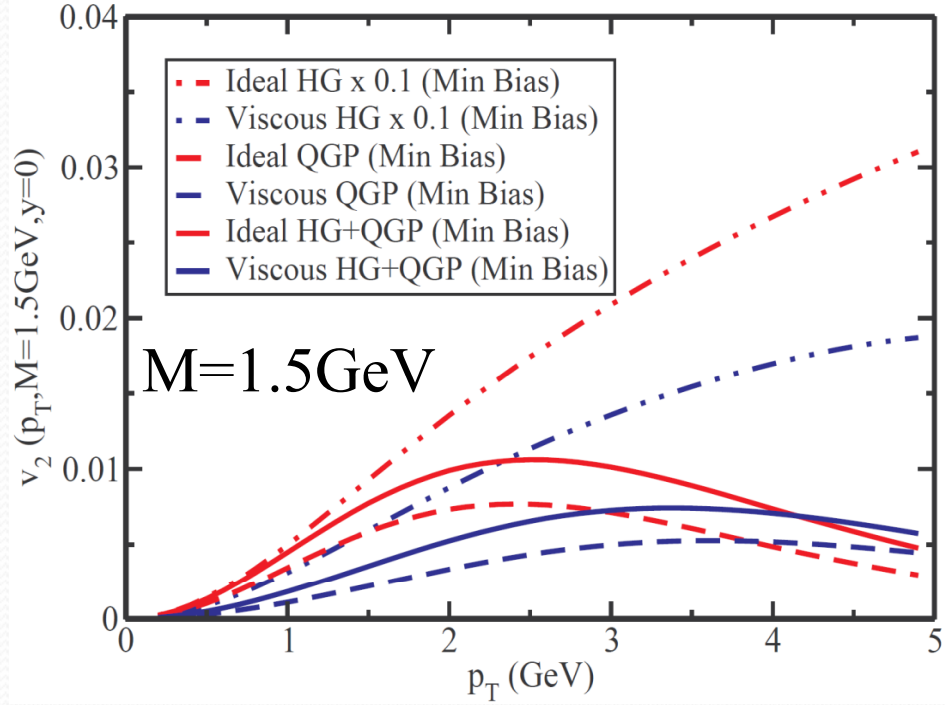


- M is extremely useful to isolate HG from QGP. At low M HG dominates and vice-versa for high M.
- R. Chatterjee et al. Phys. Rev. C 75 054909 (2007).
- We can clearly see two effects of viscosity in the $v_2(p_T)$.
  - Viscosity stops the growth of $v_2$ at large $p_T$ for the HG (dot-dashed curves)
  - Viscosity shifts the peak of $v_2$ from to higher momenta (right, solid curves). Comes from the viscous corrections to the rate: ~ $p^2$ (or $p_T^2$)

# Charmed Hadron contribution

- Since $M_q >> T$ (or $\Lambda_{QCD}$), heavy quarks must be produced perturbatively; come from early times after the nucleus-nucleus collision.

- For heavy quarks, many scatterings are needed for momentum to change appreciably.

- In this limit, Langevin dynamics applies [Moore & Teaney, Phys. Rev. C 71, 064904 (2005)]

$$\frac{dp^i}{dt} = -\eta_D p^i + \xi^i(t) \quad \langle \xi^i(t)\xi^j(0)\rangle = \kappa\delta^{ij}\delta(t) \quad \eta_D = \frac{\kappa}{2M_q T}$$

- **Charmed Hadron production:**
  - PYTHIA -> Generate a c-cbar event using nuclear parton distribution functions. (EKS98)
  - Embed the PYTHIA c-cbar event in Hydro -> Langevin dynamics to modify its momentum distribution.
  - At the end of hydro-> Hadronize the c-cbar using Peterson fragmentation.
  - PYTHIA decays the charmed hadrons -> Dileptons.

# Charmed Hadrons yield and $v_2$

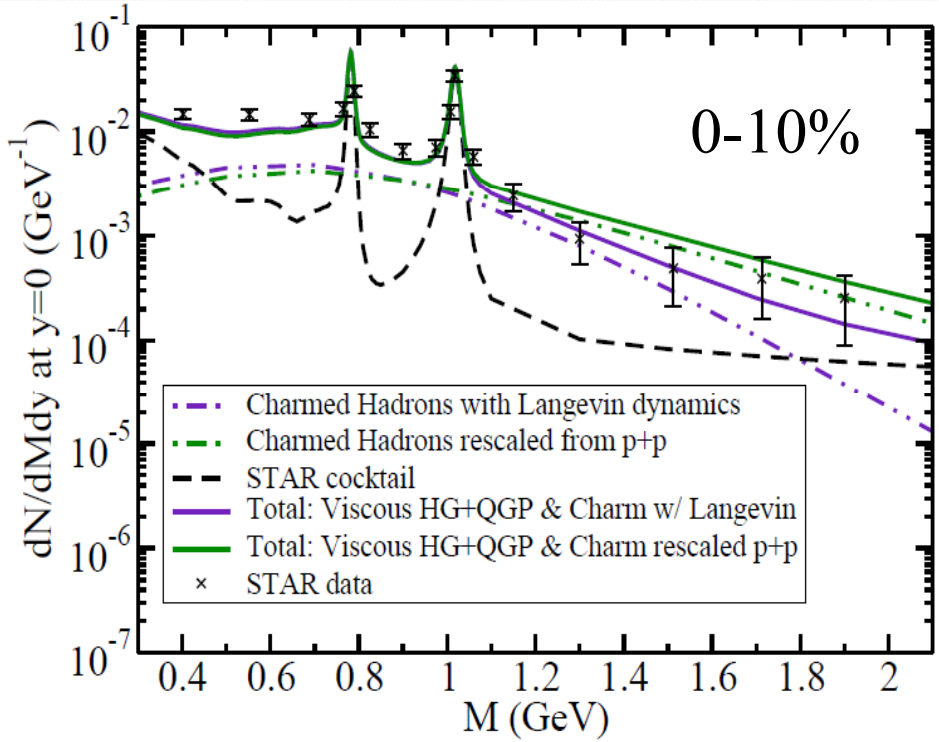


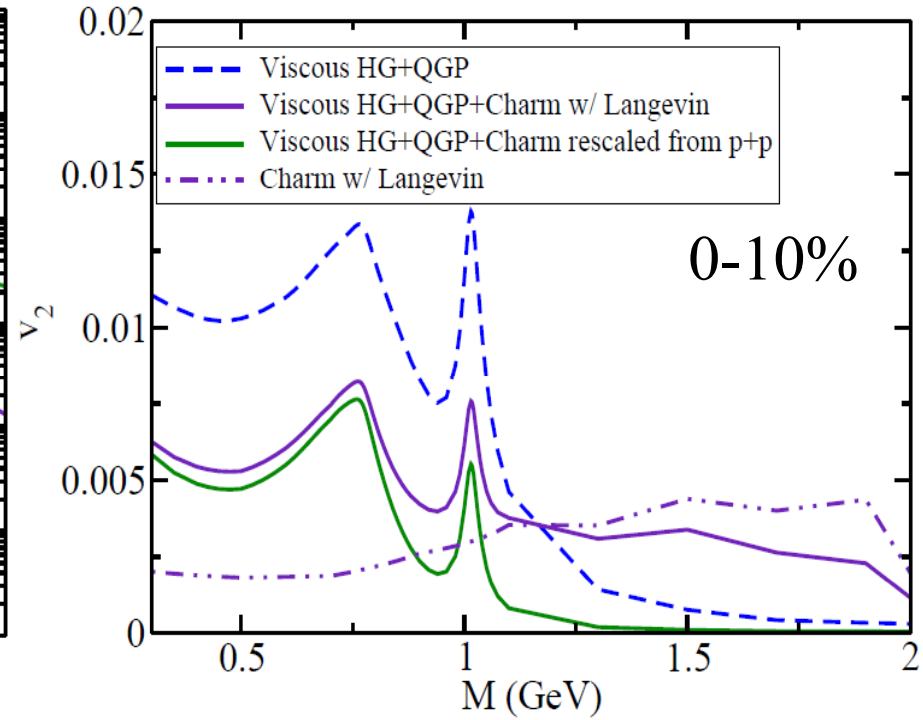


- Heavy-quark energy loss (via Langevin) affects the invariant mass yield of Charmed Hadrons (vs rescaled p+p), by increasing it in the low M region and decreasing it at high M.
- Charmed Hadrons develop a $v_2$ through energy loss (Langevin dynamics) so there is a non-zero $v_2$ in the intermediate mass region.

# Conclusion & Future work

**Conclusions**

- First calculation of dilepton yield and $v_2$ via viscous 3+1D hydrodynamical simulation.
- $v_2(p_T)$ for different invariant masses has good potential of separating QGP and HG contributions.
- Modest modification to dilepton yields owing to viscosity.
- $v_2(M)$ is reduced by viscosity and the shape is slightly broadened.
- Studying yield and $v_2$ of leptons coming from charmed hadrons allows to investigate heavy quark energy loss.

**Future work**

- Include cocktail's yield and $v_2$ with viscous hydro evolution.
- Include the contribution from $4\pi$ scattering.
- Include Fluctuating Initial Conditions (IP-Glasma) and PCE.
- Results for LHC are on the way.

# A specials thanks to:

Charles Gale
Clint Young
Björn Schenke
Sangyong Jeon
Jean-François Paquet
Igor Kozlov
Ralf Rapp

# Born, HTL, and Lattice QCD

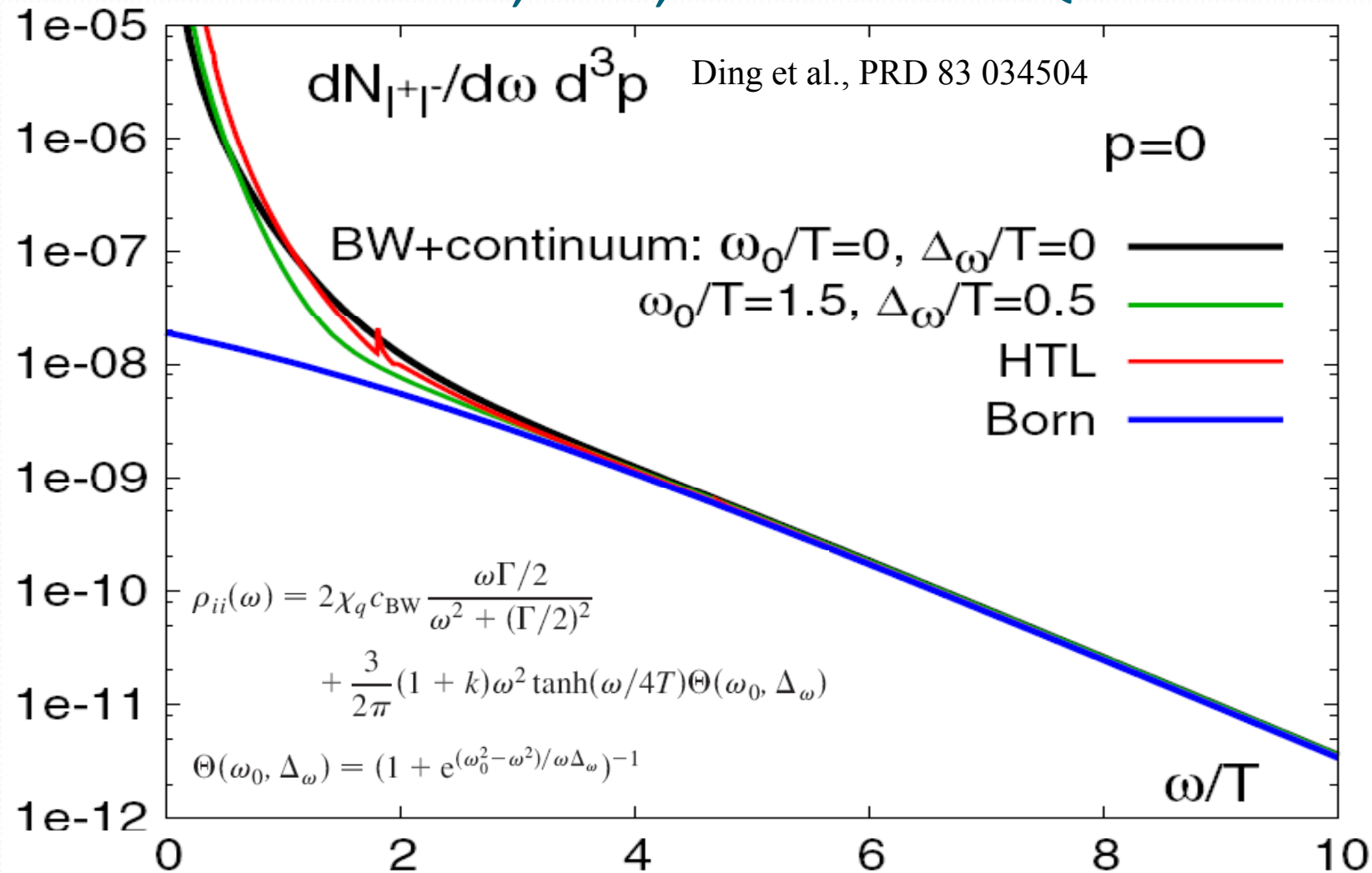

# Forward scattering amplitude results

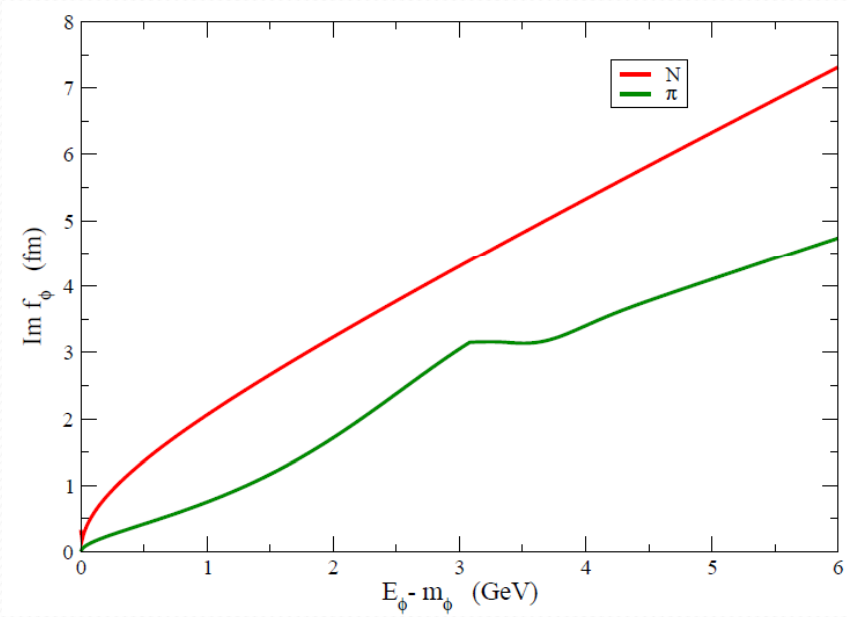


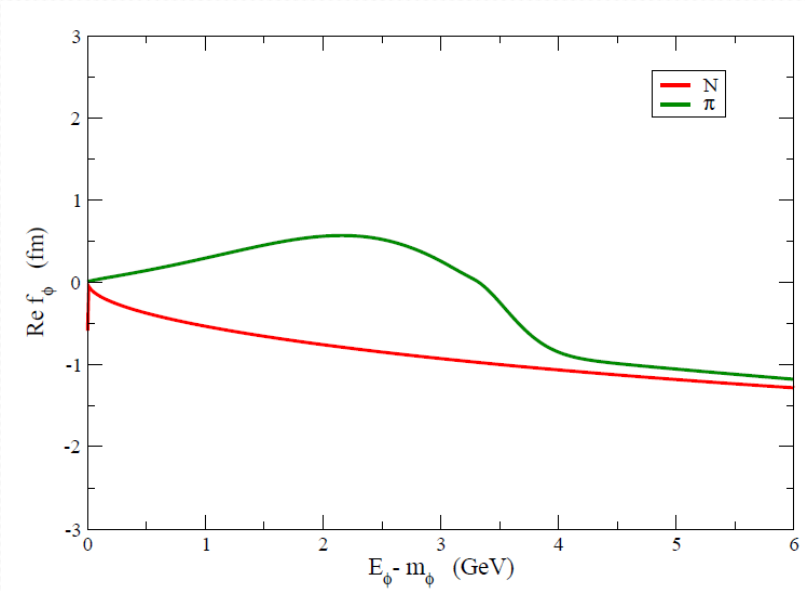


$$f_{\phi a}^{\text{total}}\left(E_\phi\right) = g\left(E_\phi\right) f_{\phi a}^{\text{low}}\left(E_\phi\right) + \left(1 - g\left(E_\phi\right)\right) f_{\phi a}^{\text{high}}\left(E_\phi\right)$$

$$g\left(E_\phi\right) = \begin{cases} \exp\left[\frac{\left(E_\phi - b\right)}{\sigma}\right] & E_\phi \geq b \\ 1 & E_\phi \leq b \end{cases}$$

Vujanovic et al., PRC 80 044907

# Dispersion relation

- The dispersion relation

$$\mathrm{Re}\, f_{Va}(E_V) = \mathrm{Re}\, f_{Va}(0) + \frac{2E_V^2}{\pi} P.V. \int_{m_V}^{\infty} \frac{\mathrm{Im}[f_{Va}(E')]}{E'(E'^2 - E_V^2)} dE'$$

- The $\phi$ dispersion graphs

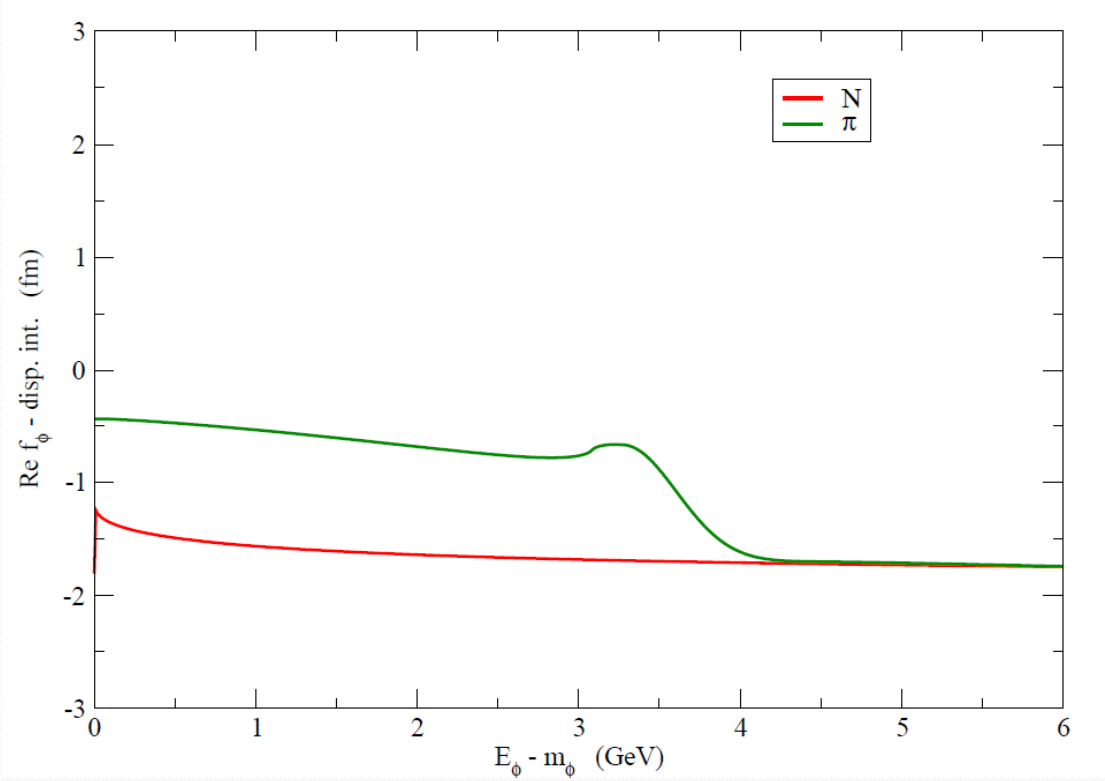


Vujanovic et al., PRC 80 044907

# $V_2$ including charm at Min Bias

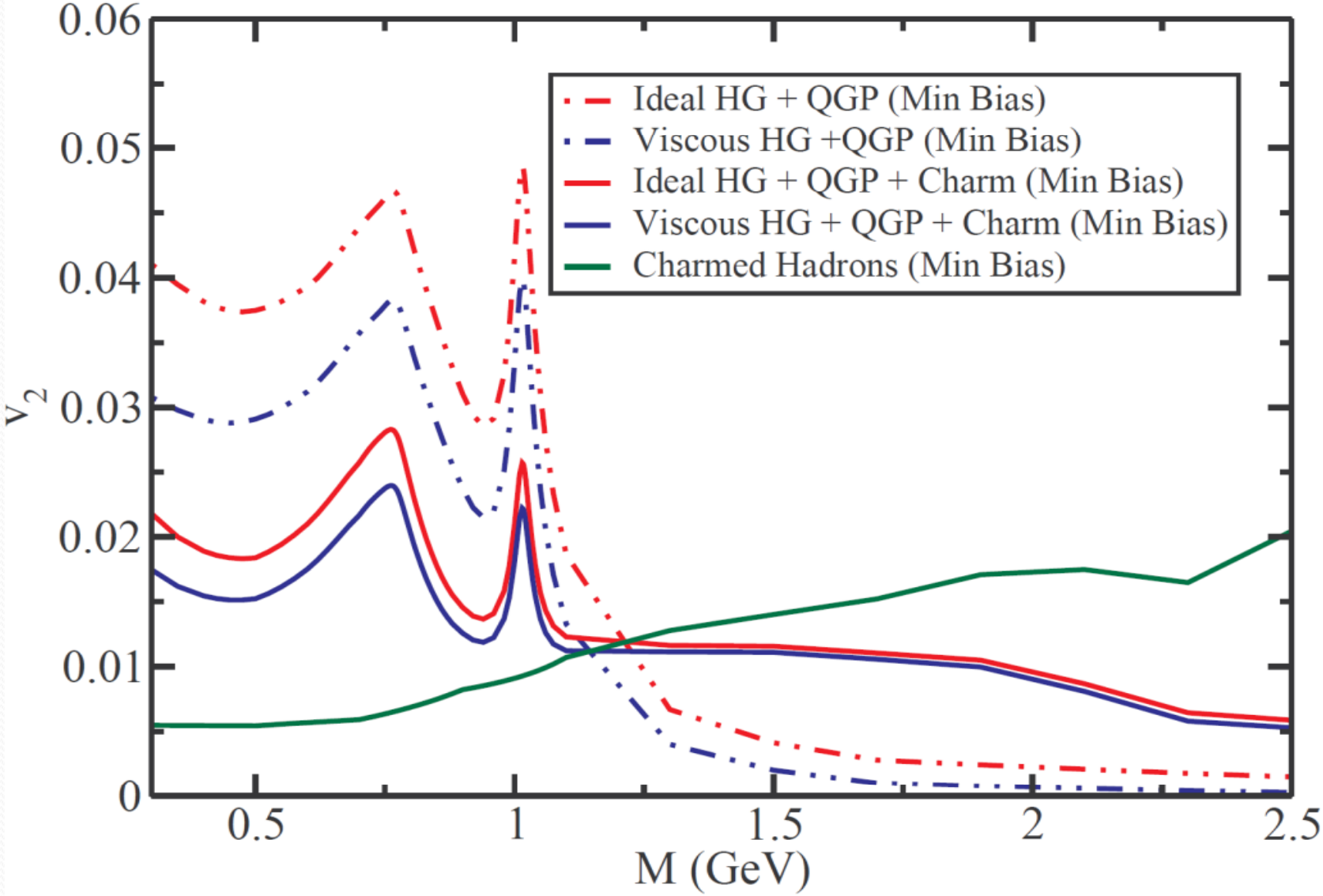

# Some aspects of dilepton production in HIC

**Qun Wang**
University of Science and Technology of China (USTC)

**J.Deng, Q.Wang, N.Xu, P.-f. Zhuang, PLB701,581(2010);**
**H.-j. Xu, H.-f. Chen, X.Dong, Q.Wang, Y.-f. Zhang, PRC85, 024906(2012)**

**Thermal radiation workshop, RBRC-BNL, Dec 4-7, 2012**

# Outline

1. Introduction: a very brief timeline (history) of dilepton production in HIC (R. Rapp's talk, I. Tserruya's talk)
2. Vector meson contribution via Vector Meson Dominance model (VDM)
3. T_eff as probe to EOS of dense matter
4. Comparison with STAR data
5. Summary and conclusion

# Di-lepton sources in HIC

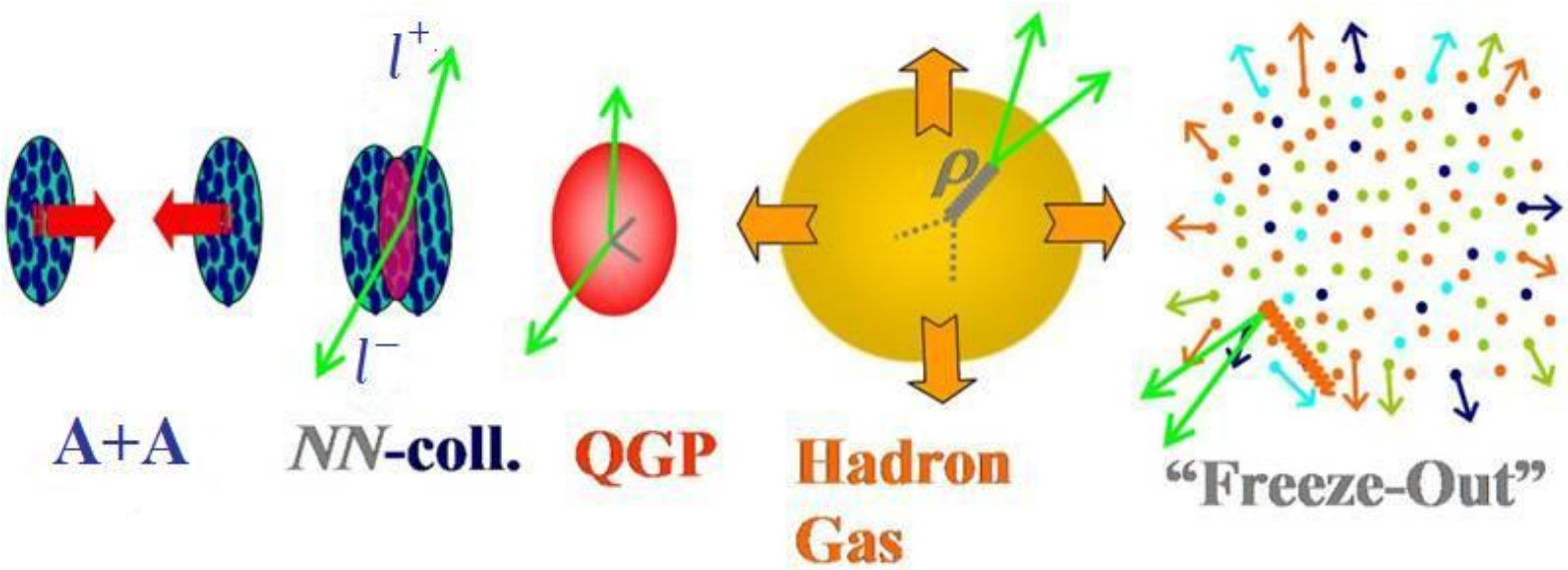


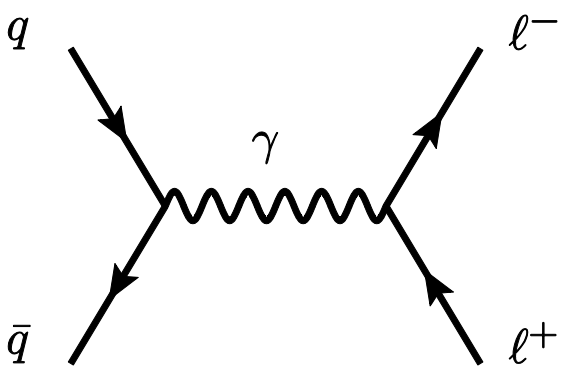


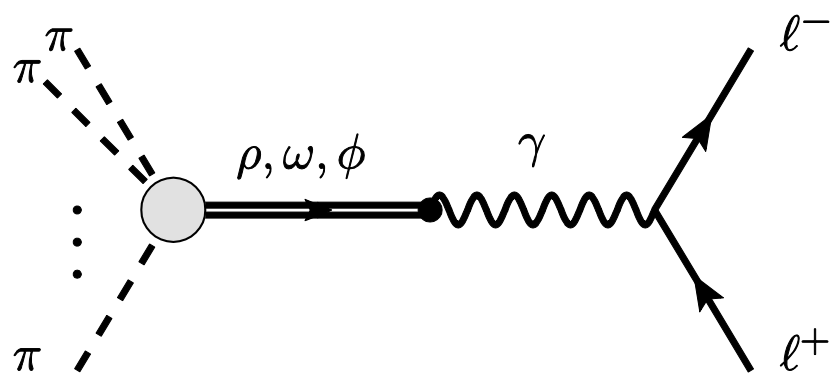

# A little history (1)

## Why dileptons ?

**(1985) McLerran & Toimela, PRD31, 545**
**(1990) Braaten,Pisarski,Yuan, PRL64, 2242**
**(1993) Shuryak,Xiong, PRL70, 2241**

- Suffer less interaction after their production
- Emitted in the whole space-time volume of the fireball
- Provide crucial information of the medium properties created by HIC

Earlier experiments

**(1997) DLS collaboration, PRL79,1229**
**(1998) DLS collaboration, PRC57,1865**

- Rare production
- Complex background

Ca+Ca, C+C, C+Ca, d+Ca

M<0.7 GeV

# A little history (2)

Low statistics

(1998) HELIOS-3, EPJC 5, 63
(1998) CERES/NA45, PLB422,405
(2000) NA50, EPJC 13,69

**Low mass enhancement**

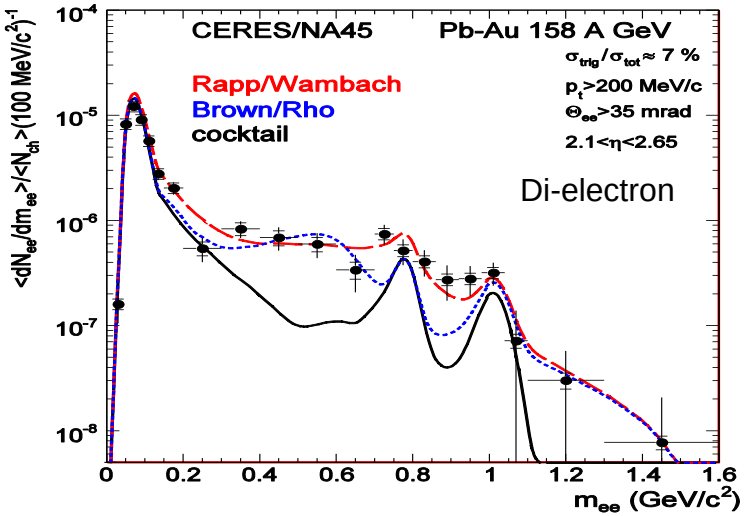


High statistics

(2006) NA60, PRL96,162302

**In-medium rho spectra**

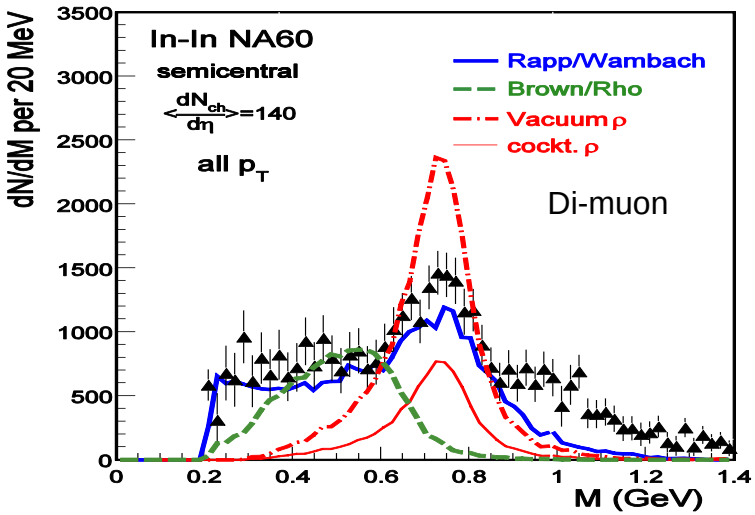

# A little history (3)

Low statistics

(2004) Brown & Rho, Phys.Rept 398, 301

**Broadening spectra vs Dropping mass**

High statistics

(2006) van Hees & Rapp. PRL97, 102301
(2008) Ruppert, Gale, et al. PRL100, 162301
(2007) Dusling, Teaney & Zahed. PRC75, 024908

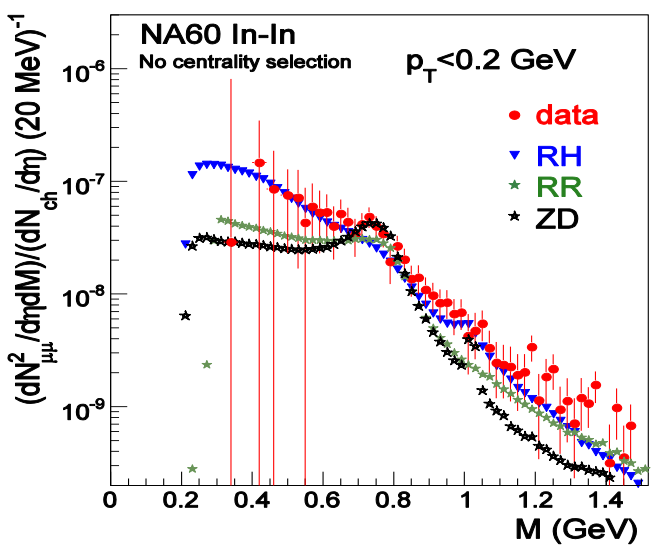


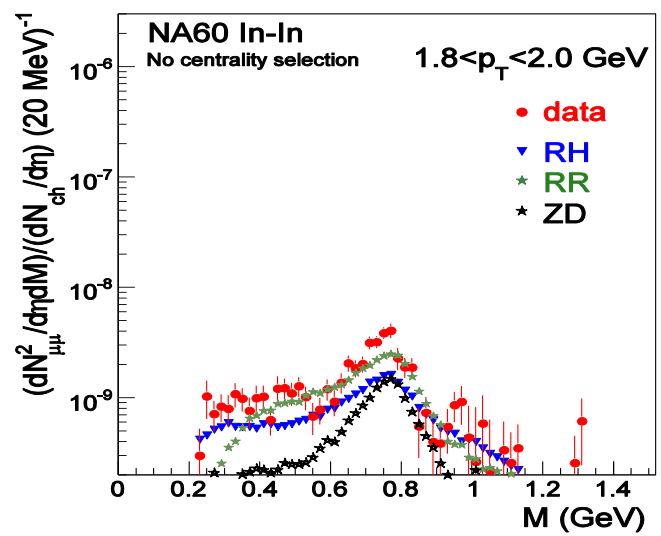

# A little history (4)

RHIC energy

(2010) PHENIX, PRC81, 034911
(2011) J. Zhao, JPG38 , 124134

**PHENIX puzzle**

Future

- STAR-BES
- LHC
- CMB

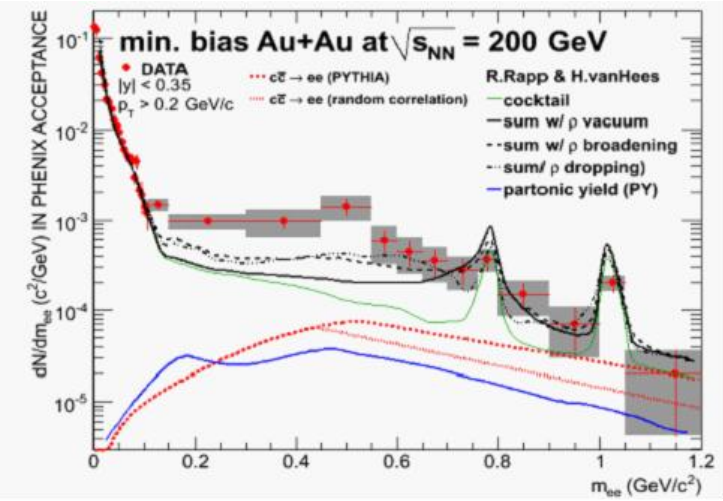


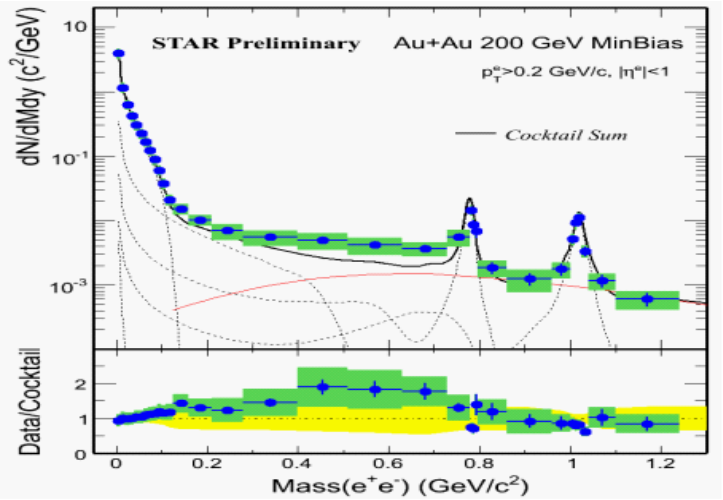

# A little history (5)

RHIC energy

(2009) Rapp, Wambach, 0901.3289
(2012) Linnyk et al, PRC85, 024910
(2012) Xu, et al, PRC85, 024906

phenomenology study

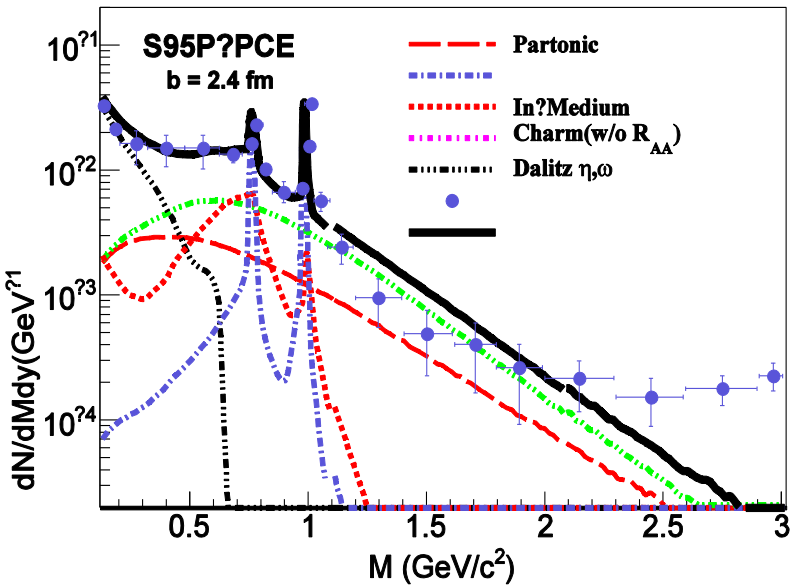


- **PHENIX puzzle**
- **The signals from BES**
- **v2, HBT**
- **etc. ……**

(2006) Chatterjee , et al. PRC75, 054909
(2008) Dusling et al. NPA809, 246
(2011) Deng, et al. PLB701,581
(2011) Mohanty, et al. PRC84, 024903
……

# Invariant mass spectra

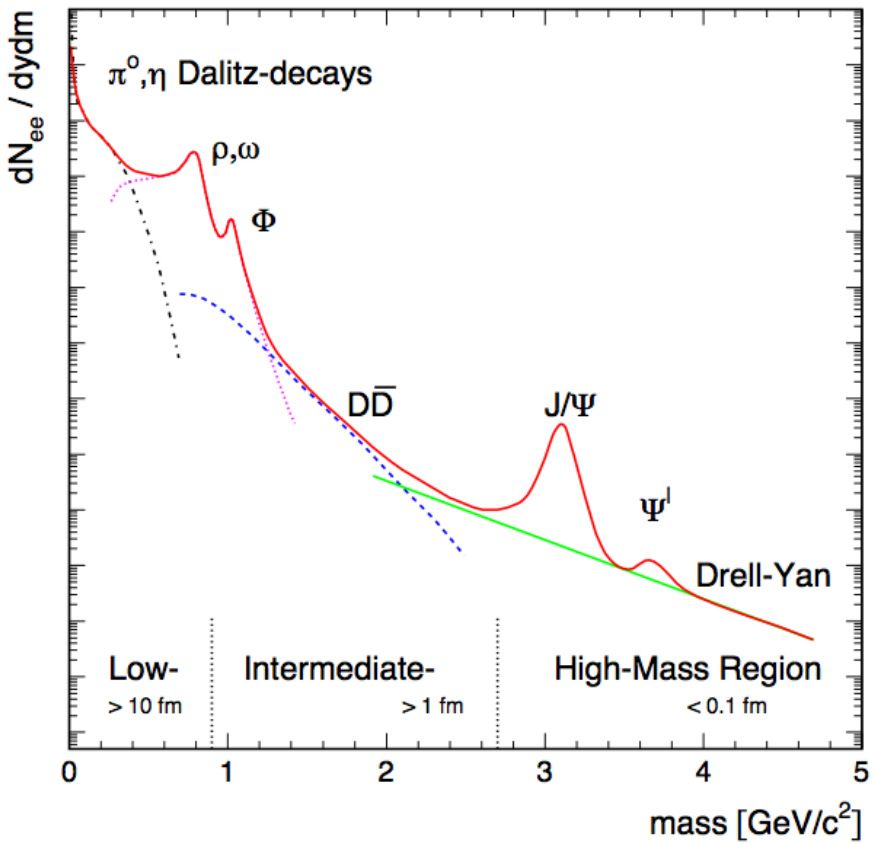


| | |
|---|---|
| LMR | **Chiral symmetry restoration, Vector meson production, in-medium effect** |
| IMR | **Heavy quark, QGP thermal radiation** |
| HMR | **Heavy quarkonia, Drell-Yan** |

# Effective temperature for hadrons and dileptons

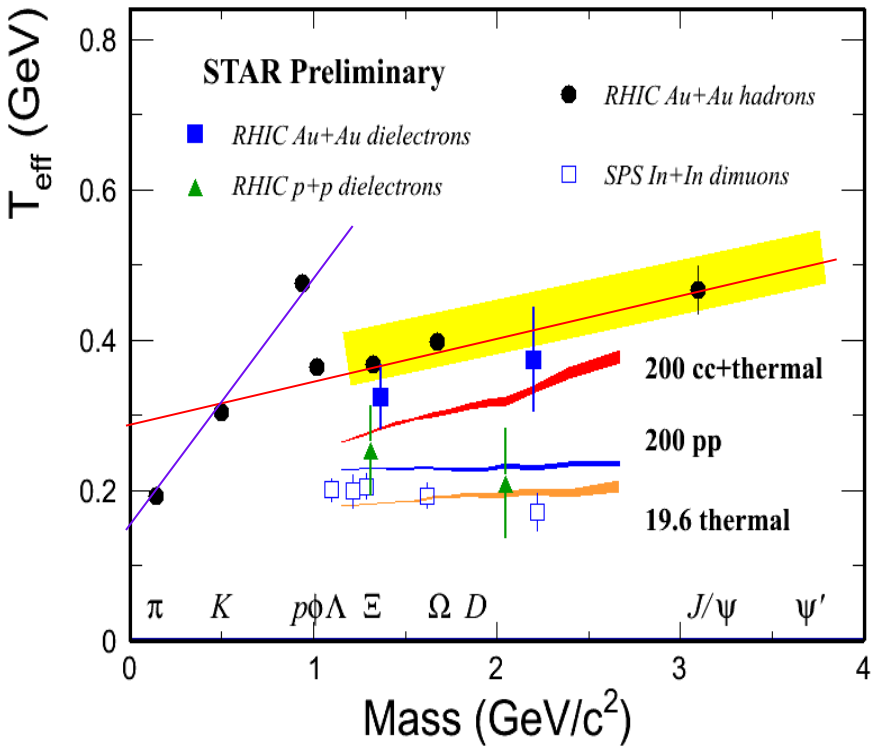


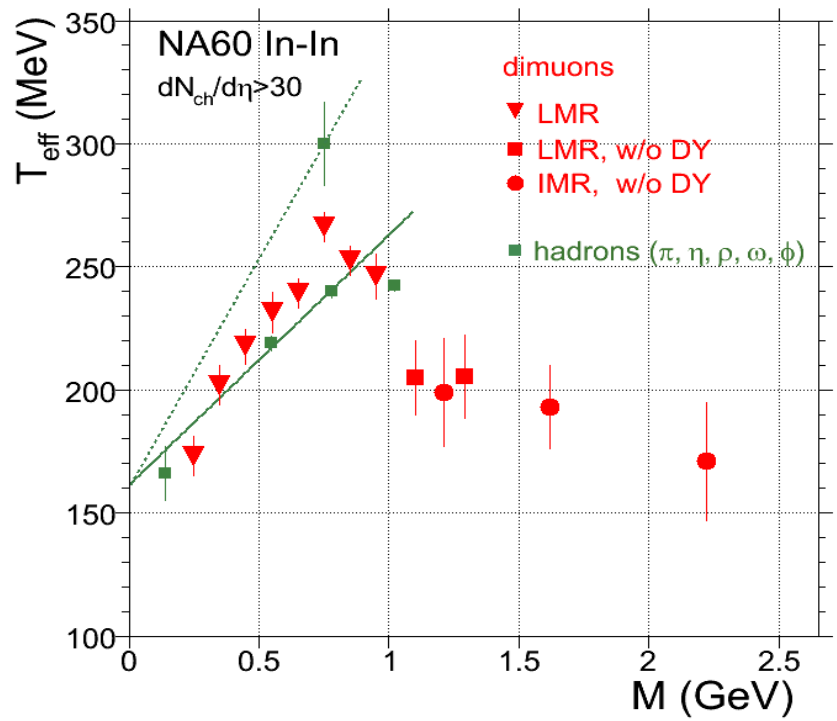


$$T_{\rm eff} = T_0 + M v_T^2$$

**The transition tregion may signal a transition from a hadronic source to a partonic source**

**NA60, PRL100, 022302(2008); EPJC59, 607(2009)**

# Strategy

- Dilepton production in Au+Au collisions at 200 GeV in IMR, QGP phase: q-qbar annihilation; Hadron phase: D_ρ with vertices ρπX (X: all mesons below 1300 GeV), and vertices of ρNN* and ρNΔ* (N* and Δ*: baryon resonances); D_ω with vertices ωρπ, ωπππ; and D_φ with vertices φKK-bar.
- Space-time evolution of medium is described by a 2+1 ideal hydro model, different EOS are used for hydro-simulation.
- Slope parameters and elliptic flows show distinct features from two phases
- Comparison to recent STAR data.

# Hydrodynamics for HIC

- **Assumption: thermalization, Ideal or Viscous**
- **Inputs: EOS, initial conditions, freeze-out conditions**
- **Outputs: space-time evolution**
- **Comparison with data: pt-spectra, flows, …**
- **Further application: fluctuation & correlation, non-equilbrium statistics, ...**

**Baym, Friman, Blaizot et al 86', Rischke 98', Kolb, Huovinen, Heinz, 00-01', Romatschke, 08', Song, Heinz, 08', Schenke, Jeon, Gale, 10' , Pang, Q.W., Wang 12', ……**

# Vector Meson Dominance Model (VDM)

- VDM (Kroll, Lee, Zumino, 67'). The Lagrangian for ρπγe-system:

$$
\begin{aligned}
L &= (D_\mu \pi)^*(D^\mu \pi) - m_\pi^2 \pi^* \pi - \frac{1}{4} G_{\mu\nu} G^{\mu\nu} + \frac{1}{2} m_\rho^2 \rho_\mu \rho^\mu \\
&\quad + \bar{\psi}(i\gamma_\mu D_A^\mu - m)\psi - \frac{1}{4} F_{\mu\nu} F^{\mu\nu} - \boxed{\frac{e}{2g} F_{\mu\nu} G^{\mu\nu}}
\end{aligned}
$$

Photon-rho coupling

where

$$
\begin{aligned}
D^\mu &= \partial^\mu + ig\rho^\mu + ieA^\mu \qquad & F^{\mu\nu} &= \partial^\mu A^\nu - \partial^\nu A^\mu \\
D_A^\mu &= \partial^\mu - ieA^\mu \qquad & G^{\mu\nu} &= \partial^\mu \rho^\nu - \partial^\nu \rho^\mu
\end{aligned}
$$

- EOM for EM field

$$
\partial_\sigma F^{\alpha\sigma} \approx e\bar{\psi}\gamma^\alpha \psi - \frac{e}{g} m_\rho^2 \rho^\alpha
$$

(keep terms linear in e/g)

$$
\boxed{
\begin{aligned}
J^\alpha = e\bar{\psi}\gamma^\alpha\psi &\rightarrow -\frac{e m_\rho^2}{g}\rho^\alpha \\
\langle J^\alpha(x) J^\beta(y)\rangle &\rightarrow \frac{e^2 m_\rho^4}{g^2}\langle \rho^\alpha(x)\rho^\beta(y)\rangle \\
\Pi_\gamma(x,y) &\rightarrow \frac{e^2 m_\rho^4}{g^2} D_\rho^{\alpha\beta}(x,y)
\end{aligned}
}
$$

# Dilepton emission rate (1)

**In-medium rate**

$$\frac{d^8N}{d^4x d^4p} = -\frac{\alpha}{4\pi^4}\frac{1}{M^2} n_B(p\cdot u) L(M) \mathrm{Im}\Pi_\gamma^R(p)$$

$$L(M) = \left(1+\frac{2m_l^2}{M^2}\right)\sqrt{1-\frac{4m_l^2}{M^2}}$$

u: fluid velocity
T: temperature
Π_γ and n_B depend on space-time via u and T

**Photon selfenery (VDM + quark)**

$$\mathrm{Im}\Pi_\gamma^R = \begin{cases} \sum_{V=\rho,\omega,\phi} e^2 \left(\frac{m_V^2}{g_V}\right)^2 \mathrm{Im}D_V & \text{hadronic source} \\ -\frac{N_c M^2}{12}\left(1+\frac{\alpha_S}{\pi}\right)\sum_{i=u,d,s} e_i^2 & \text{quark source} \end{cases}$$

**Imaginary part of Retarded propagator of rho meson**

$$\mathrm{Im}D_V(M,q,T) = \frac{1}{3}\mathrm{Im}D_V^L(M,q,T) + \frac{2}{3}\mathrm{Im}D_V^T(M,q,T)$$

$$\mathrm{Im}D_V^{L,T}(M,q,T) = \frac{\mathrm{Im}\Sigma_V^{L,T}(M,q,T)}{|M^2-(m_V^0)^2+\Sigma_V^{L,T}(M,q,T)|^2}$$

# Dilepton emission rate (2)

- **Freezeout (FO) dilepton rate is related to FO vector meson rate. Most of ρ mesons decay inside medium. But most of ω and φ meson decays take place after FO due to their long life time.**

$$\frac{dN_{l\bar{l}}^{fo}}{d^4p} = \frac{\alpha}{3}\left(\frac{e}{g}\right)^2 \frac{m_V}{\Gamma_V}\frac{dN_V^{fo}}{d^4p}$$

$$\frac{dN_V^{fo}}{d^4p} = \frac{g_s^\rho}{4\pi^4}\int_{T_f} d\Sigma_\mu p^\mu \mathrm{Im} D_V n_B(p\cdot u)$$

Freezeout Emission rate of vector meson

Freezeout hypersurface

In-vacuum vector meson propagator

# Rho self energy (1)

Chanfray,Schuck, NPA555,329(1993);
Herrmann,Friman,Noerenberg, NPA560(1993);
Rapp,Gale, PRC 60,024903(1999);
Gale,Lichard, PRD 49,3338(1994);

Meson Contribution
X = π, ω, h1(1170)
a1(1260), π'(1300)

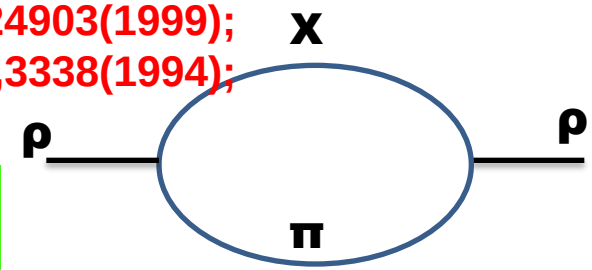


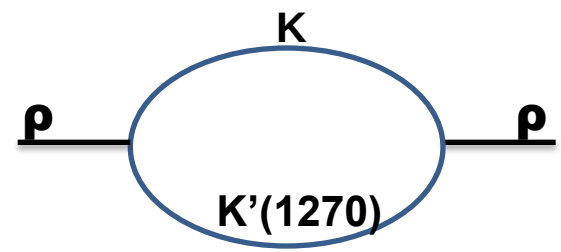


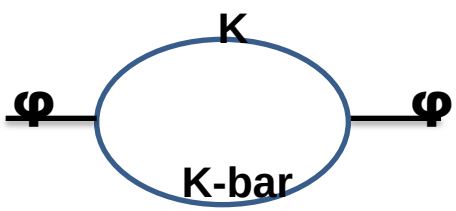


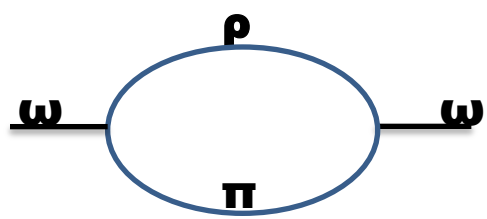


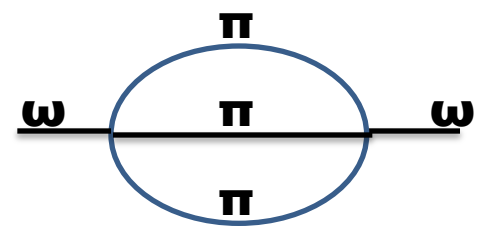


Baryon Contribution:
N(1700), N(1720), N(1900)
N(2000), N(2080), N(2090)
N(2100), N(2190),
Δ(1700), Δ(1900), Δ(1905),
Δ(1940), Δ(2000)

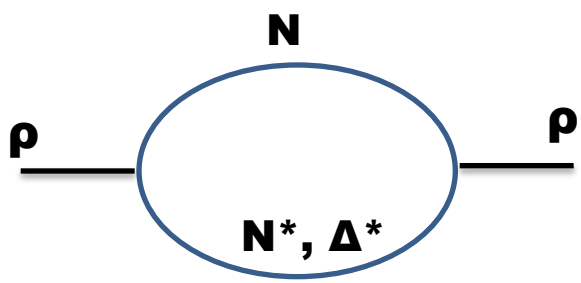


Eletsky, Belkacem,
Ellis, Kapusta,
PRC 64, 035202(2001);
Eletsky, Kapusta,
PRC 59, 2757(1999)

# Rho self energy (2)
# Re and Im from mesons

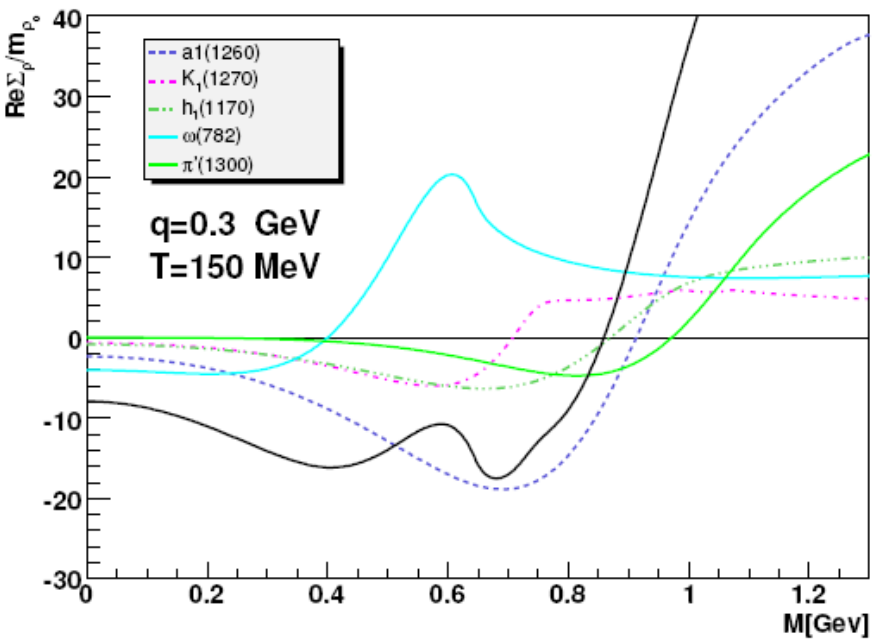


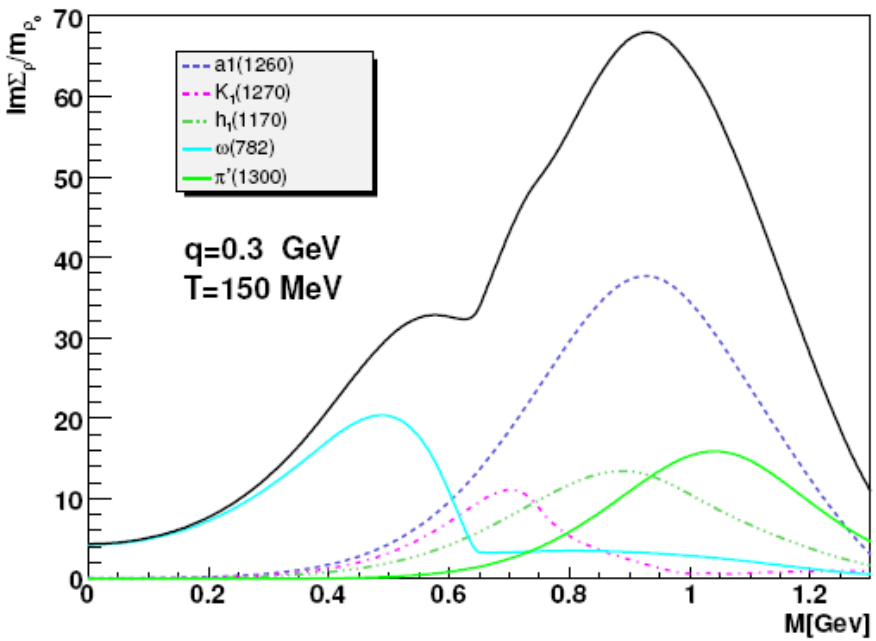


**Rapp & Gale, PRC 60,024903(1999)**

# Rho self energy (3): Im D_ρ w/o NN*+NΔ* contribution

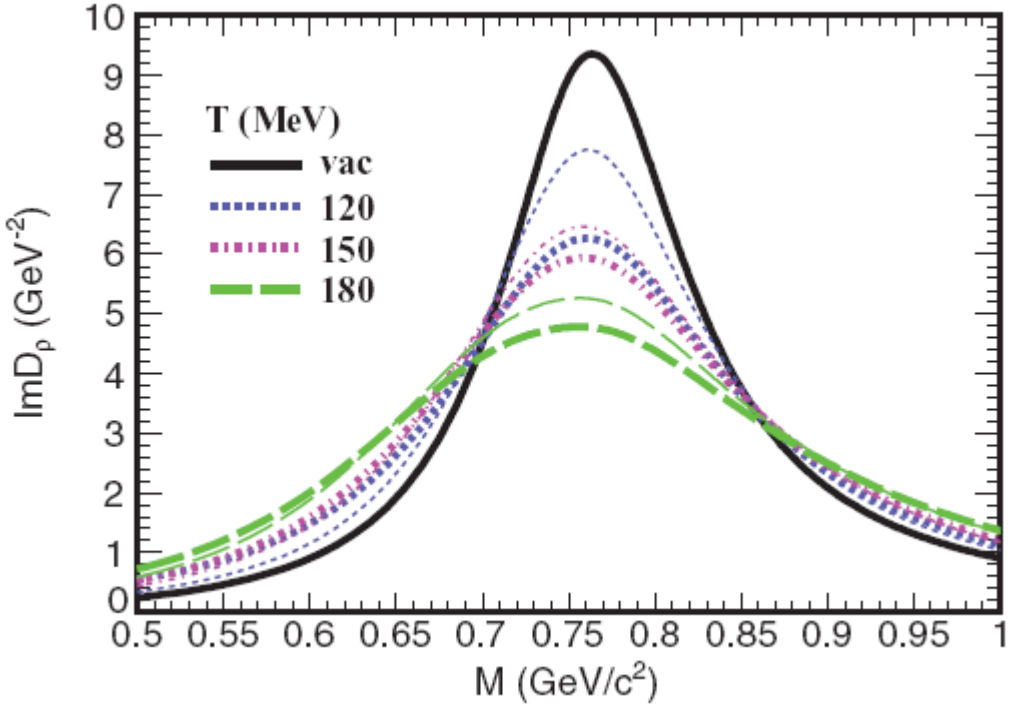


The imaginary parts of the in-medium ρ meson propagators (or in-medium spectral functions) with (thick lines) and without (thin lines) baryonic contributions. The chemical potentials in the PCE EOS are used.

**The imaginary part of the porpagator is sensitive to temperature, but insensitive to its momentum.**

# Im of ω and φ propagator

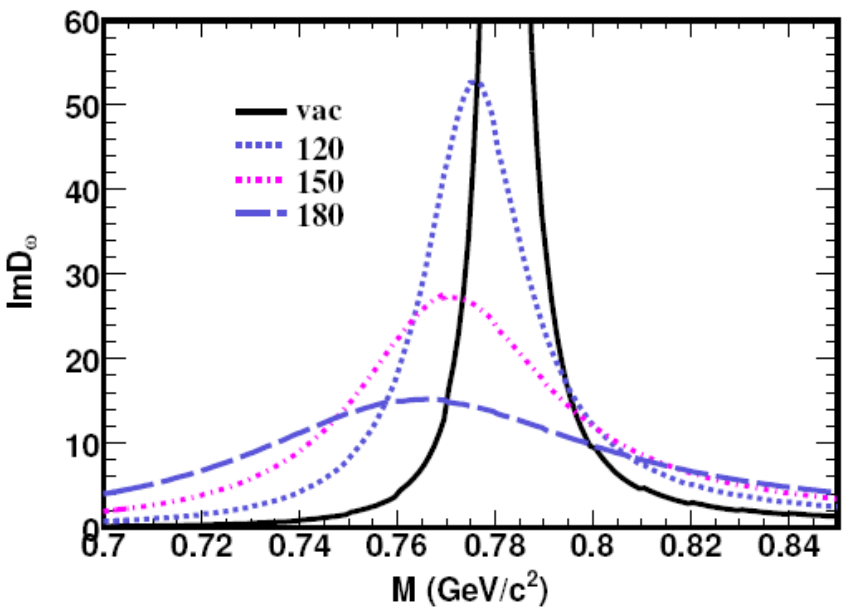


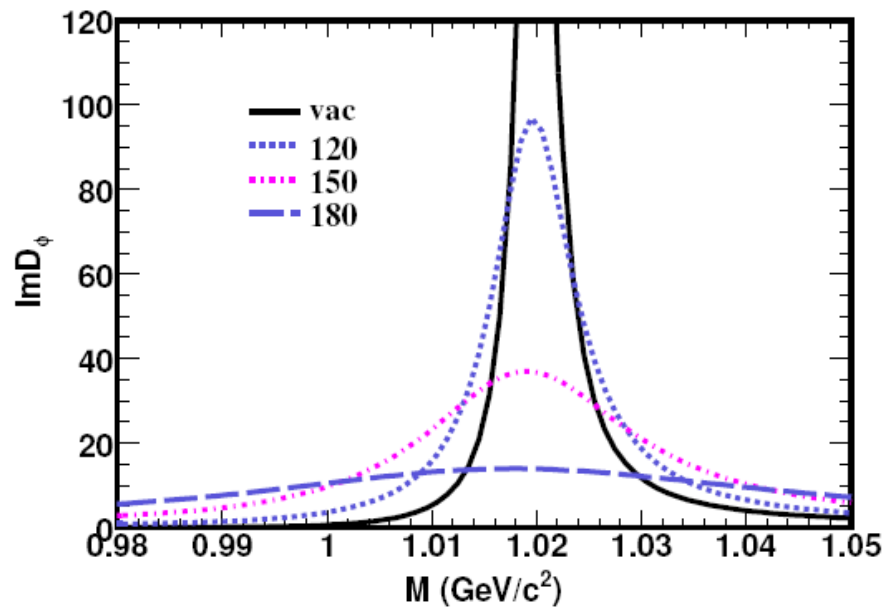

# T_eff as probe to EOS of dense matter

# Transverse flow: slope parameter

$$\frac{d^4N}{p_T dp_T M dM d\phi_p} \approx -\frac{\alpha}{2\pi^4}\frac{1}{M^2}\left(1+\frac{2m^2}{M^2}\right)\sqrt{1-\frac{4m^2}{M^2}} \times \int d^4x \exp\left[\frac{1}{T}\gamma_T M_T v_T p_T \cos(\phi_v-\phi_p)\right] K_0\left(\frac{\gamma_T M_T}{T}\right) \mathrm{Im}\Pi^R$$

$$M_T = \sqrt{M^2+p_T^2}$$

differential rate

space-time integral

transverse fluid velocity

azimuthal angle of fluid

**spectra in transverse momentum and invariant mass**

$$\frac{d^2N}{m_T dm_T M dM} \sim \sqrt{\frac{\overline{T}}{\overline{\gamma}_T}}\frac{\sqrt{m_T+M}}{m_T}\exp\left(-\frac{m_T+M}{T_{eff}}\right)$$

$$m_T \equiv M_T - M$$

slope parameter

$$T_{eff} \sim \begin{cases} \overline{T}+M^*\overline{v}_T^2, & \text{for } p_T \ll M \\ \overline{T}\sqrt{\frac{1+\overline{v}_T}{1-\overline{v}_T}}, & \text{for } p_T \gg M \end{cases}$$

# Dense or hot QCD matter EOS

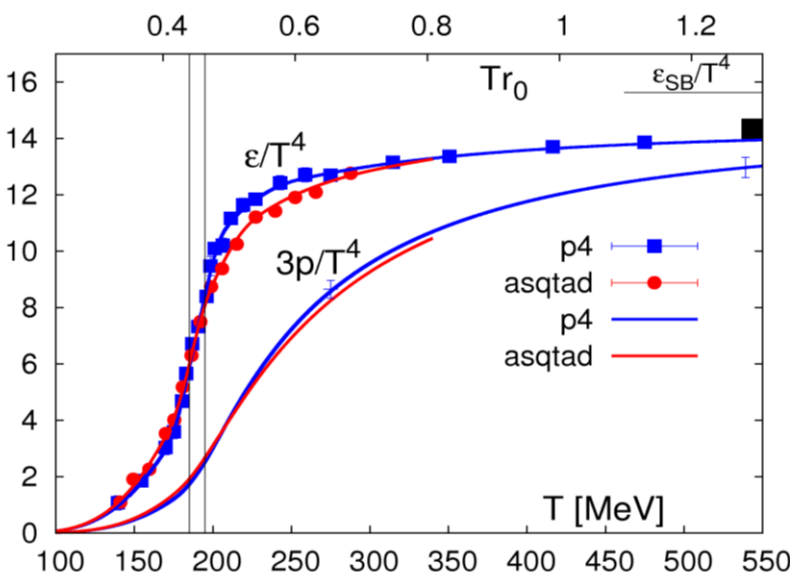


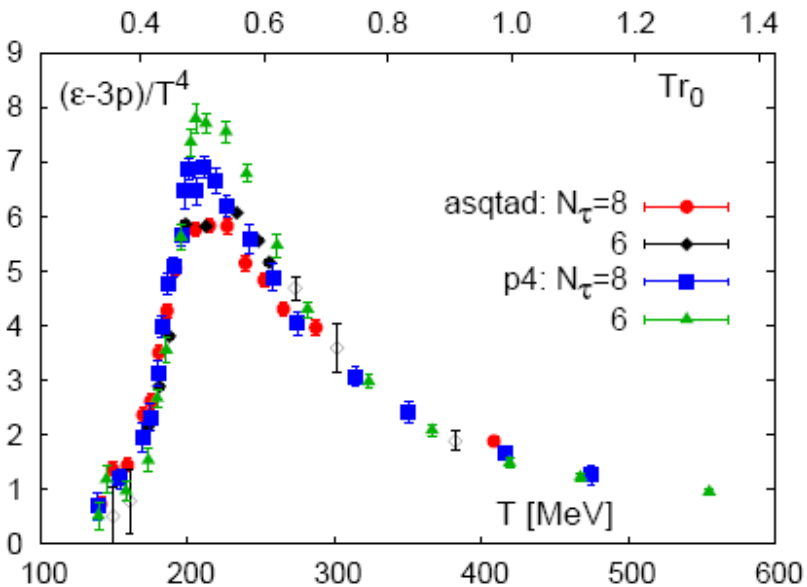


*Bernard et al, (MILC) PRD 75 (07) 094505,*
*Cheng et al, (RBC-Bielefeld) PRD 77, 014511(2008);*

*Bazavov et al, (HotQCD), Phys.Rev.D80, 014504(2009).*

# Four equations of state (EOS)

**Massless ideal QGP**

$$\epsilon = 3p = 16T^4$$

**Resonance Hadron gas**

**[Braun-Munzinger, Redlich, Stachel, nucl-th/0304013]**

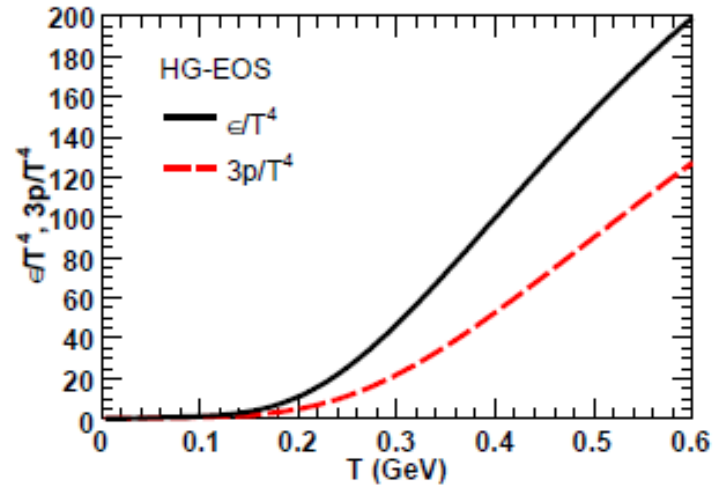


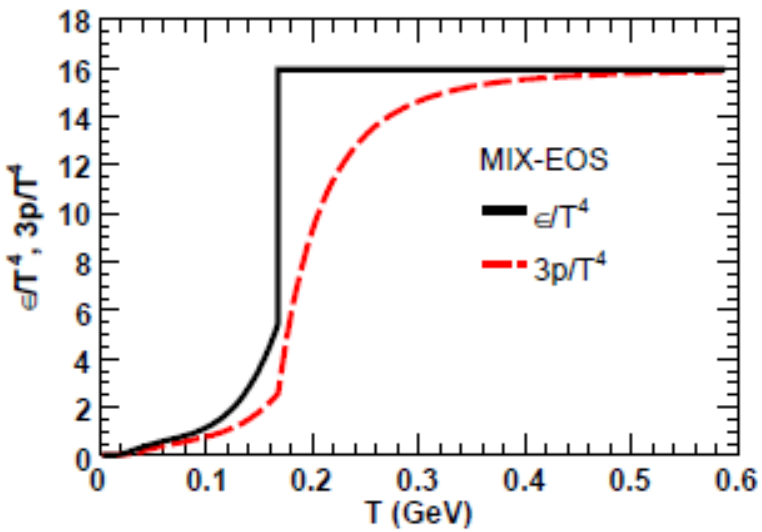


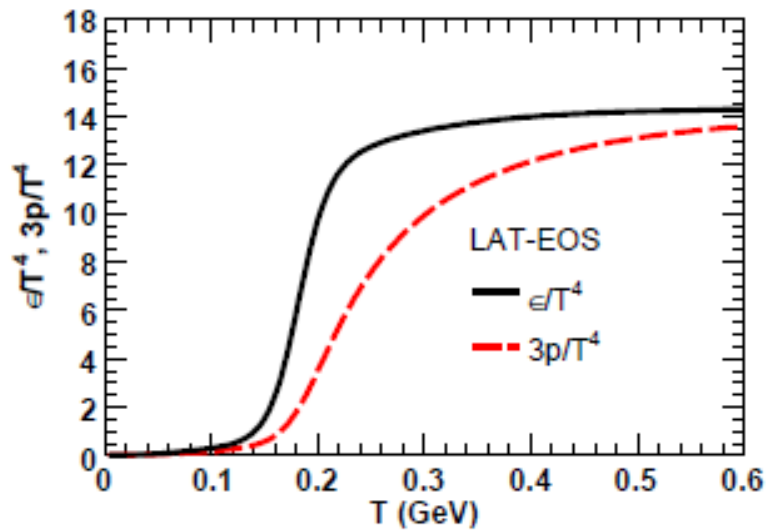

# Time evolution of the rate

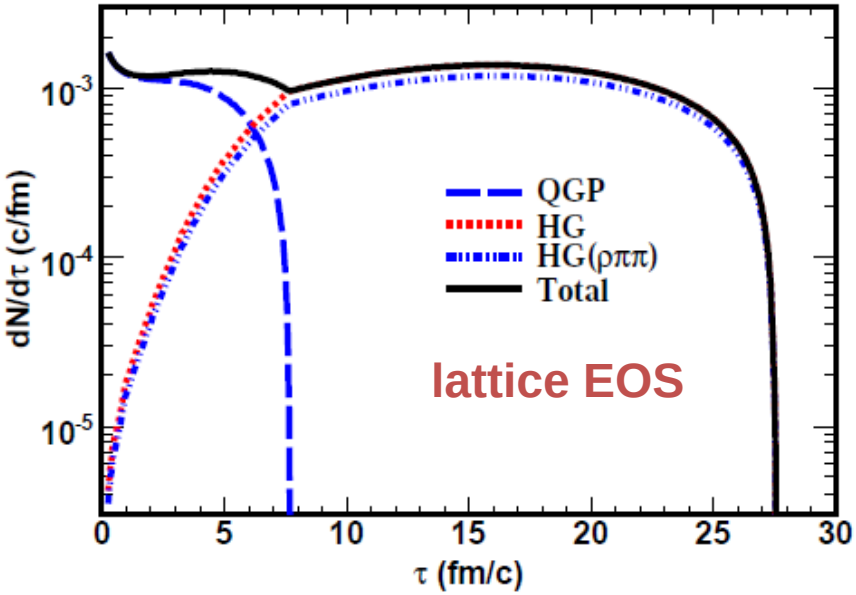


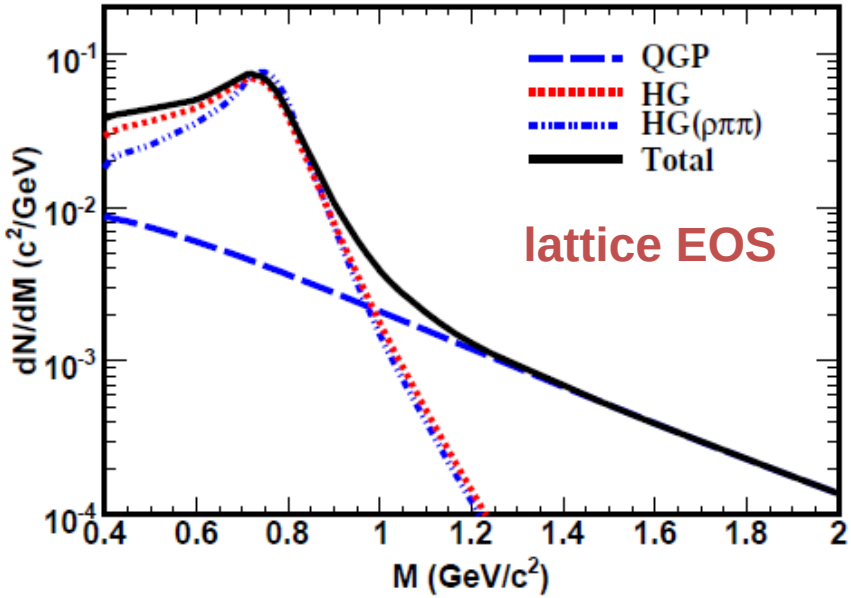


**Differential multiplicity as functions of the dilepton invariant mass and proper time. The lattice EOS is used. The unit is arbitrary.**
**The contributions from QGP and HG are shown in dashed and dotted lines.**

# Slope parameter: pt and EOS dependence

$$T_{eff} \sim T\sqrt{\frac{1+v_T}{1-v_T}}$$

pt dependence

EOS dependence

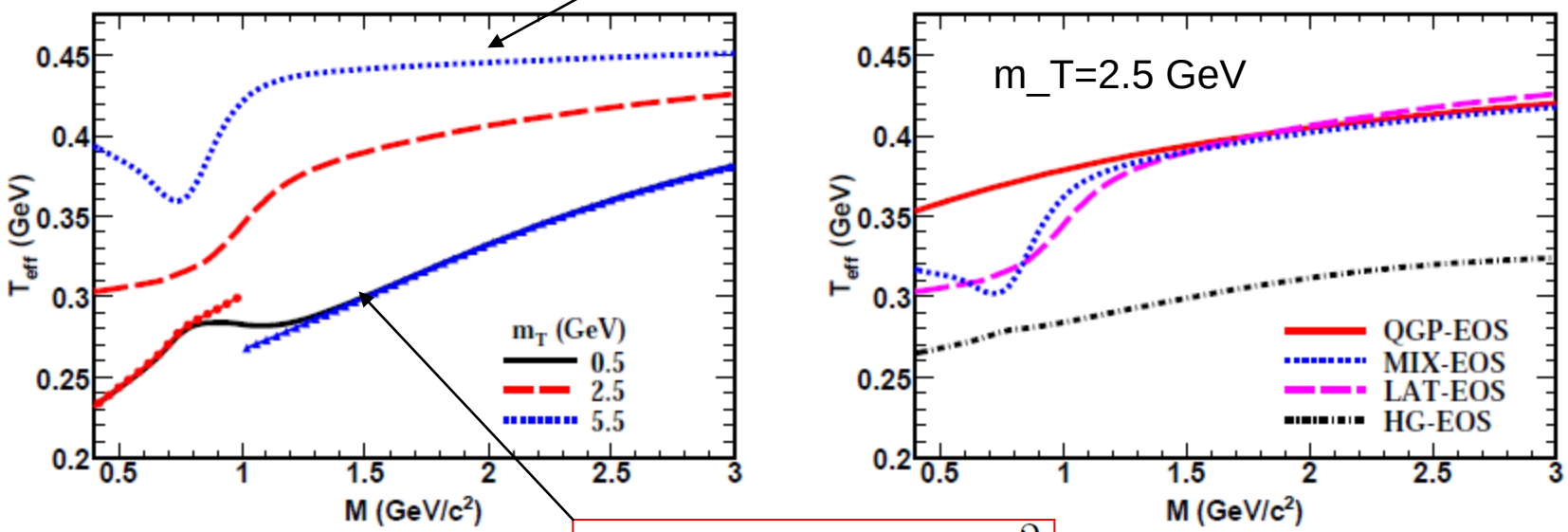


$$T_{eff} \sim T + M^* v_T^2$$

**Slope parameter as functions of *M* for the mixed phase (left panel) and the lattice (right panel) EOS. The results for different values of *mT* are shown in the solid, dashed and dotted lines. The lines with hollowed circles/triangles are extracted from the HG/QGP components.**

# Slope parameter: parameter dependence

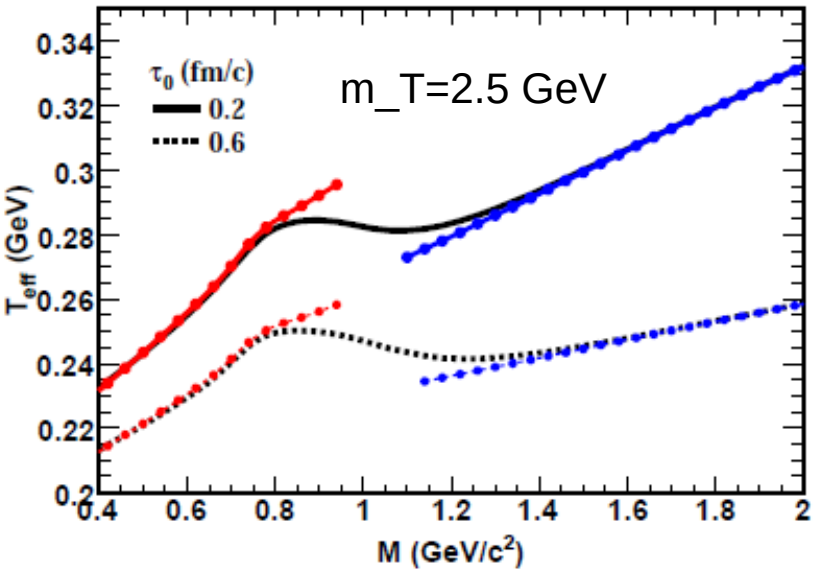


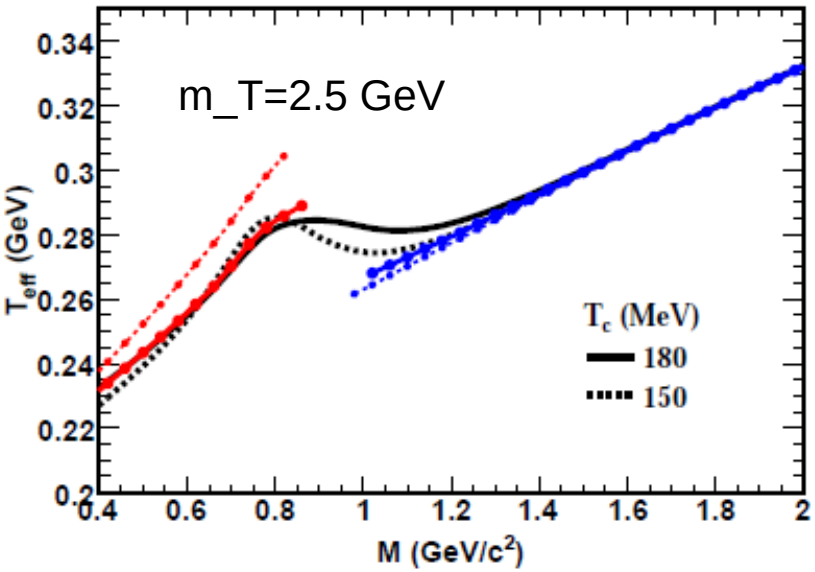


**Parameter dependences of the slope parameter with the lattice EOS. Left panel: the initial time for the hydrodynamic evolution τ0= 0.2; 0.6 fm/c. Right panel: the phase transition temperature *Tc* = 180, 150 MeV. m_T=2.5 GeV.**

# Elliptic flow v2 and R

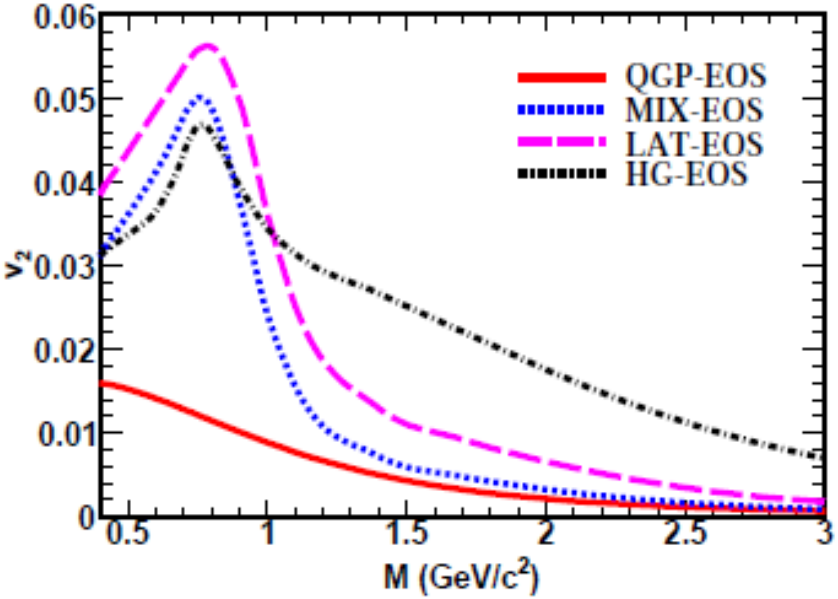


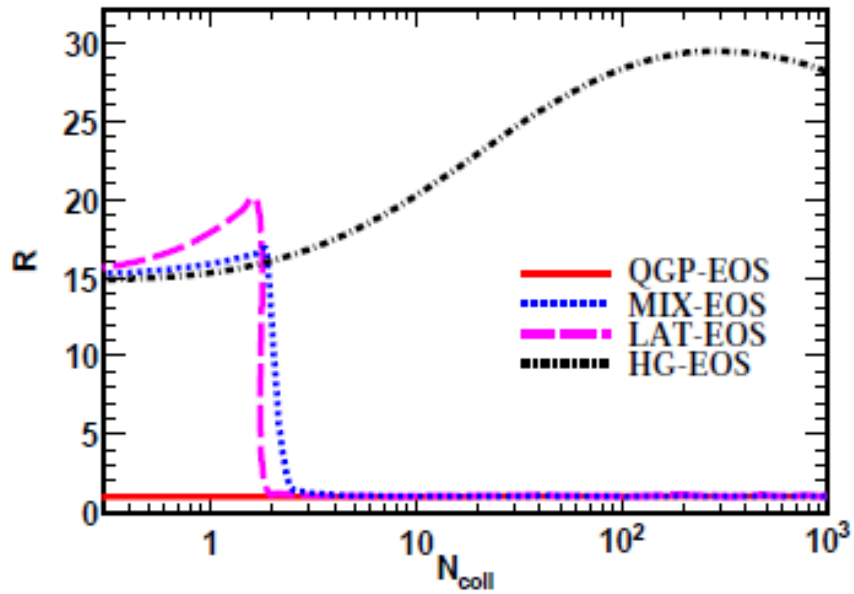


$$v_2(p_T, M) = \langle \cos(2\phi_p) \rangle$$

$$R = \frac{dN/dM_T^2 dp_T^2 dy|_{M_T=2.6GeV, p_T=2GeV}}{dN/dM_T^2 dp_T^2 dy|_{M_T=2.6GeV, p_T=0GeV}}$$

Asakawa,Ko,Levai, PRL70,398(1993).

# Comparison to STAR dilepton data

# Transverse momentum spectra

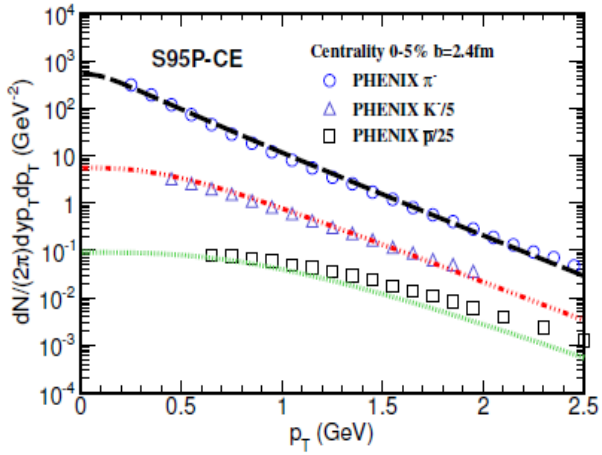


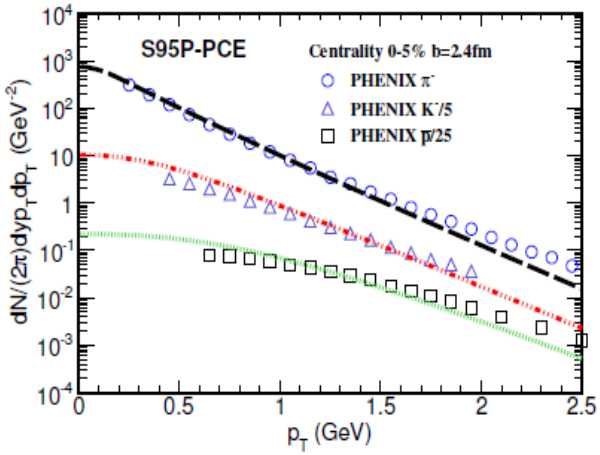


| | $\pi$ | $\rho/\pi$ | $\omega/\pi$ | $\phi/\pi$ |
|---|---|---|---|---|
| CE | 312.65 | $5.95 \times 10^{-2}$ | $5.7 \times 10^{-2}$ | $1.27 \times 10^{-2}$ |
| PCE | 349.47 | $7.8 \times 10^{-2}$ | $9 \times 10^{-2}$ | $2.8 \times 10^{-2}$ |
| PHENIX | 281.8 | $1.03 \times 10^{-1}$ | $8.98 \times 10^{-2}$ | $2.14 \times 10^{-2}$ |
| STAR | - | $1.69 \times 10^{-1}$ | - | $2.65 \times 10^{-2}$ |

**Parameters**

- S95-CE:
e0=40 GeV/fm^3,
τ0=0.4 fm,
T0=375 MeV,
Tf=128 MeV

- S95-PCE:
e0=60 GeV/fm^3,
τ0=0.4 fm,
T0=413 MeV,
Tf=140 MeV

# Cocktail of in-medium and freezeout contribution in full space

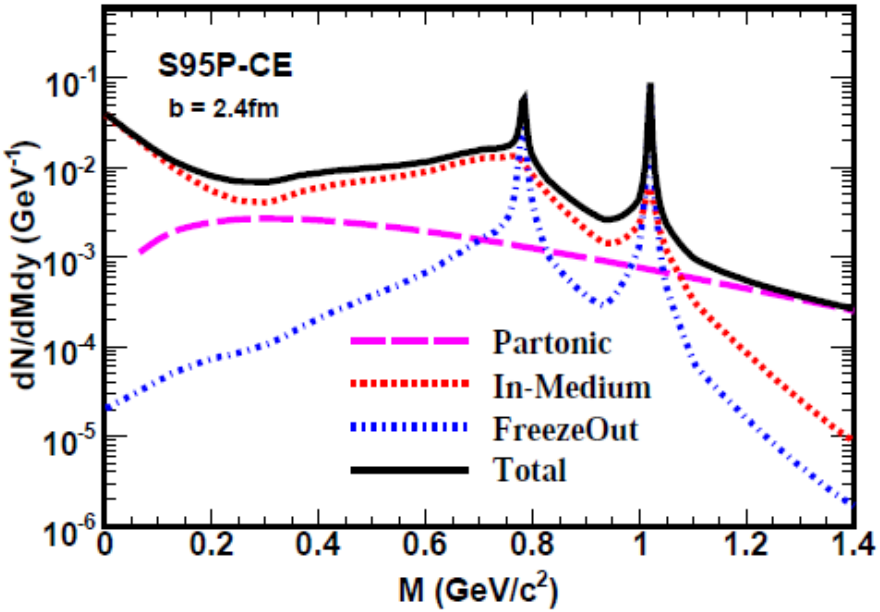


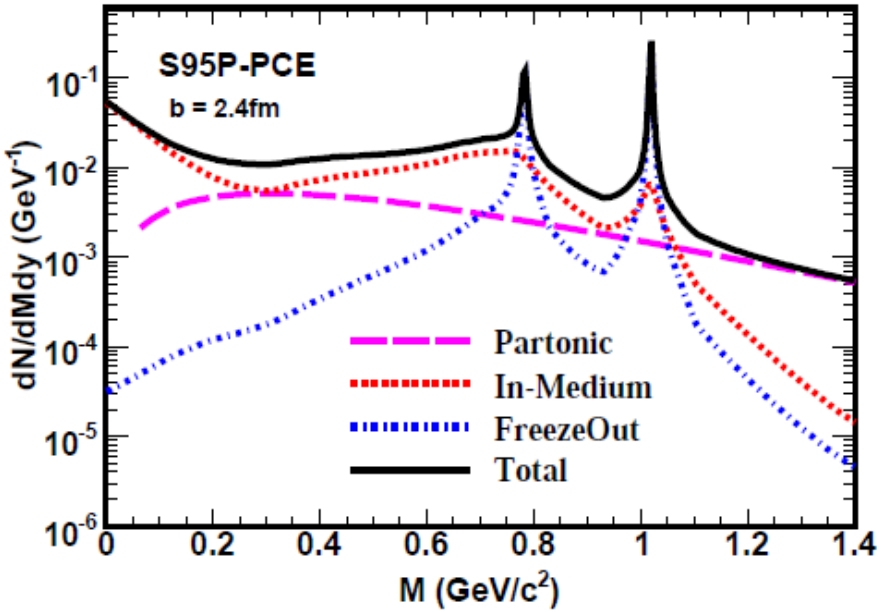


**Total = Partonic + In-medium hadronic + Freezeout**

# Semi-leptonic decays of charm hadrons

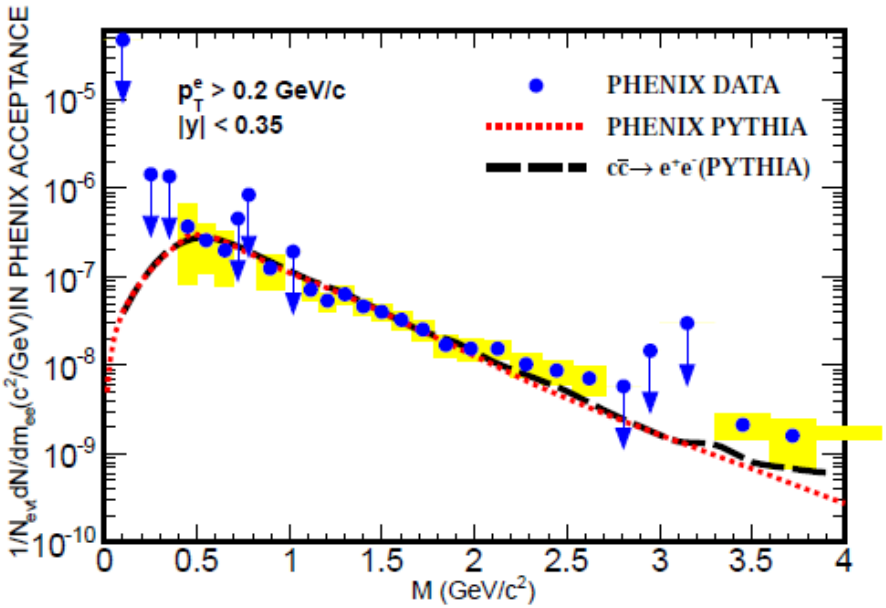


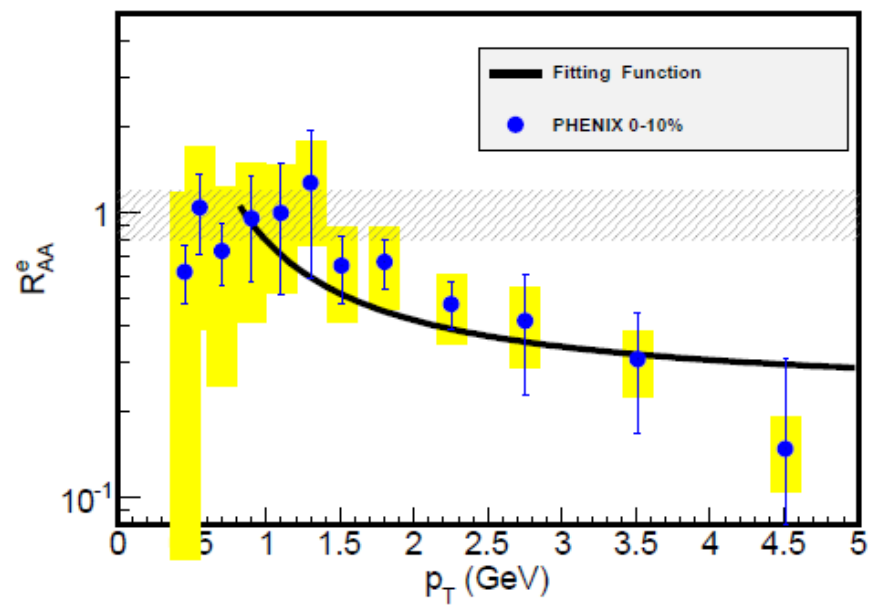


Re-scaled di-electron cross section from charm mesons of semi-leptonic decays in p+p collisions by PYTHIA.

the nuclear modification factor for nonphotonic electrons in central Au+Au collisions from the PHENIX.

Branch ratios from PDG: $D^{\pm}, D^0, D^s, \Lambda^c$

# Comparison with STAR preliminary data

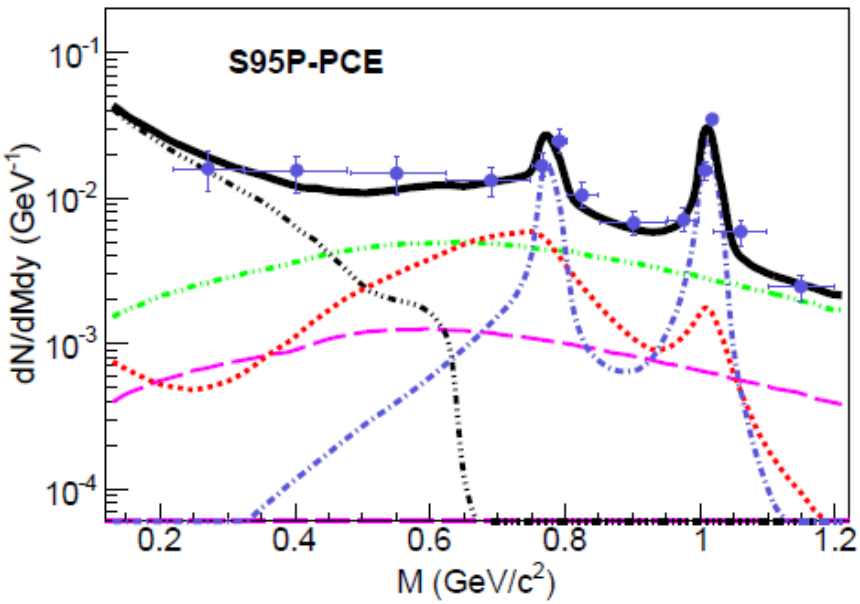


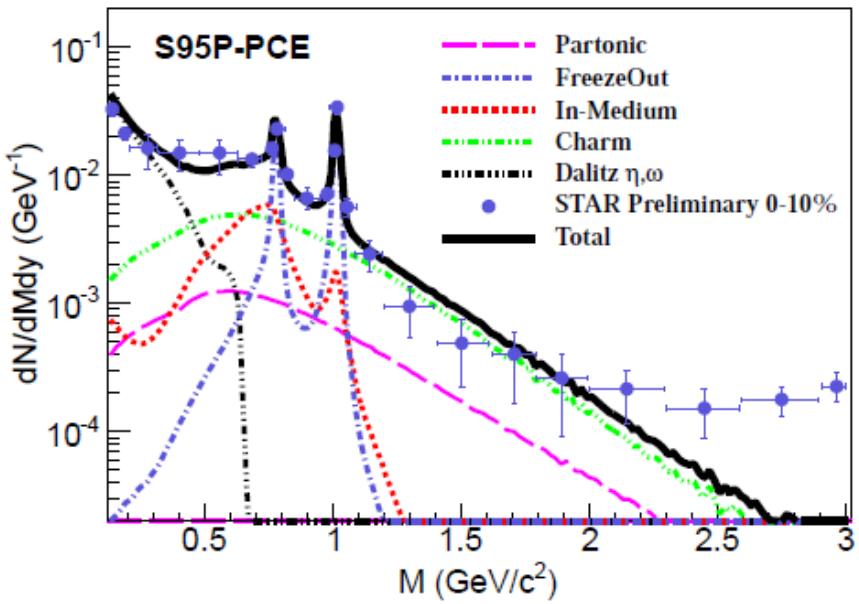


Comparison with STAR preliminary data in most central (0-10%) Au+Au collisions with the STAR acceptance.

STAR acceptance: $|\eta^e| < 1, p_T^e > 0.2 GeV, |y^{ee}| < 1$

# Summary and Conclusion

- T_eff of di-lepton can serve as a probe to EOS of the dense matter in high energy HIC
- Rho meson self-energy from meson resonances below 1300 MeV and baryon resonances (from ρNN*+ρNΔ* couplings) are taken into account
- In-medium and freezeout contributions are identified, open charm contribution is modeled
- Comparison with STAR data is made with good agreement

# Thanks!

# Direct Photon Spectra and Elliptic Flow in 2.76 TeV Pb-Pb Collisions from ALICE

Martin Wilde

on behalf of the ALICE Collaboration

Westfälische Wilhelms-Universität Münster

December 5, 2012

# Table of Contents


1. Direct Photon Production and the ALICE Detector

2. Part I: Direct Photon Spectra
   - Analysis Strategy
   - Detection of Converted Photons and $\pi^0$s
   - Inclusive Photon Results in pp and Pb-Pb
   - Decay Photon Background Calculation
   - Direct Photon Results in pp and Pb-Pb

3. Part II: Direct Photon $v_2$
   - Analysis Strategy
   - Inclusive Photon $v_2$ Analysis
   - Decay Photon $v_2$
   - Direct Photon $v_2$

# Direct Photons in pp and Pb-Pb Collisions

## Direct Photons - Definition

Photons that are not produced by particle decays

Prompt Photons: In pp and Pb-Pb

- Calculable within NLO pQCD
- Predominant source in pp
- Signal scales with number of binary collisions in Pb-Pb
- Fragmentation photons may be modified by parton energy loss in the medium

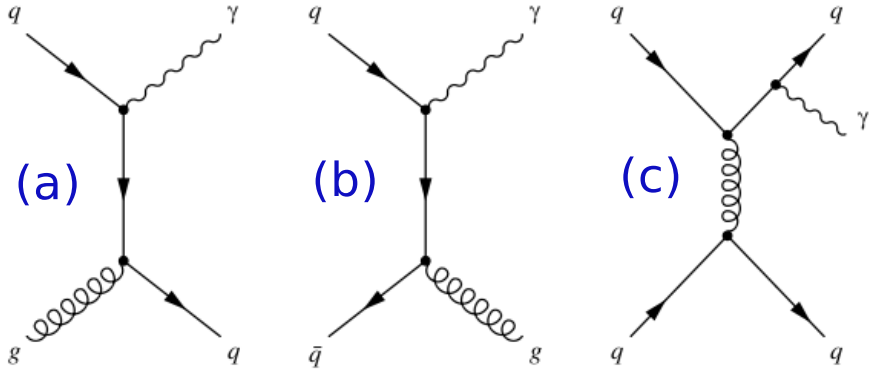


(a) Quark-gluon Compton scattering

(b) Quark-Anti-quark annihilation

(c) Fragmentation photons (bremsstrahlung)

Measurement of direct photons in pp is an ideal test for pQCD

# Direct Photons in Pb-Pb Collisions

## Additional sources of direct photons in Pb-Pb collisions

### Jet-Medium Interactions:

- Scattering of hard partons with thermalized partons
- In medium (photon) bremsstrahlung emitted by quarks

### Thermal Photons:

- Scattering of thermalized particles

  QGP: $q\bar{q} \rightarrow g\gamma$ and $qg \rightarrow q\gamma$ (+NLO)

  HHG (hot hadronic gas): Hadronic interactions (e.g. $\pi^+\pi^- \rightarrow \gamma\rho_0$)
- Exponentially decreasing but dominant at low $p_T$

2006 J. Phys. G: Nucl. Part. Phys. 32 1295

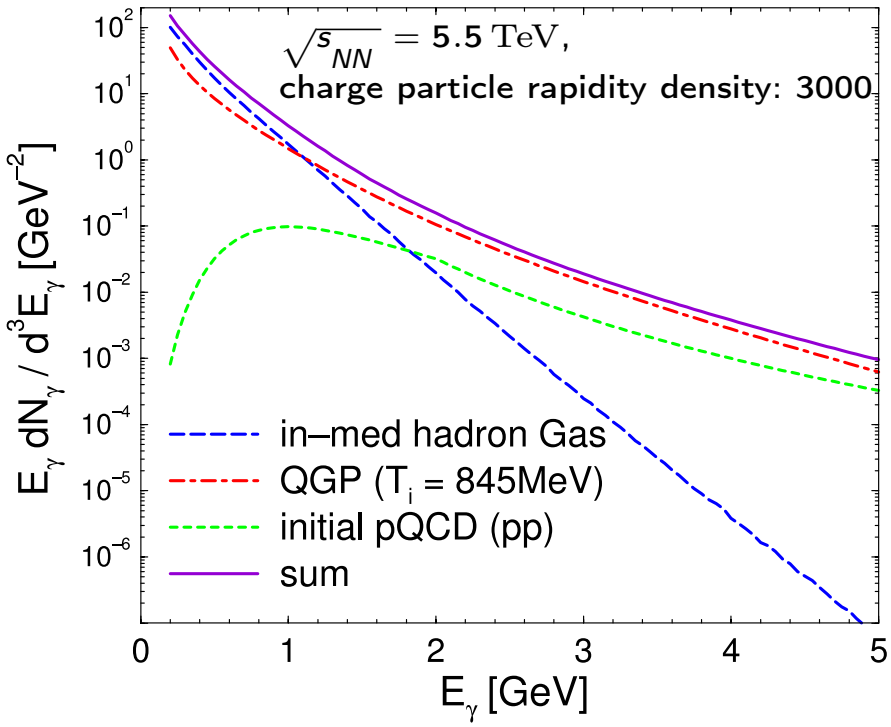


Photons leave medium unaffected, an ideal probe to study HI collisions

# The ALICE Detector and Data Sample

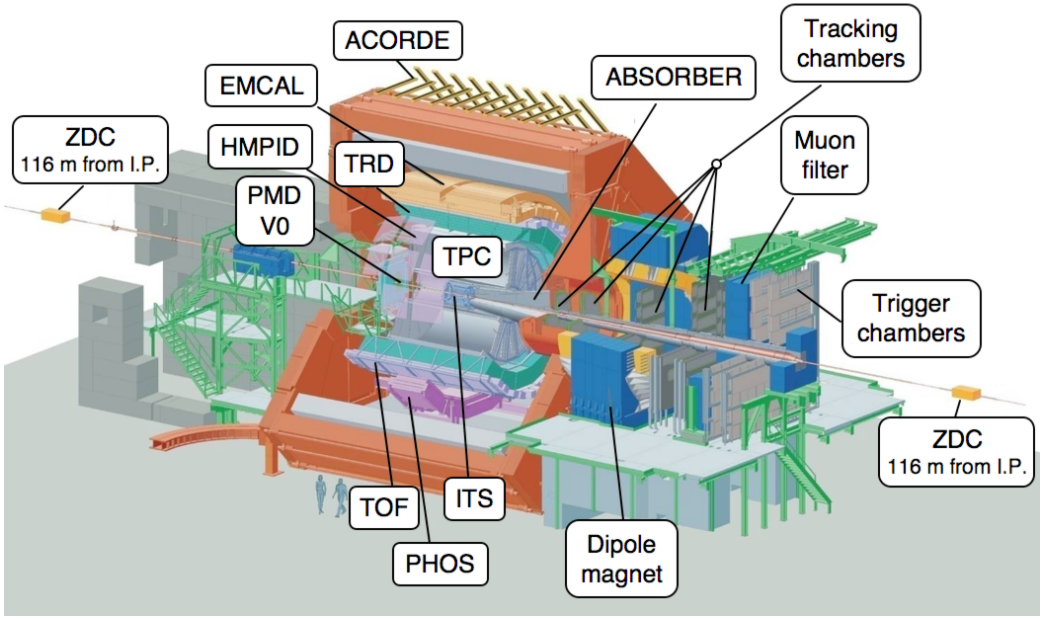


pp, $\sqrt{s} = 7\,\mathrm{TeV}$:

- Data sample: $3.54 \times 10^8$ events (min. bias)
- Monte Carlo: Pythia-Perugia0 and Phojet

Pb-Pb, $\sqrt{s_{NN}} = 2.76\,\mathrm{TeV}$:

- Data sample: $17 \times 10^6$ min. bias events
- Monte Carlo: Hijing (min. bias plus enriched events with high $p_T$ $\pi^0$s)

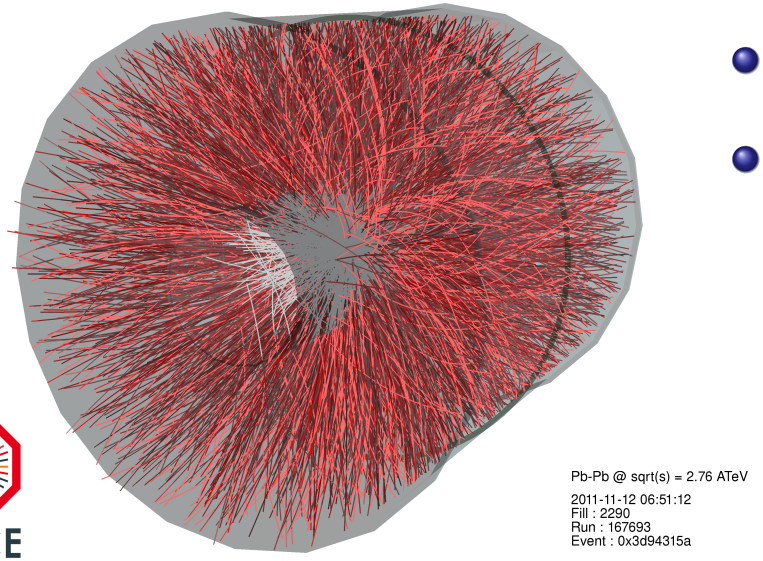


Photons are measured via their conversion products in ITS and TPC

# Part I: Direct Photon Spectra

# General Strategy of the Analysis

## Subtraction Method

$$\gamma_{\text{direct}} = \gamma_{\text{inc}} - \gamma_{\text{decay}} = (1 - \frac{\gamma_{\text{decay}}}{\gamma_{\text{inc}}}) \cdot \gamma_{\text{inc}}$$

- Inclusive photons: measure all photons that are produced
- Decay photons: calculated from measured particle spectra with photon decay branches ($\pi^0$, $\eta$, ...)

## Double Ratio

$$\frac{\gamma_{\text{inc}}}{\pi^0} / \frac{\gamma_{\text{decay}}}{\pi^0_{\text{param}}} \approxeq \frac{\gamma_{\text{inc}}}{\gamma_{\text{decay}}} \qquad \text{if} > 1 \text{ direct photon signal}$$

$\rightarrow$ advantage of ratio method: cancellation of uncertainties

- Photons and $\pi^0$s (and $\eta$) are measured via conversion method $\pi^0 \rightarrow \gamma\gamma$, $\gamma \rightarrow e^+e^-$

# Photon Reconstruction with ITS and TPC

## Secondary Vertex Algorithm - V0 Particles

- Charged tracks with large impact parameter are paired
- Candidates with a small DCA $\rightarrow$ V0 candidate
- Most abundant particle species: $K_s^0$, $\Lambda$, $\bar{\Lambda}$ or $\gamma$
- Photon conversion probability in $|\eta| < 0.9$ up to $R = 180\,\mathrm{cm}$ at 8.5%

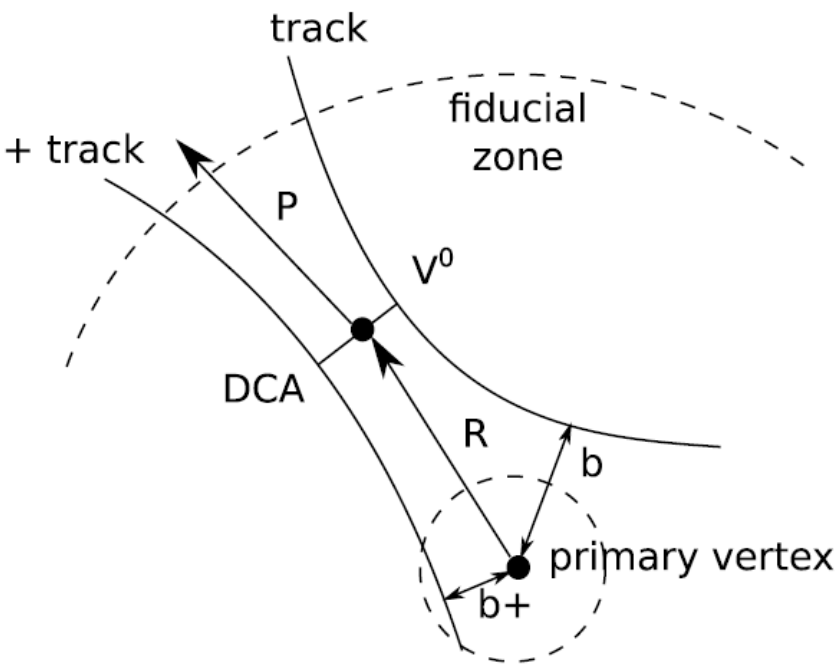


- Cuts on the decay topology of photons and electron track properties $\rightarrow$ Purity at 90% at $2\,\mathrm{GeV/c}$ for 0-40% Pb-Pb events
- Background is mainly combinatorial - Strange particle contribution negligible

# Photon Corrections and Invariant Cross Section for pp

- Raw $\gamma$ spectrum in pp and Pb-Pb corrected for:
  - purity ($\mathcal{P}$)
  - efficiency ($\mathcal{E}$)
  - conversion probability ($\mathcal{C}$)

  and secondary photon candidates subtracted

- Inclusive photon cross section in pp: $E\frac{\mathrm{d}^3\sigma}{\mathrm{d}p^3} = \frac{1}{2\pi}\frac{\sigma_{MB_{OR}}}{N_{events}}\frac{1}{p_T}\frac{\mathcal{P}}{\mathcal{C}\mathcal{E}}\frac{N^{\gamma_{prim}}}{\Delta y \Delta p_T}$

Main sources of uncertainty:

- Material budget of the detector $\sim$ 4.5%
- Efficiency estimation by cut variations

  $p_T < 5\,\mathrm{GeV}$: pp $\sim$ 3%, Pb-Pb $\sim$ 6%

  $p_T > 5\,\mathrm{GeV}$: pp $\sim$ 6%, Pb-Pb $\sim$ 15%

  e.g. geometrical cuts, detector PID, sharing of tracks between sec. vertices

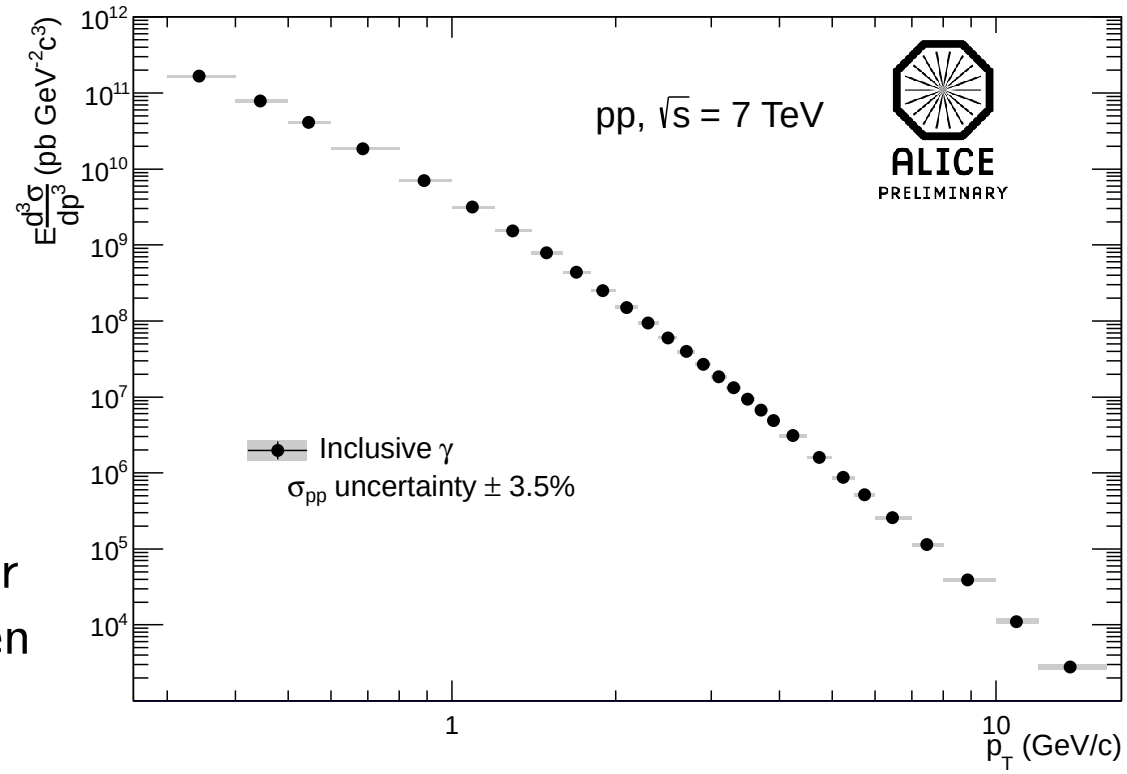

# Inclusive Photon Invariant Yield in Pb-Pb

- Two centrality selections: 0-40% and 40-80% (central and peripheral)

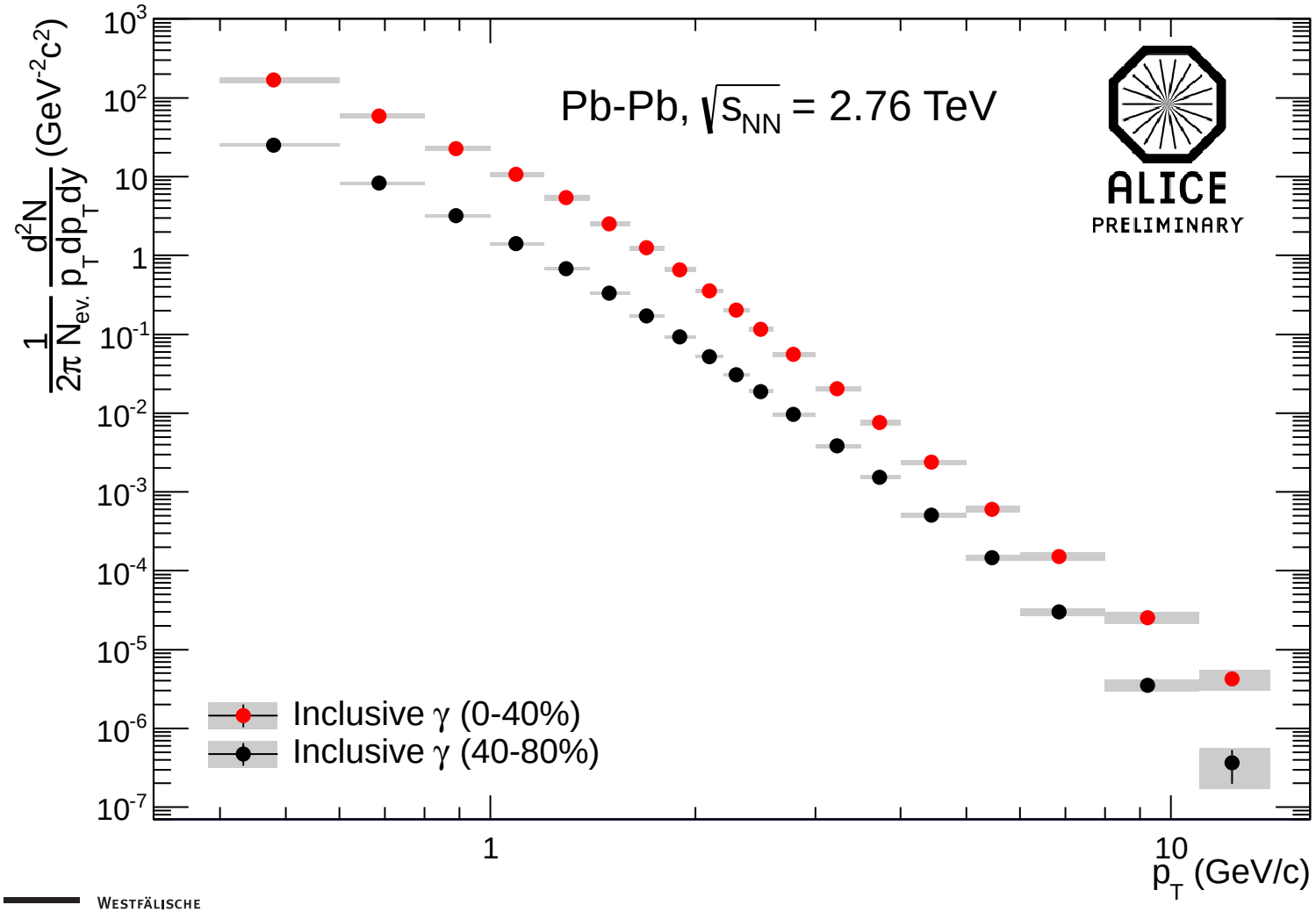

# $\pi^0$ and $\eta$ Reconstruction via Conversion

## Neutral pion and $\eta$ (pp only) based on converted photons

Measurement based on identical set of photons as used for photon results

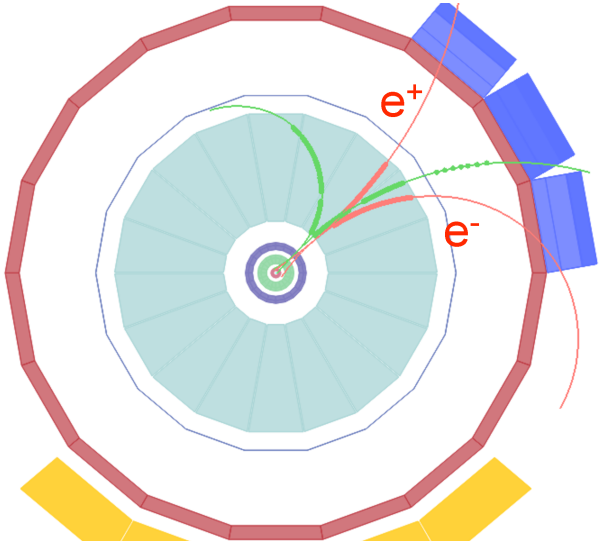


- Inv. mass calculated for all photon pairs in an event
- Combinatorial background obtained via mixed event technique
- Raw $\pi^0$ spectrum obtained by peak integration
- Efficiency and acceptance estimated with MC simulations
- For more details see:
  - pp at TeV: Phys. Lett. B 717, 162 (arXiv:1205.5724)
  - Pb-Pb and pp at 2.76TeV: published soon, similar method

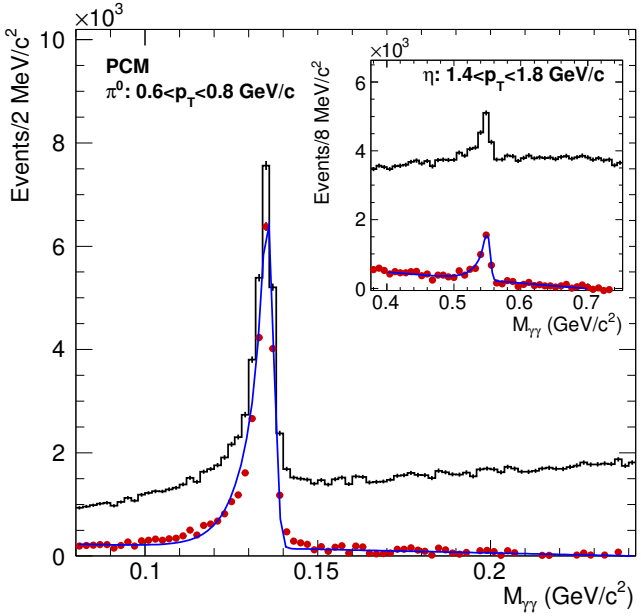

# Cocktail Generator

Decay photon spectra are obtained via calculation

- Based on a fit to measured $\pi^0$ and $\eta$ (in pp)
- Other meson spectra obtained via $m_T$-scaling
- Incorporated mesons: $\pi^0$, $\eta$, $\eta'$, $\omega$, $\phi$ and $\rho_0$

$m_T$-Scaling:
Same shape of cross sections, $f(m_T)$, of various mesons
$$E\frac{d^3\sigma_m}{dp^3} = C_m \cdot f(m_T)$$

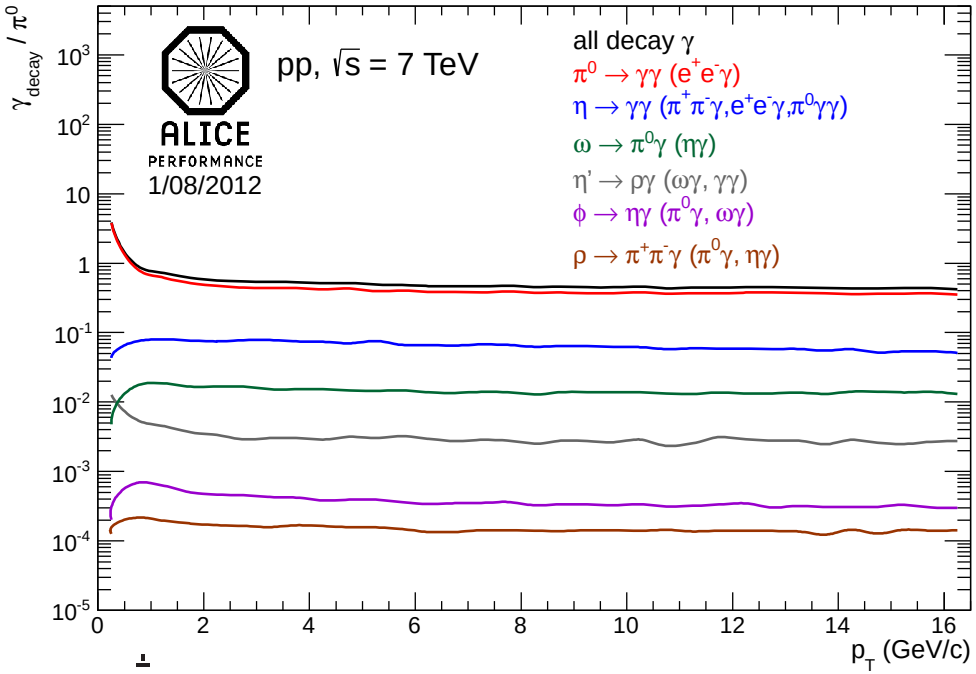


| Meson ($C_m$) | Mass | Decay Branch | B. Ratio |
|---|---|---|---|
| $\pi^0$ | 134.98 | $\gamma\gamma$ | 98.789% |
| | | $e^+e^-\gamma$ | 1.198% |
| $\eta$ | 547.3 | $\gamma\gamma$ | 39.21% |
| | | $\pi^+\pi^-\gamma$ | 4.77% |
| (0.48) | | $e^+e^-\gamma$ | $4.9 \cdot 10^{-3}$ |
| $\rho_0$ | 770.0 | $\pi^+\pi^-\gamma$ | $9.9 \cdot 10^{-3}$ |
| (1.0) | | $\pi^0\gamma$ | $7.9 \cdot 10^{-4}$ |
| $\omega$ | 781.9 | $\pi^0\gamma$ | 8.5% |
| (0.9) | | $\eta\gamma$ | $6.5 \cdot 10^{-4}$ |
| $\eta'$ | 957.8 | $\rho^0\gamma$ | 30.2% |
| | | $\omega\gamma$ | 3.01% |
| (0.25) | | $\gamma\gamma$ | 2.11% |
| $\phi$ | 1019.5 | $\eta\gamma$ | 1.3% |
| | | $\pi^0\gamma$ | $1.25 \cdot 10-3$ |
| (0.35) | | $\omega\gamma$ | $< 5\%$ |

Phys. Rev. C (arXiv:1110.3929)

# Direct Photons in pp Collisions at 7 TeV

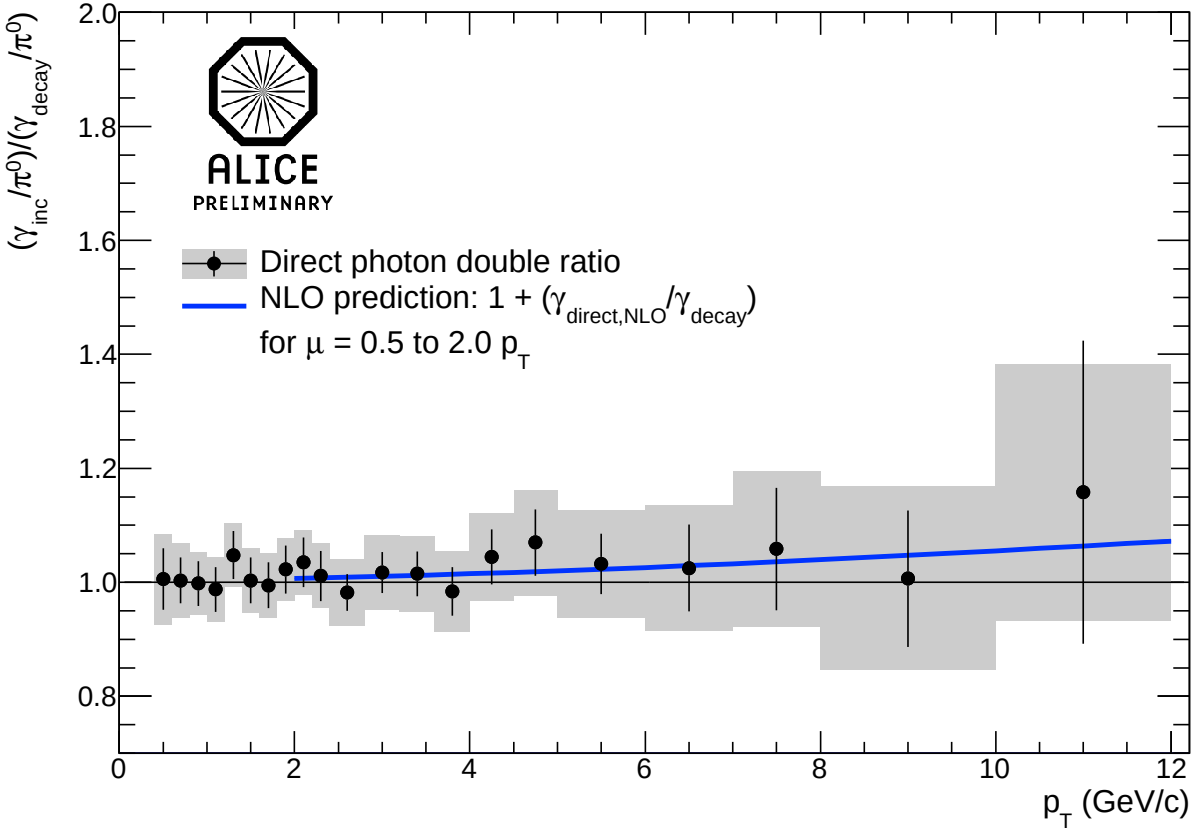


In the ratio uncertainties related to:

- normalization
- $\pi^0$ measurement
- rec. efficiency

partially or exactly canceled

Direct photon signal in pp at 7 TeV is consistent with zero

- The NLO double ratio prediction is plotted as $\mathcal{R}_{NLO} = 1 + \frac{\gamma_{direct,NLO}}{\gamma^{decay}_{cocktail}}$
- Measurement is consistent with the expected direct photon signal

# Double Ratio - Pb-Pb 2.76 TeV - peripheral

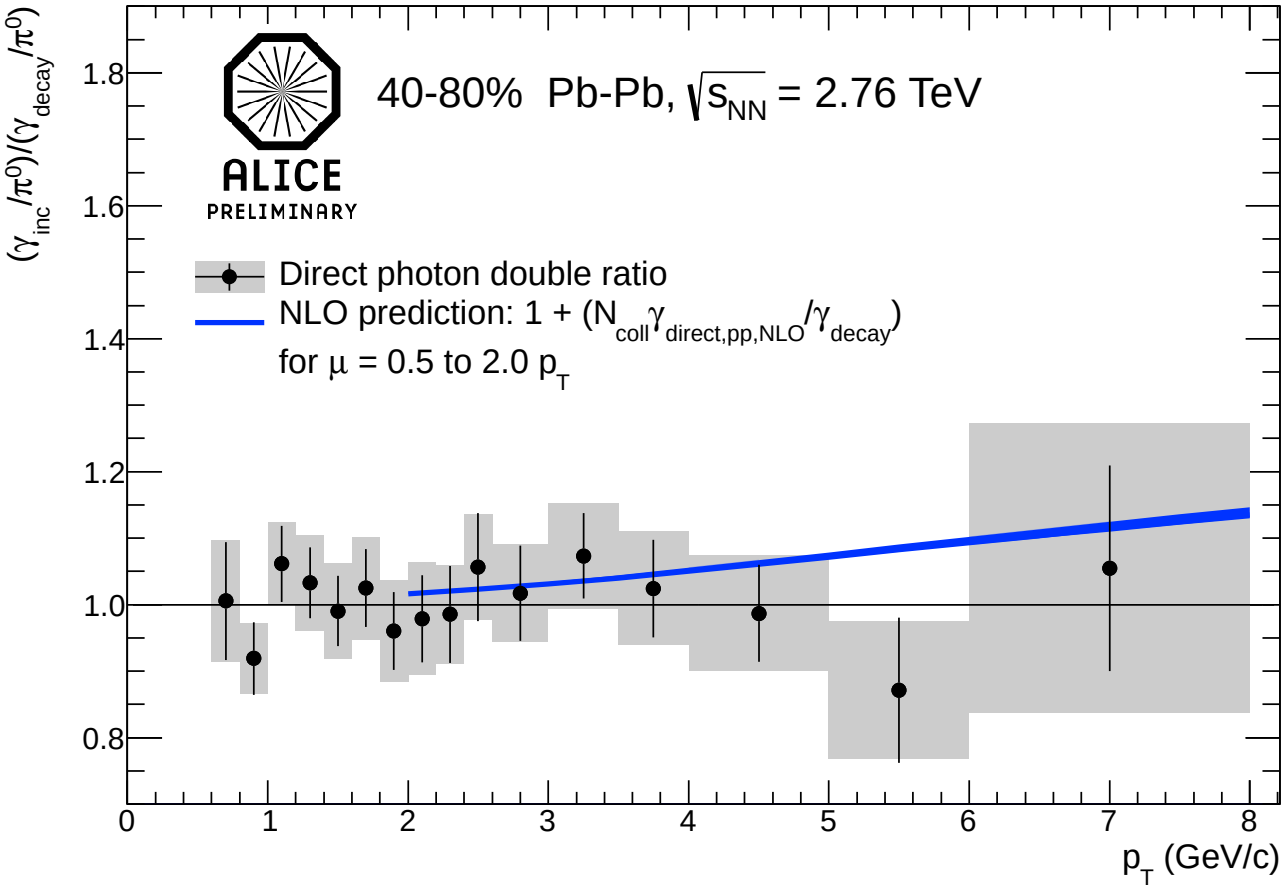


Double ratio for peripheral events shows no excess at any value of $p_T$

- Measurement is consistent with the expected direct photon signal
- pp NLO predictions scaled with $N_{coll}$

# Double Ratio - Pb-Pb 2.76 TeV - central

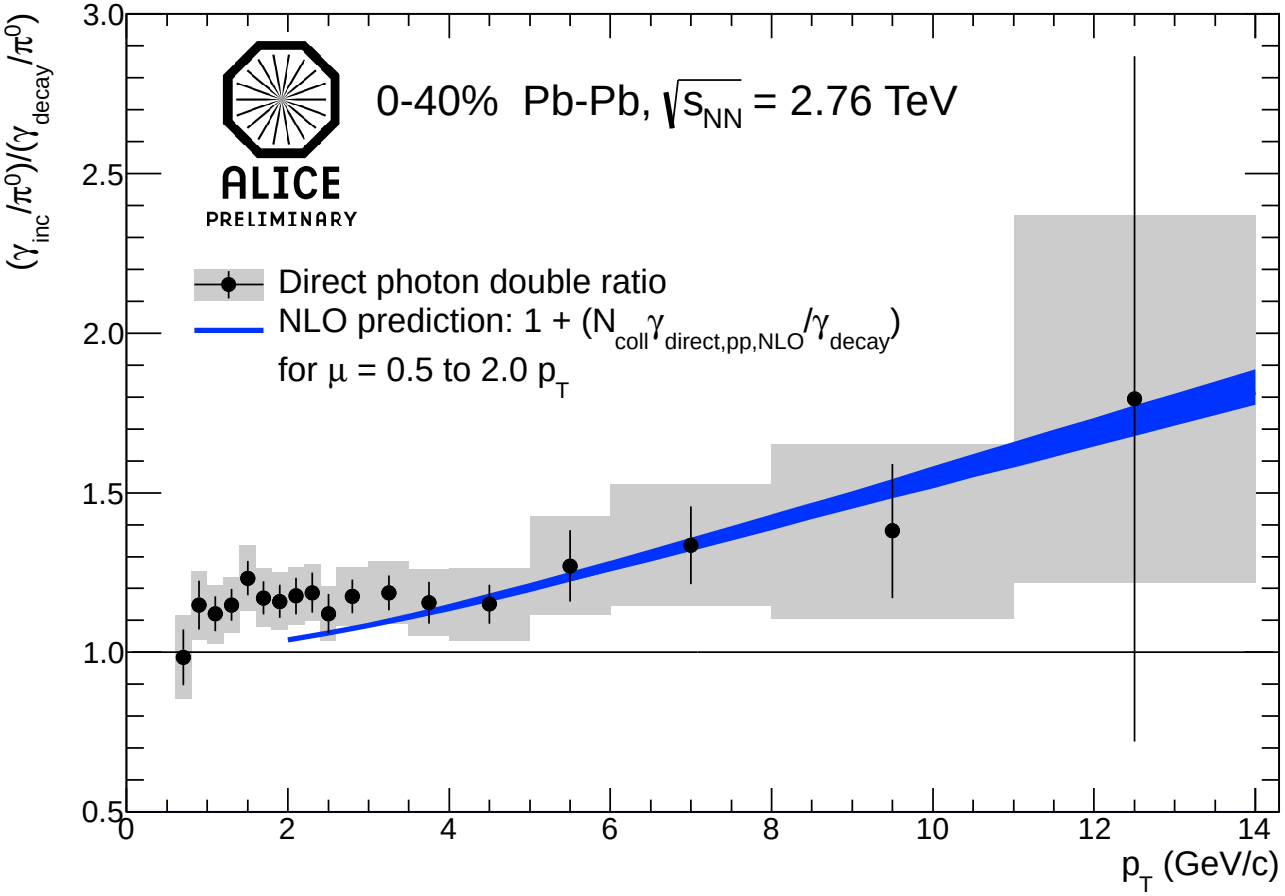


Clear extra yield of 20% for $p_T < 2\,\mathrm{GeV/c}$
$N_{coll}$ scaled pp NLO in agreement with high $p_T$ direct photons

# Double Ratio - Pb-Pb 2.76 TeV - central

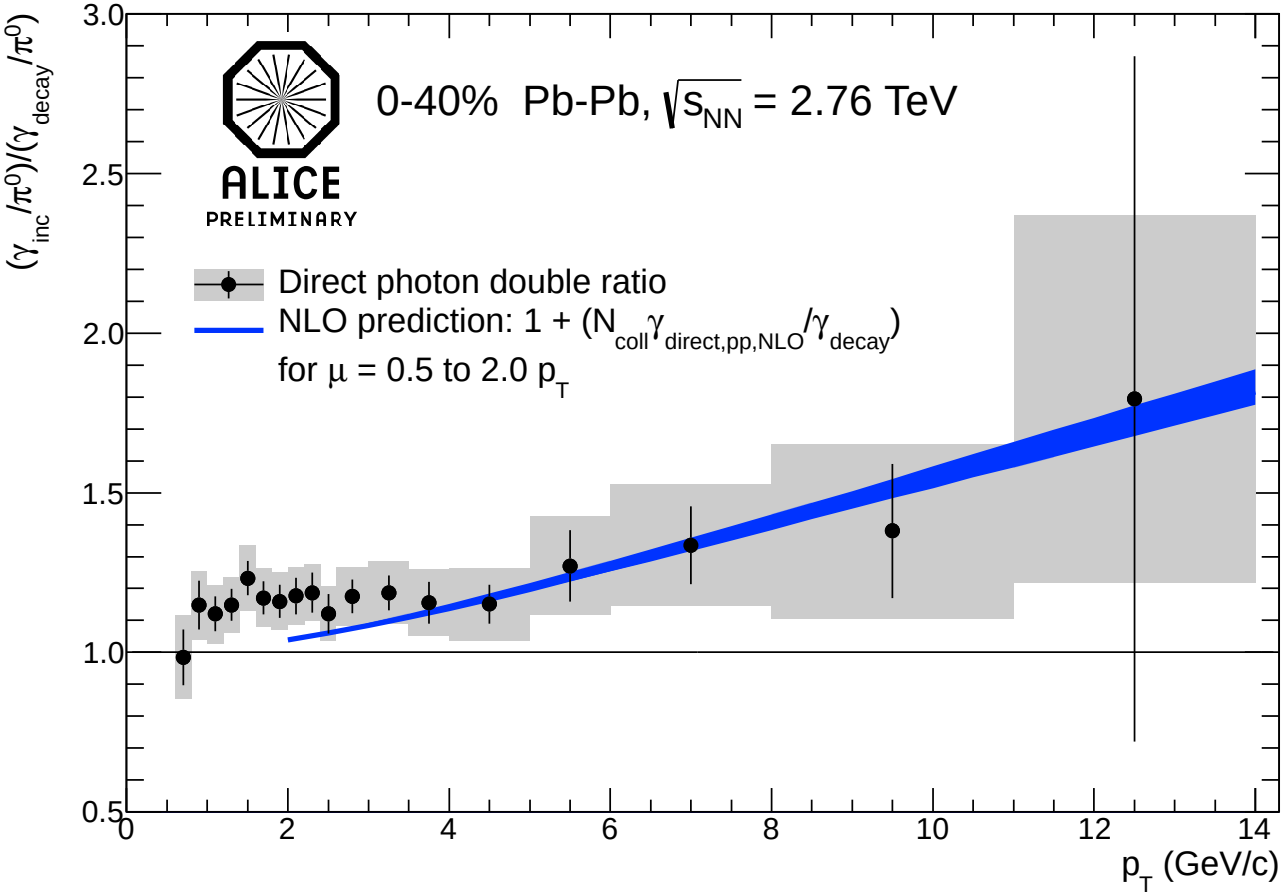


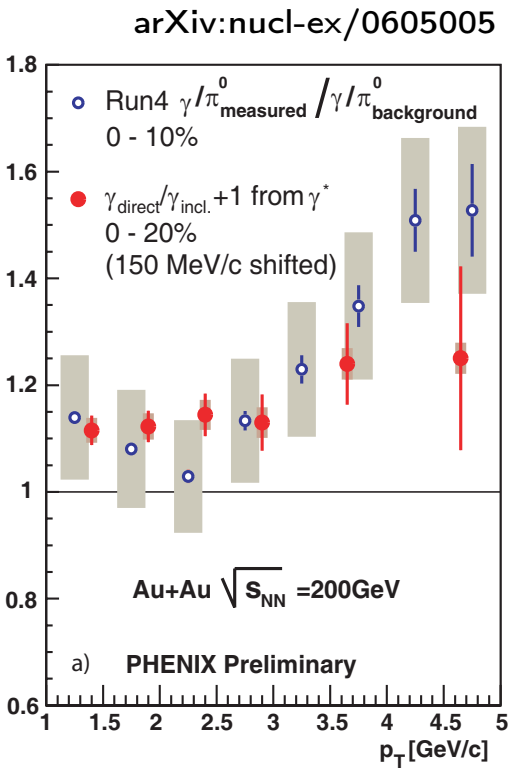


Clear extra yield of 20% for $p_T < 2\,\mathrm{GeV/c}$
$N_{coll}$ scaled pp NLO in agreement with high $p_T$ direct photons

- Similar to low $p_T$ direct photon observation by PHENIX

# Results of Pb-Pb Direct Photons at 2.76 TeV

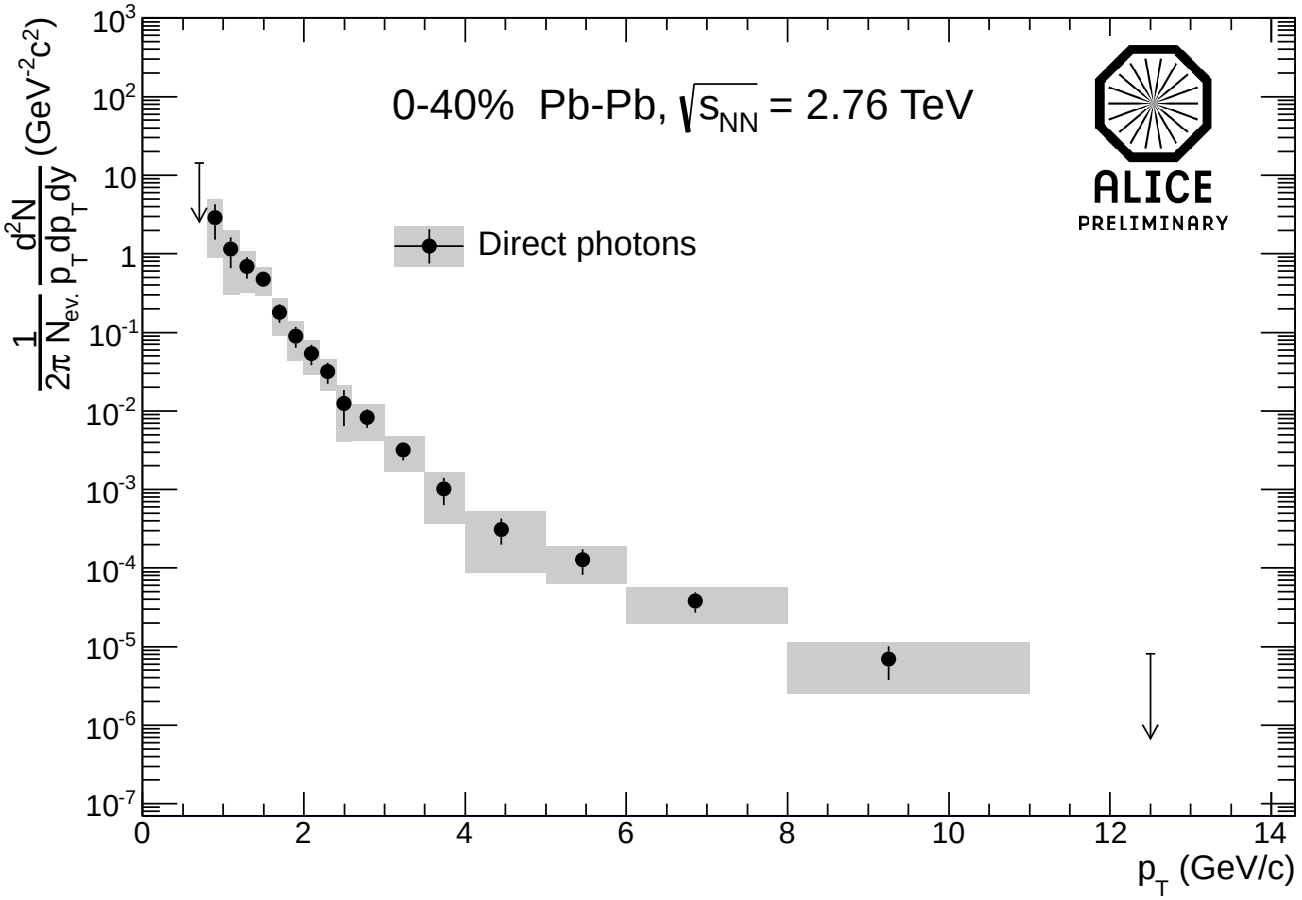


Direct Photon Spectrum for central Pb-Pb events

Spectrum derived from double ratio by:

$$\gamma_{direct} = (1 - \frac{\gamma_{decay}}{\gamma_{inc}}) \cdot \gamma_{inc}$$

# Results of Pb-Pb Direct Photons at 2.76 TeV

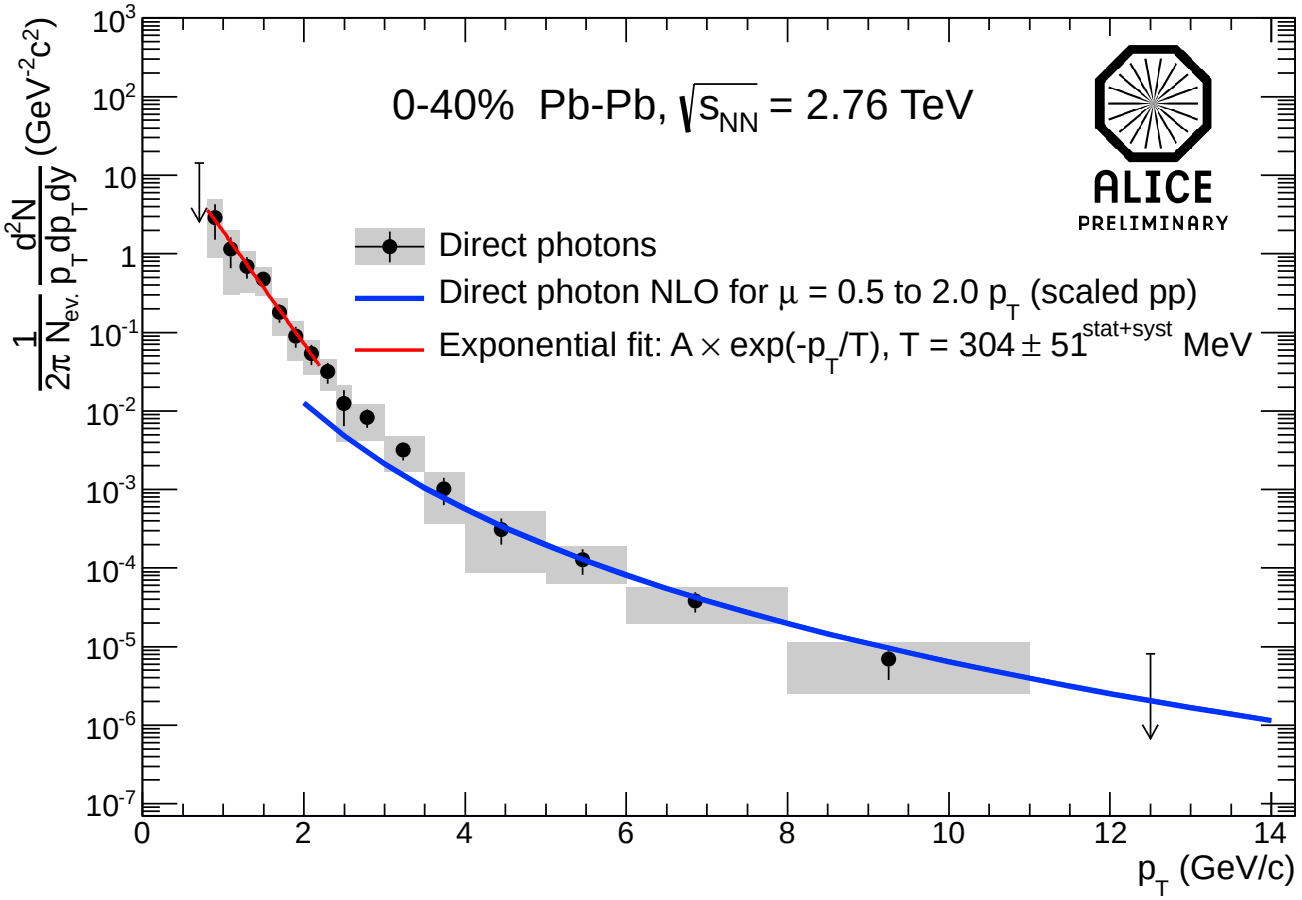


Direct Photon Spectrum for central Pb-Pb events

Spectrum derived from double ratio by:

$$\gamma_{direct} = (1 - \frac{\gamma_{decay}}{\gamma_{inc}}) \cdot \gamma_{inc}$$

- NLO predictions in agreement with spectrum ($p_T > 4\,\mathrm{GeV/c}$)
- At low $p_T$ ($< 2.2\,\mathrm{GeV/c}$) spectrum fitted with an exponential
  $\rightarrow$ slope parameter $T = 304 \pm 51^{\mathrm{stat+syst}}\,\mathrm{MeV}$
- Intermediate region: superposition of low and high $p_T$ direct photons

# Conclusions I: Direct Photon Spectra

- Statistical analysis of direct photons based on converted photons via double ratio
- With current uncertainties no significant direct photon signal in pp and peripheral Pb-Pb
- Direct photon signal is consistent with expectation from NLO pQCD

- In central Pb-Pb:
  Low $p_T$ direct photon signal, exponential in shape
- Similar excess measured at RHIC interpreted as thermal signal

  Slope parameter:
  - $T_{ALICE} = 304 \pm 51^{\mathrm{stat+syst}}\ \mathrm{MeV}$ (0-40%)
  - $T_{PHENIX} = 221 \pm 19^{\mathrm{stat}} \pm 19^{\mathrm{syst}}\ \mathrm{MeV}$ (0-20%)

  arxiv:0804.4168 PRL 104 (132301) 2010

# Part II: Direct Photon $v_2$

# What can we learn from direct photon $v_2$?

Initial azimuthal asymmetry in coordinate space in non-central A+A
$\Rightarrow$ asymmetry in momentum space

$$\frac{dN}{d\phi} = \frac{1}{2\pi}\left(1 + 2\sum_{n\geq 1} v_n \cos(n(\phi - \Psi_n^{RP}))\right)$$

- $v_2$: elliptic flow, collective expansion at low $p_T$
- $v_2$ at high $p_T$: path length dependence of in-medium parton energy loss

Thermal Photon $v_2$

- Constrains onset of direct photon production
  - Early production $\rightarrow$ small flow
  - Late production $\rightarrow$ hadron-like flow

ideal hydro th. photon $v_2$ for different QGP formation times $\tau_0$

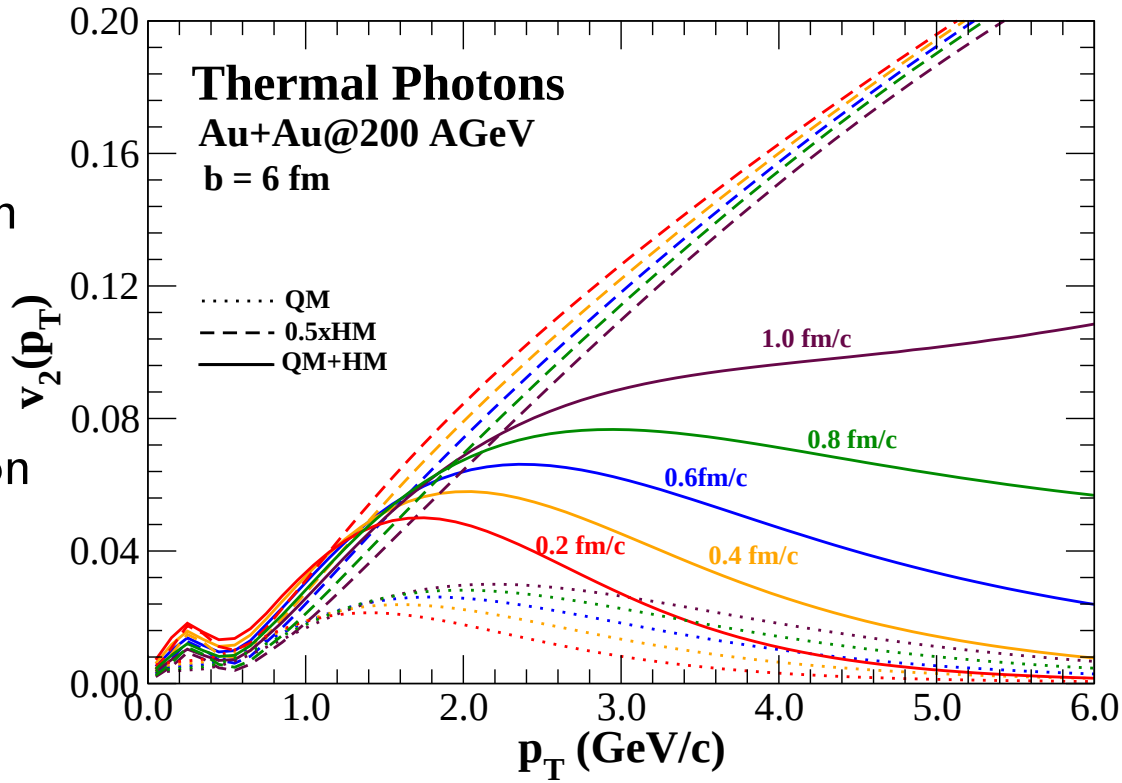


arXiv:0809.0548 [nucl-th]

# General Strategy of the $v_2$ Analysis

Direct photon $v_2$ obtained via comparison between measured and calculated decay photon $v_2$

$$v_2^{\text{direct } \gamma} = \frac{R \cdot v_2^{\text{inc } \gamma} - v_2^{\text{decay } \gamma}}{R-1}$$

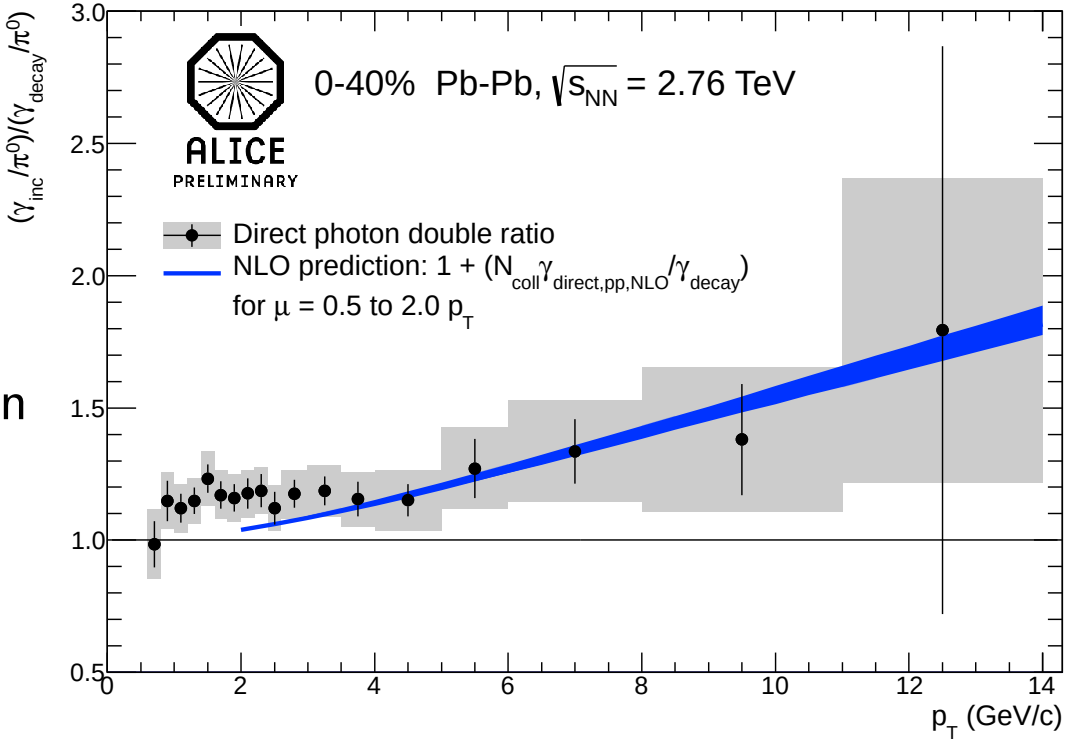


Factor $R$ represents the direct photon double ratio

- $R \cdot v_2^{\text{inc } \gamma}$: weighted inclusive photon $v_2$ due to extra photons compared to background
- $v_2^{\text{decay } \gamma}$: calculated decay photon $v_2$ from cocktail calculation

# Inclusive Photon $v_2$ Analysis

$v_2$ given by the reaction plane

$$v_2 = \langle \cos(2(\phi - \Psi_2^{RP})) \rangle$$

Extracted via this formula or by a fit

Event Plane angle determined by using the VZERO detector

- VZEROA: $2.8 < \eta < 5.1$
- VZEROC: $-3.7 < \eta < -1.7$

Reaction plane resolution obtained by the three sub-event method

Relation of RP to EP:

$$v_2 = \frac{v_2^{EP}}{\langle \cos(2\Psi_2^{EP} - \Psi_2^{RP}) \rangle} = \frac{v_2^{\mathrm{raw}}}{\text{resolution}}$$

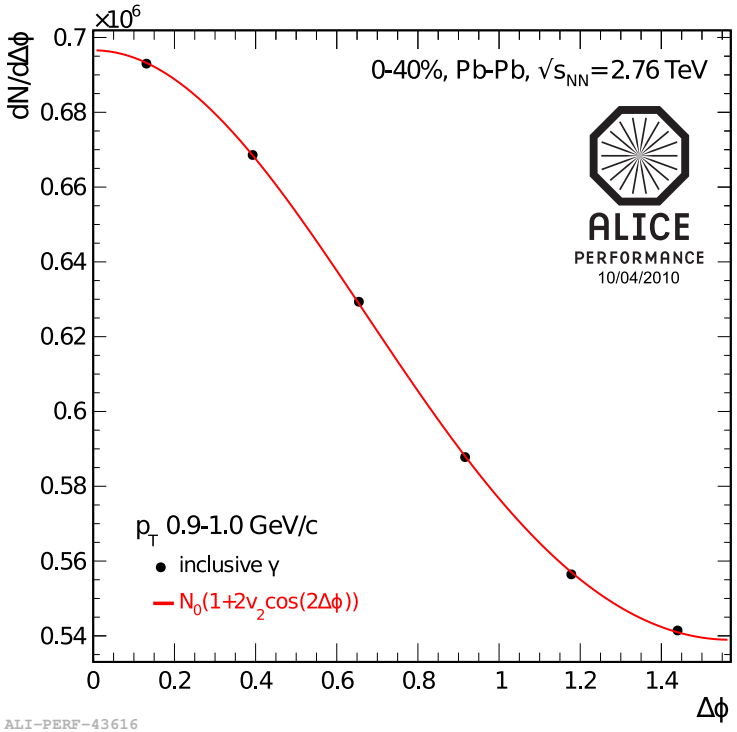


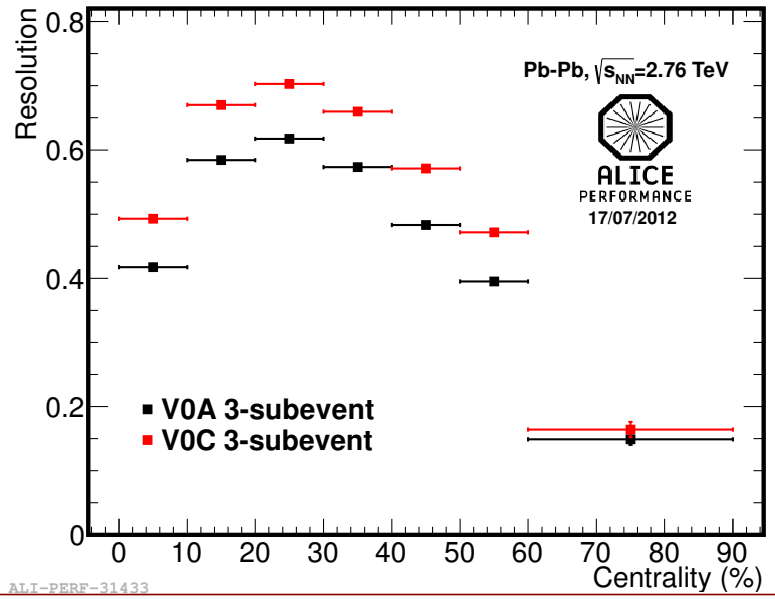

# Inclusive Photon $v_2$ Results 0-40%

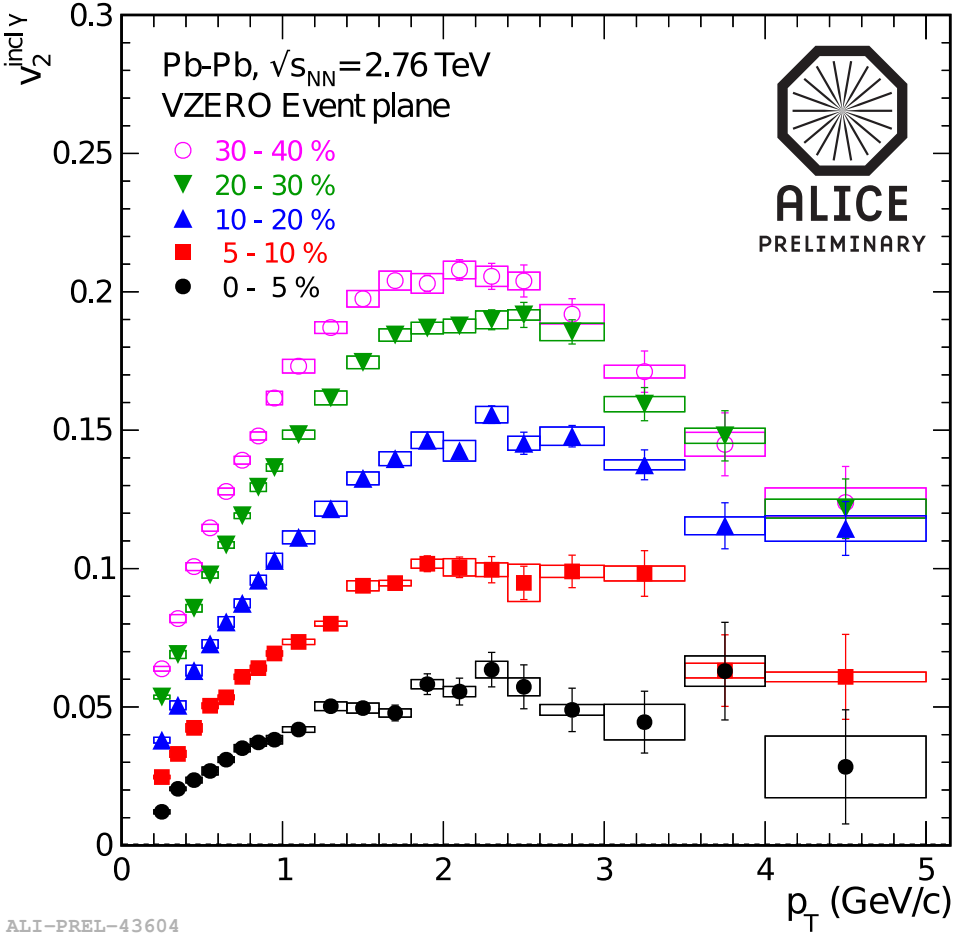


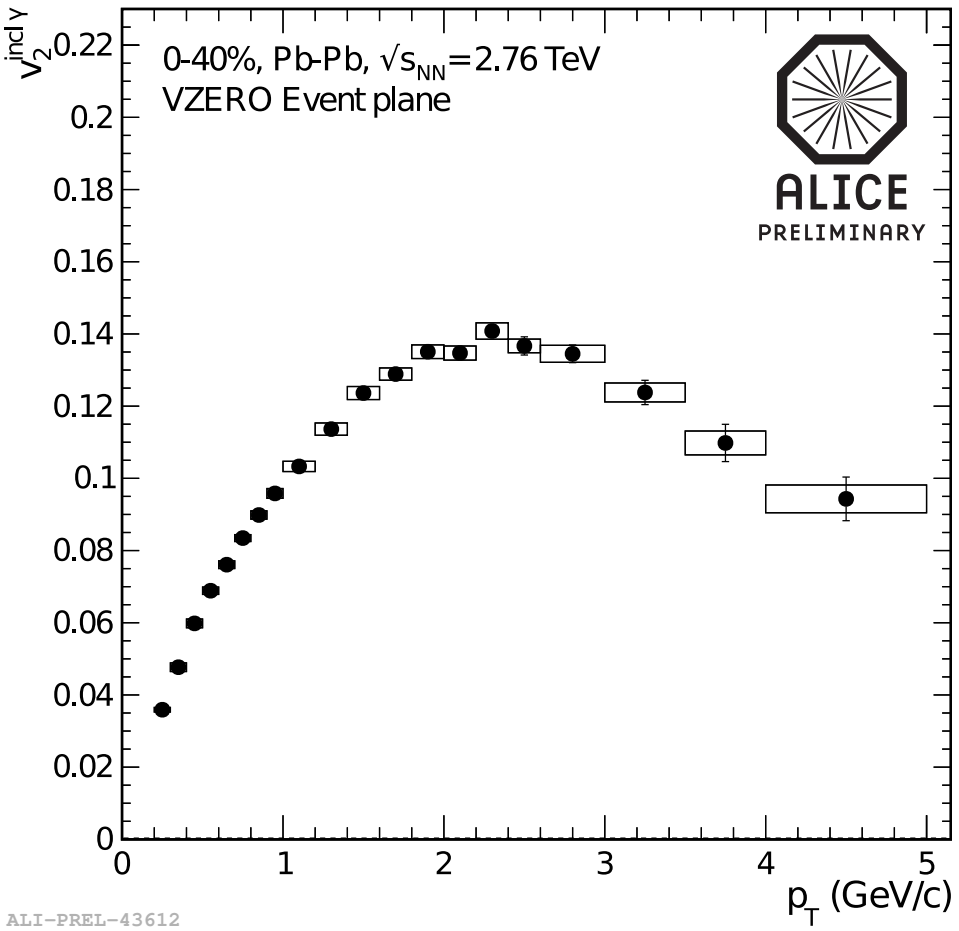


- Magnitude of $v_2$ increases with decreasing centrality
- Similar $v_2$ to hadrons
- Expected behavior, main contributions are decay photons

# Cocktail Simulation and Decay Photon $v_2$

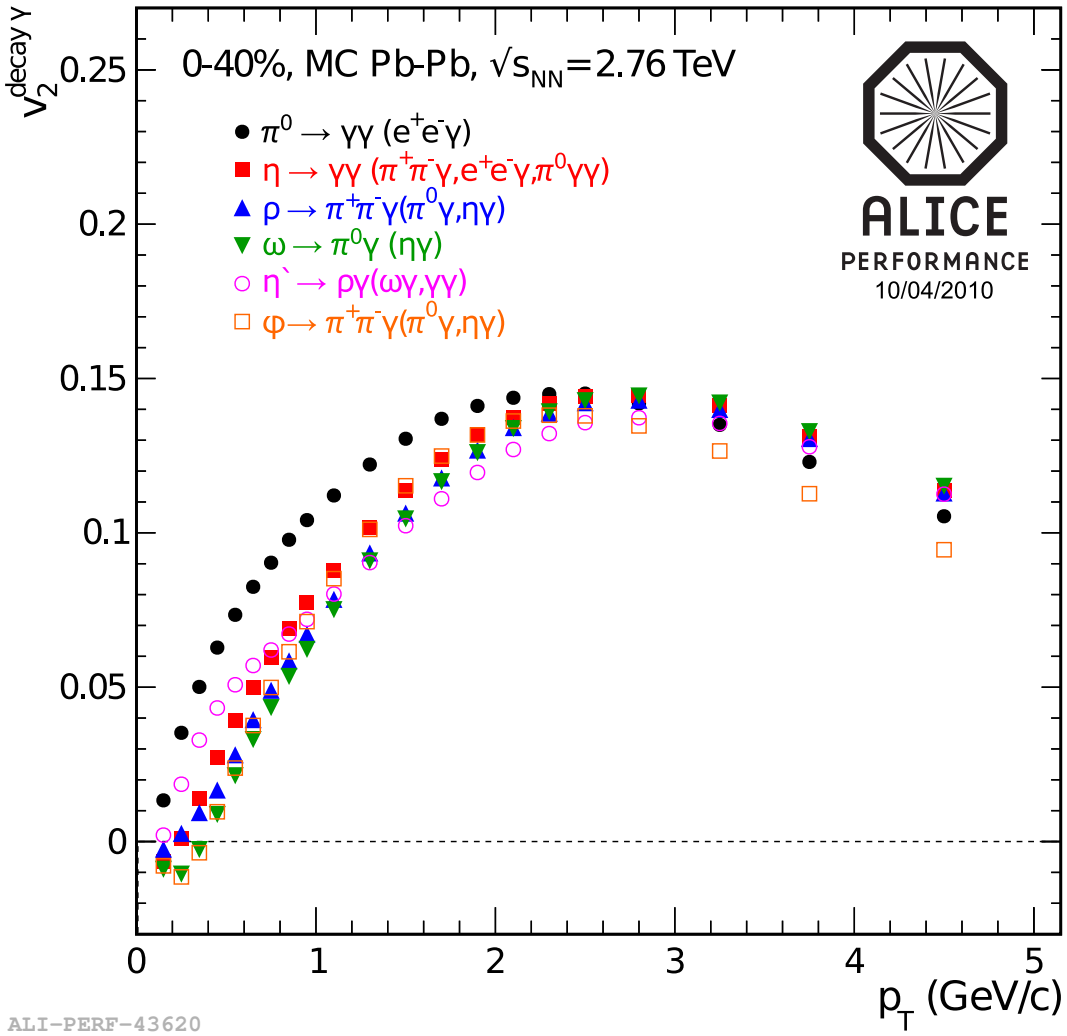


- Spectra of other mesons with photon decay branches obtained by $m_T$ scaling
- Assumption: $v_2^{\pi^0} = v_2^{\pi^\pm}$
- $v_2$ of various mesons (X) calculated via $KE_T$ (quark number) scaling from $v_2^{\pi^\pm}$
- Decay photon $v_2^X$ obtained by cocktail calculation

$$v_2^X(p_T^X) = v_2^{\pi^\pm}\left(\sqrt{(KE_T^X + m^{\pi^\pm})^2 - (m^{\pi^\pm})^2}\right)$$

with:

$$KE_T = m_T - m = \sqrt{p_T^2 + m^2} - m$$

# Comparison of Inclusive and Decay $v_2$

- Above 3 GeV/c inclusive photons significantly smaller than decay photons

→ Direct photon $v_2$ contribution with $v_2^{\mathrm{direct}} < v_2^{\mathrm{inc}}$

- Below 3 GeV/c consistent within uncertainties

→ Either contribution of direct photons with similar $v_2$ or no direct photons

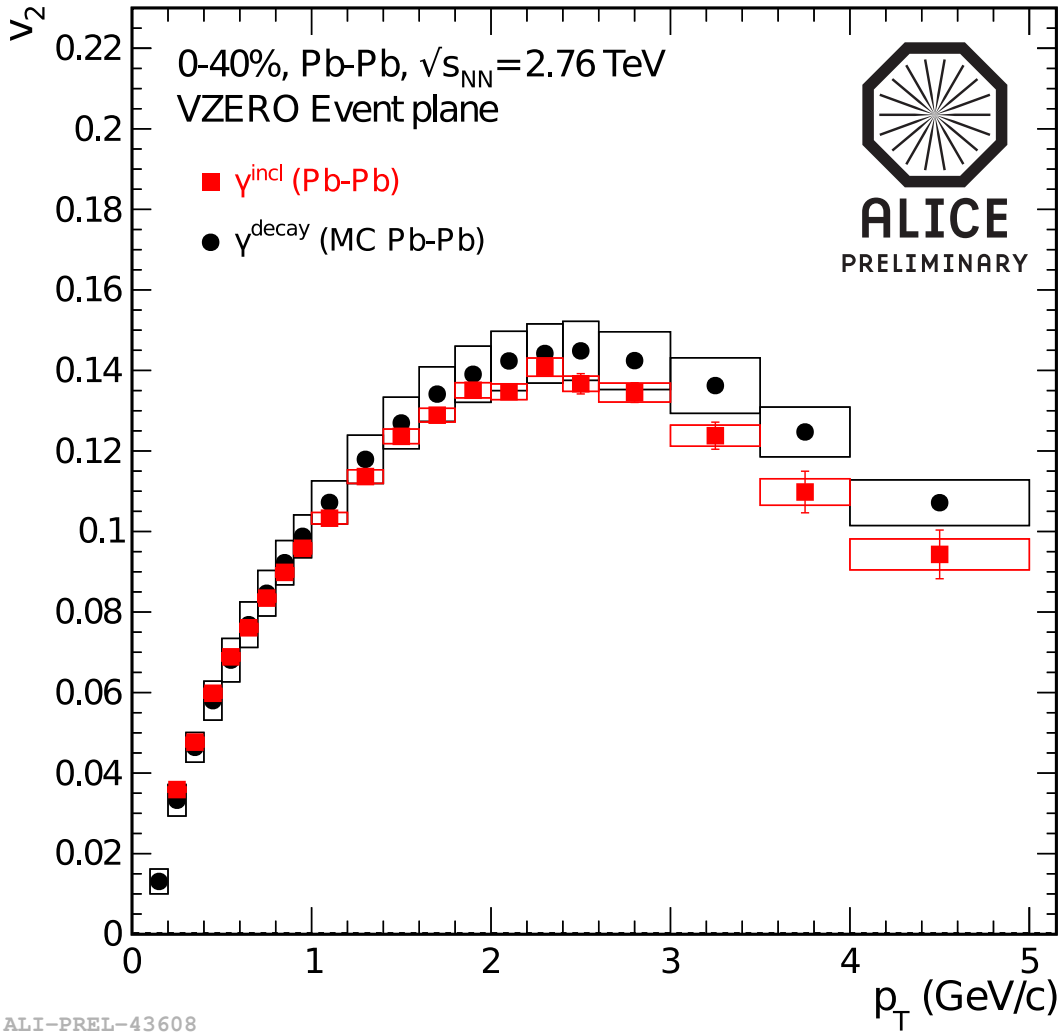

# Direct Photon $v_2$ 0-40% and Conclusions II

- Significant direct photon $v_2$ for $p_T < 3\,\mathrm{GeV/c}$ measured
- Magnitude of $v_2$ comparable to hadrons
- Result points to late production times of direct photons after flow is established
- Large inverse slope parameter of low $p_T$ direct photon spectrum favours earlier production times
- Similar direct photon $v_2$ results seen by PHENIX

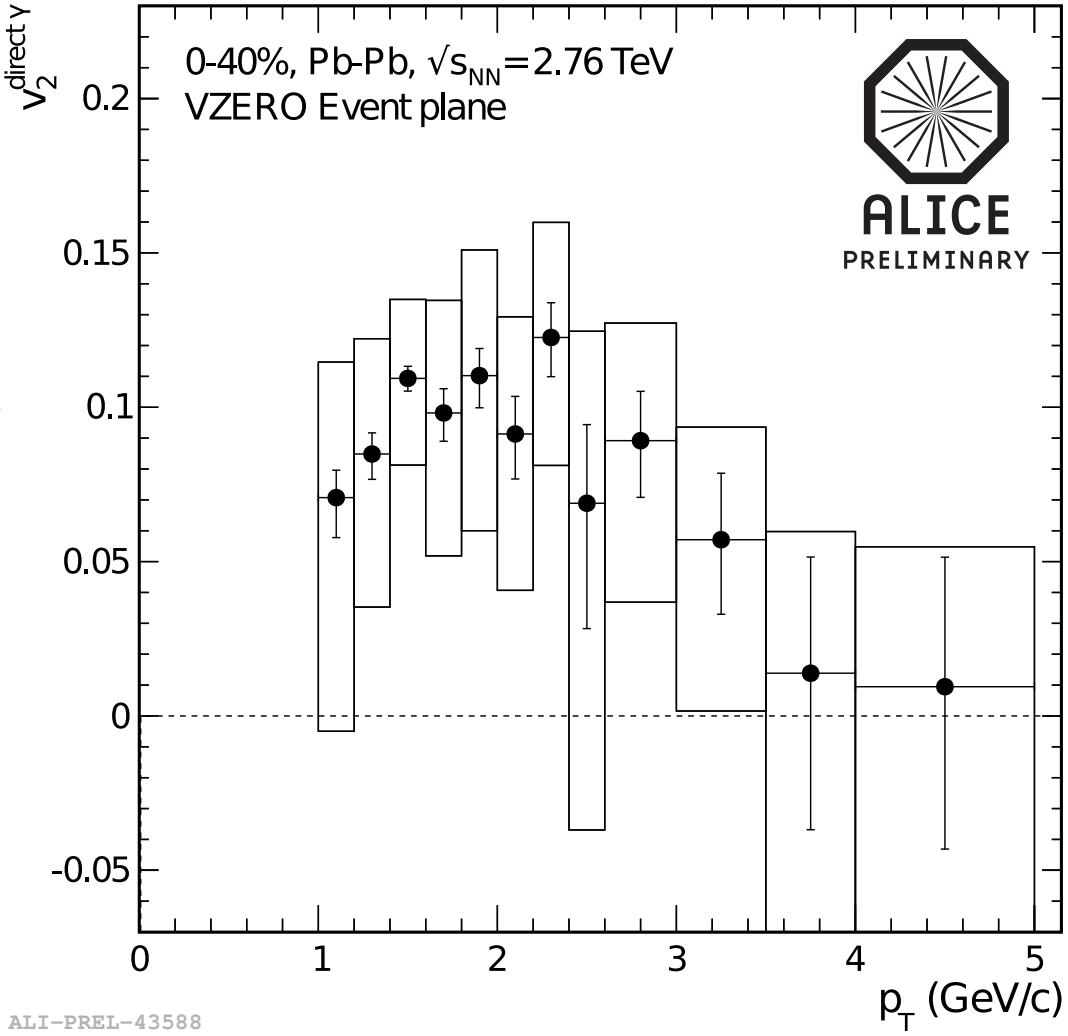

# Backup Slides

# Denominator Ratio: Cocktail Generator Pb-Pb Results

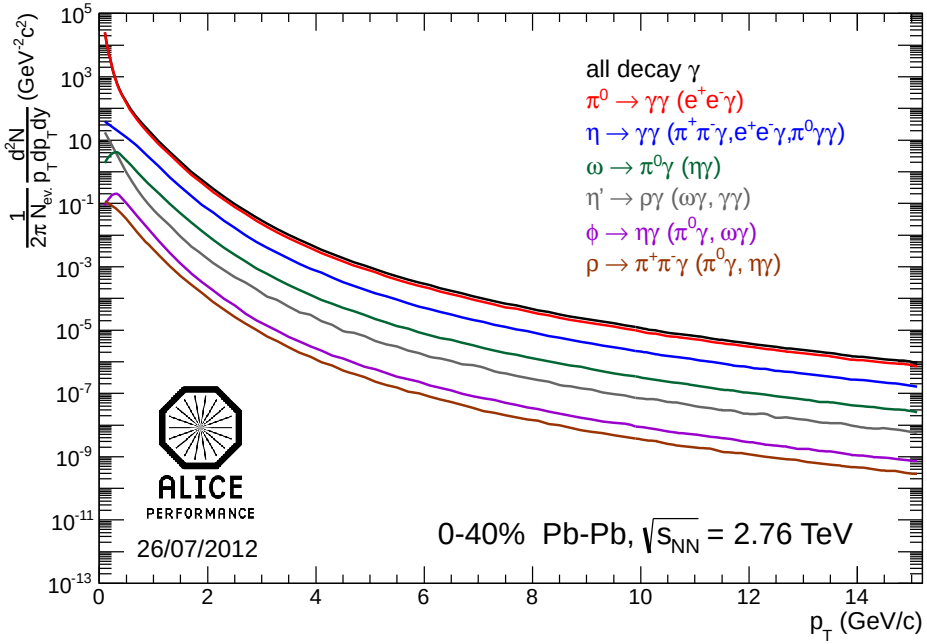


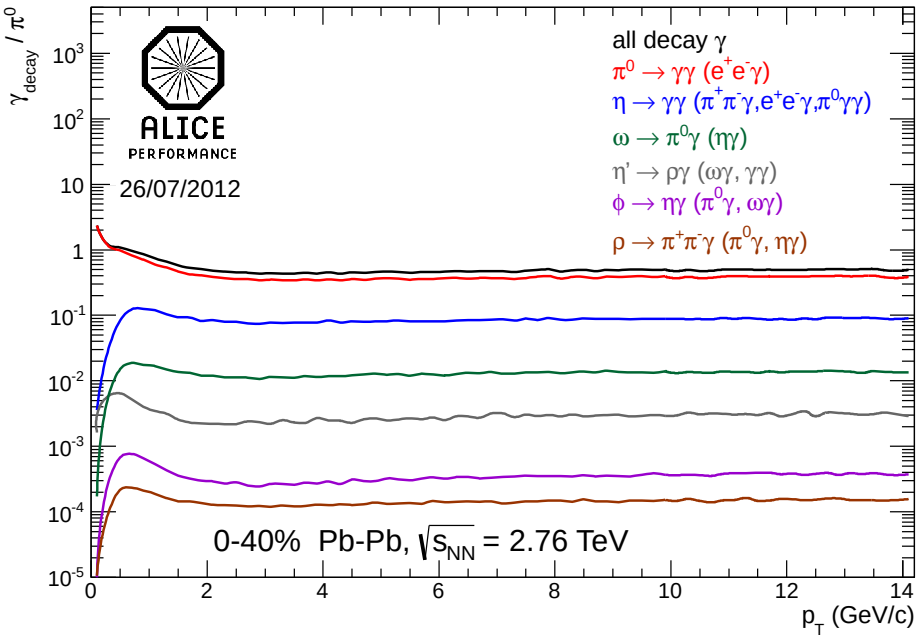


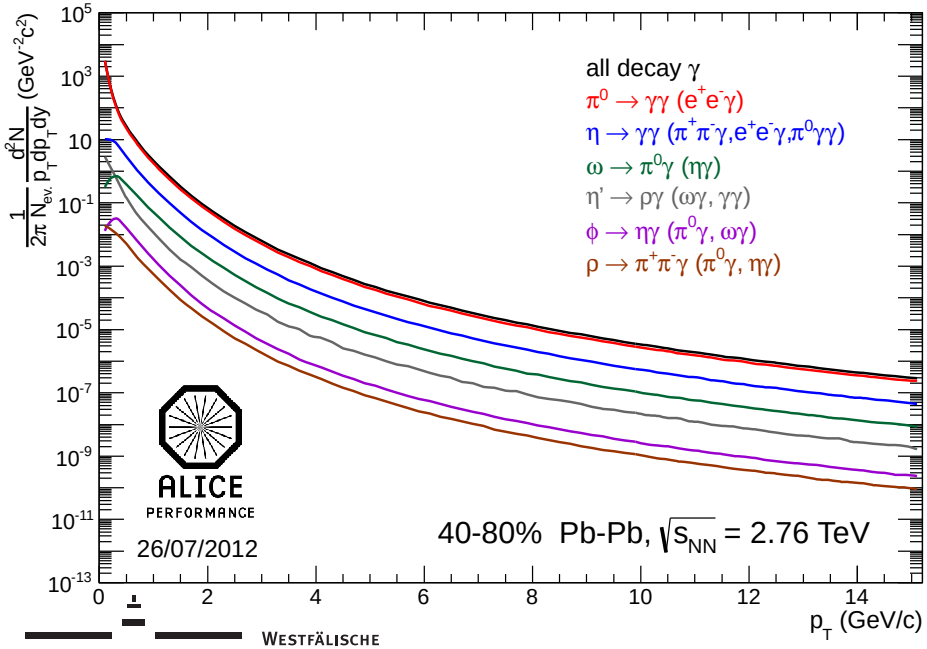


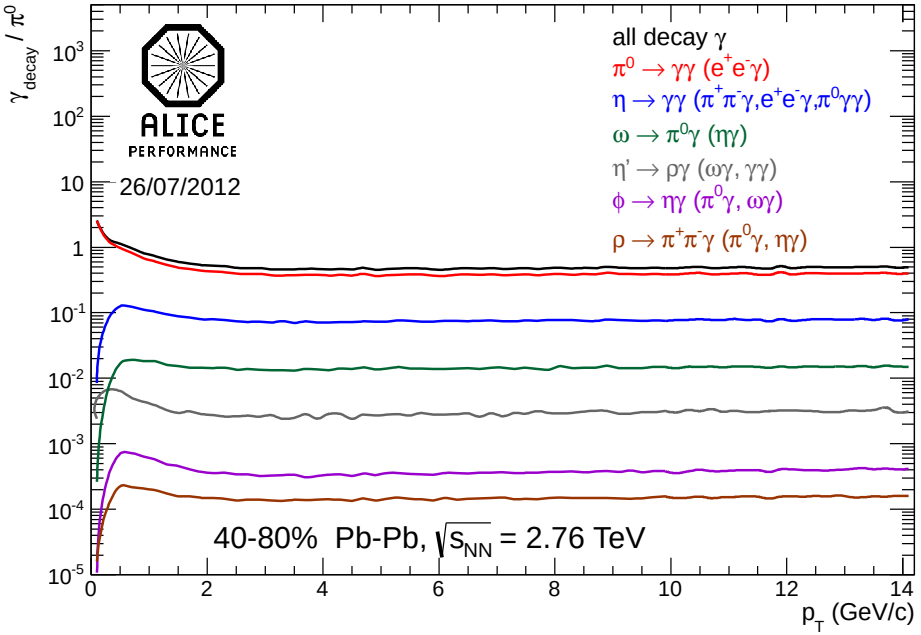

# Combined Fit for Direct Photons

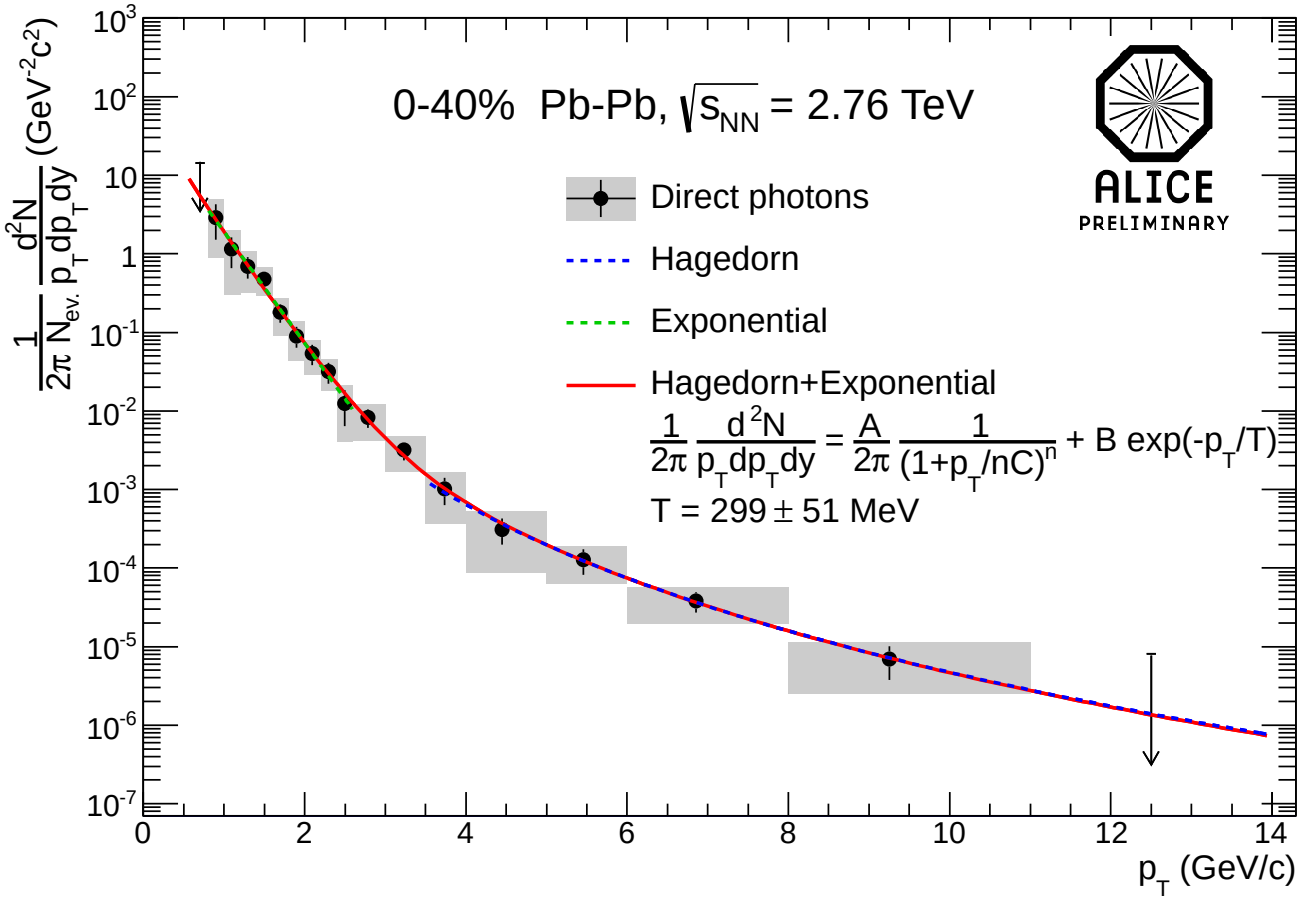


Combined fit (Hagedorn + Exponential) gives similar result for the inverse slope parameter $T$ as for the exponential only fit

# Systematic Cut Studies pp

- Cut Variations for $\gamma$ and $\pi^0$:

| Cut Name | Std. value | Variation 1 | Variation 2 | Variation 3 |
|---|---|---|---|---|
| Electron dEdx | -4,5$\sigma$ | -4,4$\sigma$ | -3,4$\sigma$ | - |
| Pion dEdx | 1,-10$\sigma$ | 2,1$\sigma$ | 2,0.5$\sigma$ | 2,0.5$\sigma$ |
| Min. p $e^+/e^-$ | 0.4 GeV/c | 0.4 GeV/c | 0.4 GeV/c | 0.3 GeV/c |
| Find. Cls. TPC | 0.35 | 0.6 | - | - |
| Photon $\chi^2$ | 20 | 30 | 10 | - |
| $q_t$ | 0.05 | 0.07 | 0.03 | - |
| min. $p_t$ $e^+/e^-$ | 50 MeV/c | 75 MeV/c | 100 MeV/c | - |
| photon $\eta$, $\pi^0$ $y$ | 0.9, 0.8 | 0.8, 0.7 | 1.2, 0.9 | - |
| min. R | 5 cm - 180 cm | 2.8 cm - 180 cm | 10 cm - 180 cm | - |

  - V0s with shared electrons rejected
  - Purity for different centralities used
  - TOF and $\alpha$ cut not used for pp
  - R cut already considered for material budget

- $\pi^0$ yield extraction:
  - Three different integration windows
  - Different Numbers of mixed events for bg, different mixed event bins (n V0s, n tracks)

- Cocktail simulation:
  - Two different fits
  - Variation of the $m_t$ scaling factors ($\eta$ measured)

# Systematic Cut Studies Pb-Pb

- Cut Variations for $\gamma$ and $\pi^0$:

| Cut Name | Std. value | Variation 1 | Variation 2 | Variation 3 |
|---|---|---|---|---|
| Electron dEdx | -3,5$\sigma$ | -4,5$\sigma$ | -2.5,4$\sigma$ | - |
| Pion dEdx | 3,-10$\sigma$ | 2.5,-10$\sigma$ | 3.5,-10$\sigma$ | 3,-10$\sigma$ |
| Min. p $e^+/e^-$ | 0.4 GeV/c | 0.4 GeV/c | 0.4 GeV/c | 0.3 GeV/c |
| Find. Cls. TPC | 0.6 | 0.7 | 0.35 | - |
| Photon $\chi^2$ | 10 | 5 | 20 | - |
| $q_t$ | 0.05 | 0.03 | 0.07 | - |
| min. $p_t$ $e^+/e^-$ | 50 MeV/c | 75 MeV/c | 100 MeV/c | - |
| photon $\eta$, $\pi^0$ $y$ | 0.75, 0.7 | 0.9, 0.8 | 0.8, 0.7 | - |
| min. R | 5 cm - 180 cm | 2.8 cm - 180 cm | 10 cm - 180 cm | - |
| $\alpha$ meson central | 0.65 | 1.00 | - | - |
| $\alpha$ meson peripheral | 0.8 | 1.00 | - | - |
| TOF | -5,-5$\sigma$ | -3,-5$\sigma$ | -2,-5$\sigma$ | - |

  - V0s with shared electrons rejected
  - Purity for different centralities used

- $\pi^0$ yield extraction:
  - Three different integration windows
  - Different Numbers of mixed events for bg, different mixed event bins (n V0s, n tracks)

- Cocktail simulation:
  - Two different fits, with and without blast wave
  - Variation of the $m_t$ scaling factors

# PHENIX Direct Photon $v_2$ Results

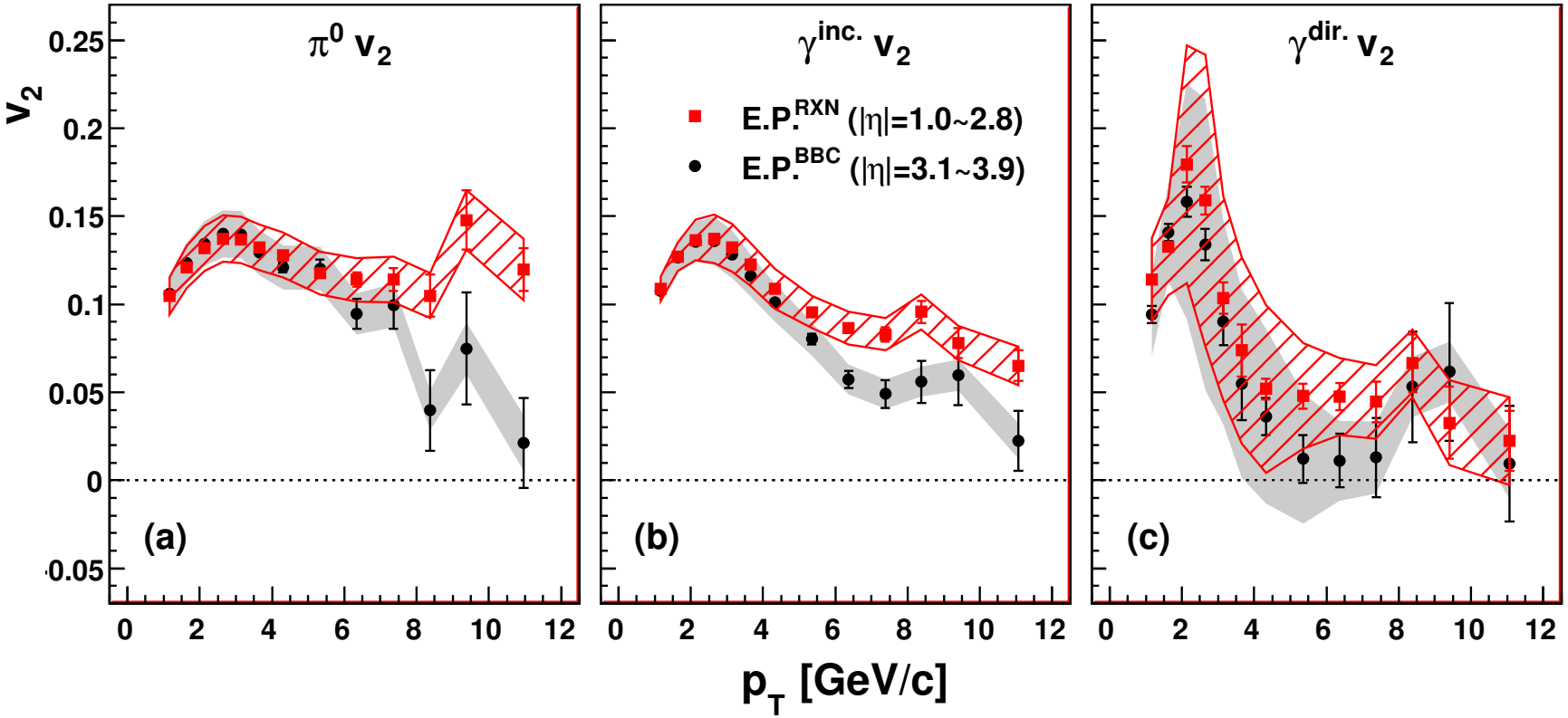

# Future dilepton measurements from STAR Upgrades

Zhangbu Xu
(Brookhaven National Lab)

- Free Quarks
  - Color Screening of Heavy Quarkonia
- Excited Vacuum
  - Novel symmetries in QCD
  - Dileptons as tool to systematically study Chiral Symmetry Restoration
- Projections from STAR Upgrades
  - Inner TPC Upgrade (iTPC) and Beam Energy Scan (II)
  - Muon Telescope Detector (dimuon and e-$\mu$)
  - Heavy-Flavor Tracker (HFT)

# 1. FREE QUARKS
# 2. EXCITED VACUUM

Quark Matter 1995



## 1. TWO PUZZLES OF MODERN PHYSICS

The status of our present theoretical structure can be summarized as follows:

**QCD** (strong interaction)
$SU(2) \times U(1)$ **Theory** (electroweak)
**General Relativity** (gravitation).

However, in order to apply these theories to the real world, we need a set of about 18 parameters, all of unknown origins. Thus, this theoretical edifice cannot be considered complete.

The two outstanding puzzles that confront us today are:

i) **Missing symmetries** - All present theories are based on symmetry, but most symmetry quantum numbers are *not* conserved.

ii) **Unseen quarks** - All hadrons are made of quarks; yet, no individual quark can be seen.

These two puzzles have been with us for several decades, beginning with parity nonconservation in the fifties and $CP$ and time reversal violations in the sixties. They are perhaps of an equal profundity as the puzzles which faced our predecessors around the turn of the century.

1. Color Screening of Quarkonia
2. In-medium ρ spectral function



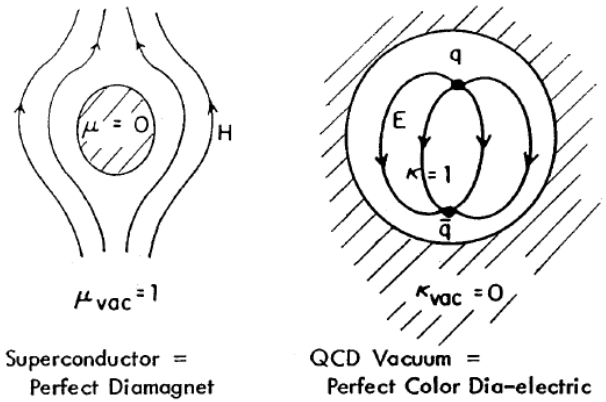


**Figure 1.** Superconductivity in QED vs. quark confinement in QCD.

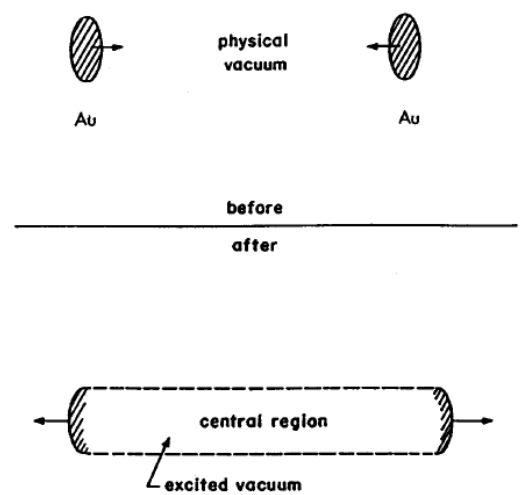


**Figure 2.** Vacuum excitation through relativistic heavy ion collisions.

# Dilepton Mass Ranges

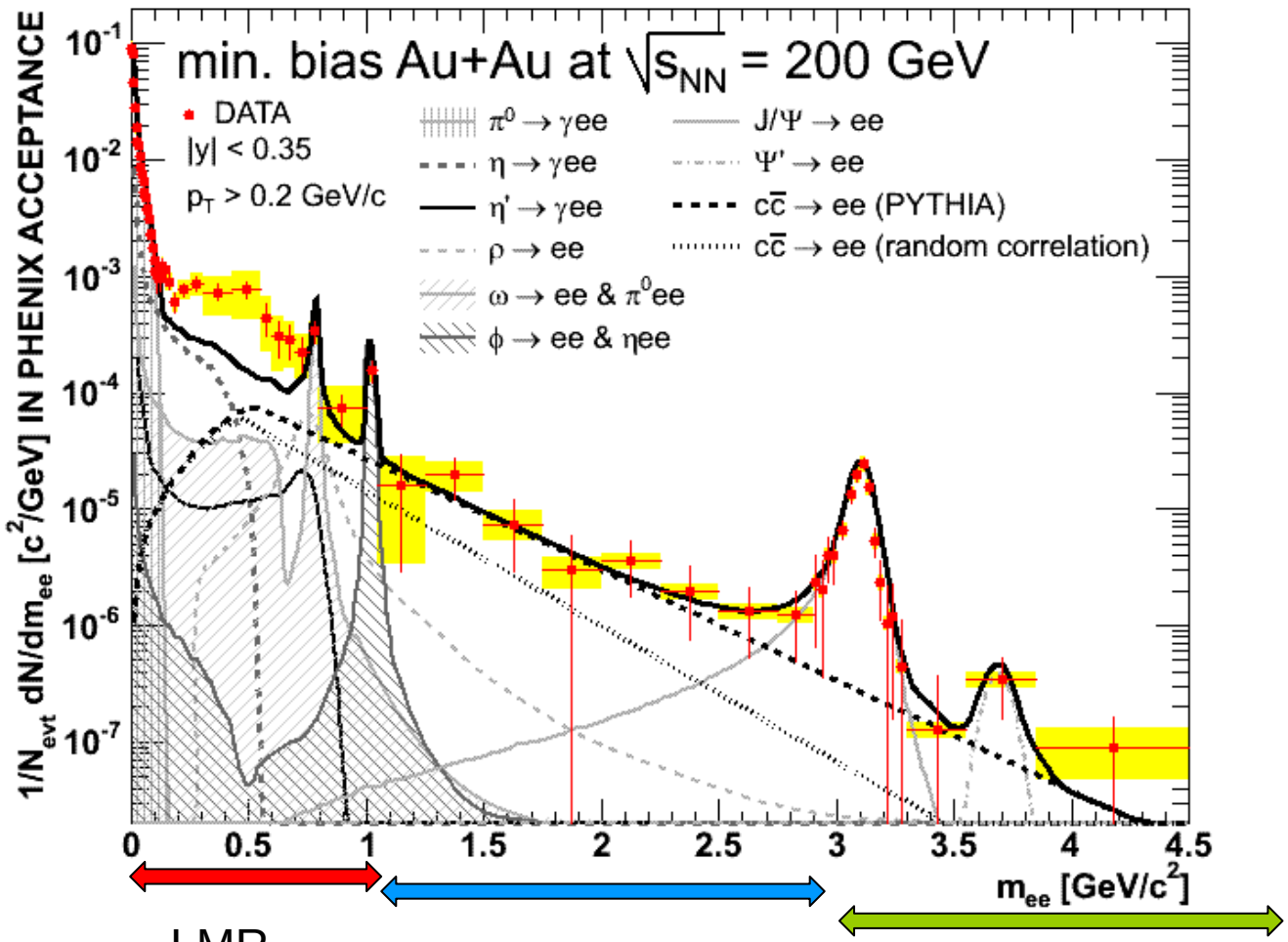


LMR

$\rho \to e^+e^-$

$\pi\eta\phi\omega$

IMR

$q\ \bar{q} \to l^+l^-$

$c \to l$

HMR

$J/\Psi$, DY, $\Upsilon$(1,2,3)

# NCQ Scaling

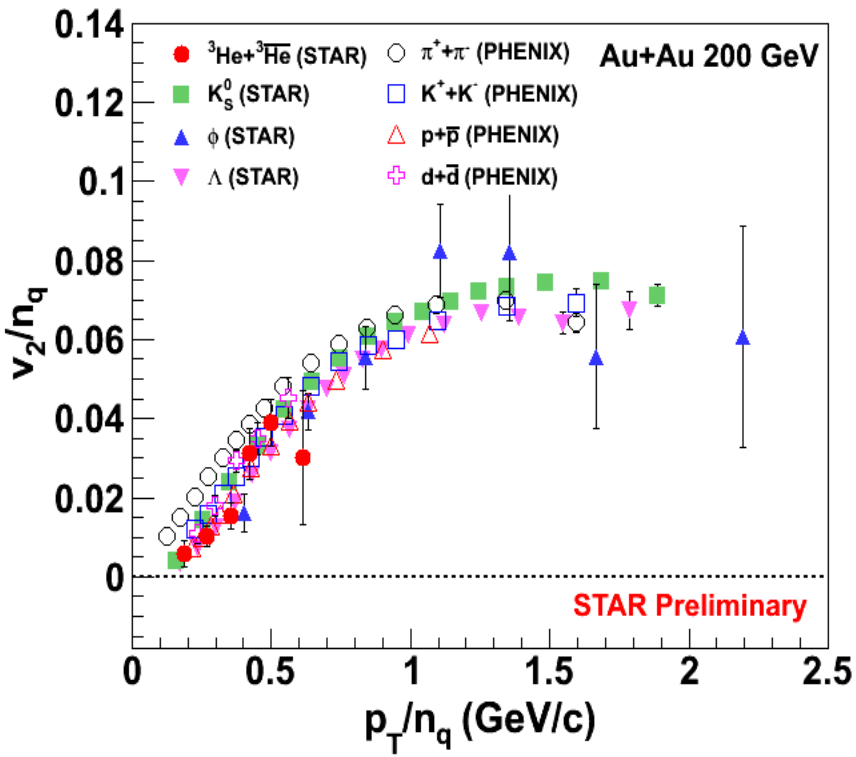


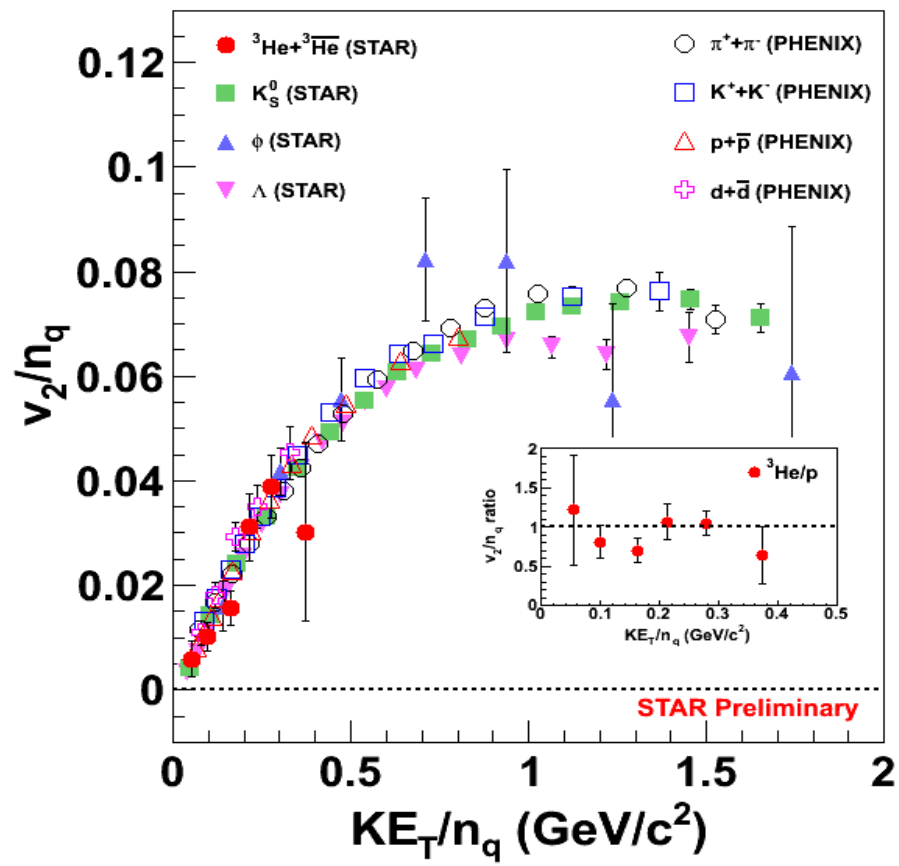


STAR, arXiv:0909.0566 [nucl-ex]

PHENIX, PRL 99, 052301 (2007)

d(p+n) : $n_q = 2 \times 3$ $\quad$ $^3$He(2p+n) : $n_q = 3 \times 3$

- Number of **constituent quark** scaling holds well for $v_2$ of $^3$He.

# Flow of Heavy Quarks

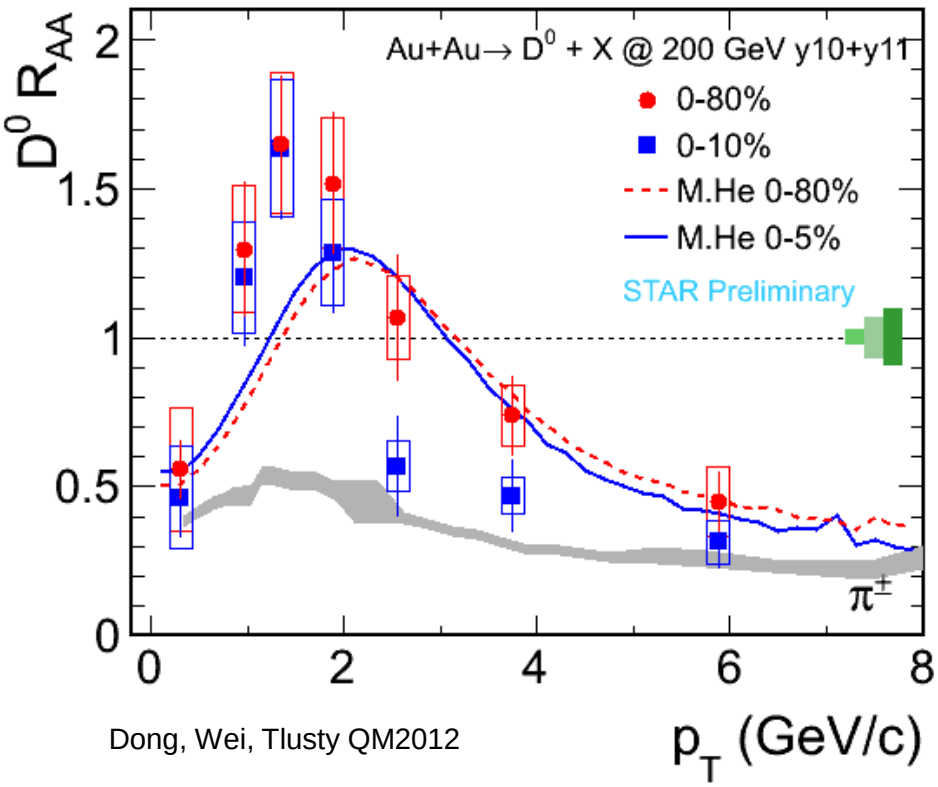


Dong, Wei, Tlusty QM2012

First measurement of directly reconstructed Charmed hadron radial flow at RHIC

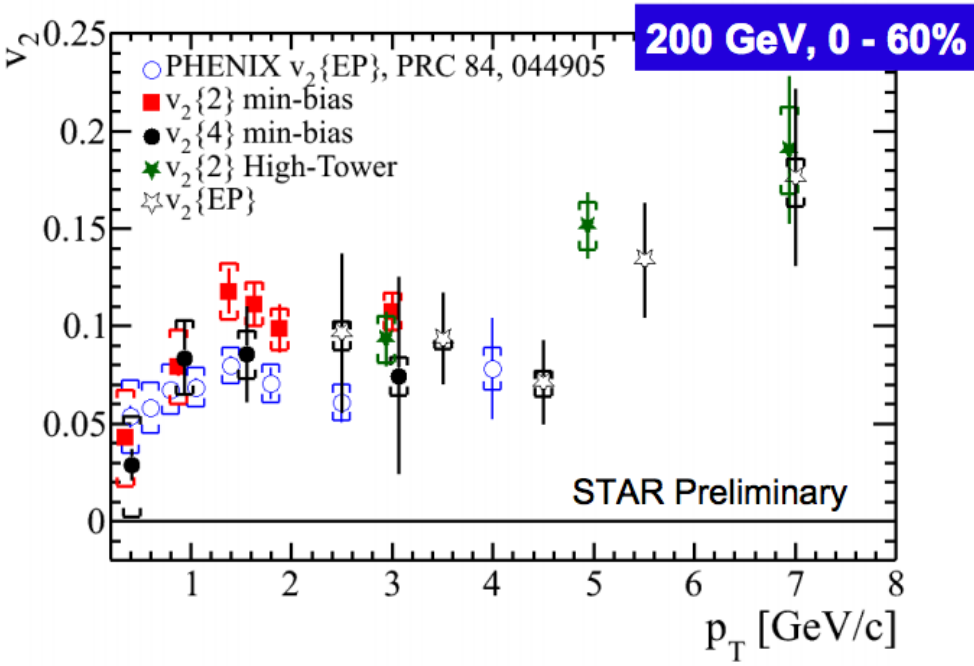


Elliptic flow of
Electrons from heavy-flavor hadrons
Different flow methods:
large flow at low pt
Jet contribution at high pt

# J/ψ $p_T$ dependence in A+A

PHENIX: PRL98(2007)232301 STAR: arXiv: 1208.2736, Trzeciak, Xie

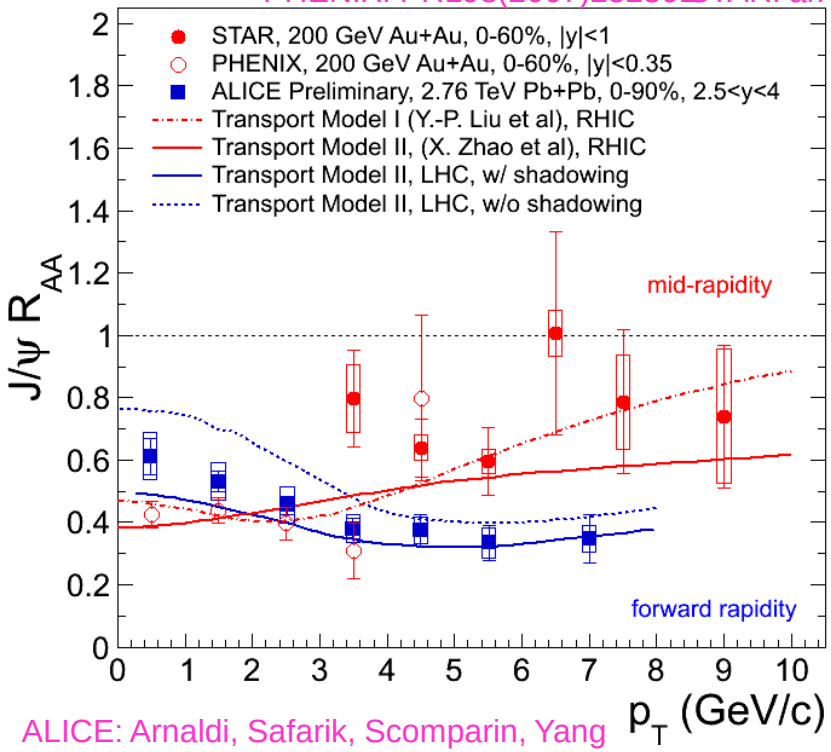


ALICE: Arnaldi, Safarik, Scomparin, Yang

CMS: Mironov, Moon, Roland

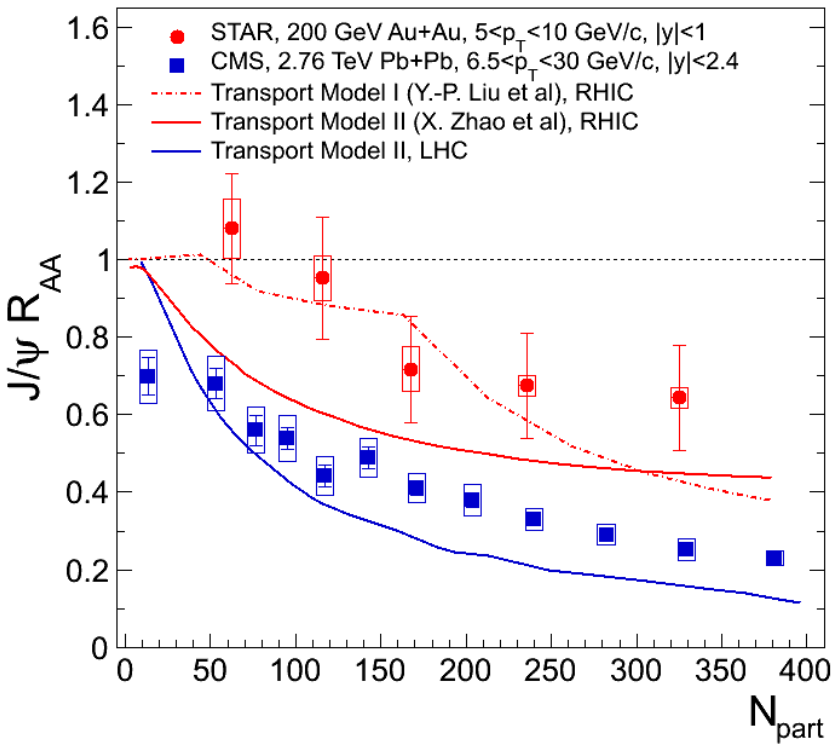


J/ψ $R_{AA}$ decreases from low to high $p_T$ at LHC.

J/ψ $R_{AA}$ increases from low to high $p_T$ at RHIC.

At high $p_T$, J/ψ more suppressed at LHC.

Models incorporating color screening andrecombination can consistently describe the J/ψ suppression pattern and flow measurements.

# Suppression without flow

RHIC:
large suppression, zero flow
LHC:
less suppression, hints of flow

**Color Screening and quark coalescence**

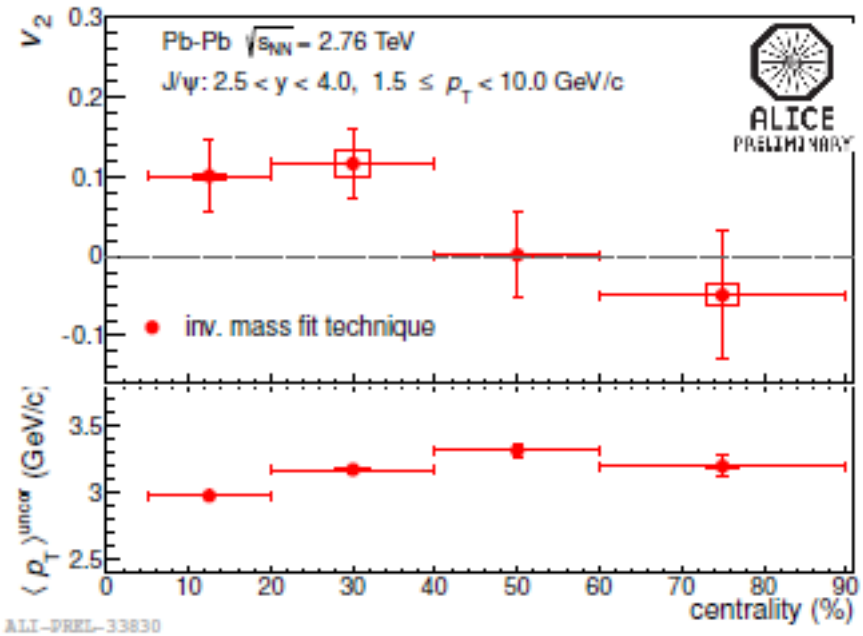


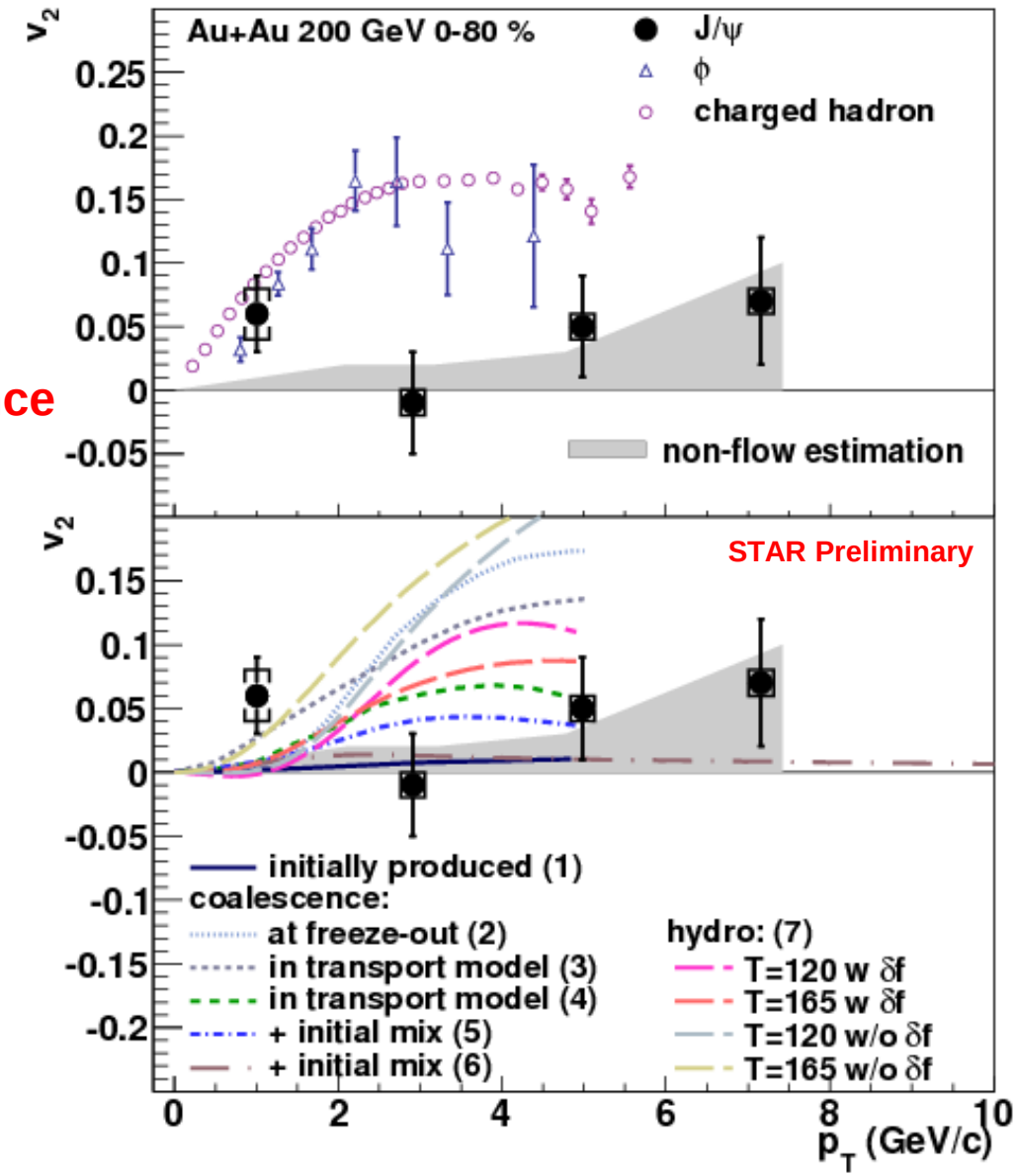

# ϒ Suppression in A+A

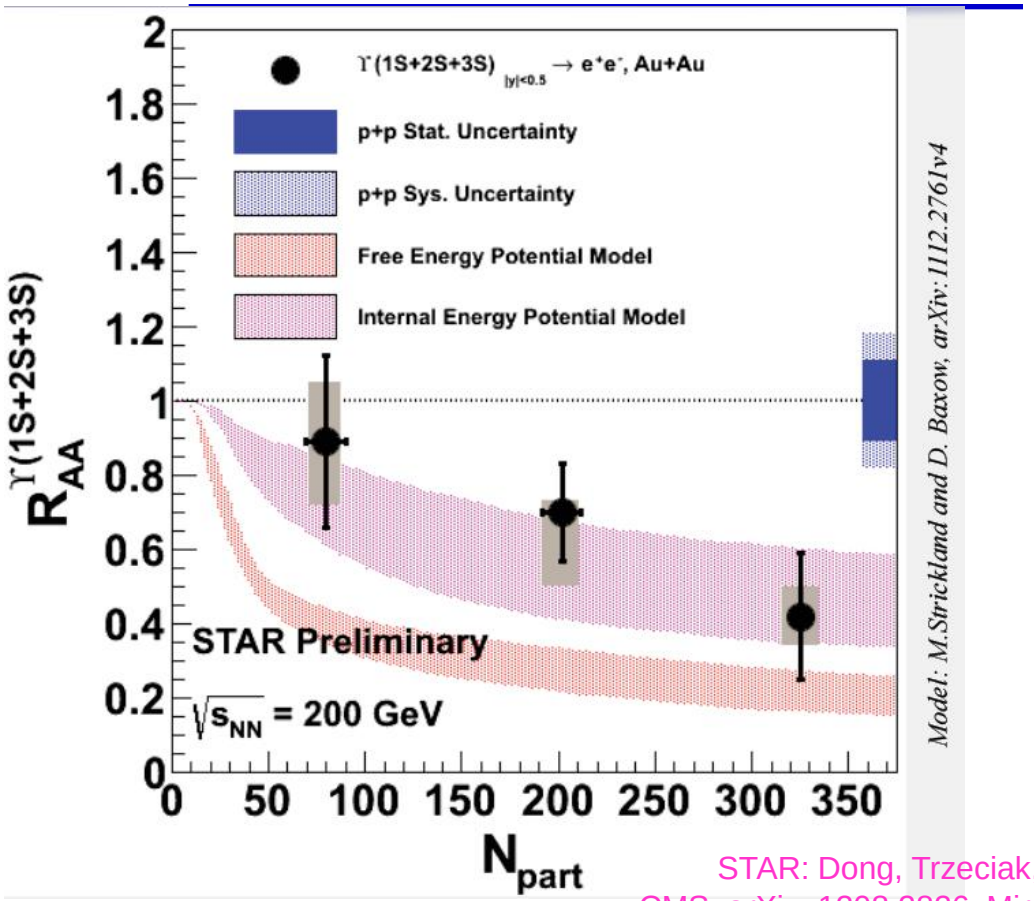


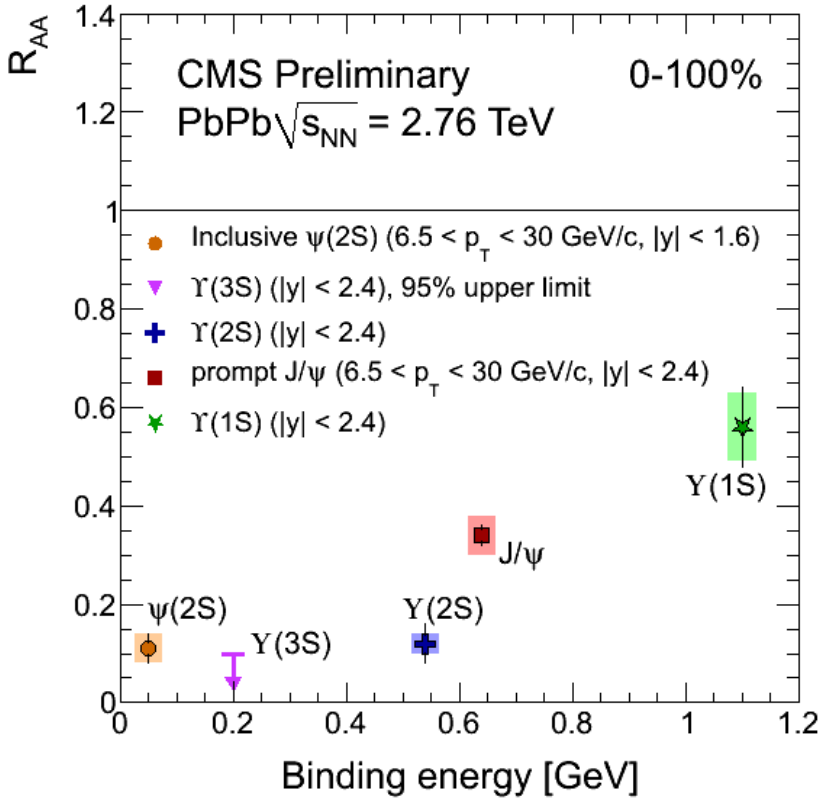


STAR: Dong, Trzeciak, Xie (QM2012)
CMS: arXiv: 1208.2826, Mironov, Rangel, Roland

**ϒ(1s) suppression magnitude consistent with excited states suppression.**

**ϒ(2S) strongly suppressed, ϒ(3S) completely melted.**

**Last piece of convincing evidence: color screening features of hot, dense medium in light of RHIC and LHC precise quarkonium measurements.**

# Novel Symmetries

## Local Parity Violation

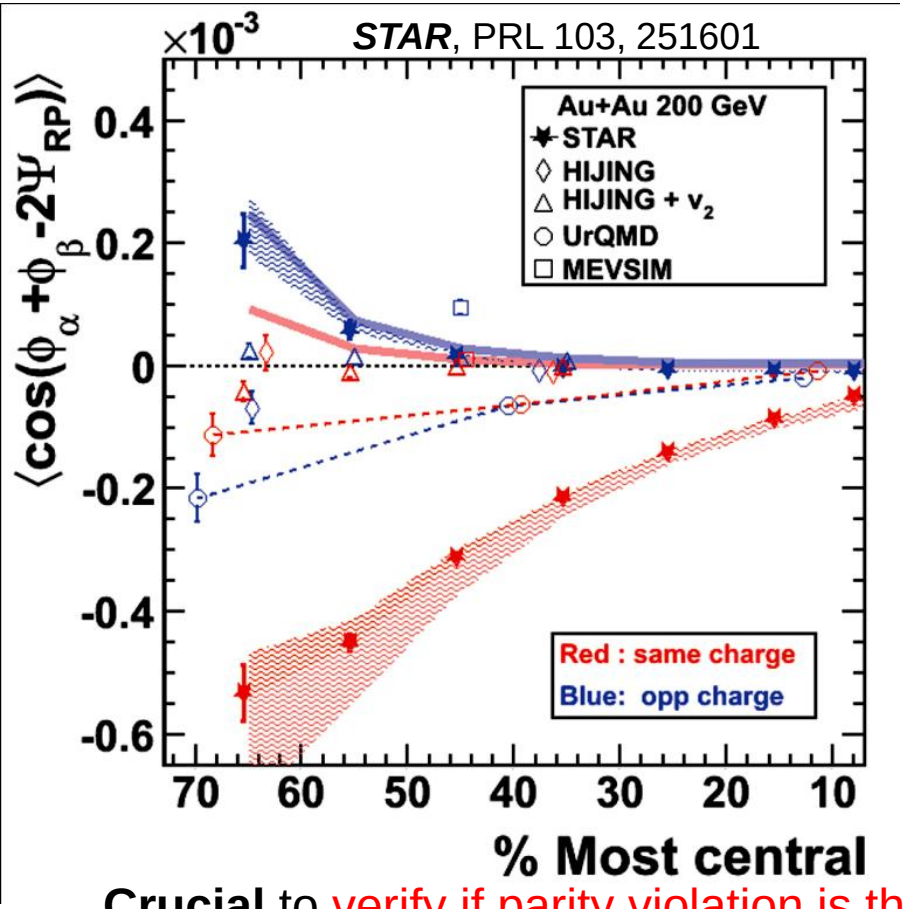


**Crucial** to verify if parity violation is the **correct explanation**

**U+U collisions:** collisions with **more $v_2$** and **less B field** than Au+Au

## Chiral Symmetry

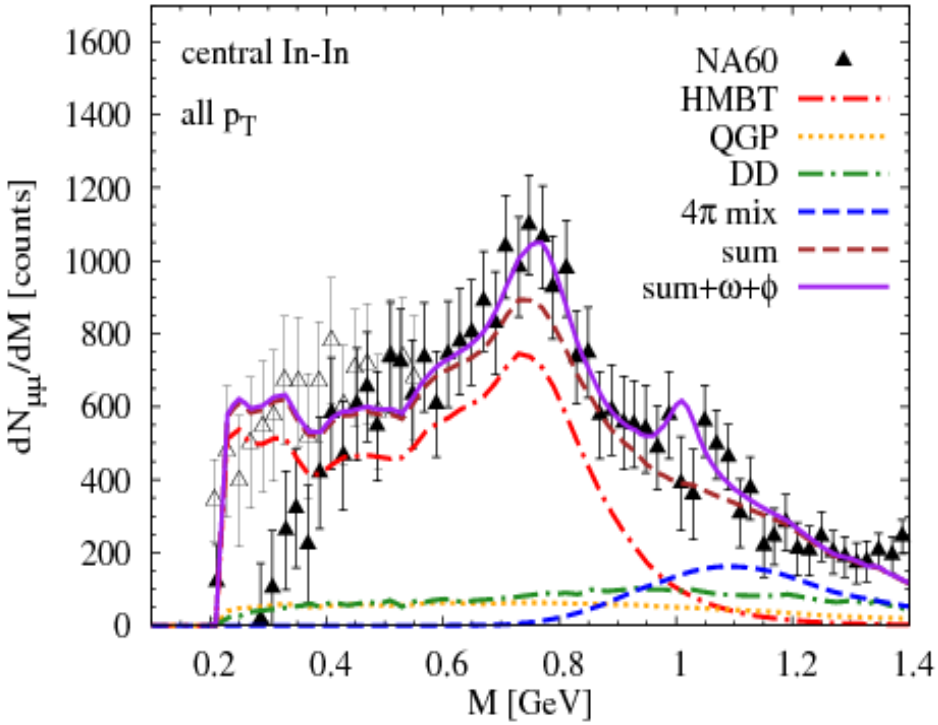

# Medium Effect on Vector Meson

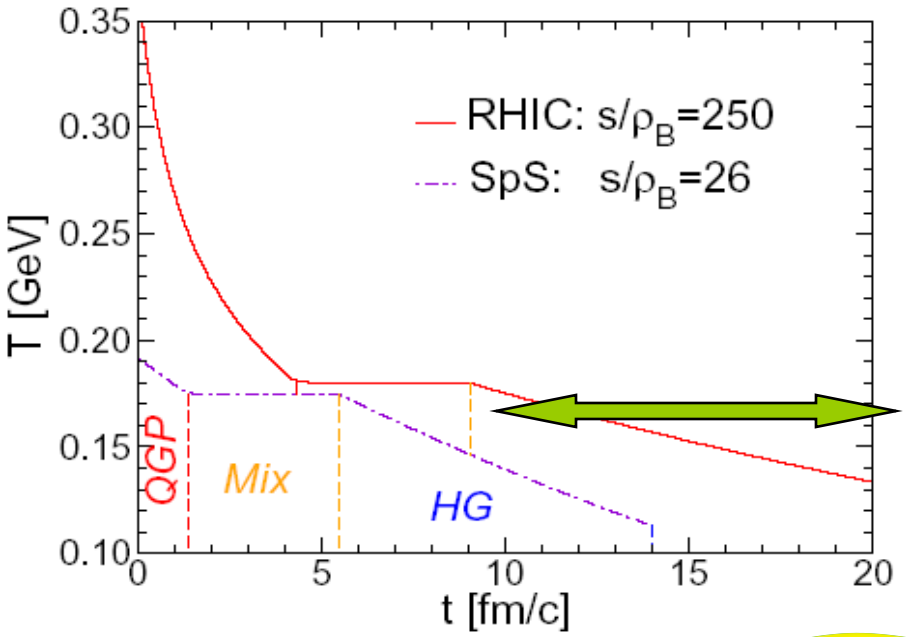


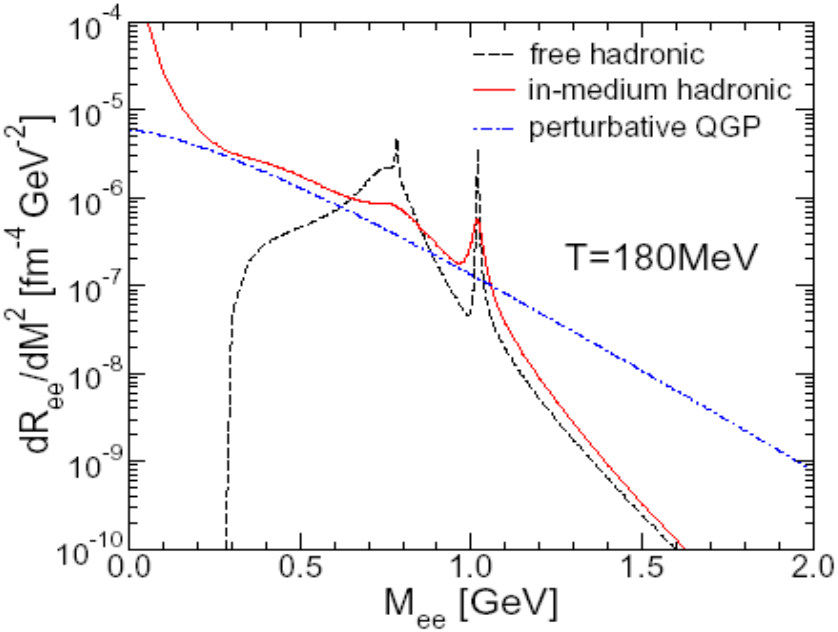


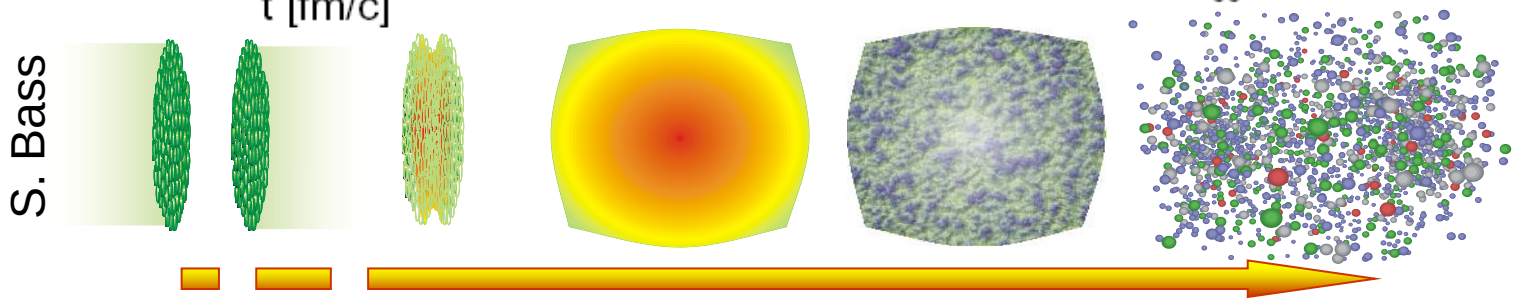


- Vector Meson Properties
- Thermal Dileptons

R. Rapp, hep-ph/0010101

# Energy dependence of di-electron spectra

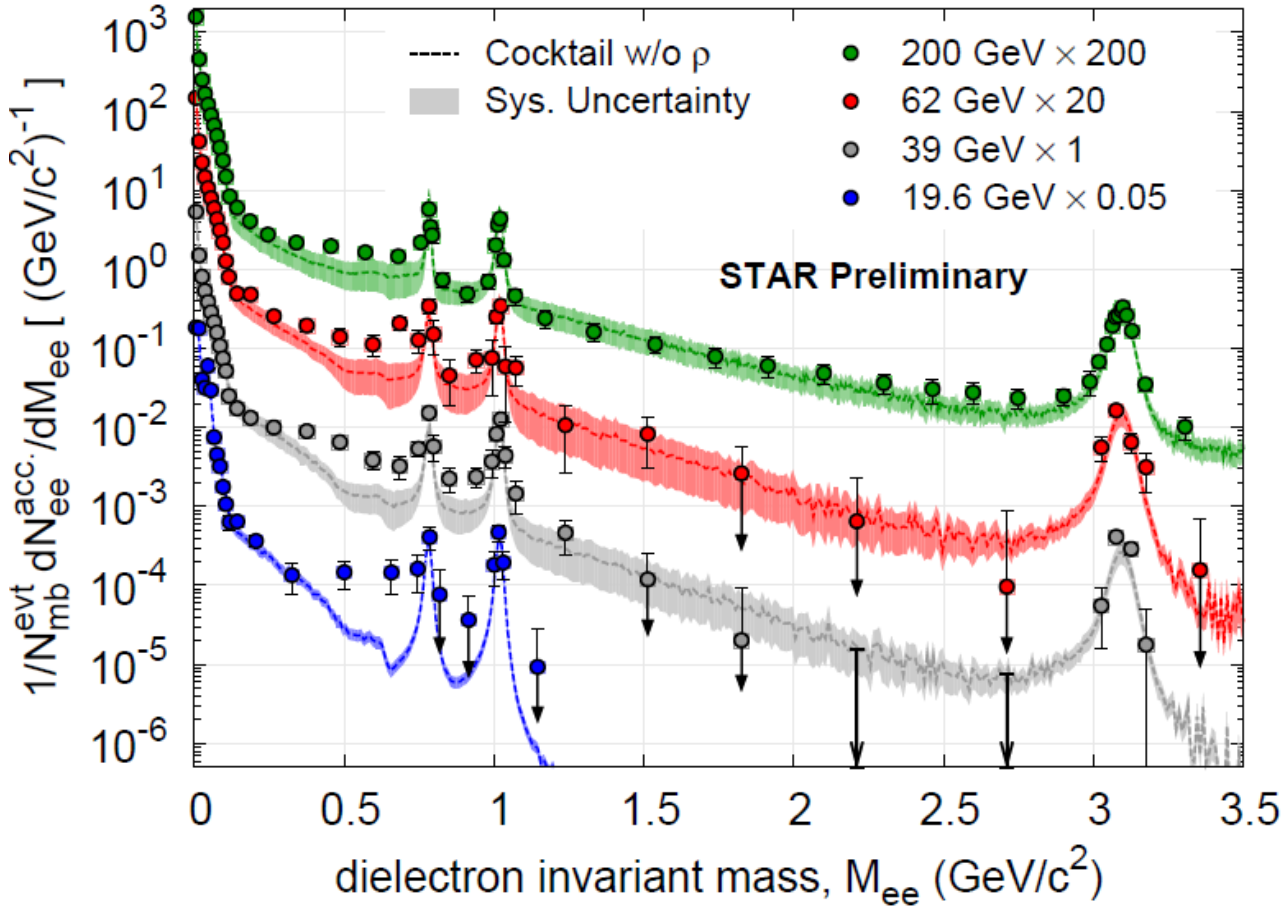


**QM2012** STAR: Dong, Geurts, Huang, Huck

**systematically study the di-electron continuum from 19.6, 39, 62.4 and 200 GeV.**

**Observe enhancement above cocktails in low mass range (~0.5 GeV/$c^2$)**

# Direct photon spectra and elliptic flow

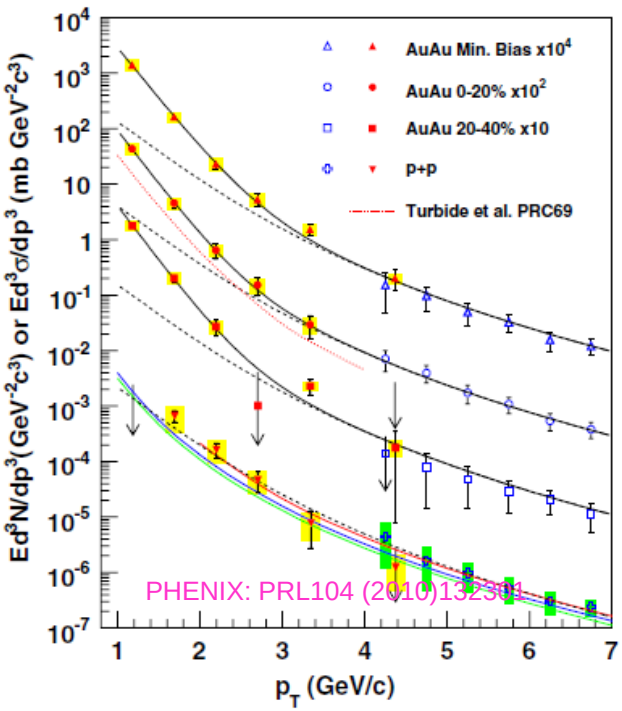


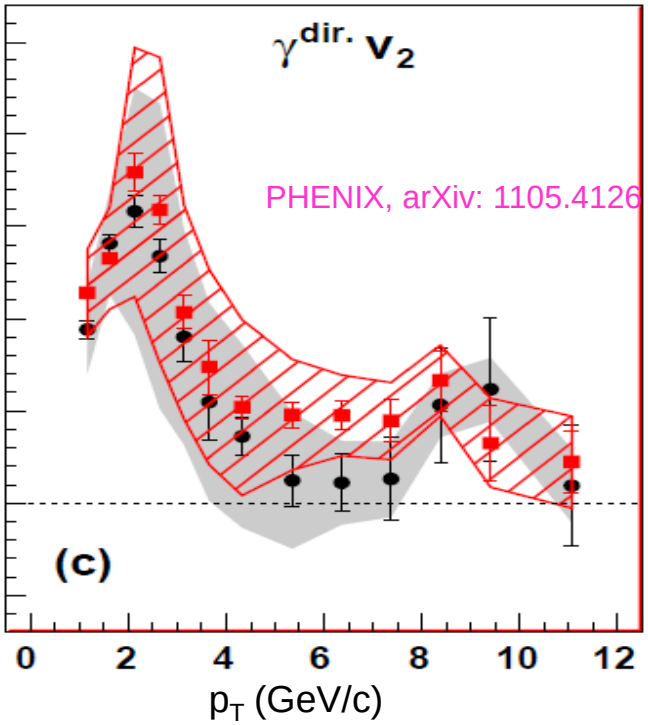


- Low $p_T$ direct photon elliptic flow measurement could provide direct constraints on QGP dynamics ($\eta/s$, T, $t_0$…).
- Excess of direct photon yield over p+p: $T_{eff}$=221 ± 19 ± 19 MeV in 0-20% Au+Au; substantial positive $v_2$ observed at $p_T$<4 GeV/c.
- Di-lepton $v_2$ versus $p_T$ & $M_{ll}$: probe the properties of the medium from hadron-gas dominated to QGP dominated. (R. Chatterjee, D. K. Srivastava, U. Heinz, C. Gale, PRC75(2007)054909)

Gale, Ruan, Tserruya, QM2012

# Di-electron $v_2$ at 200 GeV Au+Au

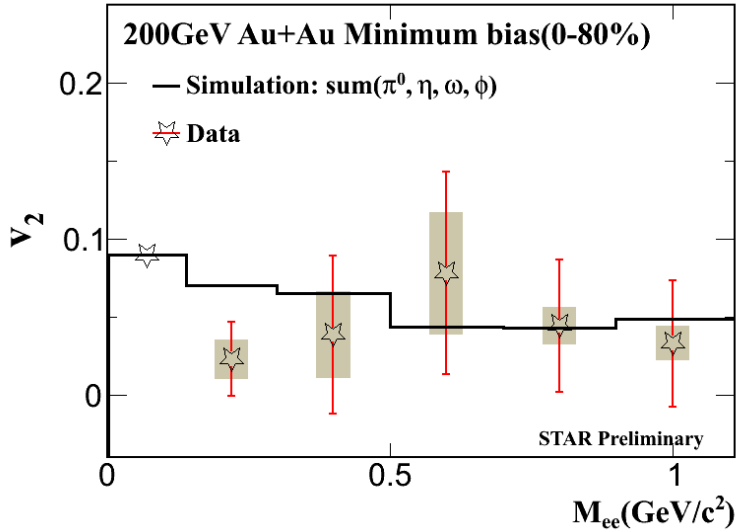


Cocktail simulation is consistent with the measured di-electron $v_2$ at $M_{ee}$<1.1 GeV/c2.

Need a factor of two more data to be sensitive to hardon gas and QGP contribution, in addition to independent measurements to disentangle ccbar correlation contribution

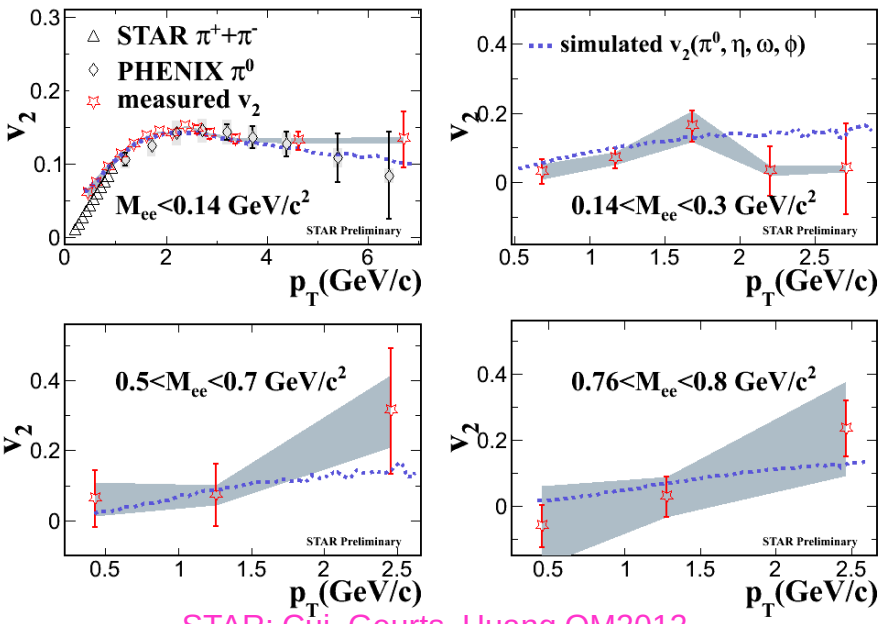


STAR: Cui, Geurts, Huang QM2012

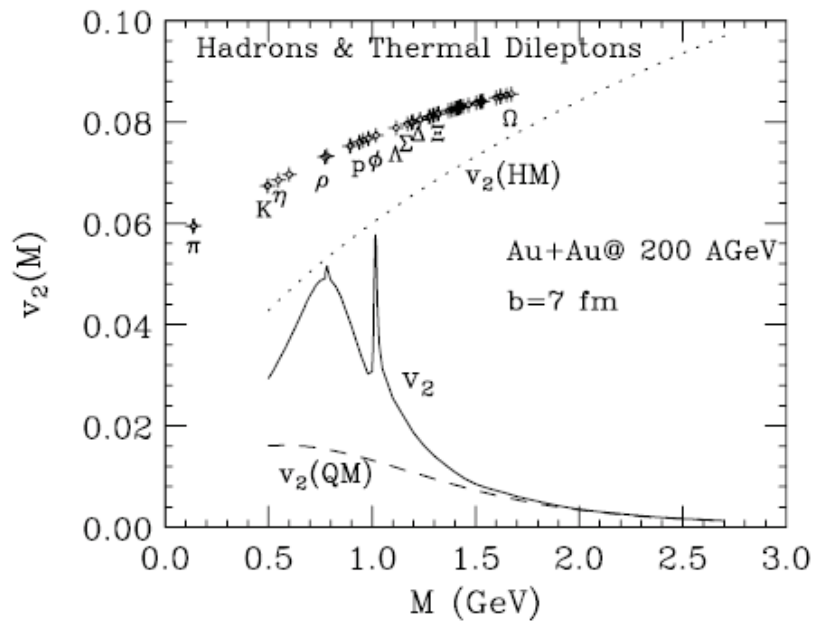


R. Chatterjee, D. K. Srivastava, U. Heinz, C. Gale, PRC75(2007)054909)

# Quantify the Enhancements

Temperature dependence of rho spectral function

1. Beam energy range where final state is similar
2. Initial state and temperature evolution different
3. Density dependence by Azimuthal dependence ($v_2$)
4. Use centrality dependence as another knob
5. Direct photon results should match with extrapolation

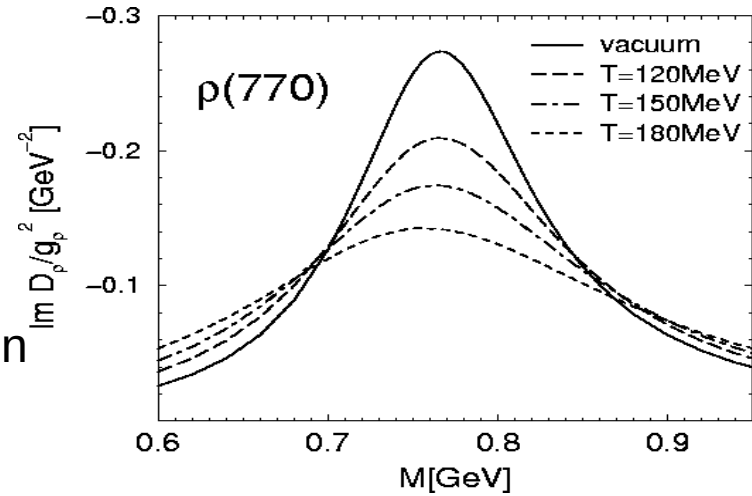


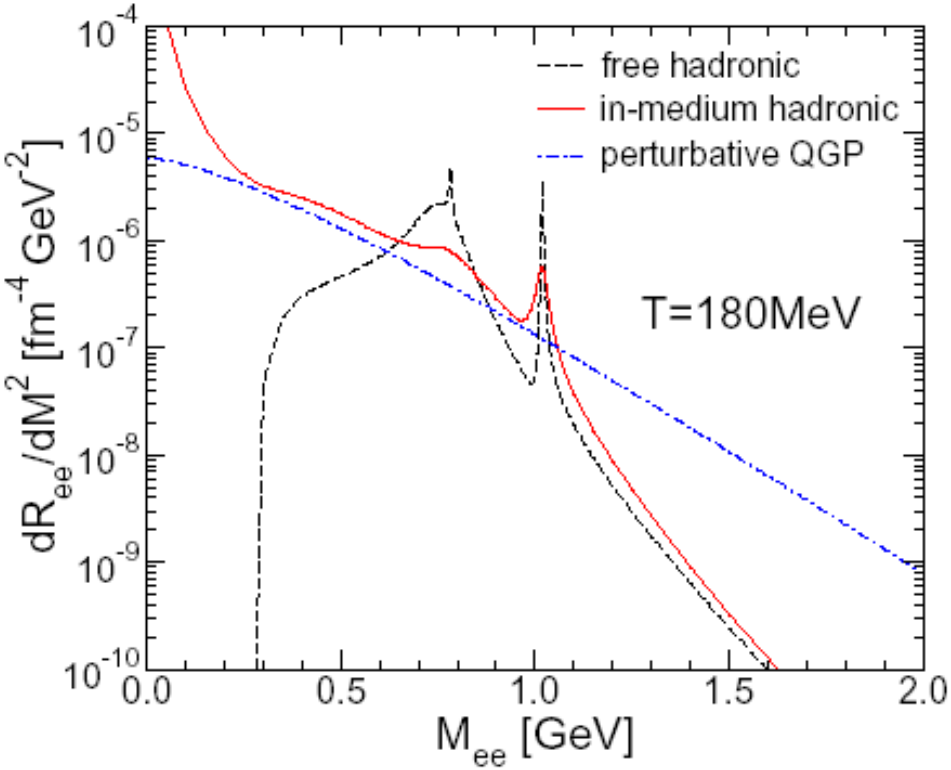


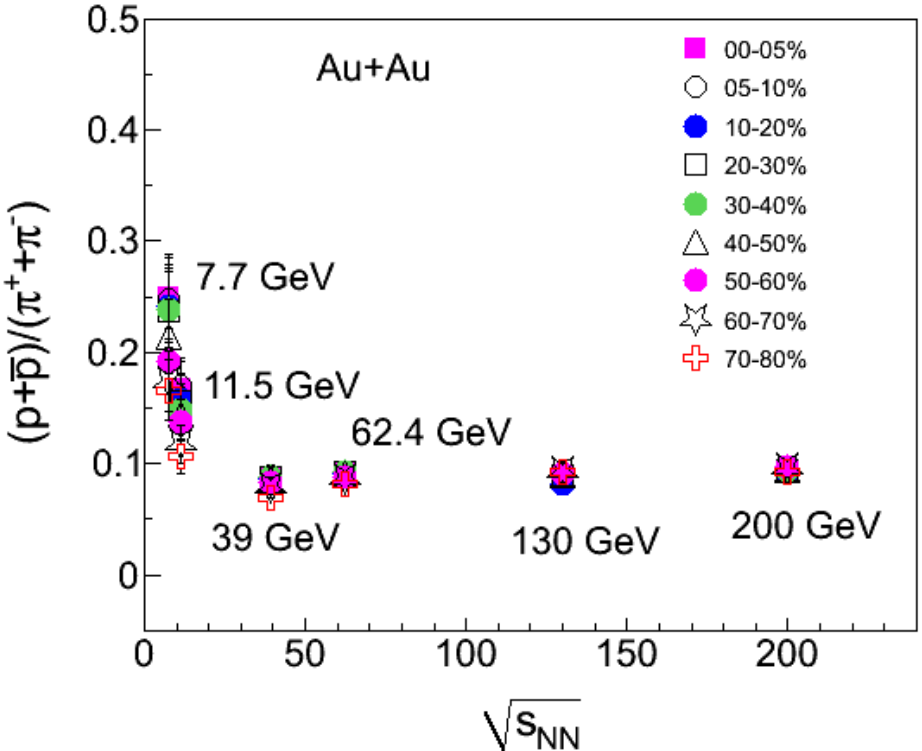

# A tool to study Chiral Symmetry Restoration

Gale,Ruan, QM2012

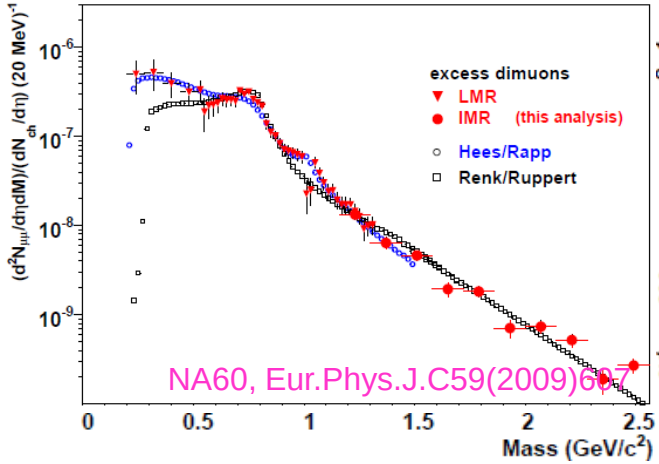


NA60, Eur.Phys.J.C59(2009)607

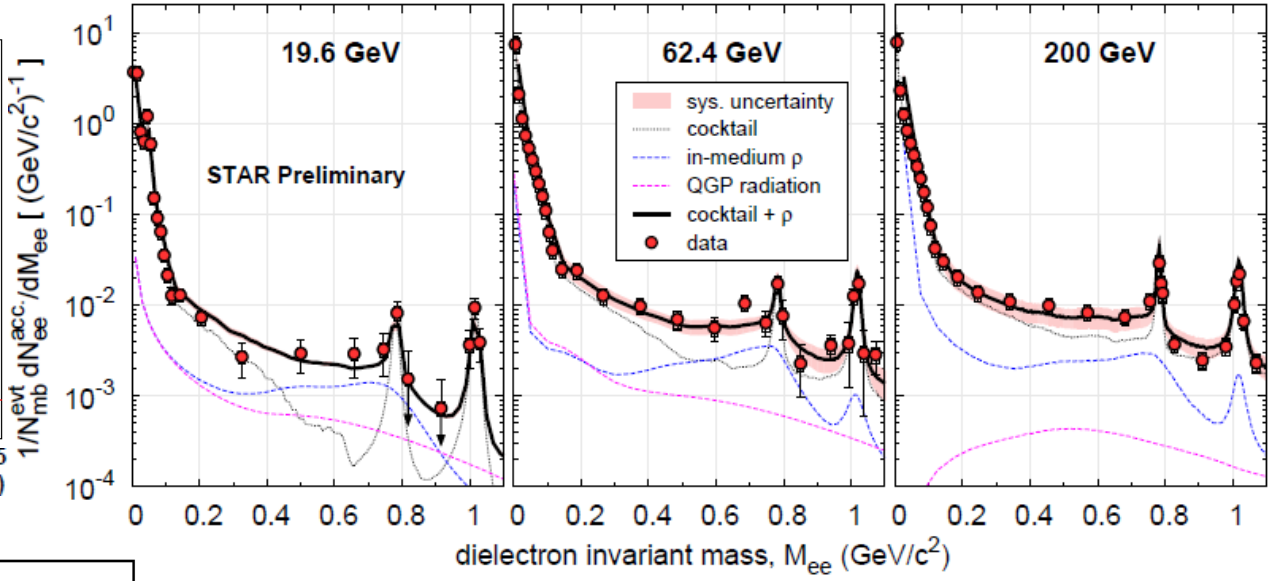


STAR: Cui, Dong, Geurts, Huang, Huck

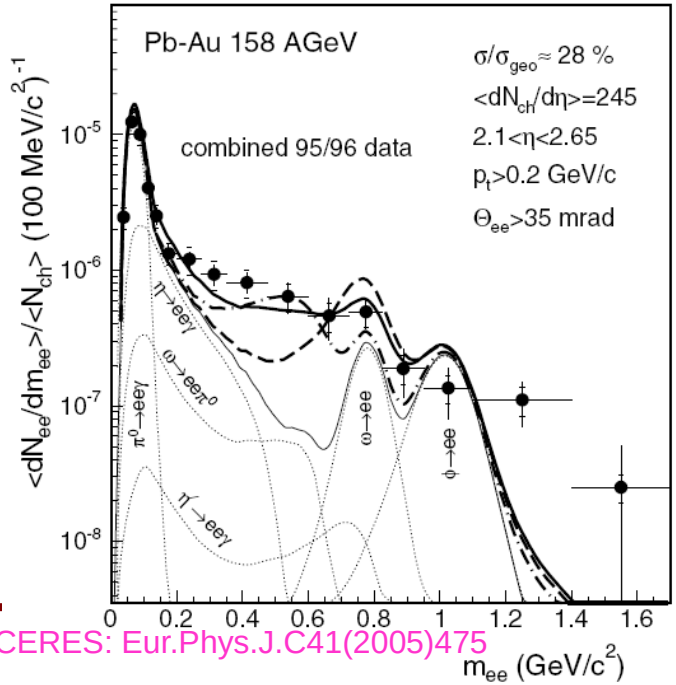


CERES: Eur.Phys.J.C41(2005)475

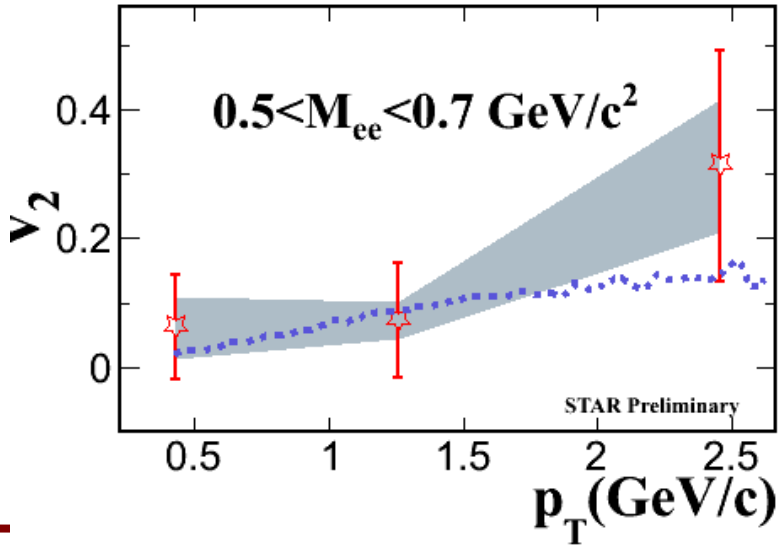

# Issues and Solutions

Low signal to background ratio at LMR
Charm semileptonic decay ("irreducible background")

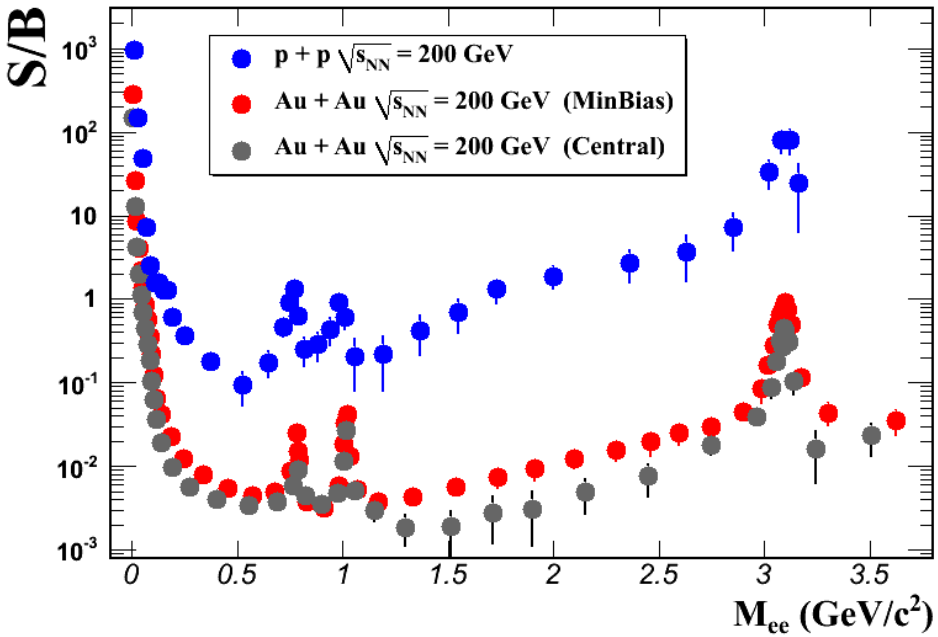


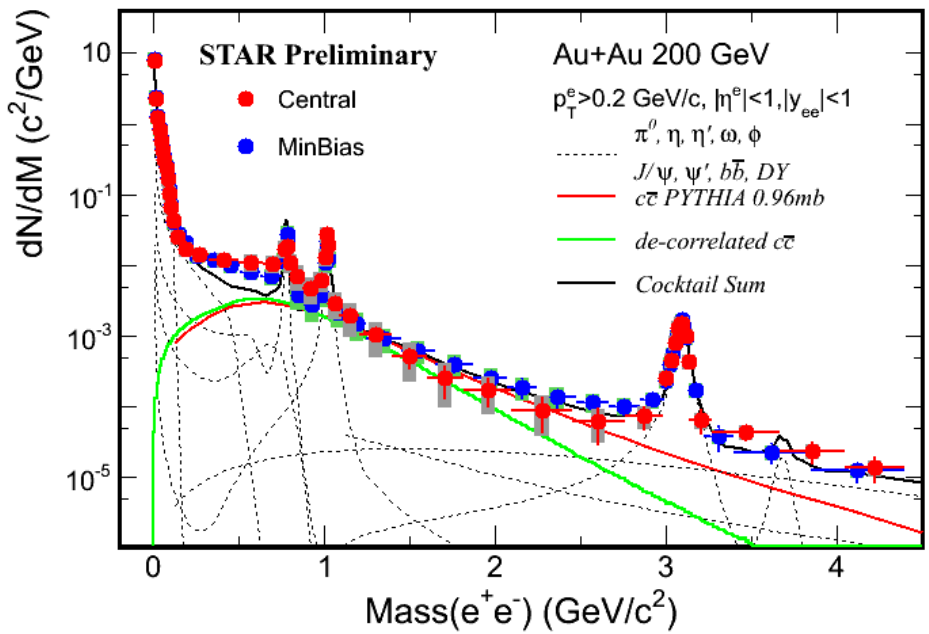


PHENIX:
Cherenkov+EMC for electron ID
Hadron Blind Detector (HBD)
reduce Dalitz decay electron pairs

STAR:
TPC dE/dx+TOF for electron ID
BES dilepton at SPS energy
Unique μ+e pair from MTD+EMC
Same rapidity and kinematics

# Must move from "Hints" → "Definitive Answers"

## Beam Energy Scan (BES) Phase II

e-cooling for low energy RHIC operation

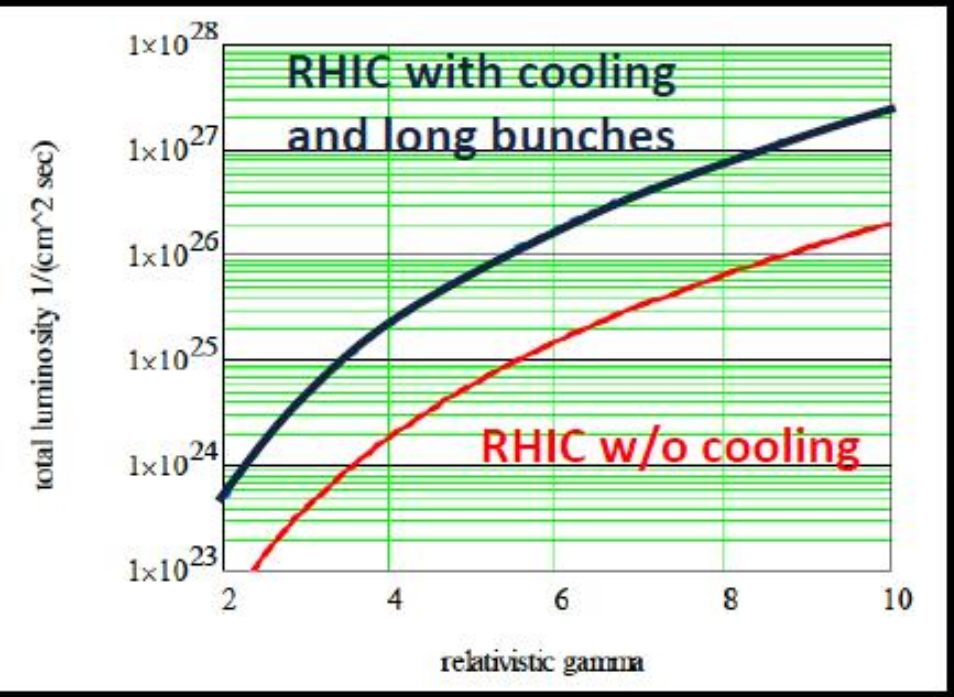


High brightness SRF electron gun or Fermilab Pelletron for 10x L

Nagle, "RHIC Future", QM2012

Increased acceptance for STAR and PHENIX

STAR Inner TPC Readout
Improved tracking and dE/dx PID
Extend η coverage 1.0-1.7

# What is the upgrade?

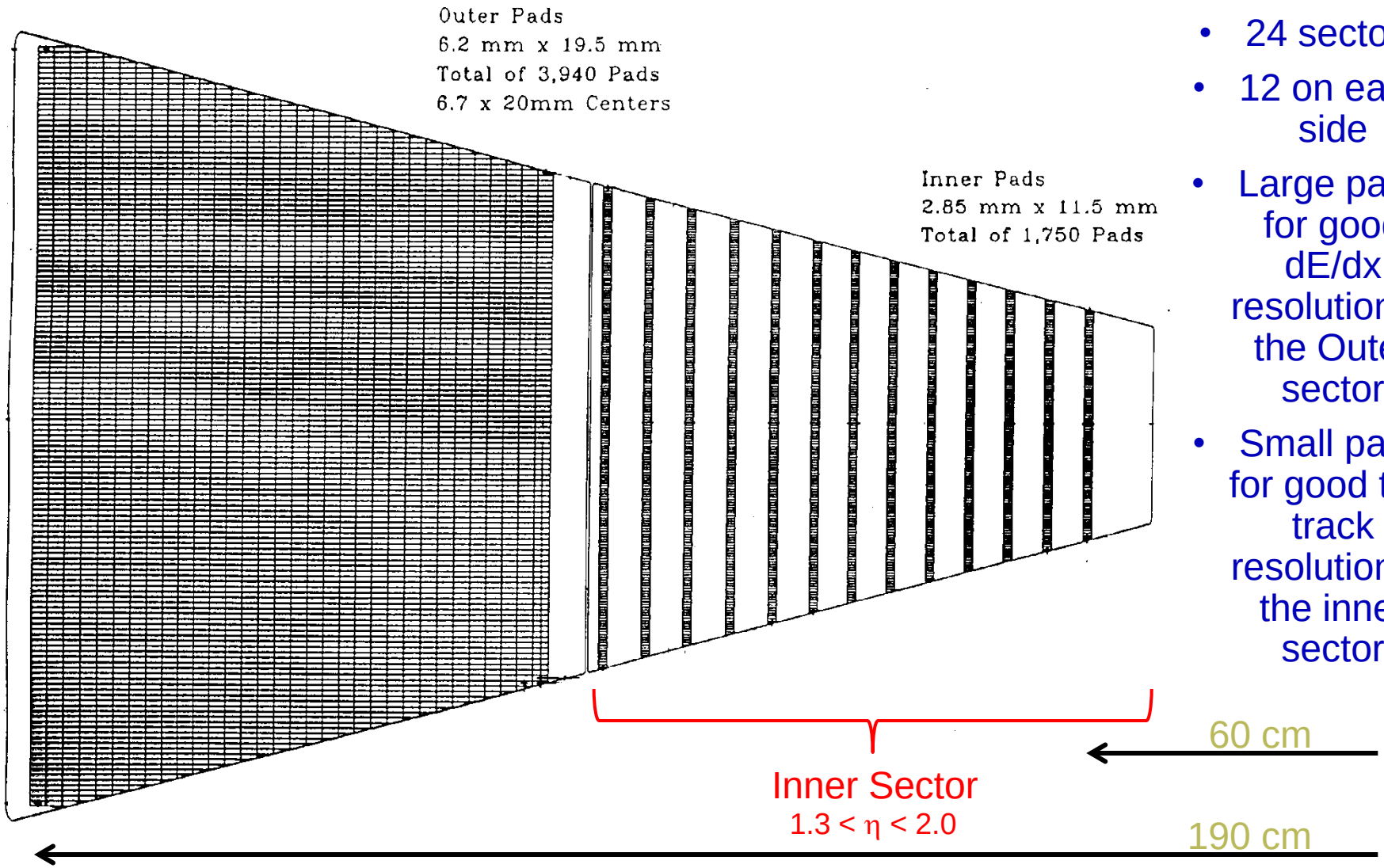


- 24 sectors
- 12 on each side
- Large pads for good dE/dx resolution in the Outer sector
- Small pads for good two track resolution in the inner sector

More pad rows and larger pads in the inner sector

# Why do it?

- Physics Motivations
  - Study of the QCD phase diagram (Beam Energy Scan Phase II)
    1. Increase eta coverage for hadron acceptance and correlations
    2. Improve low-pt coverage for hyperon reconstruction
    3. Increase dE/dx resolution for particle identification
    4. High eta coverage for fixed-target datasets
  - Study of the QGP Properties
    1. A tool to systematically map chiral symmetry restoration
    2. Improve low-pt coverage for weak-decay reconstruction
    3. Heavy-Flavor physics by improving acceptance and dE/dx
    4. Identified high-pt hadron spectra and correlation for understanding jet properties
  - Spin structure in polarized p+p collisions
    1. Improved forward tracking with FGT+EEMC
    2. Interference Fragmentation Functions at high x
    3. Rapidity dependence of Lambda hyperon polarization
- Reduce space charge distortion induced by charge leak from the Gating Grid
- Eliminate the concern about issues related to wire aging

# Benefit to dilepton in a nutshell

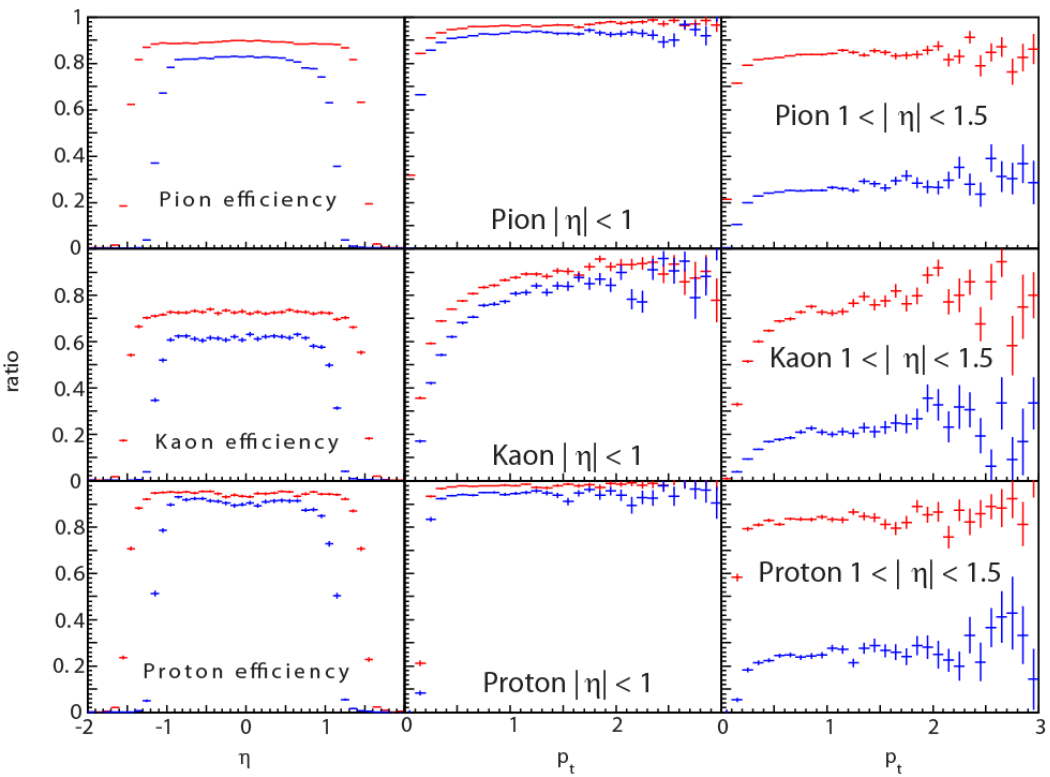


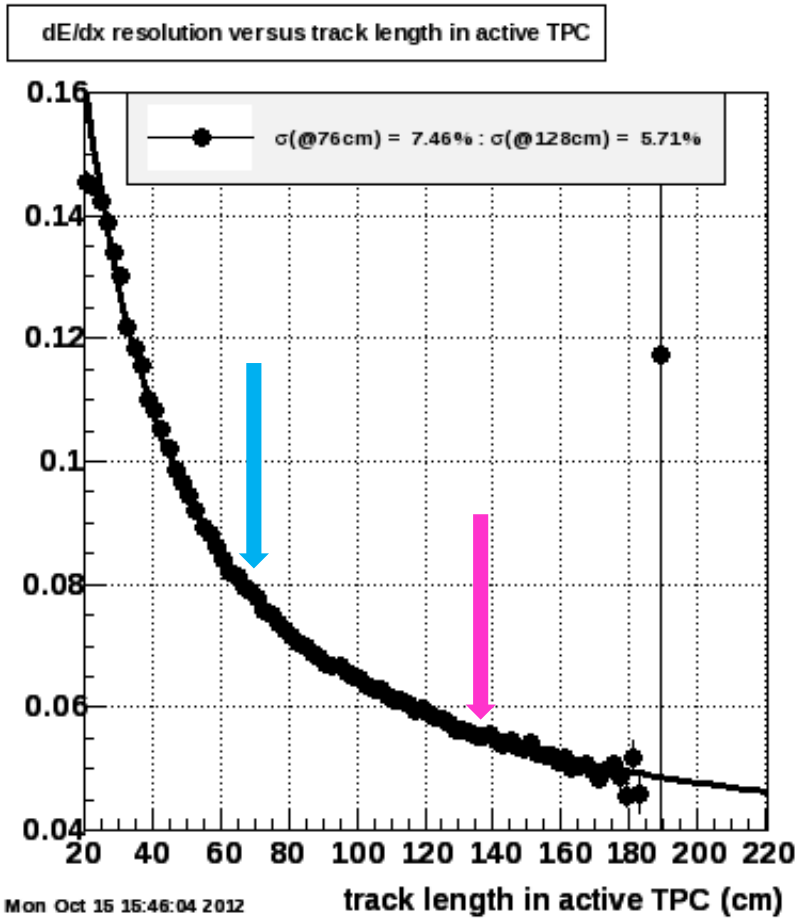


Improve dE/dx resolution and acceptance

# Improve electron PID for dilepton program

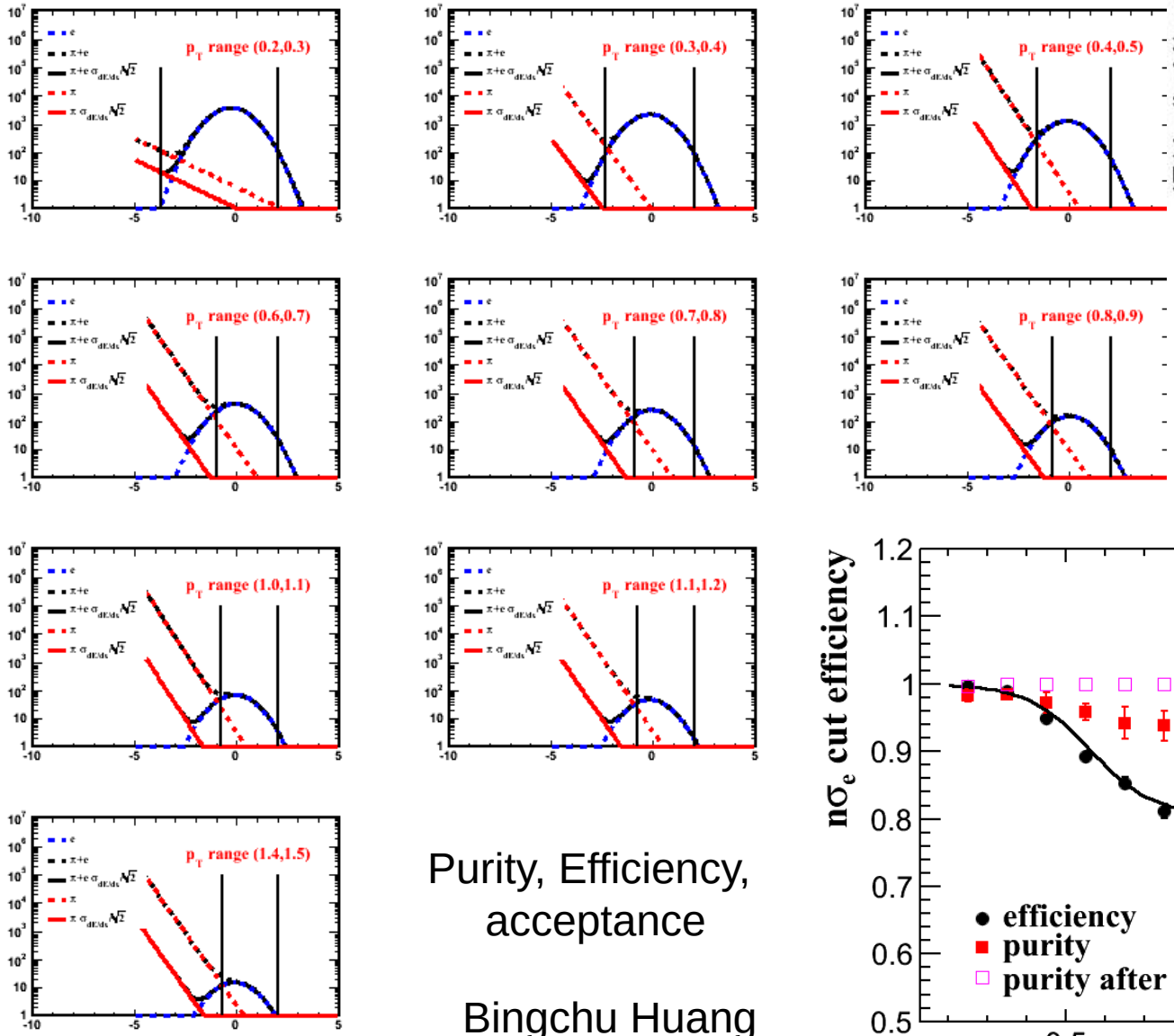


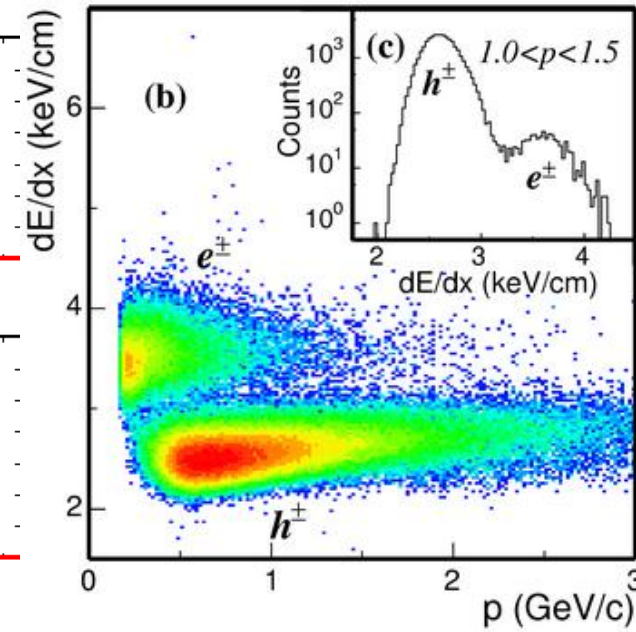


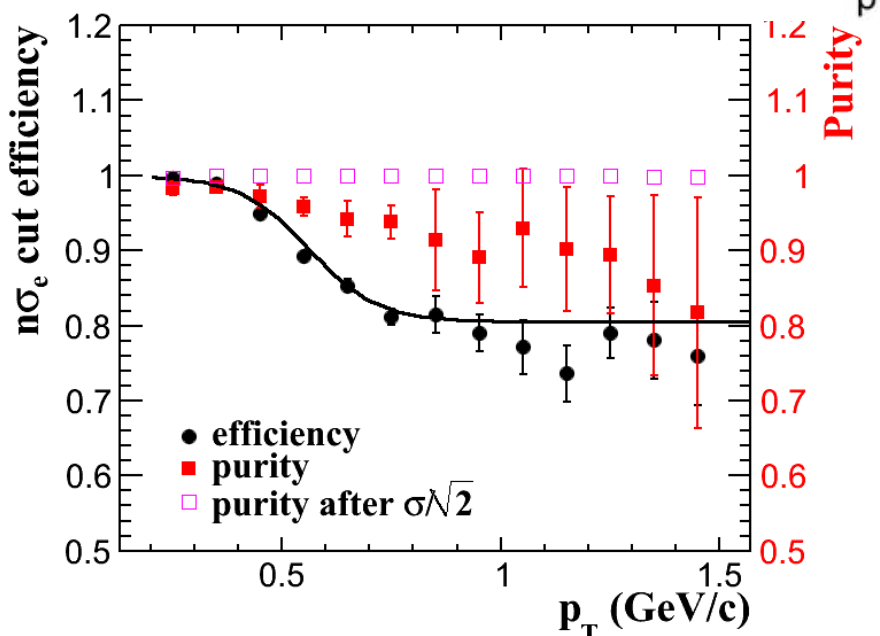


Purity, Efficiency, acceptance

Bingchu Huang

# Summary of iTPC upgrade event timeline

- Discuss the necessary tracking upgrade between -2<eta<-1 for eSTAR (2011)
- Identify iTPC as a crucial step for eSTAR upgrade (10/11)
- Discussion of possible iTPC upgrade before eRHIC
  http://drupal.star.bnl.gov/STAR/system/files/UclaUpgrade_jt.pdf
  Jim Thomas (LBL)
  UCLA Upgrade Workshop, December 2011
- iTPC Upgrade group discussions/talks at BNL (02/01/2012)
  http://drupal.star.bnl.gov/STAR/event/2012/02/14/estar-task-force-biweekly-meeting
- iTPC session at BNL upgrade workshop (06/11/2012)
  decision to move toward an iTPC project
  outline the necessary steps
- Upgrade Session at STAR Collaboration Meeting (08/07/2012)
  Establish iTPC geometry for simulation, possible collaboration institutes
  http://drupal.star.bnl.gov/STAR/system/files/iTPC_Collaboration_Upgrade2012_0.pdf
- Establish simulation/tracking framework (09/12)
- Cost Estimates and Technical Driven Schedule
  to Steve Vigdor and Tribble Committee (09/12)
- Possible Chinese group involvements (10/12)
- STAR R&D Review (10/12)
- Upgrade Workshop (11/12)
- Draft Proposal to upgrade group (2013) Proposal to Collaboration
- Electronics R&D prototype and engineer drawings (2013)
- Prototype Sector (2013—2014)

# Future STAR HFT and MTD

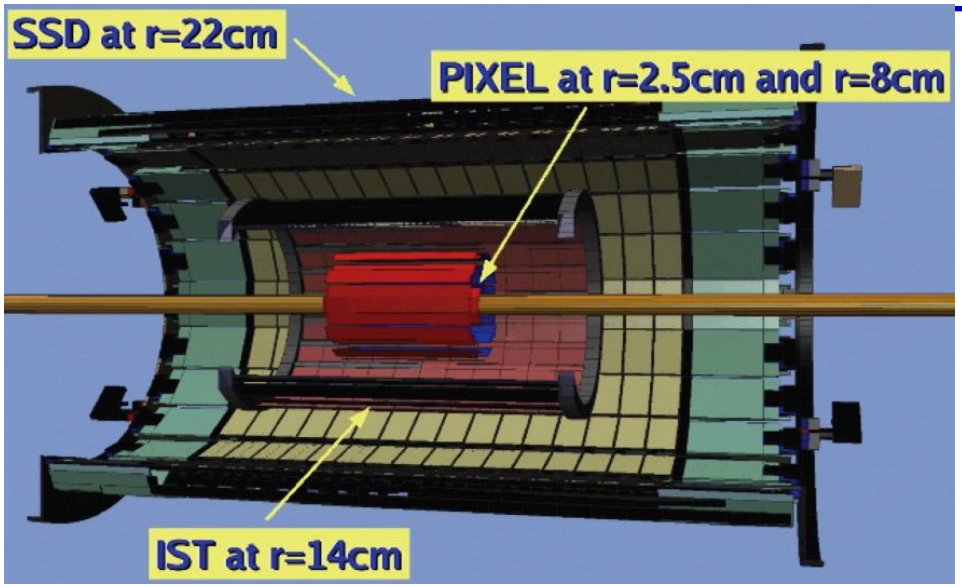


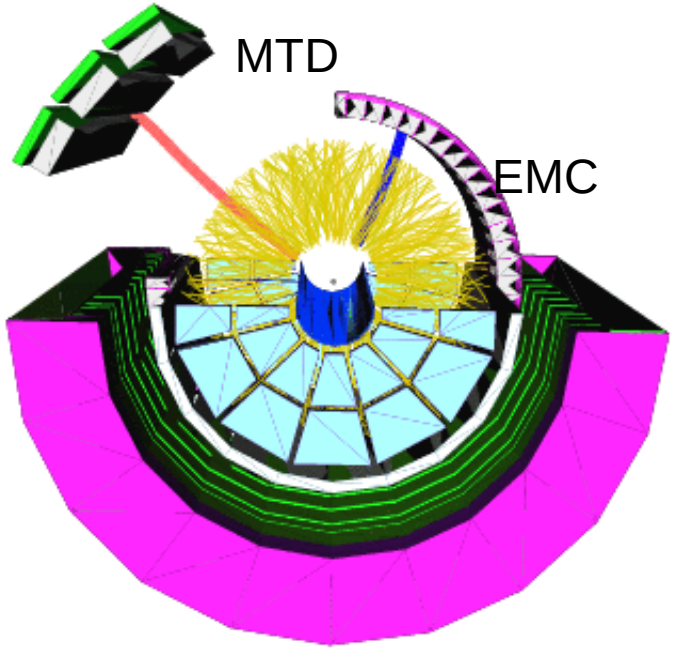


PIXEL:

- high hit resolution: 20.7μm X 20.7μm pitch
  - low thickness: 0.4% $X_0$

- ❑ Muon identification
- ❑ Muon trigger

- ❑ **significantly enhance STAR capability on measuring heavy flavor production at RHIC**
  - Direct reconstruction of D mesons at both low $p_T$ and high $p_T$
  - B→J/ψ→μμ +X, disentangle upsilon ϒ(1S/2S/3S).
- ❑ **Study QGP thermal dilepton radiation**
  - Understanding background charm decorrelation through e-muon correlation.

# Concept Design of the STAR-MTD

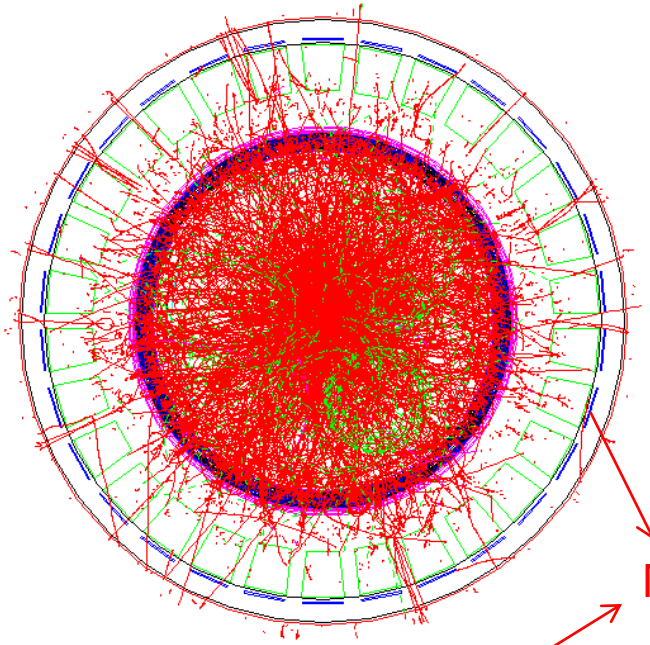

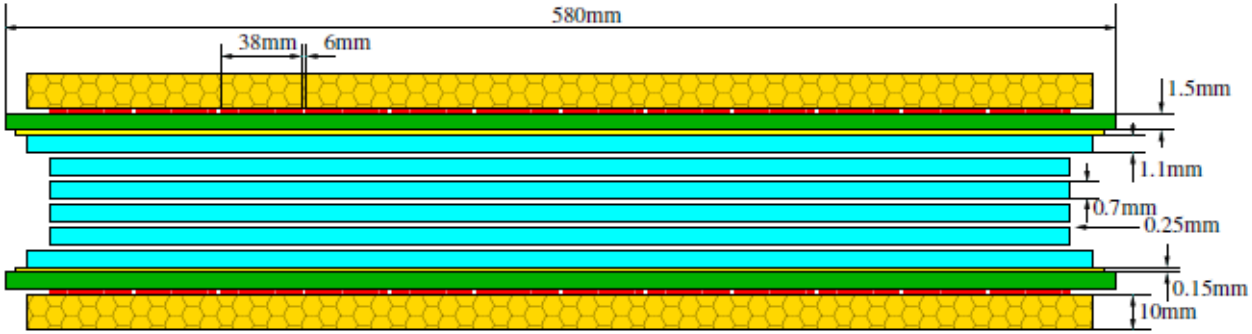


MTD

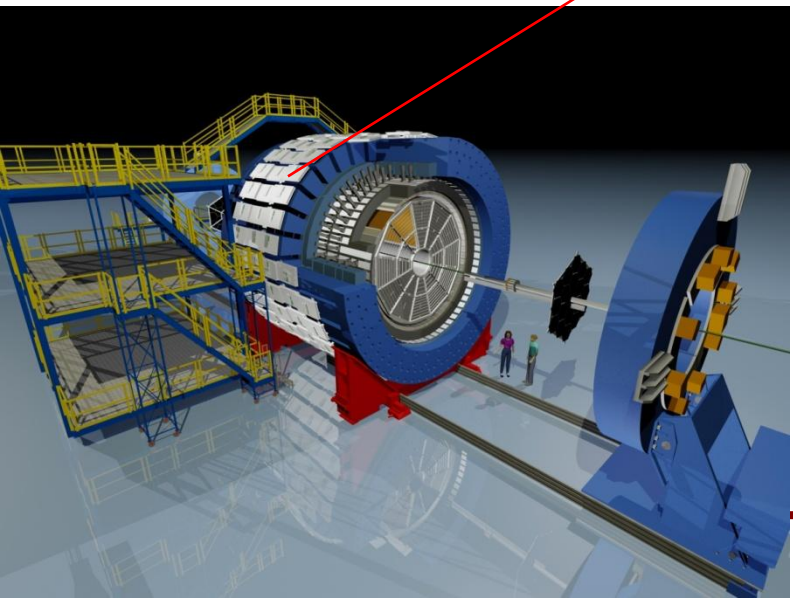

Multi-gap Resistive Plate Chamber (MRPC): gas detector, avalanche mode

A detector with long-MRPCs covers the whole iron bars and leave the gaps in-between uncovered. Acceptance: 45% at $|\eta|<0.5$

118 modules, 1416 readout strips, 2832 readout channels

Long-MRPC detector technology, electronics same as used in STAR-TOF

# High Mass Di-muon Capabilities

Z. Xu, BNL LDRD 07-007; L. Ruan et al., Journal of Physics G: Nucl. Part. Phys. 36 (2009) 095001

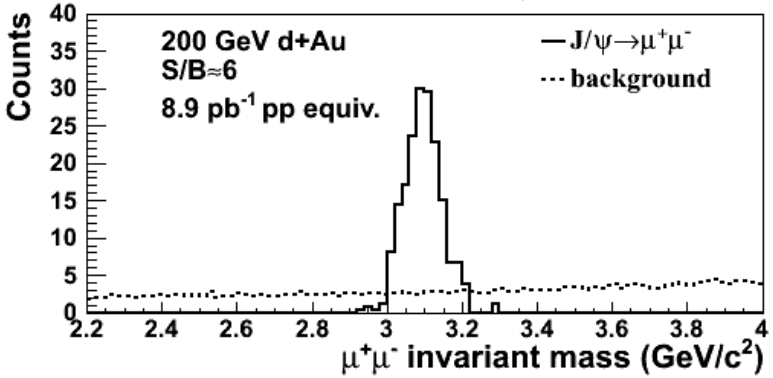


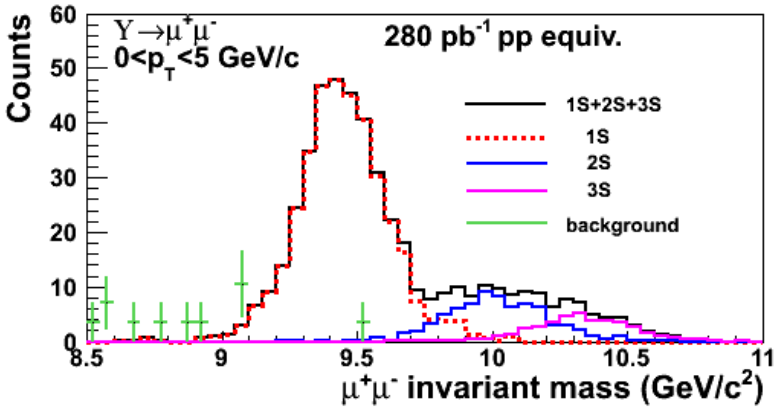


1. J/ψ: S/B=6 in d+Au and S/B=2 in central Au+Au
2. With HFT, study B→J/ψ X; J/ψ→μμ using displaced vertices
3. Excellent mass resolution: separate different upsilon states

Heavy flavor collectivity and color screening, quarkonia production mechanisms:

J/ψ $R_{AA}$ and $v_2$; upsilon $R_{AA}$ …

Quarkonium dissociation temperatures – Digal, Karsch, Satz

| state | $J/\psi(1S)$ | $\chi_c(1P)$ | $\psi'(2S)$ | $\Upsilon(1S)$ | $\chi_b(1P)$ | $\Upsilon(2S)$ | $\chi_b(2P)$ | $\Upsilon(3S)$ |
|---|---|---|---|---|---|---|---|---|
| $T_d/T_c$ | 2.10 | 1.16 | 1.12 | $> 4.0$ | 1.76 | 1.60 | 1.19 | 1.17 |

# Future Measurement Projection

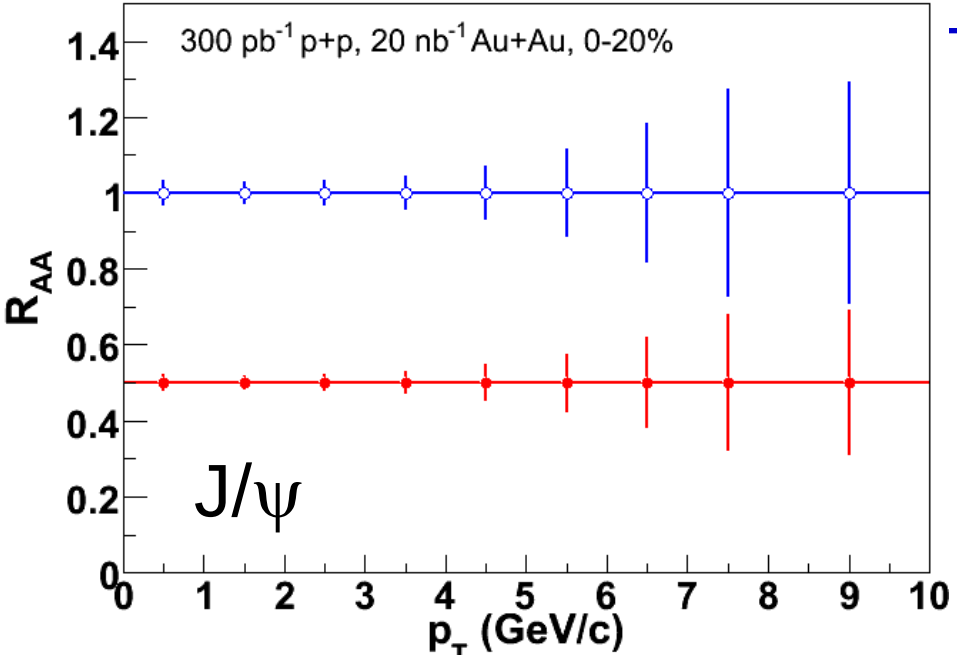


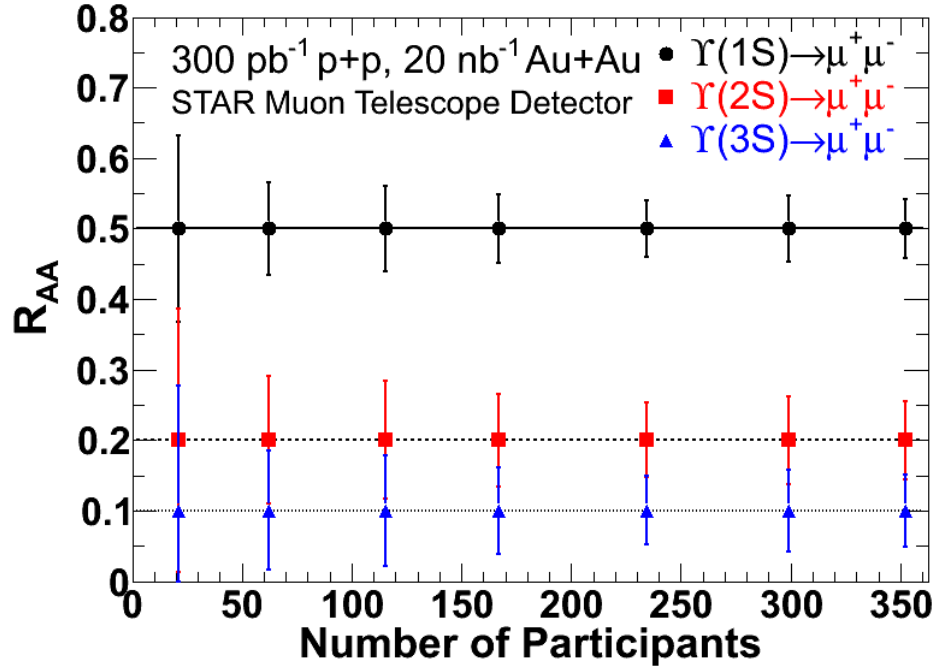


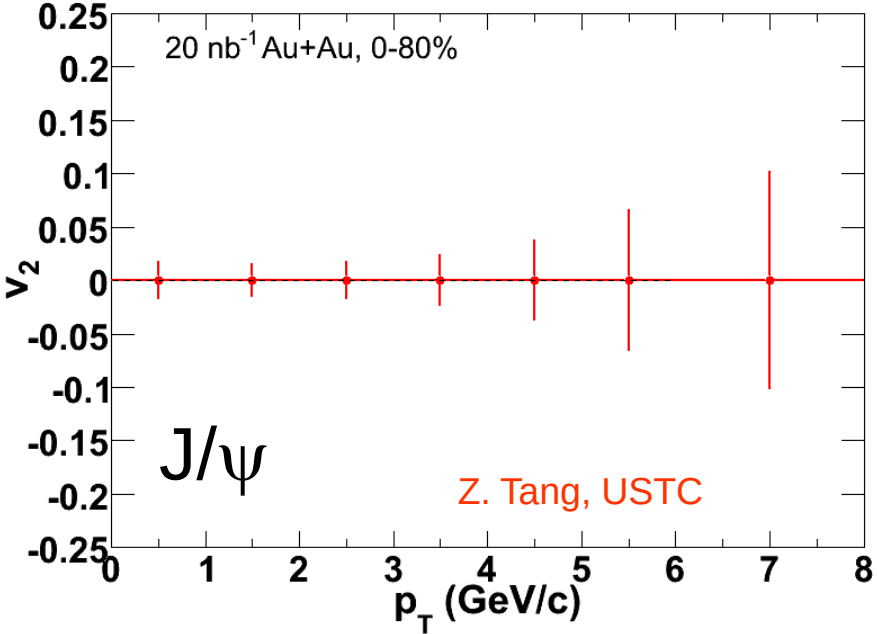


J/ψ $R_{AA}$ and $v_2$;
Y (1S, 2S, 3S) $R_{AA}$ versus $N_{part}$…

Different Upsilon states in 500 GeV p+p collisions can be measured with good precision from 12 weeks run.

# Distinguish Heavy Flavor and Initial Lepton Pair Production: e-muon Correlation

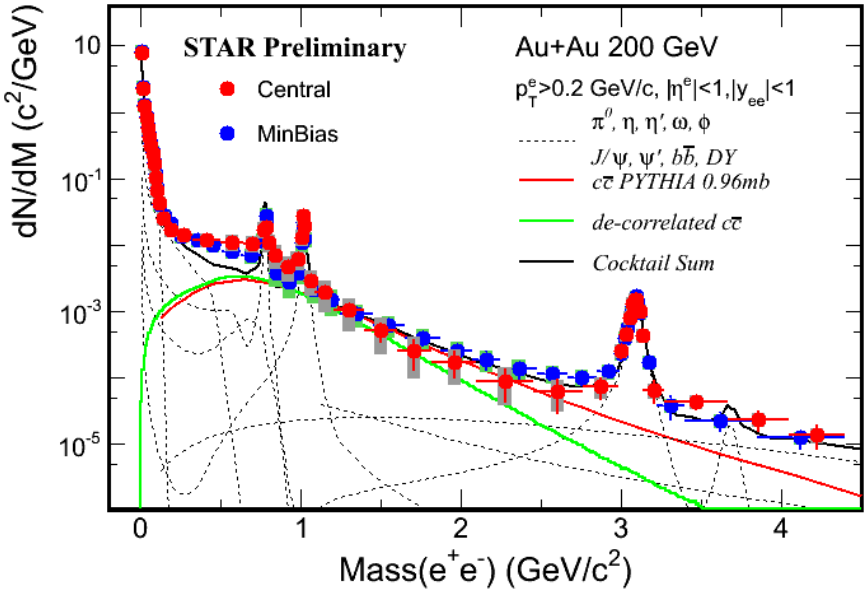


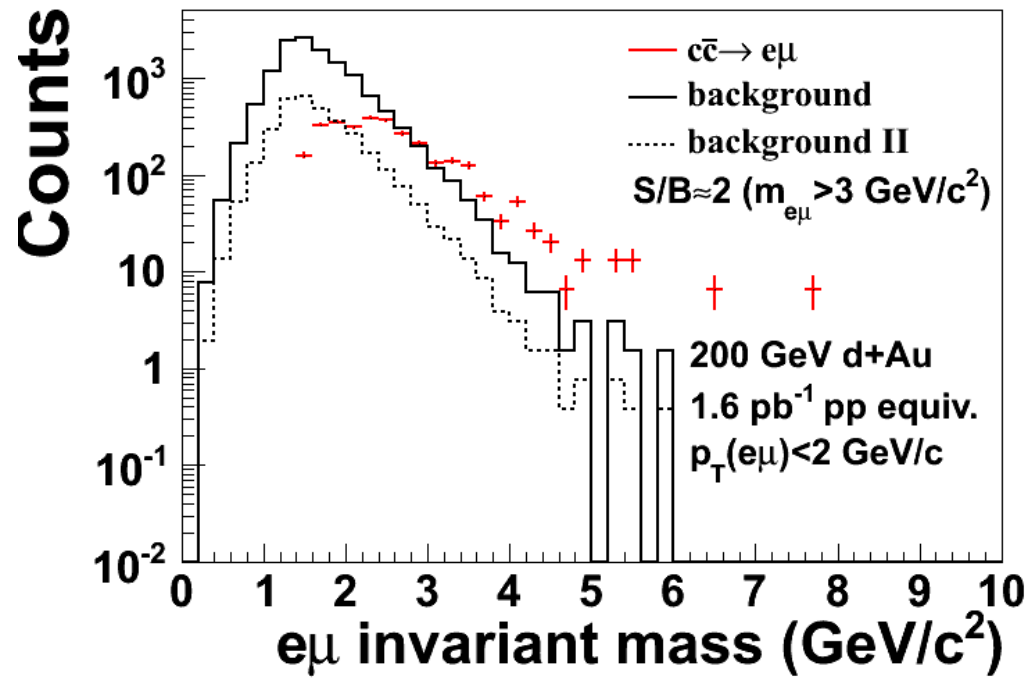


eμ correlation simulation with Muon Telescope Detector at STAR from ccbar:

S/B=2 ($M_{eu}$>3 GeV/c2 and $p_T(e\mu)$<2 GeV/c)

S/B=8 with electron pairing and tof association

MTD: construction starts in FY2011;
project completion in FY2014

# MTD in Run12

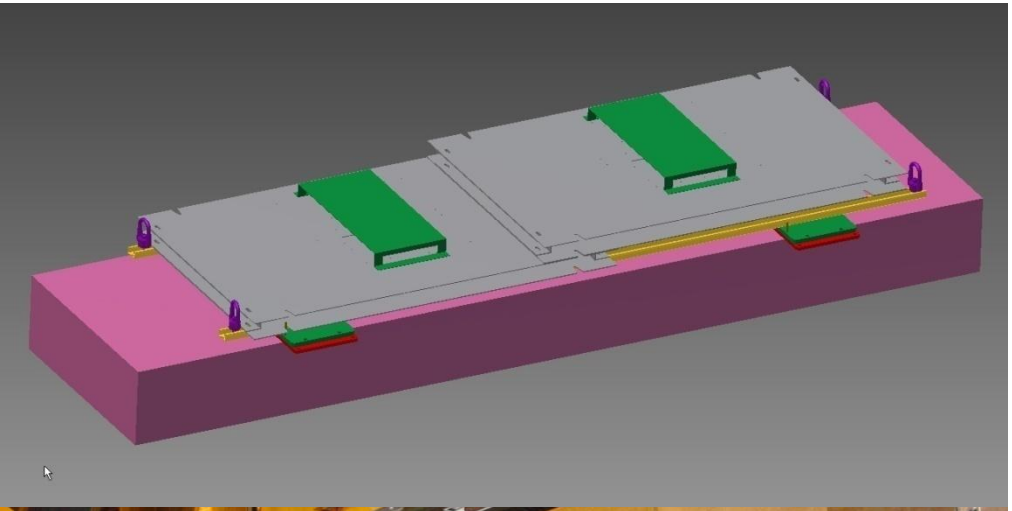

Two-pack system for the installation, designed by B. Llope and J. Scheblein, proven to be successful.

MRPC built at USTC and Tsinghua, trays assembled at UT-Austin.

For Run 12, 13 trays on three backlegs installed by STSG. Fully integrated into STAR Data Acquisition system since Jan. 2012. Successfully took MTD triggered events since Feb. 2012.

# MTD Performance from Run 12

e-muon

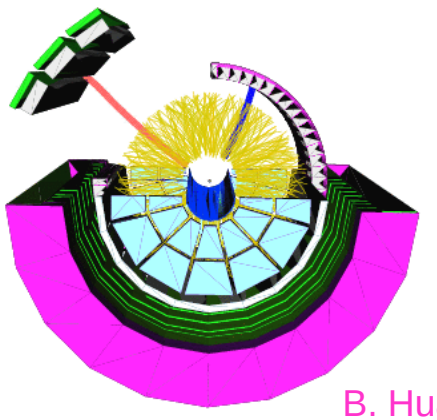

di-muon

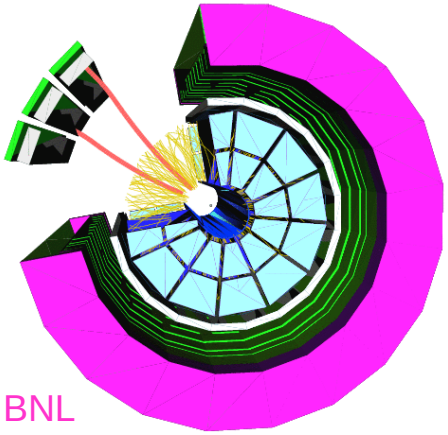

B. Huang, BNL

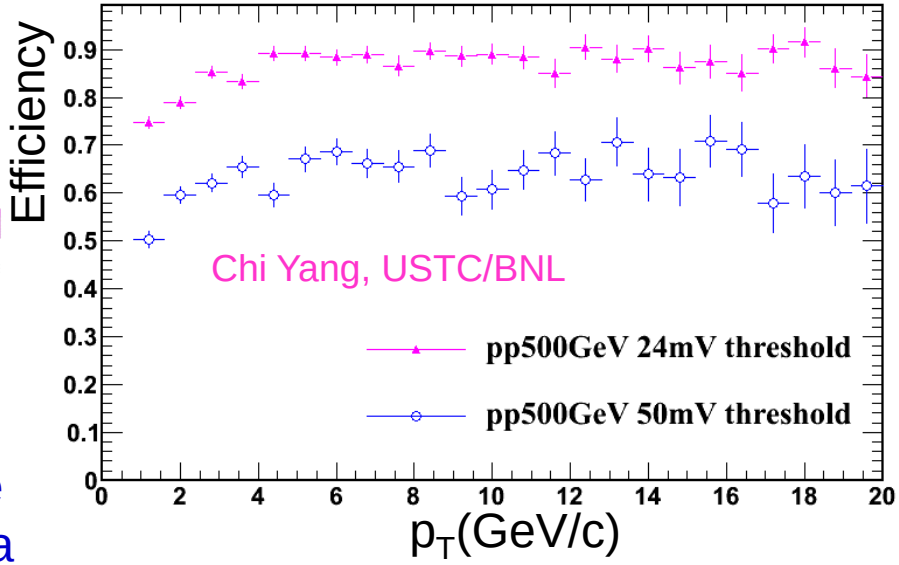


Commissioned e-muon (coincidence of single MTD hit and BEMC energy deposition above a certain threshold) and di-muon triggers, event display for
Cu+Au collisions shown above.

Determined the electronics threshold for the future runs, achieve 90% efficiency at threshold 24 mV

Intrinsic timing and spatial resolution: < 100 ps and 1~2 cm, respectively.

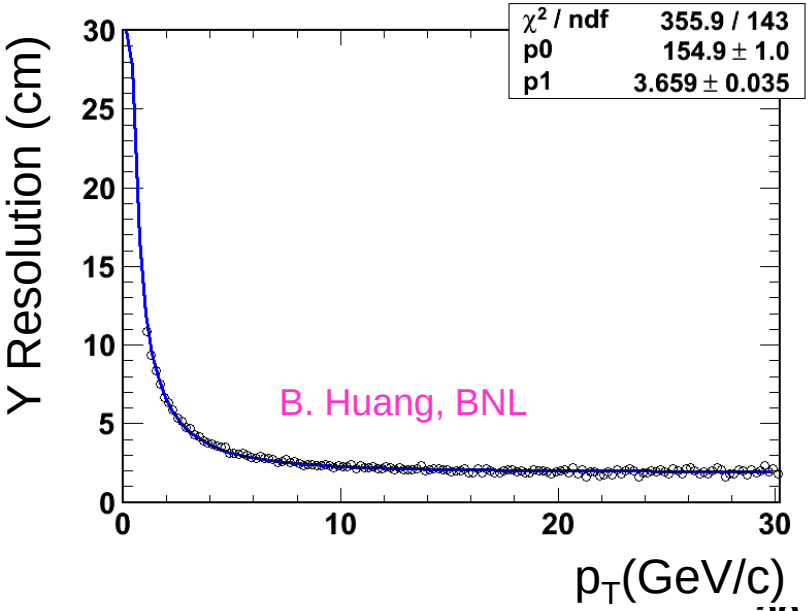

# MTD for Run 13

L-R: John, Bob, Bill, Matt, Tim, Chris, Chi, Hui, Wangmei, Alex, Anthony
Not shown: Bingchu and Shuai

By Nov. 13th, 63% of the MTD system was installed at STAR for Run 2013, electronics commissioning is on-going.
Superseded the milestone (43%) for Run 2013.

# Understanding Symmetry and Degree Of Freedom

- RHIC is the best facility to study novel symmetries and critical point:
  - flexible machine to change conditions beam species (magnetic field), BES (turn on/off QGP)
  - Large Acceptance (good for both LPV and chiral symmetry)
  - Excellent lepton PID (both electrons and muons at midrapidity, who else has that!)
- Since the beginning of physics, symmetry considerations have provided us with an extremely powerful and useful tool in our effort to understand nature. Gradually they have **become the backbone of our theoretical formulation of physical laws**.

  — Tsung-Dao Lee
  *Particle Physics and an Introduction to Field Theory* (1981), 177

- Novel Symmetries:
  - beam energy: deconfinement, chiral symmetry
  - Beam species: magnetic field
- Medium effect on vector mesons (chiral symmetry, resonant states):
  - beam energy;
  - Spectra and $v_2$ vs $M_{l+l-}$
- HFT+MTD upgrade
  - First glimpse of dilepton spectra around $\rho_0$ and $1<M<3$GeV
  - Heavy-flavor flow
- Future+
  - iTPC+Phase II BES
  - **Detailed studies of DOF**

# Thermal Radiation Workshop

**December 5-7, 2012**

**Physics Department**
**Small Seminar Room**

~ ~ ~ ~ ~ ~ ~ ~ ~ ~ ~ ~ ~ ~

## Wednesday, Dec 5th

**08:30-08:45 Registration**

08:45-09:00 Welcome: *N. Samios*
09:00-09:40 Thermal dileptons: *R. Rapp*
09:40-10:20 Glasma effect on dilepton and thermal photon: *L. McLerran*

**10:20-10:50 Coffee Break**

10:50-11:30 Dileptons from PHSD model: *O. Linnyk*
11:30-12:00 Di-electron spectra from 200 GeV p+p and Au+Au with the HBD from PHENIX: *I. Ravinovich*
12:00-12:30 Di-electron spectra from 200 GeV p+p and Au+Au from STAR: *B. Huang*

**12:30-02:00 Lunch Break**

02:00-02:40 Thermal dileptons from NA60 and possible future opportunities at SPS: *A. Drees*
02:40-03:20 Results on virtual photon production at SIS: resume and prospects: *T. Galatyuk*

**03:20-03:50 Coffee Break**

03:50-04:30 Future dilepton measurements: *I. Tserruya*
04:30-05:10 Future dilepton measurements from STAR: *Z. Xu*

**05:10-06:00 Discussion Session**

## Thursday, Dec 6th

09:00-09:40 Anisotropy of photon production in magnetic field: *V. Skokov*
09:40-10:20 Photon decay in strong magnetic field in heavy-ion collisions: *K. Tuchin*

**10:20-10:50 Coffee Break**

10:50-11:30 Cold nuclear matter effect on dilepton and photon production: *Z. Kang*
11:30-12:00 Direct photon spectra and elliptic flow in 2.76 TeV Pb+Pb collisions from ALICE: *M. Wilde*
12:00-12:30 Thermal photon yield and elliptic flow in 200 GeV Au+Au collisions from PHENIX: *R. Petti*

**12:30-02:00 Lunch Break**

Back to Contents

02:00-02:40 Dilepton production at RHIC energy: *Q. Wang*
02:40-03:20 Lattice QCD study of spectral function and EM emission rate: *H.-T. Ding*

**03:20-03:50 Coffee Break**

03:50-04:20 Di-electron production in 200 GeV d+Au collisions from PHENIX: *D. Sharma*
04:20-04:50 Di-electron production in Au+Au collisions from 19.6 to 62 GeV from STAR: *P. Huck*
04:50-05:20 Connection between dilepton data and chiral symmetry restoration: *P. Hohler*

**05:20-06:00 Discussion**

**06:30-08:00 Dinner at Brookhaven Center South Room**

## Friday, Dec 7th

09:00-09:40 Initial state and hydrodynamic evolution in heavy-ion collisions: *B. Schenke*
09:40-10:20 Viscosity effect on thermal photon production: *K. Dusling*

**10:20-10:50 Coffee Break**

10:50-11:30 Thermal dileptons at RHIC: *G. Vujanovic*
11:30-12:00 Di-electron measurement with ALICE at the LHC: *R. Averbeck*

12:00-12:30 Di-electron elliptic flow measurements in 200 GeV Au+Au from STAR: *X. Cui*

**12:30-02:00 Lunch Break**

02:00-02:40 Photon and dilepton emission from the hadronization process: *G. Chen*
02:40-03:20 Thermal photon from NLO calculation: *D. Teaney*

**03:20-03:50 Coffee Break**

03:50-04:30 New ideas about photons/dileptons: *E. Shuryak*

**04:30-06:00 Discussion**

Back to Contents

Thermal Radiation Workshop
December 5-7, 2012

# List of Registered Participants

| Name | Affiliation | E-Mail Address |
|---|---|---|
| Yasuyuki Akiba | RIKEN | akiba@bnl.gov |
| Ermias Atomssa | Stony Brook Univ | etatomssa@gmail.com |
| Ralf Averbeck | EMMI & GSI | R.Averbeck@gsi.de |
| Henner Buesching | Univ of Frankfurt | buschin@ikf.uni-frankfurt.de |
| Joseph Butterworth | Rice Univ | sbutter482@aol.com |
| Guangyao Chen | Texas A&M Univ | glorychern@neo.tamu.edu |
| William Christie | BNL | christie@bnl.gov |
| Xiangli Cui | BNL | cuixl@rcf.rhic.bnl.gov |
| Gabor David | BNL | david@bnl.gov |
| Heng-Tong Ding | BNL | htding@quark.phy.bnl.gov |
| Axel Drees | Stony Brook Univ | axel.drees@stonybrook.edu |
| Xin Dong | LBNL | XDong@lbl.gov |
| Kevin Dusling | North Carolina State Univ | kevin_dusling@ncsu.edu |
| Rainer Fries | Texas A&M Univ | rjfries@comp.tamu.edu |
| Tetyana Galatyuk | TU Darmstadt / GSI | t.galatyuk@gsi.de |
| Charles Gale | McGill Univ | gale@physics.mcgill.ca |
| Frank Geurts | Rice Univ | geurts@rice.edu |
| Yi Guo | BNL | yiguo@rcf.rhic.bnl.gov |
| Paul Hohler | Cyclotron Inst at Texas A&M Univ | pmhohler@comp.tamu.edu |
| Patrick Huck | LBNL | phuck@lbl.gov |
| Bingchu Huang | BNL | huangbc@bnl.gov |
| Zhongbo Kang | LANL | zkang@quark.phy.bnl.gov |
| Volker Koch | LBNL | vkoch@lbl.gov |
| Dmitry Kotov | PNPI | kotovdo@rcf.rhic.bnl.gov |
| Shu Lin | BNL | slin@bnl.gov |
| Olena Linnyk | Univ of Giessen | linnyk@fias.uni-frankfurt.de |
| Larry McLerran | BNL | mclerran@bnl.gov |
| Agnes Mocsy | Pratt Inst | mocsyagi@gmail.com |
| Richard Petti | Stony Brook Univ | richard.petti@gmail.com |
| Ralf Rapp | Texas A&M Univ | rapp@comp.tamu.edu |
| Ilia Ravinovich | Weizmann Inst of Science | Ilia.Ravinovich@weizmann.ac.il |
| Sky Rolnick | Univ of CA, Riverside | skymeson@gmail.com |
| Lijuan Ruan | BNL | ruan@bnl.gov |
| Takao Sakaguchi | BNL | takao@bnl.gov |
| Bjoern Schenke | BNL | bschenke@bnl.gov |
| Deepali Sharma | Stony Brook Univ | deepali@rcf.rhic.bnl.gov |
| Edward Shuryak | Stony Brook Univ | shuryak@me.com |
| Vladimir Skokov | BNL | vvskokov@gmail.com |
| Derek Teaney | Stony Brook Univ | derek.teaney@stonybrook.edu |
| Itzhak Tserruya | Weizmann Institute of Science | Itzhak.Tserruya@weizmann.ac.il |
| Giorgio Torrieri | Frankfurt University | torrieri@phys.columbia.edu |
| Kirill Tuchin | Iowa State Univ | tuchink@gmail.com |
| Gojko Vujanovic | McGill University | gojkov@physics.mcgill.ca |
| Qun Wang | Univ Science & Technology of China | qunwang@ustc.edu.cn |
| Martin Wilde | Institut for Kernphysik WWU Muenster | m_wild03@uni-muenster.de |
| Kefeng Xin | Rice Univ | kefeng.xin@rice.edu |
| Zhangbu Xu | BNL | xzb@bnl.gov |
| Chi Yang | BNL | chiyang@rcf.rhic.bnl.gov |
| Shuai Yang | BNL | syang@rcf.rhic.bnl.gov |

Back to Contents

# RIKEN BNL Research Center Proceedings

Volume 112 – RBRC Scientific Review Committee Meeting, November 6-8, 2012
Volume 111 – Forward Physics at RHIC, July 30-Aug 1, 2012 – BNL-98400-2012
Volume 110 – P- and CP-odd Effects in Hot and Dense Matter, June 25-27, 2012 – BNL-98398-2012
Volume 109 – New Horizons for Lattice Computations with Chiral Fermions, May 14-18, 2012 – BNL-98392-2012
Volume 108 – Hyperon-Hyperon Interactions and Searches for Exotic Di-Hyperons in Nuclear Collisions, February 29 – March 2, 2012 – BNL-97035-2012
Volume 107 – Future Directions in High Energy QCD, October 20-22, 2011 – BNL-98119-2011
Volume 106 – Fluctuations, Correlations and RHIC Low Energy Runs, October 3-5, 2011 – BNL-96514-2011
Volume 105 – Opportunities for Polarized He-3 in RHIC and EIC, September 28-30, 2011 – BNL-96418-2011
Volume 104 – Brookhaven Summer Program on Quarkonium Production in Elementary and Heavy Ion Collisions, June 6-18, 2011 – BNL-96171-2011
Volume 103 – Opportunities for Drell-Yan Physics at RHIC, May 11-13, 2011 – BNL-95236-2011-2011
Volume 102 – Initial State Fluctuations and Final-State Particle Correlations, February 2-4, 2011 – BNL-94704-2011
Volume 101 – RBRC Scientific Review Committee Meeting, October 27-29, 2010 – BNL-94589-2011
Volume 100 – Summer Program on Nucleon Spin Physics, July 14-27, 2010 – BNL-96163-2011
Volume 99 – The Physics of W and Z Bosons, June 24-25, 2010 – BNL-94287-2010
Volume 98 – Saturation, the Color Glass Condensate and the Glasma: What Have we Learned from RHIC? – May 10-12, 2010 – BNL-94271-2010
Volume 97 – RBRC Scientific Review Committee Meeting, October 21-22, 2009 – BNL-90674-2009
Volume 96 – P- and CP-Odd Effects in Hot and Dense Matter, April 26-30, 2010 – BNL-94237-2010
Volume 95 – Progress in High-pT Physics at RHIC, March 17-19, 2010 – BNL-94214-2010
Volume 94 – Summer Program on Nucleon Spin Physics at LBL, June 1-12, 2009
Volume 93 – PHENIX Spinfest School 2009 at BNL - July 1-31, 2009. BNL-90343-2009
Link: PHENIXSpinfestSchool2009@BNL
Volume 92 – PKU-RBRC Workshop on Transverse Spin Physics, June 30 - July 4, 2008, Beijing, China – BNL-81685-2008
Volume 91 – RBRC Scientific Review Committee Meeting, November 17-18, 2008 – BNL-81556-2008
Volume 90 – PHENIX Spinfest School 2008 at BNL, August 4-8, 2008 – BNL-81478-2008
Volume 89 – Understanding QGP through Spectral Functions and Euclidean Correlators, April 23-25, 2008 – BNL-81318-2008
Volume 88 – Hydrodynamics in Heavy Ion Collisions and QCD Equation of State, April 21-22, 2008 – BNL-81307-2008
Volume 87 – RBRC Scientific Review Committee Meeting, November 5-6, 2007 – BNL-79570-2007
Volume 86 – Global Analysis of Polarized Parton Distributions in the RHIC Era, October 8, 2007 – BNL-79457-2007
Volume 85 – Parity-Violating Spin Asymmetries at RHIC-BNL, April 26-27, 2007 – BNL-79146-2007
Volume 84 – Domain Wall Fermions at Ten Years, March 15-17, 2007 – BNL 77857-2007
Volume 83 – QCD in Extreme Conditions, July 31 - August 2, 2006 – BNL-76933-2006
Volume 82 – RHIC Physics in the Context of the Standard Model, June 18-23, 2006 – BNL-76863-2006
Volume 81 – Parton Orbital Angular Momentum (Joint RBRC/University of New Mexico Workshop) February 24-26, 2006 – BNL-75937-2006
Volume 80 – Can We Discover the QCD Critical Point at RHIC?, March 9-10, 2006 – BNL-75692-2006
Volume 79 – Strangeness in Collisions, February 16-17, 2006 – BNL-79763-2008
Volume 78 – Heavy Flavor Productions and Hot/Dense Quark Matter, December 12-14, 2005 – BNL-76915-2006
Volume 77 – RBRC Scientific Review Committee Meeting, October 10-12, 2005 – BNL-52649-2005

Back to Contents

Volume 76 – Odderon Searches at RHIC, September 27-29, 2005 – BNL-75092-2005
Volume 75 – Single Spin Asymmetries, June 1-3, 2005 – BNL-74717-2005
Volume 74 – RBRC QCDOC Computer Dedication and Symposium on RBRC QCDOC, May 26, 2005 – BNL-74813-2005
Volume 73 – Jet Correlations at RHIC, March 10-11, 2005 – BNL-73910-2005
Volume 72 – RHIC Spin Collaboration Meetings XXXI (January 14, 2005), XXXII (February 10, 2005), XXXIII (March 11, 2005) – BNL-73866-2005
Volume 71 – Classical and Quantum Aspects of the Color Glass Condensate – BNL-73793-2005
Volume 70 – Strongly Coupled Plasmas: Electromagnetic, Nuclear & Atomic – BNL-73867-2005
Volume 69 – RBRC Scientific Review Committee – BNL-73546-2004
Volume 68 – Workshop on the Physics Programme of the RBRC and UKQCD QCDOC Machines – BNL-73604-2004
Volume 67 – High Performance Computing with BlueGene/L and QCDOC Architectures
Volume 66 – RHIC Spin Collaboration Meeting XXIX, October 8-9, 2004, Torino Italy – BNL-73534-2004
Volume 65 – RHIC Spin Collaboration Meetings XXVII (July 22, 2004), XXVIII (September 2, 2004), XXX (December 6, 2004) – BNL-73506-2004
Volume 64 – Theory Summer Program on RHIC Physics – BNL-73263-2004
Volume 63 – RHIC Spin Collaboration Meetings XXIV (May 21, 2004), XXV (May 27, 2004), XXVI (June 1, 2004) – BNL-72397-2004
Volume 62 – New Discoveries at RHIC, May 14-15, 2004 – BNL- 72391-2004
Volume 61 – RIKEN-TODAI Mini Workshop on "Topics in Hadron Physics at RHIC", March 23-24, 2004 – BNL-72336-2004
Volume 60 – Lattice QCD at Finite Temperature and Density – BNL–72083-2004
Volume 59 – RHIC Spin Collaboration Meeting XXI (January 22, 2004), XXII (February 27, 2004), XXIII (March 19, 2004)– BNL-72382-2004
Volume 58 – RHIC Spin Collaboration Meeting XX – BNL-71900-2004
Volume 57 – High pt Physics at RHIC, December 2-6, 2003 – BNL-72069-2004
Volume 56 – RBRC Scientific Review Committee Meeting – BNL-71899-2003
Volume 55 – Collective Flow and QGP Properties – BNL-71898-2003
Volume 54 – RHIC Spin Collaboration Meetings XVII, XVIII, XIX – BNL-71751-2003
Volume 53 – Theory Studies for Polarized pp Scattering – BNL-71747-2003
Volume 52 – RIKEN School on QCD "Topics on the Proton" – BNL-71694-2003
Volume 51 – RHIC Spin Collaboration Meetings XV, XVI – BNL-71539-2003
Volume 50 – High Performance Computing with QCDOC and BlueGene – BNL-71147-2003
Volume 49 – RBRC Scientific Review Committee Meeting – BNL-52679
Volume 48 – RHIC Spin Collaboration Meeting XIV – BNL-71300-2003
Volume 47 – RHIC Spin Collaboration Meetings XII, XIII – BNL-71118-2003
Volume 46 – Large-Scale Computations in Nuclear Physics using the QCDOC – BNL-52678
Volume 45 – Summer Program: Current and Future Directions at RHIC – BNL-71035
Volume 44 – RHIC Spin Collaboration Meetings VIII, IX, X, XI – BNL-71117-2003
Volume 43 – RIKEN Winter School – Quark-Gluon Structure of the Nucleon and QCD – BNL-52672
Volume 42 – Baryon Dynamics at RHIC – BNL-52669
Volume 41 – Hadron Structure from Lattice QCD – BNL-52674
Volume 40 – Theory Studies for RHIC-Spin – BNL-52662
Volume 39 – RHIC Spin Collaboration Meeting VII – BNL-52659
Volume 38 – RBRC Scientific Review Committee Meeting – BNL-52649
Volume 37 – RHIC Spin Collaboration Meeting VI (Part 2) – BNL-52660

Back to Contents

Volume 36 – RHIC Spin Collaboration Meeting VI – BNL-52642
Volume 35 – RIKEN Winter School – Quarks, Hadrons and Nuclei – QCD Hard Processes and the Nucleon Spin – BNL-52643
Volume 34 – High Energy QCD: Beyond the Pomeron – BNL-52641
Volume 33 – Spin Physics at RHIC in Year-1 and Beyond – BNL-52635
Volume 32 – RHIC Spin Physics V – BNL-52628
Volume 31 – RHIC Spin Physics III & IV Polarized Partons at High Q^2 Region – BNL-52617
Volume 30 – RBRC Scientific Review Committee Meeting – BNL-52603
Volume 29 – Future Transversity Measurements – BNL-52612
Volume 28 – Equilibrium & Non-Equilibrium Aspects of Hot, Dense QCD – BNL-52613
Volume 27 – Predictions and Uncertainties for RHIC Spin Physics & Event Generator for RHIC Spin Physics III – Towards Precision Spin Physics at RHIC – BNL-52596
Volume 26 – Circum-Pan-Pacific RIKEN Symposium on High Energy Spin Physics – BNL-52588
Volume 25 – RHIC Spin – BNL-52581
Volume 24 – Physics Society of Japan Biannual Meeting Symposium on QCD Physics at RIKEN BNL Research Center – BNL-52578
Volume 23 – Coulomb and Pion-Asymmetry Polarimetry and Hadronic Spin Dependence at RHIC Energies – BNL-52589
Volume 22 – OSCAR II: Predictions for RHIC – BNL-52591
Volume 21 – RBRC Scientific Review Committee Meeting – BNL-52568
Volume 20 – Gauge-Invariant Variables in Gauge Theories – BNL-52590
Volume 19 – Numerical Algorithms at Non-Zero Chemical Potential – BNL-52573
Volume 18 – Event Generator for RHIC Spin Physics – BNL-52571
Volume 17 – Hard Parton Physics in High-Energy Nuclear Collisions – BNL-52574
Volume 16 – RIKEN Winter School - Structure of Hadrons - Introduction to QCD Hard Processes – BNL-52569
Volume 15 – QCD Phase Transitions – BNL-52561
Volume 14 – Quantum Fields In and Out of Equilibrium – BNL-52560
Volume 13 – Physics of the 1 Teraflop RIKEN-BNL-Columbia QCD Project First Anniversary Celebration – BNL-66299
Volume 12 – Quarkonium Production in Relativistic Nuclear Collisions – BNL-52559
Volume 11 – Event Generator for RHIC Spin Physics – BNL-66116
Volume 10 – Physics of Polarimetry at RHIC – BNL-65926
Volume 9 – High Density Matter in AGS, SPS and RHIC Collisions – BNL-65762
Volume 8 – Fermion Frontiers in Vector Lattice Gauge Theories – BNL-65634
Volume 7 – RHIC Spin Physics – BNL-65615
Volume 6 – Quarks and Gluons in the Nucleon – BNL-65234
Volume 5 – Color Superconductivity, Instantons and Parity (Non?)-Conservation at High Baryon Density – BNL-65105
Volume 4 – Inauguration Ceremony and Non-Equilibrium Many Body Dynamics – BNL-64912
Volume 3 – Hadron Spin-Flip at RHIC Energies – BNL-64724
Volume 2 – Perturbative QCD as a Probe of Hadron Structure – BNL-64723
Volume 1 – Open Standards for Cascade Models for RHIC – BNL-64722

Back to Contents

Li Keran

**Nuclei as heavy as bulls**
**Through collision**
**Generate new states of matter.**
**T.D. Lee**

©CCASTA

**Organizers**

Yasuyuki Akiba (RIKEN Nishina Center/RBRC)
Axel Drees (Stony Brook University)
Rainer Fries (Texas A&M)
Charles Gale (McGill University)
Lijuan Ruan (BNL)

**RIKEN BNL Research Center**
Bldg. 510A, Brookhaven National Laboratory
Upton, NY 11973-5000, USA

December 2012